Conceptual Site Model, Investigation and Remediation of Releases and Groundwater Protection and Evaluation, Red Hill Bulk Fuel Storage Facility

JOINT BASE PEARL HARBOR-HICKAM, O‘AHU, HAWAI‘I

Administrative Order on Consent in the Matter of Red Hill Bulk Fuel Storage Facility, EPA Docket Number RCRA 7003-R9-2015-01 and DOH Docket Number 15-UST-EA-01, Attachment A, Statement of Work Section 6.2, Section 7.1.2, Section 7.2.2, and Section 7.3.2

July 27, 2018
Revision 00

Comprehensive Long-Term Environmental Action Navy
Contract Number N62742-12-D-1829, CTO18F0126

This page intentionally left blank

Conceptual Site Model, Investigation and Remediation of Releases and Groundwater Protection and Evaluation, Red Hill Bulk Fuel Storage Facility

JOINT BASE PEARL HARBOR-HICKAM, O'AHU, HAWAI'I

Administrative Order on Consent in the Matter of Red Hill Bulk Fuel Storage Facility, EPA Docket Number RCRA 7003-R9-2015-01 and DOH Docket Number 15-UST-EA-01, Attachment A, Statement of Work Section 6.2, Section 7.1.2, Section 7.2.2, and Section 7.3.2

July 27, 2018
Revision 00

Prepared for:

Defense Logistics Agency Energy
8725 John J Kingman Rd Suite 4950
Fort Belvoir, VA 22060-6222

Prepared by:

AECOM Technical Services, Inc.
1001 Bishop Street, Suite 1600
Honolulu, HI 96813-3698

Prepared under:

Comprehensive Long-Term Environmental Action Navy
Contract Number N62742-12-D-1829, CTO18F0126

This page intentionally left blank

EXECUTIVE SUMMARY

This *Conceptual Site Model* (CSM) document provides a basis for evaluating contaminant transport pathways and the potential for exposure of human receptors to potentially impacted drinking water in support of the *Investigation and Remediation of Petroleum Product Releases and Groundwater Protection and Evaluation* project, at Red Hill Bulk Fuel Storage Facility ("the Facility"), Joint Base Pearl Harbor-Hickam (JBPHH), Hawai'i. The Facility is owned by the United States (U.S.) Navy (DON; "Navy") and operated by Defense Logistics Agency (DLA).

This document has been prepared under Statement of Work Sections 6 and 7 of the *Administrative Order on Consent* (AOC) *In the Matter of Red Hill Bulk Fuel Storage Facility* (EPA Docket No: RCRA 7003-R9-2015-01; DOH Docket No: 15-UST-EA-01) (EPA Region 9 and DOH 2015). The AOC was issued by the U.S. Environmental Protection Agency (EPA) Region 9 and State of Hawai'i Department of Health (DOH) (EPA Region 9 and DOH 2015) to the Navy/DLA in response to a release of an estimated 27,000 gallons of Jet Fuel Propellant (JP)-8 from one of the Facility's underground fuel storage tanks (Tank 5) that was confirmed and reported to DOH on January 23, 2014. The tanks are located above a major groundwater aquifer, which is used to feed both Navy and City and County of Honolulu drinking water supply wells and shafts.

The CSM was developed in accordance with the *CSM Development and Update Plan* (DON 2017k) to identify and evaluate the site-specific characteristics and processes that control the fate and transport of jet fuel (light non-aqueous-phase liquid [LNAPL]) and its constituent chemicals (petroleum hydrocarbons) from the source of the release (an underground fuel storage tank[s] at the Facility), through the vadose and saturated zones, and on to potential receptors (e.g., residential receptors exposed via the drinking water pathway). The CSM is an evolving tool that will continue to be updated as new information becomes available.

This CSM document is organized into seven detailed modules that describe the site-specific data and information, or lines of evidence (LOEs), used to develop the current version of the CSM and evaluate remaining uncertainties. These seven modules are summarized in Table ES-1, which identifies the LOEs to date, the remaining uncertainties, and the activities planned to help fill existing data gaps and help address the uncertainties.

Overall, the current CSM indicates that LNAPL released from Red Hill fuel storage tanks has entered the vadose zone at various areas beneath Red Hill. LNAPL entering the vadose zone encounters a complex geology in the surrounding volcanic layers that vary significantly in their permeability and overall geometry. Consequently, LNAPL will migrate laterally through high-permeability zones underlain by low-permeability layers. Vertical migration is likely manifested through clinker bridges, and highly fractured zones. As LNAPL moves through the pore spaces, some of it will be trapped in poorly connected fractures, voids, and pores. The LNAPL tends to preferentially migrate toward the predominant dip direction of 10–12 degrees to the south-southwest (between 190 and 210 degrees). Once the LNAPL encounters the water table, its vertical migration potential is minimized due to the density difference between LNAPL and water. Soluble components (monitored by analyzing groundwater samples for chemicals of potential concern [COPCs]) would enter the groundwater through either dissolution from LNAPL in the vadose zone due to infiltrating water or through dissolution of LNAPL in the saturated zone close to the water table. Currently, no LNAPL has been measured in the water table monitoring wells. However, analytical data indicate the possible presence of LNAPL in close proximity to RHMW02 or at the water table upgradient of RHMW02. The thermal study conducted in October 2017 shows evidence that residual LNAPL is primarily limited to a depth of 30 feet (ft) beneath the top of wells RHMW02 and RHMW03 (inside the lower access tunnel) and is being biodegraded. General transport of COPCs in the dissolved

plume is in the southwest direction toward Red Hill Shaft. Migration to the southeast and northwest is limited by the extent of lower-permeability materials (valley fill and saprolite) extending below the water table in the valleys bounding the Facility. Attenuation of COPCs in the dissolved plume in the saturated zone limit the extent of the existing small dissolved plume before reaching Red Hill Shaft under present conditions and within the context of historical releases.

Key findings from recently completed studies, field work, and computer simulations include:

- Long-term monitoring (LTM) and associated studies indicate that the 2014 release from Tank 5 had minimal or no impacts to groundwater at Red Hill.
- Based on thermal Natural Source-Zone Depletion (NSZD) studies, LTM and other studies indicate that LNAPL has reached residual saturation within approximately 30 feet beneath the tanks and has not reached groundwater.
- Geologic information about the formation of lava tubes indicates that these will not act as preferential pathways for contaminants to flow between Red Hill and City and County of Honolulu Board of Water Supply (BWS) water supply wells.
- Seismic studies indicate that extensive saprolite zones exist beneath stream valleys on both sides of Red Hill (including South Hālawa Stream and Moanalua Valley) and that these extend significantly below the water table, acting as a barrier to groundwater contamination.
- While the geology is heterogeneous beneath Red Hill resulting in localized hydraulic gradients, overall flow appears to be highly influenced by clinker zones that provide a preferential pathway to Red Hill Shaft.
- Natural attenuation is occurring in both the unsaturated and saturated zones, and acts to degrade contaminants in the environment.
- Risk-based decision criteria (RBDC) have been developed that are protective of human health in regards to COPCs that may potentially impact public water supplies.
- Data collected as part of recent synoptic water level studies are assisting with the ongoing development of aquifer hydraulic property estimates and groundwater flow conditions in the area of the site.

Table ES-1: Summary of CSM Modules

Conceptual Model	Uncertainty	Ongoing, Planned, or Proposed Activity	Purpose
Module A: Physical Setting			
The 144-acre underground fuel storage Facility is located in south-central O'ahu approximately 2–3 miles east of Pearl Harbor, within the Red Hill ridge that divides South Hālawa Valley from Moanalua Valley on southwest flank of O'ahu's Ko'olau Mountain Range. The Facility's twenty 250-foot-tall,12.5-million-gallon fuel storage tanks store and supply fuel for military operations in Hawai'i and throughout the Pacific. The tank bottoms are situated approximately 100–130 ft above an underlying basal aquifer that is a major municipal and military drinking water source and is considered an irreplaceable resource with a high vulnerability to contamination. Below the surface soil and saprolite of Red Hill ridge, geologic formations consist largely of basalt with varying layers with materials exhibiting high and low permeability, containing occasional voids. In the surrounding valleys, sedimentary deposits are underlain by weathered basalt (saprolite) and unweathered basalt. In the Red Hill area, the basal aquifer water table lies at approximately 20 ft mean sea level. Groundwater in the Pearl Harbor vicinity generally flows toward the harbor, although potential exists for variances in localized flow directions depending on geologic formations and other factors.	• Nature of subsurface geology in North and South Hālawa Valleys and Moanalua Valley • Groundwater levels and hydraulic gradients in the site vicinity • Extent of perched groundwater on north side of Red Hill and adjacent South Hālawa Valley floor	• Install at least one test boring adjacent to a seismic survey transect location. • Continue a borehole geophysical and video logging program during installation of additional monitoring wells on Red Hill and in North and South Hālawa Valleys. • Incorporate in the modeling effort the results of the recently completed Red Hill monitoring well elevation survey, gyroscopic survey, and synoptic water level measurements. • Collect water elevation data on Red Hill and in South Hālawa Valley existing wells in the vicinity (e.g., Hālawa Correctional Facility).	• Enable direct correlation of observed geologic conditions with interpreted results of seismic survey transect at that location. • Better define the nature of subsurface geology in the valleys and support the groundwater flow and contaminant fate and transport modeling efforts. • Develop input parameters for groundwater flow modeling. Improve understanding of flow resulting from various pumping conditions. Further define actual groundwater flow directions and assess the potential for transport of contaminants to potential downgradient exposure points. • Further define the extent of the perched water zone and the extent that water recharge from the Hālawa Quarry area influences it.
Module B: Facility Construction and Operations			
The Facility's 20 fuel storage tanks were field-constructed of steel-lined concrete in the early 1940s. They are connected to a fuel pumping station at Pearl Harbor via a tunnel system. Kerosene-based jet fuels stored at the Facility have included JP-5, JP-8, and NATO-grade F-24; the tanks currently contain kerosene-based JP-5 and F-24 and F-76 Diesel Fuel-Marine.	• Facility construction and operation issues are addressed by other sections of the AOC Statement of Work (EPA Region 9 and DOH 2015).		
Module C: LNAPL Release and Source-Zone Migration Model			
During Tank 5 refilling operations following a routine 3-year inspection and refurbishment process conducted every 20 years, a release of approximately 27,000 gallons of JP-8 was confirmed and reported to DOH in writing on January 23, 2014. During that month, a fuel hydrocarbon seep confirmed to be JP-8 was observed on a tunnel wall below Tank 5, and soil vapor monitoring points installed beneath the tank exhibited a sharp increase in hydrocarbon vapor concentrations. Potential migration pathways include through gaps between the tank's steel lining and inner side of its concrete shell, and through cracks in the concrete shell into higher-permeability rock surrounding the concrete. Subsequent analysis indicated the cause of the release to be defective workmanship in welding by the tank refurbishment contractor, poor inspection, and ineffective quality control.	• Migration routes of LNAPL following a tank release	• Employ a statistical LNAPL holding model incorporating information regarding the 2014 Tank 5 release. • Measure vertical temperature profiles in key monitoring wells for evidence of biodegradation. • Collect and evaluate natural attenuation parameter (NAP) data (e.g., dissolved oxygen and dissolved methane in groundwater and in the soil vapor monitoring points). • Conduct an infiltration study. • Deploy carbon traps on Red Hill and inside the Facility tunnels to measure hydrocarbon-based carbon dioxide efflux to the surface and through the tunnel system.	• Better understand how LNAPL releases migrate through the subsurface, and estimate the amount of LNAPL that can be retained in the release area underlying the Red Hill tank farm without causing unacceptable risks to nearby receptors. • Indicate vertical distribution of LNAPL beneath selected tanks at the Facility. • Better understand where LNAPL biodegradation is occurring. • Determine if the observed mass discharge in groundwater can originate from LNAPL present in the unsaturated zone alone, or if LNAPL is likely present at the water table in the saturated zone. • Use data to calculate NSZD rate at the Facility, and in turn estimate the chronic release rate of fuel that will not result in unacceptable risk to nearby receptors.
Module D: Vadose Zone Model			
The Facility tanks are surrounded by rock in the vadose (i.e., unsaturated) zone, which consists primarily of basalt flows in complex, alternating layers. These heterogeneous layers vary from extremely high to extremely low permeability, with a corresponding varying ability to transmit or hold LNAPL depending on the layer's type and micro-pore structure (i.e., high ability in high-permeability a'ā and thin pāhoehoe flows; low ability in massive a'ā and massive pāhoehoe flows; limited transmissivity but high holding capacity in a'ā clinker zones). Geologic and water saturation characteristics in the rock surrounding the tanks will cause LNAPL to spread as it moves through the rock. As LNAPL moves through the larger pore spaces, some of it will be trapped in poorly connected fractures and blocked by surface tension and capillary forces of moisture, especially water held in the smaller pores. Hawaiian volcanic rocks vary in porosity and permeability depending on the emplacement process, lava type, genesis, flow thickness, flow rate, extent, cooling rate, and weathering. Permeability is typically highest in the relatively thick, unweathered rubbly a'ā clinker zones and intensely fractured zones or lava tubes of pāhoehoe flows. Permeability is much lower in the interior portions of massive flows, weathered interflows, intrusive rocks (dikes/sills), ash beds, and weathered rocks (saprolite)/soil horizons, which can impede vertical flow and horizontally flow across valleys. Generally, the vertical permeability of the basalt is orders of magnitude lower than the horizontal permeability. Horizontal permeability is higher in the direction that the lava flowed.	• Potential extent of LNAPL movement away from the Facility fuel tanks	• Collect core samples during installation of new monitoring wells for petrographic analyses, and prepare detailed geologic logs. Inspect the cores for presence of LNAPL.	• Measure residual saturation values to determine capacity of the basalt to retain LNAPL.

Conceptual Model	Uncertainty	Ongoing, Planned, or Proposed Activity	Purpose
Module E: Saturated Zone Model			
Groundwater flow and solute transport are controlled by the hydraulic and physical properties of the hydrogeologic units (HGUs), including hydraulic conductivity, effective porosity, specific yield, specific storage, and dispersivity. Fresh groundwater inflow originates as deep infiltration of precipitation and seepage from surface water features. According to the United States Geological Survey (USGS), estimates of recharge for O'ahu for recent conditions (2010 land cover and 1978–2007 rainfall) differ from predevelopment recharge values by only a few percent (Izuka et al. 2018). Spatial distribution of recharge mimics the orographic rainfall pattern—recharge is highest on windward slopes and mountain peaks below the top of the trade-wind inversion. Groundwater outflow includes withdrawals from wells and natural groundwater discharge to springs, streams, wetlands, and submarine seeps. Under predevelopment conditions, groundwater withdrawal was negligible and natural groundwater discharge probably was approximately equal to recharge. Under recent conditions, natural groundwater discharge has been reduced by the pumping well withdrawals. Data collected by the USGS for groundwater levels, saltwater/freshwater interface, spring flow, and stream base-flow indicate an overall reduction in aquifer storage for most areas where groundwater has been extracted; this has caused groundwater levels to decline (Izuka et al. 2018). Water sources in the Hālawa Quarry/cement plant area north of South Hālawa Valley likely increase groundwater recharge rates locally, create zones of shallow water, and appear to increase the water table elevation in the basal aquifer in the area north of South Hālawa Valley.	• Groundwater flow directions and rates in the groundwater model area • Thickness and extent of HGUs in the groundwater model area • Geologic features that may act as preferred groundwater flow pathways or barriers • Hydraulic properties of Basalt HGU (basal aquifer) • Groundwater recharge and discharge rates	• Incorporate results of recently completed high-precision Red Hill monitoring well elevation survey in the model, and future survey results for Hālawa Shaft, Moanalua, and Tripler Army Medical Center wells. • Collect groundwater level data from additional monitoring wells planned for installation on Red Hill and in North and South Hālawa Valleys. Calibrate groundwater model to reflect the new data. • Collect groundwater level data to represent both non-pumping conditions and various combinations of pumping of water supply wells in the area. Collect groundwater level measurements from intervals deeper below the water table. • Incorporate results of recently completed synoptic water level study. • Evaluate geospatial datasets from recent USGS studies. Evaluate boring data from the Honolulu Area Rapid Transit study for further integration into cross sections within the groundwater model domain. Collect additional hydrogeologic data and prepare detailed borehole geologic logs of deep borings in areas beneath North and South Hālawa Valleys, including near Hālawa Shaft. • Collect hydrogeologic data from additional monitoring wells now being installed by the Navy. Evaluate available geophysical methods to identify potential surveys at the land surface and in borings that may be effective considering the geologic complexities, anthropogenic interferences and other limitations of applying geophysical methods at this site. • Collect additional data needed for calibrating groundwater flow model to refine aquifer hydraulic properties, which include transmissivity, hydraulic conductivity, heterogeneity and anisotropy, storativity, and specific yield. • Incorporate results of ongoing regional-scale USGS aquifer test with synoptic monitoring of groundwater levels in approximately 25 monitoring wells and pumping rates of supply wells located near the Facility. • Develop a more detailed conceptual model of the water balance (hydrologic budget) at the Hawaiian Cement plant, crushing facility, and Hālawa Quarry. • Further evaluate new and existing data regarding perched water in monitoring wells in South Hālawa Valley and proposed wells to the north. • Conduct planned infiltration tests for surface soil above the Facility. • If available, obtain updated estimates of groundwater recharge and discharge along the coast from USGS modeling studies currently underway.	• Enable more accurate determinations of hydraulic heads and hydraulic gradients. • Further define direction and rate of migration of groundwater potentially impacted by COPCs from the Facility. Further define spatial distribution of hydraulic heads (groundwater levels) and hydraulic gradients in areas extending northward to Hālawa Shaft, near the Red Hill Shaft water development tunnel, and in areas extending southward to Moanalua and Tripler Wells. • Define the potentiometric surface, which will reflect horizontal hydraulic gradients at the water table. Measure the vertical hydraulic gradient at the selected locations. • Evaluate effects of pumping water supply wells on hydraulic gradients. • Estimate extent and thickness of the HGUs in the model area. Better define the depths of older alluvial sediment fill and saprolite in areas beneath North and South Hālawa Valleys and Moanalua Valley to improve understanding of hydraulic gradients and groundwater flow directions. Further improve the geologic model. • Support further evaluation of geologic features that may act as preferred groundwater flow pathways or barriers. Better define the spatial distribution of clinker zones, paleo-channels, faults, dense low-permeability lava flows and dikes in the primary area of interest for groundwater modeling. • Calibrate groundwater flow model using an iterative process to reasonably match the new data by adjusting the aquifer hydraulic properties in the model within the range of reported values from other studies. • Evaluate the local hydrologic budget and better estimate groundwater recharge rates in the cement plant/quarry area. Integrate results with the groundwater balance for the entire model area and input the refined groundwater recharge rates to the numerical groundwater model. • Help define the contiguous or isolated nature of the perched water zone in South Hālawa Valley. Update the CSM to describe the perched water locations and depths (elevations). • Determine degree to which recharge rates are reduced by the thick clayey saprolitic soil overlying the Red Hill Facility. • Update the groundwater model to specify rate of natural groundwater discharge that occurs along the coast, if estimates become available; if not, further evaluate these data gaps.
Module F: Fate and Transport of LNAPL and Dissolved COPCs in Groundwater			
Attenuation studies, in the vadose zone as NSZD and in the dissolved groundwater plume as monitored natural attenuation (MNA), provide strong evidence of biodegradation. Occurrence of LNAPL is primarily limited to a depth of 30 ft beneath wells RHMW02 and RHMW03 and is being biodegraded based on thermal, soil vapor, and carbon trap studies. Attenuation of dissolved-plume COPCs in the saturated zone limits the extent of the existing small dissolved plume before reaching Red Hill Shaft under present conditions and within the context of historical releases. Spatial and temporal trends in COPCs, NAP data, and fuel studies provide strong evidence that active and robust attenuation processes are responsible for COPC degradation within groundwater plume under the tank farm. Profiles of total petroleum hydrocarbons–diesel-range organics (TPH-d) from site data are consistent with soluble components of jet fuel. The available chromatograms from RHMW02 groundwater samples are all consistent with chromatograms for biodegraded kerosene-type fuels (e.g., JP-5 and JP-8). Petroleum fuels are composed primarily of hydrocarbons (nonpolar) that have distinctive chromatographic profiles. The majority of the fuel is not water soluble, and the chromatographic profiles are useful in distinguishing LNAPL from soluble fuel components and biodegraded material, Polar compounds are present in the groundwater, indicating ongoing biodegradation.	• LNAPL distribution and holding capacity at the water table • Plume attenuation rates • Accuracy of very low COPC detections • Applicability of risk-based decision criteria (RBDC) as final decision criteria • Spatial distribution of COPC concentrations dissolved in groundwater between the Facility and water supply wells in North Hālawa Valley and Moanalua Valley • Source area extent, mass loading, and natural attenuation rates	• Proceed with planned installation and sampling of new monitoring wells in North and South Hālawa Valleys and on southern flank of Red Hill. • Evaluate results of ongoing natural attenuation study (DON 2017g), including microcosm studies, recharge to groundwater measurements, sheen samplers, NAP data, and mass flux/mass discharge calculations.	• Use newly obtained data to better define the nature and extent of COPCs between the Facility and the water supply wells. • Determine natural attenuation rates following NSZD concepts and multiple LOEs.
Module G: Exposure Model			
Historical releases (prior to 2005) are considered the main source of impacts to groundwater at the Facility. Other releases (e.g., spills or leaks in the fuel system) may have occurred or may occur in the future. Potentially contaminated media are unconsolidated materials, volcanic rock within the tunnels, soil/rock vapor within the tunnels, tunnel air, groundwater beneath the Facility, and offsite surface water where groundwater may discharge. Human receptors that may contact onsite or offsite Facility-impacted media are Facility occupational workers, construction workers, and visitors, and offsite residents. Among the potentially complete exposure pathways identified, the primary one is offsite residents using tap water sourced from the Red Hill Shaft water supply well. These receptors could be exposed to chemicals in tap water via direct ingestion and dermal contact, and via inhalation while showering/bathing. Exposure by ecological receptors is considered incomplete or insignificant.	• Unidentified sources and migration routes	• Continue groundwater flow and solute transport modeling and implement the planned sentinel well network described in the *Sentinel Well Network Development Plan* (DON 2017l).	• Monitor past and potential future releases from the Facility; identify possibility of unidentified sources and migration routes.

CONTENTS

Executive Summary iii

Contents vii

Acronyms and Abbreviations xv

Well Name Cross-Reference Table xix

1. Conceptual Site Model Development and Structure 1-1

- 1.1 Purpose of the CSM 1-1
- 1.2 CSM Development Approach 1-2
- 1.3 CSM Updates and Refinement 1-3
- 1.4 Organization and Key Elements of the CSM 1-4

2. Module A: Physical Setting 2-1

- 2.1 Site Location 2-1
- 2.2 Surrounding Populations and Land Use 2-1
- 2.3 Climate 2-1
- 2.4 Vegetation and Wildlife 2-2
- 2.5 Archaeological Sites 2-2
- 2.6 Topography 2-2
- 2.7 Site Volcanic Rocks 2-3
- 2.8 Site Soils 2-4
- 2.9 Surface Water 2-4
- 2.10 Groundwater 2-4
- 2.11 Water Supply Wells 2-6
- 2.12 Red Hill Long-Term Monitoring System 2-7
  - 2.12.1 Soil Vapor Monitoring System 2-7
  - 2.12.2 Groundwater Monitoring Network 2-7
- 2.13 Uncertainty Analysis 2-10
- 2.14 Addressing Uncertainties 2-10

3. Module B: Facility Construction and Operations 3-1

- 3.1 Construction and Physical Characteristics of the Facility 3-1
- 3.2 Fuel Types 3-2
- 3.3 Uncertainty Analysis 3-4
- 3.4 Addressing Uncertainties 3-4

4. Module C: LNAPL Release and Source-Zone Migration Model 4-1

- 4.1 Summary of Previous Investigations and Environmental Actions 4-1
- 4.2 History of January 2014 JP-8 Release from Tank No. 5 4-2
- 4.3 Construction Practices and Materials 4-3
  - 4.3.1 Bottom Drain 4-5
  - 4.3.2 Tunnel Floor Pipe Bedding and Sumps 4-5
- 4.4 Post-2014-Release Monitoring Results 4-5
- 4.5 2014 Release Conceptual Model 4-6
- 4.6 Uncertainty Analysis 4-7
- 4.7 Addressing Uncertainties 4-7

5. Module D: Vadose Zone Model 5-1

5.1 Macro-Scale Geologic Features 5-1
5.1.1 Lava Flows 5-2
5.1.2 Geologic Cross Sections 5-3
5.1.3 Overall Occurrence of Rock Types 5-3
5.1.4 Permeability 5-7
5.2 Micro-Scale Geologic Features 5-9
5.2.1 Assessment of Subsurface Heterogeneity 5-9
5.2.2 Geologic Features and LNAPL Movement 5-11
5.2.3 Petrographic Analyses 5-12
5.2.4 Assessment of Geologic Features and Natural Processes Affecting LNAPL 5-13
5.3 Uncertainty Analysis 5-14
5.4 Addressing Uncertainties 5-14
6. Module E: Saturated Zone Model 6-1
6.1 Previous Groundwater Levels and Recently Collected Hydrogeologic Data 6-1
6.1.1 May 2006 Regional Aquifer Pumping Test 6-2
6.1.2 Quarterly Groundwater Monitoring 6-2
6.1.3 November 2016 Synoptic Monitoring 6-3
6.1.4 Recently Collected Hydrogeologic Data 6-3
6.1.5 2017 High Precision Well Survey 6-6
6.1.6 Gyroscopic Corrections 6-6
6.1.7 2017/2018 Synoptic Monitoring 6-7
6.1.8 2017 Seismic Survey 6-9
6.2 Hydraulic Gradients and Groundwater Flow Directions 6-10
6.2.1 May 2006 Pumping Test 6-10
6.2.2 May 2015 Pumping Test 6-10
6.2.3 November 2016 Synoptic Monitoring 6-11
6.2.4 2017/2018 Synoptic Monitoring 6-12
6.3 Hydraulic Properties of Hydrogeologic Units 6-21
6.3.1 Caprock 6-21
6.3.2 Valley Fill 6-22
6.3.3 Basalt 6-22
6.3.4 Site-Area Aquifer Testing and Analysis of Hydraulic Parameters 6-24
6.4 2005 USGS Regional SUTRA Model 6-25
6.4.1 Model Domain 6-25
6.4.2 Representation of Groundwater Flow System 6-25
6.4.3 Model Results 6-26
6.5 2007 Red Hill Groundwater Flow Model 6-28
6.5.1 Model Domain 6-28
6.5.2 Representation of Groundwater Flow System 6-28
6.5.3 Model Results 6-28
6.6 Red Hill 2018 Groundwater Flow Model Area Groundwater Balance 6-29
6.6.1 Boundary Influx and Outflux 6-29
6.6.2 Groundwater Recharge 6-30
6.6.3 Groundwater Discharge 6-31
6.7 General Groundwater Chemistry Distribution 6-31

6.8 Assessment of LOEs for Groundwater Flow 6-37
6.9 Uncertainty Analysis 6-38
6.10 Addressing Uncertainties 6-38
6.10.1 Groundwater Flow Directions and Rates 6-39
6.10.2 Thickness and Extent of Hydrogeologic Units 6-39
6.10.3 Preferential Pathways and Barriers 6-40
6.10.4 Hydraulic Properties of Basalt HGU 6-40
6.10.5 Groundwater Recharge and Discharge Rates 6-40

7. Module F: Fate and Transport of LNAPL and Dissolved COPCs in Groundwater 7-1

7.1 LNAPL Distribution, Fuel Type, and Evidence of Weathering 7-1
7.1.1 LNAPL Distribution in the Unsaturated Zone 7-1
7.1.2 LNAPL Distribution at the Water Table 7-2
7.1.3 Dissolved-Phase Fuel Type and Evidence of Weathering 7-3
7.2 Dissolved-Phase COPCs Detected in Groundwater 7-4
7.3 Natural Attenuation 7-7
7.3.1 Natural Source-Zone Depletion 7-8
7.3.2 Monitored Natural Attenuation 7-16
7.4 Groundwater Flow and CF&T Modeling 7-23
7.4.1 Source Area Modeling 7-23
7.4.2 Solute Transport Parameters 7-24
7.5 Uncertainty Analysis 7-25
7.6 Addressing Uncertainties 7-26
7.6.1 Nature and Extent of Contamination 7-26
7.6.2 Source Area Extent, Mass Loading, and Natural Attenuation Rates 7-26

8. Module G: Exposure Model 8-1

8.1 Chemical Sources and Releases 8-1
8.2 Potentially Affected Media 8-2
8.3 Potential Receptors 8-2
8.3.1 Human Receptors 8-2
8.3.2 Ecological Receptors 8-3
8.4 Potentially Complete Exposure Pathways 8-3
8.5 Incomplete or Insignificant Pathways 8-3
8.6 Potential Exposure to LNAPL 8-4
8.7 Uncertainties 8-4
8.8 Addressing Uncertainties 8-5

9. References 9-1

APPENDIXES

A Cumulative Historical Groundwater Monitoring Results and COPC Concentration Graphs

B Fate and Transport Analyses

FIGURES

1-1	Red Hill Bulk Fuel Storage Facility and Vicinity	1-5
1-2	Pictorial CSM	1-7
2-1	County Land Use Ordinance Map	2-13
2-2	State Land Use Districts	2-15
2-3	Land Cover	2-17
2-4	Generalized Surficial Geology of O'ahu	2-19
2-5	Conceptual Cross Section View of O'ahu Hydrogeology	2-21
2-6	Aquifer Systems in the Groundwater Model Area	2-23
2-7	Water Supply Wells in the Groundwater Model Area	2-25
2-8	Soil Vapor Monitoring Point Construction Details	2-27
2-9	Existing and Proposed Groundwater Monitoring and Test Boring Locations	2-29
4-1	Summary of Environmental Actions at Red Hill	4-9
4-2	Soil Vapor Measurements Prior to and Following 2014 Release	4-11
5-1	Geologic Cross Section Key Plan	5-15
5-2	Geologic Cross Section A–A′	5-17
5-3	Geologic Cross Section A–A′ Extended	5-19
5-4	Geologic Cross Section B–B′ (View Looking East)	5-21
5-5	Cross Section B–B′ Extended (View Looking East)	5-23
5-6	Geologic Cross Section C–C′	5-25
5-7	Geologic Cross Section D–D′	5-27
5-8	Geologic Cross Section E–E′	5-29
5-9	Cross Section F–F′ Āliamanu Crater Section	5-31
5-10	Cross Section of Red Hill Shaft Water Development Tunnel	5-33
5-11	Logs of Formations in Tank Excavations (Barrel Logs)	5-35
5-12	Glacioeustatic Fluctuations of Sea Level and Hawaiian Pleistocene Shorelines	5-37
5-13	Micro-Scale LNAPL Vadose Zone Mobility and Retention	5-39
6-1	Hydrographs of RHMW07 vs. RHMW02 and OWDFMW01	6-43
6-2	Hydrographs of RHMW07 vs. RHMW06 and HDMW2253-03	6-45
6-3	Time-Series Graphs of Wells RHMW02 and RHMW03	6-47
6-4	Cross Section B–B′ with Westbay Data (View Looking East)	6-49
6-5	November 2016 Groundwater Levels	6-51

6-6 Time-Series Plots of Water Level Data at Area Monitoring Wells during 2015 USGS Pumping Test at Red Hill Shaft and Hālawa Shaft 6-53

6-7 Groundwater Levels in RHMW04 and RHMW07 and Pumping Rates during May 2015 6-55

6-8 Time 1: Red Hill Shaft Off (At Max Recovery), Hālawa Shaft Average Pumping 01/15/2018 6:00 6-57

6-9 Time 2: Red Hill Shaft At Max Pumping Hālawa Shaft Average Pumping 01/19/2018 21:10 6-59

6-10 Time 3: Red Hill Shaft Business as Usual Pumping, Hālawa Shaft Off 02/05/2018 19:00 6-61

6-11 Time 4: Red Hill Shaft Business as Usual Hālawa Shaft at Maximum Pumping 02/16/2018 5:00 6-63

6-12 Time 5: Red Hill Shaft Business as Usual Hālawa Shaft Average Pumping 02/19/2018 13:00 6-65

6-13 Head Differences Between - Time 1: Red Hill Shaft Off (At Max Recovery), Hālawa Shaft Average Pumping 01/15/2018 6:00 Time 2: Red Hill Shaft At Max Pumping, Hālawa Shaft Average Pumping 01/19/2018 21:10 6-67

6-14 Head Differences Between - Time 3: Red Hill Shaft Business as Usual Pumping Usual Pumping Hālawa Shaft Off 02/05/2018 19:00 Time 4: Red Hill Shaft Business as Usual Pumping Hālawa Shaft at Maximum Pumping 02/16/2018 5:00 6-69

6-15 Cooper-Jacob Drawdown and Recovery Plots (RHMW01, RHMW02, RHMW03, RHMW04, RHMW05, and RHMW06) 6-71

6-16 Cooper-Jacob Drawdown and Recovery Plots (RHMW07, RHMW08, RHMW09, RHMW10, RHMW11 Zones 1 and 2) 6-73

6-17 Cooper-Jacob Drawdown and Recovery Plots (RHMW11 Zones 3, 4, 5, 6, 7, and 8) 6-75

6-18 Cooper-Jacob Drawdown and Recovery Plots (Hālawa Deep Monitor Well (2253-03), Hālawa Deep Monitor Well Chase Tube, Ka'amilo Deep, Hālawa BWS Deep Monitor, OWDFMW01, and TAMC-MW2) 6-77

6-19 Cooper-Jacob Drawdown and Recovery Plots (Moanalua Deep, Moanalua DH43, 'Aiea Navy, Hālawa Shaft, and USGS RHMW11 Zone 8) 6-79

6-20 Distance Drawdown at Time 2 6-81

6-21 SUTRA and Interim Model Domains 6-83

6-22 SUTRA Model Layer 1 Water Levels (ft msl) 6-85

6-23 SUTRA Model Layer 1 Hydraulic Conductivity (ft/day) 6-87

6-24 SUTRA Model Saltwater-Freshwater Interface (ft msl) 6-89

6-25 Current and Previous Groundwater Model Areas 6-91

6-26 Location of Observation Wells for Synoptic Water Level Study Simulated by TEC 2007 6-93

6-27 Water Levels, May 2006 Pumping Test 6-95
6-28 Simulated 10-Year Capture Zones by Rotzoll (2014) for Red Hill Shaft Not Pumping 6-97
6-29 Current Conceptual Groundwater Balance 6-99
6-30 Average Recharge within the Model Area 6-101
6-31 Chemical Composition of Groundwater in Red Hill Monitoring Wells 6-103
6-32 Specific Conductivity Anomaly: OWDFMW1, RHMW06, RHMW07, HDMW2253-03 –624 ft 6-105
6-33 Specific Conductivity Anomaly: OWDFMW1, RHMW06, RHMW07, HDMW2253-03 –624 ft (K/cl vs. Chloride) 6-107
6-34 Specific Conductivity Anomaly: OWDFMW1, RHMW06, RHMW07, HDMW2253-03 –624 ft (Na/Cl vs. Chloride 6-109
6-35 Specific Conductivity Anomaly: OWDFMW1, RHMW06, RHMW07, HDMW2253-03 –624 ft (Ca/Mg vs. Chloride 6-111
6-36 Estimated Local Meteorological Water Line 6-113
7-1 COPC Concentration Graphs of Historical Groundwater Monitoring Results 7-27
7-2 Range of VOC Concentrations and Fuel Weathering Observed in Below-Tank Soil Vapor Wells 7-31
7-3 Use of PID Monitoring Combined with Lab Analysis to Track Release and Subsequent Weathering of LNAPL Fuel for Tank 5 7-33
7-4 Conceptual Illustration of Carbon Dioxide Flux to Ground Surface and Tunnels 7-35
7-5 Net (Background Corrected) Temperature Profiles for Facility Wells (Well Air Temperatures Method), Highlighting Clinker Zones and Inferred LNAPL Intervals 7-37
8-1 Human Health Exposure Pathway Evaluation 8-7

TABLES

2-1 Existing and Proposed Wells in the Red Hill Groundwater Monitoring Network 2-8
3-1 Types of Fuel Historically and Currently Stored in the Facility's Fuel Storage Tanks 3-2
4-1 Summary of Previous Red Hill Investigations 4-1
5-1 Geologic Media in Red Hill 5-11
6-1 RHMW11 Westbay Zone Summary 6-4
6-2 RHMW11 Hydraulic Conductivity Estimates Derived from Pneumatic Testing and Laboratory Analyses 6-5
6-3 Summary of Gyroscopic Survey Results and Calculated Tape Correction Factors 6-6

6-4	Well and Transducer Information	6-8
6-5	Summary of Barometric Responses	6-13
6-6	Summary of Cooper Jacob Approximation Calculation Components	6-17
6-7	Summary of Cooper Jacob Approximation Estimates of Transmissivity and Storativity, and Derived Hydraulic Conductivity	6-19
6-8	Previous Estimates of Aquifer Properties Based on Data Developed in 2006	6-20
6-9	Hydraulic Parameters Developed from Local Numerical Flow Model Calibration at the Facility (DON 2007)	6-24
6-10	Estimated Average Annual Groundwater Inflows and Outflows from Model Boundaries, 2017	6-29
6-11	Major Ion Composition of Groundwater Samples Collected from Red Hill Monitoring Wells, November 2016	6-32
6-12	Groundwater Chemistry Data Compiled by the University of Hawai'i Water Resources Research Center for Geothermal Study	6-35
7-1	Findings and Conclusions of Soil Vapor Investigation	7-10
7-2	Summary of Total NSZD Rates from the Tank Farm in Units of Gallons per Year	7-14
7-3	Vertical Distribution of LNAPL Intervals Indicated by Net (Background-Corrected) Temperature Profiles from Three Facility Monitoring Wells	7-15
7-4	Summary of Microcosm and Microbial Study Preliminary Results by Monitoring Well	7-19
7-5	C vs. t Coefficients, Half-Lives, and First-Order Model Fit Parameters for the COPCs at RHMW02 (September 2005 to April 2018)	7-20
7-6	C vs. d Rate Attenuation Rates and Biodegradation Rates for COPCs Along RHMW02-RHMW01 Transect (includes detected COPCs at both wells only)	7-21
7-7	Transport Parameters Used in Previous Navy CF&T Model	7-24

PHOTOGRAPHS

5-1	Pāhoehoe Flows	5-41
5-2	Pāhoehoe Flows	5-43
5-3	Pāhoehoe Flows	5-45
5-4	A'ā Permeability	5-47
5-5	Weathered A'ā Clinker	5-49
5-6	Saprolite	5-51

This page intentionally left blank

ACRONYMS AND ABBREVIATIONS

λ	biodegradation rate coefficient
$\delta^{18}O$_CORR	ratio between the heavy and light isotopes of oxygen in the water sample to those ratios in an isotopic standard derived from seawater (corrected) in parts per mil (o/oo)
$\delta^{2}H$_CORR	ratio between the heavy and light isotopes of hydrogen in the water sample to those ratios in an isotopic standard derived from seawater (corrected) in parts per mil (o/oo)
°F	degrees Fahrenheit
µg/L	micrograms per liter
Alk	alkanity
AOC	Administrative Order on Consent
AVGAS	aviation gasoline
bgs	below ground surface
BP	before present
Br	bromide
BTEX	benzene, toluene, ethylene, and xylene
btoc	below top of casing
BWS	Board of Water Supply, City and County of Honolulu
C vs. d	concentration vs. distance
C vs. t	concentration vs. time
Ca	calcium
CF&T	contaminant fate and transport
CH_4	methane
Cl	chloride
CO_3	carbonate
COPC	chemical of potential concern
CSM	conceptual site model
CWRM	Commission on Water Resource Management
DLA	Defense Logistics Agency
DLNR	Department of Land and Natural Resources, State of Hawai‘i
DO	dissolved oxygen
DOE	Department of Energy, United States
DOH	Department of Health, State of Hawai‘i
DON	Department of the Navy, United States
EAL	Environmental Action Level
EPA	Environmental Protection Agency, United States
EPH	extractable petroleum hydrocarbon
F	fluoride
F-76	Diesel Fuel-Marine
Fe^{2+} or Fe(II)	ferrous iron
FID	flame ionization detector
ft	foot/feet
ft/d	feet per day
ft/ft	feet per foot
ft^2/d	square feet per day
gal/acre/yr	gallons per acre per year
gal/yr	gallons per year

1	GWPP	*Groundwater Protection Plan*
2	HART	Honolulu Area Rapid Transit
3	HCO_3	bicarbonate
4	HFB	hydraulic flow barrier
5	HGU	hydrogeologic unit
6	ID	identification
7	ITRC	Interstate Technology Regulatory Council
8	JBPHH	Joint Base Pearl Harbor-Hickam
9	JP	Jet Fuel Propellant
10	k	first-order rate coefficient
11	K	hydraulic conductivity [or potassium]
12	K_h	horizontal hydraulic conductivity
13	k_{point}	concentration vs. time attenuation rate coefficient
14	K_v	vertical hydraulic conductivity
15	LAT	lower access tunnel
16	LMWL	Local Meteoric Water Line
17	LNAPL	light non-aqueous-phase liquid
18	LOD	limit of detection
19	LOE	line of evidence
20	LTM	long-term monitoring
21	m	meter
22	m/s	meter per second
23	MADEP	Massachusetts Department of Environmental Protection
24	meq/L	milli-equivalents per liter
25	Mg	magnesium
26	mg/L	milligrams per liter
27	mgd	million gallons per day
28	MNA	monitored natural attenuation
29	MOGAS	motor gasoline
30	msl	mean sea level
31	MTBE	methyl tert-butyl ether
32	n	number of samples
33	Na	sodium
34	NAD	North American Datum
35	NAP	natural attenuation parameter
36	NATO	North Atlantic Treaty Organization
37	NAVFAC	Naval Facilities Engineering Command
38	NO_3	nitrogen
39	NPDES	National Pollutant Discharge Elimination System
40	NSFO	Navy Special Fuel Oil
41	NSZD	natural source-zone depletion
42	NWIS	National Water Information System
43	o/oo	parts per mil
44	ORP	oxidation-reduction potential
45	OSHA	Occupational Safety and Health Administration
46	OWDF	Oily Waste Disposal Facility
47	PAH	polynuclear aromatic hydrocarbon
48	PEST	Parameter Estimation
49	PIANO	paraffin, isoparaffin, aromatic, naphthene, and olefin

PID	photoionization detector
ppbv	parts per billion by volume
qPCR	polymerase chain reaction
R^2	coefficient of determination
RBDC	risk-based decision criteria
RCRA	Resource Conservation and Recovery Act
RQD	rock quality designation
RSL	Regional Screening Level
SiO_2	silica dioxide
SME	subject matter expert
SO_4, SO_4^{2-}	sulfate
SOW	scope of work
SSRBL	site-specific risk-based level
SVE	soil vapor extraction
SVM	soil vapor monitoring
SVOC	semivolatile organic compound
SWAP	Source Water Assessment Program
$t_{1/2}$	half-life for a given COPC
TAMC	Tripler Army Medical Center
TGM	*Technical Guidance Manual for the Implementation of the Hawaii State Contingency Plan*
TIC	tentatively identified compound
TIRM	Tank Inspection, Repair, and Maintenance
TOC	total organic carbon
TPH	total petroleum hydrocarbons
TPH-d	total petroleum hydrocarbons – diesel range organics
TPH-g	total petroleum hydrocarbons – gasoline range organics
TPH-o	total petroleum hydrocarbons – residual range organics (i.e., TPH-oil)
TUA	Tank Upgrade Alternatives
Turb	turbidity
U.S.	United States
UH	University of Hawai‘i
UHM	University of Hawai‘i at Mānoa
UIC	Underground Injection Control
USGS	United States Geological Survey
VOC	volatile organic compound
VPH	volatile petroleum hydrocarbon
WP	work plan
WRRC	Water Resources Research Center, University of Hawai‘i
yr	year

This page intentionally left blank

WELL NAME CROSS-REFERENCE TABLE

Well ID	DLNR ID	USGS Site ID	Known Aliases
Fort Shafter Monitor	2053-10		
Moanalua Deep	2153-005	212123157535501	Moanalua Fresh Water Mon. Well
TAMC1	2153-007		
TAMC2	2153-008		
Manaiki T24	2153-009		Moanalua T24 (DLNR)
Moanalua 1	2153-010		
Moanalua 2	2153-011		
Moanalua 3	2153-012		
TAMC-MW2	2153-013	212144157534701	TAMC MW2 TAMC-MW-2
Moanalua DH43	2253-002	212225157533001	
Hālawa Deep Monitor Well (2253-03)	2253-003	212241157535501	Hālawa Deep HDMW HDMW2253-03
Hālawa Deep Monitor Well Chase Tube	2253-003	212241157535502	Hālawa Deep Chase Tube
RHMW06	2253-004	212226157534101	
RHMW07	2253-005	212222157535201	
RHMW08	2253-007	212216157535801	
RHMW09	2253-008	212209157535201	
RHMW10	2253-009	212213157533901	
RHMW11	2253-011	212226157535001	
Red Hill Shaft	2254-001	212225157542601	Red Hill Shaft (S11) RHMW2254-01 Navy Supply Well 2254-01
UMW-1	2254-02M	212229157541501	South Hālawa Alluvium MW-1 HCF shallow monitoring well Hālawa Correctional Facility MW
ʻAiea Hālawa Shaft	2255-032	212253157554301	Hālawa Shaft (S5) Navy Hālawa Shaft
Hālawa T-45	2255-033		
Hālawa BWS Deep Monitor	2255-040	212233157552302	Hālawa TZ Well Hālawa deep monitor well near Hālawa T45 (2255-33)
ʻAiea Navy	2256-010	212238157561101	ʻAiea US Navy (187-B) ʻAiea boat harbor well
Pearl City III	2257-003		
Hālawa Shaft	2354-001	212305157542601	Hālawa Shaft (S12)
Kaʻamilo Deep	2355-015	212340157552301	Kaʻamilo Deep Monitor
OWDFMW01		212214157542601	OWDFMW08 (former name) OWDFMW1
RHMW01		212214157535401	
RHMW02		212216157534701	
RHMW03		212219157533901	
RHMW04		212231157532901	
RHMW05		212210157540201	

This page intentionally left blank

1. Conceptual Site Model Development and Structure

This *Conceptual Site Model* (CSM) document was developed to provide a basis for evaluating contaminant transport pathways and the potential for exposure of human receptors to potentially impacted drinking water in support of the *Investigation and Remediation of Petroleum Product Releases and Groundwater Protection and Evaluation* project, at Red Hill Bulk Fuel Storage Facility ("the Facility"), Joint Base Pearl Harbor-Hickam (JBPHH), Hawai'i. As shown on Figure 1-1, the Facility is located approximately 2.5 miles northeast of Pearl Harbor, on the low ridge (Red Hill) between South Hālawa and Moanalua Valleys. The Facility is owned by the United States (U.S.) Navy (DON; "Navy") and operated by Defense Logistics Agency (DLA).

The project is being performed under Statement of Work Sections 6 and 7 of the *Administrative Order on Consent* (AOC) *In the Matter of Red Hill Bulk Fuel Storage Facility* (EPA Docket No: RCRA 7003-R9-2015-01; DOH Docket No: 15-UST-EA-01) (EPA Region 9 and DOH 2015). The AOC was issued by the U.S. Environmental Protection Agency (EPA) Region 9 and State of Hawai'i Department of Health (DOH) (EPA Region 9 and DOH 2015) to the Navy/DLA in response to a release of an estimated 27,000 gallons of Jet Fuel Propellant (JP)-8 from one of the Facility's underground fuel storage tanks (Tank 5) that was confirmed and reported to DOH on January 23, 2014. The bottoms of the Facility's tanks are located approximately 100–130 feet (ft) above a major groundwater aquifer, which is used to feed both Navy and City and County of Honolulu drinking water supply wells and shafts.

The AOC Statement of Work outlines eight sections that set forth the tasks and requirements the Navy/DLA will undertake to comply with the Order (EPA Region 9 and DOH 2015). The *Work Plan* (WP) */ Scope of Work* (SOW) (DON 2017a) for the current project presents the process, tasks, and deliverables that address the goals and requirements of Section 6 (Investigation and Remediation of Releases) and Section 7 (Groundwater Protection and Evaluation). This CSM was prepared in accordance with the *CSM Development and Update Plan* (DON 2017k), one of the derivative deliverables prepared to supplement the project WP/SOW.

1.1 PURPOSE OF THE CSM

The CSM (1) integrates and evaluates available regional and site-specific information and data as required to identify and (if possible) quantify the physical and chemical parameters and processes that control the nature, extent, fate, and transport of petroleum products (light non-aqueous-phase liquid [LNAPL]) and their constituent chemicals in the vadose and saturated zones at the Facility; (2) identifies exposure routes to potential human receptors as potentially complete, potentially complete but insignificant, or incomplete as required to assess risks to human receptors; and (3) describes site-specific conditions that may affect the feasibility of alternatives for remediating groundwater and other environmental media (e.g., vadose zone soil and soil vapor) impacted by LNAPL or its constituent chemicals. This CSM also provides a basis for developing preliminary input parameters for numerical groundwater flow modeling. An interim groundwater flow model has been developed to inform the interim environmental analysis and (2) identify data gaps for further evaluation. The interim groundwater flow model will be used in the development of the groundwater flow model that will be presented in the *Groundwater Flow Model Report* required per AOC Section 7.1.3 that is anticipated for submittal in December 2018.

The CSM is an evolving tool that will continue to be updated as new information (e.g., well, seismic, natural attenuation) becomes available. Refinements to the CSM will be used in ongoing modeling and remediation efforts.

The CSM presents currently available data to help evaluate LNAPL degradation and migration and dissolved-phase mass discharge (flux) in the subsurface. Factors related to attenuation of LNAPL (natural source-zone depletion [NSZD]) and dissolved-phase constituents (monitored natural attenuation [MNA]) are currently being evaluated, incorporating the concepts for NSZD as described by the Interstate Technology Regulatory Council (ITRC) (ITRC 2009a) and other references; preliminary results are presented in Appendix B. The interim modeling effort is focused on flow and will not directly rely on natural attenuation as part of various scenario evaluations, but currently available natural attenuation data and interpretations will be included for reference. As additional natural attenuation data become available, the data will be evaluated and included for support of the fate and transport modeling effort.

1.2 CSM DEVELOPMENT APPROACH

This CSM was developed using an evidence-based approach to identify and evaluate the site-specific characteristics and processes that control the fate and transport of jet fuel (LNAPL) and its constituent chemicals (petroleum hydrocarbons) from the source of release (an underground fuel storage tank at the Facility), through the vadose and saturated zones, and on to potential receptors (e.g., residential receptors exposed via the drinking water pathway). The graphical model presented on Figure 1-2 illustrates key elements of the CSM and cross-references to the seven detailed modules presented in subsequent sections of this document.

The CSM incorporates information about tank design, construction, fuel storage history, and potential pathways for migration of LNAPL and its constituent chemicals into the vadose and saturated zones to improve the understanding of LNAPL movement, retention, and degradation mechanisms. For example, the CSM describes how LNAPL releases would likely move from a tank leak point by characterizing the spatial distribution of interconnected pore spaces (e.g., clinker zones) and low-porosity, low-permeability massive a'ā and pāhoehoe flows. The CSM also contributes to the evaluation of the potential for lateral spreading, vertical transport, and retention of LNAPL in the subsurface, including the effects of capillary moisture in water-filled fractures and other voids and pore spaces within the thick sequence of massive basalt flows, volcanic tuff, and clinker layers that form the vadose and saturated zones. These CSM components provide a basis for estimating the extent and volume of LNAPL that could be retained in the vadose zone, locating potential pathways for transport of LNAPL to the saturated zone, and evaluating the fate and transport of dissolved petroleum product constituents in groundwater.

The CSM describes the hydrogeologic characteristics of geologic units in the vadose and saturated zones based on detailed geologic descriptions from barrel logs, boring logs, and published reports of other hydrogeologic investigations to estimate the direction(s) of flow and locations where LNAPL could accumulate in the vadose zone if released from one of the Facility's fuel storage tanks. The evaluation also includes:

- Review of Tank 5 release history, fuel types, leak rates, and volume estimates
- Assessment of potential leak locations and pathways for migration of LNAPL and its constituent chemicals from the fuel storage tanks into the vadose and saturated zones
- Evaluation of retention of LNAPL at both macro-scale (e.g., ponding on low-permeability units, retention on surface of individual clinkers/other clasts, lava tubes, boundaries of individual flows) and micro-scale (e.g., pore, micro-fractures retention)
- Studies of natural attenuation and degradation of jet fuels

- Evaluation of site-specific groundwater data (natural attenuation parameters [NAPs] and microbial analyses) (as described in DON 2017f)
- Evaluation of vertical flow velocities based on correlation between groundwater levels, precipitation, groundwater recharge rates, and soil vapor data

This CSM was prepared in accordance with current guidance, including but not limited to the following:

- *Standard Guide for Development of Conceptual Site Models and Remediation Strategies for Light Nonaqueous-Phase Liquids Released to the Subsurface*, ASTM E2531-06(2014) (ASTM 2014b)
- *Standard Guide for Developing Conceptual Site Models for Contaminated Sites*, ASTM E1689-95 (reapproved 2014) (ASTM 2014a)
- *Environmental Cleanup Best Management Practices: Effective Use of the Project Life Cycle Conceptual Site Model* (EPA 2011)
- *Evaluating Natural Source Zone Depletion at Sites with LNAPL, Interstate Technology Regulatory Council* (ITRC 2009a)
- *Evaluating LNAPL Remedial Technologies for Achieving Project Goals* (ITRC 2009b)
- LNAPL Conceptual Site Model module in: *LNAPL Training Part 2: LNAPL Characterization and Recoverability – Improved Analysis* (ITRC 2008)
- Section 3.3 Conceptual Site Models in: *Technical Guidance Manual for the Implementation of the Hawaii State Contingency Plan* (TGM) (DOH 2016)
- *Conceptual Site Model Tool*, Naval Facilities Engineering Command (NAVFAC) Technology Transfer, Environmental Restoration website (URL: http://t2.serdp-estcp.org/t2template.html#tool=CSM&page=S1)

1.3 CSM UPDATES AND REFINEMENT

As new data are obtained, the Red Hill CSM will be refined and updated on an as-needed basis through an iterative process designed to promote collaboration between the Navy, Regulatory Agencies, and AOC subject matter experts (SMEs). This iterative process is designed to ensure that the updated CSM adequately represents current site-specific conditions and processes that affect the LNAPL degradation and migration in the subsurface. The refinement will continue until the investigative and data evaluation phases of the project are complete.

Newly obtained data that are being evaluated and integrated into the Red Hill CSM as appropriate include but are not limited to the following:

- Additional analytical data representing various media (e.g., vapor, soil, and LNAPL), NAPs, and general groundwater chemistry
- Data from additional monitoring wells and borings (e.g., subsurface geology, groundwater levels)
- Chemical distribution summary figures indicating the locations of chemical of potential concern (COPC) concentrations above project action levels and the estimated lateral and vertical extent of contamination

- Hydrogeologic data (2017–2018 synoptic water level study) and modeling results indicating the direction of groundwater flow
- Evaluation of additional natural attenuation data
- Additional geologic data from a seismic study conducted in December 2017 and other sources (e.g., existing reports or other documentation, geologic mapping of Hālawa Quarry) as needed to refine cross sections depicting subsurface geology as well as the characteristics of various geologic units
- Identification of existing buildings, structures, and infrastructure changes that might affect subsurface conditions or provide preferential transport pathways (e.g., addition of underground piping, roads, surface water bodies, neighboring property operations and land uses, geographical features)
- Identification of changes in surrounding land use that could affect exposure pathways and pose potentially unacceptable risk to human receptors
- Advanced evaluation of specific environmental hazards (risk assessments)

1.4 ORGANIZATION AND KEY ELEMENTS OF THE CSM

The CSM is organized into seven modules that describe the site-specific data and information, or lines of evidence (LOEs), used to develop the current version of the CSM, and evaluate remaining uncertainties:

- Module A: Physical Setting (Section 2)
- Module B: Facility Construction and Operations (Section 3)
- Module C: LNAPL Release and Source-Zone Migration Model (Section 4)
- Module D: Vadose Zone Model (Section 5)
- Module E: Saturated Zone Model (Section 6)
- Module F: Fate and Transport of LNAPL and Dissolved COPCs in Groundwater (Section 7)
- Module G: Exposure Model (Section 8)

Each module concludes by identifying uncertainties and describing additional investigation activities needed to fill data gaps and reduce the uncertainties. The results will be used to refine and update the CSM in future updates, in turn supporting the groundwater modeling effort.

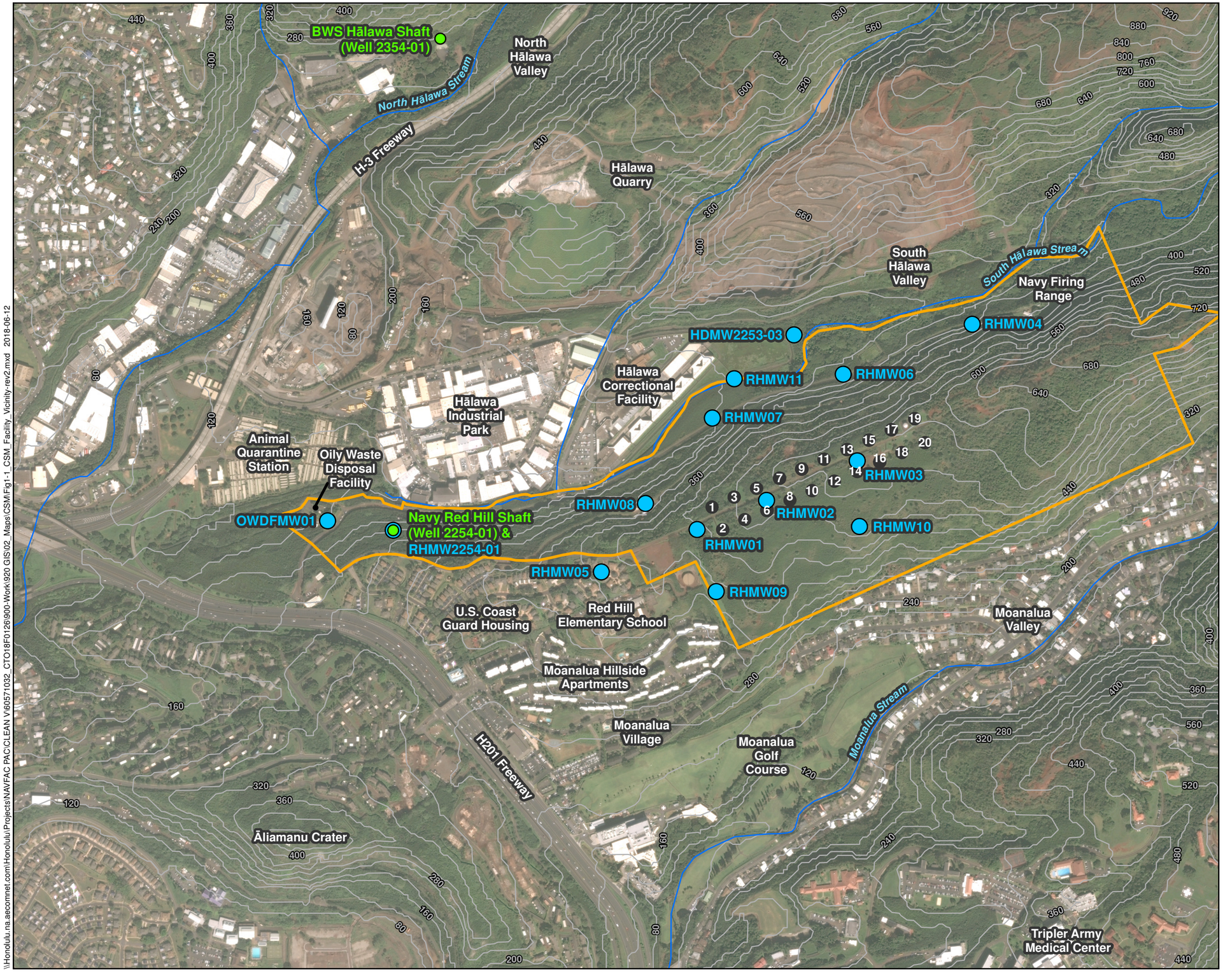

Location Map

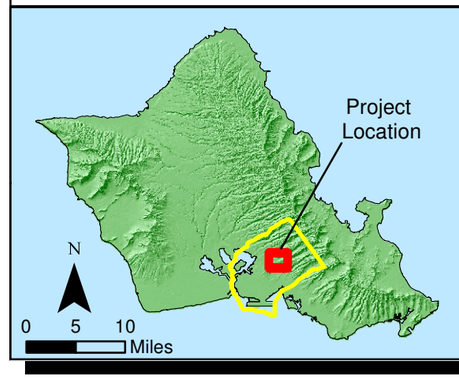

Legend

- Groundwater Monitoring Location
- Water Supply Well
- Red Hill Facility Boundary
- Stream
- Topographic Contour (feet above mean sea level)
- Red Hill Fuel Storage Tank
- Groundwater Model Area

Notes

1. Map projection: NAD 1983 UTM Zone 4N
2. Base Map: DigitalGlobe, Inc. (DG) and NRCS. Publication_Date: 2015

N

0 1,000 2,000 Feet

Figure 1-1
Red Hill Bulk Fuel Storage Facility and Vicinity
Conceptual Site Model
Investigation and Remediation of Releases and Groundwater Protection and Evaluation
Red Hill Bulk Fuel Storage Facility
JBPHH, O'ahu, Hawai'i

\\Honolulu.na.aecomnet.com\Honolulu\Projects\NAVFAC PAC\CLEAN V\60571032_CTO18F0126\900-Work\920 GIS\02_Maps\CSM\Fig1-1_CSM_Facility_Vicinity-rev2.mxd 2018-06-12

This page intentionally left blank

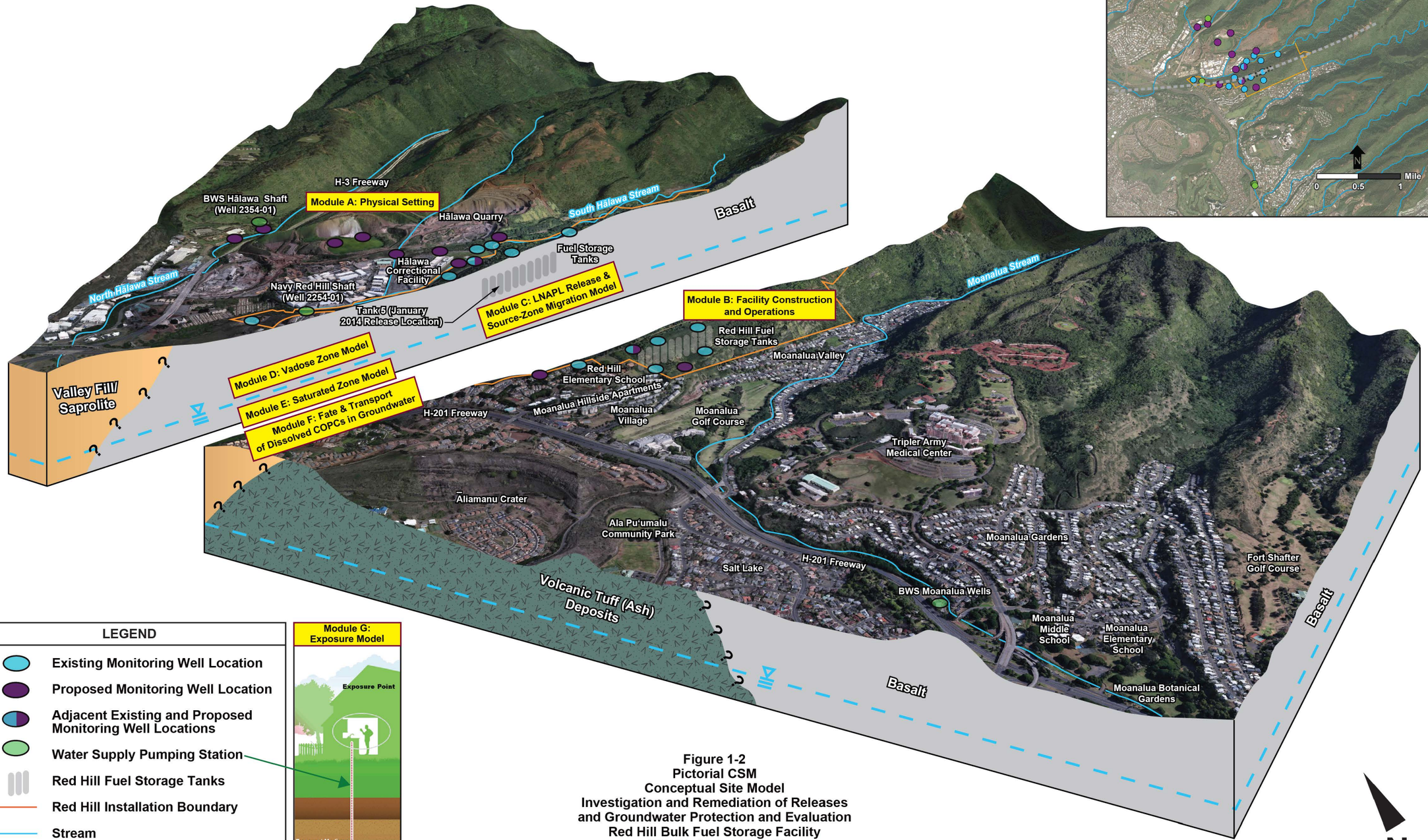

Figure 1-2
Pictorial CSM
Conceptual Site Model
Investigation and Remediation of Releases
and Groundwater Protection and Evaluation
Red Hill Bulk Fuel Storage Facility
JBPHH, Oʻahu, Hawaiʻi

S:\Projects\NAVFAC PAC\CLEAN IV\60481245CTO 0053\900-Work\921 Graphics\CSM Native\Red Hill_RI_ACrater Moanalua Hill.ai 07/27/2017

This page intentionally left blank

2. Module A: Physical Setting

2.1 SITE LOCATION

The 144-acre Facility is located in south-central O'ahu, approximately 2–3 miles east of Pearl Harbor, within the Red Hill ridge that divides South Hālawa Valley from Moanalua Valley on the southwest flank of O'ahu's Ko'olau Mountain Range (Figure 1-1). The Facility contains 20 large-capacity fuel storage tanks installed underground within Red Hill; these tanks are collectively referred to as the tank farm.

2.2 SURROUNDING POPULATIONS AND LAND USE

Populated areas closest to the Facility are 'Aiea to the west and Honolulu to the south and east. Honolulu is heavily urbanized and densely populated.

Figure 2-1 shows zoning established by County land use ordinance, and Figure 2-2 shows State land use districts. As shown on Figure 2-1, the Facility is located on land zoned by the County as a mix of F-1 Federal and Military and P-1 Restricted Preservation districts. All major structures at the Facility are located underground.

Preservation land is located east and northeast of the Facility boundary. To the southeast are residential single-family homes in Moanalua Valley; a high cliff face with a 100–200 ft elevation difference exists between the Facility and this residential area. Southwest of the tank farm area on the lower southwest flank of Red Hill are the public Red Hill Elementary School and residential apartments, and further west is U.S. Coast Guard Housing on F-1 Military land. North of the western segment of the Facility boundary in South Hālawa Valley is the State Animal Quarantine Station, private businesses in Hālawa Industrial Park, and the State-operated Hālawa Correctional Facility (see Figure 1-1). To the north of the Correctional Facility at the lower reaches of an inter-valley ridge that forms the north wall of South Hālawa Valley is the open-pit Hālawa Quarry operated by the Hawaiian Cement Company.

The H-201 Moanalua Freeway transits approximately 350–700 ft beyond the Facility's southwest boundary and intersects with the H-1 and H-3 Freeways at the Hālawa Interchange, approximately 1,800 ft west. The H-3 Freeway transits northeast from the interchange through North Hālawa Valley and on to O'ahu's windward side.

2.3 CLIMATE

The subtropical climate of O'ahu is warm and humid; prevailing northeast trade winds and ocean currents are dominating factors in the climate. Ocean temperatures are approximately 75–85 degrees Fahrenheit (°F) at Honolulu, and air temperatures in O'ahu average 70°–85°F, with the warmest months being June–October. Northeasterly winds persist most of the year, and the northeastern (windward) sides of the island are commonly the wettest due to orographic lifting and cooling of marine air, producing precipitation.

O'ahu has two general seasons for precipitation: October–April is considered the wet season and May–September the dry season. Although precipitation can be as high as 300 inches per year in some places on the island, most of O'ahu receives 20–75 inches per year. Precipitation is most commonly in the form of rain and is at a maximum between 2,000 ft and 4,000 ft mean sea level (msl).

On the Koʻolau Range's leeward slopes, precipitation generally increases up-valley as elevation increases, and decreases down-valley. Average annual precipitation in upper North Hālawa Valley and Moanalua Valley, near the ridge line of the Koʻolau Mountains, is approximately 139 and 137 inches, respectively (USGS 2017b, 2017a). Downgradient in North Hālawa Valley near municipal water supply well Hālawa Shaft, formerly active precipitation gages (2005–2009) have recorded average annual precipitation of 35–41 inches (USGS 2017c, 2017d).

2.4 VEGETATION AND WILDLIFE

The aboveground portion of the site is inhabited by non-native vegetation, including koa haole scrub, disturbed habitat, and landscaped areas (Figure 2-3). Koa haole grows throughout Oʻahu, primarily in areas that have been disturbed by grazing or human activities. The scrub community on Red Hill is dominated by koa haole (*Leucaena leucocephala*), guinea grass (*Panicum maximum*), and Chinese violet (*Asystasia gangetica*). The disturbed habitat is composed of weedy plant species that can withstand frequent disturbance by human activities or natural events. Although this vegetation does support some wildlife species, the habitat is considered to be of very low quality and is primarily used by introduced, common urban species. The onsite habitat is not considered sensitive and is dominated by introduced plant and animal species that have replaced native species. No native or sensitive species were observed in a 1995 biological survey of the area (DON 1996); while no subsequent threatened or endangered species surveys are known to have been conducted at the Facility, anticipated federal- or state-listed threatened or endangered species are not known or expected to be present on site (DON 2005). The endangered Hawaiian hoary bat (*ōpeʻapeʻa*; *Lasiurus cinereus semotus*) could conceivably use the trees; therefore, requirements stipulated in the Categorical Exclusions are followed, and field personnel coordinate with the Navy's Natural and Cultural Resources personnel to obtain clearance prior to mobilizing for field work in areas containing trees.

2.5 ARCHAEOLOGICAL SITES

An archeological survey report prepared for the Facility (DON 2015b) included an inventory-level pedestrian survey of 170 acres and a line-of-sight survey of 77 acres where the terrain was too steep or otherwise inaccessible. The report concluded that ranching and military activities in the 20th century had a substantial impact across much of the Facility area, although limited areas with intact traditional Hawaiian sites still persist. Fourteen historical sites were identified within the Facility boundaries, including Hawaiian residential, cultural, religious, and agricultural areas, plantation and ranching sites, and military sites. Ten of these sites were recommended for listing on the National Registry of Historic Places. Locations and access routes for field work (e.g., monitoring well installation) are checked for proximity to identified archaeological sites prior to commencing field work, and field personnel are instructed to stop work and notify the Navy's Natural and Cultural Resources and/or pertinent State (e.g., State Historic Preservation Office) personnel if any indications of possible archaeological findings are encountered during field work.

2.6 TOPOGRAPHY

Four major geomorphic provinces define the island of Oʻahu: two volcanic mountain ranges (Waiʻanae and Koʻolau), the Schofield Plateau, and the coastal plains, which form the northwest and south island margins (Stearns and Vaksvik 1935). The Koʻolau volcano is a shield (dome) volcano; the east (windward) half of it is "missing" because of collapse due to catastrophic mass wasting (Walker 1990). The pali (cliff line) on the windward side of the range defines the predominantly stream-eroded, back-collapsed scarp. In the south/central part of the range, the leeward flank of the shield volcano is eroded into a series of parallel ridges and stream-carved valleys extending generally perpendicular from the Koʻolau crest, which trends northwest–southeast.

Red Hill is one such leeward ridge, descending 5 miles from the Koʻolau crest at approximately 2,200 ft msl southwest to the coastal plain. The surface elevation of Red Hill in the tank farm area is approximately 420–560 ft msl. The ridge's northwest and southeast flanks drop steeply to South Hālawa Valley and Moanalua Valley, where valley floor elevations in the tank farm area are approximately 200 ft msl and 100–160 ft msl, respectively. North of South Hālawa Valley and a low inter-valley ridge lies the larger North Hālawa Valley.

2.7 SITE VOLCANIC ROCKS

As indicated on Figure 2-4, the Facility is located within the Koʻolau Volcanic series. The Koʻolau formation at Red Hill consists of the basaltic lava flows that erupted from a fissure line approaching 30 miles in length and trending in a northwest rift zone (Wentworth and MacDonald 1953). Both pāhoehoe and aʻā lava flows are present in the Koʻolau formation. The valleys on either side of Red Hill ridge were formed as a result of fluvial erosion and are filled with sedimentary deposits (alluvium and colluvium), also known as valley fill, underlain by residual (weathered basalt), also known as saprolite. Saprolite zones in Hawaiʻi are typically around 75 ft thick but can be 300 ft thick or greater beneath the valley floors or in areas of high precipitation. The results of a recently conducted seismic survey in North and South Hālawa Valleys, Red Hill, and Moanalua Valley (DON 2018d) found valley fill and saprolite to extend much deeper in the valleys surrounding Red Hill, particularly in the center of the valleys and below the streambeds. The role of saprolite as a low-permeability barrier that can impede the flow of groundwater and transport of dissolved constituents is discussed in Module D: Vadose Zone Model (Section 5).

The southeastern third of Koʻolau volcano's remnant shield (which includes the site vicinity) experienced a rejuvenation stage of volcanism. Most rejuvenation-stage volcanoes lie south of the erosional valleys carved out of the Koʻolau shield and are interbedded with alluvial and marine sediments. These rejuvenation-stage vents and associated flows and ash deposits compose the Honolulu volcanic series. These eruptions did not occur in rapid succession, but were scattered over the last 900,000 years (Walker 1990). Salt Lake Tuff, named for Salt Lake Crater east of Pearl Harbor, consists of subaerial gray to brown tuff containing nodules of dunite (Stearns and Vaksvik 1935). It is as thick as 300 ft, contains upright tree molds, and passes beneath sea level. It overlies Āliamanu Tuff. The Āliamanu Tuff, named for Āliamanu Crater east of Pearl Harbor, is composed of water-laid gray to black or grayish-brown tuff, rounded gravel, and (in tunnels) large vesicular bombs and spatter (Stearns and Vaksvik 1935). It is separated from the overlying Salt Lake Tuff by red soil and typically overlies older alluvium.

West and southwest of the Facility, substantial thicknesses of heterogeneous sediments occur on the coastal plains in southern Oʻahu around Pearl Harbor. These terrestrial and marine sediments and reef limestone deposits form a wedge up to 1,000 ft thick, commonly referred to as caprock, and overlie the lava flows of the basaltic aquifer. Overall, the caprock has lower hydraulic conductivity than the basaltic rocks, and it confines the underlying basal aquifer in the Pearl Harbor and Honolulu areas. Rejuvenation stage volcanics, caprock deposits, deep-stream valley fill sediments, and saprolite all have the potential to impede groundwater flow.

The presence of nearly horizontal beds of lava flows with variable strike and dip and alternately greater and lesser resistance to erosion at the site have been described in previous investigations and observed during site reconnaissance activities. Rapid erosion of the less-resistant beds, such as aʻā clinker, has resulted in undercutting of the more resistant massive aʻā and pāhoehoe layers. The flows vary from evenly bedded, relatively flat, and continuous to undulating and uneven.

A'ā clinker is composed of gravel- and cobble-size rubble that resembles a conglomerate. It is usually loosely held together unless it has been welded together by heat. A'ā clinker is extremely permeable and is subject to more rapid chemical weathering processes. Vertical fractures present are also subject to rapid weathering. Similarly, the nearly horizontal contacts between pāhoehoe lava flows, which are absent of a'ā clinker, are susceptible to weathering. Rock layers with denser, more closely spaced fracturing appear more extensively weathered.

A detailed description of site-specific geology and hydrogeology, including hydraulic characteristics of volcanic rock and the nature of valley fill, is presented in Module D: Vadose Zone Model and Module E: Saturated Zone Model (Sections 5 and 6, respectively).

2.8 SITE SOILS

Soils in the vicinity of Facility are mapped as Helemano-Wahiawā association consisting of well-drained, moderately fine textured and fine textured soils (USDA SCS 1972). The surfaces of the basaltic flows have been weathered to form reddish-brown clayey silt, which is the basis for the local name of "Red Hill." These soils typically range from nearly level to moderately sloping and occur in broad areas dissected by very steep gulches. They formed in material weathered from basalt and consist of clays and clayey gravels to a depth of approximately 10 ft below ground surface (bgs). Along the slopes, the basaltic bedrock is covered with approximately 10–30 ft of Ko'olau residuum. These soils were derived from weathering of the underlying basalt bedrock or were deposited as alluvium/colluvium. The younger alluvium/colluvium deposits were derived from fractured basalts and tuff. Beneath the surficial soils, alternating layers of clay and fractured basalts are encountered at depth. The western slope of Red Hill is generally barren of soil and consists of outcropping basalt lava flows to the valley floor.

2.9 SURFACE WATER

Surface water bodies in the vicinity of the tank farm include South Hālawa Stream (approximately 600–800 ft to the north), North Hālawa Stream (approximately 4,000–4,500 ft to the northwest), and Moanalua Stream (approximately 1,700–2,000 ft to the south) (Figure 1-1). Potential recharge (runon and operational water use) from the Hālawa Quarry north of the tank farm area may also impact groundwater flow in this area. In the area of Hālawa Valley, stream flow is isolated from the basal groundwater table and is over deeply weathered rock. These flows may contribute water to perched groundwater within alluvial material (valley fill). Most precipitation percolates to the freshwater-lens aquifer and does not maintain base flows in the streams (Izuka 1992). Groundwater that flows beneath the Facility does not intercept surface water inland of the ocean shoreline (DON 2007). Both South Hālawa Stream and Moanalua Stream (to the north and south of Red Hill ridge, respectively) are located approximately 100 ft or more above the groundwater table in the vicinity of the Facility. The bottoms of the Facility's fuel storage tanks are located at least 50 ft below the bottom of these streams.

2.10 GROUNDWATER

Groundwater in Hawai'i exists in two principal aquifer types: basal and caprock. Perched groundwater has also been reported in the Facility area. A conceptual cross section view of O'ahu hydrogeology depicting the basal groundwater freshwater–saltwater interface, low-permeability caprock, and perched water zones is presented on Figure 2-5.

The basal aquifer exists as a lens of fresh water floating on and displacing seawater within the pore spaces, fractures, and voids of the basalt that forms the underlying mass of each Hawaiian island. Near the shoreline and at lower elevations within the coastal plains, groundwater in the basal aquifer

is typically confined by the overlying caprock and is under pressure. Waters that flow freely to the surface from wells that tap the basal aquifer are referred to as artesian. The basal aquifer beneath the Facility is included in the Oahu Sole Source Aquifer (also known as the Southern Oahu Basal Aquifer), designated a Sole Source Aquifer in 1987 under Section 1424(e) of the Safe Drinking Water Act (61 Fed. Reg. 47752). Sole Source Aquifers are those that are the sole or principal drinking water source for an area, and which, if contaminated, would create a significant hazard to public health. Groundwater in the area of the Facility is on the boundary of the Waimalu and Moanalua Aquifer Systems of the Pearl Harbor and Honolulu Aquifer Sectors, respectively. The aquifers are classified as basal, unconfined, flank-type and are currently used as a drinking water source. The aquifers are considered fresh, with less than 250 milligrams per liter (mg/L) of chloride, and are considered an irreplaceable resource with a high vulnerability to contamination (Mink and Lau 1990). These aquifer systems underlie the Waimalu, North Hālawa, South Hālawa, Moanalua, and Kalihi Valleys, as shown on Figure 2-6. Red Hill ridge is an administrative boundary between these aquifer systems, but is not actually a hydrogeologic boundary because there are no geochemical or physical attributes that distinguish between these two aquifer systems at this location (DON 2007).

The second type of aquifer is the caprock aquifer, which consists of various kinds of unconfined and semi-confined groundwater. Commonly, the caprock consists of a thick sequence of nearly impermeable clays, coral, and basalt that separates the caprock aquifer from the basal aquifer. The impermeable nature of these materials and the artesian nature of the basal aquifer severely restrict the downward migration of groundwater from the upper caprock aquifer. However, the caprock is located downgradient of the Facility and the surrounding valleys; therefore, this aquifer is not present in the site vicinity. While the caprock aquifer does not extend to the Red Hill Shaft drinking water supply well or the tank farm area, it is present in makai (seaward) portions of the study area and may influence the flow of groundwater.

Groundwater elevations in the southern O'ahu region range from 0 ft msl near the shoreline to approximately 30 ft msl at the southern O'ahu and Schofield water region boundary. The groundwater elevation in the project vicinity is approximately 20 ft msl. Nearshore, the water is typically under artesian pressure because it is confined by caprock, unless hydraulic heads are decreased by pumping or climatic conditions. Groundwater in the vicinity of Pearl Harbor, including Red Hill, generally flows toward the harbor, but the potential exists for variances in the localized flow directions from the anticipated regional flow pattern.

The Facility is located inland and to the east of the Hawai'i State Underground Injection Control (UIC) Line, as indicated on Figure 2-6. The UIC Line indicates the border between groundwater that is or is not (i.e., aquifers shoreward of the line) considered a potential source of drinking water by the State of Hawai'i. The EPA, however, does not recognize this boundary and considers the area shoreward of the UIC Line to be a potential source of drinking water.

Shallow groundwater (at times identified as a perched zone) has been encountered in the site vicinity. A shallow perched water-bearing zone was encountered during investigations conducted at the former Oily Waste Disposal Facility (OWDF) (DON 1996), Hālawa Correctional Facility (Dames & Moore 1991; EKNA 1999), the City and County of Honolulu Hālawa Bus Facility (Kimura 2000), and Tripler Hospital (ECC 2000) (see Table 2-13 in DON [2017b]). Shallow perched water-bearing zones were also encountered during drilling of onsite monitoring wells RHMW04 at approximately 183–228 ft msl (DON 2007), and RHMW08 in two zones at approximately 214–217 and 193–198 ft msl. Shallow groundwater was observed at the recently installed monitoring well

RHMW11 on the South Hālawa Valley floor at approximately 110–115 ft msl with continuous saturation within the saprolite (perched conditions not observed) (DON 2018c).

As indicated conceptually on Figure 2-5, dikes are not expected to occur in the Facility area, but do occur further inland. Where present, the dikes' low permeability can impede the flow of groundwater and confine groundwater in localized compartments, resulting in localized deviances from average groundwater levels. Dikes are often less than 10 ft wide, but can extend vertically and laterally for long distances. Furthermore, dike complexes can form where individual dikes intersect at various angles. Dikes and dike complexes can intersect similarly low-permeability, nearly horizontal lava flows, collectively inhibiting lateral and vertical groundwater flow and resulting in high-level groundwater impoundments.

Details on site-specific hydrogeology are presented in Module D: Vadose Zone Model and Module E: Saturated Zone Model (Sections 5 and 6, respectively).

2.11 WATER SUPPLY WELLS

Locations of water supply wells in the groundwater model area are shown on Figure 2-7; additional detail on these wells is presented in the *Groundwater Model Evaluation Plan* (DON 2017i). The Hālawa/Red Hill/Moanalua area provides approximately 25 percent of the drinking water for urban Honolulu. Drinking water supply wells of primary concern for the investigation due to their proximity to the Facility tanks and pumping capacities are Red Hill Shaft, Hālawa Shaft, and Moanalua Wells (see Figure 2-7):

- The Navy's Red Hill Shaft (Hawai'i Well Identification [ID] 2254-01) is a potable water pumping station operated by NAVFAC Hawaii, Utilities and Energy Division. The pumping station is located within the Facility's lower tunnel system approximately 2,600 ft makai (seaward) of the Facility tanks. The station pumps groundwater from a water development tunnel (also called an infiltration gallery) that extends from the pumping station 1,260 ft east and southeast to within 1,530 ft of Tank 1, the nearest fuel storage tank. The pumping station supplies the JBPHH water distribution system, which serves approximately 65,200 military customers. Average pumping rates at Red Hill Shaft are [redacted] million gallons per day (mgd).
- Hālawa Shaft (2354-01) is located approximately 4,400 ft northwest of the tank farm. It is a municipal water supply well operated by the City and County of Honolulu Board of Water Supply (BWS). The pumping station is located in an underground pump room approximately 150 ft bgs. Groundwater is pumped from a water development tunnel to provide municipal drinking water for O'ahu. The tunnel extends from the pumping station 919 ft northeast, and comes within 4,600 ft of the Facility tanks at the closest point between the two. The average pumping rate is 7.0–12.1 mgd.
- Moanalua Wells Moanalua 1 (2153-10), Moanalua 2 (2153-11), and Moanalua 3 (2153-12) are located approximately 6,650 ft south of the Facility tanks and are operated by BWS. Groundwater pumped from these wells also supplies municipal drinking water for O'ahu. The average pumping rate (as channeled and measured at Moanalua 1) is 1.0–4.3 mgd.

Currently, it is presumed that the above wells represent key components in the most significant exposure pathway to human receptors from a Facility fuel release due to their known or suspected pumping influence on the aquifer beneath the Facility, the size of their drinking water distribution system(s), proximity to the Facility, and the potential groundwater flow direction relative to the

Facility. BWS projects an increase of 15–21 percent in water use in central O'ahu from 2012 demand levels of 17.2 mgd (BWS 2016).

2.12 RED HILL LONG-TERM MONITORING SYSTEM

The Facility has a network of soil vapor and groundwater monitoring points that are sampled periodically in accordance with the Red Hill *Groundwater Protection Plan* (GWPP) (DON 2014b) and long-term monitoring (LTM) *Work Plan/Sampling and Analysis Plan* (DON 2015c); all results are reported to DOH.

2.12.1 Soil Vapor Monitoring System

The Facility's soil vapor monitoring (SVM) system consists of 47 probes installed during previous investigations in angle boreholes beneath each of the 18 active Facility tanks. One angle boring is located under each tank, and two to three probes are installed in each boring. The three probe positions are referred to as shallow (near tank access), middle (near centerline of tank), and deep (near outer opposite edge of the tank). Construction details are shown on Figure 2-8. Each probe is used to withdraw vapor from these three isolated segments of the borehole via a pump and sampled in the field using a hand-held organic compound photoionization detector (PID). Total volatile organic vapors are measured down to 1 part per billion by volume (ppbv) and compared to baseline measurements from the same location. Increasing concentrations over time have been used as an indication of fuel leaks at the tested tank. SVM points have been monitored on a monthly basis at a minimum since 2008 (DON 2008a). The monitoring reports are currently included as Appendix A of the Navy's *Quarterly Release Response Reports* to DOH (DON 2014a).

2.12.2 Groundwater Monitoring Network

The Red Hill groundwater LTM program began in February 2005, when the network consisted of three wells; additional wells have subsequently been added to the network both before and after the 2014 Tank 5 release. As of the Second Quarter 2018 groundwater monitoring event, 14 groundwater monitoring locations are included in the network (see Figure 2-9 and Table 2-1): one sampling point adjacent to the Red Hill Shaft water supply well (2254-01) and 13 groundwater monitoring wells (RHMW01 through RHMW11, HDMW2253-03, and OWDFMW01) installed in the basal aquifer within or near the Facility. An additional nine monitoring wells and one test boring are currently proposed for installation within the Facility boundaries and in North and South Hālawa Valleys to extend the network and improve understanding of regional geology, hydrogeology, and local groundwater flow in support of the investigation's groundwater modeling efforts (DON 2017f).

Groundwater monitoring has been conducted on a quarterly basis at a minimum since 2005. Each monitoring event's sampling program, the screening criteria, and analytical results are presented in quarterly groundwater monitoring reports to DOH, currently presented as Appendix C of the Navy's *Quarterly Release Response Reports* (DON 2014a). Analytical parameters and discussion of COPC trends in groundwater are presented in Section 7.2.

Well elevation and gyroscopic surveys were recently conducted at the Red Hill monitoring locations to improve the accuracy of groundwater elevation measurements, which are critical to the groundwater modeling effort due to the regional aquifer's extremely low gradients. Elevations of all existing monitoring locations were resurveyed in Summer 2017 using high-precision Second Order, Class I techniques (DON 2018a) to establish accurate top-of-casing elevations, for which variable data had been reported by previous surveys, and to establish standard measuring point(s) for each monitoring location. For wells existing during the 2007 Facility investigation (DON 2007), corrections based on the resurveyed elevations were all under -0.5 ft except for RHMW2254-01

(-5.0 ft). Additionally, field gyroscopic directional surveys were conducted at all existing monitoring wells (except RHMW01 due to its small diameter) to determine whether any wells deviate from true vertical; tape correction factors calculated for all wells based on three-dimensional modeling of the field data were less than -0.1 ft except for RHMW09 (-0.24 ft). Gyroscopic correction factors for manually collected depth to water measurements have been provided to stakeholders.

Existing and proposed monitoring wells in the Red Hill groundwater monitoring network are summarized in Table 2-1.

Table 2-1: Existing and Proposed Wells in the Red Hill Groundwater Monitoring Network

Monitoring Well / Sampling Point	Location and Approximate Distance from Tank Farm	Installation Date	Rationale for Inclusion in Network
Existing [a]			
RHMW2254-01	Inside Adit 3 lower access tunnel near Red Hill Shaft; 2,600 ft W of Tank 1	2005	Monitor groundwater at Red Hill Shaft (Navy Supply Well 2254-01).
RHMW01	Inside lower access tunnel SW of Tanks 1–2	2001	Monitor groundwater directly under tank farm.
RHMW02	Inside lower access tunnel near Tank 6	2005	Monitor groundwater directly under tank farm.
RHMW03	Inside lower access tunnel near Tank 14	2005	Monitor groundwater directly under tank farm.
RHMW04	Northeast of tank farm; 850 ft NE of Tank 19	2005	Monitor background conditions in basal aquifer.
RHMW05	Inside lower access tunnel between tank farm and Red Hill Shaft; 1,000 ft SW of Tank 2 (1,700 ft SE of Red Hill Shaft)	2009	Monitor groundwater between tank farm and Red Hill Shaft.
RHMW06	North of tank farm, between tank farm and Hālawa Quarry; 550 ft NE of Tank 15	2014	Monitor groundwater between tank farm and Hālawa Shaft (BWS Supply Well 2354-01).
RHMW07	North of tank farm, between tank farm and Hālawa Correctional Facility; 600 ft NW of Tank 3	2014	Monitor groundwater between tank farm and Hālawa Shaft.
RHMW08	West of tank farm, between tank farm and Hālawa Industrial Park; 550 ft W of Tank 1	2016	Monitor groundwater west of tank farm, in general area between tank farm and Red Hill Shaft.
RHMW09	Between tank farm and Moanalua Valley residential area; 450 ft S of Tank 2	2016	Monitor groundwater southwest of tank farm.
RHMW10	Between tank farm and Moanalua Valley residential area; 400 ft S of Tank 14	2017	Monitor groundwater south of tank farm.
RHMW11 [b]	North side of South Hālawa Stream; 900 ft N of Tank 5	2017	Determine if valley fill and saprolite extend below the water table in South Hālawa Valley. Evaluate groundwater flow directions in South Hālawa Valley, groundwater quality between Red Hill and Hālawa Shaft, and potential presence for perched groundwater conditions throughout the entire thickness of the vadose zone in South Hālawa Valley.
HDMW2253-03 (Hālawa Deep Monitor Well)	East of Hālawa Correctional Facility; 1,000 ft N of Tank 13	2000	Monitor groundwater between tank farm and Hālawa Shaft.
OWDFMW01	At OWDF in western portion of Facility; 3,100 ft W of Tank 1 (550 ft W of Red Hill Shaft)	1998	Monitor groundwater west of Red Hill Shaft.

Monitoring Well / Sampling Point	Location and Approximate Distance from Tank Farm	Installation Date	Rationale for Inclusion in Network
Proposed [c]			
RHMW01R	Inside lower access tunnel adjacent to RHMW01, SW of Tanks 1–2	[2018]	Provide capability to detect LNAPL at the groundwater surface, which cannot be achieved by RHMW01 since it is screened below the water table surface.
RHMW07D	Adjacent to RHMW07, between tank farm and Hālawa Correctional Facility; 600 ft NW of Tank 3	[2018]	Evaluate water level elevations in discrete vertical zones adjacent to RHMW07 to further evaluate the basal aquifer groundwater table elevation at this location and evaluate the potential for preferential pathways in both shallow and deeper portions of the basal aquifer between Red Hill tank farm and Hālawa Shaft.
RHMW12	In South Hālawa Valley north of Hālawa Correctional Facility; 1,600 ft NW of Tank 1	[2018]	Evaluate groundwater flow north of tank farm in South Hālawa Valley, and groundwater recharge southeast of the former quarry pit where water used by the quarry is discharged. Further define geometry of valley fill sediments and saprolite layers in South Hālawa Valley.
RHMW13	In South Hālawa Valley north of HDMW2253-03; 1,200 ft NW of Tank 15	[2018]	Evaluate groundwater flow north of the tank farm in upper South Hālawa Valley, and groundwater quality to the northwest of Tank 5. Further define geometry of valley fill sediments and saprolite layers in South Hālawa Valley.
RHMW14	Northwest side of South Hālawa Stream; 550 ft NW of Tank 1	[2018]	Determine extent of valley fill and saprolite in the area. Evaluate groundwater quality and groundwater flow directions in South Hālawa Valley, and the potential presence for perched groundwater conditions throughout the entire thickness of the vadose zone in the area.
RHMW15	West of RHMW05 in the upper extent of the Red Hill Shaft; 1,550 SW of Tank 1	[2018]	Improve assessment of the effects of pumping at Red Hill Shaft. Further characterize lithology and evaluate groundwater quality adjacent to the upper reaches of the Red Hill Shaft water development tunnel.
RHMW17	Northwest of North Hālawa Stream and just southeast of Hālawa Shaft; 4,040 ft NW of Tank 1 (400 ft S of BWS Hālawa Shaft)	[2018]	Determine if valley fill and saprolite extend below the water table in North Hālawa Valley. Evaluate groundwater quality and (with RHMW18) groundwater flow directions in North Hālawa Valley. Assess effects of pumping at Hālawa Shaft on surrounding water table. Evaluate potential presence for perched groundwater conditions throughout the entire thickness of the vadose zone in the area.
RHMW18	Northwest of North Hālawa Stream; 4,300 ft NW of Tank 1 (950 ft SW of BWS Hālawa Shaft)	[2018]	Determine if valley fill and saprolite extend below the water table in North Hālawa Valley. Evaluate groundwater quality and (with RHMW18) groundwater flow directions in North Hālawa Valley. Assess effects of pumping at Hālawa Shaft on the surrounding water table. Evaluate potential presence for perched groundwater conditions.
RHMW19	Between tank farm and Moanalua Valley, between RHMW09 and RHMW10; 550 ft SE of Tank 6	[2018]	Evaluate groundwater flow directions in the area, and groundwater quality toward Moanalua Valley.

[a] All existing locations except RHMW2254-01, RHMW01, and HDMW2253-03 are screened across the water table surface. RHMW2254-01 is an unscreened sampling point in the water development tunnel near the input to the Red Hill Shaft pumping station. RHMW01's screened interval is below the water table surface. HDMW2253-03 is an open-hole deep monitor well operated by the State of Hawai'i Department of Land and Natural Resources (DLNR).
[b] RHMW11 was installed as a multi-level Westbay-system well, with eight discrete sampling zones extending from the elevation of the basal water table surface to approximately 300 ft below that elevation.
[c] Completion type of the proposed wells (i.e., conventional well with standard casing and slotted screen or multi-level Westbay-system well) is currently under review. Installation dates for proposed wells are projected (DON 2017f); exact locations are subject to change.

2.13 UNCERTAINTY ANALYSIS

Although uncertainty remains regarding groundwater levels and hydraulic gradients in the site vicinity due to apparent extremely flat water level gradients, the unreliability of previously available well elevation data for the Red Hill groundwater monitoring wells has been mitigated by the recently completed high-precision well elevation survey (DON 2018a) and development of water level tape correction factors based on the gyroscopic survey.

The extent of shallow groundwater encountered on the north side of Red Hill and the adjacent South Hālawa Valley floor is unknown: it may be semi-contiguous or contiguous along the flank of Red Hill and/or the valley floor, or may occur only in isolated regions, as has been observed in the few well locations where it has been reported (see Section 2.10). There is uncertainty about the degree to which recharge from the Hālawa Quarry and cement plant affects groundwater levels.

Uncertainty in the total depth of saprolite in the North and South Hālawa Valleys exists because the seismic surveys completed along several transects allows for an interpreted but not a measured depth to the top and bottom of saprolite. Data collected from RHMW11 allow for some corroboration of interpreted depth at nearby transect locations. However, because RHMW11 is not collocated with any of the seismic survey transects, the ability to directly correlate with seismic survey interpretations is limited.

2.14 ADDRESSING UNCERTAINTIES

The following ongoing, planned, or proposed activities are designed to help resolve the uncertainties described in Section 2.13.

The planned installation of several monitoring wells in North and South Hālawa Valleys will include collection of continuous rock core samples (DON 2017f). A detailed geologic boring log of each new monitoring well will be generated. As part of this effort, RHMW11 has recently been installed as a Westbay system multi-level well and is completed approximately 300 ft below the water table surface. Newly proposed wells will be installed as either a Westbay system multi-level well or conventional monitoring well (i.e., standard casing and slotted screen) based on input from the regulators. Following completion of coring, a comprehensive borehole geophysical program will be conducted within each borehole where a Westbay system multi-level well is installed. Video logging will be performed in all boreholes, regardless of well construction. The results will be used to better define the nature of subsurface geology in the valleys and support the groundwater flow and contaminant fate and transport (CF&T) modeling efforts.

Resolving uncertainty regarding groundwater levels and hydraulic gradients in the site vicinity is an important objective of recently completed, ongoing, and planned investigations. These investigations include the recently completed well elevation survey (DON 2018a) and gyroscopic survey (DON 2016b) for Red Hill groundwater monitoring wells, synoptic water level measurements recently collected by the U.S. Geological Survey (USGS) (USGS 2017e), and installation of new monitoring

wells at Red Hill and in North and South Hālawa Valleys (DON 2017f). These new data will be used to develop input parameters for groundwater flow modeling. The synoptic water level study will also improve understanding of flow resulting from various pumping conditions. The results will help further define actual groundwater flow directions and assess the potential for transport of contaminants to potential downgradient exposure points.

Uncertainty associated with the depth of top and bottom of saprolite, interpreted by evaluation of the seismic surveys, will be further resolved with installation of at least one test boring adjacent to at least one seismic survey transect (see Figure 2-9). Continuous coring and geophysical logging of the test boring will allow direct correlation of observed geologic conditions with seismic survey interpretation at that location.

This page intentionally left blank

'Aiea
Ford Island
Joint Base Pearl Harbor-Hickam
Tripler Army Medical Center
Honolulu International Airport

Zoning - Land Use Ordinance Categories

Country	Public	Residential	F-1 Federal/Military
Preservation	Industrial	Apartment	State Jurisdiction
Agriculture	Business	Resort	

\\honolulu\Honolulu\Projects\NAVFAC PAC\CLEAN IV\60481245CTO 0053\900-Work\920 GIS\02_Maps\CSM\Fig2-1_CSM_Zoning_rev3.mxd 3/28/2018

Location Map

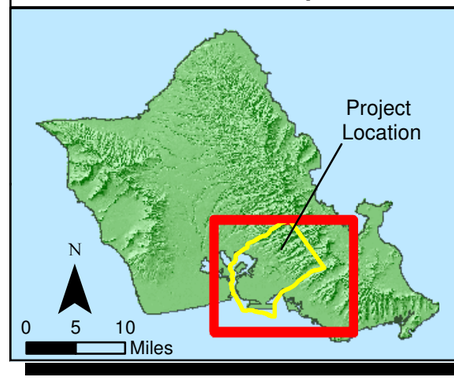

Legend

- Groundwater Model Area
- Red Hill Installation Boundary and Fuel Storage Tanks
- Highway or Freeway
- Stream

Notes

1. Map projection: NAD 1983 UTM Zone 4N
2. Base Map: DigitalGlobe, Inc. (DG) and NRCS. Publication_Date: 2015
3. Land Use Ordinance Data Source: Honolulu Land Information System (HoLIS): Zoning - Land Use Ordinance, 9/26/2017.

N

0 5,000 10,000 15,000 Feet

Figure 2-1
County Land Use Ordinance Map
Conceptual Site Model
Investigation and Remediation of Releases and Groundwater Protection and Evaluation
Red Hill Bulk Fuel Storage Facility
JBPHH, O'ahu, Hawai'i

This page intentionally left blank

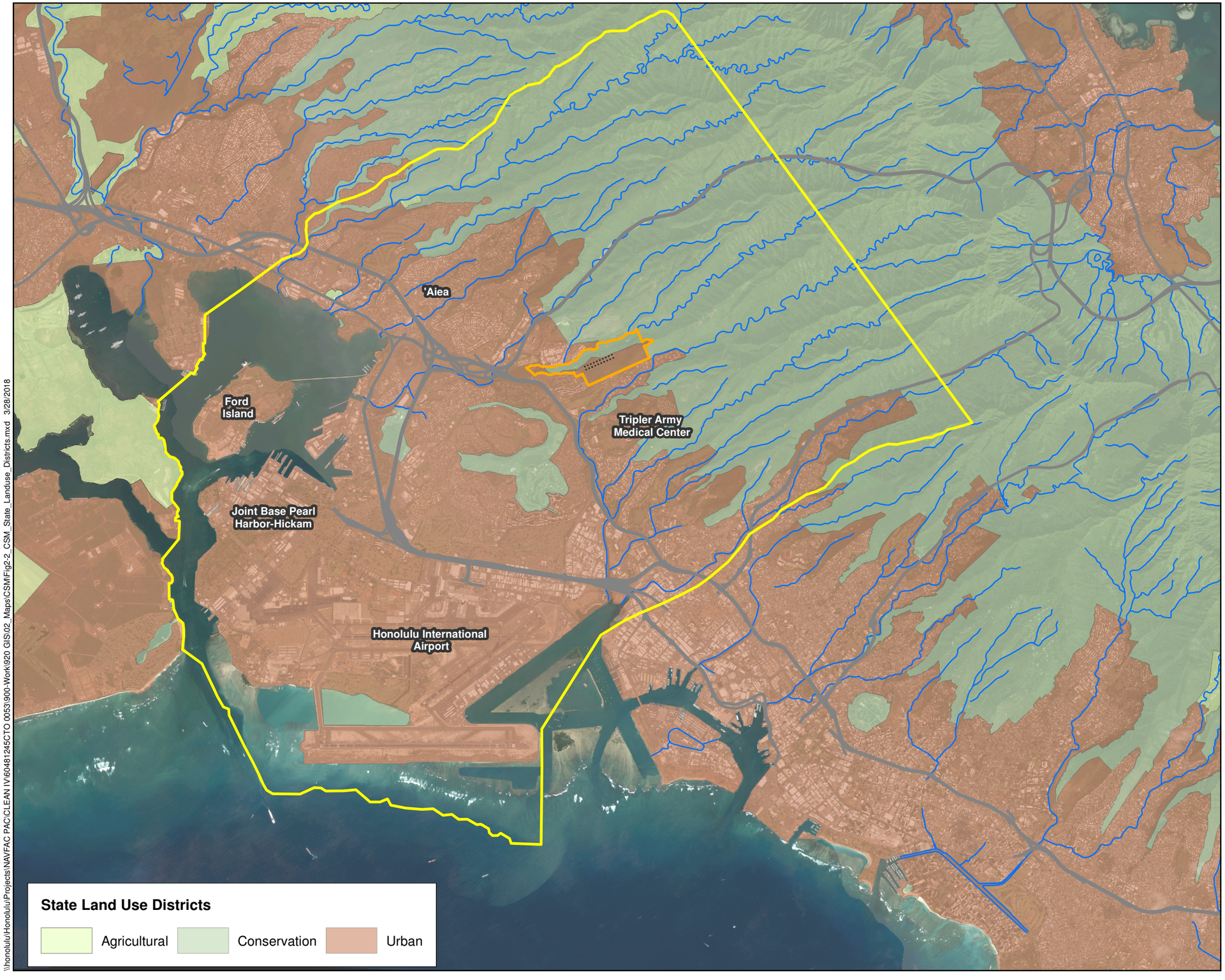

Figure 2-2
State Land Use Districts
Conceptual Site Model
Investigation and Remediation of Releases and Groundwater Protection and Evaluation
Red Hill Bulk Fuel Storage Facility
JBPHH, O'ahu, Hawai'i

\\honolulu\Honolulu\Projects\NAVFAC PAC\CLEAN IV\60481245CTO 0053\900-Work\920 GIS\02_Maps\CSM\Fig2-2_CSM_State_Landuse_Districts.mxd 3/28/2018

This page intentionally left blank

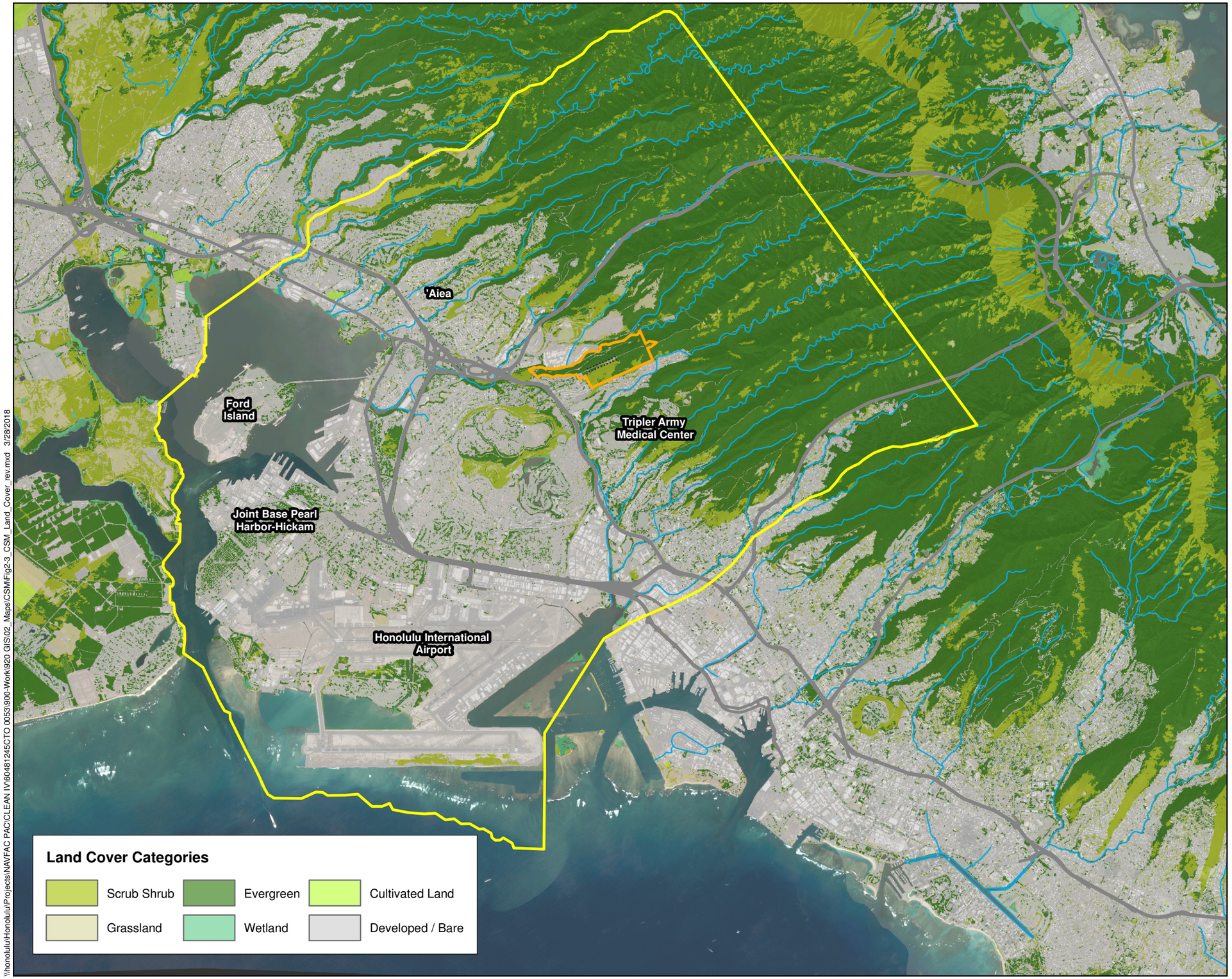

\\honolulu\Honolulu\Projects\NAVFAC PAC\CLEAN IV\60481245CTO 0053\900-Work\920 GIS\02_Maps\CSM\Fig2-3_CSM_Land_Cover_rev.mxd 3/28/2018

Location Map

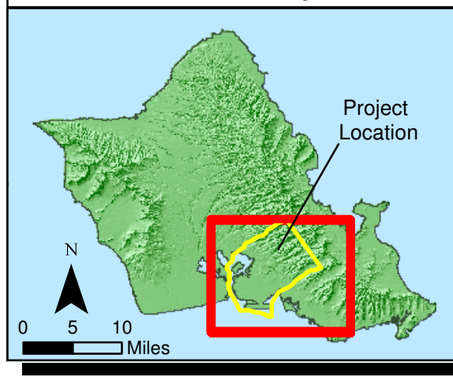

Legend

- Groundwater Model Area
- Red Hill Installation Boundary and Fuel Storage Tanks
- Highway or Freeway
- Stream

Notes

1. Map projection: NAD 1983 UTM Zone 4N
2. Base Map: DigitalGlobe, Inc. (DG) and NRCS. Publication_Date: 2015
3. Land cover imagery source: NOAA Office for Coastal Management: Digital Coast - 2011 C-CAP Land Cover of Oahu, Hawaii (coast.noaa.gov)

N

0 5,000 10,000 15,000 Feet

Figure 2-3
Land Cover
Conceptual Site Model
Investigation and Remediation of Releases and Groundwater Protection and Evaluation
Red Hill Bulk Fuel Storage Facility
JBPHH, O'ahu, Hawai'i

This page intentionally left blank

S:\Projects\NAVFAC PAC\CLEAN IV\60477080CTO 0053\900-Work\921 Graphics\PID_Wp\Fig3_GenSurficial_Geology.ai

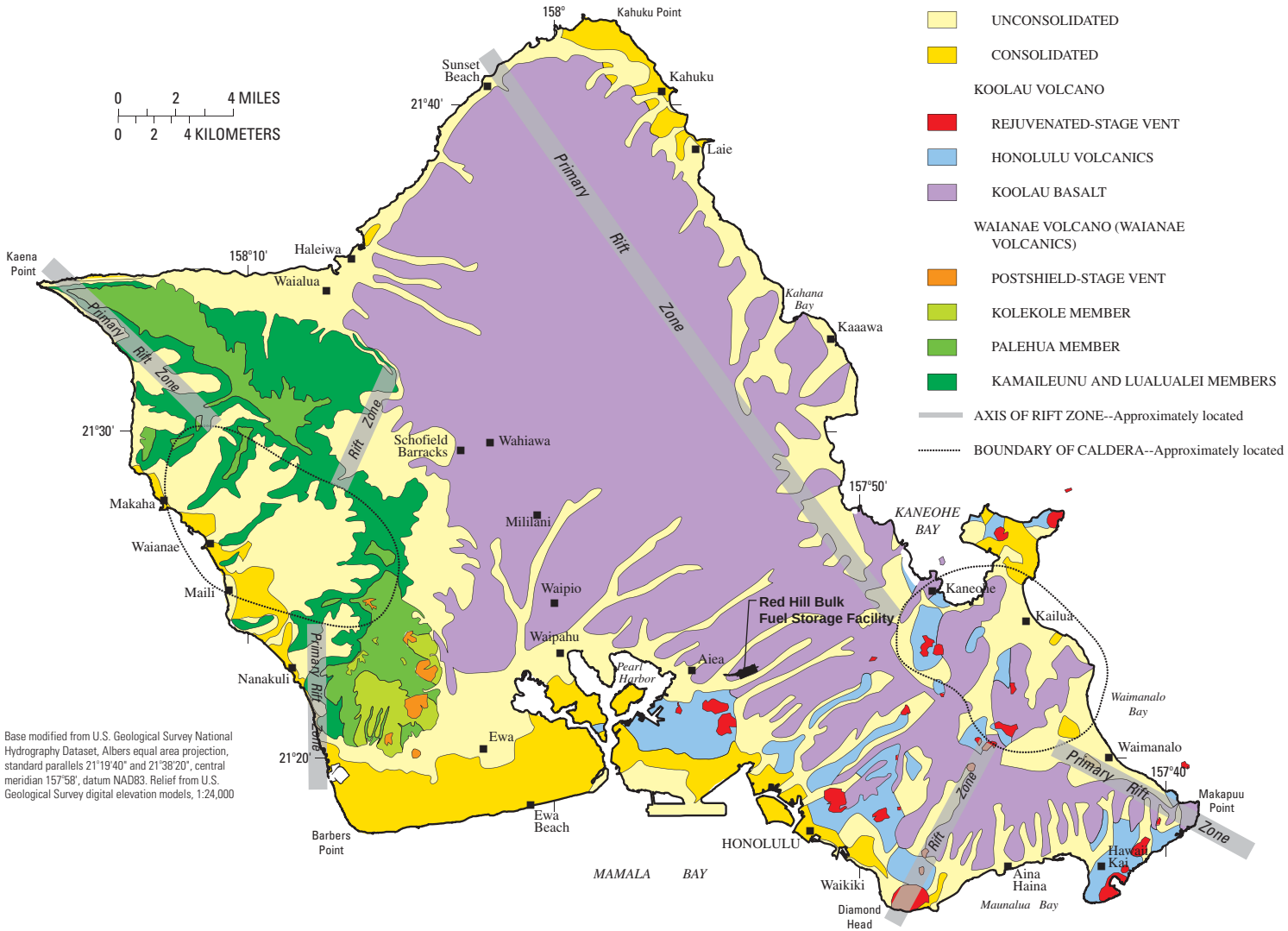

Note:
Modified from Stearns (1939); Langenheim and Clague (1987); Presley et al. 1997.

Figure 2-4
Generalized Surficial Geology of O'ahu
Conceptual Site Model
Investigation and Remediation of Releases and Groundwater Protection and Evaluation
Red Hill Bulk Fuel Storage Facility
JBPHH, O'ahu, Hawai'i

This page intentionally left blank

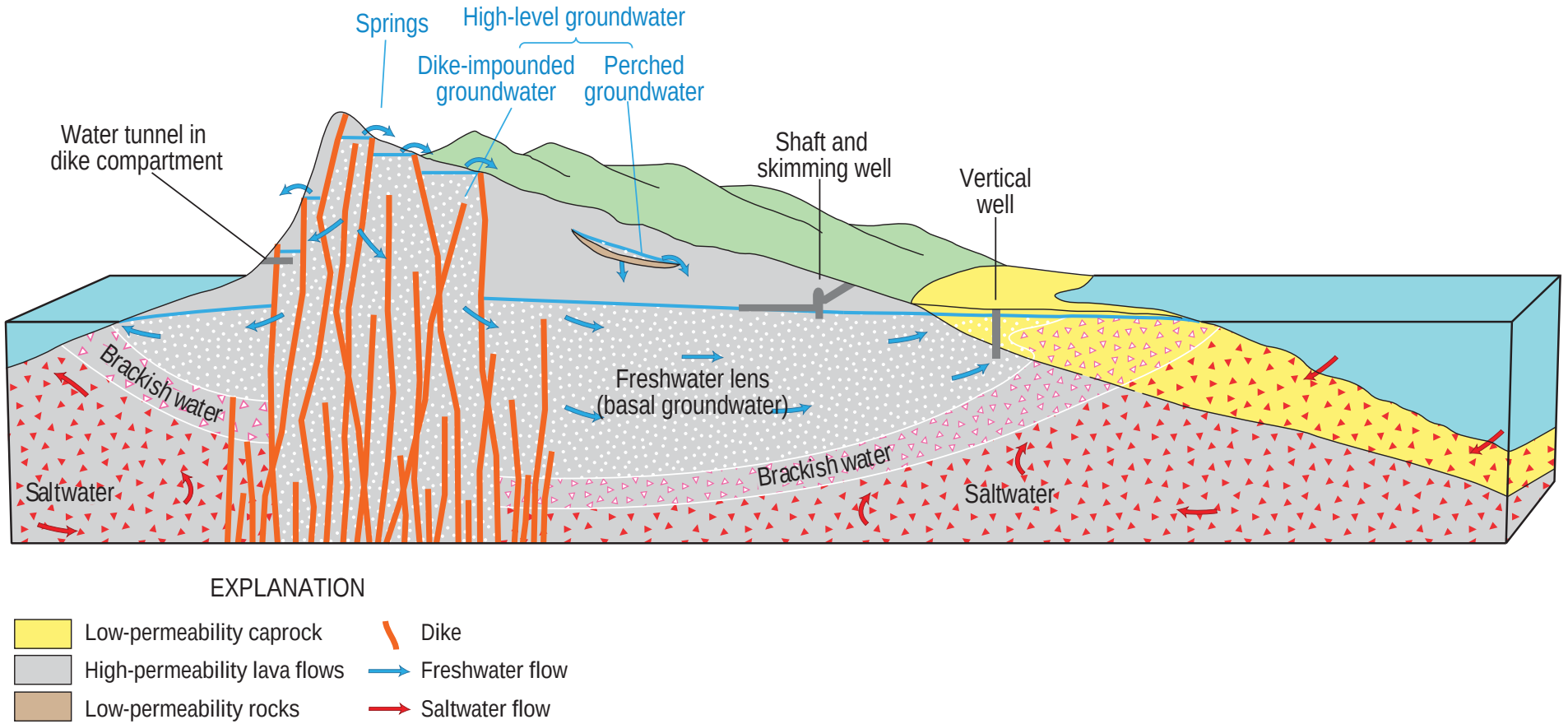

Source: Izuka et al. (2016 [2018]), Figure 21; as modified from Oki et al. (1999)

Figure 2-5
Conceptual Cross Section View of O'ahu Hydrogeology
Conceptual Site Model
Investigation and Remediation of Releases and Groundwater Protection and Evaluation
Red Hill Bulk Fuel Storage Facility
JBPHH, O'ahu, Hawai'i

This page intentionally left blank

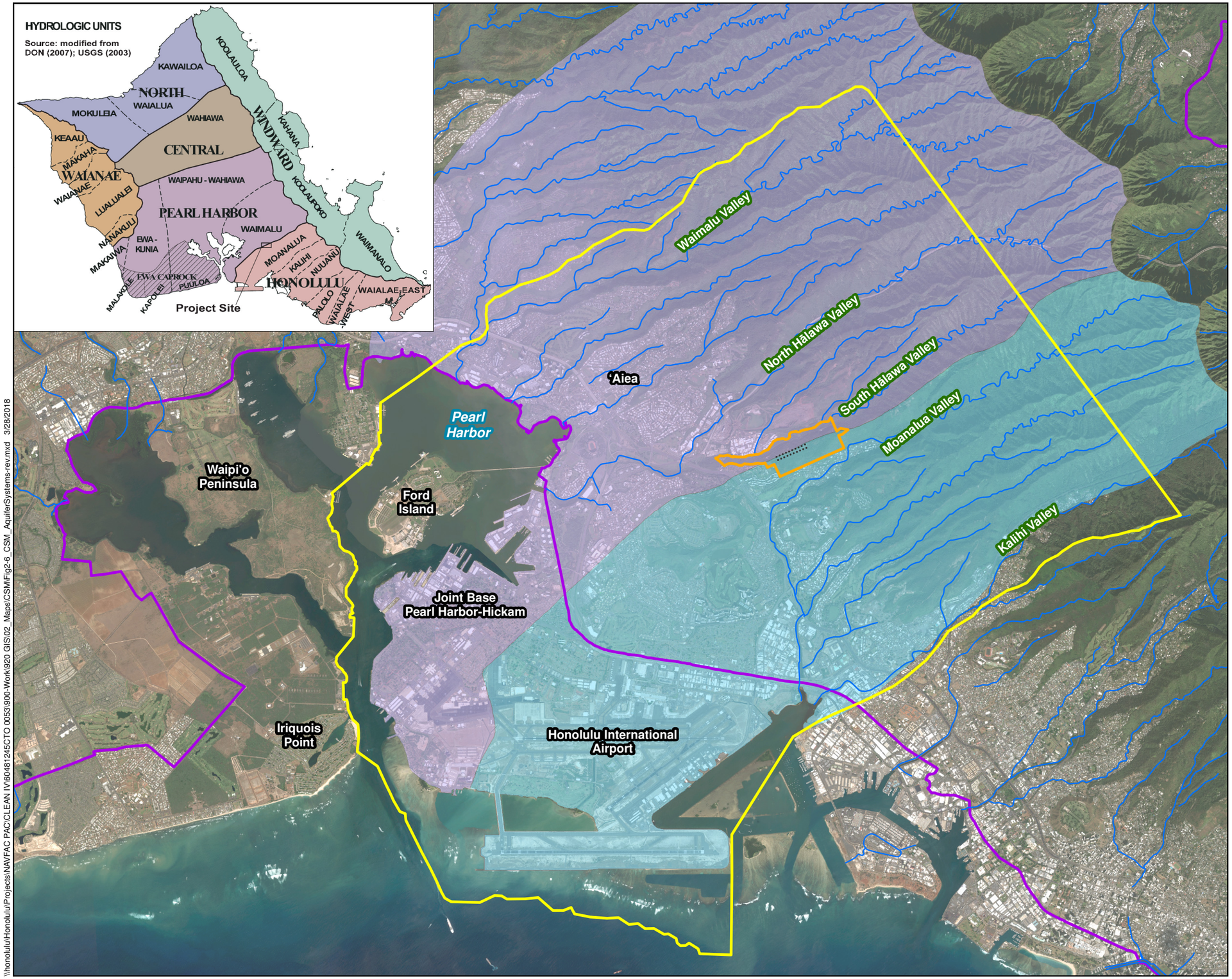

Location Map

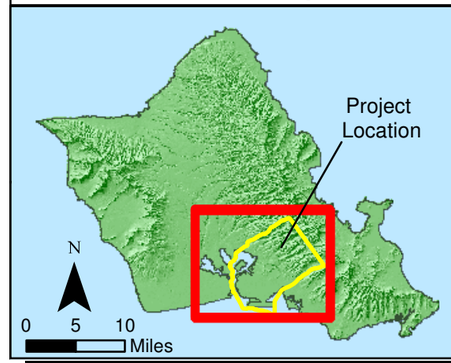

Legend

- Waimalu Aquifer
- Moanalua Aquifer
- Groundwater Model Area
- Underground Injection Control Line
- Stream
- Red Hill Installation Boundary and Fuel Storage Tanks

Notes

1. Map projection: NAD 1983 UTM Zone 4N
2. Base Map: DigitalGlobe, Inc. (DG) and NRCS. Publication_Date: 2015

N

0 5,000 10,000 15,000 Feet

Figure 2-6
Aquifer Systems in the Groundwater Model Area
Conceptual Site Model
Investigation and Remediation of Releases and Groundwater Protection and Evaluation
Red Hill Bulk Fuel Storage Facility
JBPHH, O'ahu, Hawai'i

\\honolulu\Honolulu\Projects\NAVFAC PAC\CLEAN IV\60481245CTO 0053\900-Work\920 GIS\02_Maps\CSM\Fig2-6_CSM_AquiferSystems-rev.mxd 3/28/2018

This page intentionally left blank

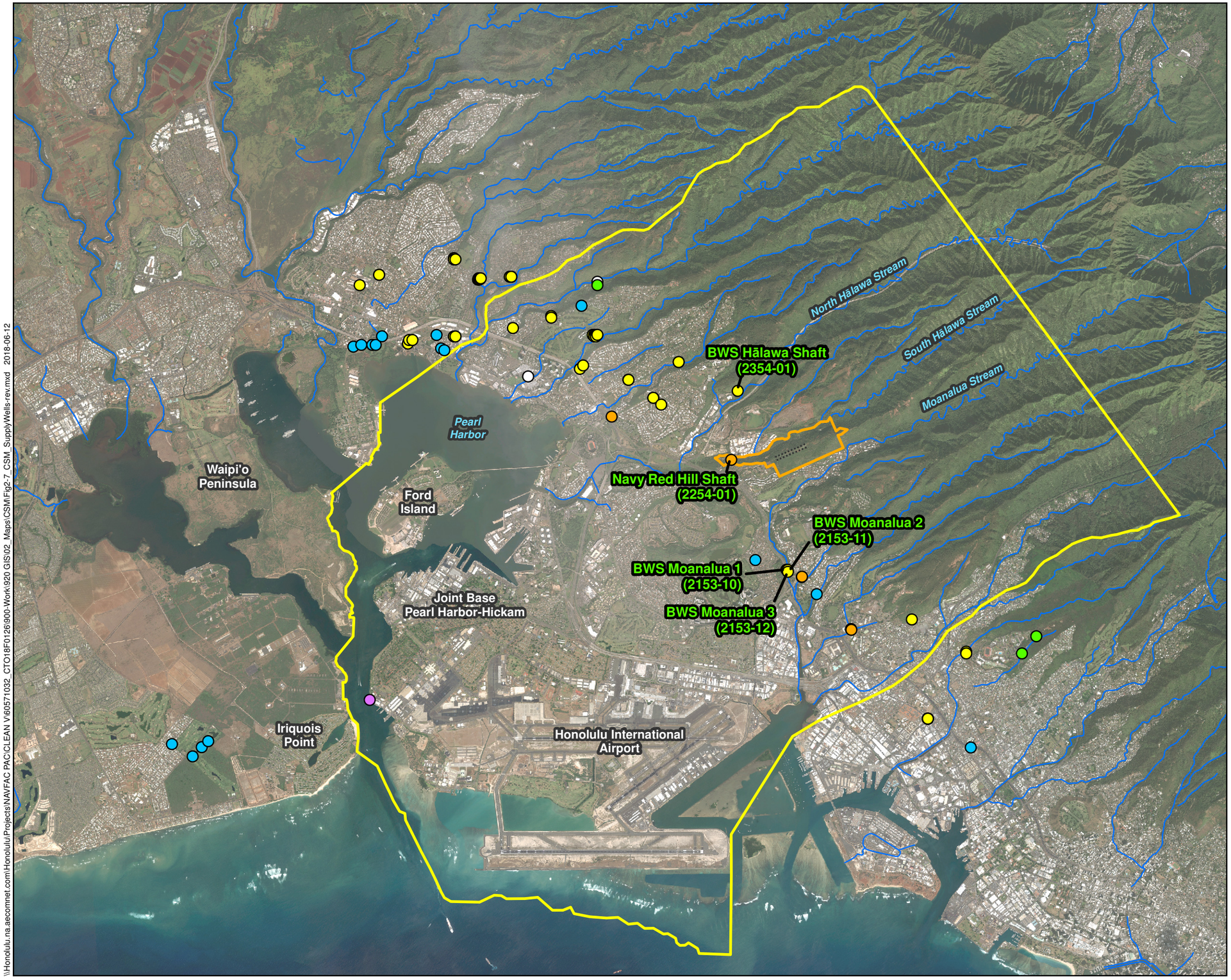

Location Map

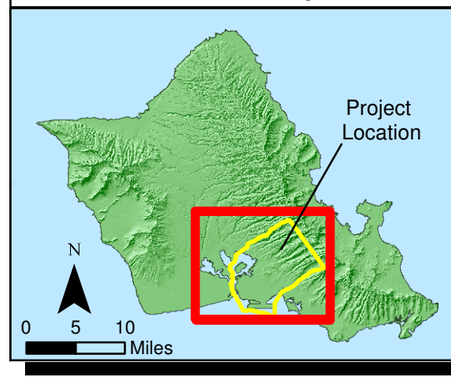

Legend

Supply Well

- Agriculture
- Domestic
- Industrial
- Irrigation
- Military
- Municipal
- Stream
- Groundwater Model Area
- Red Hill Facility Boundary and Fuel Storage Tanks

Notes

1. Map projection: NAD 1983 UTM Zone 4N
2. DigitalGlobe, Inc. (DG) and NRCS. Publication_Date: 2015

N

0 5,000 10,000 15,000 Feet

Figure 2-7
Water Supply Wells
in the Groundwater Model Area
Conceptual Site Model
Investigation and Remediation of Releases
and Groundwater Protection and Evaluation
Red Hill Bulk Fuel Storage Facility
JBPHH, O'ahu, Hawai'i

\\Honolulu.na.aecomnet.com\Honolulu\Projects\NAVFAC PAC\CLEAN V\60571032_CTO18F0126\900-Work\920 GIS\02_Maps\CSM\Fig2-7_CSM_SupplyWells-rev.mxd 2018-06-12

This page intentionally left blank

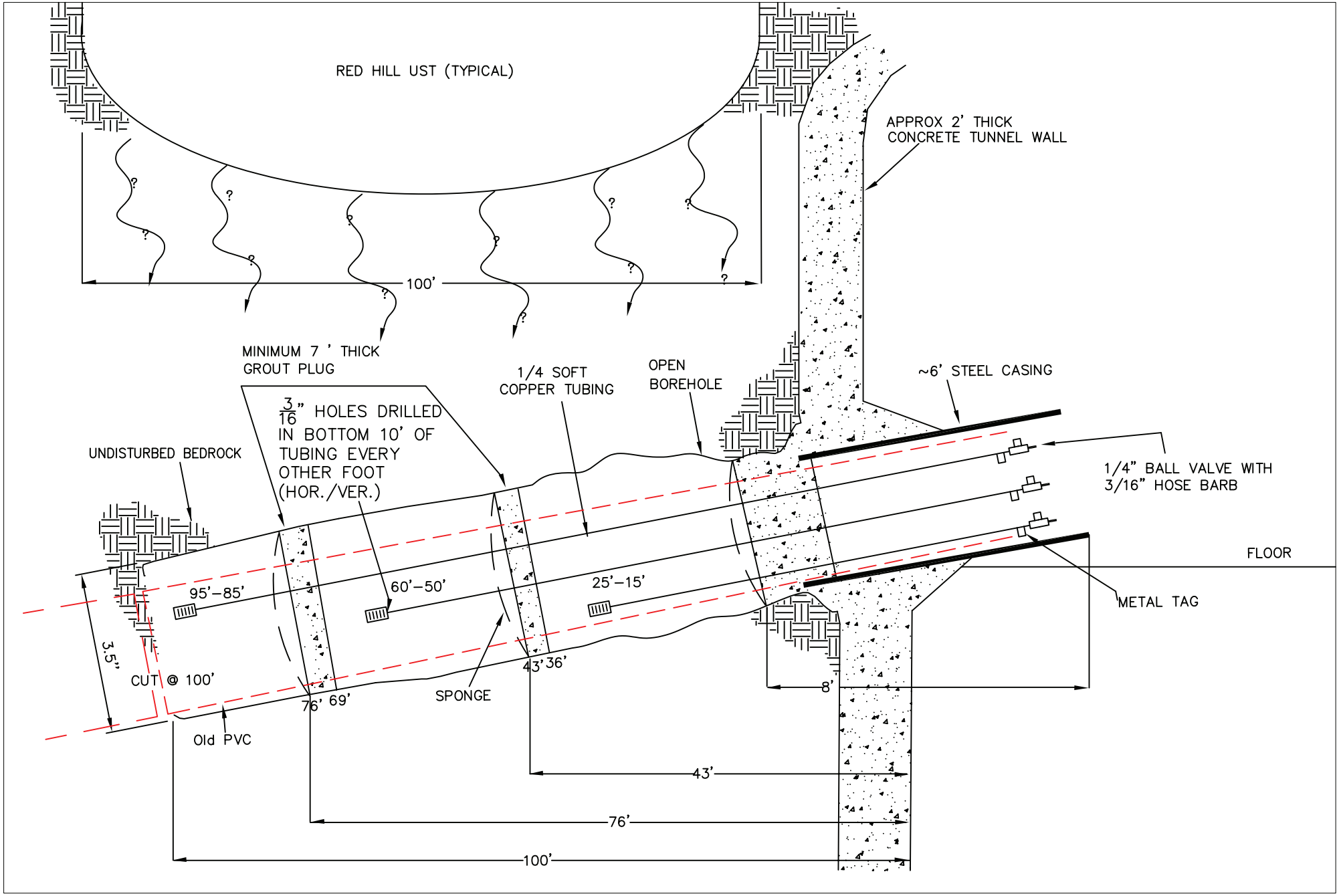

Source: DON (2007), Figure 2-2

Figure 2-8
Soil Vapor Monitoring Point Construction Details
Conceptual Site Model
Investigation and Remediation of Releases and Groundwater Protection and Evaluation
Red Hill Fuel Storage Facility
O'ahu, Hawai'i

This page intentionally left blank

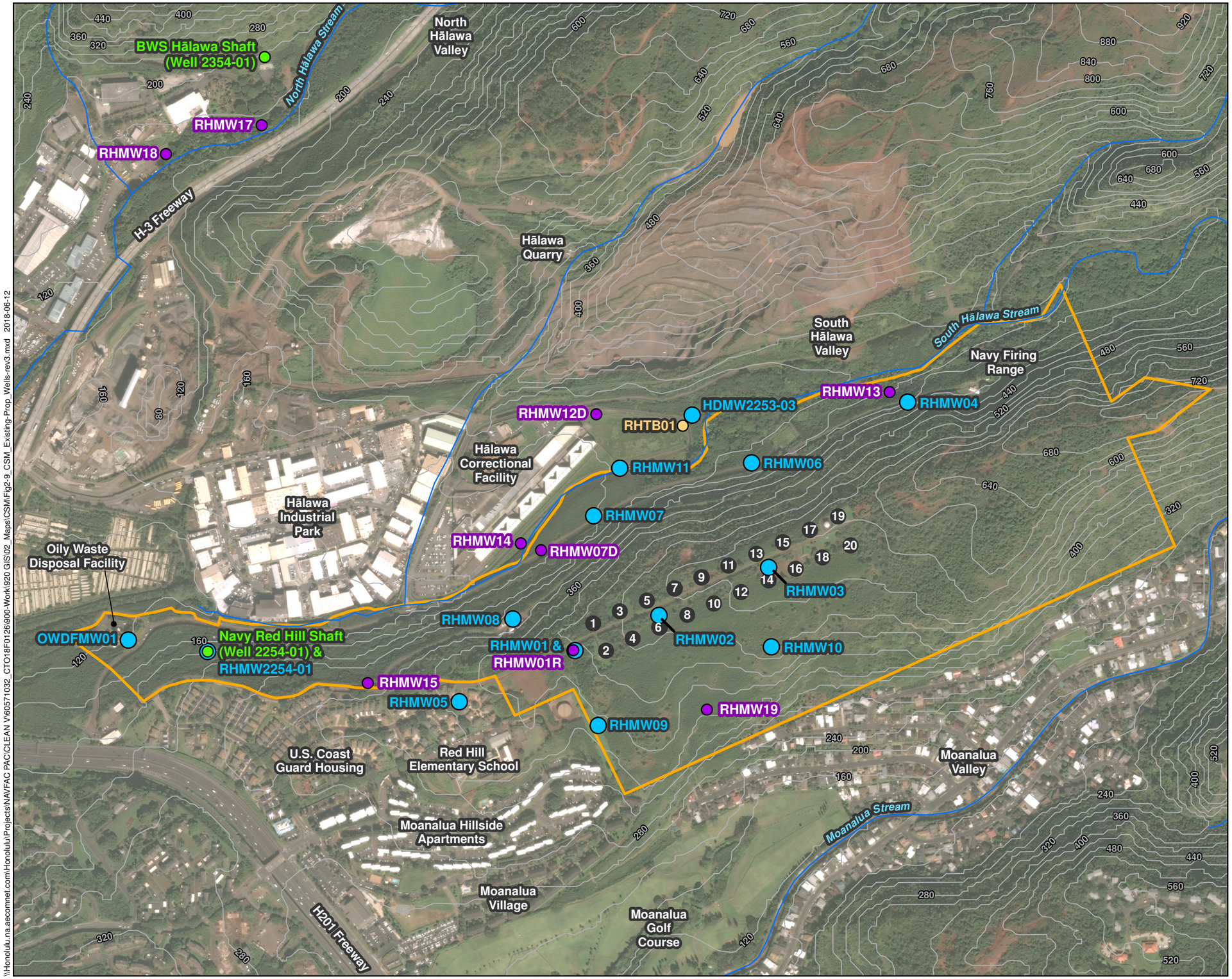

Location Map

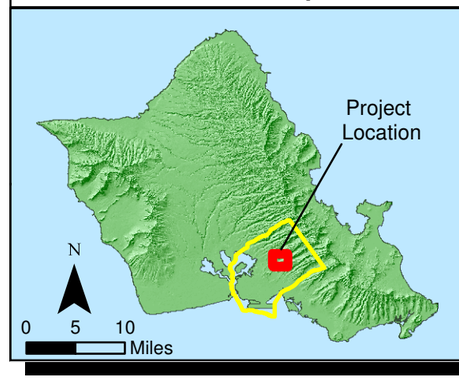

Legend

- Groundwater Monitoring Location (existing)
- Proposed Monitoring Well Location (exact location subject to change)
- Proposed Test Boring Location (exact location subject to change)
- Water Supply Well
- Stream
- Topographic Contour (feet mean sea level)
- Red Hill Facility Boundary
- Red Hill Fuel Storage Tank
- Groundwater Model Area

Notes

1. Map projection: NAD 1983 UTM Zone 4N
2. Base Map: DigitalGlobe, Inc. (DG) and NRCS. Publication_Date: 2015
3. Coordinates: NAD 1983 UTM Zone 4N

N

0 500 1,000 2,000 Feet

Figure 2-9
Existing and Proposed Groundwater Monitoring and Test Boring Locations
Conceptual Site Model
Investigation and Remediation of Releases and Groundwater Protection and Evaluation
Red Hill Bulk Fuel Storage Facility
JBPHH, O'ahu, Hawai'i

\\Honolulu.na.aecomnet.com\Honolulu\Projects\NAVFAC PAC\CLEAN V\60571032_CTO18F0126\900-Work\920 GIS\02_Maps\CSM\Fig2-9_CSM_Existing-Prop_Wells-rev3.mxd 2018-06-12

This page intentionally left blank

3. Module B: Facility Construction and Operations

As shown on Figure 1-2, the Facility's complex of 20 fuel storage tanks were constructed underground within the thick sequence of volcanic rocks that form Red Hill. The tanks are currently used to store fuel for JBPHH operations, and have provided fuel for military operations in Hawai'i and throughout the Pacific since the Facility was completed in the early 1940s. Each tank is approximately 250 ft in height and 100 ft in diameter, with a capacity of approximately 12.5 million gallons. The tanks are constructed of concrete shell lined by steel, and 18 of them are currently active. The Facility tanks extend vertically through a 250-ft-thick sequence of massive basalt layers, inter-bedded tuff deposits, and breccia zones. The Facility was declared a National Historic Civil Engineering Landmark by the American Society of Civil Engineers in 1995.

3.1 Construction and Physical Characteristics of the Facility

The tanks were constructed in two parallel rows of ten tanks, i.e., ten pairs of tanks, connected by short access tunnels to main upper and lower access tunnels that transit between the two parallel rows. These main access tunnels contain light rail systems, water and electrical facilities, and fuel pipelines. In the lower tunnel, each short access tunnel branches off from the main service tunnel and terminates at a "face-wall" under each tank. Ancillary piping extends from each face-wall to connect to fuel transmission lines that run approximately 2.5 miles from the Facility to a fuel pumping station at Pearl Harbor. The configuration of these fuel transmission lines (since the mid-2000s) is as follows (NPS 2015):

- 32-inch-diameter – Diesel Fuel-Marine (F-76)
- 18-inch-diameter – JP-5
- 16-inch-diameter – JP-8/F-24
- 16-inch-diameter between Red Hill and Pearl City – out of service, decommissioned, and abandoned in place (formerly JP-5, aviation gasoline [AVGAS], and motor gasoline [MOGAS])

The tanks are spaced 200 ft on center, separated from each other by 100 ft of igneous rock. The tops of the tanks are approximately 110–175 ft bgs, and the bottoms of the tanks are approximately 350–450 ft bgs, 123–151 ft msl (DON 2016a) and approximately 100–130 ft above the basal aquifer water table (the tanks are installed at slightly increasing elevations moving upslope; i.e., the bottoms of Tanks 1–2 are approximately 30 ft lower than Tanks 19–20).

Each tank was constructed by excavating the igneous rock formation of Red Hill to create a chamber for the tank, which was then lined with reinforced concrete and a ¼-inch-thick steel liner. The primary structure of each tank consists of an upper dome, barrel, and lower dome. The upper dome was constructed first. Rock was excavated to create a cavity for the upper dome. Steel framing and liner plates were then installed, followed by filling the cavity between the liner plates and lava rock with reinforced concrete, 4 ft thick. After the upper dome was constructed, the barrel and lower dome were excavated and the rock face was sealed with spray-applied concrete (gunite). The barrel is constructed of reinforced concrete (2.5 ft thick minimum at the top, 4 ft thick minimum at the bottom). Steel angles were cast into the concrete for installation of the steel liner. The concrete tank was lined with ¼-inch-thick steel plates, which were attached by welding to the imbedded steel, and butt welded together at all plate edges. After the barrel was constructed, it was pre-stressed by injecting grout between the reinforced concrete and lava rock. The lower dome is similarly constructed of reinforced concrete and lined with ¼-inch-thick steel plates. The floor of the lower

dome is flat and consists of ½-inch-thick steel plates (DON 2016a). During construction, all lava tubes were carefully sealed with concrete plugs to help eliminate potential preferential pathways.

The pressurized grouting procedure is further detailed in a Red Hill Facility construction report prepared by the Historic American Engineering Record (NPS 2015, p. 30):

> "*The bedrock sides of the tank excavation were coated with Gunite, approximately 6" thick, consolidating 'any loose rock to protect the workers excavating the vault and building the tank inside the vault.' The original contractors filled the joint between the reinforced-concrete shell and the Gunite on the bedrock with pressurized grout, after the concrete shell had cured. A former Supply Center Fuel Department Superintendent* [James Gammon] *provided further explanation about the purpose and steps of Gunite and grout placement:*
>
> > "*The purpose of grouting was to seal any cold joints in the reinforced concrete shell or in the gunited rock, … AND to pre-stress the tank structure with a compressive force that would counter the force of the hydrostatic pressure when the tank was filled with fuel…. [In] some areas of the vault that were not gunited during excavation [the step of] grouting would have consolidated the rock as well as sealed the joint between the rock and the reinforced concrete.*"

During the same period as tank construction, the Red Hill Shaft water development tunnel was constructed (see Section 2.11).

3.2 FUEL TYPES

Historically, types of fuel stored at the Facility have included Diesel Oil, Navy Special Fuel Oil (NSFO), Navy Distillate, F-76, AVGAS, and MOGAS. Originally, Tanks 3–20 contained NSFO and Tanks 1 and 2 stored diesel oil. Over time, each tank has been converted to store a variety of different fuel types (DON 2002). Conversion of tanks to store aviation fuel (jet fuel and AVGAS) began in the early 1960s (NPS 2015). Kerosene-based jet fuels stored at the Facility have included JP-5, JP-8, and North Atlantic Treaty Organization (NATO)-grade F-24. Based on discussions with Navy Region Hawai'i, there is no intent to store volatile fuels (such as MOGAS or AVGAS) in the future.

As indicated in Table 3-1, the fuel storage tanks currently contain JP-5, F-24, and F-76.

Table 3-1: Types of Fuel Historically and Currently Stored in the Facility's Fuel Storage Tanks

Tank ID	Date (Current Status [a])	Fuel Type	Tank ID	Date (Current Status [a])	Fuel Type
F-1	10/26/1942	Diesel Oil	**F-2**	09/28/1942	Diesel Oil
	02/04/1970	JP-5		1962	JP-5
	2006	Empty (removed from service)		early 2000s	JP-8
	Current (Inactive)	Empty		Current (Active)	F-24 Jet Fuel
F-3	01/26/1943	Navy Special Fuel Oil	**F-4**	11/15/1942	Navy Special Fuel Oil
	08/27/1970	Navy Distillate		02/17/1971	Navy Distillate
	04/03/1973	Diesel Fuel-Marine		06/06/1973	Diesel Fuel-Marine
	12/26/1973	JP-5		01/26/1974	JP-5
	early 2000s	JP-8		early 2000s	JP-8
	Current (Active)	F-24 Jet Fuel		Current (Active)	F-24 Jet Fuel

Tank ID	Date (Current Status [a])	Fuel Type
F-5	12/19/1942	Navy Special Fuel Oil
	04/06/1970	Empty
	12/29/1971	Navy Distillate
	10/1974	JP-5
	early 2000s	JP-8
	2017	F-24 Jet Fuel
	Current (Active)	Empty
F-6	12/30/1942	Navy Special Fuel Oil
	03/29/1970	Empty
	02/29/1970	Navy Distillate
	10/1974	JP-5
	01/15/1982	Diesel Fuel-Marine
	07/22/1994	Empty
	05/19/1995	JP-5
	04/15/1998	Empty
	early 2000s	JP-8
	Current (Active)	F-24 Jet Fuel
F-7	03/16/1943	Navy Special Fuel Oil
	05/04/1971	Navy Distillate
	09/11/1973	Diesel Fuel-Marine
	04/25/1995	Empty
	1996	JP-5
	Current (Active)	JP-5
F-8	03/02/1943	Navy Special Fuel Oil
	05/21/1971	Navy Distillate
	09/12/1973	Diesel Fuel-Marine
	04/13/1995	Empty
	1996	JP-5
	Current (Active)	JP-5
F-9	02/14/1943	Navy Special Fuel Oil
	06/23/1972	Navy Distillate
	09/13/1973	Diesel Fuel-Marine
	09/14/1959	Empty
	05/30/1996	JP-5
	Current (Active)	JP-5
F-10	01/26/1943	Navy Special Fuel Oil
	06/29/1972	Navy Distillate
	09/01/1973	Diesel Fuel-Marine
	10/03/1995	Empty
	1996	JP-5
	Current (Active)	JP-5
F-11	02/11/1943	Navy Special Fuel Oil
	06/29/1972	Navy Distillate
	10/1973	Diesel Fuel-Marine
	late 1990s	JP-5
	Current (Active)	JP-5
F-12	03/19/1943	Navy Special Fuel Oil
	04/28/1970	Empty
	05/26/1972	Navy Distillate
	01/29/1981	Diesel Fuel-Marine
	08/24/1994	Empty
	07/25/1995	Diesel Fuel-Marine
	late 1990s	JP-5
	Current (Active)	JP-5
F-13	03/23/1943	Navy Special Fuel Oil
	04/21/1976	Diesel Fuel-Marine
	12/01/1994	Empty
	10/04/1995	JP-5
	2000	Diesel Fuel-Marine
	Current (Active)	JP-5
F-14	03/21/1943	Navy Special Fuel Oil
	03/13/1973	Navy Distillate
	10/25/1973	Navy Special Fuel Oil
	08/26/1975	Navy Distillate
	04/12/1981	Diesel Fuel-Marine
	01/19/1995	Empty
	04/29/1996	JP-5
	2000	Diesel Fuel-Marine
	Current (Active)	JP-5

Tank ID	Date (Current Status [a])	Fuel Type	Tank ID	Date (Current Status [a])	Fuel Type
F-15	04/29/1943	Navy Special Fuel Oil	**F-16**	05/08/1943	Navy Special Fuel Oil
	10/27/1972	Navy Distillate		11/10/1971	Navy Distillate
	09/14/1973	Diesel Fuel-Marine		06/15/1975	Diesel Fuel-Marine
	10/02/1998	Empty		05/25/1994	Empty
	1998	Diesel Fuel-Marine		10/01/1998	JP-5
				11/04/1998	Empty
				1998	Diesel Fuel-Marine
	Current (Active)	F-76 Diesel Fuel-Marine		Current (Active)	F-76 Diesel Fuel-Marine
F-17	5/23/1943	Navy Special Fuel Oil	**F-18**	06/13/1942	Navy Special Fuel Oil
	03/30/1960	Empty		03/30/1960	Empty
	12/11/1964	AVGAS		05/1963	JP-5 (for leak tests)
	08/29/1968	MOGAS		08/18/1964	AVGAS
	01/15/1969	JP-5		10/30/1968	Empty
				01/10/1969	JP-5
	Current (Active)	Empty		Current (Active)	JP-5
F-19	06/13/1943	Navy Special Fuel Oil	**F-20**	07/20/1943	Navy Special Fuel Oil
	03/30/1960	Empty		03/30/1960	Empty
	01/17/1964	JP-5		06/14/1964	JP-5
	10/1985	Empty		12/28/1971	Empty
	2007	Empty (removed from service)		04/04/1972	JP-5
	Current (Inactive)	Empty		Current (Active)	JP-5

Source: DON (2005), Red Hill Groundwater LTM reports (DON 2018e). Current status as of June 2018.
[a] Active status indicates a tank is currently available for use, but does not necessarily indicate the tank is currently filled. Inactive status indicates a tank is currently not available for use.

3.3 UNCERTAINTY ANALYSIS

As noted in Section 3.2, the Navy has no plans to alter the types of fuels stored at the Facility. Issues related to tank integrity and upgrade alternatives are being addressed by other sections of the AOC Statement of Work (EPA Region 9 and DOH 2015).

3.4 ADDRESSING UNCERTAINTIES

Future activities relevant to Facility construction and operation are being addressed by other sections of the AOC Statement of Work (EPA Region 9 and DOH 2015): Section 2 Tank Inspection, Repair, and Maintenance (TIRM); Section 3 Tank Upgrade Alternatives (TUA); Section 4 Release Detection / Tank Tightness Testing; Section 5 Corrosion and Metal Fatigues Practices; and Section 8 Risk/Vulnerability Assessment.

4. Module C: LNAPL Release and Source-Zone Migration Model

This module provides appropriate models for evaluating possible release scenarios. Understanding how fuel could leak and migrate into the surrounding rock formations from the 2014 Tank 5 release can provide insights on how fuel that may be released at other tanks within the tank farm could migrate in the source-zone area. The release and migration model presented below includes specific detail about the causes of the Tank 5 release in January 2014 and assessment of potential migration pathways intrinsic to the construction of the tanks and surrounding facilities; it includes:

- Previous investigations and the Red Hill LTM network
- Location of possible release point(s) within the tank based on construction, measurements, and observations
- Possible locations and means that leaking fuel could enter the surrounding rock formation

Migration pathways for fuel/LNAPL from the tank source to the surrounding rock formation were assessed by reviewing the following:

- Tank designs and plans
- Construction "as built" plans
- Documented construction practices
- Modifications and upgrades
- Documented leaks in and around the Red Hill tank farm

4.1 Summary of Previous Investigations and Environmental Actions

Previous environmental investigations at the Facility since 1998 are summarized in Table 4-1.

Table 4-1: Summary of Previous Red Hill Investigations

Investigation	Summary	COPCs and Other Parameters Investigated
Facility Site Characterization and Investigation (DON 1999, 2002)	A two-phase investigation was initiated in 1998 to evaluate presence of petroleum constituents. The investigation included drilling and sampling of slant borings under all 20 Facility tanks and two vertical borings within the lower access tunnel west of the tanks; installation and sampling of one groundwater monitoring well (now named RHMW01); and a screening-level risk assessment. Results indicated that petroleum had been released from several Facility tanks, as observed in core samples and indicated by the groundwater data. The Phase II report recommended a comprehensive assessment of human health risks potentially associated with the Facility. The DOH Solid Waste Branch requested that quarterly groundwater monitoring be conducted, a Tier 3 risk assessment be conducted to evaluate the risk to Red Hill Shaft (Navy Supply Well 2254-01), and a contingency plan be developed to protect the well from future contamination.	TPH-g, TPH-d, TPH-o, TPH-kerosene, VOCs, PAHs, SVOCs, and hydrocarbon fingerprint

Investigation	Summary	COPCs and Other Parameters Investigated
Technical Report (DON 2007)	An environmental investigation and risk assessment initiated in 2004 included installation of SVM points in angle borings drilled under the Facility tanks and three groundwater monitoring wells (RHMW02, RHMW03, and RHMW04) in the lower tunnel. Rock core, groundwater, and soil vapor samples were collected and analyzed; a three-dimensional groundwater model was developed to simulate CF&T; and a Tier 3 human health risk assessment was conducted. The risk assessment found the primary potential risk to be from a hypothetical future scenario where groundwater beneath the tank farm was extracted for residential tapwater use. The CF&T modeling estimated the quantity, time, and distance a release of JP-5 fuel would result in benzene exceeding federal and state criteria at the Red Hill Shaft water supply well. The report recommended developing mitigation steps for a contingency plan, which was subsequently developed as the Red Hill GWPP (DON 2008b).	VOCs, alkalinity, fixed gases, metals, anions, MADEP VPH/EPH fractions, TPH-g, TPH-d, TPH-o, and percent solids
Tank 17 Removal Action Report (DON 2008c)	A limited removal action and site characterization investigation was conducted in June 2008 after approximately 4 gallons of JP-5 fuel were released from overhead piping in the Facility. Following the removal action, the report's Environmental Hazard Analysis determined that the release posed no further significant environmental hazards.	TPH-g, TPH-d, VOCs, PAHs, and flashpoint
Type 1 Letter Report (DON 2010)	After a reported TPH-d concentration in an October 2008 groundwater sample from RHMW02 exceeded the SSRBL, an investigation was conducted to provide a report to DOH in accordance with the Red Hill GWPP (DON 2008b). The 2010 investigation re-evaluated the DON (DON 2007) groundwater model assumptions/results and the Tier 3 risk assessment results. The re-evaluation of the 2007 groundwater model found local groundwater flow direction to be from the tank farm toward Red Hill Shaft, and a regional component flowing toward the northwest. The re-evaluation of the 2007 risk assessment found that its conclusions remained valid. An additional groundwater monitoring well (RHMW05) was installed west of the tank farm and added to the Red Hill groundwater monitoring network.	TPH-g, TPH-d, VOCs, MADEP VPH/EPH fractions, PAHs, and lead

CF&T contaminant fate and transport
EPH extractable petroleum hydrocarbon
MADEP Massachusetts Department of Environmental Protection
PAH polynuclear aromatic hydrocarbon
SSRBL site-specific risk-based level
SVOC semivolatile organic compound
TPH-d TPH-diesel range organics
TPH-g TPH-gasoline range organics
TPH-o TPH-residual range organics (i.e., TPH-oil)
VOC volatile organic compound
VPH volatile petroleum hydrocarbon

A summary of all key environmental actions and milestones is provided on Figure 4-1.

A chronological listing of regulatory issues and submitted documents regarding Facility tank petroleum releases, as of August 21, 2014, is presented in Appendix A of the 2014 *Interim Update* to the Red Hill GWPP (DON 2014b).

4.2 HISTORY OF JANUARY 2014 JP-8 RELEASE FROM TANK NO. 5

During Tank 5 refilling operations, a fuel release was discovered and verbally reported to DOH on January 13, 2014. A release of JP-8 from Tank 5 was confirmed and reported to DOH in writing on January 23, 2014. The volume of fuel lost from Tank 5 was estimated at 27,000 gallons. The following timeline of the 2014 release was compiled from the AOC Section 2.2 *Tank Inspection, Repair, and Maintenance* (TIRM) *Report* (NAVFAC EXWC 2016), the Tank 5 *Initial Release*

Response Report (DON 2014a), and the Navy's Energy & Environmental Magazine *Currents* (Isobe 2016):

- Following a 3-year inspection and refurbishment completed in accordance with a process conducted every 20 years, Tank 5 was placed back into service on December 9, 2013, and the Navy commenced filling it with JP-8 fuel.
- Alarms were activated when initially filling Tank 5 following the tank refurbishment.
- Operators observed an unscheduled fuel movement on January 11, 2014 and confirmed a 3/16-inch drop in fuel with manual gauges by January 13, 2014. Product from Tank 5 was drained.
- A fuel hydrocarbon seep was observed below Tank 5 on the evening of January 12, 2014 in the lower cross tunnel wall near the exterior of the material encasing the lower part of the tank. A sample showed that the liquid was JP-8 fuel.
- The SVM points under Tank 5 exhibited a sharp increase in hydrocarbon vapor concentrations from previously measured December 15, 2013 levels, and concentrations also increased significantly in nearby SVM points at Tanks 3, 6, 7, 8, and 9 (see Section 4.4).
- Subsequent analysis indicated faulty work by a contractor, specifically:
  - Defective workmanship in welding by the contractor was found in Tank 5.
  - Defective welds had not been discovered and corrected by the contractor due to poor inspection and ineffective quality control.
  - Seventeen unrepaired ¼-inch gas test holes drilled through the tank shell were found. These, along with defective welds on patch plates that covered the gas test holes, were deemed the underlying cause of the release. As noted in the TIRM Report (NAVFAC EXWC 2016), "*When Tank 5 was filled with fuel, the typical leak path was through defects in the seal weld, through the joint between a patch plate and the tank shell, and through the gas test hole*" (Section 9-2.1.4).

4.3 CONSTRUCTION PRACTICES AND MATERIALS

Review of Red Hill construction practices and "as-built" plans indicate potential migration pathways related to the practices and materials used.

The AOC Section 2.2 TIRM Report (NAVFAC EXWC 2016) indicates that "*Areas of* [Tank 5's] *internal steel liner appear to have separated from the concrete encasement surrounding the tank. This condition can allow water, fuel, liquid or vapor, to be trapped in a localized area between the two surfaces*" (TIRM Report Appendix AN, Section 2.1; 10/3/2014). The purpose of the gas test holes drilled in the tank shell was to "*sample for hydrocarbon vapor due to fuel which may have been in the tank shell to concrete interstice"* (TIRM Report Chapter 5-6.1), which is an industry-standard safety requirement prior to conducting welding activities "*…since hydrocarbons have been found in contact with the back wall surfaces in the past tanks*" (contractor's 2010 pre-refurbishment Tank 5 Inspection Report; TIRM Report Appendix T, Table 7-1, Note 3). In addition, the AOC Statement of Work Section 3.2 TUA *Scope of Work* (DON 2016a) notes that typical historical structural and integrity issues with the Red Hill fuel storage tanks relevant to repairing them for a future use include "*corrosion and pitting,*" "*holes in the steel liner,*" and "*defective welds in the barrel and upper and lower domes*" (TUA Scope of Work, Section 2.3).

The following summary of the design, construction, and modification of the tanks' tell-tale system

from a Red Hill construction report published by the Historic American Engineering Record can provide insight to potential leak points (NPS 2015):

- The original tell-tale leak-detection system consisted of a series of 12 vertical pipes, equally spaced around the perimeter of each tank.
- The pipes ran vertically down the inside tank wall, penetrated the lower dome, ran through the concrete plug under the tank, and ended at a monitoring station in the lower access cross tunnel near the skin valves for each tank.
- Tell-tale pipes were designed to collect any fuel that leaked through a hole in a shell plate (or through a hole in a shell-plate weld):
  - Fuel leaks to the space between the back side of the steel shell plates and the inner side of the reinforced concrete wall.
  - The tell-tale pipe would then deliver the collected fuel to the lower access cross tunnel, to indicate the presence of a leak.
  - During service intervals, the tell-tale pipes at or near the bottom of the tanks experienced significant corrosion on the external surfaces of the piping due to salt water in the bottom of the tanks (tanker ships that formerly delivered refined fuel to Pearl Harbor would intake seawater into vents in the cargo tanks during heavy weather, and the salt water was offloaded along with the fuel). Many tell-tale leak indications were found to be false due to holes corroded through the telltale piping itself (TIRM Report, Chapter 1-3.2) (NAVFAC EXWC 2016).
- During 1960–1963, the tell-tales in Tanks 17–20 were modified and improved:
  - The pipe diameter was increased to prevent clogging, and the pipe wall thickness was increased to Schedule 80, to provide corrosion allowance.
  - Tank 19 retains these tell-tale pipe improvements from the 1960–1963 period. It is not known if any of the improved tell-tales remain in Tanks 17, 18, or 20.
- During 1971–1973, two additional improvements to the tell-tale design were installed in Tanks 5, 6, and 12:
  - The pipes up into the Gauging Gallery at the top of the tank were extended to where they could be readily accessed for flushing and cleaning.
  - The exit point of the tell-tale pipes was relocated by routing through the side of the hemispherical lower tank section above the previous bottom exit point, so they would not be exposed to the corrosive effect of the tank bottom water.
- A 1977 design decision (MILCON P-060) removed the tell-tale systems from Tanks 1–16 altogether. Removal of the tell-tale systems created two problems:
  - It removed a tool for potentially identifying and locating fuel leaks.
  - It eliminated a way to drain off any rainwater that percolates down through the lava rock and finds its way into the space between the back side of the steel shell plates and the inner side of the concrete wall. The standing water could cause accelerated corrosion of the back side of the steel shell plate.

  Hundreds of small steel plates are welded to the tank walls to cover small holes through the liner plates that remained when the tell-tale pipes were removed under Project P-060.

4.3.1 Bottom Drain

The bottom drain pipe originally installed in each tank has been identified as a source of possible leaks: "*As the 8-inch-diameter pipe 'daylights' through the concrete wall at the end of the LAT* [lower access tunnel] *cross tunnel, it connected to a manually operated 8-inch gate valve, the skin valve. Due to the constant exposure to tank bottom water, holes corroded through the pipe walls of several of the bottom drain pipes; these rusted pipes were removed from service*" (NPS 2015, p. 34).

4.3.2 Tunnel Floor Pipe Bedding and Sumps

Lower tunnels could have potential migration pathways for LNAPL migration through the following:

- Contraction of the gunite during curing could create space between the gunite and rock formations around the tunnel exterior.
- Sumps, vent lines, grates, and drains.

4.4 POST-2014-RELEASE MONITORING RESULTS

Soil Vapor. Following the 2014 release, soil hydrocarbon vapor levels were collected from the three-point SVM system under the tanks. Concentrations under Tank 5 measured on December 23, 2013 and on January 15, 2014 increased as follows: from 50 to 96 ppbv (shallow), from 622 to 225,000 ppbv (middle), and from 794 to 204,000 ppbv (deep). The high concentration of 225,000 ppbv measured on January 15, 2014 initially decreased to 100,000 ppbv on February 24, 2014, but later increased even higher to 450,000 ppbv on May 1, 2014 (see Figure 4-2). This suggests that Tank 5 releases may have occurred along multiple migration pathways to the tank bottom, with some pathways taking longer than others. This concept would be consistent with the forensic analysis of the release from multiple release locations via gas test holes as the primary cause of the release, as described above in Section 4.2 (NAVFAC EXWC 2016).

Vapor concentrations also increased over pre-January 2014 conditions in nearby SVM points at Tanks 3, 6, 7, 8, and 9 but generally exhibited average vapor concentrations less than 10 percent of the Tank 5 vapor concentration over the next year (Figure 4-2, lower panel). The detection of the Tank 5 release in a large number of SVM points indicates that the existing SVM point network provides a robust system for detection of this type of release. There were also less-significant responses in tanks as distant as Tank 15 to the north during vapor monitoring on January 30, 2014. The vapor sampling points for the tanks around the Tank 5 release are located at elevations between ~80 and ~110 ft msl, are well under the elevation of the release (~180–250 ft msl), and below the elevation of the bottom of Tank 5 (~115 ft msl). Thus, some combination of lateral/downward LNAPL migration and diffusion/advective vapor migration could explain the migration of vapors from the Tank 5 release to the SVM points under the nearby tanks. The low vapor pressure of the jet fuel constituents will likely preclude any density-driven migration of jet fuel vapors.

Groundwater. Following the 2014 release, water samples were collected from drinking water supply wells Navy Red Hill Shaft, BWS Hālawa Shaft, Hālawa Wells, 'Aiea Wells, 'Aiea Gulch Wells, and Moanalua Wells. Test results indicated that no petroleum constituents had reached the groundwater drinking water supply wells in the months following the release (RHSF Task Force 2014).

Cumulative concentration graphs of Red Hill groundwater monitoring results for current COPCs dating from 2005 onward are presented in Appendix A (and further discussed in Section 7.2); the date of the 2014 release is indicated on the graphs. The graphs, current as of the First Quarter 2018 monitoring event (DON 2018e), show that exceedances of screening criteria (DOH Tier 1

Environmental Action Levels [EALs]) for total petroleum hydrocarbons (TPH) and/or naphthalenes have occurred in the monitoring wells closest to the tanks (RHMW01, RHMW02, and RHMW03) both before and after the 2014 Tank 5 release. No confirmed floating free product has been measured at any monitoring location, and no exceedances of the COPC screening criteria have been observed at sampling point RHMW2254-01 adjacent to Red Hill Shaft (Navy Supply Well 2254-01). Further discussion of dissolved-phase COPCs detected in groundwater is presented in Section 7.2.

Since the 2014 release, six additional groundwater monitoring wells to date have been added to the Red Hill network.

4.5 2014 RELEASE CONCEPTUAL MODEL

Release Point:

- Multiple breaches in the wall of Tank 5 into the space between the back side of the steel shell plates and the inner side of the reinforced concrete.
- 17 unrepaired gas test holes through the tank shell were found and were deemed the underlying cause of the release.
- Defective workmanship in welding by the contractor was found in Tank 5.
- Corrosion and pitting in interior and exterior steel tank wall.
- Multiple migration pathways from different areas, some taking different and possibly longer routes.

Release Point LOEs:

- Results of forensic analysis of the release as detailed in (NAVFAC EXWC 2016).
- Historical observations of space between the back side of the steel shell plates and the inner side of the reinforced concrete (NAVFAC EXWC 2016).
- Areas of weakness or corrosion potential such as the bottom drain pipe, tell-tale pipe penetrations (NAVFAC EXWC 2016).

Migration Pathways:

- LNAPL migrates down along the space between the back side of the steel shell plates and the inner side of the reinforced concrete to lower tank bottom.
- Some LNAPL may potentially exit into cracks in the concrete shell into higher-permeability rock types surrounding the concrete or to space between the inner side of the reinforced concrete and outer gunite-covered rock formations.
- Contraction of the gunite after curing could create space between the gunite and rock formations around the tunnel exterior.
- Potential damage to concrete and gunite associated with tank metal plate reinforcement.
- Sumps, vent lines, grates, and drains.

Migration Pathway LOEs:

- Construction design supports potential development due to cold joints, contraction, and cracking in the concrete and gunite.
- Historical observations of space between the back side of the steel shell plates and the inner side of the reinforced concrete (NAVFAC EXWC 2016).
- Appearance of a fuel hydrocarbon seep observed below Tank 5 on the evening of January 12, 2014 in the lower cross tunnel wall near the exterior of the material encasing the lower part of Tank 5.
- Monitored results of increasing soil vapor levels directly below and adjacent to Tank 5.

4.6 UNCERTAINTY ANALYSIS

Migration of the 2014 JP-8 release down along the space between the back side of the steel liner plates and the inner side of the reinforced concrete to lower tank bottom has not been verified but is based on strong evidence (e.g., historical construction documentation, forensic studies, and observation of leaking fuel near the bottom of the Tank 5 tunnel wall). Other suspected release points from corrosion and pitting in the interior and exterior steel tank wall have not been verified. Other suspected migration routes including migration to permeable rock formations outside the gunite/concrete wall, around tunnel linings, and through grates, drains, vent lines, or sumps have not been verified.

Soil vapor result uncertainties arise from the period frequency of sampling during and following the 2014 release, and from the fact that most vapor measurements have been collected with a PID that yields aggregate hydrocarbon results.

4.7 ADDRESSING UNCERTAINTIES

The following ongoing, planned, or proposed activities are designed to help resolve the uncertainties described in Section 4.6.

Vertical temperature profiles have been measured in key monitoring wells. Because LNAPL biodegradation releases heat, increases in temperature over background conditions are being used to indicate the vertical distribution of LNAPL beneath selected tanks at the Facility.

A statistical LNAPL holding model is now being used to better understand how LNAPL releases migrate through the subsurface and to estimate the amount of LNAPL that can be retained in the release area underlying the Red Hill tank farm without causing unacceptable risks to nearby receptors. Information regarding the 2014 LNAPL release at Tank 5 is being used to help improve the reliability of the holding capacity estimate.

NAP data, particularly dissolved oxygen (DO) and dissolved methane in groundwater and in the SVM points, have been collected and are being used to better understand where LNAPL biodegradation is occurring.

The lack of sheens in the Facility monitoring wells is being used to help constrain the location of any saturated zone LNAPL lenses at the Facility.

The planned infiltration study (DON 2017g) will help determine if the observed mass discharge in groundwater can originate from LNAPL present in the unsaturated zone alone, or if LNAPL is likely present at the water table in the saturated zone.

Carbon traps were deployed on Red Hill and inside the Facility tunnels to measure hydrocarbon-based carbon dioxide efflux to the surface and through the tunnel system. These data, along with thermal NSZD temperature measurements, are now being used to calculate the NSZD rate at the Facility. The NSZD rate will be used to estimate the chronic release rate of fuel that will not result in unacceptable risk to nearby receptors.

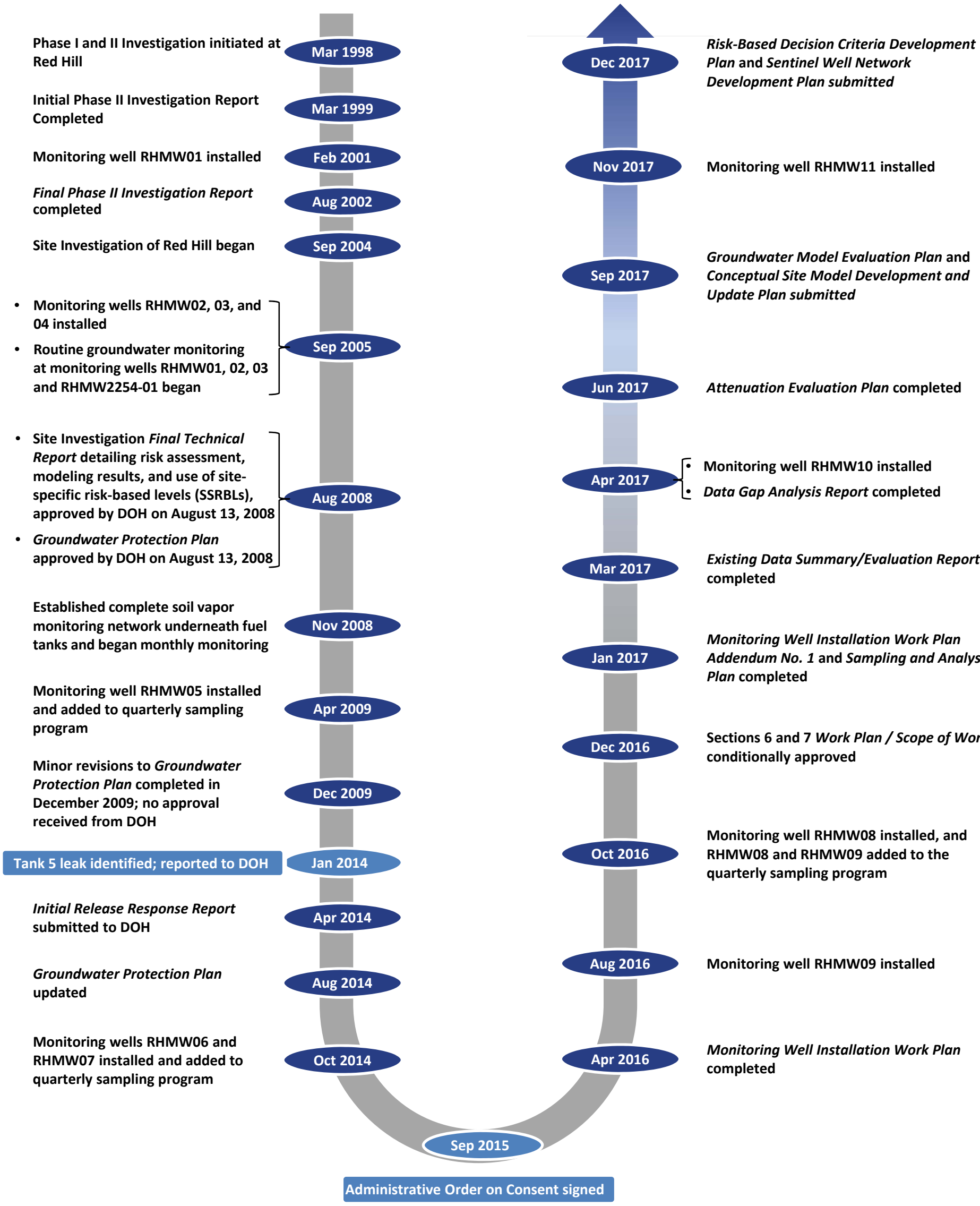

Figure 4-1
Summary of Environmental Actions at Red Hill
Conceptual Site Model
Investigation and Remediation of Releases and Groundwater Protection and Evaluation
Red Hill Bulk Fuel Storage Facility, JBPHH, O'ahu, Hawai'i

This page intentionally left blank

Linear Scale Graph of Monthly PID Monitoring Results for Below Fuel Tank Soil Vapor Wells:

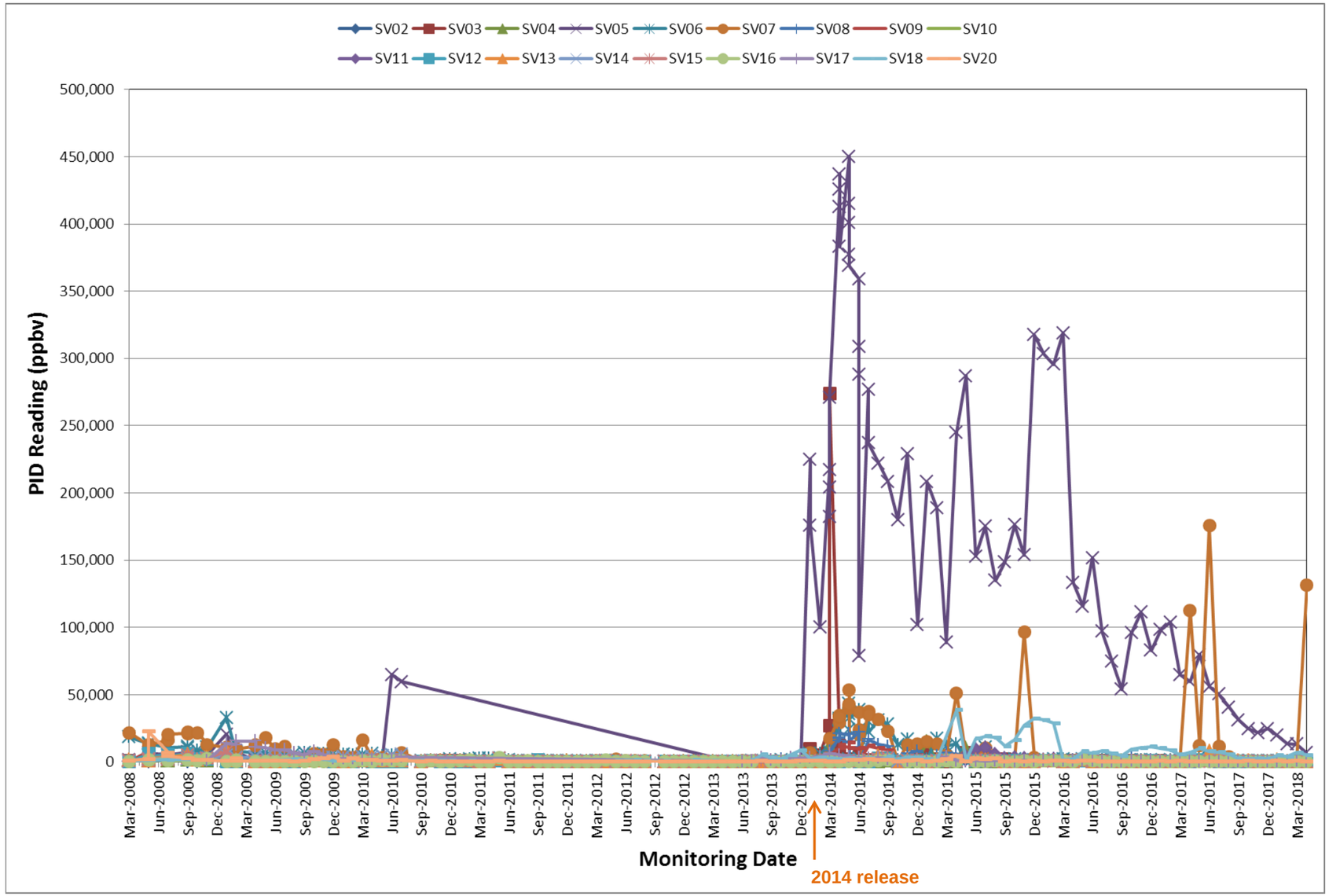

Average Yearly Total Organic Soil Vapor Concentrations by Tank, 2013 and 2014:

Tank Farm	1	3	5	7	9	11	13	15	17	19
	2	4	6	8	10	12	14	16	18	20
2013		158	203	310	156	172	132	153	1,733	
	188	188	507	226	177	128	135	127	1,328	263
2014		7,093	200,938	19,400	5,577	926	992	750	2,603	
	328	1,125	16,048	9,503	1,941	704	573	352	2,377	942

Parts per Billion by Volume

	No Data	7	5,001 - 10,000
1	< 50	8	10,001 - 20,000
2	51 - 100	9	20,001 - 50,000
3	101 - 500	10	50,001 - 100,000
4	501 - 1,000	11	100,001 - 200,000
5	1,001 - 2,000	12	200,001 - 450,000
6	2,001 - 5,000		

Figure 4-2
Soil Vapor Measurements Prior to and Following 2014 Release
Conceptual Site Model
Investigation and Remediation of Releases and Groundwater Protection and Evaluation
Red Hill Bulk Fuel Storage Facility, JBPHH, O'ahu, Hawai'i

This page intentionally left blank

5. Module D: Vadose Zone Model

The Facility tanks are surrounded by rock in the vadose (i.e., unsaturated) zone, which consists primarily of layered basalt. Although fuel was likely released into the vadose zone as a result of the January 2014 Tank 5 release, LNAPL has not been measured in any of the monitoring wells beneath the Facility or water supply wells in the area. As fuel migrates through the vadose zone, several processes redistribute and/or degrade the contaminant mass:

- *Volatilization:* Fuel releases undergo evaporative weathering by losing volatile compounds to gas-filled pore space in the vadose zone.
- *Capillary Forces:* As the LNAPL migrates through the vadose zone, some of the LNAPL mass is retained within the basalt matrix by surface tension and capillarity. The retention capacity of the vadose zone basalt is influenced by a number of factors including the characteristics of the basalt (discussed in detail within this section), the viscosity of the LNAPL, and the presence or absence of other liquids such as water. Weathering or dissolution of LNAPL in the vadose zone could also impact viscosity and LNAPL retention.
- *Dissolution:* Compounds in fuels transfer from the LNAPL into pore water that contacts the fuel.
- *Microbial degradation:* Indigenous microbial populations degrade petroleum fuels under both aerobic and anaerobic conditions.

The following subsections describe elements that may influence the migration and fate of LNAPL both at a macro-scale (Section 5.1) (i.e., geometry of geologic units, laterally continuous layers of high and low permeability, barriers) and at a micro-scale (Section 5.2) (i.e., microbial degradation, LNAPL mobility in various rock types).

5.1 MACRO-SCALE GEOLOGIC FEATURES

In the Facility area, the vadose zone surrounding the fuel tanks is heterogeneous and composed of a series of alternating layers of basalt flows that vary from high to extremely low permeability. The spatial distribution of the interconnected pore space (effective porosity) is complex and controls the migration pathways. Geologic logs and data from existing reports, new wells, and geologic mapping have been used to better define the permeable pathways of higher effective porosity, as well as low-permeability barriers to LNAPL movement.

Basalt flow layers are also present below the groundwater table in the Facility area. Information in geologic logs has been used to assess the nature and extent of low-permeability dense basalt layers, as well as high-permeability clinker zones and interflow voids between thin pāhoehoe lava flows and discontinuous, intraflow fractures that may create preferred flow pathways for groundwater and LNAPL movement in the Facility source area.

Geologic mapping and correlation of borehole geologic logs have better defined the strike and dip of the lava flows and presence of interbedded clinker units. Information from barrel logs prepared during tank construction (DON 1943) was also used to develop geologic cross sections of the tank area. These logs describe the excavated surface of the cylindrical spaces mined for the tanks and are relatively coarse descriptions. Relative to boring log information, the barrel logs provide less detail and indicate significantly thicker sections of clinker when compared to logs from nearby borings at Red Hill. As such, there are limitations to the use of data from the barrel logs. The porosity and permeability of each different geologic unit is estimated based on the geologic descriptions from the barrel logs, boring logs, and published reports from other hydrogeology investigations of the basalt.

This information was evaluated to better define the thickness and locations of permeable layers or zones, then used to estimate likely directions and locations where LNAPL could migrate if released from a tank.

In the neighboring valleys, alluvium (valley fill) is present near the ground surface. Below the alluvium, intense weathering of basaltic rocks reduces the permeability of the parent rock by altering igneous minerals to clays and oxides (saprolite). These valley fills and underlying saprolitic formations can influence groundwater flow and contaminant transport. Site-specific saprolite identification, based on data available to date, is detailed below.

5.1.1 Lava Flows

As described by Macdonald's (1941) report on the geology of the Red Hill and Waimalu Areas, O'ahu, "*The lava flows form sheets 3 to 50 feet thick, with very irregular tops and bottoms, sloping gently southwestward. Many of them thin toward the southwest. The lavas moved down the slope toward the southwest as relatively narrow streams. Their continuity along the ridge at Red Hill is therefore greater than across the ridge.*"

Hunt Jr. (1996) describes that "*Wentworth and Macdonald (1953) listed measurements for 22 historical flows on Mauna Loa and Kilauea on the island of Hawaii, which presumably are typical of flows on Oahu as well. The flows on Hawaii average about 15 miles in length and about one-half mile in width.*" Given that the distance from the NW Rift Zone of Ko'olau volcano to Red Hill is approximately 8 miles, a'ā lava flow core widths could be significantly less than one-half mile wide; potentially hundreds of feet wide.

According to Macdonald (1941), many flows thicken or thin rapidly across the ridge, and some pinch out altogether at Red Hill. This implies the existence of relatively narrow flows. If clinker bridges are present, they would be pathways for lateral and vertical flow at the edges of a lava flow, but limited in areal extent perpendicular to lava flow direction.

Lava flows are controlled by topography and follow natural drainage patterns. Recent (May 2018) thermal imagery of the flows occurring in the eastern region of Hawai'i Island show that flows do meander typically at 30–45 degrees relative to the baseline flow direction (fall line). Because lava tubes occur in pāhoehoe lava, and are generally oriented along the axis of flow within individual beds, it is unlikely that continuous lava tubes would exist between Red Hill Shaft and Hālawa Shaft, as the orientation of such a tube would be oriented transverse to the lava flow axis, and would have to remain open in subsequently weathered basalt (e.g., saprolite). If the meander (in the lava flow) were fed by a lava tube, this would imply that the lava tube would need to exceed 1 mile approximately perpendicular to the axis of the flow to intercept Hālawa Shaft. Such a lava tube would also need to dip at a very shallow angle in order to continuously intercept the upper portions of the regional basal aquifer water table, which is unlikely. An angle of less than 1 degree would be required to create a hydraulic connection via a lava tube between Red Hill and Hālawa Shaft, near the water table. This dip and orientation of a lava tube is inconsistent with conditions reported and observed in the Hawaiian islands. True dip in the vicinity of Red Hill has been measured at angles of 10–12 degrees, with a strike of 190–205 degrees. Hālawa Shaft is oriented at approximately 305 degrees from the Red Hill Facility. This conceptual lava tube would also have to stay open and competent long after the lava flow had ended. Fresh lava tubes sometimes collapse following drainage of lava from the tube and cooling. Relict lava tubes in saprolite, such as what is observed in South Hālawa Valley, as well as North Hālawa valley, are expected to collapse and/or become infilled (D. Thomas, University of Hawai'i [UH] Hilo and DOH, pers. comm. 2018).

Macdonald (1941) writes: "*The pahoehoe flows are fed by lava moving through tubes in the interior of the flow, most of them only a foot or two across but a few reaching diameters of tens of feet. Sometimes the liquid lava drains away from these tubes leaving them partly or entirely empty.*" In highly weathered basalt and saprolite sequences, such as those found below valley fill deposits in South Hālawa Valley, lava tube structures, if they were present, would generally fail and collapse. Based on the drilling of thousands of feet through similar volcanic materials on the island of Hawai'i, the occurrence of lava tubes was described as "rare" (D. Thomas, UH Hilo and DOH, pers. comm. 2018).

Lava tubes are constrained by the width of the lava flow they are contained within. With that, it is highly unlikely that there may be lava tubes from Red Hill area that would provide a conduit or pathway toward Hālawa Shaft (i.e., the unlikely geometry that would allow a lava tube somewhere near the water table under the Red Hill facility to be oriented all the way across (under or around) the saprolite in modern day North and South Hālawa Valleys, and then extend all the way to Hālawa Shaft).

5.1.2 Geologic Cross Sections

Geologic cross sections have been prepared from available geologic logs of rock cores and from field mapping (Figure 5-1 through Figure 5-9). Geologic logs from the Red Hill groundwater monitoring network, from Macdonald (1941), and from Stearns (1943) (Figure 5-10) were used to correlate the stratigraphy of the basalt flows at Red Hill. Barrel logs that were developed during the construction of the tanks also depict the stratigraphy of the rock formation (Figure 5-11). These logs encompass the 150-ft-tall cylinder interval of the tanks below the base of the dome. This is the middle 150 ft of the 250-ft-tall tanks.

Geologic mapping indicates the dip direction averages to the south-southwest in the Red Hill Area (~190–205 degrees) with a true dip of 10–12 degrees in the Red Hill area. Regionally, flows commonly dip 3–10 degrees away from the eruptive axis of the volcano (Hunt Jr. 1996), and dip direction is generally to the southwest. The average dip directions from geologic mapping in the Red Hill Area are:

- Hālawa side of Red Hill: 194 degrees
- Hālawa Quarry – Active Pit: 194 degrees
- Moanalua Water Tunnel: 192 degrees
- Moanalua side of Red Hill and Moanalua Golf Course: 202 degrees

In general, the upper stratigraphic section in Red Hill is composed predominantly of a'ā flows with some interbedded pāhoehoe flows (Figure 5-2). Field mapping also indicated a predominance of a'ā flows in exposed cliff-forming outcrops that correlate with the upper stratigraphic section. The lower section is composed primarily of thinner bedded pāhoehoe flows (see Photo 5-1). Correlation of boring logs at Red Hill indicate two well defined intervals of a'ā flows (composed of several flows with a'ā clinker layers) within the pāhoehoe section that are approximately 30–60 ft thick.

5.1.3 Overall Occurrence of Rock Types

The presence of nearly horizontal to gently dipping beds of lava flows with alternately greater and lesser resistance to erosion at the site were observed during rock coring for installation of Red Hill groundwater monitoring wells and site reconnaissance activities. No dikes were apparent in recovered cores or in observed outcrops at Red Hill.

Erosion of the less-resistant beds, such as a'ā clinker, has resulted in undercutting of the more resistant massive a'ā and pāhoehoe flows (Photo 5-2). Thinner bedded pāhoehoe flows are less resistant than massive a'ā flows (Photo 5-3). In general, flows vary from evenly bedded, relatively flat to gently dipping, and continuous to undulating and uneven.

Features or media with a high surface area to volume ratio, such as a'ā clinker and high-angle fractures, are also subject to rapid weathering. Similarly, the nearly horizontal contacts between pāhoehoe lava flows, which are absent of a'ā clinker, are susceptible to weathering. Rock layers with denser, more closely spaced fracturing also appear more extensively weathered. Vertical fractures and cooling joints are limited or bound within each flow; i.e., they do not continue into the overlying or underlying flows.

5.1.3.1 PĀHOEHOE

Pāhoehoe flows form as relatively rapidly flowing basaltic lavas that tend to spread out laterally and are typically thin. These flows have a smooth or rope-like surface texture and highly vesicular interiors (vesicles are pore spaces in the lava caused by degassing of the molten pāhoehoe lava). These flows contain voids of various sizes, and are often cracked and collapsed in places. Lava tubes are associated with pāhoehoe lava flows. Along the ridge of Red Hill, lava tubes were not encountered during coring and rates of core recovery were high with the exception of a large void encountered in the bottom of RHMW09. A 1.5-ft-thick void (potentially a lava tube) was encountered during drilling at RHMW11 situated in South Hālawa Valley (DON 2018c). Pāhoehoe flows contain voids of various sizes, and are cracked and collapsed in places. These cracks occur within individual layers, and are not vertically continuous across multiple flows. Ponding of pāhoehoe lava in depressions or on gentle slopes can result in thick accumulations of massive pāhoehoe. Interflow voids form where the irregular upper surface of a flow is not completely filled in by the viscous lava of a subsequent flow.

It is not easy to discern from boring logs massive pāhoehoe flows from high-permeability thin pāhoehoe flows. As Hunt Jr. (1996) states, most pāhoehoe flows are thin. Given that flows dip at approximately 10–12 degrees in the Red Hill area, the likelihood of ponding of pāhoehoe (i.e., resulting in massive pāhoehoe) would be low. This indicates that thin pāhoehoe flows are predominant at Red Hill (i.e., most, > 90 percent). Exposed outcrops of pāhoehoe on the South Hālawa Valley side of Red Hill reveal primarily thin-bedded flows (Photo 5-1).

The thick accumulations of pāhoehoe may represent a flow field that is divided into a number of lava flows, which at any one time form flow units with specific orientation (T. Thordarson, University of Iceland-Reykjavik, pers. comm. 2017). The flow directions vary based on the timescale of an eruption event. In addition, each lava flow can branch and is always composed of multiple lava lobes (often in the thousands). As such, lava flow fields are continuous and can cover very large areas.

On an outcrop scale (or in a drill hole), each pāhoehoe flow field is composed of multiple units defined by chilled outer margins. It can be highly difficult to define the thickness (and extent) of a flow field from outcrop patterns and even more so from drill holes.

Although vesicles are seen as small rounded holes in pāhoehoe, these pore spaces are not interconnected (Mink 1980; Hunt Jr. 1996). Thus, the total porosity of vesicular pāhoehoe may be high, but it has very low effective porosity because the vesicles are not connected and do not transmit fluids. Clinker layers are generally absent from pāhoehoe flows (Izuka et al. 2018). Although less common, lava tubes a few inches to several feet in diameter have been reported in pāhoehoe flows (Izuka et al. 2018). Larger lava tubes have also been discovered in tunneling (Hunt

Jr. 1996), and are recorded in barrel logs generated during construction of the Facility tanks. With the exception of what may be small lava tubes encountered during coring of RHMW11 and RHMW09, no other lava tubes were encountered during coring of boreholes for monitoring wells recently installed at the Facility, and core recovery rates were high.

5.1.3.2 *Aʻā*

Aʻā flows are composed of thick, massive layers of dense, hard, competent basalt flows with few fractures. Aʻā lava flows form from more viscous lava and have a rubbly surface. Aʻā lava flows are characterized by an interior or core of solid, dense, massive rock with exterior top and bottom coarse rubble or clinker zones (Photo 5-4). Massive dense aʻā core in outcrops and in cores are characterized by stretched vesicles and the absence of open fractures. The massive rock in the interior of a flow is virtually impermeable and typically has few fractures of small aperture, as reflected by high rock quality designation (RQD) values and high core recovery rates. High-angle fractures and cooling joints are limited or bound within each aʻā core flow; i.e., they do not continue into the overlying or underlying flows. Fracture apertures have also been mapped as relatively thin (and weathered in many cases), which further reduces the potential for significant vertical migration of fluids.

However, along the tops and bottoms of these dense basalt flows are zones of aʻā clinker (highly fractured or fragmented rock). The thicker aʻā clinker zones are typically composed of unconsolidated rubble with much larger pore spaces between the brittle, fragmented rock compared to the dense, hard interior portions of massive aʻā basalt flows. Clinker zones are similar to layers of coarse well-sorted gravel, where layered sequences of flows can result in widespread beds with high horizontal permeability. Clinker zones characteristically have a high proportion of pore space and surface area and are prone to weathering quickly, while the weathering of dense massive rock proceeds more slowly.

Based on outcrop exposures and rock cores, approximately 60 percent of aʻā clinker is weathered, has a high content of fine-grained material, and is of relatively low permeability at Red Hill (Photo 5-5).

5.1.3.3 *Pyroclastic Deposits*

Pyroclastic (airfall) deposits were encountered in rock cores at Red Hill. None have been observed to date in rock outcrops. These deposits are granular in nature and include ash, cinder, spatter, and larger blocks (i.e., tuff). Deposits recovered in cores are highly weathered.

Situated immediately to the south and southwest of Red Hill, the Salt Lake Tuff consists of subaerial gray to brown tuff containing nodules of dunite (Stearns and Vaksvik 1935). It is as thick as 300 ft and passes beneath sea level. It overlies Āliamanu Tuff to its northwest, which is composed of water-laid gray to black or grayish-brown tuff, rounded gravel, and (in tunnels) large vesicular bombs and spatter (Stearns and Vaksvik 1935). It is separated from the overlying Salt Lake Tuff by red soil and typically overlies older alluvium (Figure 5-9).

5.1.3.4 *Caprock Deposits*

The caprock units within the peripheral valleys have a character distinct from the lower portion of the valleys and plateaus, where the deposits often consist of terrestrial sediments that interfinger with marine sediments and limestone units, described as follows:

- *Valley Fill.* The deposits within and near the base of the valleys generally consist of fill of highly weathered and compact older alluvium that is mantled with more recent unconsolidated alluvium and colluvium (Oki 2005). The older alluvium consists of terrestrial sediments that vary in size from fine-grained particles to boulders, and is less permeable. The older alluvium has been weathered and compacted into a soft coherent mass (Wentworth 1951). The older alluvium may be hundreds of feet thick at lower altitudes, but at altitudes above approximately 400–600 ft, older alluvium may be nonexistent. These materials overlay highly weathered saprolite.

  Drilling at monitoring well RHMW11 encountered valley fill deposits to a depth of 67 ft bgs (DON 2018c). This depth is consistent with stream valley incision or erosion during prior glacio-eustatic stands of sea level. Stearns (1978) described that the Waipio low stand of the sea was minus 350± ft and lasted long enough for deep erosion along major streams (Figure 5-12). The Waipio low stand correlates with the Illinoian glacial period, about 500,000 years before present (BP), during the Pleistocene age (Stearns 1978). Deep valleys were cut during the Nebraskan glacial period (1.4 million years BP), the Kahipa low stand (Kansan glacial period; 800,000 BP), and the Waipio low stand described above, prior to subsidence of the islands. All of these low stands of the sea were of relatively long duration.

  On a regional basis, Stearns (1978) notes that "*The Waipio low stand exposed broad marine flats on which sand was abundant in many places. The drop in sea level lasted long enough for all major streams to cut their channels to levels well below present sea level along the coasts. Considerable erosion of the sedimentary caprock of the Honolulu artesian basin took place, resulting in numerous leaks, now the sites of artesian springs.*" Sherrod et al. (2007) has mapped (after the original mapping by Stearns) the valley fill deposits as 'Older Alluvium.'

- *Coastal Caprock.* A wedge of calcareous and volcanogenic sediment overlies the basal volcanics that ranges from nearly 1,000 ft thick near the coast and gradually thins and interfingers with increasing volcanogenic-sediments consisting of older weathered consolidated alluvium and more recent unconsolidated alluvium and colluvium near the valley mouths. The confining, less-permeable properties of the coastal caprock are due primarily to the presence of fine-grained layers and weathering of basalt-derived material (Hunt Jr. 1996).

5.1.3.5 SAPROLITE

Based on previously collected rock cores, the horizon of soils and highly weathered basalt described as saprolite on the Red Hill ridge is approximately 15–25 ft thick (Photo 5-6). Saprolite is weathered rock material that retains textural features of the parent rock. Intense weathering of basaltic rocks can significantly reduce the permeability of the parent rock by transforming igneous minerals to clays and oxides (Hunt Jr. 1996). Site soils on the ridges and side slopes are mapped as Helemano-Wahiawā association, consisting of well-drained, moderately fine textured and fine-textured clay-rich soils derived from basalt parent rock that give the soils its characteristic red color (USDA SCS 1972). These soils are identified throughout the confines of the Facility and extend more than one-half mile up-slope from Tanks 19 and 20.

Based on previously collected rock cores, the horizon of soils and saprolite on Red Hill ridge is approximately 15–25 ft thick. The depth of valley fill and saprolite in the valleys surrounding Red Hill, particularly in the center of the valleys and below the streambeds, is not yet well defined. However, during recent coring of monitoring well RHMW11, located in South Hālawa Valley, saprolite was encountered at approximately 68 ft bgs and extended to a depth of 279 ft bgs, or

approximately 87 ft below the expected depth of the regional basal groundwater table (approximately 20 ft msl); see Figure 5-4 and Figure 5-5) (DON 2018c). This depth is consistent with the description in Section 2.7 that saprolite zones are typically around 75 ft thick but can be 300 ft thick or greater beneath the valley floors or in areas of high precipitation.

An inspection and interpretation of the logs of cuttings (not cores) conducted for Hālawa Deep Monitor Well (HDMW2253-003) and Waimalu Deep Monitor Well (2456-005) found the following:

- Hālawa Deep Monitor Well (HDMW2253-003): Alluvium (cuttings with clay) at 0–60 ft bgs, saprolite (weathered basalt) at 60–285 ft bgs, and less-weathered to unweathered basalt from 285 ft bgs to total depth.
- Waimalu Deep Monitor Well (2456-005): Alluvium (basalt boulder with dark brown silty sand) at 0–30 ft bgs, saprolite (weathered basalt) at 30–350 ft bgs, and less-weathered basalt at 350 ft to total depth.

Based on data developed from those two well locations, the thickness of saprolite beneath alluvium/valley fill deposits is on the order of 225–320 ft thick with an average of approximately 270 ft. These numbers are consistent with and compare to those of Oki (2005, Figures 21 and 22).

According to Hunt Jr. (1996), the effectiveness of steep geohydrologic barriers "*may diminish inland from the coast with increasing altitude and decreasing penetration of the valleys into the underlying basalt. The boundary between the Pearl Harbor and Moanalua areas has been revised from South Halawa Valley to North Halawa Valley (fig. 5) following Eyre (P.R. Eyre, U.S. Geological Survey, written commun., 1991). Eyre reasoned that North Halawa Valley is deeper than South Halawa Valley and, therefore, is a more appropriate boundary between the two areas. This interpretation is consistent with Wentworth (1951). The curved trend of this barrier reflects an assumed paleodrainage pattern in southern Oahu before island subsidence and sediment infilling of the valleys. The Kaimuki area is bounded on the east by the Kaau rift zone and, perhaps, by valley fill in Palolo Valley (fig. 5).*"

Borehole geophysical data collected in RHMW11 and in Hālawa Deep Monitor Well (HDMW2253-03) are consistent with each other and indicate the presence of saprolite to a depth of approximately 279 ft bgs. Review of the HDMW2253-03 geologic log based on drill cuttings indicates clays consistent with saprolite development from 68.5 to 279 ft bgs. Additionally, the geologic core log of RHMW11 (DON 2018c) illustrates saprolite consistent with the interpreted saprolite depth at HDMW2253-03.

Seismic Profiling Survey. A survey was conducted in December 2017 along nine transects in the Red Hill area to map stratigraphy and hydrogeologic boundaries beneath North Hālawa Valley, South Hālawa Valley, and Moanalua Valley (DON 2018d). Seismic reflection results show the geometry and depth to key hydrostratigraphic boundaries within the upper 1,000 ft bgs. Key reflectors include the base of alluvium or top of saprolite, top of water-saturated (possibly perched) sediments, and the contact between weathered basalt (saprolite) and unweathered basalt.

5.1.4 Permeability

5.1.4.1 PĀHOEHOE PERMEABILITY

According to Hunt Jr. (1996): "*The mixture of voids and fractures in pahoehoe flows imparts high intrinsic permeability similar to that of carbonate rocks. Vertical permeability elements in pahoehoe include cooling joints; collapse features; skylights or holes in the roofs of large lava tubes; and*

large, open cracks where lava is pushed up into humps and pressure ridges. Lateral permeability elements in pahoehoe include drained lava tubes and interflow voids (small depressions in the irregular upper surface of a lava flow that are not filled in by the viscous lava of the subsequent flow).” In general, thin pāhoehoe lava flows have porosity fractures that result in high permeability, whereas thicker pāhoehoe flows are more massive with much lower effective porosity and permeability.

5.1.4.2 *A'ā Permeability*

The smaller effective porosity of massive a'ā cores can result in extremely low vertical permeability, especially when the rock is not fractured. The principal vertical permeability of a massive a'ā core is imparted by wide, regularly spaced cooling joints, which are typically low-permeability features. The a'ā lava flows may also act as localized confining layers in the basal aquifer system. The smaller effective porosity of massive a'ā cores suggests permeability several orders of magnitude less than a'ā clinker or thin-bedded pāhoehoe. Hunt Jr. (1996) describes marginal clinker at the periphery of an a'ā flow may provide local avenues of high vertical permeability in lava sequences and that such flow-margin clinker bridges may be more prevalent in sequences of thinner flows than in thicker flows.

A'ā clinker is composed of gravel- and cobble-size rubble that resembles a conglomerate. It is usually loosely held together unless it has been welded together by heat. Borehole geologic logs and core photos from the Facility area show the a'ā clinkers are loose fragmented rock, evidenced by much lower RQD values and low rates of core recovery that are attributable to erosion of unconsolidated rock fragments and sediment by water circulating around the core bit during drilling.

The thicker, unweathered a'ā clinker zones have large interconnected pore spaces (macro-pores), high effective porosity, and high permeability. A'ā clinker is subject to more rapid chemical weathering processes, and once it has significantly weathered, its permeability is reduced. Often the thinner clinker beds are found to be highly weathered and clayey.

Clinker zones that are unweathered characteristically have high horizontal permeability. Based on outcrop exposures and rock cores, approximately 60 percent of a'ā clinker is weathered, has a high content of fine-grained material, and is of relatively low permeability at Red Hill (Photo 5-5). From Hunt Jr. (1996): “*The areal extent of lava flows is much larger than their typical thickness of about 10 ft. Wentworth and Macdonald (1953, p. 31) listed measurements for 22 historical flows on Mauna Loa and Kilauea on the island of Hawaii (fig. 8), which presumably are typical of flows on Oahu as well. The flows on Hawaii average about 15 mi in length and about one-half mile in width. Individual flows can be traced and mapped on the surface of young, unweathered volcanoes. Areal correlation of flows in the subsurface requires careful drilling and collection of core samples or drill cuttings, detailed description and petrographic study of the samples, and borehole geophysical logging. These data are not collected routinely in Hawaii, and there are few instances when data are sufficient for lateral tracing of subsurface flows.*”

5.1.4.3 *Permeability of Pyroclastic Deposits*

Due to the highly weathered nature of pyroclastic deposits at Red Hill, their porosity and permeability are similar to those of granular sediments, with similar grain size and degree of sorting. Fine-grained ash is less permeable than coarser pyroclastic deposits, and its permeability may be reduced further by degree of welding, weathering, or compaction (Visher and Mink 1964; Hunt Jr. 1996). According to Visher and Mink (1964), volcanic tuffs of the Honolulu volcanic series are among the most impervious rocks.

The position of the Salt Lake and Āliamanu Tuffs being situated immediately to the south and southwest of Red Hill may have significant influence on groundwater flow in the Red Hill area. The Salt Lake Tuff is as thick as 300 ft and passes beneath sea level, and the underlying Āliamanu Tuff to its northwest was water-laid and typically overlies older alluvium.

5.1.4.4 INFLUENCE OF HĀLAWA QUARRY

As shown on Figure 5-5, rock quarrying operations over decades have removed considerable quantities of material. The active quarry pit immediately north of South Hālawa Valley currently has a floor elevation of approximately 196 ft msl. To the west of the active pit lies a formerly active quarry pit, which is now partially filled with sediment and used as a sedimentation/runoff control basin for the cement plant operation. The active pit is separated from South Hālawa Valley by a ridge approximately 300 ft msl. With this configuration, the approximately 500-ft-wide by 1,200-ft-long active quarry pit acts as a collection basin that increases the natural groundwater recharge rate in that area and may, along with other local sources of recharge, affect groundwater levels in the basal aquifer beneath the pit.

5.2 MICRO-SCALE GEOLOGIC FEATURES

The Facility's fuel storage tanks are situated in the vadose zone, which is more than 100 ft thick (beneath the tanks) in the area. The tanks are surrounded by volcanic rock that consists of relatively thick, dense, massive basalt flows, with basaltic a'ā clinker zones of variable thickness. Some a'ā clinker zones also contain fine-grained, clayey soil created by weathering. The tank bottoms are approximately 100–130 ft above the groundwater table. Although LNAPL was released from leakage from Tank 5 in January 2014 as well as other tanks historically (DON 2002), no LNAPL has been measured in any of the monitoring wells beneath or near the Facility or water supply wells in the area. The absence of LNAPL in groundwater is attributable, in part, to the physical properties of the geologic units in the basalt that inhibit vertical migration, as further described below.

5.2.1 Assessment of Subsurface Heterogeneity

Geologic logs and photographs of basalt cores from the Red Hill area show that the vadose zone surrounding the fuel tanks is composed of a heterogeneous series of layered basalt flows. Both types of basalt, pāhoehoe and a'ā, are present.

Within the heterogeneous layered basalt formation that composes the vadose zone surrounding the fuel tanks, the spatial distribution of interconnected pore spaces (effective porosity) is the result of the basalt lava flow genesis and subsequent sub-aerial weathering that may occur prior to the next flow. Viewed within a smaller area, the movement of molten lava is complex and unpredictable, but the flows generally move downhill due to gravitational force. Nonetheless, the available geologic information from boring logs and core photos can be integrated with geologic observations of local basalt outcrops, as well as photos of active lava flows on the island of Hawai'i, to characterize the physical properties of basalt that affect LNAPL movement and groundwater migration.

Clinker (bridges) at the periphery of an a'ā flow may provide local avenues of high vertical permeability (Hunt Jr. 1996). Sequences of thin lava flows in Hawai'i typically form highly permeable aquifers, with horizontal hydraulic conductivity (K_h) values of hundreds to tens of thousands of feet per day (ft/d) (Izuka et al. 2018). Hunt Jr. (1996) compared the permeability of massive a'ā vs. high permeability lava flows and concluded: "*In contrast, the smaller effective porosity of massive aa cores suggests permeability several orders of magnitude less than aa clinker or thin-bedded pahoehoe.*" Most of the O'ahu pāhoehoe flows are thin (Hunt Jr. [1996]; J. Kronen, AECOM, personal communication, 2017) and therefore are likely to exhibit higher permeability.

Geologic observations and reports by the USGS also reveal that the interior portions of the dense, massive a'ā basalt flows typically have very low primary porosity, low permeability (hydraulic conductivity), and low effective porosity. Within the dense basalt flow interiors, a small amount of secondary porosity is attributable to fractures formed during cooling. These cooling fractures are typically short in length and confined within an individual flow. Borehole logs and core photos from Red Hill monitoring well borings reveal that the cooling fractures typically have very narrow apertures, and most are just hairline cracks. On the other hand, more intensely fractured zones and loose rubble logged as a'ā clinker occur along the exterior portions of basalt flows, due to rapid cooling and fragmentation of the lava flow surface as it solidifies from the molten lava material (Hunt Jr. 1996).

The heterogeneous nature of the basalt is revealed in the geologic log of the Red Hill Shaft water development tunnel prepared by the USGS (Stearns 1943). That log, reproduced as Figure 5-10, recorded water inflow rates measured by the USGS as the tunnel was being constructed. The log shows that flow rates dramatically increased as the tunnel penetrated beyond 550 ft, which is attributable to a large increase in permeability of the basalt formation. On Figure 5-10, the relatively thin "top clinker" logged in the first 550 ft of the tunnel's upper lift produced essentially no groundwater. The tunnel was described as "dry" during tunneling out to about 480 ft from the shaft. Subsequent tunneling of this section, but at a lower level (lift), produced about 3.5 mgd. Progressing beyond 480 ft, the tunnel produced greater water inflows. At 730 ft the flow was recorded to be 5 mgd. After reaching 980 ft, the flow recorded was 12 mgd. From that point forward, the rate of inflow encountered in the tunnel became much larger. In the last 200 ft of the tunnel, 980–1,180 ft from the shaft, the groundwater inflows increased from 12 mgd to 29 mgd. The thicker clinker zone shown on the geologic log (Stearns 1943) produced the majority of the groundwater. This 200-ft clinker produced about 8 times more water than the clinker and pāhoehoe logged in the initial 480 ft of the tunnel. In summary, by the end of the Red Hill water development tunneling project, the groundwater inflow had increased from approximately 5 mgd to 29 mgd in the last 500 ft of that tunnel. The end of this water development tunnel is located near RHMW05.

Lying beneath the vadose zone, this same basalt formation comprises the volcanic rock aquifer described in several hydrogeology reports. The hydraulic conductivity of flank lavas is dependent on such features as thickness of the flows, thickness of clinker zones associated with a'ā flows, frequency and extension of fractures, and occurrence of lava tubes associated with pāhoehoe flows. Hydraulic conductivity ranges from several hundred to several thousand ft/d in highly permeable dike-free flank lavas, and is typically orders of magnitude higher in the horizontal direction than in the vertical direction (DON 2007).

K_h tends to be several times greater parallel to the direction of lava flows (i.e., downslope) than perpendicular to the flows (Nichols, Shade, and Hunt Jr. 1996). On a regional scale, USGS reports indicate the volcanic rock aquifer has high K_h, 1,500–4,500 ft/d. However, this aquifer has much lower vertical hydraulic conductivity (K_v), 7.5 ft/d, which is about 200–600 times lower than the K_h. Total porosity of the volcanic rock aquifer ranges between 5 and 50 percent, but the effective porosity is approximately 4–5 percent (Oki 1998; Whittier et al. 2004; Oki 2005; Izuka et al. 2018).

Rotzoll, El-Kadi, and Gingerich (2007) analyzed 238 aquifer tests of wells in Hawai'i basalt and found that hydraulic conductivity is lognormally distributed and ranges over several orders of magnitude, from 1 to 8,000 ft/d. The arithmetic mean, geometric mean, and median values of hydraulic conductivity for dike-free volcanic rocks were respectively 1,700, 900, and 1,200 ft/d.

5.2.2 Geologic Features and LNAPL Movement

For the purpose of evaluating LNAPL movement at the Facility, the geologic media was divided into five classes, as indicated in Table 5-1.

Table 5-1: Geologic Media in Red Hill

Media Type	Ability to Transmit, Hold LNAPL
Massive a'ā flows	Limited
A'ā clinker with fine-grained sediments	Limited LNAPL transmissivity but high holding capacity
High-permeability a'ā clinker	High
Massive pāhoehoe flows	Limited
High-permeability thin pāhoehoe flows	High

Geologic logs of core taken from the Facility often indicate that thin clinker zones were weathered as the top of a flow was exposed at ground surface. Considering the weathering processes reported by the USGS (Hunt Jr. 1996), fine-grained residuum would be created as the lava flow top and side clinkers were weathered at land surface for extensive periods. This weathering, including erosion and and saprolitic development of clays, would cause the surfaces of clinkers formed along the top and sides of a'ā flows to have lower permeability and lower effective porosity than non-weathered clinkers. Thinner clinker beds are often highly weathered throughout the entire thickness of the bed. The eroded fines and clay-rich matrix in the weathered clinkers would have a high capillary threshold entry pressure because water is tightly held by surface tension and capillary forces. The high threshold entry pressure must be overcome to allow LNAPL to enter water-saturated fine-grained residuum.

Conversely, the interior portions of larger, thicker clinker zones would be less affected by the weathering processes described by the USGS (Hunt Jr. 1996) because those clinkers would be more distant from subaerial exposure at the land surface. Thus interior portions of larger, thicker clinker zones would contain little eroded and clay-rich materials, and thus may have extremely high permeability and high effective porosity. Intergranular porosity of such clinker zones is analogous to well-sorted, coarse gravel deposits (Hunt Jr. 1996). Widespread beds of clinker contribute high horizontal permeability to a layered sequence of lava flows (Hunt Jr. 1996). As a site-specific example, the high rates of water inflow logged by the USGS in the Red Hill Shaft water development tunnel (Figure 5-10) show that the thick clinker zone encountered at the end of the tunnel has extremely high hydraulic conductivity. Additionally, clinker zones formed along the sides of lava flows may provide conduits or "clinker bridges." Where unweathered, such clinker bridges may allow LNAPL to migrate vertically between massive basalt flow layers.

Directly beneath the Facility's fuel storage tanks, the relatively dense, low-permeability massive basalt layers and the weathered layers as noted above would impede downward migration of LNAPL and water. But the thicker, non-weathered, high-permeability clinker zones create preferred flow pathways for fluids to move laterally. A LNAPL would move primarily in down-dip directions, while a gas or vapor lighter than air would move primarily in up-dip directions, although if the release had significant hydraulic head, the head would drive some LNAPL up-dip and across-dip as well. Although the jet fuel vapors are heavier than air, the low vapor pressure of the jet fuel constituents limits the amount of partitioning into the vapor phase, and further limits any density-driven migration of the vapors. The LNAPL released from a fuel tank would likely move from the leak point(s) along interconnected void spaces that may exist immediately outside the tank, and then into the surrounding rock with permeable zones. The available data show the geometry of the

geologic features that contain large interconnected pore spaces (macro-pores) where LNAPL is most likely to move. In addition, because the Facility's ventilation system operates under a slight vacuum, vapors within the vadose zone are expected to move toward the tunnel, and be expelled through the exhaust system.

Cooling fractures exist within interior portions of both types of lava flows. In a fracture filled with LNAPL, the pressure head of the LNAPL is equal to the connected vertical height of the LNAPL in the fracture and other fractures directly connected with it. However, where thin fractures contain moisture or water droplets, the water will impede the influx of LNAPL and reduce the relative permeability for LNAPL. Moisture held in fine-grained materials within weathered clinker will also cause very low relative permeability for the LNAPL. As previously described, fractures are generally limited to individual flows and often have small apertures, contain weathered materials, and have been subjected to secondary mineralization. Compared to water, the higher viscosity of jet fuel will impede LNAPL movement through small pore spaces, especially small water-filled fractures within the massive dense a'ā basalt layers (Figure 5-13).

Thus LNAPL would enter and move preferentially through clinker zones and/or thin pāhoehoe flows of high permeability and high effective porosity. Macro-pores pose the least capillary water resistance and thus are the preferred pathways. After LNAPL moves downward through macro-pores to the top of a dense, low-porosity, low-permeability lava bed, the LNAPL would move down-dip and spread laterally along the base of the permeable zones.

As LNAPL moves through interconnected macro-pores, such as those in the larger, thicker non-weathered clinker zones or thin pāhoehoe, some of the LNAPL will be retained in the pore spaces. Surface tension and capillary forces of water in the smaller pore spaces of small fractures and other pore spaces filled with fine-grained residuum will impede and trap the LNAPL. The LNAPL volume permanently retained in the pore space is defined as "residual saturation." Collecting data for residual saturation and other physical properties of the basalt layers will provide a basis for estimating the extent of LNAPL movement and mobility in the vadose zone and for estimating the source area for the numerical groundwater flow and CF&T modeling.

If LNAPL moving in a fracture were to reach the groundwater level, the accumulated weight of LNAPL in the fracture, within the individual a'ā flow will depress the LNAPL–water interface within the fracture. In rock that has been wetted by water first, LNAPL will enter a given fracture only if the pressure of LNAPL exceeds the capillary pressure of water in the fracture entrance. Where a fracture containing LNAPL penetrates below the groundwater surface, the LNAPL is proportional to the connected vertical height of LNAPL in the fracture above the groundwater level. This LNAPL pressure is balanced by the buoyancy of the LNAPL created by the greater density of the groundwater below.

5.2.3 Petrographic Analyses

Core samples are currently being collected for petrographic analysis from archived cores. Further petrographic sampling will be conducted from the RHMW01R core inside the Facility tunnel, adjacent to existing well RHMW01 (see Figure 2-9) (DON 2017f). The purpose is to characterize residual LNAPL and mobility characteristics in rock core and in turn characterize the vadose zone and fluid properties that affect LNAPL movement (DON 2017g). The core samples will be sent to a petrographic laboratory for evaluation of residual LNAPL, estimation of residual fuel and fuel mobility, and effective porosity. The following pertains directly to the RHMW01R planned coring:

- If the core is found to contain LNAPL, the lab analyses will include determining the LNAPL and water contents (percent saturations), as well as the LNAPL residual saturation. Residual saturation is defined as the LNAPL volume that will be permanently retained in the pore space.
- If no LNAPL is detected, the core samples will be selected for lab testing of residual saturation after the samples are saturated with jet fuel in the lab. Cores selected will represent the range of rock types most likely to provide pathways for LNAPL movement (i.e., those with effective porosity). Prior to these lab analyses, appropriate quantities of JP-8, F-24, or similar kerosene-based fuel will be sent to the laboratory for measuring the fuel properties, including viscosity, density, and interfacial tensions. Fluorescence of the fuel will also be tested. After introducing the LNAPL to saturate the selected core samples, those samples will be analyzed to measure the LNAPL residual saturations (DON 2017h).

Because some of the thin pāhoehoe cores may not include any of the key pāhoehoe secondary porosity features (e.g., voids and fractures), the attempt to introduce LNAPL into the core during the petrophysical test may be unsuccessful. In this case, the data may be used to indicate the ability of the surface of the pāhoehoe to hold LNAPL, but the results of the petrophysical test will not be used as the primary indication of the pāhoehoe LNAPL capacity.

5.2.4 Assessment of Geologic Features and Natural Processes Affecting LNAPL

In summary, the updated geologic CSM described in this report has better defined the spatial distribution, orientation, and physical characteristics of the basalt layers, and thus provides a basis for evaluating the LNAPL movement beneath the Facility tanks. The available geologic logs and core photos from the Facility area reveal that thick clinker layers in the basalt are composed of loose rubble and large interconnected macro-pores. Although much less common, open fractures with substantial aperture thickness and lava tubes may also exist, but are not expected to be laterally continuous or extend between flows. Geologic features with extensive interconnected macro-pores, such as thick clinker beds, clinker bridges, and thin pāhoehoe flows, appear to be the primary pathways for LNAPL movement.

Future LNAPL releases would likely move from a fuel tank leak point into basalt layers containing macro-pores (e.g., thick, non-weathered clinker zones, lava tubes, and interflow voids), then the LNAPL would move primarily downward and down-dip through clinker or an open fracture until being impeded by the top of a dense massive layer of low-porosity, low-permeability basalt (or until LNAPL had reached residual saturation). The LNAPL would then spread horizontally on top of lower permeability flows until fractures, clinker bridges or other vertical conduits are encountered where it can migrate downward until encountering another lower permeability layer. Based on available information, the dense interiors of the basalt flows may have an effective porosity of 1–2 percent, whereas the thick, non-weathered clinkers may have an effective porosity of 20–30 percent. Interconnected macro-pores appear to be more prevalent in the thicker clinker beds. Thus most of the LNAPL would move within those thicker clinker zones, and in the same direction as the dip of the low-permeability lava beds. The LNAPL would also spread laterally in the clinker zones and thin pāhoehoe flows, but the movement would be primarily down the dip of the lava beds. If LNAPL entered a pāhoehoe lava tube, the LNAPL would move within the confined walls of the lava tube, generally downslope within that lava flow layer.

Movement of LNAPL through thin, weathered clinker layers and fractures containing fine-grained sediments would be restricted by capillary forces created by moisture in the smaller pore spaces. Water held by surface tension and capillary forces in those small pore spaces would cause the relative permeability for LNAPL to be very low. Compared to water, the higher viscosity of jet fuel

will also restrict LNAPL movement through small pore spaces. Additional residual saturation data will be collected to enable estimates of volume of LNAPL potentially retained and extent of LNAPL in the vadose zone beneath the tanks (DON 2017g).

Available time-series data from the Facility source area (see Appendix A) show dissolved TPH-diesel range organics (TPH-d) and naphthalene initially increased in the nearby monitoring well RHMW02 after the January 2014 JP-8 fuel release, and decreased through time thereafter. The same COPCs were detected but at lower concentrations in subsequent samples from monitoring well RHMW01 located to the southwest. These data show decreasing concentrations through time as well as with distance from the source area. Together with the spatial distribution of NAP concentrations, the data indicate natural attenuation mechanisms are causing decreases in the COPC concentrations. Natural attenuation processes are described further in Module F: Fate and Transport of LNAPL and Dissolved COPCs in Groundwater (Section 7).

5.3 UNCERTAINTY ANALYSIS

At this point in the study, the main uncertainty is the potential extent of LNAPL movement away from the Facility fuel tanks. Historically, no LNAPL has been measured in monitoring wells at the site, and only isolated odors and staining have been observed in cores collected adjacent to the tanks within borings, and no LNAPL seeps/staining have been observed during field surface mapping at the site. RHMW02, however, has had historical levels of TPH-d exceeding solubility limits indicating a potential for the occurrence of LNAPL.

5.4 ADDRESSING UNCERTAINTIES

The following ongoing, planned, or proposed activities are designed to help resolve the uncertainties described in Section 5.3.

To help determine the potential extent of LNAPL movement away from the Facility fuel tanks, core samples are being collected for petrographic analyses of the capacity of the basalt to retain LNAPL. A core boring will be drilled to install a new monitoring well (RHMW01R) adjacent to RHMW01 inside the Facility tunnel system, which will have a screen interval intersecting the water table (DON 2017f). A detailed geologic log will be prepared during the core drilling. Core samples from this boring will be inspected for the presence of LNAPL on site during drilling, then preserved and shipped for the lab petrographic analyses. If no LNAPL is detected, then selected core samples will be saturated in the lab to measure residual saturation values that reasonably represent the geologic units beneath the Facility.

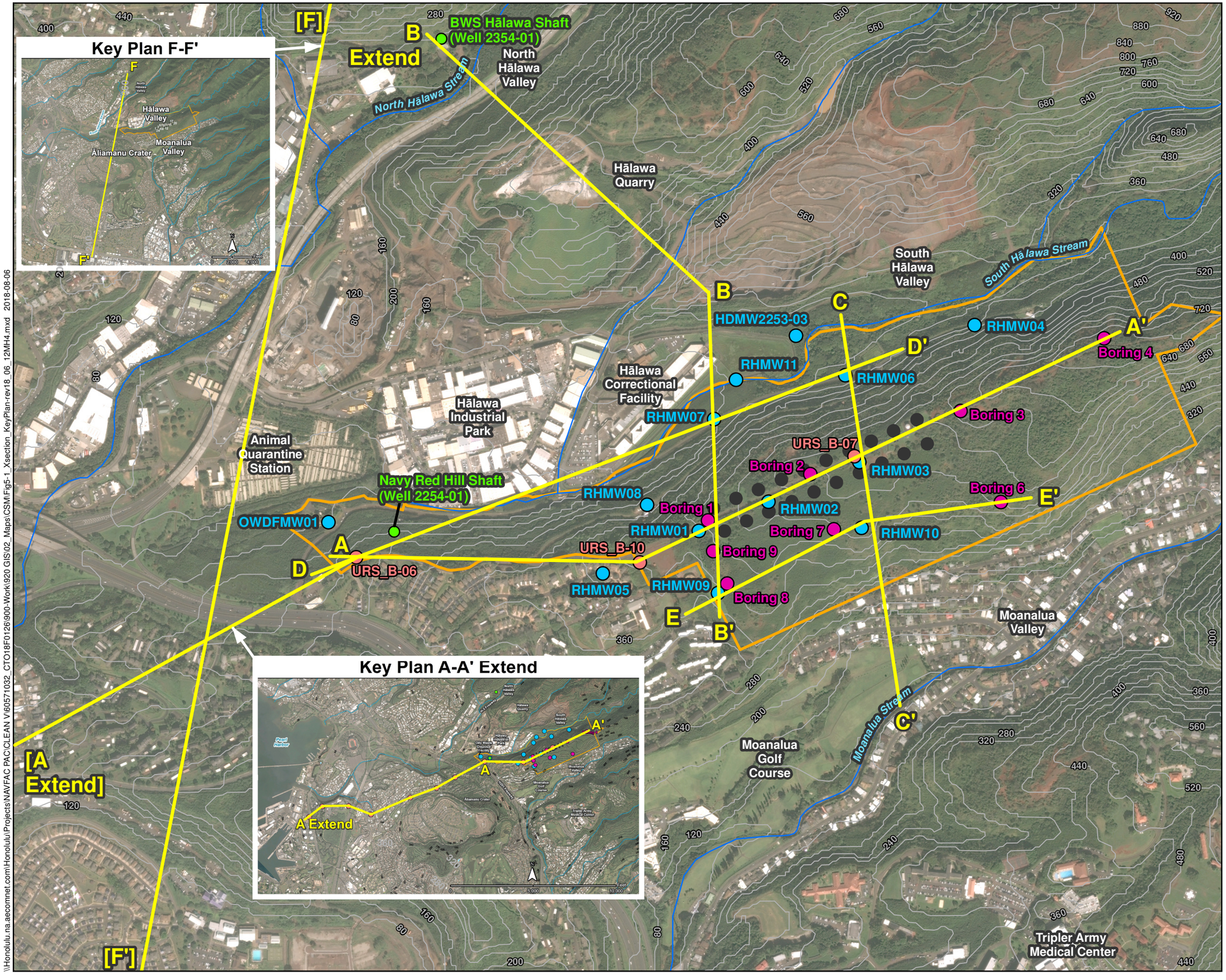

Location Map

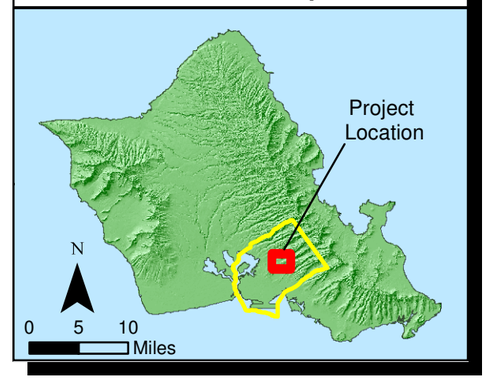

Legend

- Macdonald 1941 Boring Location
- URS 2012 Boring Location
- Red Hill Monitoring Well Boring Location
- Water Supply Well
- Stream
- Topographic Contour (feet above mean sea level)
- Red Hill Installation Boundary and Fuel Storage Tanks

Notes

1. Map projection: NAD 1983 UTM Zone 4N
2. Base Map: DigitalGlobe, Inc. (DG) and NRCS. Publication_Date: 2015
3. Yellow lines correspond to geologic cross sections presented on Figures 5-2 (A-A'), 5-3 (A-A' Extended), 5-4 (B-B'), 5-5 (B-B' Extended), 5-6 (C-C'), 5-7 (D-D'), 5-8 (E-E'), and 5-9 (F-F').

N

0 500 1,000 2,000 Feet

Figure 5-1
Geologic Cross Section Key Plan
Conceptual Site Model
Investigation and Remediation of Releases and Groundwater Protection and Evaluation
Red Hill Bulk Fuel Storage Facility
JBPHH, O'ahu, Hawai'i

\\Honolulu.na.aecomnet.com\Honolulu\Projects\NAVFAC PAC\CLEAN V\60571032_CTO18F01269\00-Work\920 GIS\02_Maps\CSM\Fig5-1_Xsection_KeyPlan-rev18_06_12MH4.mxd 2018-08-06

This page intentionally left blank

A

A'

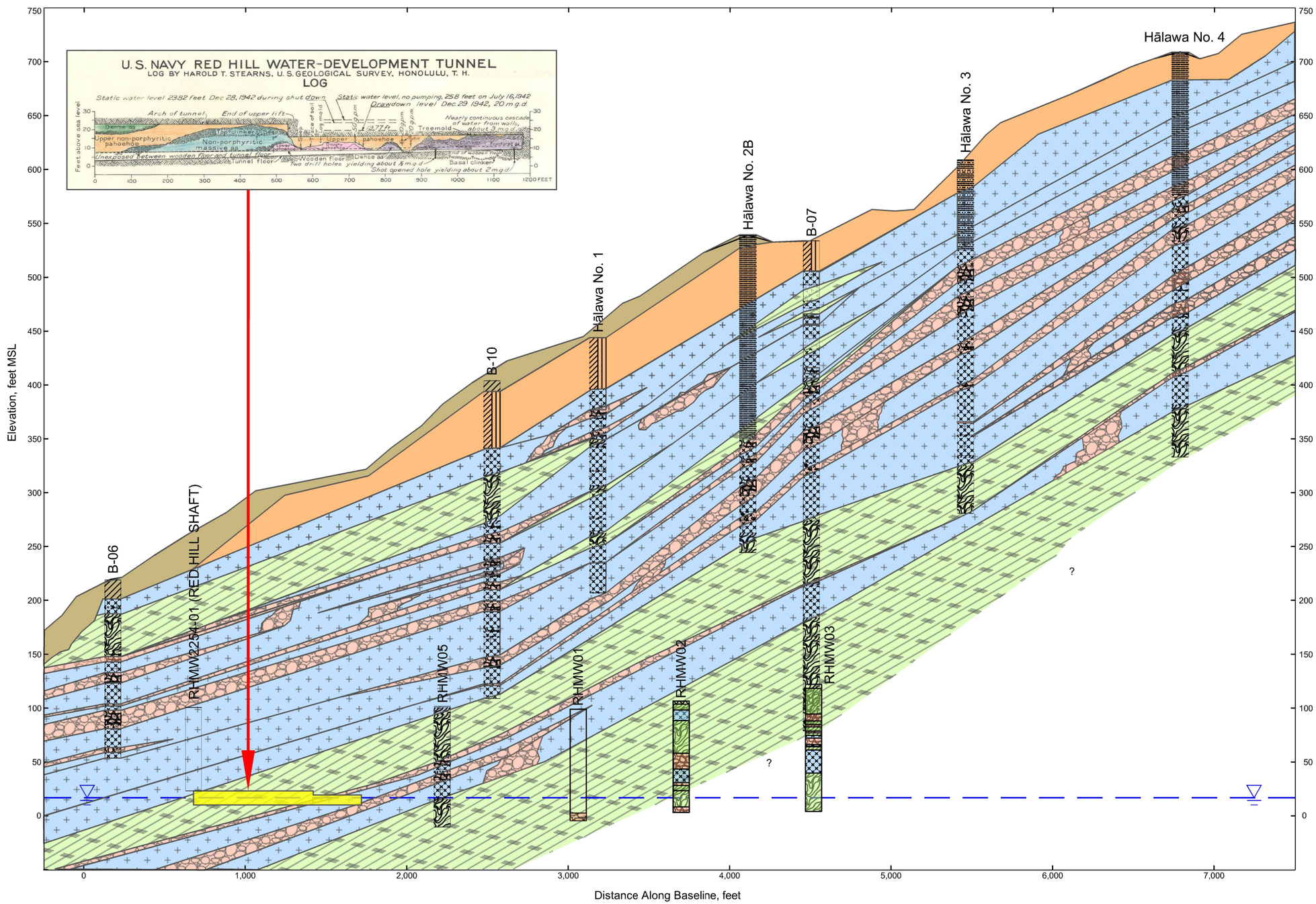

Note: Vertical exaggeration = 1H : 7V (approximate)

Key Plan

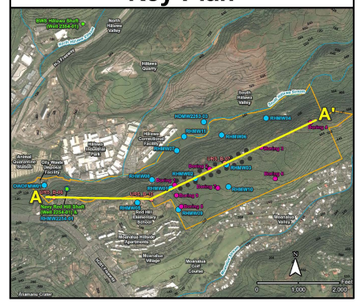

Legend

- Alluvium
- Saprolite
- Massive A'ā Basalt
- A'ā Clinker
- Pāhoehoe
- Groundwater Surface (Approximate)

Notes

1. B-06, -07, and -10: DON 2012
2. Hālawa No.1, -2B, -3, and -4: Macdonald 1941
3. RHMW01: DON 2002
4. RHMW02, 03: DON 2007

S:\Projects\NAVFAC PAC\CLEAN 1\N0571032_CTO18F0128\900--Work\910 CAD\20--SHEETS\cross--sections\Fig5--2_CrossSect--A'.dwg 08/01/18 12:04 PM Nomad

Figure 5-2
Cross Section A-A'
Conceptual Site Model
Investigation and Remediation of Releases and Groundwater Protection and Evaluation
Red Hill Bulk Fuel Storage Facility, JBPHH, O'ahu, Hawai'i

This page intentionally left blank

Key Plan A-A' Extend

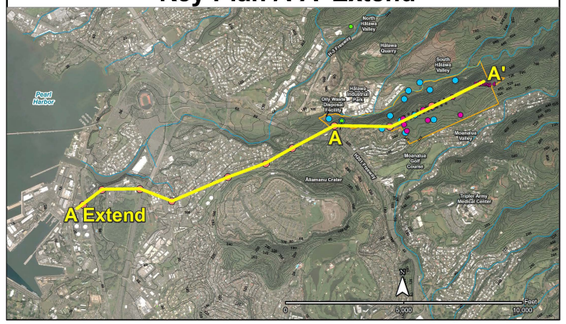

Legend

- Alluvium
- Saprolite
- Massive A'ā Basalt
- A'ā Clinker
- Pāhoehoe
- Groundwater Surface (Approximate)
- Volcanic Tuff
- Marine Limestone

Notes

1. B-01, -02, -03, -04, -05, -06, -07, -8, -9, and -10: DON 2012
2. Hālawa No.1, -2B, -3, and -4: Macdonald 1941

A Extend

A'

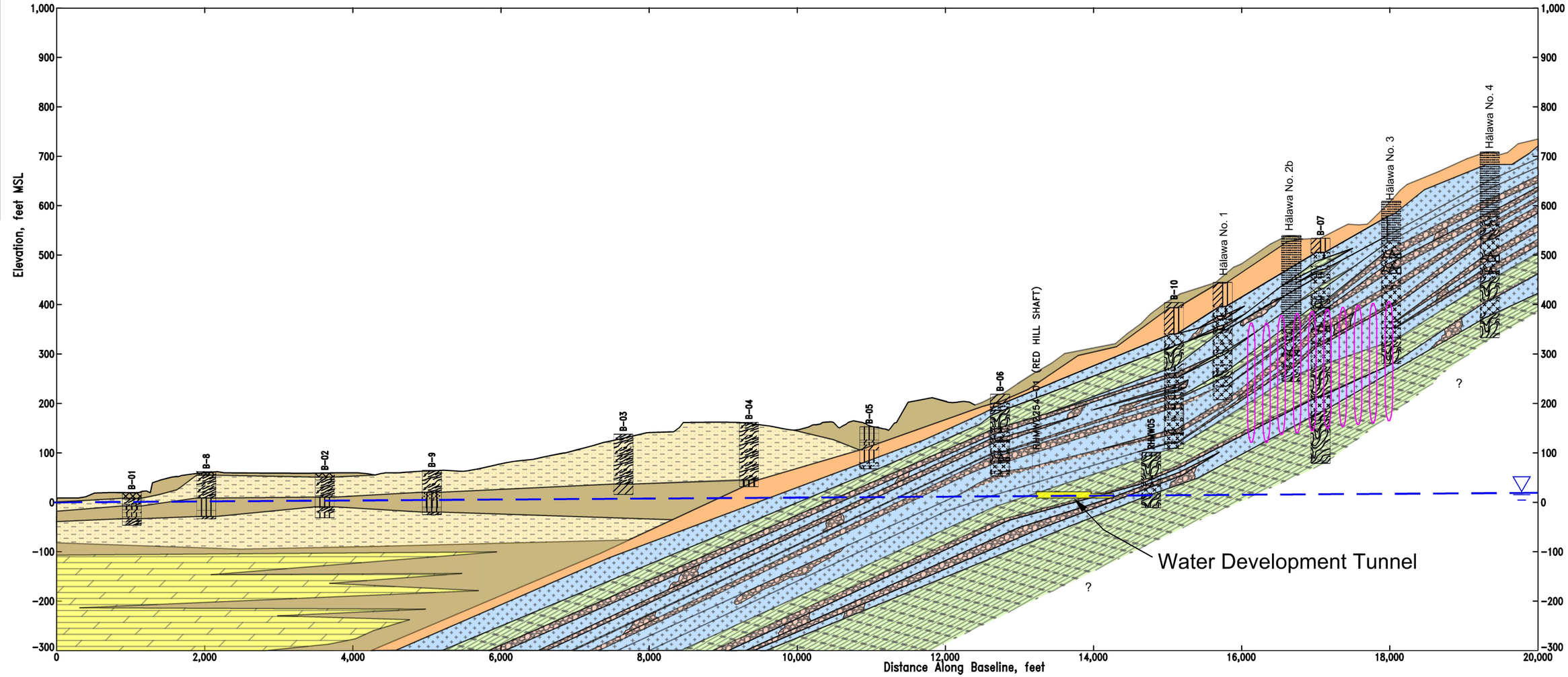

Note: Vertical exaggeration = 1H : 7V (approximate)

S:\Projects\NAVFAC PAC\CLEAN V\60071032_CTO18\2018\900-Work\010 CAD\20-SHEETS\cross-section\Vpgs-3_CrossSect-A'_Extend.dwg 06/01/18 11:55 AM Nomos

Figure 5-3
Cross Section A-A' Extended
Conceptual Site Model
Investigation and Remediation of Releases and Groundwater Protection and Evaluation
Red Hill Bulk Fuel Storage Facility, JBPHH, O'ahu, Hawai'i

This page intentionally left blank

B (Northwest)

Bend in Section

(Southeast) (North)

B' (South)

South Hālawa Valley

Elevation, feet MSL

550 500 450 400 350 300 250 200 150 100 50 0 -50 -100 -150 -200 -250 -300

3,400 3,600 3,800 4,000 4,200 4,400 4,600 4,800 5,000 5,200 5,400 5,600 5,800 6,000 6,200 6,400 6,600 6,800 7,000

Hālawa Quarry Excavation

RHMW11 (Projected 170' West)

South Hālawa Stream

RHMW07

OC11B

RHMW08 Projected 592' East

Hālawa No. 1

Hālawa No. 9

RHMW09

Tank 1

Tank 2

GW 168.0 ft. msl
(Dames and Moore,10/1991)

GW 99.84 ft. msl
(1/4/2018)

GW 22.81 ft. msl
(RHMW07 11/2016)

GW 18.80 ft. msl
(RHMW08 11/2016)

GW 18.64 ft. msl
(RHMW09 11/2016)

0 300 600 900

SCALE FEET

Horizontal Scale: 1" = 300', Vertical Scale: 1" = 150'

Note: Vertical exaggeration = 1H : 2V (approximate)

Key Plan

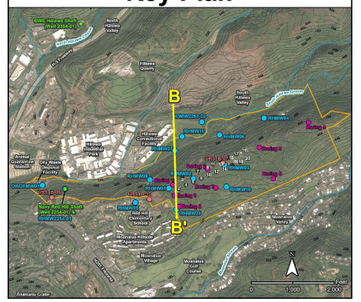

Legend

- Alluvium
- Saprolite
- Basalt - A'ā Clinker
- Basalt - Massive A'ā
- Basalt Pāhoehoe
- Measured Groundwater (date)

Notes

1. RHMW07: DON 2015a
2. RHMW09: DON 2017e
3. Hālawa No.1, 9: Macdonald 1941
4. Outcrop OC11B: Field Notes 2017
5. As-Built Barrel Log: DON 1943

S:\Projects\NAVFAC PAC\CLEAN V\60571032_CTO18F0126\GIS-Work\910 CAD\2D-SHEETS\cross-sections\Fig5-4_CrossSecB-B'.dwg 08/01/18 12:08 PM NomocL

Figure 5-4
Cross Section B-B' (View Looking East)
Conceptual Site Model
Investigation and Remediation of Releases and Groundwater Protection and Evaluation
Red Hill Bulk Fuel Storage Facility, JBPHH, O'ahu, Hawai'i

This page intentionally left blank

Key Plan

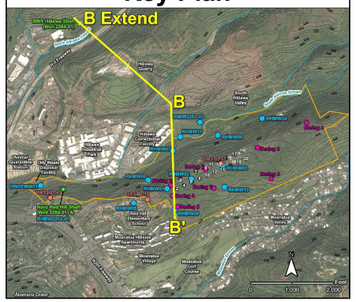

Legend

- Alluvium
- Saprolite
- Basalt - A'ā Clinker
- Basalt - Massive A'ā
- Basalt Pāhoehoe
- Measured Groundwater (date)

Notes

1. RHMW07: DON 2015a
2. RHMW09: DON 2017e
3. Hālawa No.1, 9: Macdonald 1941
4. Outcrop OC11B: Field Notes 2017
5. As-Built Barrel Log: DON 1943

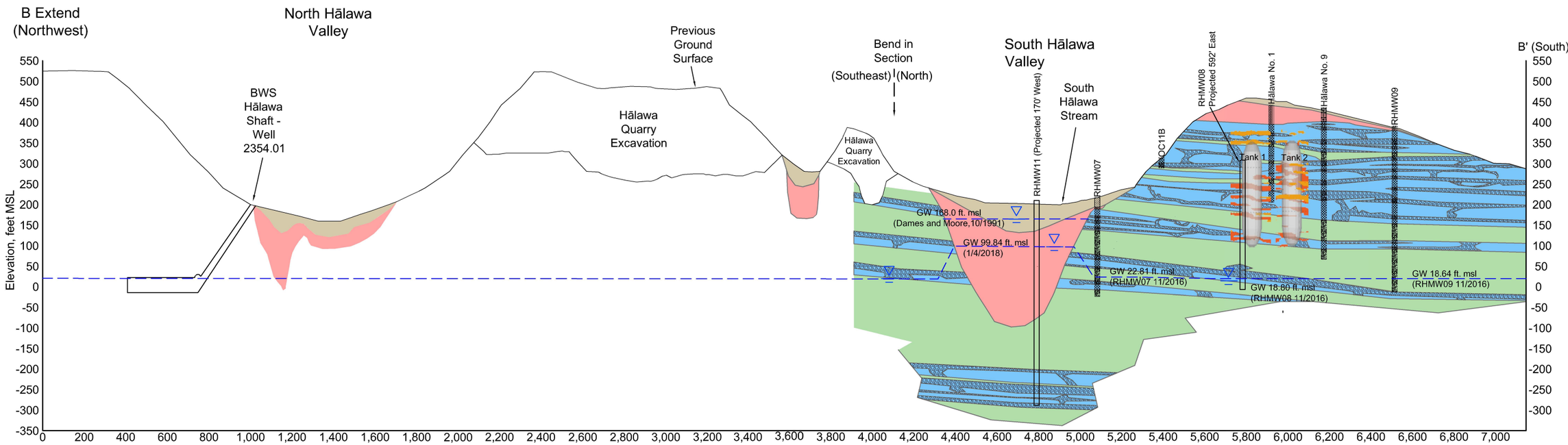

Note: Vertical exaggeration = 1H : 2V (approximate)

500' 0 500' 1000'

Horizontal Scale: 1" = 500', Vertical Scale: 1" = 250'

S:\Projects\NAVFAC PAC\CLEAN V\Rb571032_CTO18F0128\900-Work\010 CAD\20-SHEETS\cross-sections\Fig5-5_CrossSec_B-B'_Extend.dwg 08/01/18 12:12 PM NomoL

Figure 5-5
Cross Section B-B' Extended (View Looking East)
Conceptual Site Model
Investigation and Remediation of Releases and Groundwater Protection and Evaluation
Red Hill Bulk Fuel Storage Facility, JBPHH, O'ahu, Hawai'i

This page intentionally left blank

Key Plan

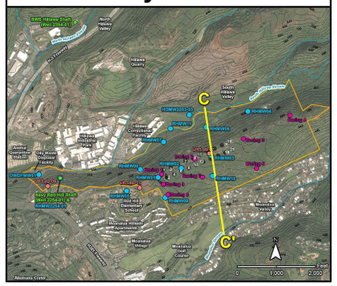

Legend

- Alluvium
- Saprolite
- Massive A'ā Basalt
- A'ā Clinker
- Pāhoehoe
- Groundwater Surface (Approximate)

Notes

1. RHMW06: DON 2015a
2. RHMW10: DON 2017e
3. B-07: DON 2012
4. Outcrops 060, OC08: Field Notes 2017

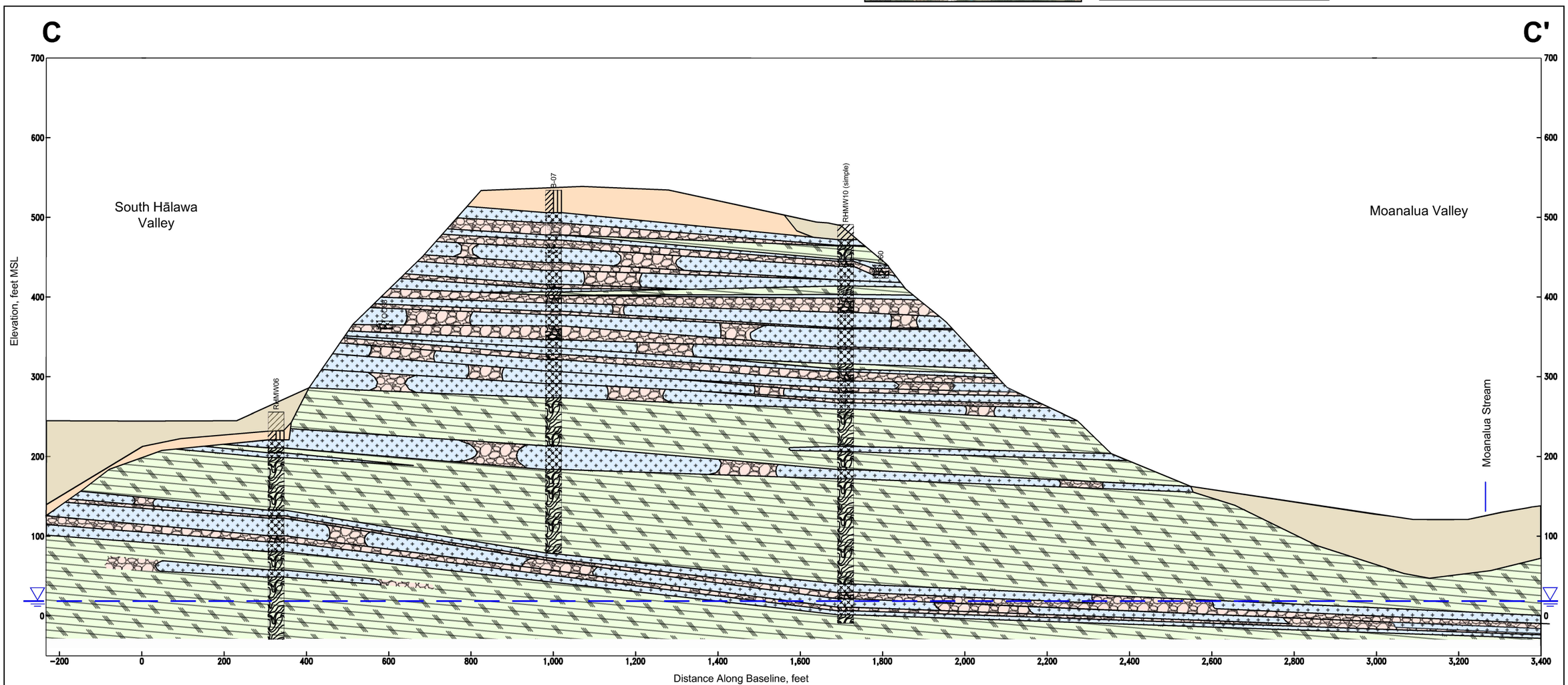

Note: Vertical exaggeration = 1H : 2V (approximate)

S:\Projects\NAVFAC PAC\JEAN V\60071092_2701RF0181\600-Work\V10 CAD\10-SHEETS\cross-sections\Fig5-6_CrossSectionC-C'.dwg 08/01/18 12:17 PM Norvell

Figure 5-6
Cross Section C - C'
Conceptual Site Model
Investigation and Remediation of Releases and Groundwater Protection and Evaluation
Red Hill Bulk Fuel Storage Facility, JBPHH, O'ahu, Hawai'i

This page intentionally left blank

Key Plan

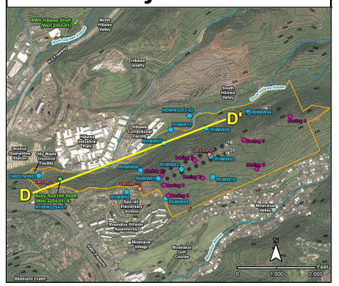

Legend

- Alluvium
- Saprolite
- Massive A'ā Basalt
- A'ā Clinker
- Pāhoehoe
- Groundwater Surface (Approximate)

Notes

1. RHMW06, RHMW07: DON 2015a
2. B-06: DON 2012

D

D'

B-06

South Hālawa Stream

South Hālawa Stream

South Hālawa Stream

RHMW07

RHMW06

?

?

Elevation, feet MSL

350
300
250
200
150
100
50
0
-50

0
500
1,000
1,500
2,000
2,500
3,000
3,500
4,000
4,500
5,000
5,500
6,000

Distance Along Baseline, feet

Note: Vertical exaggeration = 1H : 7V (approximate)

S:\Projects\NAVFAC PAC\CLEAN V\60571032_CTO18F0126\900--Work\910 CAD\20--SHEETS\cross--sections\Fig6--7_CrossSecD--D'.dwg 08/01/18 12:20 PM Nemoto

Figure 5-7
Cross Section D-D'
Conceptual Site Model
Investigation and Remediation of Releases and Groundwater Protection and Evaluation
Red Hill Bulk Fuel Storage Facility, JBPHH, O'ahu, Hawai'i

This page intentionally left blank

E

E'

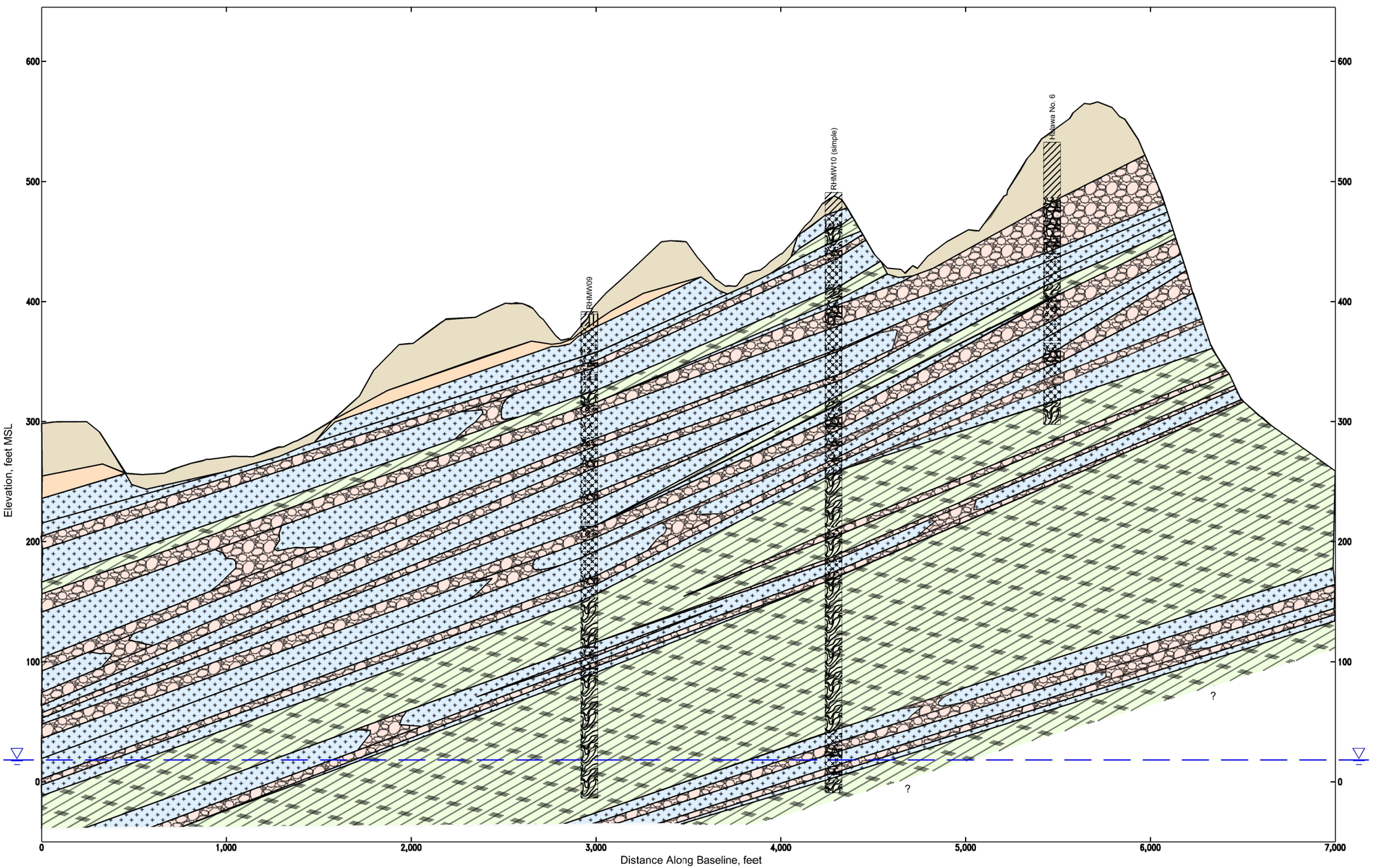

Note: Vertical exaggeration = 1H : 7V (approximate)

Key Plan

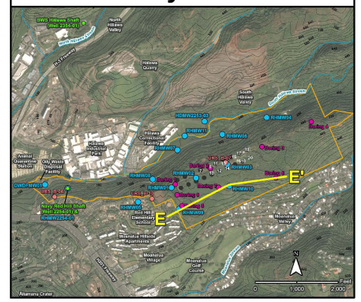

Legend

- Alluvium
- Saprolite
- Massive A'ā Basalt
- A'ā Clinker
- Pāhoehoe
- Groundwater Surface (Approximate)

Notes

1. RHMW09, RHMW10: DON 2017e
2. Halawa No.6: Macdonald 1941

S:\Projects\NAVFAC PACY\CLEAN V\60571032_CTO18\F0126\X00--Work\X10 CAD\X20--SHEETS\cross--sections\Fig5--8_CrossSectE--E'.dwg 08/01/18 12:24 PM Nomod.

Figure 5-8
Cross Section E-E'
Conceptual Site Model
Investigation and Remediation of Releases and Groundwater Protection and Evaluation
Red Hill Bulk Fuel Storage Facility, JBPHH, O'ahu, Hawai'i

This page intentionally left blank

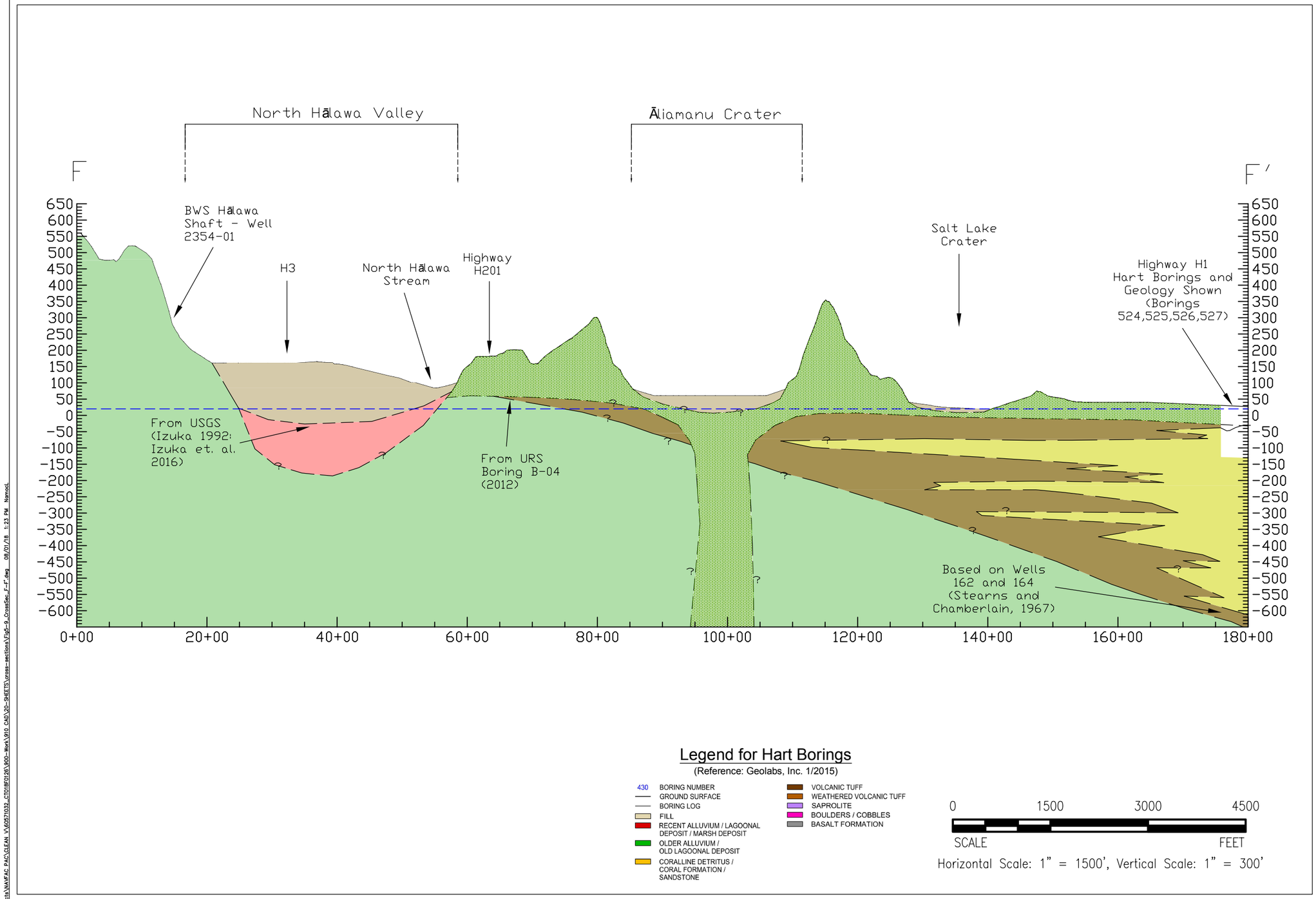

Key Plan

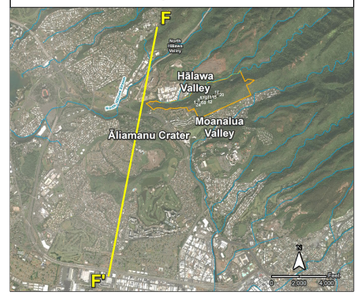

Legend

- Alluvium
- Saprolite
- Older Alluvium
- Honolulu Volcanics - Tuff
- Ko'olau Volcanic Series - Basalt & lava flows
- Coral and Coralline Sediments
- Groundwater Surface (approximate)

Legend for Hart Borings

(Reference: Geolabs, Inc. 1/2015)

- 430 BORING NUMBER
- GROUND SURFACE
- BORING LOG
- FILL
- RECENT ALLUVIUM / LAGOONAL DEPOSIT / MARSH DEPOSIT
- OLDER ALLUVIUM / OLD LAGOONAL DEPOSIT
- CORALLINE DETRITUS / CORAL FORMATION / SANDSTONE
- VOLCANIC TUFF
- WEATHERED VOLCANIC TUFF
- SAPROLITE
- BOULDERS / COBBLES
- BASALT FORMATION

0 1500 3000 4500

SCALE FEET

Horizontal Scale: 1" = 1500', Vertical Scale: 1" = 300'

S:\Projects\NAVFAC PAC\CLEAN_V\60571032_CTO18F0126\900-Work\910_CAD\20-SHEETS\cross-sections\Fig5-9_CrossSec_F-F'.dwg 08/01/18 1:23 PM Nomocl

Figure 5-9
Cross Section F-F' Āliamanu Crater Section
Conceptual Site Model
Investigation and Remediation of Releases and Groundwater Protection and Evaluation

This page intentionally left blank

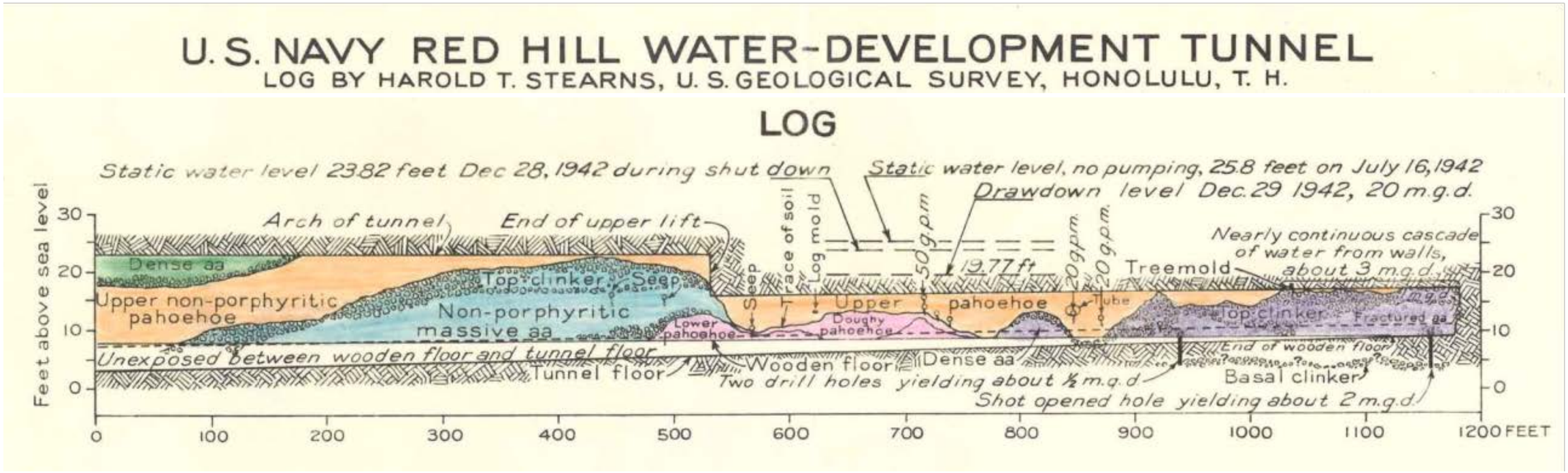

The heterogeneous nature of the basalt is revealed in the geologic log of the Red Hill Shaft water development tunnel (i.e., the infiltration gallery) prepared by the USGS (Stearns 1943).

Figure 5-10
Cross Section of Red Hill Shaft Water Development Tunnel
Conceptual Site Model
Investigation and Remediation of Releases and Groundwater Protection and Evaluation
Red Hill Bulk Fuel Storage Facility, JBPHH, O'ahu, Hawai'i

This page intentionally left blank

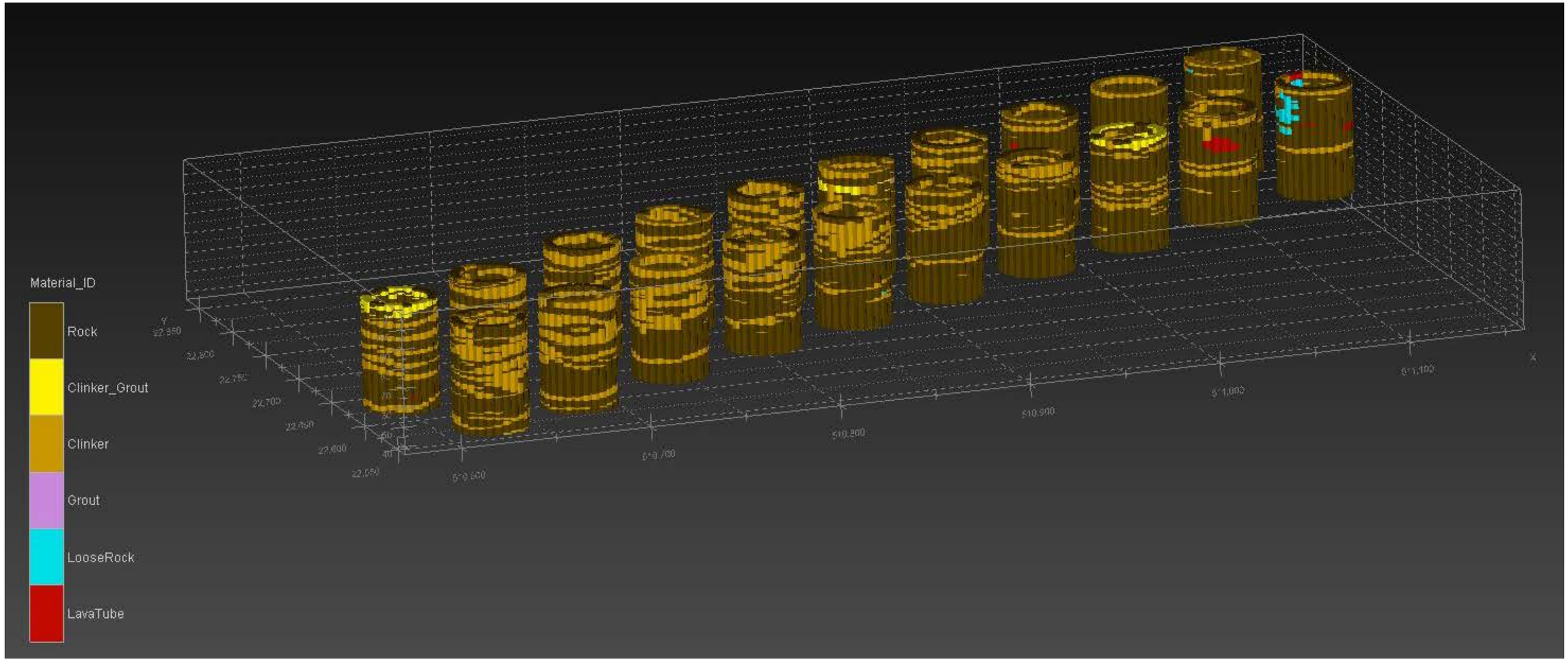

Figure 5-11
Logs of Formations in Tank Excavations (Barrel Logs)
Conceptual Site Model
Investigation and Remediation of Releases and Groundwater Protection and Evaluation
Red Hill Bulk Fuel Storage Facility, JBPHH, O'ahu, Hawai'i

This page intentionally left blank

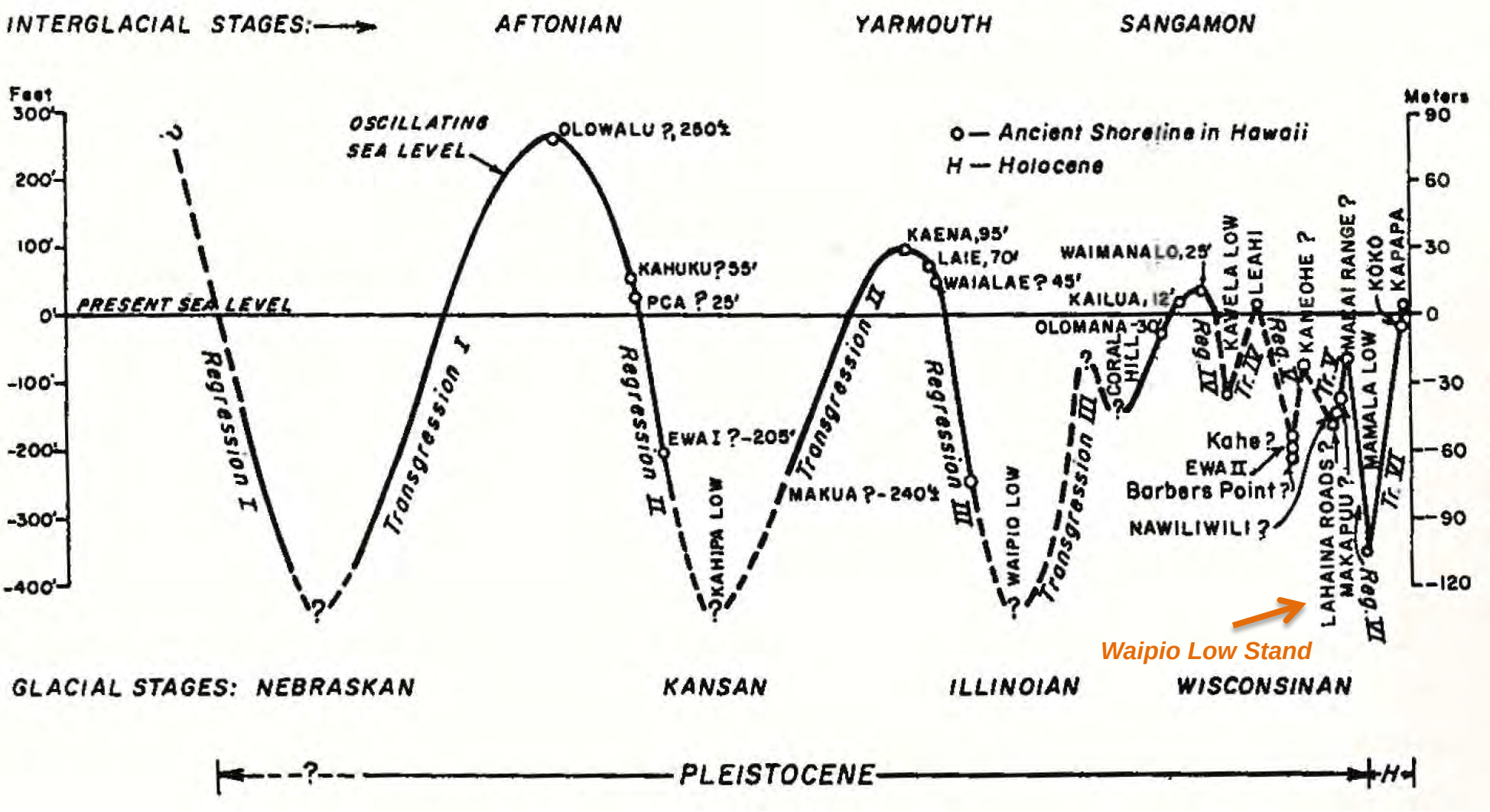

Source: Stearns (1978, Figure 1). The Waipio low stand of the sea was minus 350± feet and lasted long enough for deep erosion along major streams. It correlates with the Illinoian glacial period, about 500,000 years before present, Pleistocene age. **The drop in sea level lasted long enough for all major streams to cut their channels to levels well below present sea level along the coasts**." Stearns (1978)
Note: Sherrod et al. (2007) has mapped (after the original mapping by Stearns) the valley fill deposits as 'Older Alluvium.'

Figure 5-12
Glacioeustatic Fluctuations of Sea Level and Hawaiian Pleistocene Shorelines
Conceptual Site Model
Investigation and Remediation of Releases and Groundwater Protection and Evaluation
Red Hill Bulk Fuel Storage Facility, JBPHH, O'ahu, Hawai'i

This page intentionally left blank

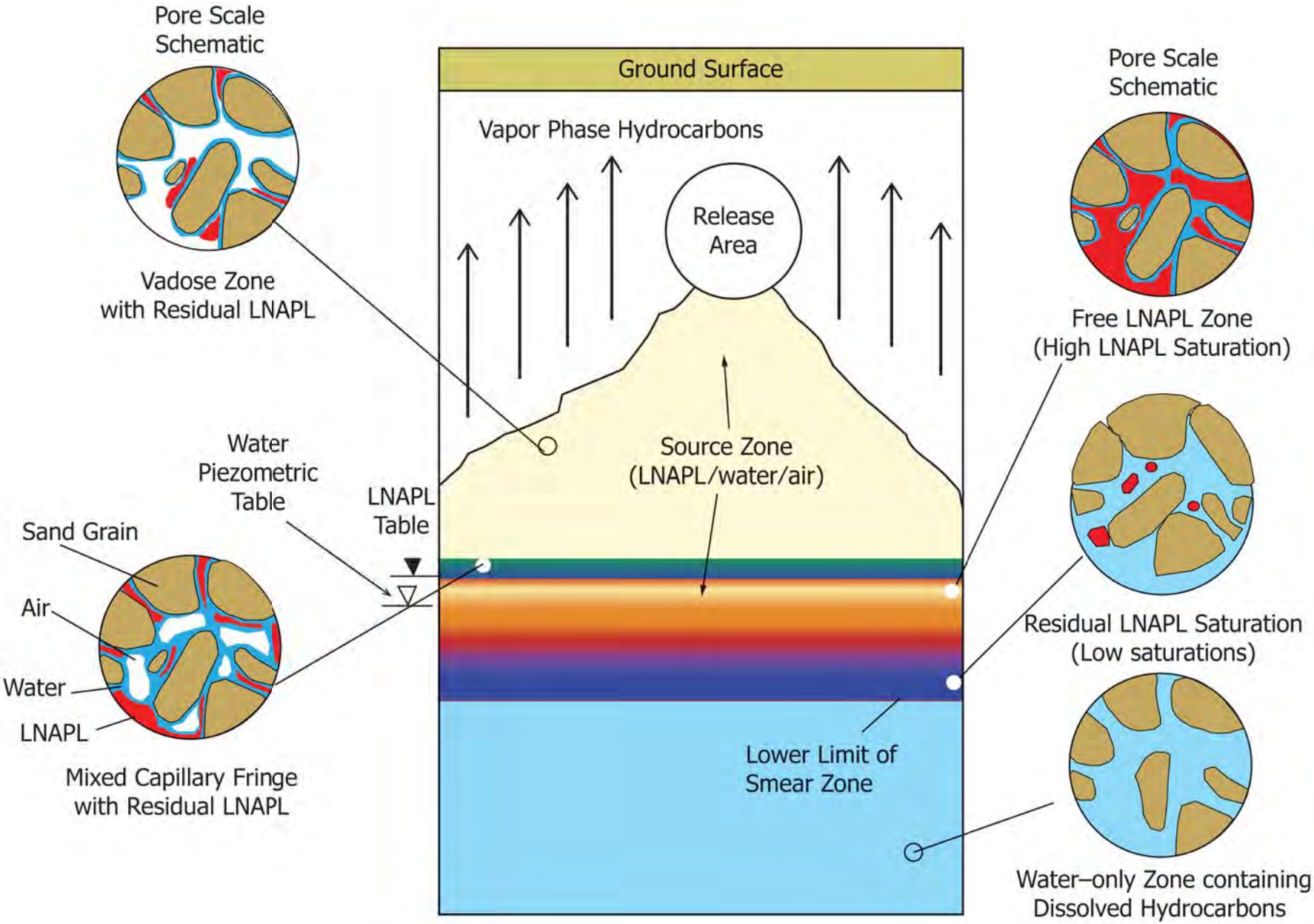

NOTE 1—During the early stages of an LNAPL release, LNAPL can be mobile (free) in all zones.
NOTE 2—The schematic is intended to convey generalized zones, not the dynamics of an active LNAPL release.

LPANL= light non-aqueous-phase liquid
COC = chemical of concern
(From Huntley and Beckett 2002)

Source: ASTM (2014b)

Figure 5-13
Micro-Scale LNAPL Vadose Zone Mobility and Retention
Conceptual Site Model
Investigation and Remediation of Releases and Groundwater Protection and Evaluation
Red Hill Bulk Fuel Storage Facility
JBPHH, O'ahu, Hawai'i

Copyright ASTM International
Provided by IHS under license with ASTM
No reproduction or networking permitted without license from IHS
Licensee=AECOM EW & Canada/5906698006; 04/24/2017 19:54:08 MDT

This page intentionally left blank

Thin bedded pāhoehoe flows are predominant in the lower section at Red Hill.

Photo 5-1
Local Geology – Pāhoehoe Flows
Conceptual Site Model
Investigation and Remediation of Releases and Groundwater Protection and Evaluation
Red Hill Bulk Fuel Storage Facility, JBPHH, O'ahu, Hawai'i

This page intentionally left blank

Erosion of the less-resistant beds, such as a‘ā clinker, has resulted in undercutting of the more resistant massive a‘ā and pāhoehoe layers.

Photo 5-2
Local Geology – Pāhoehoe Flows
Conceptual Site Model
Investigation and Remediation of Releases and Groundwater Protection and Evaluation
Red Hill Bulk Fuel Storage Facility, JBPHH, O'ahu, Hawai'i

This page intentionally left blank

Thinner bedded pāhoehoe flows are overlain by thicker, more resistant a‘ā flows.

Photo 5-3
Local Geology – Pāhoehoe Flows
Conceptual Site Model
Investigation and Remediation of Releases and Groundwater Protection and Evaluation
Red Hill Bulk Fuel Storage Facility, JBPHH, O'ahu, Hawai'i

This page intentionally left blank

Base of a‘ā lava flow

A‘ā lava flows are characterized by an interior or core of solid, dense, massive rock with exterior top and bottom coarse rubble or clinker zones. Clinker zones are similar to layers of coarse well-sorted gravel, where layered sequences of flows can result in widespread beds with high horizontal permeability. The smaller effective porosity of massive a‘ā cores can result in extremely low vertical permeability. The principal vertical permeability of a massive a‘ā core is imparted by wide, regularly spaced cooling joints, which are typically low-permeability features.

Massive core and top of a‘ā lava flow

Photo 5-4
Local Geology – A‘ā Permeability
Conceptual Site Model
Investigation and Remediation of Releases and Groundwater Protection and Evaluation
Red Hill Bulk Fuel Storage Facility, JBPHH, O'ahu, Hawai'i

This page intentionally left blank

Approximately 60% of a‘ā clinker is weathered and of relatively low permeability at Red Hill.

Photo 5-5
Local Geology – Weathered A‘ā Clinker
Conceptual Site Model
Investigation and Remediation of Releases and Groundwater Protection and Evaluation
Red Hill Bulk Fuel Storage Facility, JBPHH, O'ahu, Hawai'i

This page intentionally left blank

Saprolite outcrops in several locations on the ridge at Red Hill.

Photo 5-6
Local Geology – Saprolite
Conceptual Site Model
Investigation and Remediation of Releases and Groundwater Protection and Evaluation
Red Hill Bulk Fuel Storage Facility, JBPHH, O'ahu, Hawai'i

This page intentionally left blank

6. Module E: Saturated Zone Model

The hydrogeologic CSM provides a framework for assessing the hydrogeology of the Facility and surrounding area, and for evaluating the feasibility of investigation methodologies and potential remedial alternatives. To evaluate potential COPC migration in groundwater, the CSM describes groundwater flow in the Facility area as well as the surrounding areas that may be potentially impacted from fuel releases and includes water supply wells and shafts. Accordingly, the CSM provides the conceptual hydrogeologic basis for the numerical groundwater modeling. Specific hydrogeologic information needed for site characterization and modeling includes:

- Hydrogeologic unit (HGU) characteristics:
  - Basalt (including zones of weathered basalt/saprolite), Caprock and Valley Fill HGU geometry, and hydraulic properties
  - Perched/elevated groundwater zone areas, genesis, and potential effects on contaminant migration
  - Geologic structures that may affect groundwater flow
  - Preferred pathways for groundwater flow (e.g., clinker)
- Hydraulic heads, gradients, and groundwater flow:
  - Synoptic monitoring data to evaluate pumping and non-pumping conditions
  - Time-series hydrographs and potentiometric maps
  - External factors such as seasonal changes, barometric pressure, ocean tides, earth tides, and recharge
- Water balance for groundwater model domain:
  - Groundwater flow rates (mass flux rates) along each perimeter boundary
  - Groundwater recharge and discharge locations and rates
  - Pumping well/shaft locations, construction, and withdrawal rates

The following subsections describe the hydrogeologic CSM based on currently available data. The HGU characteristics were detailed in Section 5.

6.1 Previous Groundwater Levels and Recently Collected Hydrogeologic Data

Although useful information was provided by previous groundwater studies at the Facility, there is some uncertainty in the groundwater levels and hydraulic gradients in the site vicinity (due to extremely flat gradients and measurement error), as detailed in the *Existing Data Report* (DON 2017b) and *Data Gap Analysis Report* (DON 2017d). Resolving this uncertainty is an important objective of the site investigations now underway and the recent 2017/2018 synoptic monitoring. The following discussion is based on the data currently available. This section discusses previously collected data and data collected as part of the current investigation including:

- Aquifer pumping tests and synoptic water level studies
- Water levels measured during quarterly sampling events
- 2017 high precision survey of water level measuring point elevations

- 2017 gyroscopic survey
- 2017 seismic survey

These data are being evaluated collectively and are used to better understand the groundwater flow conditions in and around the site.

6.1.1 May 2006 Regional Aquifer Pumping Test

A regional groundwater aquifer pumping test conducted in May 2006 (DON 2007) showed that pumping of Red Hill Shaft (Navy Supply Well 2254-01) for approximately 1 week at above-average rates (approximately [redacted] mgd) lowered groundwater elevations substantially near the pumping well and created a hydraulic capture zone along the Red Hill Shaft. This pumping increased the generally gentle southwesterly gradient in the Facility area, but no response was noted in the Hālawa Deep Monitor Well (2253-03) (HDMW2253-03) located approximately 3,700 ft northeast from Red Hill Shaft. However, HDMW2253-03 is a deep open borehole that is used to monitor the freshwater / saltwater interface in the area, and this well may not respond in a manner similar to shallow water table wells in the vicinity. Other wells monitored near the Facility did show a clear hydraulic response to pumping of Red Hill Shaft. Additional discussion of the 2006 regional groundwater aquifer pumping test is presented in Sections 6.2 and 6.3.4.

During this test, the highest pumping rates reported for Red Hill Shaft approached [redacted] mgd for several periods as long as 1 day. During those periods, the largest drawdown measured at Red Hill Shaft was approximately 7 ft (DON 2007). Due to the construction of these types of tunnel wells, including both Red Hill and Hālawa Shaft, drawdown in the pools or wet wells (which are fed by water infiltration tunnels) may not be indicative of actual drawdown or heads in the aquifer. This must be considered during evaluation of data. In addition to traditional methods of aquifer testing evaluation, analysis of synoptic pumping using analytical methods, which represent line sinks, will also be considered.

6.1.2 Quarterly Groundwater Monitoring

In June 2008, monitoring began with quarterly or monthly measurements of depth to groundwater in wells RHMW01 through RHMW03. Monitoring wells RHMW04, RHMW05, OWDFMW01, HDMW2253-03, and RHMW2254-01 were subsequently added to the groundwater monitoring program. Data from the more recently installed wells are available beginning in October 2014 for RHMW06 and RHMW07, October 2016 for RHMW08 and RHMW09, May 2017 for RHMW10, and December 2017 for the new multi-level well RHMW11. Farther away from the Facility, water levels in other wells in the model domain have also been measured at various times by other agencies, including USGS and BWS.

Time-series graphs of groundwater levels (hydrographs) for select Red Hill monitoring network wells are provided on Figure 6-1 to Figure 6-3, which show temporal fluctuations attributable to seasonal variations in recharge rates and pumping of large water supply wells/shafts. Of particular interest are the plots showing the water levels in RHMW07 relative to those in other monitoring wells (Figure 6-1 and Figure 6-2) because the RHMW07 levels initially seemed to be unusually high. However, resurveying of all the wellhead measurement points has verified the accuracy of the data. Now that a sufficient period of monitoring data are available, it is clear the RHMW07 data reflect similar fluctuations over seasonal time scales, and therefore, RHMW07 appears to be hydraulically connected with the basal aquifer (see Figure 6-1 and Figure 6-2). But as will be discussed later, RHMW07 did not respond to short-term 2017/2018 synoptic monitoring pumping as did the other Red Hill area wells. RHMW07 also had a differing barometric response than the other Red Hill area

wells. The time-series graphs for monitoring wells RHMW02 and RHMW03 beneath the storage tanks at the Facility shown on Figure 6-3 reflect seasonal fluctuations and the pumping effects of Red Hill Shaft. The noticeable uptrend in water levels in these wells that began in early 2016 is attributable to the pump problems at Red Hill Shaft that curtailed pumping through November 2016 (Figure 6-3).

Groundwater levels at RHMW07 are higher than at wells further south in the Facility area. As evidenced by barometric responses and water level responses during the 2017/2018 synoptic water monitoring period, there may be a partial impediment to hydraulic communication between this well and the basal aquifer in which the surrounding Red Hill monitoring wells are completed. Additionally, the potential for higher groundwater recharge rates in the cement plant and quarry area, other natural recharge processes such as direct infiltration of rainfall and streambed seepage, and the barrier effect of the deeply weathered basalt/saprolite could be contributing to the higher hydraulic head observed in RHMW07. Based on available data, geologic information, and field observations, groundwater levels at RHMW07 may need to be further evaluated. Considering that all these Red Hill monitoring wells are completed in the basal aquifer, with screen intervals at approximately the same elevations, a possible explanation for the higher groundwater levels at RHMW07 is the barrier effect of the recently discovered deep saprolite zone at RHMW11, as described further in Section 6.1.4.

Groundwater elevations in HDMW2253-03 may not represent water table conditions because this well is constructed as an open borehole that extends deep below the freshwater lens. HDMW2253-03 was purposely constructed with an open zone from 250 to 1,575 ft bgs to monitor the depth and thickness of the saltwater/freshwater transition zone. Water levels in HDMW2253-03 are typically a few tenths of a foot higher than the chase tube completed with an open pipe in the annular space between the inner casing and the borehole at an elevation approximately equal to the regional basal aquifer water level. Also, as described in Section 6.7, the water in the deep monitoring well is saltier than in the surrounding groundwater. These factors indicate that deeper, saltier, groundwater may be rising up through HDMW2253-03 and discharging into the fresh basal aquifer.

6.1.3 November 2016 Synoptic Monitoring

In November 2016, wells in the primary area of interest were measured during a synoptic monitoring event by the USGS and the Navy. Water level data from this event are shown on Figure 6-5. Red Hill Shaft had been shut down in February 2016 due to mechanical problems, and through November 2016, only occasional, very limited short-term pumping was reported by the Navy. Thus, these synoptic data reflect non-to-very-limited-pumping conditions for Red Hill Shaft while Hālawa Shaft pumping continued at relatively low operational rates, typical for November.

6.1.4 Recently Collected Hydrogeologic Data

New Westbay monitoring well RHMW11 was drilled and constructed in late 2017 in accordance with the Red Hill *Monitoring Well Installation Work Plan* (DON 2016b). At the RHMW11 location, low-permeability saprolite, which consists of clay-rich materials and weathered basalt, extends to a depth of approximately 87 ft below the regional basal groundwater table (as recorded at the time of drilling). RHMW11 was completed with eight discrete sampling intervals (also referred to as zones) that are independently sealed and isolated using a series of Westbay System packers (as illustrated on Figure 6-4). The well is constructed with Zone 1 being the deepest zone, each subsequent zone being completed at a shallower depth, and Zone 8 being the uppermost or shallowest zone (DON 2018c). New hydraulic head data have been obtained from RHMW11 that show the water table in the upper saprolite is actually much higher than previously estimated at that location. The upper three sampling intervals (Zone 6 through Zone 8) show there is a continuously saturated zone within the saprolite

(Figure 6-4). The uppermost interval (Zone 8) shows the water table elevation is at approximately 108 ft msl, as of June 2018. The five deeper sampling intervals (Zone 1 through zone 5) in RHMW11 are completed in unweathered basalt at depths below the saprolite. Hydraulic head measurements in those zones are approximately 18–19 ft msl (Figure 6-5). The hydraulic head data from RHMW11 also show a pronounced downward hydraulic gradient (with a minor exception in the case of Zone 3), which is much stronger downward within the saprolite zone than in the unweathered basalt aquifer.

Table 6-1: RHMW11 Westbay Zone Summary

Zone Identifier	Zone Top (ft bgs)	Zone Bottom (ft bgs)	Zone Top (elevation ft msl)	Zone Bottom (elevation ft msl)	Generalized Geology	Zone Water Level (elevation ft msl)
Zone 8	159.3	204.5	51.06	5.86	Saprolite	105.55
Zone 7	209.8	239.8	0.56	-29.44	Saprolite	70.97
Zone 6	245.0	255.5	-34.64	-45.14	Saprolite	66.40
Zone 5	277.3	290.3	-66.94	-79.94	Basalt	18.49
Zone 4	330.5	342.8	-120.14	-132.44	Basalt	18.48
Zone 3	347.8	367.0	-137.44	-156.64	Basalt	18.26
Zone 2	394.0	420.3	-183.64	-209.94	Basalt	18.41
Zone 1	450.3	469.5	-239.94	-259.14	Basalt	18.00

Notes: Approximate land surface elevation = 210.36 ft msl.
Water levels reported in zones measured on 3/5/2018.

The saprolite zone encountered at RHMW11 creates a barrier to groundwater flow because of the lower hydraulic conductivity of the saturated clayey weathered basalt material and higher groundwater levels, as also evidenced by seismic refraction and reflection profiles obtained in the valley as discussed in Section 6.1.8 (DON 2018d). Pneumatic testing of select zones in RHMW11, including Zones 6, 7, and 8, was conducted following well construction (DON 2018c). Pneumatic test data from RHMW11 zones 6, 7 and 8 were treated like slug withdrawal tests and analyzed using three different techniques (Hvorslev 1951; Bouwer and Rice 1976; Hilton H. Cooper, Bredehoeft, and Papadopulos 1967). Tests in Zones 6, 7, and 8, as well as laboratory analysis of cores collected during drilling from the borehole in Zone 8, show that the hydraulic conductivity of saprolite and weathered basalt in the upper three sampling intervals is very low compared to unweathered basalt (see Table 6-2). The subsurface extent of this saprolite barrier away from RHMW11 and the seismic lines is not well known. However, this saprolite zone most likely formed beneath a deeply incised paleo-valley below the present-day South Hālawa Stream. Thus, the deep saprolite zone likely trends generally east to west, which is consistent with the geologic log of HDMW2253-03 that also shows deep weathered basalt (saprolite) extending to a roughly similar depth as at RHMW11. Higher groundwater recharge rates in the area north of RHMW07 (e.g., infiltration in the Ko'olau Mountains, streambed, and quarry pond/impoundment infiltration) may also contribute to the higher groundwater levels at RHMW11 and RHMW07. Recharge rates are likely higher in the upslope areas of the Ko'olau Mountains where precipitation rates increase and low permeability saprolite layers over the basalt are absent or thin.

Table 6-2: RHMW11 Hydraulic Conductivity Estimates Derived from Pneumatic Testing and Laboratory Analyses

Slug Test Zone	K (Hvorslev 1951) ft/d	K (Hvorslev 1951) cm/sec	K (Bouwer & Rice 1976) ft/d	K (Bouwer & Rice 1976) cm/sec	K (Cooper et al. 1967) ft/d	K (Cooper et al. 1967) cm/sec	Date	Zone Geology / Feature
Zone 8	9.2E-02	3.2E-05	1.0E-01	3.5E-05	7.1E-02	2.5E-05	12/13/2017	Saprolite
Zone 7	1.2E-01	4.2E-05	1.3E-01	4.6E-05	1.1E-01	3.8E-05	12/9/2017	Saprolitic clinker zone
Zone 7	2.6E-01	9.2E-05	2.8E-01	9.9E-05	2.7E-01	9.7E-05	12/11/2017	Saprolitic clinker zone
Zone 6	3.4E-01	1.2E-04	2.8E-01	9.9E-05	1.7E-01	6.0E-05	12/7/2017	Saprolite
Zone 5	—	—	—	—	—	—	—	Lava tube
Zone 4	—	—	—	—	—	—	—	Pāhoehoe
Zone 3	—	—	—	—	—	—	—	Pāhoehoe
Zone 2	—	—	—	—	—	—	—	Clinker zone
Zone 1	—	—	—	—	—	—	—	Clinker zone
Minimum	9.2E-02	3.2E-05	1.0E-01	3.5E-05	7.1E-02	2.5E-05		
Maximum	3.4E-01	1.2E-04	2.8E-01	9.9E-05	2.7E-01	9.7E-05		

RHMW11 Laboratory Test Results

Tested Zone	Core Depth (ft bgs)	K (ft/d)	K (cm/sec)	Sample ID	Zone Geology / Feature
Zone 8	162.6–163.6	2.49E-05	8.8E-09	ERH443B-V	Saprolite
Zone 8	162.6–163.6	2.21E-05	7.8E-09	ERH443B-H	Saprolite
Zone 8	174.3–175.0	1.26E-05	4.5E-09	ERH443C-V	Saprolite
Zone 8	174.3–175.0	1.57E-05	5.5E-09	ERH443C-V	Saprolite
Zone 8	189.5–190.0	8.50E-05	3.00E-08	ERH443D-V	Saprolite
Zone 8	189.5–190.0	7.99E-06	2.82E-09	ERH443D-H	Saprolite
	Minimum	7.99E-06	2.8E-09		
	Maximum	8.50E-05	3.0E-08		

— no data; slug test data from these intervals could not be evaluated due to high hydraulic conductivity of the basalt.
K hydraulic conductivity

Based on the existence of the saprolite in the upper three zones at RHMW11, it is concluded that the unweathered basalt basal aquifer beneath the saprolite is under confining conditions. While the majority of the monitoring wells within the Red Hill monitoring network appear to be in unconfined conditions, there are a few notable exceptions in addition to RHMW11. These exceptions are:

- RHMW07
- OWDFMW01
- Hālawa Deep Monitor Well (2253-03)

Wells completed in neighboring valleys (e.g., Moanalua) may also be completed in confined conditions beneath saprolite, but there are limited data to support a definitive conclusion. Wells completed in the caprock closer to the coast may also be in confined conditions, but are not the principle focus of this analysis.

Other wells have uncertain completion, and therefore, it is difficult to draw conclusions from the data. These wells include:

- Moanalua DH43
- Hālawa Deep Monitor Well Chase Tube

6.1.5 2017 High Precision Well Survey

As many as four wellhead surveys have been conducted for the Red Hill monitoring wells at different times. In addition, the measuring points used over the years to determine water elevations may have changed for individual wells, and there may be differences in measuring points used by various contractors. Results of the high precision survey conducted in Summer–Fall 2017 address this issue for future monitoring (DON 2018a). However, past groundwater elevations should be used with caution when evaluating absolute groundwater elevations, but may be appropriate for evaluating trends.

6.1.6 Gyroscopic Corrections

Well gyroscopic field surveys, three-dimensional modeling of gyroscopic data, and evaluation of gyroscopic data were conducted to determine if any of the wells deviate from true vertical and, if deviations occur, to calculate correction factors that can be applied to groundwater level measurements for true vertical depths. As depicted in Driscoll (1986, Figure 10.66), wells are typically neither perfectly plumb nor perfectly aligned. Assessment of the plumbness and alignment of each well is required to determine the degree to which a well's apparent depth deviates from its actual depth. Because the hydraulic conductivity of the regional basal aquifer in the Red Hill area is so high, relatively flat groundwater gradients are developed. Since groundwater flows from high hydraulic head to low hydraulic head, highly accurate water level elevations are needed to develop an understanding of local and regional gradients. The following wells are evaluated in this CSM: RHMW02 – RHMW10, HDMW2253-03, OWDFMW01, and RHMW11 (multi-level well). The calculated correction factors (Table 6-3) were provided to the USGS on May 1, 2018. The USGS used the results of the high-precision survey and gyroscopic corrections in the water level elevations on the National Water Information System (NWIS) website for the 2017/2018 synoptic monitoring.

Table 6-3: Summary of Gyroscopic Survey Results and Calculated Tape Correction Factors

Well ID	Survey Y (State Plane Zone 3 NAD 1983 ft) [a]	Survey X (State Plane Zone 3 NAD 1983 ft) [a]	Survey Top of Casing (Z) (ft msl) [a]	Inside Diameter of Well (inches) [b]	Measured Depth to Water with Tape from Top of Casing (ft bgs) [c]	3D Model of Vertical Plumb Depth (ft bgs)	Tape Correction Factor (ft)
RHMW02	74282.05	1675639.24	104.60	1.94	85.54	85.48	-0.06
RHMW03	74610.90	1676391.37	120.90	1.94	101.78	101.74	-0.04
RHMW04	75742.78	1677345.53	312.11	3.83	293.03	293.01	-0.02
RHMW05	73690.63	1674268.20	101.31	1.93	82.18	82.17	-0.01
RHMW06	75327.62	1676274.46	259.09	3.81	240.28	240.27	-0.01
RHMW07	74964.68	1675189.75	220.39	3.81	197.58	197.57	-0.01
RHMW08	74257.02	1674635.42	310.43	3.81	291.63	291.60	-0.03
RHMW09	73527.70	1675221.52	395.37	3.81	376.73	376.49	-0.24
RHMW10	74066.93	1676410.03	495.59	3.81	476.45	476.36	-0.09
HDMW2253-03	75654.10	1675867.45	226.68	8.00	206.80	206.79	-0.01
OWDFMW01	74112.72	1671997.20	138.14	3.81	119.07	119.04	-0.03
RHMW11(Westbay) Zones 1–5	75290.37	1675370.69	211.26	1.40	191.37	191.28	-0.09

Well ID	Survey Y (State Plane Zone 3 NAD 1983 ft) [a]	Survey X (State Plane Zone 3 NAD 1983 ft) [a]	Survey Top of Casing (Z) (ft msl) [a]	Inside Diameter of Well (inches) [b]	Measured Depth to Water with Tape from Top of Casing (ft bgs) [c]	3D Model of Vertical Plumb Depth (ft bgs)	Tape Correction Factor (ft)
RHMW11(Westbay) Zone 6	75290.37	1675370.69	211.26	1.40	139.26	139.19	-0.07
RHMW11(Westbay) Zone 7	75290.37	1675370.69	211.26	1.40	136.03	135.97	-0.07
RHMW11(Westbay) Zone 8	75290.37	1675370.69	211.26	1.40	107.13	107.08	-0.05

NAD North American Datum
[a] Source: *Well Elevation Survey Report* (DON 2018a)
[b] Source: Monitoring well construction logs
[c] Source: *Final Fourth Quarter 2017 - Quarterly Groundwater Monitoring Report* (DON 2018b) and recently collected field data for RHMW11

6.1.7 2017/2018 Synoptic Monitoring

From July 2017 through March 2018, depth to water wells in the primary area of interest were measured during a synoptic monitoring event by the USGS, BWS, and Navy. The *Final Synoptic Water Level Study Work Plan* dated August 10, 2017 from the USGS lays out this program (USGS 2017e). The purpose of the continuous water-level monitoring was to provide data that will lead to an improved understanding of the groundwater-flow system in the Hālawa area. Groundwater levels were monitored in 23 wells to document spatial and temporal variations in groundwater levels under typical and controlled withdrawal conditions. An attempt was made to coordinate controlled withdrawal conditions designed to provide data that can be used to interpret the short-term, aquifer-wide response of the aquifer to withdrawals. However, the USGS could not mandate specific withdrawal conditions because overriding water-purveyor constraints related to meeting water demand limited the water-purveyors' ability to maintain the exact planned rates of withdrawal. Most groundwater-level data collected as part of this effort were made publicly available online through the NWIS database. Groundwater levels were monitored for multiple months in 23 wells in the Hālawa, Moanalua, and 'Aiea areas. Data were recorded at 10-minute intervals. Details of the monitoring plan are provided below.

The pumping scenarios were as follows:

1. Withdrawing water from Moanalua Wells 1, 2, and 3 at a high rate while both Hālawa Shaft and Red Hill Shaft withdraw water at typical rates.
2. Allowing Red Hill Shaft to recover for approximately 5 days while Hālawa Shaft pumped at a near constant rate.
3. Withdrawing water from Red Hill Shaft at a nearly steady rate for approximately 4.5 days while Hālawa Shaft was withdrawing water at a typical and near constant rate.
4. Allowing Hālawa Shaft to recovery for approximately 10 days while Red Hill Shaft was pumping under normal operational conditions (on and off in response to water system demands).

5. Withdrawing water from Hālawa Shaft at a high rate for 10 days while Red Hill Shaft was pumping under normal operational conditions.
6. Withdrawing water from Hālawa Shaft at a normal rate while Red Hill Shaft was pumping under normal operational conditions.

Groundwater levels were monitored in 23 existing wells in the Hālawa area. The 23 wells include two wells that are actively being monitored for groundwater levels by the BWS using shaft encoders. The Navy has requested but not yet received these data. Near the end of the synoptic monitoring period, transducers were also installed in a shallow monitoring well (UMW-1) at the Hālawa Correctional Facility. Monitoring in RHMW11 consisted of Westbay pressure transducers in all 8 zones of RHMW11, and a vented pressure transducer in the Westbay center tube with pumping port 8 open, monitored by the USGS. Based on the *Final Synoptic Water Level Study Work Plan* (USGS 2017e), the USGS is expected to issue a draft report documenting the data collected during the monitoring period. The non-interpretive report will be provided to SMEs for comment (two-week comment period) and will follow the standard USGS review, approval, and publication process. The final report is expected to be published and made available on the internet in 2018.

The well and transducer information is summarized in Table 6-4.

Table 6-4: Well and Transducer Information

DLNR ID	USGS SITE ID	Well ID	Transducer
3-2153-05	212123157535501	Moanalua Deep	700H vented
3-2153-13	212144157534701	TAMC-MW2	700H vented
3-2253-02	212225157533001	Moanalua DH43	700H vented
3-2253-03	212241157535502	Hālawa Deep Monitor Well Chase Tube	700H vented
3-2253-03	212241157535501	Hālawa Deep Monitor Well (2253-03)	700H vented
3-2253-04	212226157534101	RHMW06	700H vented
3-2253-05	212222157535201	RHMW07	700H vented
3-2254-01	212225157542601	Red Hill Shaft	700H vented
3-2254-02M	212229157541501	UMW-1	700H vented
3-2255-32	212253157554301	ʻAiea Hālawa Shaft	700H vented
3-2255-40	212233157552302	Hālawa BWS Deep Monitor	700H vented
3-2256-10	212238157561101	ʻAiea Navy	700H vented
3-2354-01	212305157542601	Hālawa Shaft	700H vented
3-2355-15	212340157552301	Kaʻamilo Deep	700H vented
—	212214157542601	OWDFMW01	700H vented
—	212214157535401	RHMW01	700 non-vented
—	212216157534701	RHMW02	700H vented
—	212219157533901	RHMW03	700H vented
—	212231157532901	RHMW04	700H vented
—	212210157540201	RHMW05	700H vented
—	212216157535801	RHMW08	700H vented
—	212209157535201	RHMW09	700H vented
—	212213157533901	RHMW10	700H vented
3-2253-11	212226157535001	RHMW11 - Zone 8	700H vented
3-2253-11	212226157535001	RHMW11 - Zone 8	nonvented MOSDAX
3-2253-11	212226157535001	RHMW11 - Zone 7	nonvented MOSDAX
3-2253-11	212226157535001	RHMW11 - Zone 6	nonvented MOSDAX

DLNR ID	USGS SITE ID	Well ID	Transducer
3-2253-11	212226157535001	RHMW11 - Zone 5	nonvented MOSDAX
3-2253-11	212226157535001	RHMW11 - Zone 4	nonvented MOSDAX
3-2253-11	212226157535001	RHMW11 - Zone 3	nonvented MOSDAX
3-2253-11	212226157535001	RHMW11 - Zone 2	nonvented MOSDAX
3-2253-11	212226157535001	RHMW11 - Zone 1	nonvented MOSDAX
2255-033	—	Hālawa T-45	shaft encoder
2153-009	—	Manaiki T24	shaft encoder
2-2153-10	—	Moanalua 1	—
3-2153-11	—	Moanalua 2	—
3-2153-12	—	Moanalua 3	—
3-2153-07	—	TAMC1	—
3-2153-08	—	TAMC2	—

— no data available or not applicable

Data from the transducers were evaluated by the USGS, and those that did not meet their acceptance criteria were not released in the final approved dataset. Unfortunately, the data from both the primary and backup transducers in Red Hill Shaft did not meet USGS acceptance criteria during the period of recovery and pump testing of Red Hill Shaft, and therefore, no data are available for that period.

The Navy is continuing to evaluate the recent synoptic data. This evaluation is ongoing. Once the analysis is complete, it will be integrated into an updated CSM or future report.

6.1.8 2017 Seismic Survey

Nine seismic profiles were acquired in the Red Hill area over 9 days in December 2017 (DON 2018d). The objectives were to map stratigraphy and hydrogeologic boundaries beneath three valleys: North Hālawa Valley (Transects A, B, and C); South Hālawa Valley (Transects D, E, F, and G); and Moanalua Valley (Transects H and I). Seismic data quality were generally very good with: 1) clear first arrivals needed to obtain shallow seismic velocity distributions and 2) observable reflections noted between surface wave and seismic refraction signals to map large-contrast subsurface boundaries. Seismic refraction results constrain seismic velocities for the upper 100 ft and tie those velocities to nearby well logs and to other published results from Hawai'i to help constrain travel time to depth conversions for the seismic reflection results. Seismic reflection results show the geometry and depth to key hydrostratigraphic boundaries within the upper 1,000 ft below land surface. Key reflectors include the base of alluvium or top of saprolite, top of water saturated (possibly perched) sediments, and the contact between weathered basalt (saprolite) and unweathered basalt.

Valley fill sediments are constrained to the upper 60 ft below land surface in all three valleys. Saturated and/or competent saprolite are mapped from surface to hundreds of feet bgs. Those observations are consistent with v- and/or u-shaped saprolite base geometries across the valleys with the maximum saprolite thickness below surface stream flow locations. The saprolite base extends to hundreds of feet below sea level in portions of North and South Hālawa Valleys. The depth to the base of the saprolite was constrained by only one short profile beneath Moanalua Valley. The depth to these key hydrostratigraphic boundaries in South Hālawa Valley are consistent with lithologic log interpretations from nearby monitoring wells. The seismic images could not detect the geometry or depth of the regional or basal water table, in part due to shallow and confined perched water systems and the lack of large physical property contrasts (seismic velocity and density) at this basal water

system boundary. The seismic images also do not constrain volcanic stratigraphy (e.g., individual volcanic flows, lava tubes) beneath the top of unweathered basalt unit due to complexities in the seismic wavefield within this layered basalt system.

The Red Hill seismic survey yielded information on key hydrostratigraphic boundaries in the valleys. The seismic velocity and reflection results from this study allow definition of four hydrostratigraphic units. Seismic velocities that are consistent with dry alluvium, as measured by seismic velocities less than 1,000 meters per second (m/s), extend up to 60 ft deep in all three valleys. These shallow alluvial sediments overlie saprolite, as defined by velocities between 1,000 and 1,500 m/s. The thickness of dry saprolite layer ranges from 0 to 100 ft thick. With increasing depth and rock density, saprolite increases in seismic velocity to greater than 1,500 m/s. Also, with saturation, seismic velocities in both alluvium and saprolite exceed 1,500 m/s. These zones extend in depth for a few hundred feet beneath portions of all three valleys. Unaltered basalts exceed a seismic velocity of 3,000 m/s. These velocities are observed along the valley margins and at depth beneath each valley. The highly weathered volcanic rocks extend to about 300 ft below sea level beneath portions of North Hālawa and South Hālawa valleys. The depth and saprolite base geometry is less constrained beneath Moanalua Valley. The greatest depth to saprolite base is consistent with the surface expression of the streams that drain the valleys. These transects and interpretations were used to refine the CSM.

6.2 HYDRAULIC GRADIENTS AND GROUNDWATER FLOW DIRECTIONS

Groundwater levels near the Facility are strongly influenced by local heterogeneities and the pumping rates and locations of large-capacity supply wells, as indicated by the results of three regional pumping tests conducted in May 2006, May 2015, and July 2017 through March 2018. Notwithstanding the local heterogeneities, in a larger sense groundwater flow follows the regional flow patterns.

6.2.1 May 2006 Pumping Test

The results from the regional groundwater pumping test of Red Hill Shaft conducted in May 2006 did not indicate any hydraulic response in wells on the northern edge of South Hālawa Valley during pumping of Red Hill Shaft (DON 2007); however, monitoring points in that area were sparse. Conversely, wells monitored near the Facility did show a clear hydraulic response to pumping of Red Hill Shaft. Even though data points were sparse to the north of the Facility, the evaluation of the May 2006 pumping test suggested that a groundwater barrier may exist beneath South Hālawa Valley (DON 2007).

In 2010, the Navy re-evaluated groundwater level measurements collected in May 2006 (DON 2007) to prepare revised water table potentiometric maps for the site area for pumping and non-pumping conditions (DON 2010). Those data show that when the Navy was operating Red Hill Shaft at normal capacity (pumping approximately [redacted] mgd), the principal hydraulic gradient was toward the southwest from the tank farm area toward Red Hill Shaft. The report also suggested the hydraulic gradient from the area just north of the Facility may be toward the west-northwest (DON 2010). The report also indicated the southwesterly gradient was approximately 0.00022 (foot per foot [ft/ft]), and the northwesterly gradient appeared to be less.

6.2.2 May 2015 Pumping Test

During May 2015, the USGS and BWS conducted a pumping test of the Hālawa Shaft while monitoring water level elevations in a number of monitoring wells. These wells included Hālawa T-45, OWDFMW01, RHMW04, RHMW07, Moanalua DH43, TAMC-MW2, and Moanalua Deep.

Pumping rates at Hālawa Shaft and Red Hill Shaft during May 2015 and time-series plots of water level data available from monitoring wells are shown on Figure 6-6.

For the May 2015 test, pumping of BWS Hālawa Shaft was suspended during the period of May 8–13, 2015. Subsequently, Hālawa Shaft was pumped at a much higher rate, approximately 14 mgd, for the period of May 14–20, 2015. The pumping rate decreased starting on May 21 to approximately 8–9 mgd, then held steady at approximately 6 mgd during May 23–28. Red Hill Shaft pumping rates varied substantially on a daily basis throughout May 2015, as shown on Figure 6-7.

Variations in pumping rates from Hālawa Shaft and Red Hill Shaft during the May 2015 pumping test tend to complicate and obscure relationships between pumping rates and the measured drawdowns. Data were not collected from several monitoring wells in the Red Hill area. Both of these limitations create uncertainty in evaluating the available data. Nonetheless, the May 2015 pumping test data support these observations:

- Groundwater levels fluctuated daily by small amounts (approximately 0.1 ft) in both Red Hill monitoring wells located adjacent to South Hālawa Valley (RHMW04 and RHMW07).
- There appear to be water level fluctuations attributable to barometric pressure changes at both RHMW04 and RHMW07 that are a large part of the total daily fluctuations.
- The barometric effects appear to be larger at RHMW07 than RHMW04; however, there are other factors that may cause such minor fluctuations, such as transducer properties and electronic/strain gauge drift.
- During the test period, RHMW04 showed an overall water level decline (i.e., water level at beginning of test compared to water level at end of test) of approximately 0.1 ft, while well RHMW07 showed an overall decline of about 0.05 ft.
- The largest groundwater level increase during this period was about 0.35 ft (RHMW04), when the pumping rate at Hālawa Shaft stopped during May 7–14 and Red Hill Shaft was pumping daily at rates varying from [redacted] mgd.
- The largest water level decline was about 0.45 ft (RHMW04) between May 14 and May 21, 2015 when Hālawa Shaft was pumping the maximum rate of approximately 14 mgd and Red Hill Shaft was pumping daily at rates varying from [redacted] mgd.

Overall, the data from the May 2015 pumping test indicate that pumping both these water supply sources, Hālawa Shaft and Red Hill Shaft, affect groundwater levels in the South Hālawa Valley area. These water level changes were relatively small in magnitude.

6.2.3 November 2016 Synoptic Monitoring

Observations related to water level elevations calculated for this synoptic monitoring event are consistent with observations for other similar monitoring events. The absence of steep gradients at the site and near the vicinity is consistent with the presence of very high hydraulic conductivity zones in the regional basal aquifer. With the exception of wells RHMW07, HDMW2253-03, and DH43, the data reflect a very low hydraulic gradient along and in the vicinity of Red Hill ridge (RHMW01 through RHMW05 and OWDFMW01) with groundwater elevations of approximately 19 ft msl with slightly lower elevations immediately to the north (RHMW06 and RHMW08) and south (RHMW09) of the tank farm. The groundwater elevations decrease to the west toward Pearl Harbor to approximately 17 ft msl. Because pumping from Red Hill Shaft had been minimal in the preceding months, this distribution of hydraulic heads at the site represents a minimally stressed system. However, in the absence of strong gradients, the groundwater flow direction cannot be

determined with great confidence. Rather, the observation for other events holds true for this event: hydraulic heads along the ridge are slightly higher than the adjacent flanks. The significance of this distribution of heads has not yet been fully defined.

6.2.4 2017/2018 Synoptic Monitoring

All of the wells were monitored with vented (i.e., gauged on differential) transducers, except RHMW01, which was too small in diameter to accommodate a vented transducer. Instead a smaller-diameter non-vented (i.e., absolute or total) transducer was used in RHMW01. The USGS installed a vented transducer in the center tube of RHMW11, which was opened to the Zone 8 pumping port. Separately non-vented transducers were locked into each of the 8 zones. These zones are different from all of the other wells because the other wells are open to atmosphere at the top. However, for the synoptic water level study, the pumping port in Zone 8 was open to allow monitoring with a USGS transducer, and water level data derived from the Westbay MOSDAX transducer in Zone 8 does not represent "shut-in" conditions.

The first step in analyzing the data was to look for effects of barometric pressure, seasonal water level changes, earth tides, ocean tides, precipitation/recharge, and pumping from various wells and shafts.

While the skeletal structure of an aquifer may restrict some of the increase in barometric pressure at the land surface from translating to the water in the aquifer, an open top well will allow the full increase to load onto the water level inside the well. This will produce an imbalance in pressure. The ratio of the barometric pressure change and the change in water level is called barometric efficiency. In a confined aquifer an increase in barometric pressure will typically cause a decrease in water level inside the well. In an unconfined aquifer, there may be a time lag between increased barometric pressure at the surface and a change at the water level. This is primarily governed by a term called hydraulic diffusivity (transmissivity divided by storativity). Other factors that can affect barometric efficiency are well-skin (or clogged well screen) and well-bore storage. A water table aquifer deep below a perfect confining unit may possibly transmit none of the pressure change.

Numerous methods have been developed to determine barometric efficiency. A graphical method described in a USGS Paper prepared in cooperation with the U.S. Air Force Aeronautical Systems Center in Marietta, Georgia was used for this study (Gonthier 2007).

Because the majority of the transducers in this synoptic study are vented to the atmosphere via a tube, the effects of barometric pressure change do not affect measured pressures. However, the unvented transducers typically do require barometric correction.

Barometric pressure was monitored at five locations and reported by the USGS. If plots of water levels and barometric pressure versus time indicated long-term seasonal trends (as was observed in all wells in the summer and fall of 2017), then the data were first de-trended. Nearly continuous raw water levels and barometric pressures were plotted on X:Y line graphs. Passing storm fronts should theoretically result in many series of sub-parallel loops. By convention, a slope of -1.0 for these loops translates to a 100% barometric efficiency in a classic confined aquifer response. While this is not traditionally performed with vented transducers, this analysis was performed for all wells in the synoptic monitoring program.

While a barometric response would be expected in RHMW01 and RHMW11 Zones 1–5 (in the unweathered basalt basal aquifer), no response is apparent in RHMW01 using the graphical method (Gonthier 2007) nor is one apparent in plots of barometric pressure and water levels versus time for

this well. This observation is not yet understood. Another enigmatic response is observed in RHMW07 data. While this well was monitored with a vented transducer, it responded with a relatively high (~70%) efficiency in a classic confined aquifer response. There was no observed evidence of a time lag in the water level barometric pressure versus time plots.

One explanation for this type of response could be a plugged vent tube or failed desiccant. In the May 2015 pumping test, there were water level fluctuations potentially attributable to barometric pressure changes at both RHMW04 and RHMW07. In 2015 the barometric effects appeared to be larger at RHMW07 than RHMW04; however, other thus far unexplained factors may have caused these fluctuations.

The responses in RHMW11 Zones 1–5 are all near positive 1.0, which is opposite of what is typically observed with unvented transducers with open well tops. However, this is typical for zones that are isolated from the atmosphere as well as with Westbay monitoring zones and below packers (personal communication with Dave Larssen, July 3, 2018). All five of the zones in the unweathered basalt were highly efficient. All three of the zones completed in saprolite did not respond to barometric changes; instead the three zones continued to come into equilibrium throughout the monitoring period, indicative of low hydraulic conductivity of the saprolite.

Barometric response is also apparent but not as highly correlated in Moanalua DH43, Moanalua Deep, and ʻAiea Hālawa Shaft.

The summary of barometric responses is provided in Table 6-5.

Table 6-5: Summary of Barometric Responses

Well ID	Manual Slope	Summary of Response
RHMW01	-	No Response
RHMW02	-	No Response
RHMW03	-	No Response
RHMW04	-	No Response
RHMW05	-	No Response
RHMW06	-	No Response
RHMW07	-0.70	Yes
RHMW08	-	No Response
RHMW09	-	No Response
RHMW10	-	No Response
OWDFMW01	-	No Response
Moanalua DH43	-0.40	Weak response
TAMC-MW2	-0.53	Weak response
Moanalua Deep	-0.56	Weak response
Kaʻamilo Deep	-	No Response
ʻAiea Navy	-	No Response
Hālawa Deep Monitor Well (2253-03)	-	No Response
Hālawa Deep Monitor Well Chase Tube	-	No Response
Hālawa BWS Deep Monitor	-	No Response
ʻAiea Hālawa Shaft	-	Pumping Well. No response apparent.
Red Hill Shaft	-	Pumping Well. No response apparent.
Hālawa Shaft	-	Pumping Well. No response apparent.

Well ID	Manual Slope	Summary of Response
RHMW11 Zone 1	1.0	Yes; positive slope
RHMW11 Zone 2	1.0	Yes; positive slope
RHMW11 Zone 3	1.0	Yes; positive slope
RHMW11 Zone 4	1.0	Yes; positive slope
RHMW11 Zone 5	1.0	Yes; positive slope
RHMW11 Zone 6	-	No Response
RHMW11 Zone 7	-	No Response
RHMW11 Zone 8	-	No Response

Following evaluation of barometric efficiency, synoptic data were plotted along with ocean tides, earth tides, streamflow, and precipitation. Visually, the latter three do not appear to correlate with water levels in the Red Hill area wells. Some wells (e.g., 'Aiea Navy) do appear to be tidally influenced.

Water level data were corrected for barometric changes where appropriate and then plotted to estimate hydraulic properties. Water levels were plotted for five different periods listed below:

- Time 1 – Red Hill Shaft off for ~5 days, Hālawa Shaft average pumping (0600 January 15, 2018)
- Time 2 – Red Hill Shaft on steady for ~4 days, Hālawa Shaft average pumping (2110 January 19, 2018)
- Time 3 – Red Hill Shaft business as usual, Hālawa Shaft off (1900 February 5, 2018)
- Time 4 – Red Hill Shaft business as usual, Hālawa Shaft maximum pumping (0500 February 16, 2018)
- Time 5 – Red Hill Shaft business as usual,- Hālawa Shaft average pumping (1300 February 18, 2018)

Groundwater elevations for these five times were plotted on Figure 6-8 through Figure 6-12.

A description of each period is provided below:

Time 1

Time 1 represents a period when Red Hill Shaft had been offline and water levels had been allowed to recover for approximately 5 days. During this time, Hālawa Shaft was pumping steadily at average rates. On Figure 6-8, groundwater elevations along the ridge of the Facility ranged from 18.64 ft msl at RHMW03, 18.61 ft at RHMW01 and RHMW02, to 18.47 ft at OWDFMW01. With the exception of RHMW07 (22.54 ft), RHMW11 Zones 6 through 8 (71.17 to 98.77 ft), HDMW2253-03 (19.41 ft), and HDMW2253-03 Chase Tube (19.13), the water levels generally decline off the two flanks of the ridge (to the northwest and southeast). In general, water levels are higher to the south in Moanalua Valley (Moanalua DH43, TAMC-MW2 and Moanalua Deep). Water levels in the northwest corner of the Figure 6-8 range from 15.82 ft at the 'Aiea Hālawa Shaft (an active pumping shaft) to 16.49 ft at Ka'amilo Deep. While the general trend across the entire Figure 6-8 is from the south and east toward the northwest, the trends are more complicated around the Facility. This may be a product of well purpose (e.g., water supply, shallow groundwater monitoring, and deep saltwater/freshwater interface monitoring), well construction (open vertical hole, horizontal shaft, filter-packed and

cased), and the density of wells in the Facility area. Water levels gently slope toward the west-southwest along the ridge, but as mentioned above, dip away at the flanks (sub-parallel with surface topography). The water levels in the unweathered basalt in RHMW11 (Zones 1 through 5) comport with the majority of the other Red Hill monitoring wells; however, the water levels in the saprolite zone stand much higher than the regional water levels in the basal aquifer. This suggests a continuously saturated saprolite zone. RHMW07 water levels stand about 4 ft above the others nearby in the basal aquifer. Water levels in HDMW2253-03 and HDMW2253-03 Chase Tube display an upward vertical gradient possibly indicating that deeper saltier water may be rising up through the long-open-hole monitoring well and discharging to create a mound of saltier water in the fresh basal aquifer. Water levels at the principal production shafts (Red Hill Shaft and Hālawa Shaft) are depicted in pink. Because of the lengths of the shafts, these levels likely represent a composite of the heads in the aquifer along the length of the open shaft. Water levels measured during pumping often need to consider frictional losses associated with filter pack and screen, but these may not be important in these unlined shafts. There are potentially other wells and shafts in the area that may have been pumping during this period. These include ʻAiea Hālawa Shaft, the BWS Moanalua Wells 1, 2, and 3, and TAMC water supply wells located in the vicinity of Moanalua Elementary School. These may all complicate interpretation of these water levels. Because of the heterogeneities in geology, well depth, and construction, no attempt has been made to contour the water levels. The patterns described on Figure 6-8 represent an extremely gentle groundwater gradient, and despite the considerable effort to reduce errors, the remaining residual errors are probably on the order of a few tenths of a foot. Therefore, making further interpretations in the Red Hill area may not provide a better understanding of groundwater conditions in the area.

Time 2

Time 2 represents a period when Red Hill Shaft had been pumping steadily for about 4.5 days at about [redacted] mgd. During this time, Hālawa Shaft was pumping steadily at an average rate. On Figure 6-9, groundwater elevations along the ridge of the Facility ranged from 18.20 ft at RHMW03, 18.14 ft at RHMW02, 18.13 ft at RHMW01, and 17.94 ft at OWDFMW01. Again, water levels generally decline off to the flanks of the ridge. The same patterns observed at RHMW07, RHMW11 Zones 6, 7 and 8, and HDMW2253-03 Chase Tube at Time 1 continue in Time 2 (as well as Times 3, 4, and 5). The differences between Time 1 and Time 2 are discussed below.

Head Difference Between Time 1 and Time 2

The water levels displayed on Figure 6-13 represent the water level fluctuations observed in response to pumping Red Hill shaft steadily at approximately [redacted] mgd for about 4.5 days. Drawdowns associated with this pumping are also contoured into ovals of approximately equal drawdown for interpretation to be discussed later (this interpretation is ongoing). The drawdown is greatest in the wells that are nearest to Red Hill Shaft and drawdown declines away from Red Hill Shaft. The drawdown contours generally describe nearly concentric ovals with the primary orientation approximately northeast to southwest. Not all of the indicated fluctuation in wells (especially the distal wells) is thought to be associated with pumping at Red Hill Shaft, nor are the changes observed in RHMW07, RHMW11 (Zones 6, 7, and 8), or the HDMW53-03 Chase Tube. Across the rest of Figure 6-13, water level roles generally decline on the order of 0.1 to 0.2 but this may be due to effects other than the pumping of Red Hill Shaft and are within the range of probable error.

Time 3

Time 3 represents a period when Red Hill Shaft was pumping in response to demands and typically turned off and on several times per day. This was termed "business as usual". During this time, Hālawa Shaft had been shut off for approximately 9 days. On Figure 6-10, groundwater elevations

along the ridge of the Facility ranged from 18.63 ft at RHMW03, 18.59 ft at RHMW02, 18.62 ft at RHMW02, and 18.42 ft at OWDFMW01. With the exceptions noted in Time 1, the water levels generally decline off the two flanks of the ridge (to the northwest and southeast). In general, water levels are higher to the south in Moanalua Valley (Moanalua DH43, TAMCMW-2 and Moanalua Deep) and lower in the northwest area. Again, while the general trend across the entire Figure 6-10 is toward the northwest, the trends are more complicated around the Facility.

Time 4

Time 4 represents a period when Red Hill Shaft was pumping business as usual. During this time, Hālawa Shaft was pumped at an above average rate for approximately 10 days. Hālawa Shaft pumping rates have not yet been provided to the Navy. On Figure 6-11, groundwater elevations along the ridge of the Facility ranged from 18.41 ft at RHMW03, 18.38 ft at RHMW02, 18.36 ft at RHMW01, and 18.19 ft at OWDFMW01. The other general patterns noted above continue in Time 4. Lower water level (12.32 ft) was noted at Hālawa Shaft during this period of heavy pumping. The differences between Time 3 and Time 4 are discussed below.

Head Difference Between Time 3 and Time 4

The water levels displayed on Figure 6-14 represent the water level fluctuations observed in response to heavier-than-normal pumping of Hālawa Shaft as compared to Time 3 when this well was offline for several days. While there is significant drawdown in Hālawa Shaft itself, it is not clear whether the drawdown indicated at Hālawa BWS Deep Monitor, OWDFMW01, RHMW01, RHMW02, RHMW03, RHMW04, RHMW06, RHMW08, RHMW09, RHMW10, and the 5 deeper zones in RHMW11 is due to pumping at Hālawa Shaft or Red Hill Shaft. However, it does not display the pattern of nearly concentric ovals that was observed at the end of Time 2. Further analysis of these data is underway.

Time 5

Time 5 represents a period when Red Hill Shaft was pumping business as usual. During this time, Hālawa Shaft was pumping steadily at an average rate. On Figure 6-12, groundwater elevations along the ridge of the Facility ranged from 18.51 ft at RHMW03, 18.47 ft at RHMW02, 18.51 ft at RHMW01, and 18.19 ft at OWDFMW01. The other local and regional trends noted above continued for Time 5.

Drawdown was also plotted versus the logarithm of pumping time (or the ratio of time since pumping started divided by time since pumping stopped for recovery) (Figure 6-15 through Figure 6-19). Distance of each of these wells was computed from the center of the clinker zones from the last 200 ft of Red Hill Shaft. The slopes of these semi-logarithmic lines and the x-intercepts were recorded. These values were then used to calculate transmissivity and storativity using the Cooper-Jacob approximation to the Theis equation (H.H. Cooper Jr. and Jacob 1946). To convert transmissivity to hydraulic conductivity, it is first necessary to know the aquifer thickness. Because the basalt is thousands of feet deep, the high horizontal to vertical anisotropy, and the shallow depths of most wells and shafts, this value would not meet the classic definition of aquifer thickness. Instead, three different values are assumed for this conversion. The results are presented in Table 6-6 and Table 6-7.

Table 6-6: Summary of Cooper Jacob Approximation Calculation Components

Well ID	Distance to RHS (ft)	Drawdown ΔS (ft)	Drawdown T_0 (min)	Drawdown T_0 (day)	Recovery ΔS' (ft)	Residual Drawdown	Comments
RHMW01	1,480	0.30	100	0.069	0.18	0	
RHMW02	2,100	0.30	160	0.111	0.18	0	
RHMW03	2,920	0.29	160	0.111	0.17	0	
RHMW04	4,140	0.28	370	0.257	0.18	0	
RHMW05	660	0.30	75	0.052	0.18	0	Late time does not respond similarly
RHMW06	3,100	0.24	140	0.097	0.14	0.005	
RHMW07	2,000	NA	NA	NA	NA	NA	Does not appear to respond to pumping
RHMW08	1,250	0.30	70	0.049	0.17	0	
RHMW09	1,630	0.30	140	0.097	0.17	0	
RHMW10	2,820	0.30	170	0.118	0.18	0	
RHMW11 Zone 1	2,350	0.22	150	0.104	0.18	0	
RHMW11 Zone 2	2,350	0.24	270	0.188	0.15	0.01	
RHMW11 Zone 3	2,350	0.24	210	0.146	0.15	0.005	
RHMW11 Zone 4	2,350	0.24	240	0.167	0.16	0.01	
RHMW11 Zone 5	2,350	0.25	240	0.167	0.15	0.005	
RHMW11 Zone 6	2,350	NA	NA	NA	NA	NA	No clear trend
RHMW11 Zone 7	2,350	NA	NA	NA	NA	NA	No clear trend
RHMW11 Zone 8	2,350	NA	NA	NA	NA	NA	No clear trend, water levels rose during pumping
RHMW11 Zone 8	2,350	NA	NA	NA	NA	NA	USGS Transducer. No clear trend, water levels rose during pumping
Hālawa Deep Monitor Well (2253-03)	2,960	NA	NA	NA	NA	NA	Unclear drawdown trend, no apparent recovery trend
Hālawa Deep Monitor Well Chase Tube	2,960	NA	NA	NA	NA	NA	No apparent recovery, very small drawdown
OWDFMW01	1,660	0.32	130	0.090	0.15	0	
Hālawa BWS Deep Monitor	6,560	NA	NA	NA	NA	NA	Unclear drawdown trend, no apparent recovery trend
Ka'amilo Deep	9,960	NA	NA	NA	NA	NA	Unclear drawdown trend, no apparent recovery trend
TAMC-MW2	3,380	0.2	420	0.292	NA	NA	No apparent recovery

Well ID	Distance to RHS (ft)	Drawdown ΔS (ft)	Drawdown T_0 (min)	Drawdown T_0 (day)	Recovery ΔS' (ft)	Residual Drawdown	Comments
Moanalua Deep	6,350	NA	NA	NA	NA	NA	Unclear drawdown trend, no apparent recovery trend
Moanalua DH43	4,630	0.29	900	0.625	0.16	0.005	
Hālawa Shaft	14,150	NA	NA	NA	NA	NA	Operating production well
ʻAiea Navy	10,730	NA	NA	NA	NA	NA	No clear recovery

Table 6-7: Summary of Cooper Jacob Approximation Estimates of Transmissivity and Storativity, and Derived Hydraulic Conductivity

	Drawdown					Recovery			
	Transmissivity (ft^2/d)	K (ft/d) - 20 ft	K (ft/d) - 50 ft	K (ft/d) - 100 ft	Storativity	Transmissivity (ft^2/d)	K (ft/d) - 20 ft	K (ft/d) - 50 ft	K (ft/d) - 100 ft
RHMW01	627,197	31,360	12,544	6,272	0.045	490,797	24,540	9,816	4,908
RHMW02	627,197	31,360	12,544	6,272	0.036	504,820	25,241	10,096	5,048
RHMW03	648,825	32,441	12,976	6,488	0.019	519,668	25,983	10,393	5,197
RHMW04	671,997	33,600	13,440	6,720	0.023	490,797	24,540	9,816	4,908
RHMW05	627,197	31,360	12,544	6,272	0.169	490,797	24,540	9,816	4,908
RHMW06	783,997	39,200	15,680	7,840	0.018	631,025	31,551	12,621	6,310
RHMW08	627,197	31,360	12,544	6,272	0.044	519,668	25,983	10,393	5,197
RHMW09	627,197	31,360	12,544	6,272	0.052	519,668	25,983	10,393	5,197
RHMW10	627,197	31,360	12,544	6,272	0.021	490,797	24,540	9,816	4,908
RHMW11 Zone 1	855,269	42,763	17,105	8,553	0.036	490,797	24,540	9,816	4,908
RHMW11 Zone 2	783,997	39,200	15,680	7,840	0.060	588,957	29,448	11,779	5,890
RHMW11 Zone 3	783,997	39,200	15,680	7,840	0.047	588,957	29,448	11,779	5,890
RHMW11 Zone 4	783,997	39,200	15,680	7,840	0.053	552,147	27,607	11,043	5,521
RHMW11 Zone 5	752,637	37,632	15,053	7,526	0.051	588,957	29,448	11,779	5,890
OWDFMW01	855,269	42,763	17,105	8,553	0.017	588,957	29,448	11,779	5,890
TAMC-MW2	940,796	47,040	18,816	9,408	0.054	NA	NA	NA	NA
Moanalua DH43	648,825	32,441	12,976	6,488	0.043	552,147	27,607	11,043	5,521

ft^2/d square feet per day
K hydraulic conductivity
NA not applicable

Data from the most recent synoptic study were first published on NWIS in May 2018. Initial analysis of the synoptic data was performed using the Cooper-Jacob 1946 method because of its ease of operation, but additional analyses are being performed. The Cooper-Jacob approximation to the Theis method is operationally elegant and appropriate at late pumping times, specifically when $(r^2S)/(4Tt)$ is less than 0.05. Based on the calculations below and previously presented assumptions, the method should be valid for the 4.5-day sustained pumping ending at time 2 for wells with approximately 4,000 ft of Red Hill Shaft. RHMW04 is approximately at the limit of acceptable use of this method. Because of the high hydraulic conductivities in the basalt and the relatively modest drawdowns observed in the monitoring wells, the Cooper-Jacob approximation is appropriate due to the flow being essentially horizontal and laminar (non-turbulent). Turbulent losses may, however, need to be considered when evaluating data from the pumping wells themselves.

These values are similar to the ranges reported for the 2006 data shown in Table 6-8.

Table 6-8: Previous Estimates of Aquifer Properties Based on Data Developed in 2006

Well		ΔS	Transmissivity (ft^2/d)	Assumed Aquifer Thicknesses		
				K (ft/d) - 20 ft	K (ft/d) - 50 ft	K (ft/d) - 100 ft
OWDFMW08	Drawdown Composite	0.41	1,100,000	57,000	23,000	11,000
	Recovery	0.58	800,000	40,000	16,000	8,000
RHMW02	Drawdown Composite	0.68	680,000	34,000	14,000	6,800
	Recovery	0.60	770,000	39,000	15,000	7,700
RHMW03	Drawdown Composite	0.60	770,000	39,000	15,000	7,700
	Recovery	0.54	860,000	43,000	17,000	8,600
HDMW2253-03	Drawdown Composite	0.28	1,700,000	83,000	33,000	17,000
	Recovery	0.47	990,000	49,000	20,000	9,900
RHMW04	Drawdown Composite	0.41	1,100,000	57,000	23,000	11,000
	Recovery	0.60	770,000	39,000	15,000	7,700
TAMCMW2	Recovery	0.26	1,800,000	89,000	36,000	18,000
Red Hill Shaft	Drawdown Composite	1.2	390,000	19,000	7,700	3,900
	Recovery	0.60	770,000	39,000	15,000	7,700

K hydraulic conductivity

The hydraulic conductivity values are highly dependent on the assumption of aquifer thickness, so these should be used with caution and with an understanding of this limitation.

Logarithm of distance versus drawdown (at time 2) was also plotted on a single x:y scatter plot and a linear trend was manually fitted (see Figure 6-20). The slope of this line and x-intercept were recorded and used in the Cooper-Jacob distance-drawdown method and then the following parameters were calculated:

T 810,000 square feet per day (ft^2/d)

S 0.023

Review of the results of the distance drawdown evaluation yields similar values as the time drawdown calculations for transmissivity and storativity.

RHMW11 Zones 6 and 7, Moanalua DH43, RHMW07, and HDMW2253-03 Chase Tube are all outliers for this general trend. This suggests that they are all distinct from the other wells completed in the unweathered basalt basal aquifer. This could be due to well construction, fine-grained material (saprolite or valley fill) in the screen interval, and/or hydraulic barriers. RHMW07 time drawdown plot did not indicate it was responding to pumping of Red Hill Shaft. In addition, this well enigmatically appeared to respond to barometric changes although it had a vented transducer.

Data from Time 4 (maximum sustained pumping of Hālawa Shaft) are being evaluated. While there appear to be responses in several of the wells to sustained, heavier Hālawa Shaft pumping, responses in wells in the Red Hill Area are difficult to interpret because of the distance from Hālawa Shaft, the discontinuous pumping of Red Hill Shaft, and local hydrogeologic conditions (e.g., locally confining conditions, other hydrogeologic barriers).

Other work that is currently underway or being contemplated include:

- Other pump test analysis techniques
- Additional evaluation of barometric responses
- Continued monitoring of RHMW11 and the Hālawa Correctional Facility shallow monitoring well (UMW-1)
- Hydraulic tomography
- Analytic element modeling
- Additional calibration of hydraulic conductivity and anisotropy of the 2018 groundwater flow model based on the 2017/2018 synoptic data
- Evaluation of areal and streambed infiltration/recharge

The results of additional analyses will be presented in either an update to the CSM of future report.

6.3 HYDRAULIC PROPERTIES OF HYDROGEOLOGIC UNITS

Groundwater flow and solute transport are controlled by the hydraulic and physical properties of the HGUs, including hydraulic conductivity, effective porosity, specific yield, specific storage, and dispersivity. For sites in O'ahu, estimated parameter values have been reported in Nichols, Shade, and Hunt Jr. (1996), Hunt Jr. (1996), Oki (1998, 2005), Izuka et al. (2018), and others. The following is a summary of the information provided in those reports.

6.3.1 Caprock

Hydraulic conductivity of the caprock spans several orders of magnitude depending on material type. The older alluvium, including fine-grained muds and saprolite (thoroughly weathered volcanic rock), have hydraulic conductivities ranging from approximately 0.01 to 1 ft/d (Wentworth 1938). Sands have an estimated hydraulic conductivity ranging from 1 to 1,000 ft/d (Hutcheson et al. 1996). Coral gravels and reef limestone deposits have hydraulic conductivities of several thousands of ft/d (Oki 1998). Souza and Voss (1987) estimated an effective K_h of 0.15 ft/d for caprock. Although the permeability varies greatly with material type, in general, the caprock acts as a low-permeability confining unit atop the basal aquifer near the coastline (Visher and Mink 1964).

The 2005 USGS groundwater model (Oki 2005) used a range of values for hydraulic conductivity of the caprock, depending on location and rock type. For the upper limestone unit in the caprock, the K_v was 25 ft/d and the K_h was 2,500 ft/d. For the low-permeability units of the caprock, the USGS study

used hydraulic conductivities ranging from 0.01 to 0.6 ft/d (Oki 2005). A more recent USGS groundwater model (Rotzoll 2012) of the Pearl Harbor area distinguished K_h along the general lava-flow direction (longitudinal K_h) from K in perpendicular to the general lava-flow direction (transverse K_h). The model used the following hydraulic conductivity values for the caprock: 0.3 ft/d, 0.2 ft/d, and 0.3 ft/d (K_h longitudinal, K_h transverse, and K_v, respectively).

6.3.2 Valley Fill

Hydraulic conductivity estimates of valley fill deposits range from 0.019 to 0.37 ft/d (Wentworth 1938). In the Pearl Harbor area, the 2005 USGS groundwater model (Oki 2005) used 0.058 ft/d for both K_h and K_v of this unit. The valley fill deposits are underlain by weathered basalt (saprolite) of low permeability that also impedes groundwater flow (Oki 2005).

According to the most recent pertinent USGS report (Izuka et al. 2018), specific-yield values used in numerical models for the Caprock HGU, which includes valley fill deposits, have ranged between 0.04 and 0.2 (Souza and Voss 1987; Oki 1998; Gingerich and Voss 2005; Oki 2005; Rotzoll, El-Kadi, and Gingerich 2007; Rotzoll 2012).

6.3.3 Basalt

The diverse rock textures encompassed by the three types of lava that comprise the basal aquifer in the immediate vicinity of the site (massive a'ā, pāhoehoe, a'ā clinker) impart a complex porosity distribution to the lavas (Hunt Jr. 1996). In a layered sequence of lava flows, several types of primary porosity are present:

- Vesicular – small isolated gas vesicles that form in molten lava
- Fracture – joints, cracks, and bedding-plane separations
- Intergranular – fragmental rock, including cinders, rubble, and clinkers
- Conduits – large openings such as lava tubes and interflow voids

Vesicles are poorly connected and contribute little to effective porosity. Estimates of the total porosity of various volcanic rocks on O'ahu range from 5 to 51 percent, with a median value of approximately 43 percent; values of effective porosity may be lower by as much as a factor of 10 (Hunt Jr. 1996). Fracture and intergranular porosity can form a pervasive network of small openings that facilitates diffuse groundwater flow. Conduits, such as lava tubes, provide avenues for highly channelized flow. However, these conduits may be impeded by collapse and infilling of the more rapidly weathering lava tubes. Intact lava tubes are quite rare and discussed in further detail in Section 5.1.1.

Hawaiian volcanic rocks vary in porosity and permeability depending on the emplacement process, lava type, genesis, flow thickness, flow rate, extent, cooling rate, and weathering. Permeability is typically highest in the relatively thick, unweathered rubbly a'ā clinker zones and intensely fractured zones or lava tubes of pāhoehoe flows. Permeability is much lower in the interior portions of massive flows, weathered interflows, intrusive rocks (dikes/sills), ash beds, and weathered rocks (saprolite)/soil horizons, which can impede vertical flow. Even slight weathering of the basalt along flow tops and fractures results in clay mineral formation and low permeability.

The permeability of lava flows in the Pearl Harbor area generally is high. The main elements of lava flows contributing to the permeability are a'ā clinker zones, voids along the contacts between flows, cooling joints perpendicular to flow surfaces, and lava tubes developed in pāhoehoe flows.

Consequently, the regional K_h of these volcanic rocks generally ranges from hundreds to thousands of ft/d (Hunt Jr. 1996; Oki 2005). Because of the extremely high permeability, horizontal water-table gradients in these rocks are small (on the order of 1 ft/mile). K_h in the lava flows is often anisotropic. Hydraulic conductivity is often much greater parallel to the lava flows than perpendicular to the flows (Oki 2005).

According to the most recent regional USGS report (Izuka et al. 2018), estimates of K_h for dike-free lava-flow aquifers on O'ahu range between 500 and 5,000 ft/d (Hunt Jr. 1996). Aquifer test results show K_h values of 26–5,000 ft/d, with the majority of results between 200 and 1,500 ft/d (Wentworth 1938; Visher and Mink 1964; Takasaki and Valenciano 1969; Izuka et al. 2018; Rosenau, Lubke, and Nakahara 1971; Soroos 1973; Williams and Soroos 1973; Dale 1978; Mink 1980; Eyre 1983; Eyre, Ewart, and Shade 1986). Values of K_h used in calibrated numerical models range from approximately 100 to 7,500 ft/d (Eyre, Ewart, and Shade 1986; Souza and Voss 1987; Oki 1998; Gingerich and Voss 2005; Whittier et al. 2004; Rotzoll, El-Kadi, and Gingerich 2007).

Where the basalt has not been intruded by dikes (as in the study area), K_h values generally range from hundreds to thousands of ft/d (Soroos 1973; Mink 1980; Hunt Jr. 1996). Souza and Voss (1987) estimated the ratio of K_v to K_h is 0.05. For the volcanic rock aquifer in the Pearl Harbor area, the 2005 USGS regional groundwater model (Oki 2005) used a value of 4,500 ft/d for K_h along the general lava-flow direction (longitudinal K_h) and 1,500 ft/d for K in perpendicular (tranverse K_h) to the general lava-flow direction (transverse K_h). The same model used 7.5 ft/d for K_v of the volcanic rock aquifer (Oki 2005). A more recent USGS groundwater model of the Pearl Harbor area (Rotzoll 2012) used 1,350 ft/d for longitudinal K_h, 675 ft/d for transverse K_h, and 6.8 ft/d for K_v.

Weathering reduces the hydraulic conductivity of volcanic rocks (Mink 1980). Saprolite (thoroughly weathered volcanic rock) is soft and rich in clay minerals may be found in deposits 100–300 ft thick, and has very low hydraulic conductivity (DON 2007). According to the USGS (Oki 2005), the R.M. Towill Corporation reported a hydraulic conductivity of 0.058 ft/d for weathered basalt beneath Waiawa Stream Valley based on an injection test. Wentworth (1938) estimated the hydraulic conductivity of weathered basalt to be between 0.083 and 0.128 ft/d based on laboratory parameter tests on core samples. Recent December 2017 preliminary hydraulic conductivities derived from pneumatic slug testing within saprolite layers of the packered zones of RHMW11 (multi-level well with eight zones) ranged from 0.0033 to 0.026 ft/d, and hydraulic conductivities derived from laboratory core tests within the upper zone of the saprolite ranged from 7.99E-06 to 8.50E-05 ft/d.

Specific storage is the volume of water released from storage per unit decline in hydraulic head in the aquifer, per unit area of the aquifer. In the Pearl Harbor area, specific storage was estimated to range from 10^{-4} to 10^{-7} per foot (Williams and Soroos 1973). For unconfined parts of aquifers, specific yield plays a more significant role than specific storage. Specific yield is defined as the volume of water that a saturated rock or soil will yield by gravity drainage divided by the total volume of rock or soil, and is usually expressed as a percentage. Specific yield is less than the effective porosity because some portion of the water is held by surface tension and capillary forces and will not drain by gravity.

Specific yield values used for the volcanic-rock aquifer in regional groundwater models and reported by the USGS (Izuka et al. 2018) range between 0.03 and 0.1 percent (Eyre, Ewart, and Shade 1986; Souza and Voss 1987; Oki et al. 1996; Oki 1998; Gingerich and Voss 2005; Oki 2005; Rotzoll, El-Kadi, and Gingerich 2007; Whittier et al. 2010; Rotzoll 2012). In the Facility area, reported values for specific storage and specific yield values were derived from numerical modeling analysis of the

regional aquifer pumping test conducted in May 2006, the results of which are summarized in the following subsection (DON 2007).

6.3.4 Site-Area Aquifer Testing and Analysis of Hydraulic Parameters

Hydraulic conductivity values for the Basalt HGU in the Facility area were recently obtained from hydraulic tests performed in RHMW11, which augment the hydraulic parameter values derived from previous numerical modeling analysis of data collected from the regional groundwater aquifer pumping test conducted in May 2006 (see also Sections 6.1 and 6.2). Section 6.1 describes the results of hydraulic tests conducted in RHMW11 (Table 6-2). These tests show the saprolite and weathered basalt have extremely low hydraulic conductivities but the deeper unweathered basalt has very high hydraulic conductivity. The May 2006 numerical analysis was conducted using the local groundwater flow model for the 2007 Red Hill project, which is summarized in more detail in Section 6.5. The aquifer pumping test was conducted in May 2006 by the Navy in coordination with BWS, the State of Hawai'i Department of Land and Natural Resources (DLNR) and its Commission on Water Resource Management (CWRM), and the U.S. Army Corps of Engineers. For the 2006 test, the primary pumping well was Red Hill Shaft. Groundwater level monitoring was performed via transducers and data loggers in several wells in the Red Hill area, including the Red Hill monitoring wells and other wells near Red Hill Shaft and Hālawa Shaft. The collected field data were compared to simulated water levels from corresponding wells to calibrate hydraulic conductivity and other hydrogeologic properties for a local groundwater flow model.

The 2006 pumping test period covered approximately 1 month, from May 10, 2006 to June 1, 2006, although some data loggers recorded water levels earlier. The main pumping test was initiated by completely shutting off Red Hill Shaft between May 12 and May 19, which allowed the water levels near the well to recover from pumping stresses. During this same period, BWS Hālawa Shaft and the BWS Moanalua Wells maintained their regular pumping schedules and rates. After the recovery period, Red Hill Shaft was subjected to a period of above-average pumping between May 19 and May 26; the 10-year average pumping rate for the well is approximately [redacted] mgd, and during the above-average pumping period the pumping rate alternated between [redacted] mgd.

The local groundwater flow model for the 2007 Red Hill project was calibrated for both steady-state and dynamic, or "transient," conditions (DON 2007, Appendix L). The steady-state calibration was conducted by (1) selecting representative hydraulic parameters of the major stratigraphic units from literature values, (2) simulating water table elevations using average recharge and pumping conditions for the period between 1996 and 2005, and (3) iteratively running the groundwater flow model, using a Parameter Estimation (PEST) algorithm (Doherty 2000), until the differences between the measured and simulated groundwater elevations were minimized. Thirty pumping wells located in the local model area were used to define the steady-state water table elevations. Table 6-9 provides the hydraulic parameters derived using this modeling approach with PEST; these hydraulic parameter values are specified in the final 2007 calibrated numerical flow model (DON 2007).

Table 6-9: Hydraulic Parameters Developed from Local Numerical Flow Model Calibration at the Facility (DON 2007)

Hydrogeologic Unit	Horizontal, Longitudinal K (ft/d)	Horizontal, Transversal K (ft/d)	Vertical K (ft/d)	Effective Porosity	Specific Storage (per ft)	Specific Yield
Caprock	115	115	115	0.10	3.05 × 10-5	0.10
Valley Fill	0.066	0.066	0.066	0.15	1.52 × 10-5	0.12
Basalt	4,428	1,476	7.4	0.05	1.07 × 10-5	0.031

K hydraulic conductivity

6.4 2005 USGS REGIONAL SUTRA MODEL

A modeling study of the aquifer in the Pearl Harbor region was conducted by the USGS (Oki 2005) to evaluate the impacts of the valley fill barriers and of redistribution of groundwater withdrawals on water levels and salinity in the aquifer. This density-dependent groundwater flow and solute transport model was developed using a finite element code SUTRA (version 2D3D.1), which is appropriate for evaluating saltwater intrusion in coastal systems. A summary of that model and associated report are presented below, focusing on the aspects relevant to the current modeling objectives and domain.

6.4.1 Model Domain

The SUTRA model domain covers the current Red Hill project study area, with the southeast boundary lying approximately at the same location. The model extends into Pearl Harbor and into the ocean to represent the saltwater flow dynamics.

The model is discretized into 56 rows, 72 columns, and 76 layers of nodes. The rows and columns are deformed such that the elements are boundary fitted to the simulation domain, while the layers are stacked vertically. A variable-grid spacing includes fine discretization in the upper part of the aquifer and near areas of groundwater discharge. Figure 6-21 shows the simulation domain of the SUTRA model in relation to the current model area.

The top of the model is set at sea level; therefore, the model does not explicitly include that portion of the saturated zone above sea level up to the water table. The overall aquifer transmissivity was noted to be only underestimated by less than 1 percent using this configuration.

The model extends to a depth of 5,906 ft below msl to include the saltwater system down to an assumed aquifer bottom. Inflow of freshwater from lateral upgradient boundaries occurs between altitudes of -3 ft and -984 ft, with no-flow conditions farther below.

6.4.2 Representation of Groundwater Flow System

The groundwater flow system in the basalt aquifer consists of a freshwater lens overlying saltwater. Recharge to the freshwater lens system occurs due to infiltration of rainfall and inflow into the area of interest from upstream areas. Recharge was estimated using reported relationships between annual recharge and annual rainfall depending on agricultural conditions. Maps of the area presented indicate that there has been little if any cultivation within the model area since the mid-1970s. Recharge for the transient model was averaged over periods ranging from 5 to 20 years.

Groundwater discharge occurs as pumping, discharge to onshore springs, and diffuse discharge through the caprock to Pearl Harbor and the ocean. Groundwater pumping from the basalt aquifer increased through the 1970s and declined thereafter following closure of sugarcane plantations. Withdrawal from the caprock was mainly from its upper limestone unit and is currently used mainly for landscape and golf course irrigation or industrial purposes. The major Pearl Harbor Springs within the current model area include Pearl Harbor Springs at Kalauao and Kalauao Spring. Main spring discharge occurs from areas where the basalt is exposed or a break in the land surface occurs. Reported relationships between spring discharge and water level measured at a Pearl Harbor well were used to quantify discharge; a high correlation was found for Waiawa and Waimano-Waiau Springs. Diffuse seeps also occur where the caprock is thin.

Uniform hydraulic properties for the basalt aquifer were used to calibrate the model. The modeled estimate of longitudinal K_h was 4,500 ft/d, and transverse K_h was 1,500 ft/d. These values were also

used by other researchers. Uniform anisotropic aquifer properties were used in the model to avoid creating an overly complex model that could not be justified based on existing information.

Several geologic controls to groundwater flow are represented in the model. Low-permeability valley fill deposits and weathered volcanic rock beneath the valley fill deposits impede groundwater movement and can create differences in groundwater levels on opposite sides of the valley. Nearer the coast, some of the valleys may consist of terrestrial sediments inter-fingered with marine sediments and limestone units. Inland, above an altitude of around 30 ft, the base of the valley fill material typically consists of older alluvium that may be hundreds of feet thick in lower altitudes but non-existent above altitudes of 400–600 ft.

In Kalihi Valley along the southeastern boundary of the current model area, the thickness of valley fill deposits likely exceeds 1,000 ft, forming an effective barrier to flow. A site beneath Waiawa Valley along the northwestern boundary of the model area reportedly had weathered basalt extending to depths of 50–100 ft below sea level. Valley fill barriers and underlying weathered basalt associated with Waimalu and North Hālawa Streams within the model area may impede the flow of groundwater. Waimalu Valley reportedly contains sedimentary material and weathered basalt to depths greater than 200 ft below msl, while North Hālawa Valley contains alluvial and colluvial material at depths below sea level, with weathered basalt extending even farther below (Oki 2005).

Older alluvium deposits in the valleys have a low hydraulic conductivity reportedly estimated between 0.013 ft/d to 1.08 ft/d (three samples), while alluvium without reference to weathering was reportedly estimated to have a hydraulic conductivity ranging from 0.019 to 0.37 ft/d. Valley fill barriers were assigned an isotropic value for hydraulic conductivity of 0.058 ft/d.

Weathering of the basalt is dominated by chemical processes that are enhanced by percolating water in high rainfall areas and under streams where the saprolite (weathered basalt) thicknesses are greater. Weathered basalt hydraulic conductivity was estimated to be 0.083 ft/d to 0.128 ft/d, although higher values, as much as 283 ft/d, and lower values, as low as 0.0028 ft/d, were also estimated and attributed to variability in macro-porosity among samples.

Coastal sedimentary deposits and underlying weathered basalt form a caprock confining unit above the basalt aquifer. The caprock includes zones of low to high hydraulic conductivity; however, the overall effect is that of a low hydraulic conductivity modeled at 0.15 ft/d by Souza and Voss (1987). The Oki (2005) model simulates the caprock as an upper limestone unit (K_v and K_h of 25 and 2,500 ft/d, respectively) and a low-permeability unit (isotropic hydraulic conductivity value of 0.6 ft/d).

Modeled effective porosity for the basalt (including clinker zones and surrounding basalt) in the current model area was 0.04; the upper limestone unit had an effective porosity of 0.2; and all other rock types had an effective porosity value of 0.1. Storage properties of the basalt aquifer are related to the porosity. The specific storage was modeled to range from 7.5×10^{-6} per foot to 7.8×10^{-6} per foot for effective porosity values ranging from 0.02 to 0.2.

6.4.3 Model Results

The USGS model (Oki 2005) provides useful insights about the aquifer system. Figure 6-22 shows the simulated water table elevation (water levels in Layer 1) at the end of the simulation (in 2000), as extracted from the base case model results. The simulated water levels are at msl within the caprock near the coastline and increase further inland within the basalt aquifer. Higher water levels were also simulated in North Hālawa Valley, probably from additional mounding of recharge within the lower

hydraulic conductivity valley fill material. The longitudinal hydraulic conductivity of the top layer of the model was extracted and is shown on Figure 6-23.

The simulated elevation of the saltwater interface (50 percent salinity contour) within the current model area at the end of the simulation (in 2000), as extracted from the base case model results is shown on Figure 6-24. The saltwater interface elevation is similar to that obtained by the Ghyben-Herzberg Principle in the Red Hill area and along the northeastern boundary of the study area. The calculated interface depth decreases rapidly within the caprock nearer the shoreline and surfaces at the coastline.

Sensitivity to valley fill barriers was reported to be about a few tenths of a foot difference in water levels within the Red Hill study area for when the barriers were varied from absent to very deep as compared to the base case simulation. Reducing pumping in Hālawa Shaft by 5.66 mgd and increasing pumping in Pearl City III well by the same amount produced a change in the interface elevation by less than 15 ft under both these locations. For the case of shifting the Hālawa Shaft pumping well to Kunia III (2401-04), the interface depth change was less than 10 ft at Hālawa Shaft (Oki 2005).

Sensitivity of saltwater intrusion to reducing pumping in Hālawa Shaft by 5.66 mgd with and without valley fill barriers indicated that the saltwater intrusion impact due to pumping changes in Hālawa Shaft is larger when there is no valley fill barrier than when the simulation included or deepened the valley fill barrier.

The following points summarize the findings of the model by Oki (2005) that appear relevant to the current Red Hill CSM:

- The model provides ranges of aquifer parameter values representative of the site region.
- Water levels in the caprock are close to sea level nearer to the ocean. The saltwater interface computed using the Ghyben-Herzberg Principle (at a depth of 40 times the water elevation above msl) would be similarly close to the coastline outside of the harbor. The saltwater interface as represented by the 50 percent seawater concentration was simulated to be adjacent to the ocean shoreline. The saltwater interface depth was simulated to be 850–900 ft in the Red Hill area which is consistent with the Ghyben-Herzberg Principle
- Truncating the aquifer below the water table had a negligible impact on transmissivity. Therefore, transmissivity of freshwater is not sensitive to freshwater depth under Red Hill. Pumping changes of [redacted] mgd moves the saltwater interface depth by less than 15 ft. This would have a negligible impact on the freshwater transmissivity.
- Valley fill and underlying weathered basalt form low hydraulic conductivity barriers that control flow and water levels across the barrier.
- Seasonal water level fluctuations were approximately 2.5 ft after 2000. Water level measurement errors of as large as 0.3 ft can occur due to barometric fluctuations within a matter of a week.
- Uniform material property values (homogeneous conditions) for each of the geologic units were adequate to calibrate the model to water levels and chlorides measured at select wells.
- Calibration was not sensitive to the assumed thicknesses of the valley fill barriers.

6.5 2007 RED HILL GROUNDWATER FLOW MODEL

The 2007 modeling study of the area around Red Hill conducted by the Navy (DON 2007) included a groundwater flow and transport assessment to evaluate current and potential future risk to human health associated with drinking water potentially impacted by petroleum compounds from past or future releases to the environment. That model includes the current Red Hill project study area, and was designed for similar objectives.

6.5.1 Model Domain

The 2007 Red Hill model was developed in two stages. First, the regional island-wide model of O'ahu's Source Water Assessment Program (SWAP) was modified to represent a more recent period from 1996 to 2005 by updating land use, recharge, pumping rates and observed water levels (Whittier et al. 2004). The model was then used to establish boundary conditions to a local-scale model of Red Hill and adjacent areas. Figure 6-25 shows the domains of the 2007 regional and local models compared to that of the current Red Hill project model. The 2007 regional model had a grid size that varied from 150 ft in the region of Red Hill to 1,000 ft in the outer regions of the model. The regional model consisted of two numerical layers.

The 2007 local model had a grid size that varied from 30 ft in the region of Red Hill to 600 ft in the outer regions of the model. The model consisted of seven numerical layers.

6.5.2 Representation of Groundwater Flow System

The conceptualization of the groundwater flow system components is similar to that presented by the USGS (Oki 2005), as discussed above. The regional model treated the valley fill using the hydraulic flow barrier (HFB) conditions available in MODFLOW. The local model simulated the valley fill explicitly in the five major valleys in the area (Waimalu, North Hālawa, South Hālawa, Moanalua, and Kalihi Valleys). However, the 2007 model did not address saltwater intrusion as did the USGS study (Oki 2005) instead it focused on the specific objectives of the DON (2007) study. Cross sections of the valley topography were analyzed to evaluate the depth of the valley fill for the local model.

Calibrated hydraulic parameters for the local model are similar to the USGS model of Oki (2005). As presented previously in Table 6-9, the basalt hydraulic conductivities were 4,428, 1,476, and 7.4 ft/d for the longitudinal horizontal, transverse horizontal, and vertical directions, respectively. Isotropic hydraulic conductivity values were assigned to the Valley Fill and Caprock at 0.066 ft/d and 115 ft/d, respectively.

6.5.3 Model Results

A transient calibration was also conducted with the local model for synoptic water level studies between May 10 and June 1, 2006. The simulation was conducted for a period of 17 days. Pumping at Red Hill Shaft was varied in a controlled manner, and resulting water level responses were measured at several surrounding wells (reproduced on Figure 6-26).

Figure 6-27 reproduces the pumping rate at Red Hill Shaft, and simulated and observed water level signals at the observation wells of Figure 6-26. The calibration is noted to be good for all wells except for Red Hill Shaft where simulated responses were more muted than observed. This may be a function of frictional losses, the way the tunnel and pool are constructed, and/or the method/location that water levels are measured. The simulated response at the Hālawa wells (Figure 6-27) was noted to be larger than observed indicating a larger effective simulated connectivity between Red Hill Shaft and these wells than indicated by the observations.

Capture zones created from the calibrated steady-state simulation indicated that capture at the Hālawa Shaft was not intersecting the Red Hill Facility area. The 2007 model also showed that pumping the Red Hill Shaft at average and maximum rates created a capture zone extending across the Facility.

Sensitivity analyses of the valley fill hydraulic conductivity indicated little difference in the water table except that increasing the conductivity caused the water table to decline beneath the valleys.

In 2014, Rotzoll used the 2007 model to further evaluate the impact of flow in the aquifer resulting from a simulated shutdown of the Navy Red Hill Shaft pumping (Rotzoll 2014). Capture zones developed for this simulation also indicated that capture at the Hālawa Shaft was not intersecting the Facility footprint. Figure 6-28 shows the 10-year capture zones computed by the DON (2007) simulation with Red Hill Shaft on, and by the Rotzoll (2014) simulation with Red Hill Shaft not pumping.

6.6 RED HILL 2018 GROUNDWATER FLOW MODEL AREA GROUNDWATER BALANCE

Fresh groundwater inflow originates as deep infiltration of precipitation and seepage from surface water features. Spatial distribution of recharge mimics the orographic rainfall pattern—recharge is highest on windward slopes and mountain peaks below the top of the trade-wind inversion. Human activity also affects recharge in some areas (Izuka et al. 2018).

Groundwater outflow includes withdrawals from wells and natural groundwater discharge to springs, streams, wetlands, and submarine seeps. Under predevelopment conditions, groundwater withdrawal was negligible and natural groundwater discharge probably was approximately equal to recharge. Under recent conditions, natural groundwater discharge (e.g., springs, submarine discharge) has been reduced by the pumping well withdrawals. Data collected by the USGS for groundwater levels, saltwater/freshwater interface, spring flow, and stream base-flow indicate an overall reduction in aquifer storage for most areas where groundwater has been developed (Izuka et al. 2018).

The available information for groundwater inflows and outflows has been collected and evaluated to characterize the groundwater balance for the groundwater model area, as described below.

6.6.1 Boundary Influx and Outflux

The 2018 Red Hill groundwater flow model area perimeter boundaries are shown on Figure 2-6 and Figure 6-25. Table 6-10 provides the estimated average annual groundwater inflows and outflows from each model boundary, and the information sources. Figure 6-29 illustrates the current conceptual groundwater balance.

Table 6-10: Estimated Average Annual Groundwater Inflows and Outflows from Model Boundaries, 2017

Source	Rate (mgd)
Northwest inflow	0
Southeast inflow	0
Northeast inflow	22.4
Recharge	30.3
Well discharge	-31.46
Spring discharge	-12.12
Seafloor groundwater discharge (calculated based on balancing the above inflows and discharges)	-9.12

6.6.2 Groundwater Recharge

Groundwater recharge from direct infiltration of precipitation and streambed seepage are important components of the CSM for groundwater and surface water. The principal surface water features in the primary area of interest include North Hālawa Stream, South Hālawa Stream, and Moanalua Stream. Where the water table lies below the streams, as is the case in the Facility area, in addition to recharge from precipitation, it is important to properly account for interactions between groundwater and surface water. The streams in the Facility area do not receive groundwater discharge because the groundwater table elevation is substantially below ground surface. Rather, seepage through the streambed during streamflow periods causes groundwater recharge. The relationships between surface water and groundwater are being evaluated and integrated within the CSM. This will be updated as data are further evaluated

Groundwater recharge in the 2007 model area was assigned to the upper model layer using rainfall-recharge regressions developed by Shade and Nichols (1996), with land use areas updated (Rotzoll and El-Kadi 2007). For the current groundwater modeling, the groundwater recharge component of the water balance was further updated based on the information from more recent USGS reports.

These recent USGS studies provide detailed maps of groundwater recharge rates (Engott et al. 2015; Izuka et al. 2018), and used as inputs to the CSM and groundwater model. North of the Facility, the Hālawa Quarry and Hawaiian Cement plant operations have modified the natural watershed topography and likely changed groundwater recharge rates in the area. The latest USGS report (Izuka et al. 2018) presents a map of recharge rates for recent conditions (2010 land cover, 1978–2007 rainfall). The other recent USGS report (Engott et al. 2015) provides a comprehensive water budget analysis and estimates of the spatial distribution of groundwater recharge rate. Results of the USGS analyses include maps covering the entire modeling area that show recharge rates estimated for drought conditions. Geospatial datasets from the USGS (received in September 2017) have been used to initially estimate the areal distribution of groundwater recharge rates in the groundwater flow model. For the model domain, the total groundwater recharge rate is calculated to be 30.3 mgd based on the data from the USGS (Engott et al. 2015). Figure 6-30 shows the distribution of groundwater recharge rates throughout the model domain.

Recharge rates reported by these recent USGS studies will be further evaluated and may need to be modified in some areas to account for anthropogenic effects possibly not considered by the USGS. For instance, the USGS studies appear to possibly not consider the accumulation of storm water runoff into the open pits of the Hālawa Quarry and seepage outflow discharge due to operations or the impounded stream east of the quarry. In addition, the cement plant operations just west of the quarry show substantial areas where cement truck washing and crushed rock washing cause process water discharges to the ground surface. Seepage from those areas may increase groundwater recharge rates.

On the other hand, natural groundwater recharge rates are substantially reduced by the extensive pavement area in the Hālawa Industrial Park and Hālawa Correctional Facility. Increased runoff from those areas reduces infiltration and diverts runoff flows and seepage to increase groundwater recharge in the adjacent non-paved areas. Another feature that affects groundwater recharge is the clay-rich saprolitic soil that is present at the ground surface, is of substantial thickness and extends throughout the Facility vicinity. This thick clayey soil cover probably reduces the recharge rates in the Red Hill area, especially at the surface of Red Hill. Also, extensive building roofs and pavements create nearly impermeable coverage of the land surface in the light industrial area immediately north of the Facility which also reduces recharge rates locally.

In combination, these surface features may substantially modify groundwater recharge rates, which could affect groundwater flow directions locally near the Facility, and thus will be incorporated into the numerical groundwater model.

6.6.3 Groundwater Discharge

Groundwater leaves the model area from pumping well withdrawals, springs, and seafloor seepage, as further described below.

6.6.3.1 Water Supply Well Pumping

Groundwater discharge from the modeling area occurs primarily by pumping of water supply wells and shafts. In the Rotzoll and El-Kadi (2007) steady-state calibrated model, each pumping well was assigned the average pumping rate for 1996 to 2005. For the model refinement, the pumping rate of each well will be updated based on available information from the DLNR CWRM, USGS, and BWS.

According to the USGS (Izuka et al. 2018), the CWRM database of user-reported water withdrawals was used to compile groundwater pumping information. For the period after 2000, the USGS worked closely with CWRM to ensure that the most current data were analyzed for the 2016 USGS study (Izuka et al. 2018). Withdrawal values for wells with data, along with well-construction information, were compiled from CWRM's database and BWS.

6.6.3.2 Spring Discharge

Natural groundwater discharge also occurs as diffuse seepage near the coast, and as discharge to springs that occur along the edge of the interface of basalt with caprock. Two springs are located within the study domain: Pearl Harbor Springs at Kalauao, and Kalauao Spring. Pearl Harbor Springs at Kalauao has considerable discharge, while discharge at Kalauao Spring is relatively minor and was neglected in the previous (Oki 2005; Rotzoll and El-Kadi 2007) modeling efforts. The estimated rates of discharge from seeps and springs are not provided in the recent USGS reports (Engott et al. 2015; Izuka et al. 2018). Oki (1998, 2005) used available data to develop linear-regression equations for each of the major spring areas relating spring discharge to groundwater levels in the Navy 'Aiea Well (2256-10). Discharge from the Pearl Harbor springs was correlated with on the head in the aquifer at the Navy 'Aiea Well: discharge is high when head in the aquifer is high, and discharge is low when head in the aquifer is low. In the 2007 local Red Hill groundwater model (Rotzoll and El-Kadi 2007) and the 2018 Red Hill groundwater flow model, the spring discharge rates were based on the regression analysis by the USGS (Oki 1998). Based on available information, average annual spring discharge is 12.12 mgd for 2017. The seafloor groundwater discharge is estimated as a closure term of water balance to be 9.12 mgd.

6.7 General Groundwater Chemistry Distribution

The major ion composition of groundwater samples collected from Red Hill area monitoring wells in November 2016 is shown in Table 6-11. Values in the table are provided in mg/L, and expressed as milli-equivalents per liter (meq/L). Major ion composition of the groundwater is shown on Figure 6-31, which is a trilinear plot of the data in Table 6-11. On the trilinear plot, the colored dots indicate the well location from which samples were collected.

Preparing a trilinear plot is useful for interpreting groundwater analysis data because it facilitates visual comparison of the major chemical components in water samples that may reflect the effects of recharge, aquifer interactions, and chemical sources on natural groundwater. Each data point on the trilinear plot shows the composition of the water sample as a percentage of total ions, in meq/L. A plot of several samples from different locations in a study area is often useful to identify mixtures of

different water types (Hem 1985). Mixing of two distinct water types is seen as a linear trend in the data points on the trilinear diagram for samples lying between the two distinct water-type endpoints.

Table 6-11: Major Ion Composition of Groundwater Samples Collected from Red Hill Monitoring Wells, November 2016

Monitoring Well / Sampling Point	Unit	Ca	Mg	Na	K	CO_3	HCO_3	Cl	SO_4
RHMW2254-01	mg/L	15.8	15.4	42.2	2.23	1.7	67.4	72.3	18.5
	meq/L	0.78842	1.26742	1.8357	0.057088	0.0561	1.10536	2.03886	0.3848
RHMW01	mg/L	11.5	9.88	35.2	1.9	1.7	94.4	39.4	4.5
	meq/L	0.57385	0.813124	1.5312	0.04864	0.0561	1.54816	1.11108	0.0936
RHMW02	mg/L	12.6	24.8	53.6	2.44	1.7	196	39	1.2
	meq/L	0.62874	2.04104	2.3316	0.062464	0.0561	3.2144	1.0998	0.02496
RHMW03	mg/L	25	33.4	104	3.7	1.7	285	47.2	45.7
	meq/L	1.2475	2.74882	4.524	0.09472	0.0561	4.674	1.33104	0.95056
RHMW04	mg/L	16.9	18.6	34.7	1.96	1.7	75.2	72.8	9.8
	meq/L	0.84331	1.53078	1.50945	0.050176	0.0561	1.23328	2.05296	0.20384
RHMW05	mg/L	7.85	13.2	136	4.93	1.7	98.1	157	46.5
	meq/L	0.391715	1.08636	5.916	0.126208	0.0561	1.60884	4.4274	0.9672
RHMW06	mg/L	35.1	54.9	165	2.33	1.7	108	365	81.8
	meq/L	1.75149	4.51827	7.1775	0.059648	0.0561	1.7712	10.293	1.70144
RHMW07	mg/L	55.5	71.9	150	3.04	1.7	119	411	67.9
	meq/L	2.76945	5.91737	6.525	0.077824	0.0561	1.9516	11.5902	1.41232
RHMW08	mg/L	32.7	12	109	5.68	1.7	50.8	169	58.2
	meq/L	1.63173	0.9876	4.7415	0.145408	0.0561	0.83312	4.7658	1.21056
RHMW09	mg/L	12.9	11.6	36.6	2.11	1.7	66.5	51.5	10.1
	meq/L	0.64371	0.95468	1.5921	0.054016	0.0561	1.0906	1.4523	0.21008
HDMW2253-03	mg/L	12.9	17.5	57.1	0.608	1.7	50	84.7	27.6
	meq/L	0.64371	1.44025	2.48385	0.0155648	0.0561	0.82	2.38854	0.57408
OWDFMW01	mg/L	115	220	350	7.64	1.7	161	1070	368
	meq/L	5.7385	18.106	15.225	0.195584	0.0561	2.6404	30.174	7.6544

Ca calcium
Cl chloride
CO_3 carbonate
HCO_3 bicarbonate
K potassium
Mg magnesium
mg/L milligrams per liter
Na sodium
SO_4 sulfate

Major ion data for the Red Hill area groundwater samples plotted on this trilinear diagram show a distinct mixing trend. Water from RHMW07 is composed mainly of the sodium-chloride type, and lies at one end of the mixing trend. The water sample from RHMW07 is very similar to rainfall water shown on the trilinear plot reported by the USGS (Visher and Mink 1964). Water at OWDFMW01 is similar to the sodium-chloride type water at RHMW07, but with slightly more magnesium. The other end point of the mixing trend is represented by samples from wells RHMW02 and RHMW03, in which sodium and bicarbonate are the dominant ions. This type of water is typical of the basal basalt aquifer in the Pearl Harbor area as described by Visher and Mink (1964), and plot in the same area of

the Figure 6-31 trilinear plot as the November 2016 samples from RHMW01, RHMW02, and RHMW03.

Additional groundwater chemistry data have recently been compiled by the University of Hawai'i at Mānoa (UHM) Water Resources Research Center (WRRC) as part of a Department of Energy (DOE)-funded geothermal assessment study and provided to the Navy by UHM (see Table 6-12). These groundwater samples were collected as part of statewide geothermal resource assessment funded by the DOE. As part of that effort, the Navy (NAVFAC) facilitated the collection of water samples from a suite of monitoring wells located on Navy facilities. Samples were collected at 12 wells in the NAVFAC monitoring network and were analyzed for major ions, trace metals, and oxygen and hydrogen isotopes. UHM also compared these data from the Red Hill area with four samples collected elsewhere on O'ahu by UHM and data collected by the USGS for the National Water Quality Assessment 2001 (https://pubs.usgs.gov/wri/wri034305/).

Even though these data have not been published, some are relevant and useful for the CSM of groundwater flow, as described below. Overall the major ion concentrations reported in the UHM groundwater data are comparable to the general water chemistry data in Table 6-11 and consistent with Figure 6-31.

One of the most meaningful natural geochemical parameters in groundwater is chloride because it is less reactive than other major ions with the crystalline rock, sediment, and soils through which groundwater moves. Chloride is also relatively unaffected by bacterial reactions and biodegradation processes. Samples from wells nearest the Red Hill fuel tanks show the lowest chloride concentrations, which range from 37 to 47 mg/L in wells RHMW02, RHMW01, and RHMW03, respectively. In contrast, chloride concentrations range from about 420 mg/L at wells RHMW06 and RHMW07 to about 1,100 mg/L at Well OWDFMW01. The deep water sample from HDMW2253-03 (624 ft) contained chloride at 1,874 mg/L, while the shallow sample from the same well collected at 50 ft depth contained chloride at only 88 mg/L. For comparison, the sample from Hālawa Shaft contained chloride at 120 mg/L. Bivariate plots were developed to evaluate conductivity in groundwater (Figure 6-32 through Figure 6-35). HDMW2253-03 has a relatively high chloride signature (along with associated ions) that is also influencing surrounding wells such as RHMW06 and RHMW07. OWDFMW01 also has a relatively high chloride signature, but this is likely due to past operations.

The spatial distribution of the chloride concentrations are consistent with, and provide additional support for, the conceptual model of the groundwater flow pattern in the Facility area that is described above (Sections 6.1 and 6.2). Specifically, the pattern of chloride concentrations suggests that chloride is being added to the relatively fresh groundwater flow system in the area north of South Hālawa Stream. As this higher-chloride groundwater flows southward, it is being diluted by lower-chloride groundwater flowing southwestward beneath South Hālawa Stream and the Facility. Mixing of the higher chloride water flowing from the north with the lower chloride water flowing from the northeast and east, the resulting chloride concentration is reflected in the sample of Red Hill Shaft, approximately 90 mg/L.

UHM also provided stable isotopic measurements of oxygen and hydrogen for the groundwater samples. In particular, these data include (1) the ratio of the "heavy" isotope of hydrogen ^{2}H to the common and "lighter" isotope ^{1}H; and (2) the ratio of the heavy isotope of oxygen ^{18}O to the common and lighter isotope ^{16}O. The values are expressed as a ratio between the heavy and light isotopes in the water sample to those ratios in an isotopic standard derived from seawater. The units are parts per mil (o/oo) and designated $\delta^{2}H$ for hydrogen and $\delta^{18}O$ for oxygen. To facilitate

interpretation, these isotopic data are typically plotted on an X-Y graph with $\delta^{18}O$ on the X axis and $\delta^{2}H$ on the Y axis. Factors affecting the isotopic composition of water include the temperature of precipitation, the distance the water vapor travels before precipitation, latitude, and amount of evaporation. Nonetheless, most groundwater samples for $\delta^{18}O$ and $\delta^{2}H$ plot closely to the Global Meteoric Water Line where: $\delta^{2}H = 8*\delta^{18}O+10$. However, there is also some regional variability in the relationship between $\delta^{2}H$ and $\delta^{18}O$, which is referred to as the Local Meteoric Water Line (LMWL). The estimated LMWL for the site is shown on Figure 6-36, along with data from several Red Hill monitoring network wells.

In the preliminary UHM analyses of these data provided to the Navy, UHM performed a regression analysis to provide a preliminary LMWL based on reasonable assumptions and the available data. This preliminary LMWL is very similar to the LMWL developed by UHM and the USGS for Hawai'i and Maui Islands. The RHMW well samples plot along the LMWL except for OWDFMW1, which falls well to the right of the LMWL. Two processes are commonly viewed as causing such a deviation from the LMWL: (1) direct evaporation of the water prior to deep infiltration; and (2) geothermal influence due to isotopic exchange of water oxygen with oxygen in the silicates in the rocks (which are isotopically much heavier than the water).

For the Red Hill area groundwater sample data, evaporation of the water prior to deep infiltration (groundwater recharge) is one explanation for this deviation in the OWDFMW01 data. In addition, past operations in this area may have also resulted in these water quality anomalies.

As described in the UHM evaluation, these isotopic data for groundwater are useful for estimating the effective (volume-weighted average) elevation that the groundwater recharge occurred. Studies done by the USGS and UHM have shown a strong correlation between the isotopic composition of rainfall and the elevation where that rainfall reached the ground surface. The relationship between the isotopic composition of rainfall and elevation varies depending on whether or not the rainfall occurred above the trade wind inversion elevation and whether the rainfall occurred on the windward or leeward slope of an island. For East Maui, it was found that for elevations less than 1,900 meters (m) (6,200 ft) the following relationship between recharge elevation and the δ18O values:

- Windward slopes: Recharge Elevation (m msl) = $-860*\delta^{18}O$
- Leeward slopes: Recharge Elevation (m msl) = $-810*\delta^{18}O$

Using this relationship, the Red Hill area monitoring well data were used by UHM to estimate that groundwater recharge occurred over an elevation range of approximately 2,100 ft. This estimate is based on the difference in the $\delta^{18}O$ value at HDMW2253-03 (-2.93 in shallow sample from 50 ft depth) and RHMW03 (-3.72). UHM found that $\delta^{18}O$ values for RHMW04, RHMW06, RHMW07, and HDMW2253-03 are consistent with lower elevation recharge, while the $\delta^{18}O$ values for the other Red Hill area wells and wells at the Moanalua and Honolulu International Country Club are consistent with middle- to higher-elevation recharge. These and other data may suggest recharge from various locations/elevations is flowing along different flow paths generally paralleling the primary lava flows from the Ko'olau range during the shield-building phase. In summary, the stable isotope groundwater data for oxygen and hydrogen are consistent with the conceptual model of the groundwater recharge and flow pattern in the Red Hill Facility area that is described above (Sections 6.1 and 6.2).

Table 6-12: Groundwater Chemistry Data Compiled by the University of Hawai'i Water Resources Research Center for Geothermal Study

Well No.	Name	Date	Specific Conduc-tivity	pH	ORP	Alk	DO (mg/L)	Turb	NO_3	Ca	Mg	K	Na	Br	Cl	F	SiO_2	SO_4	HCO_3	CO_3	Hydrogen 2/1 ratio	Oxygen 18/16 ratio	δ^{18}O_CORR	δ^{2}H_CORR
HDMW2253-03 Deep Sample																								
3-2253-003	HDMW@-624ft	3/6/2017	5,500	7.15	41	31	7.2	—	0.2	320.9	279.4	15.9	473.8	6.4	1,874.0	0.01	39.2	247.2	37.8	18.6	-11.45	-3.06	-12.98	-3.41
Red Hill Outside Wells																								
OWDFMW1	OWDFMW1	7/19/2016	4,042	8.02	117	166	4.0	67.0	1.6	106.1	244.9	7.3	368.5	3.0	1,059.0	0.05	51.4	321.1	202.5	99.6	-20.14	-3.40	-21.59	-3.61
3-2253-005	RHMW07	7/19/2016	1,869	7.26	152	97	2.6	1.7	0.9	61.2	82.6	3.0	162.3	1.4	431.0	0.06	76.2	72.6	118.3	58.2	-13.22	-2.96	-13.81	-3.04
3-2253-007	RHMW08	1/11/2017	1,001	8.20	168	56	4.7	2.0	n0.5	32.4	18.9	5.6	108.6	0.6	169.0	0.23	45.6	79.0	68.3	33.6	-16.70	-3.60	-17.13	-3.65
3-2253-003	HDMW@-50ft	3/6/2017	485	6.71	56	45	5.1	—	0.2	11.8	15.5	0.4	50.7	0.2	88.0	0.06	65.0	27.6	54.9	27.0	-11.80	-2.90	-12.14	-2.93
3-2253-004	RHMW06	7/19/2016	1,568	6.93	193	100	6.3	4.2	0.6	45.2	74.2	2.4	198.9	1.3	416.0	0.06	74.3	94.6	122.0	60.0	-12.85	-3.01	-13.42	-3.09
RHMW04	RHMW04	7/19/2016	437	6.50	201	56	8.6	6.0	0.6	18.6	18.8	2.3	33.8	0.3	74.0	0.06	57.1	10.9	68.3	33.6	-11.61	-3.03	-11.94	-3.06
Red Hill Tunnel Wells																								
3-2254-001	RHMW2254-01	1/9/2017	450	7.54	171	54	8.6	-4.4	0.0	16.7	15.7	2.5	41.8	0.3	89.0	0.07	49.1	15.2	65.9	32.4	-10.30	-3.20	-10.64	-3.23
RHMW05	RHMW05	2/7/2017	844	7.91	119	90	8.3	-2.2	1.0	7.8	12.8	4.9	138.8	0.5	148.0	0.33	86.5	46.2	109.8	54.0	-13.00	-3.30	-13.39	-3.34
RHMW01	RHMW01	2/6/2017	333	6.87	-19	92	0.5	-5.8	0.4	—	—	—	—	—	40.9	—	—	4.6	112.0	—	—	—	—	—
RHMW02	RHMW02	2/7/2017	519	6.54	-37	188	0.1	-2.1	0.4	13.4	25.7	2.3	53.0	0.1	37.0	0.64	91.3	0.4	229.4	112.8	-11.80	-3.20	-12.11	-3.22
RHMW03	RHMW03	1/12/2017	802	6.77	198	252	3.0	-0.5	1.8	24.5	32.2	3.3	98.2	0.2	47.0	0.18	86.2	44.2	307.4	151.2	-17.90	-3.70	-18.22	-3.72
BWS Wells																								
3-2354-001	Hālawa Shaft	3/6/2017	560	—	—	52	—	—	0.5	27.0	23.0	2.5	38.0	0.4	120.0	—	—	—	—	—	—	—	—	—

— no data

δ^{18}O_CORR ratio between the heavy and light isotopes of oxygen in the water sample to those ratios in an isotopic standard derived from seawater (corrected) in parts per mil (o/oo)
δ^{2}H_CORR ratio between the heavy and light isotopes of hydrogen in the water sample to those ratios in an isotopic standard derived from seawater (corrected) in parts per mil (o/oo)
Alk alkalinity
Br bromide
Ca calcium
Cl chloride
CO_3 carbonate
DO dissolved oxygen
F fluoride
HCO_3 bicarbonate
K potassium
Mg magnesium
NO_3 nitrogen
ORP oxidation-reduction potential
SiO_2 silica dioxide
SO_4 sulfate
Turb turbidity

This page intentionally left blank

6.8 ASSESSMENT OF LOEs FOR GROUNDWATER FLOW

The regional groundwater head gradients are from east to west within the study domain. Local-scale heterogeneities including clinker zones with large contrasts in hydraulic properties cause local variations in these flow gradients. Multiple LOEs exist for the conceptual model of groundwater flow directions in the Facility area, including:

- Groundwater levels measured throughout the Facility area of interest are consistent with the regional groundwater levels and flow directions reported in previous studies, which include those by the USGS (Oki 2005) and DON (2007, 2010).
- Spatial distributions of groundwater level elevations measured in the Red Hill area monitoring wells show hydraulic gradients are generally southwestward beneath the Facility, even when Red Hill Shaft was not pumping in November 2016. However, the gradient at Red Hill is extremely gentle and is also affected by local heterogeneities.
- Quarterly water level data from 2007 to present show that RHMW07 fluctuations closely correspond with other water table monitoring wells and are representative of groundwater levels in the basal aquifer.
- Borehole geologic logs show a deep saprolite zone occurs beneath South Hālawa Valley and forms a low-permeability barrier to groundwater flow. At new monitoring well RHMW11, this saprolite extends to approximately 87 ft below the regional basal groundwater table. New data from multiple intervals in RHMW11 show the saprolite zone is continuously saturated and the groundwater levels in the saprolite are still equilibrating but indicate a downward vertical hydraulic gradient, and the water table is much higher than at the nearby well RHMW07 and other Red Hill wells. However, the lateral and vertical extent of the saprolite has not been delineated particularly in the upper portion of South Hālawa Valley.
- Groundwater flows from areas of higher recharge to areas lower recharge or discharge. Recharge occurs as a result of direct infiltration of rainfall, seepage from streams and other water sources at the land surface. Recharge rates are spatially distributed throughout the groundwater model area such that higher recharge occurs at higher land surface elevations as recently estimated by the USGS.
- Water sources in the Hālawa Quarry/cement plant area north of South Hālawa Valley as well as other local recharge sources may increase groundwater recharge rates locally, create shallow perched water zones, and increase the water table elevation in the basal aquifer in the area north of South Hālawa Valley.
- The geologic log of Red Hill Water Development Tunnel (i.e., Red Hill Shaft) shows a highly permeable clinker zone in the last couple hundred feet of the tunnel. Groundwater contours reflect a converging flow pattern toward the eastern end of the water tunnel.
- Time-series water level data from the May 2006 pumping test of Red Hill Shaft and the USGS/BWS May 2015 pumping test of Hālawa Shaft suggest there is a hydraulic barrier located north of monitoring well RHMW07.
- Pump test data from the 2017/2018 synoptic monitoring indicate that RHMW07; RHMW11 Zones 6, 7, and 8; Hālawa Deep Monitoring Well (HDMW2253-03) chase tube and others do not respond to pumping from Red Hill Shaft or Hālawa Shaft.
- Trends in major chemical components in groundwater from monitor wells indicates mixing of two main groundwater types, a sodium-chloride type water from the area north of South Hālawa Valley and sodium-bicarbonate type from the southeast.

- Groundwater chemistry data from Red Hill area wells compiled and evaluated by UHM, which include major ions and stable isotopes of oxygen and hydrogen, support the conceptual model of the groundwater recharge and flow pattern in the Red Hill Facility area described above.

Groundwater levels measured throughout the Facility area of interest are consistent with the regional groundwater levels and flow directions reported in previous studies, which include those by the USGS (Oki 2005) and DON (2007, 2010).

6.9 UNCERTAINTY ANALYSIS

Uncertainties associated with the Saturated Zone Model include insufficient data and information regarding:

- *Groundwater flow directions and rates in the groundwater model area.* Recently, the direction and rate of migration of groundwater potentially impacted by COPCs from the Facility has been better defined. Accurate hydraulic heads (groundwater levels) and hydraulic gradients in the area of existing Red Hill groundwater monitoring wells were recently established by the high-accuracy survey of wellhead elevations (DON 2018a). Nonetheless, some uncertainty remains in the spatial distribution of hydraulic heads and hydraulic gradients in the area extending northward to Hālawa Shaft and in the area extending from the Facility southward to the Moanalua and TAMC Wells. In addition, it is not clear what the reported Hālawa Shaft water levels represent because details on the measuring point used for water level measurements have not been obtained.
- *The thickness and extent of HGUs in the groundwater model area.* In particular, better definition of the depths of older alluvial sediment fill and saprolite in areas beneath North and South Hālawa Valleys is needed.
- *Geologic features that may act as preferred groundwater flow pathways or barriers.* Clinker zones, paleo-channels, faults, dense low-permeability lava flows, and lava tubes in the primary area of interest result in heterogeneities that may affect local gradients. Sensitivity analyses help bound many of these factors.
- *Hydraulic properties of the Basalt HGU (the basal aquifer).* Additional data are needed to calibrate the groundwater flow model and refine aquifer hydraulic properties, including transmissivity, hydraulic conductivity, heterogeneity, anisotropy, storativity, and specific yield. These are being developed from the 2017/2018 synoptic monitoring dataset.
- *Groundwater recharge and discharge rates.* Recharge and discharge rates at Red Hill, the cement plant, crushing facility, and quarry to the north are not yet defined. The degree to which recharge rates are reduced by the thick clayey saprolitic soil overlying the Red Hill Facility is also not well defined. Total groundwater discharge flux out of the model area is currently unknown. Flow monitoring of larger springs in the Pearl Harbor area is being conducted by the USGS, and these data are available from the USGS website, but total groundwater discharge flux out of the model area is not being measured and are not reported in recent USGS reports (Engott et al. 2015; Izuka et al. 2018).

6.10 ADDRESSING UNCERTAINTIES

The following ongoing, planned or proposed activities are designed to help resolve the uncertainties described in Section 6.9.

6.10.1 Groundwater Flow Directions and Rates

A high-precision well elevation survey has recently been completed to more accurately determine the measuring point elevations of all wells in the Red Hill groundwater monitoring network (DON 2018a). Data from this survey will enable more accurate determinations of hydraulic heads and hydraulic gradients using the available groundwater level measurements.

Similar groundwater level data from additional monitoring well locations are needed to better define the direction and rate of migration of groundwater potentially impacted by COPCs from the Facility, and to further define the spatial distribution of hydraulic heads (groundwater levels) and hydraulic gradients in the areas extending northward to Hālawa Shaft, near the Red Hill Shaft water development tunnel, and in the area extending southward to the Moanalua and TAMC Wells. Accordingly, additional monitoring wells are planned or currently being installed at selected key locations to provide these data (see Figure 2-9) (DON 2017f). Furthermore, the numerical-model-simulated water levels at wells that are currently monitored for regional flow conditions will be evaluated in a similar manner to the monitoring data to establish if the simulations are consistent with observations.

Groundwater level elevation data are needed to represent both non-pumping conditions and various combinations of pumping these wells. The additional monitoring wells will need to be completed with intake intervals that measure groundwater levels (hydraulic heads) to define the potentiometric surface, which will reflect horizontal hydraulic gradients at the water table. Hydraulic head measurements are also needed from intervals deeper below the water table to measure the vertical hydraulic gradient at the selected locations. The 2017–2018 USGS synoptic study of pumping and water level monitoring data are being analyzed to establish the aquifer response to non-pumping and various pumping conditions to help better define the hydraulic properties that affect regional groundwater flow.

Additional data to define hydraulic heads and gradients have been collected from the Westbay system in RHMW11 where a shallow saturated zone appears to extend to the water table within saprolite, and will be collected from additional monitoring wells in the area south of Hālawa Shaft and elsewhere in Hālawa Valley.

Groundwater data obtained from the new monitoring wells will be used to further define the actual groundwater flow directions, and the updated groundwater model will be calibrated to reflect those new data. As part of the investigation, the potential for transient and/or local groundwater flow northwestward from the Facility (see Section 6.9) will also be evaluated.

6.10.2 Thickness and Extent of Hydrogeologic Units

Geologic maps showing the Caprock HGU thickness and elevation of the top of the Basalt HGU were published in recent USGS studies (Izuka et al. 2018). For these maps, the geospatial datasets have been obtained from the USGS are now being evaluated to estimate the extent and thickness of the HGUs in the model area. However, additional hydrogeologic data are needed to better define the depths of older alluvial sediment fill and saprolite in areas beneath North and South Hālawa Valleys. Detailed borehole geologic logs of deep borings in those areas would reduce this uncertainty. Borings from the Honolulu Area Rapid Transit (HART) study were evaluated for integration into cross sections within the groundwater model domain to further improve the geologic model. Valley fill/saprolite may locally affect groundwater movement, and additional data will help improve the understanding of hydraulic gradients and groundwater flow directions. One of the sensitivity models prepared during the interim groundwater flow modeling evaluated the existence and effect of saprolite in the North and South Hālawa Valley. The results indicate that groundwater flow is not

sensitive to the existence of saprolite in South Hālawa Valley based on the assumptions used in this analysis. The Navy is currently planning at least one new boring for installing a monitoring well in North Hālawa Valley to provide geologic data to define the valley fill and saprolite thickness immediately south of Hālawa Shaft.

6.10.3 Preferential Pathways and Barriers

Hydrogeologic data are being collected from the Red Hill area monitoring wells now being installed. These data will support further evaluation of geologic features that may act as preferred groundwater flow pathways or barriers. Similar data will also be needed from additional monitoring well locations. Together these data will be evaluated to better define the spatial distribution of clinker zones, paleo-channels, faults, dense low-permeability lava flows and dikes in the primary area of interest for groundwater modeling. Recent analysis (see further discussion in Section 5) of primary basalt flow directions relative to the formation of lava tubes in pāhoehoe at Red Hill indicate that it would be highly unlikely for a lava tube to extend in the direction of Hālawa Shaft from Red Hill. In addition, any such tube would be intersected by valley fill and saprolite in South and North Hālawa Valleys, which would prevent it from acting as a preferential pathway from Red Hill to Hālawa Shaft. Available geophysical methods will be evaluated to identify potential surveys at the land surface and in borings that may be effective considering the geologic complexities, anthropogenic interferences, and other limitations of applying geophysical methods at this site.

6.10.4 Hydraulic Properties of Basalt HGU

The new monitoring wells being installed will include borehole geologic/geophysical logs and core samples for further characterizing the physical properties of the Basalt HGU (basal aquifer), such as was recently obtained from monitoring well RHMW11. However, additional data are needed for calibrating the groundwater flow model to refine aquifer hydraulic properties, which include transmissivity, hydraulic conductivity, heterogeneity, anisotropy, storativity, and specific yield.

The existing 2007 groundwater model was calibrated using pumping test data from May 2006, when fewer monitoring wells were available near the Facility. Since 2007, the only new information relevant to aquifer hydraulic properties in the modeling area is the USGS dataset collected in May 2015 while the BWS Hālawa Shaft pumping was being pumped and the 2017/2018 synoptic monitoring under various pumping conditions. Other wells in the Hālawa and Moanalua area were also being pumped during that time, but the pumping data appear to be incomplete. Variable pumping rates add further uncertainty in evaluating the data.

To address the uncertainty, a regional-scale aquifer test with synoptic monitoring of groundwater levels in monitoring wells and pumping rates of supply wells located near the Facility was recently completed. As requested by the Navy, the USGS performed synoptic monitoring of 23 monitoring wells while the supply wells are pumped in sequence at controlled flow rates and continuously monitored (USGS 2017e). Using these regional pumping test data, the groundwater flow model will be calibrated using an iterative process to reasonably match these data by adjusting the aquifer hydraulic properties in the model within the range of reported values from other studies. The flow model calibration will be complete when the refined model simulations reasonably match the time-series drawdown and recovery data, the measured hydraulic gradients, and groundwater level contour maps for non-pumping and pumping conditions.

6.10.5 Groundwater Recharge and Discharge Rates

A more detailed conceptual model of the water balance (hydrologic budget) at the cement plant, crushing facility, and quarry is being developed to better estimate groundwater recharge rates in that

area. These data will be important to evaluate the local hydrologic budget of that area, and will be used to refine the estimated recharge rates. Results of this local water balance analysis will be integrated with the groundwater balance for the entire model area, and the refined groundwater recharge rates will be input to the numerical groundwater model.

A number of monitoring wells in South Hālawa Valley and to the north have encountered shallow, possibly perched, groundwater, which is further indication of the increase in local groundwater recharge rates and/or an indicator of lower permeability materials. A pressure transducer was placed in one of the shallow monitoring wells at the Hālawa Correctional Facility. Based on review of the most recent data on the USGS website the water table elevation in this well is approximately 150 ft above msl. In context the heads in the basal aquifer are generally 18 to 20 ft above msl, while the most recent (but still equilibrating saprolite zones in RHMW11 are 70 to 105 ft above msl. As described in Module A: Physical Setting (Section 2), further evaluation of new and existing data will be conducted to help define the contiguous or isolated nature of this shallow water zone. The CSM will be updated to describe the perched water locations and depths (elevations).

Infiltration tests are now being considered for surface soil above the Facility to determine the hydraulic parameters of the thick clayey saprolitic soil overlying the Red Hill Facility.

Natural groundwater discharge also occurs along the coast, and thus the groundwater model update needs to specify the rate of this flux. Updated estimates of groundwater recharge and discharge may become available from the USGS modeling studies currently underway. If not, however, the impact of these data gaps will be further evaluated during the modeling.

This page intentionally left blank

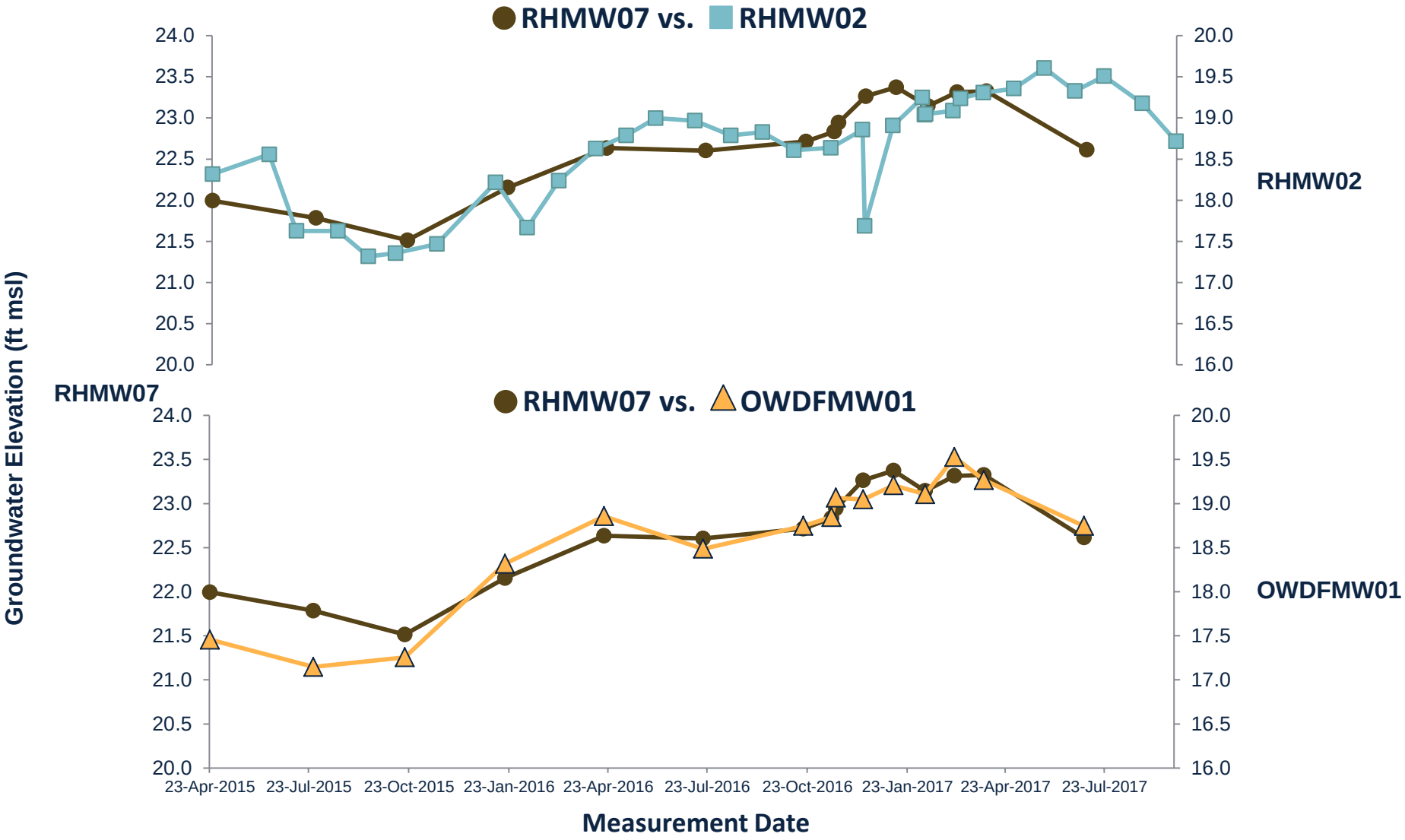

Figure 6-1
Hydrographs of RHMW07 vs. RHMW02 and OWDFMW01
Conceptual Site Model
Investigation and Remediation of Releases and Groundwater Protection and Evaluation
Red Hill Bulk Fuel Storage Facility, JBPHH, O'ahu, Hawai'i

This page intentionally left blank

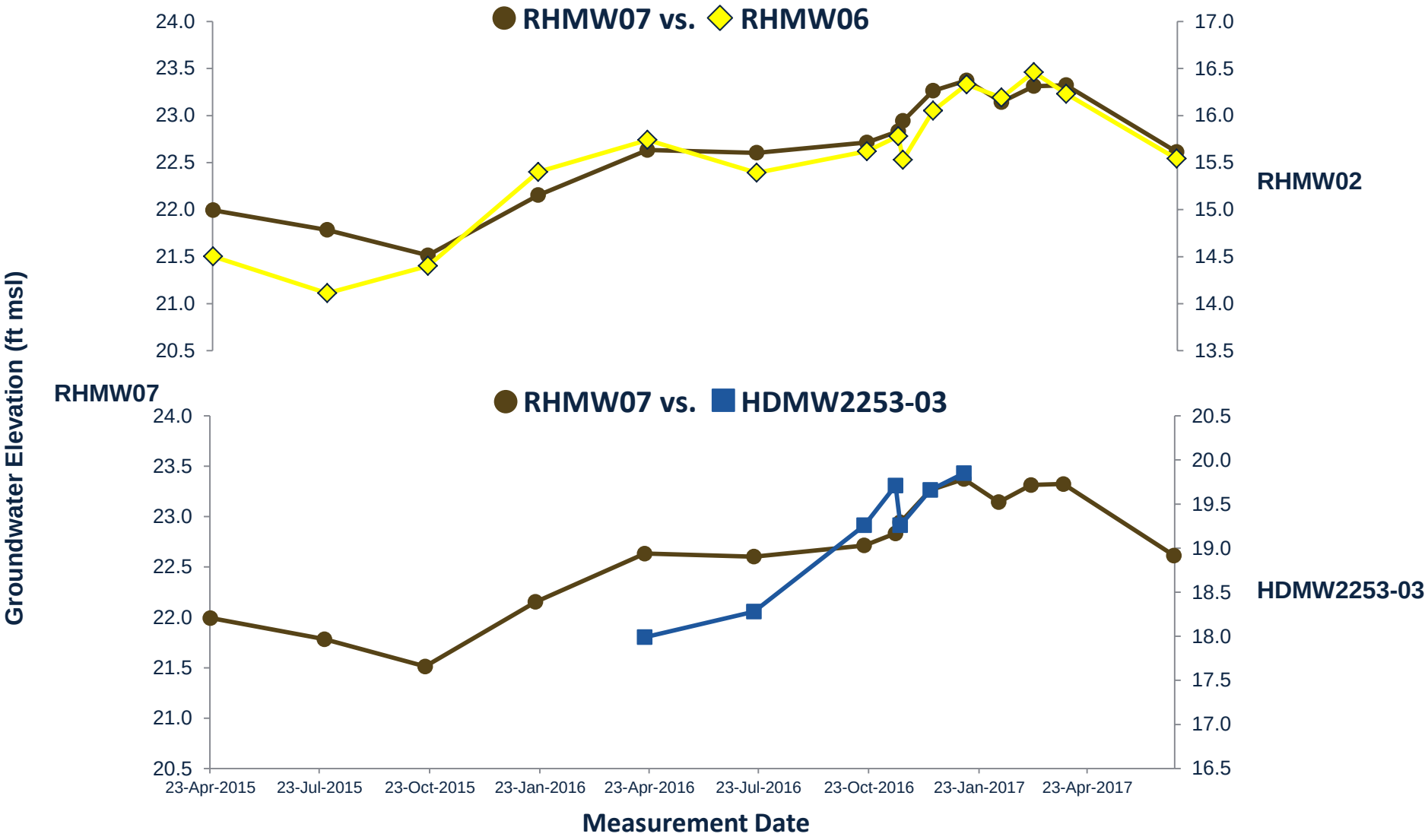

Figure 6-2
Hydrographs of RHMW07 vs. RHMW06 and HDMW2253-03
Conceptual Site Model
Investigation and Remediation of Releases and Groundwater Protection and Evaluation
Red Hill Bulk Fuel Storage Facility, JBPHH, O'ahu, Hawai'i

This page intentionally left blank

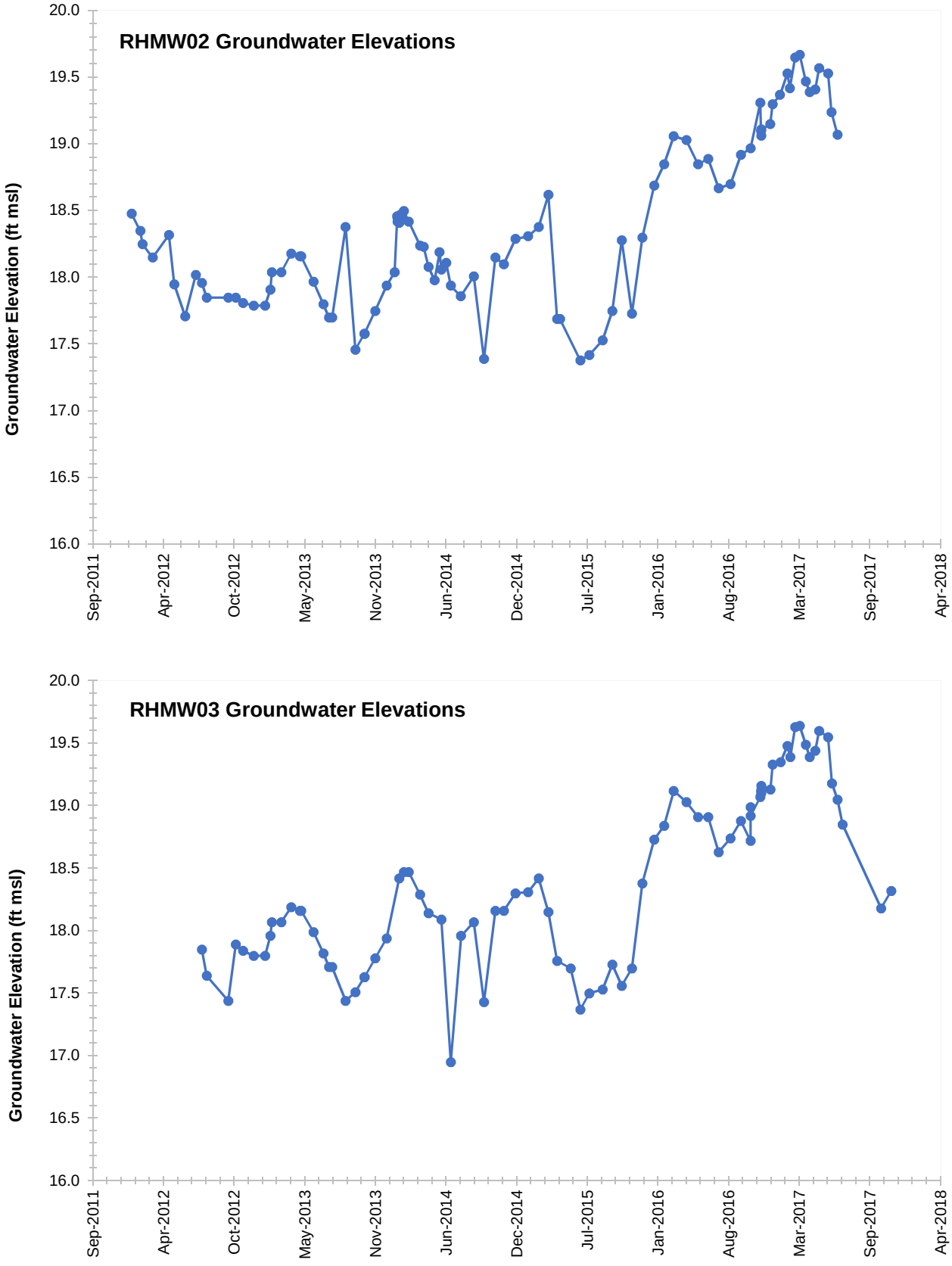

Figure 6-3
Time-Series Graphs of Wells RHMW02 and RHMW03
Conceptual Site Model
Investigation and Remediation of Releases and Groundwater Protection and Evaluation
Red Hill Bulk Fuel Storage Facility, JBPHH, O'ahu, Hawai'i

This page intentionally left blank

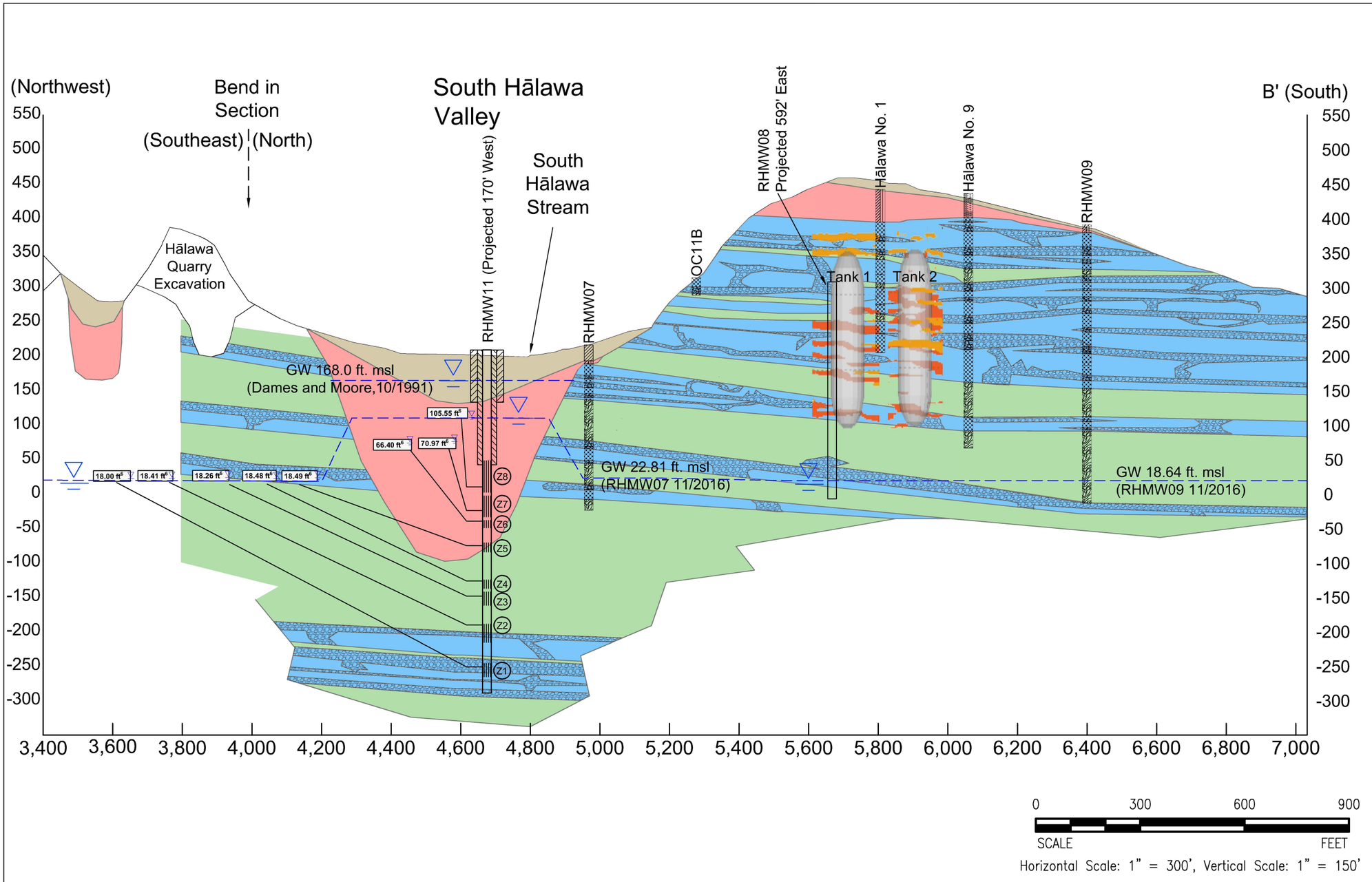

Key Plan

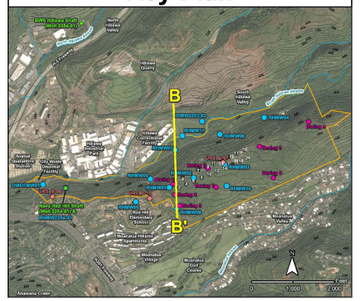

Legend

- Valley Fill
- Saprolite
- Basalt - A'ā Clinker
- Basalt - Massive A'ā
- Basalt Pāhoehoe
- Measured Groundwater (date)

Notes

1. RHMW07: DON 2015a
2. RHMW09: DON 2017e
3. Hālawa No.1, 9: Macdonald 1941
4. Outcrop OC11B: Field Notes 2017
5. Clinker in As-Built Barrel Log: DON 1943

S:\Projects\NAVFAC PAC\CLEAN V\60571032_CTO1BF0126\900-Work\910 CAD\20-SHEETS\cross-sections\Fig6-4_CrossSecB-B'.dwg 08/01/18 12:42 PM Nomod

Figure 6-4
Cross Section B-B' (View Looking East)
Conceptual Site Model
Investigation and Remediation of Releases and Groundwater Protection and Evaluation
Red Hill Bulk Fuel Storage Facility, JBPHH, O'ahu, Hawai'i

This page intentionally left blank

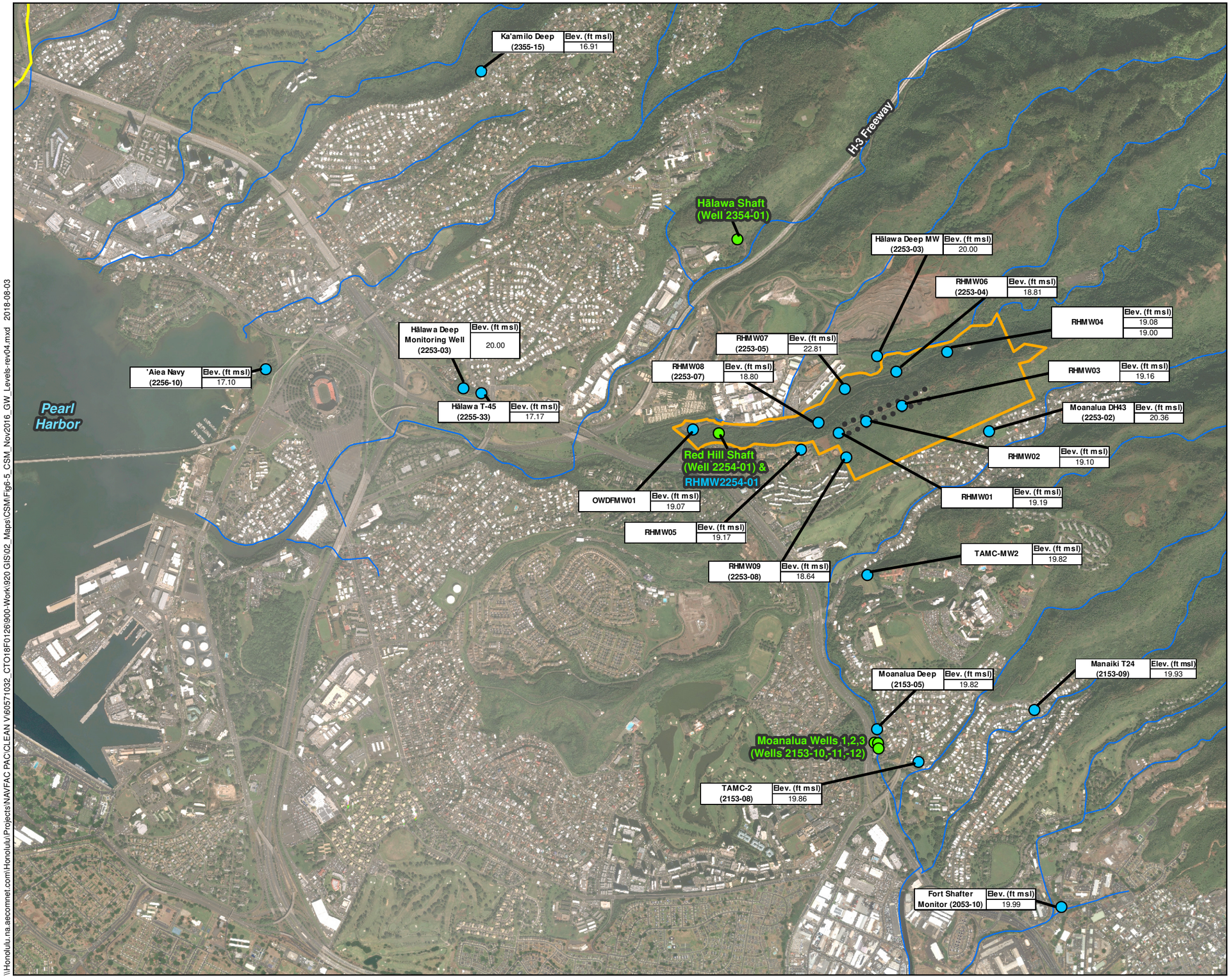

Location Map

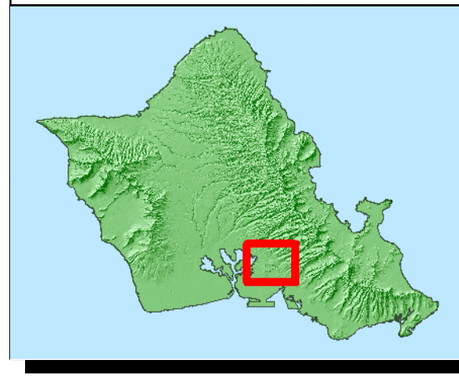

Legend

- Groundwater Monitoring Location
- Water Supply Well
- Stream
- Red Hill Facility Boundary and Fuel Storage Tanks
- Groundwater Model Area

Notes

1. Map projection: NAD 1983 UTM Zone 4N
2. DigitalGlobe, Inc. (DG) and NRCS. Publication_Date: 2015
3. Definitions:
   - BWS Honolulu Board of Water Supply
   - ft foot or feet
   - msl mean sea level
   - MW monitoring well
   - NM not measured
4. All water levels were measured on 11/18/2016. Measurements were collected between 8:00am and 11:20am.

N

0 1,250 2,500 5,000 Feet

Figure 6-5
November 2016 Groundwater Levels
Conceptual Site Model
Investigation and Remediation of Releases and Groundwater Protection and Evaluation
Red Hill Bulk Fuel Storage Facility
JBPHH, O'ahu, Hawai'i

\\Honolulu.na.aecomnet.com\Honolulu\Projects\NAVFAC PAC\CLEAN V\60571032_CTO18F0126\900-Work\920 GIS\02_Maps\CSM\Fig6-5_CSM_Nov2016_GW_Levels-rev04.mxd 2018-08-03

This page intentionally left blank

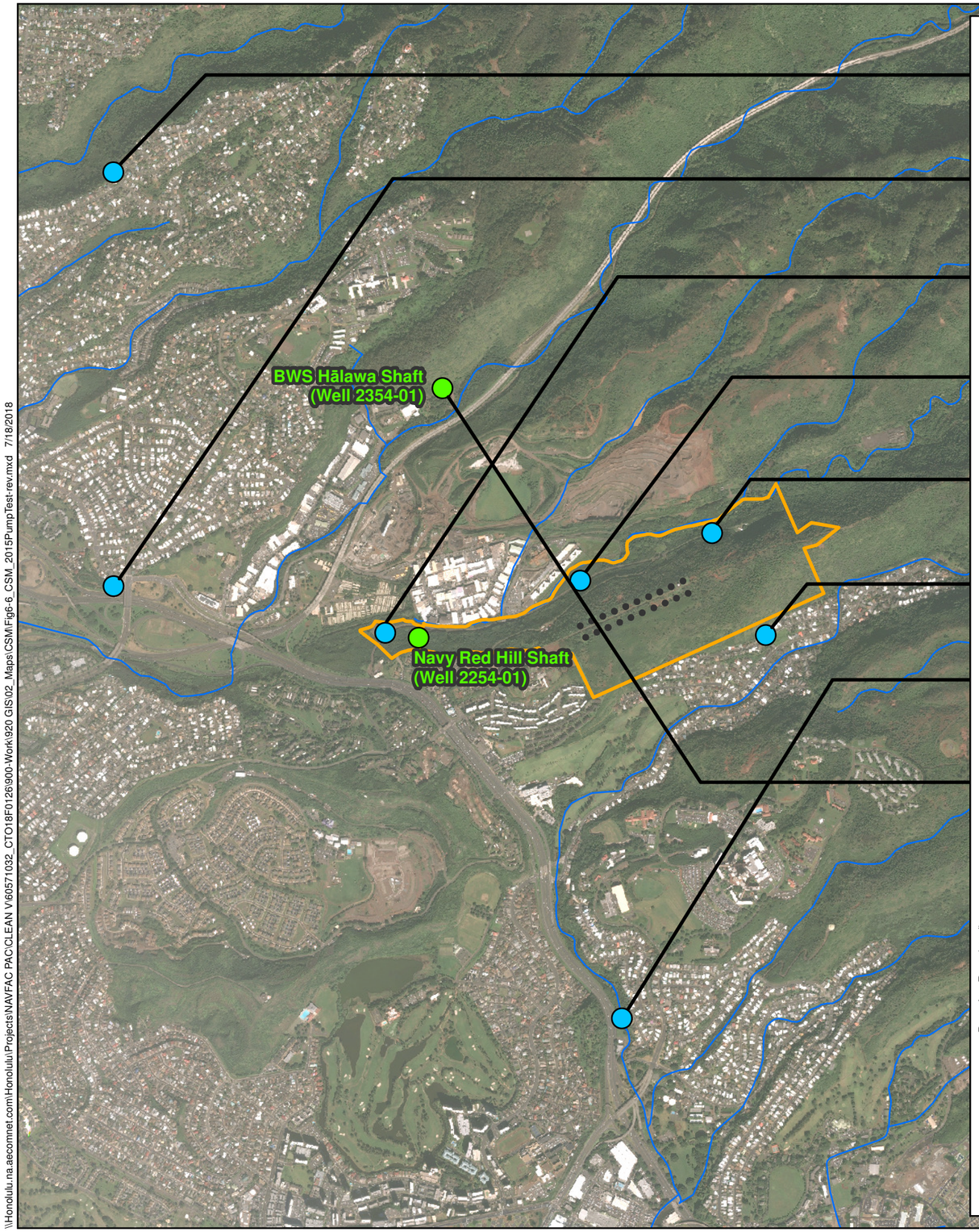

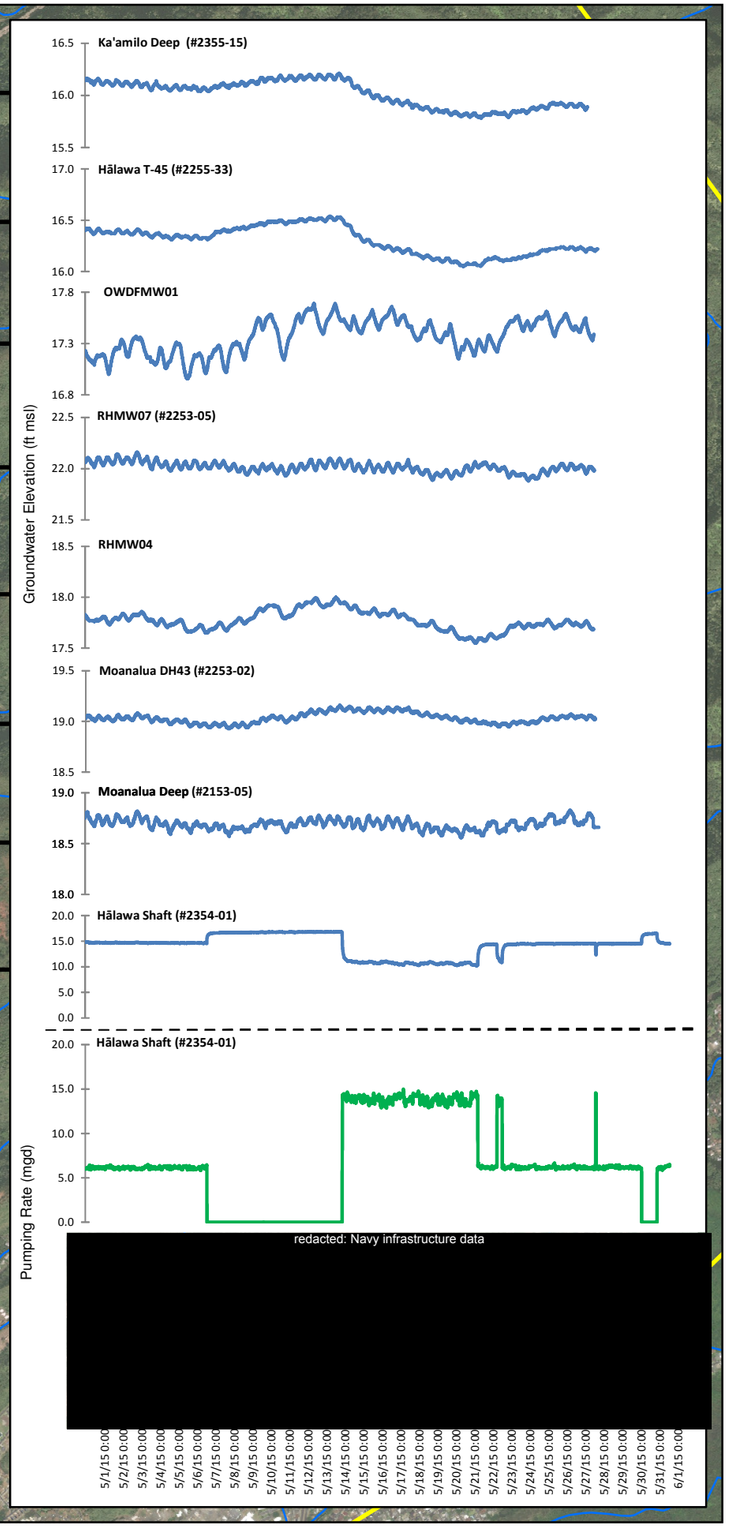

Location Map

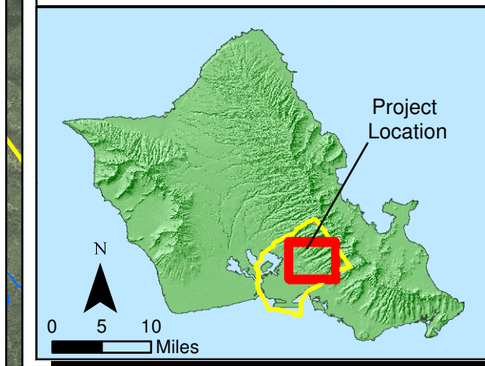

Legend

- Monitoring / Observation Well
- Water Supply Well
- Stream
- Red Hill Facility Boundary and Fuel Storage Tanks
- Stream

Notes

1. Map projection: NAD 1983 UTM Zone 4N
2. DigitalGlobe, Inc. (DG) and NRCS. Publication_Date: 2015

N

0 1,250 2,500 5,000 Feet

Figure 6-6
Time-Series Plots of Water Level Data at Area Monitoring Wells during 2015 USGS Pumping Test at Red Hill Shaft and Hālawa Shaft
Conceptual Site Model
Investigation and Remediation of Releases and Groundwater Protection and Evaluation
Red Hill Bulk Fuel Storage Facility
JBPHH, O'ahu, Hawai'i

\\Honolulu.na.aecomnet.com\Honolulu\Projects\NAVFAC PAC\CLEAN V\60571032_CTO18F01260\900-Work\920 GIS\02_Maps\CSM\Fig6-6_CSM_2015PumpTest-rev.mxd 7/18/2018

This page intentionally left blank

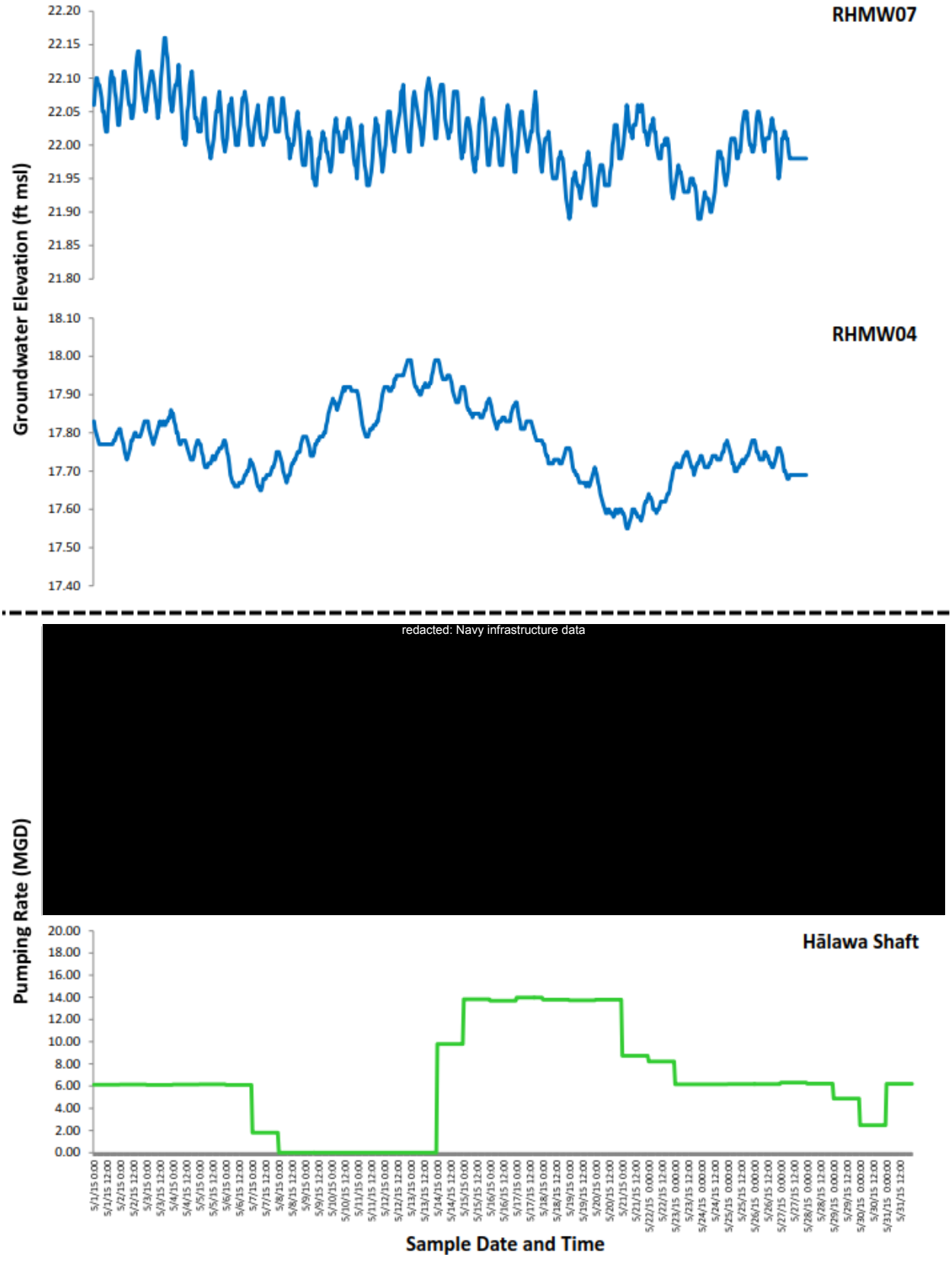

Figure 6-7
Groundwater Levels in RHMW04 and RHMW07 and Pumping Rates during May 2015
Conceptual Site Model
Investigation and Remediation of Releases and Groundwater Protection and Evaluation
Red Hill Bulk Fuel Storage Facility, JBPHH, O'ahu, Hawai'i

This page intentionally left blank

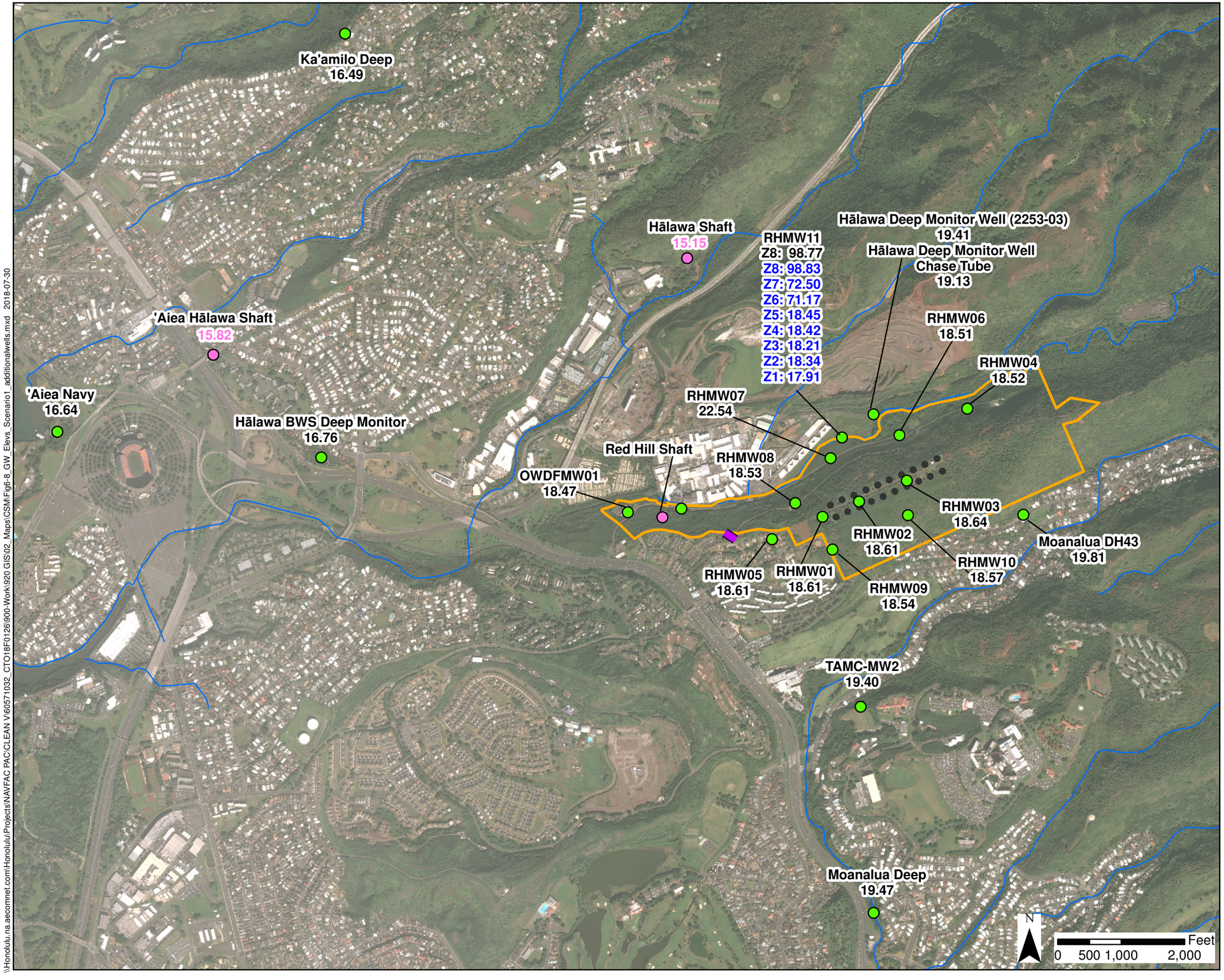

Location Map

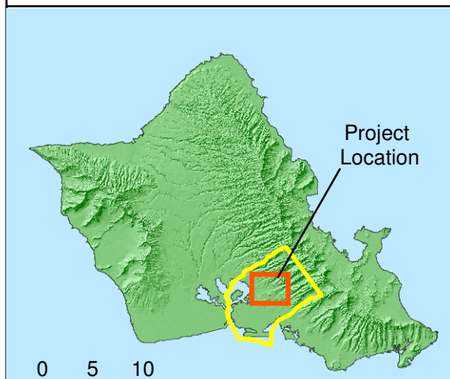

Legend

- Clinker
- Red Hill Fuel Storage Tank
- Supply Well
- Monitoring Well
- Groundwater Model Area
- Red Hill Bulk Fuel Storage Facility Boundary
- Stream

Notes

1. Map projection: NAD 1983 Hawaii State Plane Zone 3 (feet)
2. DigitalGlobe, Inc. (DG) and NRCS. Publication_Date: 2015

Z1: 17.91 indicates measurement was made in a Westbay pumping port

15.15 indicates measurement was made in a pumping well

Figure 6-8
Time 1: Red Hill Shaft Off (At Max Recovery), Hālawa Shaft Average Pumping 01/15/2018 6:00
Conceptual Site Model
Investigation and Remediation of Releases and Groundwater Protection and Evaluation
Red Hill Bulk Fuel Storage Facility
JBPHH, O'ahu, Hawai'i

\\Honolulu.na.aecomnet.com\Honolulu\Projects\NAVFAC PAC\CLEAN V\60571032_CTO18F0126\900-Work\920 GIS\02_Maps\CSM\Fig6-8_GW_Elevs_Scenario1_additionalwells.mxd 2018-07-30

This page intentionally left blank

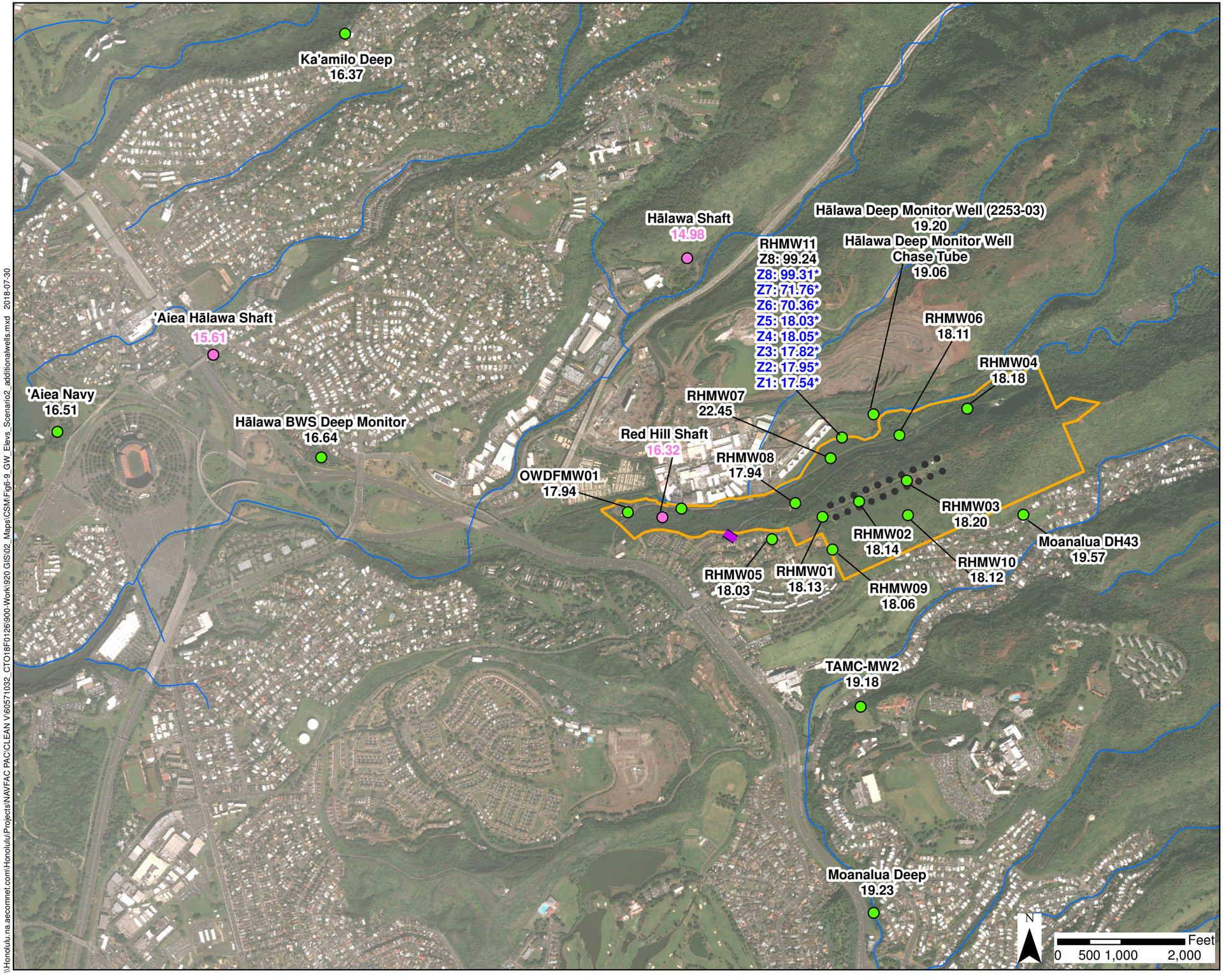

Location Map

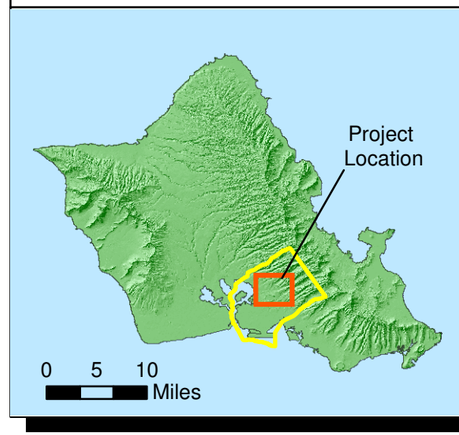

Legend

- Clinker
- Red Hill Fuel Storage Tank
- Supply Well
- Monitoring Well
- Groundwater Model Area
- Red Hill Bulk Fuel Storage Facility Boundary
- Stream

Notes

1. Map projection: NAD 1983 Hawaii State Plane Zone 3 (feet)
2. DigitalGlobe, Inc. (DG) and NRCS. Publication_Date: 2015

Z1: 17.91 indicates measurement was made in a Westbay pumping port

15.15 indicates measurement was made in a pumping well

Figure 6-9
Time 2: Red Hill Shaft At Max Pumping
Hālawa Shaft Average Pumping 01/19/2018 21:10
Conceptual Site Model
Investigation and Remediation of Releases and Groundwater Protection and Evaluation
Red Hill Bulk Fuel Storage Facility
JBPHH, O'ahu, Hawai'i

\\Honolulu.na.aecomnet.com\Honolulu\Projects\NAVFAC PAC\CLEAN V\60571032_CTO18F0126\900-Work\920 GIS\02_Maps\CSM\Fig6-9_GW_Elevs_Scenario2_additionalwells.mxd 2018-07-30

This page intentionally left blank

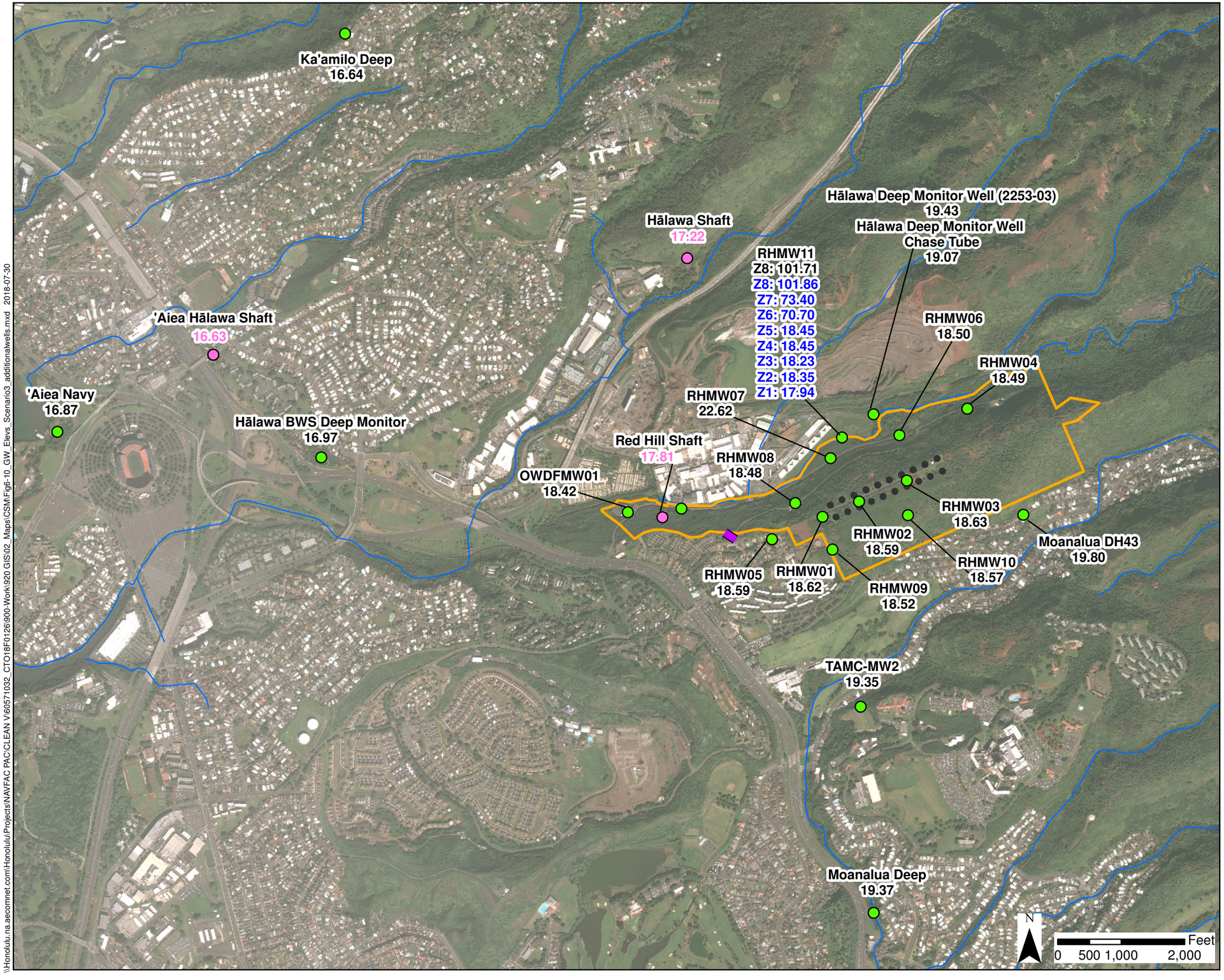

Location Map

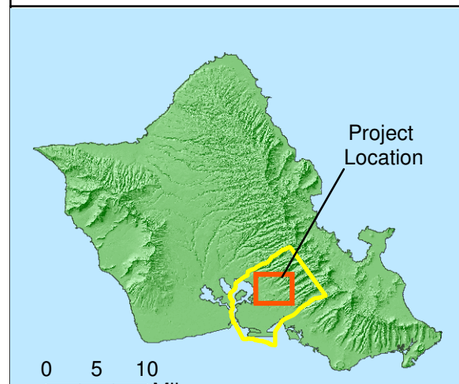

Legend

- Clinker
- Red Hill Fuel Storage Tank
- Supply Well
- Monitoring Well
- Groundwater Model Area
- Red Hill Bulk Fuel Storage Facility Boundary
- Stream

Notes

1. Map projection: NAD 1983 Hawaii State Plane Zone 3 (feet)
2. DigitalGlobe, Inc. (DG) and NRCS. Publication_Date: 2015

Z1: 17.91 indicates measurement was made in a Westbay pumping port

15.15 indicates measurement was made in a pumping well

Figure 6-10
Time 3: Red Hill Shaft Business as Usual Pumping
Hālawa Shaft Off 02/05/2018 19:00
Conceptual Site Model
Investigation and Remediation of Releases and Groundwater Protection and Evaluation
Red Hill Bulk Fuel Storage Facility
JBPHH, O'ahu, Hawai'i

\\Honolulu.na.aecomnet.com\Honolulu\Projects\NAVFAC PAC\CLEAN V\60571032_CTO18F0126\900-Work\920 GIS\02_Maps\CSM\Fig6-10_GW_Elevs_Scenario3_additionalwells.mxd 2018-07-30

This page intentionally left blank

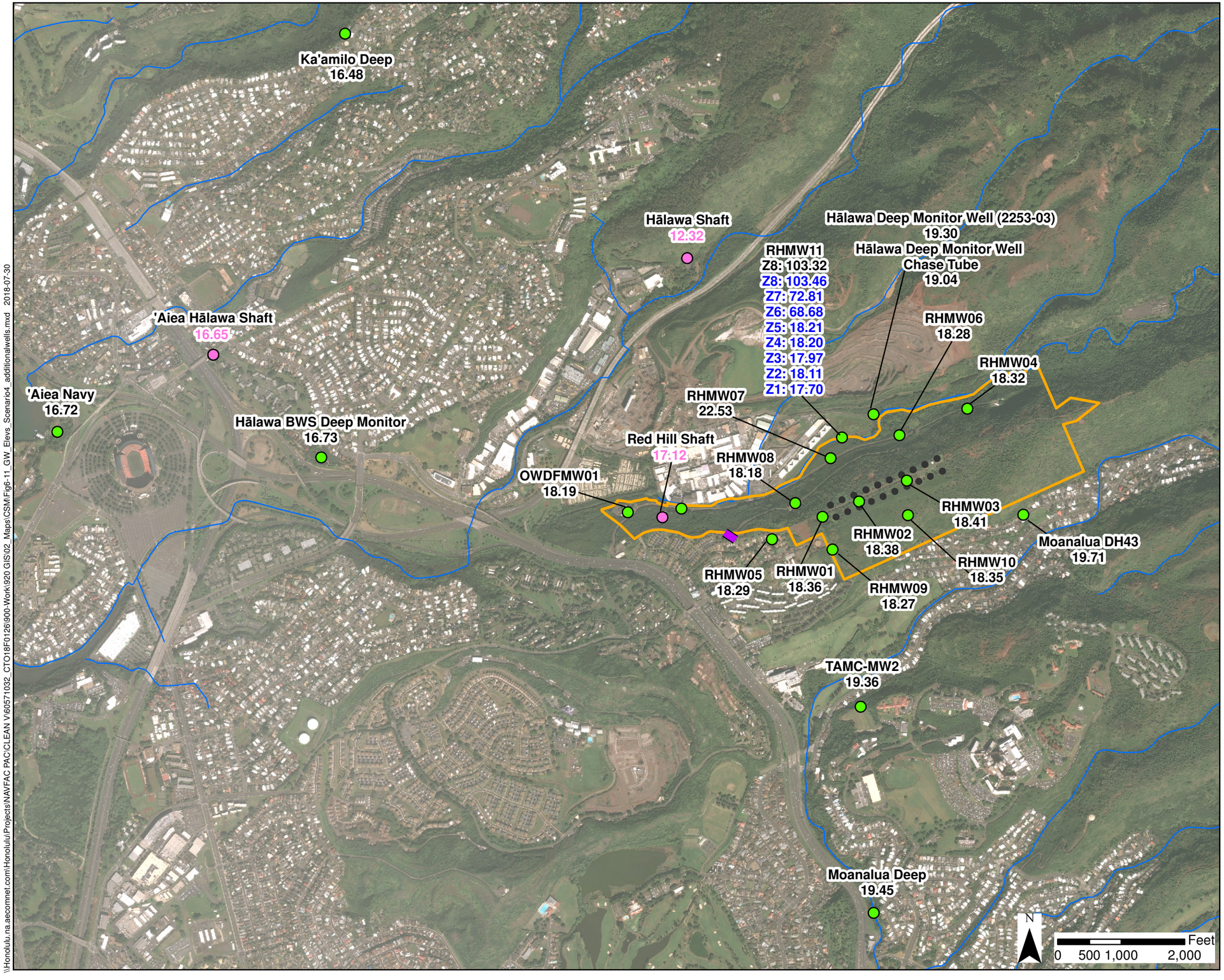

\\Honolulu.na.aecomnet.com\Honolulu\Projects\NAVFAC PAC\CLEAN V\60571032_CTO18F0126\900-Work\920 GIS\02_Maps\CSM\Fig6-11_GW_Elevs_Scenario4_additionalwells.mxd 2018-07-30

Location Map

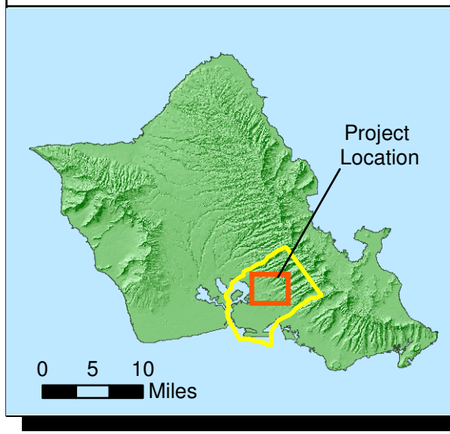

Legend

- Clinker
- Red Hill Fuel Storage Tank
- Supply Well
- Monitoring Well
- Groundwater Model
- Red Hill Bulk Fuel Storage Facility Boundary
- Stream

Notes

1. Map projection: NAD 1983 Hawaii State Plane Zone 3 (feet)
2. DigitalGlobe, Inc. (DG) and NRCS. Publication_Date: 2015

Z1: 17.91 indicates measurement was made in a Westbay pumping port

15.15 indicates measurement was made in a pumping well

Figure 6-11
Time 4: Red Hill Shaft Business as Usual
Hālawa Shaft at Maximum Pumping 02/16/2018 5:00
Conceptual Site Model
Investigation and Remediation of Releases and Groundwater Protection and Evaluation
Red Hill Bulk Fuel Storage Facility
JBPHH, O'ahu, Hawai'i

This page intentionally left blank

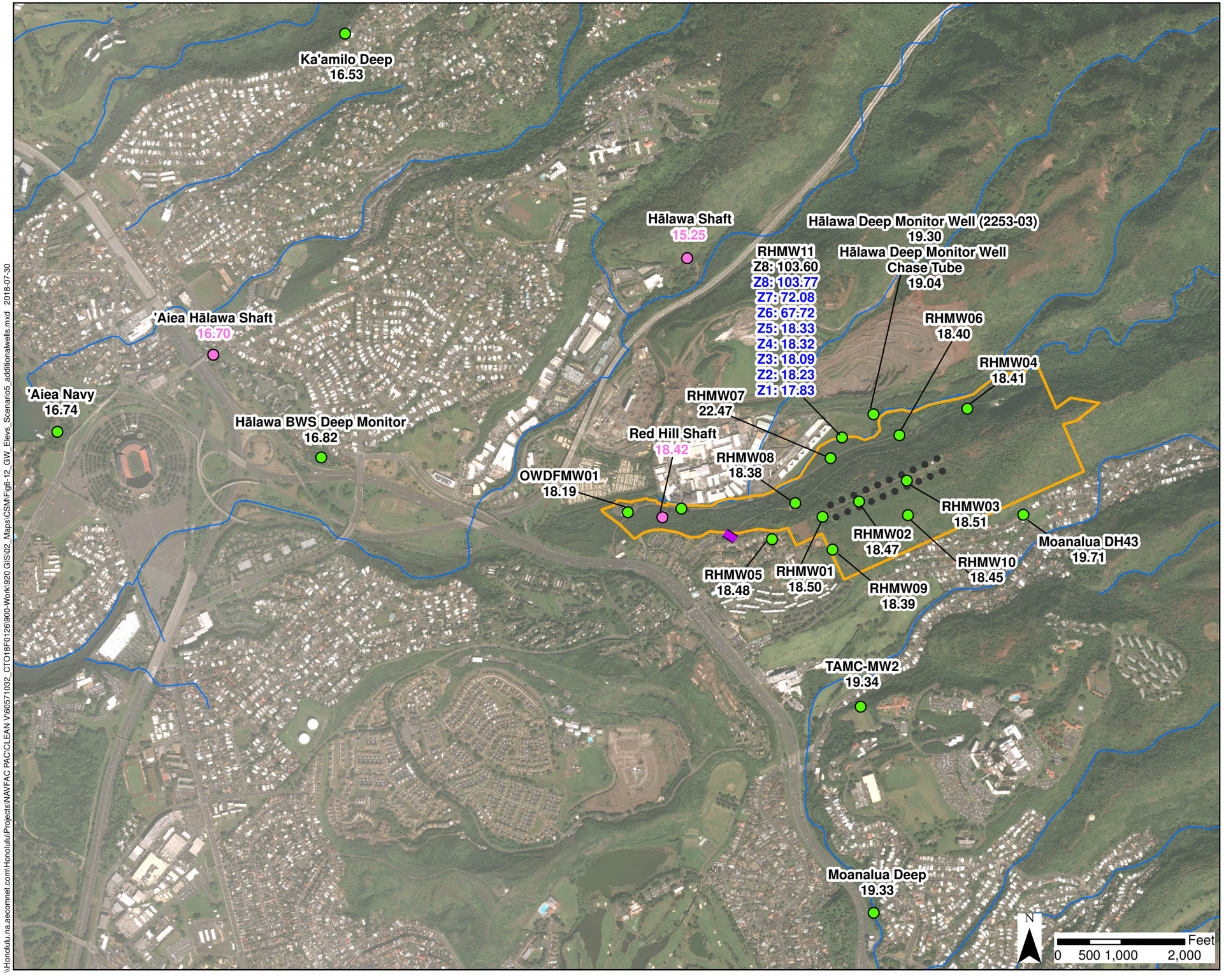

\\Honolulu.na.aecomnet.com\Honolulu\Projects\NAVFAC PAC\CLEAN V\60571032_CTO18F0126\900-Work\920 GIS\02_Maps\CSM\Fig6-12_GW_Elevs_Scenario5_additionalwells.mxd 2018-07-30

Location Map

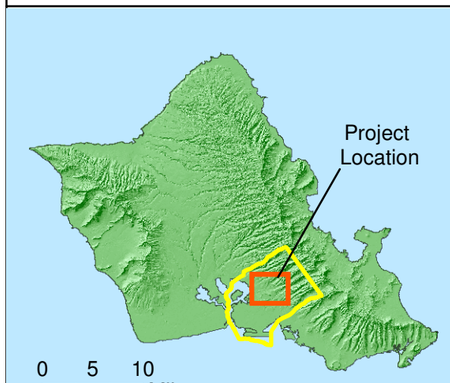

Legend

- Clinker
- Red Hill Fuel Storage Tank
- Supply Well
- Monitoring Well
- Groundwater Model Area
- Red Hill Bulk Fuel Storage Facility Boundary
- Stream

Notes

1. Map projection: NAD 1983 Hawaii State Plane Zone 3 (feet)
2. DigitalGlobe, Inc. (DG) and NRCS. Publication_Date: 2015

Z1: 17.91 indicates measurement was made in a Westbay pumping port

15.15 indicates measurement was made in a pumping well

Figure 6-12
Time 5: Red Hill Shaft Business as Usual
Hālawa Shaft Average Pumping 02/19/2018 13:00
Conceptual Site Model
Investigation and Remediation of Releases and Groundwater Protection and Evaluation
Red Hill Bulk Fuel Storage Facility
JBPHH, O'ahu, Hawai'i

This page intentionally left blank

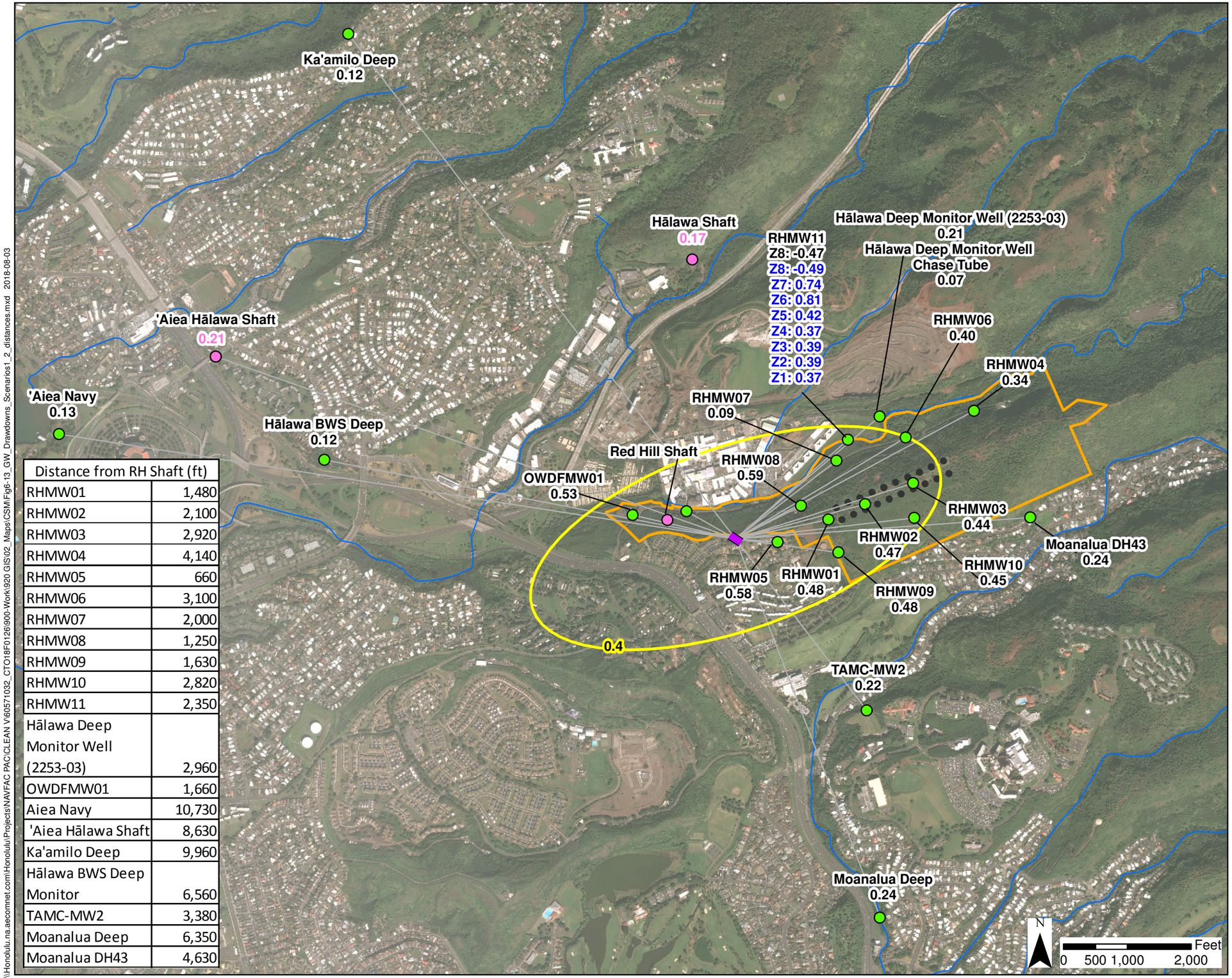

Distance from RH Shaft (ft)	
RHMW01	1,480
RHMW02	2,100
RHMW03	2,920
RHMW04	4,140
RHMW05	660
RHMW06	3,100
RHMW07	2,000
RHMW08	1,250
RHMW09	1,630
RHMW10	2,820
RHMW11	2,350
Hālawa Deep Monitor Well (2253-03)	2,960
OWDFMW01	1,660
Aiea Navy	10,730
'Aiea Hālawa Shaft	8,630
Ka'amilo Deep	9,960
Hālawa BWS Deep Monitor	6,560
TAMC-MW2	3,380
Moanalua Deep	6,350
Moanalua DH43	4,630

Notes

1. Map projection: NAD 1983 Hawaii State Plane Zone 3 (feet)
2. DigitalGlobe, Inc. (DG) and NRCS. Publication_Date: 2015

Z1: 17.91 indicates measurement was made in a Westbay pumping port

15.15 indicates measurement was made in a pumping well

Figure 6-13
Head Differences Between -
Time 1: Red Hill Shaft Off (At Max Recovery), Hālawa Shaft Average Pumping 01/15/2018 6:00
Time 2: Red Hill Shaft At Max Pumping, Hālawa Shaft Average Pumping 01/19/2018 21:10
Conceptual Site Model
Investigation and Remediation of Releases and Groundwater Protection and Evaluation
Red Hill Bulk Fuel Storage Facility
JBPHH, O'ahu, Hawai'i

\\Honolulu.na.aecomnet.com\Honolulu\Projects\NAVFAC PAC\CLEAN V\60571032_CTO18F0126900-Work\920 GIS\02_Maps\CSM\Fig6-13_GW_Drawdowns_Scenarios1_2_distances.mxd 2018-08-03

This page intentionally left blank

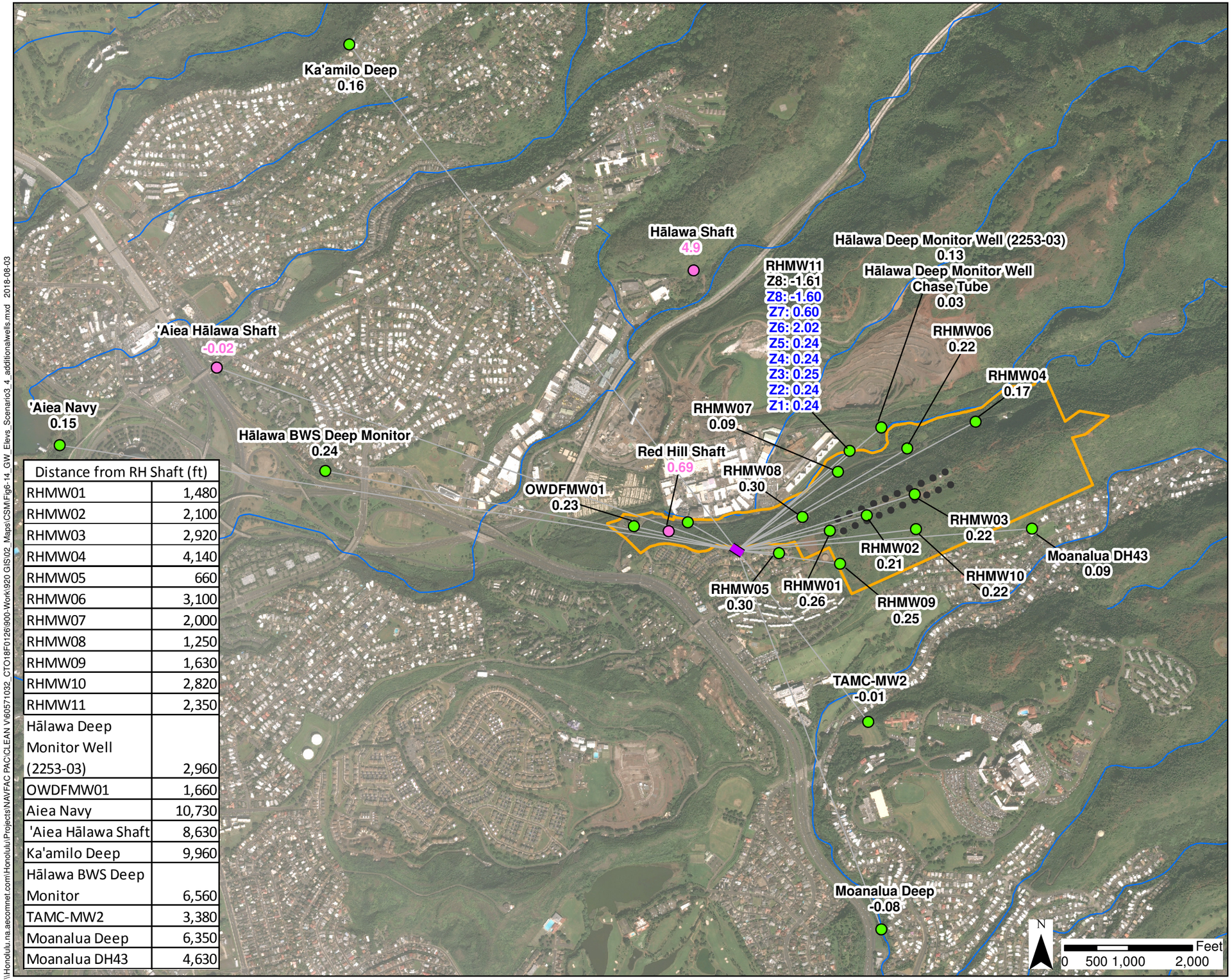

Distance from RH Shaft (ft)	
RHMW01	1,480
RHMW02	2,100
RHMW03	2,920
RHMW04	4,140
RHMW05	660
RHMW06	3,100
RHMW07	2,000
RHMW08	1,250
RHMW09	1,630
RHMW10	2,820
RHMW11	2,350
Hālawa Deep Monitor Well (2253-03)	2,960
OWDFMW01	1,660
Aiea Navy	10,730
'Aiea Hālawa Shaft	8,630
Ka'amilo Deep	9,960
Hālawa BWS Deep Monitor	6,560
TAMC-MW2	3,380
Moanalua Deep	6,350
Moanalua DH43	4,630

\\Honolulu.na.aecomnet.com\Honolulu\Projects\NAVFAC PAC\CLEAN V\60571032_CTO18F01269\900-Work\920 GIS\02_Maps\CSM\Fig6-14_GW_Elevs_Scenario3_4_additionalwells.mxd 2018-08-03

Figure 6-14
Head Differences Between -
Time 3: Red Hill Shaft Business as Usual Pumping
Hālawa Shaft Off 02/05/2018 19:00
Time 4: Red Hill Shaft Business as Usual
Hālawa Shaft at Maximum Pumping 02/16/2018 5:00
Conceptual Site Model
Investigation and Remediation of Releases and Groundwater Protection and Evaluation
Red Hill Bulk Fuel Storage Facility
JBPHH, O'ahu, Hawai'i

This page intentionally left blank

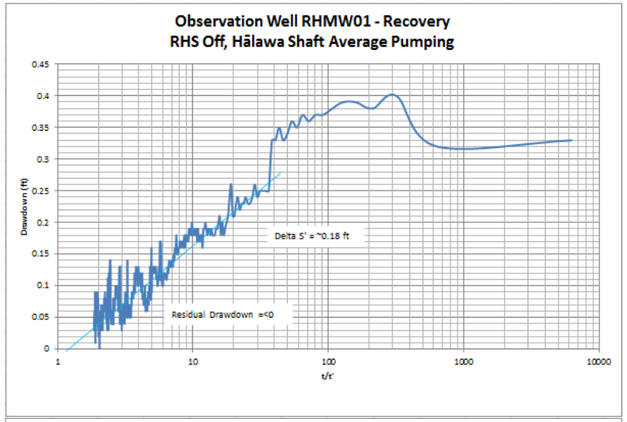

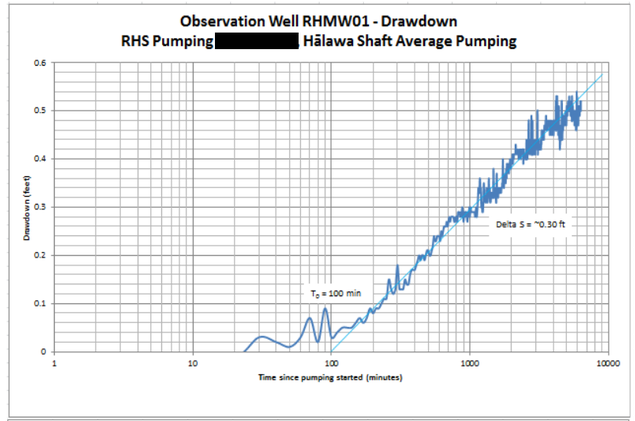

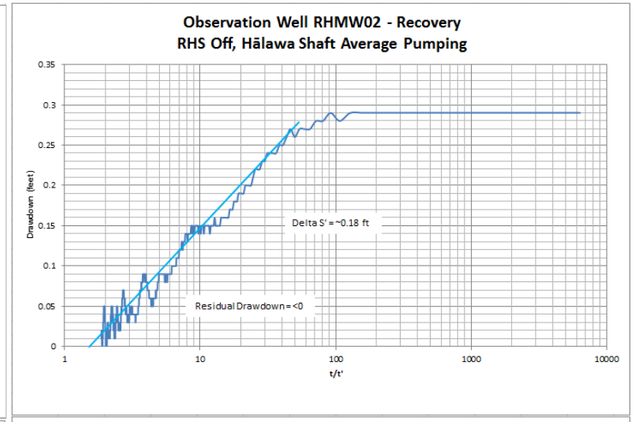

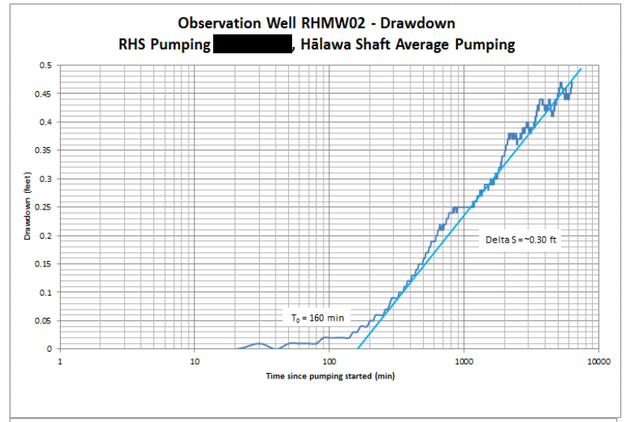

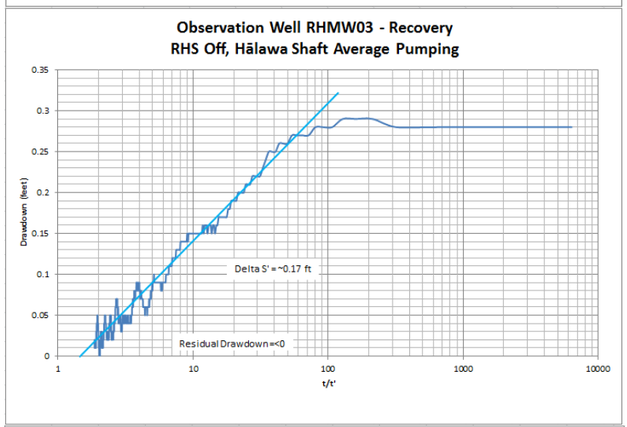

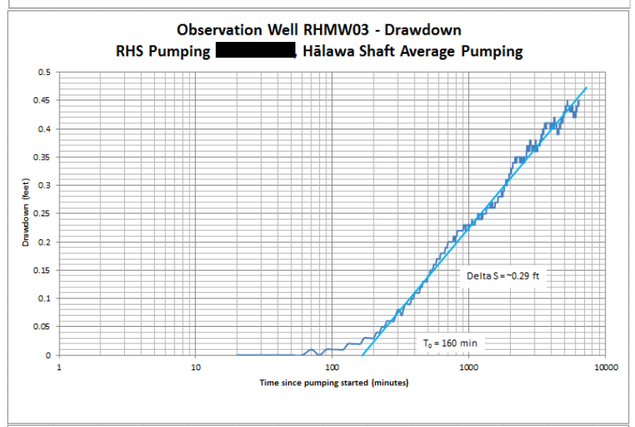

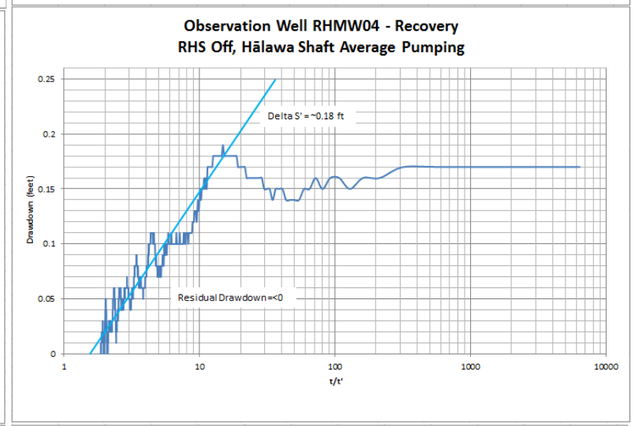

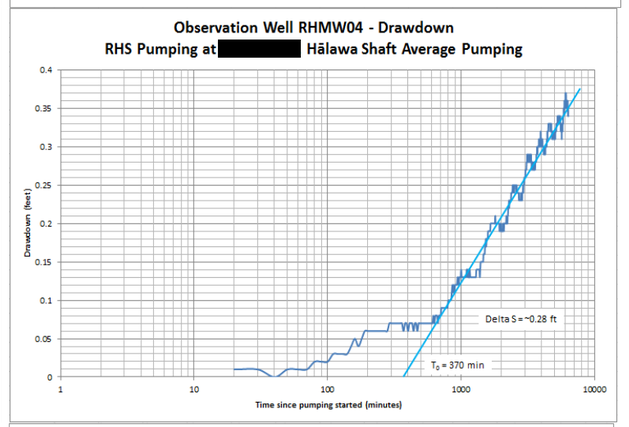

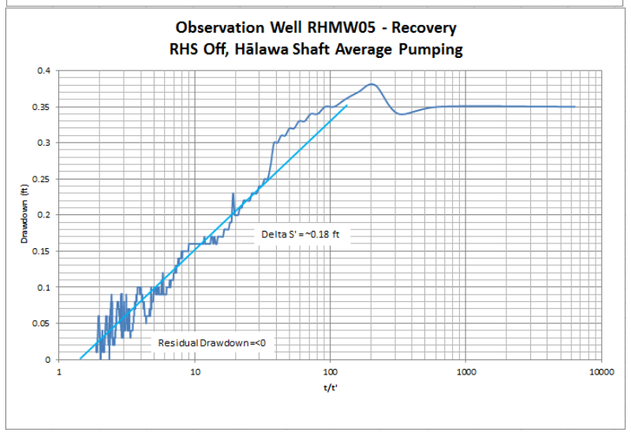

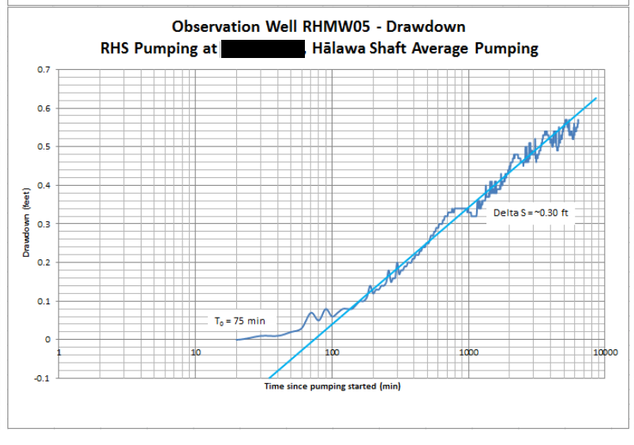

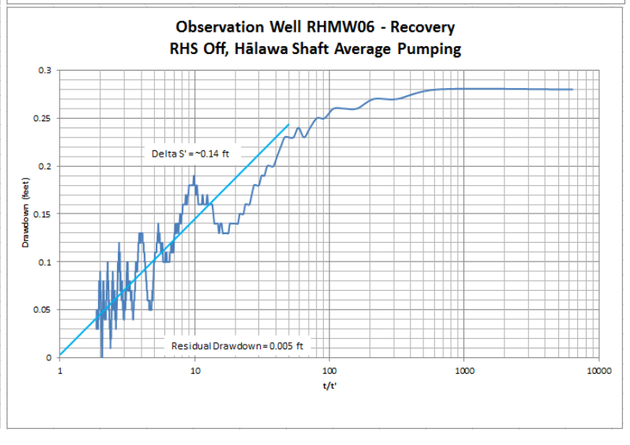

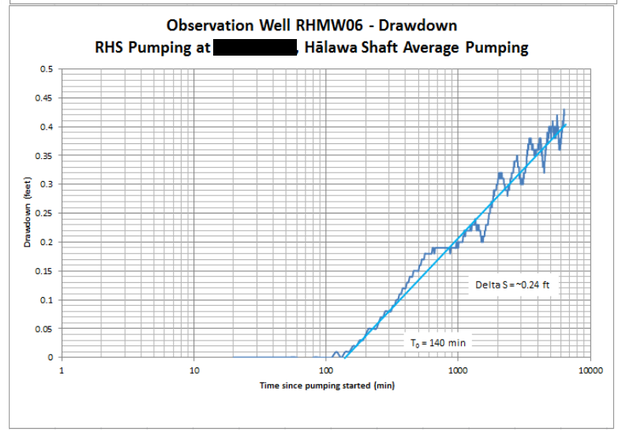

Figure 6-15
Cooper-Jacob Drawdown and Recovery Plots (RHMW01, RHMW02, RHMW03, RHMW04, RHMW05, and RHMW06)
Red Hill Bulk Fuel Storage Facility and Vicinity
Conceptual Site Model
Investigation and Remediation of Releases and Groundwater Protection and Evaluation
Red Hill Bulk Fuel Storage Facility
JBPHH, O'ahu, Hawai'i

This page intentionally left blank

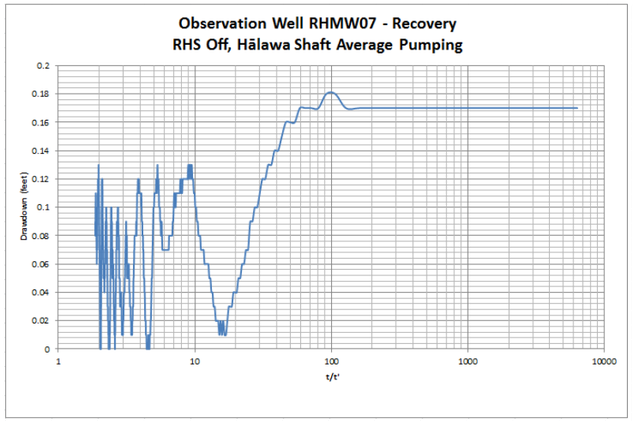

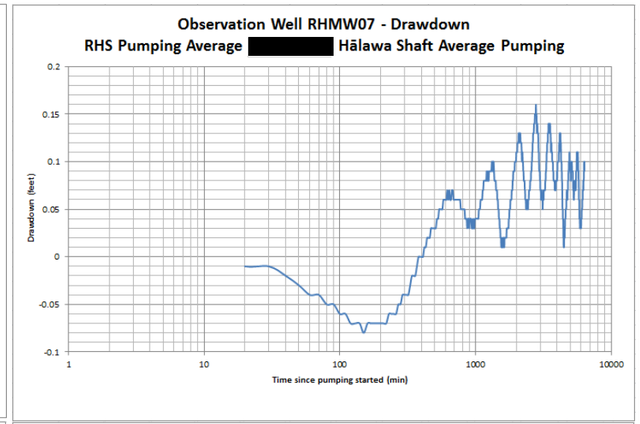

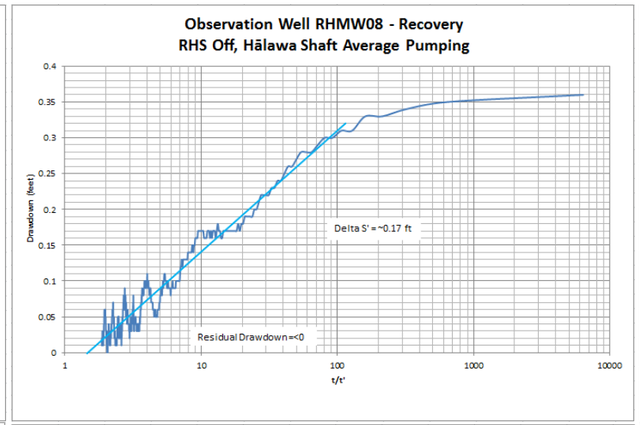

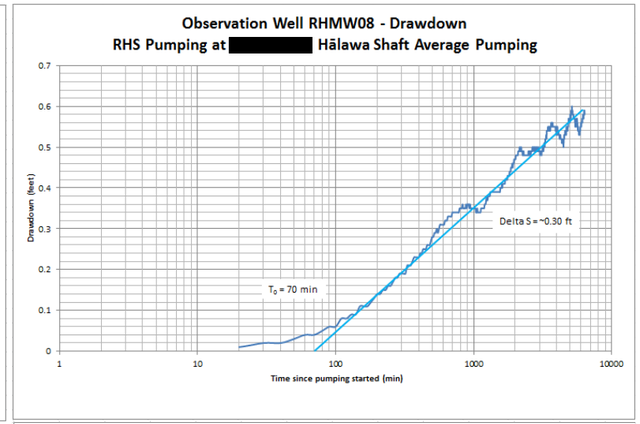

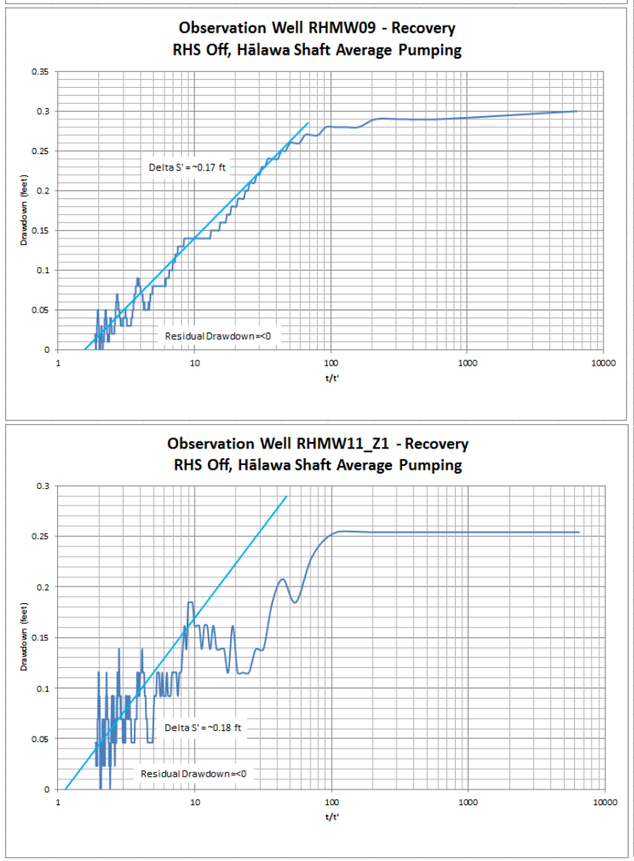

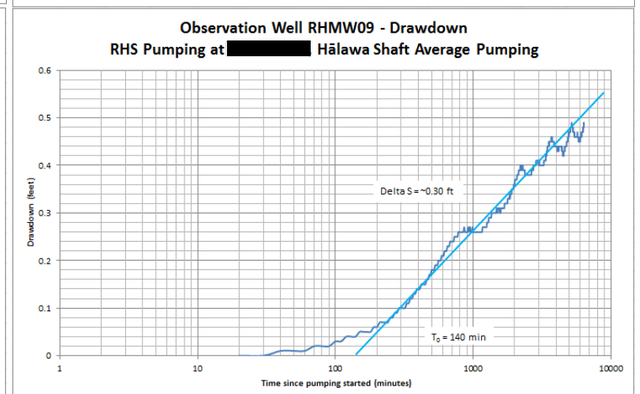

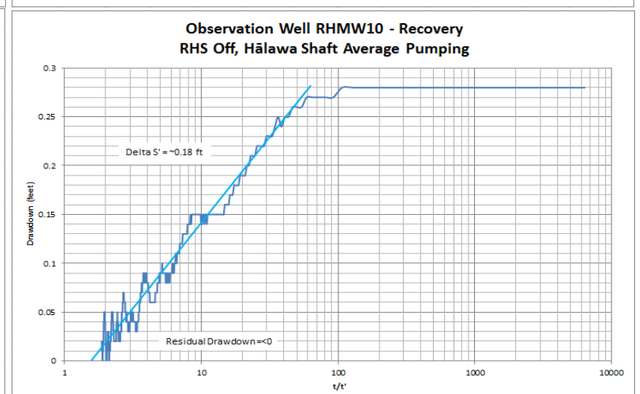

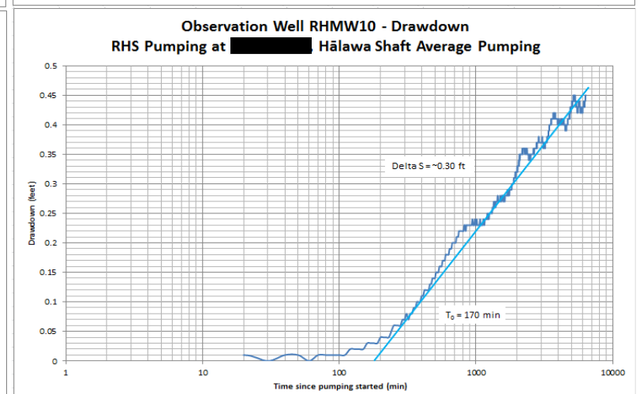

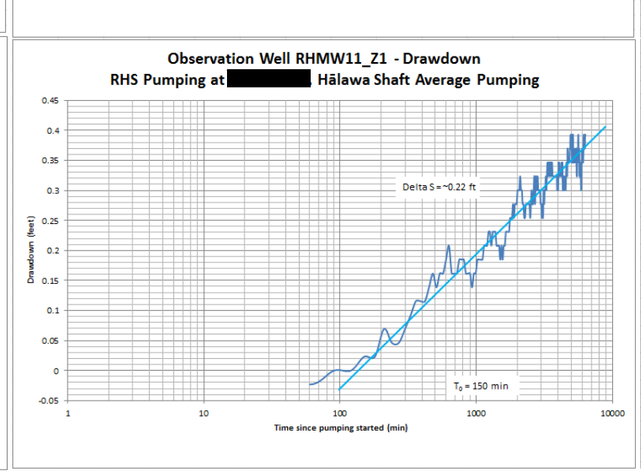

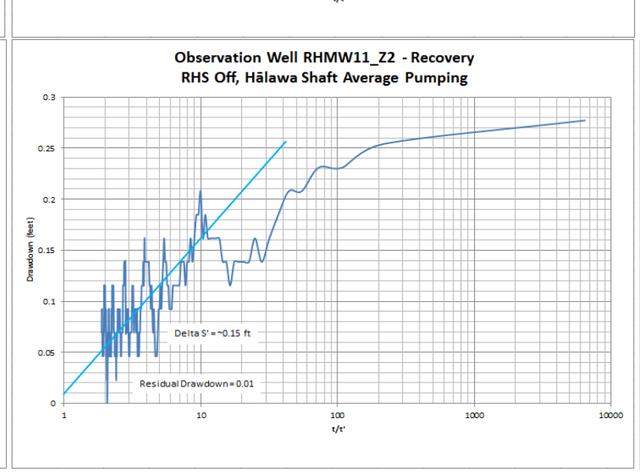

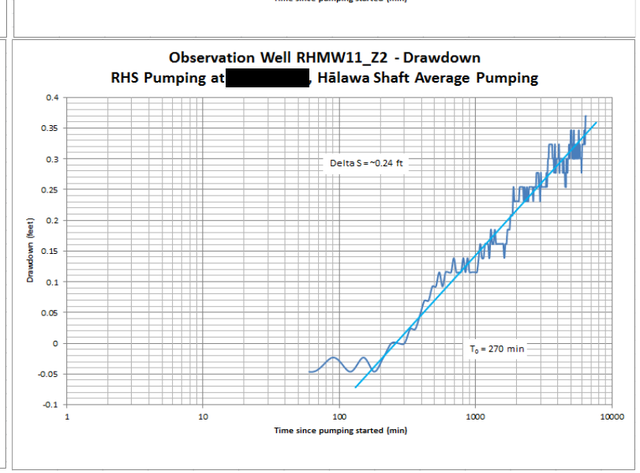

Figure 6-16
Cooper-Jacob Drawdown and Recovery Plots (RHMW07, RHMW08, RHMW09, RHMW10, RHMW11 Zones 1 and 2)
Red Hill Bulk Fuel Storage Facility and Vicinity
Conceptual Site Model
Investigation and Remediation of Releases and Groundwater Protection and Evaluation
Red Hill Bulk Fuel Storage Facility
JBPHH, O‘ahu, Hawai‘i

This page intentionally left blank

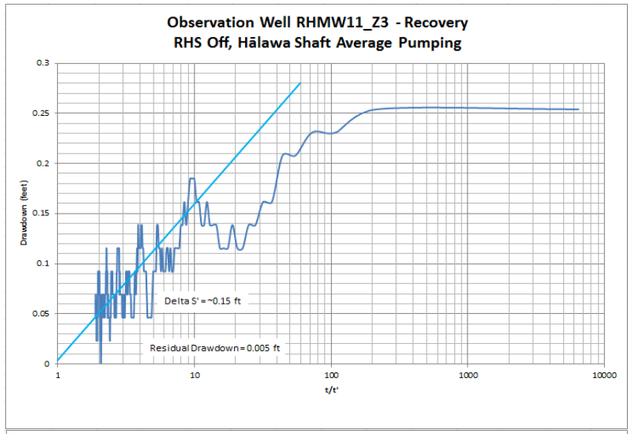

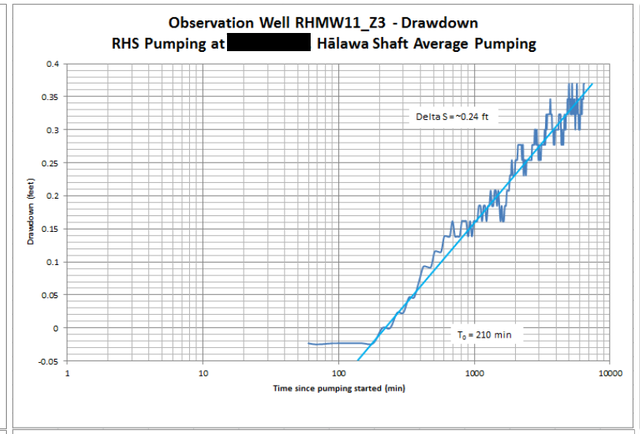

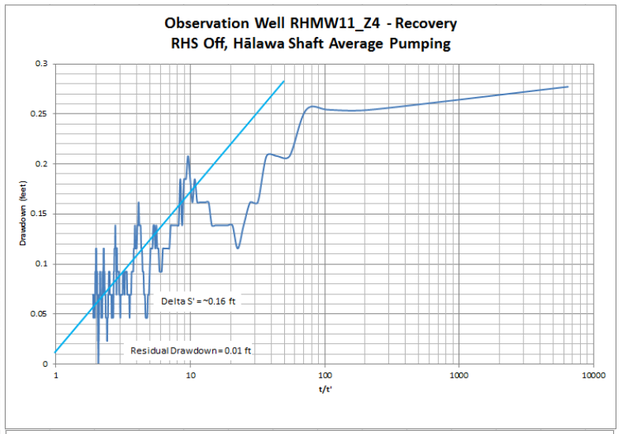

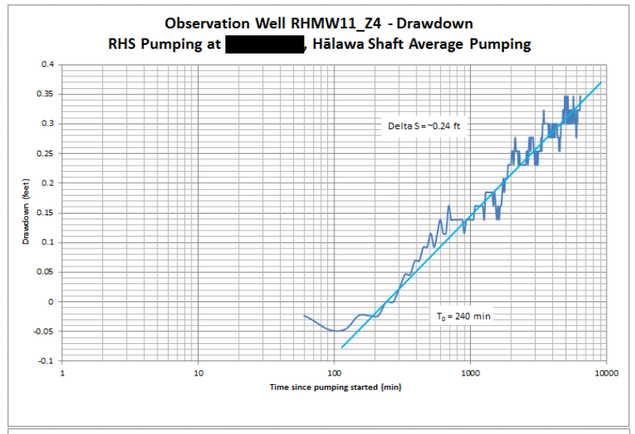

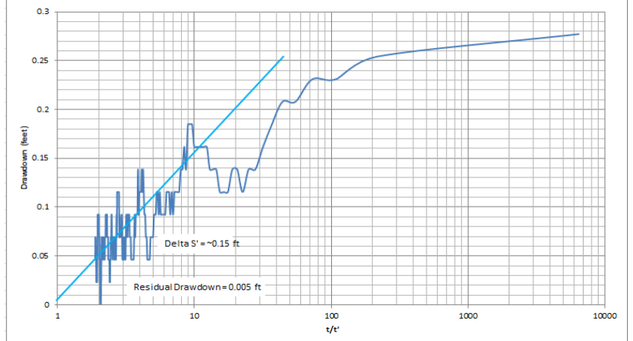

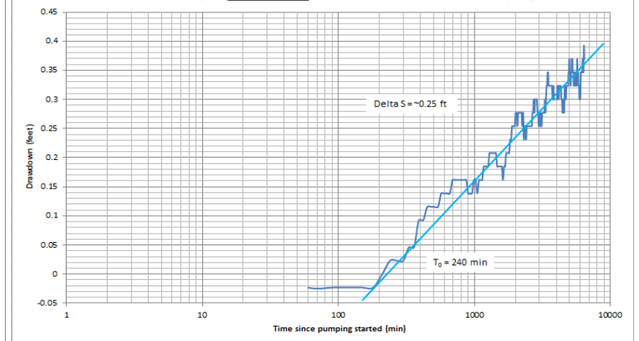

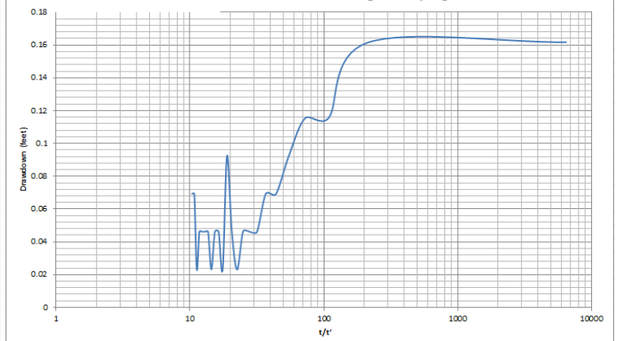

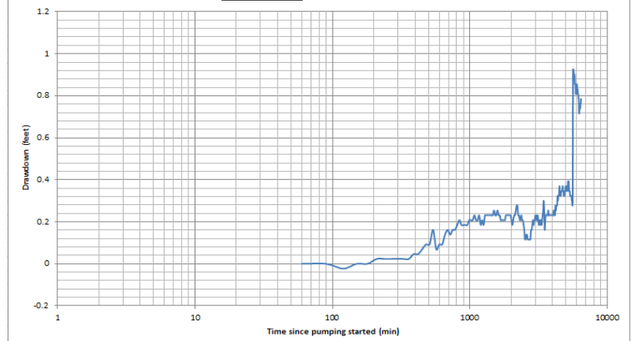

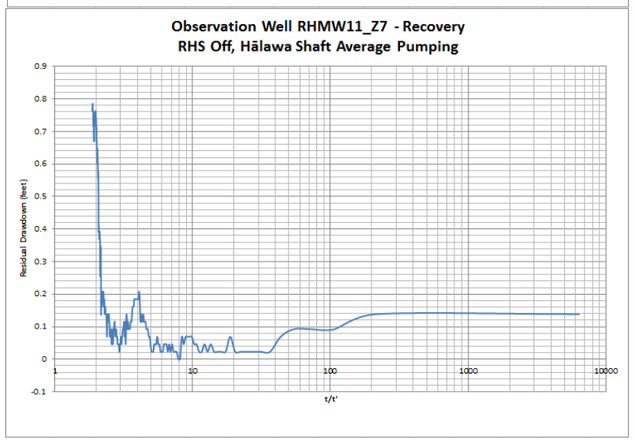

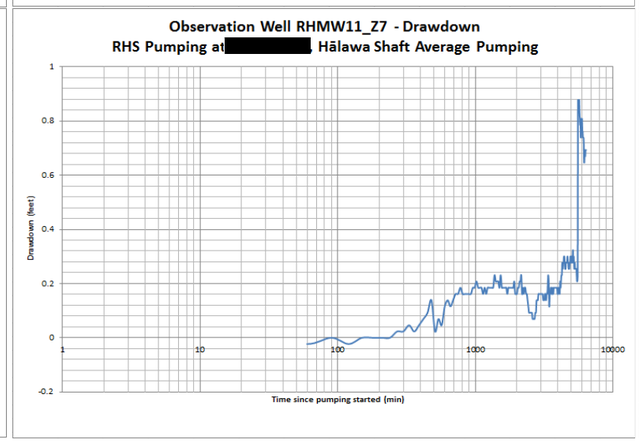

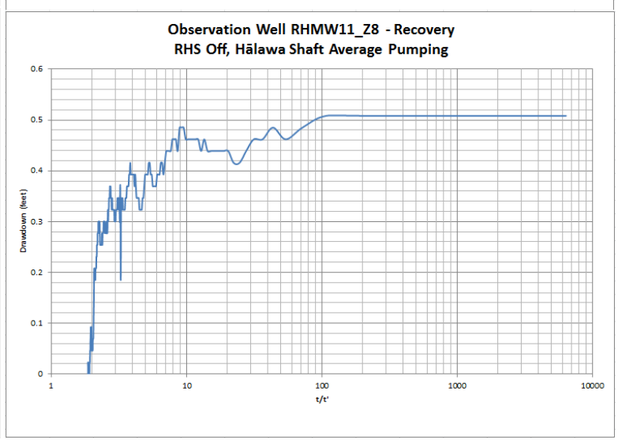

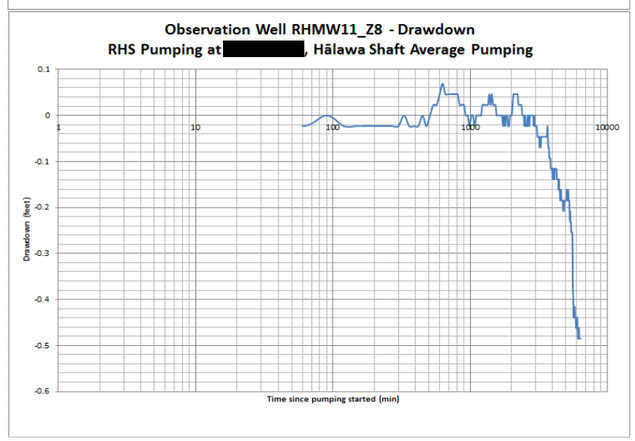

Figure 6-17
Cooper-Jacob Drawdown and Recovery Plots (RHMW11 Zones 3, 4, 5, 6, 7, and 8)
Red Hill Bulk Fuel Storage Facility and Vicinity
Conceptual Site Model
Investigation and Remediation of Releases and Groundwater Protection and Evaluation
Red Hill Bulk Fuel Storage Facility
JBPHH, Oʻahu, Hawaiʻi

This page intentionally left blank

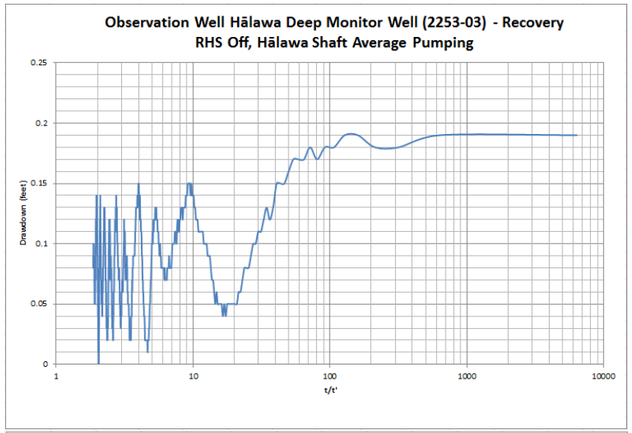

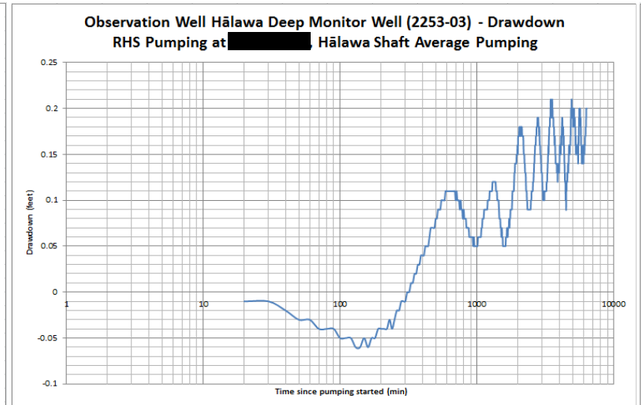

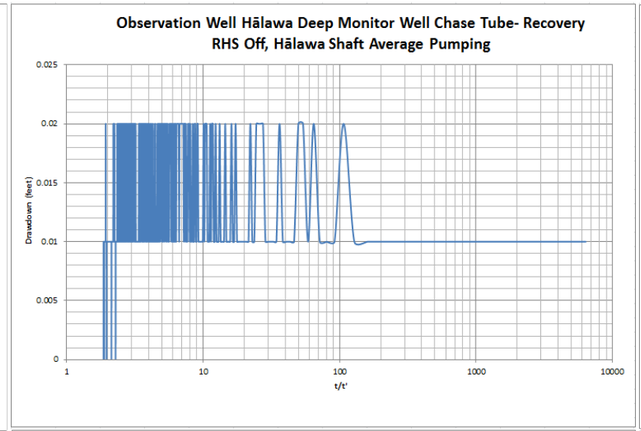

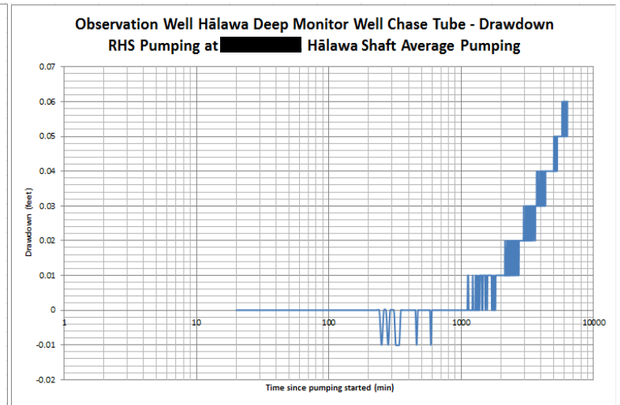

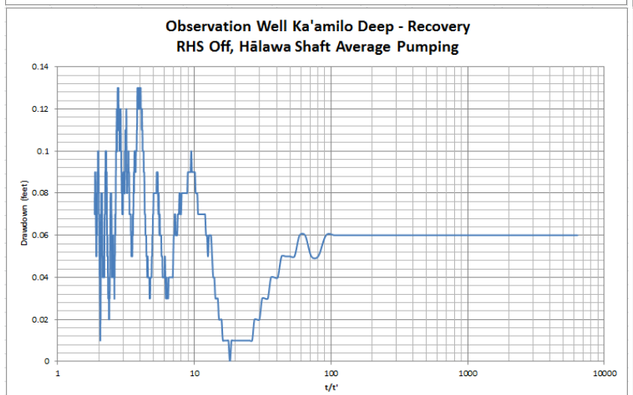

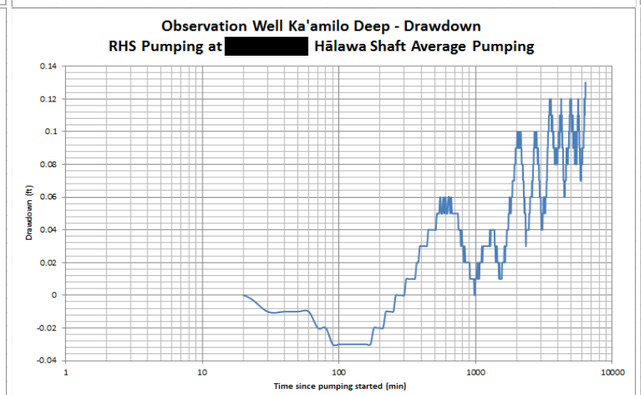

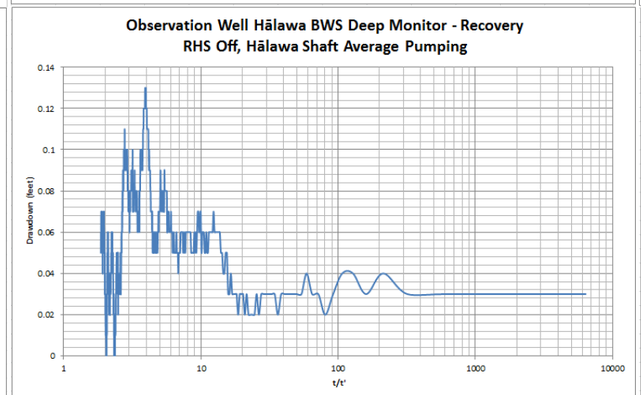

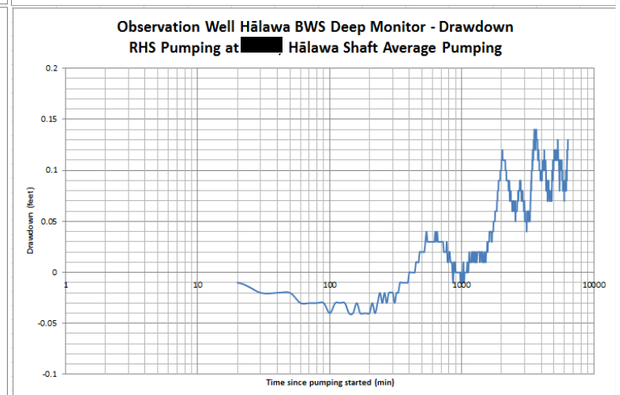

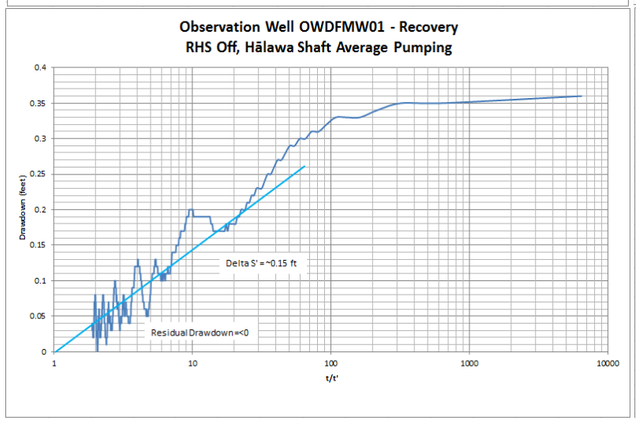

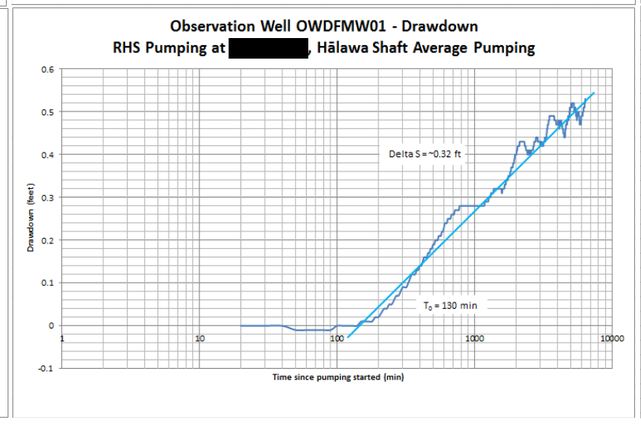

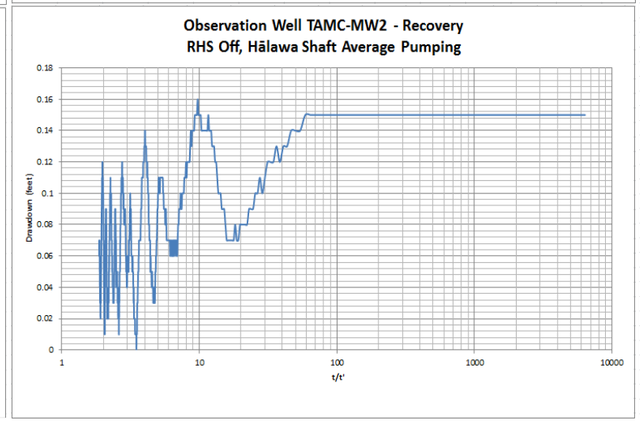

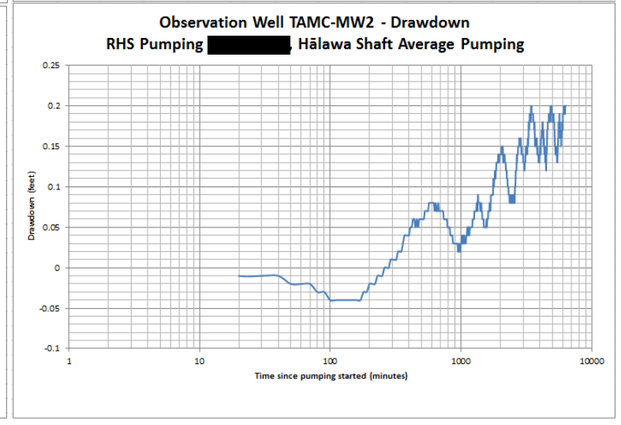

Figure 6-18
Cooper-Jacob Drawdown and Recovery Plots (Hālawa Deep Monitor Well (2253-03), Hālawa Deep Monitor Well Chase Tube, Ka'amilo Deep, Hālawa BWS Deep Monitor, OWDFMW01, and TAMC-MW2)
Red Hill Bulk Fuel Storage Facility and Vicinity
Conceptual Site Model
Investigation and Remediation of Releases and Groundwater Protection and Evaluation
Red Hill Bulk Fuel Storage Facility
JBPHH, O'ahu, Hawai'i

This page intentionally left blank

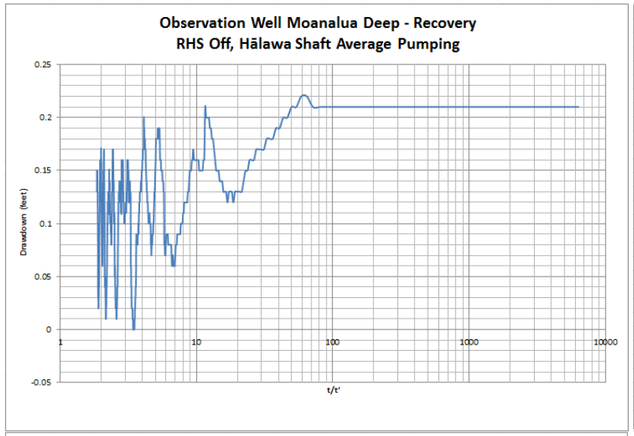

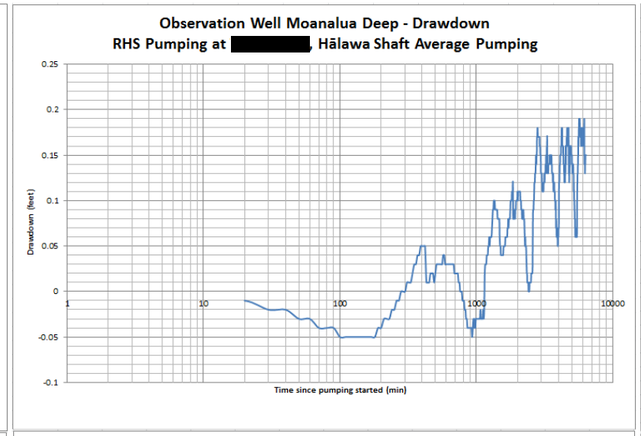

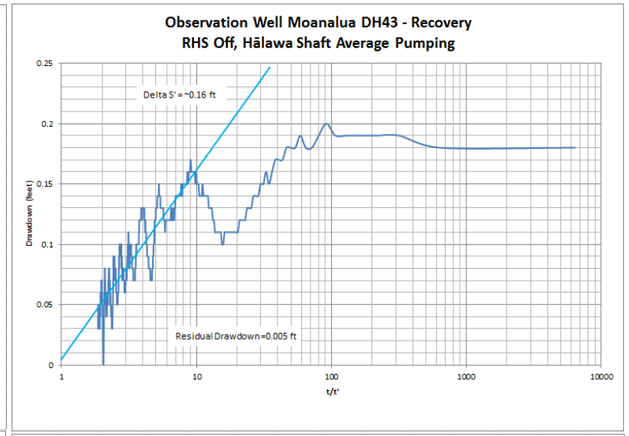

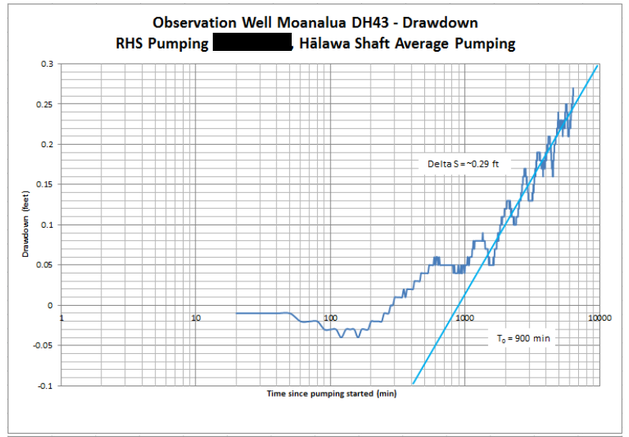

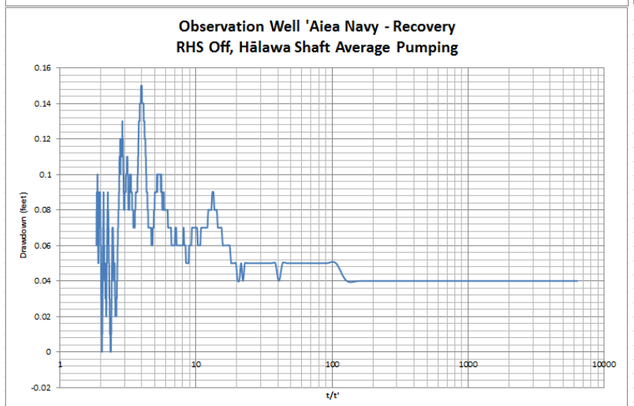

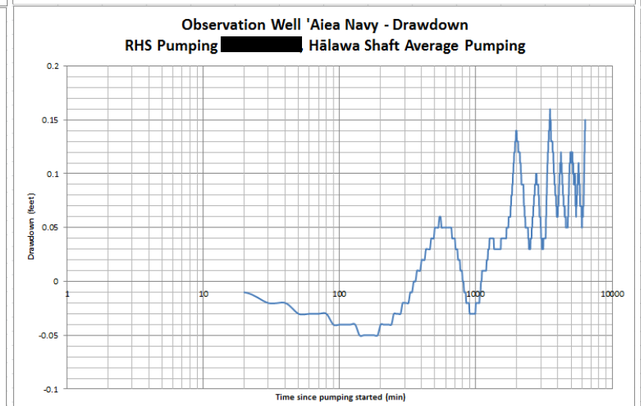

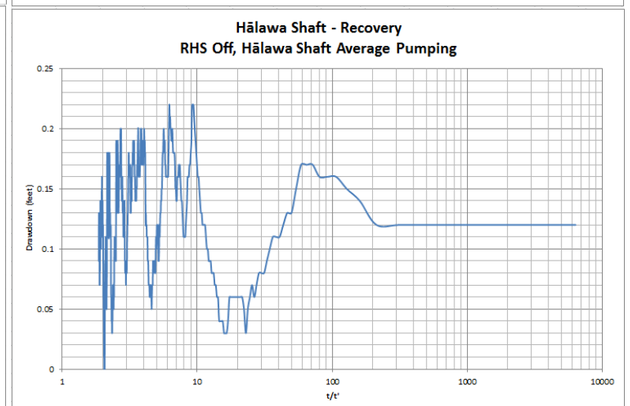

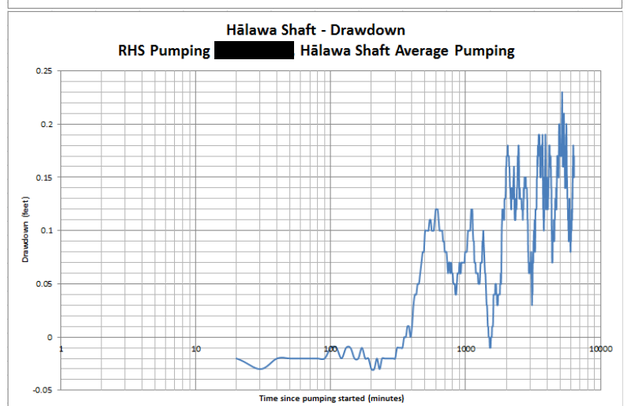

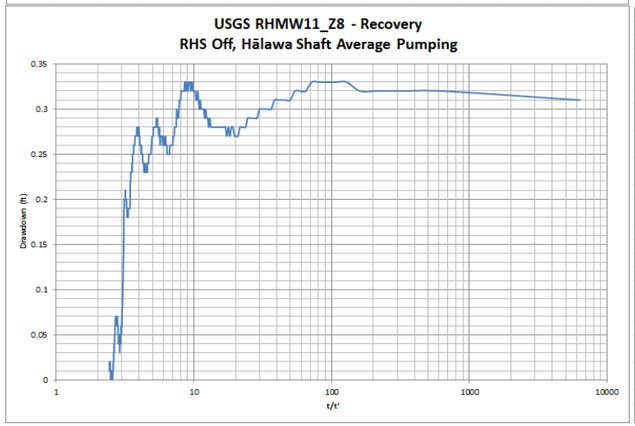

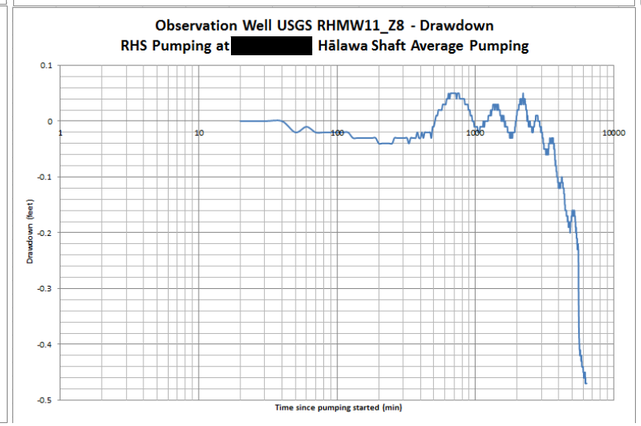

Figure 6-19
Cooper-Jacob Drawdown and Recovery Plots (Moanalua Deep, Moanalua DH43, ʻAiea Navy, Hālawa Shaft, and USGS RHMW11 Zone 8)
Red Hill Bulk Fuel Storage Facility and Vicinity
Conceptual Site Model
Investigation and Remediation of Releases and Groundwater Protection and Evaluation
Red Hill Bulk Fuel Storage Facility
JBPHH, Oʻahu, Hawaiʻi

This page intentionally left blank

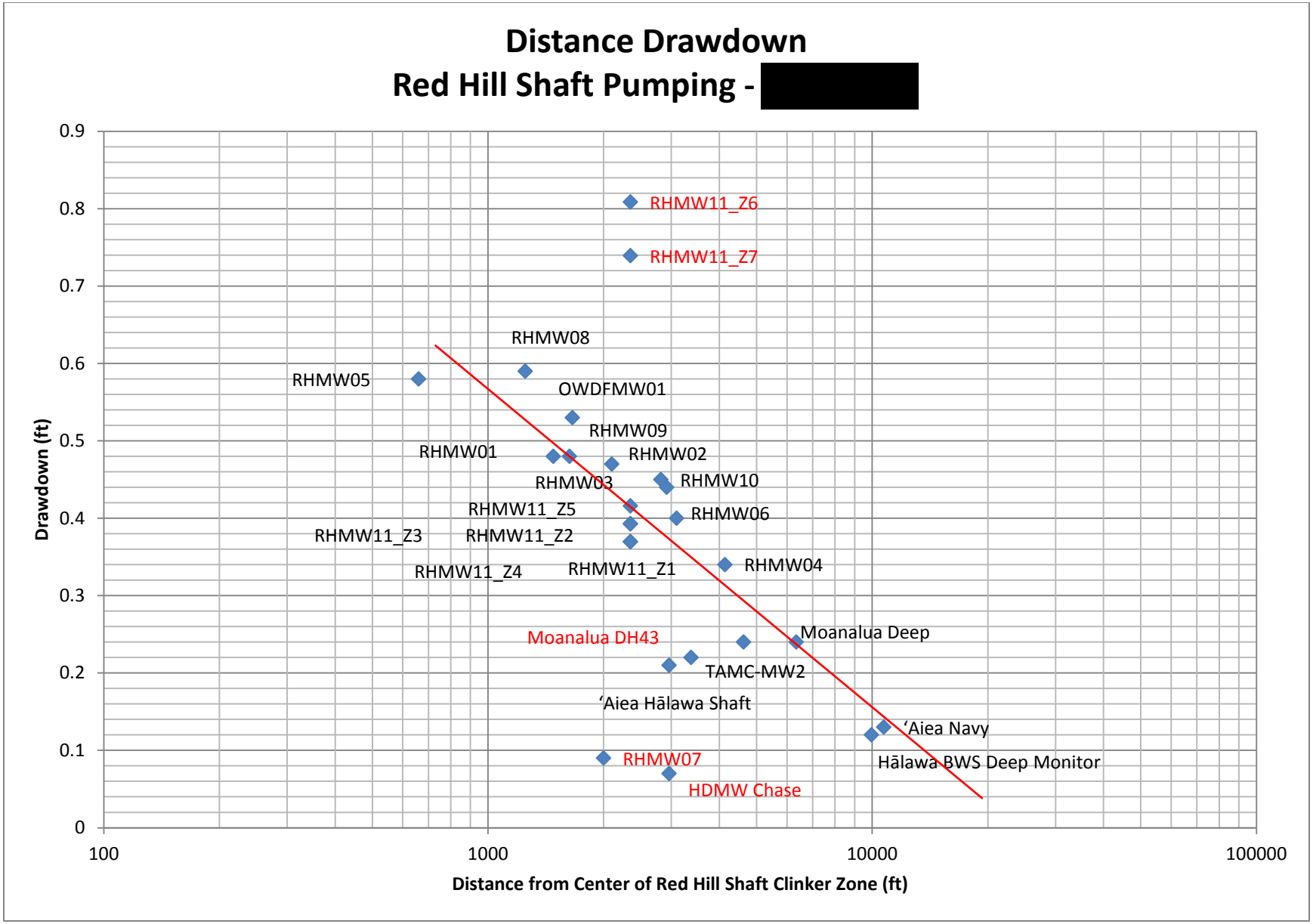

Figure 6-20
Distance Drawdown at Time 2
Conceptual Site Model
Investigation and Remediation of Releases and Groundwater Protection and Evaluation
Red Hill Bulk Fuel Storage Facility
JBPHH, O'ahu, Hawai'i

This page intentionally left blank

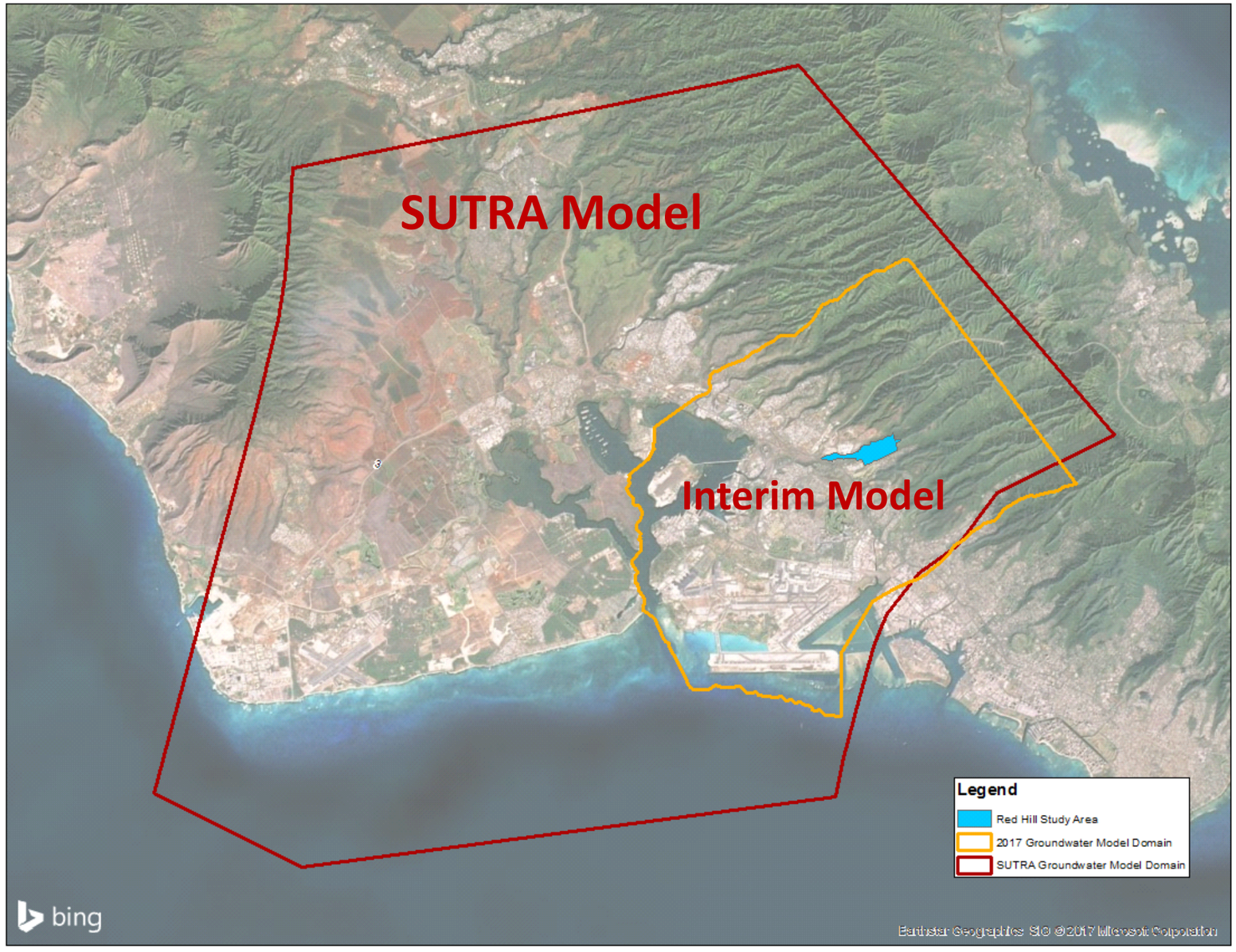

Location Map

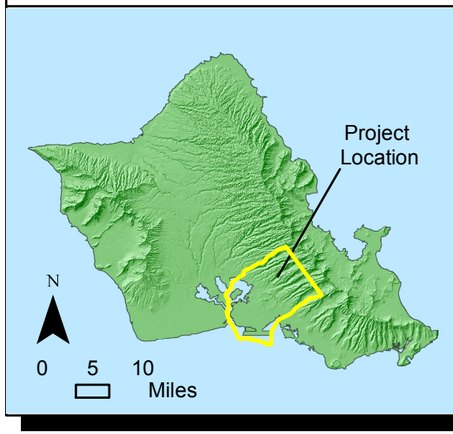

Notes

1. Map projection: NAD 1983 Hawaii State Plane Zone 3 feet

N

0 10,000 20,000 40,000 Feet

Figure 6-21
SUTRA and Interim Model Domains
Conceptual Site Model
Investigation and Remediation of Releases and Groundwater Protection and Evaluation
Red Hill Bulk Fuel Storage Facility,
JBPHH, O'ahu, Hawai'i

\\Honolulu.na.aecomnet.com\Honolulu\Projects\NAVFAC PAC\CLEAN V\60571032_CTO18F01260\900-Work\920 GIS\02_Maps\CSM\Fig6-21_CSM_SUTRA_Intrm_Mod_Domains.mxd 7/18/2018

This page intentionally left blank

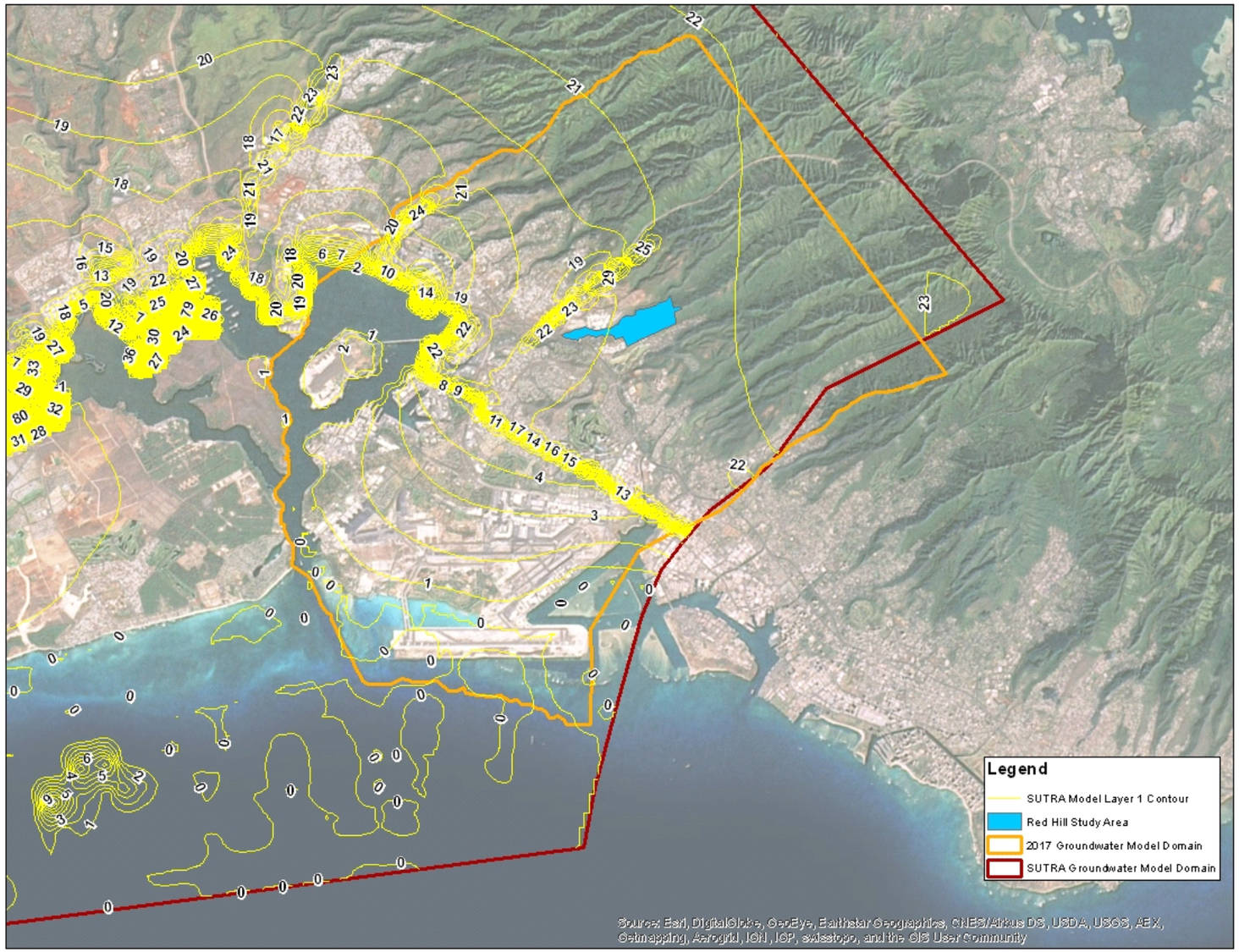

Location Map

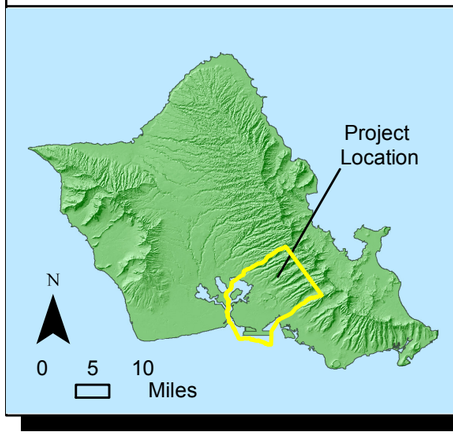

Notes

1. Map projection: NAD 1983 Hawaii State Plane Zone 3 feet

N

0 5,000 10,000 20,000 Feet

Figure 6-22
SUTRA Model Layer 1 Water Levels (ft msl)
Conceptual Site Model
Investigation and Remediation of Releases and Groundwater Protection and Evaluation
Red Hill Bulk Fuel Storage Facility,
JBPHH, O'ahu, Hawai'i

\\Honolulu.na.aecomnet.com\Honolulu\Projects\NAVFAC PACIFIC\CLEAN V\60571032_CTO18F01269\00-Work\20 GIS\02_Maps\CSM\Fig6-22_CSM_SUTRA_Layer1_Water_Levels.mxd 7/18/2018

This page intentionally left blank

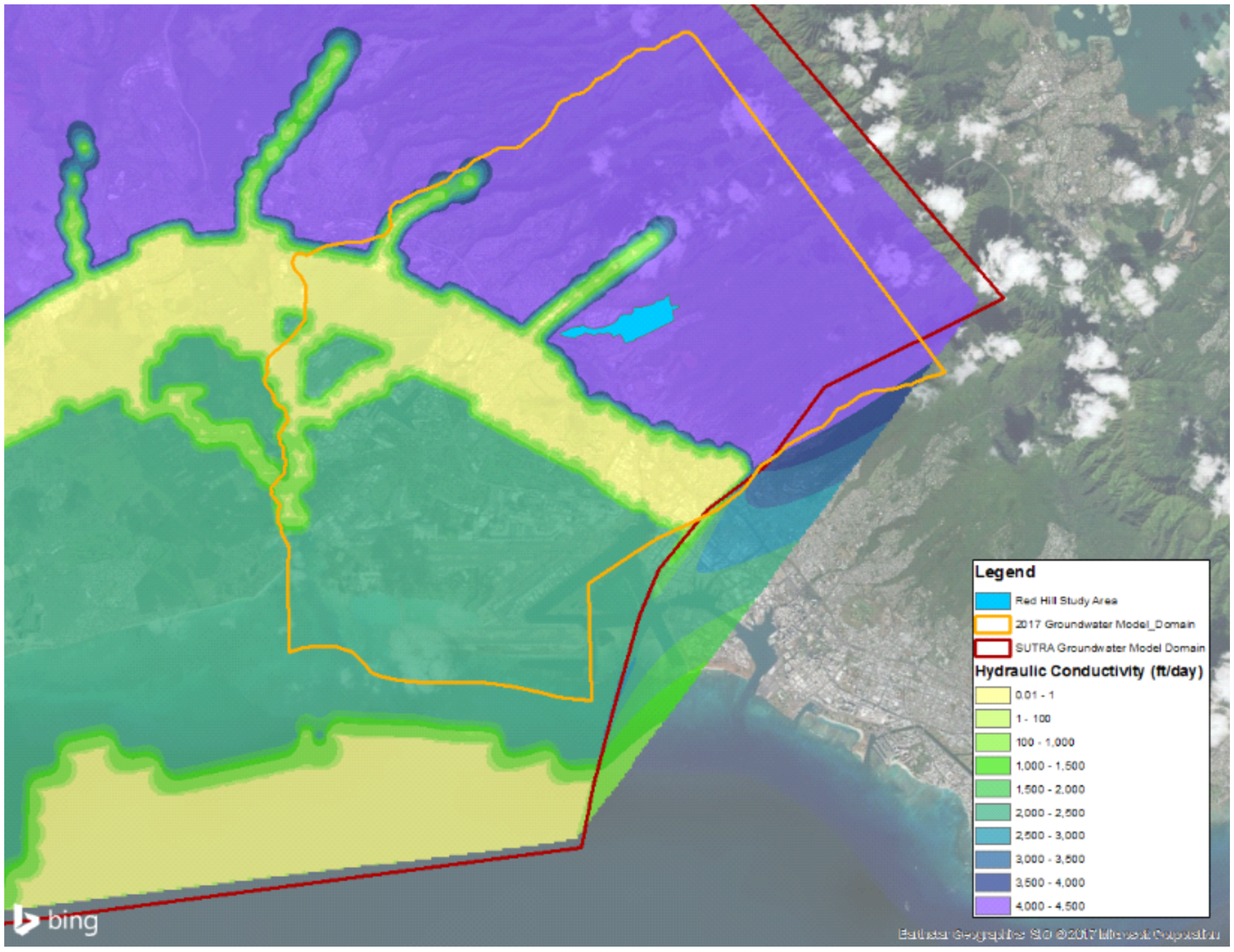

Location Map

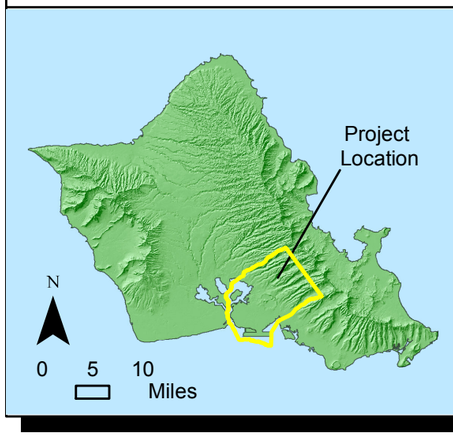

Notes

1. Map projection: NAD 1983 Hawaii State Plane Zone 3 feet

N

0 5,000 10,000 20,000 Feet

Figure 6-23
SUTRA Model Layer 1
Hydraulic Conductivity (ft/day)
Conceptual Site Model
Investigation and Remediation of Releases and Groundwater Protection and Evaluation
Red Hill Bulk Fuel Storage Facility,
JBPHH, O'ahu, Hawai'i

\\Honolulu.na.aecomnet.com\Honolulu\Projects\NAVFAC PAC\CLEAN V\60571032_CTO18F0126\900-Work\920 GIS\02_Maps\CSM\Fig6-23_CSM_SUTRA_Layer1_Hydraulic_Condctvty.mxd 7/18/2018

This page intentionally left blank

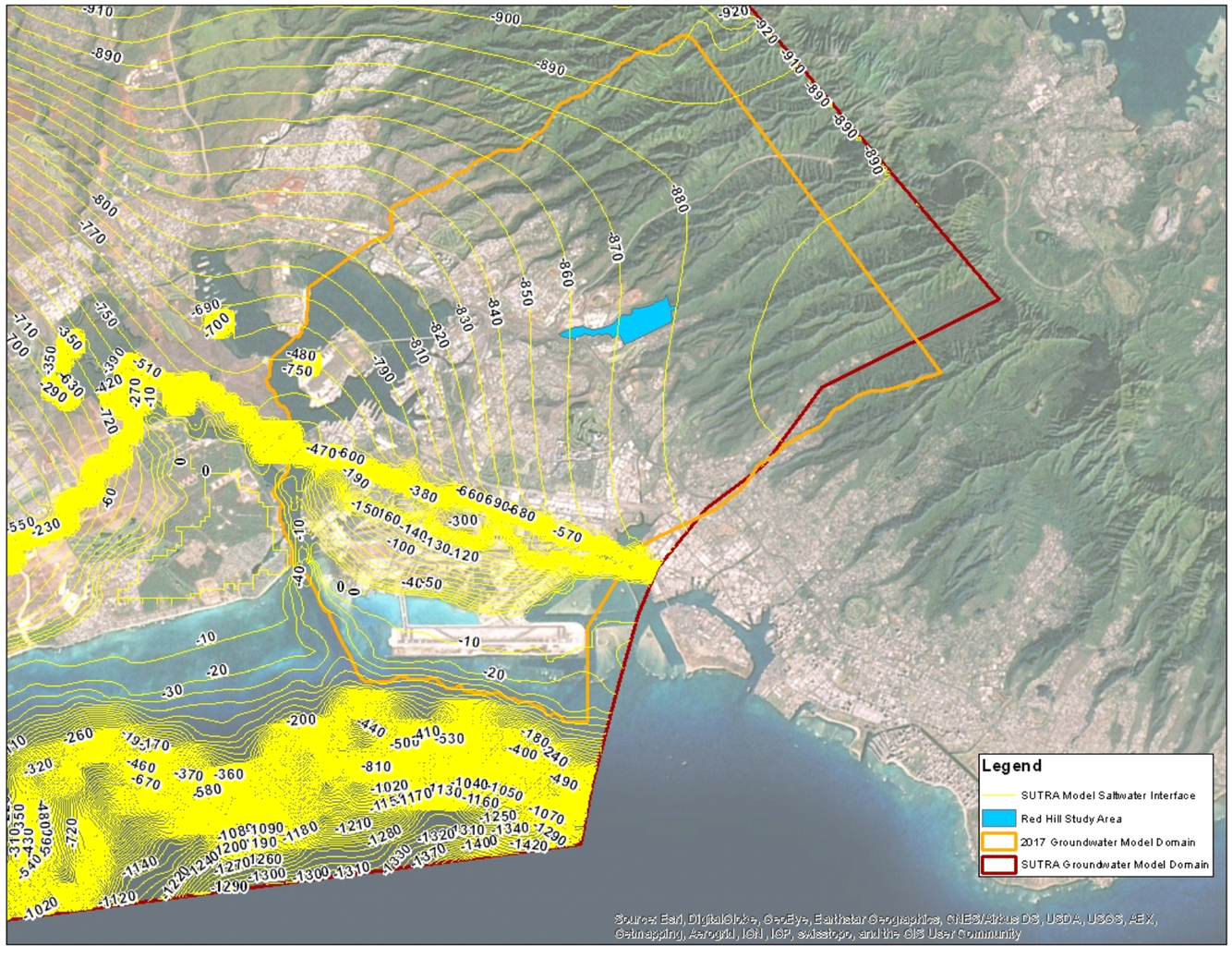

Location Map

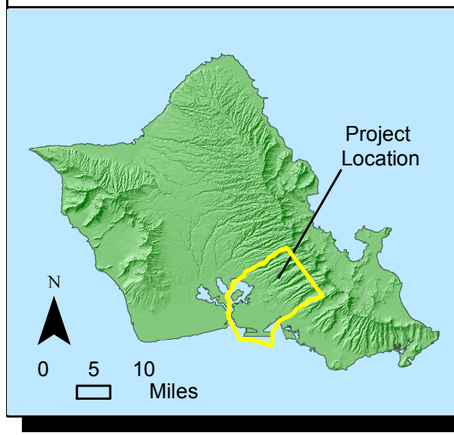

Notes

1. Map projection: NAD 1983 Hawaii State Plane Zone 3 feet

N

0 5,000 10,000 20,000 Feet

Figure 6-24
SUTRA Model Simulated Saltwater-Freshwater Interface (ft msl)
Conceptual Site Model
Investigation and Remediation of Releases and Groundwater Protection and Evaluation
Red Hill Bulk Fuel Storage Facility, JBPHH, O'ahu, Hawai'i

\\Honolulu.na.aecomnet.com\Honolulu\Projects\NAVFAC PAC\CLEAN V\60571032_CTO18F01269\00-Work\920 GIS\02_Maps\CSMFig6-24_CSM_SUTRA_Simultd_SaltFreshWater_Interface.mxd 7/18/2018

This page intentionally left blank

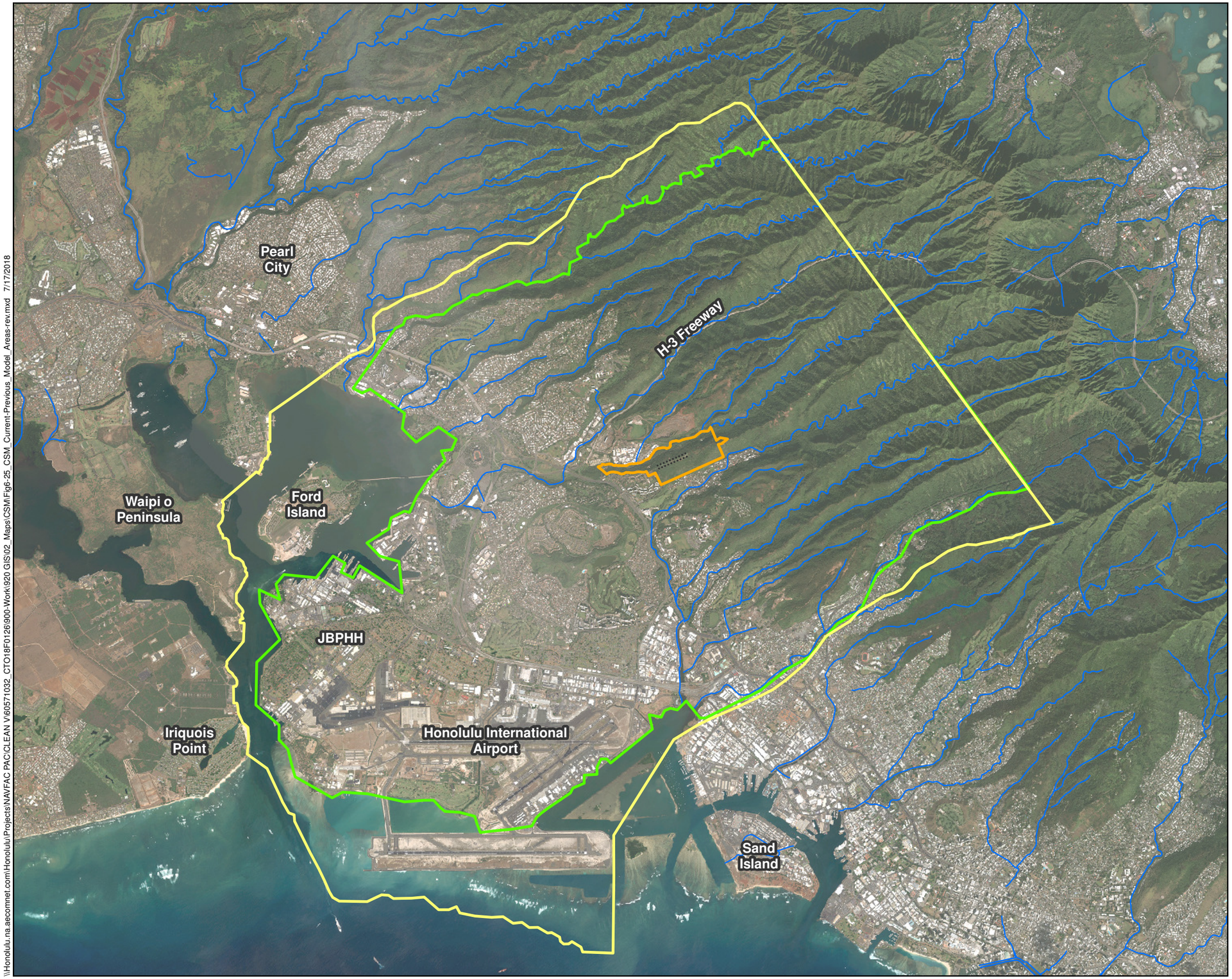

Location Map

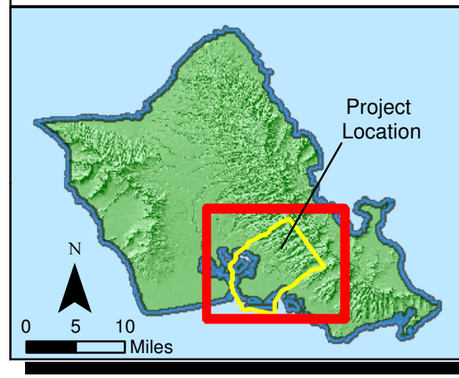

Legend

- Current Groundwater Model Area
- 2007 Groundwater Model Area
- 2004 Regional Model Area (see Location Map)
- Red Hill Facility Boundary and Fuel Storage Tanks
- Stream

Notes

1. Map projection: NAD 1983 UTM Zone 4N
2. DigitalGlobe, Inc. (DG) and NRCS. Publication_Date: 2015
3. 2007 Navy Red Hill model: DON (2007)
   2004 DOH SWAP model: Whittier et al. (2004)

N

0 5,000 10,000 15,000 Feet

Figure 6-25
Current and Previous Groundwater Model Areas
Conceptual Site Model
Investigation and Remediation of Releases and Groundwater Protection and Evaluation
Red Hill Bulk Fuel Storage Facility
JBPHH, O'ahu, Hawai'i

\\Honolulu.na.aecomnet.com\Honolulu\Projects\NAVFAC PAC\CLEAN V\60571032_CTO18F0126\900-Work\920 GIS\02_Maps\CSM\Fig6-25_CSM_Current-Previous_Model_Areas-rev.mxd 7/17/2018

This page intentionally left blank

S:\Projects\NAVFAC PAC\CLEAN V\60571032_CTO18F0126\900-Work\921 Graphics\01_TUA Support\CSM\Fig6-26_Observation Wells.ai

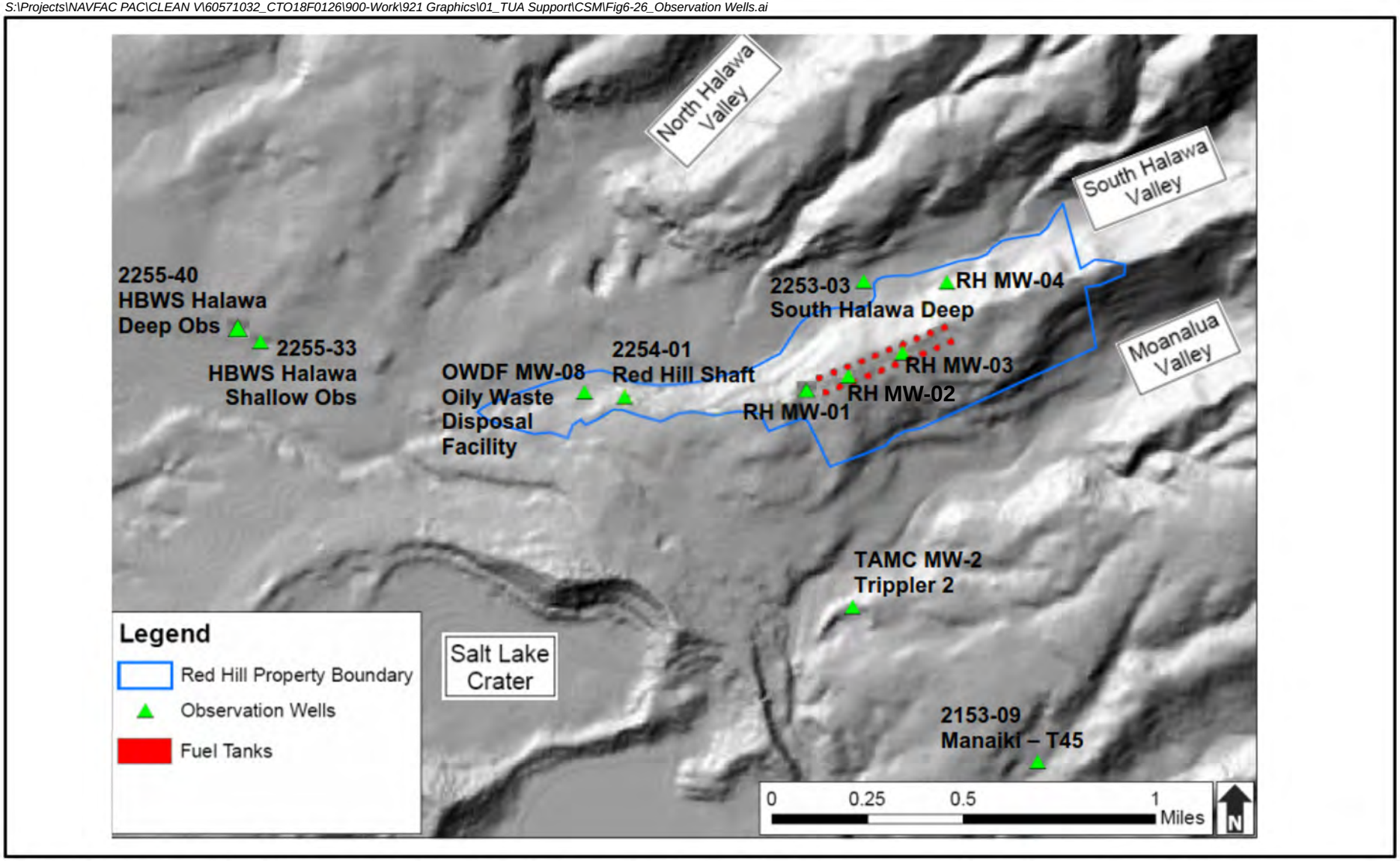

Source: U.S. Department of the Navy. 2007. *Red Hill Bulk Fuel Storage Facility, Final Technical Report*. Prepared by TEC, Inc. for Commander Naval Facilities Engineering Command, Pacific. August.

Figure 6-26
Location of Observation Wells for Synoptic Water Level Study Simulated by TEC 2007
Red Hill Bulk Fuel Storage Facility and Vicinity
Conceptual Site Model
Investigation and Remediation of Releases and Groundwater Protection and Evaluation
Red Hill Bulk Fuel Storage Facility
JBPHH, O'ahu, HI

This page intentionally left blank

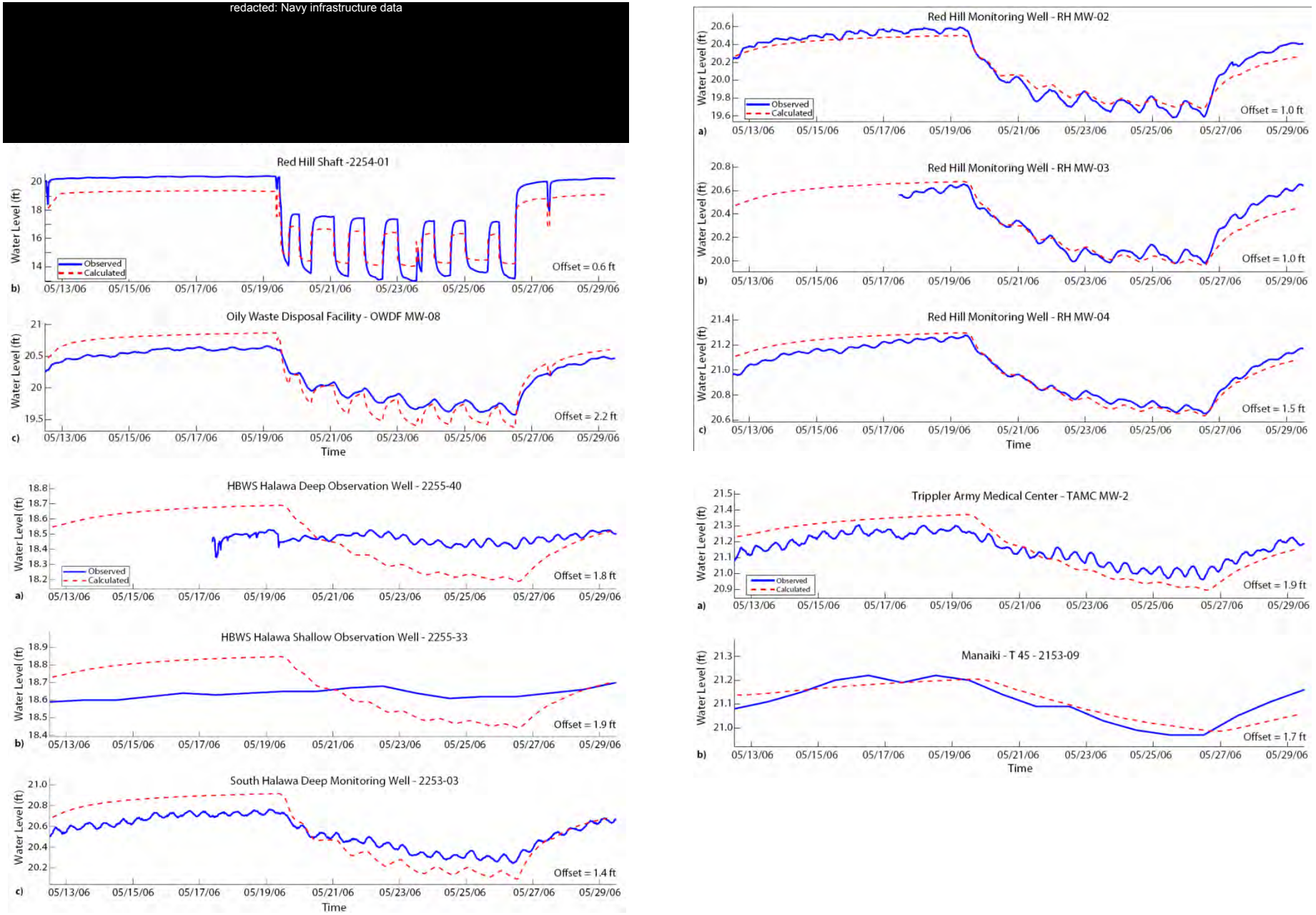

Source: DON (2007, Appendix L)

Figure 6-27
Water Levels, May 2006 Pumping Test
Conceptual Site Model
Investigation and Remediation of Releases and Groundwater Protection and Evaluation
Red Hill Bulk Fuel Storage Facility, JBPHH, O'ahu, Hawai'i

This page intentionally left blank

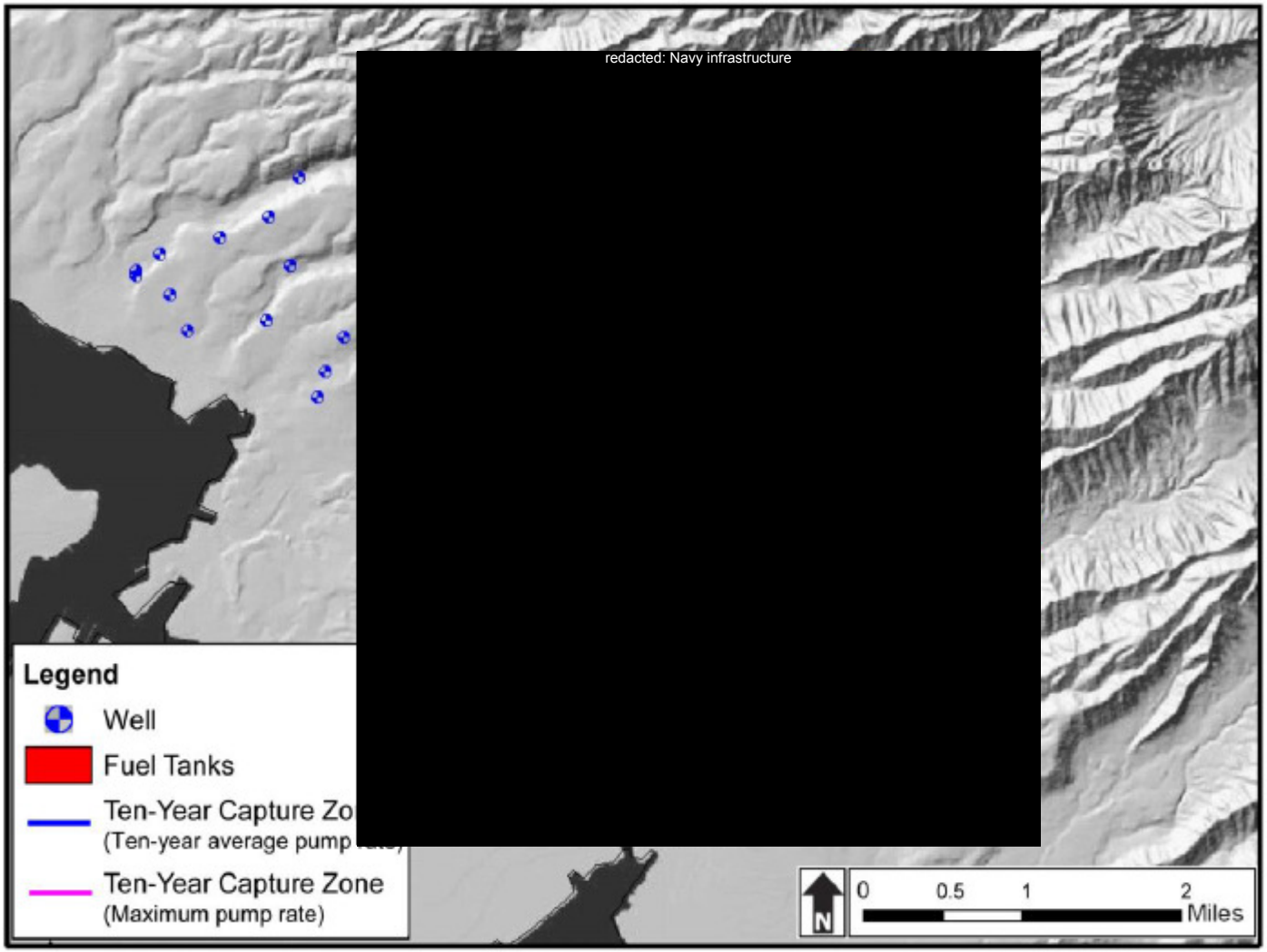

Source: Rotzoll, K. 2014. "Addendum to Rotzoll and El-Kadi (2007) Numerical Ground-Water Flow Simulation for Red Hill Fuel Storage Facilities, NAVFAC Pacific, Oahu, Hawaii." To: J. Shimabuku, NAVFAC HI; E. Lau, HBWS; cc: R. Whittier, HDOH; A. El-Kadi, University of Hawaii. January 29. Water Resources Research Center, University of Hawaii.

Figure 6-28
Simulated 10-Year Capture Zones by Rotzoll (2014) for Red Hill Shaft Not Pumping
Red Hill Bulk Fuel Storage Facility and Vicinity
Conceptual Site Model
Investigation and Remediation of Releases and Groundwater Protection and Evaluation
Red Hill Bulk Fuel Storage Facility
JBPHH, Oʻahu, Hawaiʻi

This page intentionally left blank

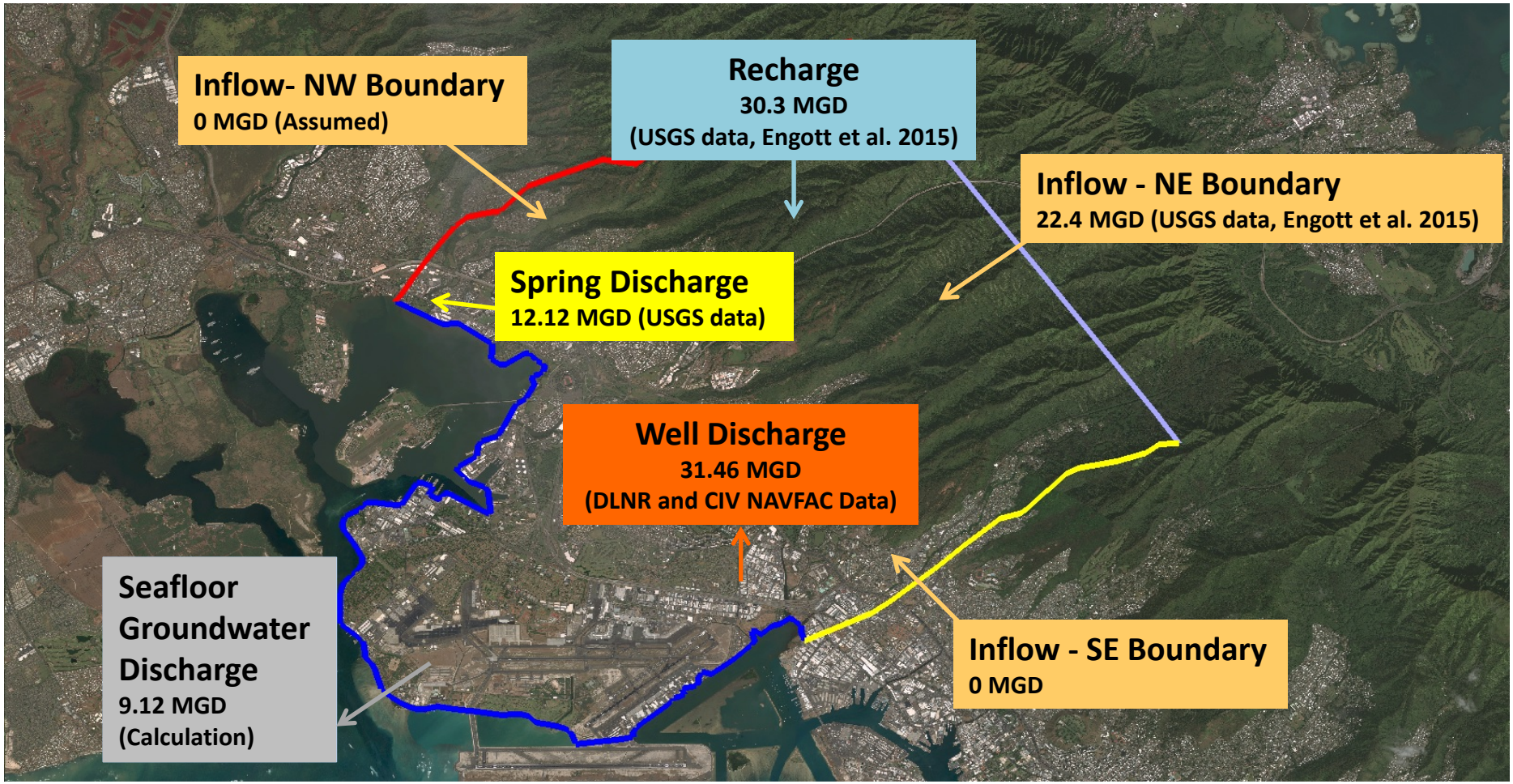

Figure 6-29
Current Conceptual Groundwater Balance
Conceptual Site Model
Investigation and Remediation of Releases and Groundwater Protection and Evaluation
Red Hill Bulk Fuel Storage Facility, JBPHH, O'ahu, Hawai'i

This page intentionally left blank

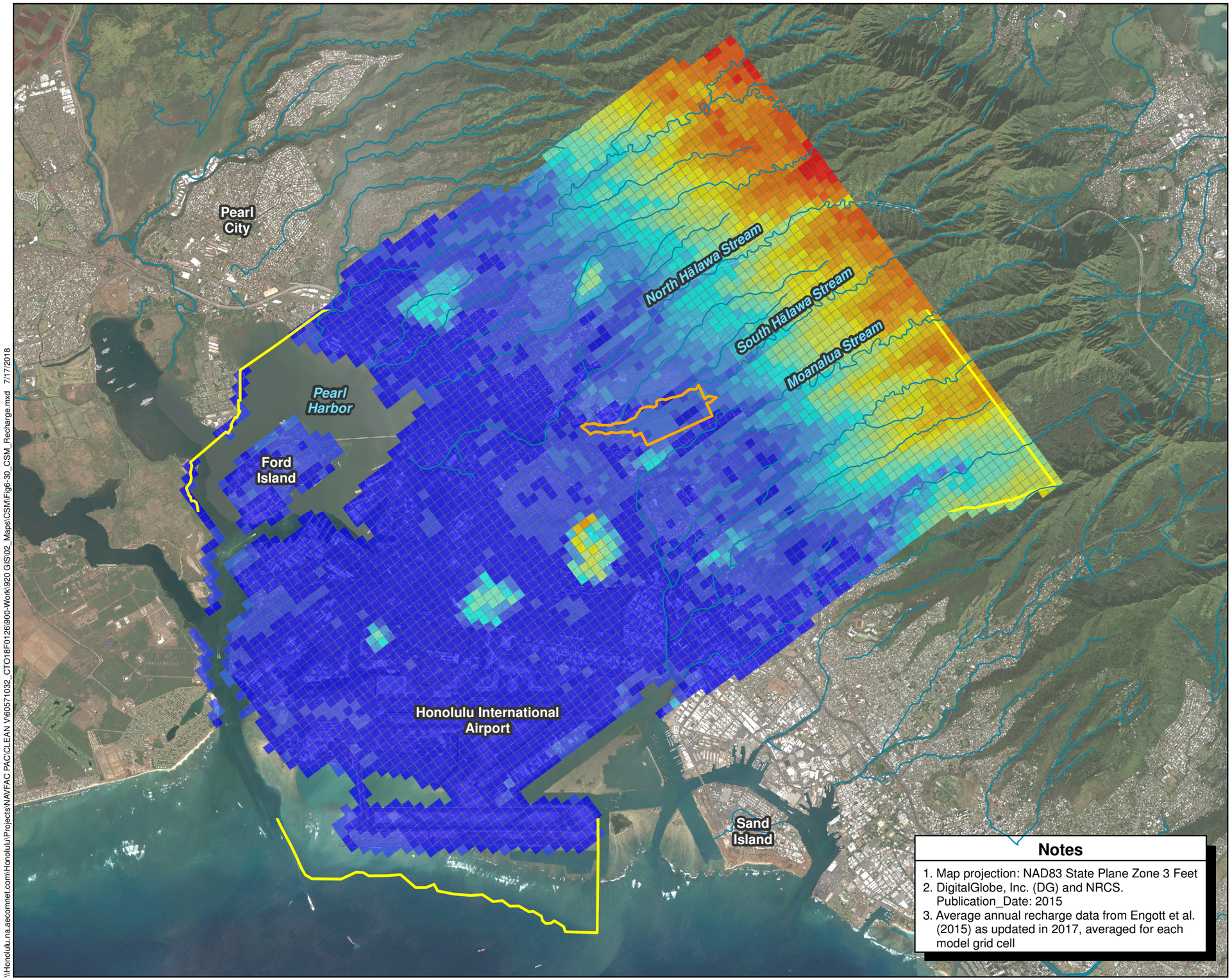

Location Map

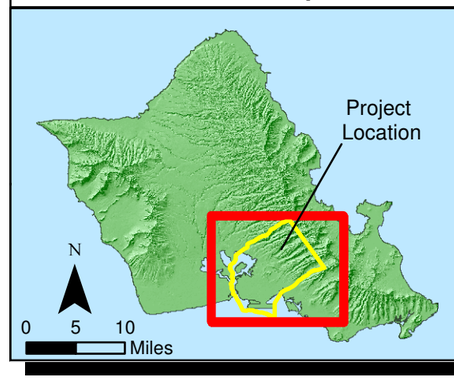

Legend

- Groundwater Model Area
- Red Hill Bulk Fuel Storage Facility Boundary
- Stream

Average Recharge (inches/year)

0.0 - 5.0	40.0 - 45.0
5.0 - 10.0	45.0 - 50.0
10.0 - 15.0	50.0 - 55.0
15.0 - 20.0	55.0 - 60.0
20.0- 25.0	60.0- 65.0
25.0 - 30.0	65.0 - 70.0
30.0 - 35.0	70.0 - 75.0
35.0- 40.0	75.0 - 80.0

Notes

1. Map projection: NAD83 State Plane Zone 3 Feet
2. DigitalGlobe, Inc. (DG) and NRCS. Publication_Date: 2015
3. Average annual recharge data from Engott et al. (2015) as updated in 2017, averaged for each model grid cell

N

0 5,000 10,000 15,000 Feet

Figure 6-30
Average Recharge within the Model Area
Conceptual Site Model
Investigation and Remediation of Releases and Groundwater Protection and Evaluation
Red Hill Bulk Fuel Storage Facility
JBPHH, O'ahu, Hawai'i

\\Honolulu.na.aecomnet.com\Honolulu\Projects\NAVFAC PAC\CLEAN V\60571032_CTO18F0126\900-Work\920 GIS\02_Maps\CSM\Fig6-30_CSM_Recharge.mxd 7/17/2018

This page intentionally left blank

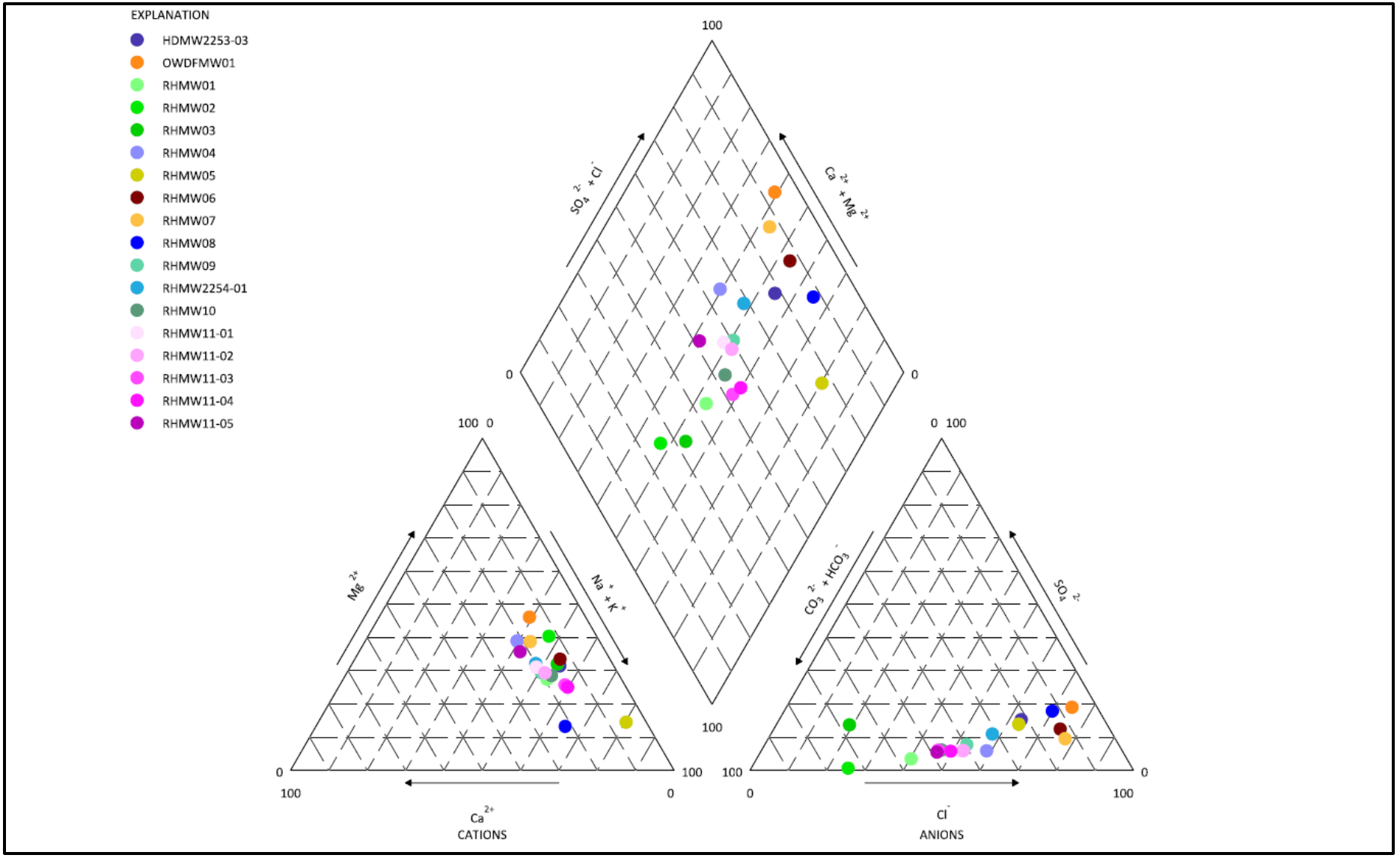

Figure 6-31
Chemical Composition of Groundwater in Red Hill Monitoring Wells
Red Hill Bulk Fuel Storage Facility and Vicinity
Conceptual Site Model
Investigation and Remediation of Releases and Groundwater Protection and Evaluation
Red Hill Bulk Fuel Storage Facility
JBPHH, O‘ahu, Hawai‘i

This page intentionally left blank

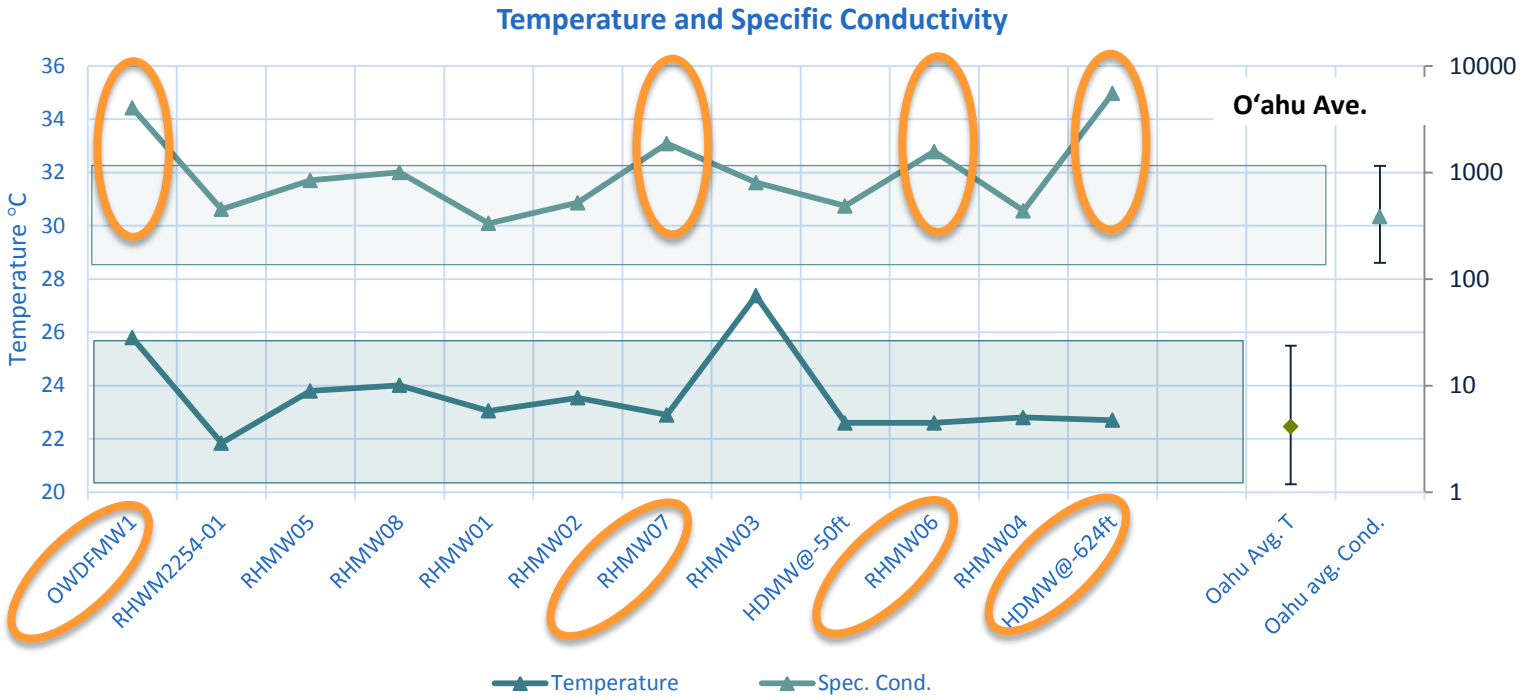

Figure 6-32
Specific Conductivity Anomaly: OWDFMW1, RHMW06, RHMW07, HDMW2253-03 –624 ft
Conceptual Site Model
Investigation and Remediation of Releases and Groundwater Protection and Evaluation
Red Hill Bulk Fuel Storage Facility
JBPHH, O'ahu, Hawai'i

This page intentionally left blank

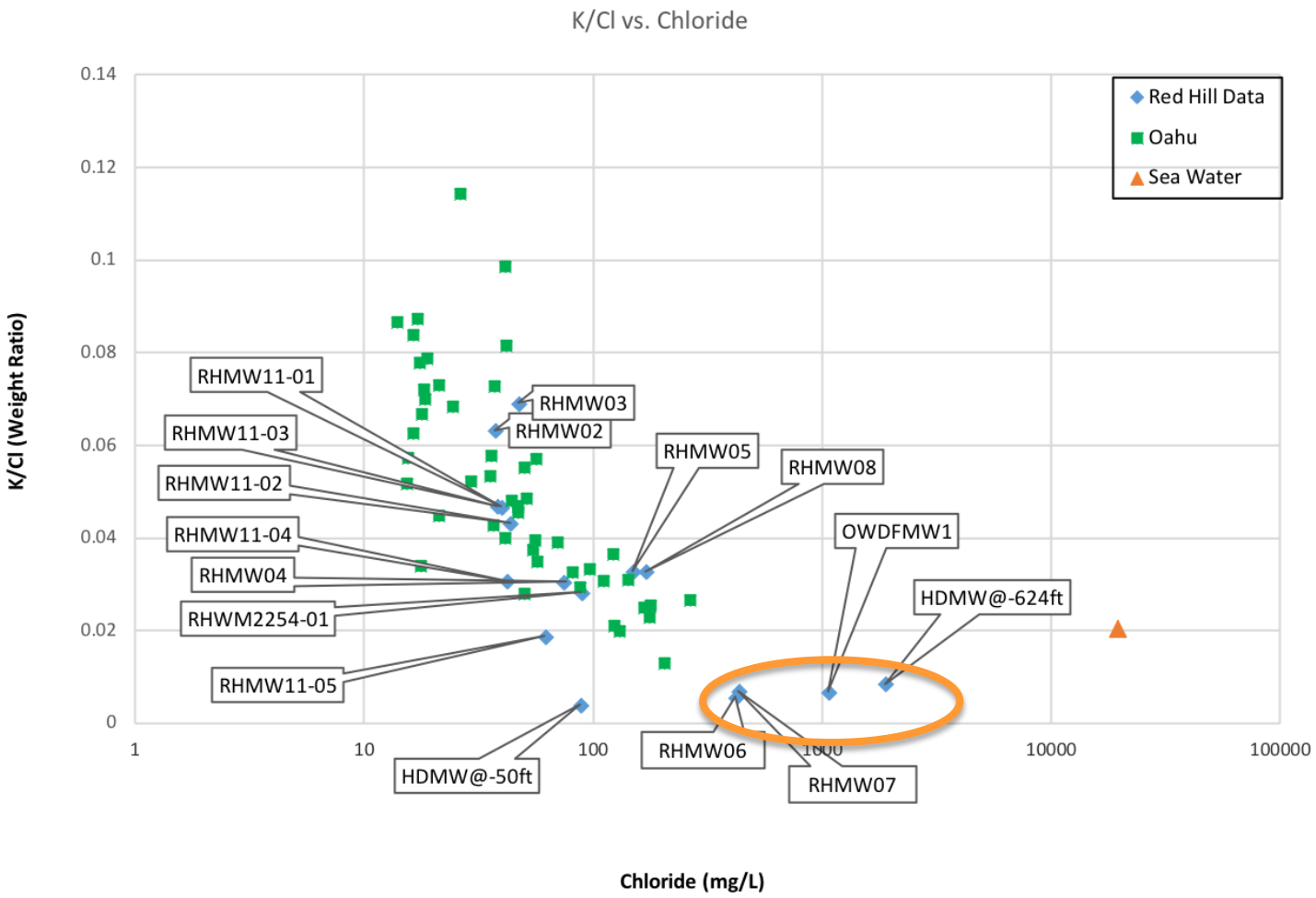

Figure 6-33
Specific Conductivity Anomaly: OWDFMW1, RHMW06, RHMW07, HDMW2253-03 –624 ft (K/cl vs. Chloride)
Conceptual Site Model
Investigation and Remediation of Releases and Groundwater Protection and Evaluation
Red Hill Bulk Fuel Storage Facility
JBPHH, O'ahu, Hawai'i

This page intentionally left blank

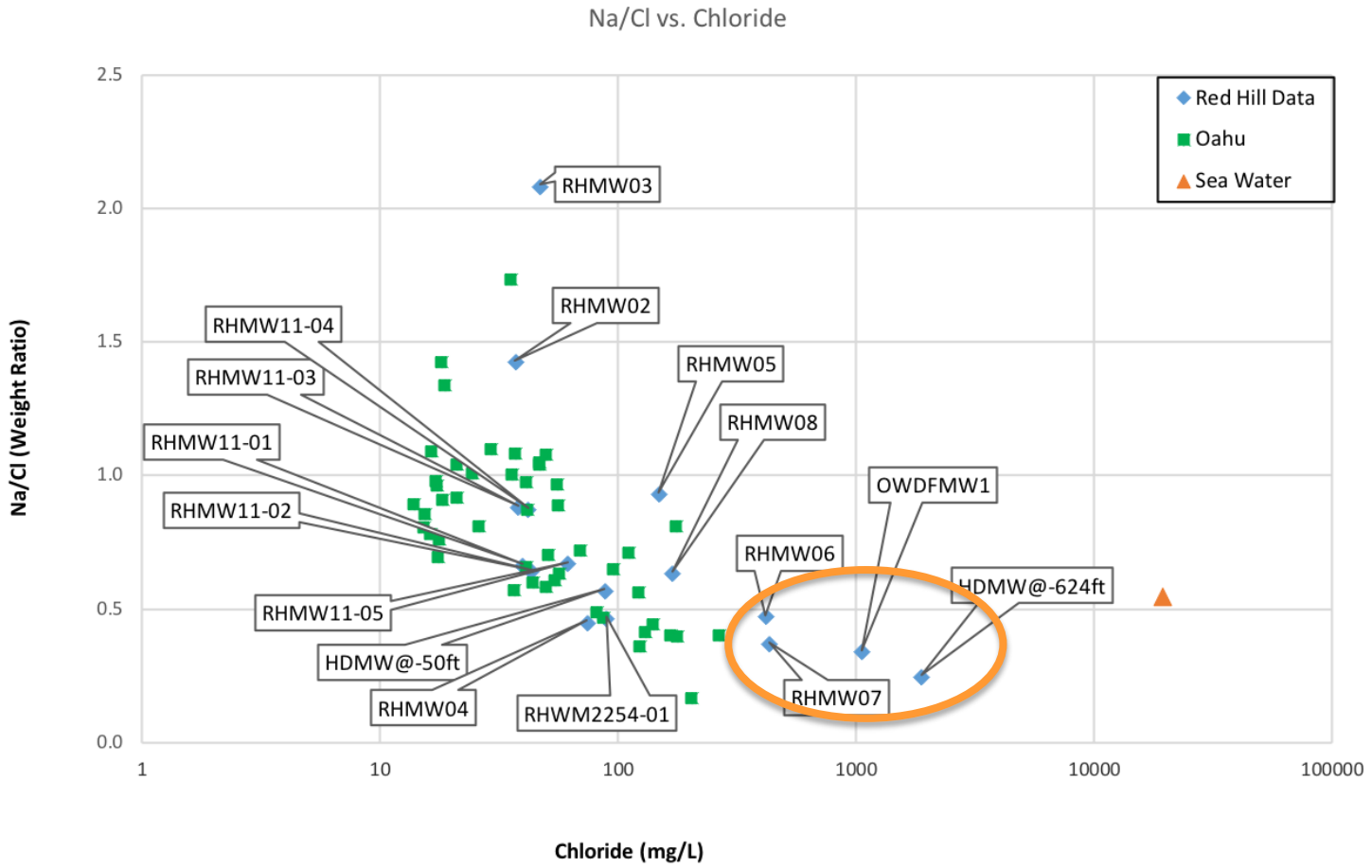

Figure 6-34
Specific Conductivity Anomaly: OWDFMW1, RHMW06, RHMW07, HDMW2253-03 –624 ft (Na/Cl vs. Chloride)
Conceptual Site Model
Investigation and Remediation of Releases and Groundwater Protection and Evaluation
Red Hill Bulk Fuel Storage Facility
JBPHH, O'ahu, Hawai'i

This page intentionally left blank

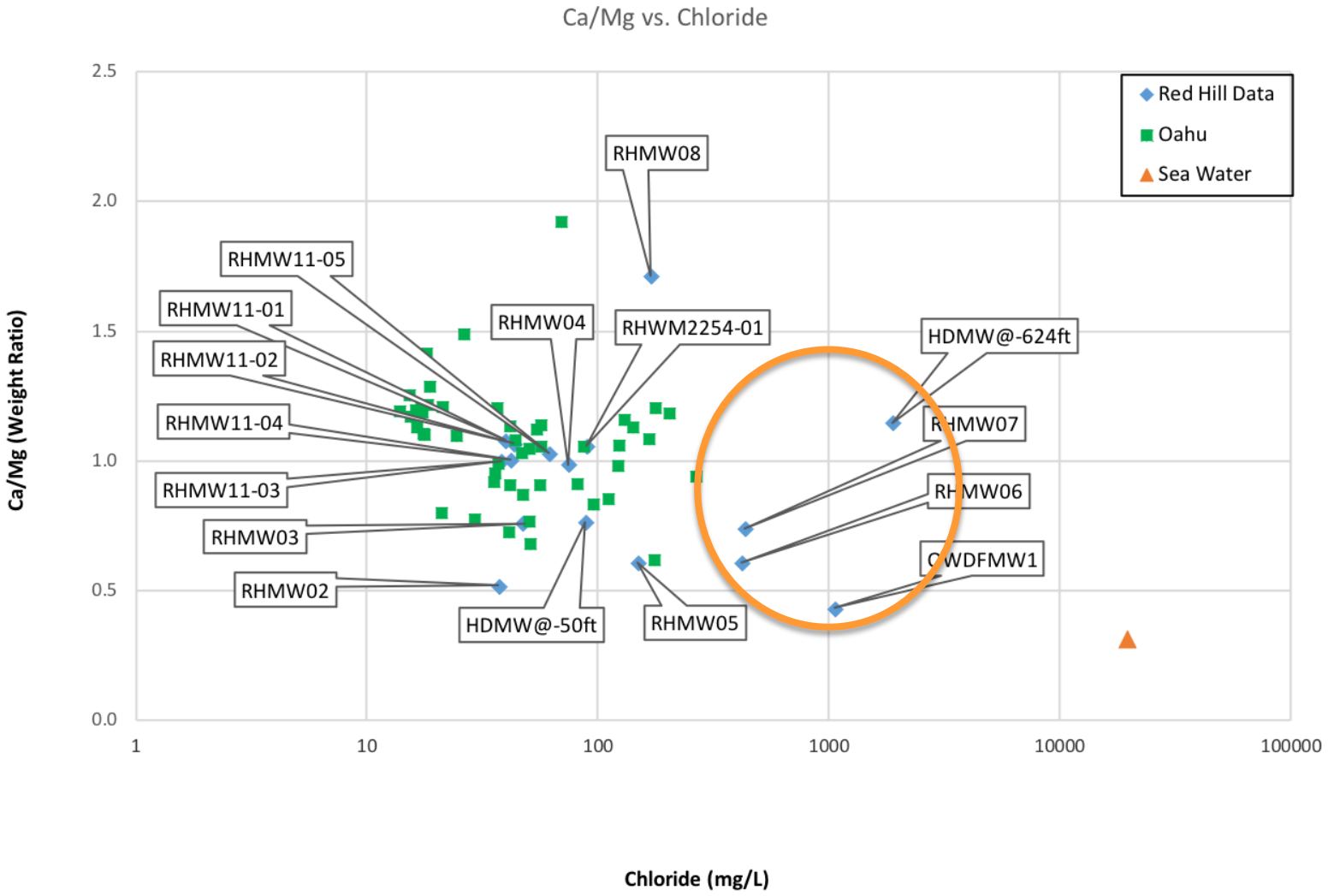

Figure 6-35
Specific Conductivity Anomaly: OWDFMW1, RHMW06, RHMW07, HDMW2253-03 –624 ft (Ca/Mg vs. Chloride)
Conceptual Site Model
Investigation and Remediation of Releases and Groundwater Protection and Evaluation
Red Hill Bulk Fuel Storage Facility
JBPHH, O'ahu, Hawai'i

This page intentionally left blank

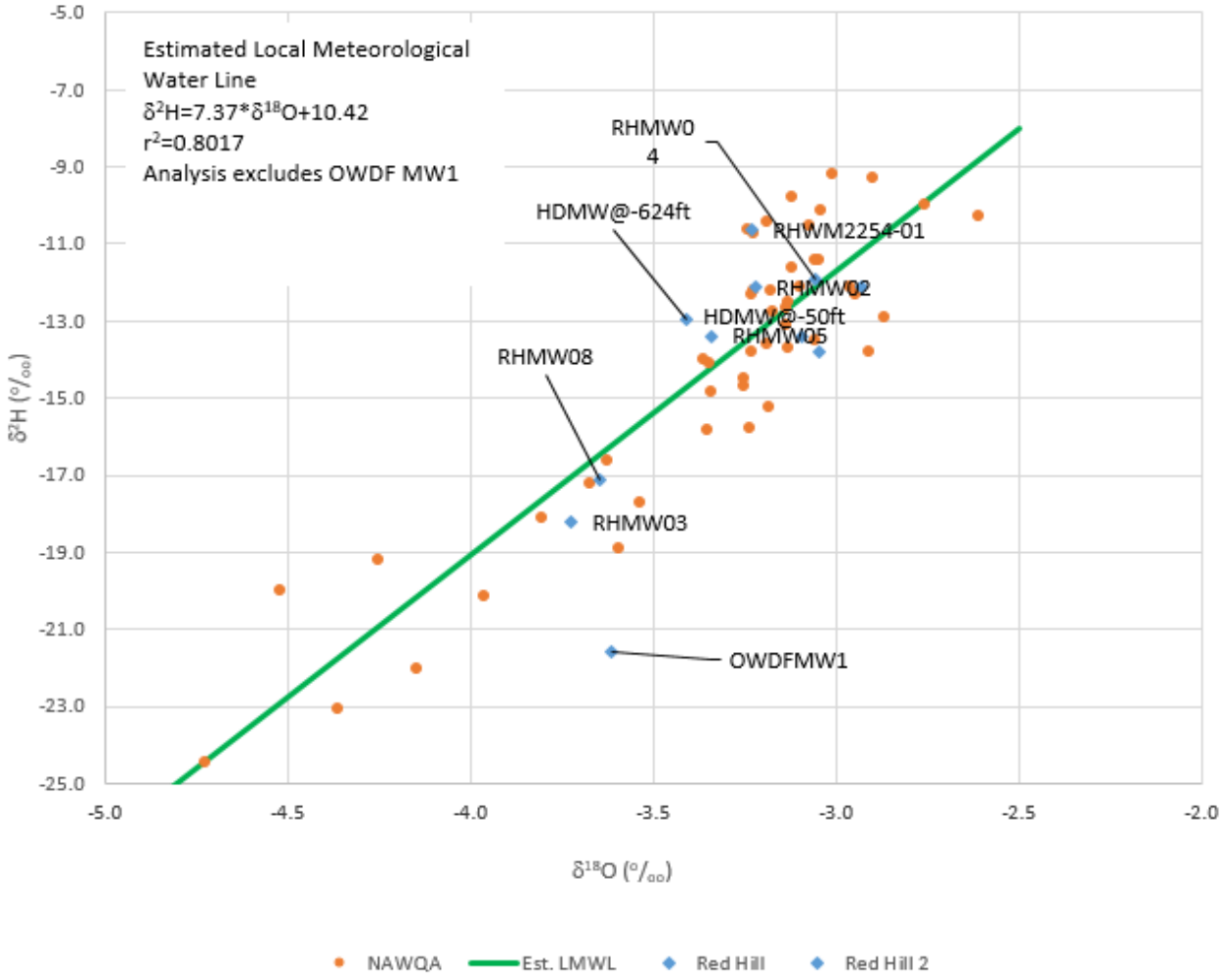

Figure 6-36
Estimated Local Meteorological Water Line
Conceptual Site Model
Investigation and Remediation of Releases and Groundwater Protection and Evaluation
Red Hill Bulk Fuel Storage Facility
JBPHH, O'ahu, Hawai'i

This page intentionally left blank

7. Module F: Fate and Transport of LNAPL and Dissolved COPCs in Groundwater

Potential vadose zone and groundwater transport pathways are identified based on the spatial and temporal trends of COPCs in groundwater from both historical and future sampling conducted at the site, and the results of previous groundwater flow and CF&T modeling. Evaluations of LNAPL migration are based on direct observation in core samples, and indirectly based on vapor samples, temperature surveys, and petrographic studies. Fate is discussed within the context of fuel properties and attenuation studies both in the vadose zone as NSZD and in the dissolved groundwater plume as MNA processes.

7.1 LNAPL Distribution, Fuel Type, and Evidence of Weathering

This subsection documents the distribution of LNAPL in the subsurface at the Facility, the evidence concerning the type of fuel released, and the weathering of that fuel. A thorough discussion of LNAPL release and migration based on the construction of the tank farm and influence of the complex underlying geology (geometry, rock characteristics, volcanic features) is presented in Module C: LNAPL Release and Source-Zone Migration Model (Section 4) and Module D: Vadose Zone Model (Section 5), respectively.

7.1.1 LNAPL Distribution in the Unsaturated Zone

Historical data and preliminary data from the *Attenuation Evaluation Plan* (DON 2017g) have been used to evaluate the distribution of LNAPL within the vadose zone at the Facility. Specifically, (1) the thermal NSZD investigation has been used to evaluate the vertical distribution of LNAPL in the unsaturated zone (see Section 7.3.1.4 and Appendix B.1), and (2) observations of soil contamination while drilling angle borings under the tanks between 1998 and 2002 (DON 1999, 2002) have been used to evaluate the presence of LNAPL below individual tanks (Appendix B.1 Figure 3-3). These data suggest the following LNAPL distribution in the vadose zone:

- Based on the temperature profiles for Facility wells, LNAPL is inferred to be present within the top one-third of the unsaturated zone between the LAT and the water table (i.e., within a depth interval of 70–110 ft msl (see Section 7.3.1.4).
- Based on the angle boring investigations conducted between 1998 and 2002, LNAPL staining and/or sheens were observed in unsaturated-zone soils below Tanks 1, 9, 11, 13, 14, and 16.
- Based on the angle boring investigations conducted between 1998 and 2002, petroleum odors (but no staining or sheens) were noted below Tanks 2–8, 12, and 18–20. No evidence of petroleum impacts was observed below Tanks 10, 15, and 17.
- Based on monthly SVM conducted since 2008, there has been no significant recent release of LNAPL from any tank since 2008 except for the 2014 release from Tank 5 (see Section 7.3.1.4 and Appendix B.3).
- LNAPL is present in the vicinity of Tank 5 has penetrated only the upper portion of the unsaturated zone. Previous investigations have confirmed that (1) the vadose zone and saturated zone beneath the Facility are composed of zones of high horizontal permeability, interconnected at the site scale; (2) low-permeability zones of unfractured basalt may be barriers to the movement of fluids through the vadose zone and groundwater flow; and (3) valley fill sediments are fine-grained and have the potential to form low-permeability flow barriers. Saprolite occurring beneath valley fill sediments also has the potential to form

a low-permeability flow barrier, which could further impede the transfer of fluids or groundwater. Dikes may be barriers, but have not been observed at the site.

7.1.2 LNAPL Distribution at the Water Table

Historical observations and monitoring data from Facility monitoring wells have been used to evaluate the LNAPL distribution at the water table.

7.1.2.1 Observation of LNAPL in Monitoring Wells

No LNAPL has been observed in any Facility monitoring well since 2014 (i.e., after the January 2014 Tank 5 release event). Prior to 2014, the available records regarding LNAPL observations do not provide a clear indication of the presence or absence of LNAPL in individual wells. Discussions with DOH (Bob Whittier, pers. comm. 2018) indicate that a small sheen may have been present in an early sampling event for RHMW02 prior to the 2014 release.

7.1.2.2 Evidence of LNAPL Based on COPC Concentrations in Monitoring Wells

Dissolved-phase concentrations of COPCs in groundwater and chromatographic profiles of TPH analysis may be useful as indirect indicators in evaluating the presence of LNAPL in groundwater, when used collectively as multiple LOEs. Based on the evaluation of the chromatograms, there is no evidence of the presence of LNAPL in any of the groundwater samples collected from monitoring wells at the Facility. For the four monitoring wells located adjacent to or immediately downgradient from the tanks, the dissolved-phase COPC concentrations support the following observations:

- In monitoring well RHMW03, total dissolved-phase concentrations of fuel constituents are relatively low (< 0.5 mg/L since 2005), with limited depletion of groundwater electron acceptors (oxygen, nitrate, and sulfate) and no measurable methane production. The groundwater data in this area suggest the presence of a low-concentration dissolved plume, potentially one that is driven by infiltration/leaching processes, and do not indicate the presence of LNAPL in the saturated zone upgradient of RHMW03.
- Monitoring well RHMW02 exhibits the highest concentrations of total dissolved-phase fuel constituents among the Facility monitoring wells (approximately 2–7 mg/L since 2005). Much of these concentrations are in the form of polar compounds associated with the biodegradation of petroleum. The concentrations of naphthalene, 1-methylnaphthalene, and 2-methylnaphthalene are equal to or greater than the expected concentration based on the effective solubility of these compounds in jet fuel. However, concentrations of benzene, toluene, ethylbenzene, and xylene (BTEX) are very low (generally less than 1 microgram per liter [µg/L]). Although COPC concentrations have varied over time, the observed concentration ranges are similar for the monitoring periods before and after the 2014 Tank 5 release. The MNA sampling parameters indicate high levels of biodegradation occurring in the vicinity of this well, as key electron acceptors are depleted and high concentrations of dissolved methane are present (sometimes greater than 10 mg/L). Taken together, these data suggest the presence of weathered LNAPL (i.e., pre-2005 release) in the immediate vicinity of RHMW02 or within the saturated zone upgradient from this well. Based on the angle boring investigations conducted during 1998–2002 (DON 1999, 2002), this LNAPL may have originated from Tank 9, 11, or 13. The monitoring data indicate it is likely that the 2014 Tank 5 release did not impact groundwater and impacts to groundwater are more likely attributable to historical releases.
- Monitoring well RHMW01 exhibits the next highest dissolved-phase fuel constituent concentrations (approximately 0.1–1 mg/L since 2005), which may have some hydraulic

connection to monitoring well RHMW02 located upgradient. Electron acceptors are depleted, and methane is present in the 0.2–7 mg/L range, since 2005. These data are consistent with the natural attenuation of dissolved constituents in groundwater and do not suggest the presence of LNAPL within the saturated zone between RHMW02 and RHMW01.

- Monitoring well RHMW05 is located between the tank farm area and the Red Hill Shaft water development tunnel. Groundwater at this location exhibits low concentrations of fuel hydrocarbons (typically less than 0.05 mg/L). These data do not suggest the presence of LNAPL within the saturated zone between RHMW01 and RHMW05.

7.1.3 Dissolved-Phase Fuel Type and Evidence of Weathering

Characterization of TPH in groundwater is presented in Appendix B.7, including description of jet fuel composition, partition to water, and biodegradation, as well as an assessment of what constituents compose the TPH in groundwater from RHMW02, the only current well with TPH-d (hydrocarbons within the middle distillates or diesel range) exceeding DOH EALs. The analysis presented in Appendix B.7 is summarized below. No LNAPL has been measured in the monitoring wells at the Facility. Consequently, the evaluation of fuel type and weathering has relied on the available dissolved-phase COPC monitoring results, particularly the dissolved TPH-d results and chromatograms.

7.1.3.1 Dissolved-Phase Fuel Type

The mixture of individual constituents in TPH-d in monitoring well RHMW02 is consistent with a jet fuel release. The TPH-d is composed of soluble components of jet fuels or kerosene (i.e., the base fuel for jet fuels), which include:

- Substituted benzenes (primarily C3- and C4-benzenes: substituted benzenes with side chains containing three and four carbons)
- Naphthalene and C1-substituted naphthalenes (i.e., 1-methylnaphthalene and 2-methylnaphthalene)
- C2+ substituted naphthalenes
- It is evident that the dissolved TPH-d in RHMW02 is from a jet fuel release that is weathered based on the aromatic hydrocarbons found in the groundwater and the predominance of metabolites. Appendix B.7 Sections 3.1, 3.3, 4.1, and 4.2 include more-detailed discussions of what constituents compose the aromatic hydrocarbons in the groundwater and associated metabolites.

7.1.3.2 Evidence of Dissolved-Phase TPH Weathering

The TPH chromatographic profiles or fingerprints show the following evidence of weathering:

- Profiles consistent with soluble components of jet fuel. The presence of naphthalene, C1-naphthalenes, as well as C2+naphthalenes is evident. There is also evidence of C4-benzenes. Lighter components are partially lost in the extraction and concentration of the extract prior to analysis; thus, lighter substituted benzenes, if present, would not be detected in the TPH-d analysis.
- Presence of a "hump" in the chromatograms that extends beyond the end of the jet/kerosene carbon range (C16+) (see Appendix B.7 Figure 3-11 and associated discussion). Unweathered petroleum fuels are composed primarily of hydrocarbons (nonpolar) that have

distinctive chromatographic profiles seen as evenly distributed peaks spanning the carbon range of the fuel. The presence of a hump with unevenly distributed peaks beyond the fuel carbon range is likely due to polar matter that could be metabolites from biodegradation. Silica gel treatment (used to remove polar material) of the groundwater extract used for measuring TPH-d removes between 40% and 85% of the RHMW02 dissolved TPH-d concentration, indicating that a significant amount of polar compounds is present in the groundwater. The dissolved organics in RHMW02 are a mixture of hydrocarbons and polar metabolites, indicating ongoing biodegradation.

- Certain compounds that are relatively resistant to biodegradation are typically found in low concentrations in unweathered fuel, but become relatively enriched in the weathered fuels as the more degradable compounds are consumed. Some of the compounds detected as tentatively identified compounds (TICs) in RHMW02 are these more recalcitrant compounds (e.g., naphtheno-benzenes); these compounds would likely not be detectable in a plume originating from an unweathered fuel release. The detection of these compounds in RHMW02 indicates that the dissolved-phase plume is originating from weathered fuel (see Appendix B.7 Section 4.2, Table 4-3).
- Methane is consistently detected in RHMW02, indicating anaerobic (i.e., methanogenic) biodegradation of fuel constituents.

7.2 DISSOLVED-PHASE COPCS DETECTED IN GROUNDWATER

The Red Hill groundwater monitoring network is described in Section 2.12.2. Groundwater samples are currently analyzed for the following constituents: COPCs (including TPH-gasoline range organics [TPH-g], TPH-d, TPH-residual range organics [TPH-o], benzene, ethylbenzene, toluene, xylenes, 1-methylnaphthalene, 2-methylnaphthalene, and naphthalene); fuel additives (including phenol and 2-[2-ethoxymethoxy]-ethanol); lead scavengers (including 1,2-dichloroethane and 1,2-dibromoethane; for newly installed monitoring wells only); and NAPs (including nitrate, sulfate, chloride, nitrate-nitrite as nitrogen, alkalinity, ferrous iron, methane, DO, oxidation-reduction potential (ORP), and TPH-d/o with silica gel cleanup). Groundwater samples have also been analyzed for general groundwater chemistry, which is further discussed in Section 6.7.

Current and historical COPCs, fuel additives, and lead scavenger results are compared against the screening criteria, which is partially based on the most current DOH Table D-1b EALs (i.e., groundwater EALs for sites where groundwater is a current or potential drinking water resource and the nearest surface water body is greater than 150 m from release site) (DOH 2017) where available. For analytes without EALs, the screening criterion is based on most current EPA Regional Screening Levels (RSLs) (EPA 2018). TPH-d and benzene results from select monitoring wells (i.e., RHMW01, RHMW02, and RHMW03) are also compared to Site-Specific Risk-Based Levels (SSRBLs), which were established in the latest Red Hill GWPP (DON 2014b) and subsequently presented in the AOC Statement of Work Sections 6 and 7 scoping completion letter (EPA Region 9 and DOH 2016) (DON 2017k).

One approach for evaluating COPC plume trends is plotting COPC concentrations over time at each monitoring location, as well as spatial graphing of contaminant concentrations versus distance downgradient along the plume flow path over multiple sampling events. Historical Red Hill groundwater monitoring results indicate that most COPCs, and in general the highest detected COPC concentrations, occur in well RHMW02. Seasonal variations (i.e., wet and dry season effects) are not evident. Cumulative results of historical groundwater monitoring and graphs of COPC concentrations over time are presented in Appendix A. COPC concentration graphs for TPH-g, TPH-d, TPH-o, BTEX, 1-methylnaphthalene, 2-methylnaphthalene, and naphthalene are shown in

relation to monitoring well locations on Figure 7-1. Additional discussions of COPC and NAP results are discussed in the quarterly groundwater monitoring reports (DON 2018e).

Quarterly groundwater monitoring analytical results through April 2018 for the 14 monitoring locations are summarized below. A more detailed evaluation of the data is presented in Appendix B.7 Section 5.2.6 and Attachments B.7.2, B.7.3, and B.7.4.

- *RHMW2254-01* is a sampling point located inside the infiltration gallery of Navy Supply Well 2254-01 (Red Hill Shaft). Detections of TPH-g, TPH-d, TPH-o, and polynuclear aromatic hydrocarbons (PAHs) occurred occasionally during monitoring events between 2005 and October 2017, but no COPCs have been detected above the screening criteria. The highest TPH-d concentration (67 µg/L) was detected during the June 2005 monitoring event (the second sampling event performed at this sampling point), much lower than the screening criterion (400 µg/L). Fuel additives have never been detected at this sampling point or in any of the other wells in the monitoring network. Naphthalenes have not been detected since March 2014. Toluene was detected during four monitoring events, but may be attributed to field or laboratory artifact based on reported trip blank contamination during the October 2015 and January 2016 events.
- *RHMW01*, an in-tunnel monitoring well located southwest of the tank farm, was installed in 2001 (DON 2002). TPH-d is consistently detected at RHMW01, with the most recent DOH screening criterion exceedance during the First Quarter (January) 2016 monitoring event. TPH-d has never exceeded the SSRBL. Evaluation of the chromatographic profiles indicates fuel biodegradation by-products. TPH-o was detected frequently, and TPH-o exceeded its screening criteria (500 µg/L) during monitoring events in 2005. TPH-g, benzene, and toluene were detected occasionally at concentrations below the screening criteria during monitoring events between 2005 and 2017. Naphthalene (0.037–5.98 µg/L), 1-methylnaphthalene (0.0068 J–9.44 µg/L), and 2-methylnaphthalene (0.0058 J–3.07 µg/L) were detected below the respective screening criteria (17, 10, and 10 µg/L) periodically before October 2016 but have not been detected since. Evaluation of historical quality control data indicates that some pre-October 2016 results were affected by matrix interferences, and that some results may be attributable to field or laboratory artifacts due to detections reported in the laboratory and field blanks.
- *RHMW02*, an in-tunnel monitoring well located next to Tank 6, was installed in 2005 (DON 2007). TPH-g is regularly detected at RHMW02 and exceeded the screening criterion (300 µg/L) during 2012 and 2013 monitoring events. TPH-d is also regularly detected; concentrations exceeded the screening criterion in all monitoring events and exceeded the SSRBL (4,500 µg/L) in 2008, 2014, 2015, and 2016. TPH-o was detected below the 500-µg/L screening criterion in most monitoring events from April 2015 to April 2017, but has not been detected since. 1-Methylnaphthalene, 2-methylnaphthalene, and naphthalene regularly exceeded their screening criteria (10, 10, and 17 µg/L) during monitoring events between 2005 and 2017. The TPH chromatographic signature and the results of the TPH-d with silica gel treatment analysis indicate that the reported TPH-d results are a mixture consistent with jet-fuel-soluble components and biodegradation by-products. Benzene, ethylbenzene, toluene, and total xylenes were also detected in most events between 2005 and 2017 at trace concentrations below the screening criteria.
- *RHMW03*, an in-tunnel monitoring well located next to Tank 14, was installed in 2005 (DON 2007). TPH-d and TPH-o have been regularly detected at concentrations below the respective screening criteria (400 and 500 µg/L). TPH-g, toluene, and PAHs were

occasionally detected at trace concentrations below screening criteria between 2005 and 2017. Benzene, ethylbenzene, and xylenes have never been detected.

- *RHMW04*, an outside-tunnel monitoring well located northeast of the tank farm, was installed in 2005 as a background monitoring location (DON 2007). TPH-d, TPH-o, benzene, toluene, and PAHs were occasionally detected below screening criteria, but none have been detected since July 2016.
- *RHMW05*, an inside-tunnel monitoring well located southwest of the tank farm and southeast of sampling point RHMW2254-01, was installed in 2009. Benzene, ethylbenzene, and xylenes have never been detected. TPH-g, TPH-o, toluene, 1-methylnaphthalene, 2-methylnaphthalene, and naphthalene have been detected occasionally below the respective screening criteria (300, 500, 40, 10, 10, and 17 µg/L). TPH-d was detected occasionally between 2005 and 2016, exceeded the screening criterion of 400 µg/L during monitoring events in 2009 and 2010, but had detections below screening criteria until January 2016. No COPCs have been detected after January 2016.
- *RHMW06 & RHMW07*, outside-tunnel monitoring wells located north of the tank farm, were installed in 2014 in response to the January 2014 release (DON 2015a). TPH-g, benzene, ethylbenzene, and xylenes have never been detected. TPH-d, TPH-o, toluene, and PAHs were occasionally detected below screening criteria. No COPCs have been detected after March 2017.
- *RHMW08 & RHMW09*, outside-tunnel monitoring wells located west of Tank 1, were installed in 2016 as part of the AOC Statement of Work Sections 6 and 7 investigation (DON 2017a). No COPCs have been detected at RHMW09. At RHMW08, no COPCs have been detected above the screening criteria. Only TPH-d and TPH-o have been detected at RHMW08, both at estimated values below the respective screening criteria (400 and 500 µg/L). Due the very low concentrations, it is not possible to assess if the TPH chromatographic signatures are related to fuels or biogenic sources.
- *RHMW10*, an outside-tunnel monitoring well located south of Tank 14, was installed in April 2017 as part of the AOC Statement of Work Sections 6 and 7 investigation (DON 2017a). TPH-d and TPH-o were detected at concentrations below their respective screening criteria (400 and 500 µg/L) during the May 2017 and October 2017 events; evaluation of the groundwater and the drilling source water TPH results from that event indicates potential contamination from drilling activities. No COPCs were detected in the subsequent monitoring events.
- *RHMW11*, a multi-level outside-tunnel well located north of the tank farm at the Hālawa Correctional Facility, was installed in November 2017 as part of the AOC Statement of Work Sections 6 and 7 investigation (DON 2017a). RHMW11 was first sampled (at five monitoring zones RHMW11-01 through RHMW11-05) during the First Quarter 2018 groundwater monitoring event. No COPCs were detected.
- *HDMW2253-03* (Hālawa Deep Monitor Well 2253-03), an outside-tunnel well located north of the tank farm at the Hālawa Correctional Facility, was installed in 2000 by DLNR. COPCs have been detected below screening criteria with the exception of TPH-d (600 µg/L) exceeding the screening criterion (400 µg/L) during the January 2013 quarterly monitoring event. Most TPH-d results were estimated values and were often flagged as not matching a fuel pattern. All other COPCs either have not been detected or have been detected below their respective screening criteria and/or flagged because of laboratory and/or field blank contamination. No COPCs have been detected since July 2016. HDMW2253-03 was not

sampled during quarterly and monthly monitoring events from April to July 2017 due to experimental testing conducted by CWRM and UH.

- *OWDFMW01*, located at the former OWDF west of Navy Supply Well 2254-01 (Red Hill Shaft), was installed in 1998 (DON 2000). TPH-d exceeded the screening criterion during quarterly monitoring events in 2010 and between 2012 and 2015. TPH-o was detected at concentrations below the screening criterion during monitoring events in 2015–2017. Evaluation of the analytical chromatograms indicates that the reported TPH-d and TPH-o detections are from non-petroleum sources, based on the chromatograms showing a non-petroleum chemical signature. All other COPCs have been detected below their respective screening criteria.

Appendix B.7 presents a detailed evaluation of jet fuel chemistry, site dissolved-phase hydrocarbon composition and attenuation, COPC spatial and temporal trends, and analytical data usability. These multiple LOEs were evaluated to assess the presence of LNAPL at the Facility at or near the groundwater table, as well as to assess the impact of the 2014 JP-8 release to the site groundwater. It was concluded that impacts to groundwater from the jet fuel release seem to be localized in the area of RHMW02, and that natural attenuation is occurring at the site based on groundwater COPC and NAP concentrations at RHMW02 and to a lesser extent at RHMW01 and RHMW03. The available data suggest the presence of weathered LNAPL (i.e., pre-2005 release) in the immediate vicinity of RHMW02 or within the saturated zone upgradient of this well. The groundwater monitoring data indicate it is likely that the 2014 Tank 5 release did not impact groundwater and impacts to groundwater are more likely attributable to historical releases.

As part of the analytical data usability assessment, Appendix B.7 Attachment B.7.2 and B.7.3 present an evaluation of the COPC detections at the Navy Supply Well groundwater monitoring location (Red Hill Shaft; RHMW2254-01) and the currently identified background monitoring well (RHMW04). The evaluations indicate that there is currently no evidence that the 2014 JP-8 release impacts, if any, reached the Navy Supply Well and the background well and any impacts to groundwater are more likely attributable to historical leaks. Additionally, Appendix B.7 Attachment B.7.4 presents an evaluation of low-level detections of naphthalene that seem to be in many wells (except for RHMW02 and RHMW01) around the same time. Evaluation of the data indicates that low-level detections (i.e., less than 0.1 µg/L) of naphthalene in outlying wells are not consistent with LNAPL transport through either the vadose or saturated zones. Due to the uncertainties in the data, these low-level detections are not considered as evidence of impacts from the Facility without additional supporting LOEs.

7.3 NATURAL ATTENUATION

This subsection summarizes natural attenuation studies being conducted at Red Hill. These data will be further described as part of the Sections 6 and 7 technical support document for the AOC Statement of Work Section 3 TUA. As additional data become available, the natural attenuation sections will be updated to reflect current knowledge.

The *Attenuation Evaluation Plan* (DON 2017g) describes the technical approach and additional data used to further evaluate natural attenuation processes for petroleum source depletion. All these additional data are being evaluated and integrated to refine the CSM of natural attenuation and source depletion processes. Two different types of attenuation were identified in the *Attenuation Evaluation Plan*: NSZD (Section 7.3.1) and MNA (Section 7.3.2). NSZD guidance generally addresses LNAPL source zones, while MNA guidance (e.g., Wiedemeier et al. 1999a,b) primarily addresses attenuation of dissolved plumes emanating from a source zone.

7.3.1 Natural Source-Zone Depletion

In 2009, the ITRC published a document describing the NSZD approach, which is a straightforward, quantitative mass balance method to estimate the rates at which quantities of liquid fuels (LNAPLs) are being naturally lost from a petroleum source zone due to the combined effects of sorption, volatilization, dissolution, and aerobic and anaerobic biodegradation (ITRC 2009a).

NSZD is the active process whereby LNAPL is degraded in the subsurface by biodegradation and other naturally occurring processes. For this CSM, LNAPL consists of petroleum hydrocarbons in the form of various fuels. NSZD rates have been measured at many LNAPL sites and can be quantified by measuring the magnitude and distribution of subsurface temperatures, and then calculating the net heat flux being generated by biodegradation processes.

In NSZD, fuel hydrocarbons (LNAPLs) are attenuated by natural processes, primarily aerobic and anaerobic biodegradation. NSZD processes are active both in the unsaturated and saturated zone. These biodegradation processes are not limited to highly soluble hydrocarbon compounds in the LNAPL but can also remove relatively insoluble compounds in the LNAPL. NSZD rates can be measured using several different methods, and the resulting rates can be in the range of a few hundred to a few thousand gallons of LNAPL biodegraded per acre per year.

NSZD is now emerging as an important remediation approach for petroleum hydrocarbon sites. As described in Garg et al. (2017), a variety of methods have been used to obtain NSZD rates, as summarized below.

7.3.1.1 Migration of LNAPL and Dissolution

Geologic and water saturation characteristics in the rock surrounding the tanks will cause LNAPL to spread as it moves through the rock. As LNAPL moves through the larger pore spaces, some of it will be trapped in poorly connected fractures and blocked by surface tension and capillary forces of moisture, especially water held in the smaller pores. Hydrocarbon constituents dissolve from a LNAPL source and are transported in solution by groundwater, as described by the ITRC (2009a).

Even though it is possible to recover LNAPL from a source zone, LNAPL below the point of residual saturation will remain, and dissolution by water contact will continue to the solubility limits of compounds in the LNAPL (ITRC 2009a). Effective solubility represents the maximum equilibrium concentration of a constituent from a multicomponent LNAPL mixture in groundwater at a specific temperature and pressure (EPA 1995). Effective solubility of an individual LNAPL constituent is a product of its mole fraction in the LNAPL and solubility of the constituents in its pure non-aqueous phase (ITRC 2009a). Solubility of jet fuel is a focus of Appendix B.7 Forensics and Data Evaluation - Groundwater (summarized in Section 7.1.3.1).

7.3.1.2 Volatilization and Diffusion in the Unsaturated Zone

Petroleum constituents in LNAPL also volatilize and biodegrade by microbial and/or enzymatic activity (ITRC 2009a). Volatile constituents move by diffusion from areas of higher concentration to areas of lower concentration. Hydrocarbon vapors preferentially migrate from the LNAPL source toward the ground surface, but are typically biodegraded aerobically in the presence of oxygen before they reach the surface. Diffusion is usually the dominant mechanism for vapor-phase transport in unsaturated porous media under most conditions (Rockhold, Yarwood, and Selker 2004) and is a function of a constituent's air diffusion coefficient and the air-filled porosity of the soil. Diffusion and advective vapor migration are faster in soils and rock with more air-filled effective porosity (ITRC 2009a). Sites with more air-filled porosity will have higher diffusion rates, more

oxygen influx, and more aerobic biodegradation compared to anaerobic biodegradation. This will be addressed in more detail in the forthcoming Sections 6 and 7 interim environmental analysis.

7.3.1.3 New Conceptual Model for Biodegradation at LNAPL Sites

A recent report in the journal *Groundwater Monitoring & Remediation* reviewed extensive research on natural attenuation and petroleum source depletion processes during the last 35 years and presented the key findings related to natural attenuation of petroleum (Garg et al. 2017). That report includes results of long-term research studies of petroleum degradation that were initiated in 1983 by the USGS and subsequent studies of natural attenuation processes by Arizona State University and Colorado State University. Those in-depth research studies were integrated to develop a comprehensive mass-balance and reactive-transport model (Ng et al. 2014, 2015). The paper by Garg et al. (2017) indicates that methanogenic processes are likely responsible for most of the NSZD at sand/silt/clay sites impacted by LNAPL. This is because the sand/silt/clay impedes rapid diffusion of oxygen and creates anaerobic zones where methanogenic processes are active.

Methanogenesis is a complicated, multiple-step, syntrophic process that involves two groups of organisms that cooperatively degrade the complex petroleum compounds: one group degrades the byproducts of another group and ensures that the overall reaction is thermodynamically favorable. In anaerobic LNAPL zones, fermenters biodegrade hydrocarbons and form dissolved hydrogen and/or acetate, and then methanogens use the hydrogen and/or acetate to form methane (Garg et al. 2017). The presence of methane in groundwater or unsaturated LNAPL source zones indicates that NSZD processes are active.

As reported by Garg et al. (2017), methanogenic biodegradation of LNAPL occurs at a much higher rate than was generally thought a few years ago, and methanogenesis is increasingly accepted as a dominant process for NSZD. Most of the NSZD occurs via direct outgassing within the pore space adjacent to the entrapped oil, where low-solubility hydrocarbons are biodegraded without entering the bulk dissolved phase in groundwater (Ng et al. 2014). In the saturated zone, direct outgassing from the LNAPL may be accompanied by ebullition, which brings carbon dioxide and methane into the vadose zone. As these gases travel toward the surface, naturally occurring methane-oxidizing bacteria convert the methane to carbon dioxide.

While methanogenesis is likely the dominant process for degradation of petroleum LNAPL in the saturated and smear zones (Garg et al. 2017), it may not be as important in the unsaturated zone at the Facility because the unsaturated zone underlying the tank farm area is deep with some extremely high-permeability media that allow oxygen to enter and serve as an electron acceptor for aerobic biodegradation. The NSZD measurements described below have been performed at the Facility, and will help determine if biodegradation is occurring, determine where aerobic vs. anaerobic processes dominate, and provide NSZD rate information for the Facility.

7.3.1.4 Measuring NSZD at the Facility

Biodegradation of petroleum in the unsaturated zone generates carbon dioxide, potentially methane, and heat and will deplete oxygen. To further evaluate this, studies of natural attenuation and source depletion processes were conducted that included (1) a soil vapor study, (2) a carbon trap study, and (3) a thermal NSZD investigation. These studies, presented in Appendix B.3, B.2, and B.1, respectively, are summarized below.

Soil Vapor Study. A soil vapor study was conducted that involved collection of soil vapor samples from the shallow, middle, and deep soil vapor probes that currently exist underneath the tanks; from vapor pins installed in the upper tunnel; and from sampling points on the surface of Red Hill. The

samples were analyzed for concentrations of oxygen, carbon dioxide, volatile organic compounds (VOCs), and methane. The soil vapor study was designed to help address the following study questions:

1. Is there evidence of recent or historical fuel releases at one or more of the tanks?
2. Is LNAPL present below the tanks?
3. Is NSZD occurring?
4. Can vapor monitoring help quantify the magnitude of NSZD?
5. Can vapor monitoring help detect new LNAPL fuel releases?
6. Are vadose zone petroleum vapors a significant source of impacts in the tunnels?

Field monitoring and laboratory analysis of soil vapors was conducted in October/November 2017. Investigation results support evidence of releases and NSZD, an evaluation of the utility of SVM to track releases, the NSZD of LNAPL fuel as expressed in the vapor emissions, and insights as to the source of petroleum VOCs in the tunnels. Soil vapor study results are summarized in Table 7-1.

Table 7-1: Findings and Conclusions of Soil Vapor Investigation

Question	Answer	Discussion
Evidence of Releases and NSZD		
1. Is there evidence of recent or historical fuel releases at one or more of the tanks?	YES. The soil vapor results suggest a historical release of LNAPL fuel at Tank 5 and, at the other tanks, low-level vapor-phase releases associated with ongoing Facility operations.	As shown on Figure 7-2, the soil vapor monitoring showed a range of total VOC concentrations and differences in alkane composition for the below-tank soil vapor wells. Together, these data indicate the presence of weathered LNAPL fuel below Tank 5. For the other tanks, the target analyte results along with visual evaluation of the FID chromatograms indicate low levels of unweathered or lightly weathered petroleum vapors likely associated with ongoing Facility operations combined with less volatile compounds likely associated with highly weathered historical releases. The low levels of unweathered petroleum vapors are consistent with minor vapor-phase emissions typical of any fuel storage operation.
2. Is LNAPL present below the tanks?	YES. The soil vapor results suggest the presence of weathered LNAPL fuel below Tank 5.	Angle borings completed below some of the other tanks provided visual evidence of LNAPL at the time the borings were installed (1998–2002) (DON 1999, 2002). For these other tanks, the presence of LNAPL is not reflected in the quantitative analysis of soil vapor samples collected in October/November 2017; however, many of the FID chromatograms show an unresolved hump of less-volatile compounds potentially consistent with the presence of highly weathered LNAPL (see Appendix B.3 Attachment B.3.2).
3. Is NSZD occurring?	YES. As discussed above, the soil vapor results suggest that significant biological weathering of the LNAPL below Tank 5 has occurred since the 2014 release. This is consistent with other LOEs supporting biological NSZD.	The conclusion of biological weathering of LNAPL releases is supported by the following observations: • The petroleum vapor fingerprint from below Tank 5 is consistent with weathered LNAPL associated with the 2014 release. • The vapor testing below other tanks indicates that the LNAPL visually observed in borings completed below these tanks in 1998–2002 (DON 1999, 2002) is depleted in VOCs. • Field monitoring and laboratory analysis indicate high oxygen concentrations (13.7–20.6%) in all the below-tank soil vapor wells, supporting aerobic biodegradation. • Thermal monitoring indicates ongoing biological NSZD (see Appendix B.1).

Question	Answer	Discussion
Utility of Soil Vapor Monitoring Data		
4. Can vapor monitoring help detect new LNAPL fuel releases?	YES. Monthly PID screening of the soil vapor wells with laboratory confirmation for those with elevated PID readings is likely to be a reliable method for detecting any new LNAPL releases of jet fuel.	As shown on Figure 7-3, monthly PID monitoring clearly reflects the LNAPL fuel release from Tank 5 that occurred in January 2014. If future PID monitoring suggests a new release, laboratory analysis by TO-15 PIANO can be used to confirm that the observed PID spike is associated with a new release. Following the Tank 5 release, elevated PID readings (>25,000 ppbv) were observed in nine soil vapor wells (below Tank 5 and three adjacent tanks), indicating that the existing soil vapor well network provides a robust system for release detection. Evaluation of the available PID monitoring data (2008–present) (DON 2008a) indicates that the 2014 Tank 5 release was the only significant release event during that monitoring period.
5. Can vapor monitoring help quantify the magnitude of NSZD?	YES. Monthly PID monitoring appears to track decreases in petroleum vapor concentration over time associated with weathering of LNAPL releases. The TO-15 PIANO analysis provides detailed information on the petroleum VOC vapor composition that can be used to evaluate the degree of biological weathering.	As shown on Figure 7-3, the monthly PID monitoring shows a decrease in PID readings at Tank 5 from 2014 to 2017 following the 2014 release event. The TO-15 PIANO analysis in November 2017 indicated a depletion of n-alkanes resulting in a relative enrichment of cycloalkanes confirming the occurrence of biological weathering (Figure 7-3, right panel). These data indicate that monthly PID monitoring combined with periodic laboratory analyses can serve to document both the magnitude and mechanism of NSZD. Results presented in Appendix B.3 Section 4 show that monthly PID monitoring conducted since 2008 has also documented the occurrence of NSZD below Tanks 3, 6, 7, 8, and 9.
Risk Assessment		
6. Are vadose zone petroleum vapors a significant source of impacts in the tunnels?	NO. Facility operations are the primary source of petroleum vapors in the tunnels. Any soil vapors entering the tunnel are highly diluted by the tunnel ventilation system.	The magnitude and sources of petroleum vapors in the tunnels were evaluated using PID readings and qualitative observations. These data suggest that: • Petroleum vapor concentrations in the tunnels are higher than in outdoor air. • Although vapor flow is from the vadose zone into the tunnel, any soil vapors entering the tunnels are highly diluted by ambient air from the tunnel ventilation system. • The primary source of the petroleum vapors in the tunnels is active operations at the Facility.

FID flame ionization detector
PIANO paraffin, isoparaffin, aromatic, naphthene, and olefin

For locations where the monitoring well screen extends above and below the water table, concentrations of VOCs and NAPs (i.e., oxygen, carbon dioxide, and methane) can be used to monitor biodegradation of petroleum at the water table. Thus, to further evaluate biodegradation activity at and near the water table, vapor samples were collected from selected wells. The selected locations included monitoring wells in the source area where the screen straddles the groundwater table. At each monitoring well, a vapor sample was collected at a point directly above the groundwater level in the well and analyzed for the same gases analyzed from the SVM probes, described above. These vapor concentration data are being evaluated in conjunction with the vapor data from the SVM points and the other groundwater COPC and NAP analysis data.

Carbon Trap Study. LNAPL biodegradation generates carbon dioxide, which was measured using a chamber-based sampling device or carbon traps at the surface, and by analyzing the vertical concentration gradient and applying diffusion calculations.

The carbon dioxide efflux method (or "carbon trap" method) is one of a variety of methods (as described in Garg et al. 2017) that have been used to obtain NSZD rates. This method measures the amount of carbon dioxide being generated through the biodegradation of LNAPL. The carbon

dioxide is captured using two carbon dioxide sorbent elements composed of soda lime (consisting primarily of calcium hydroxides), which are contained in a canister, over LNAPL zones (McCoy et al. 2014). The carbon dioxide generated by LNAPL biodegradation is transported to the surface by diffusion, and in some cases advection, and is trapped in one sorbent element. The other sorbent element prevents atmospheric carbon dioxide from being captured by the first sorbent element. Traps are typically deployed in receivers in the field for 14 days and then sent to the laboratory. The carbon-14 fraction (^{14}C correction) is also measured in the lab so that "modern carbon" (e.g., carbon dioxide generated from biodegradation of recent plant material) can be separated from "ancient carbon" (carbon dioxide associated with the biodegradation of fossil fuel). The efflux rate of ancient carbon is used to calculate a NSZD rate in units of gallons per acre per year (gal/acre/yr). Due to the unique construction of the Facility, conventional carbon traps were used to measure carbon dioxide flux at the ground surface, and modified carbon cartridges were used to measure carbon dioxide flux from the basalt into the tunnels.

*NSZD Rate Based on Tunnel Carbon Dioxide Flux***.** The ventilation system in the upper and lower access tunnels creates a negative pressure gradient within the tank access tunnels (i.e., a pressure gradient from the basalt into the tunnel), so that any advective gas flow is from the unsaturated zone into the tunnels (see Appendix B.3). As a result, the tunnels act like a soil vapor extraction (SVE) system and can capture ancient (i.e., petrogenic) carbon dioxide generated through biological NSZD occurring in the unsaturated zone.

Carbon dioxide concentrations in the tunnels were measured through the collection of 24-hour air samples pumped through carbon trap cartridges. The concentration of ancient carbon in each sample was determined using two methods: either (1) assuming a standard fraction of modern carbon in contemporary living material (Hua, Barbetti, and Rakowski 2013) or (2) using a site-specific value. This ancient carbon was attributed to petroleum NSZD. The flux of ancient carbon through the tunnel was calculated by multiplying the excess ancient carbon concentration by the tunnel air flow. Tunnel air flow was estimated using either (1) the design air flow rate in the tunnels or (2) a modified flow rate accounting for ventilation system maintenance (based on communications with the Navy: December 5, 2017 email message from John Floyd to Curtis C. Stanley, GSI Environmental, "RE: 4671 Tunnel Ventilation Questions for Navy"). Based on this range of calculation inputs, the NSZD rate attributable to ancient carbon entering the tunnels was calculated as between 3,400 and 6,400 gallons per year (gal/yr).

NSZD Rate Based on Ground Surface Carbon Dioxide Flux. Carbon traps were also installed on the top and sides of the tank farm (transverse to the tank farm) either near known impact areas or on clinker zone outcrops. All ground surface carbon traps showed low or zero NSZD based on the ancient carbon captured, indicating that carbon dioxide flux to the ground surface is low and variable. The NSZD rates estimated using individual carbon traps ranged from zero gal/acre/yr to 84 gal/acre/yr. Based on the trap data and the total ground surface area for carbon dioxide efflux, the NSZD rate attributable to ground surface carbon dioxide flux from the top and sides of the tank farm is 1,000 gal/yr.

Conclusions. The majority of the NSZD is from the tunnel acting like a partial SVE system, pulling carbon dioxide from the basalt into the tunnels (Figure 7-4). Thicker arrows on Figure 7-4 indicate greater flux; location of tanks, traps, and biodegradation zones are approximate. The two NSZD rates (flux to the tunnels and flux to the ground surface) are additive, so the total NSZD rate at the tank farm is between 4,400 and 7,400 gal/yr.

Furthermore, if less than 0.5% of the air flow through the tunnel originates from the vadose zone (rather than the tunnel entrances), then the resulting ventilation of the vadose zone would be sufficient to provide 100% of the oxygen needed to support the observed NSZD while maintaining vadose zone oxygen concentrations above 19%. Thus, only a small amount of leakage through the tunnel walls is required to provide sufficient air flow through the unsaturated zone to sustain aerobic biodegradation.

Thermal NSZD Investigation. A thermal NSZD investigation was conducted using two methods in the field to measure vertical temperature profiles in wells in the Facility, with both methods producing similar data. These data were then used to determine the general vertical location of LNAPL at each location and the corresponding NSZD rates for that LNAPL.

Vertical temperature profiles were obtained from three existing monitoring wells (RHMW01, RHMW02, and RHMW03) and one background well (RHMW05). These profiles were then used to quantify NSZD rates at the tank farm.

Two methods were employed to obtain temperature measurements: Well Air Temperatures Method and Wall Temperatures Method. In the Well Air Temperatures Method, the thermocouple for temperature measurement was fed through a hole in a well plug; a weight was attached to a line attached to the end of the thermocouple; and the assembly was fed down the well. In the Wall Temperatures Method, the thermocouple was attached to a pipe test ball plug, which was fed down the well and inflated, thus pressing the thermocouple against the inside wall of the monitoring well. Both methods provided similar thermal profiles, so the NSZD rates were calculated for both methods and averaged.

By performing two different calculations, a range in the NSZD rates was obtained:

- The Net Temperatures Method used the net (background-corrected) temperature profiles to remove seasonal and tunnel heating effects to calculate heat fluxes going upward into the atmosphere and downward into the groundwater, and then these heat fluxes were used to calculate a total NSZD rate. This is the most common method used to calculate NSZD rates using temperature.
- The Thermal Profiles Method is an alternate method where the raw (not background-corrected) temperatures were used with a thermodynamic model (the Hillel [1982] model) to correct for seasonal effects in the temperature data.

NSZD Results. All the NSZD rates for both calculation methods were relatively similar, which increases the confidence in the accuracy of these results. Measured NSZD rates using the Net Temperatures Method for calculation and averaged results from the Well Air Temperatures and Wall Temperatures Methods are shown below. These are considered the most accurate calculations for NSZD rates of all the methods.

- RHMW01: 140 gal/acre/yr of NSZD
- RHMW02: 640 gal/acre/yr of NSZD
- RHMW03: 1,500 gal/acre/yr of NSZD

Typical NSZD rates measured at other hydrocarbon release sites range from hundreds to thousands of gallons per acre per year (Garg et al. 2017), so these values are consistent with other hydrocarbon releases that are being biodegraded by NSZD biodegradation processes.

The distribution matches the site conceptual model where known past releases have been associated with the tanks near RHMW02 and RHMW03 (DON 1999, 2002; see Section 4.1). RHMW01 is located just southwest of the tank farm. RHMW05 showed virtually no NSZD, which was expected since it was the background well and was furthest from the tank farm.

In addition to measuring NSZD rates from the temperature profiles using the Net Temperatures and Thermal Profiles Methods of calculation, a supporting calculation was done to estimate the NSZD rate indicated by the increase in temperature seen in groundwater underlying the tank farm (the Groundwater Temperatures Method). This measurement was of the same magnitude as the vertical heat flux moving into groundwater from the vertical temperature profiles, again increasing the confidence in the NSZD calculation methods.

Assuming the three thermal NSZD measurements are representative samples of NSZD within the tank farm, an average NSZD rate for the entire tank farm was calculated in gallons per year (gal/yr). Taking an average of all the NSZD rates (759 gal/acre/yr) and multiplying this by the area encompassed tby the tank farm (13.1 acres), the total NSZD rate comes to 9,935 gal/year or about 10,000 gal/acre/yr. To establish a range of values for the total NSZD at the tank farm, the standard deviation of the total NSZD rate of all three wells using the Net Temperatures Method was calculated. This value is 7,334 gal/yr. Therefore, the average total NSZD rate at the tank farm is between 2,600 and 17,300 gal/yr. Total NSZD rates in units of gal/yr are shown in Table 7-2. The Bottom NSZD Rate is the rate going downward through the unsaturated zone that results in a change in groundwater temperature. The Top NSZD Rate is the rate at the top of the unsaturated zone at a specific well location.

Table 7-2: Summary of Total NSZD Rates from the Tank Farm in Units of Gallons per Year

Well	Net Temperatures Method	Thermal Profiles Method	Groundwater Temperatures Method
Bottom NSZD Rate (gal/yr)			
RHMW01	1,633	2,183	—
RHMW02	2,056	2,494	—
RHMW03	2,452	3,869	—
Average	2,047	2,849	1,284
Top NSZD Rate (gal/yr)			
RHMW01	217	730	—
RHMW02	6,296	6,804	—
RHMW03	17,151	17,664	—
Average	7,888	8,401	—
Total NSZD Rate (gal/yr)			
RHMW01	1,850	2,913	—
RHMW02	8,352	9,303	—
RHMW03	19,603	21,533	—
Average	**9,935**	**11,250**	—

— no data

Although there is some uncertainty regarding how NSZD rates change over time at an individual site, there is a general conceptual model that NSZD rates may be relatively constant provided there is a continuing source term. Even as biodegradation acts first on easily biodegradable compounds and then progresses to less-biodegradable compounds, the overall NSZD rate (i.e., mass of petroleum

degraded per year) may remain relatively constant (e.g., Garg et al. 2017). For example, for the purpose of evaluating past and future attenuation, USGS researchers at the Bemidji National Crude Oil Release site assumed constant NSZD rates over the lifetime of the crude oil release that occurred at that site in 1979 (Ng et al. 2014, 2015).

Vertical LNAPL Distribution Inferred from Temperature Profiles. In addition to providing NSZD rates, the temperature data also indicate the general location of biodegradation reactions occurring in the subsurface. Because high oxygen levels were observed at all depths within the unsaturated zone (see Appendix B.3), the heat-generating degradation reactions were assumed to be occurring with the LNAPL intervals. Thus, the LNAPL intervals in each well were determined by analyzing the temperature gradients in the net (background-corrected) temperature profiles (profiles of the difference between the raw temperature recorded at each depth relative to the upper and lower access tunnels minus the raw temperature calculated at the same depth for the background well, RHMW05). From these data, the general location of LNAPL biodegradation reactions in these wells was in the intervals shown in Table 7-3 and on Figure 7-5. On Figure 7-5, each scale shows depth below the tunnel floor, with the elevation scale (ft msl) on the far left. As shown on this figure, the interval of the LNAPL does not correspond directly with the location of the clinker zones at these locations. This indicates that other geologic media, such as thin pāhoehoe layers, are able to transmit and hold LNAPL.

Table 7-3: Vertical Distribution of LNAPL Intervals Indicated by Net (Background-Corrected) Temperature Profiles from Three Facility Monitoring Wells

Monitoring Well	Top of Casing Elevation (ft msl)	Approximate Top of LNAPL (ft btoc)	Approximate Bottom of LNAPL (ft btoc)	Approximate Top of LNAPL (ft msl)	Approximate Bottom of LNAPL (ft msl)
RHMW01	102.0	20	30	82	72
RHMW02	104.6	0	30	105	75
RHMW03	121.9	10	45	111	76

Note: All three wells are installed in the lower access tunnel of the Facility.
btoc below top of casing

At many NSZD sites, the intervals of the LNAPL and the intervals of the heat generation are not collocated because methanogenic processes degrade the LNAPL near and in the water table, and then methane is produced. This methane then diffuses toward the surface, but is oxidized by naturally occurring bacteria in a reaction zone between the top of the LNAPL and the surface. This methane oxidization zone is where the heat is generated in this type of system.

Within the tank farm area, however, the unsaturated zone is characterized by high oxygen concentrations and no detectable methane both in well headspace samples collected immediately above the water table and soil vapor well samples collected from 10 to 30 ft below the fuel tanks (see Appendix B.3). These results indicate that heat generation within the unsaturated zone at the tank farm area is attributable to direct aerobic degradation of petroleum constituents within LNAPL-impacted intervals.

The location of the LNAPL inferred by the net temperature measurements does correlate to historical data regarding LNAPL releases. At RHMW03, angle borings drilled in 1998 at Tank 16, located near RHMW03, detected LNAPL staining/discoloration down to 40 ft msl (approximately 22 ft above the water table) (DON 1999). This compares to the net temperature signal that indicated the presence of LNAPL between approximately 110 and 75 ft msl (Figure 7-5).

The net temperature signal at RHMW02, located from 0 to 30 ft below the tunnel, is consistent with a release of LNAPL from Tank 5 in 2014 that did not make it down to the water table.

7.3.2 Monitored Natural Attenuation

Several processes are known to cause a reduction in the concentration and/or mass of a contaminant dissolved in groundwater via MNA. Processes that result in a change in a contaminant's aqueous-phase concentration, but not of the total contaminant mass in groundwater, are termed nondestructive. Processes that result in the reduction of contaminant mass are referred to as destructive. Nondestructive processes include advection, hydrodynamic dispersion (mechanical dispersion and diffusion), sorption, dilution, and volatilization. Destructive processes include aerobic and anaerobic biodegradation, and in some cases, abiotic degradation. A key concept is that MNA methods focus on the attenuation of dissolved groundwater plumes or vapor plumes, while NSZD methods are focused on measuring attenuation in source zones.

7.3.2.1 KEY MNA PROCESSES

Hydrodynamic dispersion is the process whereby a groundwater plume mixes with clean water as the plume migrates through a porous medium. This mixing occurs as a result of two processes: mechanical dispersion due to the change in groundwater flow paths as groundwater migrates through a porous medium, and molecular diffusion of contaminants from high-concentration to low-concentration zones. There is currently a re-evaluation of the importance of both the mechanical dispersion vs. diffusion process, but in general, dispersion is a second-order process (i.e., typically does not serve as the primary natural attenuation process).

Sorption is a non-destructive process in which organic compounds are sorbed to the matrix of the water-bearing unit and is represented by a retardation factor (Wiedemeier, Rifai, et al. 1999). Sorption is controlled by both the characteristics of the chemicals (chemicals that are more hydrophobic will exhibit more sorption) and the soil (soils with more organic material will be able to sorb more chemicals). The amount of sorption is described using a "retardation factor" that reflects two key factors: (1) the degree to which a particular constituent moves slower than groundwater seepage velocity, and (2) the ratio of total constituent mass per volume of aquifer matrix to the volume of dissolved constituents.

Back-diffusion occurs where porous, low-permeability geologic material is in long-term contact with LNAPL or dissolved plumes. First, dissolved contaminants enter porous, low-permeability materials like clays (or fine-grained material in weathered clinker) by the physical process of diffusion (movement of dissolved constituents from areas of high to low concentration). When matrix diffusion is active over several years, significant contaminant mass can be stored in low-permeability zones. Then, after source material (e.g., LNAPL) is removed by remediation and/or NSZD, back-diffusion from these fine-grained units can serve as long-term ongoing sources of dissolved constituents to groundwater.

In MNA, biodegradation is the process where naturally occurring bacteria biodegrade fuel constituents to end-products such as carbon dioxide. Bacteria typically will utilize an electron acceptor compound that is present in groundwater, soil, or the air and then produce carbon dioxide.

Common electron acceptors for MNA reactions in the unsaturated and saturated zones include oxygen for aerobic reactions and nitrate, sulfate, and/or ferric iron for anaerobic reactions. Another reaction is methanogenic, where one class of fermenting bacteria can ferment hydrocarbons to dissolved hydrogen and/or acetate, and then the hydrogen/acetate is utilized by methanogens to produce methane and carbon dioxide.

7.3.2.2 MICROBIAL INVESTIGATIONS

Two microbial studies of natural attenuation capacity at Red Hill due to biodegradation are ongoing:

- A microcosm study designed to estimate the bulk attenuation rate due to biodegradation for several constituents of concern under aerobic and anaerobic conditions. Microcosms were constructed with site groundwater from RMHW01 and RHMW02 and are being monitored over an extended period to assess degradation rates.
- A microbial parameter study to assess levels of several functional genes associated with aerobic and anaerobic degradation of BTEX, alkane, and/or PAH degradation and can be used as an indicator for biodegradation capacity of petroleum hydrocarbon degradation. The tests involve polymerase chain reaction (qPCR)-based analyses of site groundwater from RHMW01, RHMW02, RHMW03, and RHMW04. The results provide a snapshot of the microbial community present at the Facility, including those capable of petroleum hydrocarbon degradation. Data from a single sampling event (October 25, 2017) are available for evaluation.
- Additional tests that focus on additional microbial parameters (BioTrap samplers) are intended to be performed at a later date.

Collectively, the results of these tests help to establish if key organisms are present, active, and degrading hydrocarbons at rates that help to limit migration. These data serve not only as a LOE for attenuation but also as site-specific input values for subsequent fate and transport modeling. The preliminary data and analysis of these ongoing studies are presented in Appendix B.6 and summarized below.

Microcosm Results. Rate coefficients were calculated for individual constituents using available time-series concentration data and assuming that degradation fits a first-order relationship. Rapid biodegradation under aerobic conditions was observed in the microcosms from RHMW02; all constituents were degraded with half-lives of less than 1 week, and several less than 1 day. Aerobic biodegradation rates at this location are consistent with those reported by Kao et al. (2006) for benzene, toluene, and xylene and 1,2,4-trimethylbenzene (half-lives ranging from 0.8 to 6 days) and Landmeyer et al. (1998) for naphthalene (half-life of 0.8 day). The data indicate that strong degradation capacity can be stimulated at this location when oxygen is present. Slower biodegradation rates were observed in the aerobic microcosms from RHMW01, although all constituents exhibited a concentration decrease over the monitoring period. Complete degradation of all constituents was observed in microcosms from RHMW01 within 79 days. Current aerobic half-life estimates at RHMW01 for the constituents included in the test range from 8 days (m-, p-xylene) to 25 days (benzene).

Little or no biodegradation has been observed under anaerobic conditions in microcosms from either RHMW01 or RHMW02 over the first 5 months of monitoring. Concentrations for this set of microcosms were relatively unchanged and generally followed similar trends as those of the sterile controls. The lack of initial activity in anaerobic microcosms is not unexpected and likely reflects a commonly observed lag period as the microbial cultures acclimated to the initially aerobic reactor

conditions (due to the introduction of oxygen during field sampling). Reducing conditions have been established in these anaerobic microcosms, and these conditions may lead to more significant degradation of petroleum hydrocarbons in these microcosms during future monitoring events.

Microbial Parameters (QuantArray-Petro). Samples from all four wells contained measurable levels of several functional genes associated with aerobic and anaerobic degradation of BTEX, alkane, and/or PAHs based on the QuantArray-Petro analysis. This is a strong indicator for biodegradation capacity.

RHMW02 and RHMW04 had several aerobic biomarkers, including the highest levels of PM1, which is associated with BTEX and methyl tert-butyl ether (MTBE) degradation. RHMW04 is a background well outside the area of groundwater impacts and is screened in an aerobic portion of the groundwater-bearing unit, while RHMW02 is screened in a much more reducing portion of the groundwater-bearing unit based on low DO levels (historically below 1 mg/L) and elevated methane levels (4.5 mg/L during the October 2017 monitoring event). In addition, the microcosm study showed that the RHMW02 microbial community could be easily stimulated to degrade petroleum hydrocarbons aerobically when oxygen was added to the bottles. Relative to RHMW02 and RHMW04, wells RHMW01 and RHMW03 generally had lower levels of aerobic biomarkers and higher levels of anaerobic biomarkers, consistent with the existing groundwater sampling data showing dissolved petroleum constituents and low DO concentrations at these locations. However, based on data from historic monitoring events, well RHMW03 does not show geochemical indicators of intense anaerobic activity, with relatively little sulfate depletion and no methane production over the past 2 years.

Samples from all four wells had moderate to high levels of benzyl coenzyme, which is a biomarker of anaerobic BTEX degradation, while RHMW01 and RHMW02 had measurable levels of biomarkers associated with anaerobic PAH degradation (e.g., naphthalenes). RHMW01 and RHMW02 also had the highest levels of eubacteria, which can be used as a bulk indicator of microbial abundance. This is consistent with the diversity of aerobic and anaerobic biomarkers measured in samples from these wells. Collectively, these data provide significant evidence that biodegradation of petroleum hydrocarbons can occur at these locations.

Conclusions. The results of these microbial studies are largely consistent with concentration trends and geochemical conditions at the Facility. Specifically, petroleum hydrocarbon concentrations are relatively high at RHMW02 and then attenuate significantly moving away from this well. The molecular data suggest that a combination of anaerobic and aerobic processes is responsible for this attenuation, although the potential for rapid aerobic degradation (as observed in the microcosms) is restricted somewhat by the low availability of oxygen in the vicinity of RHMW02. Degradation rates are apparently slower at RHMW01 based on the available microcosm data, but the molecular data provide another LOE that biodegradation within the plume is contributing to the attenuation observed at RHMW01.

There is also significant biodegradation potential at RHMW03 and in the background well RHMW04 due to the presence of abundant DO and multiple biomarkers for aerobic and anaerobic degradation. While the concentrations of petroleum hydrocarbons are relatively low at RHMW03 and RHMW04 (where the hydrocarbons might be attributed to analytical issues and/or oils associated with drilling fluids), the data suggest that biodegradation would help attenuate any contaminants in the vicinity of these wells.

Preliminary study results for the four monitoring wells are summarized in Table 7-4.

Table 7-4: Summary of Microcosm and Microbial Study Preliminary Results by Monitoring Well

Monitoring Well	Range of Aerobic Biodegradation Rate Coefficients (1/day) (from Microcosm Study)	Range of Anaerobic Biodegradation Rate Coefficients (1/day) (from Microcosm Study)	Presence and Abundance of Biomarkers for Aerobic Biodegradation?	Presence and Abundance of Biomarkers for Anaerobic Biodegradation?
RHMW01	8 days to 25 days	Degradation not yet observed	Yes	Yes
RHMW02	< 1 day to 7 days	Degradation not yet observed	Yes	Yes
RHMW03	Not included in study	Not included in study	Yes	Yes
RHMW04	Not included in study	Not included in study	Yes	Yes

7.3.2.3 MNA MEASUREMENT METHODS

MNA protocols divide MNA measurement methods into three different LOEs described in the EPA's (1999) MNA Directive:

- *LOE 1 (primary data).* Demonstrate a loss of contaminant mass or reduction in concentration in groundwater.
- *LOE 2 (secondary data)* Show conditions are conducive to MNA success using geochemical data.
- *LOE 3.* Use special microcosm or field studies to demonstrate "proof of concept" of a particular attenuation process. The microcosm study and microbial parameters fit in this category and are described in Section 7.3.2.2 and Appendix B.6.

According to this directive, the first LOE is always used to demonstrate MNA, the second LOE is often used, and the third LOE is used less frequently. Since publication of the EPA directive in 1999, new technologies and approaches have blurred the lines on which MNA measurement methods fit under which LOEs.

LOE 1 Evaluations: Existing groundwater monitoring data at the Facility are being analyzed now to demonstrate LOE 1, loss of contaminants. Changes in COPC concentrations over time at individual monitoring locations are being used to evaluate plume duration. Changes in COPC concentrations between monitoring locations along the same flow pathway (i.e., concentration vs. distance [C vs. d] analysis) are being used to evaluate plume attenuation. Based on the current groundwater flow model, RHMW02 and RHMW01 are in the same flow path within the Red Hill Shaft capture zone. Concentrations vs. distance analyses are being applied to evaluate concentration changes from RHMW02 to RHMW01 and from RHMW02 to RHMW2254-01 (i.e., Red Hill Shaft).

LOE 2 Evaluations: Tables, graphs, and figures of the NAP data from the Facility are currently being prepared as part of LOE 2. MNA processes are being evaluated by measuring the consumption of oxygen, nitrate, and sulfate and the production of ferrous iron and methane in the area of the groundwater plume as part of LOE 2. The analysis involves a comparison of upgradient and cross-gradient geochemical conditions outside of the plume to geochemical conditions inside the plume.

LOE 3 Evaluations: Microcosm tests, both aerobic and anaerobic were conducted for LOE 3, as described in Section 7.3.2.2 and Appendix B.6. Additional testing of LOE 3 using biotraps (stable isotope probes), devices with radiolabeled site constituents that are inserted in monitoring wells, may also be conducted to evaluate if subsurface conditions are conducive for biodegradation.

Chemical fingerprinting of both groundwater and vapor samples has been performed to determine if and how much weathering has occurred in areas impacted by hydrocarbon vapors and dissolved constituents as well as provide forensic data to better understand LNAPL releases. These analyses are presented in Appendix B.7 and Appendix B.3.

7.3.2.4 EVALUATION USING NATURAL ATTENUATION PARAMETERS

Primary (#1) and secondary (#2) LOEs were evaluated to demonstrate whether natural attenuation processes are occurring at the Facility. The two evaluations, presented in Appendix B.4 and Appendix B.5, respectively, are summarized below.

Analysis of Primary MNA Data. Natural attenuation processes at the Facility were evaluated using primary LOEs (i.e., temporal and spatial contaminant concentrations) from the Facility groundwater monitoring network. Where data are available, first-order rate coefficients and associated half-lives were calculated for monitoring wells RHMW01 and RHMW02 at the Facility. COPCs include 1-methylnaphthalene, 2-methylnaphthalene, and naphthalene. These data serve as a LOE for COPC attenuation and will provide site-specific input values for ongoing fate and transport modeling at the Facility.

BTEX data were not analyzed in this study, given their low concentrations and/or limited datasets (i.e., benzene and toluene). TPH-d was included in the analysis; however, due to laboratory analytical issues associated with the TPH-d method such as variations in extraction efficiency and absence of silica gel clean-up (see Appendix B.7), the TPH-d results have high uncertainty.

Two types of first-order attenuation rate coefficients were calculated to evaluate LOE 1 MNA processes at the Facility:

- *Plume Duration (Concentration vs. Time [C vs. t] analysis):* Based on analysis of COPC concentrations over time, concentration trends (increasing, stable, or decreasing) and effects of attenuation processes on plume duration were evaluated.
- *Plume Attenuation (C vs. d analysis):* Based on changes in COPC concentrations between different monitoring locations, COPC attenuation within the groundwater flow system was evaluated.

*Plume Duration***:** *C vs. t Attenuation Rate Coefficient (k_{point}).* C vs. t first-order rate coefficients and half-lives were calculated at monitoring well RHMW01 (TPH-d only) and RHMW02. Full results are presented in Appendix B.4, and results for RHMW02 are summarized in Table 7-5.

Table 7-5: C vs. t Coefficients, Half-Lives, and First-Order Model Fit Parameters for the COPCs at RHMW02 (September 2005 to April 2018)

COPC	k (per yr)	$t_{1/2}$ (yr)	n	R^2	p-value
TPH-d	-0.04	16.1	63	0.0821	***0.023***
1-Methylnaphthalene	-0.05	14.6	63	0.0161	0.322
2-Methylnaphthalene	0.03	**	63	0.0032	0.658
Naphthalene	0.03	**	63	0.0085	0.472

** Half-lives are not reported for 2-methylnaphthalene and naphthalene because attenuation rates were positive.
Bold italics: p-value = less than 0.05 (reject null hypothesis H_o: slope = 0)
k first-order rate coefficient
n number of samples
R^2 coefficient of determination
$t_{1/2}$ half-life
yr year

Plume Attenuation: C vs. d. For monitoring wells RHMW02 and RHMW01, C vs. d first-order rate coefficients (k) and half-lives were calculated using the entire historical groundwater dataset (2005 to March 2018). The locations of these monitoring wells align with the expected direction of groundwater flow through the tank farm (west-southwesterly direction), and the current groundwater model indicates that they are on the same flow path. First-order attenuation rates were calculated for each monitoring event where a COPC was detected in both monitoring wells. The average attenuation rate and standard deviation are presented in Table 7-6. In addition, for each paired measurement, a biodegradation rate was calculated using the method of Buscheck and Alcantar (1995) method to separate the contributions of biodegradation and dispersion in the overall C vs. d attenuation rates. These results are also presented in Table 7-6.

Table 7-6: C vs. d Rate Attenuation Rates and Biodegradation Rates for COPCs Along RHMW02-RHMW01 Transect (includes detected COPCs at both wells only)

COPC	n	k (per day) *	$t_{1/2}$ (day)	λ (per day)	$t_{1/2}$ (day)
TPH-d	57	-0.05 ± 0.01	13.8	-0.05 ± 0.01	15.0
1-Methylnaphthalene	11	-0.13 ± 0.05	5.1	-0.11 ± 0.05	6.5
2-Methylnaphthalene	14	-0.12 ± 0.05	5.6	-0.10 ± 0.05	7.0
Naphthalene	26	-0.11 ± 0.04	6.2	-0.09 ± 0.04	7.6

* Attenuation rates are presented as mean ± standard deviation
λ biodegradation rate coefficient (per day)

A similar analysis was conducted using all paired measurements where a COPC was detected in either RHMW02 or RHMW01. For this analysis, the limit of detection (LOD) was used in place of non-detect results. This approach increased the number of paired measurements that could be used to calculate C vs. d attenuation rates and biodegradation rates. However, this approach resulted in little change (20%) in the average attenuation rate for each COPC (see Appendix B.4). For TPH-d, C vs. d attenuations rates were calculated using TPH-d results, TPH-d with silica gel cleanup, and total organic carbon (TOC) results. C vs. d attenuations rates were similar (0.04 per day to 0.05 per day) for all three analytical methods (see Appendix B.4).

Plume Attenuation: RHMW02 to Red Hill Shaft. Similar to the analysis of COPC concentrations in RHMW02 and RHMW01, the change in COPC concentration between RHMW02 and Red Hill Shaft can be used to estimate COPC attenuation rates. However, because Red Hill Shaft is a pumping well that captures groundwater flow from a large area, a modified evaluation method is required to account for dilution of COPCs caused by mixing of the plume with clean water. This calculation method is presented in Appendix B.4 The C vs. d attenuation rate coefficient for COPC migration from RHMW02 to Red Hill Shaft was evaluated only for naphthalene, because naphthalene has been the most commonly detected individual COPC at Red Hill Shaft (detections for 12 of 63 monitoring events from 2005 to March 2018). Two attenuation rates were calculated based on two estimates of travel time from RHMW02 to Red Hill Shaft: (1) the travel time from the base case groundwater flow model (95 days) and (2) the travel time for the base case model including a clinker zone connecting the Facility source area to the Red Hill Shaft (45 days). The resulting attenuation rates were 0.0075 per day and 0.016 per day, respectively, corresponding to a half-life of 43–92 days. These half-lives are much larger than the half-life calculated for naphthalene between RHMW02 and RHMW01 (6.2 days; see Table 7-6).

Conclusions. Groundwater monitoring data from the Facility over the monitoring period of 2005 to April 2018 have been used to evaluate plume duration and plume attenuation. These evaluations support the following observations:

- *Plume Duration:* COPC concentrations at individual monitoring locations vary over time, exhibiting both increases and decreases in concentration. However, at RHMW02, the monitoring location with the highest COPC concentrations, most of the COPCs show little or no overall long-term concentration trend (i.e., the overall concentration trend is stable over the monitoring period).
- *Plume Attenuation:* COPC concentrations generally decrease from the source area (represented by RHMW02) to downgradient monitoring locations (RHMW01 and Red Hill Shaft). C vs d attenuation half-lives range from 5 to 14 days for the analysis of concentration changes from RHMW02 to RHMW01, while half-lives range from 43 to 92 days for the analysis of concentration changes from RHMW02 to Red Hill Shaft. Although both analyses support the conclusion that biodegradation is contributing to the natural attenuation of COPCs within groundwater, the estimated attenuation rate is 6–8 times slower for analysis of concentration changes from RHMW02 to Red Hill Shaft compared to RHMW02 to RHMW01.
- Both evaluations of C vs d attenuation rates depend on important assumptions:
  - *RHMW02 to RHMW01:* This analysis assumes that RHMW02 and RHMW01 are in the same flow path (i.e., the COPCs present in RHMW01 originated in the vicinity of RHMW02). If the COPCs in RHMW01 actually originate from a lower-strength source (or a more distant source), then the analysis would overestimate true attenuation rate.
  - *RHMW02 to Red Hill Shaft:* This analysis assumes that the very low naphthalene concentrations detected in Red Hill Shaft (i.e., <0.1 µg/L) reflect the actual naphthalene concentration in the Red Hill Shaft water rather than false-positive artifacts of laboratory analysis. For example, for a number of sampling events in 2013 and 2014, low concentrations of naphthalene (<0.1 µg/L) were detected in most or all of the groundwater samples, including those from wells upgradient of the Facility source area (see Appendix B.7 for additional discussion of the uncertainty associated with the low concentration detections of naphthalene). If the actual naphthalene concentrations in Red Hill Shaft are lower than those indicated by the laboratory detections, then the analysis would underestimate the true attenuation rate.
- Taken together, analysis of RHMW02 to RHMW01 and RHMW02 to Red Hill Shaft likely represents the possible range of plume attenuation rates for COPCs in groundwater at the Facility (i.e., an attenuation half-life of 5–14 days or 43–92 days). Based on the currently available information, it is difficult to conclude which estimate is more reliable.

Analysis of Secondary MNA Data. Natural attenuation processes at the Facility were also evaluated using secondary LOEs (i.e., geochemical data; electron acceptor concentrations) from the Facility groundwater monitoring network. Concentrations of the following analytes were considered: total alkalinity, nitrate as nitrogen (NO_3^-), ferrous iron (Fe^{2+} or Fe[II]), sulfate (SO_4^{2-}), and methane (CH_4). Methane concentration measurements from 2005 and 2006 were not included in this analysis because these samples were collected using a bailer, likely leading to low bias in the results due to loss of methane during sample collection. In addition, field measurements of DO (O_2) and ORP were incorporated in the MNA analysis. COPCs considered for this study were TPH-d, 1-methylnaphthalene, 2-methylnaphthalene, and naphthalene. Where sufficient data are available, relationships between electron acceptor concentrations (and field parameters) and COPC concentrations were identified using time-series, spatial contour maps, and X-Y plots for all monitoring wells.

Spatial and temporal concentration trends for electron acceptors (O_2, NO_3^-, SO_4^{2-}) and metabolic byproducts (Fe^{2+}, CH_4) provide strong evidence for aerobic and anaerobic petroleum hydrocarbon degradation within the tank farm area. In the area of the highest COPC concentrations (RHMW01 and RHMW02), electron acceptors (O_2, NO_3^-, SO_4^{2-}) are depleted (or have low concentrations) and concentrations of metabolic byproducts (Fe^{2+}, CH_4) are elevated relative to the monitoring locations outside and upgradient of the tank farm area (Appendix B.5). As expected from MNA processes, higher TPH-d concentrations correspond to (1) lower sulfate concentrations and (2) higher dissolved-methane concentrations. Low DO concentrations and negative ORP values further support the presence of anaerobic conditions within the tank farm area. These secondary LOEs, combined with COPC attenuation rates and half-lives (see Appendix B.4), provide strong evidence of active and robust biodegradation of COPCs within the tank farm.

7.4 GROUNDWATER FLOW AND CF&T MODELING

Following the CSM, interim numerical groundwater flow modeling is being used to further quantify the groundwater flow system and improve understanding of groundwater flow. Numerical modeling may also serve to refine the CSM for the *Groundwater Flow Model Report*. Details of the planned technical approach are described in the *Groundwater Model Evaluation Plan* (DON 2017i). The interim groundwater flow model will be described in the forthcoming AOC Statement of Work Sections 6 and 7 support document for the Section 3 TUA; initial submittal of the Section 7 deliverable *Groundwater Flow Model Report* is scheduled concurrent with initial submittal of the *Investigation and Remediation of Releases Report* in December 2018. Finally, a numerical fate and transport model will be based on the Regulator-approved flow model and natural attenuation data. The initial *CF&T Model Report* will be submitted 6 months after Regulatory Agency approval of the *Groundwater Flow Model Report*.

All available data will be evaluated to further develop the CSM for CF&T modeling, including new chemical data to be collected as part of the project WP/SOW (DON 2017a) and the *Attenuation Evaluation Plan* (DON 2017g). With the numerical groundwater flow model set up and calibrated consistent with the CSM, the CF&T modeling will utilize available information for predictive simulations of COPC migration and concentrations for assessing potential health effects to potential receptors as well as potential remedial alternatives.

Interim results of the CF&T modeling effort as well as other LNAPL modeling techniques will be used to estimate LNAPL migration for current and potential future releases, including the fraction expected to be immobilized in the vadose zone, and the fraction expected to reach groundwater. The modeling effort will also include an assessment of the potential migration of LNAPL within the saturated zone.

7.4.1 Source Area Modeling

Different methods are available for solute transport modeling to evaluate contaminant sources by history matching of available time-series concentration data. Some models involve specifying a constant concentration source or an equivalent LNAPL-water partitioning. The hydrocarbon chemistry/forensics analysis will be used to determine the likely concentrations that are generated by a LNAPL source zone, for LNAPL in both the saturated and unsaturated zones.

LNAPL modeling will be used to develop the LNAPL source term to be used in various scenarios as part of the CF&T modeling effort. A series of history-matching simulations will be performed while adjusting source concentration and mass to reflect the available COPC concentrations through time and equivalent LNAPL-water partitioning. Use of the equivalent LNAPL-water partitioning

approach will allow the MODFLOW USGS model to simulate release of COPCs from LNAPL in the source zone, by simulating both:

- A finite mass of contaminant in a source zone
- Depletion of source mass through dissolution with time

Interim modeling will be based on a conservative approach that uses a mass flux approach for evaluating potential risk to receptors and establishing SSRBLs for sentinel wells that are protective of receptors based on the current risk-based decision criteria (RBDC) (DON 2017k).

7.4.2 Solute Transport Parameters

Solute transport modeling will be applied to evaluate the new groundwater data and further refine the CSM. A dual-porosity conceptualization will be applied to delineate the fast-flow zones from the relatively stagnant zones at a sub-grid-block scale. A series of model simulations will be performed while adjusting source concentrations and mass to reflect the available COPC concentrations through time. The numerical CF&T modeling will require estimating the solute transport parameters. Previous modeling studies in the site area (DON 2007) used the values shown in Table 7-7.

Table 7-7: Transport Parameters Used in Previous Navy CF&T Model

Hydrogeologic Unit	Longitudinal Dispersivity (m)	Transverse Dispersivity (m)	Vertical Dispersivity (m)	Effective Porosity (unitless)
Caprock	5	0.5	0.05	0.10
Valley Fill	3	0.3	0.03	0.15
Basalt	34	3.4	0.34	0.05

Source: (DON 2007)
m meter

The CF&T modeling will include simulation of the COPC decay rates. History matching will be used to estimate transport parameter values for porosity, dispersivity, dual-porosity mass transfer rate term, and biodegradation half-life. The history-matching simulation process is similar to the flow model calibration process. For solute transport, the parameters are adjusted within reasonable ranges so that the simulated COPC concentrations in the plume approximately match the measured values in monitoring wells. To estimate the decay rate, the calibrated MODFLOW model will be run, holding the advection and dispersion parameters constant, while adjusting the degradation rate in a series of iterative model runs to attain results comparable to the time-series data from monitoring wells near the source and away from the source (e.g., RHMW02 and RHMW01). Since CF&T modeling can have a high degree of uncertainty, multiple models will be evaluated via a sensitivity analysis to bracket the range of observed site behavior. These models will be used for evaluating possible future conditions that bracket likely behavior.

According to the USGS, there are few reported dispersivity values available for O'ahu (Oki 2005). In 1974, dispersivity was estimated to be approximately 200 ft for the volcanic-rock aquifer in the Honolulu area, and this value likely represents a longitudinal dispersivity. Using a cross-sectional numerical model, Souza and Voss (1987) estimated the longitudinal and transverse dispersivities of the Pearl Harbor area to be 250 and 0.82 ft, respectively. Souza and Voss (1987) also estimated a vertical to longitudinal dispersivity ratio of 0.004, and stated that transverse dispersivity values vary between 0.05 and 0.33 of the longitudinal dispersivity value. The more recent USGS groundwater model (Rotzoll 2012) used the following dispersivity values for basalt: 164 ft, 8.2 ft, and 0.8 ft for

horizontal longitudinal, horizontal transverse, and vertical dispersivity, respectively. For caprock, Rotzoll 2012 used 33 ft, 1.6 ft, and 0.2 ft for horizontal longitudinal, horizontal transverse, and vertical dispersivity, respectively.

For the Red Hill local modeling area, previous CF&T modeling used longitudinal dispersivity values of 5 m, 3 m, and 34 m for caprock, valley fill, and basalt, respectively (DON 2007, Appendix L). The same model used a transverse to longitudinal dispersivity ratio of 0.1 and a vertical to longitudinal dispersivity ratio of 0.01.

Dual-porosity mass transfer rates and decay rates for COPCs at the site have not been previously established. The dual-porosity mass transfer rates will be evaluated as a calibration parameter, and sensitivity simulations will evaluate the behavior of a reasonable range of values. The decay rates of COPCs will be estimated from site investigations and laboratory studies, and evaluated as a calibration parameter.

7.5 UNCERTAINTY ANALYSIS

Recent investigation activities and a comprehensive review of historical investigation results have significantly improved the conceptual model for the fate and transport of LNAPL and dissolved COPCs at the Facility. However, remaining key uncertainties include:

- *LNAPL distribution at the water table:* LNAPL has not measured in any of the existing monitoring wells. However, the presence and distribution of LNAPL at the water table at other locations within the vicinity of the tanks is less certain.
- *LNAPL holding capacity at the water table:* The absence of LNAPL in existing monitoring wells provides evidence that prior LNAPL releases have not resulted in a laterally extensive lens of LNAPL at the water table below the tanks. However, the LNAPL holding capacity at the water table (i.e., the volume of LNAPL per unit area within an extensive LNAPL lens) is difficult to estimate from available data because extensive LNAPL lenses have not been detected in monitoring wells.
- *Plume attenuation rates:* Plume attenuation rates (C vs. d rates) have been estimated based on data from limited paired locations (i.e., RHMW02, RHMW01 and Red Hill Shaft). The small number of monitoring locations available for this analysis increases the uncertainty in the results.
- *Accuracy of very low COPC detections:* The historical groundwater monitoring dataset includes sporadic detections on some COPCs at some locations at very low concentrations (e.g., less than 0.1 µg/L for individual COPCs; less than 50 µg/L for TPH analyses). During some monitoring events, these low-level detections have occurred in most or all wells sampled, including wells upgradient from the active parts of the Facility. The reliability of these very low detections is uncertain (see Appendix B.7).
- *Applicability of RBDC as final decision criteria:* RBDCs have been developed as screening levels for the initial evaluation of Facility monitoring results (DON 2017k). Some RBDCs (e.g., naphthalene) are close to the LOD for sample analytical results. Final decision criteria for Facility COPCs will be developed in the future.

In addition, the spatial distribution of COPC concentrations dissolved in groundwater between the Facility and the water supply wells in North Hālawa Valley and Moanalua Valley is not well understood. The presence of hydrocarbons in shallow perched zones underlying the Hālawa Correctional Facility further complicates this.

The extent of the source area, COPC mass loading rates, and site-specific values for natural attenuation rates of the COPCs are uncertain. Compositional changes in released kerosene-based fuels over time are unknown. Site-specific values for COPC sorption and degradation rates are not currently available.

7.6 ADDRESSING UNCERTAINTIES

The following ongoing, planned, or proposed activities are designed to help resolve the uncertainties described in Section 7.5.

Additional hydrogeologic and chemical data are currently being collected as described in the project WP/SOW (DON 2017a) and subsequent derivative deliverables. Many of the data obtained during the investigation will be applicable and useful for refining and updating the CSM, but some data gaps and uncertainties still remain, as described in the *Data Gap Analysis Repor*t (DON 2017d) and summarized below. Either these data gaps will be filled during the investigation or conservative assumptions will be made during development and refinement of the CSM and groundwater modeling effort.

7.6.1 Nature and Extent of Contamination

Additional data are being collected to better define the spatial distribution of COPC concentrations dissolved in groundwater surrounding the Facility. To fulfill these data needs, monitoring wells are being installed and sampled for detailed groundwater quality analyses to characterize the spatial distribution of COPC concentrations. Similar groundwater quality data from additional monitoring well locations, which were recently planned (DON 2017f), will better define the nature and extent of COPCs between the Facility and the water supply wells.

7.6.2 Source Area Extent, Mass Loading, and Natural Attenuation Rates

To reduce potential uncertainties, additional data collection activities have been undertaken, including:

- *Microcosm Studies:* In addition to potentially deploying biotraps to obtain degradation rates, laboratory microcosm studies are being performed to estimate aerobic and anaerobic rates.
- *Recharge to Groundwater Measurements:* A better understanding of vadose zone LNAPL dissolution rates is needed. Measuring the recharge rate into Red Hill will help reduce the current uncertainty about the importance of this process.
- *Sheen Samplers:* If sheens are present in the wells, then sheen samplers would be deployed to better understand the chemistry and composition of the sheen material (a sheen is an extremely thin layer of LNAPL that may exist on the surface of the water table). However, no sheens were observed during the Fall 2017 sampling event, and the samplers were not deployed. This device will be used in existing monitoring wells to analyze hydrocarbon sheens if present.
- *NAP Data:* NAP data were collected and are now being analyzed to demonstrate whether biodegradation of LNAPL and dissolved-plume constituents is occurring.
- *Mass Flux/Mass Discharge Calculations:* Order-of-magnitude mass discharge calculations are being developed to better understand the magnitude of the existing release and the magnitude of a future release that could impact water supply shafts.

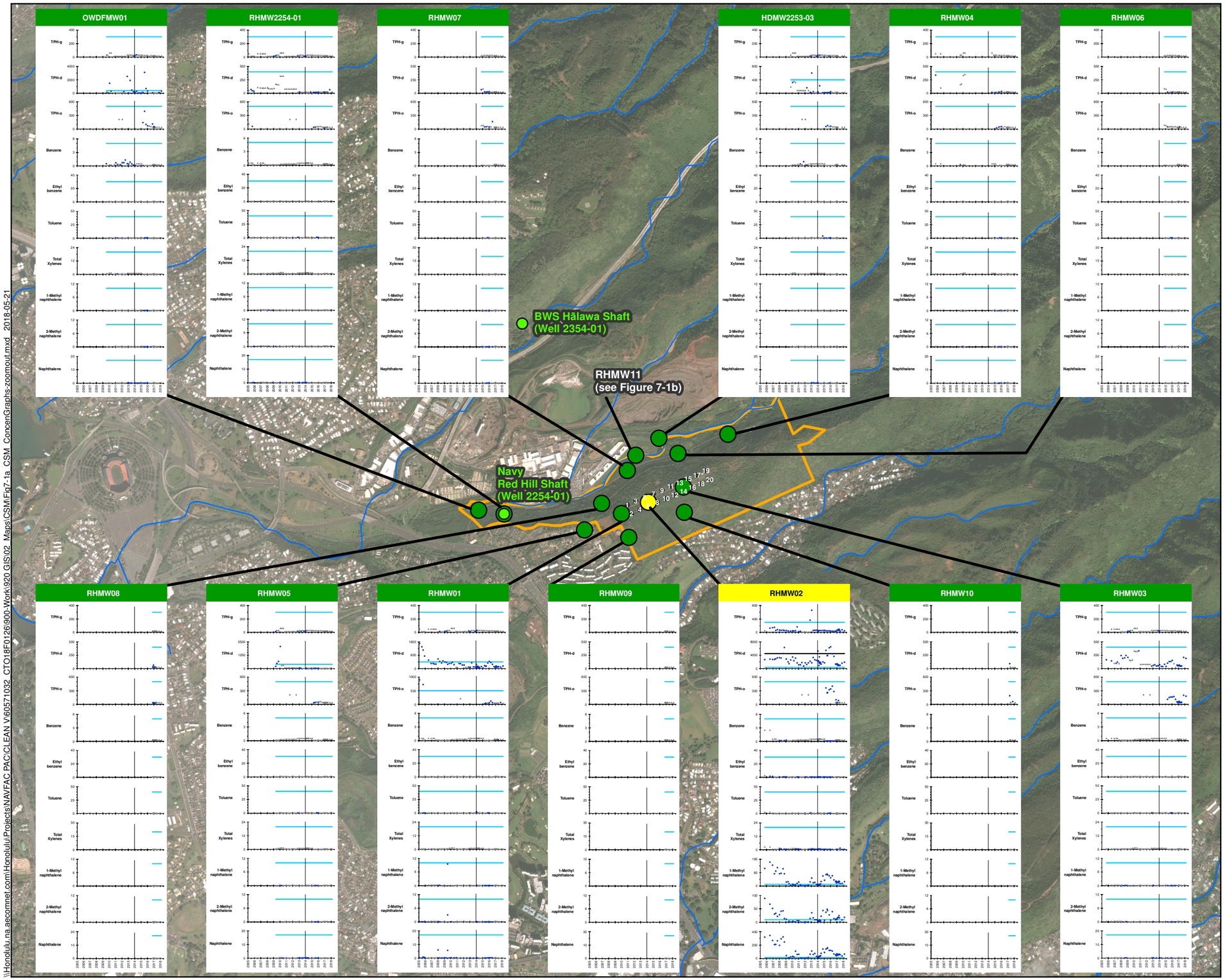

Location Map

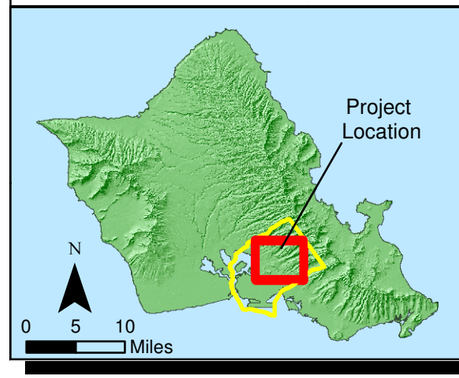

Legend

- Red Hill Facility Boundary and Fuel Storage Tanks
- Stream
- Water Supply Well

Groundwater Monitoring Location:

- Without Current COPC Exceedances
- With Current COPC Exceedances

Graph Legend:

- Detected Concentration
- Non-Detect Concentration
- Regulatory Screening Level (DOH)
- Site-Specific Risk-Based Level (SSRBL)
- 2014 Tank 5 Release

2013 2014 2015

Notes

1. Map projection: NAD 1983 UTM Zone 4N
2. Base Map: DigitalGlobe, Inc. (DG) and NRCS. Publication_Date: 2015
3. Source: *Final First Quarter 2018 - Quarterly Groundwater Monitoring Report* (DON 2018a)
4. All results in parts per billion (ppb or micrograms per liter)

N

0 1,250 2,500 5,000 Feet

Figure 7-1a
COPC Concentration Graphs of Historical Groundwater Monitoring Results
Conceptual Site Model
Investigation and Remediation of Releases and Groundwater Protection and Evaluation
Red Hill Bulk Fuel Storage Facility
JBPHH, O'ahu, Hawai'i

\\Honolulu.na.aecomnet.com\Honolulu\Projects\NAVFAC PAC\CLEAN V\60571032 CTO18F01260\900-Work\920 GIS\02 Maps\CSM\Fig7-1a CSM ConcenGraphs-zoomout.mxd 2018-05-21

This page intentionally left blank

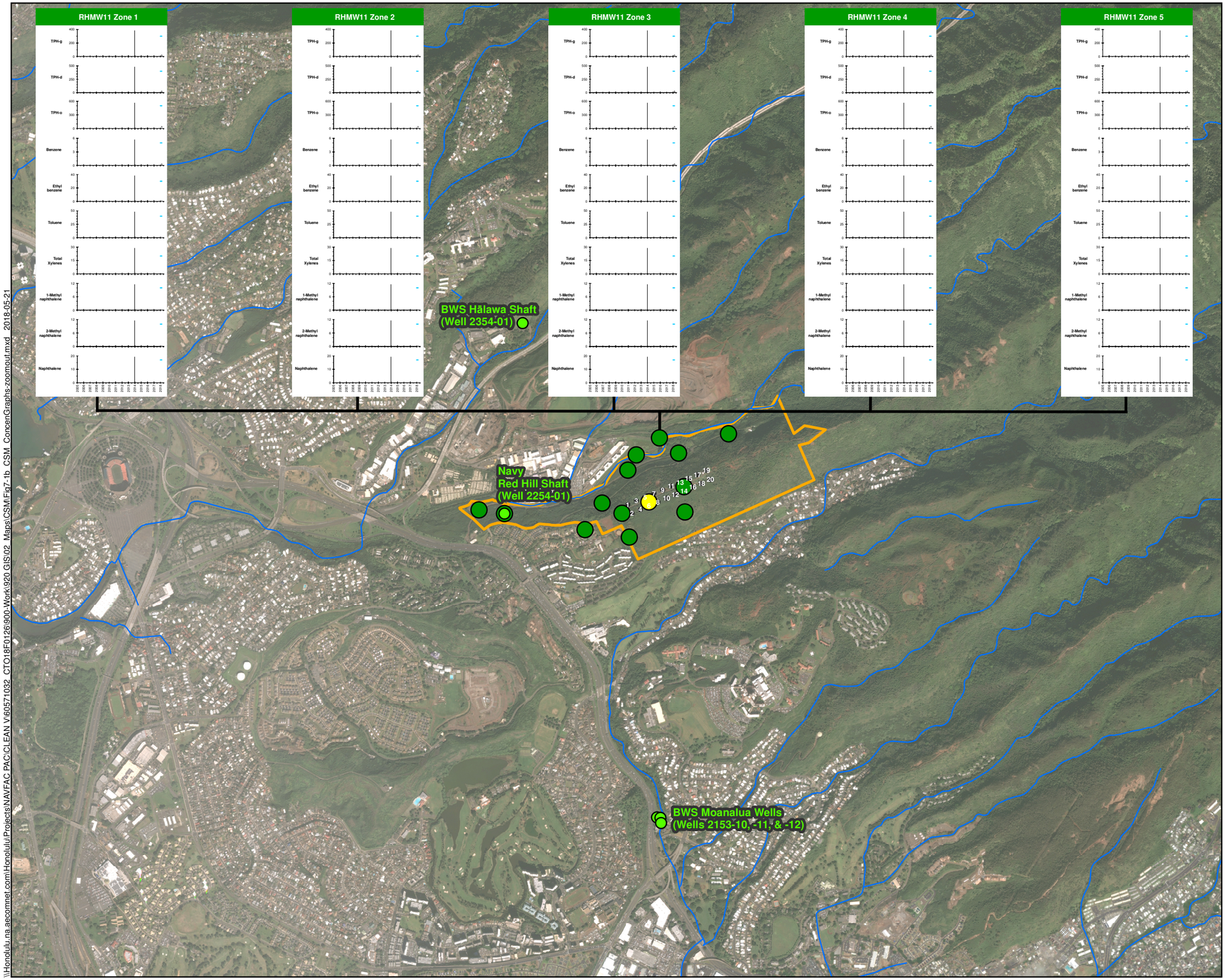

Location Map

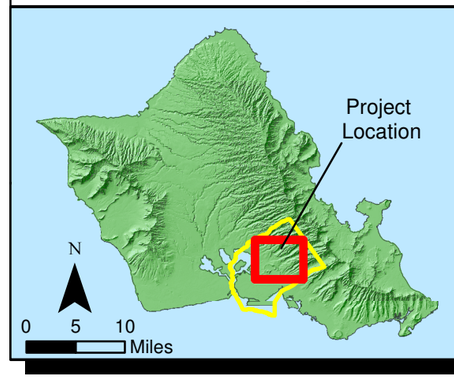

Legend

- Red Hill Facility Boundary and Fuel Storage Tanks
- Stream
- Water Supply Well

Groundwater Monitoring Location:

- Without Current COPC Exceedances
- With Current COPC Exceedances

Graph Legend:

- Detected Concentration
- Non-Detect Concentration
- Regulatory Screening Level (DOH)
- Site-Specific Risk-Based Level (SSRBL)
- 2014 Tank 5 Release

2013 2014 2015

Notes

1. Map projection: NAD 1983 UTM Zone 4N
2. Base Map: DigitalGlobe, Inc. (DG) and NRCS. Publication_Date: 2015
3. Source: *Final First Quarter 2018 - Quarterly Groundwater Monitoring Report* (DON 2018a)
4. All results in parts per billion (ppb or micrograms per liter)

N

0 1,250 2,500 5,000 Feet

Figure 7-1b
COPC Concentration Graphs of Historical Groundwater Monitoring Results
Conceptual Site Model
Investigation and Remediation of Releases and Groundwater Protection and Evaluation
Red Hill Bulk Fuel Storage Facility
JBPHH, O'ahu, Hawai'i

\\Honolulu.na.aecomnet.com\Honolulu\Projects\NAVFAC PAC\CLEAN V\60571032 CTO18F01126\900-Work\920 GIS\02 Maps\CSM\Fig7-1b CSM ConcenGraphs-zoomout.mxd 2018-05-21

This page intentionally left blank

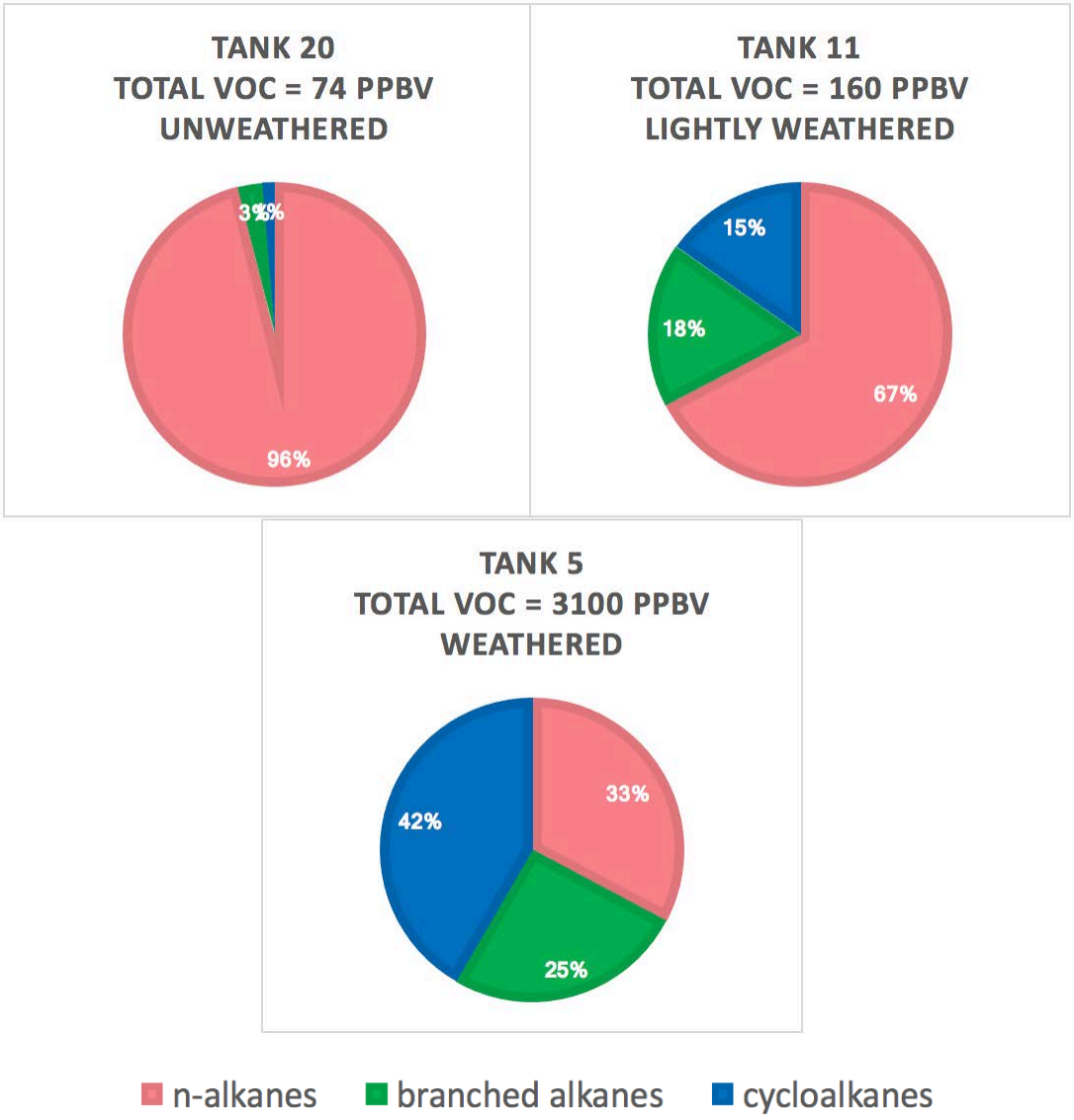

Figure 7-2
Range of VOC Concentrations and Fuel Weathering Observed in Below-Tank Soil Vapor Wells
Conceptual Site Model
Investigation and Remediation of Releases
and Groundwater Protection and Evaluation
Red Hill Bulk Fuel Storage Facility
JBPHH, O‘ahu, Hawai‘i

This page intentionally left blank

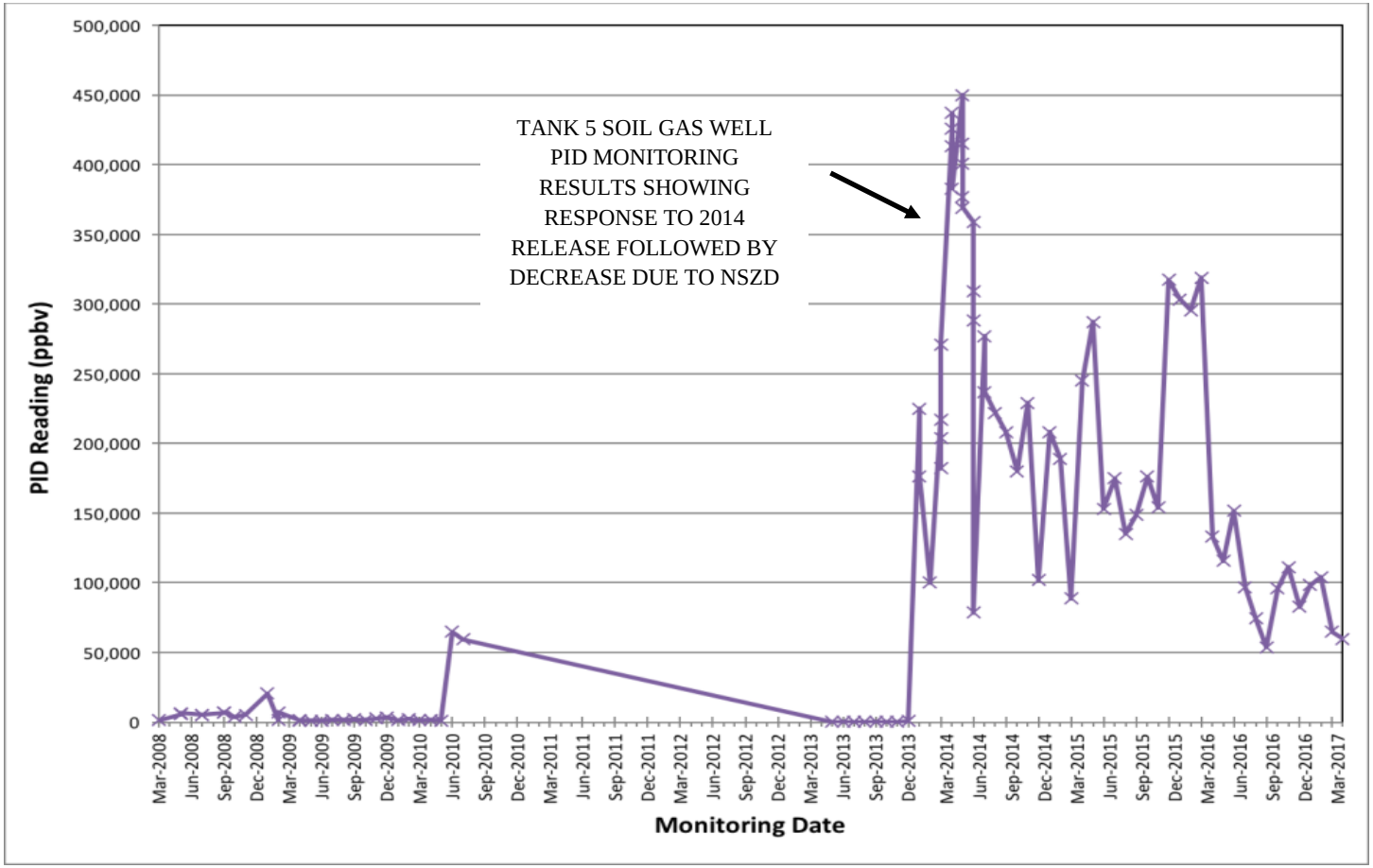

LAB ANAYSIS OF VAPORS BELOW TANK 5 COLLECTED IN NOV. 2017 SHOWING BIOLOGICAL WEATHERING (I.E., ENRICHMENT IN CYCLOALKANES)

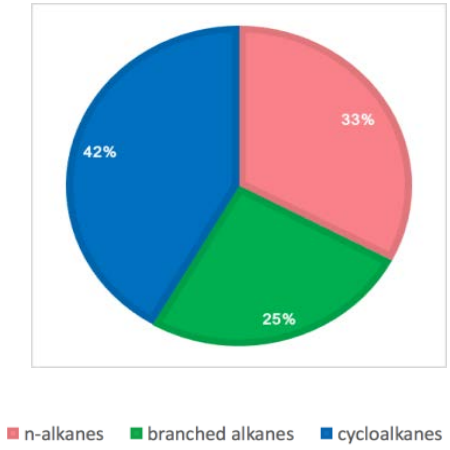

Figure 7-3
Use of PID Monitoring Combined with Lab Analysis to Track Release and Subsequent Weathering of LNAPL Fuel for Tank 5
Conceptual Site Model
Investigation and Remediation of Releases
and Groundwater Protection and Evaluation
Red Hill Bulk Fuel Storage Facility
JBPHH, Oʻahu, Hawaiʻi

This page intentionally left blank

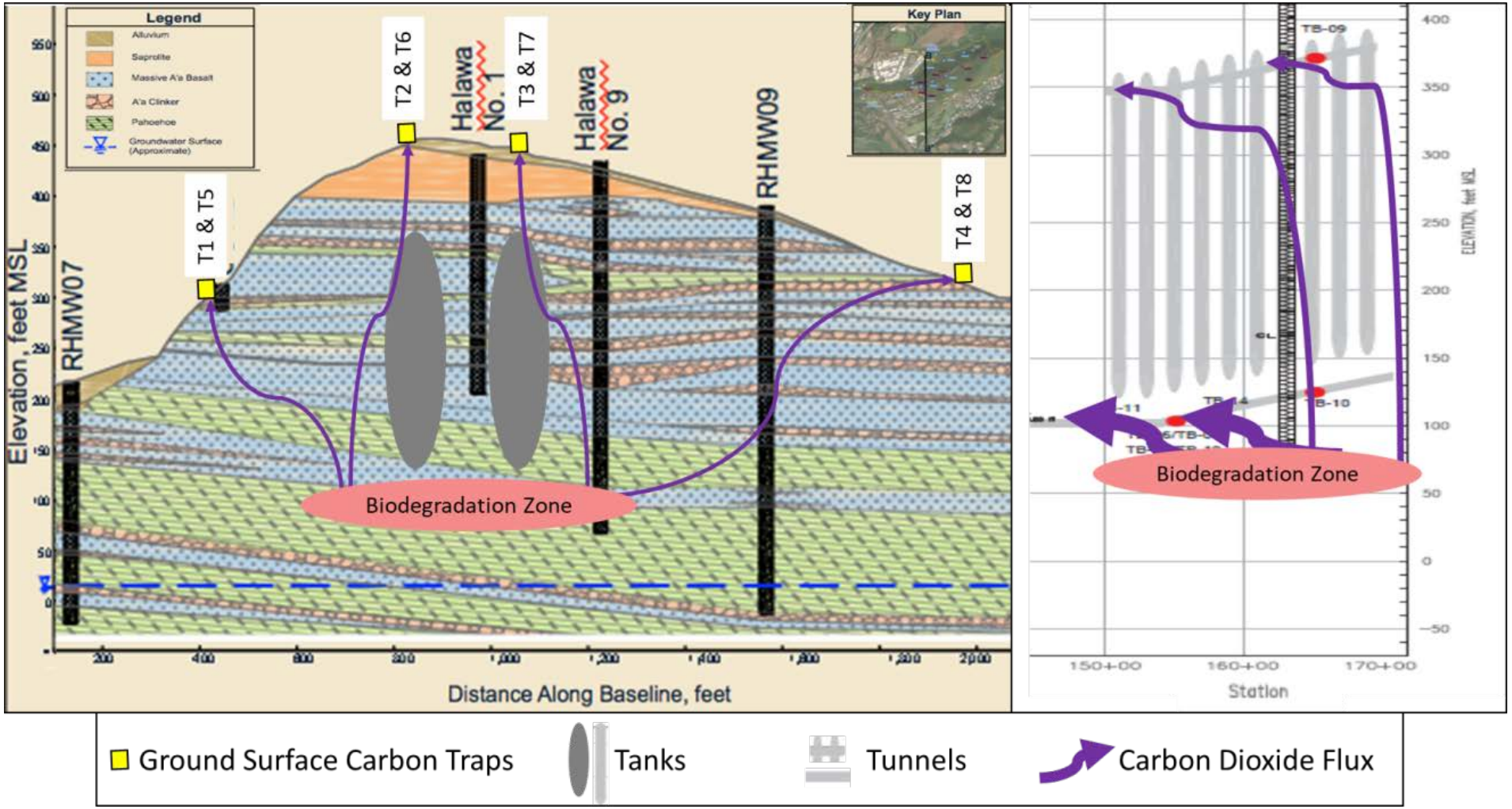

Figure 7-4
Conceptual Illustration of Carbon Dioxide Flux to Ground Surface and Tunnels
Conceptual Site Model
Investigation and Remediation of Releases
and Groundwater Protection and Evaluation
Red Hill Bulk Fuel Storage Facility
JBPHH, O'ahu, Hawai'i

This page intentionally left blank

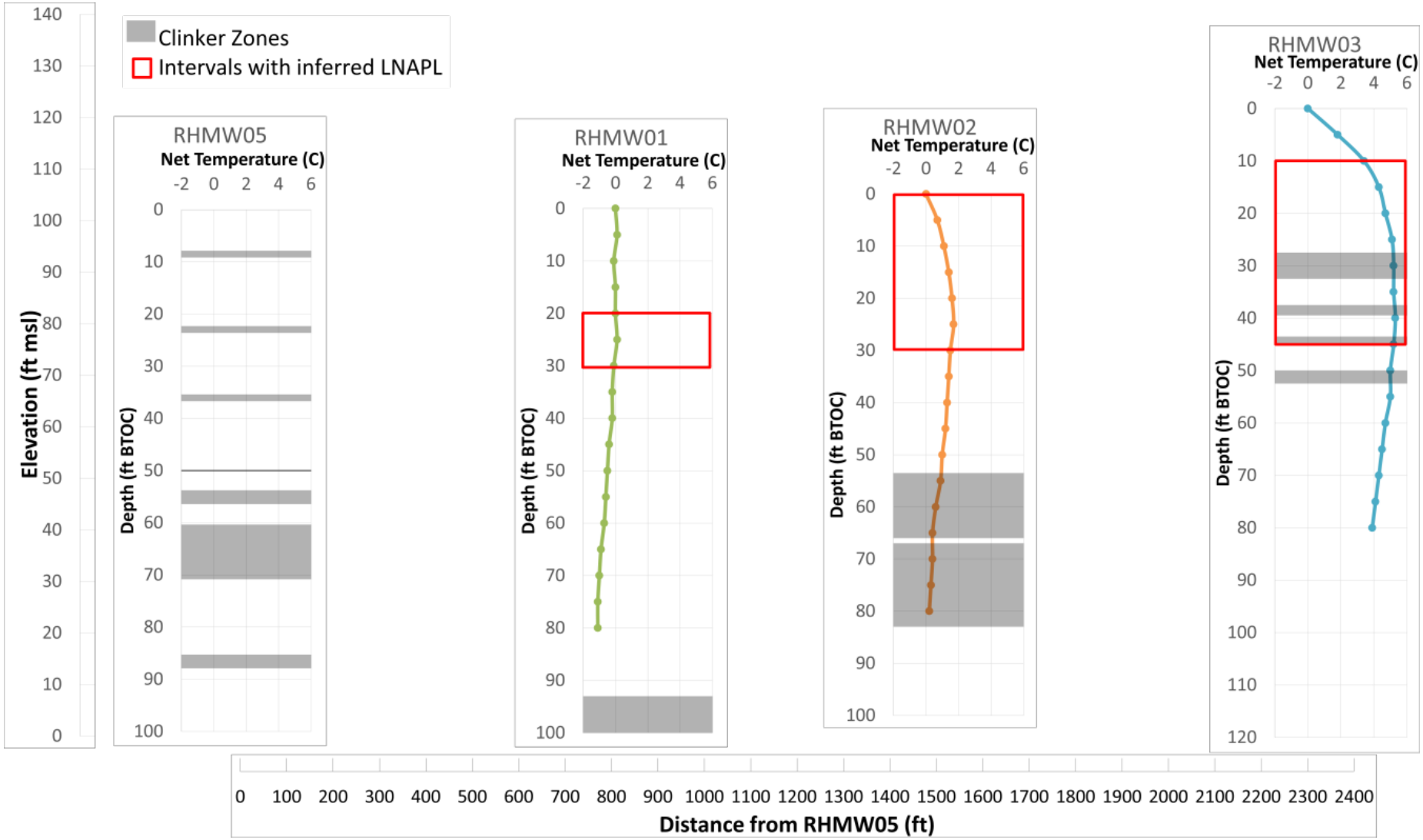

Figure 7-5
Net (Background Corrected) Temperature Profiles for Facility Wells (Well Air Temperatures Method), Highlighting Clinker Zones and Inferred LNAPL Intervals
Conceptual Site Model
Investigation and Remediation of Releases and Groundwater Protection and Evaluation
Red Hill Bulk Fuel Storage Facility
JBPHH, O‘ahu, Hawai‘i

This page intentionally left blank

8. Module G: Exposure Model

The exposure model evaluates the potential for exposure to COPCs in site media for receptors (human and ecological) that might contact those media. It is also referred to as a risk-based CSM (e.g., in the *Risk-Based Decision Criteria Development Plan*; DON 2017k). The exposure model identifies the chemical sources and migration routes, exposure media and pathways, and potential receptors. It is used to guide the evaluation of potential exposures for human health and ecological receptors so that relevant pathways, exposure routes, and ultimately risks can be evaluated in the human health risk assessment. The primary purpose of the risk-based exposure model is to represent chemical sources, exposure pathways, and receptors (that are potentially complete) that may warrant additional evaluation of risk concerns. Only potentially complete exposure pathways are evaluated quantitatively in the risk assessment, consistent with EPA (1989) guidance. While evaluation of ecological receptors was conducted as part of risk-based CSM for completeness, the potential receptors of primary interest are those who could be exposed to COPCs through water-supply sources, in accordance with the AOC.

A complete exposure pathway includes all the following elements:

- Chemical source(s)
- Affected media
- Chemical release and transport mechanisms
- Routes of exposure
- Human and/or environmental receptors

The absence of any one of these elements results in an incomplete exposure pathway, which does not warrant further evaluation. The refined risk-based exposure model (Figure 8-1) visually depicts the potential current and future exposure pathways at the Facility.

Each identified exposure route has been assessed as potentially complete, potentially complete but insignificant, or incomplete in accordance with the following criteria:

- *Potentially complete:* exposure pathways that include all the above elements
- *Potentially complete but insignificant:* exposure pathways identified as potentially complete but not likely to pose a potential for adverse effects to human health or ecological receptors
- *Incomplete:* exposure pathways lacking at least one of the above elements are not complete and therefore will not affect human health or ecological receptors

8.1 Chemical Sources and Releases

The Facility contains 18 active and 2 inactive underground fuel storage tanks that are operated by the Navy. The tanks are accessed via a tunnel system that connects to Pearl Harbor. Kerosene-based jet fuels stored at the Facility have included JP-5, JP-8, and F-24. In January 2014, the Navy reported that JP-8 fuel was released from Tank 5. However, historical releases (prior to 2005) are considered to be the main source of impacts to groundwater at the Facility. The 2014 release did not result in COPC concentrations in groundwater outside of their historical range. Other releases (e.g., spills or leaks in the fuel system) in the tunnels may have occurred or may occur in the future, leading to contamination of unconsolidated materials, volcanic rock, soil/rock vapor and air in the tunnels, and groundwater.

8.2 POTENTIALLY AFFECTED MEDIA

Potentially contaminated media at the Facility site are unconsolidated materials, volcanic rock within the tunnels, soil vapor within the tunnels, tunnel air, groundwater beneath the Facility, and offsite surface water where groundwater may discharge.

Soil or rock may be contaminated directly by spills or leaks from the fuel tanks or associated components of the fuel system. Although the fuel tanks are constructed of steel-lined concrete, released fuels could migrate to the underlying soil if the integrity of the concrete containers is compromised. Volatile components of such releases could migrate as soil vapor and could affect the air in the tunnels.

As the Facility overlies the Waiawa System of the Pearl Harbor Aquifer Sector and the Moanalua System of the Honolulu Aquifer Sector (see Figure 2-6), fuel releases can migrate to groundwater beneath the Facility. The depth from ground surface to groundwater beneath the site and in downgradient areas ranges from approximately 80 ft bgs at Red Hill Shaft to as much as 400–500 ft bgs in the tank farm area. Water supply wells near the Facility are transport mechanisms in potentially complete groundwater exposure pathways. The Navy's Red Hill Shaft and the BWS municipal water supply wells Hālawa Shaft and Moanalua Wells represent the most significant pathways to human receptors due to their known or suspected pumping influence on the aquifer beneath the Facility, the size of their drinking water distribution system(s), and location relative to potential downgradient groundwater flow direction from the Facility. Water supply wells identified within the groundwater model domain are shown on Figure 2-7 and further discussed in Section 2.11.

As groundwater within the unconfined basalt aquifer at the Facility migrates toward the ocean, it dips below and becomes confined by overlying caprock. The confining action of the caprock produces artesian groundwater flow and creates numerous springs around Pearl Harbor, but not near the Facility.

The nearest surface water bodies, South Hālawa and Moanalua Streams, are approximately 600 ft and 1,800 ft away from the nearest tanks, respectively. However, these are both intermittent streams that lie at higher elevations than the basal aquifer and are not expected to receive groundwater discharge from the basal aquifer.

8.3 POTENTIAL RECEPTORS

8.3.1 Human Receptors

The human receptors that may contact onsite or offsite Facility-impacted media are Facility occupational workers, construction workers, and visitors, and offsite residents:

- Onsite occupational workers are people who work at the Facility. They are anticipated to spend their work day within the tunnels or on Facility grounds outside the tunnels.
- Construction workers also work at the Facility but are assumed to work in excavations at the Facility as part of tunnel construction or maintenance or in utility trenches. These work activities would expose construction workers to soil or rock beneath the concrete floors of the tunnel system.
- Visitors to the Facility are assumed to have similar activities as occupational workers. They are anticipated to spend their work day within the tunnel system or on Facility grounds outside the tunnels.

- Offsite residents who use U.S. Navy Supply Well 2254-01 (Red Hill Shaft) (located approximately 2,600 ft west of the nearest underground fuel storage tank) as their tap water source are potential receptors for site chemicals that migrate via groundwater from Facility releases.
- Offsite residents who use BWS' Hālawa Shaft and/or Moanalua Wells as their tap water source are potential receptors for site chemicals that migrate via groundwater from Facility releases.
- Other offsite receptors may include people who might access groundwater discharge locations near Pearl Harbor.

8.3.2 Ecological Receptors

A preliminary risk assessment conducted as part of a previous Facility investigation concluded that there were no significant pathways for ecological receptors (DON 2002). DON (2007) notes that both South Hālawa Stream and Moanalua Stream are impaired streams and do not support aquatic life, with nutrient inputs, pathogens, turbidity and exotic species due to urban runoff, storm sewers, and other sources of disturbance. Further, groundwater occurs 80 ft beneath the stream beds and does not discharge to the streams. The artesian features near Pearl Harbor noted in Section 2.10 are considered too far away (Pearl Harbor is approximately 2.5 miles from the tank farm area) to pose a significant concern for any ecological receptor at those locations. For these reasons, ecological exposures are considered incomplete or insignificant and are not further evaluated for the Facility.

8.4 POTENTIALLY COMPLETE EXPOSURE PATHWAYS

Incidental ingestion, dermal contact, and inhalation of particulates are potentially complete surface and subsurface soil exposure pathways for construction workers at the Facility. Construction workers may be exposed via these pathways in construction or maintenance excavations or in utility trenches that are dug beneath the concrete floors of the tunnels.

Volatile components of fuels released to soil in the tunnels or released via spills or leaks in the active fuel systems may migrate to indoor air in the tunnels. All receptors in the tunnels are potentially exposed to these chemicals via inhalation of tunnel air. Although this pathway is considered potentially complete, the tunnels are well ventilated, which would limit buildup of volatile chemicals in air. Further, any potential vapor intrusion from soil releases into the tunnels could not be differentiated from other sources within the tank complex. Finally, because the Facility is an active work place, any potential occupational exposure to chemicals at the workplace is assumed to be covered under the Navy's Occupational Safety and Health Administration (OSHA) program.

Tap water at the Facility comes from the public water supply. Therefore, occupational workers, construction workers, and visitors that use tap water at the Facility could be exposed to chemicals in tap water via ingestion and dermal absorption while washing hands. Bathing is not a realistic scenario for onsite receptors, however, so dermal exposure is considered an insignificant pathway.

Offsite residents that use the Red Hill Shaft water supply as their tap water source could be exposed to chemicals in tap water via direct ingestion and dermal contact. They may also be exposed to volatile chemicals via inhalation while showering/bathing.

8.5 INCOMPLETE OR INSIGNIFICANT PATHWAYS

Direct contact with surface and subsurface soil is not anticipated for occupational workers or visitors in the tunnels because the tunnels are concrete-lined and soil is not exposed.

Contact with tap water for all receptors in the tunnels is limited to direct ingestion and dermal contact while washing hands. Workers and visitors are not expected to shower at the site and therefore, inhalation and dermal contact while showering are not complete pathways.

Because the depth to groundwater precludes direct contact, all other direct groundwater exposure pathways are considered incomplete for Facility receptors. Even excavations in the tunnels would not be deep enough to contact groundwater at the Facility.

Vapor intrusion from groundwater at the site is possible but considered insignificant compared to other pathways because of the depth to groundwater.

The vapor intrusion pathway for nearby residents is also considered an insignificant pathway. This is due to the depth of groundwater in the residential areas adjacent to the Facility (at least 80 ft bgs), and the fact that the vast majority of the fuels stored at the Facility have very little volatile content.

Potential exposure to groundwater used as offsite irrigation water and at groundwater discharge locations near Pearl Harbor is considered insignificant. A quantitative evaluation of these supplementary, lower-exposure pathways is not warranted as the evaluation and protection of residential tap water exposures would also be protective of the other water-related pathways.

8.6 POTENTIAL EXPOSURE TO LNAPL

There is potential exposure to LNAPL by workers in the tunnels, but that is covered under the Navy's OSHA program. LNAPL migration is being evaluated as part of the AOC Statement of Work Section 3 TUA, and attenuation is being evaluated as part of both the interim environmental analysis and CSM. Finally, it is possible that LNAPL could reach Navy Supply Well 2254-01 (Red Hill Shaft), but contingencies will be put in place as described in the GWPP (DON 2014b) so that human health is protected in the event LNAPL impacts drinking water.

The DOH EAL approach considers the presence of LNAPL to represent a "free product" scenario and does not apply risk-based criteria to LNAPL-impacted media. However, the gross contamination EALs, which consider aspects of solubility and saturation limits, may be used for preliminary comparisons of LNAPL-related data.

8.7 UNCERTAINTIES

Various uncertainties are associated with the identification of potential sources, migration routes, receptors, and exposure pathways.

Although the 2014 fuel release from Tank 5 was detected, other releases may have occurred at the Facility where the types of chemicals that may have been released are unknown. The planned sentinel well network described in the *Sentinel Well Network Development Plan* (DON 2017l) will function as a tool to monitor past and potential releases from the Facility.

A pathway from the Facility to Red Hill Shaft has been identified as a possible chemical migration route. Uncertainty is associated with other possible migration routes to drinking water supply wells (e.g., Hālawa Shaft and Moanalua Wells) and other areas where groundwater might discharge.

Uncertainty is also associated with potential exposure via pathways that are considered insignificant. Because of the conservative nature of the evaluation of exposure and risk to residents, however, any potential risk via these other pathway is assumed to be addressed by the residential risk evaluation.

Although land use at the Facility is not expected to change in the future, a hypothetical land use change would warrant a re-evaluation of potential receptors and exposure pathways.

8.8 ADDRESSING UNCERTAINTIES

As described in Section 8.7, the main uncertainties with risk-based exposure model are those associated with the possibility of unidentified sources and migration routes. These are addressed by the groundwater flow and solute transport modeling and the extensiveness of the planned sentinel groundwater monitoring network, especially where it is focused on the water supply wells (see Section 2.11).

This page intentionally left blank

Contributing Source	Transport Mechanism & Exposure Medium	Exposure Route*	Receptors			
			Offsite Resident (Adult/Child)	Onsite Occupational Worker	Onsite Construction Worker	Onsite Visitor
Releases from Red Hill Fuel Storage Tanks						
Surface Soil	Direct Contact with Surface Soil [a]	Ingestion:	Incomplete	Incomplete	**Potentially Complete**	Incomplete
		Dermal:	Incomplete	Incomplete	**Potentially Complete**	Incomplete

Rationale: The only contact with potentially contaminated soil would occur within the Facility tunnels. There are no current (or anticipated future) residents within the tunnels, and the concrete foundation precludes any soil exposure for occupational workers or Facility visitors. For these receptors, the exposure pathway for surface soil is incomplete.

Within the Facility, only construction workers (utility workers) in an excavation would be potentially exposed to soil, which is otherwise inaccessible.

Subsurface Soil	Direct Contact with Subsurface Soil	Ingestion:	Incomplete	Incomplete	**Potentially Complete**	Incomplete
		Dermal:	Incomplete	Incomplete	**Potentially Complete**	Incomplete

Rationale: The only contact with potentially contaminated soil would occur within the Facility tunnels. There are no current (or anticipated future) residents within the tunnels, and the concrete walkways preclude any soil exposure for occupational workers or Facility visitors. For these receptors, the exposure pathway for surface soil is incomplete.

Within the Facility, only construction workers (utility workers) in an excavation would be potentially exposed to soil, which is otherwise inaccessible.

Volatilization & Dispersion to Tunnel Air		Inhalation:	Incomplete	**Potentially Complete**	**Potentially Complete**	**Potentially Complete**

Rationale: Inhalation of soil vapor VOCs in ambient air is not a complete pathway for residents because any soil contamination is localized at the Facility, where there are no current residents and where future residential use is not likely.

Volatile components of fuels could migrate to indoor air within the Facility and inhalation inside contaminated tunnels is a potentially complete exposure pathway for these receptors. Because the Facility is an active workplace, however, any occupational exposures to volatile chemicals within the tunnels are assumed to be covered under the Navy's OSHA programs.

Infiltration to Groundwater		Ingestion:	**Potentially Complete**	**Potentially Complete**	**Potentially Complete**	**Potentially Complete**
		Dermal:	**Potentially Complete**	Insignificant	Insignificant	Insignificant
		Inhalation (Bathing/Showering):	**Potentially Complete**	Incomplete	Incomplete	Incomplete
		Inhalation/ Vapor Intrusion:	Insignificant	Insignificant	Insignificant	Insignificant

Rationale: Direct exposure to chemicals in tap water (ingestion and dermal contact) and inhalation of VOCs while bathing are considered potentially complete pathways for residents that use groundwater in the area as a drinking water source.

All onsite receptors could potentially be exposed to drinking water at the Facility, due to the proximity of Red Hill Shaft downgradient of the Facility. Offsite receptors could be exposed to drinking water from Red Hill Shaft, Hālawa Shaft, and Moanalua Wells. Bathing, however, is not a realistic scenario for onsite receptors. Therefore, while dermal exposure (washing hands) is possible, the dermal pathway for onsite receptors is considered insignificant.

Due to the depth to groundwater across the site (between 400–500 ft bgs at the tank farm and approximately 80 ft bgs at Red Hill Shaft), there is not a complete exposure pathway for construction workers in an excavation.

Inhalation of indoor or outdoor air is considered insignificant because groundwater is too deep for any appreciable migration of VOCs to indoor or outdoor air to occur; any such exposure is expected to be insignificant compared to exposure via the direct use of tap water for residents and insignificant for people in the tunnels compared to VOC inputs to tunnel air from releases to soil and current Facility operations.

Groundwater Discharge to Surface Water		All Pathways:	Incomplete	Incomplete	Incomplete	Incomplete

Rationale: In the Facility vicinity, there are no known surface water bodies that receive groundwater discharges. Although there might be groundwater discharge locations close to Pearl Harbor, any potential exposure to offsite receptors at these locations is considered insignificant as Pearl Harbor is approximately 2.5 miles from the tank farm area.

Use of Groundwater for Irrigation		All Pathways:	Insignificant	Incomplete	Incomplete	Incomplete

Rationale: Groundwater could be used to irrigate gardens at local residences. Ingestion of or dermal contact with irrigation water is expected to be minimal, and exposure to volatile COPCs in groundwater would be limited given the expected high rate of volatilization to outdoor air during irrigation. Further, exposure to volatile or non-volatile components of COPCs is expected to be insignificant for residential gardeners compared to direct contact of groundwater as a drinking water source. There is not a complete relevant pathway for onsite receptors.

* A potentially complete exposure pathway includes all of the following elements:
- Sources and type of chemicals present
- Affected media
- Chemical release and transport mechanisms
- Known and potential routes of exposure
- Known or potential human receptors

Insignificant exposure pathway: pathway is potentially complete, but not likely to pose a potential for adverse effects to human health.
Incomplete exposure pathway: pathway is not complete and therefore will not affect human health.

Figure 8-1
Human Health Exposure Pathway Evaluation

This page intentionally left blank

9. References

ASTM International. 2014a. *Standard Guide for Developing Conceptual Site Models for Contaminated Sites*. E1689-95 (Reapproved 2014). West Conshohocken, PA.

———. 2014b. *Standard Guide for Development of Conceptual Site Models and Remediation Strategies for Light Nonaqueous-Phase Liquids Released to the Subsurface*. E2531-06(2014). West Conshohocken, PA.

Bouwer, Herman, and R. C. Rice. 1976. "A Slug Test for Determining Hydraulic Conductivity of Unconfined Aquifers with Completely or Partially Penetrating Wells." *Water Resources Research* 12 (3): 423–428. https://doi.org/10.1029/WR012i003p00423.

Buscheck, T. E., and C. M. Alcantar. 1995. "Regression Techniques and Analytical Solutions to Demonstrate Intrinsic Bioremediation." In *Intrinsic Bioremediation (Proceedings from the Third International In Situ and On-Site)*. Columbus, OH: Battelle Press.

Board of Water Supply, City and County of Honolulu (BWS). 2016. *2016 Water Master Plan*. Prepared by CDM Smith. October.

Cooper, H.H., Jr., and C.E. Jacob. 1946. "A Generalized Graphical Method for Evaluating Formation Constants and Summarizing Well Field History." *Transactions, American Geophysical Union* 27 (4).

Cooper, Hilton H., John D. Bredehoeft, and Istavros S. Papadopulos. 1967. "Response of a Finite-Diameter Well to an Instantaneous Charge of Water." *Water Resources Research* 3 (1): 263–269. https://doi.org/10.1029/WR003i001p00263.

Dale, R. H. 1978. *A Ground-Water Inventory of the Waialua Basal-Water Body, Island of Oahu, Hawaii*. Open-File Report 78-24. Prepared in cooperation with Board of Water Supply, City and County of Honolulu, Honolulu, Hawaii. U.S. Geological Survey.

Dames & Moore. 1991. *Site Characterization, Halawa Medium Security Facility, Halawa Valley, Oahu, Hawaii*. D&M Job Number 0314-147-037. October 25.

Department of Health, State of Hawaii (DOH). 2016. *Technical Guidance Manual for the Implementation of the Hawaii State Contingency Plan*. Interim Final. Honolulu, HI: Hazard Evaluation and Emergency Response Office. September.

———. 2017. *Evaluation of Environmental Hazards at Sites with Contaminated Soil and Groundwater, Hawai'i Edition*. Hazard Evaluation and Emergency Response. Revised 2017. Fall.

Doherty, J. L. 2000. *PEST: Model Independent Parameter Estimation, Preface to the 4th Edition*. Watermark Numerical Computing.

Department of the Navy (DON). 1943. *Log of Formations in Tank Excavation, Tank Barrels 1–20 [1941–1943]*. Pacific Naval Air Bases.

———. 1996. *Phase I Remedial Investigation Report, Red Hill Oily Waste Disposal Facility, Fleet and Industrial Supply Center, Pearl Harbor, Oahu, Hawaii*. Prepared by Ogden Environmental and Energy Services Co., Inc., Honolulu, HI. Pearl Harbor, HI: Pacific Division, Naval Facilities Engineering Command. January.

———. 1999. *Initial Phase II Site Characterization Report, Fleet Industrial Supply Center Bulk Fuel Storage Facility at Red Hill*. Prepared by Ogden Environmental and Energy Services Co., Inc., Honolulu, HI. Pearl Harbor, HI: Pacific Division, Naval Facilities Engineering Command. March.

———. 2000. *Remedial Investigation Phase II, Red Hill Oily Waste Disposal Facility, Halawa, Oahu, Hawaii*. Prepared by Earth Tech, Inc., Honolulu, HI. Volume I, Technical Report. Pearl Harbor, HI: Pacific Division, Naval Facilities Engineering Command. September.

———. 2002. *Red Hill Bulk Fuel Storage Facility Investigation Report (Final) for Fleet Industrial Supply Center (FISC), Oahu, Hawaii*. Prepared by AMEC Earth & Environmental, Inc., Huntsville, AL. Pearl Harbor, HI: Pacific Division, Naval Facilities Engineering Command. August.

———. 2005. *Red Hill Bulk Fuel Storage Facility Work Plan, Pearl Harbor, Hawaii*. Prepared by The Environmental Company, Inc. (TEC), Honolulu, HI; and AMEC Earth & Environmental, Inc., Honolulu, HI. Pearl Harbor, HI: Naval Facilities Engineering Command, Pacific. June.

———. 2007. *Red Hill Bulk Fuel Storage Facility Final Technical Report, Pearl Harbor, Hawaii*. Prepared by TEC Inc., Honolulu, HI. Pearl Harbor, HI: Naval Facilities Engineering Command, Pacific. August.

———. 2008a. *Monthly Soil Vapor Monitoring Reports, Red Hill Bulk Fuel Storage Facility*. 2008–present. Prepared for Naval Facilities Engineering Command, Hawaii, JBPHH, HI.

———. 2008b. *Red Hill Bulk Fuel Storage Facility Final Groundwater Protection Plan, Pearl Harbor, Hawaii*. Prepared by TEC Inc. Includes December 2009 Revisions to the Red Hill Groundwater Protection Plan. Pearl Harbor, HI: Naval Facilities Engineering Command, Pacific. January.

———. 2008c. *Tank 17 Removal Action Report, Red Hill Fuel Storage Facility, Pearl Harbor, Oahu, Hawaii*. Prepared by TEC Inc., Honolulu, HI. Pearl Harbor, HI: Commander, Navy Region Hawaii, Environmental Department, Code N45. September.

———. 2010. *Type 1 Letter Report – Re-Evaluation of the Tier 3 Risk Assessment/Groundwater Model & Proposed Course of Action Red Hill Bulk Fuels Storage Facility, Pearl Harbor, HI*. Prepared by TEC Inc. Prepared for Naval Fleet Engineering Service Center and Pearl Harbor Naval Base Fleet Industrial Supply Center. May 4.

———. 2012. *FY11SRM Repair of Red Hill Fuel Tunnel, Geotechnical Data Report*. Prepared by URS Corporation. August 3.

———. 2014a. *Tank 5 Initial and Quarterly Release Response Reports, Red Hill Bulk Fuel Storage Facility, JBPHH, Oahu, Hawaii*. April 2014–present. Prepared by Commander Navy Region Hawaii Environmental Department, Code N45, JBPHH, HI.

———. 2014b. *Interim Update, Red Hill Bulk Fuel Storage Facility Final Groundwater Protection Plan, Pearl Harbor, Hawaii. (January 2008)*. Pearl Harbor, HI: Naval Facilities Engineering Command, Pacific. August.

———. 2015a. *Draft Monitoring Well Installation Report, Red Hill Bulk Fuel Storage Facility, Joint Base Pearl Harbor-Hickam, Hawaii*. Prepared by Battelle, Columbus, OH; and Parsons, South Jordan, UT. JBPHH HI: Naval Facilities Engineering Command, Hawaii. March.

———. 2015b. *Final Archaeological Inventory Survey of the Red Hill Fuel Facility, Joint Base Pearl Harbor-Hickam, O'ahu, Hawai'i. Tax Map Key (TMK): (1) 1-1-012:003 and 004 (Both, Portions); and TMK (1) 9-9-010:001, 006, 026 (All, Portions), and 050*. Prepared by International Archaeology, LLC, Honolulu, HI. Pearl Harbor, HI: Pacific Division, Naval Facilities Engineering Command. August.

———. 2015c. *Work Plan/Sampling and Analysis Plan, Long-Term Groundwater and Soil Vapor Monitoring, Red Hill Bulk Fuel Storage Facility, Joint Base Pearl Harbor-Hickam, Oahu,*

Hawaii. Prepared by Element Environmental, LLC, Aiea, HI. JBPHH HI: Naval Facilities Engineering Command, Hawaii. September.

———. 2015d. *Red Hill Tank Complex, Soil Vapor Sampling Results for August 2015*. Letter Report from A. Y. Poentis, Navy Region Hawaii, Regional Environmental Department; to: R. Takaba, Hawaii State Department of Health, Environmental Management Division, Solid and Hazardous Waste Branch, Underground Storage Tank Section. September 8.

———. 2016a. *3.2 Tank Upgrade Alternatives (TUA), Scope of Work Outline Final Submission, Red Hill Fuel Storage Facility, NAVSUP FLC Pearl Harbor, HI (PRL), Joint Base Pearl Harbor-Hickam*. Administrative Order on Consent In the Matter of Red Hill Bulk Fuel Storage Facility EPA Docket No. RCRA 7003-R9-2015 01 DOH Docket No. 15-UST-EA-01. Prepared by Enterprise Engineering, Inc., Freeport, ME. JBPHH HI: Naval Facilities Engineering Command, Pacific. September.

———. 2016b. *Monitoring Well Installation Work Plan, Red Hill Bulk Fuel Storage Facility, Joint Base Pearl Harbor-Hickam, O'ahu, Hawai'i; August 29, 2016*. Prepared by AECOM Technical Services, Inc., Honolulu, HI. Prepared for Defense Logistics Agency Energy, Fort Belvoir, VA, under Naval Facilities Engineering Command, Hawaii, JBPHH HI.

———. 2017a. *Work Plan / Scope of Work, Investigation and Remediation of Releases and Groundwater Protection and Evaluation, Red Hill Bulk Fuel Storage Facility, Joint Base Pearl Harbor-Hickam, O'ahu, Hawai'i; January 4, 2017, Revision 02*. Prepared by AECOM Technical Services, Inc., Honolulu, HI. Prepared for Defense Logistics Agency Energy, Fort Belvoir, VA, under Naval Facilities Engineering Command, Hawaii, JBPHH HI.

———. 2017b. *Existing Data Summary and Evaluation Report for Groundwater Flow and Contaminant Fate and Transport Modeling, Red Hill Bulk Fuel Storage Facility, Joint Base Pearl Harbor-Hickam, O'ahu, Hawai'i; March 5, 2017, Revision 00*. Prepared by AECOM Technical Services, Inc., Honolulu, HI. Prepared for Defense Logistics Agency Energy, Fort Belvoir, VA, under Naval Facilities Engineering Command, Hawaii, JBPHH HI.

———. 2017c. *Groundwater Flow Model Progress Report 01, Red Hill Bulk Fuel Storage Facility, Joint Base Pearl Harbor-Hickam, O'ahu, Hawai'i; April 5, 2017, Revision 00*. Prepared by AECOM Technical Services, Inc., Honolulu, HI. Prepared for Defense Logistics Agency Energy, Fort Belvoir, VA, under Naval Facilities Engineering Command, Hawaii, JBPHH HI.

———. 2017d. *Data Gap Analysis Report, Investigation and Remediation of Releases and Groundwater Protection and Evaluation, Red Hill Bulk Fuel Storage Facility, Joint Base Pearl Harbor-Hickam, O'ahu, Hawai'i; April 25, 2017, Revision 00*. Prepared by AECOM Technical Services, Inc., Honolulu, HI. Prepared for Defense Logistics Agency Energy, Fort Belvoir, VA, under Naval Facilities Engineering Command, Hawaii, JBPHH HI.

———. 2017e. *Groundwater Flow Model Progress Report 02, Red Hill Bulk Fuel Storage Facility, Joint Base Pearl Harbor-Hickam, O'ahu, Hawai'i; August 4, 2017, Revision 00*. Prepared by AECOM Technical Services, Inc., Honolulu, HI. Prepared for Defense Logistics Agency Energy, Fort Belvoir, VA, under Naval Facilities Engineering Command, Hawaii, JBPHH HI.

———. 2017f. *Monitoring Well Installation Work Plan Addendum 02, Investigation and Remediation of Releases and Groundwater Protection and Evaluation, Red Hill Bulk Fuel Storage Facility, Joint Base Pearl Harbor-Hickam, O'ahu, Hawai'i; August 25, 2017, Revision 00*. Prepared by AECOM Technical Services, Inc., Honolulu, HI. Prepared for Defense Logistics Agency Energy, Fort Belvoir, VA, under Naval Facilities Engineering Command, Hawaii, JBPHH HI.

———. 2017g. *Attenuation Evaluation Plan, Investigation and Remediation of Releases and Groundwater Protection and Evaluation, Red Hill Bulk Fuel Storage Facility, Joint Base Pearl Harbor-Hickam, O'ahu, Hawai'i; September 1, 2017, Revision 00*. Prepared by AECOM Technical Services, Inc., Honolulu, HI. Prepared for Defense Logistics Agency Energy, Fort Belvoir, VA, under Naval Facilities Engineering Command, Hawaii, JBPHH HI.

———. 2017h. *Sampling and Analysis Plan Addendum 01, Investigation and Remediation of Releases and Groundwater Protection and Evaluation, Red Hill Bulk Fuel Storage Facility, Joint Base Pearl Harbor-Hickam, O'ahu, Hawai'i; September 1, 2017, Revision 00*. Prepared by AECOM Technical Services, Inc., Honolulu, HI. Prepared for Defense Logistics Agency Energy, Fort Belvoir, VA, under Naval Facilities Engineering Command, Hawaii, JBPHH HI.

———. 2017i. *Groundwater Model Evaluation Plan, Investigation and Remediation of Releases and Groundwater Protection and Evaluation, Red Hill Bulk Fuel Storage Facility, Joint Base Pearl Harbor-Hickam, O'ahu, Hawai'i; September 8, 2017, Revision 00*. Prepared by AECOM Technical Services, Inc., Honolulu, HI. Prepared for Defense Logistics Agency Energy, Fort Belvoir, VA, under Naval Facilities Engineering Command, Hawaii, JBPHH HI.

———. 2017j. *Risk-Based Decision Criteria Development Plan, Investigation and Remediation of Releases and Groundwater Protection and Evaluation, Red Hill Bulk Fuel Storage Facility, Joint Base Pearl Harbor-Hickam, O'ahu, Hawai'i; December 11, 2017, Revision 00*. Prepared by AECOM Technical Services, Inc., Honolulu, HI. Prepared for Defense Logistics Agency Energy, Fort Belvoir, VA, under Naval Facilities Engineering Command, Hawaii, JBPHH HI.

———. 2017k. *Sentinel Well Network Development Plan, Investigation and Remediation of Releases and Groundwater Protection and Evaluation, Red Hill Bulk Fuel Storage Facility, Joint Base Pearl Harbor-Hickam, O'ahu, Hawai'i; December 11, 2017, Revision 00*. Prepared by AECOM Technical Services, Inc., Honolulu, HI. Prepared for Defense Logistics Agency Energy, Fort Belvoir, VA, under Naval Facilities Engineering Command, Hawaii, JBPHH HI.

———. 2018a. *Well Elevation Survey Report, Red Hill Bulk Fuel Storage Facility, Joint Base Pearl Harbor-Hickam, O'ahu, Hawai'i*. Prepared by AECOM Technical Services, Inc., Honolulu, HI. Prepared for Defense Logistics Agency Energy, Fort Belvoir, VA, under Naval Facilities Engineering Command, Hawaii, JBPHH HI.

———. 2018b. *Final Fourth Quarter 2017 - Quarterly Groundwater Monitoring Report, Red Hill Bulk Fuel Storage Facility, Joint Base Pearl Harbor-Hickam, O'ahu, Hawai'i*. Prepared by AECOM Technical Services, Inc. JBPHH HI: Naval Facilities Engineering Command, Hawaii. January.

———. 2018c. *Technical Memorandum, Testing and Verification of Packer Integrity at RHMW11, Red Hill Bulk Fuel Storage Facility, Joint Base Pearl Harbor-Hickam, O'ahu, Hawai'i; February 9, 2018*. JBPHH HI: Naval Facilities Engineering Command, Hawaii. February.

———. 2018d. *Seismic Profiling to Map Hydrostratigraphy in the Red Hill Area, Red Hill Bulk Fuel Storage Facility, Joint Base Pearl Harbor-Hickam, O'ahu, Hawai'i; March 30, 2018, Revision 00*. Prepared by Lee Liberty and James St. Claire, Boise State University, Boise, ID, For AECOM Technical Services, Inc., Honolulu, HI. Boise State University Technical Report BSU CGISS 18-01. Prepared for Defense Logistics Agency Energy, Fort Belvoir, VA, under Naval Facilities Engineering Command, Hawaii, JBPHH HI.

———. 2018e. *Final First Quarter 2018 - Quarterly Groundwater Monitoring Report, Red Hill Bulk Fuel Storage Facility, Joint Base Pearl Harbor-Hickam, O'ahu, Hawai'i*. Prepared by AECOM Technical Services, Inc. JBPHH HI: Naval Facilities Engineering Command, Hawaii. July.

Driscoll, F. G. 1986. *Groundwater and Wells*. 2nded. St. Paul, MN: Johnson Screens.

Environmental Chemical Corporation (ECC). 2000. *Removal of Underground Storage Tank TAMC 137-4, Building 137, Tripler Army Medical Center, Oahu, Hawaii*. Prepared for Department of Army Headquarters, United States Army Garrison, Hawaii. September.

Edward K. Noda and Associates, Inc. (EKNA). 1999. *Closure Report: Halawa Medium Security Facility, Existing UST Closure Actions, 99-902 Moanalua Road, Aiea, Hawaii, 96701*. Prepared for State of Hawaii, Department of Accounting and General Services Division of Public Works. June.

Engott, J. A., A. G. Johnson, M. Bassiouni, and S. K. Izuka. 2015. *Spatially Distributed Groundwater Recharge for 2010 Land Cover Estimated Using a Water-Budget Model for the Island of O'ahu, Hawai'i*. Scientific Investigations Report 2015–5010. Prepared in cooperation with the State of Hawai'i Commission on Water Resource Management and the City and County of Honolulu Board of Water Supply. U.S. Geological Survey.

Environmental Protection Agency, United States (EPA). 1989. *Risk Assessment Guidance for Superfund, Volume I: Human Health Evaluation Manual (Part A)*. Interim Final. EPA/540/1-89/002. Office of Emergency and Remedial Response. December.

———. 1995. *Light Nonaqueous Phase Liquids*. Ground Water Issue. EPA/540/S-95/500. Washington, DC: Office of Research and Development, Office of Solid Waste and Emergency Response. July.

———. 1999. *Use of Monitored Natural Attenuation at Superfund, RCRA Corrective Action, and Underground Storage Tank Sites*. OSWER 9200.4-17P. Office of Solid Waste and Emergency Response. April.

———. 2011. *Environmental Cleanup Best Management Practices: Effective Use of the Project Life Cycle Conceptual Site Model*. Quick Reference Fact Sheet. EPA 542-F-11-011. Office of Solid Waste and Emergency Response. July.

———. 2018. *Regional Screening Levels for Chemical Contaminants at Superfund Sites*. EPA Office of Superfund. May.

Environmental Protection Agency, United States, Region 9; and Department of Health, State of Hawaii (EPA Region 9 and DOH). 2015. *Administrative Order on Consent In the Matter of Red Hill Bulk Fuel Storage Facility, EPA Docket No: RCRA 7003-R9-2015-01; DOH Docket No: 15-UST-EA-01*. September.

———. 2016. "Final Scoping for AOC SOW Sections 6 and 7, and Navy's Proposed Chemical of Potential Concern (COPC) Recommendations," February 4, 2016. Letter from Bob Pallarino, EPA Red Hill Project Coordinator, and Steven Chang, DOH Red Hill Project Coordinator, to: James A. K. Miyamoto, Naval Facilities Engineering Command, Hawaii, Joint Base Pearl Harbor-Hickam.

Eyre, P. R. 1983. *The Effects of Pumpage, Irrigation Return, and Regional Ground-Water Flow on the Water Quality at Waiawa Water Tunnel, Oahu, Hawaii*. Water-Resources Investigations Report 83–4097. U.S. Geological Survey.

Eyre, P. R., C. Ewart, and P. J. Shade. 1986. *Hydrology of the Leeward Aquifers, Southeast Oahu, Hawaii: Regional Analysis of the Southern Oahu Ground-Water Flow System*. Water-Resources Investigations Report 85-4270. U.S. Geological Survey.

Garg, S., C. J. Newell, P. R. Kulkarni, D. C. King, D. T. Adamson, M. I. Renno, and T. Sale. 2017. "Overview of Natural Source Zone Depletion: Processes, Controlling Factors, and Composition Change." *Groundwater Monitoring & Remediation*, July. https://doi.org/10.1111/gwmr.12219.

Gingerich, S. B., and C. I. Voss. 2005. "Three-Dimensional Variable-Density Flow Simulation of a Coastal Aquifer in Southern Oahu, Hawaii, USA." *Hydrogeology Journal* 13 (2): 436–450. https://doi.org/10.1007/s10040-004-0371-z.

Gonthier, G. J. 2007. *A Graphical Method for Estimation of Barometric Efficiency from Continuous Data—Concepts and Application to a Site in the Piedmont, Air Force Plant 6, Marietta, Georgia*. Scientific Investigation Report 2007-5111. Prepared in cooperation with the U.S. Air Force Aeronautical Systems Center, Marietta, Georgia. U.S. Geological Survey.

Hem, J. D. 1985. *Study and Interpretation of the Chemical Characteristics of Natural Water*. Water-Supply Paper 2254. 3rd Ed. U.S. Geological Survey.

Hillel, D. 1982. *Introduction to Soil Physics*. San Diego, CA: Academic Press.

Hua, Q., M. Barbetti, and A. Z. Rakowski. 2013. "Atmospheric Radiocarbon for the Period 1950–2010." *Radiocarbon* 55 (4): 2059–72.

Hunt Jr., C. D. 1996. *Geohydrology of the Island of Oahu, Hawaii*. Professional Paper 1412-B. Regional Aquifer-System Analysis—Oahu, Hawaii. U.S. Geological Survey.

Huntley, D., and G. D. Beckett. 2002. *Evaluating Hydrocarbon Removal from Source Zones and Its Effect on Dissolved Plume Longevity and Magnitude*. API Publication 4715. American Petroleum Institute, Regulatory Analysis and Scientific Affairs Department.

Hutcheson, M. S., D. Pedersen, N. D. Anastas, J. Fitzgerald, and D. Silverman. 1996. "Beyond TPH: Health-Based Evaluation of Petroleum Hydrocarbon Exposures." *Regulatory Toxicology and Pharmacology* 24 (1): 85–101. https://doi.org/10.1006/rtph.1996.0066.

Hvorslev, M.J. 1951. "Time Lag and Soil Permeability in Ground-Water Observations." Bulletin No. 36. Vicksburg, MS: Waterways Experiment Station, Corps of Engineers, U.S. Army. April.

Isobe, K. 2016. "Navy Intensifies Modernization of Red Hill Bulk Fuel Storage Facility." *Currents—The Navy's Energy and Environmental Magazine*, Fall 2016.

Interstate Technology & Regulatory Council (ITRC). 2008. *LNAPL Training Part 2: LNAPL Characterization and Recoverability – Improved Analysis*. ITRC Internet-Based Training Program. Co-sponsored by the EPA Office of Superfund Remediation and Technology Innovation.

———. 2009a. *Evaluating Natural Source Zone Depletion at Sites with LNAPL*. LNAPL-1. Prepared by the ITRC LNAPLs Team. April.

———. 2009b. *Evaluating LNAPL Remedial Technologies for Achieving Project Goals*. LNAPL-2. Washington, DC: Prepared by the ITRC LNAPLs Team. December.

Izuka, S. K. 1992. *Geology and Stream Infiltration of North Halawa Valley, Oahu, Hawaii*. Prepared in cooperation with the State of Hawaii Department of Transportation. Honolulu, HI. Water-Resources Investigations Report 91-4197. U.S. Geological Survey.

Izuka, S. K., J. A. Engott, K. Rotzoll, M. Bassiouni, A. G. Johnson, L. D. Miller, and A. Mair. 2018. *Volcanic Aquifers of Hawai'i—Hydrogeology, Water Budgets, and Conceptual Models*. Ver. 2.0, March 2018. Scientific Investigations Report 2015–5164. Water Availability and Use Science Program. U.S. Geological Survey.

Kao, C. M., W. Y. Huang, L. J. Chang, T. Y. Chen, H. Y. Chien, and F. Hou. 2006. "Application of Monitored Natural Attenuation to Remediate A Petroleum-Hydrocarbon Spill Site." *Water Science & Technology* 53 (2): 321–328.

Kimura International, Inc. (Kimura). 2000. *Release Response Report: City & County of Honolulu, Halawa Bus Facility, 99-999 Iwaena Street, Honolulu, Hawaii*. Prepared for Fuel Oil Polishing Company, Inc. August.

Landmeyer, J. E., F. H. Chapelle, M. D. Petkewich, and P. M. Bradley. 1998. "Assessment of Natural Attenuation of Aromatic Hydrocarbons in Groundwater Near A Former Manufactured-Gas Plant, South Carolina, USA." *Environmental Geology* 34 (4): 279–292.

Langenheim, V. M., and D. A. Clague. 1987. "The Hawaiian-Emperor Volcanic Chain, Part II, Stratigraphic Framework of Volcanic Rocks of the Hawaiian Islands." In *Volcanism in Hawaii*, v. 1, chap. 1, pp. 55–84. Professional Paper 1350. U.S. Geological Survey.

Macdonald, G. A. 1941. *Geology of the Red Hill and Waimalu Areas, Oahu, in Relation to the Underground Fuel Storage Project of the U.S. Navy*. February 21, 1941 Report Attachment to Letter from H. T. Stearns, U.S. Geological Survey Geologist in Charge, Hawaiian Ground-Water Investigations, to: Capt. H. F. Bruns, Public Works Office, Pearl Harbor, February 26, 1941. Honolulu, HI: U.S. Geological Survey.

McCoy, K., J. Zimbron, T. Sale, and M. Lyverse. 2014. "Measurement of Natural Losses of LNAPL Using CO_2 Traps." *Groundwater* 53: 658–667.

Mink, John F. 1980. *State of the Groundwater Resources of Southern Oahu*. Honolulu, HI: Board of Water Supply, City and County of Honolulu.

Mink, John F., and L. Stephen Lau. 1990. *Aquifer Identification and Classification for Oahu: Groundwater Protection Strategy for Hawaii*. Technical Report No. 179. Honolulu, HI: University of Hawaii, Water Resources Research Center. November 1987; rev. February 1990.

Naval Facilities Engineering Command, Engineering and Expeditionary Warfare Center (NAVFAC EXWC). 2016. *Red Hill Facility Tank Inspection, Repair, and Maintenance Report, Administrative Order on Consent (AOC) Statement of Work (SOW), Section 2.2*. Site Specific Report SSR-NAVFAC EXWC-CI-1655. 11 October.

Ng, G.-H. C., B. A. Bekins, I. M. Cozzarelli, M. J. Baedecker, P. C. Bennett, and R. T. Amos. 2014. "A Mass Balance Approach to Investigating Geochemical Controls on Secondary Water Quality Impacts at a Crude Oil Spill Site Near Bemidji, MN." *Journal of Contaminant Hydrology* 164: 1–15. https://doi.org/10.1016/j.jconhyd.2014.04.006.

Ng, G.-H. C., B. A. Bekins, I. M. Cozzarelli, M. J. Baedecker, P. C. Bennett, R. T. Amos, and W. N. Herkelrath. 2015. "Reactive Transport Modeling of Geochemical Controls on Secondary Water Quality Impacts at a Crude Oil Spill Site Near Bemidji, MN." *Water Resources Research* 51: 4156–183. https://doi.org/10.1002/2015WR016964.

Nichols, W. D., P. J. Shade, and C. D. Hunt Jr. 1996. *Summary of the Oahu, Hawaii, Regional Aquifer-System Analysis*. Professional Paper 1412-A. Regional Aquifer-System Analysis—Oahu, Hawaii. U.S. Geological Survey.

National Park Service (NPS). 2015. *Historic American Engineering Record: U.S. Naval Base, Pearl Harbor, Red Hill Underground Fuel Storage System*. Photographs; Written Historical and Descriptive Data. Washington, DC: U.S. Department of the Interior.

Oki, D. S. 1998. *Geohydrology of the Central Oahu, Hawaii, Ground-Water Flow System and Numerical Simulation of the Effects of Additional Pumping*. Water-Resources Investigations

Report 97–4276. Prepared in Cooperation with the Honolulu Board of Water Supply. U.S. Geological Survey.

———. 2005. *Numerical Simulation of the Effects of Low-Permeability Valley-Fill Barriers and the Redistribution of Ground-Water Withdrawals in the Pearl Harbor Area, Oahu, Hawaii*. Scientific Investigations Report 2005-5253. U.S. Geological Survey.

Oki, D. S., and A. Brasher. 2003. *Environmental Setting and the Effects of Natural and Human-Related Factors on Water Quality and Aquatic Biota, Oahu, Hawaii*. Water-Resources Investigations Report 03-4156. Honolulu, HI: U.S. Geological Survey.

Oki, D. S., S. B. Gingerich, and R. L. Whitehead. 1999. "Hawaii." In *Ground Water Atlas of the United States: Segment 13 - Alaska, Hawaii, Puerto Rico and the U.S. Virgin Islands*. HA 730-N. U.S. Geological Survey.

Oki, D. S., W. R. Souza, E. I. Bolke, and G. R. Bauer. 1996. *Numerical Analysis of Ground-Water Flow and Salinity in the Ewa Area, Oahu, Hawaii*. Open-File Report 96-442. Prepared in Cooperation with the State of Hawaii Commission on Water Resource Management. U.S. Geological Survey.

Presley, T. K., J. M. Sinton, and M. Pringle. 1997. "Postshield Volcanism and Catastrophic Mass Wasting of the Waianae Volcano, Oahu, Hawaii." *Bulletin of Volcanology* 58 (8): 597–616. https://doi.org/10.1007/s004450050165.

Red Hill Fuel Storage Facility Task Force, State of Hawai'i (RHSF Task Force). 2014. *Report to the Twenty-Eighth Legislature, State of Hawaii, 2015, Pursuant To Senate Concurrent Resolution 73 Requesting the Department of Health to Convene a Task Force to Study the Effects of the January 2014 Fuel Tank Leak at the Red Hill Fuel Storage Facility*. December.

Rockhold, M. L., R. R. Yarwood, and J. S. Selker. 2004. "Coupled Microbial and Transport Processes in Soils." *Vadose Zone J.* 3: 368–383. https://doi.org/10.2113/3.2.368.

Rosenau, J. C., E. R. Lubke, and R. H. Nakahara. 1971. *Water Resources of North-Central Oahu, Hawaii*. Geological Survey Water-Supply Paper 1899-D. Prepared in cooperation with the State of Hawaii, Department of Land and Natural Resources, Division of Water and Land Development. U.S. Geological Survey.

Rotzoll, K. 2012. *Numerical Simulation of Flow in Deep Open Boreholes in a Coastal Freshwater Lens, Pearl Harbor Aquifer, O'ahu, Hawai'i*. Scientific Investigations Report 2012-5009. Prepared in Cooperation with the Honolulu Board of Water Supply. Reston, VA: U.S. Geological Survey.

———. 2014. "Addendum to Rotzoll and El-Kadi (2007) Numerical Ground-Water Flow Simulation for Red Hill Fuel Storage Facilities, NAVFAC Pacific, Oahu, Hawaii." To: J. Shimabuku, NAVFAC HI; E. Lau, HBWS; cc: R. Whittier, HDOH; A. El-Kadi, University of Hawaii. January 29. Water Resources Research Center, University of Hawaii.

Rotzoll, K., and A. I. El-Kadi. 2007. *Numerical Ground-Water Flow Simulation for Red Hill Fuel Storage Facilities, NAVFAC Pacific, Oahu, Hawaii*. Prepared for The Environmental Company (TEC). Appendix L in: Department of the Navy (2007), *Red Hill Bulk Fuel Storage Facility Final Technical Report, Pearl Harbor, Hawaii*; Naval Facilities Engineering Command, Pacific. Honolulu, HI: University of Hawaii, Water Resources Research Center. August.

Rotzoll, K., A. I. El-Kadi, and S. B. Gingerich. 2007. "Estimating Hydraulic Properties of Volcanic Aquifers Using Constant-Rate and Variable-Rate Aquifer Tests." *JAWRA Journal of the American Water Resources Association* 43 (2): 334–345. https://doi.org/10.1111/j.1752-1688.2007.00026.x.

Shade, P. J., and W. D. Nichols. 1996. *Water Budget and the Effects of Land-Use Changes on Ground-Water Recharge, Oahu, Hawaii*. Professional Paper 1412-C. Regional Aquifer-System Analysis—Oahu, Hawaii. U.S. Geological Survey.

Sherrod, D. R., J. M. Sinton, S. E. Watkins, and K. M. Brunt. 2007. "Geologic Map of the State of Hawai'i, Sheet 3—Island of O'ahu." Open-File Report 2007-1089.

Soroos, R. L. 1973. *Determination of Hydraulic Conductivity of Some Oahu Aquifers with Step-Drawdown Test Data*. M.S. Thesis, Univ. of Hawaii, Honolulu, HI.

Souza, W. R., and C. I. Voss. 1987. "Analysis of an Anisotropic Coastal Aquifer System Using Variable-Density Flow and Solute Transport Simulation." *Journal of Hydrology* 92 (1–2): 17–41.

Stearns, H. T. 1939. *Geologic Map and Guide of the Island of Oahu, Hawaii*. Bulletin 2. Prepared in cooperation with the Geological Survey. Honolulu: Hawaii (Terr.) Department of Public Lands, Division of Hydrography.

———. 1943. "Letter from H. T. Stearns, Senior Geologist, U.S. Geological Survey, to: O. E. Meinzer, Division of Ground Water, U.S. Geological Survey, Washington, DC," January 18, 1943.

———. 1978. *Quaternary Shorelines in the Hawaiian Islands*. Bernice P. Bishop Museum Bulletin 237. Honolulu, HI: Bishop Museum Press.

Stearns, H. T., and T. K. Chamberlain. 1967. "Deep Cores of Oahu, Hawaii and Their Bearing on the Geologic History of the Central Pacific Basin." *Pacific Science* 21 (2): 153–165.

Stearns, H. T., and K. N. Vaksvik. 1935. *Geology and Groundwater Resources of the Island of Oahu, Hawaii*. Bulletin 1. Prepared in cooperation with the Geological Survey. Honolulu: Hawaii (Terr.) Department of Public Lands, Division of Hydrography.

Takasaki, K. J., and S. Valenciano. 1969. *Water in the Kahuku Area, Oahu, Hawaii*. Water Supply Paper 1874. U.S. Geological Survey.

United States Department of Agriculture, Soil Conservation Service (USDA SCS). 1972. *Soil Survey of Islands of Kauai, Oahu, Maui, Molokai, and Lanai, State of Hawaii*. In cooperation with the University of Hawaii Agricultural Experiment Station. Washington, DC. August. https://www.nrcs.usda.gov/wps/portal/nrcs/surveylist/soils/survey/state/?stateId=HI.

United States Geological Survey (USGS). 2003. *Environmental Settings and Effects of Natural and Human-Related Factors on Water Quality and Aquatic Biota, Oahu, Hawaii*. Water Resources Investigation Report 03-4156.

———. 2017a. *National Water Information System - Moanalua Precipitation Gauge*. https://nwis.waterdata.usgs.gov/nwis/inventory/?site_no=212359157502601&agency_cd=USGS. Accessed October 2017.

———. 2017b. *National Water Information System - North Halawa Valley Precipitation Gauge*. https://nwis.waterdata.usgs.gov/nwis/inventory/?site_no=212428157511201&agency_cd=USGS. Accessed October 2017.

———. 2017c. *USGS 212304157542201 771.9 N Halawa Rain Gage Nr Honolulu, Oahu, HI*. https://waterdata.usgs.gov/nwis/dv?cb_00045=on&format=html&site_no=212304157542201&referred_module=sw&period=&begin_date=2005-01-01&end_date=2017-07-07. Accessed July 2017.

———. 2017d. *USGS 212346157533701 772.1 N Halawa Rain Gage Nr Aiea, Oahu, HI*. https://waterdata.usgs.gov/nwis/dv?cb_00045=on&format=html&site_no=212346157533701&re

ferred_module=sw&period=&begin_date=2005-01-01&end_date=2017-07-06. Accessed July 2017.

———. 2017e. *Final Synoptic Water Level Study Work Plan, Hālawa Area, O'ahu, Hawai'i*. Honolulu, HI: Pacific Islands Water Science Center. August 10.

Visher, F. N., and J. F. Mink. 1964. *Ground-Water Resources in Southern Oahu, Hawaii*. Geological Survey Water Supply Paper 1778. Prepared in Cooperation with the State of Hawaii, Department of Land and Natural Resources, Division of Water and Land Development. U.S. Geological Survey.

Walker, G. P. L. 1990. "Geology and Volcanology of the Hawaiian Islands." *Pacific Science* 44 (4): 315–347.

Wentworth, C. K. 1938. *Geology and Ground Water Resources of the Palolo-Waialae District*. Honolulu, HI: Board of Water Supply.

———. 1951. *Geology and Groundwater Resources of the Honolulu-Pearl Harbor Area, Oahu, Hawaii*. Honolulu, HI: City and County of Honolulu, Board of Water Supply.

Wentworth, C. K., and G. A. MacDonald. 1953. *Structures and Forms of Basaltic Rocks in Hawaii*. Geological Survey Bulletin 994. U.S. Geological Survey.

Whittier, R. B., K. Rotzoll, S. Dhal, A. I. El-Kadi, C. Ray, and D. Chang. 2010. "Groundwater Source Assessment Program for the State of Hawaii, USA: Methodology and Example Application." *Hydrogeology Journal* 18 (3): 711–723. https://doi.org/10.1007/s10040-009-0548-6.

Whittier, R. B., K. Rotzoll, S. Dhal, A. I. El-Kadi, C. Ray, G. Chen, and D. Chang. 2004. *Hawaii Source Water Assessment Report*. Prepared for the Hawai'i Department of Health, Safe Drinking Water Branch. University of Hawai'i, Water Resources Research Center.

Wiedemeier, T. H., H. S. Rifai, C. J. Newell, and J. T. Wilson. 1999. *Natural Attenuation of Fuels and Chlorinated Solvents in the Subsurface*. New York: John Wiley & Sons, Inc.

Wiedemeier, T. H., J. T. Wilson, D. H. Kampbell, R. N. Miller, and J. E. Hansen. 1999a. *Technical Protocol for Implementing Intrinsic Remediation with Long-Term Monitoring for Natural Attenuation of Fuel Contamination Dissolved in Groundwater. Vols. I & II*. San Antonio, TX: Air Force Center for Environmental Excellence, Technology Transfer Division. March.

———. 1999b. *Technical Protocol for Implementing Intrinsic Remediation with Long-Term Monitoring for Natural Attenuation of Fuel Contamination Dissolved in Groundwater. Volume II*. San Antonio, TX: Air Force Center for Environmental Excellence, Technology Transfer Division. March.

Williams, J. A., and R. L. Soroos. 1973. *Evaluation of Methods of Pumping Test Analyses for Application to Hawaiian Aquifers*. Technical Report No. 70. Submitted to Board of Water Supply, City and County of Honolulu, Honolulu, HI.

Appendix A:
Cumulative Historical Groundwater Monitoring Results and COPC Concentration Graphs (DON 2018e)

This page intentionally left blank

Appendix A.1:
Cumulative Historical Groundwater Monitoring Results

Table A.1-1: Cumulative Groundwater COPC Results
First Quarter 2018 - Quarterly Groundwater Monitoring Report, Red Hill Bulk Fuel Storage Facility, JBPHH, O'ahu, Hawai'i

			Method	8015						8260					8260SIM		8011	8270			8270/8270 Mod.	
				TPH-d	TPH-g ****	TPH-o	TPH-g ****	1,2-Dibromoethane *****	1,2-Dichloroethane *****	Benzene	Ethylbenzene	Naphthalene	Toluene	Xylenes, Total (p/m-, o-xylene)	1,2-Dibromoethane *****	1,2-Dichloroethane *****	1,2-Dibromoethane *****	1-Methylnaphthalene	2-Methylnaphthalene	Naphthalene	Phenol	2-(2-Methoxyethoxy)-ethanol
			Unit	(µg/L)	(µg/L)	(µg/L)	(µg/L)	(µg/L)	(µg/L)	(µg/L)	(µg/L)	(µg/L)	(µg/L)	(µg/L)	(µg/l)	(µg/L)	(µg/L)	(µg/L)	(µg/L)	(µg/L)	(µg/L)	(µg/L)
			Screening Criterion	400	300	500	300	0.04	5.0	5.0	30	17	40	20	0.04	5.0	0.04	10	10	17	300	800
			SSRBL	4500	—	—	—	—	—	750	—	—	—	—	—	—	—	—	—	—	—	—
Well Name	Sample ID	Date Sampled		Result	Result	Result	Result	Result	Result	Result	Result	Result	Result	Result	Result	Result	Result	Result	Result	Result	Result	Result
RHMW2254-01	RH-B-001	2/16/2005[be]		< 50 U	< 50 U	< 100 U	—	<0.0083 U	< 0.50 U	< 0.50 U	< 0.50 U	—	**1.0**	< 0.50 U	—	—	—	—	< 0.020 U	< 0.020 U	—	—
	RH-B-002	2/16/2005[bf]		< 53 U	< 50 U	< 110 U	—	<0.0081 U	< 0.50 U	< 0.50 U	< 0.50 U	—	**1.2**	< 0.50 U	—	—	—	—	< 0.022 U	< 0.022 U	—	—
	RH-B-003	2/16/2005*[bf]		< 50 U	< 50 U	< 100 U	—	<0.0082 U	< 0.50 U	< 0.50 U	< 0.50 U	—	**0.81**	< 0.50 U	—	—	—	—	< 0.021 U	< 0.021 U	—	—
	RH-B-004	6/28/2005[ae]		**43 J**	< 13 U	—	—	< 0.00096 U	< 0.50[b] U	< 0.50[b] U	< 0.50[b] U	—	< 0.50[b] U	< 0.50[b] U	—	—	—	—	< 0.020[b] U	< 0.020[b] U	—	—
	RH-B-005	6/28/2005*[ae]		**67 Z**	< 13 U	—	—	< 0.00096 U	< 0.50[b] U	< 0.50[b] U	< 0.50[b] U	—	< 0.50[b] U	< 0.50[b] U	—	—	—	—	< 0.020[b] U	< 0.020[b] U	—	—
	RH-B-006	6/28/2005*[af]		**58 Z**	< 13 U	—	—	< 0.00096 U	< 0.50[b] U	< 0.50[b] U	< 0.50[b] U	—	< 0.50[b] U	< 0.50[b] U	—	—	—	—	< 0.021[b] U	< 0.021[b] U	—	—
	RH-B-007	9/8/2005[ae]		**45 J**	< 13 U	**59 J**	—	< 0.00096 U	< 0.12 U	< 0.14 U	< 0.13 U	—	< 0.11 U	< 0.22 U	—	—	—	—	< 0.020[b] U	**0.085**	—	—
	RH-B-008	9/8/2005[af]		< 50 U	< 13 U	< 28 U	—	< 0.00096 U	< 0.12 U	< 0.14 U	< 0.13 U	—	< 0.11 U	< 0.22 U	—	—	—	—	< 0.020[b] U	< 0.020[b] U	—	—
	RH-B-009	9/8/2005*[af]		< 50[d] U	< 13 U	<100[d] U	—	< 0.00096 U	< 0.12 U	< 0.14 U	< 0.13 U	—	< 0.11 U	< 0.22 U	—	—	—	—	< 0.020[b] U	**0.045**	—	—
	RHMW2254W01	9/20/2005[bd]		—	—	—	—	< 0.50 U	< 0.50 U	< 0.50 U	< 0.50 U	< 1.0 U	< 0.50 U	< 0.50 U	—	—	—	—	—	—	—	—
	RH-B-010	12/6/2005[ae]		**38 J**	< 13 U	—	—	< 0.0096[b] U	< 0.12 U	< 0.14 U	< 0.13 U	—	< 0.11 U	< 0.22 U	—	—	—	—	**0.038**	**0.036**	—	—
	RH-B-011	12/6/2005*[ae]		**24 J**	< 13 U	—	—	< 0.0094[b] U	< 0.12 U	< 0.14 U	< 0.13 U	—	< 0.11 U	< 0.22 U	—	—	—	—	**0.022**	**0.024**	—	—
	RH-B-012	12/7/2005[af]		< 20 U	< 13 U	—	—	< 0.0095[b] U	< 0.12 U	< 0.14 U	< 0.13 U	—	< 0.11 U	< 0.22 U	—	—	—	—	**0.0071 J**	**0.011 J**	—	—
	RHMW2254-01-GW02	7/10/2006[ad]		< 110 U	< 50 U	—	—	< 0.50 U	< 0.50 U	< 0.50 U	< 0.50 U	< 1.0 U	< 0.50 U	< 0.50 U	—	—	—	< 0.26 U	< 0.26 U	< 0.26 U	—	—
	RHMW2254-01-GW06	12/5/2006[ad]		< 100 U	< 50 U	—	—	< 0.50 U	< 0.50 U	< 0.50 U	< 0.50 U	< 1.0 U	< 0.50 U	< 0.50 U	—	—	—	< 0.25 U	< 0.25 U	< 0.25 U	—	—
	RHMW2254-01-WG07	3/27/2007[a]		< 98 U	< 50 U	—	—	< 0.50 U	< 0.50 U	< 0.50 U	< 0.50 U	< 1.0 U	< 0.50 U	< 0.50 U	—	—	—	< 0.24 U	< 0.24 U	< 0.24 U	—	—
	RHMW2254-01-WG08	6/12/2007[a]		< 98 U	< 50 U	—	—	< 0.50 U	< 0.50 U	< 0.50 U	< 0.50 U	< 1.0 U	< 0.50 U	< 0.50 U	—	—	—	< 0.25 U	< 0.25 U	< 0.25 U	—	—
	RHMW2254-01-WG0	9/10/2007[a]		< 97 U	< 50 U	—	—	< 0.20 U	< 0.20 U	< 0.20 U	< 0.20 U	< 0.44 U	< 0.27 U	< 0.36 U	—	—	—	< 0.25 U	< 0.25 U	< 0.25 U	—	—
	RHMW2254-01-WG10	1/15/2008[a]		< 102 U	< 10.0 U	—	—	< 0.310 U	< 0.150 U	< 0.120 U	< 0.310 U	< 0.620 U	< 0.310 U	< 0.620 U	—	—	—	< 0.0150 U	< 0.0150 U	< 0.0310 U	—	—
	RHMW2254-01-WG10.1	2/6/2008[a]		< 100 U	—	—	—	—	—	—	—	—	—	—	—	—	—	—	—	—	—	—
	RHMW2254-01-WG10.1	2/6/2008[a]		< 10.3 U	—	—	—	—	—	—	—	—	—	—	—	—	—	—	—	—	—	—
	RHMW2254-01-WG11	4/15/2008[a]		< 86.0 U	< 10.0 U	—	—	< 0.310 U	< 0.150 U	< 0.120 U	< 0.310 U	< 0.620 U	< 0.310 U	< 0.620 U	—	—	—	**0.0435 J**	**0.0561**	< 0.0332 U	—	—
	RHMW2254-01-WG12	7/29/2008[a]		< 83.3 U	< 10.0 U	—	—	< 0.310 U	< 0.150 U	< 0.120 U	< 0.310 U	< 0.620 U	< 0.310 U	< 0.620 U	—	—	—	< 0.0156 U	< 0.0156 U	< 0.0323 U	—	—
	RHMW2254-01-WG13	10/22/2008[a]		< 84.2 U	< 10.0 U	—	—	< 0.310 U	< 0.150 U	< 0.120 U	< 0.310 U	< 0.620 U	< 0.310 U	< 0.620 U	—	—	—	**0.0276 J**	< 0.0150 U	**0.0466 J**	—	—
	RHMW2254-WG13B	12/16/2008[c]		—	—	—	—	< 0.310 U	< 0.150 U	< 0.120 U	< 0.310 U	< 0.620 U	< 0.310 U	< 0.93 U	—	—	—	—	—	—	—	—
	RHMWA01-WG13B	12/16/2008*[c]		—	—	—	—	< 0.310 U	< 0.150 U	< 0.120 U	< 0.310 U	< 0.620 U	< 0.310 U	< 0.93 U	—	—	—	—	—	—	—	—
	RHMW2254-01-WG14	2/4/2009[a]		< 92.0 U	**14.0 J**	—	—	< 0.310 U	< 0.150 U	< 0.120 U	< 0.310 U	< 0.620 U	< 0.310 U	< 0.620 U	—	—	—	< 0.0161 U	< 0.0161 U	< 0.0333 U	—	—
	RHMW2254-01-WG15	5/13/2009[a]		< 169 U	**19.1 J**	—	—	< 0.310 U	< 0.150 U	< 0.120 U	< 0.310 U	< 0.620 U	< 0.310 U	< 0.620 U	—	—	—	< 0.0156 U	**0.0180 J**	< 0.0323 U	—	—
	RHMW2254-01-WG16	7/15/2009[a]		< 163 U	< 30.0 U	—	—	< 0.310 U	< 0.150 U	< 0.120 U	< 0.310 U	< 0.620 U	< 0.310 U	< 0.620 U	—	—	—	< 0.0165 U	< 0.0165 U	< 0.0341 U	—	—
	RHMW2254-WG17	10/14/2009[a]		< 158 U	< 30 U	—	—	< 0.31 U	< 0.15 U	< 0.12 U	< 0.31 U	< 0.62 U	< 0.31 U	< 1 U	—	—	—	< 0.017 U	< 0.017 U	< 0.0352 U	—	—
	RHMW2254-01-WG18	1/27/2010		< 320 U	< 60.0 U	—	—	< 0.620 U	< 0.300 U	< 0.240 U	< 0.620 U	< 1.24 U	< 0.620 U	< 1.24 U	—	—	—	< 0.0316 U	< 0.0316 U	**0.0375 J**	—	—
	RHMW2254-01-WG19	4/13/2010		< 320 U	< 60.0 U	—	—	< 0.620 U	< 0.300 U	< 0.240 U	< 0.620 U	< 1.24 U	< 0.620 U	< 1.24 U	—	—	—	< 0.0330 U	< 0.0330 U	< 0.0682 U	—	—
	RHMW2254-01-WG20	7/13/2010		< 320 U	< 60.0 U	—	—	< 0.620 U	< 0.300 U	< 0.240 U	< 0.620 U	< 1.24 U	< 0.620 U	< 1.24 U	—	—	—	< 0.0320 U	< 0.0320 U	< 0.0664 U	—	—
	ES004	10/19/2010		< 80.0 U	—	—	< 12.12 U	< 0.40 U	< 0.28 U	< 0.32 U	< 0.46 U	—	< 0.34 U	< 0.38 U	—	—	—	< 0.12 U	< 0.12 U	< 0.10 U	—	—
	ES014	1/20/2011		< 80.8 U	—	—	< 12.12 U	< 0.40 U	< 0.28 U	< 0.32 U	< 0.46 U	—	< 0.34 U	< 0.38 U	—	—	—	< 0.12 U	< 0.12 U	< 0.10 U	—	—
	ES019	4/19/2011		< 80.8 U	—	—	< 12.12 U	< 0.40 U	< 0.28 U	< 0.32 U	< 0.46 U	—	< 0.34 U	< 0.38 U	—	—	—	< 0.12 U	< 0.12 U	< 0.10 U	—	—
	ES040	7/20/2011		< 80.8 U	—	< 212.0 U	< 12.12 U	< 0.40 U	< 0.28 U	< 0.32 U	< 0.46 U	—	< 0.34 U	< 0.38 U	—	—	—	< 0.12 U	< 0.12 U	< 0.10 U	—	—
	ES050	10/25/2011		< 80.8 U	—	—	< 12.12 U	< 0.40 U	< 0.28 U	< 0.32 U	< 0.46 U	—	< 0.34 U	< 0.38 U	—	—	—	< 0.12 U	< 0.12 U	< 0.10 U	—	—
	ES062	2/1/2012		< 80.8 U	—	—	< 12.12 U	< 0.40 U	< 0.28 U	< 0.32 U	< 0.46 U	—	< 0.34 U	< 0.38 U	—	—	—	< 0.12 U	< 0.12 U	< 0.10 U	—	—
	ES074	4/17/2012		< 80.8 U	—	—	< 12.12 U	< 0.40 U	< 0.28 U	< 0.32 U	< 0.46 U	—	< 0.34 U	< 0.38 U	—	—	—	< 0.12 U	< 0.12 U	< 0.10 U	—	—
	ES077	7/17/2012		< 80.8 U	—	< 212.0 U	< 12.12 U	< 0.40 U	< 0.28 U	< 0.32 U	< 0.46 U	—	< 0.34 U	< 0.38 U	—	—	—	< 0.12 U	< 0.12 U	< 0.10 U	—	—
	ES006	10/22/2012		< 20 U	—	—	**18 BJ**	< 0.50 U	< 0.50 U	< 0.50 U	< 0.50 U	—	**0.71 J**	< 1.0 U	—	—	—	< 0.050 U	< 0.050 U	**0.037 J**	—	—
	ES014	1/29/2013		**22 J,HD**	—	—	< 30 U	< 0.50 U	< 0.50 U	< 0.50 U	< 0.50 U	—	< 0.50 U	< 1.0 U	—	—	—	< 0.050 U	< 0.050 U	**0.052 J**	—	—
	ES023	4/23/2013		< 20 U	—	—	< 30 U	< 0.50 U	< 0.50 U	< 0.50 U	< 0.50 U	—	< 0.50 U	< 1.0 U	—	—	—	< 0.051 U	< 0.051 U	< 0.051 U	—	—
	ES032	7/23/2013		< 20 U	—	—	< 30 U	< 0.50 U	< 0.50 U	< 0.50 U	< 0.50 U	—	< 0.50 U	< 1.0 U	—	—	—	< 0.050 U	< 0.050 U	**0.099 J**	—	—

Table A.1-1: Cumulative Groundwater COPC Results (cont'd)
First Quarter 2018 - Quarterly Groundwater Monitoring Report, Red Hill Bulk Fuel Storage Facility, JBPHH, O'ahu, Hawai'i

		Method	8015						8260					8260SIM		8011	8270			8270/8270 Mod.	
			TPH-d	TPH-g ****	TPH-o	TPH-g ****	1,2-Dibromoethane *****	1,2-Dichloroethane *****	Benzene	Ethylbenzene	Naphthalene	Toluene	Xylenes, Total (p/m-, o-xylene)	1,2-Dibromoethane *****	1,2-Dichloroethane *****	1,2-Dibromoethane *****	1-Methylnaphthalene	2-Methylnaphthalene	Naphthalene	Phenol	2-(2-Methoxyethoxy)-ethanol
		Unit	(µg/L)	(µg/L)	(µg/L)	(µg/L)	(µg/L)	(µg/L)	(µg/L)	(µg/L)	(µg/L)	(µg/L)	(µg/L)	(µg/l)	(µg/L)	(µg/L)	(µg/L)	(µg/L)	(µg/L)	(µg/L)	(µg/L)
		Screening Criterion	400	300	500	300	0.04	5.0	5.0	30	17	40	20	0.04	5.0	0.04	10	10	17	300	800
		SSRBL	4500	—	—	—	—	—	750	—	—	—	—	—	—	—	—	—	—	—	—
Well Name	Sample ID	Date Sampled	Result	Result	Result	Result	Result	Result	Result	Result	Result	Result	Result	Result	Result	Result	Result	Result	Result	Result	Result
RHMW2254-01	ES041	10/22/2013	< 20 U	—	—	**13 BJ**	< 0.50 U	< 0.50 U	< 0.50 U	< 0.50 U	—	< 0.50 U	< 1.0 U	—	—	—	< 0.050 U	< 0.050 U	**0.036 J**	—	—
(cont'd)	ES050	1/16/2014	< 20 U	—	—	—	< 0.50 U	< 0.50 U	< 0.50 U	< 0.50 U	—	< 0.50 U	< 1.0 U	—	—	—	< 0.049 U	< 0.049 U	**0.046 J**	—	—
	ES060	1/29/2014	< 20 U	—	—	**16 BJ**	< 0.50 U	< 0.50 U	< 0.50 U	< 0.50 U	—	< 0.50 U	< 1.0 U	—	—	—	< 0.050 U	< 0.050 U	**0.049 J**	—	—
	ES067	3/6/2014	< 20 U	—	—	—	—	—	< 0.50 U	< 0.50 U	—	< 0.50 U	< 1.0 U	—	—	—	< 0.050 U	< 0.050 U	**0.081 J**	—	—
	ES075	3/26/2014	< 10 U	—	—	—	—	—	< 0.50 U	< 0.50 U	—	< 0.50 U	< 1.0 U	—	—	—	< 0.050 U	< 0.050 U	< 0.050 U	—	—
	ES085	4/22/2014	< 10 U	—	—	< 30 U	< 0.50 U	< 0.50 U	< 0.50 U	< 0.50 U	—	< 0.50 U	< 1.0 U	—	—	—	< 0.049 U	< 0.049 U	< 0.049 U	—	—
	ES094	5/28/2014	< 12 U	—	—	—	—	—	< 0.50 U	< 0.50 U	—	< 0.50 U	< 1.0 U	—	—	—	< 0.050 U	< 0.050 U	< 0.050 U	—	—
	ES102	6/24/2014	< 12 U	—	—	—	—	—	< 0.50 U	< 0.50 U	—	< 0.50 U	< 1.0 U	—	—	—	< 0.049 U	< 0.049 U	< 0.049 U	—	—
	ES107	7/22/2014	< 12 U	—	—	< 30 U	< 0.50 U	< 0.50 U	< 0.50 U	< 0.50 U	—	< 0.50 U	< 1.0 U	—	—	—	< 0.048 U	< 0.048 U	< 0.048 U	—	—
	ES117	10/28/2014	**22 J,HD**	—	—	< 30 U	< 0.50 U	< 0.50 U	< 0.50 U	< 0.50 U	—	< 0.50 U	< 1.0 U	—	—	—	< 0.097 U	< 0.049 U	< 0.049 U	—	—
	ES125	1/27/2015	< 12 U	—	—	< 30 U	< 0.50 U	< 0.50 U	< 0.50 U	< 0.50 U	—	< 0.50 U	< 1.0 U	—	—	—	< 0.10 U	< 0.050 U	< 0.050 U	—	—
	ES134	4/21/2015	**14 BJ**	< 25 U	**37 BJ**	—	< 0.20 U	—	< 0.10 U	< 0.10 U	—	< 0.10 U	< 0.20 U	< 0.010 U	< 0.015 U	< 0.0040 U	< 0.0050 UJ	< 0.0050 UJ	< 0.0050 UJ	—	—
	ES149	7/21/2015	**17 J**	< 25 U	**42 J**	—	< 0.20 U	—	< 0.10 U	< 0.10 U	—	< 0.10 U	< 0.20 U	—	< 0.015 U	< 0.0040 U	< 0.0050 U	< 0.0050 U	< 0.0050 U	—	—
	ERH009	10/20/2015	**16 BJ**	< 25 U	< 53 UB	—	< 0.20 U**	—	< 0.10 U**	< 0.10 U**	—	**0.990 Tb****	< 0.20 U**	—	< 0.015 U	< 0.0040 U	< 0.0050 U	< 0.0050 UB	< 0.0050 UB	—	—
	ERH021	1/20/2016	**21 BJ**	< 25 U	< 54 UB	—	< 0.20 U	—	< 0.10 U	< 0.10 U	—	**0.16 TbJ**	< 0.20 U	—	< 0.015 U	< 0.0040 U	< 0.0050 U	< 0.0050 U	< 0.0050 U	—	—
	ERH037	4/20/2016	< 21 UB	< 25 U	<61 UB	—	—	—	< 0.10 U	**0.10 J**	—	< 0.10 U	< 0.20 U	—	—	—	< 0.0050 U	< 0.0050 U	< 0.0050 U	—	—
	ERH051	7/20/2016	< 21 U	< 25 U	< 52 UBF	—	—	—	< 0.10 U	< 0.10 U	—	< 0.10 U	< 0.20 U	—	—	—	< 0.0050 U	< 0.0050 U	< 0.0050 UBF	—	—
	ERH088/092	10/18/2016*	< 25 U	—	< 40 U	< 18 UJ	—	—	< 0.30 U	< 0.50 U	—	< 0.30 U	< 0.30 U	—	—	—	< 0.10 U	< 0.10 U	< 0.10 U	< 4.00 U	< 80.0 UJ
	ERH115/116	11/14/2016*	< 25 U	—	< 40 U	< 18 U	—	—	< 0.30 U	< 0.50 U	—	< 0.30 U	< 0.30 U	—	—	—	< 0.10 U	< 0.10 U	< 0.10 U	< 4.00 U	< 80.0 U
	ERH135/137	12/12/2016*	**14 J**	—	**16 J**	< 18 U	—	—	< 0.30 U	< 0.50 U	—	< 0.30 U	< 0.30 U	—	—	—	< 0.10 U	< 0.10 U	< 0.10 U	< 4.00 U	< 80.0 U
	ERH161/162	1/10/2017*	< 25 U	—	< 40 U	< 18 U	—	—	< 0.30 U	< 0.50 U	—	< 0.30 U	< 0.30 U	—	—	—	< 0.10 U	< 0.10 U	< 0.10 U	< 4.00 U	< 80.0 U
	ERH205/206	2/7/2017*	< 25 U	—	< 40 U	< 18 U	—	—	< 0.30 U	< 0.50 U	—	< 0.30 U	< 0.30 U	—	—	—	< 0.10 U	< 0.10 U	< 0.10 U	< 4.00 U	< 80.0 U
	ERH257/258	3/6/2017*	< 25 U	—	< 40 U	< 18 U	—	—	< 0.30 U	< 0.50 U	—	< 0.30 U	< 0.30 U	—	—	—	< 0.10 U	< 0.10 U	< 0.10 U	< 4.00 U	< 80.0 U
	ERH292/293	4/3/2017*	< 25 U	—	< 40 U	< 18 U	—	—	< 0.30 U	< 0.50 U	—	< 0.30 U	< 0.30 U	—	—	—	< 0.10 U	< 0.10 U	< 0.10 U	< 4.00 U	< 80.0 U
	ERH329/330	5/1/2017*	< 25 U	—	< 41 U	< 18 U	—	—	< 0.30 U	< 0.50 U	—	< 0.30 U	< 0.30 U	—	—	—	< 0.10 U	< 0.10 U	< 0.10 U	< 4.00 U	< 80.0 U
	ERH349/350	6/6/2017*	< 25 U	—	< 41 U	< 18 U	—	—	< 0.30 U	< 0.50 U	—	< 0.30 U	< 0.30 U	—	—	—	< 0.10 U	< 0.10 U	< 0.10 U	< 4.00 U	< 80.0 U
	ERH378/379	7/5/2017*	< 25 U	—	< 41 U	< 18 U	—	—	< 0.30 U	< 0.50 U	—	< 0.30 U	< 0.30 U	—	—	—	< 0.10 U	< 0.10 U	< 0.10 U	< 4.00 U	< 80.0 U
	ERH409/410	10/24/2017*	**65 J**	—	< 40 U	< 18 U	—	—	< 0.30 U	< 0.50 U	—	< 0.30 U	< 0.30 U	—	—	—	< 0.10 U	< 0.10 U	< 0.10 U	< 4.00 U	< 80.0 U
	ERH542/543	3/14/2018*	< 25 UJ	—	< 40 U	< 18 U	—	—	< 0.30 U	< 0.50 U	—	< 0.30 U	< 0.30 U	—	—	—	< 0.10 U	< 0.10 U	< 0.10 U	< 4.00 U	< 80.0 U

Table A.1-1: Cumulative Groundwater COPC Results (cont'd)
First Quarter 2018 - Quarterly Groundwater Monitoring Report, Red Hill Bulk Fuel Storage Facility, JBPHH, O'ahu, Hawai'i

		Method	8015						8260					8260SIM		8011	8270			8270/8270 Mod.	
			TPH-d	TPH-g ****	TPH-o	TPH-g ****	1,2-Dibromoethane *****	1,2-Dichloroethane *****	Benzene	Ethylbenzene	Naphthalene	Toluene	Xylenes, Total (p/m-, o-xylene)	1,2-Dibromoethane *****	1,2-Dichloroethane *****	1,2-Dibromoethane *****	1-Methylnaphthalene	2-Methylnaphthalene	Naphthalene	Phenol	2-(2-Methoxyethoxy)-ethanol
		Unit	(µg/L)	(µg/L)	(µg/L)	(µg/L)	(µg/L)	(µg/L)	(µg/L)	(µg/L)	(µg/L)	(µg/L)	(µg/L)	(µg/l)	(µg/L)	(µg/L)	(µg/L)	(µg/L)	(µg/L)	(µg/L)	(µg/L)
		Screening Criterion	400	300	500	300	0.04	5.0	5.0	30	17	40	20	0.04	5.0	0.04	10	10	17	300	800
		SSRBL	4500	—	—	—	—	—	750	—	—	—	—	—	—	—	—	—	—	—	—
Well Name	Sample ID	Date Sampled	Result	Result	Result	Result	Result	Result	Result	Result	Result	Result	Result	Result	Result	Result	Result	Result	Result	Result	Result
RHMW01	RH-W-001	2/17/2005[b]	**1,400 Y**	< 50[b] U	**770 O**	—	< 0.0083[b] U	< 0.50[b] U	< 0.50[b] U	< 0.50[b] U	—	< 0.50[b] U	< 0.50[b] U	—	—	—	—	**0.14**	**0.25**	—	—
	RH-W-002	2/17/2005*[b]	**1,500**	< 50[b] U	**890**	—	< 0.0082[b] U	< 0.50[b] U	< 0.50[b] U	< 0.50[b] U	—	< 0.50[b] U	< 0.50[b] U	—	—	—	—	**0.057**	**0.21**	—	—
	RH-W-003	6/28/2005[a]	**1,300 Z**	< 13 U	—	—	< 0.00096 U	< 0.50[b] U	< 0.50[b] U	< 0.50[b] U	—	< 0.50[b] U	< 0.50[b] U	—	—	—	—	**0.054**	**0.073**	—	—
	RH-W-004	6/28/2005*[a]	**1,100 Z**	< 13 U	—	—	<0.00095[d] U	< 0.50[b] U	< 0.50[b] U	< 0.50[b] U	—	< 0.50[b] U	< 0.50[b] U	—	—	—	—	**0.051**	**0.055**	—	—
	RH-W-005	9/8/2005[a]	**950 Y**	< 13 U	**540 O**	—	< 0.00096 U	< 0.12 U	< 0.14 U	< 0.13 U	—	**0.15 J**	< 0.22 U	—	—	—	—	**0.038**	**0.83**	—	—
	RH-W-006	9/8/2005*[a]	**1,100 Y**	< 13 U	**720 O**	—	< 0.00096 U	< 0.12 U	< 0.14 U	< 0.13 U	—	**0.15 J**	< 0.22 U	—	—	—	—	**0.038**	**0.78**	—	—
	RHMW01W01	9/20/2005[b]	—	—	—	—	< 0.50 U	< 0.50 U	< 0.50 U	< 0.50 U	< 1.0 U	< 0.50 U	< 0.50 U	—	—	—	—	—	—	—	—
	RH-W-007	12/6/2005[a]	**670 Z**	< 13 U	—	—	< 0.0096 U	< 0.12 U	< 0.14 U	< 0.13 U	—	**0.12 J**	< 0.33 U	—	—	—	—	**0.098**	**0.51**	—	—
	RH-W-008	12/6/2005*[a]	**740 Z**	< 13 U	—	—	< 0.0095 U	< 0.12 U	< 0.14 U	< 0.13 U	—	< 11 U	< 0.33 U	—	—	—	—	**0.11**	**0.48**	—	—
	RHMW01-GW02	7/10/2006[ad]	**509**	< 50 U	—	—	< 0.50 U	< 0.50 U	< 0.50 U	< 0.50 U	< 1.0 U	< 0.50 U	< 0.50 U	—	—	—	< 0.25 U	< 0.25 U	< 0.25 U	—	—
	RHMW01-GW06	12/5/2006[ad]	**303**	< 50 U	—	—	< 0.50 U	< 0.50 U	< 0.50 U	< 0.50 U	< 1.0 U	< 0.50 U	< 0.50 U	—	—	—	< 0.25 U	< 0.25 U	< 0.25 U	—	—
	RHMW01-WG07	3/27/2007[ad]	**307**	< 50 U	—	—	< 0.50 U	< 0.50 U	< 0.50 U	< 0.50 U	< 1.0 U	< 0.50 U	< 0.50 U	—	—	—	< 0.25 U	< 0.25 U	< 0.25 U	—	—
	RHMW01-WG08	6/12/2007[ad]	**274**	< 50 U	—	—	< 0.50 U	< 0.50 U	< 0.50 U	< 0.50 U	< 1.0 U	< 0.50 U	< 0.50 U	—	—	—	< 0.25 U	< 0.25 U	< 0.25 U	—	—
	RHMW01-WG09	9/10/2007[a]	**261**	< 50 U	—	—	< 0.20 U	< 0.20 U	< 0.20 U	< 0.20 U	< 0.44 U	< 0.27 U	< 0.36 U	—	—	—	< 0.25 U	< 0.25 U	< 0.25 U	—	—
	RHMW01-WG10	1/15/2008[a]	**574**	< 10.0 U	—	—	< 0.310 U	< 0.150 U	< 0.120 U	< 0.310 U	**5.98**	< 0.310 U	< 0.620 U	—	—	—	**0.0640**	**0.0478 J**	**0.210**	—	—
	RHMW01-WG11	4/15/2008[a]	**427 J**	**13.6 J**	—	—	< 0.310 U	< 0.150 U	< 0.120 U	< 0.310 U	< 0.620 U	< 0.310 U	< 0.620 U	—	—	—	**0.101**	**0.0789**	**0.216**	—	—
	RHMW01-WG12	7/29/2008[a]	**327 J**	< 10.0 U	—	—	< 0.310 U	< 0.150 U	< 0.120 U	< 0.310 U	< 0.620 U	< 0.310 U	< 0.620 U	—	—	—	< 0.0150 U	< 0.0150 U	**0.114**	—	—
	RHMW01-WG13	10/22/2008[a]	**459**	< 10.0 U	—	—	< 0.310 U	< 0.150 U	< 0.120 U	< 0.310 U	< 0.620 U	< 0.310 U	< 0.620 U	—	—	—	< 0.0150 U	< 0.0150 U	**0.103**	—	—
	RHMW01-WG14	2/4/2009[a]	**387 J**	**14.4 J**	—	—	< 0.310 U	< 0.150 U	< 0.120 U	< 0.310 U	< 0.620 U	< 0.310 U	< 0.620 U	—	—	—	< 0.0165 U	< 0.0165 U	**0.173**	—	—
	RHMW01-WG15	5/13/2009[a]	**373 J**	**16.6 J**	—	—	< 0.310 U	< 0.150 U	< 0.120 U	< 0.310 U	< 0.620 U	< 0.310 U	< 0.620 U	—	—	—	< 0.0150 U	< 0.0150 U	**0.182**	—	—
	RHMW01-WG16	7/15/2009[a]	**248 J**	< 30.0 U	—	—	< 0.310 U	< 0.150 U	< 0.120 U	< 0.310 U	< 0.620 U	< 0.310 U	< 0.620 U	—	—	—	**9.44**	**3.07**	**5.61**	—	—
	RHMW01-WG17	10/14/2009[a]	**299 F**	< 30 U	—	—	< 0.31 U	< 0.15 U	< 0.12 U	< 0.31 U	< 0.62 U	< 0.31 U	< 1 U	—	—	—	< 0.0174 U	< 0.0174 U	**0.193**	—	—
	RHMW01-WG18	1/27/2010	**312 J**	< 60.0 U	—	—	< 0.620 U	< 0.300 U	< 0.240 U	< 0.620 U	< 1.24 U	< 0.620 U	< 1.24 U	—	—	—	< 0.0334 U	**0.0559**	**0.330**	—	—
	RHMW01-WG19	4/13/2010	**377 J**	< 60.0 U	—	—	< 0.620 U	< 0.300 U	< 0.240 U	< 0.620 U	< 1.24 U	< 0.620 U	< 1.24 U	—	—	—	< 0.0322 U	< 0.0322 U	< 0.0666 U	—	—
	RHMW01-WG20	7/13/2010	**228 J**	< 60.0 U	—	—	< 0.620 U	< 0.300 U	< 0.240 U	< 0.620 U	< 1.24 U	< 0.620 U	< 1.24 U	—	—	—	< 0.0316 U	< 0.0316 U	**0.184**	—	—
	ES009	11/3/2010	< 80.8 U	—	—	< 12.12 U	< 0.40 U	< 0.28 U	< 0.32 U	< 0.46 U	—	< 0.34 U	< 0.38 U	—	—	—	< 0.12 U	< 0.12 U	**0.17 J**	—	—
	ES015	1/20/2011	< 80.8 U	—	—	< 12.12 U	< 0.40 U	< 0.28 U	< 0.32 U	< 0.46 U	—	< 0.34 U	< 0.38 U	—	—	—	< 0.12 U	< 0.12 U	< 0.10 U	—	—
	ES033	4/28/2011	**300**	—	—	< 12.12 U	< 0.40 U	< 0.28 U	< 0.32 U	< 0.46 U	—	< 0.34 U	< 0.38 U	—	—	—	< 0.12 U	< 0.12 U	< 0.10 U	—	—
	ES041	7/20/2011	**290**	—	< 212.0 U	< 12.12 U	< 0.40 U	< 0.28 U	< 0.32 U	< 0.46 U	—	< 0.34 U	< 0.38 U	—	—	—	< 0.12 U	< 0.12 U	**0.12 J**	—	—
	ES057	11/2/2011	**210**	—	—	< 12.12 U	< 0.40 U	< 0.28 U	< 0.32 U	< 0.46 U	—	< 0.34 U	< 0.38 U	—	—	—	< 0.12 U	< 0.12 U	< 0.10 U	—	—
	ES069	2/14/2012	**210 ++**	—	—	< 12.12 U	< 0.40 U	< 0.28 U	< 0.32 U	< 0.46 U	—	< 0.34 U	< 0.38 U	—	—	—	< 0.12 U	< 0.12 U	< 0.10 U	—	—
	ES075	4/17/2012	< 80.8 U	—	—	< 12.12 U	< 0.40 U	< 0.28 U	< 0.32 U	< 0.46 U	—	< 0.34 U	< 0.38 U	—	—	—	< 0.12 U	< 0.12 U	< 0.10 U	—	—
	ES088	7/20/2012	< 80.8 U	—	—	< 12.12 U	< 0.40 U	< 0.28 U	< 0.32 U	< 0.46 U	—	< 0.34 U	< 0.38 U	—	—	—	< 0.12 U	< 0.12 U	**0.13 J**	—	—
	ES001	10/22/2012	**85 J,HD**	—	—	**20 BJ**	< 0.50 U	< 0.50 U	< 0.50 U	< 0.50 U	—	< 0.50 U	< 1.0 U	—	—	—	< 0.050 U	< 0.050 U	< 0.050 U	—	—
	ES010	2/4/2013	**79**	—	—	**13 J**	< 0.50 U	< 0.50 U	< 0.50 U	< 0.50 U	—	< 0.50 U	< 1.0 U	—	—	—	< 0.050 U	< 0.050 U	**0.10 J**	—	—
	ES019	4/22/2013	**340 HD**	—	—	< 30 U	< 0.50 U	< 0.50 U	< 0.50 U	< 0.50 U	—	< 0.50 U	< 1.0 U	—	—	—	< 0.052 U	< 0.052 U	< 0.052 U	—	—
	ES028	7/22/2013	**99 HD**	—	—	< 30 U	< 0.50 U	< 0.50 U	< 0.50[1] U	< 0.50[1] U	—	< 0.50[1] U	<1.0[1] U	—	—	—	< 0.050 U	< 0.050 U	**0.048 J**	—	—
	ES037	10/21/2013	**92 HD**	—	—	**15 BJ**	< 0.50 U	< 0.50 U	< 0.50 U	< 0.50 U	—	< 0.50 U	< 1.0 U	—	—	—	< 0.052 U	< 0.052 U	< 0.052 U	—	—
	ES048	1/15/2014	**250 HD**	—	—	—	< 0.50 U	< 0.50 U	< 0.50 U	< 0.50 U	—	**2.5**	< 1.0 U	—	—	—	**0.040 J**	**0.039 J**	**0.062 J**	—	—
	ES056	1/28/2014	**130 HD**	—	—	**26 BJ**	< 0.50 U	< 0.50 U	< 0.50 U	< 0.50 U	—	**1.3**	< 1.0 U	—	—	—	< 0.050 U	< 0.050 U	**0.045 J**	—	—
	ES062	2/24/2014	**89 HD**	—	—	< 30 U	< 0.50 U	< 0.50 U	< 0.50 U	< 0.50 U	—	< 0.50 U	< 1.0 U	—	—	—	< 0.050 U	< 0.050 U	**0.037 J**	—	—
	ES064	3/5/2014	**93**	—	—	—	—	—	< 0.50 U	< 0.50 U	—	< 0.50 U	< 1.0 U	—	—	—	< 0.050 U	**0.038 J**	< 0.050 U	—	—
	ES069	3/10/2014	**38 HD**	—	—	—	—	—	< 0.50 U	< 0.50 U	—	< 0.50 U	< 1.0 U	—	—	—	< 0.052 U	< 0.052 U	< 0.052 U	—	—
	ES072	3/25/2014	**82 HD**	—	—	—	—	—	< 0.50 U	< 0.50 U	—	< 0.50 U	< 1.0 U	—	—	—	< 0.051 U	< 0.051 U	< 0.051 U	—	—
	ES077	4/7/2014	**140 HD**	—	—	—	—	—	< 0.50 U	< 0.50 U	—	< 0.50 U	< 1.0 U	—	—	—	< 0.050 U	< 0.050 U	< 0.050 U	—	—

Table A.1-1: Cumulative Groundwater COPC Results (cont'd)
First Quarter 2018 - Quarterly Groundwater Monitoring Report, Red Hill Bulk Fuel Storage Facility, JBPHH, O'ahu, Hawai'i

		Method	8015						8260					8260SIM		8011	8270			8270/8270 Mod.	
			TPH-d	TPH-g ****	TPH-o	TPH-g ****	1,2-Dibromoethane *****	1,2-Dichloroethane *****	Benzene	Ethylbenzene	Naphthalene	Toluene	Xylenes, Total (p/m-, o-xylene)	1,2-Dibromoethane *****	1,2-Dichloroethane *****	1,2-Dibromoethane *****	1-Methylnaphthalene	2-Methylnaphthalene	Naphthalene	Phenol	2-(2-Methoxyethoxy)-ethanol
		Unit	(µg/L)	(µg/L)	(µg/L)	(µg/L)	(µg/L)	(µg/L)	(µg/L)	(µg/L)	(µg/L)	(µg/L)	(µg/L)	(µg/l)	(µg/L)	(µg/L)	(µg/L)	(µg/L)	(µg/L)	(µg/L)	(µg/L)
		Screening Criterion	400	300	500	300	0.04	5.0	5.0	30	17	40	20	0.04	5.0	0.04	10	10	17	300	800
		SSRBL	4500	—	—	—	—	—	750	—	—	—	—	—	—	—	—	—	—	—	—
Well Name	Sample ID	Date Sampled	Result	Result	Result	Result	Result	Result	Result	Result	Result	Result	Result	Result	Result	Result	Result	Result	Result	Result	Result
RHMW01	ES080	4/21/2014	**88 HD**	—	—	< 30 U	< 0.50 U	< 0.50 U	< 0.50 U	< 0.50 U	—	< 0.50 U	< 1.0 U	—	—	—	< 0.050 U	< 0.050 U	< 0.050 U	—	—
(cont'd)	ES091	5/27/2014	**66 HD**	—	—	—	—	—	< 0.50 U	< 0.50 U	—	< 0.50 U	< 1.0 U	—	—	—	< 0.051 U	< 0.051 U	< 0.051 U	—	—
	ES098	6/23/2014	**77**	—	—	—	—	—	< 0.50 U	< 0.50 U	—	< 0.50 U	< 1.0 U	—	—	—	< 0.050 U	< 0.050 U	< 0.050 U	—	—
	ES103	7/21/2014	**67 HD**	—	—	< 30 U	< 0.50 U	< 0.50 U	< 0.50 U	< 0.50 U	—	< 0.50 U	< 1.0 U	—	—	—	< 0.051 U	< 0.051 U	< 0.051 U	—	—
	ES113	10/27/2014	**120 J,HD**	—	—	< 30 U	< 0.50 U	< 0.50 U,IH	< 0.50 U	< 0.50 U	—	< 0.50 U	< 1.0 U	—	—	—	< 0.10 U	< 0.052 U	< 0.052 U	—	—
	ES120X	1/27/2015	**33 HD**	—	—	< 30 U	< 0.50 U	< 0.50 U	< 0.50 U	< 0.50 U	—	< 0.50 U	< 1.0 U	—	—	—	< 0.11 U	< 0.054 U	< 0.054 U	—	—
	ES130	4/20/2015	**170 Y**	< 25 U	**23 BJ**	—	< 0.20 U	—	< 0.10 U	< 0.10 U	—	< 0.10 U	< 0.20 U	< 0.010 U	< 0.015 U	< 0.0040 U	**0.014 J**	**0.0093 J**	**0.056 J**	—	—
	ES143	6/25/2015	**130 Y**	—	**40 J**	—	—	—	—	—	—	—	—	—	—	—	**0.0068 JX**	**0.0058 JX**	**0.040 X**	—	—
	ES145	7/20/2015	**150 Y**	< 25 U	**21 J**	—	< 0.20 U	—	< 0.10 U	< 0.10 U	—	< 0.10 U	< 0.20 U	—	< 0.015 U	< 0.0040 U	**0.014 JX**	**0.013 J**	**0.057**	—	—
	ERH011	10/20/2015	**330 BY**	< 25 U	< 54 UB	—	< 0.20 U**	—	< 0.10 U**	< 0.10 U**	—	**0.42 J,**,Tb**	< 0.20 U**	—	< 0.015 U	< 0.0040 U	**0.037**	**0.024 B**	**0.20 B**	—	—
	ERH024	1/20/2016	**430 BY**	< 25 U	**60 BJ**	—	< 0.004 U	< 0.020 U	< 0.10 U	< 0.10 U	—	**0.17 JTb**	< 0.20 U	—	< 0.015 U	< 0.0040 U	**0.029 X**	**0.023 X**	**0.18**	—	—
	ERH039	4/20/2016	**360 Y**	< 25 U	< 120 LB	—	—	—	< 0.10 U	< 0.10 U	—	< 0.10 U	< 0.20 U	—	—	—	**0.024 X**	**0.014 J,X**	**0.23**	—	—
	ERH053	7/20/2016	**250 Y**	< 25 U	**59 J**	—	—	—	< 0.10 U	< 0.10 U	—	< 0.10 U	< 0.20 U	—	—	—	**0.032 XJV**	**0.0068 XJV**	**0.21**	—	—
	ERH090	10/17/2016	**120**	—	< 40 U	< 18 U	—	—	< 0.30 U	< 0.50 U	—	< 0.30 U	< 0.30 U	—	—	—	< 0.10 U	< 0.10 U	< 0.10 U	< 4.00 U	< 80.0 UJ
	ERH117	11/14/2016	**94**	—	< 40 U	< 18 U	—	—	< 0.30 U	< 0.50 U	—	< 0.30 U	< 0.30 U	—	—	—	< 0.10 U	< 0.10 U	< 0.10 U	< 4.00 U	< 80.0 U
	ERH143	12/13/2016	< 96 U	—	< 40 U	< 18 U	—	—	< 0.30 U	< 0.50 U	—	< 0.30 U	< 0.30 U	—	—	—	< 0.10 U	< 0.10 U	< 0.10 U	< 4.00 U	< 80.0 U
	ERH172	1/11/2017	**88**	—	< 40 U	< 18 U	—	—	< 0.30 U	< 0.50 U	—	< 0.30 U	< 0.30 U	—	—	—	< 0.10 U	< 0.10 U	< 0.10 U	< 4.00 U	< 80.0 U
	ERH223	2/8/2017	**150**	—	< 40 U	< 18 U	—	—	< 0.30 U	< 0.50 U	—	< 0.30 U	< 0.30 U	—	—	—	< 0.10 U	< 0.10 U	< 0.10 U	< 4.00 U	< 80.0 U
	ERH275	3/8/2017	**83**	—	< 40 U	< 18 U	—	—	< 0.30 U	< 0.50 U	—	< 0.30 U	< 0.30 U	—	—	—	< 0.10 U	< 0.10 U	< 0.10 U	< 4.00 U	< 80.0 U
	ERH310	4/3/2017	**97**	—	< 40 U	< 18 U	—	—	< 0.30 U	< 0.50 U	—	< 0.30 U	< 0.30 U	—	—	—	< 0.10 U	< 0.10 U	< 0.10 U	< 4.00 U	< 80.0 U
	ERH332	5/1/2017	**110**	—	< 40 U	< 18 U	—	—	< 0.30 U	< 0.50 U	—	< 0.30 U	< 0.30 U	—	—	—	< 0.10 U	< 0.10 U	< 0.10 U	< 4.00 U	< 80.0 U
	ERH352	6/5/2017	**98**	—	< 40 U	< 18 U	—	—	**0.18 J**	< 0.50 U	—	< 0.30 U	< 0.30 U	—	—	—	< 0.10 U	< 0.10 U	< 0.10 U	< 4.00 U	< 80.0 U
	ERH383	7/5/2017	**110**	—	< 40 U	< 18 U	—	—	< 0.30 U	< 0.50 U	—	< 0.30 U	< 0.30 U	—	—	—	< 0.10 U	< 0.10 U	< 0.10 U	< 4.00 U	< 80.0 U
	ERH412/413	10/25/2017*	**86**	—	**67**	< 18 U	< 0.50 U	< 0.30 U	< 0.30 U	< 0.50 U	—	< 0.30 U	< 0.30 U	—	—	—	< 0.10 U	< 0.10 U	< 0.10 U	< 4.00 U	< 80.0 U
	ERH545	3/12/2018	**150**	—	< 40 U	< 18 U	—	—	< 0.30 U	< 0.50 U	—	< 0.30 U	< 0.30 U	—	—	—	< 0.10 U	< 0.10 U	< 0.10 U	< 4.00 U	< 80.0 U

Table A.1-1: Cumulative Groundwater COPC Results (cont'd)
First Quarter 2018 - Quarterly Groundwater Monitoring Report, Red Hill Bulk Fuel Storage Facility, JBPHH, O'ahu, Hawai'i

		Method	8015						8260					8260SIM		8011	8270			8270/8270 Mod.	
			TPH-d	TPH-g ****	TPH-o	TPH-g ****	1,2-Dibromoethane *****	1,2-Dichloroethane *****	Benzene	Ethylbenzene	Naphthalene	Toluene	Xylenes, Total (p/m-, o-xylene)	1,2-Dibromoethane *****	1,2-Dichloroethane *****	1,2-Dibromoethane *****	1-Methylnaphthalene	2-Methylnaphthalene	Naphthalene	Phenol	2-(2-Methoxyethoxy)-ethanol
		Unit	(µg/L)	(µg/L)	(µg/L)	(µg/L)	(µg/L)	(µg/L)	(µg/L)	(µg/L)	(µg/L)	(µg/L)	(µg/L)	(µg/l)	(µg/L)	(µg/L)	(µg/L)	(µg/L)	(µg/L)	(µg/L)	(µg/L)
		Screening Criterion	400	300	500	300	0.04	5.0	5.0	30	17	40	20	0.04	5.0	0.04	10	10	17	300	800
		SSRBL	4500	—	—	—	—	—	750	—	—	—	—	—	—	—	—	—	—	—	—
Well Name	Sample ID	Date Sampled	Result	Result	Result	Result	Result	Result	Result	Result	Result	Result	Result	Result	Result	Result	Result	Result	Result	Result	Result
RHMW02	RHMW02W01	9/20/2005[b]	**2,660**	< 50 U	—	—	< 2.5 U	< 2.5 U	< 2.5 U	< 2.5 U	**283 J**	< 2.5 U	< 2.5 U	—	—	—	**104**	**88.5**	**120**	—	—
	RHMW02Q01	9/20/2005*[b]	**2,500**	< 50 U	—	—	< 2.5 U	< 2.5 U	< 2.5 U	< 2.5 U	**319**	< 2.5 U	< 2.5 U	—	—	—	**102**	**87.2**	**123**	—	—
	RHMW02-GW02	7/10/2006[a]	**2,800**	**124**	—	—	< 0.50 U	< 0.50 U	< 0.50 U	**1.3**	**343**	< 0.50 U	< 0.50 U	—	—	—	**142**	**65.8**	**171**	—	—
	RHMW05-GW02	7/10/2006*[a]	**2,790**	**119**	—	—	< 2.5 U	< 2.5 U	< 2.5 U	< 2.5 U	**335**	< 2.5 U	< 2.5 U	—	—	—	**133**	**67.1**	**180**	—	—
	RHMW02-GW06	12/5/2006[a]	**2,600**	**110**	—	—	< 0.50 U	< 0.50 U	< 0.50 U	**1.2**	**257**	< 0.50 U	< 0.50 U	—	—	—	**124**	**45.1**	**160**	—	—
	RHMWA01-GW06	12/5/2006*[a]	**2,690**	**138**	—	—	< 0.50 U	< 0.50 U	< 0.50 U	**1.1**	**269**	< 0.50 U	< 0.50 U	—	—	—	**114**	**51.1**	**147**	—	—
	RHMW02-WG07	3/27/2007[a]	**2,750 O**	**122 O**	—	—	< 0.50 U	< 0.50 U	< 0.50 U	< 0.50 U	**196 O**	< 0.50 U	< 0.50 U	—	—	—	**72.1 O**	**30.3 O**	**105 O**	—	—
	RHMWA01-WG07	3/27/2007*[a]	**2,250 O**	**148 O**	—	—	< 0.50 U	< 0.50 U	< 0.50 U	< 0.50 U	**207 O**	< 0.50 U	< 0.50 U	—	—	—	**59.4 O**	**26.2 O**	**90.1 O**	—	—
	RHMW02-WG08	6/12/2007[a]	**2,750**	**52.5 J**	—	—	< 0.50 U	< 0.50 U	< 0.50 U	< 0.50 U	**209**	< 0.50 U	< 0.5 U	—	—	—	**67.3**	**26.5**	**87.2**	—	—
	RHMWA01-WG08	6/12/2007*[a]	**2,900**	**56.5 J**	—	—	< 0.50 U	< 0.50 U	< 0.50 U	< 0.50 U	**207**	< 0.50 U	< 0.50 U	—	—	—	**88.3**	**33**	**128**	—	—
	RHMW02-WG09	9/10/2007[a]	**2,810**	**76 J**	—	—	< 0.20 U	< 0.20 U	< 0.20 U	< 0.20 U	**206**	< 0.27 U	< 0.36 U	—	—	—	**109**	**21.5**	**144**	—	—
	RHMWA01-WG09	9/10/2007*[a]	**3,180**	**78.2 J**	—	—	< 0.20 U	< 0.20 U	< 0.2 U	< 0.20 U	**264**	< 0.27 U	< 0.38 U	—	—	—	**102**	**19.7**	**136**	—	—
	RHMW02-WG10	1/15/2008[a]	**2,310**	**64.3 J**	—	—	< 0.310 U	< 0.150 U	**0.170 J**	< 0.310 U	**195**	< 0.310 U	**1.06**	—	—	—	**67.0**	**23.8**	**93.6**	—	—
	RHMWA01-WG10	1/15/2008*[a]	**3,230**	**66.2 J**	—	—	< 0.310 U	< 0.150 U	**0.170 J**	**0.350 J**	**194**	< 0.310 U	**1.10**	—	—	—	**73.2**	**27.6**	**102**	—	—
	RHMW02-WG11	4/15/2008[a]	**3,120**	**58.9 J**	—	—	< 0.310 U	< 0.150 U	< 0.120 U	< 0.310 U	**290**	< 0.310 U	**0.740 J**	—	—	—	**75.8**	**34.5**	**73.0**	—	—
	RHMWA01-WG11	4/15/2008*[a]	**3,020**	**58.9 J**	—	—	< 0.310 U	< 0.150 U	**0.150 J**	< 0.310 U	**293**	< 0.310 U	**0.750 J**	—	—	—	**71.9**	**40.8**	**105**	—	—
	RHMW02-WG12	7/29/2008[a]	**4,470**	**61.7 J**	—	—	< 0.310 U	< 0.150 U	< 0.120 U	**0.580 J**	**320**	< 0.310 U	< 0.620 U	—	—	—	**102**	**31.5**	**140**	—	—
	RHMWA01-WG12	7/29/2008*[a]	**3,640**	**61.2 J**	—	—	< 0.310 U	< 0.150 U	**0.120 J**	**0.560 J**	**309**	< 0.310 U	< 0.620 U	—	—	—	**96.0**	**42.2**	**132**	—	—
	RHMW02-WG13	10/22/2008[a]	**4,540**	**52.8 J**	—	—	< 0.310 U	< 0.150 U	**0.140 J**	**0.450 J**	**239**	< 0.310 U	**0.450 J**	—	—	—	**72.1**	**13.7**	**97.4**	—	—
	RHMWA01-WG13	10/22/2008*[a]	**6,300**	**52.9 J**	—	—	< 0.310 U	< 0.150 U	**0.150 J**	**0.420 J**	**245**	< 0.310 U	**0.490 J**	—	—	—	**62.4**	**12.7**	**82.3**	—	—
	RHMW02-WG14	2/4/2009[a]	**2,840**	**52.3 J**	—	—	< 0.310 U	< 0.150 U	**0.260 J**	**0.490 J**	**42.8**	< 0.310 U	**0.400 J**	—	—	—	**21.2**	**10.5**	**15.2**	—	—
	RHMWA01-WG14	2/4/2009*[a]	**2,840**	**54.3 J**	—	—	< 0.310 U	< 0.150 U	**0.240 J**	**0.520 J**	**43.0**	< 0.310 U	**0.470 J**	—	—	—	**22.8**	**11.1**	**16.6**	—	—
	RHMW02-WG15	5/13/2009[a]	**1,620**	**39.1 J**	—	—	< 0.310 U	< 0.150 U	< 0.120 U	< 0.310 U	< 0.620 U	< 0.310 U	**0.310 J**	—	—	—	**17.9**	**0.136**	**1.17**	—	—
	RHMWA01-WG15	5/13/2009*[a]	**2,000**	**36.7 J**	—	—	< 0.310 U	< 0.150 U	< 0.120 U	< 0.310 U	< 0.620 U	< 0.310 U	< 0.620 U	—	—	—	**24.6**	**0.107**	**1.08**	—	—
	RHMW02-WG16	7/15/2009[a]	**1,450**	< 30.0 U	—	—	< 0.310 U	< 0.150 U	< 0.120 U	< 0.310 U	**10.1**	< 0.310 U	< 0.620 U	—	—	—	**13.2**	**3.66**	**8.37**	—	—
	RHMWA01-WG16	7/15/2009*[a]	**1,300**	< 30.0 U	—	—	< 0.310 U	< 0.150 U	< 0.120 U	< 0.310 U	**11.2**	< 0.310 U	< 0.620 U	—	—	—	**10.6**	**2.58**	**6.71**	—	—
	RHMW02-WG17	10/13/2009[ad]	**2,570**	**36.9 F**	—	—	< 0.31 U	< 0.15 U	< 0.12 U	< 0.31 U	**23.3**	< 0.31 U	< 1 U	—	—	—	**2.46**	**0.486**	**6.77**	—	—
	RHMWA01-WG17	10/13/2009*[a]	**2,570**	< 30 U	—	—	< 0.31 U	< 0.15 U	< 0.12 U	< 0.31 U	**20.0**	< 0.31 U	< 1 U	—	—	—	**4.03**	**0.783**	**7.82**	—	—
	RHMW02-WG18	1/26/2010	**2,130**	**42.3 J**	—	—	< 0.620 U	< 0.300 U	< 0.240 U	< 0.620 U	**31.5**	< 0.620 U	< 1.24 U	—	—	—	**9.03**	**3.85**	**17.3**	—	—
	RHMWA01-WG18	1/26/2010*	**3,410**	**38.1 J**	—	—	< 0.620 U	< 0.300 U	< 0.240 U	< 0.620 U	**9.30**	< 0.620 U	< 1.24 U	—	—	—	**8.26**	**2.65**	**15.7**	—	—
	RHMW02-WG19	4/13/2010	**2,350**	**39.3 J**	—	—	< 0.620 U	< 0.300 U	< 0.240 U	< 0.620 U	**20.6**	< 0.620 U	< 1.24 U	—	—	—	**6.61**	**1.69**	**14.3**	—	—
	RHMWA01-WG19	4/13/2010*	**2,080**	**39.0 J**	—	—	< 0.620 U	< 0.300 U	< 0.240 U	< 0.620 U	**21.4**	< 0.620 U	< 1.24 U	—	—	—	**5.90**	**1.90**	**12.7**	—	—
	RHMW02-WG20	7/13/2010	**3,060**	**46.5 J**	—	—	< 0.620 U	< 0.300 U	< 0.240 U	< 0.620 U	**107**	< 0.620 U	**0.690 J**	—	—	—	**7.43**	**1.06**	**59.9**	—	—
	RHMWA01-WG20	7/13/2010*	**3,110**	**45.4 J**	—	—	< 0.620 U	< 0.300 U	< 0.240 U	< 0.620 U	**102**	< 0.620 U	**0.660 J**	—	—	—	**7.05**	**0.937**	**61.1**	—	—
	ES002	10/18/2010	**1,700 ++**	—	—	**150 ++**	< 0.40 U	< 0.28 U	< 0.32 U	**0.25 J**	—	< 0.34 U	**0.60 J**	—	—	—	**15**	**5.0**	**59**	—	—
	ES003	10/18/2010*	**1,700 ++**	—	—	**160 ++**	< 0.40 U	< 0.28 U	< 0.32 U	**0.32 J**	—	< 0.34 U	**0.51 J**	—	—	—	**15**	**6.3**	**54**	—	—
	ES010	1/18/2011	**1,100 ++**	—	—	**17 J++**	< 0.40 U	< 0.28 U	< 0.32 U	**0.29 J**	—	< 0.34 U	**0.48 J**	—	—	—	**19**	**3.6**	**57**	—	—
	ES011	1/18/2011*	**1,100 ++**	—	—	**20 ++**	< 0.40 U	< 0.28 U	< 0.32 U	**0.25 J**	—	< 0.34 U	**0.58 J**	—	—	—	**23**	**5.6**	**63**	—	—
	ES020	4/19/2011	**1,100 ++**	—	—	**24 ++**	< 0.40 U	< 0.28 U	< 0.32 U	< 0.46 U	—	< 0.34 U	**0.41 J**	—	—	—	**5.1**	**0.43**	**3.5**	—	—
	ES021	4/19/2011*	**1,100 ++**	—	—	**29 ++**	< 0.40 U	< 0.28 U	< 0.32 U	< 0.46 U	—	< 0.34 U	**0.41 J**	—	—	—	**5.2**	**0.53**	**4.2**	—	—
	ES037	7/19/2011	**1,100**	—	< 212.0 U	< 12.12 U	< 0.40 U	< 0.28 U	< 0.32 U	< 0.46 U	—	< 0.34 U	< 0.38 U	—	—	—	**0.85**	**0.16 J**	**2.2**	—	—
	ES038	7/19/2011*	**1,800**	—	< 212.0 U	< 12.12 U	< 0.40 U	< 0.28 U	< 0.32 U	< 0.46 U	—	< 0.34 U	< 0.38 U	—	—	—	**0.90**	**0.12 J**	**2.7**	—	—
	ES046	10/24/2011	**750**	—	—	< 12.12 U	< 0.40 U	< 0.28 U	< 0.32 U	< 0.46 U	—	< 0.34 U	< 0.38 U	—	—	—	**0.53**	**0.15 J**	**0.80**	—	—
	ES047	10/24/2011*	**730**	—	—	< 12.12 U	< 0.40 U	< 0.28 U	< 0.32 U	< 0.46 U	—	< 0.34 U	< 0.38 U	—	—	—	**0.62**	**0.20**	**1.0**	—	—
	ES061	1/26/2012	**1,700**	—	—	< 12.12 U	< 0.40 U	< 0.28 U	< 0.32 U	**0.30 J**	—	< 0.34 U	< 0.38 U	—	—	—	**0.57**	**0.17 J**	**1.7**	—	—

Table A.1-1: Cumulative Groundwater COPC Results (cont'd)
First Quarter 2018 - Quarterly Groundwater Monitoring Report, Red Hill Bulk Fuel Storage Facility, JBPHH, O'ahu, Hawai'i

		Method	8015						8260					8260SIM		8011	8270			8270/8270 Mod.	
			TPH-d	TPH-g ****	TPH-o	TPH-g ****	1,2-Dibromoethane *****	1,2-Dichloroethane *****	Benzene	Ethylbenzene	Naphthalene	Toluene	Xylenes, Total (p/m-, o-xylene)	1,2-Dibromoethane *****	1,2-Dichloroethane *****	1,2-Dibromoethane *****	1-Methylnaphthalene	2-Methylnaphthalene	Naphthalene	Phenol	2-(2-Methoxyethoxy)-ethanol
		Unit	(µg/L)	(µg/L)	(µg/L)	(µg/L)	(µg/L)	(µg/L)	(µg/L)	(µg/L)	(µg/L)	(µg/L)	(µg/L)	(µg/l)	(µg/L)	(µg/L)	(µg/L)	(µg/L)	(µg/L)	(µg/L)	(µg/L)
		Screening Criterion	400	300	500	300	0.04	5.0	5.0	30	17	40	20	0.04	5.0	0.04	10	10	17	300	800
		SSRBL	4500	—	—	—	—	—	750	—	—	—	—	—	—	—	—	—	—	—	—
Well Name	Sample ID	Date Sampled	Result	Result	Result	Result	Result	Result	Result	Result	Result	Result	Result	Result	Result	Result	Result	Result	Result	Result	Result
RHMW02	ES071	4/16/2012	**1,200**	—	—	< 12.12 U	< 0.40 U	< 0.28 U	< 0.32 U	< 0.46 U	—	< 0.34 U	< 0.38 U	—	—	—	**0.30**	< 0.12 U	**0.86**	—	—
(cont'd)	ES072	4/16/2012*	**1,100**	—	—	< 12.12 U	< 0.40 U	< 0.28 U	< 0.32 U	**0.23 J**	—	< 0.34 U	< 0.38 U	—	—	—	**1.2**	**0.61**	**2.9**	—	—
	ES082	7/18/2012	**1,700 ++**	—	< 212.0 U	< 12.12 U	< 0.40 U	< 0.28 U	< 0.32 U	< 0.46 U	—	< 0.34 U	**0.43 J**	—	—	—	**4.7**	**0.88**	**17**	—	—
	ES002	10/22/2012	**2,200 HD**	—	—	**320 B**	< 0.50 U	< 0.50 U	< 0.50 U	**0.18 J**	—	**0.59 J**	**0.51 J**	—	—	—	**24**	**14**	**63**	—	—
	ES003	10/22/2012*	**1,800 HD**	—	—	**360 B**	< 0.50 U	< 0.50 U	< 0.50 U	**0.18 J**	—	**0.60 J**	**0.47 J**	—	—	—	**21**	**12**	**61**	—	—
	ES011	1/28/2013	**1,700 HD**	—	—	**660**	< 0.50 U	< 0.50 U	< 0.50 U	**0.21 J**	—	< 0.50 U	**0.65 J**	—	—	—	**47**	**35**	**110**	—	—
	ES012	1/28/2013*	**1,500 HD**	—	—	**650**	< 0.50 U	< 0.50 U	< 0.50 U	**0.24 J**	—	< 0.50 U	**0.69 J**	—	—	—	**41**	**31**	**100**	—	—
	ES020	4/22/2013	**2,600 HD**	—	—	**54**	< 0.50 U	< 0.50 U	< 0.50 U	**0.21 J**	—	< 0.50 U	**0.58 J**	—	—	—	**16**	**13**	**53**	—	—
	ES021	4/22/2013*	**3,300 HD**	—	—	**56**	< 0.50 U	< 0.50 U	< 0.50 U	**0.21 J**	—	< 0.50 U	**0.58 J**	—	—	—	**20**	**16**	**61**	—	—
	ES029	7/22/2013	**2,500 HD**	—	—	**55**	< 0.50 U	< 0.50 U	< 0.50[1] U	**0.17[1] J**	—	< 0.50[1] U	**0.45[1] J**	—	—	—	**21**	**9.1**	**73**	—	—
	ES030	7/22/2013*	**2,600 HD**	—	—	**61**	< 0.50 U	< 0.50 U	< 0.50[1] U	**0.19[1] J**	—	< 0.50[1] U	**0.50[1] J**	—	—	—	**18**	**6.6**	**67**	—	—
	ES038	10/21/2013	**2,400 HD**	—	—	**48 BJ**	< 0.50 U	< 0.50 U	< 0.50 U	**0.14 J**	—	< 0.50 U	**0.37 J**	—	—	—	**9.0**	**9.0**	**30**	—	—
	ES039	10/21/2013*	**2,400 HD**	—	—	**63 B**	< 0.50 U	< 0.50 U	< 0.50 U	< 0.50 U	—	< 0.50 U	**0.37 J**	—	—	—	**7.5**	**7.5**	**25**	—	—
	ES046	1/15/2014	**5,000**	—	—	—	< 0.50 U	< 0.50 U	< 0.50 U	**0.17 J**	—	< 0.50 U	**0.48 J**	—	—	—	**6.0**	**4.9**	**18**	—	—
	ES047	1/15/2014*	**5,200**	—	—	—	< 0.50 U	< 0.50 U	< 0.50 U	**0.17 J**	—	< 0.50 U	**0.45 J**	—	—	—	**5.3**	**4.3**	**17**	—	—
	ES057	1/28/2014	**2,300 HD**	—	—	**50 B**	< 0.50 U	< 0.50 U	**0.14 J**	**0.20 J**	—	< 0.50 U	**0.38 J**	—	—	—	**8.8**	**5.4**	**18**	—	—
	ES058	1/28/2014*	**2,100 HD**	—	—	**52 B**	< 0.50 U	< 0.50 U	**0.15 J**	**0.20 J**	—	< 0.50 U	**0.34 J**	—	—	—	**9.0**	**5.9**	**18**	—	—
	ES063	2/24/2014	**2,200 HD**	—	—	**40 J**	< 0.50 U	< 0.50 U	< 0.50 U	**0.15 J**	—	< 0.50 U	**0.29 J**	—	—	—	**5.2**	**2.5**	**15**	—	—
	ES065	3/5/2014	**2,100**	—	—	—	—	—	< 0.50 U	**0.15 J**	—	< 0.50 U	**0.29 J**	—	—	—	**2.6**	**1.5**	**10**	—	—
	ES066	3/5/2014*	**2,200**	—	—	—	—	—	< 0.50 U	**0.15 J**	—	< 0.50 U	**0.32 J**	—	—	—	**3.9**	**2.9**	**13**	—	—
	ES070	3/10/2014	**930**	—	—	—	—	—	< 0.50 U	< 0.50 U	—	< 0.50 U	**0.30 J**	—	—	—	**3.7**	**2.5**	**11**	—	—
	ES071	3/10/2014*	**890**	—	—	—	—	—	< 0.50 U	< 0.50 U	—	< 0.50 U	**0.31 J**	—	—	—	**4.2**	**3.0**	**12**	—	—
	ES073	3/25/2014	**1,700 HD**	—	—	—	—	—	< 0.50 U	**0.15 J**	—	< 0.50 U	**0.38 J**	—	—	—	**9.0**	**4.9**	**33**	—	—
	ES074	3/25/2014*	**1,700 HD**	—	—	—	—	—	< 0.50 U	**0.16 J**	—	< 0.50 U	**0.41 J**	—	—	—	**8.1**	**4.0**	**33**	—	—
	ES078	4/7/2014	**3,500 HD**	—	—	—	—	—	< 0.50 U	**0.18 J**	—	< 0.50 U	**0.40 J**	—	—	—	**6.2**	**4.4**	**25**	—	—
	ES079	4/7/2014*	**3,300 HD**	—	—	—	—	—	< 0.50 U	< 0.50 U	—	< 0.50 U	**0.33 J**	—	—	—	**9.0**	**7.6**	**31**	—	—
	ES081	4/21/2014	**1,900**	—	—	**53**	< 0.50 U	< 0.50 U	< 0.50 U	**0.17 J**	—	< 0.50 U	**0.43 J**	—	—	—	**8.7**	**8.1**	**31**	—	—
	ES082	4/21/2014*	**1,500**	—	—	**50**	< 0.50 U	< 0.50 U	< 0.50 U	**0.16 J**	—	< 0.50 U	**0.42 J**	—	—	—	**8.3**	**7.7**	**32**	—	—
	ES092	5/27/2014	**1,500 HD**	—	—	—	—	—	< 0.50 U	< 0.50 U	—	< 0.50 U	**0.31 J**	—	—	—	**9.3**	**2.7**	**34**	—	—
	ES093	5/27/2014*	**1,300 HD**	—	—	—	—	—	< 0.50 U	< 0.50 U	—	< 0.50 U	**0.32 J**	—	—	—	**7.8**	**1.5**	**28**	—	—
	ES099	6/23/2014	**1,800**	—	—	—	—	—	< 0.50 U	**0.16 J**	—	< 0.50 U	**0.40 J**	—	—	—	**11**	**3.4**	**38**	—	—
	ES100	6/23/2014*	**1,600**	—	—	—	—	—	< 0.50 U	**0.18 J**	—	< 0.50 U	**0.37 J**	—	—	—	**12**	**4.5**	**41**	—	—
	ES104	7/21/2014	**1,200 HD**	—	—	**48 J**	< 0.50 U	< 0.50 U	< 0.50 U	< 0.50 U	—	< 0.50 U	**0.36 J**	—	—	—	**25**	**20**	**71**	—	—
	ES105	7/21/2014*	**1,300 HD**	—	—	**49 J**	< 0.50 U	< 0.50 U	< 0.50 U	< 0.50 U	—	< 0.50 U	**0.33 J**	—	—	—	**26**	**22**	**76**	—	—
	ES114	10/27/2014	**2,000 J,HD**	—	—	**57**	< 0.50 U	< 0.50 U,IH	< 0.50 U	**0.15 J**	—	< 0.50 U	**0.32 J**	—	—	—	**59**	**43**	**140**	—	—
	ES115	10/27/2014	**2,000 J,HD**	—	—	**53**	< 0.50 U	< 0.50 U,IH	< 0.50 U	**0.14 J**	—	< 0.50 U	**0.29 J**	—	—	—	**54**	**36**	**130**	—	—
	ES126	1/28/2015	**1,100 HD**	—	—	**54**	< 0.50 U	< 0.50 U	< 0.50 U	**0.16 J**	—	< 0.50 U	**0.35 J**	—	—	—	**34**	**7.6 J**	**90**	—	—
	ES127	1/28/2015*	**1,700 HD**	—	—	**59**	< 0.50 U	< 0.50 U	< 0.50 U	**0.17 J**	—	< 0.50 U	**0.35 J**	—	—	—	**25**	**2.7 J**	**63**	—	—
	ES131	4/20/2015	**5,200 Y**	**46 J**	**360 L**	—	< 0.20 U	—	**0.090 J**	**0.18 J**	—	< 0.10 U	**0.26 J**	< 0.010 U	< 0.015 U	< 0.0040 U	**31 JD**	**15 JD**	**39 JD**	—	—
	ES132	4/20/2015*	**5,400 Y**	**47 J**	**360 L**	—	< 0.20 U	—	**0.080 J**	**0.19 J**	—	< 0.10 U	**0.30 J**	< 0.010 U	< 0.015 U	< 0.0040 U	**68 JD**	**37 JD**	**140 JD**	—	—
	ES144	6/25/2015	**3,800 Y**	—	**250 L**	—	—	—	—	—	—	—	—	—	—	—	**71 JD**	**48 JD**	**150 JD**	—	—
	ES146	7/20/2015	**3,900 Y**	**40 J**	**240 L**	—	< 0.20 U	—	< 0.10 U	**0.16 J**	—	**0.060 J**	**0.26 J**	—	< 0.015 U	< 0.0040 U	**65 JD**	**43 JD**	**150 JD**	—	—
	ES147	7/20/2015*	**3,200 Y**	**41 J**	**260 L**	—	< 0.20 U	—	**0.10 J**	**0.17 J**	—	< 0.10 U	**0.27 J**	—	< 0.015 U	< 0.0040 U	**66 D**	**43 D**	**160 D**	—	—
	ERH012	10/20/2015	**6,100 BY**	**47 J**	**310 BL**	—	< 0.20 U**	—	**0.090 J,****	**0.29 J,****	—	**0.30 J,**,Tb**	**0.32 J,****	—	— U	< 0.0040 U	**60 D**	**27 BD**	**120 BD**	—	—
	ERH013	10/20/2015*	**6,200 BY**	**47 J**	**320 BL**	—	< 0.20 U**	—	**0.090 J,****	**0.26 J,****	—	**0.49 J,**,Tb**	**0.30 J,****	—	— U	< 0.0040 U	**57 D**	**24 BD**	**88 BD**	—	—

Table A.1-1: Cumulative Groundwater COPC Results (cont'd)
First Quarter 2018 - Quarterly Groundwater Monitoring Report, Red Hill Bulk Fuel Storage Facility, JBPHH, O'ahu, Hawai'i

		Method	8015						8260					8260SIM		8011	8270			8270/8270 Mod.	
			TPH-d	TPH-g ****	TPH-o	TPH-g ****	1,2-Dibromoethane *****	1,2-Dichloroethane *****	Benzene	Ethylbenzene	Naphthalene	Toluene	Xylenes, Total (p/m-, o-xylene)	1,2-Dibromoethane *****	1,2-Dichloroethane *****	1,2-Dibromoethane *****	1-Methylnaphthalene	2-Methylnaphthalene	Naphthalene	Phenol	2-(2-Methoxyethoxy)-ethanol
		Unit	(µg/L)	(µg/L)	(µg/L)	(µg/L)	(µg/L)	(µg/L)	(µg/L)	(µg/L)	(µg/L)	(µg/L)	(µg/L)	(µg/l)	(µg/L)	(µg/L)	(µg/L)	(µg/L)	(µg/L)	(µg/L)	(µg/L)
		Screening Criterion	400	300	500	300	0.04	5.0	5.0	30	17	40	20	0.04	5.0	0.04	10	10	17	300	800
		SSRBL	4500	—	—	—	—	—	750	—	—	—	—	—	—	—	—	—	—	—	—
Well Name	Sample ID	Date Sampled	Result	Result	Result	Result	Result	Result	Result	Result	Result	Result	Result	Result	Result	Result	Result	Result	Result	Result	Result
RHMW02	ERH025	1/20/2016	**6,500 BY**	**36 J**	**340 BL**	—	< 0.20 U	—	**0.080 J**	**0.014 J**	—	**0.070 TbJ**	**0.21 J**	—	< 0.015 U	< 0.0040 U	**48 D**	**7.9 D**	**120 D**	—	—
(cont'd)	ERH040	4/20/2016	**4,400 Y**	**35 J**	**390 L**	—	—	—	< 0.10 U	**0.17 J**	—	< 0.10 U	**0.16 J**	—	—	—	**59 D**	**38 D**	**100 D**	—	—
	ERH041	4/20/2016*	**3,700 Y**	**35 J**	**400 L**	—	—	—	**0.070 J**	**0.17 J**	—	< 0.10 U	**0.18 J**	—	—	—	**61 D**	**39 D**	**110 D**	—	—
	ERH054	7/20/2016	**3,600 Y**	**31 JS**	**280 L**	—	—	—	**0.070 J**	< 0.10 UF	—	< 0.10 U	< 0.20 UF	—	—	—	**36 D**	**13 D**	**67 D**	—	—
	ERH055	7/20/2016*	**3,200 Y**	**30 JS**	**270 L**	—	—	—	**0.080 J**	< 0.10 UF	—	< 0.10 U	< 0.20 UF	—	—	—	**33 D**	**12 D**	**62 D**	—	—
	ERH091	10/19/2016	**1,300**	—	< 40 U	**35**	—	—	< 0.30 U	< 0.50 U	—	< 0.30 U	< 0.30 U	—	—	—	**25**	**9.2**	**49**	< 4.00 U	< 80.0 UJ
	ERH124	11/15/2016	**1,300**	—	**100**	**26**	—	—	< 0.30 U	< 0.50 U	—	< 0.30 U	< 0.30 U	—	—	—	**29**	**12**	**58**	< 4.00 U	< 80.0 U
	ERH144	12/13/2016	**1,300**	—	< 40 U	< 18 U	—	—	< 0.30 U	< 0.50 U	—	< 0.30 U	**0.19 J**	—	—	—	**17**	**11**	**40**	< 4.00 U	< 80.0 U
	ERH174	1/10/2017	**1,400**	—	**42**	**63**	—	—	< 0.30 U	< 0.50 U	—	< 0.30 U	**0.26 J**	—	—	—	**25**	**11**	**69**	< 4.00 U	< 80.0 U
	ERH216	2/7/2017	**1,000**	—	< 40 U	**65**	—	—	< 0.30 U	< 0.50 U	—	< 0.30 U	**0.23 J**	—	—	—	**22**	**16**	**57**	< 4.00 U	< 80.0 U
	ERH265	3/7/2017	**1,200**	—	< 40 U	**73**	—	—	< 0.30 U	< 0.50 U	—	< 0.30 U	< 0.30 U	—	—	—	**22**	**17**	**49**	< 4.00 U	< 80.0 U
	ERH300	4/4/2017	**940**	—	**84**	**57**	—	—	< 0.30 U	< 0.50 U	—	< 0.30 U	< 0.30 U	—	—	—	**20**	**17**	**52**	< 4.00 U	< 80.0 U
	ERH334	5/1/2017	**1000**	—	< 40	**94**	—	—	< 0.30 U	< 0.50 U	—	< 0.30 U	< 0.30 U	—	—	—	**28**	**24**	**65**	< 4.00 U	< 80.0 U
	ERH354	6/5/2017	**1000**	—	< 40 U	**65**	—	—	< 0.30 U	< 0.50 U	—	< 0.30 U	< 0.30 U	—	—	—	**25**	**16**	**62**	< 4.00 U	< 80.0 U
	ERH391	7/6/2017	**1000**	—	< 40 U	**33**	—	—	< 0.30 U	< 0.50 U	—	< 0.30 U	**1.4 J**	—	—	—	**14**	**1.5**	**56**	< 4.00 U	< 80.0 U
	ERH415/416	10/23/2017*	**1600**	—	< 40 U	**76**	< 0.50 U	< 0.30 U	< 0.30 U	< 0.50 U	—	< 0.30 U	**0.26 J**	—	—	—	**15**	**8.6**	**38** J	< 4.00 U	< 80.0 U
	ERH547/548	3/13/2018*	**1900**	—	< 40 U	**47**	—	—	< 0.30 U	< 0.50 U	—	< 0.30 U	**0.37 J**	—	—	—	**25**	**18**	**65**	< 4.00 U	< 80.0 U

Table A.1-1: Cumulative Groundwater COPC Results (cont'd)
First Quarter 2018 - Quarterly Groundwater Monitoring Report, Red Hill Bulk Fuel Storage Facility, JBPHH, O'ahu, Hawai'i

		Method	8015						8260					8260SIM		8011	8270			8270/8270 Mod.	
			TPH-d	TPH-g ****	TPH-o	TPH-g ****	1,2-Dibromoethane *****	1,2-Dichloroethane *****	Benzene	Ethylbenzene	Naphthalene	Toluene	Xylenes, Total (p/m-, o-xylene)	1,2-Dibromoethane *****	1,2-Dichloroethane *****	1,2-Dibromoethane *****	1-Methylnaphthalene	2-Methylnaphthalene	Naphthalene	Phenol	2-(2-Methoxyethoxy)-ethanol
		Unit	(µg/L)	(µg/L)	(µg/L)	(µg/L)	(µg/L)	(µg/L)	(µg/L)	(µg/L)	(µg/L)	(µg/L)	(µg/L)	(µg/l)	(µg/L)	(µg/L)	(µg/L)	(µg/L)	(µg/L)	(µg/L)	(µg/L)
		Screening Criterion	400	300	500	300	0.04	5.0	5.0	30	17	40	20	0.04	5.0	0.04	10	10	17	300	800
		SSRBL	4500	—	—	—	—	—	750	—	—	—	—	—	—	—	—	—	—	—	—
Well Name	Sample ID	Date Sampled	Result	Result	Result	Result	Result	Result	Result	Result	Result	Result	Result	Result	Result	Result	Result	Result	Result	Result	Result
RHMW03	RHMW03W01	9/20/2005[b]	**162 J**	< 0.50 U	—	—	< 0.50 U	< 0.50 U	< 0.50 U	< 0.50 U	< 1.0 U	< 0.50 U	< 0.50 U	—	—	—	< 0.24 U	< 0.24 U	< 0.24 U	—	—
	RHMW03-GW02	7/10/2006[ad]	**142 J**	< 50 U	—	—	< 0.50 U	< 0.50 U	< 0.50 U	< 0.50 U	< 1.0 U	< 0.50 U	< 0.50 U	—	—	—	< 0.25 U	< 0.25 U	< 0.25 U	—	—
	RHMW03-GW06	12/5/2006[ad]	< 100 U	< 50 U	—	—	< 0.50 U	< 0.50 U	< 0.50 U	< 0.50 U	< 1.0 U	< 0.50 U	< 0.50 U	—	—	—	< 0.25 U	< 0.25 U	< 0.25 U	—	—
	RHMW03-WG07	3/27/2007[a]	**95.7 J**	< 50 U	—	—	< 0.50 U	< 0.50 U	< 0.50 U	< 0.50 U	< 1.0 U	< 0.50 U	< 0.50 U	—	—	—	< 0.25 U	< 0.25 U	< 0.25 U	—	—
	RHMW03-WG08	6/12/2007[a]	**123 J**	< 50 U	—	—	< 0.50 U	< 0.50 U	< 0.50 U	< 0.50 U	< 1.0 U	< 0.50 U	< 0.50 U	—	—	—	< 0.25 U	< 0.25 U	< 0.25 U	—	—
	RHMW03-WG09	9/10/2007[a]	< 96 U	< 50 U	—	—	< 0.20 U	< 0.20 U	< 0.20 U	< 0.20 U	< 0.44 U	< 0.27 U	< 0.36 U	—	—	—	< 0.25 U	< 0.25 U	< 0.25 U	—	—
	RHMW03-WG10	1/15/2008[a]	**242 J**	< 10.0 U	—	—	< 0.310 U	< 0.150 U	< 0.120 U	< 0.310 U	< 0.620 U	< 0.310 U	< 0.620 U	—	—	—	< 0.0156 U	< 0.0156 U	< 0.0323 U	—	—
	RHMW03-WG11	4/15/2008[a]	**190 J**	< 10.0 U	—	—	< 0.310 U	< 0.150 U	< 0.120 U	< 0.310 U	< 0.620 U	< 0.310 U	< 0.620 U	—	—	—	**0.0268 J**	**0.0279 J**	< 0.0341 U	—	—
	RHMW03-WG12	7/29/2008[a]	**199 J**	< 10.0 U	—	—	< 0.310 U	< 0.150 U	< 0.120 U	< 0.310 U	< 0.620 U	< 0.310 U	< 0.620 U	—	—	—	**0.0294 J**	< 0.0156 U	**0.0689 J**	—	—
	RHMW03-WG13	10/22/2008[a]	**244 J**	< 10.0 U	—	—	< 0.310 U	< 0.150 U	< 0.120 U	< 0.310 U	< 0.620 U	< 0.310 U	< 0.620 U	—	—	—	**0.0658**	**0.0937**	**0.219**	—	—
	RHMW03-WG14	2/4/2009[a]	**207 J**	**16.1 J**	—	—	< 0.310 U	< 0.150 U	< 0.120 U	< 0.310 U	< 0.620 U	< 0.310 U	< 0.620 U	—	—	—	< 0.0161 U	< 0.0161 U	< 0.0333 U	—	—
	RHMW03-WG15	5/13/2009[a]	< 161 U	**14.8 J**	—	—	< 0.310 U	< 0.150 U	< 0.120 U	< 0.310 U	< 0.620 U	< 0.310 U	< 0.620 U	—	—	—	< 0.0152 U	< 0.0152 U	< 0.0313 U	—	—
	RHMW03-WG16	7/15/2009[a]	< 150 U	< 30.0 U	—	—	< 0.310 U	< 0.150 U	< 0.120 U	< 0.310 U	< 0.620 U	< 0.310 U	< 0.620 U	—	—	—	< 0.0158 U	< 0.0158 U	< 0.0326 U	—	—
	RHMW03-WG17	10/14/2009[a]	< 163 U	< 30 U	—	—	< 0.31 U	< 0.15 U	< 0.12 U	< 0.31 U	< 0.62 U	< 0.31 U	< 1 U	—	—	—	< 0.0169 U	< 0.0169 U	< 0.0348 U	—	—
	RHMW03-WG18	1/27/2010	< 330 U	< 60.0 U	—	—	< 0.620 U	< 0.300 U	< 0.240 U	< 0.620 U	< 1.24 U	< 0.620 U	< 1.24 U	—	—	—	< 0.0322 U	< 0.0322 U	< 0.0666 U	—	—
	RHMW03-WG19	4/13/2010	< 320 U	< 60.0 U	—	—	< 0.620 U	< 0.300 U	< 0.240 U	< 0.620 U	< 1.24 U	< 0.620 U	< 1.24 U	—	—	—	< 0.0322 U	< 0.0322 U	< 0.0666 U	—	—
	RHMW03-WG20	7/13/2010	< 324 U	< 60.0 U	—	—	< 0.620 U	< 0.300 U	< 0.240 U	< 0.620 U	< 1.24 U	< 0.620 U	< 1.24 U	—	—	—	< 0.0322 U	< 0.0322 U	< 0.0666 U	—	—
	ES001	10/18/2010	**330 ++**	—	—	< 12.12 U	< 0.40 U	< 0.28 U	< 0.32 U	< 0.46 U	—	< 0.34 U	< 0.38 U	—	—	—	< 0.12 U	< 0.12 U	< 0.10 U	—	—
	ES012	1/19/2011	< 80.8 U	—	—	< 12.12 U	< 0.40 U	< 0.28 U	< 0.32 U	< 0.46 U	—	< 0.34 U	< 0.38 U	—	—	—	< 0.12 U	< 0.12 U	< 0.10 U	—	—
	ES025	4/20/2011	< 80.8 U	—	—	< 12.12 U	< 0.40 U	< 0.28 U	< 0.32 U	< 0.46 U	—	< 0.34 U	< 0.38 U	—	—	—	< 0.12 U	< 0.12 U	< 0.10 U	—	—
	ES035	7/19/2011	< 80.8 U	—	< 212.0 U	< 12.12 U	< 0.40 U	< 0.28 U	< 0.32 U	< 0.46 U	—	< 0.34 U	< 0.38 U	—	—	—	< 0.12 U	< 0.12 U	< 0.10 U	—	—
	ES049	10/24/2011	< 80.8 U	—	—	< 12.12 U	< 0.40 U	< 0.28 U	< 0.32 U	< 0.46 U	—	< 0.34 U	< 0.38 U	—	—	—	< 0.12 U	< 0.12 U	< 0.10 U	—	—
	ES060	1/26/2012	< 80.8 U	—	—	< 12.12 U	< 0.40 U	< 0.28 U	< 0.32 U	< 0.46 U	—	< 0.34 U	< 0.38 U	—	—	—	< 0.12 U	< 0.12 U	< 0.10 U	—	—
	ES073	4/16/2012	< 80.8 U	—	—	< 12.12 U	< 0.40 U	< 0.28 U	< 0.32 U	< 0.46 U	—	< 0.34 U	< 0.38 U	—	—	—	< 0.12 U	< 0.12 U	< 0.10 U	—	—
	ES081	7/18/2012	< 80.8 U	—	< 212.0 U	< 12.12 U	< 0.40 U	< 0.28 U	< 0.32 U	< 0.46 U	—	< 0.34 U	< 0.38 U	—	—	—	< 0.12 U	< 0.12 U	< 0.10 U	—	—
	ES004	10/22/2012	**45 J,HD**	—	—	< 30 U	< 0.50 U	< 0.50 U	< 0.50 U	< 0.50 U	—	**0.54 J**	< 1.0 U	—	—	—	< 0.050 U	< 0.050 U	**0.029 J**	—	—
	ES013	1/28/2013	**59 HD**	—	—	< 30 U	< 0.50 U	< 0.50 U	< 0.50 U	< 0.50 U	—	< 0.50 U	< 1.0 U	—	—	—	**0.10 J**	**0.069 J**	**0.32**	—	—
	ES022	4/22/2013	**69 HD**	—	—	< 30 U	< 0.50 U	< 0.50 U	< 0.50 U	< 0.50 U	—	< 0.50 U	< 1.0 U	—	—	—	< 0.053 U	< 0.053 U	< 0.053 U	—	—
	ES031	7/22/2013	**48 J,HD**	—	—	< 30 U	< 0.50 U	< 0.50 U	< 0.50[1] U	< 0.50[1] U	—	< 0.50[1] U	<1.0[1] U	—	—	—	< 0.050 U	< 0.050 U	**0.064 J**	—	—
	ES040	10/21/2013	**54 HD**	—	—	**23 BJ**	< 0.50 U	< 0.50 U	< 0.50 U	< 0.50 U	—	< 0.50 U	< 1.0 U	—	—	—	< 0.050 U	< 0.050 U	< 0.050 U	—	—
	ES059	1/28/2014	**74**	—	—	**20 BJ**	< 0.50 U	< 0.50 U	< 0.50 U	< 0.50 U	—	< 0.50 U	< 1.0 U	—	—	—	< 0.050 U	< 0.050 U	**0.15 J**	—	—
	ES083	4/21/2014	**39 HD**	—	—	< 30 U	< 0.50 U	< 0.50 U	< 0.50 U	< 0.50 U	—	< 0.50 U	< 1.0 U	—	—	—	< 0.049 U	< 0.049 U	**0.11 J**	—	—
	ES106	7/22/2014	**37 HD**	—	—	< 30 U	< 0.50 U	< 0.50 U	< 0.50 U	< 0.50 U	—	< 0.50 U	< 1.0 U	—	—	—	< 0.047 U	< 0.047 U	< 0.047 U	—	—
	ES116	10/27/2014	**80 J,HD**	—	—	< 30 U	< 0.50 U	< 0.50 U,IH	< 0.50 U	< 0.50 U	—	< 0.50 U	< 1.0 U	—	—	—	< 0.11 U	< 0.054 U	< 0.054 U	—	—
	ES123	1/28/2015	**39 HD**	—	—	< 30 U	< 0.50 U	< 0.50 U	< 0.50 U	< 0.50 U	—	< 0.50 U	< 1.0 U	—	—	—	< 0.097 U	< 0.048 U	< 0.048 U	—	—
	ES133	4/20/2015	**100 BY**	< 25 U	**110 BL**	—	< 0.20 U	—	< 0.10 U	< 0.10 U	—	< 0.10 U	< 0.20 U	< 0.010 U	< 0.015 U	< 0.0040 U	**0.015 J**	**0.0083 J**	**0.035 J**	—	—
	ES148	7/20/2015	**130 Y**	< 25 U	**150 L**	—	< 0.20 U	—	< 0.10 U	< 0.10 U	—	< 0.10 U	< 0.20 U	—	< 0.015 U	< 0.0040 U	< 0.0052 U	< 0.0052 U	< 0.0052 U	—	—
	ERH014	10/20/2015	**130 BY**	< 25 U	**160 BL**	—	< 0.20 U**	—	< 0.10 U**	< 0.10 U**	—	**0.40 J,**,Tb**	< 0.20 U**	—	< 0.015 U	< 0.0040 U	**0.0039 J**	**0.0034 BJ**	**0.0094 BJ**	—	—
	ERH026	1/20/2016	**150 BY**	< 25 U	**160 BL**	—	< 0.20 U	—	< 0.10 U	< 0.10 U	—	**0.14 TbJ**	< 0.20 U	—	< 0.015 U	< 0.0040 U	< 0.0050 U	< 0.0050 U	< 0.0050 U	—	—
	ERH042	4/20/2016	< 95 YUB	< 25 U	< 170 BL	—	—	—	< 0.10 U	< 0.10 U	—	< 0.10 U	< 0.20 U	—	—	—	**0.0084 J**	**0.0075 J**	< 0.0050 U	—	—
	ERH056	7/20/2016	< 70 YUB	< 25 U	**110 J**	—	—	—	< 0.10 U	< 0.10 U	—	< 0.10 U	< 0.20 U	—	—	—	**0.0073 J**	**0.0040 J**	< 0.0050 UF	—	—
	ERH093	10/19/2016	**65**	—	**59**	< 18 U	—	—	< 0.30 U	< 0.50 U	—	< 0.30 U	< 0.30 U	—	—	—	< 0.10 U	< 0.10 U	< 0.10 U	< 4.00 U	< 80.0 UJ
	ERH125	11/15/2016	**51**	—	**42**	< 18 U	—	—	< 0.30 U	< 0.50 U	—	< 0.30 U	< 0.30 U	—	—	—	< 0.10 U	< 0.10 U	< 0.10 U	< 4.00 U	< 80.0 U
	ERH152	12/14/2016	**56**	—	**49**	< 18 U	—	—	< 0.30 U	< 0.50 U	—	< 0.30 U	< 0.30 U	—	—	—	< 0.10 U	< 0.10 U	< 0.10 U	< 4.00 U	< 80.0 U
	ERH181	1/12/2017	**51**	—	**46**	< 18 U	—	—	< 0.30 U	< 0.50 U	—	< 0.30 U	< 0.30 U	—	—	—	< 0.10 U	< 0.10 U	< 0.10 U	< 4.00 U	< 80.0 U

Table A.1-1: Cumulative Groundwater COPC Results (cont'd)
First Quarter 2018 - Quarterly Groundwater Monitoring Report, Red Hill Bulk Fuel Storage Facility, JBPHH, O'ahu, Hawai'i

		Method	8015						8260					8260SIM		8011	8270			8270/8270 Mod.	
			TPH-d	TPH-g ****	TPH-o	TPH-g ****	1,2-Dibromoethane *****	1,2-Dichloroethane *****	Benzene	Ethylbenzene	Naphthalene	Toluene	Xylenes, Total (p/m-, o-xylene)	1,2-Dibromoethane *****	1,2-Dichloroethane *****	1,2-Dibromoethane *****	1-Methylnaphthalene	2-Methylnaphthalene	Naphthalene	Phenol	2-(2-Methoxyethoxy)-ethanol
		Unit	(µg/L)	(µg/L)	(µg/L)	(µg/L)	(µg/L)	(µg/L)	(µg/L)	(µg/L)	(µg/L)	(µg/L)	(µg/L)	(µg/l)	(µg/L)	(µg/L)	(µg/L)	(µg/L)	(µg/L)	(µg/L)	(µg/L)
		Screening Criterion	400	300	500	300	0.04	5.0	5.0	30	17	40	20	0.04	5.0	0.04	10	10	17	300	800
		SSRBL	4500	—	—	—	—	—	750	—	—	—	—	—	—	—	—	—	—	—	—
Well Name	Sample ID	Date Sampled	Result	Result	Result	Result	Result	Result	Result	Result	Result	Result	Result	Result	Result	Result	Result	Result	Result	Result	Result
RHMW03	ERH231	2/8/2017	**67**	—	**71**	< 18 U	—	—	< 0.30 U	< 0.50 U	—	< 0.30 U	< 0.30 U	—	—	—	< 0.10 U	< 0.10 U	< 0.10 U	< 4.00 U	< 80.0 U
(cont'd)	ERH268	3/7/2017	**55**	—	**41**	< 18 U	—	—	< 0.30 U	< 0.50 U	—	< 0.30 U	< 0.30 U	—	—	—	< 0.10 U	< 0.10 U	< 0.10 U	< 4.00 U	< 80.0 U
	ERH303	4/4/2017	**47**	—	**47**	< 18 U	—	—	< 0.30 U	< 0.50 U	—	< 0.30 U	< 0.30 U	—	—	—	< 0.10 U	< 0.10 U	< 0.10 U	< 4.00 U	< 80.0 U
	ERH303	5/1/2017	**50**	—	**46**	< 18 U	—	—	< 0.30 U	< 0.50 U	—	< 0.30 U	< 0.30 U	—	—	—	< 0.10 U	< 0.10 U	< 0.10 U	< 4.00 U	< 80.0 U
	ERH356	6/6//2017	**46**	—	**36 J**	< 18 U	—	—	< 0.30 U	< 0.50 U	—	< 0.30 U	< 0.30 U	—	—	—	< 0.10 U	< 0.10 U	< 0.10 U	< 4.00 U	< 80.0 U
	ERH392	7/6//2017	**49**	—	**46**	< 18 U	—	—	< 0.30 U	< 0.50 U	—	< 0.30 U	< 0.30 U	—	—	—	< 0.10 U	< 0.10 U	< 0.10 U	< 4.00 U	< 80.0 U
	ERH418/419	10/23/2017*	**210**	—	**200**	< 18 U	< 0.50 U	< 0.30 U	< 0.30 U	< 0.50 U	—	< 0.30 U	< 0.30 U	—	—	—	< 0.10 U	< 0.10 U	< 0.10 U	< 4.00 U	< 80.0 U
	ERH550	3/12/2018	**190**	—	**180**	< 18 U	—	—	< 0.30 U	< 0.50 U	—	< 0.30 U	< 0.30 U	—	—	—	< 0.10 U	< 0.10 U	< 0.10 U	< 4.00 U	< 80.0 U

Table A.1-1: Cumulative Groundwater COPC Results (cont'd)
First Quarter 2018 - Quarterly Groundwater Monitoring Report, Red Hill Bulk Fuel Storage Facility, JBPHH, O'ahu, Hawai'i

		Method	8015						8260					8260SIM		8011	8270			8270/8270 Mod.	
			TPH-d	TPH-g ****	TPH-o	TPH-g ****	1,2-Dibromoethane *****	1,2-Dichloroethane *****	Benzene	Ethylbenzene	Naphthalene	Toluene	Xylenes, Total (p/m-, o-xylene)	1,2-Dibromoethane *****	1,2-Dichloroethane *****	1,2-Dibromoethane *****	1-Methylnaphthalene	2-Methylnaphthalene	Naphthalene	Phenol	2-(2-Methoxyethoxy)-ethanol
		Unit	(µg/L)	(µg/L)	(µg/L)	(µg/L)	(µg/L)	(µg/L)	(µg/L)	(µg/L)	(µg/L)	(µg/L)	(µg/L)	(µg/l)	(µg/L)	(µg/L)	(µg/L)	(µg/L)	(µg/L)	(µg/L)	(µg/L)
		Screening Criterion	400	300	500	300	0.04	5.0	5.0	30	17	40	20	0.04	5.0	0.04	10	10	17	300	800
		SSRBL	4500	—	—	—	—	—	750	—	—	—	—	—	—	—	—	—	—	—	—
Well Name	Sample ID	Date Sampled	Result	Result	Result	Result	Result	Result	Result	Result	Result	Result	Result	Result	Result	Result	Result	Result	Result	Result	Result
RHMW04	RHMW04W01	9/19/2005[a,b]	**338**	< 50.0 U	—	—	< 0.50 U	< 0.50 U	< 0.50 U	< 0.50 U	< 1.0 U	< 0.50 U	< 0.50 U	—	—	—	< 0.28 U	< 0.28 U	< 0.28 U	—	—
	RHMW04-GW02	7/10/2006[a,b]	< 100 U	< 50.0 U	—	—	< 0.50 U	< 0.50 U	< 0.50 U	< 0.50 U	< 1.0 U	< 0.50 U	< 0.50 U	—	—	—	< 0.26 U	< 0.26 U	< 0.26 U	—	—
	RHMW04-WG-01	8/4/2009[a]	<157 U	< 30.0 U	—	—	< 0.310 U	< 0.150 U	< 0.120 U	< 0.310 U	< 0.620 U	< 0.310 U	< 0.620 U	—	—	—	< 0.0162 U	< 0.0162 U	<0.0335 U	—	—
	RHMWA01-WG-01	8/4/2009*[a]	<161 U	< 30.0 U	—	—	< 0.310 U	< 0.150 U	**0.250 J**	< 0.310 U	< 0.620 U	< 0.310 U	< 0.620 U	—	—	—	< 0.0167 U	< 0.0167 U	<0.0344 U	—	—
	RHMW04-WG-02	10/13/2009[ab]	<169 U	< 30.0 U	—	—	< 0.31 U	< 0.15 U	< 0.12 U	< 0.31 U	< 0.62 U	< 0.31 U	< 0.62 U	—	—	—	< 0.0172 U	< 0.0172 U	<0.0356 U	—	—
	RHMWA01-WG-02	10/13/2009*[ab]	<174 U	< 30.0 U	—	—	< 0.31 U	< 0.15 U	< 0.12 U	< 0.31 U	< 0.62 U	< 0.31 U	< 0.62 U	—	—	—	< 0.0169 U	< 0.0169	< 0.0348 U	—	—
	RHMW04-WG-03	1/26/2010	<334 U	< 60.0 U	—	—	< 0.620 U	< 0.300 U	< 0.240 U	< 0.620 U	< 1.24 U	< 0.620 U	< 1.24 U	—	—	—	<0.0326 U	<0.0326 U	<0.0674 U	—	—
	RHMWA01-WG-03	1/26/2010*	<330 U	< 60.0 U	—	—	< 0.620 U	< 0.300 U	< 0.240 U	< 0.620 U	< 1.24 U	< 0.620 U	< 1.24 U	—	—	—	<0.0338 U	<0.0338 U	<0.0696 U	—	—
	RHMW04-WG-04	4/26/2010	<348 U	< 60.0 U	—	—	< 0.620 U	< 0.300 U	< 0.240 U	< 0.620 U	< 1.24 U	< 0.620 U	< 1.24 U	—	—	—	< 0.0352 U	< 0.0352 U	<0.0730 U	—	—
	RHMWA01-WG-04	4/26/2010*	<352 U	< 60.0 U	—	—	< 0.620 U	< 0.300 U	< 0.240 U	< 0.620 U	< 1.24 U	< 0.620 U	< 1.24 U	—	—	—	< 0.0352 U	< 0.0352 U	<0.0730 U	—	—
	ES112	7/23/2014	**17 J,HD**	—	—	< 30 U	< 0.50 U	< 0.50 U	< 0.50 U	< 0.50 U	—	< 0.50 U	< 1.0 U	—	—	—	< 0.052 U	< 0.052 U	< 0.052 U	—	—
	ES119	10/29/2014	< 12 U	—	—	< 30 U	< 0.50 U	< 0.50 U	< 0.50 U	< 0.50 U	—	< 0.50 U	< 1.0 U	—	—	—	< 0.099 U	< 0.050 U	< 0.050 U	—	—
	ES129	1/29/2015	**10 J,HD**	—	—	< 30 U	< 0.50 U	< 0.50 U	< 0.50 U	< 0.50 U	—	< 0.50 U	< 1.0 U	—	—	—	< 0.10 U	< 0.052 U	< 0.052 U	—	—
	ES139	4/22/2015	< 21 U	< 25 U	**25 BJ**	—	< 0.20 U	—	< 0.10 U	< 0.10 U	—	< 0.10 U	< 0.20 U	< 0.010 U	< 0.015 U	< 0.0040 UJ	< 0.0050 U	< 0.0050 U	< 0.0050 U	—	—
	ES156	8/20/2015	**24 BJ**	< 25 U	**40 BJ**	—	< 0.20 U	—	< 0.10 U	< 0.10 U	—	< 0.10 U	< 0.20 U	—	< 0.015 U	< 0.0040 U	< 0.0050 U	**0.0059 J**	**0.0075 J**	—	—
	ERH006	10/19/2015	< 22 UB	< 25 U	< 53 UB	—	< 0.20 U**	—	**0.08 J,****	< 0.10 U**	—	**0.420 J****	< 0.20 U**	—	< 0.015 U	< 0.0040 U	**0.0043 J**	**0.0047 BJ**	**0.0051 BJ**	—	—
	ERH019	1/19/2016	**36 BJ**	< 25 U	**52 BJ**	—	< 0.20 U	—	< 0.10 U	< 0.10 U	—	< 0.10 U	< 0.20 U	—	< 0.015 U	< 0.0040 U	< 0.0050 U	< 0.0050 U	< 0.0050 U	—	—
	ERH020	1/19/2016	**29 BJ**	< 25 U	< 53 UB	—	< 0.20 U	—	< 0.10 U	< 0.10 U	—	**0.11 TbJ**	< 0.20 U	—	< 0.015 U	< 0.0040 U	< 0.0050 U	< 0.0050 U	< 0.0050 U	—	—
	ERH034	4/19/2016	< 20 UB	< 25 U	<33 UB	—	—	—	< 0.10 U	< 0.10 U	—	< 0.10 U	< 0.20 U	—	—	—	< 0.0050 U	< 0.0050 U	< 0.0050 U	—	—
	ERH048	7/19/2016	< 22 UF	< 25 U	< 55 UBF	—	—	—	< 0.10 U	< 0.10 U	—	< 0.10 U	< 0.20 U	—	—	—	**0.0070 J**	**0.0068 J**	**0.18**	—	—
	ERH096	10/25/2016	< 25 U	—	< 40 U	< 18 U	—	—	< 0.30 U	< 0.50 U	—	< 0.30 U	< 0.30 U	—	—	—	< 0.10 U	< 0.10 U	< 0.10 U	< 4.00 U	< 80.0 U
	ERH128	11/14/2016	< 25 U	—	< 40 U	< 18 U	—	—	< 0.30 U	< 0.50 U	—	< 0.30 U	< 0.30 U	—	—	—	< 0.10 U	< 0.10 U	< 0.10 U	< 4.00 U	< 80.0 U
	ERH138	12/13/2016	< 25 U	—	< 40 U	< 18 U	—	—	< 0.30 U	< 0.50 U	—	< 0.30 U	< 0.30 U	—	—	—	< 0.10 U	< 0.10 U	< 0.10 U	< 4.00 U	< 80.0 U
	ERH166	1/9/2017	< 25 U	—	< 40 U	< 18 U	—	—	< 0.30 U	< 0.50 U	—	< 0.30 U	< 0.30 U	—	—	—	< 0.10 U	< 0.10 U	< 0.10 U	< 4.00 U	< 80.0 U
	ERH208	2/6/2017	< 25 U	—	< 40 U	< 18 U	—	—	< 0.30 U	< 0.50 U	—	< 0.30 U	< 0.30 U	—	—	—	< 0.10 U	< 0.10 U	< 0.10 U	< 4.00 U	< 80.0 U
	ERH260	3/6/2017	< 25 U	—	< 40 U	< 18 U	—	—	< 0.30 U	< 0.50 U	—	< 0.30 U	< 0.30 U	—	—	—	< 0.10 U	< 0.10 U	< 0.10 U	< 4.00 U	< 80.0 U
	ERH295	4/3/2017	< 25 U	—	< 40 U	< 18 U	—	—	< 0.30 U	< 0.50 U	—	< 0.30 U	< 0.30 U	—	—	—	< 0.10 U	< 0.10 U	< 0.10 U	< 4.00 U	< 80.0 U
	ERH381	7/5/2017	< 25 U	—	< 40 U	< 18 U	—	—	< 0.30 U	< 0.50 U	—	< 0.30 U	< 0.30 U	—	—	—	< 0.10 U	< 0.10 U	< 0.10 U	< 4.00 U	< 80.0 U
	ERH421	10/24/2017	< 25 U	—	< 40 U	< 18 U	—	—	< 0.30 U	< 0.50 U	—	< 0.30 U	< 0.30 U	—	—	—	< 0.10 U	< 0.10 U	< 0.10 U	< 4.00 U	< 80.0 U
	ERH552	3/14/2018	< 25 U	—	< 40 U	< 18 U	—	—	< 0.30 U	< 0.50 U	—	< 0.30 U	< 0.30 U	—	—	—	< 0.10 U	< 0.10 U	< 0.10 U	< 4.00 U	< 80.0 U

Table A.1-1: Cumulative Groundwater COPC Results (cont'd)
First Quarter 2018 - Quarterly Groundwater Monitoring Report, Red Hill Bulk Fuel Storage Facility, JBPHH, O'ahu, Hawai'i

			Method	8015						8260					8260SIM		8011	8270			8270/8270 Mod.	
				TPH-d	TPH-g ****	TPH-o	TPH-g ****	1,2-Dibromoethane *****	1,2-Dichloroethane *****	Benzene	Ethylbenzene	Naphthalene	Toluene	Xylenes, Total (p/m-, o-xylene)	1,2-Dibromoethane *****	1,2-Dichloroethane *****	1,2-Dibromoethane *****	1-Methylnaphthalene	2-Methylnaphthalene	Naphthalene	Phenol	2-(2-Methoxyethoxy)-ethanol
			Unit	(µg/L)	(µg/L)	(µg/L)	(µg/L)	(µg/L)	(µg/L)	(µg/L)	(µg/L)	(µg/L)	(µg/L)	(µg/L)	(µg/l)	(µg/L)	(µg/L)	(µg/L)	(µg/L)	(µg/L)	(µg/L)	(µg/L)
			Screening Criterion	400	300	500	300	0.04	5.0	5.0	30	17	40	20	0.04	5.0	0.04	10	10	17	300	800
			SSRBL	4500	—	—	—	—	—	750	—	—	—	—	—	—	—	—	—	—	—	—
Well Name	Sample ID	Date Sampled		Result	Result	Result	Result	Result	Result	Result	Result	Result	Result	Result	Result	Result	Result	Result	Result	Result	Result	Result
RHMW05	RHMW05-WG15	5/13/2009[a]		**200 J**	**13.2 J**	—	—	< 0.310 U	< 0.150 U	< 0.120 U	< 0.310 U	< 0.620 U	< 0.310 U	< 0.620 U	—	—	—	< 0.0158 U	< 0.0158 U	< 0.0326 U	—	—
	RHMW05-WG16	7/15/2009[a]		**491**	< 30.0 U	—	—	< 0.310 U	< 0.150 U	< 0.120 U	< 0.310 U	< 0.620 U	< 0.310 U	< 0.620 U	—	—	—	< 0.0165 U	< 0.0165 U	< 0.0341 U	—	—
	RHMW05-WG17	10/13/2009[ad]		**673**	< 30 U	—	—	< 0.31 U	< 0.15 U	< 0.12 U	< 0.31 U	< 0.62 U	< 0.31 U	< 1 U	—	—	—	< 0.017 U	< 0.017 U	< 0.0352 U	—	—
	RHMW05-WG18	1/26/2010		**2,060**	< 60.0 U	—	—	< 0.620 U	< 0.300 U	< 0.240 U	< 0.620 U	< 1.24 U	< 0.620 U	< 1.24 U	—	—	—	**0.0207 J**	**0.0246 J**	< 0.0712 U	—	—
	RHMW05-WG19	4/13/2010		< 300 U	< 60.0 U	—	—	< 0.620 U	< 0.300 U	< 0.240 U	< 0.620 U	< 1.24 U	< 0.620 U	< 1.24 U	—	—	—	**0.0335 J**	< 0.0326 U	**0.0752 J**	—	—
	RHMW05-WG20	7/13/2010		< 320 U	< 60.0 U	—	—	< 0.620 U	< 0.300 U	< 0.240 U	< 0.620 U	< 1.24 U	< 0.620 U	< 1.24 U	—	—	—	< 0.0316 U	< 0.0316 U	**0.0643 J**	—	—
	ES005	10/20/2010		< 80.8 U	—	—	< 12.12 U	< 0.40 U	< 0.28 U	< 0.32 U	< 0.46 U	—	< 0.34 U	< 0.38 U	—	—	—	< 0.12 U	< 0.12 U	< 0.10 U	—	—
	ES013	1/19/2011		< 80.8 U	—	—	< 12.12 U	< 0.40 U	< 0.28 U	< 0.32 U	< 0.46 U	—	< 0.34 U	< 0.38 U	—	—	—	< 0.12 U	< 0.12 U	< 0.10 U	—	—
	ES024	4/20/2011		< 80.8 U	—	—	< 12.12 U	< 0.40 U	< 0.28 U	< 0.32 U	< 0.46 U	—	< 0.34 U	< 0.38 U	—	—	—	< 0.12 U	< 0.12 U	< 0.10 U	—	—
	ES039	7/19/2011		< 80.8 U	—	< 212.0 U	< 12.12 U	< 0.40 U	< 0.28 U	< 0.32 U	< 0.46 U	—	< 0.34 U	< 0.38 U	—	—	—	< 0.12 U	< 0.12 U	< 0.10 U	—	—
	ES051	10/25/2011		< 80.8 U	—	—	< 12.12 U	< 0.40 U	< 0.28 U	< 0.32 U	< 0.46 U	—	< 0.34 U	< 0.38 U	—	—	—	< 0.12 U	< 0.12 U	< 0.10 U	—	—
	ES063	2/1/2012		< 80.8 U	—	—	< 12.12 U	< 0.40 U	< 0.28 U	< 0.32 U	< 0.46 U	—	< 0.34 U	< 0.38 U	—	—	—	< 0.12 U	< 0.12 U	< 0.10 U	—	—
	ES070	4/16/2012		< 80.8 U	—	—	< 12.12 U	< 0.40 U	< 0.28 U	< 0.32 U	< 0.46 U	—	< 0.34 U	< 0.38 U	—	—	—	< 0.12 U	< 0.12 U	< 0.10 U	—	—
	ES079	7/17/2012		< 80.8 U	—	< 212.0 U	< 12.12 U	< 0.40 U	< 0.28 U	< 0.32 U	< 0.46 U	—	< 0.34 U	< 0.38 U	—	—	—	< 0.12 U	< 0.12 U	< 0.10 U	—	—
	ES080	7/17/2012*		< 80.8 U	—	< 212.0 U	< 12.12 U	< 0.40 U	< 0.28 U	< 0.32 U	< 0.46 U	—	< 0.34 U	< 0.38 U	—	—	—	< 0.12 U	< 0.12 U	< 0.10 U	—	—
	ES005	10/22/2012		**17 J,HD**	—	—	**15 BJ**	< 0.50 U	< 0.50 U	< 0.50 U	< 0.50 U	—	**0.31 J**	< 1.0 U	—	—	—	< 0.050 U	< 0.050 U	**0.038 J**	—	—
	ES015	1/29/2013		**62 HD**	—	—	< 30 U	< 0.50 U	< 0.50 U	< 0.50 U	< 0.50 U	—	< 0.50 U	< 1.0 U	—	—	—	< 0.050 U	< 0.050 U	**0.075 J**	—	—
	ES024	4/23/2013		**27 J**	—	—	**15 J**	< 0.50 U	< 0.50 U	< 0.50 U	< 0.50 U	—	< 0.50 U	< 1.0 U	—	—	—	< 0.048 U	< 0.048 U	**0.033 J**	—	—
	ES033	7/23/2013		< 20 U	—	—	< 30 U	< 0.50 U	< 0.50 U	< 0.50 U	< 0.50 U	—	< 0.50 U	< 1.0 U	—	—	—	< 0.051 U	< 0.051 U	**0.033 J**	—	—
	ES042	10/22/2013		< 20 U	—	—	**17 BJ**	< 0.50 U	< 0.50 U	< 0.50 U	< 0.50 U	—	< 0.50 U	< 1.0 U	—	—	—	< 0.051 U	< 0.051 U	**0.17 J**	—	—
	ES049	1/16/2014		< 20 U	—	—	—	< 0.50 U	< 0.50 U	< 0.50 U	< 0.50 U	—	< 0.50 U	< 1.0 U	—	—	—	< 0.050 U	< 0.050 U	< 0.050 U	—	—
	ES061	1/29/2014		**16 J,HD**	—	—	**23 BJ**	< 0.50 U	< 0.50 U	< 0.50 U	< 0.50 U	—	< 0.50 U	< 1.0 U	—	—	—	< 0.050 U	< 0.050 U	**0.064 J**	—	—
	ES068	3/6/2014		< 21 U	—	—	—	—	—	< 0.50 U	< 0.50 U	—	< 0.50 U	< 1.0 U	—	—	—	< 0.050 U	< 0.050 U	**0.038 J**	—	—
	ES076	3/26/2014		**17 J,HD**	—	—	—	—	—	< 0.50 U	< 0.50 U	—	< 0.50 U	< 1.0 U	—	—	—	< 0.050 U	< 0.050 U	**0.092 J**	—	—
	ES084	4/22/2014		< 10 U	—	—	< 30 U	< 0.50 U	< 0.50 U	< 0.50 U	< 0.50 U	—	< 0.50 U	< 1.0 U	—	—	—	< 0.051 U	< 0.051 U	**0.066 J**	—	—
	ES095	5/28/2014		< 12 U	—	—	—	—	—	< 0.50 U	< 0.50 U	—	< 0.50 U	< 1.0 U	—	—	—	< 0.049 U	< 0.049 U	< 0.049 U	—	—
	ES101	6/24/2014		< 12 U	—	—	—	—	—	< 0.50 U	< 0.50 U	—	< 0.50 U	< 1.0 U	—	—	—	< 0.051 U	< 0.051 U	< 0.051 U	—	—
	ES108	7/22/2014		< 12 U	—	—	< 30 U	< 0.50 U	< 0.50 U	< 0.50 U	< 0.50 U	—	< 0.50 U	< 1.0 U	—	—	—	< 0.049 U	< 0.049 U	< 0.049 U	—	—
	ES118	10/28/2014		**16 J,HD**	—	—	< 30 U	< 0.50 U	< 0.50 U	< 0.50 U	< 0.50 U	—	< 0.50 U	< 1.0 U	—	—	—	< 0.096 U	< 0.048 U	< 0.048 U	—	—
	ES124	1/27/2015		< 13 U	—	—	< 30 U	< 0.50 U	< 0.50 U	< 0.50 U	< 0.50 U	—	< 0.50 U	< 1.0 U	—	—	—	< 0.096 U	< 0.048 U	< 0.048 U	—	—
	ES135	4/21/2015		**17 BJ**	< 25 U	**34 BJ**	—	< 0.20 U	—	< 0.10 U	< 0.10 U	—	< 0.10 U	< 0.20 U	< 0.010 U	< 0.015 U	< 0.0040 U	< 0.0050 UJ	< 0.0050 UJ	< 0.0050 UJ	—	—
	ES142	6/25/2015		**15 J**	—	**41 J**	—	—	—	—	—	—	—	—	—	—	—	**0.0046 J**	**0.0029 J**	< 0.0050 U	—	—
	ES150	7/21/2015		**18 J**	< 25 U	**44 J**	—	< 0.20 U	—	< 0.10 U	< 0.10 U	—	< 0.10 U	< 0.20 U	—	< 0.015 U	< 0.0040 U	**0.0041 J**	**0.0036 J**	**0.0058 J**	—	—
	ERH010	10/20/2015		**20 BJ**	< 25 U	<54 UB	—	< 0.20 U**	—	< 0.10 U**	< 0.10 U**	—	**0.59 **, Tb**	< 0.20 U**	—	< 0.015 U	< 0.0040 U	**0.0050 J**	**0.0066 BJ**	**0.0074 BJ**	—	—
	ERH022	1/20/2016		**27 BJ**	< 25 U	**45 BJ**	—	< 0.20 U	—	< 0.10 U	< 0.10 U	—	**0.18 TbJ**	< 0.20 U	—	< 0.015 U	< 0.0040 U	< 0.0050 U	**0.0031 J**	< 0.0050 U	—	—
	ERH023	1/20/2016		**26 BJ**	< 25 U	**44 BJ**	—	< 0.20 U	—	< 0.10 U	< 0.10 U	—	**0.12 TbJ**	< 0.20 U	—	< 0.015 U	< 0.0040 U	< 0.0050 U	**0.0039 J**	**0.0046 J**	—	—
	ERH038	4/20/2016		< 22 UB	< 25 U	< 65 UB	—	—	—	< 0.10 U	< 0.10 U	—	< 0.10 U	< 0.20 U	—	—	—	< 0.0050 U	< 0.0050 U	< 0.0050 U	—	—
	ERH052	7/20/2016		< 21 U	< 25 U	< 52 UBF	—	—	—	< 0.10 U	< 0.10 U	—	< 0.10 U	< 0.20 U	—	—	—	< 0.0050 U	< 0.0050 U	< 0.0050 UBF	—	—
	ERH089	10/19/2016		< 25 U	—	< 40 U	< 18 U	—	—	< 0.30 U	< 0.50 U	—	< 0.30 U	< 0.30 U	—	—	—	< 0.10 U	< 0.10 U	< 0.10 U	< 4.00 U	< 80.0 UJ
	ERH126	11/15/2016		< 25 U	—	< 40 U	< 18 U	—	—	< 0.30 U	< 0.50 U	—	< 0.30 U	< 0.30 U	—	—	—	< 0.10 U	< 0.10 U	< 0.10 U	< 4.00 U	< 80.0 U
	ERH136	12/12/2016		< 25 U	—	< 40 U	< 18 U	—	—	< 0.30 U	< 0.50 U	—	< 0.30 U	< 0.30 U	—	—	—	< 0.10 U	< 0.10 U	< 0.10 U	< 4.00 U	< 80.0 U
	ERH164	1/10/2017		< 25 U	—	< 40 U	< 18 U	—	—	< 0.30 U	< 0.50 U	—	< 0.30 U	< 0.30 U	—	—	—	< 0.10 U	< 0.10 U	< 0.10 U	< 4.00 U	< 80.0 U
	ERH212	2/7/2017		< 25 U	—	< 40 U	< 18 U	—	—	< 0.30 U	< 0.50 U	—	< 0.30 U	< 0.30 U	—	—	—	< 0.10 U	< 0.10 U	< 0.10 U	< 4.00 U	< 80.0 U
	ERH278	3/8/2017		< 25 U	—	< 40 U	< 18 U	—	—	< 0.30 U	< 0.50 U	—	< 0.30 U	< 0.30 U	—	—	—	< 0.10 U	< 0.10 U	< 0.10 U	< 4.00 U	< 80.0 U
	ERH295	4/3/2017		< 25 U	—	< 40 U	< 18 U	—	—	< 0.30 U	< 0.50 U	—	< 0.30 U	< 0.30 U	—	—	—	< 0.10 U	< 0.10 U	< 0.10 U	< 4.00 U	< 80.0 U

Table A.1-1: Cumulative Groundwater COPC Results (cont'd)
First Quarter 2018 - Quarterly Groundwater Monitoring Report, Red Hill Bulk Fuel Storage Facility, JBPHH, O'ahu, Hawai'i

		Method	8015						8260					8260SIM		8011	8270			8270/8270 Mod.	
			TPH-d	TPH-g ****	TPH-o	TPH-g ****	1,2-Dibromoethane *****	1,2-Dichloroethane *****	Benzene	Ethylbenzene	Naphthalene	Toluene	Xylenes, Total (p/m-, o-xylene)	1,2-Dibromoethane *****	1,2-Dichloroethane *****	1,2-Dibromoethane *****	1-Methylnaphthalene	2-Methylnaphthalene	Naphthalene	Phenol	2-(2-Methoxyethoxy)-ethanol
		Unit	(µg/L)	(µg/L)	(µg/L)	(µg/L)	(µg/L)	(µg/L)	(µg/L)	(µg/L)	(µg/L)	(µg/L)	(µg/L)	(µg/l)	(µg/L)	(µg/L)	(µg/L)	(µg/L)	(µg/L)	(µg/L)	(µg/L)
		Screening Criterion	400	300	500	300	0.04	5.0	5.0	30	17	40	20	0.04	5.0	0.04	10	10	17	300	800
		SSRBL	4500	—	—	—	—	—	750	—	—	—	—	—	—	—	—	—	—	—	—
Well Name	Sample ID	Date Sampled	Result	Result	Result	Result	Result	Result	Result	Result	Result	Result	Result	Result	Result	Result	Result	Result	Result	Result	Result
RHMW05	ERH338	5/1/2017	< 25 U	—	< 40 U	< 18 U	—	—	< 0.30 U	< 0.50 U	—	< 0.30 U	< 0.30 U	—	—	—	< 0.10 U	< 0.10 U	< 0.10 U	< 4.00 U	< 80.0 U
(cont'd)	ERH357	6/6/2017	< 25 U	—	< 40 U	< 18 U	—	—	< 0.30 U	< 0.50 U	—	< 0.30 U	< 0.30 U	—	—	—	< 0.10 U	< 0.10 U	< 0.10 U	< 4.00 U	< 80.0 U
	ERH387	7/5/2017	< 25 U	—	< 40 U	< 18 U	—	—	< 0.30 U	< 0.50 U	—	< 0.30 U	< 0.30 U	—	—	—	< 0.10 U	< 0.10 U	< 0.10 U	< 4.00 U	< 80.0 U
	ERH423	10/24/2017	< 25 U	—	< 40 U	< 18 U	—	—	< 0.30 U	< 0.50 U	—	< 0.30 U	< 0.30 U	—	—	—	< 0.10 U	< 0.10 U	< 0.10 U	< 4.00 U	< 80.0 U
	ERH554	3/13/2018	< 25 U	—	< 40 U	< 18 U	—	—	< 0.30 U	< 0.50 U	—	< 0.30 U	< 0.30 U	—	—	—	< 0.10 U	< 0.10 U	< 0.10 U	< 4.00 U	< 80.0 U

Table A.1-1: Cumulative Groundwater COPC Results (cont'd)
First Quarter 2018 - Quarterly Groundwater Monitoring Report, Red Hill Bulk Fuel Storage Facility, JBPHH, O'ahu, Hawai'i

		Method	8015						8260					8260SIM		8011	8270			8270/8270 Mod.	
			TPH-d	TPH-g ****	TPH-o	TPH-g ****	1,2-Dibromoethane *****	1,2-Dichloroethane *****	Benzene	Ethylbenzene	Naphthalene	Toluene	Xylenes, Total (p/m-, o-xylene)	1,2-Dibromoethane *****	1,2-Dichloroethane *****	1,2-Dibromoethane *****	1-Methylnaphthalene	2-Methylnaphthalene	Naphthalene	Phenol	2-(2-Methoxyethoxy)-ethanol
		Unit	(µg/L)	(µg/L)	(µg/L)	(µg/L)	(µg/L)	(µg/L)	(µg/L)	(µg/L)	(µg/L)	(µg/L)	(µg/L)	(µg/l)	(µg/L)	(µg/L)	(µg/L)	(µg/L)	(µg/L)	(µg/L)	(µg/L)
		Screening Criterion	400	300	500	300	0.04	5.0	5.0	30	17	40	20	0.04	5.0	0.04	10	10	17	300	800
		SSRBL	4500	—	—	—	—	—	750	—	—	—	—	—	—	—	—	—	—	—	—
Well Name	Sample ID	Date Sampled	Result	Result	Result	Result	Result	Result	Result	Result	Result	Result	Result	Result	Result	Result	Result	Result	Result	Result	Result
RHMW06	RHMW06-GW-01	10/21/2014	<86 U	< 20 U	<86 U	—	< 0.50 U	< 0.100 U	< 0.200 U	< 0.50 U	—	< 0.30 U	< 0.30 U	—	—	< 0.020 U	< 0.011 U	**0.0064 J**	< 0.053 U	—	—
	RHMW06-GW-02	1/23/2015[d]	<76 U	< 20 U	<76 U	—	< 0.50 U	< 0.100 U	< 0.200 U	< 0.50 U	—	< 0.30 U	< 0.30 U	—	—	< 0.020 U	< 0.010 U	< 0.010 U	< 0.052 U	—	—
	ES140	4/23/2015	**20 J**	< 25 U	**47 BJ**	—	< 0.20 U	—	< 0.10 U	< 0.10 U	—	< 0.10 U	< 0.20 U	< 0.010 U	< 0.015 U	< 0.0040 UJ	< 0.0052 U	< 0.0052 U	< 0.0052 U	—	—
	ES155	7/28/2015	< 20 U	< 25 U	< 50 U	—	< 0.20 U	—	< 0.10 U	< 0.10 U	—	< 0.10 U	< 0.20 U	—	< 0.015 U	< 0.0040 U	< 0.0050 U	< 0.0050 U	< 0.0050 U	—	—
	ERH004	10/19/2015	**17 BJ**	< 25 U	< 53 UB	—	< 0.20 U**	—	< 0.10 U**	< 0.10 U**	—	**1.1 ****	< 0.20 U**	—	< 0.015 U	< 0.0040 U	< 0.0050 U	< 0.0050 UB	< 0.0050 UB	—	—
	ERH005	10/19/2015	< 21 UB	< 25 U	< 53 UB	—	< 0.20 U**	—	< 0.10 U**	< 0.10 U**	—	**0.50 ****	< 0.20 U**	—	< 0.015 U	< 0.0040 U	< 0.0050 U	< 0.0050 UB	< 0.0050 UB	—	—
	ERH018	1/19/2016	**21 BJ**	< 25 U	< 54 UB	—	< 0.20 U	—	< 0.10 U	< 0.10 U	—	**0.10 TbJ**	< 0.20 U	—	< 0.015 U	< 0.0040 U	< 0.0050 U	< 0.0050 U	< 0.0050 U	—	—
	ERH033	4/19/2016	<28 UB	< 25 U	<48 UB	—	—	—	< 0.10 U	< 0.10 U	—	< 0.10 U	< 0.20 U	—	—	—	< 0.0050 U	< 0.0050 U	< 0.0050 U	—	—
	ERH047	7/19/2016	<23 U	< 25 U	< 56 UBF	—	—	—	< 0.10 U	< 0.10 U	—	< 0.10 U	< 0.20 U	—	—	—	< 0.0050 U	< 0.0050 U	< 0.0050 UBF	—	—
	ERH097	10/19/2016	< 25 U	—	< 40 U	< 18 U	—	—	< 0.30 U	< 0.50 U	—	< 0.30 U	< 0.30 U	—	—	—	< 0.10 U	< 0.10 U	< 0.10 U	< 4.00 U	< 80.0 UJ
	ERH120	11/14/2016	< 25 U	—	< 40 U	< 18 U	—	—	< 0.30 U	< 0.50 U	—	< 0.30 U	< 0.30 U	—	—	—	< 0.10 U	< 0.10 U	< 0.10 U	< 4.00 U	< 80.0 U
	ERH139	12/12/2016	< 25 U	—	< 40 U	< 18 U	—	—	< 0.30 U	< 0.50 U	—	< 0.30 U	< 0.30 U	—	—	—	< 0.10 U	< 0.10 U	< 0.10 U	< 4.00 U	< 80.0 U
	ERH168	1/9/2017	< 25 U	—	< 40 U	< 18 U	—	—	< 0.30 U	< 0.50 U	—	< 0.30 U	< 0.30 U	—	—	—	< 0.10 U	< 0.10 U	< 0.10 U	< 4.00 U	< 80.0 U
	ERH210	2/7/2017	< 25 U	—	< 40 U	< 18 U	—	—	< 0.30 U	< 0.50 U	—	< 0.30 U	< 0.30 U	—	—	—	< 0.10 U	< 0.10 U	< 0.10 U	< 4.00 U	< 80.0 U
	ERH284	3/7/2017	< 25 U	—	**47**	< 18 U	—	—	< 0.30 U	< 0.50 U	—	< 0.30 U	< 0.30 U	—	—	—	< 0.10 U	< 0.10 U	< 0.10 U	< 4.00 U	< 80.0 U
	ERH319	4/3/2017	< 25 U	—	< 40 U	< 18 U	—	—	< 0.30 U	< 0.50 U	—	< 0.30 U	< 0.30 U	—	—	—	< 0.10 U	< 0.10 U	< 0.10 U	< 4.00 U	< 80.0 U
	ERH369	7/4/2017	< 25 U	—	< 40 U	< 18 U	—	—	< 0.30 U	< 0.50 U	—	< 0.30 U	< 0.30 U	—	—	—	< 0.10 U	< 0.10 U	< 0.10 U	< 4.00 U	< 80.0 U
	ERH425	10/23/2017	< 25 U	—	< 40 U	< 18 U	—	—	< 0.30 U	< 0.50 U	—	< 0.30 U	< 0.30 U	—	—	—	< 0.10 U	< 0.10 U	< 0.10 U	< 4.00 U	< 80.0 U
	ERH556	3/12/2018	< 25 U	—	< 40 U	< 18 U	—	—	< 0.30 U	< 0.50 U	—	< 0.30 U	< 0.30 U	—	—	—	< 0.10 U	< 0.10 U	< 0.10 U	< 4.00 U	< 80.0 U

Table A.1-1: Cumulative Groundwater COPC Results (cont'd)
First Quarter 2018 - Quarterly Groundwater Monitoring Report, Red Hill Bulk Fuel Storage Facility, JBPHH, O'ahu, Hawai'i

		Method	8015						8260					8260SIM		8011	8270			8270/8270 Mod.	
			TPH-d	TPH-g ****	TPH-o	TPH-g ****	1,2-Dibromoethane *****	1,2-Dichloroethane *****	Benzene	Ethylbenzene	Naphthalene	Toluene	Xylenes, Total (p/m-, o-xylene)	1,2-Dibromoethane *****	1,2-Dichloroethane *****	1,2-Dibromoethane *****	1-Methylnaphthalene	2-Methylnaphthalene	Naphthalene	Phenol	2-(2-Methoxyethoxy)-ethanol
		Unit	(µg/L)	(µg/L)	(µg/L)	(µg/L)	(µg/L)	(µg/L)	(µg/L)	(µg/L)	(µg/L)	(µg/L)	(µg/L)	(µg/l)	(µg/L)	(µg/L)	(µg/L)	(µg/L)	(µg/L)	(µg/L)	(µg/L)
		Screening Criterion	400	300	500	300	0.04	5.0	5.0	30	17	40	20	0.04	5.0	0.04	10	10	17	300	800
		SSRBL	4500	—	—	—	—	—	750	—	—	—	—	—	—	—	—	—	—	—	—
Well Name	Sample ID	Date Sampled	Result	Result	Result	Result	Result	Result	Result	Result	Result	Result	Result	Result	Result	Result	Result	Result	Result	Result	Result
RHMW07	RHMW07-GW-01	10/20/2014	**57 J**	< 20 U	<78 U	—	< 0.50 U	< 0.100 U	< 0.200 U	< 0.50 U	—	< 0.30 U	< 0.30 U	—	—	< 0.020 U	< 0.0096 U	**0.0084 J**	< 0.048 U	—	—
	RHMW07-GW-01FD	10/20/2014	**66 J**	< 20 U	<77 U	—	< 0.50 U	< 0.100 U	< 0.200 U	< 0.50 U	—	< 0.30 U	< 0.30 U	—	—	< 0.020 U	< 0.010 U	**0.0060 J**	< 0.050 U	—	—
	RHMW07-GW-02	1/22/2015[d]	<75 U	< 20 U	<75 U	—	< 0.50 U	< 0.100 U	< 0.200 U	< 0.50 U	—	< 0.30 U	< 0.30 U	—	—	< 0.020 U	< 0.011 U	< 0.011 U	< 0.055 U	—	—
	RHMW07-GW-02FD	1/22/2015[d*]	<81 U	< 20 U	<81 U	—	< 0.50 U	< 0.100 U	< 0.200 U	< 0.50 U	—	< 0.30 U	< 0.30 U	—	—	< 0.020 U	< 0.010 U	< 0.010 U	< 0.050 U	—	—
	ES141	4/23/2015	**26 J**	< 25 U	**47 BJ**	—	< 0.20 U	—	< 0.10 U	< 0.10 U	—	< 0.10 U	< 0.20 U	< 0.010 U	< 0.015 U	< 0.0040 UJ	< 0.0052 U	< 0.0052 U	< 0.0052 U	—	—
	ES154	7/27/2015	**22 J**	< 25 U	**48 J**	—	< 0.20 U	—	< 0.10 U	< 0.10 U	—	< 0.10 U	< 0.20 U	—	< 0.015 U	< 0.0040 U	**0.0051 J**	**0.0095 J**	**0.0060 J**	—	—
	ERH003	10/19/2015	**26 BJ**	< 25 U	< 59 UB	—	< 0.20 U**	—	< 0.10 U**	< 0.10 U**	—	**0.640 ****	< 0.20 U**	—	< 0.015 U	< 0.0040 U	**0.0067 J**	**0.010 BJ**	**0.010 BJ**	—	—
	ERH017	1/19/2016	**28 BJ**	< 25 U	**44 BJ**	—	< 0.20 U	—	< 0.10 U	< 0.10 U	—	< 0.10 U	< 0.20 U	—	< 0.015 U	< 0.0040 U	**0.0046 J**	**0.0077 J**	**0.0038 J**	—	—
	ERH032	4/19/2016	<26 UB	< 25 U	< 52 UB	—	—	—	< 0.10 U	< 0.10 U	—	< 0.10 U	< 0.20 U	—	—	—	< 0.0050 U	<0.0036 UB	< 0.0050 U	—	—
	ERH045	7/19/2016	< 22 U	< 25 U	< 53 UBF	—	—	—	< 0.10 U	< 0.10 U	—	< 0.10 U	< 0.20 U	—	—	—	< 0.0050 U	**0.0037 J**	< 0.0050 UBF	—	—
	ERH046	7/19/2016	< 22 UF	< 25 U	**160 O**	—	—	—	< 0.10 U	< 0.10 U	—	< 0.10 U	< 0.20 U	—	—	—	< 0.0050 U	**0.0033 J**	< 0.0050 UBF	—	—
	ERH098	10/19/2016	< 25 U	—	< 40 U	< 18 U	—	—	< 0.30 U	< 0.50 U	—	< 0.30 U	< 0.30 U	—	—	—	< 0.10 U	< 0.10 U	< 0.10 U	< 4.00 U	< 80.0 UJ
	ERH121	11/14/2016	< 25 U	—	< 40 U	< 18 U	—	—	< 0.30 U	< 0.50 U	—	< 0.30 U	< 0.30 U	—	—	—	< 0.10 U	< 0.10 U	< 0.10 U	< 4.00 U	< 80.0 U
	ERH140	12/13/2016	< 25 U	—	< 40 U	< 18 U	—	—	< 0.30 U	< 0.50 U	—	< 0.30 U	< 0.30 U	—	—	—	< 0.10 U	< 0.10 U	< 0.10 U	< 4.00 U	< 80.0 U
	ERH179	1/10/2017	< 25 U	—	< 40 U	< 18 U	—	—	< 0.30 U	< 0.50 U	—	< 0.30 U	< 0.30 U	—	—	—	< 0.10 U	< 0.10 U	< 0.10 U	< 4.00 U	< 80.0 U
	ERH218	2/8/2017	< 25 U	—	< 40 U	< 18 U	—	—	< 0.30 U	< 0.50 U	—	< 0.30 U	< 0.30 U	—	—	—	< 0.10 U	< 0.10 U	< 0.10 U	< 4.00 U	< 80.0 U
	ERH270	3/7/2017	< 25 U	—	< 40 U	< 18 U	—	—	< 0.30 U	< 0.50 U	—	< 0.30 U	< 0.30 U	—	—	—	< 0.10 U	< 0.10 U	< 0.10 U	< 4.00 U	< 80.0 U
	ERH305	4/3/2017	< 25 U	—	< 40 U	< 18 U	—	—	< 0.30 U	< 0.50 U	—	< 0.30 U	< 0.30 U	—	—	—	< 0.10 U	< 0.10 U	< 0.10 U	< 4.00 U	< 80.0 U
	ERH372	7/4/2017	< 25 U	—	< 40 U	< 18 U	—	—	< 0.30 U	< 0.50 U	—	< 0.30 U	< 0.30 U	—	—	—	< 0.10 U	< 0.10 U	< 0.10 U	< 4.00 U	< 80.0 U
	ERH427	10/25/2017	< 25 U	—	< 40 U	< 18 U	—	—	< 0.30 U	< 0.50 U	—	< 0.30 U	< 0.30 U	—	—	—	< 0.10 U	< 0.10 U	< 0.10 U	< 4.00 U	< 80.0 U
	ERH558	3/13/2018	< 25 U	—	< 40 U	< 18 U	—	—	< 0.30 U	< 0.50 U	—	< 0.30 U	< 0.30 U	—	—	—	< 0.10 U	< 0.10 U	< 0.10 U	< 4.00 U	< 80.0 U

Table A.1-1: Cumulative Groundwater COPC Results (cont'd)
First Quarter 2018 - Quarterly Groundwater Monitoring Report, Red Hill Bulk Fuel Storage Facility, JBPHH, O'ahu, Hawai'i

		Method	8015						8260					8260SIM		8011	8270			8270/8270 Mod.	
			TPH-d	TPH-g ****	TPH-o	TPH-g ****	1,2-Dibromoethane *****	1,2-Dichloroethane *****	Benzene	Ethylbenzene	Naphthalene	Toluene	Xylenes, Total (p/m-, o-xylene)	1,2-Dibromoethane *****	1,2-Dichloroethane *****	1,2-Dibromoethane *****	1-Methylnaphthalene	2-Methylnaphthalene	Naphthalene	Phenol	2-(2-Methoxyethoxy)-ethanol
		Unit	(µg/L)	(µg/L)	(µg/L)	(µg/L)	(µg/L)	(µg/L)	(µg/L)	(µg/L)	(µg/L)	(µg/L)	(µg/L)	(µg/l)	(µg/L)	(µg/L)	(µg/L)	(µg/L)	(µg/L)	(µg/L)	(µg/L)
		Screening Criterion	400	300	500	300	0.04	5.0	5.0	30	17	40	20	0.04	5.0	0.04	10	10	17	300	800
		SSRBL	4500	—	—	—	—	—	750	—	—	—	—	—	—	—	—	—	—	—	—
Well Name	Sample ID	Date Sampled	Result	Result	Result	Result	Result	Result	Result	Result	Result	Result	Result	Result	Result	Result	Result	Result	Result	Result	Result
RHMW08	ERH102	10/19/2016	< 25 U	—	< 40 U	< 18 U	—	< 0.30 U	< 0.30 U	< 0.50 U	—	< 0.30 U	< 0.30 U	—	—	< 0.02 U	< 0.10 U	< 0.10 U	< 0.10 U	< 4.00 U	< 80.0 UJ
	ERH122	11/15/2016	**33 J**	—	**32 J**	< 18 U	—	< 0.30 U	< 0.30 U	< 0.50 U	—	< 0.30 U	< 0.30 U	—	—	< 0.02 U	< 0.10 U	< 0.10 U	< 0.10 U	< 4.00 U	< 80.0 U
	ERH141	12/12/2016	**27 J**	—	**29 J**	< 18 U	—	< 0.30 U	< 0.30 U	< 0.50 U	—	< 0.30 U	< 0.30 U	—	—	< 0.02 U	< 0.10 U	< 0.10 U	< 0.10 U	< 4.00 U	< 80.0 U
	ERH157/158	12/21/2016*	**63**	—	< 40 U	< 18 U	—	< 0.30 U	< 0.30 U	< 0.50 U	—	< 0.30 U	< 0.30 U	—	—	< 0.02 U	< 0.10 U	< 0.10 U	< 0.10 U	< 4.00 U	< 80.0 U
	ERH169/170	1/11/2017*	**28 J**	—	**29 J**	< 18 U	—	< 0.30 U	< 0.30 U	< 0.50 U	—	< 0.30 U	< 0.30 U	—	—	< 0.02 U	< 0.10 U	< 0.10 U	< 0.10 U	< 4.00 U	< 80.0 U
	ERH220/221	2/6/2017*	**26 J**	—	**31 J**	< 18 U	—	< 0.30 U	< 0.30 U	< 0.50 U	—	< 0.30 U	< 0.30 U	—	—	< 0.02 U	< 0.10 U	< 0.10 U	< 0.10 U	< 4.00 U	< 80.0 U
	ERH262/263	3/6/2017*	**27 J**	—	**25 J**	< 18 U	—	< 0.30 U	< 0.30 U	< 0.50 U	—	< 0.30 U	< 0.30 U	—	—	< 0.02 U	< 0.10 U	< 0.10 U	< 0.10 U	< 4.00 U	< 80.0 U
	ERH297/298	4/4/2017*	< 25 U	—	< 40 U	< 18 U	—	< 0.30 U	< 0.30 U	< 0.50 U	—	< 0.30 U	< 0.30 U	—	—	< 0.02 U	< 0.10 U	< 0.10 U	< 0.10 U	< 4.00 U	< 80.0 U
	ERH340	5/2/2017	< 25 U	—	< 40 U	< 18 U	—	< 0.30 U	< 0.30 U	< 0.50 U	—	< 0.30 U	< 0.30 U	—	—	< 0.02 U	< 0.10 U	< 0.10 U	< 0.10 U	< 4.00 U	< 80.0 U
	ERH360	6/5/2017	< 25 U	—	< 40 U	< 18 U	—	< 0.30 U	< 0.30 U	< 0.50 U	—	< 0.30 U	< 0.30 U	—	—	< 0.02 U	< 0.10 U	< 0.10 U	< 0.10 U	< 4.00 U	< 80.0 U
	ERH376	7/4/2017	< 25 U	—	< 40 U	< 18 U	—	< 0.30 U	< 0.30 U	< 0.50 U	—	< 0.30 U	< 0.30 U	—	—	< 0.02 U	< 0.10 U	< 0.10 U	< 0.10 U	< 4.00 U	< 80.0 U
	ERH429	10/23/2017	< 25 U	—	< 40 U	< 18 U	—	—	< 0.30 U	< 0.50 U	—	< 0.30 U	< 0.30 U	—	—	—	< 0.10 U	< 0.10 U	< 0.10 U	< 4.00 U	< 80.0 U
	ERH560	3/12/2018	< 25 U	—	< 40 U	< 18 U	—	—	< 0.30 U	< 0.50 U	—	< 0.30 U	< 0.30 U	—	—	—	< 0.10 U	< 0.10 U	< 0.10 U	< 4.00 U	< 80.0 U

Table A.1-1: Cumulative Groundwater COPC Results (cont'd)
First Quarter 2018 - Quarterly Groundwater Monitoring Report, Red Hill Bulk Fuel Storage Facility, JBPHH, O'ahu, Hawai'i

		Method	8015						8260					8260SIM		8011	8270			8270/8270 Mod.	
			TPH-d	TPH-g ****	TPH-o	TPH-g ****	1,2-Dibromoethane *****	1,2-Dichloroethane *****	Benzene	Ethylbenzene	Naphthalene	Toluene	Xylenes, Total (p/m-, o-xylene)	1,2-Dibromoethane *****	1,2-Dichloroethane *****	1,2-Dibromoethane *****	1-Methylnaphthalene	2-Methylnaphthalene	Naphthalene	Phenol	2-(2-Methoxyethoxy)-ethanol
		Unit	(µg/L)	(µg/L)	(µg/L)	(µg/L)	(µg/L)	(µg/L)	(µg/L)	(µg/L)	(µg/L)	(µg/L)	(µg/L)	(µg/l)	(µg/L)	(µg/L)	(µg/L)	(µg/L)	(µg/L)	(µg/L)	(µg/L)
		Screening Criterion	400	300	500	300	0.04	5.0	5.0	30	17	40	20	0.04	5.0	0.04	10	10	17	300	800
		SSRBL	4500	—	—	—	—	—	750	—	—	—	—	—	—	—	—	—	—	—	—
Well Name	Sample ID	Date Sampled	Result	Result	Result	Result	Result	Result	Result	Result	Result	Result	Result	Result	Result	Result	Result	Result	Result	Result	Result
RHMW09	ERH103	10/25/2016	< 25 U	—	< 40 U	< 18 U	—	< 0.30 U	< 0.30 U	< 0.50 U	—	< 0.30 U	< 0.30 U	—	—	< 0.02 U	< 0.10 U	< 0.10 U	< 0.10 U	< 4.00 U	< 80.0 UJ
	ERH129	11/15/2016	< 25 U	—	< 40 U	< 18 U	—	< 0.30 U	< 0.30 U	< 0.50 U	—	< 0.30 U	< 0.30 U	—	—	< 0.02 U	< 0.10 U	< 0.10 U	< 0.10 U	< 4.00 U	< 80.0 U
	ERH146	12/12/2016	< 25 U	—	< 40 U	< 18 U	—	< 0.30 U	< 0.30 U	< 0.50 U	—	< 0.30 U	< 0.30 U	—	—	< 0.02 U	< 0.10 U	< 0.10 U	< 0.10 U	**1.1 J**	< 80.0 U
	ERH178	1/11/2017	< 25 U	—	< 40 U	< 18 U	—	< 0.30 U	< 0.30 U	< 0.50 U	—	< 0.30 U	< 0.30 U	—	—	< 0.02 U	< 0.10 U	< 0.10 U	< 0.10 U	< 4.00 U	< 80.0 U
	ERH225/247	2/8/2017*	< 25 U	—	< 40 U	< 18 U	—	< 0.30 U	< 0.30 U	< 0.50 U	—	< 0.30 U	< 0.30 U	—	—	< 0.02 U	< 0.10 U	< 0.10 U	< 0.10 U	< 4.00 U	< 80.0 U
	ERH272	3/7/2017	< 25 U	—	< 40 U	< 18 U	—	< 0.30 U	< 0.30 U	< 0.50 U	—	< 0.30 U	< 0.30 U	—	—	< 0.02 U	< 0.10 U	< 0.10 U	< 0.10 U	< 4.00 U	< 80.0 U
	ERH307/314	4/4/2017*	< 25 U	—	< 40 U	< 18 U	—	< 0.30 U	< 0.30 U	< 0.50 U	—	< 0.30 U	< 0.30 U	—	—	< 0.02 U	< 0.10 U	< 0.10 U	< 0.10 U	< 4.00 U	< 80.0 U
	ERH385	7/5/2017	< 25 U	—	< 40 U	< 18 U	—	< 0.30 U	< 0.30 U	< 0.50 U	—	< 0.30 U	< 0.30 U	—	—	< 0.02 U	< 0.10 U	< 0.10 U	< 0.10 U	< 4.00 U	< 80.0 U
	ERH431	10/24/2017	< 25 U	—	< 40 U	< 18 U	—	—	< 0.30 U	< 0.50 U	—	< 0.30 U	< 0.30 U	—	—	—	< 0.10 U	< 0.10 U	< 0.10 U	< 4.00 U	< 80.0 U
	ERH562	3/12/2018	< 25 U	—	< 40 U	< 18 U	—	—	< 0.30 U	< 0.50 U	—	< 0.30 U	< 0.30 U	—	—	—	< 0.10 U	< 0.10 U	< 0.10 U	< 4.00 U	< 80.0 U

Table A.1-1: Cumulative Groundwater COPC Results (cont'd)
First Quarter 2018 - Quarterly Groundwater Monitoring Report, Red Hill Bulk Fuel Storage Facility, JBPHH, O'ahu, Hawai'i

		Method	8015						8260					8260SIM		8011	8270			8270/8270 Mod.	
			TPH-d	TPH-g ****	TPH-o	TPH-g ****	1,2-Dibromoethane *****	1,2-Dichloroethane *****	Benzene	Ethylbenzene	Naphthalene	Toluene	Xylenes, Total (p/m-, o-xylene)	1,2-Dibromoethane *****	1,2-Dichloroethane *****	1,2-Dibromoethane *****	1-Methylnaphthalene	2-Methylnaphthalene	Naphthalene	Phenol	2-(2-Methoxyethoxy)-ethanol
		Unit	(µg/L)	(µg/L)	(µg/L)	(µg/L)	(µg/L)	(µg/L)	(µg/L)	(µg/L)	(µg/L)	(µg/L)	(µg/L)	(µg/l)	(µg/L)	(µg/L)	(µg/L)	(µg/L)	(µg/L)	(µg/L)	(µg/L)
		Screening Criterion	400	300	500	300	0.04	5.0	5.0	30	17	40	20	0.04	5.0	0.04	10	10	17	300	800
		SSRBL	4500	—	—	—	—	—	750	—	—	—	—	—	—	—	—	—	—	—	—
Well Name	Sample ID	Date Sampled	Result	Result	Result	Result	Result	Result	Result	Result	Result	Result	Result	Result	Result	Result	Result	Result	Result	Result	Result
RHMW10	ERH345/346	5/4/2017*	**89**		**190**	< 18 U	—	< 0.30 U	< 0.30 U	< 0.50 U	—	< 0.30 U	< 0.30 U	—	—	< 0.02 U	< 0.10 U	< 0.10 U	< 0.10 U	< 4.00 U	< 80.0 U
	ERH365/366	6/5/2017*	< 25 UJ	—	< 40 UJ	< 18 U	—	< 0.30 U	< 0.30 U	< 0.50 U	—	< 0.30 U	< 0.30 U	—	—	< 0.02 U	< 0.10 U	< 0.10 U	< 0.10 U	< 4.00 U	< 80.0 U
	ERH373/374	7/4/2017*	< 25 UJ	—	< 40 UJ	< 18 U	—	< 0.30 U	< 0.30 U	< 0.50 U	—	< 0.30 U	< 0.30 U	—	—	< 0.02 U	< 0.10 U	< 0.10 U	< 0.10 U	< 4.00 U	< 80.0 U
	ERH433	10/25/2017	< 25 U	—	**61**	< 18 U	—	< 0.30 U	< 0.30 U	< 0.50 U	—	< 0.30 U	< 0.30 U	—	—	< 0.02 U	< 0.10 U	< 0.10 U	< 0.10 U	< 4.00 U	< 80.0 U
	ERH564	3/13/2018	< 25 U	—	< 40 U	< 18 U	—	< 0.30 U	< 0.30 U	< 0.50 U	—	< 0.30 U	< 0.30 U	—	—	< 0.02 U	< 0.10 U	< 0.10 U	< 0.10 U	< 4.00 U	< 80.0 U

Table A.1-1: Cumulative Groundwater COPC Results (cont'd)
First Quarter 2018 - Quarterly Groundwater Monitoring Report, Red Hill Bulk Fuel Storage Facility, JBPHH, O'ahu, Hawai'i

		Method	8015						8260					8260SIM		8011	8270			8270/8270 Mod.	
			TPH-d	TPH-g ****	TPH-o	TPH-g ****	1,2-Dibromoethane *****	1,2-Dichloroethane *****	Benzene	Ethylbenzene	Naphthalene	Toluene	Xylenes, Total (p/m-, o-xylene)	1,2-Dibromoethane *****	1,2-Dichloroethane *****	1,2-Dibromoethane *****	1-Methylnaphthalene	2-Methylnaphthalene	Naphthalene	Phenol	2-(2-Methoxyethoxy)-ethanol
		Unit	(µg/L)	(µg/L)	(µg/L)	(µg/L)	(µg/L)	(µg/L)	(µg/L)	(µg/L)	(µg/L)	(µg/L)	(µg/L)	(µg/l)	(µg/L)	(µg/L)	(µg/L)	(µg/L)	(µg/L)	(µg/L)	(µg/L)
		Screening Criterion	400	300	500	300	0.04	5.0	5.0	30	17	40	20	0.04	5.0	0.04	10	10	17	300	800
		SSRBL	4500	—	—	—	—	—	750	—	—	—	—	—	—	—	—	—	—	—	—
Well Name	Sample ID	Date Sampled	Result	Result	Result	Result	Result	Result	Result	Result	Result	Result	Result	Result	Result	Result	Result	Result	Result	Result	Result
RHMW11-01	ERH573	3/21/2018	< 25 U	—	< 40 U	< 18 U	—	< 0.30 U	< 0.30 U	< 0.50 U	—	< 0.30 U	< 0.30 U	—	—	< 0.02 U	< 0.10 U	< 0.10 U	< 0.10 U	< 4.00 U	< 80.0 U
RHMW11-02	ERH575	3/22/2018	< 25 U	—	< 40 U	< 18 U	—	< 0.30 U	< 0.30 U	< 0.50 U	—	< 0.30 U	< 0.30 U	—	—	< 0.02 U	< 0.10 U	< 0.10 U	< 0.10 U	< 4.00 U	< 80.0 U
RHMW11-03	ERH579	3/27/2018	< 25 U	—	< 40 U	< 18 U	—	< 0.30 U	< 0.30 U	< 0.50 U	—	< 0.30 U	< 0.30 U	—	—	< 0.02 U	< 0.10 U	< 0.10 U	< 0.10 U	< 4.00 U	< 80.0 U
RHMW11-04	ERH577	3/27/2018	< 25 U	—	< 40 U	< 18 U	—	< 0.30 U	< 0.30 U	< 0.50 U	—	< 0.30 U	< 0.30 U	—	—	< 0.02 U	< 0.10 U	< 0.10 U	< 0.10 U	< 4.00 U	< 80.0 U
RHMW11-05	ERH581/582	3/28/2018*	< 25 U	—	< 40 U	< 18 U	—	< 0.30 U	< 0.26 U	< 0.50 U	—	< 0.30 U	< 0.30 U	—	—	< 0.02 U	< 0.10 U	< 0.10 U	< 0.10 U	< 4.00 U	< 80.0 U

Table A.1-1: Cumulative Groundwater COPC Results (cont'd)
First Quarter 2018 - Quarterly Groundwater Monitoring Report, Red Hill Bulk Fuel Storage Facility, JBPHH, O'ahu, Hawai'i

			Method	8015					8260					8260SIM		8011	8270			8270/8270 Mod.	
				TPH-d	TPH-g ****	TPH-o	TPH-g ****	1,2-Dibromoethane *****	1,2-Dichloroethane *****	Benzene	Ethylbenzene	Naphthalene	Toluene	Xylenes, Total (p/m-, o-xylene)	1,2-Dibromoethane *****	1,2-Dichloroethane *****	1,2-Dibromoethane *****	1-Methylnaphthalene	2-Methylnaphthalene	Naphthalene	Phenol	2-(2-Methoxyethoxy)-ethanol
			Unit	(µg/L)	(µg/L)	(µg/L)	(µg/L)	(µg/L)	(µg/L)	(µg/L)	(µg/L)	(µg/L)	(µg/L)	(µg/L)	(µg/l)	(µg/L)	(µg/L)	(µg/L)	(µg/L)	(µg/L)	(µg/L)	(µg/L)
			Screening Criterion	400	300	500	300	0.04	5.0	5.0	30	17	40	20	0.04	5.0	0.04	10	10	17	300	800
			SSRBL	4500	—	—	—	—	—	750	—	—	—	—	—	—	—	—	—	—	—	—
Well Name	Sample ID	Date Sampled		Result	Result	Result	Result	Result	Result	Result	Result	Result	Result	Result	Result	Result	Result	Result	Result	Result	Result	Result
HDMW2253-03	HDMW2253-03-WG-02	10/13/2009[ab]		< 185 U	< 30 U	—	—	< 0.31 U	< 0.15 U	< 0.12 U	< 0.31 U	< 0.62 U	< 0.31 U	< 0.62 U	—	—	—	< 0.0169 U	< 0.0169 U	<0.035 U	—	—
	HDMW2253-03-WG-03	1/26/2010		**322 J**	< 60.0 U	—	—	< 0.620 U	< 0.300 U	< 0.240 U	< 0.620 U	< 1.24 U	< 0.620 U	< 1.24 U	—	—	—	< 0.0500 U	< 0.0500 U	<0.103 U	—	—
	HDMW2253-03-WG-04	4/26/2010		< 352 U	< 60.0 U	—	—	< 0.620 U	< 0.300 U	< 0.240 U	< 0.620 U	< 1.24 U	< 0.620 U	< 1.24 U	—	—	—	< 0.0348 U	< 0.0348 U	<0.0720 U	—	—
	HDMW2253-03-WG-05	7/8/2010		< 320 U	< 60.0 U	—	—	< 0.620 U	< 0.300 U	< 0.240 U	< 0.620 U	< 1.24 U	< 0.620 U	< 1.24 U	—	—	—	< 0.0348 U	< 0.0348 U	**0.0596 J**	—	—
	ES006	10/21/2010		< 80.8 U	—	—	< 12.12 U	< 0.40 U	< 0.28 U	< 0.32 U	<0.46 U	—	< 0.34 U	< 0.38 U	—	—	—	< 0.12 U	< 0.12 U	< 0.10 U	—	—
	ES016	1/21/2011		< 80.8 U	—	—	< 12.12 U	< 0.40 U	< 0.28 U	< 0.32 U	<0.46 U	—	< 0.34 U	< 0.38 U	—	—	—	< 0.12 U	< 0.12 U	< 0.10 U	—	—
	ES028	4/21/2011		< 80.8 U	—	—	< 12.12 U	< 0.40 U	< 0.28 U	**0.42 J**	<0.46 U	—	< 0.34 U	< 0.38 U	—	—	—	< 0.12 U	< 0.12 U	< 0.10 U	—	—
	ES043	7/21/2011		< 80.8 U	—	< 212.0 U	< 12.12 U	< 0.40 U	< 0.28 U	< 0.32 U	<0.46 U	—	< 0.34 U	< 0.38 U	—	—	—	< 0.12 U	< 0.12 U	< 0.10 U	—	—
	ES053	10/26/2011		< 80.8 U	—	—	< 12.12 U	< 0.40 U	< 0.28 U	**0.92 J**	<0.46 U	—	< 0.34 U	< 0.38 U	—	—	—	< 0.12 U	< 0.12 U	< 0.10 U	—	—
	ES057	1/24/2012		< 80.8 U	—	< 212.0 U	< 12.12 U	< 0.40 U	< 0.28 U	< 0.32 U	<0.46 U	—	< 0.34 U	< 0.38 U	—	—	—	< 0.12 U	< 0.12 U	< 0.10 U	—	—
	ES076	4/26/2012		**160 ++**	—	—	< 12.12 U	< 0.40 U	< 0.28 U	**0.20 J**	<0.46 U	—	< 0.34 U	< 0.38 U	—	—	—	< 0.12 U	< 0.12 U	< 0.10 U	—	—
	ES083	7/19/2012		< 80.8 U	—	—	< 12.12 U	< 0.40 U	< 0.28 U	< 0.32 U	<0.46 U	—	< 0.34 U	< 0.38 U	—	—	—	< 0.12 U	< 0.12 U	< 0.10 U	—	—
	ES009	11/7/2012		**25 J,HD**	—	—	**15 BU,B**	< 0.50 U	< 0.50 U	< 0.50 U	< 0.50 U	—	< 0.50 U	< 1 U	—	—	—	< 0.050 U	< 0.050 U	< 0.050 U	—	—
	ES018	1/30/2013		**600**	—	—	< 30 U	< 0.50 U	< 0.50 U	< 0.50 U	< 0.50 U	—	< 0.50 U	< 1 U	—	—	—	< 0.050 U	< 0.050 U	**0.037 J**	—	—
	ES027	4/24/2013		**45 J**	—	—	< 30 U	< 0.50 U	< 0.50 U	< 0.50 U	< 0.50 U	—	< 0.50 U	< 1.0 U	—	—	—	< 0.052 U	< 0.052 U	**0.16 J**	—	—
	ES036	7/24/2013		< 21 U	—	—	< 30 U	< 0.50 U	< 0.50 U	< 0.50 U	< 0.50 U	—	< 0.50 U	< 1.0 U	—	—	—	< 0.047 U	< 0.047 U	**0.030 J**	—	—
	ES045	10/23/2013		< 20 U	—	—	**15 BJ**	< 0.50 U	< 0.50 U	< 0.50 U	< 0.50 U	—	< 0.50 U	< 1.0 U	—	—	—	< 0.050 U	< 0.050 U	**0.041 J**	—	—
	ES051	1/22/2014		**18 J,HD**	—	—	—	—	—	< 0.50 U	< 0.50 U	—	< 0.50 U	< 1.0 U	—	—	—	< 0.051 U	< 0.051 U	< 0.051 U	—	—
	ES052	1/22/2014*		**18 J,HD**	—	—	—	—	—	< 0.50 U	< 0.50 U	—	< 0.50 U	< 1.0 U	—	—	—	< 0.051 U	< 0.051 U	< 0.051 U	—	—
	ES055	1/27/2014		**35 J,HD**	—	—	**27 BJ**	< 0.50 U	< 0.50 U	< 0.50 U	< 0.50 U	—	< 0.50 U	< 1.0 U	—	—	—	< 0.051 U	< 0.051 U	**0.064 J**	—	—
	ES088***	4/23/2014		**220 HD**	—	—	**27 BJ**	< 0.50 U	< 0.50 U	< 0.50 U	< 0.50 U	—	< 0.50 U	< 1.0 U	—	—	—	< 0.051 U	< 0.051 U	< 0.051 U	—	—
	ES111	7/23/2014		< 12 U	—	—	< 30 U	< 0.50 U	< 0.50 U	< 0.50 U	< 0.50 U	—	< 0.50 U	< 1.0 U	—	—	—	< 0.053 U	< 0.053 U	< 0.053 U	—	—
	ES120	10/22/2014		**14 J,HD**	—	—	< 30 U	< 0.50 U	< 0.50 U	< 0.50 U	< 0.50 U	—	**3.8**	< 1.0 U	—	—	—	< 0.10 U	< 0.051 U	< 0.051 U	—	—
	ES128	1/29/2015		**16 J,HD**	—	—	< 30 U	< 0.50 U	< 0.50 U	< 0.50 U	< 0.50 U	—	< 0.50 U	< 1.0 U	—	—	—	< 0.11 U	< 0.053 U	< 0.053 U	—	—
	ES136	4/22/2015		**13 J**	< 25 U	**55 BJ**	—	< 0.20 U	—	< 0.10 U	< 0.10 U	—	**0.070 J**	< 0.20 U	< 0.010 U	< 0.015 U	< 0.0040 UJ	< 0.0052 U	< 0.0052 U	< 0.0052 U	—	—
	ES151	7/22/2015		**18 J**	< 25 U	**77 J**	—	< 0.20 U	—	< 0.10 U	< 0.10 U	—	< 0.10 U	< 0.20 U	—	< 0.015 U	< 0.0040 U	< 0.0050 U	< 0.0050 U	< 0.0050 U	—	—
	ERH001	10/19/2015		**21 BJ**	**16 J**	< 56 UB	—	< 0.20 U**	—	< 0.10 U,**	< 0.10 U**	—	**0.37 J****	< 0.20 U**	—	< 0.015 U	< 0.0040 U	< 0.0050 U	< 0.0050 UB	**0.0042 BJ**	—	—
	ERH015	1/19/2016		**43 BJ**	< 25 U	**63 BJ**	—	< 0.20 U	—	< 0.10 U	< 0.10 U	—	**0.24 TbJ**	< 0.20 U	—	< 0.015 U	< 0.0040 U	< 0.0050 U	< 0.0050 U	< 0.0050 U	—	—
	ERH029	4/19/2016		< 25 UB	< 21 UB	<48 UB	—	—	—	< 0.10 U	< 0.10 U	—	< 0.10 U	< 0.20 U	—	—	—	< 0.0050 U	< 0.0050 U	< 0.0050 U	—	—
	ERH043	7/19/2016		< 22 UF	< 25 U	<54 UBF	—	—	—	< 0.10 U	< 0.10 U	—	< 0.10 U	< 0.20 U	—	—	—	< 0.0050 U	**0.0027 J**	< 0.0050 UBF	—	—
	ERH095	10/18/2016		< 25 U	—	< 40 U	< 18 U	—	—	< 0.30 U	< 0.50 U	—	< 0.30 U	< 0.30 U	—	—	—	< 0.10 U	< 0.10 U	< 0.10 U	< 4.00 U	< 80.0 UJ
	ERH127	11/16/2016		< 25 U	—	< 40 U	< 18 U	—	—	< 0.30 U	< 0.50 U	—	< 0.30 U	< 0.30 U	—	—	—	< 0.10 U	< 0.10 U	< 0.10 U	< 4.00 U	< 80.0 U
	ERH145	12/13/2016		< 25 U	—	< 40 U	< 18 U	—	—	< 0.30 U	< 0.50 U	—	< 0.30 U	< 0.30 U	—	—	—	< 0.10 U	< 0.10 U	< 0.10 U	< 4.00 U	< 80.0 U
	ERH176	1/10/2017		< 25 U	—	< 40 U	< 18 U	—	—	< 0.30 U	< 0.50 U	—	< 0.30 U	< 0.30 U	—	—	—	< 0.10 U	< 0.10 U	< 0.10 U	< 4.00 U	< 80.0 U
	ERH214	2/7/2017		< 25 U	—	< 40 U	< 18 U	—	—	< 0.30 U	< 0.50 U	—	< 0.30 U	< 0.30 U	—	—	—	< 0.10 U	< 0.10 U	< 0.10 U	< 4.00 U	< 80.0 U
	ERH280	3/8/2017		< 25 U	—	< 40 U	< 18 U	—	—	< 0.30 U	< 0.50 U	—	< 0.30 U	< 0.30 U	—	—	—	< 0.10 U	< 0.10 U	< 0.10 U	< 4.00 U	< 80.0 U
	ERH437	10/31/2017		< 25 U	—	< 40 U	< 18 U	—	—	< 0.30 U	< 0.50 U	—	< 0.30 U	< 0.30 U	—	—	—	< 0.10 U	< 0.10 U	< 0.10 U	< 4.00 U	< 80.0 U
	ERH568	3/12/2018		< 25 U	—	< 40 U	< 18 U	—	—	< 0.30 U	< 0.50 U	—	< 0.30 U	< 0.30 U	—	—	—	< 0.10 U	< 0.10 U	< 0.10 U	< 4.00 U	< 80.0 U

Table A.1-1: Cumulative Groundwater COPC Results (cont'd)
First Quarter 2018 - Quarterly Groundwater Monitoring Report, Red Hill Bulk Fuel Storage Facility, JBPHH, O'ahu, Hawai'i

			Method	8015						8260					8260SIM		8011	8270			8270/8270 Mod.	
				TPH-d	TPH-g ****	TPH-o	TPH-g ****	1,2-Dibromoethane *****	1,2-Dichloroethane *****	Benzene	Ethylbenzene	Naphthalene	Toluene	Xylenes, Total (p/m-, o-xylene)	1,2-Dibromoethane *****	1,2-Dichloroethane *****	1,2-Dibromoethane *****	1-Methylnaphthalene	2-Methylnaphthalene	Naphthalene	Phenol	2-(2-Methoxyethoxy)-ethanol
			Unit	(µg/L)	(µg/L)	(µg/L)	(µg/L)	(µg/L)	(µg/L)	(µg/L)	(µg/L)	(µg/L)	(µg/L)	(µg/L)	(µg/l)	(µg/L)	(µg/L)	(µg/L)	(µg/L)	(µg/L)	(µg/L)	(µg/L)
			Screening Criterion	400	300	500	300	0.04	5.0	5.0	30	17	40	20	0.04	5.0	0.04	10	10	17	300	800
			SSRBL	4500	—	—	—	—	—	750	—	—	—	—	—	—	—	—	—	—	—	—
Well Name	Sample ID	Date Sampled		Result	Result	Result	Result	Result	Result	Result	Result	Result	Result	Result	Result	Result	Result	Result	Result	Result	Result	Result
OWDFMW01	OWDFMW01-WG-01	8/4/2009[a]		<171 U	< 30.0 U	—	—	< 0.310 U	< 0.150 U	**0.470**	< 0.310 U	< 0.620 U	< 0.310 U	< 0.620 U	—	—	—	< 0.0164 U	< 0.0164 U	<0.0339 U	—	—
	OWDFMW01-WG-02	10/13/2009[ab]		<167 U	< 30 U	—	—	< 0.31 U	< 0.15 U	< 0.12 U	< 0.31 U	< 0.62 U	< 0.31 U	< 0.62 U	—	—	—	< 0.0168 U	< 0.0168 U	<0.0346 U	—	—
	OWDFMW01-WG-03	1/26/2010		**1,490**	< 60.0 U	—	—	< 0.620 U	< 0.300 U	< 0.240 U	< 0.620 U	< 1.24 U	< 0.620 U	< 1.24 U	—	—	—	< 0.0320 U	< 0.0320 U	<0.0664 U	—	—
	OWDFMW01-WG-04	4/26/2010		**288 J**	< 60.0 U	—	—	< 0.620 U	< 0.300 U	< 0.240 U	< 0.620 U	< 1.24 U	< 0.620 U	< 1.24 U	—	—	—	< 0.0352 U	< 0.0352 U	<0.0730 U	—	—
	ES007	10/21/2010		< 80.8 U	—	—	< 12.12 U	< 0.40 U	< 0.28 U	< 0.32 U	<0.46 U	—	< 0.34 U	< 0.38 U	—	—	—	< 0.12 U	< 0.12 U	< 0.10 U	—	—
	ES008	10/21/2010*		< 80.8 U	—	—	< 12.12 U	< 0.40 U	< 0.28 U	< 0.32 U	<0.46 U	—	< 0.34 U	< 0.38 U	—	—	—	< 0.12 U	< 0.12 U	< 0.10 U	—	—
	ES017	1/21/2011		< 80.8 U	—	—	< 12.12 U	< 0.40 U	< 0.28 U	**0.54 J**	<0.46 U	—	< 0.34 U	< 0.38 U	—	—	—	< 0.12 U	< 0.12 U	< 0.10 U	—	—
	ES018	1/21/2011*		< 80.8 U	—	—	< 12.12 U	< 0.40 U	< 0.28 U	**0.69 J**	<0.46 U	—	< 0.34 U	< 0.38 U	—	—	—	< 0.12 U	< 0.12 U	< 0.10 U	—	—
	ES029	4/21/2011		< 80.8 U	—	—	< 12.12 U	< 0.40 U	< 0.28 U	< 0.32 U	<0.46 U	—	**0.21 J**	**0.39 J**	—	—	—	< 0.12 U	< 0.12 U	< 0.10 U	—	—
	ES031	4/21/2011*		< 80.8 U	—	—	< 12.12 U	< 0.40 U	< 0.28 U	**0.29 J**	<0.46 U	—	< 0.34 U	< 0.38 U	—	—	—	< 0.12 U	< 0.12 U	< 0.10 U	—	—
	ES044	7/21/2011		< 80.8 U	—	< 212.0 U	< 12.12 U	< 0.40 U	< 0.28 U	< 0.32 U	<0.46 U	—	< 0.34 U	< 0.38 U	—	—	—	< 0.12 U	< 0.12 U	< 0.10 U	—	—
	ES045	7/21/2011*		< 80.8 U	—	< 212.0 U	< 12.12 U	< 0.40 U	< 0.28 U	< 0.32 U	<0.46 U	—	< 0.34 U	< 0.38 U	—	—	—	< 0.12 U	< 0.12 U	< 0.10 U	—	—
	ES055	10/26/2011		< 80.8 U	—	—	< 12.12 U	< 0.40 U	< 0.28 U	< 0.32 U	<0.46 U	—	< 0.34 U	< 0.38 U	—	—	—	< 0.12 U	< 0.12 U	< 0.10 U	—	—
	ES056	10/26/2011*		< 80.8 U	—	—	< 12.12 U	< 0.40 U	< 0.28 U	**0.28 J**	<0.46 U	—	< 0.34 U	< 0.38 U	—	—	—	< 0.12 U	< 0.12 U	< 0.10 U	—	—
	ES058	1/24/2012		< 80.8 U	—	< 212.0 U	< 12.12 U	< 0.40 U	< 0.28 U	**0.70 J**	<0.46 U	—	< 0.34 U	< 0.38 U	—	—	—	< 0.12 U	< 0.12 U	< 0.10 U	—	—
	ES059	1/24/2012*		< 80.8 U	—	< 212.0 U	< 12.12 U	< 0.40 U	< 0.28 U	**0.58 J**	<0.46 U	—	< 0.34 U	< 0.38 U	—	—	—	< 0.12 U	< 0.12 U	< 0.10 U	—	—
	ES077	4/26/2012		**220 ++**	—	—	< 12.12 U	< 0.40 U	< 0.28 U	**0.71 J**	<0.46 U	—	< 0.34 U	< 0.38 U	—	—	—	< 0.12 U	< 0.12 U	< 0.10 U	—	—
	ES084	7/19/2012		< 80.8 U	—	—	< 12.12 U	< 0.40 U	< 0.28 U	**1.3**	<0.46 U	—	< 0.34 U	< 0.38 U	—	—	—	< 0.12 U	< 0.12 U	< 0.10 U	—	—
	ES008	11/7/2012		**2,500 HD**	—	—	**17 BU,B**	< 0.50 U	< 0.50 U	**0.38 BU,J**	< 0.50 U	—	< 0.50 U	< 1 U	—	—	—	< 0.050 U	< 0.050 U	**0.025 J**	—	—
	ES007	11/7/2012*		**2,500 HD**	—	—	< 30 BU,U	< 0.50 U	< 0.50 U	**0.49 BU,J**	< 0.50 U	—	< 0.50 U	< 1 U	—	—	—	< 0.050 U	< 0.050 U	**0.035 J**	—	—
	ES016	1/30/2013		**1,000**	—	—	< 30 U	< 0.50 U	< 0.50 U	**0.39 J**	< 0.50 U	—	< 0.50 U	< 1 U	—	—	—	< 0.050 U	< 0.050 U	**0.032 J**	—	—
	ES017	1/30/2013*		**1,000**	—	—	< 30 U	< 0.50 U	< 0.50 U	**0.17 J**	< 0.50 U	—	< 0.50 U	< 1 U	—	—	—	< 0.050 U	< 0.050 U	**0.039 J**	—	—
	ES025	4/24/2013		**1,900 HD**	—	—	< 30 U	< 0.50 U	< 0.50 U	**0.82 J**	< 0.50 U	—	< 0.50 U	< 1.0 U	—	—	—	< 0.051 U	< 0.051 U	**0.063 J**	—	—
	ES026	4/24/2013*		**1,600 HD**	—	—	< 30 U	< 0.50 U	< 0.50 U	**0.67 J**	< 0.50 U	—	< 0.50 U	< 1.0 U	—	—	—	< 0.050 U	< 0.050 U	**0.068 J**	—	—
	ES034	7/24/2013		**470 HD**	—	—	< 30 U	< 0.50 U	< 0.50 U	**0.42 J**	< 0.50 U	—	< 0.50 U	< 1.0 U	—	—	—	< 0.050 U	< 0.050 U	**0.081 J**	—	—
	ES035	7/24/2013*		**340 HD**	—	—	< 30 U	< 0.50 U	< 0.50 U	**0.44 J**	< 0.50 U	—	< 0.50 U	< 1.0 U	—	—	—	< 0.048 U	< 0.048 U	**0.12 J**	—	—
	ES043	10/23/2013		**170 HD**	—	—	**17 BJ**	< 0.50 U	< 0.50 U	< 0.50 U	< 0.50 U	—	< 0.50 U	< 1.0 U	—	—	—	< 0.049 U	< 0.049 U	< 0.049 U	—	—
	ES044	10/23/2013*		**200 HD**	—	—	**14 BJ**	< 0.50 U	< 0.50 U	**0.17 J**	< 0.50 U	—	< 0.50 U	< 1.0 U	—	—	—	< 0.049 U	< 0.049 U	< 0.049 U	—	—
	ES053	1/27/2014		**170 HD**	—	—	**26 BJ**	< 0.50 U	< 0.50 U	**0.15 J**	< 0.50 U	—	< 0.50 U	< 1.0 U	—	—	—	< 0.050 U	< 0.050 U	**0.093 J**	—	—
	ES054	1/27/2014*		**140 HD**	—	—	**23 BJ**	< 0.50 U	< 0.50 U	< 0.50 U	< 0.50 U	—	< 0.50 U	< 1.0 U	—	—	—	< 0.050 U	< 0.050 U	**0.085 J**	—	—
	ES086	4/23/2014		**270 HD**	—	—	< 30 U	< 0.50 U	< 0.50 U	< 0.50 U	< 0.50 U	—	< 0.50 U	< 1.0 U	—	—	—	< 0.049 U	< 0.049 U	**0.035 J**	—	—
	ES087***	4/23/2014*		**32 HD**	—	—	**31 BJ**	< 0.50 U	< 0.50 U	< 0.50 U	< 0.50 U	—	< 0.50 U	< 1.0 U	—	—	—	< 0.050 U	< 0.050 U	**0.035 J**	—	—
	ES109	7/24/2014		**17 J,HD**	—	—	< 30 U	< 0.50 U	< 0.50 U	< 0.50 U	< 0.50 U	—	< 0.50 U	< 1.0 U	—	—	—	< 0.051 U	< 0.051 U	**0.031 J**	—	—
	ES110	7/24/2014*		**15 J,HD**	—	—	< 30 U	< 0.50 U	< 0.50 U	< 0.50 U	< 0.50 U	—	< 0.50 U	< 1.0 U	—	—	—	< 0.050 U	< 0.050 U	**0.027 J**	—	—
	ES121	10/22/2014		**19 J,HD**	—	—	< 30 U	< 0.50 U	< 0.50 U	< 0.50 U	< 0.50 U	—	< 0.50 U	< 1.0 U	—	—	—	< 0.10 U	< 0.052 U	**0.047 J**	—	—
	ES122	10/22/2014*		**19 J,HD**	—	—	< 30 U	< 0.50 U	< 0.50 U,IH	< 0.50 U	< 0.50 U	—	< 0.50 U	< 1.0 U	—	—	—	< 0.10 U	< 0.052 U	< 0.052 U	—	—
	ES121X	1/26/2015		**24 J,HD**	—	—	< 30 U	< 0.50 U	< 0.50 U	< 0.50 U	< 0.50 U	—	< 0.50 U	< 1.0 U	—	—	—	< 0.10 U	< 0.052 U	< 0.052 U	—	—
	ES122X	1/26/2015*		**16 J,HD**	—	—	< 30 U	< 0.50 U	< 0.50 U	< 0.50 U	< 0.50 U	—	< 0.50 U	< 1.0 U	—	—	—	< 0.10 U	< 0.051 U	< 0.051 U	—	—
	ES137	4/22/2015		**120 Z**	< 25 U	**110 BZ**	—	< 0.20 U	—	**0.070 J**	< 0.10 U	—	< 0.10 U	< 0.20 U	< 0.010 U	**0.010 J**	< 0.0040 UJ	**0.023**	**0.017 J**	**0.025**	—	—
	ES138	4/22/2015*		**120 Z**	< 25 U	**140 BZ**	—	< 0.20 U	—	< 0.10 U	< 0.10 U	—	< 0.10 U	< 0.20 U	< 0.010 U	**0.0081 J**	< 0.0040 UJ	**0.020**	**0.015 J**	**0.023**	—	—
	ES152	7/22/2015		**3,100 Z**	< 25 U	**390 Z**	—	< 0.20 U	—	< 0.10 U	< 0.10 U	—	< 0.10 U	< 0.20 U	—	**0.012 J**	< 0.0040 U	**0.0088 J**	**0.0086 J**	**0.014 J**	—	—
	ES153	7/22/2015*		**3,000 Z**	< 25 U	**330 Z**	—	< 0.20 U	—	< 0.10 U	< 0.10 U	—	**0.060 J**	< 0.20 U	—	**0.012 J**	< 0.0040 U	**0.0096 J**	**0.0097 J**	**0.016 J**	—	—
	ERH002	10/19/2015		**680 BZ**	< 25 U	**100 BJ**	—	< 0.20 U**	—	< 0.10 U**	< 0.10 U**	—	**0.40 J****	< 0.20 U**	< 0.010 U	**0.0009 J**	< 0.0040 U	**0.019 J**	**0.013 BJ**	**0.025 BJ**	—	—
	ERH016	1/19/2016		**320 BZ**	< 25 U	**69 BJ**	—	< 0.20 U	—	< 0.10 U	< 0.10 U	—	**0.18 TbJ**	< 0.20 U	—	**0.0096 J**	< 0.0040 U	**0.030**	**0.020**	**0.024**	—	—
	ERH030	4/19/2016		<38 UB	< 13 UB	< 56 UB	—	—	—	< 0.10 U	< 0.10 U	—	< 0.10 U	< 0.20 U	—	—	—	< 0.0050 U	< 0.0050 U	< 0.0050 U	—	—

Table A.1-1: Cumulative Groundwater COPC Results (cont'd)
First Quarter 2018 - Quarterly Groundwater Monitoring Report, Red Hill Bulk Fuel Storage Facility, JBPHH, O'ahu, Hawai'i

		Method	8015						8260					8260SIM		8011	8270			8270/8270 Mod.	
			TPH-d	TPH-g ****	TPH-o	TPH-g ****	1,2-Dibromoethane *****	1,2-Dichloroethane *****	Benzene	Ethylbenzene	Naphthalene	Toluene	Xylenes, Total (p/m-, o-xylene)	1,2-Dibromoethane *****	1,2-Dichloroethane *****	1,2-Dibromoethane *****	1-Methylnaphthalene	2-Methylnaphthalene	Naphthalene	Phenol	2-(2-Methoxyethoxy)-ethanol
		Unit	(µg/L)	(µg/L)	(µg/L)	(µg/L)	(µg/L)	(µg/L)	(µg/L)	(µg/L)	(µg/L)	(µg/L)	(µg/L)	(µg/l)	(µg/L)	(µg/L)	(µg/L)	(µg/L)	(µg/L)	(µg/L)	(µg/L)
		Screening Criterion	400	300	500	300	0.04	5.0	5.0	30	17	40	20	0.04	5.0	0.04	10	10	17	300	800
		SSRBL	4500	—	—	—	—	—	750	—	—	—	—	—	—	—	—	—	—	—	—
Well Name	Sample ID	Date Sampled	Result	Result	Result	Result	Result	Result	Result	Result	Result	Result	Result	Result	Result	Result	Result	Result	Result	Result	Result
OWDFMW01	ERH031	4/19/2016	< 36 UB	<9 UB	<67 UB	—	—	—	< 0.10 U	< 0.10 U	—	< 0.10 U	< 0.20 U	—	—	—	< 0.0050 U	< 0.0050 U	< 0.0050 U	—	—
(cont'd)	ERH044	7/19/2016	< 22 UF	< 25 U	<54 UBF	—	—	—	< 0.10 U	< 0.10 U	—	< 0.10 U	< 0.20 U	—	—	—	< 0.0050 U	**0.0027 J**	< 0.0050 UBF	—	—
	ERH104/105	10/20/2016*	**54**	—	**110**	< 18 U	—	—	< 0.30 U	< 0.50 U	—	< 0.30 U	< 0.30 U	—	—	—	< 0.10 U	< 0.10 U	< 0.10 U	< 4.00 U	< 80.0 U
	ERH118/119	11/15/2016*	< 25 U	—	< 40 U	< 18 U	—	—	< 0.30 U	< 0.50 U	—	< 0.30 U	< 0.30 U	—	—	—	< 0.10 U	< 0.10 U	< 0.10 U	< 4.00 U	< 80.0 U
	ERH147/148	12/14/2016*	< 58 U	—	**46**	< 18 U	—	—	< 0.30 U	< 0.50 U	—	< 0.30 U	< 0.30 U	—	—	—	< 0.10 U	< 0.10 U	< 0.10 U	< 4.00 U	< 80.0 U
	ERH184	1/12/2017	< 25 U	—	**45**	< 18 U	—	—	< 0.30 U	< 0.50 U	—	< 0.30 U	< 0.30 U	—	—	—	< 0.10 U	< 0.10 U	< 0.10 U	< 4.00 U	< 80.0 U
	ERH227	2/9/2017	< 23 U	—	**44**	< 18 U	—	—	< 0.30 U	< 0.50 U	—	< 0.30 U	< 0.30 U	—	—	—	< 0.10 U	< 0.10 U	< 0.10 U	< 4.00 U	< 80.0 U
	ERH286	3/8/2017	< 25 U	—	< 40 U	< 18 U	—	—	< 0.30 U	< 0.50 U	—	< 0.30 U	< 0.30 U	—	—	—	< 0.10 U	< 0.10 U	< 0.10 U	< 4.00 U	< 80.0 U
	ERH321	4/4/2017	< 25 U	—	< 40 U	< 18 U	—	—	< 0.30 U	< 0.50 U	—	< 0.30 U	< 0.30 U	—	—	—	< 0.10 U	< 0.10 U	< 0.10 U	< 4.00 U	< 80.0 U
	ERH389	7/5/2017	< 25 U	—	< 40 U	< 18 U	—	—	< 0.30 U	< 0.50 U	—	< 0.30 U	< 0.30 U	—	—	—	< 0.10 U	< 0.10 U	< 0.10 U	< 4.00 U	< 80.0 U
	ERH435	10/26/2017	**110**	—	< 40 U	< 18 U	—	—	< 0.30 U	< 0.50 U	—	< 0.30 U	< 0.30 U	—	—	—	< 0.10 U	< 0.10 U	< 0.10 U	< 4.00 U	< 80.0 U
	ERH566	3/14/2018	**310 J**	—	< 40 U	< 18 U	—	—	< 0.30 U	< 0.50 U	—	< 0.30 U	< 0.30 U	—	—	—	< 0.10 U	< 0.10 U	< 0.10 U	< 4.00 U	< 80.0 U

Table A.1-1: Cumulative Groundwater COPC Results (cont'd)
First Quarter 2018 - Quarterly Groundwater Monitoring Report, Red Hill Bulk Fuel Storage Facility, JBPHH, O'ahu, Hawai'i

Table Notes:

DOH Tier 1 Environmental Action Levels, Table D-1b. Groundwater Action Levels (Groundwater IS a current or potential drinking water resource, surface water body IS NOT located within 150 meters of release site).

Background historical data are from February 2005 to July 2012.

Non-detects (from October 2012 on) are the LOD values.

Results for October 2015 sampling have been adjusted to reflect corrections from hits in the laboratory blank.

January 2008 to November 2009 depth to water measurements were entered in previous reports a tenth of a foot too high, adjustments were made to correct.

1	The holding time until analysis was exceeded by 1 day; the results may be biased low.
*	Duplicate sample
**	Samples analyzed past the EPA recommended holding time.
***	Samples ES087 and ES088 possibly switched prior to analysis.
****	TPH-g analyzed by either 8015 or 8260.
*****	Analyzed by either 8260, 8260 SIM, or 8011.
a	MDL values were used for non-detects.
b	MRL values were used for non-detects.
c	No analytical lab reports found, could not verify results.
d	No analytical lab reports available, used summary table from DOH Quarterly GW Reports.
e	Results from stilling basin, pumps offline.
f	Results from stilling basin, pumps online.
g	Analyzed by Method 6010B.
h	Analyzed by Method 6020.
i	The MRL/MDL was elevated due to a chromatographic interference.
k	Analyzed by Method 200.8.
µg/L	micrograms per liter
Grey highlight	Exceeds EAL
Bold	Detected value
B	Analyte was present in the associated method blank.
BU	Sample analyzed after holding time expired.
D	The reported result is from a dilution.
F	The compound was identified but the concentration was above the MDL and below the RL.
ICH	Initial calibration verification recovery above method CL for this analyte.
ICJ	Initial calibration verification recovery below method CL for this analyte.
IH	Calibration verification recovery below method CL for this analyte.
IJ	Calibration verification recovery above method CL for this analyte.
J	Estimated value
U	The compound was analyzed for but not detected at or above the stated limit. The stated limit is the LOD unless otherwise specified.
HD, Y, L, O, Z, H, ++	The chromatographic pattern was inconsistent with the profile of the reference fuel standard.
S	Surrogate recovery was outside quality control limits.
V	Unusual problems found with the data not defined elsewhere. Description of the problem can be found in the associated quarterly monitoring analytical data validation report.
X	Possible high bias due to matrix interference.
Tb	The analyte was also detected in the associated trip blank at a similar concentration.

Appendix A.2:
COPC Concentration Graphs

RHMW2254-01

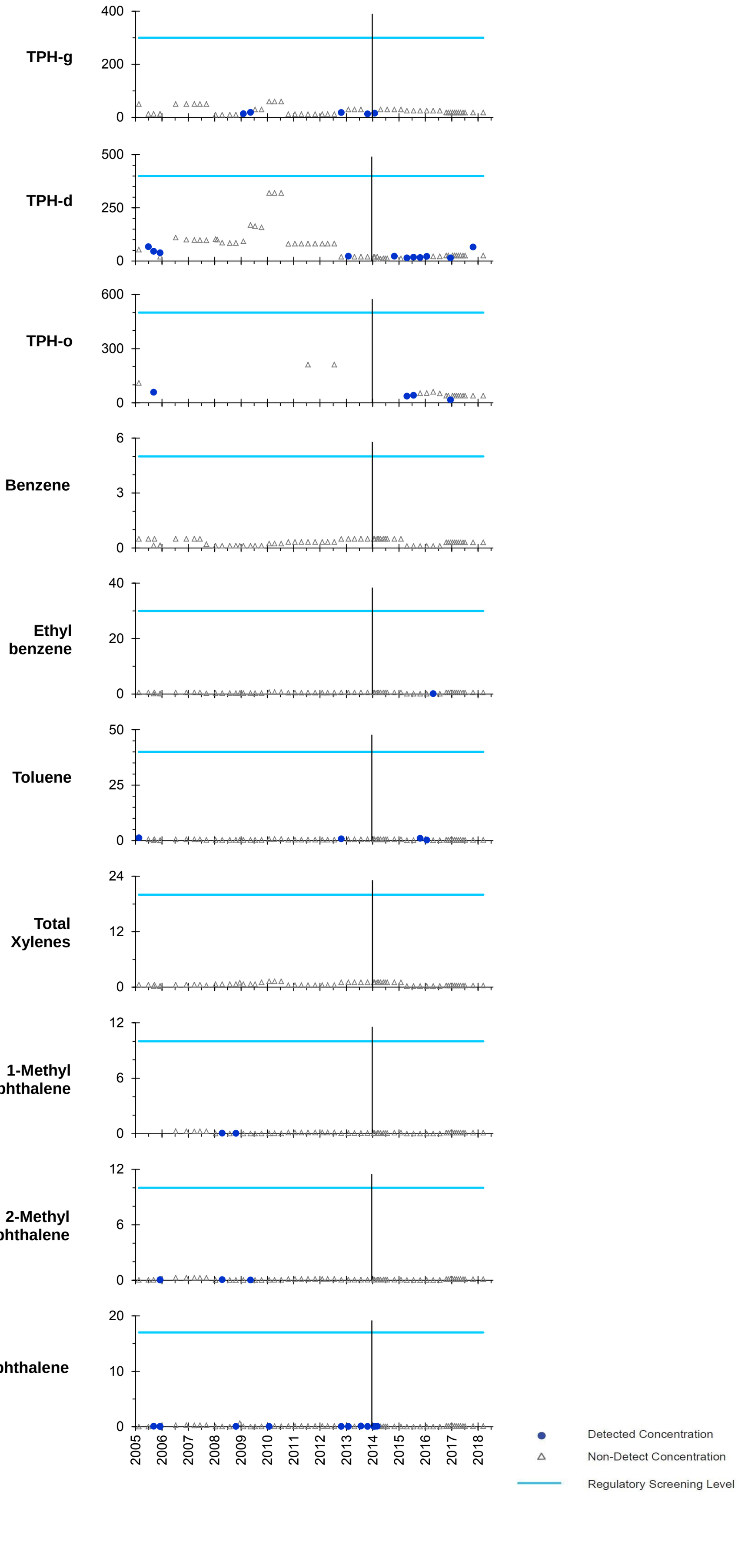
TPH-g
400
200
0
TPH-d
500
250
0
TPH-o
600
300
0
Benzene
6
3
0
Ethyl benzene
40
20
0
Toluene
50
25
0
Total Xylenes
24
12
0
1-Methyl naphthalene
12
6
0
2-Methyl naphthalene
12
6
0
Naphthalene
20
10
0
2005
2006
2007
2008
2009
2010
2011
2012
2013
2014
2015
2016
2017
2018
Detected Concentration
Non-Detect Concentration
Regulatory Screening Level

RHMW01

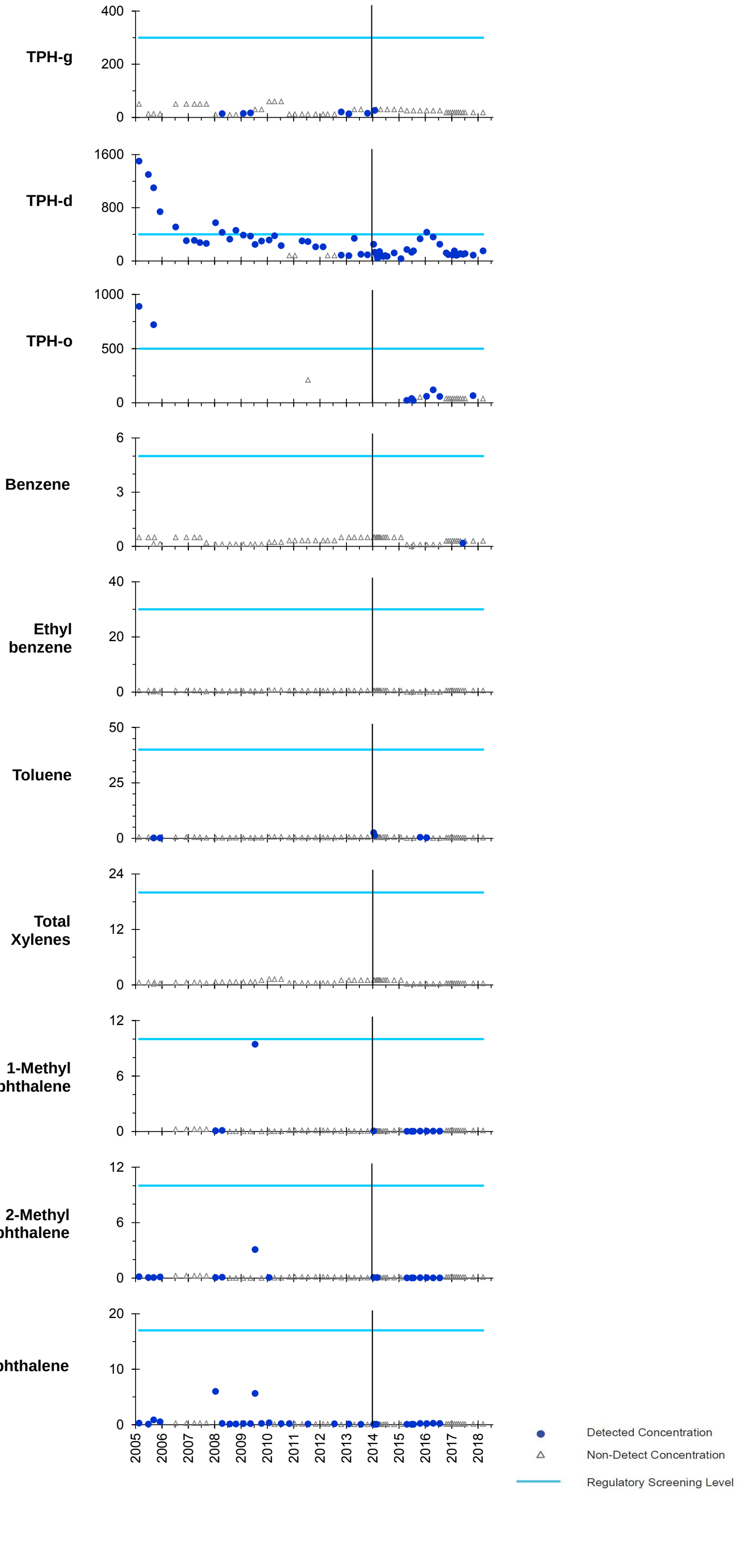
TPH-g
400
200
0
TPH-d
1600
800
0
TPH-o
1000
500
0
Benzene
6
3
0
Ethyl benzene
40
20
0
Toluene
50
25
0
Total Xylenes
24
12
0
1-Methyl naphthalene
12
6
0
2-Methyl naphthalene
12
6
0
Naphthalene
20
10
0
2005
2006
2007
2008
2009
2010
2011
2012
2013
2014
2015
2016
2017
2018
Detected Concentration
Non-Detect Concentration
Regulatory Screening Level

RHMW02

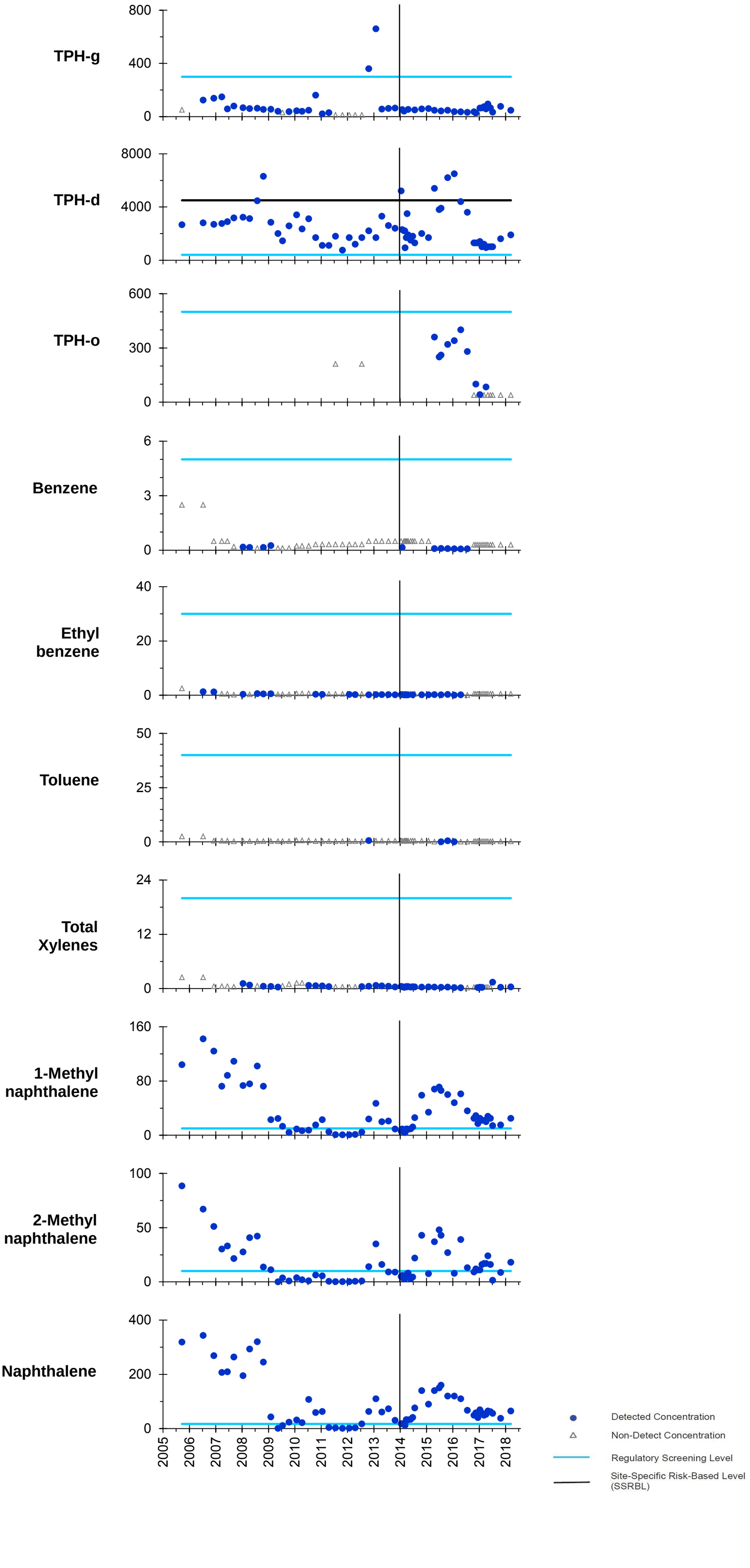
TPH-g
800
400
0
TPH-d
8000
4000
0
TPH-o
600
300
0
Benzene
6
3
0
Ethyl benzene
40
20
0
Toluene
50
25
0
Total Xylenes
24
12
0
1-Methyl naphthalene
160
80
0
2-Methyl naphthalene
100
50
0
Naphthalene
400
200
0
2005
2006
2007
2008
2009
2010
2011
2012
2013
2014
2015
2016
2017
2018
Detected Concentration
Non-Detect Concentration
Regulatory Screening Level
Site-Specific Risk-Based Level (SSRBL)

RHMW03

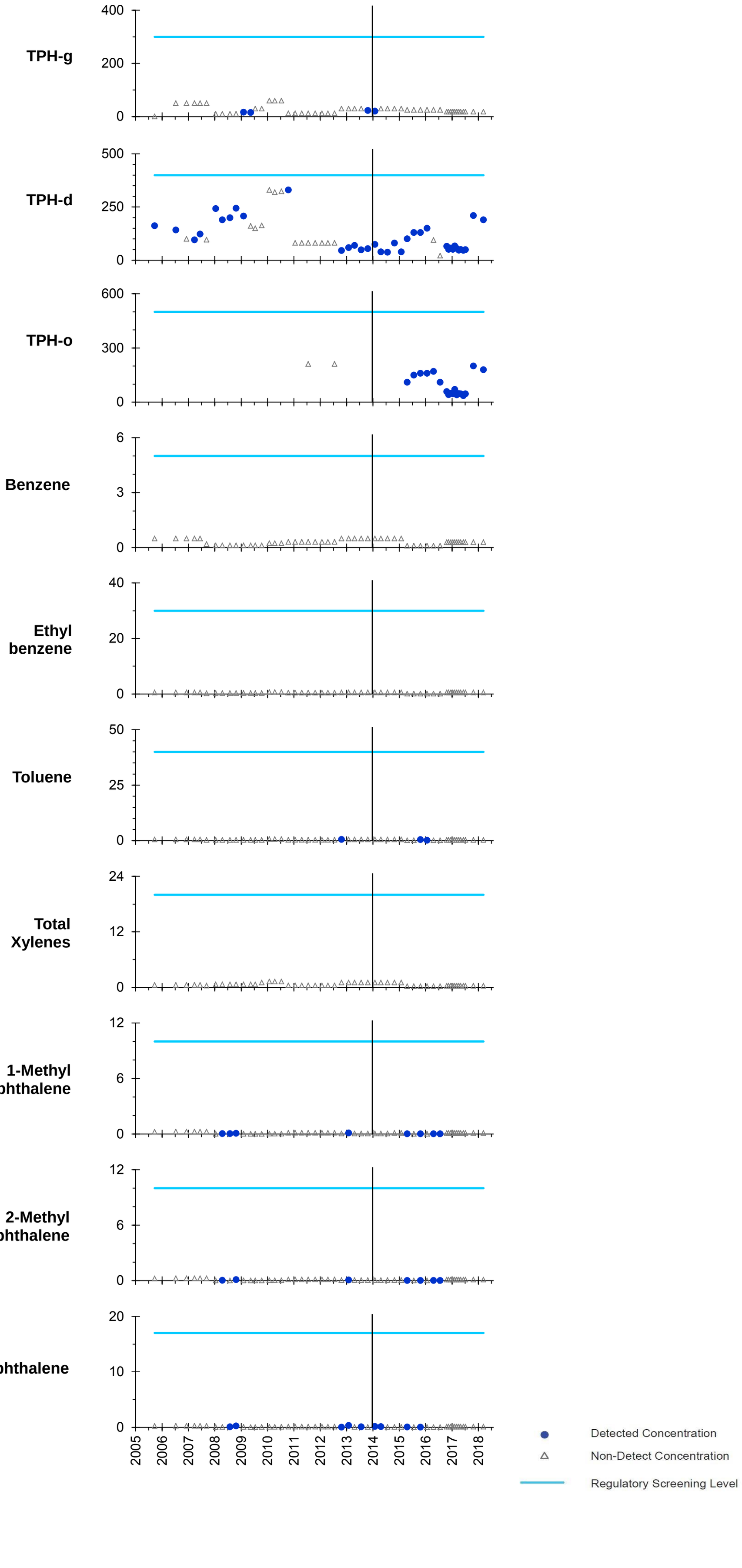
TPH-g
400
200
0
TPH-d
500
250
0
TPH-o
600
300
0
Benzene
6
3
0
Ethyl benzene
40
20
0
Toluene
50
25
0
Total Xylenes
24
12
0
1-Methyl naphthalene
12
6
0
2-Methyl naphthalene
12
6
0
Naphthalene
20
10
0
2005
2006
2007
2008
2009
2010
2011
2012
2013
2014
2015
2016
2017
2018
Detected Concentration
Non-Detect Concentration
Regulatory Screening Level

RHMW04

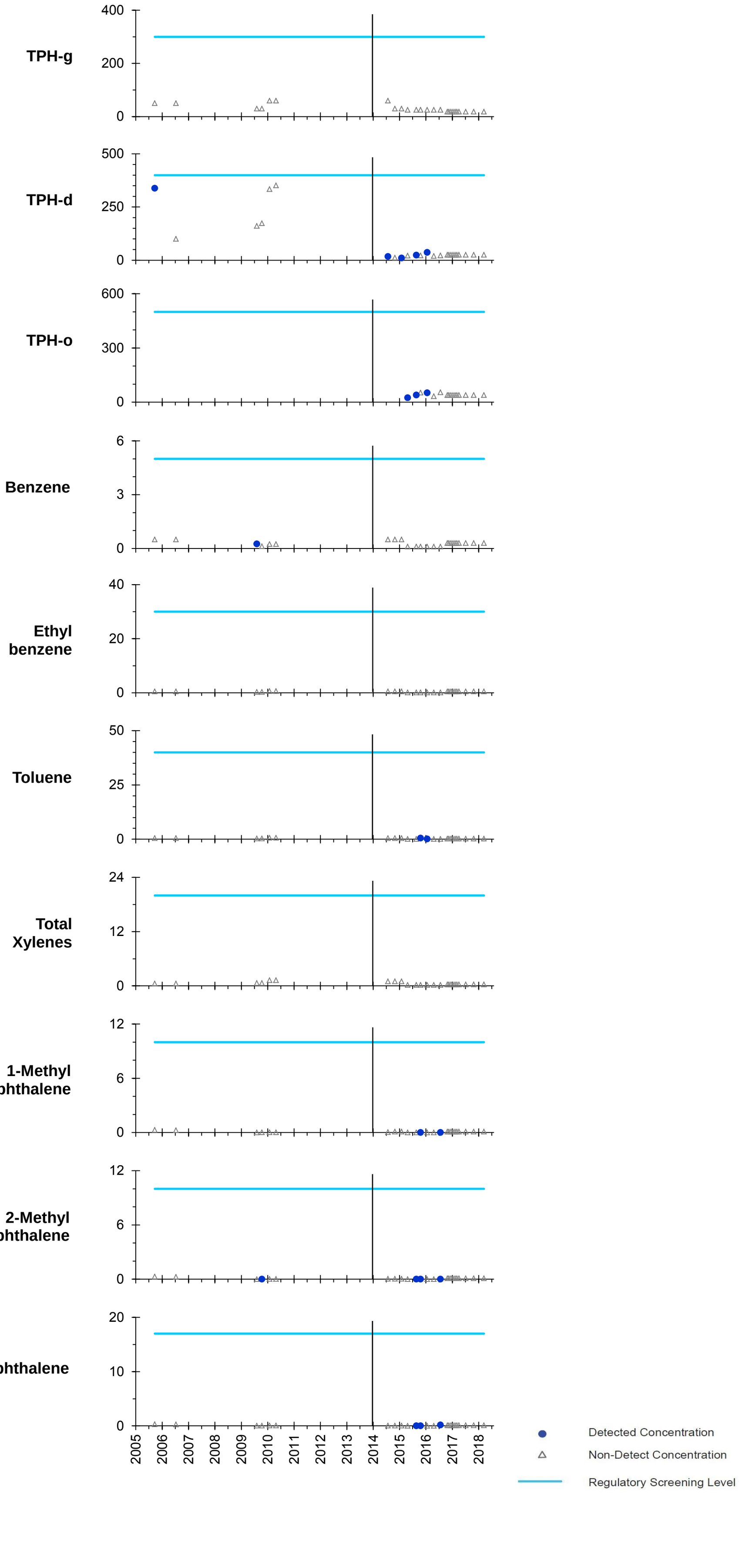
TPH-g
400
200
0
TPH-d
500
250
0
TPH-o
600
300
0
Benzene
6
3
0
Ethyl benzene
40
20
0
Toluene
50
25
0
Total Xylenes
24
12
0
1-Methyl naphthalene
12
6
0
2-Methyl naphthalene
12
6
0
Naphthalene
20
10
0
2005
2006
2007
2008
2009
2010
2011
2012
2013
2014
2015
2016
2017
2018
Detected Concentration
Non-Detect Concentration
Regulatory Screening Level

RHMW05

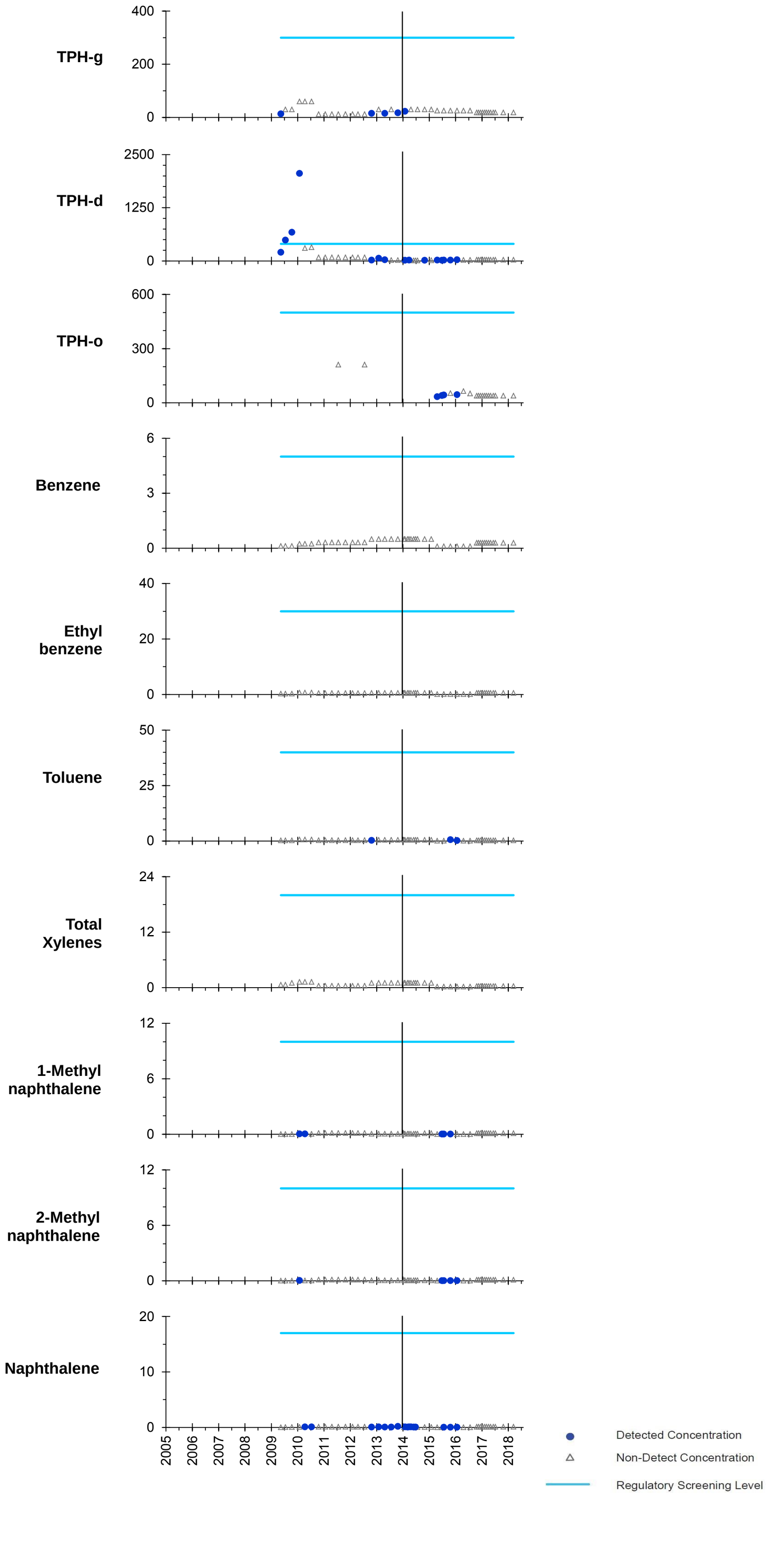
TPH-g
400
200
0
TPH-d
2500
1250
0
TPH-o
600
300
0
Benzene
6
3
0
Ethyl benzene
40
20
0
Toluene
50
25
0
Total Xylenes
24
12
0
1-Methyl naphthalene
12
6
0
2-Methyl naphthalene
12
6
0
Naphthalene
20
10
0
2005
2006
2007
2008
2009
2010
2011
2012
2013
2014
2015
2016
2017
2018
Detected Concentration
Non-Detect Concentration
Regulatory Screening Level

RHMW06

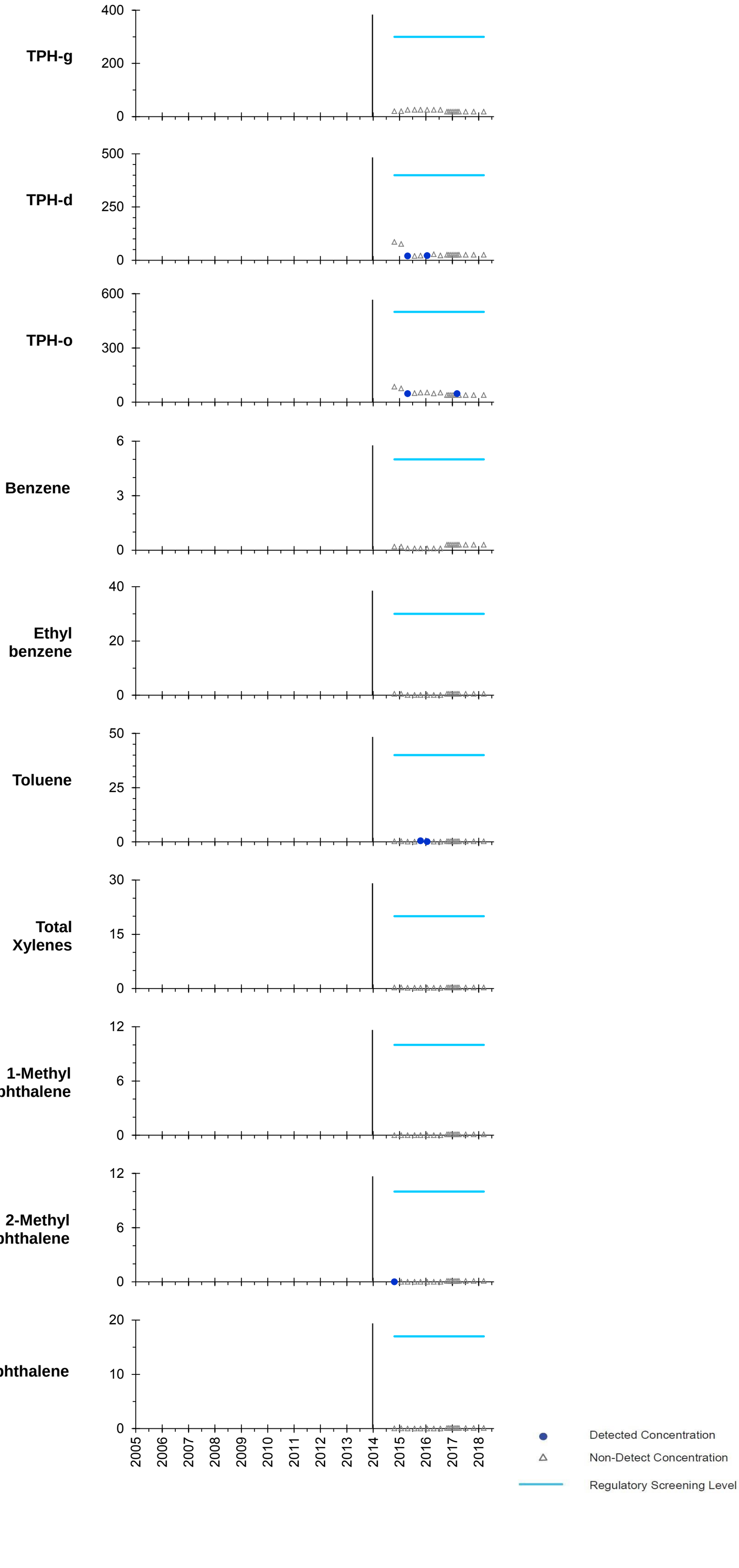
TPH-g
400
200
0
TPH-d
500
250
0
TPH-o
600
300
0
Benzene
6
3
0
Ethyl benzene
40
20
0
Toluene
50
25
0
Total Xylenes
30
15
0
1-Methyl naphthalene
12
6
0
2-Methyl naphthalene
12
6
0
Naphthalene
20
10
0
2005
2006
2007
2008
2009
2010
2011
2012
2013
2014
2015
2016
2017
2018
Detected Concentration
Non-Detect Concentration
Regulatory Screening Level

RHMW07

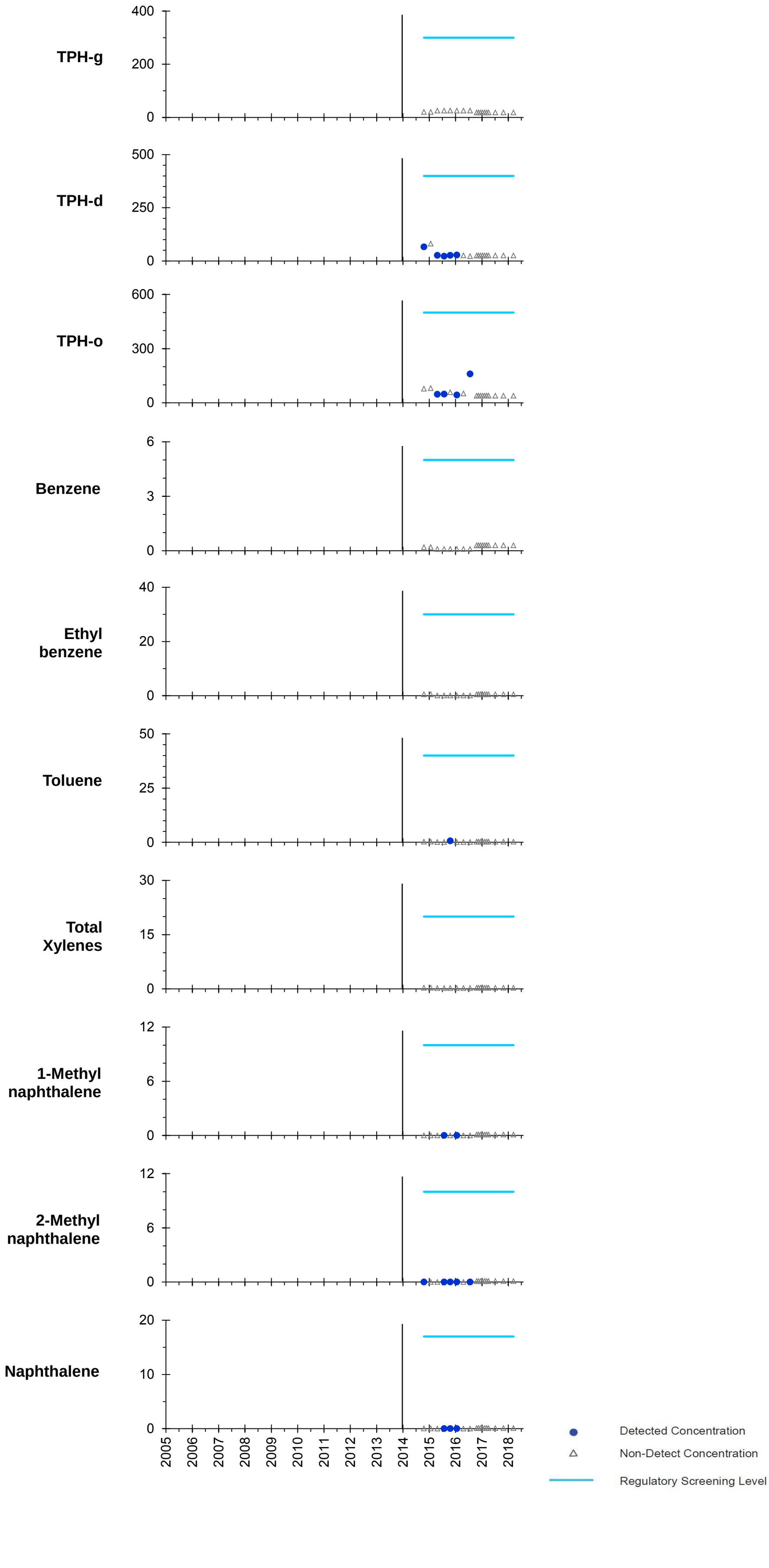
TPH-g
400
200
0
TPH-d
500
250
0
TPH-o
600
300
0
Benzene
6
3
0
Ethyl benzene
40
20
0
Toluene
50
25
0
Total Xylenes
30
15
0
1-Methyl naphthalene
12
6
0
2-Methyl naphthalene
12
6
0
Naphthalene
20
10
0
2005
2006
2007
2008
2009
2010
2011
2012
2013
2014
2015
2016
2017
2018
Detected Concentration
Non-Detect Concentration
Regulatory Screening Level

RHMW08

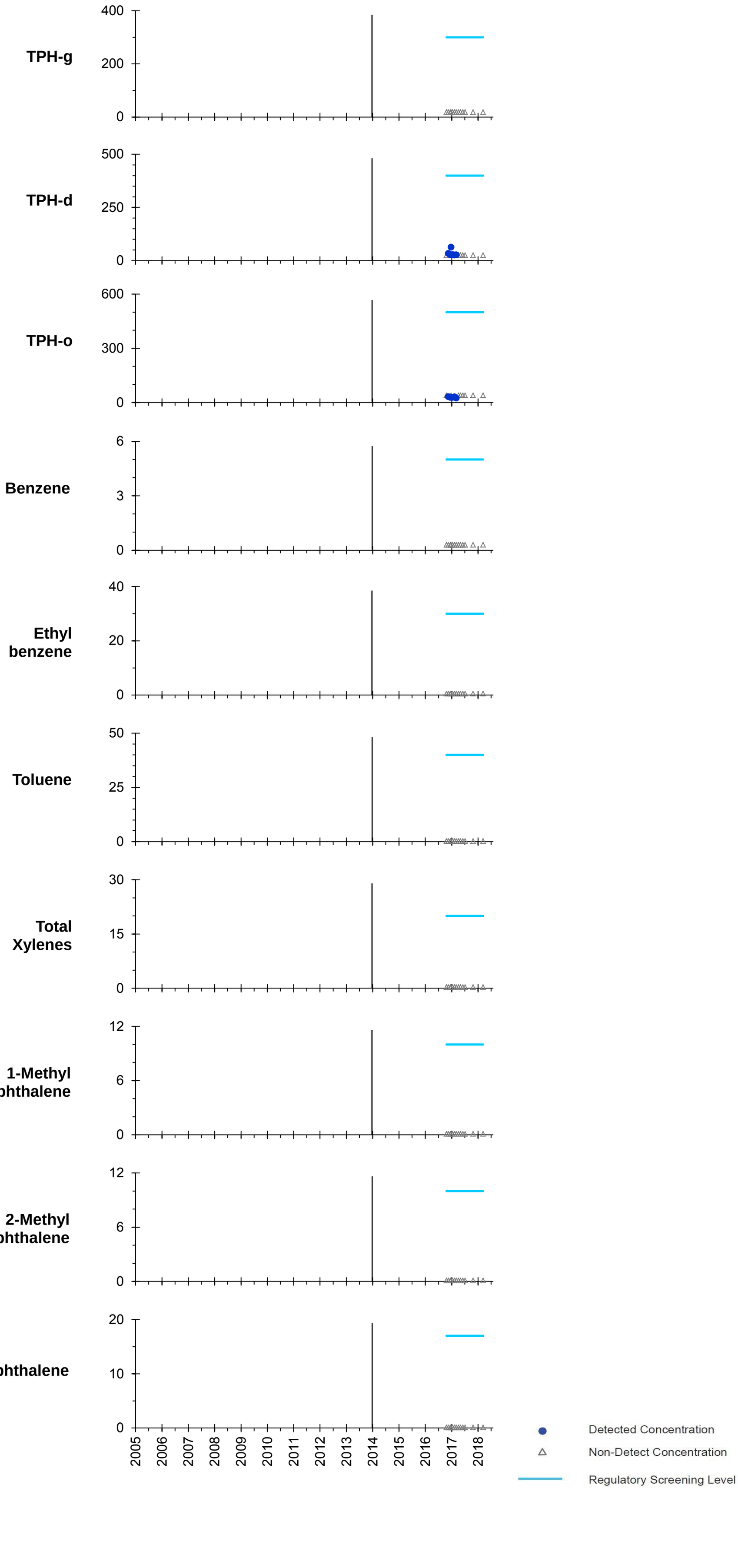
TPH-g
400
200
0
TPH-d
500
250
0
TPH-o
600
300
0
Benzene
6
3
0
Ethyl benzene
40
20
0
Toluene
50
25
0
Total Xylenes
30
15
0
1-Methyl naphthalene
12
6
0
2-Methyl naphthalene
12
6
0
Naphthalene
20
10
0
2005
2006
2007
2008
2009
2010
2011
2012
2013
2014
2015
2016
2017
2018
Detected Concentration
Non-Detect Concentration
Regulatory Screening Level

RHMW09

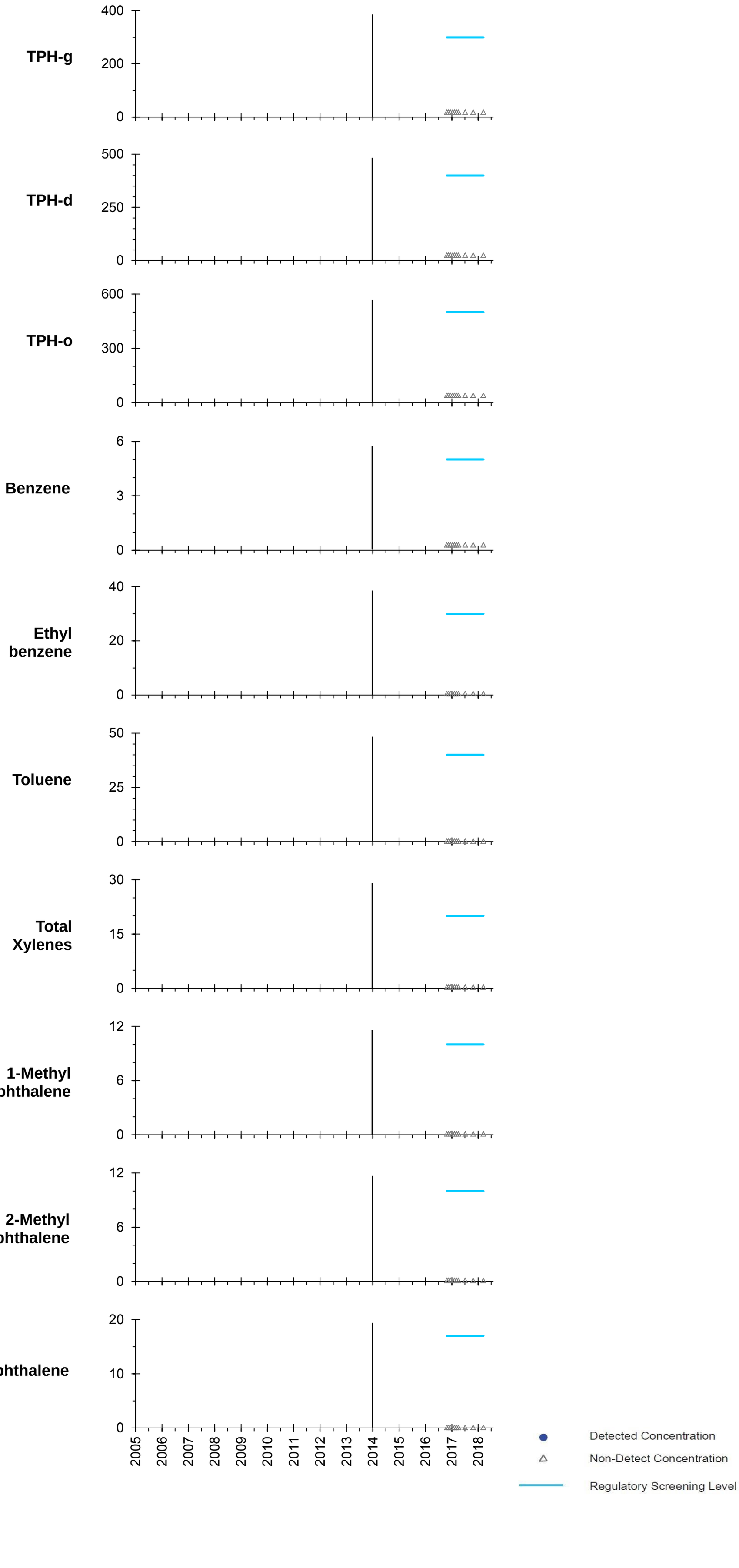
TPH-g
400
200
0
TPH-d
500
250
0
TPH-o
600
300
0
Benzene
6
3
0
Ethyl benzene
40
20
0
Toluene
50
25
0
Total Xylenes
30
15
0
1-Methyl naphthalene
12
6
0
2-Methyl naphthalene
12
6
0
Naphthalene
20
10
0
2005
2006
2007
2008
2009
2010
2011
2012
2013
2014
2015
2016
2017
2018
Detected Concentration
Non-Detect Concentration
Regulatory Screening Level

RHMW10

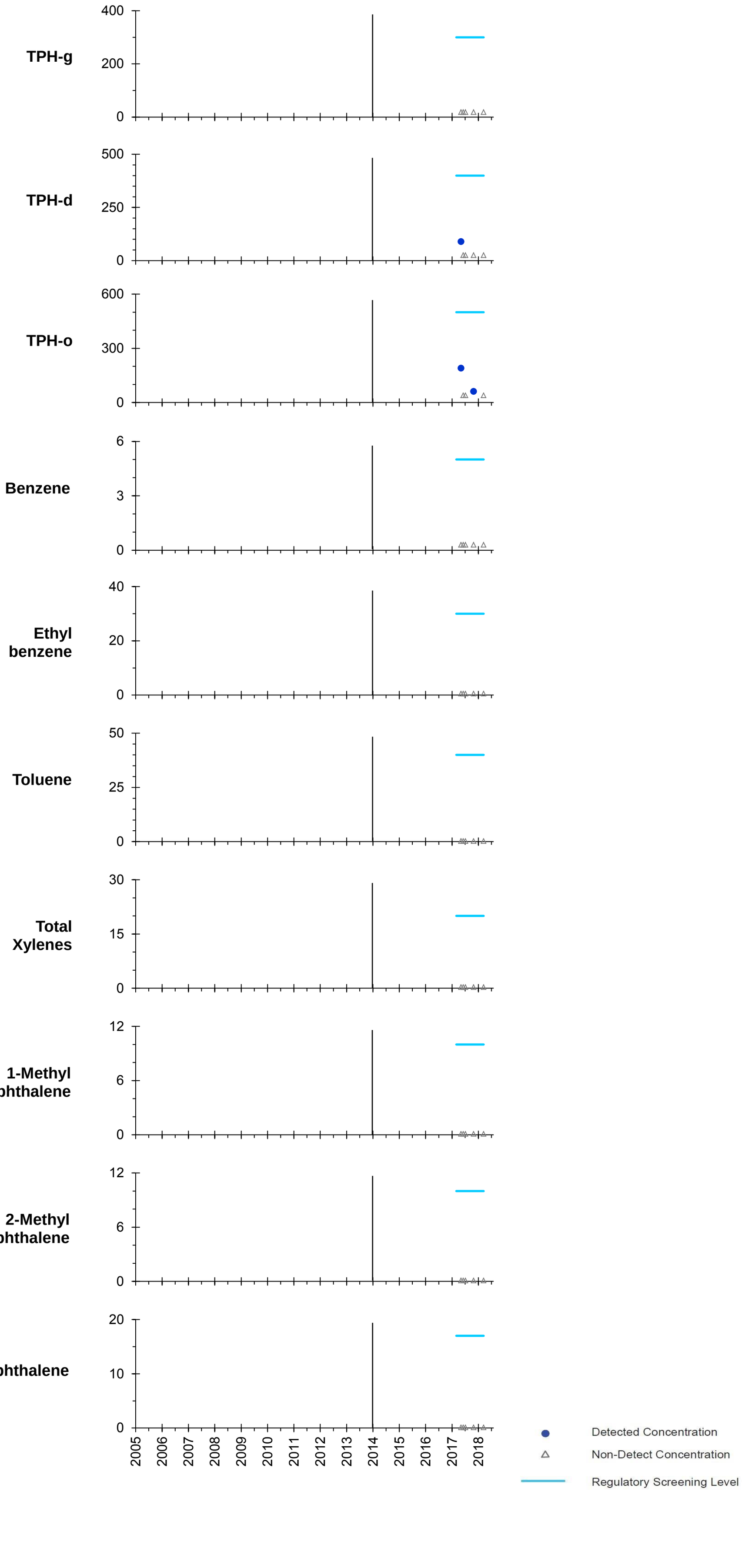
TPH-g
400
200
0
TPH-d
500
250
0
TPH-o
600
300
0
Benzene
6
3
0
Ethyl benzene
40
20
0
Toluene
50
25
0
Total Xylenes
30
15
0
1-Methyl naphthalene
12
6
0
2-Methyl naphthalene
12
6
0
Naphthalene
20
10
0
2005
2006
2007
2008
2009
2010
2011
2012
2013
2014
2015
2016
2017
2018
Detected Concentration
Non-Detect Concentration
Regulatory Screening Level

RHMW11 Zone 1

RHMW11 Zone 2

RHMW11 Zone 3

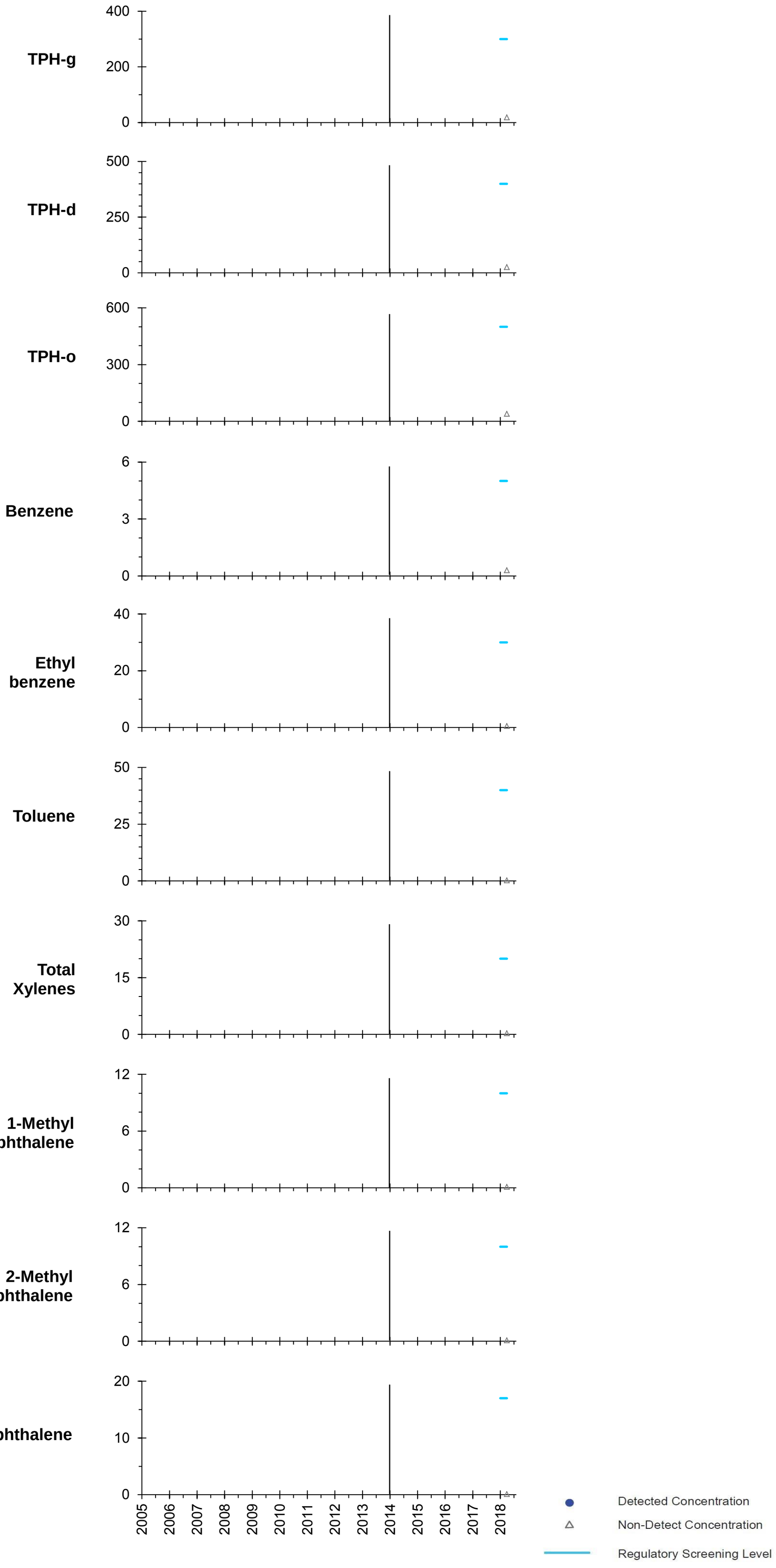

RHMW11 Zone 4

RHMW11 Zone 5

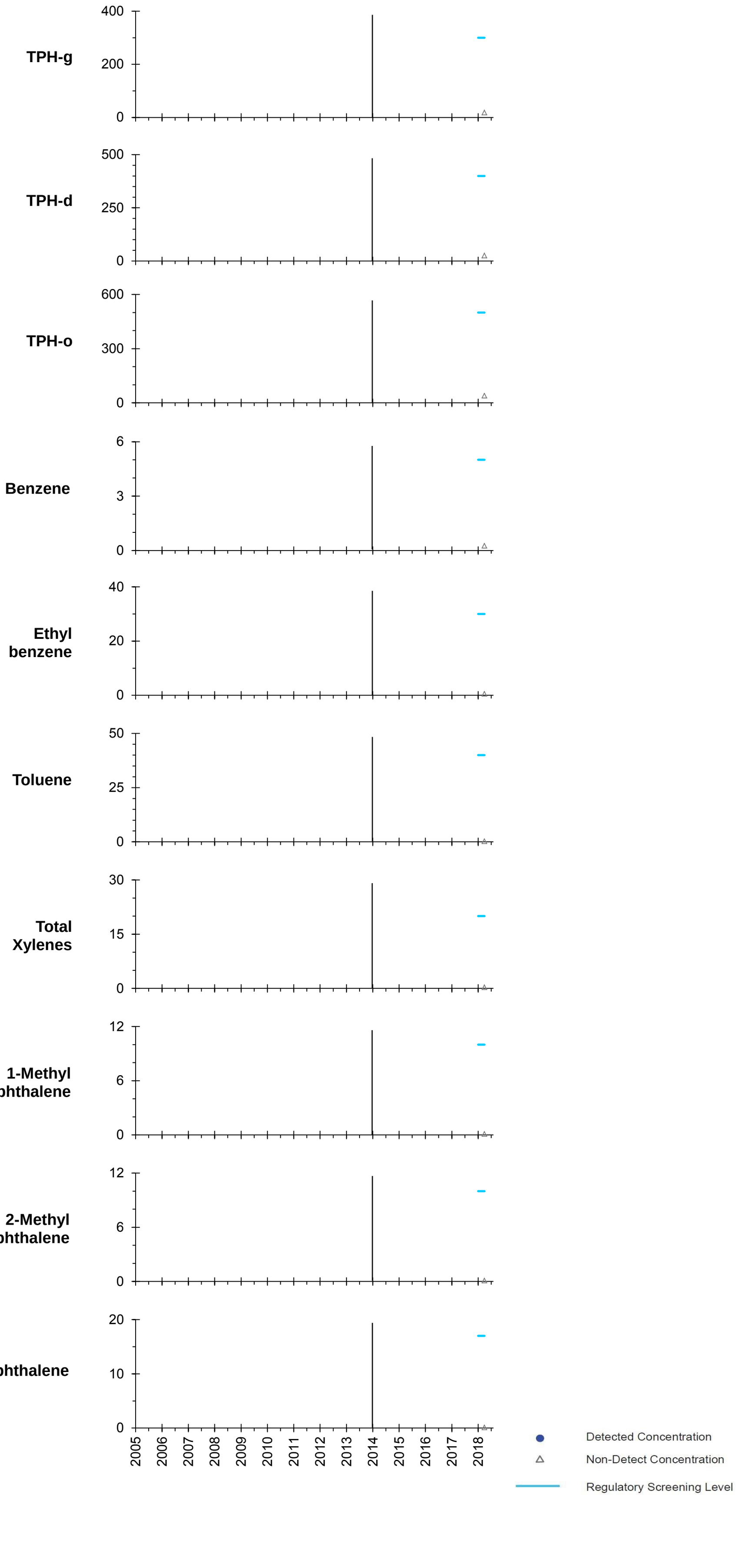

OWDFMW01

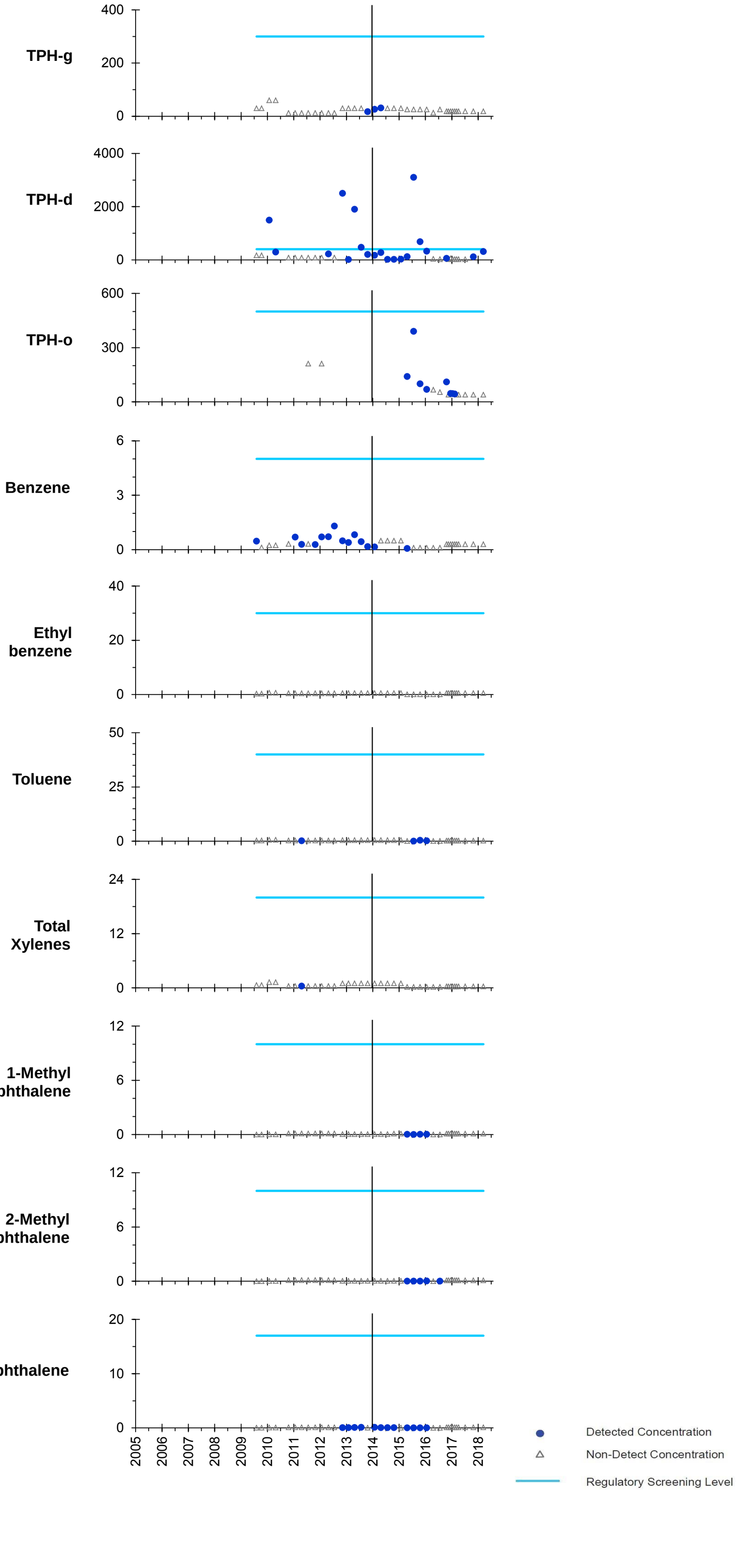
TPH-g
400
200
0
TPH-d
4000
2000
0
TPH-o
600
300
0
Benzene
6
3
0
Ethyl benzene
40
20
0
Toluene
50
25
0
Total Xylenes
24
12
0
1-Methyl naphthalene
12
6
0
2-Methyl naphthalene
12
6
0
Naphthalene
20
10
0
2005
2006
2007
2008
2009
2010
2011
2012
2013
2014
2015
2016
2017
2018
Detected Concentration
Non-Detect Concentration
Regulatory Screening Level

HDMW2253-03

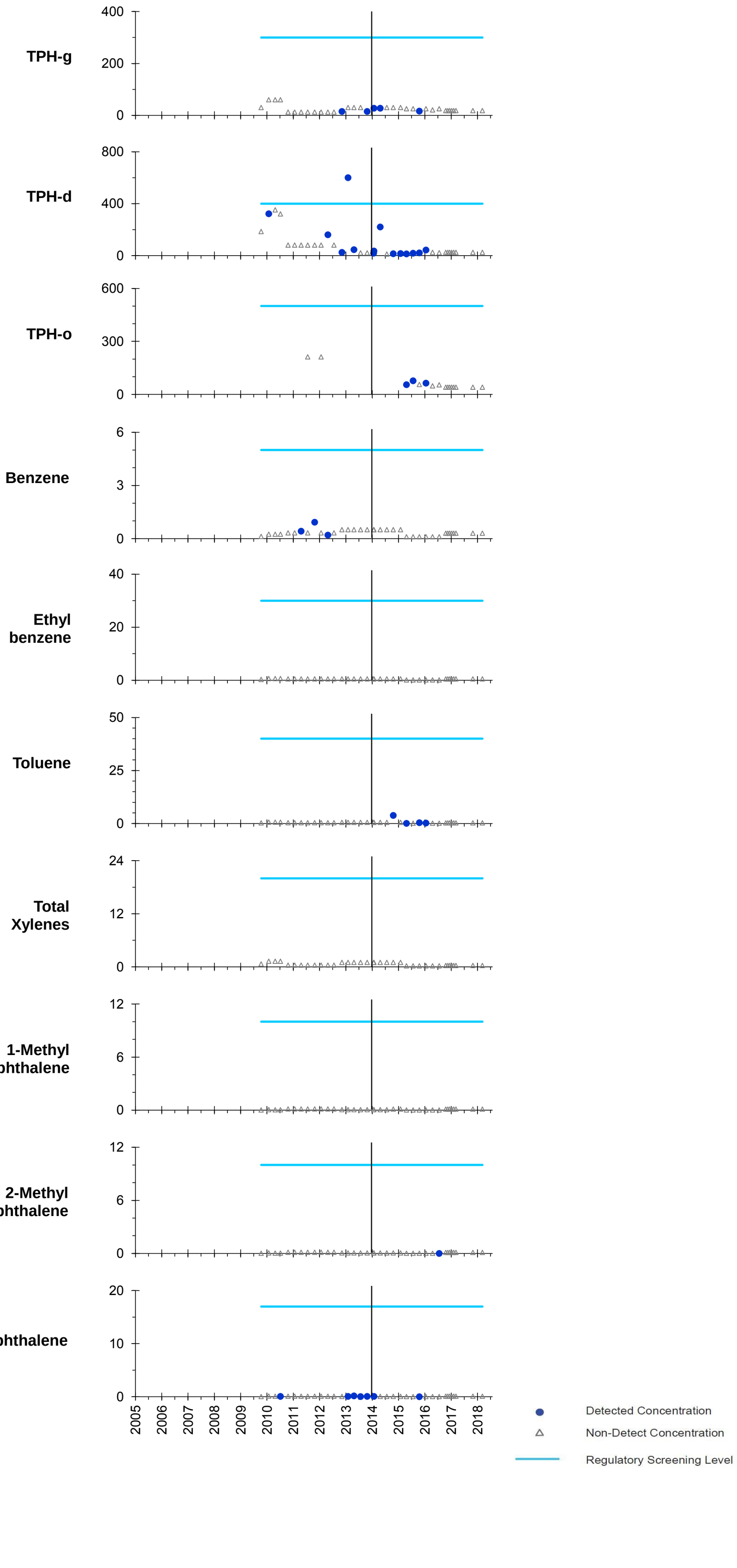
TPH-g
400
200
0
TPH-d
800
400
0
TPH-o
600
300
0
Benzene
6
3
0
Ethyl benzene
40
20
0
Toluene
50
25
0
Total Xylenes
24
12
0
1-Methyl naphthalene
12
6
0
2-Methyl naphthalene
12
6
0
Naphthalene
20
10
0
2005
2006
2007
2008
2009
2010
2011
2012
2013
2014
2015
2016
2017
2018
Detected Concentration
Non-Detect Concentration
Regulatory Screening Level

Appendix B:
Fate and Transport Analyses

B.1: Thermal NSZD Analysis

B.2: Carbon Trap NSZD Analysis

B.3: Soil Vapor Analysis

B.4: MNA Primary Lines of Evidence and Rate Calculations

B.5: MNA Secondary Lines of Evidence

B.6: Microcosm Study and Microbial Parameter Analysis

B.7: Characterization of TPH in Groundwater: Forensics

Appendix B.1:
Thermal NSZD Analysis

CONTENTS

Acronyms and Abbreviations iii

1. Introduction 1-1

1.1 Technical Background 1-1
1.2 Study Objectives 1-1
1.3 Selection of Monitoring Wells for NSZD Study 1-1
1.4 Measurement Protocols 1-3
1.4.1 Method 1: Well Air Temperature 1-3
1.4.2 Method 2: Wall Temperature 1-3
1.5 Background Location 1-7

2. NAPL Distribution Inferred from Temperature Data 2-1

3. NSZD Rates 3-1

3.1 Calculation Method 1: Net Temperatures 3-1
3.1.1 Net Temperature Profiles 3-1
3.1.2 NSZD Calculations 3-1
3.2 Calculation Method 2: Thermal Profiles 3-4
3.2.1 NSZD Calculations 3-5
3.3 Agreement Between Method 1 and Method 2 NSZD Rates 3-7
3.4 Method 3: Groundwater Temperatures 3-7

4. Conclusions 4-1

5. References 5-1

ATTACHMENTS

B.1.1 Thermal Monitoring Data

FIGURES

1-1 Location of Temperature-Profile Wells in Relation to Tank Farm 1-2

1-2 Pipe Test-Ball Plug (left) and Inflated Plug Inside Well (right) 1-3

1-3 Design of Wall Temperature Method Monitoring Device (Protective Mesh Around Test Ball and Weight Not Shown). 1-4

1-4 Polyethylene Mesh Netting Used to Secure Thermocouple Tip to Test Ball 1-4

1-5 Comparison of Raw (Not Background-Corrected) Thermal Profiles for Well Air Temperature and Wall Temperature Methods 1-5

1-6 Raw (Not Background-Corrected) Thermal Profiles for Facility Wells 1-6

2-1 Net (Background-Corrected) Temperature Profiles for Facility Wells (Well Air Temperature Method) 2-1

2-2 Net (Background-Corrected) Temperature Profiles for Facility Wells (Well Air Temperature Method) 2-3

2-3 Net (Background-Corrected) Temperature Profiles for Facility Wells (Well Air Temperature Method), Highlighting Clinker Zones (Identified from Boring Logs) and LNAPL Intervals 2-4

3-1 Area Encompassed by Tank Farm 3-3

3-2 Hillel-Corrected Raw (Not Background-Corrected) Thermal Profiles for Facility Wells (Well Air Temperature Method) 3-4

4-1 Soil Contamination at Tank Farm Observed During 1998–2002 Environmental Investigation 4-3

TABLES

1-1 Summary of Details for Monitoring Wells Used for NSZD Study 1-1

1-2 Average Temperatures in Honolulu, HI 1-2

2-1 Inferred LNAPL-Containing Intervals Indicated by Net (Background-Corrected) Temperature Profiles from Three Facility Monitoring Wells 2-2

3-1 Calculation of Bottom Heat Flux for NSZD Using Well Air Temperature Method and Net Temperatures Method 3-2

3-2 Calculation of Conversion from W/m^2 to gal/acre/yr of NSZD 3-2

3-3 Net Temperatures Method NSZD Rates for Facility Wells (Well Air Temperature Method) 3-3

3-4 Net Temperature NSZD Rates for Facility Wells (Average of Well Air Temperature and Wall Temperature Methods) 3-3

3-5 Calculation of Bottom Heat Flux for NSZD Using Well Air Temperature Method and Thermal Profiles Method 3-6

3-6 Thermal Profiles Method NSZD Rates for Facility Wells (Well Air Temperature Method) 3-6

3-7 Thermal Profiles Method NSZD Rates for Facility Wells (Average of Well Air Temperature and Wall Temperature Methods) 3-6

3-8 Water Temperatures at RHMW03 and RHMW05 3-8

3-9 Calculation of Mass of Water Flow from RHMW03 to RHMW05 3-8

3-10 Calculation of Biodegradation in Groundwater 3-9

3-11 The Bottom NSZD Rate (i.e., Associated with Downward Heat Transfer) for the Three Calculation Methods 3-9

4-1 Summary of Total NSZD Rates from the Tank Farm 4-1

ACRONYMS AND ABBREVIATIONS

btoc	below top of casing
°C	degree Celsius
cal/g/C	calorie per gram per degree Celsius
CSM	conceptual site model
DAWT	directly above the water table
ft	foot/feet
gal	gallon
gal/acre/yr	gallons per acre per year
gal/yr	gallons per year
J	joule
K	Kelvin
kg	kilogram
L	liter
LNAPL	light non-aqueous-phase liquid
m^2	square meter
m^3	cubic meter
MJ	megajoule
msl	mean sea level
NSZD	natural source-zone depletion
W	watt
yr	year

1. Introduction

This subappendix is summarized in Section 7.3.1.4 of the Conceptual Site Model (CSM) main document.

1.1 TECHNICAL BACKGROUND

Natural source-zone depletion (NSZD) is the active process whereby light non-aqueous-phase liquid (LNAPL) is degraded in the subsurface by biodegradation and other naturally occurring processes. For this document, LNAPL consists of petroleum hydrocarbons in the form of various fuels. NSZD rates have been measured at many LNAPL sites and can be quantified by measuring the magnitude and distribution of subsurface temperatures and then calculating the net heat flux being generated by biodegradation processes.

1.2 STUDY OBJECTIVES

In this study, the objectives were to determine if temperature profiles in monitoring wells in the Red Hill tank farm area can be used to:

1. Assess the vertical distribution of LNAPL based on depths with elevated temperatures.
2. Quantify the rate of NSZD based on temperature profile measurements.

Temperature profiles were collected in four existing monitoring wells at the site: RHMW01, RHMW02, RHMW03, and RHMW05.

1.3 SELECTION OF MONITORING WELLS FOR NSZD STUDY

The temperature profiles were measured in four monitoring wells at the Red Hill Bulk Fuel Storage Facility ("the Facility") from the surface to the bottom of the well. Data for existing monitoring wells were reviewed to select a number of suitable wells with the occurrence of dissolved-phase constituents (RHMW01, RHMW02, and RHMW03) as well as a background well (RHMW05). Well construction details, measured groundwater levels, and measured borehole depths are summarized in Table 1-1, as provided in the *Existing Data Summary and Evaluation Report for Groundwater Flow and Contaminant Fate and Transport Modeling, Red Hill Bulk Fuel Storage Facility*" (DON, 2017) dated March 5, 2017 and measured in the field. The locations of these wells are shown on Figure 1-1. RHMW05 was chosen as the background well because it is the furthest from the tank farm of all the wells and therefore is likely to have no impact from LNAPL in the unsaturated zone.

Table 1-1: Summary of Details for Monitoring Wells Used for NSZD Study

Well	Lower Tunnel Floor Surface (ft msl)	Top of Casing (ft msl)	Groundwater Surface as of March 5, 2017 (ft btoc)	Borehole Depth (ft btoc)	Ambient Air Temperature at Time of Measurement (October 2017) (°C)
RHMW01	102.5	102.0	83.7	99.5	26.6
RHMW02	105.7	104.6	86.4	102.4	26.4
RHMW03	122.1	120.9	102.6	116.8	26.9
RHMW05 (Background)	101.2	101.3	83.0	124.8	26.8

°C degree Celsius
ft foot/feet
btoc below top of casing
msl mean sea level

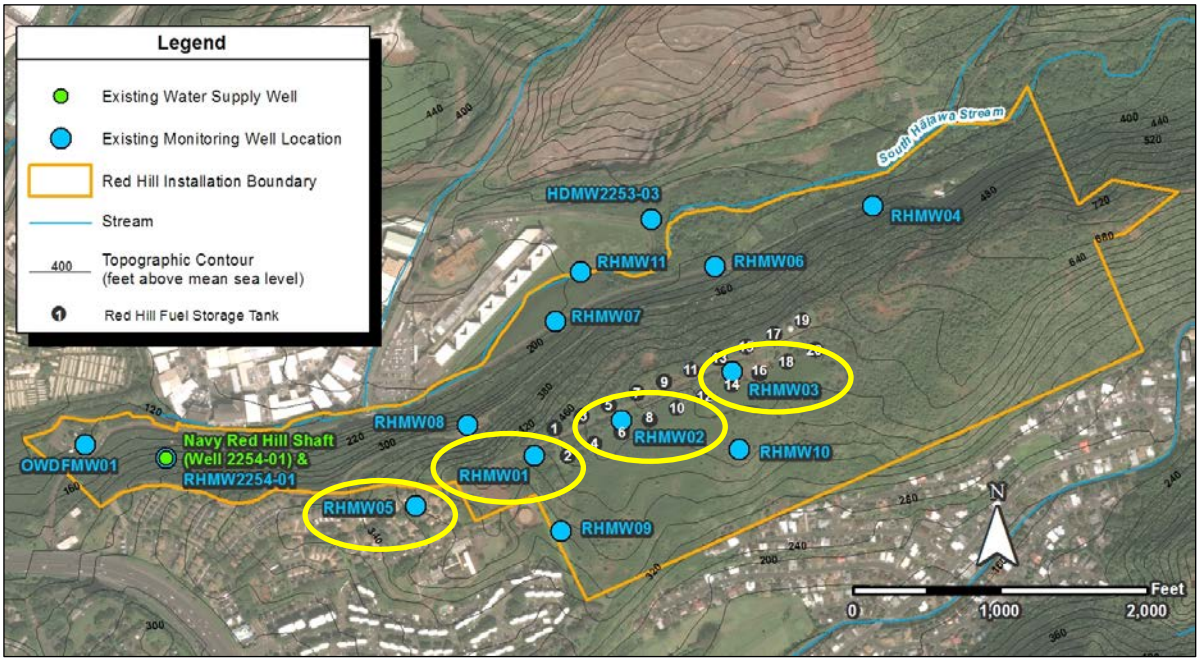

1 **Figure 1-1: Location of Temperature-Profile Wells in Relation to Tank Farm**

2 The ambient temperatures inside the tunnels at the time of measurement were fairly similar to typical
3 temperatures in Honolulu (Table 1-2). This is likely because the air in the tunnels is in relative
4 equilibrium with the ambient air because of tunnel ventilation.

5 **Table 1-2: Average Temperatures in Honolulu, HI**

Month	Average Temperature (°C)	
	Typical Year (Multi-Year Average)	2017
January	22.9	23.1
February	22.8	23.2
March	23.6	24.6
April	24.5	25.4
May	25.4	25.8
June	26.8	26.7
July	27.3	27.6
August	27.7	27.7
September	27.5	27.6
October	26.7	26.7
November	25.3	—
December	23.8	—
Overall	25.4	—

6 Source: (U.S. Climate Data 2018)
7 — no data

1.4 MEASUREMENT PROTOCOLS

Temperature measurements were obtained using high accuracy Type-T thermocouples, calibrated on July 20, 2017. Both Well Air Temperature and Wall Temperature Methods of measurement were employed because of the complicated setting at the site. It was hypothesized that open space in the wells might be subject to air flow from open screen intervals near the water table to the lower pressure tunnel environment, which might distort the formation of a temperature signal in the thermocouple. Therefore, the Wall Temperature Method was intended to reduce the impacts of this confounding factor if it occurred.

1.4.1 Method 1: Well Air Temperature

In this configuration, the thermocouple was fed through a hole in a well plug, a weight was attached to a line attached to the end of the thermocouple, and the assembly was fed down the well. The weight ensured the thermocouple wire stayed taut as temperature measurements were taken at 5-ft intervals down to the water table, then at the top, middle, and bottom of the water column. The weight and thermocouple were decontaminated with Alconox and water between each well, and a new line was used for each well. This method had the advantage of simplicity but could potentially be impacted by air flowing up the well. This air flow is caused by a negative pressure within the tunnels, which pulls air from the unsaturated zone into the tunnels. The air has the potential to distort the temperature signal from the formation on the outside of the well.

To help mitigate potential problems from this airflow, two measures were taken: (1) the wells were capped for several days before the Well Air Temperature Method was performed; and (2) the Wall Temperature Method was also performed.

1.4.2 Method 2: Wall Temperature

In the Wall Temperature Method configuration, the thermocouple was attached to a pipe test ball plug (Figure 1-2 and Figure 1-3), which was fed down the well and inflated using a bicycle tire pump at the surface up to a specific inflation pressure. A protective mesh netting was placed around the test ball and thermocouple tip to hold the tip in place next to the test ball (Figure 1-4). The inflated test ball ensured that the measurement tip of the thermocouple was pressed against the well casing, to potentially increase the accuracy of subsurface temperature readings.

Figure 1-2: Pipe Test-Ball Plug (left) and Inflated Plug Inside Well (right)

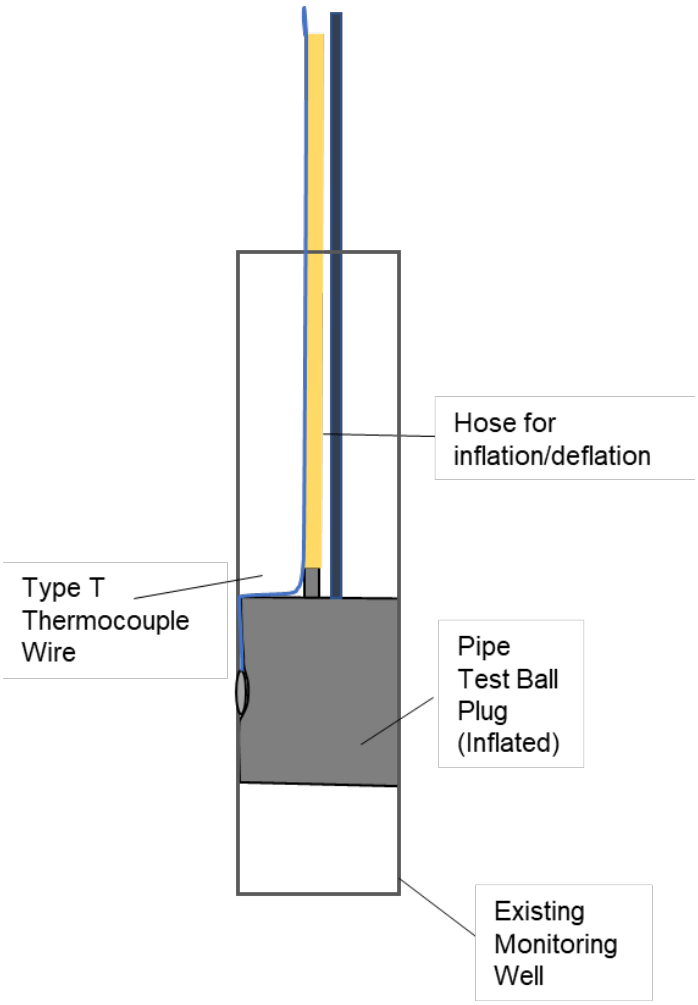

Figure 1-3: Design of Wall Temperature Method Monitoring Device (Protective Mesh Around Test Ball and Weight Not Shown).

Figure 1-4: Polyethylene Mesh Netting Used to Secure Thermocouple Tip to Test Ball

As the thermocouple, inflatable plug, and inflation/deflation hose were lowered from ground surface into the monitoring well, the assembly remained straight using a weight attached to the end of the downhole assembly.

Similar to the Well Air Temperature Method, wall temperature measurements were taken at 5-ft intervals. Measurements were taken down to no less than 5 ft above the water table. Note that the assembly using the Wall Temperature Method was not lowered into the water table in the wells to avoid cross contamination from the rubber material used in the test ball.

After evaluating the temperature readings for both methods, however, little to no difference was seen between the temperature profiles measured using the Well Air Temperature and Wall Temperature Methods (Figure 1-5). Therefore, both methods are deemed valid for performing NSZD calculations.

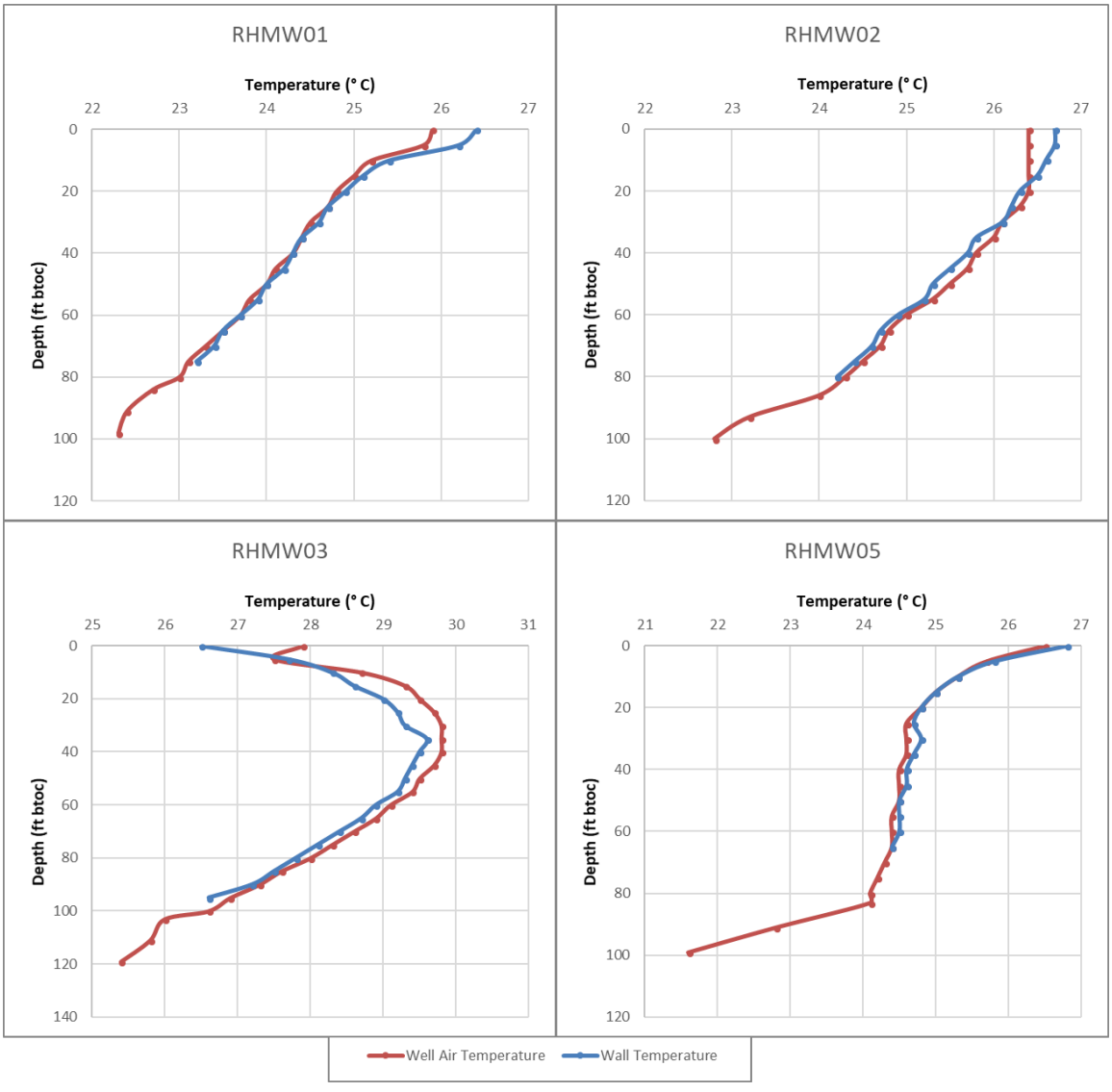

Figure 1-5: Comparison of Raw (Not Background-Corrected) Thermal Profiles for Well Air Temperature and Wall Temperature Methods

The calculations of NSZD rates were performed using both the Well Air Temperature and Wall Temperature Methods, and then those rates were averaged to arrive at final NSZD rates. For brevity, however, calculations (Sections 3.1.2 and 3.2.1) are shown using only the Well Air Temperature Method. The data for all the wells using both methods are shown on Figure 1-6 and in Attachment B.1.1. Because seasonal and daily effects cause uncertainty for the temperature measurements at the top of the raw (not background-corrected) thermal profiles (0 ft below top of casing [btoc]), the raw temperature at 0 ft btoc was assumed to be the average air temperature in Honolulu (25.4°C) (Table 1-2) for all wells for the purpose of calculating NSZD rates.

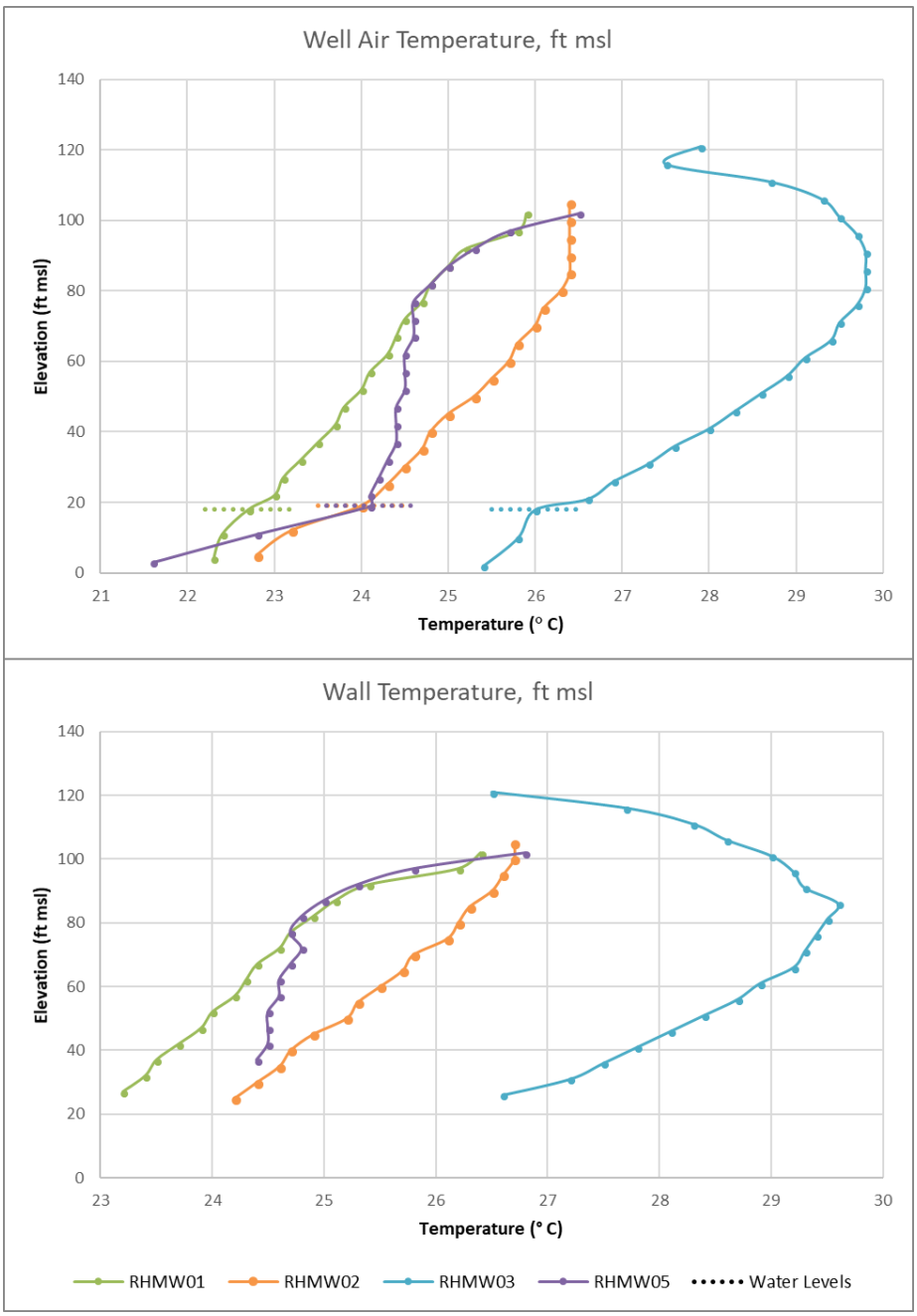

Figure 1-6: Raw (Not Background-Corrected) Thermal Profiles for Facility Wells

1.5 BACKGROUND LOCATION

RHMW05 was chosen as the background well location for net temperature calculations because it showed the least evidence of heat generation associated with biodegradation. This can easily be seen in the graph of temperature vs. depth for RHMW05 in Figure 1-5. The top approximately 20 ft btoc at RHMW05 show decreasing temperatures with depth consistent with the expected late summer/fall season shallow temperature profile. However, from approximately 20 ft btoc down to the water table, the ground temperature is fairly constant. This indicates that no heat generation is occurring within this interval, and thus no NSZD is occurring. The sharp decrease in temperature that is seen at the bottom of the graph (below 83 ft btoc) occurs once the thermocouple entered the groundwater and shows the temperature decrease that occurs within the shallow aquifer.

2. NAPL Distribution Inferred from Temperature Data

The temperature profiles were used to assess where the LNAPL is in the subsurface near each of the temperature profile monitoring wells. This was done by looking at the net (background-corrected) temperature profiles to remove the background temperature seasonal signals while preserving the temperature signal associated with LNAPL biodegradation. Net temperatures are the difference between the raw temperature recorded at each depth for a well minus the raw temperature calculated at the same depth for the background well (RHMW05) that was assumed to have no impact from LNAPL in the unsaturated zone. These net temperature profiles are shown on Figure 2-1. In the background-corrected temperature profile, the peak temperature occurs within the LNAPL biodegradation zone. The temperature gradients (i.e., change in temperature with depth) above and below this peak are used to quantify the magnitude of LNAPL biodegradation.

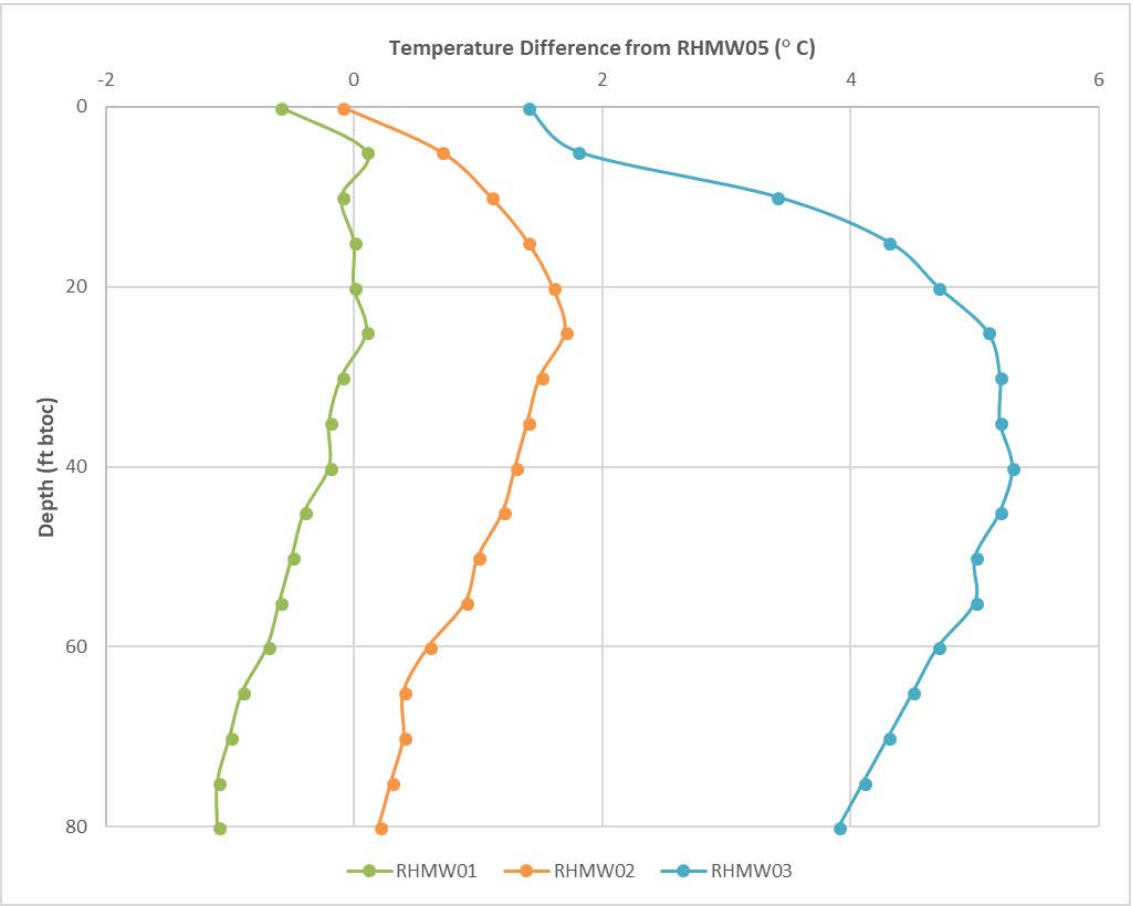

Note:

1. The net temperature profile for RHMW05 is not shown because it is the background well (i.e., temperature difference equals zero).
2. Net temperature profiles are shown for temperature data from the top of casing to 80 ft btoc, because that was the deepest measurement taken for RHMW05 above the water table.
3. The net temperature at 0 ft btoc is typically set to be 0°C for the purposes of NSZD calculations. The net temperature profiles shown on Figure 2-1 do not reflect this procedure; however, this will be assumed going forward.

Figure 2-1: Net (Background-Corrected) Temperature Profiles for Facility Wells (Well Air Temperature Method)

Using the net temperature data, the interval of biological heat generation at each well location was determined. Within the interval of heat generation, the vertical (upwards or downwards) heat flux is increasing. This is reflected in the net temperature profile through an increasing negative slope (for upward heat flux) or an increasing positive slope (for downward heat flux). Outside of the heat generation interval, the heat flux is relatively constant resulting in a relatively constant slope in the net temperature vs. elevation profile.

At many NSZD sites, anaerobic LNAPL biodegradation at or near the water table produces methane that diffuses toward the surface. This methane, in turn, is biodegraded within the unsaturated zone when it mixes with downward diffusing oxygen from the ground surface. At these sites, the bulk of the heat generation occurs in the methane degradation zone vertically removed from the LNAPL-impacted zone.

However, at the Facility, high oxygen concentrations (generally >19%) were observed at all unsaturated zone measurement locations including well headspace samples collected in close proximity to the water table and soil gas wells installed 10–30 ft below the base of the fuel tanks. In addition, no methane was detected in any unsaturated zone measurement locations (see CSM Appendix B.3). The vapor sample data indicate aerobic conditions throughout the unsaturated zone with little or no methane production/transport. Therefore, unsaturated-zone heat generation appears to be attributable to the direct aerobic biodegradation of petroleum, and the interval of heat generation is assumed to indicate the interval containing residual LNAPL.

This is highlighted on Figure 2-2, which shows the net temperature profile for each of the three wells, assuming an identical surface temperature. The intervals in each profile that have constant slopes (i.e., no LNAPL) are highlighted with dashed lines, and the areas with changing slopes (due to heat generation associated with biodegradation of petroleum) are shaded. For each temperature profile, the depth intervals with constant slopes (no LNAPL) and the depth interval with changing slope (LNAPL) were identified using professional judgement based on visual inspection of the temperature profile. These intervals are shown in Table 2-1.

Table 2-1: Inferred LNAPL-Containing Intervals Indicated by Net (Background-Corrected) Temperature Profiles from Three Facility Monitoring Wells

Monitoring Well	Top of Casing Elevation (ft msl)	Approximate Top of LNAPL (ft btoc)	Approximate Bottom of LNAPL (ft btoc)	Approximate Top of LNAPL (ft msl)	Approximate Bottom of LNAPL (ft msl)
RHMW01	102.00	20	30	82	72
RHMW02	104.60	0	30	105	75
RHMW03	120.90	10	45	111	76

Note: All three wells are installed in the lower tunnel of the Facility.

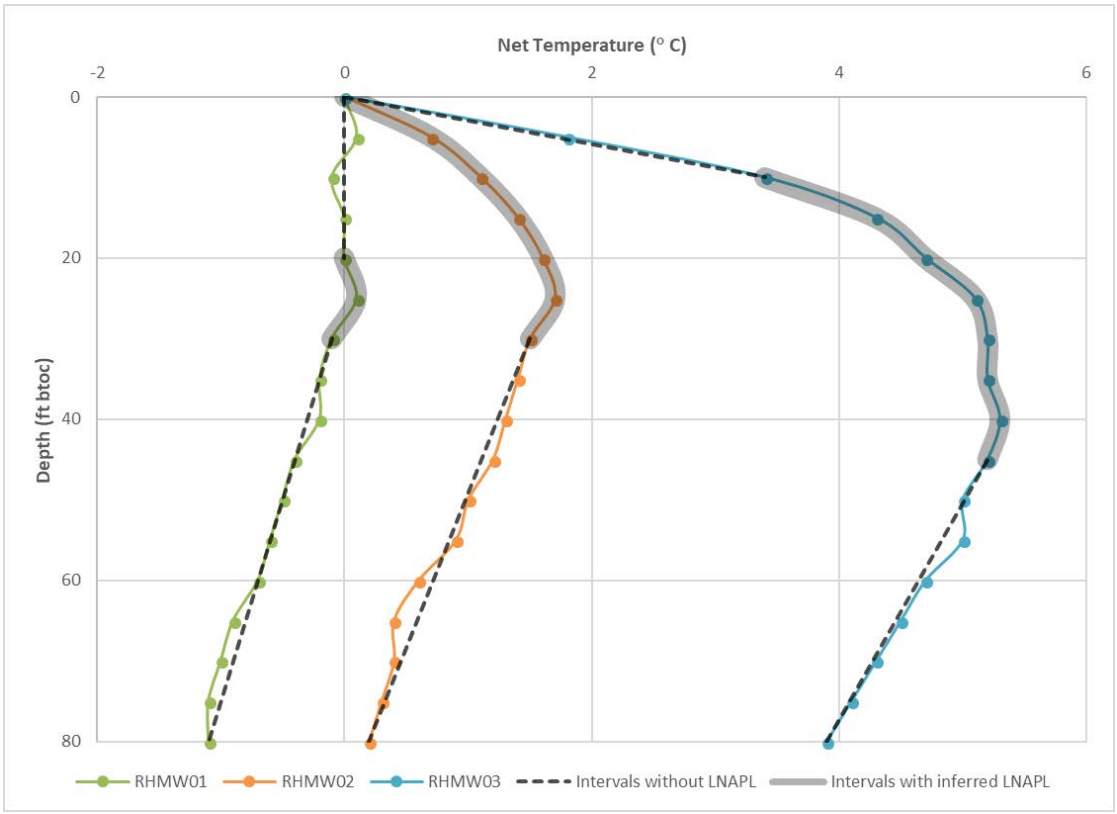

Note: Grey shading shows interval of heat generation indicating presence of LNAPL within this interval.

Figure 2-2: Net (Background-Corrected) Temperature Profiles for Facility Wells (Well Air Temperature Method)

The net temperature signal at RHMW02, measured from 0 to 30 ft below the lower tunnel floor, is consistent with a release of LNAPL from Tank 5 in 2014 that did not make it down to the water table.

As shown on Figure 2-3, the location of the LNAPL does not correspond directly with the location of the clinker zones at these locations. This indicates that other geologic media, such as thin pāhoehoe layers, may be transmitting and holding LNAPL.

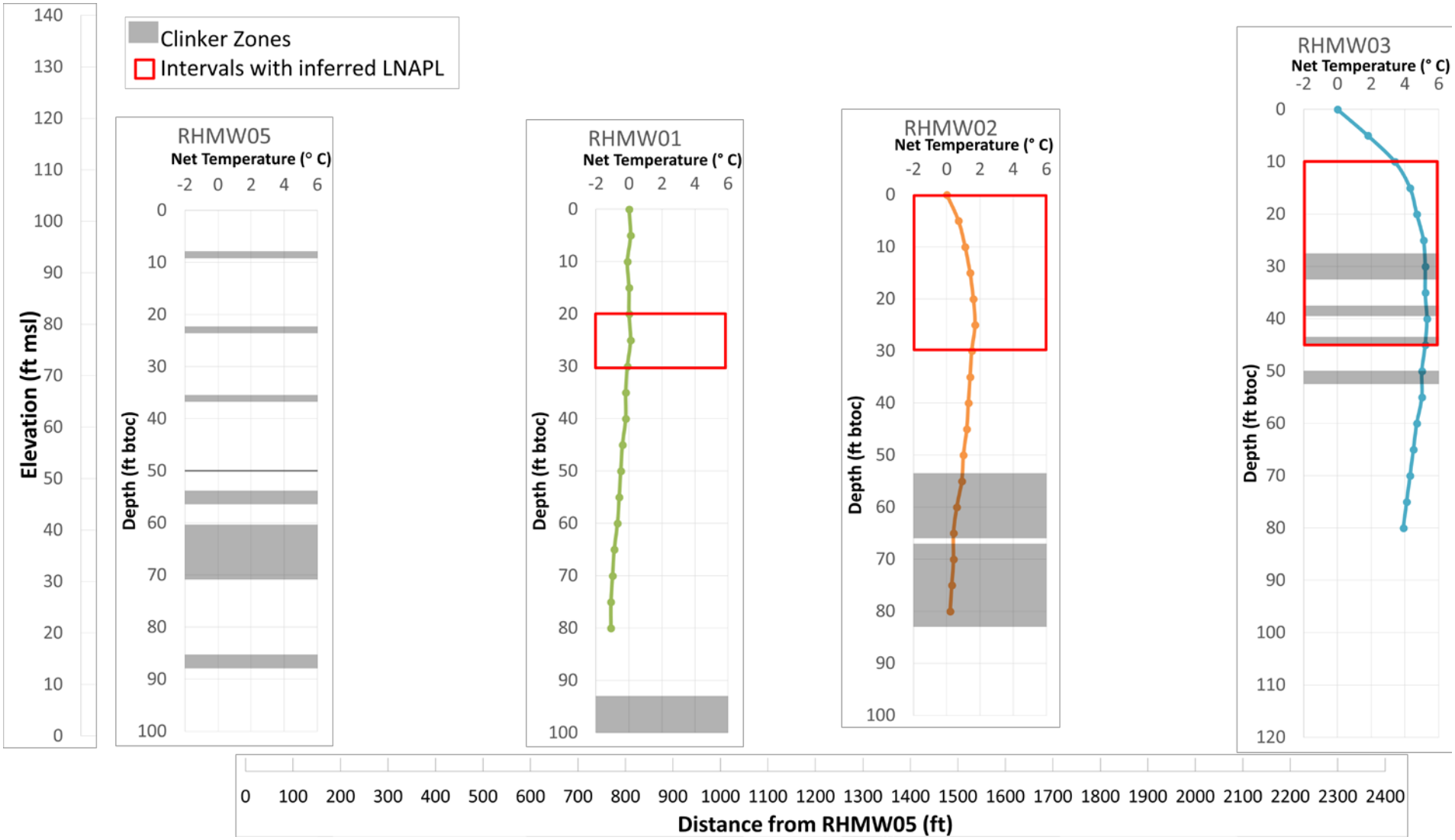

Note: Each scale shows depth below the tunnel floor, with the elevation scale (ft msl) on the far left.

Figure 2-3: Net (Background-Corrected) Temperature Profiles for Facility Wells (Well Air Temperature Method), Highlighting Clinker Zones (Identified from Boring Logs) and LNAPL Intervals

3. NSZD Rates

Three methods are used for calculating NSZD rates. Method 1 is considered the primary method and uses the net (background-corrected) temperature vertical profiles. Method 2 uses the raw (not background-corrected) thermal profiles, rather than the net (background-corrected) temperature profiles and is considered an alternative method for calculating NSZD rates. Method 3 uses differences in groundwater temperatures to calculate a bulk biodegradation rate for the entire tank farm. All three methods were employed for this assessment and are detailed in the following subsections.

3.1 CALCULATION METHOD 1: NET TEMPERATURES

3.1.1 Net Temperature Profiles

The primary method for calculating NSZD rates uses the net (background-corrected) temperature vertical profiles. These are shown on Figure 2-2, and the calculations are detailed below.

3.1.2 NSZD Calculations

To calculate the rate of NSZD occurring in the subsurface at each well, the downward heat flux going from the unsaturated zone to the water table and the upward heat flux going to the atmosphere were calculated. This was done by determining a temperature gradient from the net temperatures, then calculating a heat flux, and finally using the heat flux to calculate the NSZD rate. The temperature gradient above the heat generation interval was used to calculate the upward heat flux to the atmosphere, and the temperature gradient below the heat generation interval was used to calculate the downward heat flux to the water table. In theory, the net temperature gradients above and below the heat generation interval should be constant; however, limitations in background correction can result in small variations in the measured temperature gradient. As a result, the temperature gradient is generally estimated using as many measurement points as possible from outside the heat generation interval. Two points is the minimum number needed for this calculation, but using additional points when available provides more confidence in the result.

To obtain the value for the temperature gradient going downward toward the water table, the slope of a linear regression of all the net temperature values between 50 and 80 ft btoc (seven points) was calculated to get an average "dT/dz" value in degrees Celsius (°C) per ft. 50 ft btoc was chosen as the top of the interval for the regression because this depth is below the interval of heat generation (i.e., below the biodegradation zone), indicating a constant, and therefore reliable heat flux. 80 ft btoc was chosen as the bottom of the interval for the regression because this depth was the deepest measurement taken for RHMW05 above the water table.

The dT/dz value for the heat flux going up into the atmosphere was obtained by dividing the net temperature at 15 ft btoc by 15. This is because the average temperature at 0 ft btoc (i.e., at the base of the lower access tunnel) for all wells is assumed to have a net temperature of 0°C. A simple two-point line was used to determine this gradient, rather than a linear regression, because seasonal and daily variations in temperature within the top 30 ft can cause the slope of a regression to vary significantly from the average temperature gradient going into the atmosphere, and these variations are removed when using a simple two-point line and assuming an identical temperature at 0 ft btoc. 15 ft btoc was chosen as the bottom of the interval for the gradient calculation because it is a good compromise between having a bottom depth near the top of or above the zone of heat generation/biodegradation (for the sake of an accurate gradient) and having a bottom depth far enough below the ground surface (to remove seasonal and daily surface temperature variations). For

RHMW02 (and possibly RHMW03) the 15-ft depth is likely within the biodegradation zone. As a result, the calculated NSZD rate likely underestimates that actual degradation rate.

The dT/dz values were then multiplied by the thermal conductivity of the soil or rock (basalt in this case, with a thermal conductivity of 1.69 W/m-K) (Eppelbaum, Kutasov, and Pilchin 2014) to obtain heat fluxes into the groundwater and atmosphere in Watts per square meter (W/m^2). The calculations are shown in Table 3-1.

Table 3-1: Calculation of Bottom Heat Flux for NSZD Using Well Air Temperature Method and Net Temperatures Method

Well	Net Temp. at 50 ft btoc (°C)	Net Temp. at 80 ft btoc (°C)	Bottom dT/dz from Regression Using 7 Points (°C/ft)	Bottom Heat Flux (W/m^2)	Net Temp. at 15 ft btoc (°C)	dT/dz (°C/ft)	Top Heat Flux (W/m^2)
RHMW01	-0.5	-1.1	0.02	0.12	0.0	0.00	0.00
RHMW02	1.0	0.2	0.03	0.15	1.4	0.09	0.52
RHMW03	5.0	3.9	0.04	0.22	4.3	0.29	1.59

Note: Values are rounded. Calculations were performed using unrounded values.

These two heat fluxes were then added together, and that value converted to gallons per acre per year (gal/acre/yr) of NSZD, using the conversion from W/m^2 to gal/acre/yr, as calculated in Table 3-2.

Table 3-2: Calculation of Conversion from W/m^2 to gal/acre/yr of NSZD

Parameter	Value	Reasoning
Conversion from W to J/sec	1 J/sec-W	Known
Conversion from sec to yrs	3.2×10^7 sec/yr	Known
Conversion from m^2 to ac	4,047 m^2/ac	Known
Heat of Combustion of Jet Fuel	4.7×10^7 J/kg	(Martínez 2017)
Density of Jet Fuel	800 kg/m^3	(Martínez 2017)
Conversion from m^3 to L	1,000 L/m^3	Known
Conversion from L to gal	0.26 gal/L	Known
Conversion from W/m^2 to gal/acre/yr	898 (gal/acre/yr)/(W/m^2)	Calculation

Note: Values are rounded. Calculations were performed using unrounded values.

J joule
gal gallon
kg kilogram
L liter
m^3 cubic meter
yr year

Following this process, the following NSZD rates were calculated (Table 3-3 and Table 3-4):

Table 3-3: Net Temperatures Method NSZD Rates for Facility Wells (Well Air Temperature Method)

Well	Total Heat Flux (W/m^2)	NSZD Rate (gal/acre/yr)
RHMW01	0.12	110
RHMW02	0.67	600
RHMW03	1.81	1,622

Note: Values are rounded. Calculations were performed using unrounded values.

Table 3-4: Net Temperature NSZD Rates for Facility Wells (Average of Well Air Temperature and Wall Temperature Methods)

Well	NSZD Rate from Well Air Temperature Method (gal/acre/yr)	NSZD Rate from Wall Temperature Method (gal/acre/yr)	Average NSZD Rate (gal/acre/yr)
RHMW01	110	173	**141**
RHMW02	600	677	**638**
RHMW03	1,622	1,374	**1,498**

Note: Values are rounded. Calculations were performed using unrounded values.

Assuming the three NSZD measurements are representative samples of NSZD within the tank farm, an average NSZD rate for the entire tank farm was calculated in gallons per year (gal/yr). Taking an average of all the NSZD rates (759 gal/acre/yr) and multiplying this by the area encompassed by the tank farm (13.1 acres; Figure 3-1), the total NSZD rate comes to 9,935 gal/year or about 10,000 gal/yr.

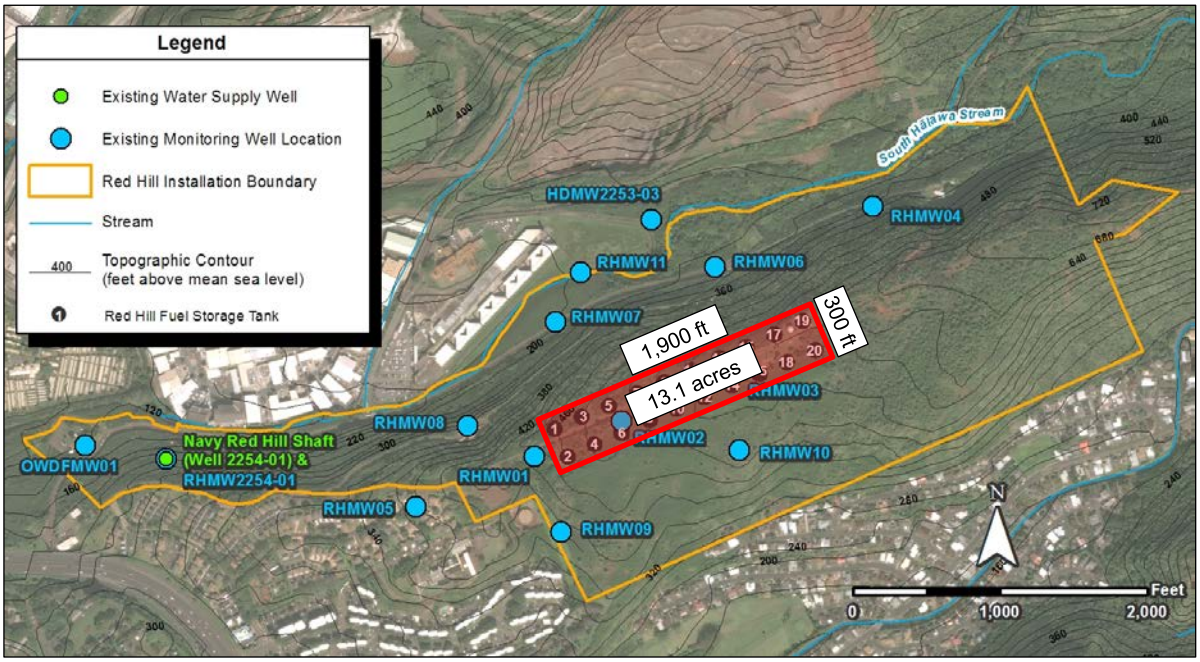

Figure 3-1: Area Encompassed by Tank Farm

3.2 CALCULATION METHOD 2: THERMAL PROFILES

The accuracy of NSZD rates calculated using Calculation Method 1 (i.e., with background correction) depends on the suitability of the background location used for the background correction. If the temperature profile at the background location is not representative of the LNAPL-impacted locations, then the use of this location for background correct can result in an over-estimation or under-estimation of the true NSZD rates. An alternative method for calculating NSZD rates is to use the raw (non-background-corrected) thermal profiles, rather than the net (background-corrected) temperature profiles. In this method, it is assumed that enough heat flux is going into the groundwater and into the atmosphere that it can be seen in the raw thermal profiles. This alternative calculation method was done to evaluate the accuracy the Net Temperatures Method approach. Attainment of similar NSZD rates using the two methods provides increased confidence in the accuracy of both methods.

To correct for seasonal variations in temperature, however, the temperature values from the raw thermal profiles were altered by the amount that a soil column would be expected to vary from average Honolulu air temperatures as calculated by Nofziger and Wu (2003) using the Hillel (1982) formula. These corrected profiles are shown on Figure 3-2.

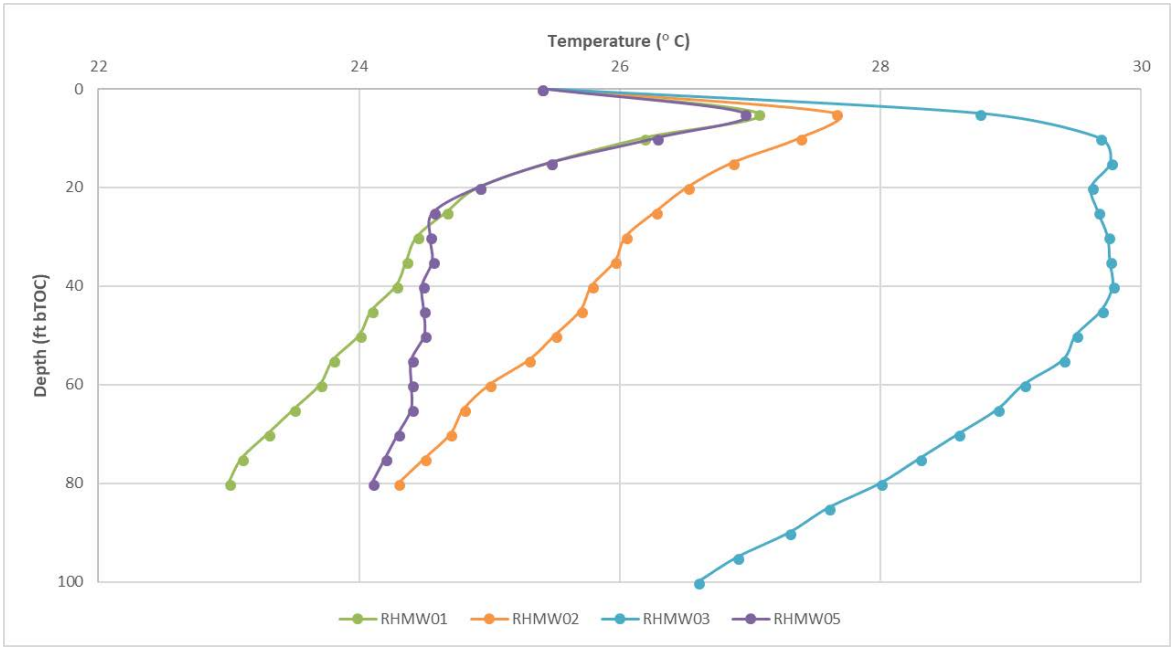

Figure 3-2: Hillel-Corrected Raw (Not Background-Corrected) Thermal Profiles for Facility Wells (Well Air Temperature Method)

Because seasonal and daily effects cause uncertainty for the temperature measurements at the top of subsurface raw thermal profiles, and the tunnel ventilation system likely introduces a seasonal temperature signal to the basalt in the Facility, the raw temperature at 0 ft btoc was assumed to be the average annual air temperature in Honolulu (25.4°C) (Table 1-2) for all wells for the purpose of calculating NSZD rates.

3.2.1 NSZD Calculations

To calculate the rate of NSZD occurring in the subsurface at each well, after correcting the profiles using the Hillel (1982) formula, the downward heat flux going from the unsaturated zone to the water table and the upward heat flux going to the atmosphere were calculated. This was done by determining a temperature gradient from the raw thermal profiles, and then calculating a heat flux and thus a NSZD rate. The temperature gradient above the heat generation interval was used to calculate the upward heat flux to the atmosphere, and the temperature gradient below the heat generation interval was used to calculate the downward heat flux to the water table.

The dT/dz values for the Thermal Profiles Method were calculated similarly as for the Net Temperatures Method. For the bottom gradient, the slope of a linear regression of all the temperature values between 50 ft btoc and the temperature directly above the water table (DAWT) (seven or eleven points, depending on the well) was calculated to get an average "dT/dz" value in degrees Celsius (°C) per foot. 50 ft btoc was chosen as the top of the interval for the regression because this depth is below the interval of heat generation (i.e., below the biodegradation zone), indicating a relatively constant, and therefore reliable, heat flux. The value DAWT was chosen as the bottom of the interval for the regression, rather than 80 ft btoc, because RHMW03 was a deeper well than the other wells.

For the upper gradient, the dT/dz value for the heat flux going into the atmosphere was obtained by subtracting the temperature at 15 ft btoc by the average air temperature in Honolulu (25.4°C), then dividing by 15. This is because, on an average basis, the temperature at 0 ft btoc (i.e., at the base of the lower tunnel) for all wells is assumed to be the same as the average air temperature in Honolulu, so this provided a way to calculate the average heat flux. A simple two-point line was used in this case, rather than a linear regression, because seasonal and daily variations in temperature within the top 30 ft can cause the slope of a regression to vary significantly from the average temperature gradient going into the atmosphere, and these variations are removed when using a simply two-point line and assuming an identical temperature at 0 ft btoc. 15 ft btoc was chosen as the bottom of the interval for the gradient calculation because it represented a good compromise between having a bottom depth near the top of or above the zone of biodegradation (for the sake of an accurate gradient) and having a bottom depth far enough below the ground surface (to remove seasonal and daily surface temperature variations). For RHMW02 (and possibly RHMW03), the 15-ft depth is likely within the biodegradation zone. As a result, the calculated NSZD rate likely underestimates that actual degradation rate.

Both lower and upper dT/dz values were then multiplied by the thermal conductivity of the soil (1.69 W/m-K) (Eppelbaum, Kutasov, and Pilchin 2014) to obtain heat fluxes into the groundwater and atmosphere in W/m^2. The calculations are shown in Table 3-5.

Table 3-5: Calculation of Bottom Heat Flux for NSZD Using Well Air Temperature Method and Thermal Profiles Method

Well	Temp. at 50 ft btoc (°C)	Temp. DAWT (°C)	dT/dz from Regression (°C/ft) [Number of Points Used]	Bottom Heat Flux (W/m^2)	Temp. at 15 ft btoc (°C)	Average Air Temp. in Honolulu (°C)	dT/dz (°C/ft)	Top Heat Flux (W/m^2)
RHMW01	24.0	23.0	0.03 [7]	0.19	25.5	25.4	0.01	0.04
RHMW02	25.5	24.3	0.04 [7]	0.22	26.9	25.4	0.10	0.56
RHMW03	29.5	26.6	0.05 [11]	0.33	29.8	25.4	0.29	1.63
RHMW05	24.5	24.1	0.01 [7]	0.07	25.5	25.4	0.01	0.04

Note: Values are rounded. Calculations were performed using unrounded values.

These two heat fluxes were then added together, and that value converted to gal/acre/yr of NSZD, using the conversion from Watts/m^2 to gallons/acre/year, as calculated in Table 3-2. The calculated NSZD rates are shown in Table 3-6 and Table 3-7.

Table 3-6: Thermal Profiles Method NSZD Rates for Facility Wells (Well Air Temperature Method)

Well	Net Heat Flux (Bottom – Top) (W/m^2)	NSZD Rate (gal/acre/yr)
RHMW01	0.23	210
RHMW02	0.78	700
RHMW03	1.97	1,766
RHMW05	0.11	100

Note: Values are rounded. Calculations were performed using unrounded values.

Table 3-7: Thermal Profiles Method NSZD Rates for Facility Wells (Average of Well Air Temperature and Wall Temperature Methods)

Well	NSZD Rate from Well Air Temperature Method (gal/acre/year)	NSZD Rate from Wall Temperature Method (gal/acre/year)	Average NSZD rate (gal/acre/yr)
RHMW01	210	235	**223**
RHMW02	700	722	**711**
RHMW03	1,766	1,525	**1,646**
RHMW05	100	69	**85**

Note: Values are rounded. Calculations were performed using unrounded values.

Assuming NSZD is happening only underneath the tank farm, an average NSZD rate was calculated in gal/yr. Note that it is assumed that all NSZD is occurring underneath the tank farm because there is no evidence of extensive migration out of the tank farm area. This would not necessarily be the case for a large, sudden release. Taking an average of the NSZD rates for RHMW01, RHMW02, and RHMW03 (ignoring the background well) gave a value of 860 gal/acre/yr. This value was multiplied by the area encompassed by the tank farm (13.1 acres; Figure 3-1), yielding a total NSZD rate of 11,250 gal/year, fairly close to that calculated using the Net Temperatures Method (Section 3.1.2).

3.3 AGREEMENT BETWEEN METHOD 1 AND METHOD 2 NSZD RATES

NSZD rates were calculated using two different calculation methods: Method 1 (Net Temperatures) and Method 2 (Thermal Profiles):

1. RHMW05 is the farthest of the four monitoring wells from the tank farm. For Method 1, RHMW05 was assumed to be unaffected by LNAPL and was used as the background location to generate net temperature profiles for the remaining locations. For Method 2 (which does not require a background location), the temperature profile for RHMW05 was processed using the same Method 2 calculation procedures applied to the other locations. The very low NSZD rate calculated for RHMW05 using Method 2 (85 gal/acre/yr) is likely an artifact of small measurement errors or natural temperature variations at this location. The extremely low NSZD rate measured at RHMW05 using Method 2 confirms it was a suitable well to serve as a background well for Method 1.
2. At the three locations within the tank area (RHMW01, RHMW02, and RHMW03), the NSZD rates calculated using the two methods were similar, providing increased confidence in the accuracy of the results (i.e., the resulting rates are not an artifact of assumptions associated with a specific calculation method). For the three locations, the average difference in NSZD rates for the two methods was only 100 gal/acre/year). For the two locations with the highest NSZD rates (RHMW02 and RHMW03), the difference in rates between the two methods was only 10%.

3.4 METHOD 3: GROUNDWATER TEMPERATURES

The groundwater temperature in the monitoring wells within the tank area (i.e., RHMW02 and RHMW03) is elevated relative to the background well (RHMW05). Elevated groundwater temperatures have been observed at other NSZD sites (e.g., Kimmel and Braids 1980). To evaluate whether the downward convection of heat associated with the observed vadose zone biodegradation is consistent with the observed increase in groundwater temperature within this area, a third method for calculating NSZD was conducted based on the heat required to heat the groundwater flowing through this area. In this method, the difference in groundwater temperatures was measured between RHMW01, RHMW02, and RHMW03 and RHMW05. The reason for this temperature difference is likely due to NSZD in the unsaturated zone, which is causing a heat flux into the groundwater that is increasing the water temperature above the temperature of the background groundwater. This method yields a partial NSZD rate that accounts only for the downward heat flux from the unsaturated zone to the groundwater. It does not account for upward heat loss from the unsaturated zone to the atmosphere. However, the results from this method are comparable to the downward heat flux portion of the unsaturated temperate profile NSZD methods.

The calculation was conducted for a range of elevated groundwater temperatures based on (1) the difference between the temperature as RHMW03 (the well with the highest temperature) and RHMW05 (the background well) and (2) the difference between the average temperature of the groundwater for RHMW01, RHMW02, and RHMW03 vs. RHMW05. The groundwater temperatures are shown in Table 3-8. The average temperature of the groundwater for RHMW01 is approximately the same temperature as the average temperature of the groundwater for RHMW05 (cooler by approximately 0.3°C), which is in line with the vadose zone temperature profile at RHMW01 that indicates only minor amounts of NSZD at this location. The average temperature of the groundwater for the other two wells had higher temperatures than RHMW05.

Table 3-8: Water Temperatures at RHMW03 and RHMW05

Well	Temp. at Top of Water Column (°C)	Temp. at Middle of Water Column (°C)	Temp. at Bottom of Water Column (°C)	Average Water Temp. (°C)
RHMW01	22.7	22.4	22.3	22.5
RHMW02	24.0	23.2	22.8	23.3
RHMW03	26.0	25.8	25.4	25.7
			Average of RHMW01, RHMW02, & RHMW03	23.8
RHMW05	24.1	22.8	21.6	22.8
			Difference	1.0 – 2.9

Note: The temperature difference range is based on (1) the difference between RHMW03 and RHMW05 and (2) the difference of the average of RHMW01, RHMW02, and RHMW03 vs. RHMW05.

Also, the mass of groundwater that would be affected by this temperature change was calculated. Note that a range of seepage velocities was used based on preliminary particle tracking model results conducted for the investigation's interim groundwater flow modeling effort reflecting the range between base model and the base model with clinker zone. This calculation is shown in Table 3-9.

Table 3-9: Calculation of Mass of Water Flow from RHMW03 to RHMW05

Parameter	Value	Reasoning
Width of Groundwater Flow	300 ft	Width of tank farm
Thickness of Heated Zone	15 ft	Screened intervals
Darcy Velocity	0.496 – 1.38 ft/day	Based on interim groundwater flow modeling
Volume of Groundwater Flow Per Year	814,680 – 2.3×10^6 ft^3/yr 2.3×10^7 – 6.4×10^7 L/yr	Calculation (300 ft × 15 ft x 0.496 ft/day × 365 days/yr; 300 ft × 15 ft × 1.38 ft/day × 365 days/yr) (1 ft^3 = 28.3 L)
Density of Water	1 kg/L	Known
Mass of Groundwater Flow Per Year	2.3×10^7 – 6.4×10^7 kg/yr 2.3×10^{10} – 6.4×10^{10} g/yr	Calculation (2.3×10^7 L/yr × 1 kg/L; 6.4×10^7 L/yr × 1 kg/L) (1 kg = 1,000 g)

Note: Values are rounded. Calculations were performed using unrounded values.

Using these data, a rate of biodegradation in the groundwater (in gallons of fuel per year) was calculated, as shown in Table 3-10.

Table 3-10: Calculation of Biodegradation in Groundwater

Parameter	Value	Reasoning
Heat Capacity of Water	1 cal/g/C	Known
Total Heat Generated (1.0°C difference)	2.3×10^{10} – 6.5×10^{10} cal/year 97,536 – 271,370 MJ/yr	Calculation ($2.3x10^{10}$ g/yr × 1.0°C × 1 cal/g/°C; $6.5x10^{10}$ g/yr × 1.0°C × 1 cal/g/°C) (1 MJ = 239,006 cal)
Total Heat Generated (2.9°C difference)	6.7×10^{10} – 1.9×10^{11} cal/year 279,746 – 778,324 MJ/yr	Calculation (2.3×10^{10} g/yr × 2.9°C × 1 cal/g/°C; $6.4x10^{10}$ g/yr × 2.9°C × 1 cal/g/°C) (1 MJ = 239,006 cal)
Heat Combustion of Jet Fuel	47 MJ/kg	Martinez (2017)
Amount of Biodegradation (1.0°C difference)	2,075 – 5,774 kg/yr **686 – 1,909 gal/yr**	Calculation (97,536 MJ/yr / 47 MJ/kg); 271,370 MJ/yr / 47 MJ/kg) (1 kg Jet Fuel = 0.33 gal Jet Fuel)
Amount of Biodegradation (2.9°C difference)	5,952 – 16,560kg/yr **1,968 – 5,476 gal/yr**	Calculation (279,746 MJ/yr / 47 MJ/kg); 778,324 MJ/yr / 47 MJ/kg) (1 kg Jet Fuel = 0.33 gal Jet Fuel)

Note: Values are rounded. Calculations were performed using unrounded values.
cal/g/°C calorie per gram per degrees Celsius

Therefore, the heat flux going into the groundwater from NSZD in the unsaturated zone is coming from the degradation of approximately 700 to 5,500 gallons of fuel per year. Comparing this to the average Bottom NSZD rate (the only heat flux that would go into the groundwater) from the Net Temperatures and Thermal Profiles Methods (average for each method), the two average Bottom NSZD rates are within this range, providing additional confidence that the elevated groundwater temperatures in these wells are attributable to the vadose zone NSZD (Table 3-11).

Table 3-11: The Bottom NSZD Rate (i.e., Associated with Downward Heat Transfer) for the Three Calculation Methods

Method	Bottom NSZD Rate (gal/yr)
Method 1: Net Temperatures	2,000 gal/yr
Method 2: Thermal Profiles	2,300 gal/yr
Method 3: Groundwater Temperatures	700 – 5,500 gal/yr

Note: Values are rounded. Calculations were performed using unrounded values.

In conclusion, the Groundwater Temperatures Method, an independent method that did not rely on vertical temperature profiles in the unsaturated zone, yielded results that match the corresponding part of the NSZD calculations from the Net Temperatures and Thermal Profiles Methods (i.e., downward heat flux parts), thereby increasing the confidence in those methods.

4. Conclusions

Two methods were used in the field to measure vertical temperature profiles in wells in the Facility with both producing similar data. These data were used to determine the general vertical location of LNAPL at each location (shown in Table 2-1) and the corresponding NSZD rates for that LNAPL.

The NSZD rates were calculated using three different methods: 1: Net Temperatures, 2: Thermal Profiles, and 3: Groundwater Temperatures. Method 3 (Groundwater Temperature) accounts for only downward heat flux from the bottom of the LNAPL zone to groundwater. The Method 3 results serve to confirm the reasonableness of Method 1 and Method 2 results, but Method 3 does not provide an estimate of the total NSZD rates at the Facility. Despite some differences between these methods, each produced fairly consistent NSZD rates among the three locations. Total NSZD rates in units of gal/yr are shown in Table 4-1.

Table 4-1: Summary of Total NSZD Rates from the Tank Farm

Well	Net Temperatures Method	Thermal Profiles Method	Groundwater Temperatures Method
Bottom NSZD Rate (gal/yr)			
RHMW01	1,600	2,200	N/A
RHMW02	2,100	2,500	N/A
RHMW03	2,500	3,900	N/A
Average	2,000	2,800	670 – 5,500
Top NSZD Rate (gal/yr)			
RHMW01	220	730	N/A
RHMW02	6,300	6,800	N/A
RHMW03	17,000	18,000	N/A
Average	7,900	8,400	N/A
Total NSZD Rate (gal/yr)			
RHMW01	1,900	2,900	N/A
RHMW02	8,400	9,300	N/A
RHMW03	20,000	22,000	N/A
Average	**9,900**	**11,000**	N/A

Note: Values are rounded. Calculations were performed using unrounded values.
N/A not applicable

The NSZD rates using the Net Temperatures Method for calculation and averaged results from the Well Air Temperature and the Wall Temperature Methods (see Table 3-4) are shown below. These are considered the most accurate calculations for NSZD rates of all the methods.

- RHMW01: 140 gal/acre/yr of NSZD
- RHMW02: 640 gal/acre/yr of NSZD
- RHMW03: 1,500 gal/acre/yr of NSZD

The calculated NSZD rates at the three locations are consistent with the understanding of historical LNAPL releases at the Facility:

1. RHMW01 is the farthest of the three monitoring wells from the tank farm, and therefore was expected to be the location least impacted by LNAPL releases. The low NSZD rate (140 gal/acre/yr) is consistent with limited LNAPL impacts.
2. RHMW02 has a relatively high NSZD rate (640 gal/acre/yr), which is expected due a known release of 27,000 gallons of fuel that occurred in early 2014 from Tank 5.
3. RHMW03 has the highest NSZD rate (1,500 gal/acre/yr). This is consistent with results of the 1998–2002 angle borings investigation (Figure 4-1) that indicated historical releases from three adjacent tanks; Tank 13, Tank 14, and Tank 16 (DON 1999, 2002; see main CSM document, Section 4.1).

The Thermal NSZD analysis confirms that biodegradation of LNAPL in the vadose zone is an important NSZD process at the Facility. In addition, the downward heat flux associated with this NSZD is sufficient to explain the elevated groundwater temperatures observed in RHMW03 and RHMW02.

As part of the concurrently published interim environmental analysis document (DON 2018), the calculated NSZD rate will be used to evaluate the LNAPL assimilative capacity at the Facility. This assimilative capacity will be used for the evaluation of hypothetical future release scenarios. To establish a range of values for the Total NSZD at the tank farm, the standard deviation of the total NSZD rate of all three wells using the Net Temperatures Method was calculated. This standard deviation is 7,300 gal/yr.

In summary, the best estimate for the total NSZD rate at the tank farm is 9,900 gallons per year, with a likely range of 2,600 to 17,200 gallons per year.

Angle Boring B-05 [a] (15°)		
Elevation (ft msl)	Observation	Date
104.01	Slight odor	1/24/2001
102.80	Odor	
101.43	Slight odor	

Angle Boring B-03 [a] (15°)		
Elevation (ft msl)	Observation	Date
102.72	Slight odor	1/31/2001
100.81	Slight odor	
100.68	Slight odor	
91.62	Slight odor	

Angle Boring B-01 [a] (15°)		
Elevation (ft msl)	Observation	Date
102.66	Odor	2/8/2001
102.14	Sheen	
102.01	Odor	
100.77	Strong odor	
100.59	Sheen	
100.38	Odor	
88.27	Odor	
87.23	Sheen	
86.95	Sheen and strong odor	
85.63	Strong odor	
84.26	Sheen and strong odor	
82.96	Odor	

Sheen was observed in drill water, but depth was not specified.

Angle Boring B-07 [a] (15°)		
Elevation (ft msl)	Observation	Date
113.96	Odor	1/17/2001
113.44	Slight odor	
111.71	Slight odor	
107.26	Odor	
105.65	Odor	
103.48	Odor	
89.86	Odor	
87.35	Odor	
86.06	Odor	
84.77	Odor	
83.42	Odor	
82.90	Odor	
81.56	Odor	

Angle Boring B-11 [a] (15°)		
Elevation (ft msl)	Observation	Date
117.98	Slight odor	12/15/2000
116.95	Strong odor	
116.56	Strong odor	
116.43	Strong odor	
116.07	Slight odor	
115.70	Strong odor	
115.52	Sheen and Strong odor	
115.31	Strong odor	
112.73	Slight odor	
108.09	Slight odor	
106.77	Strong odor	
101.75	Strong odor	
96.91	Strong odor	
94.82	Strong odor	
93.42	Strong odor	
92.59	Strong odor	

Angle Boring B-09A [a,b] (11°)		
113.9 to 113.7	Saturated	12/16/1998

Angle Boring B-09B [a,b] (11°)		
Elevation (ft msl)	Observation	Date
101.1 to 101.0	Staining	12/16/1998
100.2 to 100.1	Staining	
100.0 to 99.9	Staining	

Angle Boring B-09C [a,b] (11°)		
101.2	Staining	12/16/1998

Angle Boring B-13 [a] (15°)		
Elevation (ft msl)	Observation	Date
121.95	Odor	12/8/2000
120.92	Strong odor	
120.50	Strong odor	
119.98	Strong odor	
119.88	Sheen	

Sheen was observed in drill water at a depth of 121.95 ft msl.

Angle Boring B-19 [a] (13°)		
Elevation (ft msl)	Observation	Date
124.66	Odor	11/22/2000
123.78	Odor	
122.12	Slight odor	
121.85	Slight odor	
120.12	Slight odor	
119.60	Strong odor	

Angle Boring B-20 [a] (15°)		
Elevation (ft msl)	Observation	Date
133.54	Strong odor	3/2/2001
131.60	Strong odor	

Angle Boring B-18 [a] (13°)		
Elevation (ft msl)	Observation	Date
120.22	Slight odor	11/2/2000

Angle Boring B-16A [a,b] (11°)		
Elevation (ft msl)	Observation	Date
112.7 to 112.5	Saturation Stains	12/14/1998
111.3	Saturated	
111.1	Staining	
110.2	Saturated with Staining	
109.7	Heavy staining, slude layer	
109.3	Staining, slude layer	
108.8	Staining	
107.9	Saturation point	
107.1 to 106.6	Saturated	
106.3 to 105.9	Saturated	

Angle Boring B-16B [a,b] (11°)		
122.60	Saturated point	12/14/1998
115.7 to 115.2	Intermittent saturation	
114.2 to 113.0	Intermittent staining	
113.0 to 112.8	Heavy staining and discoloration	
112.8 to 112.4	Heavy staining	
111.8 to 111.0	Evident staining and saturation	

Angle Boring B-16C [a,b] (11°)		
119.8 to 118.9	Light discoloration	12/15/1998
115.3 to 115.2	Staining	
115.1 to 114.9	Saturated	
114.4 to 113.9	Saturation visible	
113.9 to 113.0	Staining and Saturation	
111.40	Saturation point	

Angle Boring B-02 [a] (15°)		
Elevation (ft msl)	Observation	Date
102.31	Slight odor	2/5/2001
79.74	Slight odor	

Angle Boring B-04 [a] (15°)		
Elevation (ft msl)	Observation	Date
101.97	Odor	1/29/2001
100.81	Odor	
100.50	Odor	
99.72	Slight odor	
98.58	Odor	

Angle Boring B-06 [a] (15°)		
Elevation (ft msl)	Observation	Date
105.68	Strong odor	1/19/2001
105.16	Strong odor	
103.87	Odor	
102.76	Slight odor	
101.38	Odor	
98.92	Strong odor	
97.68	Odor	
96.03	Slight odor	
94.65	Odor	
93.54	Odor	
92.14	Odor	

Angle Boring B-08 [a] (15°)		
Elevation (ft msl)	Observation	Date
113.67	Odor	1/15/2001
113.13	Odor	

Angle Boring B-12 [a] (15°)		
Elevation (ft msl)	Observation	Date
116.52	Slight odor	12/12/2000
116.05	Strong odor	
115.74	Slight odor	
109.51	Strong odor	
108.21	Strong odor	
106.92	Slight odor	
105.65	Slight odor	
102.96	Strong odor	
101.61	Slight odor	
89.78	Slight odor	
88.46	Odor	
87.12	Slight odor	

Angle Boring B-14 [a] (15°)		
Elevation (ft msl)	Observation	Date
98.15	Heavy staining on core	12/5/2000
95.51	Hydrocarbon odor and stain	
94.16	Hydrocarbon odor and stain	
92.81	Hydrocarbon odor and stain	
91.47	Hydrocarbon odor and sheen	
90.20	Hydrocarbon odor and sheen	
88.83	Hydrocarbon odor and sheen	

HDMW2253 03
RHMW04
RHMW11
RHMW06
RHMW07
RHMW03
RHMW08
RHMW02
RHMW10
RHMW01
RHMW05
RHMW09
B-01
B-02
B-03
B-04
B-05
B-06
B-07
B-08
B-09
B-10
B-11
B-12
B-13
B-14
B-15
B-17
B-18
B-19
B-20
B 09A
B 09B
B 09C
B 16A
B 16B
B 16C

Key Map

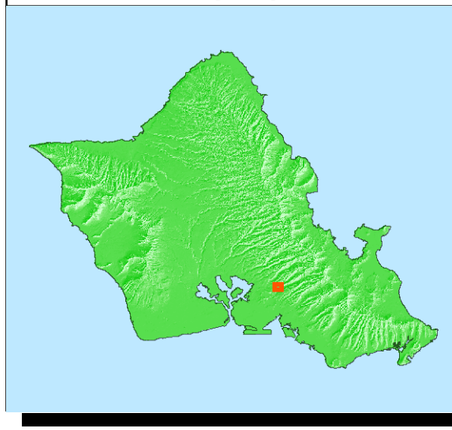

Legend

- Red Hill Fuel Storage Tank- Fuel Odor Noted in Boring Log
- Red Hill Fuel Storage Tank- Sheen or Staining Observed in Boring Log
- Red Hill Fuel Storage Tank- No Evidence of Contamination Observed in Boring Log
- Groundwater Monitoring Well- No evidence of contamination observed in boring log
- Angle Boring
- Stream
- Red Hill Facility Boundary
- Groundwater Model Area

Notes

1. Map projection: NAD 1983 UTM Zone 4N
2. DigitalGlobe, Inc. (DG) and NRCS. Publication_Date: 2015
3. References:
   a. Boring logs from DON 2002. Red Hill Bulk Fuel Storage Facility Investigation Report (Final) for Fleet Industrial Supply Center (FISC), Oahu, Hawaii. Prepared by AMEC Earth and Environmental, Inc. for NAVFAC Pacific. August.
   b. Boring logs from DON 1999. Initial Phase II Site Characterization Report, Fleet Industrial Supply Center Bulk Fuel Storage Facility at Red Hill. Prepared by Ogden Environmental and Energy Services Co., Inc. for NAVFAC Pacific. March.

* Elevations presented as "~100" are approximations made based on boring logs and notes in the text.

N

0 200 400 800 Feet

Figure 4-1
Soil Contamination at Tank Farm Observed During 1998–2002 Environmental Investigation
Red Hill Bulk Fuel Storage Facility
JBPHH, O'ahu, Hawai'i

\\Honolulu.na.aecomnet.com\Honolulu\Projects\NAVFAC PAC\CLEAN V\60571032_CTO18F0126\900-Work\920 GIS\02_Maps\CSM\FigAppB1_4-1_Red Hill_Soil Contamination.mxd 2018-06-19

5. References

Department of the Navy (DON). 1999. *Initial Phase II Site Characterization Report, Fleet Industrial Supply Center Bulk Fuel Storage Facility at Red Hill*. Prepared by Ogden Environmental and Energy Services Co., Inc., Honolulu, HI. Pearl Harbor, HI: Pacific Division, Naval Facilities Engineering Command. March.

———. 2002. *Red Hill Bulk Fuel Storage Facility Investigation Report (Final) for Fleet Industrial Supply Center (FISC), Oahu, Hawaii*. Prepared by AMEC Earth & Environmental, Inc., Huntsville, AL. Pearl Harbor, HI: Pacific Division, Naval Facilities Engineering Command. August.

———. 2017. *Existing Data Summary and Evaluation Report for Groundwater Flow and Contaminant Fate and Transport Modeling, Red Hill Bulk Fuel Storage Facility, Joint Base Pearl Harbor-Hickam, O'ahu, Hawai'i; March 5, 2017, Revision 00*. Prepared by AECOM Technical Services, Inc., Honolulu, HI. Prepared for Defense Logistics Agency Energy, Fort Belvoir, VA, under Naval Facilities Engineering Command, Hawaii, JBPHH HI.

———. 2018. *Groundwater Protection and Evaluation Considerations for the Red Hill Bulk Fuel Storage Facility, Joint Base Pearl Harbor-Hickam, O'ahu, Hawai'i; July 27, 2018, Revision 00*. AECOM Technical Services, Inc., Honolulu, HI. Prepared for Defense Logistics Agency Energy, Fort Belvoir, VA, under Naval Facilities Engineering Command, Hawaii, JBPHH HI.

Eppelbaum, L., I. Kutasov, and A. Pilchin. 2014. *Applied Geothermics*. 1st ed. Springer-Verlag Berlin Heidelberg.

Hillel, D. 1982. *Introduction to Soil Physics*. San Diego, CA: Academic Press.

Kimmel, G. E., and O. C. Braids. 1980. *Leachate Plumes in Ground Water From Babylon and Islip Landfills, Long Island, New York*. Professional Paper 1085. Prepared in cooperation with the Suffolk County Department of Environmental Control: U.S. Geological Survey.

Martínez, I. 2017. *Fuel Data for Combustion with Air*. Departamento de Motopropulsión y Termofluidodinámica, Universidad Politecnica, Madrid, Spain. http://webserver.dmt.upm.es/~isidoro/dat1/eCombus.pdf.

Nofziger, D. L., and J. Wu. 2003. *Soil Temperature Changes with Time and Depth*. http://soilphysics.okstate.edu/software/SoilTemperature/document.pdf.

U.S. Climate Data. 2018. *Climate Honolulu – Hawaii and Weather Averages Honolulu*. https://www.usclimatedata.com/climate/honolulu/hawaii/united-states/ushi0026.

Attachment B.1.1:
Thermal Monitoring Data

GSI ENVIRONMENTAL

ATTACHMENT B.1.1: THERMAL MONITORING DATA
Red Hill Bulk Fuel Storage Facility, Joint Base Pearl Harbor-Hickam, O'ahu, Hawai'i

Ambient Temperature (C)				
RHMW01	RHMW02	RHMW03	RHMW04	RHMW05
26.60	26.40	26.90	19.80	26.80

	Temperature (C)									
	Well Air Temperature, ft bTOC					Wall Temperature, ft bTOC				
Depth (ft bTOC)	RHMW01	RHMW02	RHMW03	RHMW04	RHMW05	RHMW01	RHMW02	RHMW03	RHMW04	RHMW05
0	25.90	26.40	27.90	20.60	26.50	26.40	26.70	26.50	24.80	26.80
5	25.80	26.40	27.50	23.70	25.70	26.20	26.70	27.70	25.20	25.80
10	25.20	26.40	28.70	25.20	25.30	25.40	26.60	28.30	25.00	25.30
15	25.00	26.40	29.30	25.00	25.00	25.10	26.50	28.60	24.70	25.00
20	24.80	26.40	29.50	24.40	24.80	24.90	26.30	29.00	24.10	24.80
25	24.70	26.30	29.70	24.20	24.60	24.70	26.20	29.20	23.80	24.70
30	24.50	26.10	29.80	23.90	24.60	24.60	26.10	29.30	23.70	24.80
35	24.40	26.00	29.80	23.70	24.60	24.40	25.80	29.60	23.40	24.70
40	24.30	25.80	29.80	23.60	24.50	24.30	25.70	29.50	23.50	24.60
45	24.10	25.70	29.70	23.40	24.50	24.20	25.50	29.40	23.30	24.60
50	24.00	25.50	29.50	23.30	24.50	24.00	25.30	29.30	23.20	24.50
55	23.80	25.30	29.40	23.20	24.40	23.90	25.20	29.20	23.30	24.50
60	23.70	25.00	29.10	23.10	24.40	23.70	24.90	28.90	23.10	24.50
65	23.50	24.80	28.90	23.00	24.40	23.50	24.70	28.70	23.00	24.40
70	23.30	24.70	28.60	22.90	24.30	23.40	24.60	28.40	23.00	
75	23.10	24.50	28.30	22.80	24.20	23.20	24.40	28.10	23.00	
80	23.00	24.30	28.00	22.80	24.10		24.20	27.80	22.90	
83					24.10					
84	22.70									
85			27.60	22.70				27.50	22.80	
86		24.00								
88										
90			27.30	22.60				27.20	22.80	
91	22.40				22.80					
93		23.20								
95			26.90	22.60				26.60	22.70	
96										
98	22.30									
99					21.60					
100		22.80	26.60	22.50					22.60	
103			26.00							
105				22.50					22.60	
110				22.40					22.60	
111			25.80							
115				22.40					22.50	
119			25.40							
120				22.30					22.50	
125				22.30					22.50	
130				22.20					22.40	
135				22.20					22.40	
140				22.10					22.30	
145				22.10					22.30	
150				22.10					22.20	
155				22.00					22.20	
160				22.00					22.10	
165				22.00					22.10	
170				22.00					22.00	
175				22.00					22.00	
180				21.90					22.10	
185				21.90					22.00	
190				21.80					21.90	
195				21.80					22.10	
200				21.80					21.90	
205				21.70					21.60	
210				21.70					21.70	
215				21.60					21.70	
220				21.60					21.70	
225				21.60					21.60	
230				21.50					21.60	
235				21.50					21.60	
240				21.40					21.60	
245				21.40					21.50	
250				21.30					21.50	
255				21.30					21.50	
260				21.30					21.40	
265				21.20					21.40	
270				21.20					21.30	
275				21.10					21.30	
280				21.10					21.20	
285				21.00					21.20	
289				20.90						
297				20.90						
310				20.90						

Appendix B.2:
Carbon Trap NSZD Analysis

CONTENTS

Acronyms and Abbreviations iii

1. Introduction 1-1

2. NSZD Rate Based on Tunnel Carbon Dioxide Flux 2-1

   2.1 Carbon Cartridges 2-1
   2.2 Carbon Traps 2-5

3. NSZD Rate Based on Ground Surface Carbon Dioxide Flux 3-1

4. Conclusions 4-1

5. References 5-1

ATTACHMENTS

B.2.1 E-Flux Laboratory Reports

FIGURES

2-1 Diagram Showing Carbon Dioxide Measurement Points in the Exhaust Tunnels (E1 and E2) and the Inlet Location (I1) 2-2

2-2 Diagram Showing Carbon Trap Locations in Tunnels 2-6

3-1 Carbon Trap Receiver, Trap (In Uncapped Mode), Rubber Connector, and Rain Cover 3-1

3-2 Locations for Eight Ground Surface Carbon Trap Deployments at Facility with Results in gal/acre/yr 3-2

3-3 Area Encompassed by Traps and Tank Farm for Ground Surface NSZD Calculation 3-3

4-1 Conceptual Illustration of Carbon Dioxide Flux to Ground Surface and Tunnels 4-1

TABLES

2-1 Carbon Cartridge Results 2-1

2-2 Calculation of Upper-Bound NSZD Rate from Unadjusted Carbon Cartridge Results in Upper Tunnel 2-3

2-3 Calculation of Upper-Bound NSZD Rate from Unadjusted Carbon Cartridge Results in Lower Tunnel 2-4

2-4 Total Upper-Bound NSZD Rate Calculated from Unadjusted Carbon Cartridge Results 2-4

2-5 Calculation of Lower-Bound NSZD Rate from Adjusted Carbon Cartridge Results in Upper Tunnel 2-4

2-6 Calculation of Lower-Bound NSZD Rate from Adjusted Carbon Cartridge Results in Lower Tunnel 2-5

2-7 Total Lower-Bound NSZD Rate Calculated from Adjusted Carbon Cartridge Results 2-5

2-8 Results from Tunnel Carbon Traps 2-7

3-1 Results from Ground Surface Carbon Traps 3-2

4-1 Calculation of Tunnel-Induced Ventilation of the Unsaturated Zone Required to Sustain Aerobic Conditions 4-2

ACRONYMS AND ABBREVIATIONS

^{14}C	carbon-14
cm^3	cubic centimeter
CO_2	carbon dioxide
ft^3	cubic foot
g	gram
gal	gallon
L	liter
LNAPL	light non-aqueous-phase liquid
min	minute
mol	mole
NSZD	natural source-zone depletion
O_2	oxygen
yr	year

1. Introduction

This subappendix is summarized in Section 7.3.1.4 of the Conceptual Site Model main document.

Natural source-zone depletion (NSZD) is the active process whereby light non-aqueous-phase liquid (LNAPL) is degraded in the subsurface by biodegradation and other naturally occurring processes. For this report, LNAPL consists of petroleum hydrocarbons in the form of various fuels. NSZD is now emerging as an important remediation approach for petroleum hydrocarbon sites (Garg et al. 2017). As described in Garg et al. (2017), a variety of methods have been used to obtain NSZD rates.

One such method is the carbon dioxide efflux method (or "carbon trap" method). This method measures the amount of carbon dioxide being generated through the biodegradation of LNAPL. The carbon dioxide is captured using two carbon dioxide sorbent elements comprised of soda lime (consisting primarily of calcium hydroxides), which are contained in a canister, over LNAPL zones (McCoy et al. 2014). The carbon dioxide generated by LNAPL biodegradation is transported to the surface by diffusion, and in some cases advection, and is trapped in one sorbent element. Another sorbent element prevents atmospheric carbon dioxide from being captured by the first sorbent element. Traps are typically deployed in receivers in the field for 14 days and then sent to the laboratory. The carbon-14 fraction (^{14}C correction) is also measured in the laboratory so that "modern carbon" (e.g., carbon dioxide generated from biodegradation of recent plant material) can be separated from "ancient carbon" (carbon dioxide associated with the biodegradation of fossil fuel). The efflux rate of ancient carbon is used to calculate a NSZD rate in units of gallons per acre per year. Due to the unique construction of the Facility, conventional carbon traps were used to measure carbon dioxide flux at the ground surface and modified carbon cartridges were used to measure carbon dioxide flux into the tunnels.

2. NSZD Rate Based on Tunnel Carbon Dioxide Flux

2.1 CARBON CARTRIDGES

The ventilation system in the tunnels creates a negative pressure gradient within the tank access tunnels (i.e., a pressure gradient from the basalt into the tunnel), so that advective gas flow is from the vadose zone into the tunnels (see CSM Appendix B.3). As a result, the tunnels act like a soil vapor extraction system and can capture ancient (i.e., petrogenic) carbon dioxide generated through biological NSZD occurring in the vadose zone. This reduces the carbon dioxide captured by any traps installed on the top and sides of the tank farm (Figure 3-2; Section 3). It was unknown beforehand whether this gas flow is mostly via fractures in the concrete/gunite lined tunnels or from the permeability of the concrete/gunite (competent concrete permeability to gas flow is low but measureable).

To measure any NSZD-related carbon dioxide pulled into the tunnels in this manner, a custom measurement procedure was deployed in the exhaust tunnels of the tank farm (Figure 2-1) at several locations including E1 near exhaust fan 1-A in the upper tunnel, E2 near exhaust fan 2-A in the lower tunnel, and I1 near the inlet fan at Adit 6. Carbon dioxide concentrations in the tunnels were measured through the collection of 24-hour air samples pumped through carbon trap cartridges.

The results from the carbon cartridges are shown in Table 2-1. The carbon dioxide mass sorbed on the sorbent element was corrected to remove the modern carbon signal using ^{14}C measurements (Attachment B.2.1). The unadjusted fossil fuel carbon dioxide (CO_2) (ancient carbon) calculation used a standard fraction of modern carbon in contemporary living material of 1.05 (Hua, Barbetti, and Rakowski 2013). However, the measurements from the inlet showed some non-zero fossil fuel CO_2 values, so the fraction of modern carbon in contemporary living material was altered to 1.038, so that the average of the fossil fuel CO_2 values from the inlet (I1) would be zero in the adjusted values.

The volume of air forced through the trap was then used to provide an ancient carbon concentration. This concentration of ancient carbon in the exhaust gas was multiplied by the design air flow rate of the ventilation system at the various sampling locations (Figure 2-1) to obtain an ancient carbon mass discharge rate. The mass discharge rate was then converted to a NSZD rate in units of gallons per year.

Table 2-1: Carbon Cartridge Results

Cartridge ID	Unadjusted Fossil Fuel CO_2 (g)	Adjusted Fossil Fuel CO_2 (g)	Pumping Rate (L/min)	Sample Time (min)	Sample Volume (L)
E1a	0.02	0.01	1.06	1,335	1,415
E1b	0.04	0.02	1.06	1,447	1,534
E2a	0.09	0.07	1.06	1,322	1,401
E2b	0.08	0.06	1.06	1,453	1,540
I1a	0.03	0.02	1.06	1,397	1,481
I1b	Non-detect	Non-detect	1.06	1,328	1,408

g gram
L liter
min minute

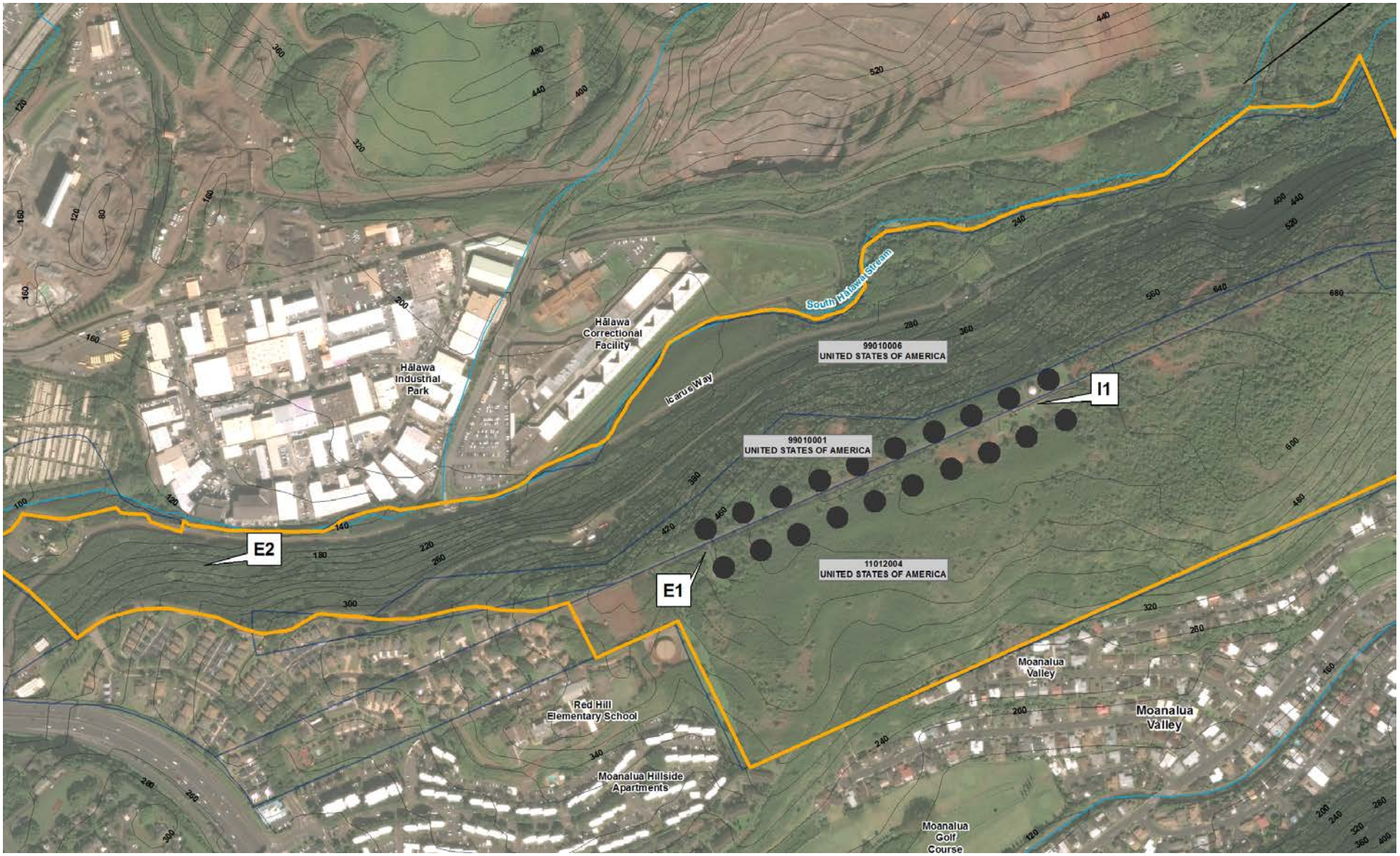

Figure 2-1: Diagram Showing Carbon Dioxide Measurement Points in the Exhaust Tunnels (E1 and E2) and the Inlet Location (I1)

The calculations using unadjusted fossil fuel CO_2 values are shown in Table 2-2, Table 2-3, and Table 2-4. This provides an upper bound for the NSZD rate based on carbon dioxide flowing into the tunnels. A lower bound was calculated by running the same calculations, but using the adjusted values and assuming a lower air flow rate through the tunnels. Based on communications with the Navy (pers. comm., December 5, 2017, email message from John Floyd to Curtis C. Stanley, GSI Environmental, "RE: 4671 Tunnel Ventilation Questions for Navy"), for 14 hours per day (58% of each day) during this sampling, air flows in the tunnels may have decreased by 50%, so, as a conservative estimate, all flows were decreased by 29% (50% decrease for 58% of the time). The calculations using adjusted fossil fuel CO_2 values and decreased flow rates are shown in Table 2-5, Table 2-6, and Table 2-7.

Table 2-2: Calculation of Upper-Bound NSZD Rate from Unadjusted Carbon Cartridge Results in Upper Tunnel

Parameter	Value	Reasoning
Average E1 Fossil Fuel CO_2	0.03 g CO_2	Calculation [(0.02 g CO_2 + 0.04 g CO_2) / 2] (Table 2-1)
Average E1 Sample Volume	1,474 L air	Calculation [(1,415 L + 1,534 L) / 2] (Table 2-1)
Average Fossil Fuel CO_2 Concentration	2.0×10^{-5} g CO_2/L air 5.8×10^{-4} g CO_2/ft^3 air	Calculation (0.03 g CO_2 / 1,474 L) 1 L = 0.0353 ft^3
Air Flow Rate in Upper Tunnel	16,000 ft^3 air/min	Red Hill Mechanical New Airflow Diagram - Scheme 3 (InSynergy Engineering 2013)
CO_2 Flow Rate in Upper Tunnel	9.2 g CO_2/min 0.2 mol CO_2/min	Calculation (5.8×10^{-4} g CO_2/ft^3 air × 16,000 ft^3 air/min) Mol weight of CO_2 = 44 g/mol
Stoichiometric Ratio of CO_2 to Jet Fuel	11 mol CO_2/mol fuel	Taken from degradation equation: $C_{11}H_{24} + 17O_2 \rightarrow 11CO_2 + 12H_2O$
Jet Fuel NSZD Rate (Upper Tunnel)	0.02 mol fuel/min 3.0 g fuel/min	Calculation (0.2 mol CO_2/min / 11 mol CO_2/mol fuel) Mol weight of fuel = 156 g/mol
Density of Jet Fuel	0.78 g fuel/cm^3 fuel	Tien et al. (2015)
Jet Fuel NSZD Rate (Upper Tunnel)	3.8 cm^3 fuel/min 0.001 gal fuel/min **529 gal fuel/yr**	Calculation (3.0 g fuel/min / 0.78 g fuel/cm^3 fuel) 1 cm^3 = 0.000264 gal 525600 min = 1 year

cm^3 cubic centimeter
ft^3 cubic foot
gal gallon
mol mole
yr year

Table 2-3: Calculation of Upper-Bound NSZD Rate from Unadjusted Carbon Cartridge Results in Lower Tunnel

Parameter	Value	Reasoning
Average E2 Fossil Fuel CO_2	0.085 g CO_2	Calculation [(0.09 g CO_2 + 0.08 g CO_2) / 2] (Table 2-1)
Average E2 Sample Volume	1,471 L air	Calculation [(1,401 L + 1,540 L) / 2] (Table 2-1)
Average Fossil Fuel CO_2 Concentration	5.8×10^{-5} g CO_2/L air 1.6×10^{-3} g CO_2/ft^3 air	Calculation (0.085 g CO_2 / 1,471 L) 1 L = 0.0353 ft^3
Air Flow Rate in Lower Tunnel	63,000 ft^3 air/min	Red Hill Mechanical New Airflow Diagram - Scheme 3 (InSynergy Engineering 2013)
CO_2 Flow Rate in Upper Tunnel	103 g CO_2/min 2.3 mol CO_2/min	Calculation (1.6×10^{-3} g CO_2/ft^3 air × 63,000 ft^3 air/min) Mol weight of CO_2 = 44 g/mol
Stoichiometric Ratio of CO_2 to Jet Fuel	11 mol CO_2/mol fuel	Taken from degradation equation: $C_{11}H_{24} + 17O_2 \rightarrow 11CO_2 + 12H_2O$
Jet Fuel NSZD Rate (Upper Tunnel)	0.21 mol fuel/min 33 g fuel/min	Calculation (2.3 mol CO_2/min / 11 mol CO_2/mol fuel) Mol weight of fuel = 156 g/mol
Density of Jet Fuel	0.78 g fuel/cm^3 fuel	Tien et al. (2015)
Jet Fuel NSZD Rate (Upper Tunnel)	43 cm^3 fuel/min 0.01 gal fuel/min **5,916 gal fuel/yr**	Calculation (33 g fuel/min / 0.78 g fuel/cm^3 fuel) 1 cm^3 = 0.000264 gal 525600 min = 1 year

Table 2-4: Total Upper-Bound NSZD Rate Calculated from Unadjusted Carbon Cartridge Results

Location	NSZD Rate (gal/year)
Upper Tunnel	529
Lower Tunnel	5,916
Both Tunnels (Total)	**6,445**

Table 2-5: Calculation of Lower-Bound NSZD Rate from Adjusted Carbon Cartridge Results in Upper Tunnel

Parameter	Value	Reasoning
Average E1 Fossil Fuel CO_2	0.015 g CO_2	Calculation [(0.01 g CO_2 + 0.02 g CO_2) / 2] (Table 2-1)
Average E1 Sample Volume	1,474 L air	Calculation [(1,415 L + 1,534 L) / 2] (Table 2-1)
Average Fossil Fuel CO_2 Concentration	1.0×10^{-5} g CO_2/L air 2.9×10^{-4} g CO_2/ft^3 air	Calculation (0.015 g CO_2 / 1,474 L) 1 L = 0.0353 ft^3
Air Flow Rate in Upper Tunnel	11,300 ft^3 air/min	Red Hill Mechanical New Airflow Diagram - Scheme 3 (InSynergy Engineering 2013). Air flow rate reduced by 29% as described in text above.
CO_2 Flow Rate in Upper Tunnel	3.3 g CO_2/min 0.074 mol CO_2/min	Calculation (2.9×10^{-4} g CO_2/ft^3 air × 11,300 ft^3 air/min) Mol weight of CO_2 = 44 g/mol
Stoichiometric Ratio of CO_2 to Jet Fuel	11 mol CO_2/mol fuel	Taken from degradation equation: $C_{11}H_{24} + 17O_2 \rightarrow 11CO_2 + 12H_2O$
Jet Fuel NSZD Rate (Upper Tunnel)	0.0067 mol fuel/min 1.1 g fuel/min	Calculation (0.074 mol CO_2/min / 11 mol CO_2/mol fuel) Mol weight of fuel = 156 g/mol
Density of Jet Fuel	0.78 g fuel/cm^3 fuel	Tien et al. (2015)
Jet Fuel NSZD Rate (Upper Tunnel)	1.3 cm^3 fuel/min 3.6×10^{-4} gal fuel/min **187 gal fuel/yr**	Calculation (1.1 g fuel/min / 0.78 g fuel/cm^3 fuel) 1 cm^3 = 0.000264 gal 525600 min = 1 year

Table 2-6: Calculation of Lower-Bound NSZD Rate from Adjusted Carbon Cartridge Results in Lower Tunnel

Parameter	Value	Reasoning
Average E2 Fossil Fuel CO_2	0.065 g CO_2	Calculation [(0.07 g CO_2 + 0.06 g CO_2) / 2] (Table 2-1)
Average E2 Sample Volume	1,471 L air	Calculation [(1,401 L + 1,540 L) / 2] (Table 2-1)
Average Fossil Fuel CO_2 Concentration	4.4×10^{-5} g CO_2/L air 1.3×10^{-3} g CO_2/ft^3 air	Calculation (0.065 g CO_2 / 1,471 L) 1 L = 0.0353 ft^3
Air Flow Rate in Lower Tunnel	44,600 ft^3 air/min	Red Hill Mechanical New Airflow Diagram - Scheme 3 (InSynergy Engineering 2013). Air flow rate reduced by 29% as described in text above.
CO_2 Flow Rate in Upper Tunnel	56 g CO_2/min 1.3 mol CO_2/min	Calculation (1.3×10^{-3} g CO_2/ft^3 air × 44,600 ft^3 air/min) Mol weight of CO_2 = 44 g/mol
Stoichiometric Ratio of CO_2 to Jet Fuel	11 mol CO_2/mol fuel	Taken from degradation equation: $C_{11}H_{24} + 17O_2 \rightarrow 11CO_2 + 12H_2O$
Jet Fuel NSZD Rate (Upper Tunnel)	0.12 mol fuel/min 18 g fuel/min	Calculation (1.3 mol CO_2/min / 11 mol CO_2/mol fuel) Mol weight of fuel = 156 g/mol
Density of Jet Fuel	0.78 g fuel/cm^3 fuel	Tien et al. (2015)
Jet Fuel NSZD Rate (Upper Tunnel)	23 cm^3 fuel/min 0.0061 gal fuel/min **3,205 gal fuel/yr**	Calculation (18 g fuel/min / 0.78 g fuel/cm^3 fuel) 1 cm^3 = 0.000264 gal 525600 min = 1 year

Table 2-7: Total Lower-Bound NSZD Rate Calculated from Adjusted Carbon Cartridge Results

Location	NSZD Rate (gal/year)
Upper Tunnel	187
Lower Tunnel	3,205
Both Tunnels (Total)	**3,392**

From these calculations, then, the NSZD rate from carbon dioxide entering the tunnels is between 3,400 and 6,400 gallons per year.

2.2 CARBON TRAPS

Two carbon traps (with a trip blank) were also sealed onto the tunnel floor at locations shown in Figure 2-2 as follows: F1 (between tanks T5 and T6 in the upper access tunnel) and F2 (between tanks T5 and T-6 in the lower access tunnel). A silicon sealer/grout was used to determine if there was a measurable carbon dioxide flux through the tunnel walls/floor. The grout was placed to allow any gas migrating directly through the concrete/gunite but not allow any transport from the tunnel air into the trap. The specific locations for trap deployment were selected to minimize the potential for disturbance during the sample period. A trip blank was placed at F2; any ancient carbon dioxide detected in the trip blank is subtracted from the ancient carbon detected in the exposed samples before calculating NSZD rates. The results from these tunnel traps are shown in Table 2-8.

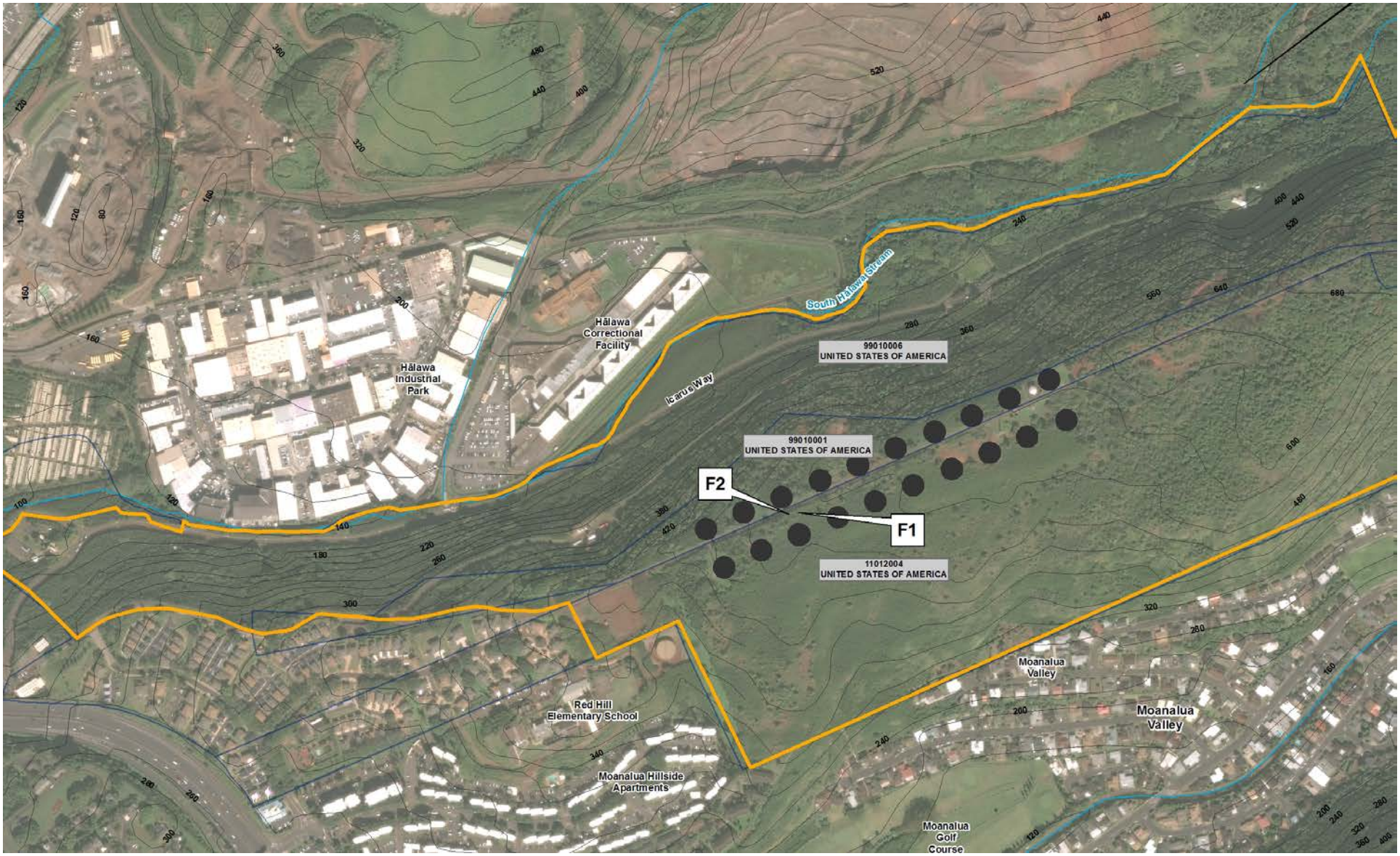

Figure 2-2: Diagram Showing Carbon Trap Locations in Tunnels

Table 2-8: Results from Tunnel Carbon Traps

Trap ID	NSZD Rate (gal/acre/yr)
F1	0
F2	10

Attachment B.2.1 explains the process of developing these values from the carbon trap measurements. The NSZD rates measured indicate that some carbon dioxide is flowing into the tunnels through the competent concrete/gunite, but at very low to zero rates. Because of their low values, the carbon dioxide flow rate through the tunnel floor is likely low. Most of the carbon dioxide flow rate into the tunnels, therefore, must be occurring through various cracks in the tunnel and not directly through the concrete/gunite.

3. NSZD Rate Based on Ground Surface Carbon Dioxide Flux

Eight carbon traps (with a trip blank) were deployed for 14 days on the top and sides of the tank farm to measure carbon dioxide efflux in the conventional manner assuming that the carbon dioxide being generated by NSZD might diffuse upwards and/or sideways out of the tank farm (E-Flux, 3185-A Rampart Road, #250D Fort Collins, CO 80521 970-492-4360). Installing carbon traps involves installing a trap receiver, placing the trap into the receiver, inserting a diffusion cap, and placing a rain cover on the entire assembly (Figure 3-1).

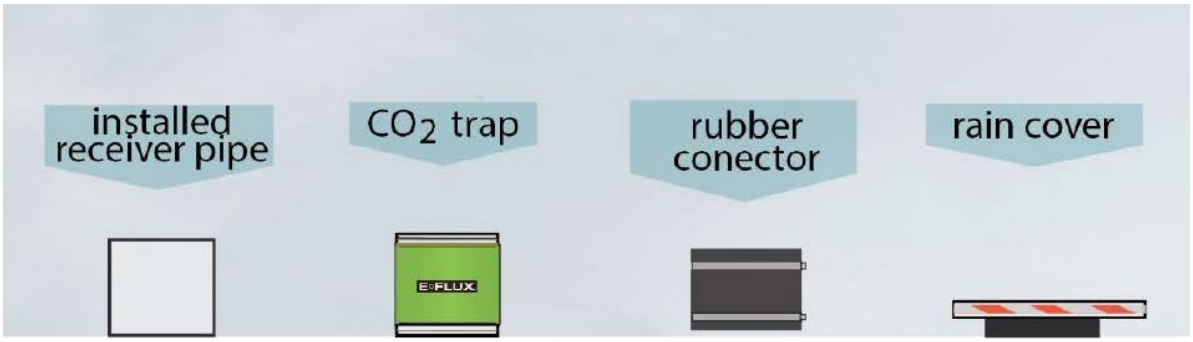

Figure 3-1: Carbon Trap Receiver, Trap (In Uncapped Mode), Rubber Connector, and Rain Cover

Eight traps were deployed on the top and sides of the tank farm using E-Flux standard operating procedures. Locations are summarized below and shown on Figure 3-1:

- A line of four traps (T1 to T4) was placed transverse to the tank farm, with one on the north side, one on the south side, and two near the top of the tank farm near Tanks 05 and 06, which is a known impact area based on soil vapor data. T1 and T4 were placed on clinker zone outcrops on the side of the tank farm. A trip blank was placed at T2; any ancient carbon dioxide detected in the trip blank is subtracted from the ancient carbon detected in the exposed samples before calculating NSZD rates.
- A second line of four traps was placed transverse to the tank farm, with one on the north side, one on the south side, and two near the top of the tank farm near Tanks 11 and 12, which is a zone with potentially less LNAPL impacts based on soil vapor data. T5 and T8 were placed on clinker zone outcrops on the side of the tank farm.

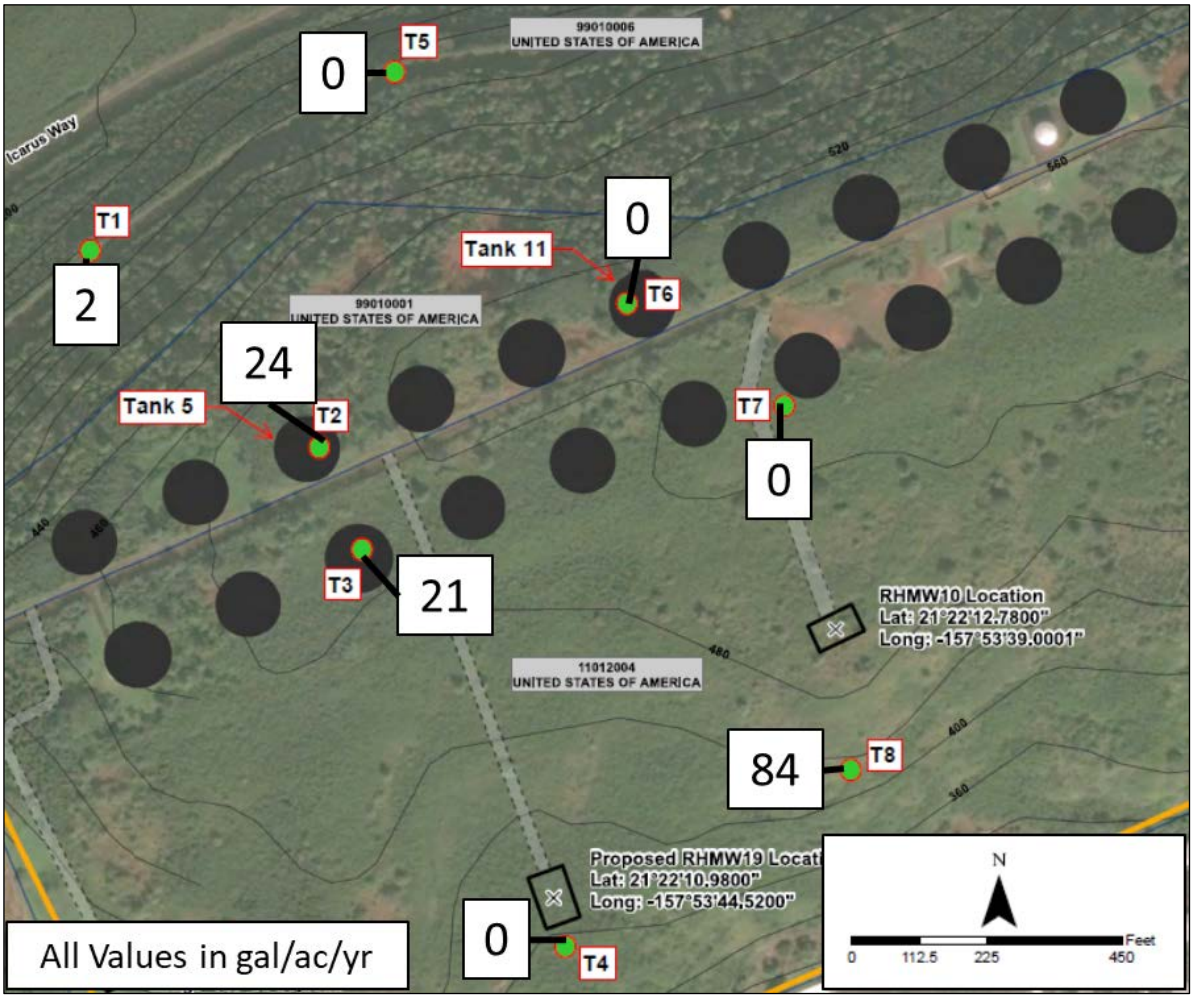

Figure 3-2: Locations for Eight Ground Surface Carbon Trap Deployments at Facility with Results in gal/acre/yr

The results from the analysis of these traps are shown in Table 3-1.

Table 3-1: Results from Ground Surface Carbon Traps

Trap ID	NSZD Rate (gal/acre/yr)
T1	2
T2	24
T3	21
T4	0
T5	0
T6	0
T7	0
T8	84

Attachment B.2.1 explains the process of developing these values from the carbon trap measurements. The rates measured by these traps were fairly low and in some cases zero, indicating that ancient carbon flux to the ground surface is low and variable. It is worth noting, however, that the largest rate measured was in one of the traps that was placed on a clinker outcrop. This suggests that the carbon dioxide from the NSZD does indeed preferentially flow laterally through the clinker zones to the surface. Assuming the ancient carbon flux from NSZD that was measured by these traps is happening in the area encompassed by the traps and the tank farm, an average NSZD rate was calculated in gallons per year. Taking an average of all the NSZD rates (16 gal/acre/year) and multiplying this by the area encompassed by the traps and the tank farm (61.1 acres; Figure 3-3), the total NSZD rate attributable to ground surface ancient carbon flux from top and sides of the tank farm comes to about 1,000 gallons per year.

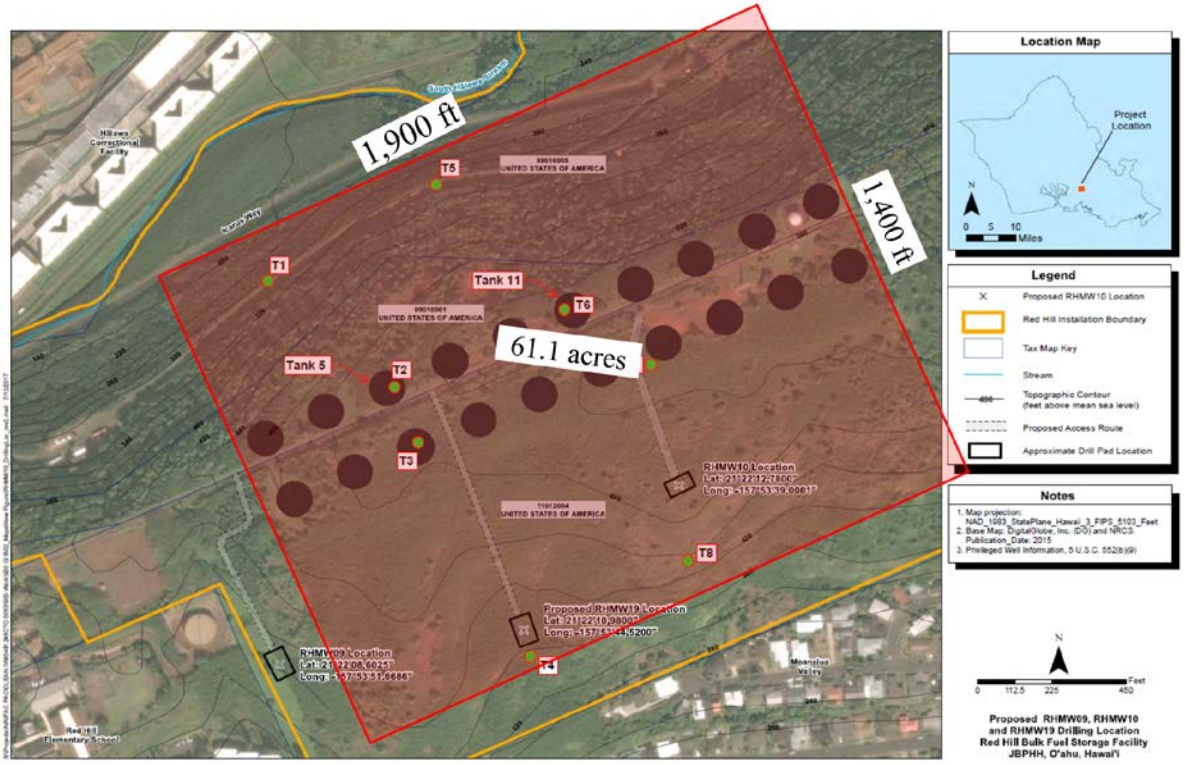

Figure 3-3: Area Encompassed by Traps and Tank Farm for Ground Surface NSZD Calculation

4. Conclusions

Carbon cartridges and traps were installed within the tunnels and on the top and sides of the tank farm. Based on the mass of ancient carbon sorbed to these cartridges and traps, an approximate NSZD rate was determined.

From the cartridges, a range of 3,400–6,400 gallons per year was calculated. Little to no NSZD was seen in the tunnel traps set on the tunnel floor, indicating that the carbon dioxide within the tunnels was mostly entering through cracks, not directly through the concrete/gunite. From the ground surface traps, a value of 1,000 gallons per year outside the tunnels was calculated.

Therefore, the majority of the NSZD is from the tunnel acting like a partial soil vapor extraction system (Figure 4-1), pulling carbon dioxide from the basalt into the tunnels. The two NSZD rates (tunnel and hill top) are additive, however, so, the total NSZD rate in the tank farm is between 4,400 and 7,400 gallons per year.

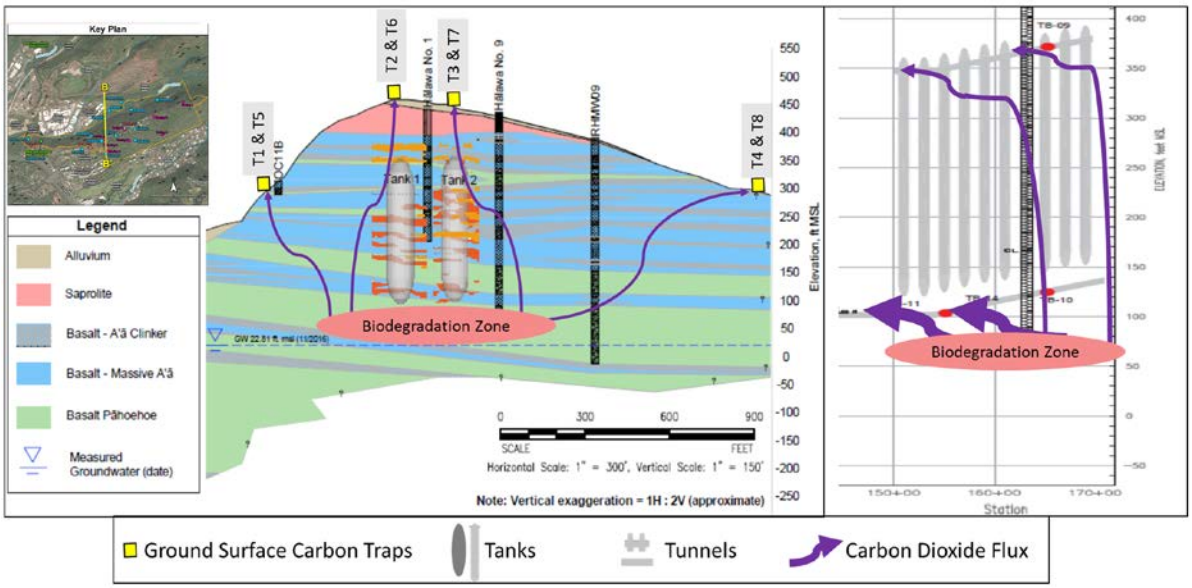

Thicker arrows indicate greater flux; location of tanks, traps, and biodegradation zones are approximate.

Figure 4-1: Conceptual Illustration of Carbon Dioxide Flux to Ground Surface and Tunnels

Furthermore, if less than 0.5% of air flow through the tunnel originates from the vadose zone (rather than the tunnel entrances), then the resulting ventilation of the vadose zone would be sufficient to provide 100% of the oxygen needed to support the observed NSZD while maintaining vadose zone oxygen concentrations above 19% (Table 4-1). Thus, only a small amount of leakage from the unsaturated zone into the tunnels through the tunnel walls is required to provide sufficient air flow through the unsaturated zone to sustain aerobic biodegradation.

Table 4-1: Calculation of Tunnel-Induced Ventilation of the Unsaturated Zone Required to Sustain Aerobic Conditions

Parameter	Value	Reasoning
NSZD Rate	6,400 gal fuel/yr 2.4 x10^7 cm^3 fuel/yr	Upper Bound NSZD Rate (Table 2-4) 1 cm^3 = 0.000264 gal
Density of Jet Fuel	0.78 g fuel/cm^3 fuel	Tien et al. (2015)
NSZD Rate	1.9 x10^7 g fuel/yr	Calculation (2.4×10^7 cm^3 fuel/yr × 0.78 g fuel/cm^3 fuel)
Molecular Weight of Jet Fuel	156 g fuel/mol fuel	Assume that Jet Fuel is $C_{11}H_{24}$
NSZD Rate	121,100 mol fuel/yr	Calculation (1.9 x10^7 g fuel/yr / 156 g fuel/mol fuel)
Stoichiometric Ratio of O_2 to Jet Fuel	17 mol O_2/mol fuel	Taken from degradation equation: $C_{11}H_{24} + 17O_2 \rightarrow 11CO_2 + 12H_2O$
O_2 Consumption Rate	2.1 x10^6 mol O_2/yr	Calculation (121,100 mol fuel/yr × 17 mol O_2/mol fuel)
Molecular Weight of O_2	32 g O_2/mol O_2	Known
O_2 consumption Rate	6.6 x10^7 g O_2/yr	Calculation (2.1 x10^6 mol O_2/yr × 32 g O_2/mol O_2)
Density of O_2	1.43 g O_2/L O_2	Known
O_2 consumption Rate	4.6 x10^7 L O_2/yr	Calculation (6.6 x10^7 g O_2/yr / 1.43 g O_2/LO_2)
Percentage of O_2 in Air	21%	Known
Air flow rate to sustain aerobic conditions in basalt	2.2 x10^8 L air/yr 7.8 x10^6 ft^3 air /yr	Calculation (4.6 x10^7 L O_2/yr / 21%) 1 L = 0.0353 ft^3
Current Air Flow Rate in Tunnels	79,000 ft^3 air/min 4.2 x10^{10} ft^3 air/yr	Sum of Upper and Lower Tunnel Flow Rates 525,600 min = 1 year
Percentage of Current Air Flow Rate in Tunnel Required to Sustain Aerobic Conditions in Basalt	0.02%	Calculation (7.8 x10^6 ft^3 air/yr / 4.2 x10^{10} ft^3 air/yr)

Note: As reported in Appendix B.3, an oxygen (O_2) concentration of 19% was seen in the unsaturated zone, suggesting that only 10% of the available O_2 is being utilized for biodegradation. Thus, up to 10 times as much air flow through the basalt might be required to sustain an average oxygen concentration of 19% in the basalt (i.e., 0.2% of the air flow through the tunnel).

5. References

Garg, S., C. J. Newell, P. R. Kulkarni, D. C. King, D. T. Adamson, M. I. Renno, and T. Sale. 2017. "Overview of Natural Source Zone Depletion: Processes, Controlling Factors, and Composition Change." *Groundwater Monitoring & Remediation*, July. https://doi.org/10.1111/gwmr.12219.

Hua, Q., M. Barbetti, and A. Z. Rakowski. 2013. "Atmospheric Radiocarbon for the Period 1950–2010." *Radiocarbon* 55 (4): 2059–072.

InSynergy Engineering. 2013. *Red Hill Mechanical New Airflow Diagram - Scheme 3*.

McCoy, K., J. Zimbron, T. Sale, and M. Lyverse. 2014. "Measurement of Natural Losses of LNAPL Using CO_2 Traps." *Groundwater* 53: 658–667.

Tien, C-J., Y-Y. Shu, S-R. Ciou, and C. S. Chen. 2015. "Partitioning of Aromatic Constituents into Water from Jet Fuels." *Arch Environ Contam Toxicol* 69: 153–162. https://doi.org/10.1007/s00244-015-0154-7.

Attachment B.2.1:
E-Flux Laboratory Reports

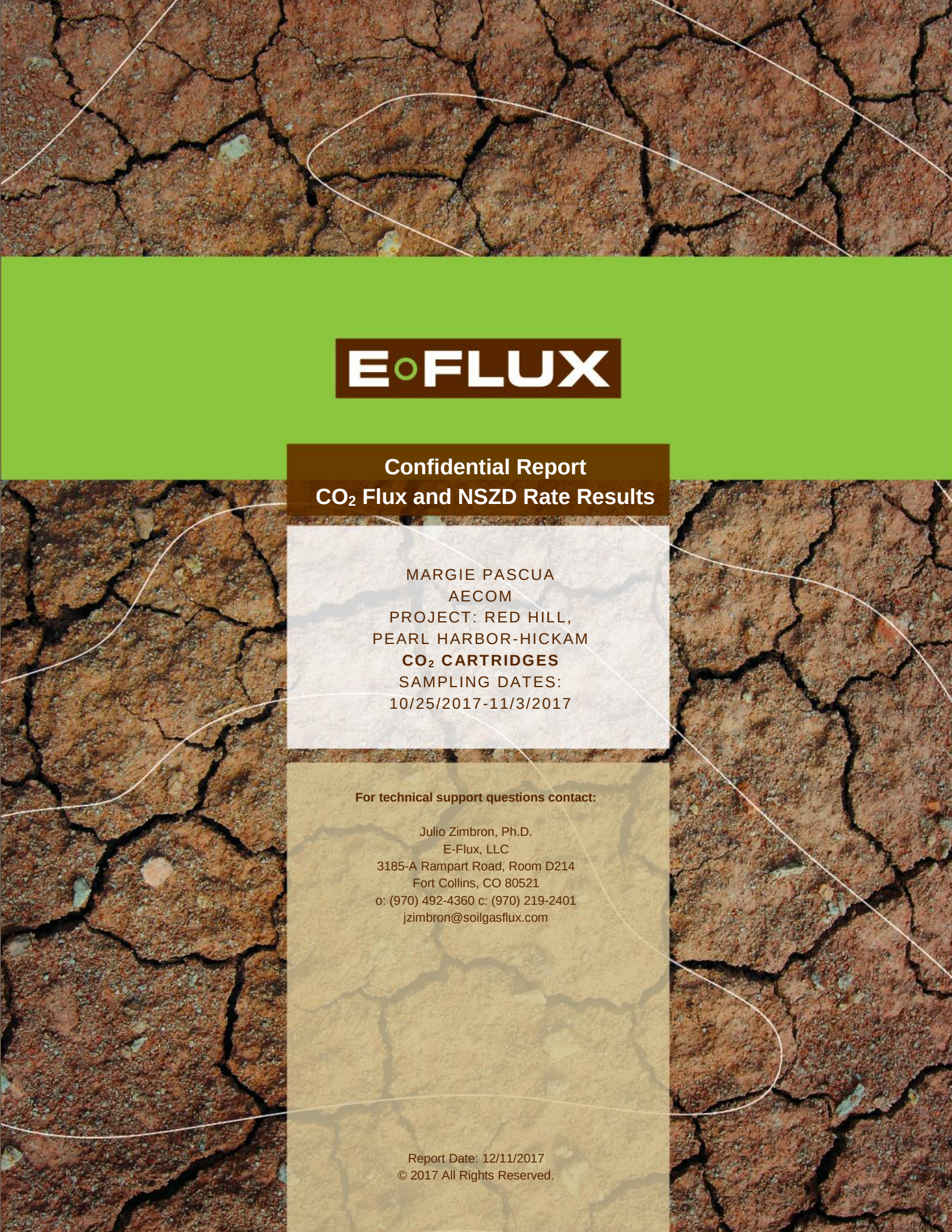

E·FLUX

Confidential Report
CO_2 Flux and NSZD Rate Results

MARGIE PASCUA
AECOM
PROJECT: RED HILL,
PEARL HARBOR-HICKAM
CO_2 CARTRIDGES
SAMPLING DATES:
10/25/2017-11/3/2017

For technical support questions contact:

Julio Zimbron, Ph.D.
E-Flux, LLC
3185-A Rampart Road, Room D214
Fort Collins, CO 80521
o: (970) 492-4360 c: (970) 219-2401
jzimbron@soilgasflux.com

Report Date: 12/11/2017
© 2017 All Rights Reserved.

©2017 All Rights Reserved

This report is for measurement of the mass of fossil fuel-derived CO_2 using cartridges. The purpose of this document is to provide sample calculations of the results reported here and to explain the basis for differentiating petroleum hydrocarbon-derived CO_2 (i.e., fossil fuel CO_2) from modern CO_2 interferences. The following topics are addressed:

- The Value of ^{14}C Analysis
- Site Specific Study Results and Applicable Notes
- Calculation Explanations
- References

The Value of the ^{14}C Analysis

How to differentiate petroleum hydrocarbon-derived CO_2 from modern CO_2 interferences.

Unimpacted soils have natural CO_2 flux generation rates, due to microbial root zone activity and/or the degradation of natural organic matter (NOM). Thus, the total CO_2 flux measured at an impacted location is the sum of both natural soil respiration processes and those related to LNAPL degradation (Sihota et al, 2011).

This report uses carbon isotopic analysis (14C) to determine the contributions to an environmental sample sorbed into CO2 cartridges from both modern and fossil fuel sources, using ASTM Method D6686-12.

Carbon Isotope Analysis Methodology

Sampling was done using CO_2 cartridges loaded with a predetermined mass of CO_2 sorbent. Upon retrieval and shipment to the lab, the samples were homogenized and analyzed for total CO_2 and ^{14}C using methods described before (McCoy et al, 2015).

Unstable isotopic analysis has been previously used to differentiate anthropogenic (due to fossil fuel-burning) and natural sources of atmospheric CO, CO_2 and methane (for example, Klouda and Connolly, 1995; Levin et al, 1995; Avery et al, 2006). Such findings are the basis of ASTM Method D6686-12, Determining the Biobased Content in Solids, Liquids and Gases Using Radiocarbon Analysis (ASTM, 2012). The technique relies on the analysis of ^{14}C, an unstable carbon isotope (with a half-life of approximately 5600 years) that is generated by cosmic rays in the atmosphere. Thus, contemporary (modern) organic carbon is ^{14}C-rich, while fossil fuel carbon is completely ^{14}C-depleted. Furthermore, contemporary samples and atmospheric samples have the same characteristic amount of ^{14}C. The detection limit of ^{14}C by accelerator mass spectrometry enables dating of samples younger than 60,000 years, while older samples (such as fossil fuels) have non-detectable ^{14}C activity (Stuiver and Polach, 1977).

For a sample that contains carbon from both modern and fossil fuel carbon sources, measurement of the ^{14}C enables quantitation of both source contributions. The fossil fuel fraction of the sample, ff_{sample}, and the remaining non-fossil fuel or contemporary fraction ($1- ff_{sample}$), are related by the following two-component mass balance:

$$Fm_{sample} = ff_{sample}\left(Fm_{ff}\right)+\left(1- ff_{sample}\right)\left(Fm_{atm}\right)$$

In this formula, Fm_{sample} is the measured modern fraction of the sample, Fm_{ff} is the fraction of modern carbon in fossil fuel ($Fm_{ff} = 0$), and Fm_{atm} is the fraction of modern carbon in contemporary living material ($Fm_{atm} = 1.05$) (Hua et al., 2013). By convention, the reporting of carbon isotope analysis is based on a 1950 NBS oxalic acid standard, synthesized when the ^{14}C atmospheric levels were lower than current ones due to nuclear tests. Thus, Fm_{sample} is reported as if the analysis was done in 1950, and Fm_{atm} is counter-intuitively larger than 1.

Expected Results and Recommendations

The fossil-fuel carbon content on the unexposed sorbent is non-zero (typically around 35%). This might be the result of either a background fossil fuel signature of the sorbent (due to processing of the chemical or mineral sources), or due to material handling (i.e., exposure to fossil fuel fumes). Although the fossil fuel CO_2 mass is very small, this error is adjusted by a travel blank correction procedure. This consists of subtracting the fossil fuel CO_2 mass from an unexposed trap (a travel blank) from those measured on the traps deployed in the field. The ^{14}C analysis is done on CO_2 sorbent subsamples, after homogenization.

©2017 All Rights Reserved

Study Results

The report and results below are based on proprietary technology to measure the fossil fuel content of an environmental sample using E-Flux CO_2 cartridges. All information contained in this report is strictly confidential to the customer. The chemical analysis is based on methods ASTM 4373-02 (Rapid Determination for Carbonate Content in Soils) and ASTM D6686-12 (Determining the Biobased Content in Solids, Liquids and Gases Using Radiocarbon Analysis).

The site specific results and interpretation are as follows:

E◦FLUX
Easy set-up. Expert results.

Project: Red Hill, Pearl Harbor-Hickam

Customer: AECOM

Customer Contact: Margie Pascua, (808) 356-5373

Report Date: 11-Dec-17

Sample ID	Deployment Dates			Raw Results (not blank corrected)					Blank Corrected Results[a] and ^{14}C Analysis (Fossil Fuel)					
	Deployed	Retrieved	Days	Moisture	Dry Sorbent Mass (g)	Num. of Reps.[b]	Avg CO_2[b]	CV CO_2[c]	Carbon Content[d] %	Carbon Content[d] (g)	Modern Carbon, As Reported[e]	Std. Dev. Modern	Adjusted Fossil Fuel Carbon[f]	Grams Of Fossil Fuel CO_2 (g)
PHHI-C1-CO2-TB	NA	NA	0.00	20.6%	4.136	2	0.91%	7.22%	-	-	65.3%	0.30%	37.8%	-
PHHI-C1-CO2-01	10/25/17 10:05	10/26/17 8:20	0.93	3.1%	4.858	2	25.92%	0.57%	25.0%	1.22	101.8%	0.40%	3.1%	0.02
PHHI-C1-CO2-02	10/26/17 8:26	10/27/17 8:33	1.00	3.0%	4.882	2	25.40%	0.77%	24.5%	1.20	100.5%	0.33%	4.3%	0.04
PHHI-C1-CO2-03	10/30/17 9:56	10/31/17 7:58	0.92	3.0%	5.005	2	28.41%	0.03%	27.5%	1.38	97.4%	0.32%	7.2%	0.09
PHHI-C1-CO2-04	10/31/17 8:00	11/1/17 8:13	1.01	2.9%	5.101	2	30.29%	0.07%	29.4%	1.50	98.3%	0.33%	6.4%	0.08
PHHI-C1-CO2-05	11/1/17 8:45	11/2/17 8:02	0.97	4.4%	4.877	2	25.57%	0.08%	24.7%	1.20	100.8%	0.30%	4.0%	0.03
PHHI-C1-CO2-06	11/2/17 8:07	11/3/17 6:15	0.92	3.0%	4.817	2	23.62%	0.99%	22.7%	1.09	104.0%	0.50%	0.9%	ND

This report contains Confidential Information and is to be delivered only to the Customer indicated above.

See following page for assumptions, project specific quality assurance/quality control information, and notes.

The Following Assumptions and General Notes apply for CO_2 traps:

a. Results are travel blank corrected but not background location corrected.
Blank Corrected Results = Raw Results - Travel Blank

b. Number of Replicates: Carbon analysis was conducted in duplicate if CV ≤ 5%. If CV > 5%, carbon analysis was conducted with triplicates (see Quality Assurance/Quality Control notes). Avg % refers to the percent of CO_2 in the dry sorbent mass before blank corrected.

c. CV is coefficient of variation, equal to the ratio of the standard deviation over the average.

d. If the cartridge carbon content is not larger than travel blank, results are reported as ND. Expressed as CO_2 not pure carbon.

e. "As reported" refers to % modern carbon at the time of development of the test (1950).

f. Adjusted fossil fuel carbon has been transformed from the "As reported" basis (1950) to present ^{14}C levels.

NA means Not Applicable.

Quality Assurance / Quality Control Notes:

- The Travel Blank (**PHHI-C1-CO2-TB**) concentration for this report was **0.91%**. Typical Travel Blank concentration is <2%.
- Cartridge tops were not saturated with CO_2, but some had appreciable CO_2 contents. The mass sorbed in the top element was up to 20% of the total mass sorbed in the whole cartridge. Because of the configuration of these cartridges, this could indicate CO_2 breakthrough from the bottom element, and total carbon may be underestimated by these results. Maximum measured top concentration was **8.20%** (sample **PHHI-C1-CO2-02.1**). Sorbent saturation is 30%.
- **PHHI-C1-CO2-06** showed non-detectable fossil fuel carbon (ND).
- ASTM 4373-02 QA/QC criteria does not provide acceptable variability (CV) standards. Similar methods (for example the carbonates in water, such as ASTM 513.02) provide typical error ≤20%. E-Flux practice is that a CV ≤5% is acceptable. *Sample **PHHI-C1-CO2-TB** had a CV of **7.22%**; this could not be brought down to acceptable levels, as there was not enough sample mass.*

Calculation Explanations

Conversion of Modern C to Fossil Fuel C

Reported modern carbon content (from carbon dating or ^{14}C analysis) is by convention at the ^{14}C levels as of the time of development of the test (1950). Due to higher current levels of ^{14}C in the environment resulting from atomic testing, current (contemporary) levels are approximately 5% higher than in 1950 (Hua et al., 2013). Thus, fossil fuel C can be found with the following conversions:

$$\%\ Modern\ C_{contemporary} = \frac{\%\ Modern\ C_{1950}}{1.05}$$

$$Contemporary\ fossil\ fuel\ C\ \% = 1 - \%\ Modern\ C_{contemporary} = 1 - \frac{\%\ Modern\ C_{1950}}{1.05}$$

Calculating Grams of Fossil Fuel CO_2

Calculating grams of fossil fuel (ff) CO_2 is based on the travel blank corrected percent fossil fuel carbon in the sample (the difference between total fossil fuel CO_2 in the sample and that of the travel blank). This is done as follows:

$$g\ CO_{2(ff)} = g\ sorbent * \left((Avg\ sample\ \%\ CO_2 * ff\ sample\ \%\ C) - (Avg\ TB\ \%\ CO_2 * ff\ TB\ \%\ C)\right)$$

N/A

©2017 All Rights Reserved

References

ASTM (2012), Method D6686-12, Determining the Biobased Content in Solids, Liquids and Gases Using Radiocarbon Analysis.

ASTM (2002), Method D4373-02, Standard Test Method for Rapid Determination of Carbonate Content of Soil.

Avery et al, (2006). Carbon isotopic characterization of dissolved organic carbon in rainwater: Terrestrial and marine influences. Atmos. Environ. p. 7539-7545.

Bauer, H.P.; Beckett, P.H.; and Bie, S.W. (1972). A Rapid Gravimetric Method for Estimating Calcium Carbonate in Soils, Plant and Soil, Vol 37, p. 689-690.

Hua, Q.; Barbetti, M.; and Rakowski, A.Z. (2013). Atmospheric Radiocarbon for the Period 1950-2010. Radiocarbon. 55(4), p. 2059-2072.

Klouda and Connolly, (1995). Radiocarbon (14C) Measurements to Quantify Sources of Atmospheric Carbon Monoxide in Urban Air. Atmos. Environ. p. 3309-3318.

Levin, I. R. Graul, Ne. Trivett. (1995). Long-term observations of atmospheric CO_2 and carbon isotopes at continental sites in Germany. Tellus., 47B, p. 23-34.

McCoy, K., Zimbron, J., Sale, T. and Lyverse, M. (2015), Measurement of Natural Losses of LNAPL Using CO2 Traps. Groundwater, 53: p. 658–667. doi:10.1111/gwat.12240.

Stuiver and Polach, (1977). Discussion. Reporting of ^{14}C data. Radiocarbon 19(3), p. 355–363.

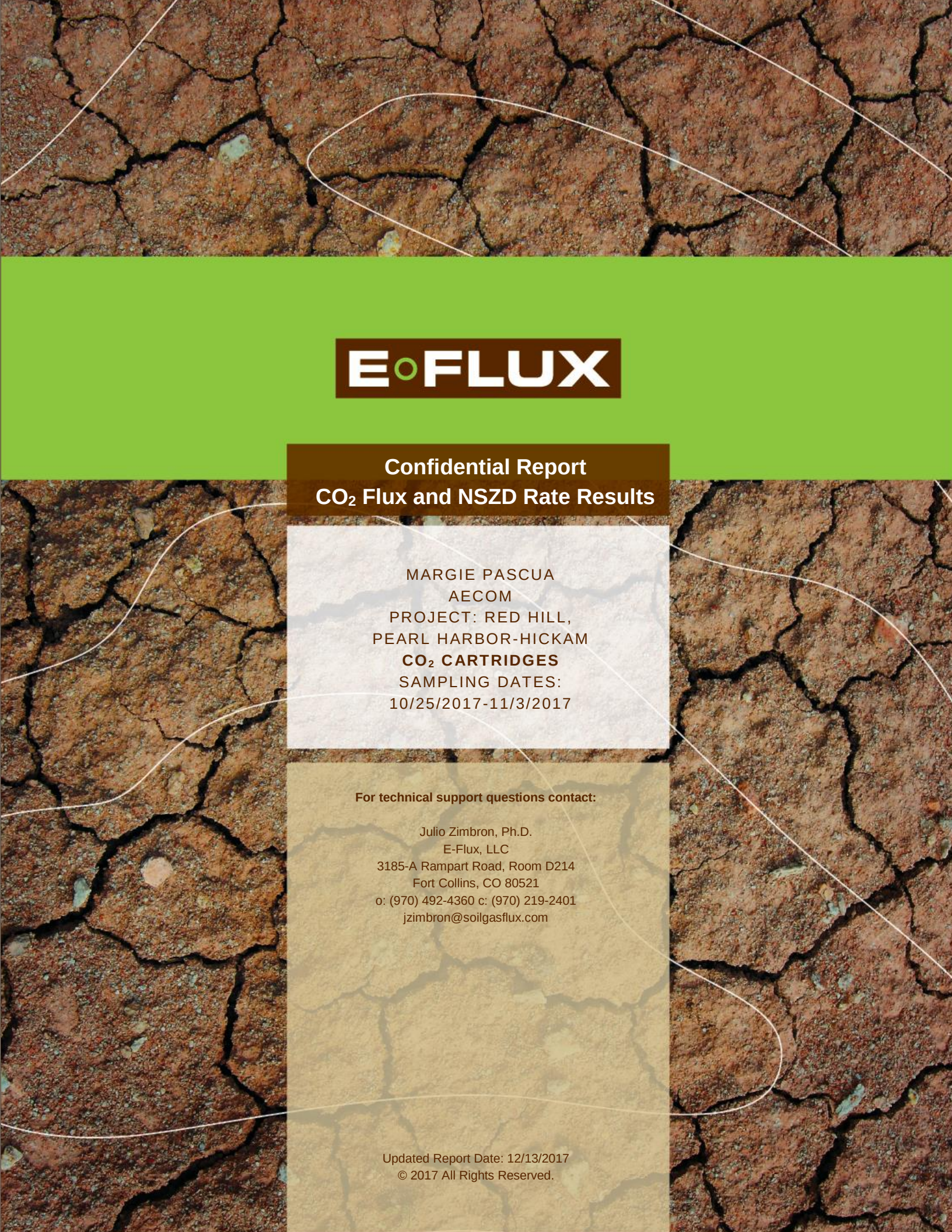

Confidential Report
CO_2 Flux and NSZD Rate Results

MARGIE PASCUA
AECOM
PROJECT: RED HILL,
PEARL HARBOR-HICKAM
CO_2 CARTRIDGES
SAMPLING DATES:
10/25/2017-11/3/2017

For technical support questions contact:

Julio Zimbron, Ph.D.
E-Flux, LLC
3185-A Rampart Road, Room D214
Fort Collins, CO 80521
o: (970) 492-4360 c: (970) 219-2401
jzimbron@soilgasflux.com

Updated Report Date: 12/13/2017
© 2017 All Rights Reserved.

©2017 All Rights Reserved

This report is for measurement of the mass of fossil fuel-derived CO_2 using cartridges. The purpose of this document is to provide sample calculations of the results reported here and to explain the basis for differentiating petroleum hydrocarbon-derived CO_2 (i.e., fossil fuel CO_2) from modern CO_2 interferences. The following topics are addressed:

- The Value of ^{14}C Analysis
- Site Specific Study Results and Applicable Notes
- Calculation Explanations
- References

The Value of the ^{14}C Analysis

How to differentiate petroleum hydrocarbon-derived CO_2 from modern CO_2 interferences.

Unimpacted soils have natural CO_2 flux generation rates, due to microbial root zone activity and/or the degradation of natural organic matter (NOM). Thus, the total CO_2 flux measured at an impacted location is the sum of both natural soil respiration processes and those related to LNAPL degradation (Sihota et al, 2011).

This report uses carbon isotopic analysis (14C) to determine the contributions to an environmental sample sorbed into CO2 cartridges from both modern and fossil fuel sources, using ASTM Method D6686-12.

Carbon Isotope Analysis Methodology

Sampling was done using CO_2 cartridges loaded with a predetermined mass of CO_2 sorbent. Upon retrieval and shipment to the lab, the samples were homogenized and analyzed for total CO_2 and ^{14}C using methods described before (McCoy et al, 2015).

Unstable isotopic analysis has been previously used to differentiate anthropogenic (due to fossil fuel-burning) and natural sources of atmospheric CO, CO_2 and methane (for example, Klouda and Connolly, 1995; Levin et al, 1995; Avery et al, 2006). Such findings are the basis of ASTM Method D6686-12, Determining the Biobased Content in Solids, Liquids and Gases Using Radiocarbon Analysis (ASTM, 2012). The technique relies on the analysis of ^{14}C, an unstable carbon isotope (with a half-life of approximately 5600 years) that is generated by cosmic rays in the atmosphere. Thus, contemporary (modern) organic carbon is ^{14}C-rich, while fossil fuel carbon is completely ^{14}C-depleted. Furthermore, contemporary samples and atmospheric samples have the same characteristic amount of ^{14}C. The detection limit of ^{14}C by accelerator mass spectrometry enables dating of samples younger than 60,000 years, while older samples (such as fossil fuels) have non-detectable ^{14}C activity (Stuiver and Polach, 1977).

For a sample that contains carbon from both modern and fossil fuel carbon sources, measurement of the ^{14}C enables quantitation of both source contributions. The fossil fuel fraction of the sample, ff_{sample}, and the remaining non-fossil fuel or contemporary fraction ($1- ff_{sample}$), are related by the following two-component mass balance:

$$Fm_{sample} = ff_{sample}\left(Fm_{ff}\right) + \left(1 - ff_{sample}\right)\left(Fm_{atm}\right)$$

In this formula, Fm_{sample} is the measured modern fraction of the sample, Fm_{ff} is the fraction of modern carbon in fossil fuel ($Fm_{ff} = 0$), and Fm_{atm} is the fraction of modern carbon in contemporary living material ($Fm_{atm} = 1.05$) (Hua et al., 2013). By convention, the reporting of carbon isotope analysis is based on a 1950 NBS oxalic acid standard, synthesized when the ^{14}C atmospheric levels were lower than current ones due to nuclear tests. Thus, Fm_{sample} is reported as if the analysis was done in 1950, and Fm_{atm} is counter-intuitively larger than 1.

Expected Results and Recommendations

The fossil-fuel carbon content on the unexposed sorbent is non-zero (typically around 35%). This might be the result of either a background fossil fuel signature of the sorbent (due to processing of the chemical or mineral sources), or due to material handling (i.e., exposure to fossil fuel fumes). Although the fossil fuel CO_2 mass is very small, this error is adjusted by a travel blank correction procedure. This consists of subtracting the fossil fuel CO_2 mass from an unexposed trap (a travel blank) from those measured on the traps deployed in the field. The ^{14}C analysis is done on CO_2 sorbent subsamples, after homogenization.

©2017 All Rights Reserved

Study Results

The report and results below are based on proprietary technology to measure the fossil fuel content of an environmental sample using E-Flux CO_2 cartridges. All information contained in this report is strictly confidential to the customer. The chemical analysis is based on methods ASTM 4373-02 (Rapid Determination for Carbonate Content in Soils) and ASTM D6686-12 (Determining the Biobased Content in Solids, Liquids and Gases Using Radiocarbon Analysis).

The site specific results and interpretation are as follows:

E-FLUX
Easy set-up. Expert results.

Project: Red Hill, Pearl Harbor-Hickam CO_2 Traps

Customer: AECOM

Customer Contact: Margie Pascua, (808) 356-5373

Updated Report Date: 13-Dec-17

Sample ID	Deployment Dates			Raw Results (not blank corrected)					Blank Corrected Results[a] and ^{14}C Analysis (Fossil Fuel)					
	Deployed	Retrieved	Days	Moisture	Dry Sorbent Mass (g)	Num. of Reps.[b]	Avg CO_2[b]	CV CO_2[c]	Carbon Content[d] %	Carbon Content[d] (g)	Modern Carbon, As Reported[e]	Std. Dev. Modern	Adjusted Fossil Fuel Carbon[f]	Grams Of Fossil Fuel CO_2 (g)
PHHI-C1-CO2-TB	NA	NA	0.00	20.6%	4.136	2	0.91%	7.22%	-	-	65.3%	0.30%	37.1%	-
PHHI-C1-CO2-01	10/25/17 10:05	10/26/17 8:20	0.93	3.1%	4.858	2	25.92%	0.57%	25.0%	1.22	101.8%	0.40%	1.9%	0.01
PHHI-C1-CO2-02	10/26/17 8:26	10/27/17 8:33	1.00	3.0%	4.882	2	25.40%	0.77%	24.5%	1.20	100.5%	0.33%	3.1%	0.02
PHHI-C1-CO2-03	10/30/17 9:56	10/31/17 7:58	0.92	3.0%	5.005	2	28.41%	0.03%	27.5%	1.38	97.4%	0.32%	6.1%	0.07
PHHI-C1-CO2-04	10/31/17 8:00	11/1/17 8:13	1.01	2.9%	5.101	2	30.29%	0.07%	29.4%	1.50	98.3%	0.33%	5.3%	0.06
PHHI-C1-CO2-05	11/1/17 8:45	11/2/17 8:02	0.97	4.4%	4.877	2	25.57%	0.08%	24.7%	1.20	100.8%	0.30%	2.8%	0.02
PHHI-C1-CO2-06	11/2/17 8:07	11/3/17 6:15	0.92	3.0%	4.817	2	23.62%	0.99%	22.7%	1.09	104.0%	0.50%	ND	ND

This report contains Confidential Information and is to be delivered only to the Customer indicated above.

See following page for assumptions, project specific quality assurance/quality control information, and notes.

The Following Assumptions and General Notes apply for CO_2 fossil fuel analysis:

a. Results are travel blank corrected but not background location corrected.
Blank Corrected Results = Raw Results - Travel Blank

b. Number of Replicates: Carbon analysis was conducted in duplicate if CV ≤ 5%. If CV > 5%, carbon analysis was conducted with triplicates (see Quality Assurance/Quality Control notes). Avg % refers to the percent of CO_2 in the dry sorbent mass before blank corrected.

c. CV is coefficient of variation, equal to the ratio of the standard deviation over the average.

d. If the cartridge carbon content is not larger than travel blank, results are reported as ND. Expressed as CO_2 not pure carbon.

e. "As reported" refers to % modern carbon at the time of development of the test (1950).

f. Adjusted fossil fuel carbon has been transformed from the "As reported" basis (1950) to present ^{14}C levels.

g. Note that for this report a value of 1.038 was used in place of 1.05 so that the average grams of fossil fuel carbon for samples PHHI-C1-CO2-05 and PHHI-C1-CO2-06 equaled 0.

NA means Not Applicable.

Quality Assurance / Quality Control Notes:

- The Travel Blank (**PHHI-C1-CO2-TB**) concentration for this report was **0.91%**. Typical Travel Blank concentration is <2%.
- Cartridge tops were not saturated with CO_2, but some had appreciable CO_2 contents. The mass sorbed in the top element was up to 20% of the total mass sorbed in the whole cartridge. Because of the configuration of these cartridges, this could indicate CO_2 breakthrough from the bottom element, and total carbon may be underestimated by these results. Maximum measured top concentration was **8.20%** (sample **PHHI-C1-CO2-02.1**). Sorbent saturation is 30%.
- ASTM 4373-02 QA/QC criteria does not provide acceptable variability (CV) standards. Similar methods (for example the carbonates in water, such as ASTM 513.02) provide typical error ≤20%. E-Flux practice is that a CV ≤5% is acceptable. *Sample **PHHI-C1-CO2-TB** had a CV of **7.22%**; this could not be brought down to acceptable levels, as there was not enough sample mass.*

Calculation Explanations

Conversion of Modern C to Fossil Fuel C

Reported modern carbon content (from carbon dating or ^{14}C analysis) is by convention at the ^{14}C levels as of the time of development of the test (1950). Due to higher current levels of ^{14}C in the environment resulting from atomic testing, current (contemporary) levels are approximately 5% higher than in 1950 (Hua et al., 2013). Thus, fossil fuel C can be found with the following conversions:

$$\%\ Modern\ C_{contemporary} = \frac{\%\ Modern\ C_{1950}}{1.05}$$

$$Contemporary\ fossil\ fuel\ C\ \% = 1 - \%\ Modern\ C_{contemporary} = 1 - \frac{\%\ Modern\ C_{1950}}{1.05}$$

Note that for this report a value of 1.038 was used in place of 1.05 so that the average grams of fossil fuel carbon for samples PHHI-C1-CO2-05 and PHHI-C1-CO2-06 equaled 0.

Calculating Grams of Fossil Fuel CO_2

Calculating grams of fossil fuel (ff) CO_2 is based on the travel blank corrected percent fossil fuel carbon in the sample (the difference between total fossil fuel CO_2 in the sample and that of the travel blank). This is done as follows:

$$g\ CO_{2(ff)} = g\ sorbent * \left((Avg\ sample\ \%\ CO_2 * ff\ sample\ \%\ C) - (Avg\ TB\ \%\ CO_2 * ff\ TB\ \%\ C)\right)$$

N/A

©2017 All Rights Reserved

References

ASTM (2012), Method D6686-12, Determining the Biobased Content in Solids, Liquids and Gases Using Radiocarbon Analysis.

ASTM (2002), Method D4373-02, Standard Test Method for Rapid Determination of Carbonate Content of Soil.

Avery et al, (2006). Carbon isotopic characterization of dissolved organic carbon in rainwater: Terrestrial and marine influences. Atmos. Environ. p. 7539-7545.

Bauer, H.P.; Beckett, P.H.; and Bie, S.W. (1972). A Rapid Gravimetric Method for Estimating Calcium Carbonate in Soils, Plant and Soil, Vol 37, p. 689-690.

Hua, Q.; Barbetti, M.; and Rakowski, A.Z. (2013). Atmospheric Radiocarbon for the Period 1950-2010. Radiocarbon. 55(4), p. 2059-2072.

Klouda and Connolly, (1995). Radiocarbon (14C) Measurements to Quantify Sources of Atmospheric Carbon Monoxide in Urban Air. Atmos. Environ. p. 3309-3318.

Levin, I. R. Graul, Ne. Trivett. (1995). Long-term observations of atmospheric CO_2 and carbon isotopes at continental sites in Germany. Tellus., 47B, p. 23-34.

McCoy, K., Zimbron, J., Sale, T. and Lyverse, M. (2015), Measurement of Natural Losses of LNAPL Using CO2 Traps. Groundwater, 53: p. 658–667. doi:10.1111/gwat.12240.

Stuiver and Polach, (1977). Discussion. Reporting of ^{14}C data. Radiocarbon 19(3), p. 355–363.

Confidential Report
CO_2 Flux and NSZD Rate Results

MARGIE PASCUA
AECOM
PROJECT: RED HILL,
PEARL HARBOR-HICKAM
CO_2 TRAPS
SAMPLING DATES:
10/23/2017-11/9/2017

For technical support questions contact:

Julio Zimbron, Ph.D.
E-Flux, LLC
3185-A Rampart Road, Room D214
Fort Collins, CO 80521
o: (970) 492-4360 c: (970) 219-2401
jzimbron@soilgasflux.com

Report Date: 12/11/2017
© 2017 All Rights Reserved.

©2017 All Rights Reserved

The purpose of this document is to provide sample calculations of the results reported here and to explain the basis for differentiating petroleum hydrocarbon-derived CO_2 (i.e., fossil fuel CO_2) from modern CO_2 interferences. The following topics are addressed:

- The Value of ^{14}C Analysis
- Site Specific Study Results and Applicable Notes
- Calculation Explanations
- References

The Value of the ^{14}C Analysis

How to differentiate petroleum hydrocarbon-derived CO_2 from modern CO_2 interferences using CO_2 flux traps.

Unimpacted soils have natural CO_2 flux generation rates, due to microbial root zone activity and/or the degradation of natural organic matter (NOM). Thus, the total CO_2 flux measured at an impacted location is the sum of both natural soil respiration processes and those related to LNAPL degradation (Sihota et al, 2011).

The CO_2 flux due to natural soil respiration can be estimated by measuring CO_2 fluxes at unimpacted locations, and subtracting such rates from the total CO_2 fluxes at LNAPL impacted locations in order to estimate CO_2 flux due to LNAPL degradation (Sihota et al, 2012). This is known as the "background correction" and assumes that the rates of natural soil respiration (i.e., modern carbon CO_2 fluxes) are similar for both impacted and unimpacted locations.

The difficulties of this approach are: a) at many industrial facilities it is difficult to find unimpacted locations, and b) the unimpacted locations have very different vegetation to that at the impacted locations. This document provides the basis to use carbon isotope analysis as a location specific correction to the total carbon CO_2 fluxes, designed to overcome the limitations of the background correction.

Carbon Isotope Analysis Methodology

Upon sampling and analysis of the samples by the methods described before (McCoy et al, 2015), the analysis for carbon isotopes is conducted on the homogenized solid samples from the CO_2 flux traps.

Unstable isotopic analysis has been previously used to differentiate anthropogenic (due to fossil fuel-burning) and natural sources of atmospheric CO, CO_2 and methane (for example, Klouda and Connolly, 1995; Levin et al, 1995; Avery et al, 2006). Such findings are the basis of ASTM Method D6686-12, Determining the Biobased Content in Solids, Liquids and Gases Using Radiocarbon Analysis (ASTM, 2012). The technique relies on the analysis of ^{14}C, an unstable carbon isotope (with a half-life of approximately 5600 years) that is generated by cosmic rays in the atmosphere. Thus, contemporary (modern) organic carbon is ^{14}C-rich, while fossil fuel carbon is completely ^{14}C-depleted. Furthermore, contemporary samples and atmospheric samples have the same characteristic amount of ^{14}C. The detection limit of ^{14}C by accelerator mass spectrometry enables dating of samples younger than 60,000

years, while older samples (such as fossil fuels) have non-detectable ^{14}C activity (Stuiver and Polach, 1977).

For a sample that contains carbon from both modern and fossil fuel carbon sources, measurement of the ^{14}C enables quantitation of both source contributions. The fossil fuel fraction of the sample, ff_{sample}, and the remaining non-fossil fuel or contemporary fraction ($1- ff_{sample}$), are related by the following two-component mass balance:

$$Fm_{sample} = ff_{sample}\left(Fm_{ff}\right)+\left(1- ff_{sample}\right)\left(Fm_{atm}\right)$$

In this formula, Fm_{sample} is the measured modern fraction of the sample, Fm_{ff} is the fraction of modern carbon in fossil fuel ($Fm_{ff} = 0$), and Fm_{atm} is the fraction of modern carbon in contemporary living material ($Fm_{atm} = 1.05$) (Hua et al., 2013). By convention, the reporting of carbon isotope analysis is based on a 1950 NBS oxalic acid standard, synthesized when the ^{14}C atmospheric levels were lower than current ones due to nuclear tests. Thus, Fm_{sample} is reported as if the analysis was done in 1950, and Fm_{atm} is counter-intuitively larger than 1.

Expected Results and Recommendations

Our results suggest that the ^{14}C-based technique offers a built-in, location specific correction for fossil fuel as an alternative to the background correction often done at these sites. Earlier data on a limited amount of samples suggested that results using the ^{14}C-correction were equivalent to the background correction (McCoy et al, 2015; Sihota et al, 2012). However, a recent compilation at 4 sites comparing results from the background correction to the ^{14}C-correction suggests that modern carbon fluxes can vary over a factor of 5x for different locations within the same site (Zimbron and Kasyon, 2015). The resulting difference between the background-corrected estimates and the fossil-fuel carbon corrected data can be up to one order of magnitude (depending on the location).

This finding suggests that the assumption implied by the background correction that the modern carbon flux is constant for an entire site might introduce large errors in the correction for petroleum-biodegradation derived CO_2 fluxes. Contrary to the background correction, the ^{14}C-based correction is collocated with the measurement, and thus spatially unbiased by uncertainties related to differences with respect to background location(s) (i.e., due to different vegetation and lithology, unknown impacts, different gas transport regimes, high sensitivity to soil moisture, etc).

The fossil-fuel carbon content on the unexposed sorbent is non-zero (typically around 30%). This might be the result of either a background fossil fuel signature of the sorbent (due to processing of the chemical or mineral sources), or due to material handling (i.e., exposure to fossil fuel fumes). Although the fossil fuel CO_2 mass is very small, this error is adjusted by a travel blank correction procedure. This consists of subtracting the fossil fuel CO_2 mass from an unexposed trap (a travel blank) from those measured on the traps deployed in the field. The ^{14}C analysis is done on CO_2 sorbent subsamples, after homogenization.

©2017 All Rights Reserved

Study Results

The report and results below are based on proprietary technology to measure the soil gas efflux. All information contained in this report is strictly confidential to the customer. The chemical analysis is based on methods ASTM 4373-02 (Rapid Determination for Carbonate Content in Soils) and ASTM D6686-12 (Determining the Biobased Content in Solids, Liquids and Gases Using Radiocarbon Analysis).

The site specific results and interpretation are as follows:

EFLUX
Easy set-up. Expert results.

Project: Red Hill, Pearl Harbor-Hickam
CO_2 Traps

Customer: AECOM

Customer Contact: Margie Pascua, (808) 356-5373

Report Date: 11-Dec-17

Sample ID	Deployment Dates			Raw Results (not blank corrected)					Blank Corrected Results[a] and ^{14}C Analysis (Fossil Fuel)								
	Deployed	Retrieved	Days	Moisture	Dry Sorbent Mass (g)	Num. of Reps. [b]	Avg CO_2[b]	CV CO_2[c]	Carbon Content[d] %	Carbon Content[d] (g)	CO_2 Flux[e] (microM/ m^2.sec)	Modern Carbon, As Reported[g]	Std. Dev. Modern	Modern CO_2 Flux (microM/ m^2.sec)	Adjusted Fossil Fuel Carbon [h]	Grams Of Fossil Fuel CO_2 (g)	Fossil Fuel CO_2 Flux (microM/ m^2.sec)	Equivalent Fossil Fuel-Based NAPL Loss Rate (gallons/ acre.yr)
PHHI-R1-CO2-TB	NA	NA	0.00	19.4%	42.099	2	0.92%	1.21%	-	-	-	64.6%	0.21%	-	38.5%	-	-	-
PHHI-R1-CO2-01	10/26/17 8:20	11/9/17 10:25	14.09	16.9%	42.991	2	1.01%	1.95%	0.1%	0.04	0.1	66.5%	0.24%	0.1	36.7%	0.01	0.0	10
PHHI-R1-CO2-02	10/23/17 13:40	11/6/17 12:20	13.94	25.7%	41.747	2	3.66%	4.35%	2.7%	1.14	2.7	93.9%	0.26%	2.6	10.6%	0.01	0.0	21
PHHI-R1-CO2-03	10/24/17 11:10	11/7/17 12:57	14.07	21.0%	44.178	2	5.08%	1.42%	4.2%	1.84	4.2	98.5%	0.29%	4.3	6.2%	ND	ND	ND
PHHI-R1-CO2-04	10/24/17 16:00	11/7/17 11:15	13.80	25.7%	41.937	2	2.48%	1.42%	1.6%	0.65	1.5	89.9%	0.26%	1.5	14.4%	0.00	0.0	2
PHHI-R1-CO2-05	10/24/17 15:10	11/7/17 11:22	13.84	20.7%	44.826	2	5.54%	4.55%	4.6%	2.07	4.9	98.3%	0.34%	4.9	6.4%	ND	ND	ND
PHHI-R1-CO2-06	10/23/17 14:35	11/6/17 12:32	13.91	21.6%	44.412	2	4.76%	0.15%	3.8%	1.71	4.0	97.6%	0.26%	4.0	7.0%	ND	ND	ND
PHHI-R1-CO2-07	10/23/17 11:30	11/6/17 12:05	14.02	24.6%	43.589	2	7.56%	2.15%	6.6%	2.90	6.7	99.6%	0.28%	6.7	5.2%	0.02	0.0	24
PHHI-R1-CO2-08	10/25/17 13:20	11/8/17 9:40	13.85	21.5%	45.130	2	5.97%	4.41%	5.0%	2.28	5.3	96.6%	0.27%	5.2	8.0%	0.06	0.1	84
PHHI-R1-CO2-09	10/25/17 12:30	11/8/17 10:00	13.90	23.7%	41.666	2	3.26%	0.23%	2.3%	0.98	2.3	94.1%	0.28%	2.3	10.4%	ND	ND	ND
PHHI-R1-CO2-10	10/26/17 8:50	11/9/17 10:55	14.09	17.8%	42.199	2	0.94%	4.78%	0.0%	0.01	0.0	68.2%	0.26%	0.0	35.0%	ND	ND	ND
PHHI-R1-CO2-TBB	NA	NA	0.00	21.0%	42.595	2	0.97%	0.61%	-	-	-	70.2%	0.21%	-	33.1%	-	-	-

This report contains Confidential Information and is to be delivered only to the Customer indicated above.

See following page for assumptions, project specific quality assurance/quality control information, and notes.

The Following Assumptions and General Notes apply for CO_2 traps:

a. Results are travel blank corrected but not background location corrected.
Blank Corrected Results = Raw Results - Travel Blank

b. Number of Replicates: Carbon analysis was conducted in duplicate if CV ≤ 5%. If CV > 5%, carbon analysis was conducted with triplicates. Avg % refers to the percent of CO_2 in the dry sorbent mass before blank corrected.

c. CV is coefficient of variation, equal to the ratio of the standard deviation over the average.

d. If trap carbon content is not larger than travel blank, results are reported as ND. Expressed as CO_2 not pure carbon.

e. Trap cross sectional area is **8.11×10^{-3}** m^2 (i.e., equivalent to a **4in** receiver pipe).

f. The flux equivalence is 1 microMole/(m^2.sec) equals **625** gallons/(acre.yr). This assumes a hydrocarbon density of **0.77** g/mL and a formula of **C_8H_{18}**.

g. "As reported" refers to % modern carbon at the time of development of the test (1950).

h. Adjusted fossil fuel carbon has been transformed from the "As reported" basis (1950) to present ^{14}C levels.

NA means Not Applicable.

Quality Assurance / Quality Control Notes:

- The Travel Blank (PHHI-R1-CO2-TB) concentration for this report was **0.92%.** Typical Travel Blank concentration is <2%. The additional travel blank (PHHI-R1-CO2-TBB) had a concentration of **0.97%.** Carbon contents were blank-corrected using **PHHI-R1-CO2-TB**.

- Trap tops were not saturated with CO_2. Maximum measured top concentration was **1.85%** (sample **PHHI-R1-CO2-01.1**). Sorbent saturation is 30%.

- Modern carbon fluxes represent the contribution of plant and microbial activity to the total carbon flux that the ^{14}C analysis corrects for. Average modern CO_2 flux was **3.16** microMole/m^2.s, with a coefficient of variation of **70%**.

- **PHHI-R1-CO2-03, PHHI-R1-CO2-05, PHHI-R1-CO2-06, PHHI-R1-CO2-09**, and **PHHI-R1-CO2-10** showed non-detectable fossil fuel CO_2 flux (ND). The totality of the CO_2 flux should be considered modern. Such samples are not included in the modern CO_2 flux average or coefficient of variation calculations.

- ASTM 4373-02 QA/QC criteria does not provide acceptable variability (CV) standards. Similar methods (for example the carbonates in water, such as ASTM 513.02) provide typical error ≤20%. E-Flux practice is that a CV ≤5% is acceptable.

Calculation Explanations

Conversion of grams CO_2 to CO_2 Flux

Calculating the CO_2 flux from grams of CO_2 involves the cross-sectional area of the trap as well as the number of days that the trap was deployed in the field. The cross-sectional area of the trap is 8.11 x 10^{-3} m^2 (for a 4in receiver). The molecular weight of CO_2 is 44 g/mol. Converting g of CO_2 to CO_2 flux is as follows:

$$\frac{\left(g\ CO_2 * \left(\frac{1\ mol\ CO_2}{44\ g\ CO_2}\right) * \left(\frac{1{,}000{,}000\ micromol\ CO_2}{mol\ CO_2}\right) * \left(\frac{1}{8.11 * 10^{-3}\ m^2}\right)\right)}{days\ in\ the\ field * \frac{24\ hr}{day} * \frac{3600\ sec}{hr}} = \frac{micro\ mol\ CO_2}{m^2 * sec}$$

Conversion of Modern C to Fossil Fuel C

Reported modern carbon content (from carbon dating or ^{14}C analysis) is by convention at the ^{14}C levels as of the time of development of the test (1950). Due to higher current levels of ^{14}C in the environment resulting from atomic testing, current (contemporary) levels are approximately 5% higher than in 1950 (Hua et al., 2013). Thus, fossil fuel C can be found with the following conversions:

$$\%\ Modern\ C_{contemporary} = \frac{\%\ Modern\ C_{1950}}{1.05}$$

$$Contemporary\ fossil\ fuel\ C\ \% = 1 - \%\ Modern\ C_{contemporary} = 1 - \frac{\%\ Modern\ C_{1950}}{1.05}$$

Calculating Grams of Fossil Fuel CO_2

Calculating grams of fossil fuel (ff) CO_2 is based on the travel blank corrected percent fossil fuel carbon in the sample (the difference between total fossil fuel CO_2 in the sample and that of the travel blank). This is done as follows:

$$g\ CO_{2(ff)} = g\ sorbent * \left((Avg\ sample\ \%\ CO_2 * ff\ sample\ \%\ C) - (Avg\ TB\ \%\ CO_2 * ff\ TB\ \%\ C)\right)$$

Calculation to Convert Carbon Flux to Equivalent LNAPL Loss Rate

The intermediate reactions for LNAPL mineralization include methanogenesis (production of methane and CO_2) and the subsequent aerobic oxidation of methane (into CO_2):

$$C_8H_{18} + 3.5\ H_2O \rightarrow 6.25\ CH_4 + 1.75\ CO_2$$

$$6.25\ CH_4 + 12.5\ O_2 \rightarrow 6.25\ CO_2 + 12.5\ H_2O$$

The overall reaction (the summation of both reactions), is:

$$C_8H_{18} + 12.5\ O_2 \rightarrow\ 9H_2O + 8\ CO_2$$

For C_8H_{18}, the molecular weight is 114.23 g/mole. Assuming an LNAPL density of 0.77 g/mL (in the upper range of gasoline, for a conservative estimate), the following unit conversion results:

$$1\frac{\mu Mole\ CO_2}{m^2\ s}$$
$$= \frac{\mu Mole\ CO_2}{m^2\ s} \times \left(\frac{1\ \mu Mole\ C_8H_{18}}{8\ \mu Mole\ CO_2}\right) \times \left(\frac{Mole}{1 \times 10^6 \mu Mole}\right) \times \left(\frac{4{,}046\ m^2}{1\ acre}\right) \times \left(\frac{3600\ s}{1\ h}\right) \times \left(\frac{24\ h}{1\ d}\right) \times \left(\frac{365\ d}{1\ yr}\right)$$
$$\times \left(\frac{114\ g\ C_8H_{18}}{1\ Mole\ C_8H_{18}}\right) \times \left(\frac{1\ mL\ C_8H_{18}}{0.77\ g\ C_8H_{18}}\right) \times \left(\frac{1\ L}{1000 mL}\right) \times \left(\frac{1\ gallon}{3.785\ L}\right) = 625\frac{gallon\ C_8H_{18}}{acre.yr}$$

Note that both the LNAPL formula and its density are assumed, and thus subject to uncertainty. If available, site specific data can be used.

Alternative assumptions on the LNAPL formula and its corresponding density generally result in slightly different conversion factors, within 10-15% of the value shown here. Thus, such uncertainty still results in an acceptable estimate.

©2017 All Rights Reserved

References

ASTM (2012), Method D6686-12, Determining the Biobased Content in Solids, Liquids and Gases Using Radiocarbon Analysis.

ASTM (2002), Method D4373-02, Standard Test Method for Rapid Determination of Carbonate Content of Soil.

Avery et al, (2006). Carbon isotopic characterization of dissolved organic carbon in rainwater: Terrestrial and marine influences. Atmos. Environ. p. 7539-7545.

Bauer, H.P.; Beckett, P.H.; and Bie, S.W. (1972). A Rapid Gravimetric Method for Estimating Calcium Carbonate in Soils, Plant and Soil, Vol 37, p. 689-690.

Hua, Q.; Barbetti, M.; and Rakowski, A.Z. (2013). Atmospheric Radiocarbon for the Period 1950-2010. Radiocarbon. 55(4), p. 2059-2072.

Klouda and Connolly, (1995). Radiocarbon (14C) Measurements to Quantify Sources of Atmospheric Carbon Monoxide in Urban Air. Atmos. Environ. p. 3309-3318.

Levin, I. R. Graul, Ne. Trivett. (1995). Long-term observations of atmospheric CO_2 and carbon isotopes at continental sites in Germany. Tellus., 47B, p. 23-34.

McCoy, K., Zimbron, J., Sale, T. and Lyverse, M. (2015), Measurement of Natural Losses of LNAPL Using CO2 Traps. Groundwater, 53: p. 658–667. doi:10.1111/gwat.12240.

Sihota, N. and U. Mayer. (2012). Characterizing vadose zone hydrocarbon biodegradation using CO2-effluxes, isotopes, and 2 reactive transport modeling. Vadose Zone Journal. Accepted for publication.

Stuiver and Polach, (1977). Discussion. Reporting of ^{14}C data. Radiocarbon 19(3), p. 355–363.

Zimbron, J. and E. Kasyon, (2015). Combined Use of Isotope Analysis and Passive CO_2 Flux Traps to Estimate Field Rates of Hydrocarbon Degradation. Battelle Remediation Conference. Miami FL, May 18-21.

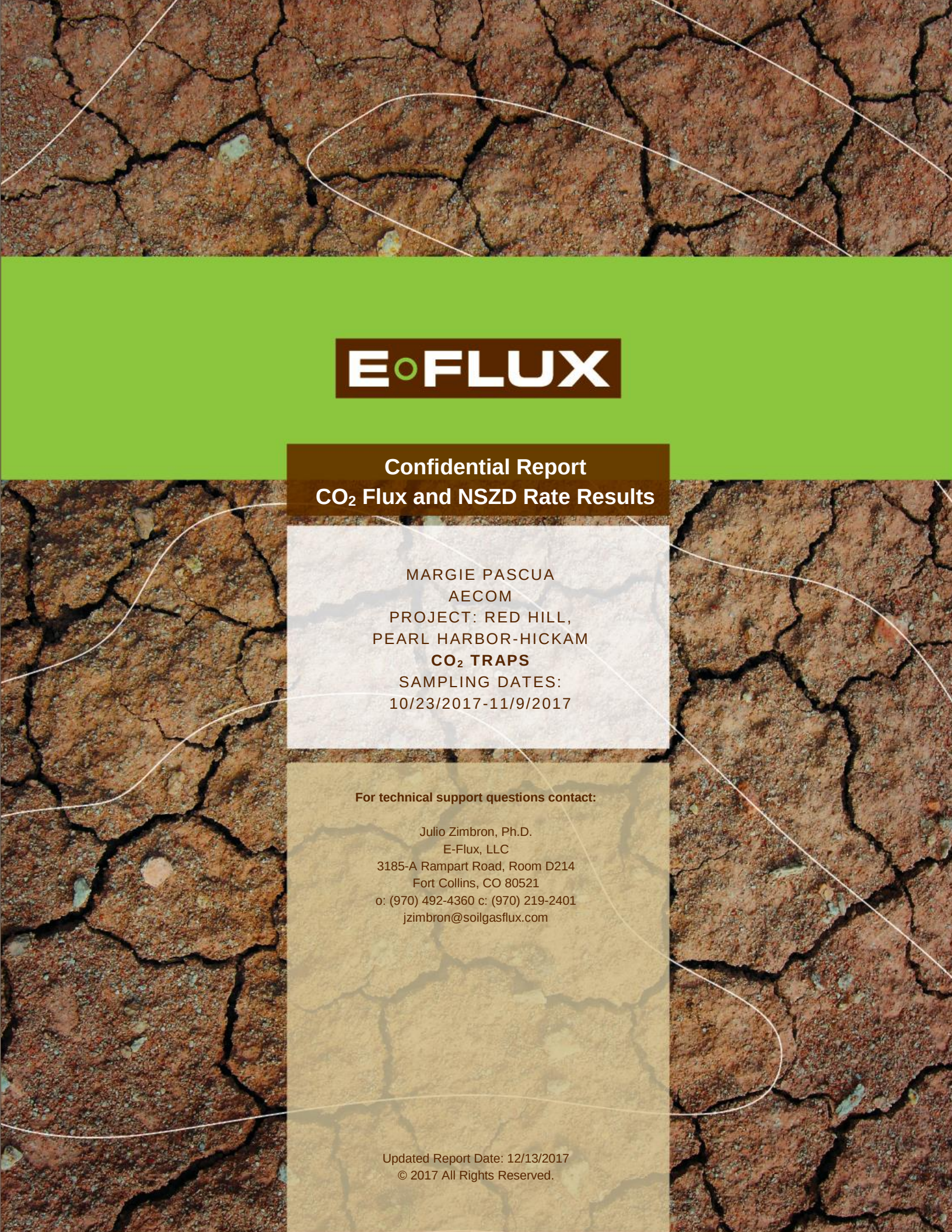

Confidential Report
CO_2 Flux and NSZD Rate Results

MARGIE PASCUA
AECOM
PROJECT: RED HILL,
PEARL HARBOR-HICKAM
CO_2 TRAPS
SAMPLING DATES:
10/23/2017-11/9/2017

For technical support questions contact:

Julio Zimbron, Ph.D.
E-Flux, LLC
3185-A Rampart Road, Room D214
Fort Collins, CO 80521
o: (970) 492-4360 c: (970) 219-2401
jzimbron@soilgasflux.com

Updated Report Date: 12/13/2017
© 2017 All Rights Reserved.

©2017 All Rights Reserved

The purpose of this document is to provide sample calculations of the results reported here and to explain the basis for differentiating petroleum hydrocarbon-derived CO_2 (i.e., fossil fuel CO_2) from modern CO_2 interferences. The following topics are addressed:

- The Value of ^{14}C Analysis
- Site Specific Study Results and Applicable Notes
- Calculation Explanations
- References

The Value of the ^{14}C Analysis

How to differentiate petroleum hydrocarbon-derived CO_2 from modern CO_2 interferences using CO_2 flux traps.

Unimpacted soils have natural CO_2 flux generation rates, due to microbial root zone activity and/or the degradation of natural organic matter (NOM). Thus, the total CO_2 flux measured at an impacted location is the sum of both natural soil respiration processes and those related to LNAPL degradation (Sihota et al, 2011).

The CO_2 flux due to natural soil respiration can be estimated by measuring CO_2 fluxes at unimpacted locations, and subtracting such rates from the total CO_2 fluxes at LNAPL impacted locations in order to estimate CO_2 flux due to LNAPL degradation (Sihota et al, 2012). This is known as the "background correction" and assumes that the rates of natural soil respiration (i.e., modern carbon CO_2 fluxes) are similar for both impacted and unimpacted locations.

The difficulties of this approach are: a) at many industrial facilities it is difficult to find unimpacted locations, and b) the unimpacted locations have very different vegetation to that at the impacted locations. This document provides the basis to use carbon isotope analysis as a location specific correction to the total carbon CO_2 fluxes, designed to overcome the limitations of the background correction.

Carbon Isotope Analysis Methodology

Upon sampling and analysis of the samples by the methods described before (McCoy et al, 2015), the analysis for carbon isotopes is conducted on the homogenized solid samples from the CO_2 flux traps.

Unstable isotopic analysis has been previously used to differentiate anthropogenic (due to fossil fuel-burning) and natural sources of atmospheric CO, CO_2 and methane (for example, Klouda and Connolly, 1995; Levin et al, 1995; Avery et al, 2006). Such findings are the basis of ASTM Method D6686-12, Determining the Biobased Content in Solids, Liquids and Gases Using Radiocarbon Analysis (ASTM, 2012). The technique relies on the analysis of ^{14}C, an unstable carbon isotope (with a half-life of approximately 5600 years) that is generated by cosmic rays in the atmosphere. Thus, contemporary (modern) organic carbon is ^{14}C-rich, while fossil fuel carbon is completely ^{14}C-depleted. Furthermore, contemporary samples and atmospheric samples have the same characteristic amount of ^{14}C. The detection limit of ^{14}C by accelerator mass spectrometry enables dating of samples younger than 60,000

years, while older samples (such as fossil fuels) have non-detectable ^{14}C activity (Stuiver and Polach, 1977).

For a sample that contains carbon from both modern and fossil fuel carbon sources, measurement of the ^{14}C enables quantitation of both source contributions. The fossil fuel fraction of the sample, ff_{sample}, and the remaining non-fossil fuel or contemporary fraction ($1- ff_{sample}$), are related by the following two-component mass balance:

$$Fm_{sample} = ff_{sample}\left(Fm_{ff}\right)+\left(1- ff_{sample}\right)\left(Fm_{atm}\right)$$

In this formula, Fm_{sample} is the measured modern fraction of the sample, Fm_{ff} is the fraction of modern carbon in fossil fuel ($Fm_{ff} = 0$), and Fm_{atm} is the fraction of modern carbon in contemporary living material ($Fm_{atm} = 1.05$) (Hua et al., 2013). By convention, the reporting of carbon isotope analysis is based on a 1950 NBS oxalic acid standard, synthesized when the ^{14}C atmospheric levels were lower than current ones due to nuclear tests. Thus, Fm_{sample} is reported as if the analysis was done in 1950, and Fm_{atm} is counter-intuitively larger than 1.

Expected Results and Recommendations

Our results suggest that the ^{14}C-based technique offers a built-in, location specific correction for fossil fuel as an alternative to the background correction often done at these sites. Earlier data on a limited amount of samples suggested that results using the ^{14}C-correction were equivalent to the background correction (McCoy et al, 2015; Sihota et al, 2012). However, a recent compilation at 4 sites comparing results from the background correction to the ^{14}C-correction suggests that modern carbon fluxes can vary over a factor of 5x for different locations within the same site (Zimbron and Kasyon, 2015). The resulting difference between the background-corrected estimates and the fossil-fuel carbon corrected data can be up to one order of magnitude (depending on the location).

This finding suggests that the assumption implied by the background correction that the modern carbon flux is constant for an entire site might introduce large errors in the correction for petroleum-biodegradation derived CO_2 fluxes. Contrary to the background correction, the ^{14}C-based correction is collocated with the measurement, and thus spatially unbiased by uncertainties related to differences with respect to background location(s) (i.e., due to different vegetation and lithology, unknown impacts, different gas transport regimes, high sensitivity to soil moisture, etc).

The fossil-fuel carbon content on the unexposed sorbent is non-zero (typically around 30%). This might be the result of either a background fossil fuel signature of the sorbent (due to processing of the chemical or mineral sources), or due to material handling (i.e., exposure to fossil fuel fumes). Although the fossil fuel CO_2 mass is very small, this error is adjusted by a travel blank correction procedure. This consists of subtracting the fossil fuel CO_2 mass from an unexposed trap (a travel blank) from those measured on the traps deployed in the field. The ^{14}C analysis is done on CO_2 sorbent subsamples, after homogenization.

©2017 All Rights Reserved

Study Results

The report and results below are based on proprietary technology to measure the soil gas efflux. All information contained in this report is strictly confidential to the customer. The chemical analysis is based on methods ASTM 4373-02 (Rapid Determination for Carbonate Content in Soils) and ASTM D6686-12 (Determining the Biobased Content in Solids, Liquids and Gases Using Radiocarbon Analysis).

The site specific results and interpretation are as follows:

EoFLUX
Easy set-up. Expert results.

Project: Red Hill, Pearl Harbor-Hickam CO_2 Traps

Customer: AECOM

Customer Contact: Margie Pascua, (808) 356-5373

Updated Report Date: 13-Dec-17

Sample ID	Deployment Dates			Raw Results (not blank corrected)					Blank Corrected Results[a] and ^{14}C Analysis (Fossil Fuel)								
	Deployed	Retrieved	Days	Moisture	Dry Sorbent Mass (g)	Num. of Reps. [b]	Avg CO_2[b]	CV CO_2[c]	Carbon Content[d] %	Carbon Content[d] (g)	CO_2 Flux[e] (microM/ m^2.sec)	Modern Carbon, As Reported[g]	Std. Dev. Modern	Modern CO_2 Flux (microM/ m^2.sec)	Adjusted Fossil Fuel Carbon [h]	Grams Of Fossil Fuel CO_2 (g)	Fossil Fuel CO_2 Flux (microM/ m^2.sec)	Equivalent Fossil Fuel-Based NAPL Loss Rate (gallons/ acre.yr)
PHHI-R1-CO2-TB	NA	NA	0.00	19.4%	42.099	2	0.92%	1.21%	-	-	-	64.6%	0.21%	-	37.8%	0	-	-
PHHI-R1-CO2-01	10/26/17 8:20	11/9/17 10:25	14.09	16.9%	42.991	2	1.01%	1.95%	0.1%	0.04	0.1	66.5%	0.24%	0.1	36.0%	0.01	0.0	9
PHHI-R1-CO2-02	10/23/17 13:40	11/6/17 12:20	13.94	25.7%	41.747	2	3.66%	4.35%	2.7%	1.14	2.7	93.9%	0.26%	2.7	9.6%	0.00	0.0	2
PHHI-R1-CO2-03	10/24/17 11:10	11/7/17 12:57	14.07	21.0%	44.178	2	5.08%	1.42%	4.2%	1.84	4.2	98.5%	0.29%	4.3	5.1%	ND	ND	ND
PHHI-R1-CO2-04	10/24/17 16:00	11/7/17 11:15	13.80	25.7%	41.937	2	2.48%	1.42%	1.6%	0.65	1.5	89.9%	0.26%	1.6	13.4%	ND	ND	ND
PHHI-R1-CO2-05	10/24/17 15:10	11/7/17 11:22	13.84	20.7%	44.826	2	5.54%	4.55%	4.6%	2.07	4.9	98.3%	0.34%	4.9	5.3%	ND	ND	ND
PHHI-R1-CO2-06	10/23/17 14:35	11/6/17 12:32	13.91	21.6%	44.412	2	4.76%	0.15%	3.8%	1.71	4.0	97.6%	0.26%	4.0	6.0%	ND	ND	ND
PHHI-R1-CO2-07	10/23/17 11:30	11/6/17 12:05	14.02	24.6%	43.589	2	7.56%	2.15%	6.6%	2.90	6.7	99.6%	0.28%	6.7	4.1%	ND	ND	ND
PHHI-R1-CO2-08	10/25/17 13:20	11/8/17 9:40	13.85	21.5%	45.130	2	5.97%	4.41%	5.0%	2.28	5.3	96.6%	0.27%	5.3	7.0%	0.03	0.1	45
PHHI-R1-CO2-09	10/25/17 12:30	11/8/17 10:00	13.90	23.7%	41.666	2	3.26%	0.23%	2.3%	0.98	2.3	94.1%	0.28%	2.3	9.4%	ND	ND	ND
PHHI-R1-CO2-10	10/26/17 8:50	11/9/17 10:55	14.09	17.8%	42.199	2	0.94%	4.78%	0.0%	0.01	0.0	68.2%	0.26%	0.0	34.3%	ND	ND	ND
PHHI-R1-CO2-TBB	NA	NA	0.00	21.0%	42.595	2	0.97%	0.61%	-	-	-	70.2%	0.21%	-	33.1%	-	-	-

This report contains Confidential Information and is to be delivered only to the Customer indicated above.

See following page for assumptions, project specific quality assurance/quality control information, and notes.

The Following Assumptions and General Notes apply for CO_2 traps:

a. Results are travel blank corrected but not background location corrected.
Blank Corrected Results = Raw Results - Travel Blank

b. Number of Replicates: Carbon analysis was conducted in duplicate if CV ≤ 5%. If CV > 5%, carbon analysis was conducted with triplicates. Avg % refers to the percent of CO_2 in the dry sorbent mass before blank corrected.

c. CV is coefficient of variation, equal to the ratio of the standard deviation over the average.

d. If trap carbon content is not larger than travel blank, results are reported as ND. Expressed as CO_2 not pure carbon.

e. Trap cross sectional area is **8.11×10^{-3}** m^2 (i.e., equivalent to a **4in** receiver pipe).

f. The flux equivalence is 1 microMole/(m^2.sec) equals **625** gallons/(acre.yr). This assumes a hydrocarbon density of **0.77** g/mL and a formula of **C_8H_{18}**.

g. "As reported" refers to % modern carbon at the time of development of the test (1950).

h. Adjusted fossil fuel carbon has been transformed from the "As reported" basis (1950) to present ^{14}C levels.

NA means Not Applicable.

Quality Assurance / Quality Control Notes:

- The Travel Blank (PHHI-R1-CO2-TB) concentration for this report was **0.92%.** Typical Travel Blank concentration is <2%. The additional travel blank (PHHI-R1-CO2-TBB) had a concentration of **0.97%.** Carbon contents were blank-corrected using **PHHI-R1-CO2-TB**.

- Trap tops were not saturated with CO_2. Maximum measured top concentration was **1.85%** (sample **PHHI-R1-CO2-01.1**). Sorbent saturation is 30%.

- Modern carbon fluxes represent the contribution of plant and microbial activity to the total carbon flux that the ^{14}C analysis corrects for. Average modern CO_2 flux was **3.20** microMole/m^2.s, with a coefficient of variation of **70%**.

- **PHHI-R1-CO2-03, PHHI-R1-CO2-04, PHHI-R1-CO2-05, PHHI-R1-CO2-06, PHHI-R1-CO2-07, PHHI-R1-CO2-09**, and **PHHI-R1-CO2-10** showed non-detectable fossil fuel CO_2 flux (ND). The totality of the CO_2 flux should be considered modern. Such samples are not included in the modern CO_2 flux average or coefficient of variation calculations.

- ASTM 4373-02 QA/QC criteria does not provide acceptable variability (CV) standards. Similar methods (for example the carbonates in water, such as ASTM 513.02) provide typical error ≤20%. E-Flux practice is that a CV ≤5% is acceptable.

Calculation Explanations

Conversion of grams CO_2 to CO_2 Flux

Calculating the CO_2 flux from grams of CO_2 involves the cross-sectional area of the trap as well as the number of days that the trap was deployed in the field. The cross-sectional area of the trap is 8.11 x 10^{-3} m^2 (for a 4in receiver). The molecular weight of CO_2 is 44 g/mol. Converting g of CO_2 to CO_2 flux is as follows:

$$\frac{\left(g\ CO_2 * \left(\frac{1\ mol\ CO_2}{44\ g\ CO_2}\right) * \left(\frac{1{,}000{,}000\ micromol\ CO_2}{mol\ CO_2}\right) * \left(\frac{1}{8.11 * 10^{-3}\ m^2}\right)\right)}{days\ in\ the\ field * \frac{24\ hr}{day} * \frac{3600\ sec}{hr}} = \frac{micro\ mol\ CO_2}{m^2 * sec}$$

Conversion of Modern C to Fossil Fuel C

Reported modern carbon content (from carbon dating or ^{14}C analysis) is by convention at the ^{14}C levels as of the time of development of the test (1950). Due to higher current levels of ^{14}C in the environment resulting from atomic testing, current (contemporary) levels are approximately 5% higher than in 1950 (Hua et al., 2013). Thus, fossil fuel C can be found with the following conversions:

$$\%\ Modern\ C_{contemporary} = \frac{\%\ Modern\ C_{1950}}{1.05}$$

$$Contemporary\ fossil\ fuel\ C\ \% = 1 - \%\ Modern\ C_{contemporary} = 1 - \frac{\%\ Modern\ C_{1950}}{1.05}$$

Note that for this report a value of 1.038 was used in place of 1.05 so that the average grams of fossil fuel carbon for samples PHHI-C1-CO2-05 and PHHI-C1-CO2-06 equaled 0.

Calculating Grams of Fossil Fuel CO_2

Calculating grams of fossil fuel (ff) CO_2 is based on the travel blank corrected percent fossil fuel carbon in the sample (the difference between total fossil fuel CO_2 in the sample and that of the travel blank). This is done as follows:

$$g\ CO_{2(ff)} = g\ sorbent * \left((Avg\ sample\ \%\ CO_2 * ff\ sample\ \%\ C) - (Avg\ TB\ \%\ CO_2 * ff\ TB\ \%\ C)\right)$$

Calculation to Convert Carbon Flux to Equivalent LNAPL Loss Rate

The intermediate reactions for LNAPL mineralization include methanogenesis (production of methane and CO_2) and the subsequent aerobic oxidation of methane (into CO_2):

$$C_8H_{18} + 3.5\ H_2O \rightarrow 6.25\ CH_4 + 1.75\ CO_2$$

$$6.25\ CH_4 + \ 12.5\ O_2 \ \rightarrow 6.25\ CO_2 + 12.5\ H_2O$$

The overall reaction (the summation of both reactions), is:

$$C_8H_{18} + 12.5\ O_2 \rightarrow \ 9H_2O + 8\ CO_2$$

For C_8H_{18}, the molecular weight is 114.23 g/mole. Assuming an LNAPL density of 0.77 g/mL (in the upper range of gasoline, for a conservative estimate), the following unit conversion results:

$$1\frac{\mu Mole\ CO_2}{m^2\ s}$$
$$= \frac{\mu Mole\ CO_2}{m^2\ s} \times \left(\frac{1\ \mu Mole\ C_8H_{18}}{8\ \mu Mole\ CO_2}\right) \times \left(\frac{Mole}{1 \times 10^6 \mu Mole}\right) \times \left(\frac{4{,}046\ m^2}{1\ acre}\right) \times \left(\frac{3600\ s}{1\ h}\right) \times \left(\frac{24\ h}{1\ d}\right) \times \left(\frac{365\ d}{1\ yr}\right)$$
$$\times \left(\frac{114\ g\ C_8H_{18}}{1\ Mole\ C_8H_{18}}\right) \times \left(\frac{1\ mL\ C_8H_{18}}{0.77\ g\ C_8H_{18}}\right) \times \left(\frac{1\ L}{1000 mL}\right) \times \left(\frac{1\ gallon}{3.785\ L}\right) = 625\frac{gallon\ C_8H_{18}}{acre.yr}$$

Note that both the LNAPL formula and its density are assumed, and thus subject to uncertainty. If available, site specific data can be used.

Alternative assumptions on the LNAPL formula and its corresponding density generally result in slightly different conversion factors, within 10-15% of the value shown here. Thus, such uncertainty still results in an acceptable estimate.

©2017 All Rights Reserved

References

ASTM (2012), Method D6686-12, Determining the Biobased Content in Solids, Liquids and Gases Using Radiocarbon Analysis.

ASTM (2002), Method D4373-02, Standard Test Method for Rapid Determination of Carbonate Content of Soil.

Avery et al, (2006). Carbon isotopic characterization of dissolved organic carbon in rainwater: Terrestrial and marine influences. Atmos. Environ. p. 7539-7545.

Bauer, H.P.; Beckett, P.H.; and Bie, S.W. (1972). A Rapid Gravimetric Method for Estimating Calcium Carbonate in Soils, Plant and Soil, Vol 37, p. 689-690.

Hua, Q.; Barbetti, M.; and Rakowski, A.Z. (2013). Atmospheric Radiocarbon for the Period 1950-2010. Radiocarbon. 55(4), p. 2059-2072.

Klouda and Connolly, (1995). Radiocarbon (14C) Measurements to Quantify Sources of Atmospheric Carbon Monoxide in Urban Air. Atmos. Environ. p. 3309-3318.

Levin, I. R. Graul, Ne. Trivett. (1995). Long-term observations of atmospheric CO_2 and carbon isotopes at continental sites in Germany. Tellus., 47B, p. 23-34.

McCoy, K., Zimbron, J., Sale, T. and Lyverse, M. (2015), Measurement of Natural Losses of LNAPL Using CO2 Traps. Groundwater, 53: p. 658–667. doi:10.1111/gwat.12240.

Sihota, N. and U. Mayer. (2012). Characterizing vadose zone hydrocarbon biodegradation using CO2-effluxes, isotopes, and 2 reactive transport modeling. Vadose Zone Journal. Accepted for publication.

Stuiver and Polach, (1977). Discussion. Reporting of ^{14}C data. Radiocarbon 19(3), p. 355–363.

Zimbron, J. and E. Kasyon, (2015). Combined Use of Isotope Analysis and Passive CO_2 Flux Traps to Estimate Field Rates of Hydrocarbon Degradation. Battelle Remediation Conference. Miami FL, May 18-21.

Appendix B.3:
Soil Vapor Analysis

CONTENTS

Acronyms and Abbreviations iv

1. Introduction 1-1

1.1 Technical Background 1-1
1.2 Study Objectives 1-2

2. Field Methods and Procedures 2-1

2.1 Selection of Sample Locations for Analysis 2-1
2.2 Installation of Shallow Soil Vapor Points 2-1
2.3 Installation of Soil Vapor Probes (Vapor Pins) through Tunnel Walls 2-3
2.4 Soil Vapor Sampling Procedures 2-3
2.5 Monitoring Well Headspace Sampling Procedures 2-4
2.6 Laboratory Analysis 2-6

3. Investigation Results 3-1

3.1 Laboratory Analysis of VOCs in Soil Vapor Samples 3-1
3.1.1 Magnitude of Petroleum Vapors 3-1
3.1.2 Composition of Petroleum Vapors 3-3
3.1.3 Tentatively Identified Compounds in Soil Vapor Samples 3-6
3.1.4 Evaluation of FID Chromatograms 3-6
3.2 Field Measurements 3-8
3.2.1 PID Readings 3-8
3.2.2 Oxygen, Carbon Dioxide, and Methane 3-8
3.2.3 Differential Pressure 3-9
3.3 Correlation between Field Measurements and Laboratory Results 3-9
3.3.1 Field PID Readings vs. Laboratory Total Quantified VOC Concentrations 3-9
3.3.2 Field vs. Laboratory Oxygen, Carbon Dioxide, and Methane Concentrations 3-10

4. Discussion of Soil Vapor Investigation Results 4-1

5. Gradient Method for Measuring NSZD 5-1

5.1 Technical Background 5-1
5.2 Gradient Method Data Collection 5-1
5.3 Soil Vapor Carbon Dioxide and Gradient Profiles 5-2
5.4 Reasons for Complex Soil Vapor Oxygen Profiles at the Facility 5-3
5.4.1 Horizontal Oxygen Migration 5-3
5.4.2 Tunnel System Acting Like Soil Vapor Extraction (SVE) System 5-4
5.5 Gradient Method Conclusions 5-5

6. References 6-1

ATTACHMENTS

B.3.1 Fingerprint Charts for Soil Vapor and Groundwater Monitoring Well Headspace Samples

B.3.2 FID Chromatograms for Soil Vapor and Groundwater Monitoring Well Headspace Samples

B.3.3 Soil Vapor Field Monitoring Results

B.3.4 Soil Vapor and Groundwater Monitoring Well Headspace Sample Analytical Results

B.3.5 LNAPL Indications from Drilling Fluids and Boring Logs for Borings Completed Below Fuel Storage Tanks (Most Borings Completed 1998–2001)

B.3.6 Laboratory Report and EDD for Soil Vapor Samples Analyzed by Alpha Analytical: Laboratory Job Number L1740493

FIGURES

1-1 Facility Tank Farm 1-1

1-2 Typical Soil Vapor Monitoring Well Construction Details 1-2

2-1 Locations of Shallow Soil Vapor Wells Installed On Top of Red Hill Near Carbon Trap Locations T2 and T6 2-2

2-2 Illustration of Connection Between Soil Vapor Well and Summa Canister 2-4

2-3 Illustration of Vapor Sample Collection from Monitoring Well 2-6

3-1 Total Concentration of Quantified VOCs in Soil Vapor Samples 3-2

3-2 Distribution of Alkanes in Soil Vapor Samples for All Samples Except Tank 5 3-4

3-3 Distribution of Alkanes in Soil Vapor Samples for Tank 5 3-5

3-4 FID Chromatograms from Representative Samples Showing Range of Unresolved Hump 3-7

3-5 Correlation Between PID Readings and Laboratory Total Target Analytes Plus TICs 3-9

3-6 Correlation Between Field- and Laboratory-Measured Oxygen Concentration 3-11

3-7 Correlation Between Field- and Laboratory-Measured Oxygen Concentration Excluding Two Low-Biased Laboratory Measurements 3-11

3-8 Correlation Between Field- and Laboratory-Measured Carbon Dioxide Concentration 3-12

4-1 Top: LNAPL Indications from Drilling Fluids; Bottom: LNAPL Indications from Boring Logs 4-2

4-2 Linear Scale Graph of Monthly PID Monitoring Results for Below Fuel Tank Soil Vapor Wells 4-4

4-3 Monthly PID Monitoring Results for Below-Tank Soil Vapor Wells 4-6

4-4 Log Scale Graph of Monthly PID Monitoring Results for Below-Tank Soil Vapor Wells 4-7

5-1 Oxygen vs. Elevation Data Collected at the Facility 5-2

5-2 Left: Soil Vapor Data Collected at Oil Field Site; Right: Actual Data from Figure 5-1 vs. Expected Pattern if Gradient Method Conditions Were Met 5-3

5-3 Vertical Location of Tank 5 in North-South Cross Section Between Tanks 5 and 6 5-4

TABLES

2-1 Petroleum VOC Analyte List for TO-15 PIANO Analysis 2-7

4-1 Study Question 1: Is There Evidence of Recent or Historical Fuel Releases at One or More of the Tanks? 4-1

4-2 Study Question 2: Is LNAPL Present below the Tanks? 4-1

4-3 Study Question 3: Is NSZD Occurring? 4-3

4-4 Study Question 4: Can Vapor Monitoring Help Detect New LNAPL Fuel Releases? 4-3

4-5 Study Question 5: Can Vapor Monitoring Help Quantify the Magnitude of NSZD? 4-5

4-6 Study Question 6: Are Vadose-Zone Petroleum Vapors a Significant Source of Impacts In the Tunnels? 4-8

4-7 Summary of PID Measurements in the Tunnels 4-9

ACRONYMS AND ABBREVIATIONS

bgs	below ground surface
cfm	cubic feet per minute
CSM	conceptual site model
ENV	Environmental Protection Agency, United States
FID	flame ionization detector
ft	foot/feet
GC	gas chromatograph/chromatograph
Hg	mercury
L	liter
LNAPL	light non-aqueous-phase liquid
mbar	millibar
mL	milliliter
MS	mass spectrum
msl	mean sea level
NAPL	non-aqueous-phase liquid
NSZD	natural source-zone depletion
PIANO	paraffin, isoparaffin, aromatic, naphthene, and olefin compounds
PID	photoionization detector
ppbv	parts per billion by volume
ppm	parts per million
ppmv	parts per million by volume
ppt	parts per thousand
SOP	standard operating procedure
SVE	soil vapor extraction
SVMP	soil vapor monitoring point
TIC	tentatively identified compound
TPH	total petroleum hydrocarbons
UCM	unresolved complex mixture
VOC	volatile organic compound

1. Introduction

This subappendix is summarized in Section 7.3.1.4 of the Conceptual Site Model (CSM) main document.

1.1 TECHNICAL BACKGROUND

The Red Hill Bulk Fuel Storage Facility (the "Facility") tank farm is a complex of 20 petroleum storage tanks constructed inside Red Hill (Figure 1-1).

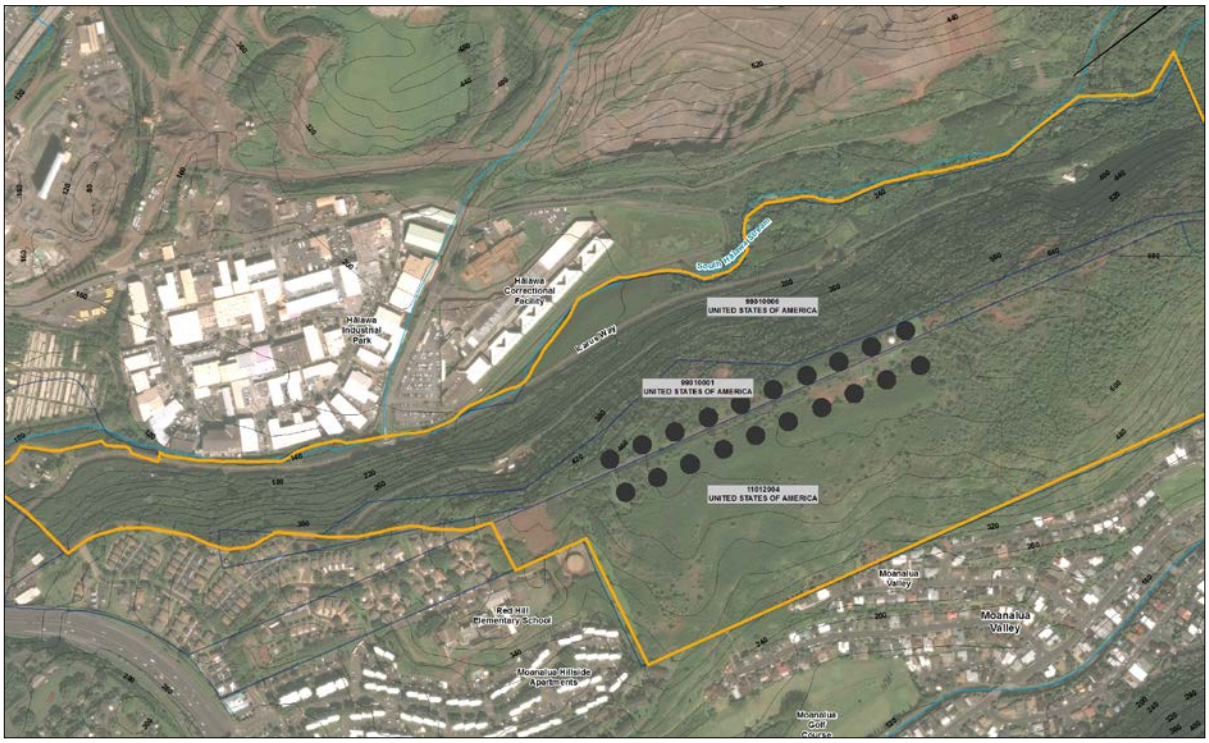

Figure 1-1: Facility Tank Farm

The 20 fuel storage tanks have been used mostly for storage of jet fuel such as JP-5 and JP-8 and to a lesser extent marine diesel fuel, fuel oil, and gasoline. Because of the predominance of jet fuel in the tanks and in the January 2014 release, this subappendix uses jet fuel as the primary reference fuel for the evaluation of the soil vapor data.

Section 3 of the CSM main document provides more detailed background information on the Facility. From 1998 to 2002, angle borings were installed below each tank. In 2006, soil vapor monitoring wells were constructed inside these existing boreholes below each tank except for Tank 1 and Tank 19, which were already permanently out of service. Two to three vapor monitoring wells were installed in each of the existing boreholes (Figure 1-2). This yielded a robust network of 47 soil vapor monitoring wells below active tanks.

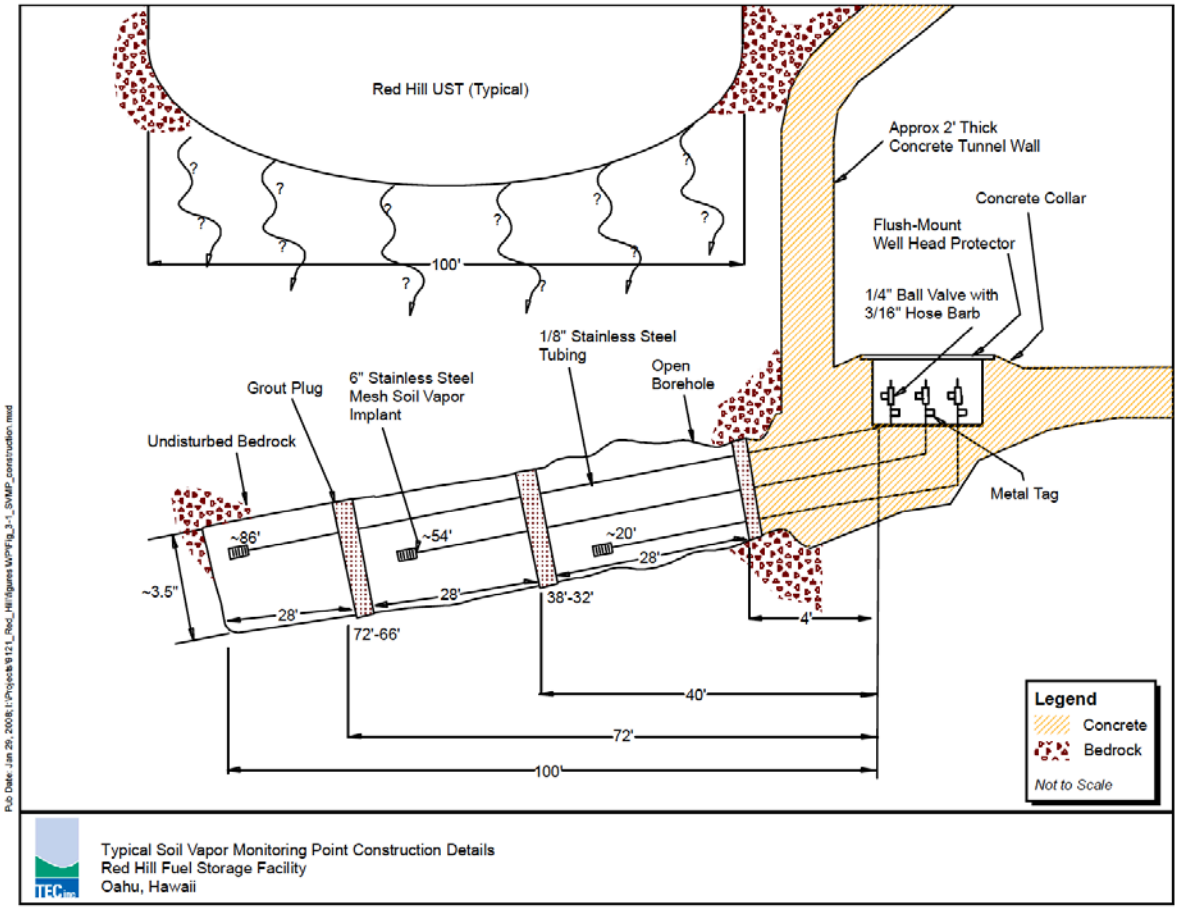

Source: TEC 2010.

Figure 1-2: Typical Soil Vapor Monitoring Well Construction Details

Historically, a small number of vapor samples had been collected for laboratory analysis of volatile organic compounds (VOCs) and total petroleum hydrocarbons (TPH). More recently, the vapor wells have been used for field screening (TEC 2010). Most of these vapor wells are monitored monthly using a field portable photoionization detector (PID) to measure total VOC concentrations. Despite the technical analysis presented in TEC (2010), PID readings alone provide little or no ability to distinguish between dissolved and light non-aqueous-phase liquid (LNAPL) petroleum contamination. Additional data may provide an improved ability to characterize sources and interpret temporal variations in PID readings.

1.2 STUDY OBJECTIVES

The vapor sampling program described in this subappendix was completed to (1) provide a better understanding of recent and historical fuel releases at the Facility, (2) support assessment of the natural source-zone depletion (NSZD) whereby LNAPL is degraded in the subsurface by biodegradation and other naturally occurring processes, and (3) assess how vapor monitoring might aid in detection of potential future LNAPL fuel releases at the Facility.

2. Field Methods and Procedures

Field measurements and collection of samples for laboratory analysis were completed between October 25 and November 2, 2017. Activities included the following:

- Field measurements and soil vapor sampling from the existing soil vapor wells below the fuel tanks
- Installation of and field measurements at two shallow soil vapor points on top of the tank farm
- Installation of and field measurements at two Cox-Colvin Vapor Pin locations in the upper tunnel
- Field measurements and well headspace vapor sampling from monitoring wells RHMW01, RHMW02, RHMW03, and RHMW04

2.1 Selection of Sample Locations for Analysis

Existing and newly installed soil vapor points and monitoring wells were selected for field measurements. This included the following:

- Forty-seven existing below-tank soil vapor wells at 18 tanks. Tanks 2–18 and Tank 20 have soil vapor monitoring wells. Tanks 1 and 19 are no longer in service and do not have soil vapor monitoring wells. All of the remaining tanks have three soil vapor monitoring wells except for Tanks 6, 10, 11, and 18, which each have two soil vapor wells. No field screening or soil vapor sampling was conducted at Tank 17 because a physical structure constructed for tank maintenance blocked access to the soil vapor wells at the time of the field investigation.
- Two shallow soil vapor wells installed on top of the tank farm above Tank 5 and Tank 11.
- Two new Vapor Pin points installed in the upper tunnel (at Tank 5 and Tank 11).
- Monitoring wells RHMW01, RHMW02, RHMW03, and RHMW04 were selected for collection of well headspace samples.

2.2 Installation of Shallow Soil Vapor Points

Shallow soil vapor sample points were installed above Tanks 5 and 11 near locations T2 and T6 (Figure 2-1). First, a hand auger was used to drill a hole to a depth of 5 feet (ft) below ground surface (bgs). 1/8-inch outside diameter nylon tubing with a porous sampling point at the end was lowered into the hole and the porous point was emplaced within 6 inches of sand (3 inches below and 3 inches above). One foot of dry bentonite was poured above the sand, and the rest of the hole was filled with hydrated bentonite in a stepwise fashion (a small amount of dry bentonite poured in, then water poured in to hydrate the bentonite; this process was repeated to the top of the hole). At the surface, a three-way valve was connected to the nylon tubing using Masterflex tubing and set so that the below-ground tubing was isolated from the atmosphere.

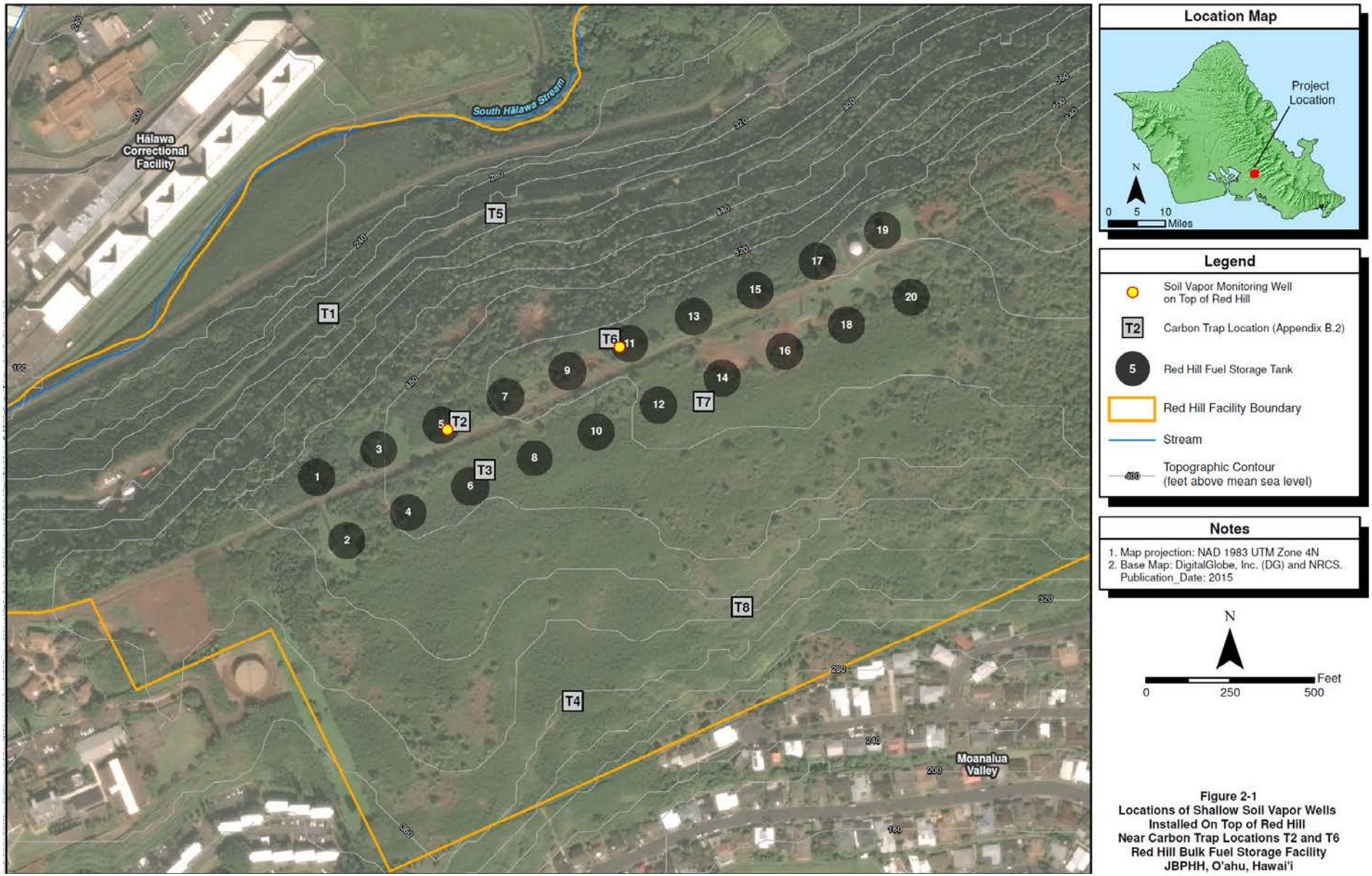

Figure 2-1
Locations of Shallow Soil Vapor Wells
Installed On Top of Red Hill
Near Carbon Trap Locations T2 and T6
Red Hill Bulk Fuel Storage Facility
JBPHH, O'ahu, Hawai'i

Figure 2-1: Locations of Shallow Soil Vapor Wells Installed On Top of Red Hill Near Carbon Trap Locations T2 and T6

2.3 INSTALLATION OF SOIL VAPOR PROBES (VAPOR PINS) THROUGH TUNNEL WALLS

Two Cox-Colvin Vapor Pins were installed in the upper tunnel: one near Tank 5 and one near Tank 11. Two additional potential Vapor Pin locations were planned at the top of the access ladders at the top of Tank 5 and Tank 11. However, site maintenance activities prevented access to the Tank 5 ladder. At Tank 11, it was determined that the required equipment could not safely be transported up the access ladder for installation of the Vapor Pin at that location.

To install each Vapor Pin, a hammer drill with an 18-inch × 5/8-inch drill bit was used to drill a hole through the tunnel wall at a height of approximately 3 ft above the floor. The drill bit was used to create a 16-inch-deep hole. The gunite wall over the native basalt was estimated to be approximately 4 inches thick based on a subtle color and texture contrast in the drill cuttings between the gunite and the basalt. For flush-mounted completion, a 1½-inch drill bit was used to over-drill the hole to a depth of 1¾ inches. The Vapor Pin was installed in accordance with the Cox-Colvin Vapor Pin installation Standard Operating Procedure (SOP) (Cox-Colvin 2016). After installation, the Vapor Pin was capped with a protective cover to prevent air flow when not sampling.

2.4 SOIL VAPOR SAMPLING PROCEDURES

Field instruments were calibrated every morning in accordance with manufacturers' instructions. Field screening was conducted at all soil vapor points (i.e., the new shallow soil vapor points, the new upper tunnel Vapor Pins, and the existing tank vapor wells). Samples for laboratory analysis were collected only from the existing tank vapor wells.

Field Screening: A minimum of 1 liter (L) of gas was purged from each soil vapor well prior to field screening. Purging was performed using either the pump in the PID or a separate pump.

- **Total VOC Concentration:** Total VOC concentrations were measured in the field using a ppb RAE PID. The PID was connected directly to the soil vapor well and the meter reading was monitored for a minimum of 1 minute until a stable reading was obtained. If the meter had not stabilized after 5 minutes, the reading at 5 minutes was recorded and the lack of stabilization was noted in the field notes.
- **Oxygen, Carbon Dioxide, and Methane:** Following completion of PID measurements, a syringe pump was used to pump 750 mL soil vapor into a Tedlar bag. A GEM5000 Landfill Gas Meter was used to measure oxygen, carbon dioxide, and methane concentrations in the bag. The meter reading typically stabilized after approximately 1 minute (500 milliliters [mL]), and the reading was recorded when the bag was almost emptied by the meter. A charcoal filter cartridge was installed in the sample line between the water filter and the Tedlar bag to prevent false positive methane readings associated with petroleum vapors in the samples. No methane was detected in any sample.
- **Differential Pressure:** Following completion of the fixed gas readings, differential pressure was measured by connecting the GEM5000 directly to the soil vapor well.

Sample Collection: At each tank, a sample was collected from the vapor monitoring well with the highest PID reading. Samples were collected into batch clean-certified 2.7-L Summa canisters (with 200 mL/min flow controller). The sample collection setup is illustrated on Figure 2-2. The sampling was completed as follows:

- **Leak Check:** The absence of leaks between the Summa and the ball valve on the soil vapor well was verified by using a syringe to induce a vacuum. The vacuum was maintained for a

minimum of 10 seconds. If any air entered the system (as evidenced by the syringe plunger not returning to the base of the syringe when the plunger was released), then the connections were tightened, and a second leak test was performed. During the field program, one Summa canister was rejected because the flow controller did not pass the leak test even after tightening the connections.

Summa Canister Sample: After passing the leak test, the syringe was used to remove air from the sample line running from the 3-way valve to the Summa canister and the 3-way valve was set to isolate the syringe while connecting the Summa to the sample point. The ball valve on the soil vapor well was opened and then the valve on the Summa canister was opened. The valves were kept open until the canister vacuum fell to less than 4 inches mercury (Hg) and were then closed. All Summas filled over a period of 10–12 minutes. A field duplicate sample was collected from soil vapor well RHSV05S below Tank 5.

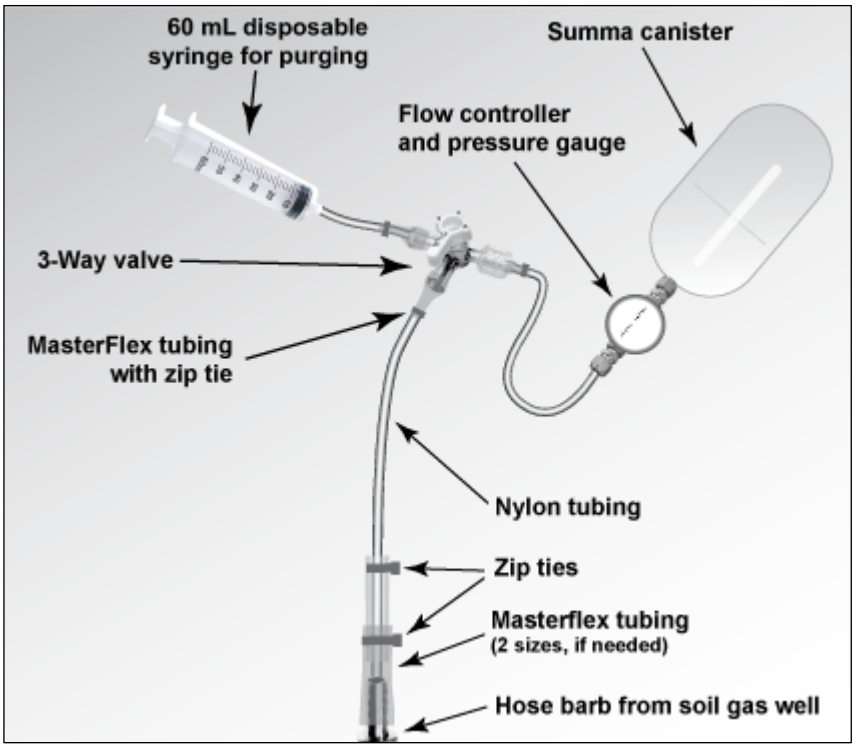

Figure 2-2: Illustration of Connection Between Soil Vapor Well and Summa Canister

2.5 MONITORING WELL HEADSPACE SAMPLING PROCEDURES

Well headspace field measurement and samples were collected from four groundwater monitoring wells: RHMW01, RHMW02, RHMW03, and RHMW04 (background).

Sample Collection: At each monitoring well, a vapor sample was collected into a batch clean-certified 2.7-L Summa canister (with 200 mL/min flow controller) as follows:

1. **Well Plugging:** At least 18 hours prior to sample collection, the vented well cap was replaced with a rubber stopper that formed a gas-tight seal and prevented gas flow through the well.

2. **Sampling Equipment:** A sample line was constructed to extend to a depth of 2 ft above the water level in the well. As shown on Figure 2-3, the 1/8-inch nylon sample line was deployed through a second rubber stopper. This second stopper had a small hole for the sample line and served to minimize vertical gas flow in the well during sample line deployment and sample collection. After the sample line was deployed to the correct depth, modeling clay was used to seal the small opening around the sample line.

3. **Sample Line Purge and Leak Check:** A disposable syringe was used to purge three line volumes of gas from the sample line. 1/8-inch tubing has a line volume of approximately 2.4 mL/ft. Following the purge, the Summa was connected, and the syringe was used to create a vacuum between the Summa and the 3-way valve to check for leaks. If leakage was detected, the hardware was tightened, and the leak check was performed again.

4. **Sample Collection:** After passing the leak test, the syringe was used to remove air from the sample line connecting the Summa canister to the 3-way valve and the 3-way valve was set to isolate the syringe while connecting the Summa to the well. The valve was opened on the Summa canister and kept open until the canister vacuum fell to less than 4 in Hg. All Summas filled over a period of 10–12 minutes.

Field Screening: At each monitoring well, after Summa sample collection, field screening was conducted using the field instruments (PID and Landfill Gas Meter).

1. **Total VOC Concentration:** The PID was connected directly to the nylon sample line and the meter was monitored for a minimum of 1 minute until a stable reading was obtained. If the meter had not stabilized after 5 minutes, the reading at 5 minutes was recorded and the lack of stabilization was noted in the field notes.

5. **Oxygen, Carbon Dioxide, and Methane:** Following completion of PID measurements, a syringe pump was used to pump 750 mL of headspace vapor into a Tedlar bag. The GEM5000 Landfill Gas Meter was used to measure oxygen, carbon dioxide, and methane concentrations in the bag. The meter reading typically stabilized after approximately 1 minute (500 mL), and the reading was recorded when the bag was almost emptied by the meter. A charcoal filter cartridge was installed in the sample line between the water filter and the Tedlar bag to prevent false positive methane readings associated with petroleum vapors in the samples. No methane was detected in any sample.

6. **Differential Pressure:** Following completion of the fixed gas readings, differential pressure was measured by connecting the GEM 5000 directly to the nylon sample line installed inside the groundwater monitoring well.

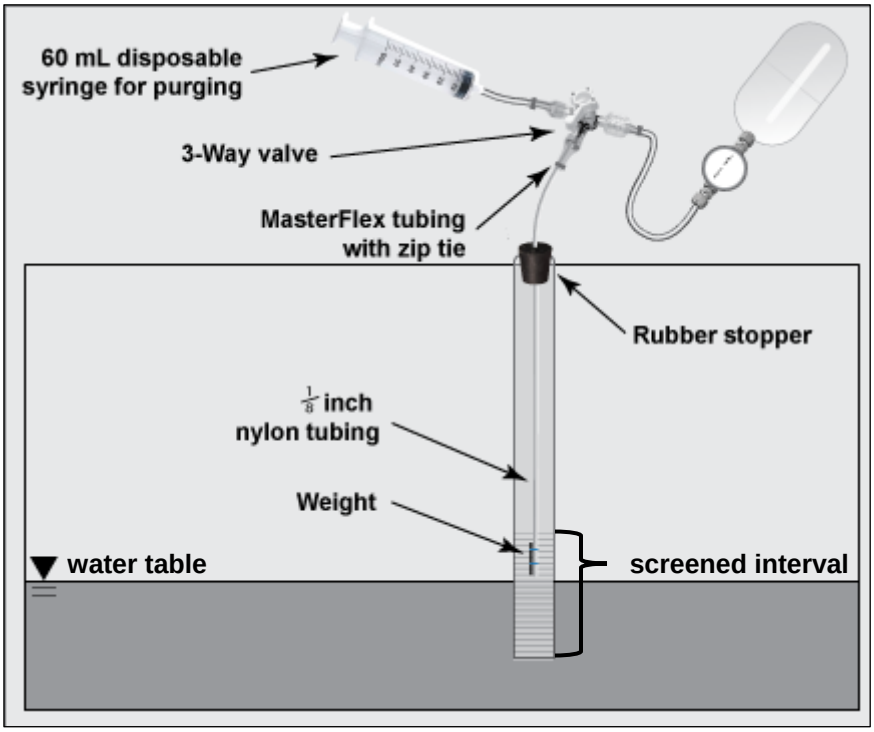

Figure 2-3: Illustration of Vapor Sample Collection from Monitoring Well

2.6 LABORATORY ANALYSIS

The Summa canister samples were shipped at ambient temperature under chain of custody control to Alpha Analytical Laboratory, Westborough, MA for analysis of volatile petroleum hydrocarbons by U.S. Environmental Protection Agency (EPA) Method TO-15 PIANO (see Table 2-1 for analyte list) and fixed gases (oxygen, carbon dioxide, methane, and nitrogen) by EPA Method 3C. Additionally, the laboratory was requested to report tentatively identified compounds (TICs).

Table 2-1: Petroleum VOC Analyte List for TO-15 PIANO Analysis

1-Decene	1,2,4,5-Tetramethylbenzene	3-Ethylhexane	Methylcyclopentane
1-Ethyl-1-Methylcyclopentane	1,3-Butadiene	3-Methylheptane	MMT
1-Heptene	1,3-Dimethyl-2-Ethylbenzene	3-Methylhexane	n-Butylbenzene
1-Hexene	1,3-Dimethyl-4-Ethylbenzene	3-Methylpentane	n-Hexane
1-Methyl-2-Ethylbenzene	1,3-Dimethyl-5-Ethylbenzene	3-Methylthiophene	N-Pentylbenzene
1-Methyl-2-Isopropylbenzene	1,3,5-Trimethylbenzene	Benzene	n-Propylbenzene
1-Methyl-2-N-Propylbenzene	1,4-Dimethyl-2-Ethylbenzene	Benzothiophene	Naphthalene
1-Methyl-3-Ethylbenzene	2-Ethylthiophene	cis-2-Pentene	Nonane (C9)
1-Methyl-3-Isopropylbenzene	2-Methyl-1-Butene	Cyclohexane	o-Xylene
1-Methyl-3-N-Propylbenzene	2-Methylheptane	Cyclopentane	Octane
1-Methyl-4-Ethylbenzene	2-Methylhexane	Decane (C10)	p/m-Xylene
1-Methyl-4-Isopropylbenzene	2-Methylnaphthalene	Dodecane (C12)	Pentane
1-Methyl-4-N-Propylbenzene	2-Methylpentane	Ethyl-Tert-Butyl-Ether	sec-Butylbenzene
1-Methylnaphthalene	2-Methylthiophene	Ethylbenzene	Styrene
1-Nonene	2,2-Dimethylpentane	Heptane	Tertiary Butanol
1-Octene	2,3-Dimethylbutane	Indane	Tertiary-Amyl Methyl Ether
1-Pentene	2,3-Dimethylhexane	Indene	Thiophene
1,2-Dibromoethane	2,3-Dimethylpentane	Isooctane	Toluene
1,2-Dichloroethane	2,3,3-Trimethylpentane	Isopentane	trans-2-Pentene
1,2-Diethylbenzene	2,3,4-Trimethylpentane	Isopropyl Ether	Tridecane
1,2-Dimethyl-3-Ethylbenzene	2,4-Dimethylhexane/ 2,2,3-Trimethylpentan	Isopropylbenzene	Undecane
1,2-Dimethyl-4-Ethylbenzene	2,4-Dimethylpentane	Methyl tert butyl ether	
1,2,4-Trimethylbenzene	2,5-Dimethylhexane	Methylcyclohexane	

3. Investigation Results

3.1 Laboratory Analysis of VOCs in Soil Vapor Samples

Soil vapor samples for laboratory analysis were collected from the soil vapor well below each fuel tank with the highest PID reading and from the headspace of RHMW01, RHMW02, RHMW03, and RHMW04. A table of laboratory analytical results for the soil vapor and well headspace samples is provided as Attachment B.3.4. The magnitude and chemical composition of soil vapor samples can be used to evaluate the occurrence of recent and historical releases of fuel from the fuel tanks and weathering of these releases.

3.1.1 Magnitude of Petroleum Vapors

Each vapor sample was analyzed for 83 petroleum constituents and seven petroleum additives (four oxygenates, two lead scavengers, and one octane booster). Seventy-four petroleum constituents and five additives (four oxygenates and one lead scavenger) were detected in one or more samples. In addition, for each sample, the laboratory estimated the concentration and used mass spectrum matching software to identify TICs with the most prominent gas chromatogram (GC) peaks that were not on the standard sample analyte list. As discussed in Section 3.1.3, the TICs included a variety of petroleum and non-petroleum compounds. The TIC concentrations were estimated based on the instrument response relative to an internal standard and, therefore, these concentrations are more uncertain than the concentrations reported for the target analytes.

The magnitude of quantified VOCs in soil vapor samples (i.e., the total concentration of target analytes and TICs) can be used to evaluate the likely presence of LNAPL below each tank. The total concentration of quantified analytes is summarized on Figure 3-1. Siloxane and silanol compounds were excluded from the TICs because these compounds are commonly associated with the laboratory equipment and were likely not present in the original samples (http://analyteguru.com/gc-gc-ms-troubleshooting-part-ii-siloxane-peak-contamination/).

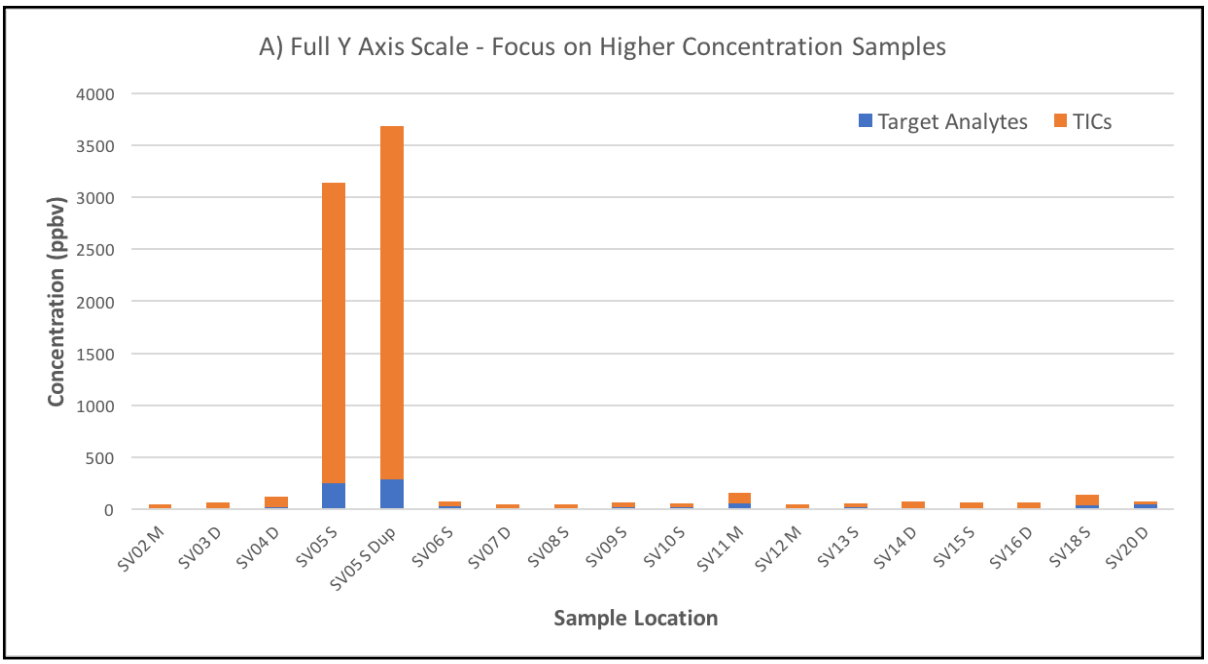

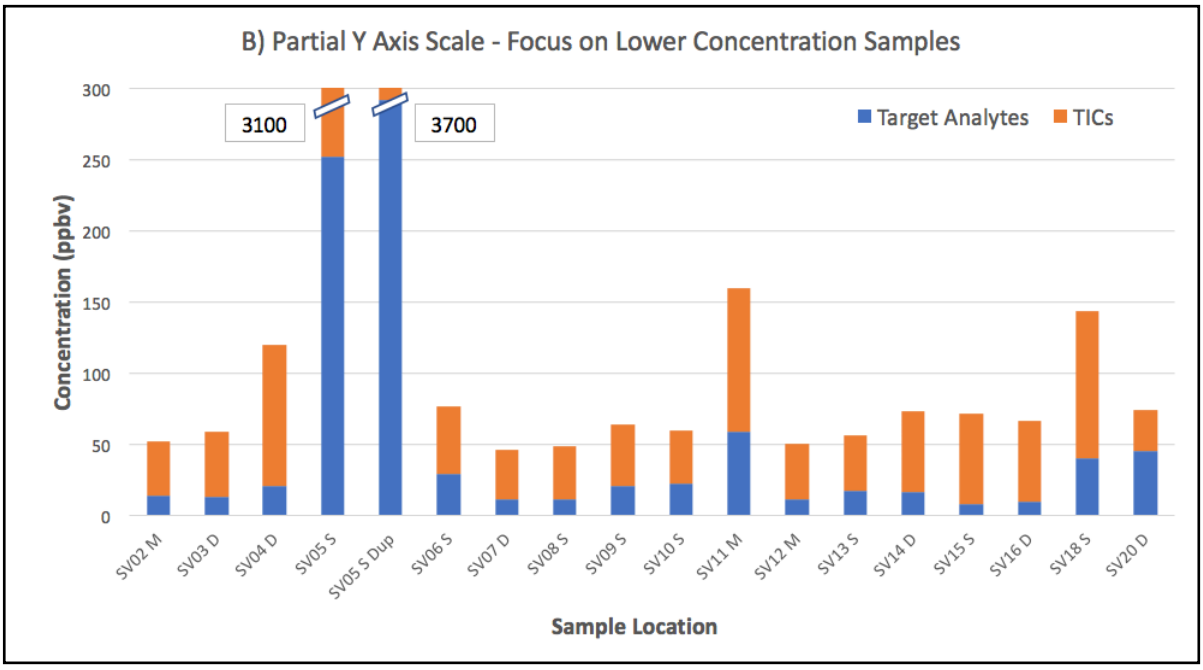

ppbv parts per billion by volume

Figure 3-1: Total Concentration of Quantified VOCs in Soil Vapor Samples

At equilibrium between liquid fuel and vapor, the vapor pressure defines the total petroleum vapor concentration in the vapor phase. The vapor pressure of fresh jet fuel is approximately 2–4 millibars (mbar) (https://www.ncbi.nlm.nih.gov/books/NBK231234/; Shepard et al. 2000). At equilibrium, this represents a petroleum vapor concentration of 2,000–4,000 parts per million by volume (ppmv) of fresh jet fuel (i.e., 1 mbar is approximately equal to 1 part per thousand [ppt]) or 1,000 parts per million [ppm]). However, the vapor pressure of fuel decreases with weathering as the more volatile components are depleted from the liquid fuel (Shepard et al. 2000).

Total VOC concentrations measured in soil vapor samples rarely approach concentrations predicted by equilibrium partitioning (McHugh and McAlary 2009). In a study evaluating soil vapors at 24 contaminated groundwater sites, the measured soil vapor concentrations ranged from 0.002% to 10% of that predicted by Henry's law, with a mean of 0.66% (Fitzpatrick and Fitzgerald 1996). Similar non-equilibrium conditions are expected at LNAPL sites because similar vapor attenuation processes (diffusion, advection, and biodegradation) prevent full equilibration in bulk soil vapor.

As shown on Figure 3-1, the magnitude of VOCs detected in the samples for the soil vapor wells varied over a relatively small range (46–160 parts per billion by volume [ppbv]) except for the duplicate samples collected from the shallow soil vapor well below Tank 5 (3,138 and 3,682 ppbv). The total concentration of target analytes plus TICs in Tank 5 (i.e., 3 ppmv and 4 ppmv) samples was equal to approximately 0.1% of the expected equilibrium vapor concentration of fresh jet fuel (2,000–4,000 ppmv). After accounting for the effects of weathering on decreasing the vapor pressure of jet fuel, the likely presence of unquantified petroleum compounds in the samples, and non-equilibrium conditions in soil vapor, the total VOC concentrations measured below Tank 5 (i.e., 0.1% of equilibrium with fresh jet fuel) are likely consistent with the presence of weathered jet fuel LNAPL in the vicinity of the sample collection point. The total VOC concentrations measured below all of the other tanks (i.e., < 0.01% of equilibrium with fresh jet fuel) are too low to be indicative of LNAPL containing a significant volatile fraction. However, as discussed in Section 3.1.4, many of these samples contained an unresolved "hump" of less-volatile constituents visible on the flame ionization detector (FID) chromatogram that may indicate the presence of heavily weathered LNAPL in the vicinity of these tanks.

Finding: The magnitude of quantified petroleum vapors in samples from the below-tank soil vapor wells indicates the presence of weathered LNAPL below Tank 5. Although the quantitative laboratory results from the other tanks are not indicative of LNAPL below these other tanks, other lines of evidence do suggest the presence of heavily weathered LNAPL below other tanks.

3.1.2 Composition of Petroleum Vapors

The mixture of petroleum compounds detected in each soil vapor sample can be used to evaluate the weathering state of the source fuel. Specifically, the distribution of alkanes provides a good marker for biological weathering. C8–C12 n-alkanes are the most prominent components of vapors from unweathered jet fuel, with lower concentrations of branched alkanes and cycloalkanes (Pleil, Smith, and Zelnick 2000, Figure 4). However, under either aerobic conditions (Kaplan et al. 1997) or anaerobic conditions (Baedecker et al. 2011), n-alkanes are readily biodegraded while branched alkanes are more slowly degraded and cycloalkanes exhibit the slowest degradation rates. As a result, branched alkanes and cycloalkanes are more dominant in vapors from more weathered fuel.

"Fingerprint" graphs for each sample are provided as Attachment B.3.1.

The distribution of alkanes in samples collected from the soil vapor wells is provided on Figure 3-2 and Figure 3-3. The distribution Figure 3-2 is consistent with unweathered or lightly weathered jet fuel; the distribution on Figure 3-3 is consistent with weathered jet fuel.

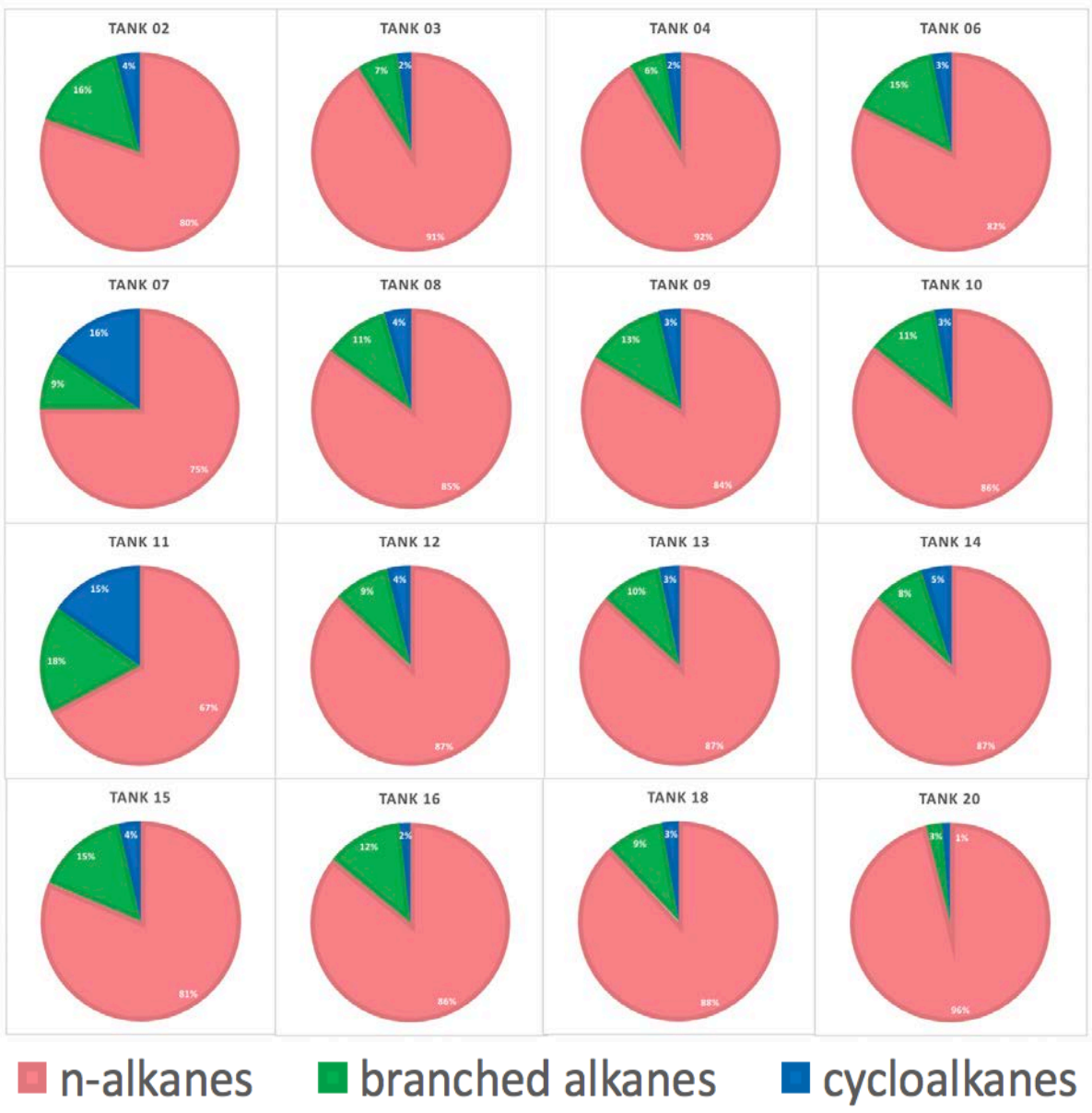

Figure 3-2: Distribution of Alkanes in Soil Vapor Samples for All Samples Except Tank 5

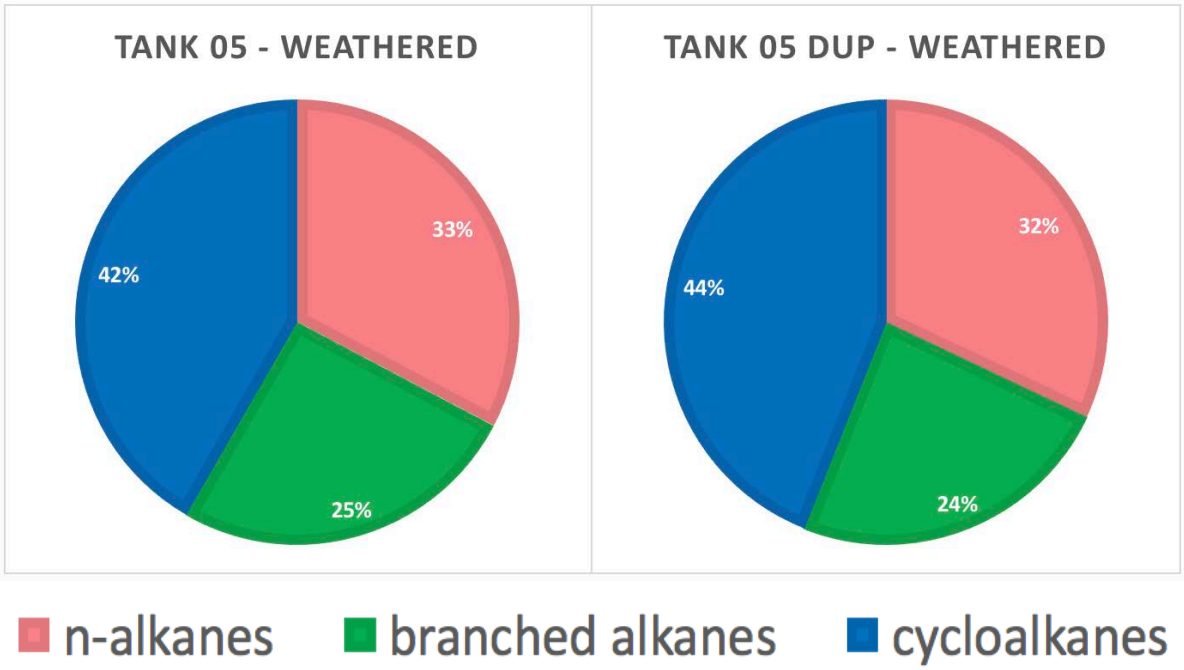

Figure 3-3: Distribution of Alkanes in Soil Vapor Samples for Tank 5

As shown on Figure 3-2, except for Tank 5, the quantified target analytes for the samples from the soil vapor wells shown an alkane distribution consistent with little or no weathering of the fuel (Kaplan et al. 1997). These samples are dominated by n-alkanes (67–96%) with much smaller percentages of branched alkanes (3–18%) and cycloalkanes (1–16%). In addition, as shown in Attachment B.3.1, most of these samples exhibit a normal distribution of n-alkanes within the range of C9 (nonane) to C13 (tridecane), consistent with the profile observed in fresh diesel vapors (e.g., Figure 4A from Pleil, Smith, and Zelnick 2000; Figure 3A from Gregg et al. 2007). Fresh diesel vapors are similar in composition to fresh jet fuel vapors.

Based on low total VOC concentration (Section 3.1.1) and the composition consistent with unweathered jet fuel, the petroleum vapors in these samples likely reflect low-level vapor-phase releases of petroleum rather than LNAPL releases. Aside from Tank 5, the total target analyte plus TIC concentration was very low (ranging from 46 ppbv to 160 ppbv); several orders of magnitude below the equilibrium vapor concentration associated with fresh jet fuel LNAPL. In addition, aside from Tank 5, the concentrations of all individual petroleum constituents (except naphthalene) were below EPA Regional Screening Levels for industrial indoor air. In other words, even undiluted, the individual VOCs detected in the below-tank soil vapor samples would not pose an indoor air exposure risk. Although the specific source(s) of these vapors were not identified through this study, low-level vapor releases at fuel storage facilities are not unexpected. Vapor releases can occur through joints, valves, and gaskets as well as during tank filling and fuel transfer operations. These types of small vapor-phase releases are difficult to completely eliminate.

In contrast to the samples from below the other tanks, the normal and duplicate vapor samples collected from below Tank 5 (Figure 3-3) exhibited a smaller percentage of n-alkanes (32–33%) and a higher percentage of branched alkanes (24–25%) and cycloalkanes (42–44%). This distribution is consistent with biologically weathered jet fuel (Kaplan et al. 1997; Baedecker et al. 2011).

Finding: Considering both the concentration and composition of petroleum vapors detected in the below-tank soil vapor wells, the results from Tank 5 are consistent with a LNAPL release that has undergone significant biological weathering, and the results from the other tanks are consistent with low level vapor-phase releases typical of any fuel storage operation.

3.1.3 Tentatively Identified Compounds in Soil Vapor Samples

An evaluation of the TICs provides additional support for the evaluation of the Tank 5 sample as weathered LNAPL. For Tank 5, all of the TICs that could be tentatively identified by the laboratory were cycloalkanes or branched alkanes with estimated concentrations in the range of 200–400 ppbv. As discussed above, the cycloalkanes and branched alkanes biodegrade more slowly than the n-alkanes and, therefore, become more predominant as the LNAPL weathers. For the other tanks, the TICs were mostly a mixture of petroleum hydrocarbons, alcohols, and ketones with much lower estimated concentrations of 1–20 ppbv.

3.1.4 Evaluation of FID Chromatograms

Middle distillate fuels such as jet fuel contain a complex mixture of petroleum compounds many of which cannot be completely separated in a laboratory GC column. As a result, an unresolved "hump" (also called an "unresolved complex mixture," UCM) is often visible at the end of the chromatogram (Tran et al. 2010). As the fuel weathers in the environment, this unresolved hump often becomes more prominent. Compounds in this unresolved hump are not quantified as either target analytes or TICs.

For each soil vapor sample, the FID chromatogram was reviewed to evaluate the presence of an unresolved hump indicative of compounds not quantified as either target analytes or TICs. For this purpose, the FID chromatogram rather than the mass spectrum (MS) detector chromatogram was used because the FID response is more consistent across petroleum compounds. Representative FID chromatograms are provided on Figure 3-4, and the full set of FID chromatograms are provided in Attachment B.3.2.

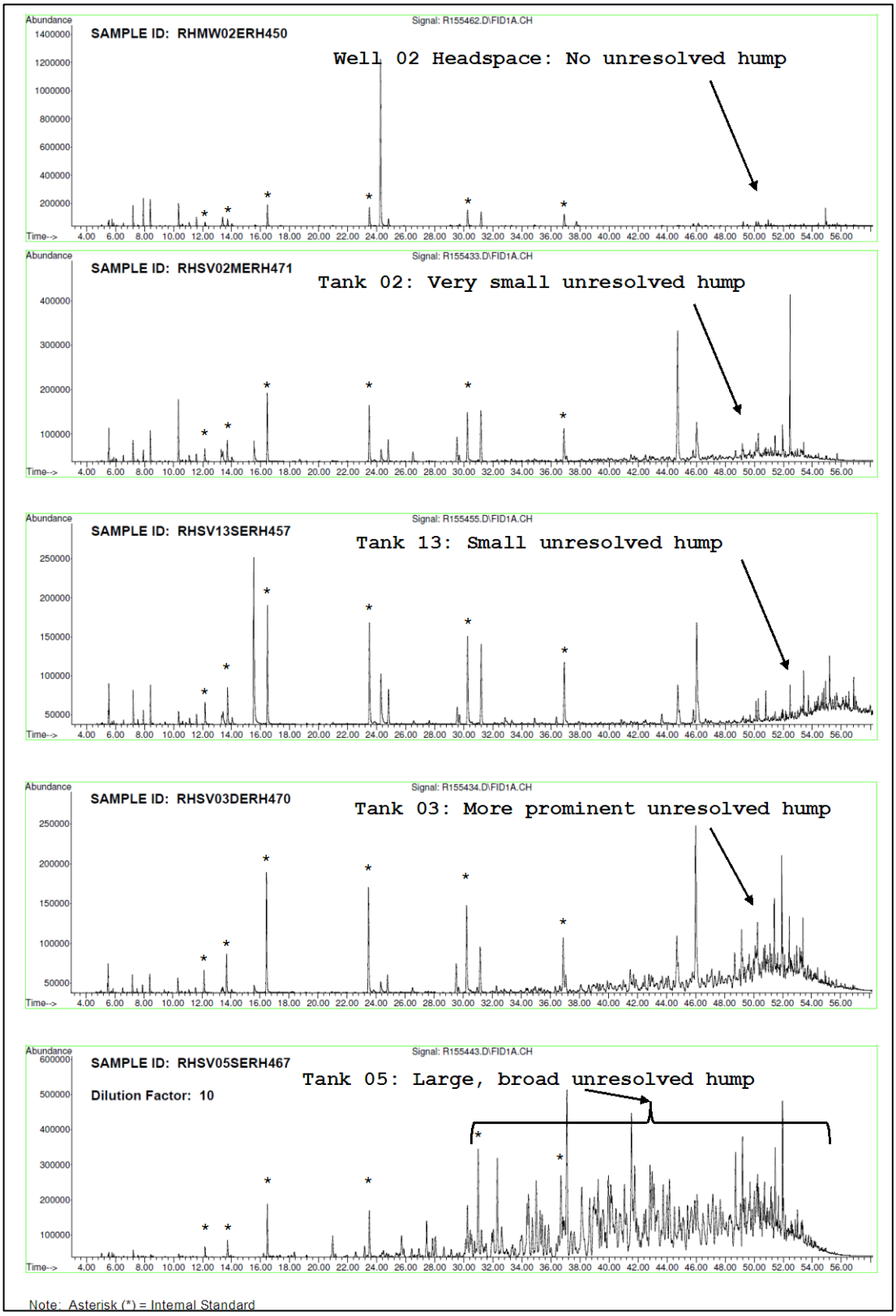

Figure 3-4: FID Chromatograms from Representative Samples Showing Range of Unresolved Hump

All of the samples collected from the below-tank soil vapors wells contained a visible unresolved hump at the end of the FID chromatogram indicating the presence of at least some unquantified lower volatility compounds in these samples. In contrast, none of the four well headspace samples contained a visible unresolved hump. For the below-tank samples, the size of this hump varied between samples indicating differing amounts of the unquantified compounds:

- **Tank 5:** The shape and magnitude of the unresolved hump is consistent with the presence of weathered LNAPL. This is consistent with the analysis of target analytes and TICs in Sections 3.1.1–3.1.3.
- **Tanks 3, 4, 7, and 18:** The shape and magnitude of the unresolved hump is consistent with the presence of heavily weathered LNAPL. For these tanks, the analysis of target analytes and TICs indicates low-level vapor-phase releases likely associated with ongoing Facility operations. Thus, the samples collected from these soil vapor wells likely consist of a mixture of unweathered (or slightly weathered) vapor releases and vapors from heavily weather petroleum LNAPL.
- **Tanks 2, 6, 9, 10, 11, 12, 13, 14, 15, 16, and 20:** The shape and magnitude of the unresolved hump is mostly consistent with fresh jet fuel vapors with contributions from heavily weathered LNAPL apparent in some of the samples. For these tanks, the analysis of target analytes and TICs is consistent with unweathered or lightly weathered jet fuel indicating likely low-level vapor-phase releases associated with ongoing Facility operations. Thus, the samples collected from these soil vapor wells likely consist of unweathered (or slightly weathered) vapor releases with a smaller component of vapors from heavily weathered petroleum LNAPL.

3.2 FIELD MEASUREMENTS

Field measurements were conducted at existing and new soil vapor points, plus RHMW01, RHMW02, RHMW03, and RHMW04 headspace. In addition, ambient readings were recorded for the tunnel and outdoor air. Field measurements included total VOC concentration by PID, and oxygen, carbon dioxide, methane concentrations and differential pressure by Landfill Gas Meter. All of the field measurements are presented in Attachment B.3.3.

3.2.1 PID Readings

PID readings at the soil vapor points ranged from 44 to 40,000 ppbv. Readings above 10,000 ppbv were recorded at seven locations (RHMW01 headspace and soil vapor wells below Tanks 5, 6, 11, 12 [two wells], and 18). However, as discussed in Section 3.3, there was a poor correlation between PID readings and the total VOC concentration measured in samples collected for laboratory analysis. Specifically, the PID reading was often much higher than the laboratory-measured total VOC concentration.

3.2.2 Oxygen, Carbon Dioxide, and Methane

High oxygen and low carbon dioxide concentrations were recorded at almost all measurement locations. For the below-tank soil vapor wells, oxygen concentrations ranged from 13.7% to 20.6%, with only two readings below 18%. Carbon dioxide concentrations ranged from 0.1% to 3.2%, with most readings less than 1%. For the well headspace samples, oxygen was 17–21% and carbon dioxide was 0.1–2.1% except for RHMW02, where oxygen was 6.6% and carbon dioxide was 8.5%. Methane was not detected in any measurement location. These results indicate an aerobic environment throughout the vadose zone. The results for the individual sample points are provided in Attachment B.3.3.

3.2.3 Differential Pressure

For 39 of the 46 below-tank soil vapor wells tested, both of the two upper-tunnel Vapor Pin points, and three of four monitoring wells, the differential pressure measurements showed a positive pressure relative to the tunnel (i.e., a pressure gradient indicating gas flow from the vadose zone into the tunnel). At most of these locations, the differential pressure was greater than 0.1 inch H_2O (i.e., > 25 pascals). For comparison, a differential pressure of 0.02 inch H_2O (5 pascals) is typically considered sufficient to support advective flow in the context of vapor intrusion mitigation (i.e., sufficient for effective sub-slab depressurization systems). These results indicate that advective air flow is from the vadose zone into the tunnels.

3.3 Correlation between Field Measurements and Laboratory Results

The correlations between field measurements and laboratory analytical results were evaluated to determine the utility of field measurements for ongoing screening and monitoring activities.

3.3.1 Field PID Readings vs. Laboratory Total Quantified VOC Concentrations

All of the below-tank soil vapor wells have been screened monthly using a PID since 2008. In order to evaluate the utility of this screening for tracking petroleum vapor concentrations going forward, examined the correlation between the October/November 2017 field PID readings and the collocated laboratory measured total VOC concentrations was evaluated (Figure 3-5).

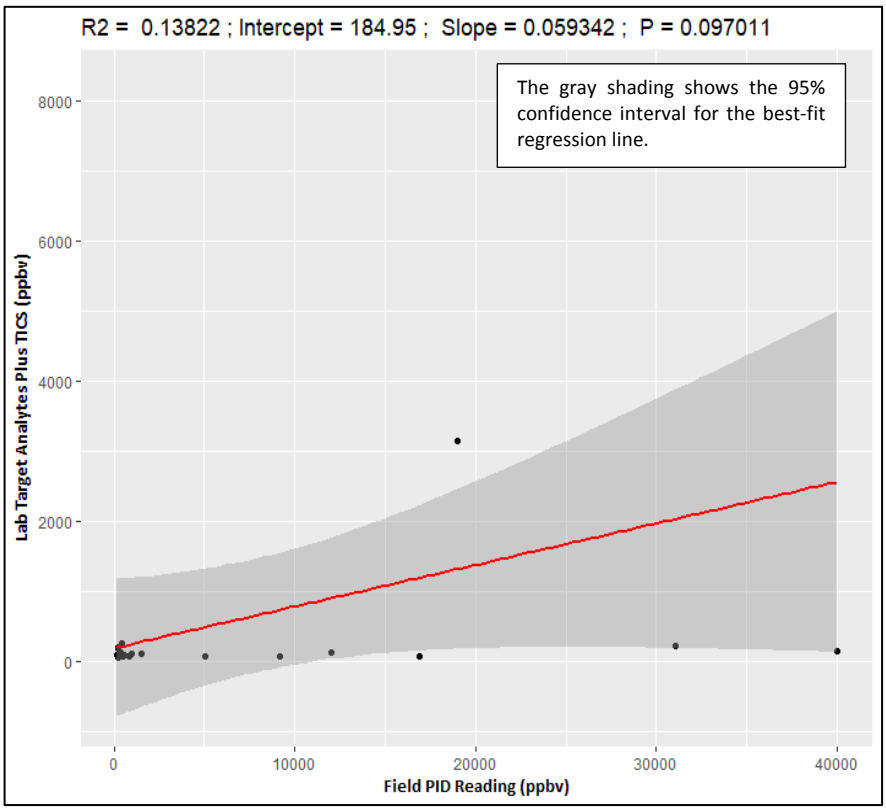

Figure 3-5: Correlation Between PID Readings and Laboratory Total Target Analytes Plus TICs

As shown on Figure 3-5, a poor correlation was observed between PID readings and laboratory-measured total VOC concentrations (Slope = 0.06, R^2 = 0.14). For Tank 5 (PID = 19,000; Laboratory = 3,100) and MW01 Headspace (PID = 23,200; Laboratory = 8,300), the sum of target analytes and TICs was in reasonable agreement with the PID reading. However, for the remaining paired measurements, the sum of target analytes and TICs ranged from 46 to 254 ppbv while the PID readings ranged from 160 to 40,000 ppbv. In addition to Tank 5, six other locations yielded PID readings above 10,000 ppbv. However, the sum of target analytes and TICs at these six locations was 254 ppbv or lower. Thus, the PID appeared to have a large false-positive rate, commonly yielding PID readings of greater than 10,000 ppbv at locations without high concentrations of laboratory measured petroleum or other VOCs. The cause(s) of these high PID readings was not determined.

Although a poor correlation between PID readings and laboratory-quantified VOCs was observed during the single monitoring event, this dataset did not allow evaluation of the utility of changes in PID readings over time for detection of new releases. As discussed in Section 4 (Question 5), for individual monitoring locations, changes in PID readings over time do appear to provide an indication of possible new LNAPL fuel releases.

3.3.2 Field vs. Laboratory Oxygen, Carbon Dioxide, and Methane Concentrations

In addition to field measurement at all locations, oxygen, carbon dioxide, and methane concentrations were measured by EPA Method 3C in all samples collected for laboratory analysis. Methane was not detected in any sample by field measurement or laboratory analysis. To evaluate the accuracy of the field measurements, the correlation between the field measurement and the laboratory measurement was evaluated.

Oxygen Concentration: As shown on Figure 3-6, a relatively poor correlation was observed between the field and laboratory measured oxygen concentrations. However, this poor correlation is attributable to two locations where the laboratory measured oxygen concentration was much lower than the field measured concentration. For both of these locations the laboratory and field-measured carbon dioxide concentrations were low (0.2–0.4%). Because low oxygen in soil vapor samples is typically accompanied by elevated carbon dioxide levels, these results suggest erroneous laboratory results for these two samples. When these two data points are removed from the dataset, a very high correlation is observed (Slope = 1.01; R^2 = 0.98, Figure 3-7). This analysis indicates high accuracy for the field measured oxygen concentrations.

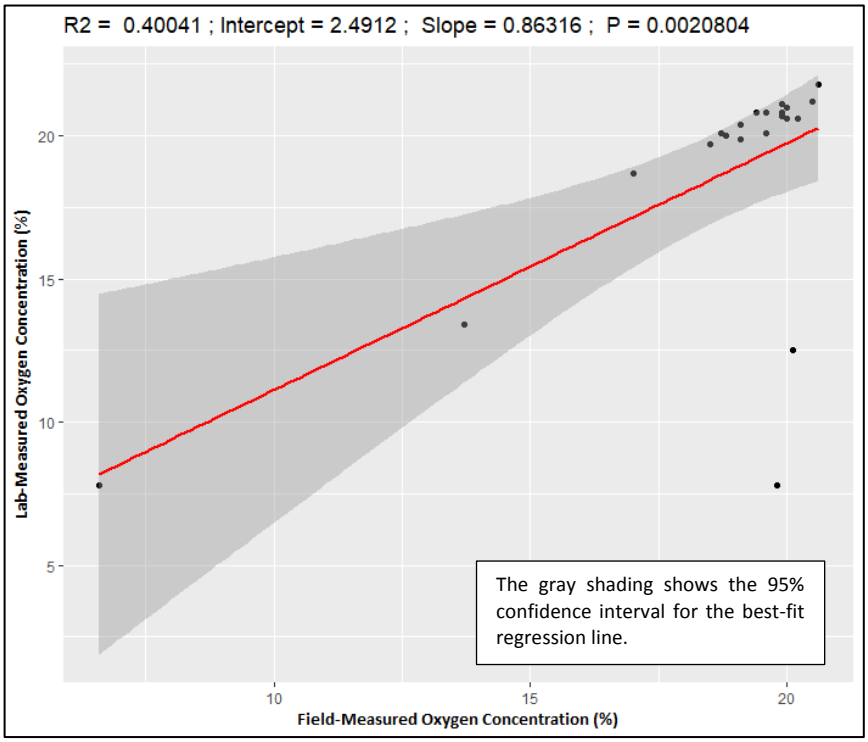

Figure 3-6: Correlation Between Field- and Laboratory-Measured Oxygen Concentration

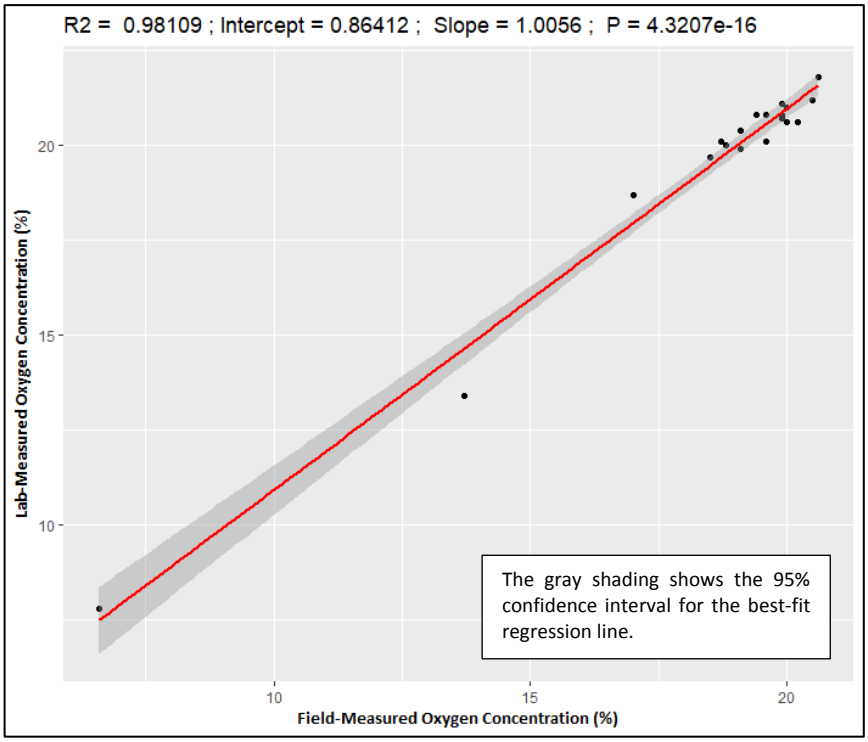

Figure 3-7: Correlation Between Field- and Laboratory-Measured Oxygen Concentration Excluding Two Low-Biased Laboratory Measurements

Carbon Dioxide Concentration: As shown on Figure 3-8, a good correlation was observed between the field and laboratory carbon dioxide concentrations (Slope = 1.08; R^2 = 0.99). This indicates high accuracy for the field-measured carbon dioxide concentrations.

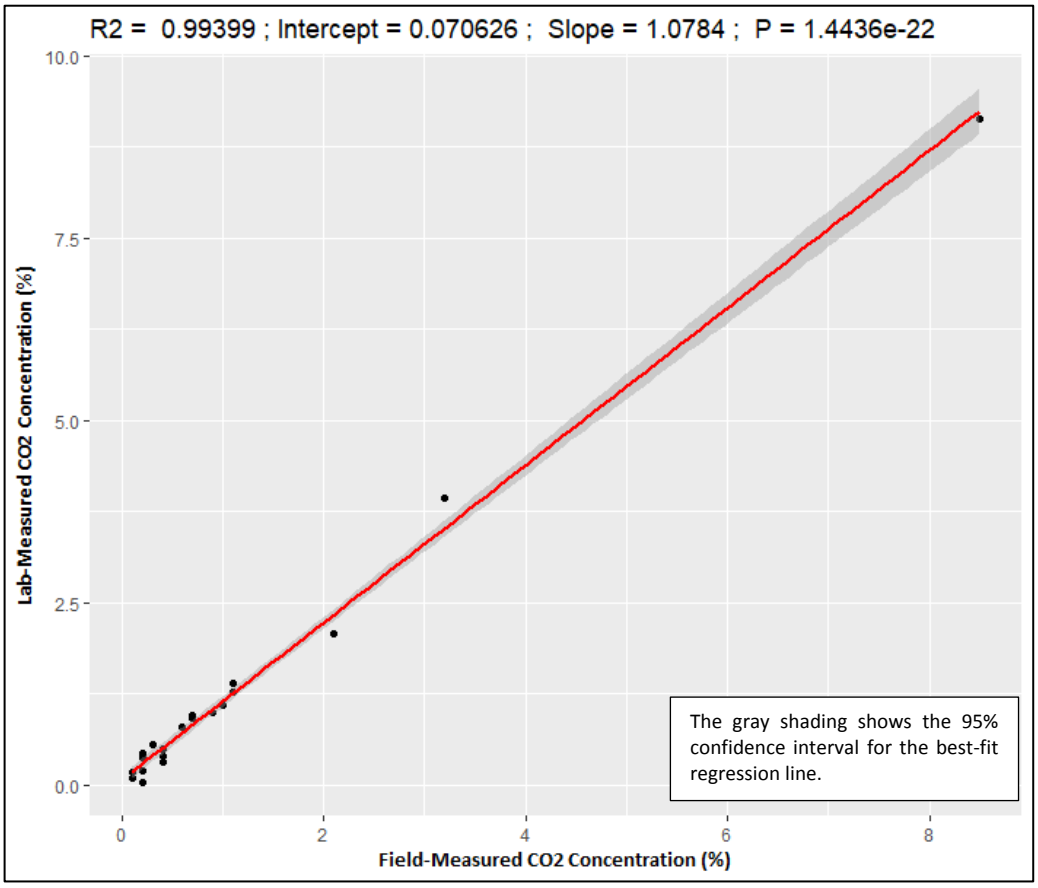

Figure 3-8: Correlation Between Field- and Laboratory-Measured Carbon Dioxide Concentration

4. Discussion of Soil Vapor Investigation Results

The purpose of the soil vapor investigation was to help address the following questions:

1. Is there evidence of recent or historical fuel releases at one or more of the tanks?
7. Is LNAPL present below the tanks?
8. Is NSZD occurring?
9. Can vapor monitoring help detect potential future LNAPL fuel releases?
10. Can vapor monitoring help quantify the magnitude of NSZD?
11. Are vadose zone petroleum vapors a significant source of impacts in the tunnels?

Findings are presented in Table 4-1 – Table 4-6.

Table 4-1: Study Question 1: Is There Evidence of Recent or Historical Fuel Releases at One or More of the Tanks?

Finding	Discussion
YES, the soil vapor results suggest an historical release of LNAPL fuel at Tank 5 and, at the other tanks, low-level vapor-phase releases associated with ongoing Facility operations.	The analysis of soil vapor samples indicates a LNAPL fuel release at Tank 5. The total VOC (i.e., sum of target analytes plus TICs) concentration in the two soil vapor samples from below Tank 5 (3 and 4 ppmv) were approximately 0.1% of equilibrium vapor concentrations for fresh jet fuel (2,000–4,000 ppmv). Accounting for non-equilibrium conditions typically observed in the subsurface and the expected reduction in vapor pressure associated with the weathering of jet fuel, the concentration of VOC vapors measured below Tank 5 is consistent with the presence of weathered jet fuel LNAPL in this area. The alkanes in this sample were predominately cycloalkanes and branched alkanes, compounds that are more resistant to biodegradation, with a lower percentage of readily biodegradable n-alkanes (Figure 3-3). This composition suggests that the LNAPL is weathered. The analysis of soil vapor samples from below the other tanks does not indicate the presence of fresh or weathered LNAPL containing measureable levels of VOCs. The total VOC concentrations at these locations (0.05–0.16 ppmv) is less than 5% of the concentration at Tank 5. In addition, the alkanes in these samples are dominated by the readily degradable n-alkanes (67–96%; Figure 3-2) indicating little or no weathering of the fuel. The low VOC concentration combined with the absence of weathering suggests low-level vapor-phase releases of fuel near these tanks are likely associated with ongoing Facility operations.

Table 4-2: Study Question 2: Is LNAPL Present below the Tanks?

Finding	Discussion
YES, the soil vapor results suggest the presence of weathered LNAPL fuel below Tank 5. Borings completed below some of the other tanks provided visual evidence of LNAPL at the time the borings were installed (1998-2012). For these other tanks, the presence of LNAPL is not reflected in the quantitative analysis soil vapor samples collected in October/November 2017; however, many of the FID chromatograms show an unresolved hump of less-volatile compounds potentially consistent with the presence of highly weathered LNAPL (see Attachment B.3.2).	The total VOC concentration and alkane composition in the soil vapor samples collected from below Tank 5 are consistent with the presence of weathered LNAPL in this area. These results suggest that significant weathering has occurred since the documented Tank 5 fuel release in 2014. Angle borings completed below the fuel tanks from 1998 to 2012 suggested the presence of LNAPL below several additional tanks, such as Tanks 1, 9, 13, 14, 16, and 17 (Figure 4-1; Attachment B.3.5). The 2017 soil vapor samples collected from below all tanks (except Tank 5) contained low concentrations of target VOCs and TICs. The distribution of alkanes in these samples (i.e., mostly n-alkanes) was consistent with unweathered or lightly weathered jet fuel likely associated with vapor-phase releases from ongoing Facility operations. However, all of these samples contained unresolved humps at the end of the FID chromatograms indicating the presence of less volatile compounds in these samples that were not quantified as target analytes or TICs (see Attachment B.3.2). The greatest amount of this material was observed in the samples from below Tanks 3, 4, 7, and 18. These results suggest that the LNAPL observed below the tanks in the 1998–2012 borings has weathered to the point that most or all of the volatile constituents have been depleted.

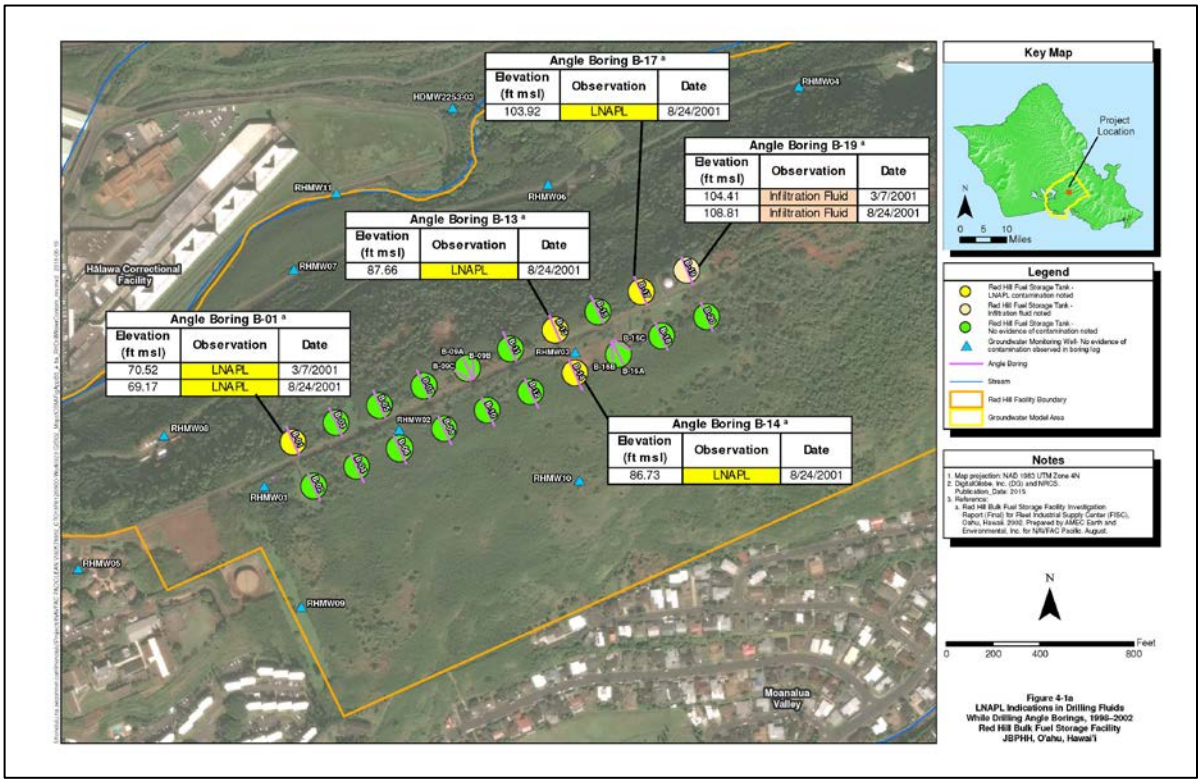

Figure 4-1a
LNAPL Indications in Drilling Fluids
While Drilling Angle Borings, 1998–2002
Red Hill Bulk Fuel Storage Facility
JBPHH, O'ahu, Hawai'i

1

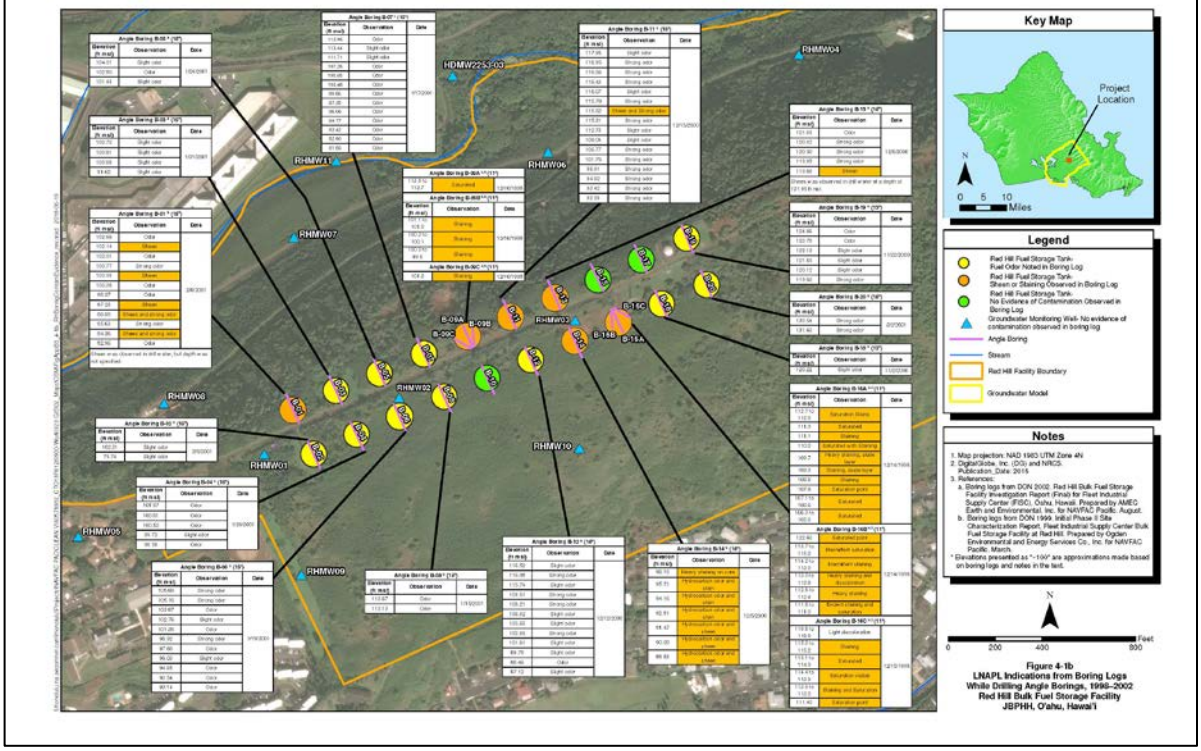

Figure 4-1b
LNAPL Indications from Boring Logs
While Drilling Angle Borings, 1998–2002
Red Hill Bulk Fuel Storage Facility
JBPHH, O'ahu, Hawai'i

2

3 Most data from 1998–2001; see Attachment B.3.5 for full-size figures.

4 **Figure 4-1: Top: LNAPL Indications from Drilling Fluids; Bottom: LNAPL Indications from Boring Logs**

Table 4-3: Study Question 3: Is NSZD Occurring?

Finding	Discussion
YES, as discussed above, the soil vapor results suggest that significant biological weathering of the LNAPL below Tank 5 has occurred since the 2014 release. This is consistent with other lines of evidence supporting biological NSZD.	The conclusion of biological weathering of LNAPL releases is supported by the following observations: • The petroleum vapor fingerprint from below Tank 5 is consistent with weathered LNAPL associated with the 2014 release. • The vapor testing below other tanks indicates that the LNAPL visually observed in borings completed below these tanks in 1998 to 2002 is depleted in VOCs. • Field monitoring and laboratory analysis indicate high oxygen concentrations (13.7–20.6%) and non-detect levels of methane (<0.1%) in all of the below-tank soil vapor wells, supporting aerobic biodegradation. Carbon dioxide concentrations are low (0.1–3.2%), but above atmospheric levels (0.04%). • Thermal monitoring indicates ongoing biological NSZD (see CSM Appendix B.1).

Table 4-4: Study Question 4: Can Vapor Monitoring Help Detect New LNAPL Fuel Releases?

Finding	Discussion
YES. Monthly PID screening of the soil vapor wells with laboratory confirmation for those with elevated PID readings is likely to be a reliable method for detecting any new LNAPL releases of jet fuel.	Although a poor correlation was observed between PID readings and laboratory measured total VOC concentrations across soil vapor monitoring wells during a single monitoring event, changes in PID readings over time do appear to provide useful information regarding possible new releases of LNAPL jet fuel. As shown on Figure 4-2, PID readings at the Tank 5 soil vapor monitoring wells spiked rapidly from less than 100 ppbv in December 2013 to greater than 200,000 ppbv in January 2014 corresponding to the 2014 Tank 5 release event. PID readings at Tank 5 peaked at 450,000 ppbv May 2014 and have then decreased over time consistent with biological weathering and other NSZD processes. In contrast, PID readings from below other tanks have rarely exceeded 100,000 ppbv since 2008. The PID monitoring results suggest that rapid increases in PID readings below a fuel tank may indicate a new release of LNAPL fuel. If a rapid increase is observed in future monitoring, laboratory analysis by TO-15 PIANO (i.e., TO-15 analysis with 90+ petroleum VOC analyte list) can be used to provide confirmation that the spike is associated with a new release. The January 2014 release event from Tank 5 resulted in PID readings >100,000 ppbv in all three soil vapor wells below Tank 5. In addition, the release event caused elevated PID readings (i.e., >25,000 ppbv) in soil vapor wells below all three adjacent tanks (i.e., in one of three soil vapor wells below Tank 3, two of two soil vapor wells below Tank 6, and three of three soil vapor wells below Tank 7). Although these readings were smaller in magnitude and shorter in duration than those observed in the Tank 5 soil vapor wells, they were clearly elevated relative to baseline (pre-release) PID readings. Thus, following the release event, elevated PID readings were observed in a total of nine soil vapor wells. This indicated that the soil vapor monitoring well network is very robust with a higher well density than needed to detect releases on the magnitude of thousands of gallons. The PID monitoring results further suggest that a large release event (i.e., thousands of gallons) results in a sustained increase in PID readings below the tank that persists for months to years. Following the January 2014 release event of 27,000 gallons at Tank 5, PID readings for the soil vapor wells below Tank 5 remained above 100,000 ppbv for approximately 30 months (i.e., until June 2016). The absence of similar sustained elevated PID readings for the soil vapor wells below the other tanks suggests that no large release events have occurred from these tanks during the period of PID monitoring (i.e., 2008 to present).

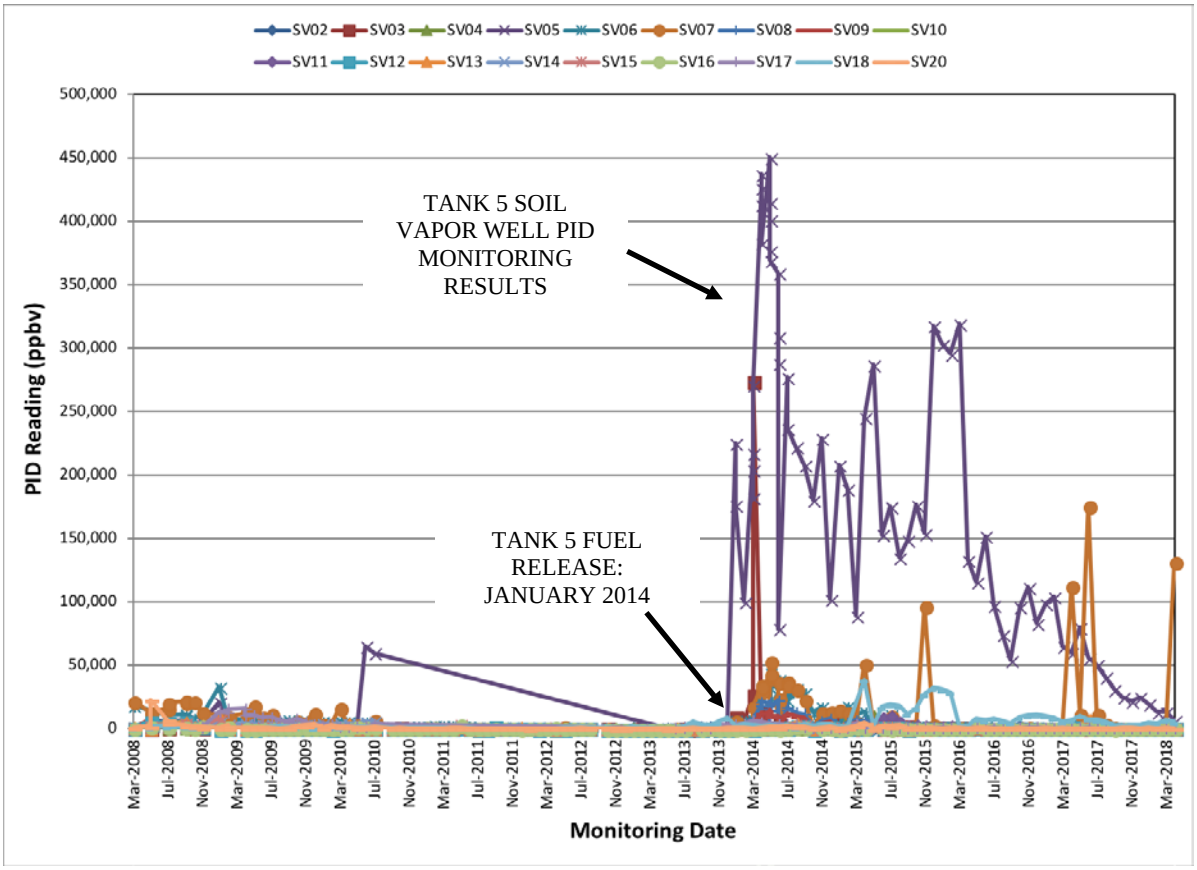

Figure 4-2: Linear Scale Graph of Monthly PID Monitoring Results for Below Fuel Tank Soil Vapor Wells

Table 4-5: Study Question 5: Can Vapor Monitoring Help Quantify the Magnitude of NSZD?

Finding	Discussion
YES, monthly PID monitoring appears to track decreases in petroleum vapor concentration over time associated with weathering of LNAPL releases. The TO-15 PIANO analysis provides detailed information on the petroleum VOC vapor composition that can be used to evaluate the degree of biological weathering.	Monthly PID monitoring of the below-tank soil vapor wells has been conducted since 2008 (Figure 4-3 and Figure 4-4). These monitoring data document below-tank petroleum impacts that pre-date the initiation of PID monitoring resulting in 2008 PID readings generally in the range of 1,000 ppbv to 10,000 ppbv. As shown on Figure 4-3 and Figure 4-4, these PID readings generally decreased over time from 2008 through 2013 consistent with NSZD of the historical fuel impacts. In early 2014, PID readings for the Tank 5 soil vapor wells increased above 200,000 ppbv corresponding with the January 2014 release from Tank 5. Smaller PID reading increases were observed for soil vapor wells below tanks adjacent to Tank 5. From 2014 to 2017, PID readings again showed a gradual decrease over time consistent with NSZD of the 2014 release. In November 2017, TO-15 PIANO analysis documented the occurrence of biological weathering of the LNAPL below Tank 5 and indicated that any LNAPL present below the other tanks is heavily weathered. Aside from the elevated PID readings associated with the Tank 5 release event in early 2014, the monthly soil vapor monitoring point (SVMP) PID monitoring has rarely shown a PID reading above 10,000 ppbv. Since August 2015, only SVMPs at Tank 5, Tank 7, and Tank 18 have exhibited PID readings above 10,000 ppbv. Although Tank 5 PID readings are typically above 10,000 ppbv, they exhibit a decreasing trend over time consistent with natural attenuation of the 2014 LNAPL release. For Tank 18, the SVMP PID readings exhibited an abrupt increase from around 2,000 ppbv to 38,000 ppbv in April 2015. From April 2015 to May 2017, 12 of the 26 monthly PID readings were above 10,000 ppbv; however, for the last 11 monthly readings (June 2017 to April 2018), 7 have been below 10,000 ppbv. For Tank 7, monthly PID readings since August 2015 have generally been less than 1,000 ppbv. However, four large 1-month spikes have been observed: 96,000 ppbv in Nov 2015, 112,000 ppbv in April 2017, 176,000 ppbv in June 2017, and 131,000 ppbv in April 2018. In April and June 2017 and April 2018, the PID readings at Tank 7 were much higher than the readings at Tank 5, suggesting that the Tank 7 readings were not associated with the 2014 Tank 5 release. For both Tank 7 and Tank 18, the laboratory analysis of vapor samples collected in late October 2017 did not show evidence of recent (i.e., 2017) LNAPL releases from these tanks. For both tanks, the total concentrations of target analytes plus TICs were much lower than observed at Tank 5, and the FID chromatograms were not indicative of fresh jet fuel vapors. However, the timing of this field sampling program (late October/early November 2017) did not correspond to the period of elevated PID readings at Tank 7 and Tank 18. Laboratory analysis of a vapor sample collected coincidently with the observation of an elevated PID reading would provide a better understanding of the cause of that elevated PID reading.

Max ppm	3.8	274	383	176	12.6	10.2	8.8	7.7	38.4	22.7
Tank	1	3	5	7	9	11	13	15	17	19
	2	4	6	8	10	12	14	16	18	20

Parts per Billion by Volume

	No Data
1	< 50
2	51 - 100
3	101 - 500
4	501 - 1,000
5	1,001 - 2,000
6	2,001 - 5,000
7	5,001 - 10,000
8	10,001 - 20,000
9	20,001 - 50,000
10	50,001 - 100,000
11	100,001 - 200,000
12	200,001 - 450,000

2008	T1–2	T3–4	T5–6	T7–8	T9–10	T11–12	T13–14	T15–16	T17–18	T19–20
24-Mar		579	1,295	21,667	405	419	1,195	600		
		827	18,567	428	246	231	347	195	662	1,133
6-May		668	5,441	12,433	7,644	2,770	640	831		
	252	1,235	13,733	4,266	5,368	6,055	2,302	1,521	1,162	2,045
29-May		685	6,523	12,867	878	1,507	3,108	2,082		
	1,785	681	13,333	607	521	3,915	2,056	1,576	1,224	22,667
3-Jul		1,504	5,195	16,000	4,238	2,318	3,464	1,541		
	1,090	898	10,560	1,764	3,212	5,374	2,816	2,395	1,844	6,976
31-Jul		1,313	5,190	20,367	1,024	1,409	3,469	2,349		
	728	1,144	10,502	804	855	4,420	2,204	936	1,679	4,201
2-Sep		1,645	6,905	21,067	1,949	3,459		2,585		
	754	1,270	11,416	1,605	1,410	5,948	2,325	1,300	1,792	2,709
29-Sep		4,425	7,149	22,100	2,714	3,157	4,872	4,746		
	553	1,454	10,456	2,397	2,266	5,794	2,101	1,461	2,515	2,796
23-Oct		1,423	3,690	21,733	1,458	1,234	1,504	1,905		
	555	1,321	8,337	1,358	1,043	2,237	2,477	788	1,481	1,609
25-Nov		1,417	5,221	12,867	2,142	1,238	2,961	2,886	980	
	3,396	893	10,683	2,780	1,825	2,066	2,666	2,594	1,262	1,208
2009										
14-Jan		4,658	20,567	10,667	4,851	2,123	8,757	7,650	13,567	
	329	1,138	32,867	7,153	5,568	11	4,798	361	996	714
5-Feb		1,756	1,824	7,718	786	425	815	1,892	12,933	
	264	746	7,624	1,263	957	226	3,042	1,738	2,099	2,553
26-Feb		2,616	7,015	9,532	930	298	713	605	15,567	
	1,912	1,920	7,936	1,289	798	463	3,080	176	915	674
1-Apr		611	1,179	12,033	241	117	362	249	15,633	
	195	608	6,857	416	194	149	3,971	87	820	645
20-Apr		573	1,326	12,700	361	333	492	351	11,000	
	704	695	6,872	484	241	245	3,385	238	963	798
27-May		568	1,123	18,233	326	210	452	251	10,567	
	1,473	740	6,940	367	194	162	3,392	86	1,146	627
29-Jun		665	1,131	9,743	425	364	516	882	8,982	
	2,141	796	6,161	491	312	274	2,912	256	1,122	663
20-Jul		1,272	1,582	11,667	704	462	667	977	9,093	
	1,360	1,354	7,120	727	424	510	3,312	245	1,597	729
28-Aug		703	1,776	3,078	515	403	622	711	6,506	
	564	751	5,901	563	352	360	3,080	269	2,156	473
24-Sep		860	1,906	2,213	708	763	791	759	5,345	
	488	846	6,917	752	539	680	3,903	356	1,549	762
29-Oct		902	1,724	6,121	710	734	1,016	708	8,051	
	999	931	5,430	762	546	675	3,199	326	1,888	2,259
19-Nov		740	2,715	5,342	928	744	1,622	673	5,115	
	305	788	6,129	877	751	1,058	3,249	327	2,209	2,789
16-Dec		800	3,418	12,633	1,410	1,142	2,026	541	2,840	
	356	726	5,549	1,382	1,141	311	3,417	301	776	3,545

2010	T1–2	T3–4	T5–6	T7–8	T9–10	T11–12	T13–14	T15–16	T17–18	T19–20
28-Jan		575	1,227	4,079	510	396	542	779	2,497	
	684	616	5,721	621	356	336	3,550	288	888	666
22-Feb		641	2,234	3,519	877	619	792	442	2,846	
	364	713	4,841	840	711	104	2,795	209	1,631	2,599
25-Mar		919	1,484	16,200	670	847	863	806	1,865	
	394	761	5,709	612	815	569	4,006	707	1,222	1,625
28-Apr		733	1,532	2,365	858	738	4,463	599	2,072	
	385	683	5,905	756	695	444	3,617	447	1,575	1,597
26-May		621	1,147	3,244	543	880	600	608	1,637	
	374	618	4,483	560	420	439	4,383	1,633	1,190	746
28-Jun		645	64,900	1,786	627	444	637	592	1,773	
	400	626	4,800	609	440	383	5,258	1,144	1,299	898
28-Jul		528	59,433	6,775	630	440	661	623	3,745	
	332	588	4,347	610	994	397	5,447	1,112	1,485	1,191
29-Sep		259		372	377	321	382	328		
	224	318	1,090	352	288	283	334	359	580	284
18-Oct		876		839	923	720	737	677		
	577	843	1,084	1,221	686	722	597	576	839	602
16-Nov		581		701	607	326	626	605		
	424	644	1,142	740	625	252	438	467	778	365
14-Dec		732		369	633	198	572	556		
	416	335	2,043	657	385	272	452	327	725	484
2011										
14-Jan		627		451	668	418	878	625		
	651	633	1,282	862	501	333	604	923	512	306
15-Feb		542		550	586	343	565	552		
	298	609	2,245	541	310	357	525	1,348	662	361
15-Mar		350		296	312	224	434	367		
	221	471	2,542	304	246	339	311	331	515	368
18-Apr		401		333	365	260	501	368		
	327	475	2,412	489	297	285	550	230	518	540
18-May		840		900	1,102	920	1,915	2,864		
	980	983	2,343	1,263	1,077	1,005	1,767	2,985	742	752
22-Jun		386		475	223	183	370	314		
	205	356	1,558	412	216	278	306	330	551	347
27-Jul		127		342	181	145	159	193		
	101	187	909	320	88	132	158	470	380	305
26-Aug		146		135	122	86	207	192		
		205	924	180	97	134	254	765	382	252
22-Sep		346		443	302	333	390	136		
	318	373	1,385	309	301	1,631	112	219	367	240
27-Oct		294		537	271	290	361	199		
	270	281	1,155	338	245	256	236	214	358	263
22-Nov		338		431	243	183	394	230		
	235	356	1,098	355	195	303	257	245	403	334
16-Dec		274		424	379	75	860	94		
	408	799	651	211	141	185	156	121	327	361
2012										
20-Jan		223		356	148	272	229	101		
	239	141	537	340	224	297	105	198	233	88
23-Feb		190		213	135	135	201	271		
	167	436	943	222	139	148	180	195	326	393
13-Mar		341		782	360	144	282	117		
	222	146	816	391	387	423	514	282	373	236
16-Apr		230		708	1,212	157	161	832		
	149	241	756	485	323	123	222	1,280	402	424
15-May		196		1,877	137	66	233	153		
	146	253	699	157	87	130	190	247	594	176
19-Jun		422		686	626	347	382	570		
	292	464	498	466	319	315	406	570	875	383
10-Jul		265		638	325	252	369	454		
	206	289	373	325	353	345	292	340	1,425	563
14-Aug		410		680	350	342	334	303		
	389	358	476	296	225	285	237	344	853	494
24-Oct		246		552	335	303	195	146		
	166	221	474	400	164	153	157	166	752	264
26-Nov		139		100	78	121	59	19		
	110	187		76	51	34	13	92	215	106
18-Dec		109			87	35	42	10		
	106	99			36	23	5	28	171	39

2013	T1–2	T3–4	T5–6	T7–8	T9–10	T11–12	T13–14	T15–16	T17–18	T19–20
31-Jan		54			66	10	3	4		
	966	423			11	8	6	13	1,423	223
28-Feb		215			133	100	44	85		
	47	87			91	98	518	77	913	296
28-Mar		52			47	14	32	13		
	12	24			23	16	16	21	572	263
25-Apr		39			59	44	43	25		
	18	39			40	62	29	36	293	182
30-May		160	221		226	158	40			
	204	135			301	73	112	56	307	95
27-Jun		35	233	676	47	27	44	59	274	
	15	26	378	402	301	44	280	51	264	137
25-Jul		179	322	583	184	138	148	90	876	
	316	130	742	176	100	101	124	76	1,197	332
29-Aug		13	161	173	39	784	255	710	3,069	
	165	192	1,066	28	1,621	270	862		5,326	581
26-Sep		49	114	253	3	52	3	14	1,716	
	306	18	566	15	3	8	12	20	3,190	323
24-Oct		277	250	396	200	321	206	181	648	
	285	295	1,485	2,013	191	221	170	173	2,333	454
21-Nov		150	120	191	133	471	83	46	3,349	
	186	159	322	88	76	140	75	163	5,227	350
23-Dec		17	794	8	13	14	11	18	3,023	
	61	14	39	6	12	11		6	8,679	787
2014										
30-Jan		9,444	176,000	6,539	2,408	374	1,109	1,025	2,980	
	11	165	3,046	2,952	483	270		139	2,116	697
24-Feb		5,290	100,000	1,187	330	307	116	65	4,069	
	135	163	6,165	601	165	215		65	3,241	571
25-Mar		274,000	271,000	17,300	5,465	53	332	372	6,391	
	146	11,800	2,169	7,880	1,148	66	261	388	2,545	242
22-Apr		2,442	383,000	33,500	12,600	167	575	623	5,221	
	739	948	31,100	21,000	3,381	290	349	302	2,082	561
27-May		1,536	369,000	43,000	10,200	959	1,615	1,071	3,827	
	697	817	31,900	15,100	2,850	810	697	348	2,856	1,451
23-Jun		3,530	78,700	495	22	17	727	260	3,138	
	183	1,233	2,747	133	10	374	824	169	2,050	1,271
21-Jul		1,215	237,000	34,900	12,000	240	1,191	1,321	2,804	
	527	735	21,900	16,800	3,640	290	634	552	2,823	2,213
27-Aug		1,050	222,000	31,400	10,200	3,218	4,638	1,916	2,954	
	199	296	31,200	12,700	3,650	2,769	1,376	1,026	1,478	1,618
25-Sep		1,298	208,000	23,000	8,583	3,185	2,562	3,159	2,056	
	1,028	614	28,000	11,600	4,093	2,338	1,295	1,226	3,679	1,561
29-Oct		254	180,000	540	185	154	205		257	
	409	194	12,600	1,196	117	144	127		2,008	283
20-Nov		919	229,000	12,800	4,102	1,182	1,208	754	998	
	309	409	17,100	5,894	2,124	1,147	678	458	3,404	983
23-Dec		2,004	102,000	13,500	5,213	1,261	1,621	886	1,319	
	811	1,483	10,900	7,996	2,225	1,075	654	470	3,421	1,516
2015										
28-Jan		10,300	208,000	15,000	87	99	85	71	282	
	3,808	14,800	2,051	237	74	63	85	63	1,762	101
27-Feb		2,231	189,000	13,200	2,689	1,056	1,309	956	877	
	160	370	17,700	4,689	1,187	609	648	333	1,398	898
26-Mar		554	88,900	5,280	4,885	2,294	2,562	1,585	3,938	
	360	814	11,500	6,634	104	1,203	1,088	884		2,211
20-Apr		436	245,000	51,300	2,410	835	1,145	651	952	
	164	339	13,300	5,860	1,175	728	434	393	38,400	4,586
28-May		6,657	287,000	3,740	2	4,184			268	
	1,285	10,500	763						1,191	29
25-Jun		435	153,000	7,341	3,074	9,065	1,594	1,239	955	
	248	295	4,536	3,323	959	897	986	531	17,200	2,456
21-Jul		880	175,000	10,200	2,383	10,200	1,431	927	275	
	243	385	11,000	3,430	823	940	500	93	19,100	1,994
27-Aug		576	135,000	1,025	859	5,595	659	1,126	1,045	
	270	406	731	549	363	1,047	892	777	18,000	2,673
23-Sep		2,316	148,667	113	44	2,584	59	193	358	
	341	460	486		71	64	148	477	11,625	455
20-Oct		619	176,267	569	476	3,045	286	277	439	
	323	627	1,881	412	380	584	320	289	16,280	697
18-Nov		469	153,867	96,503	103	2,714	125	253	1,082	
		425		93	103	207	161	735	27,153	556
17-Dec		506	317,400	3,086	420	1,071	393	338	612	
	904	323	1,620	538	403	541	418	432	32,387	1,010

2016	T1–2	T3–4	T5–6	T7–8	T9–10	T11–12	T13–14	T15–16	T17–18	T19–20
20-Jan		963	303,367	719	703	1,534	707	633	810	
	739	602	1,548	644	667	630	589	580	31,047	427
17-Feb		888	295,600	832	591	2,316	615	530	765	
	671	617	1,763	633	574	616	543	705	28,737	724
15-Mar		841	319,000	956	662	947	407	551	818	
	565	520	1,797	599	608	465	532	607	1,699	840
20-Apr		855	133,033	626	951	1,133	451	451	726	
	454	428	1,347	810	535	456	371	371	2,154	344
23-May		1,382	115,567	1,403	1,797	1,271	1,233	1,668	1,033	
	856	1,093	2,122	1,691	1,342	1,008	877	2,147	7,787	813
21-Jun		763	151,600	796	701	968	436	479	766	
	473	622	1,668	632	595	675	441	576	6,715	584
22-Jul		740	96,967	427	347	522	292	253	520	
	519	575	1,176	309	298	346	296	353	8,082	322
23-Aug		518	74,483	889	526	498	392	306	417	
	396	387	1,312	629	479	312	319	298	6,230	252
21-Sep		646	53,800	428	379	273	295	234	375	
	516	660	621	293	295	321	196	273	4,441	178
19-Oct		727	95,847	900	698	409	316	308	730	
	426	751	1,322	3,981	567	293	238	236	9,297	539
17-Nov		540	111,200	904	469	353	307	306	536	
	289	306	1,379	671	485	235	277	304	10,427	259
20-Dec		802	82,860	657	579	630	474	511	838	
	543	552	1,234	602	576	568	522	463	11,247	262
2017										
31-Jan		618	98,227	329	434	411	231	263	507	
	477	407	1,091	390	333	333	340	299	10,312	646
22-Feb		454	103,867	557	554	302	299	284	492	
	679	351	1,350	485	495	338	335	356	8,613	211
24-Mar		458	64,780	320	342	827	511	353	534	
	323	343	781	304	290	318	355	322	5,366	626
20-Apr		480	59,747	112,600	388	491	720	293	398	
	472	529	1,074	509	322	361	319	235	6,817	434
28-May		1,628	79,537	11,877	1,840	918	846	484	446	
	1,646	1,746	3,201	1,645	682	1,541	492	376	10,253	411
25-Jun		699	55,877	175,533	1,078	1,415	7,761	519	519	
	624	568	1,815	966	973	1,213	615	362	7,718	422
21-Jul		731	50,333	11,383	733	731		418	343	
	604	637	1,135	770	500	461	324	268	7,241	262
27-Aug		608	40,520	3,551	862	692		344	404	
	519	596	1,187	775	708	297	313	245	5,694	358
23-Sep		412	31,050	966	410	354	796	289	238	
	296	315	662	355	283	324	227	134	2,567	200
20-Oct		373	24,613	772	712	399	695	434	348	
	297	318	746	664	558	369	335	280	2,304	745
18-Nov		345	21,623	395	365	226	323	561	276	
	269	281	747	195	193	196	286	222	2,849	545
18-Dec		410	24,653	469	310	346	327	271	357	
	310	323	685	258	280	290	278	329	2,585	306
2018										
31-Jan		242	19,520	436	383	390	1,261	379	480	
	158	158	912	362	341	357	383	360	4,773	896
22-Feb		361	13,307	421	377	356	375	229	372	
	410	339	1,037	299	391	341	347	371	3,994	403
24-Mar		540	13,113	470	444	535	365	355	820	
	412	397	701	387	482	779	414	389	6,908	602
20-Apr		456	6,616	131,367	324	308	260	226	450	
	356	302	757	282	321	357	314	305	5,112	388
28-May		558	2,149	593	573	758	273	262	487	
	340	307	1,190	406	426	329	343	245	6,588	553

Figure 4-3: Monthly PID Monitoring Results for Below-Tank Soil Vapor Wells
Conceptual Site Model
Red Hill Bulk Fuel Storage Facility
JBPHH, O'ahu, Hawai'i

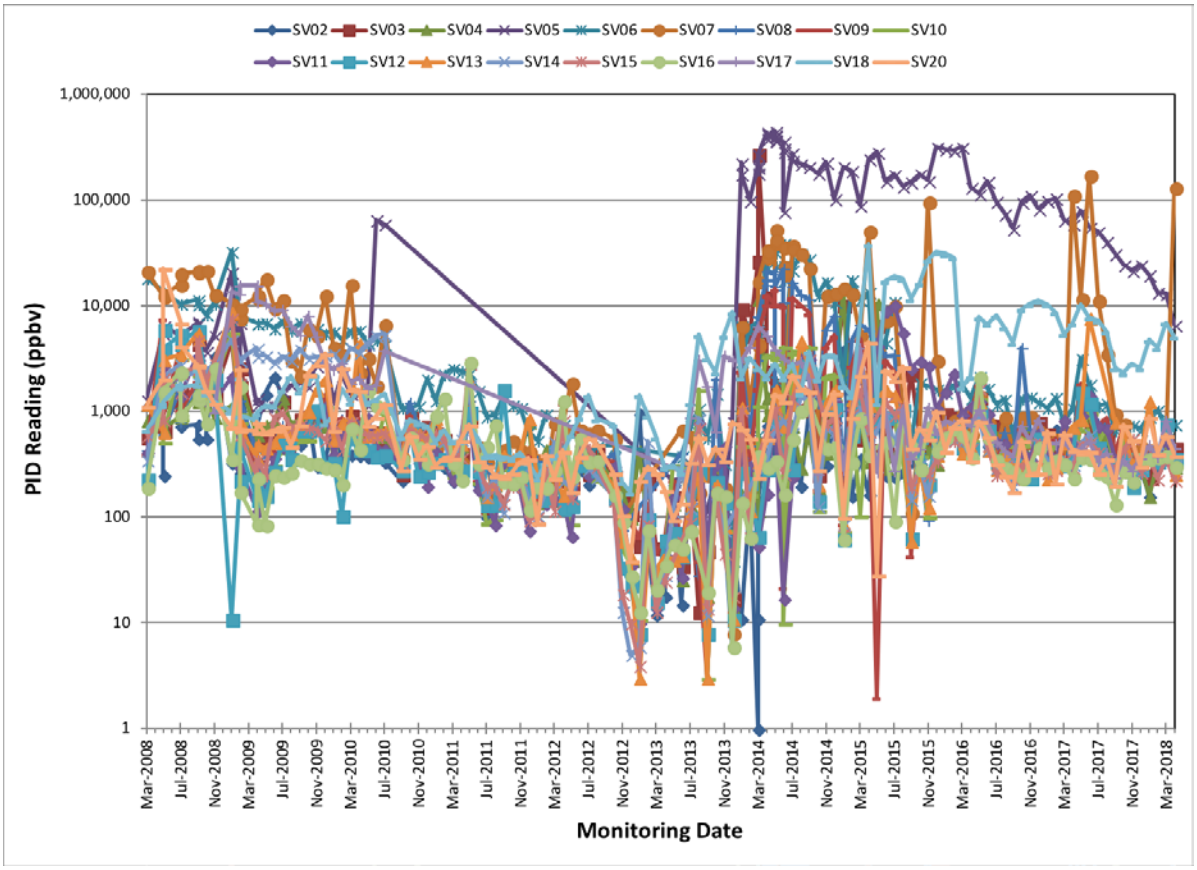

Figure 4-4: Log Scale Graph of Monthly PID Monitoring Results for Below-Tank Soil Vapor Wells

Table 4-6: Study Question 6: Are Vadose-Zone Petroleum Vapors a Significant Source of Impacts In the Tunnels?

Finding	Discussion
NO. Facility operations are the primary source of petroleum vapors in the tunnels. Any soil vapors entering the tunnel are highly diluted by the tunnel ventilation system. The magnitude and sources of petroleum vapors in the tunnels were evaluated using PID readings and qualitative observations. These data suggest that:	**Relative to outdoors, PID readings are elevated in the tunnels and in the soil vapor wells.** The PID readings showed similar petroleum vapor concentrations in the tunnels and soil vapor wells below the tanks (Table 4-7). The median PID readings in the lower tunnel and the soil vapor wells were almost identical and the maximum soil vapor well PID reading was equal to the maximum PID reading from the upper tunnel (i.e., both 40,000 ppb). In addition, as discussed in Section 3, laboratory analysis of soil vapor samples collected from the below-tank soil vapor wells suggested that elevated PID readings at these soil vapor wells are not always associated with the presence of petroleum vapors. Although PID readings above 10,000 ppbv were observed in soil vapor wells at six of the 17 tanks tested, the laboratory analysis of samples collected from these wells indicated high petroleum vapors only at Tank 5. At the other locations, the high PID readings do not appear to be associated with elevated petroleum VOC concentrations. These results suggest that the primary source of petroleum vapors in the tunnels is not petroleum vapors in the basalt.
• Petroleum vapor concentrations in the tunnels are higher than in outdoor air. • Although vapor flow is from the vadose zone into the tunnel, any soil vapors entering the tunnels are highly diluted by ambient air from the tunnel ventilation system. • The primary source of the petroleum vapors in the tunnels is active operations at the Facility.	**Any vadose zone vapors entering the tunnels are highly diluted by the tunnel ventilation system.** The tunnel ventilation system is designed to maintain a combined air flow through the upper (16,000 cubic feet per minute [cfm]) and lower (63,000 cfm) tunnels in the vicinity of the fuel tanks of 79,000 cfm (see CSM Appendix B.2, Figure 2-1). As discussed in Section 3.2.3, the tunnels have a negative pressure relative to the vadose zone such that any gas flow is from the vadose zone into the tunnels. However, the large volume of outdoor air pumped though the tunnels results in significant dilution of any soil vapors entering the tunnels. The vadose zone to tunnel dilution factor was estimated using two independent datasets: i) oxygen concentration measurements and thermal NSZD rates, and ii) ancient carbon (carbon dioxide associated with the biodegradation of fossil fuel) concentrations in the tunnels. These calculations are provided in CSM Appendix B.2. Both calculations indicated that less than 0.5% of the air in the tunnels originates from the vadose zone. In other words, any vapors entering the tunnels are diluted by > 100× with outdoor air provided by the ventilation system (i.e., an attenuation factor of < 0.01). Applying this attenuation factor to the average PID reading for the soil vapor wells (4,335 ppbv × 0.01 = 43 ppb) suggests that vadose zone soil vapors account for less than 10% of the average PID reading in the tunnels (660 ppb).
	The primary source of petroleum vapors in the tunnels is Facility operations. The observed Facility operations and distribution of petroleum vapors in the tunnels suggest that ongoing Facility operations are the primary source of petroleum vapors in the tunnels. On the first day of soil vapor well sampling (October 27, 2017), fuel was being transferred from Tank 20 using a flexible hose. The Facility personnel suggested that work be deferred in that area because disconnection of the hose would result in elevated petroleum vapors in the tunnels. As a result, sample collection at Tank 20 was deferred until three days later (October 30); even at this later date, PID readings at Tank 20 were 2,400 ppb, almost twice as high as any other locations within the lower tunnel. Note that Tanks 19 and 20 are located within a "dead end" section of the lower tunnel (i.e., beyond the Adit 6 ventilation system) and are less highly ventilated compared to the other sections of the lower tunnel. Observations and readings in the upper tunnel also suggested that the Facility operations could be a source of petroleum vapors to the tunnels. The top of each tank can be accessed from the upper tunnel by a fixed set of ladder stairs at the end of the lateral tank access tunnels. These ladder stairs are accessed directly from the upper tunnel without any door or other enclosure. During the field program, access to the top of Tank 6 was attempted for the purpose of installing a soil vapor sample point. Approximately one-third of the way up the ladder, the multigas meter being used for safety monitoring showed a petroleum vapor reading of 40 ppmv (i.e., 40,000 ppbv) and rising. A petroleum vapor concentration of 40 ppmv is –2% of the equilibrium vapor concentration for fresh jet fuel (2,000–4,000 ppmv). Based on the reading, the ladder was exited and measurements of the maximum petroleum vapor concentration in this area were not attempted. Taken together, the observations of petroleum vapors at Tank 20 in the lower tunnel and Tank 6 in the upper tunnel suggest that ongoing Facility operations are the primary source of petroleum vapors in tunnels.

Table 4-7: Summary of PID Measurements in the Tunnels

Parameter	Outdoor Air	Upper Tunnel [a]	Lower Tunnel	Soil Vapor Wells [b]
Number of Readings	2	2	17	46
Minimum (ppb)	0	180	85	44
Median (ppb)	NC	NC	581	594
Average (ppb)	78	340	660	4,335
Maximum (ppb)	155	40,000	2,400	40,000

Notes:
[a] Table includes a reading of 40,000 ppbv taken using as multigas meter approximately one-third of the way up the access ladder to the top of Tank 6. Excluding this value, the maximum PID reading within the upper tunnel was 500 ppb.
[b] Two or three soil vapor wells are installed below each of the 18 active fuel storage tanks.
NC not calculated

5. Gradient Method for Measuring NSZD

5.1 TECHNICAL BACKGROUND

Based on the results of the soil vapor sampling program (Table 4-3 and Table 4-4), NSZD is occurring at the Facility. Under certain conditions, NSZD rates can be obtained by using the gradient method by measuring the oxygen gradient from the surface (oxygen concentration of 21% of air) to a point in the subsurface where the oxygen is completely consumed. When this vertical oxygen gradient is multiplied by an effective diffusion coefficient, and if certain other conditions hold, a NSZD rate can be obtained (e.g., Johnson, Lundegard, and Liu 2006; Lundegard and Johnson 2006). The diffusive flux can be converted to a NSZD rate in units of gallons per acre per year.

The key assumptions required to apply the gradient method to calculate NSZD rates are:

- Oxygen and/or carbon dioxide concentrations in the air phase in the unsaturated zone migrate via one dimensional diffusion from the source of these compounds (for oxygen, the source is ground surface; for carbon dioxide, the location where methane/hydrocarbons are oxidized) to the sink of these compounds (for oxygen, the sink is the location where methane/hydrocarbons are oxidized; for carbon dioxide, it is the ground surface).
- Relatively uniform soil conditions in the soil column and over time so that a one-dimensional diffusion model can be applied.
- No advective source of vapor flow in the subsurface.

As the data collection activities described in the *Attenuation Evaluation Plan* (DON 2017) progressed, it became more obvious that the key assumptions above were not valid for the Facility system. This section describes applicability of the gradient method at the Facility and issues with the underlying assumptions.

5.2 GRADIENT METHOD DATA COLLECTION

The gradient method was employed using data from the following vapor measurement points designed to collect vapor samples from the surrounding basalt at different elevations:

- Bottom of the tanks using the existing soil vapor probes.
- Through the sidewall of the upper tunnel near Tanks 5 and 11 (Vapor Pin sample locations). These two locations represent a range of possible conditions from likely impacted (Tank 5) to a location with a potentially smaller impact in the middle of the tank farm (Tank 11).
- In shallow soil vapor points above/near Tanks 5 and 11.
- In the atmosphere where ambient oxygen concentrations are 21% and carbon dioxide concentrations are about 400 ppbv.

In addition, vapor samples were also collected from the screened intervals in the two nearest monitoring wells (RHMW02 and RHMW03) to Tanks 5 and 11, respectively. Because these sample locations were below any LNAPL accumulation in the unsaturated zone they were not originally intended to be used for the gradient method calculations. Data were collected at these locations principally to better understand the distribution of LNAPL below the tank farm and help interpret the site attenuation data.

A GEM5000 Landfill Gas Meter was used to collect all the oxygen and carbon dioxide data from the sampling points except for the ambient concentration in the atmosphere where literature values were used.

5.3 SOIL VAPOR CARBON DIOXIDE AND GRADIENT PROFILES

Oxygen vs. elevation data were plotted as an initial screen to determine if the gradient method could be applied at the Facility (Figure 5-1) to determine NSZD rates. In general, if the key conditions necessary to apply the gradient method are present, the oxygen vs. elevation data will plot in a relatively straight line with a negative slope (e.g., Lundegard and Johnson 2006).

The oxygen values at the lowest elevation are from two monitoring wells: RHMW02 for Tank 5 and RHMW03 for Tank 11 (note that RHMW03 is actually over 100 ft distant from Tank 11).

The oxygen levels near 100 ft above mean sea level (msl) elevation are from the vapor probes underlying the tanks, where the elevations were estimated using the general design of the probes and the angle of the borings.

The oxygen levels at about 380 ft msl correspond to Vapor Pins drilled into the sides of the upper access tunnel. The two highest elevation data points represent shallow soil vapor points installed about 5 ft into the soil at the top of the tank farm and ambient atmospheric conditions at ground surface.

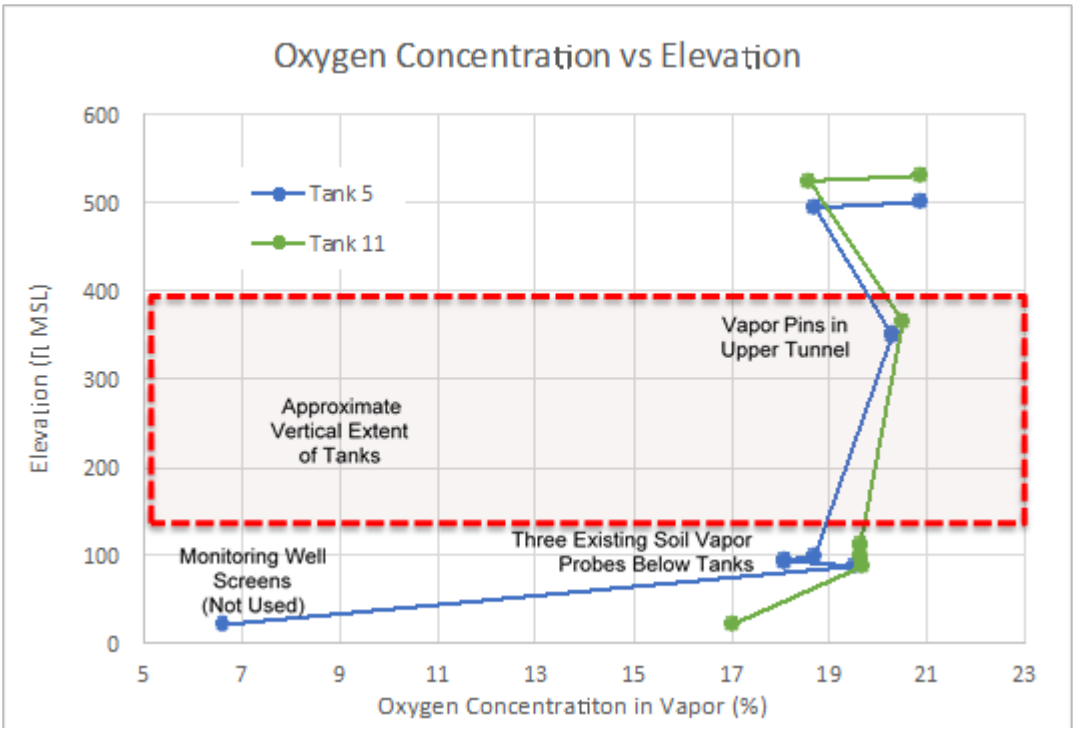

Figure 5-1: Oxygen vs. Elevation Data Collected at the Facility

At most sites where the gradient is applied successfully, a relatively constant oxygen gradient is observed in the unsaturated zone above the LNAPL body (Figure 5-2).

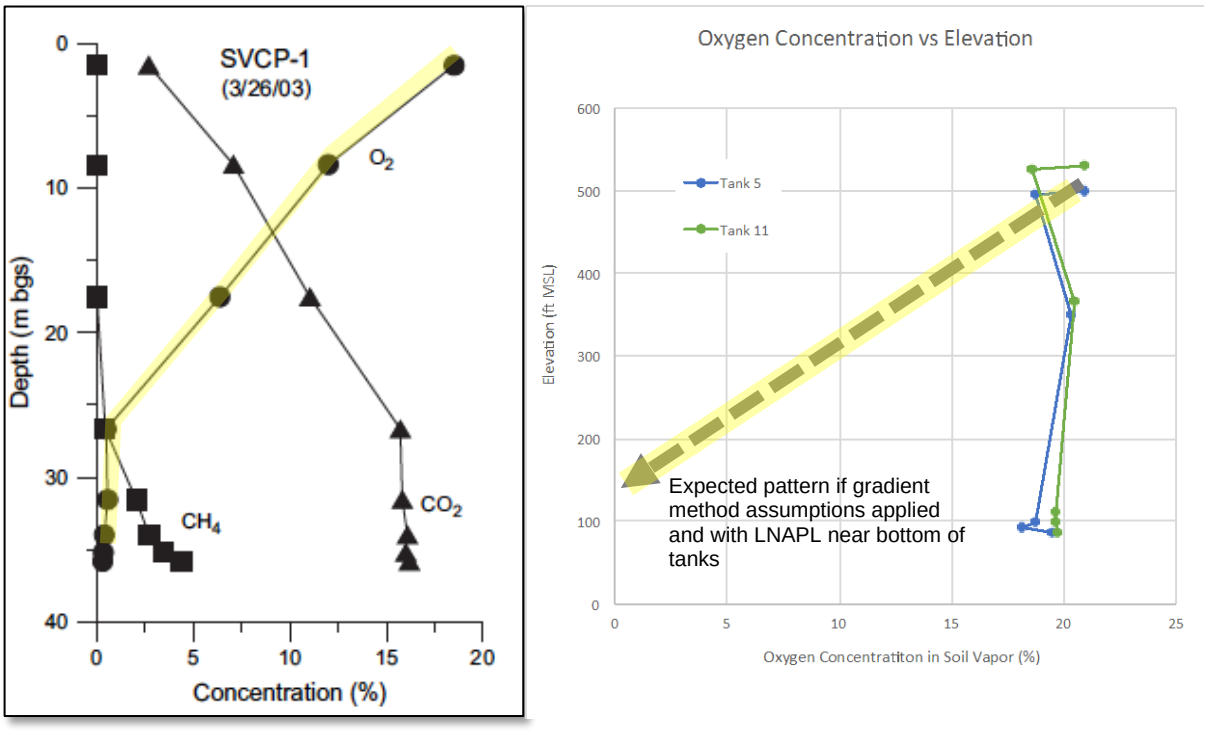

Source (left panel): Lundegard and Johnson 2006.
Yellow highlight shows oxygen gradient in unsaturated zone above the LNAPL body that is appropriate for applying the gradient method.

Figure 5-2: Left: Soil Vapor Data Collected at Oil Field Site; Right: Actual Data from Figure 5-1 vs. Expected Pattern if Gradient Method Conditions Were Met

5.4 REASONS FOR COMPLEX SOIL VAPOR OXYGEN PROFILES AT THE FACILITY

As shown on Figure 5-2 (right side), the non-linear oxygen gradient at both Tank 5 and Tank 11 locations suggests that the gradient method is not applicable at the Facility. Several confounding processes are present:

- The presence of horizontal pathways for oxygen delivery, thereby violating the assumption of a purely vertical diffusion process.
- The ventilation system within the Facility tunnel system that acts as a partial soil vapor extraction system, thereby violating the diffusion-only requirement.

5.4.1 Horizontal Oxygen Migration

The shallow vapor probe data show oxygen concentrations in the 18–19% range, lower than the 20.9% atmosphere and lower than the oxygen concentrations in the upper tunnel Vapor Pins (about 20.5% oxygen). This suggests that the soils these shallow vapor wells are screened in likely: (1) have low permeability that restricts the influx of oxygen from the surface; and/or (2) are affected by natural organic sources decaying and are thereby removing oxygen.

The relatively high oxygen concentrations in the upper tunnel near atmospheric conditions (about 20.4% oxygen) indicate that there is an influx of oxygen in this location. This may be from high-permeability clinker zones or thin pāhoehoe zones that have preferential pathways and/or very

high air-filled porosity that is allowing oxygen to diffuse in from the sides of the tank farm. As shown on Figure 5-3, there are clinker and pāhoehoe units in the vertical intervals where the tanks are located. On the figure, yellow arrows indicate geologic pathways that appear to be delivering oxygen horizontally to the tank farm.

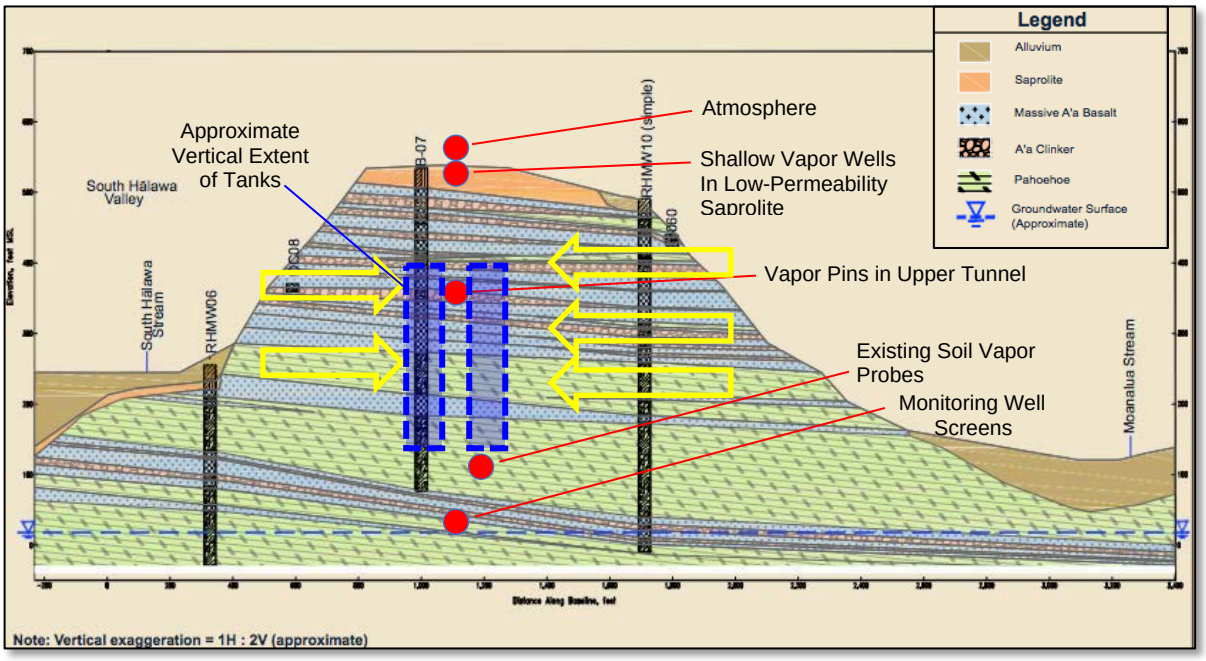

Location of tanks and sample points are approximate. Yellow arrows indicate geologic pathways that appear to be delivering oxygen horizontally to the tank farm, thereby violating the gradient method assumptions.

Figure 5-3: Vertical Location of Tank 5 in North-South Cross Section Between Tanks 5 and 6

Planning-level diffusion calculations show the horizontal pathways likely have similar capacity (within an order of magnitude) to diffuse oxygen in from the sides of the tank farm as from the vertical pathways from the top of the tank farm. Note that the presence of fine-grained material in the weathered a'ā clinker zones would reduce the ability of the clinker to transmit gas by diffusion, but only by a relatively small amount compared to the reduction in hydraulic conductivity. Consequently, the presence of fine-grained material does not likely impede the diffusion of gases significantly compared to its effect on the advection of gases and water through this material.

5.4.2 Tunnel System Acting Like Soil Vapor Extraction (SVE) System

The highly oxygenated vapor throughout the Facility oxygen profiles indicates there is a significant influx of air due to advection. As discussed in Section 3.2.3, the tunnel ventilation system results in the tunnels being kept at a lower pressure than ambient air in the basalt. Therefore, there is a net inflow of air into tunnels from the basalt. In addition to the differential pressure measurements, carbon trap data indicate that, while there is some air migration through the floor of the tunnel, most is from small cracks and fractures (see CSM Appendix B.2). Overall, the carbon trap data show:

- A small fraction of the tunnel air (less than 0.5%) (see CSM Appendix B.2) is likely drawn from the basalt via cracks and fractures in the tunnel walls/floor.

- The signal of "ancient carbon" (carbon dioxide associated with the biodegradation of fossil fuel) shows that some of the carbon dioxide leaving the tunnels originated in fossil fuels (which are depleted in carbon-14 due to their age).
- The amount of ancient carbon can be converted to a NSZD rate, and this rate is within the NSZD rate estimated by the thermal NSZD analysis (see CSM Appendix B.1).
- The tunnel is acting like a relatively inefficient SVE system, but one that efficient enough to draw air from the atmosphere to the LNAPL zones.

Because of the tunnel system and its behaving like an SVE system, the movement of oxygen near the tank farm violates the gradient method's assumption of oxygen transport by vertical gas-phase diffusion only.

5.5 GRADIENT METHOD CONCLUSIONS

Soil vapor oxygen concentrations were collected at elevations near Tanks 5 and Tank 11 in order to apply the gradient method to estimate NSZD rates. Certain geologic and contaminant transport conditions were required to apply the gradient method. The presence or absence of these conditions at the Facility was not known prior to the field investigation.

When the vertical oxygen profile data were analyzed along with carbon trap data and other attenuation data, it became clear that two of the key assumptions necessary to apply the gradient method are not found at the Facility:

- It is unlikely that oxygen transport between the surface and near the biodegradation zone is via one-dimensional gas-phase diffusion. Within the tank farm, horizontal oxygen migration pathways are likely present, thereby invalidating the one-dimensional vertical diffusion assumption.
- It is very likely that the ventilation system with the Facility tunnels is acting like a SVE system, drawing air through small cracks and fractures in the tunnel walls/floor and thereby introducing oxygen by advection. This also invalidates the one-dimensional vertical diffusion assumption. The SVE-like behavior of the tunnel system is supported by multiple lines of evidence, including:
  - Carbon trap data on the hillside are much lower than typical hydrocarbon release sites.
  - Carbon trap data in the tunnels shows high concentrations of "ancient carbon" in the carbon dioxide leaving the tunnel. This ancient carbon in the form of carbon dioxide confirms LNAPL biodegradation is ongoing, and significant amounts of the carbon dioxide is being captured by the tunnel ventilation system.
  - Soil vapor data shows the geologic media around the tanks is surprisingly high in oxygen content, indicating an active mechanism for delivering oxygen to the tanks.
  - Soil measurements show the air pressure outside the tunnels is higher than the air pressure within the tunnels.
  - Calculations show only a small amount of air leakage (< 0.5%; see CSM Appendix B.2) from the basalt into the tunnels can explain all the biodegradation being measured at the Facility.

6. References

Baedecker, M. J., R. P. Eganhouse, B. A. Bekins, and G. N. Delin. 2011. "Loss of Volatile Hydrocarbons from an LNAPL Oil Source." *Journal of Contaminant Hydrology* 126: 140–152.

Cox-Colvin, Cox-Colvin & Associates, Inc. 2016. *Standard Operating, Procedure Installation and Extraction of the Vapor Pin®*. Plain City, OH: Updated September 16.

Department of the Navy (DON). 2017. *Attenuation Evaluation Plan, Investigation and Remediation of Releases and Groundwater Protection and Evaluation, Red Hill Bulk Fuel Storage Facility, Joint Base Pearl Harbor-Hickam, O'ahu, Hawai'i; September 1, 2017, Revision 00*. Prepared by AECOM Technical Services, Inc., Honolulu, HI. Prepared for Defense Logistics Agency Energy, Fort Belvoir, VA, under Naval Facilities Engineering Command, Hawaii, JBPHH HI.

Fitzpatrick, N. A., and J. J. Fitzgerald. 1996. *An Evaluation of Vapor Intrusion into Buildings Through a Study of Field Data*. In: Proceedings of the 11th Annual Conference on Contaminated Soils, University of Massachusetts at Amherst, October 1996.

Gregg, S. D., J. L. Campbell, J. W. Fisher, and M. G. Bartlett. 2007. "Methods for the Characterization of Jet Propellent-8: Vapor and Aerosol." *Biomedical Chromatography* 21: 463–472.

Johnson, P., P. Lundegard, and Z. Liu. 2006. "Source Zone Natural Attenuation at Petroleum Hydrocarbon Spill Sites: I. Site-Specific Assessment Approach." *Groundwater Monitoring & Remediation* 26: 82–92.

Kaplan, I., Y. Galperin, S. T. Lu, and R. P. Lee. 1997. "Forensic Environmental Geochemistry: Differentiation of Different Fuel Types, Their Sources and Release Times." *Org. Geochem.* 27: 289–317.

Lundegard, P. D., and P. C. Johnson. 2006. "Source Zone Natural Attenuation at Petroleum Hydrocarbon Spill Sites: II. Application to a Former Oil Field." *Groundwater Monitoring & Remediation* 26 (4): 93–106. https://doi.org/10.1111/j.1745-6592.2006.00115.x.

McHugh, T. E., and T. McAlary. 2009. *Important Physical Processes For Vapor Intrusion: A Literature Review*. In: Proceedings of AWMA Vapor Intrusion Conference (San Diego, CA, January 28–30, 2009).

Pleil, J. D., L. B. Smith, and S. D. Zelnick. 2000. "Personal Exposure to JP-8 Jet Fuel Vapors and Exhaust at Air Force Bases." *Environmental Health Perspectives* 108 (3): 183–192.

Shepard, J. E., C. D. Nuyt, J. J. Lee, and J. E. Woodrow. 2000. *Flash Point and Chemical Composition of Aviation Kerosene (Jet A)*. In Collaboration with ARCO Products Company, Carson, CA and J. E. Woodrow Center for Environmental Sciences and Engineering, University of Nevada. Explosion Dynamics Laboratory Report FM99-4. Pasadena, CA: California Institute of Technology, Graduate Aeronautical Laboratories. April 2, Revised May 26.

TEC, Inc. (TEC). 2010. *Final Soil Vapor Sampling Monitoring Analysis Letter Report*. From Robert Whittier, Senior Hydrogeologist, to: Greg Yamasaki, Supervisory General Engineer, FISC Pearl Harbor. Contract No. N47408-04-D-8514, Task Order 054.

Tran, T. C., G. A. Logan, E. Grosjean, D. Ryan, and P. J. Marriott. 2010. "Use of Comprehensive Two-Dimensional Gas Chromatography/Time-of-Flight Mass Spectrometry for the Characterization of Biodegradation and Unresolved Complex Mixtures in Petroleum." *Geochimica et Cosmochimica Acta* 74: 6468–484.

Attachment B.3.1:
Fingerprint Charts for Soil Vapor and Groundwater Monitoring Well Headspace Samples

ATTACHMENT B.3.1: FINGERPRINT CHARTS FOR SOIL VAPOR AND GROUNDWATER MONITORING WELL HEADSPACE SAMPLES
Red Hill Bulk Fuel Storage Facility, Joint Base Pearl Harbor-Hickam, O'ahu, Hawai'i

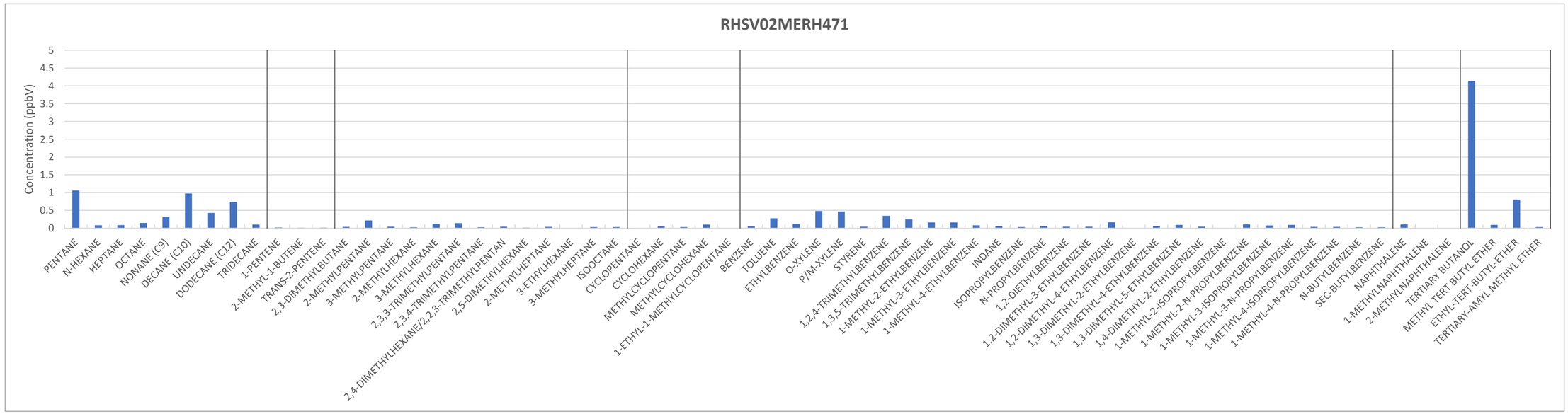

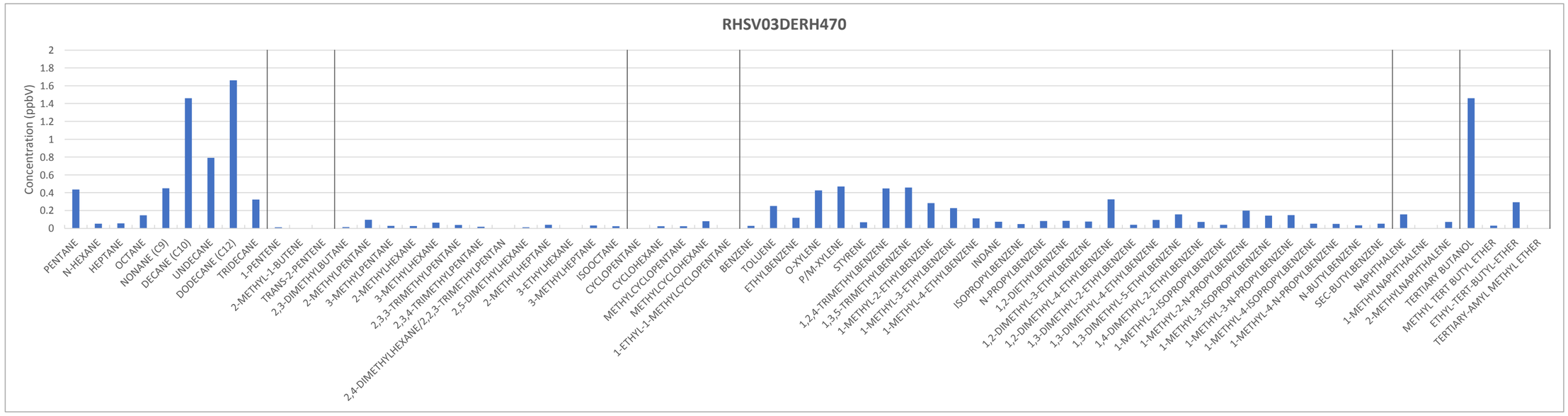

ATTACHMENT B.3.1: FINGERPRINT CHARTS FOR SOIL VAPOR AND GROUNDWATER MONITORING WELL HEADSPACE SAMPLES
Red Hill Bulk Fuel Storage Facility, Joint Base Pearl Harbor-Hickam, O'ahu, Hawai'i

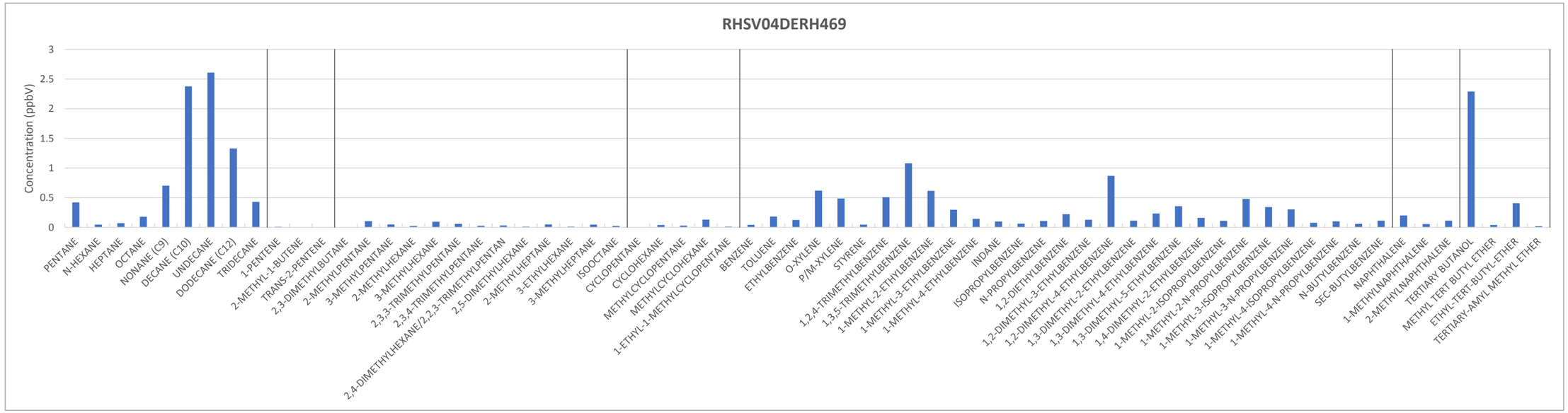

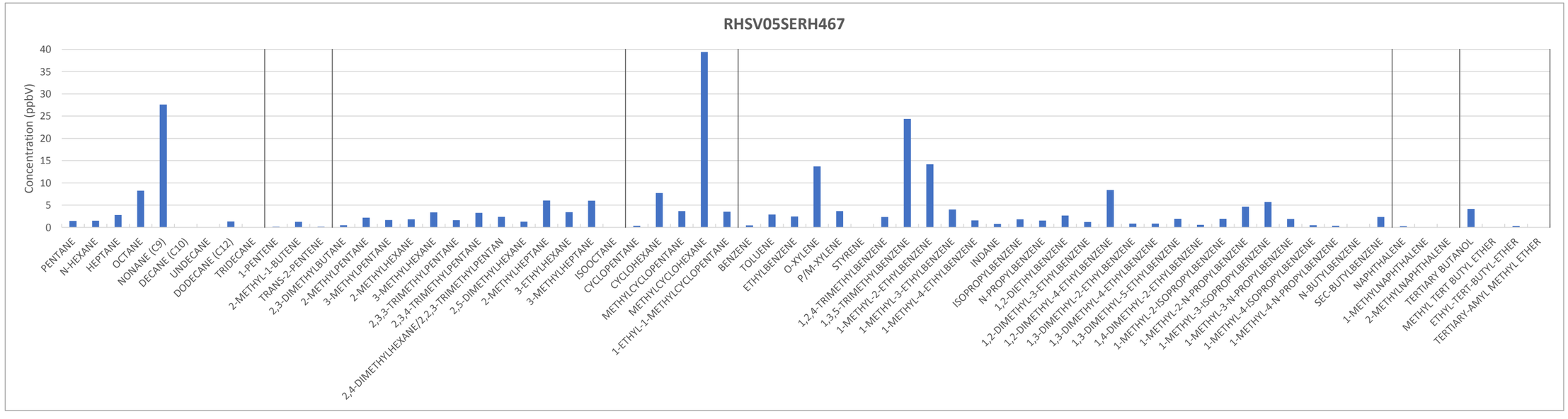

ATTACHMENT B.3.1: FINGERPRINT CHARTS FOR SOIL VAPOR AND GROUNDWATER MONITORING WELL HEADSPACE SAMPLES
Red Hill Bulk Fuel Storage Facility, Joint Base Pearl Harbor-Hickam, O'ahu, Hawai'i

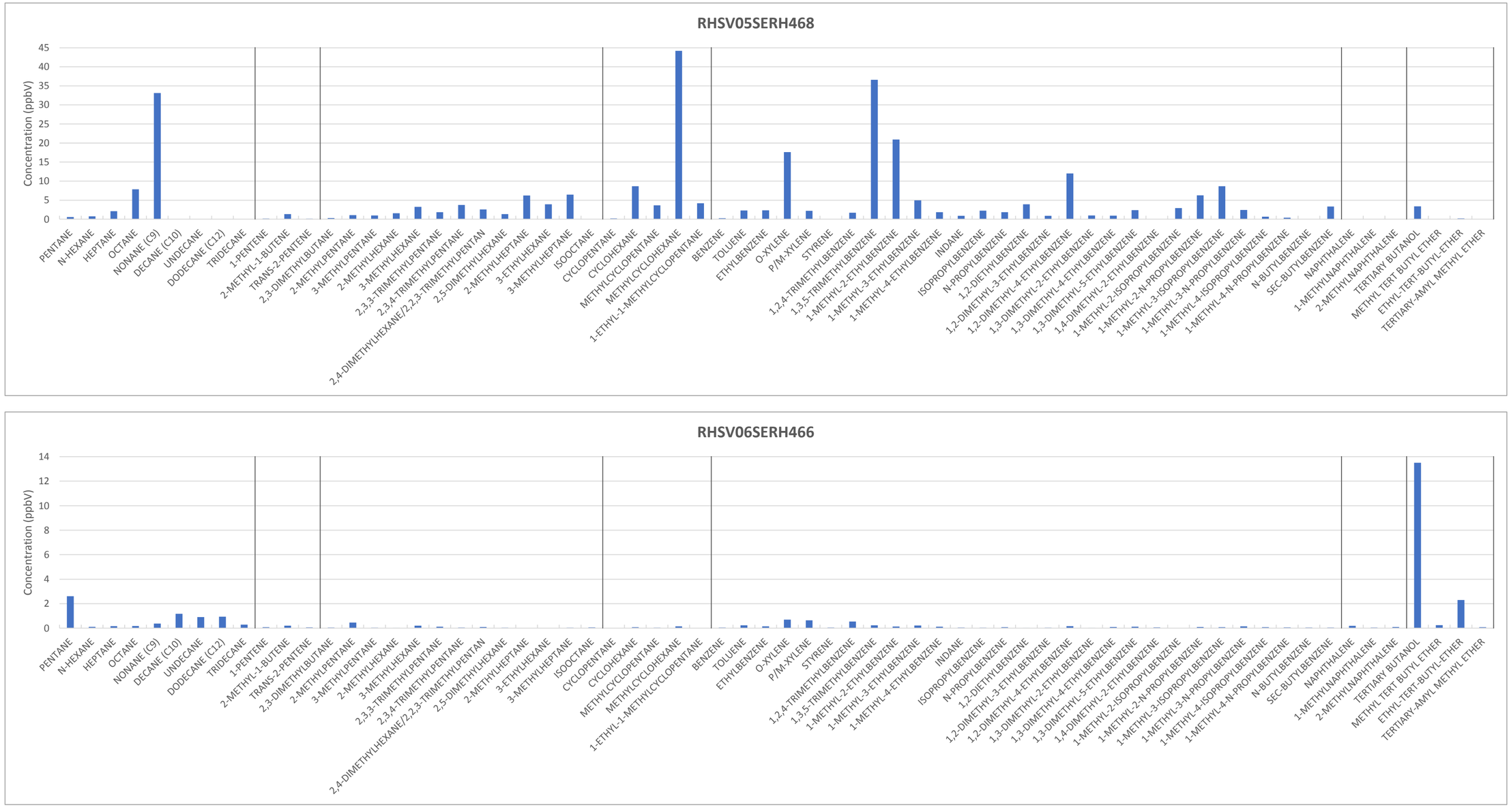

ATTACHMENT B.3.1: FINGERPRINT CHARTS FOR SOIL VAPOR AND GROUNDWATER MONITORING WELL HEADSPACE SAMPLES
Red Hill Bulk Fuel Storage Facility, Joint Base Pearl Harbor-Hickam, O'ahu, Hawai'i

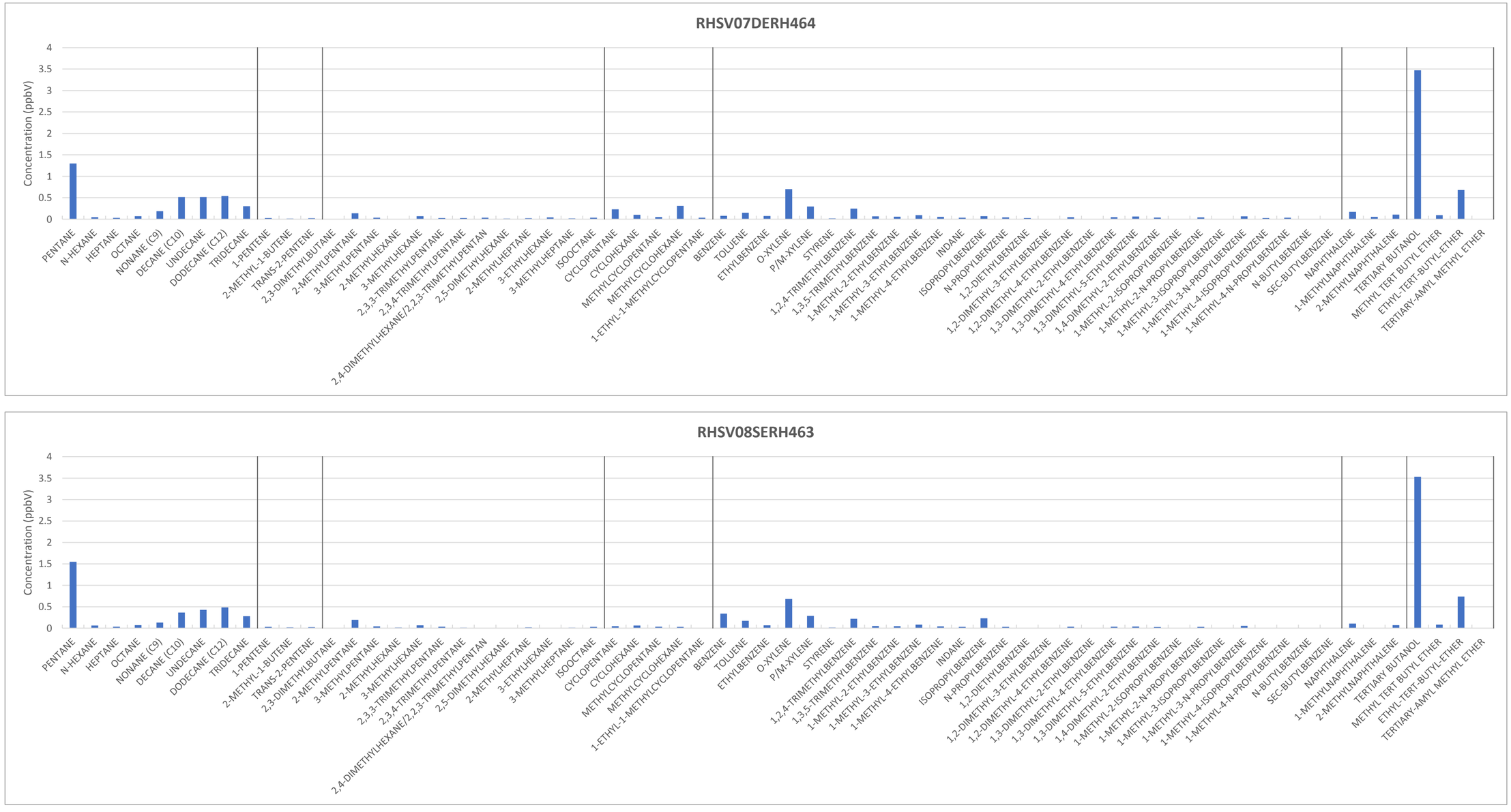

ATTACHMENT B.3.1: FINGERPRINT CHARTS FOR SOIL VAPOR AND GROUNDWATER MONITORING WELL HEADSPACE SAMPLES
Red Hill Bulk Fuel Storage Facility, Joint Base Pearl Harbor-Hickam, O'ahu, Hawai'i

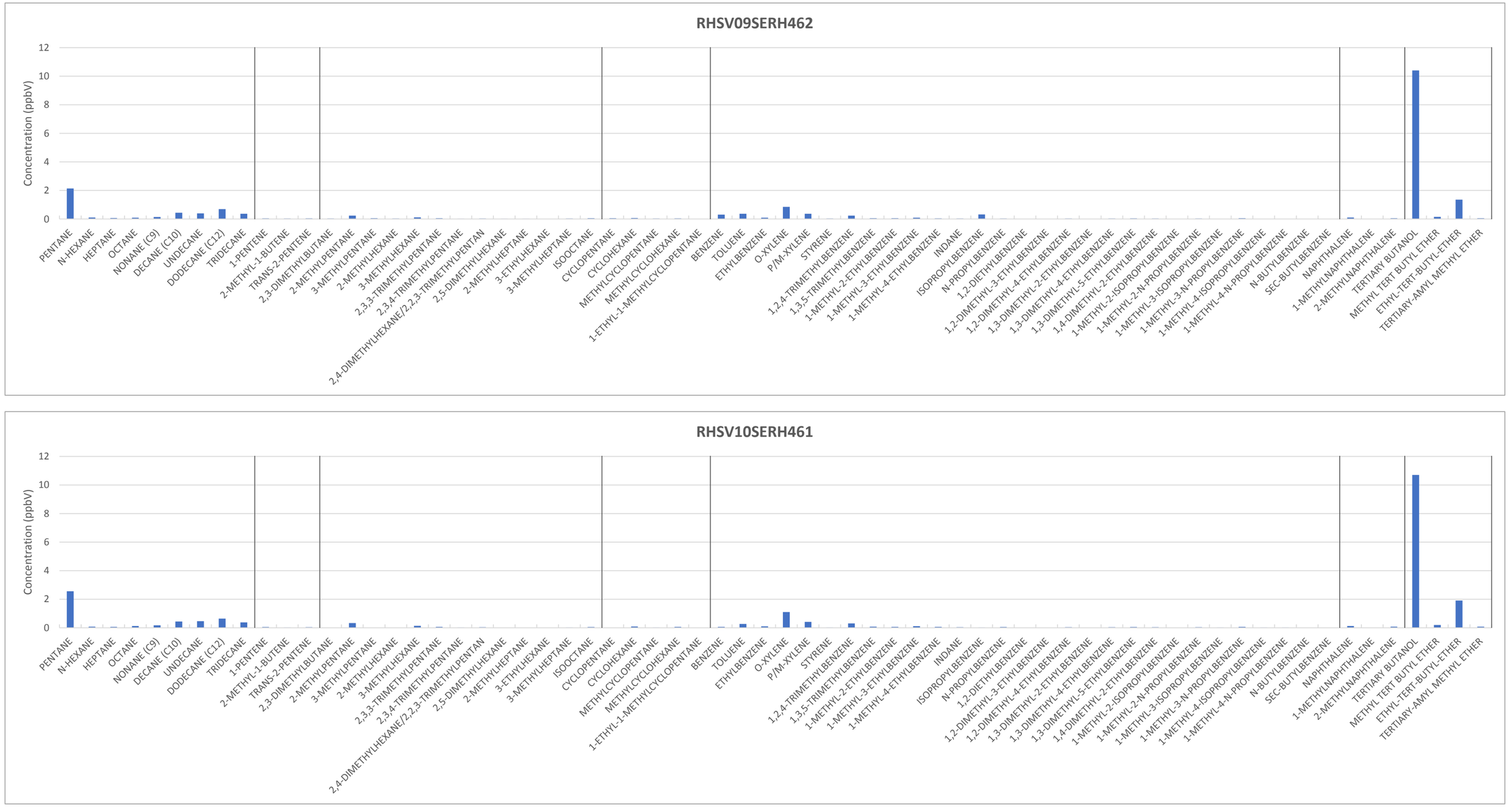

ATTACHMENT B.3.1: FINGERPRINT CHARTS FOR SOIL VAPOR AND GROUNDWATER MONITORING WELL HEADSPACE SAMPLES
Red Hill Bulk Fuel Storage Facility, Joint Base Pearl Harbor-Hickam, O'ahu, Hawai'i

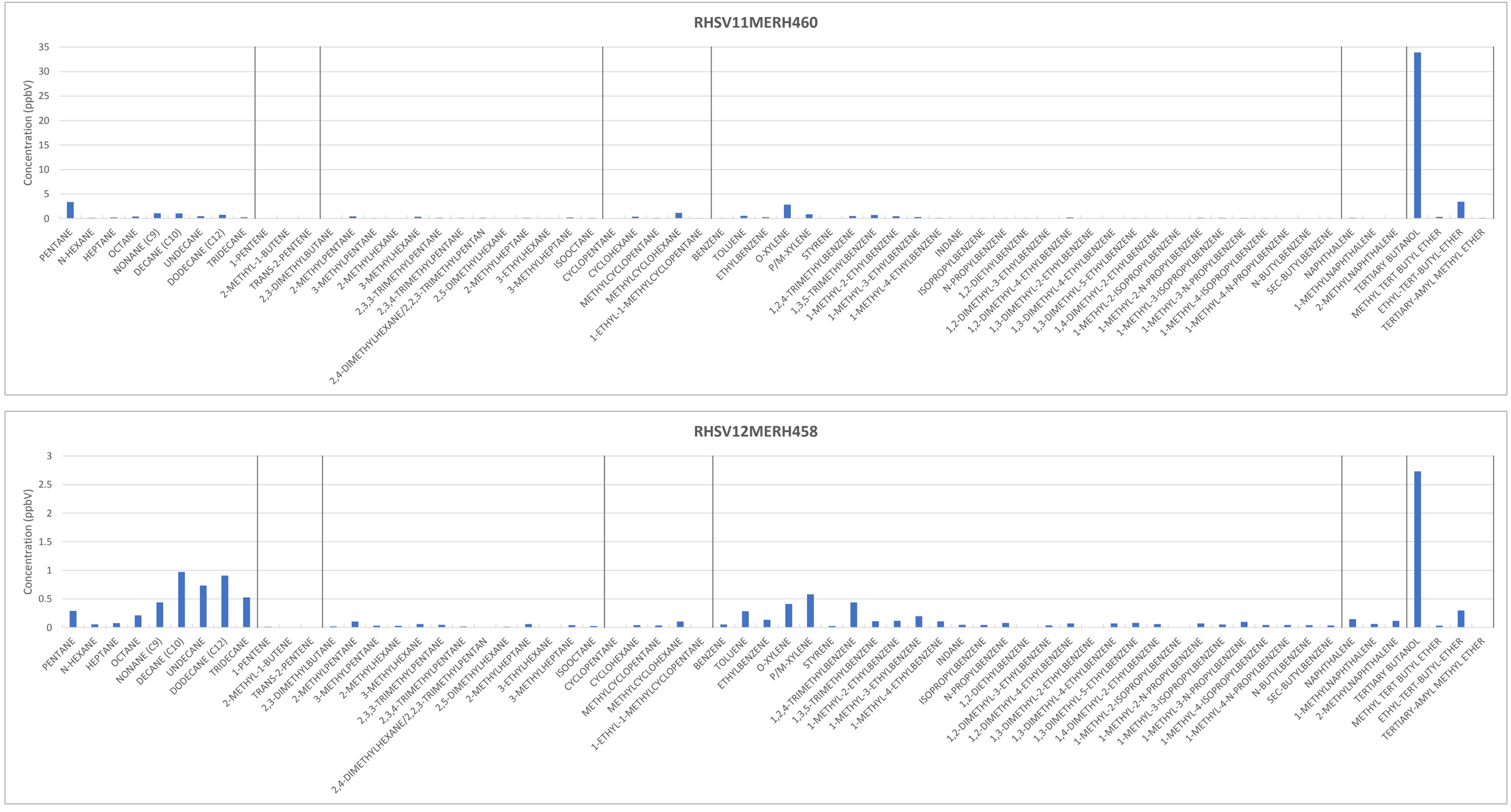

ATTACHMENT B.3.1: FINGERPRINT CHARTS FOR SOIL VAPOR AND GROUNDWATER MONITORING WELL HEADSPACE SAMPLES
Red Hill Bulk Fuel Storage Facility, Joint Base Pearl Harbor-Hickam, O'ahu, Hawai'i

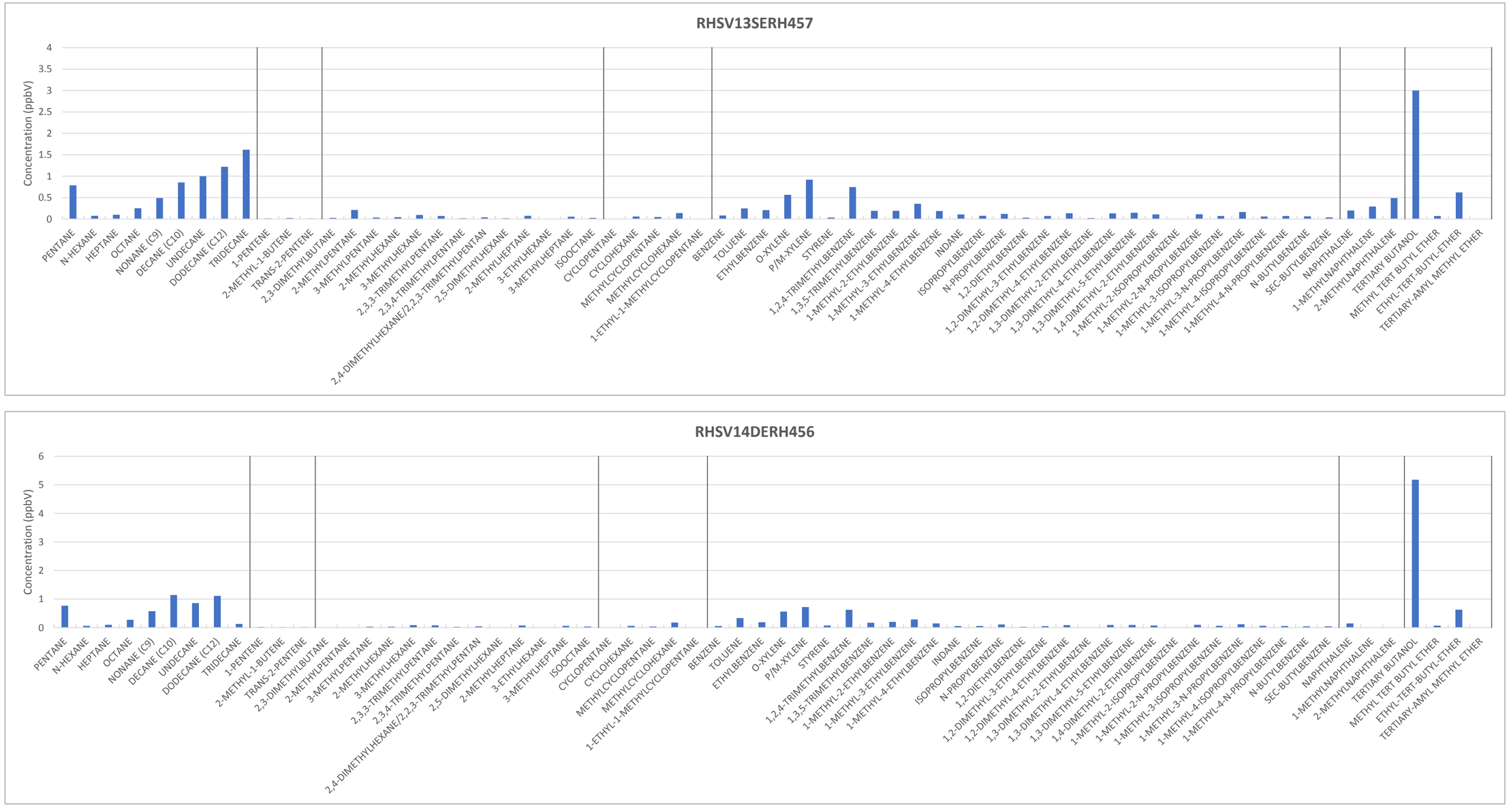

ATTACHMENT B.3.1: FINGERPRINT CHARTS FOR SOIL VAPOR AND GROUNDWATER MONITORING WELL HEADSPACE SAMPLES
Red Hill Bulk Fuel Storage Facility, Joint Base Pearl Harbor-Hickam, O'ahu, Hawai'i

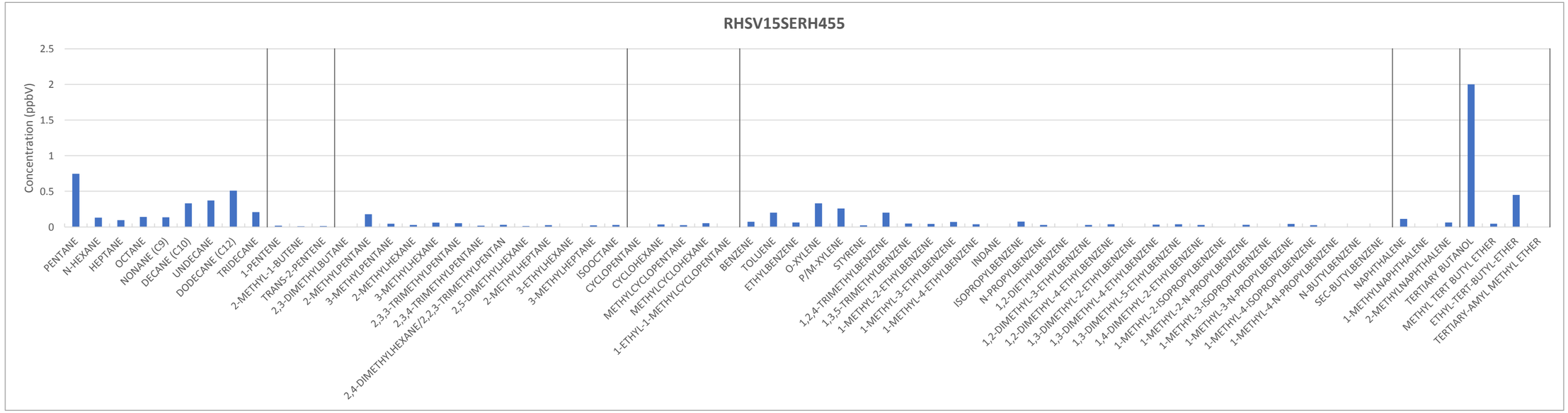

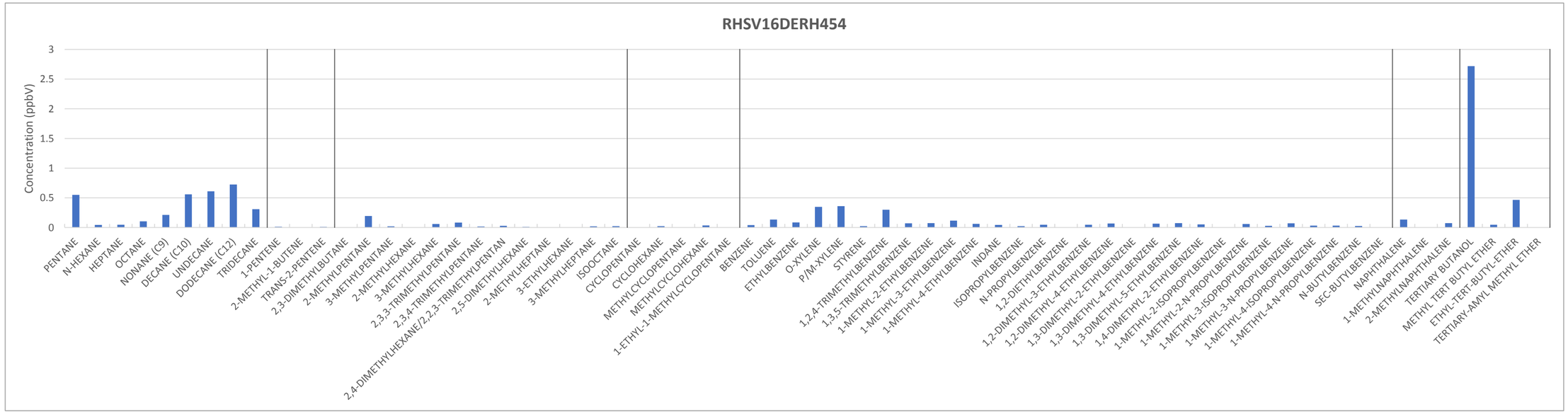

ATTACHMENT B.3.1: FINGERPRINT CHARTS FOR SOIL VAPOR AND GROUNDWATER MONITORING WELL HEADSPACE SAMPLES
Red Hill Bulk Fuel Storage Facility, Joint Base Pearl Harbor-Hickam, O'ahu, Hawai'i

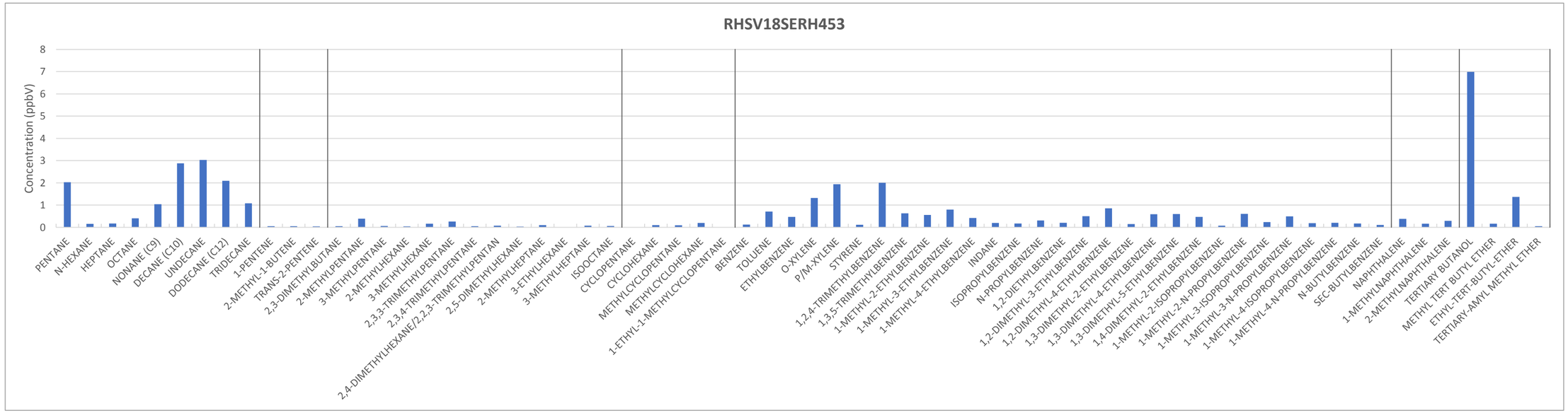

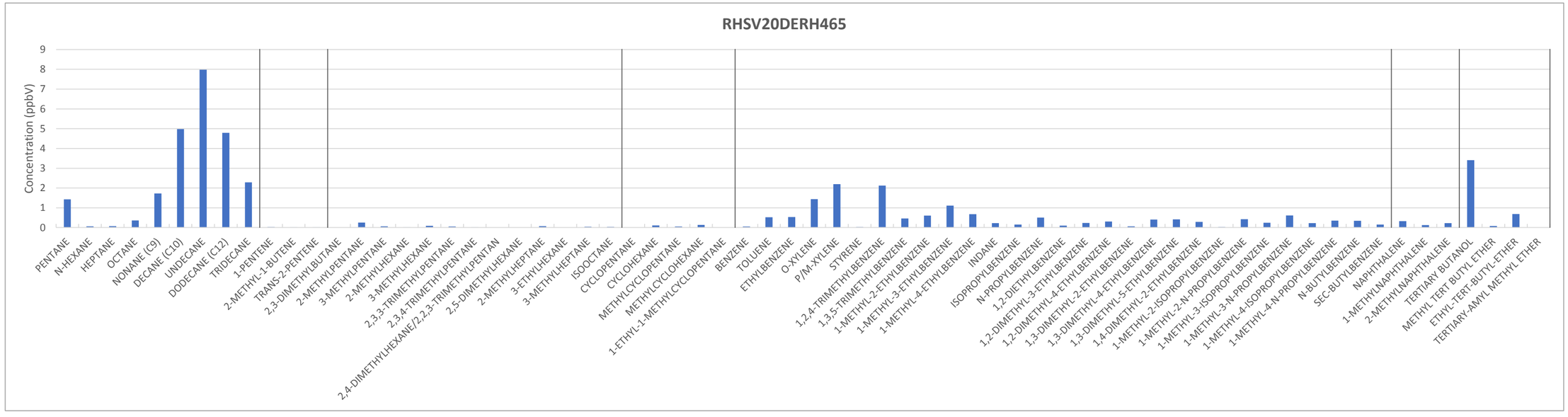

ATTACHMENT B.3.1: FINGERPRINT CHARTS FOR SOIL VAPOR AND GROUNDWATER MONITORING WELL HEADSPACE SAMPLES
Red Hill Bulk Fuel Storage Facility, Joint Base Pearl Harbor-Hickam, O'ahu, Hawai'i

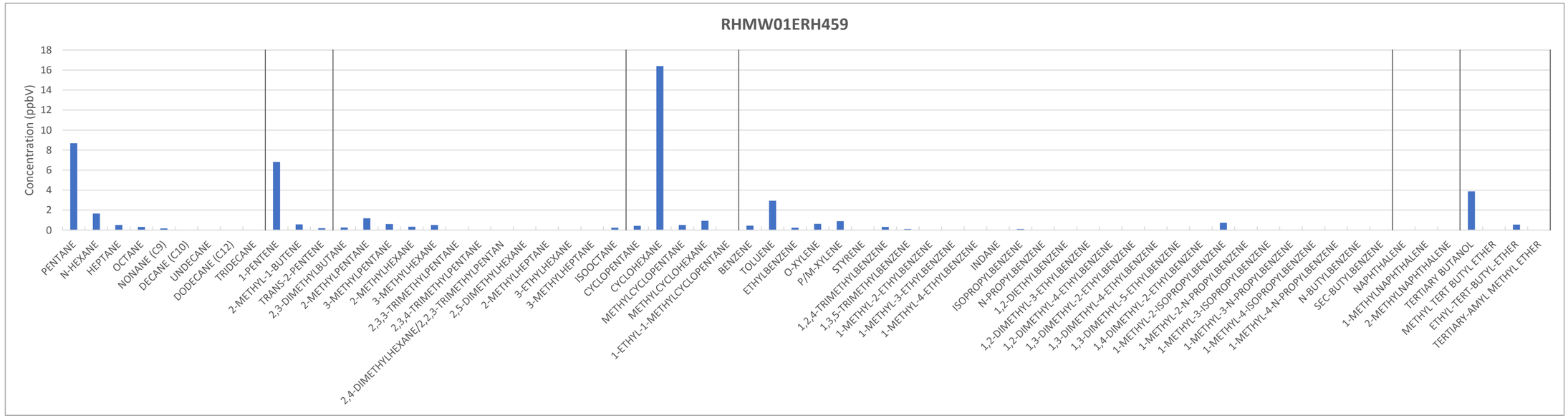

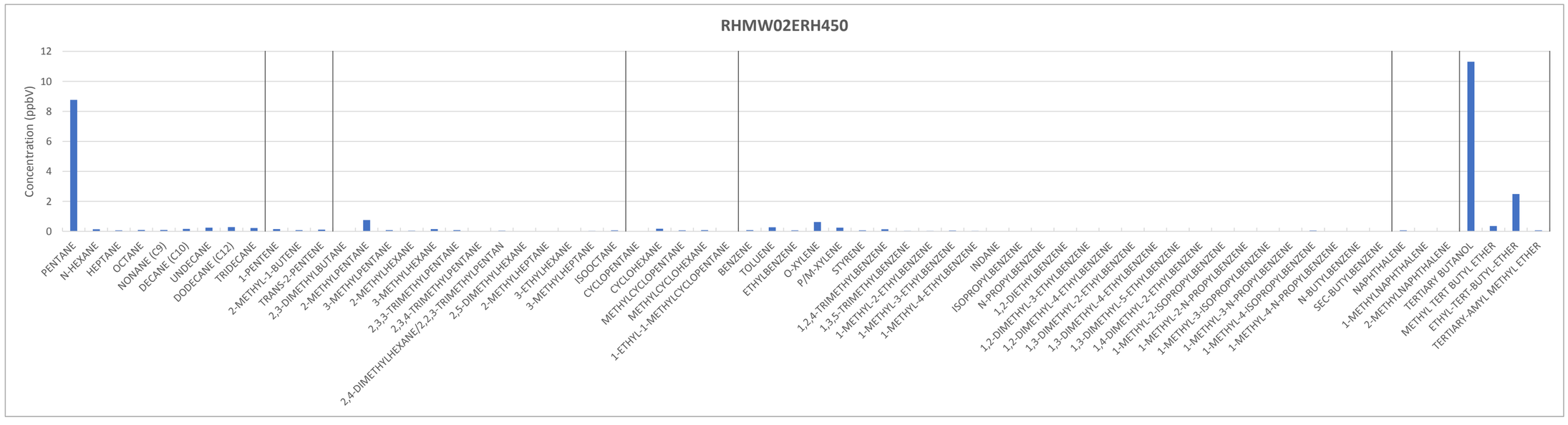

ATTACHMENT B.3.1: FINGERPRINT CHARTS FOR SOIL VAPOR AND GROUNDWATER MONITORING WELL HEADSPACE SAMPLES
Red Hill Bulk Fuel Storage Facility, Joint Base Pearl Harbor-Hickam, O'ahu, Hawai'i

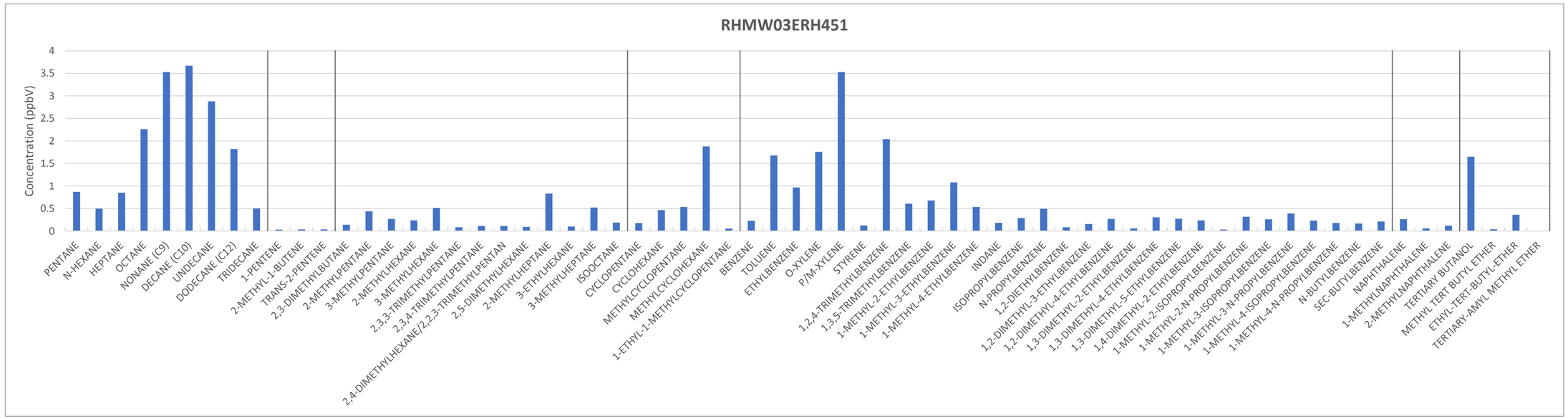

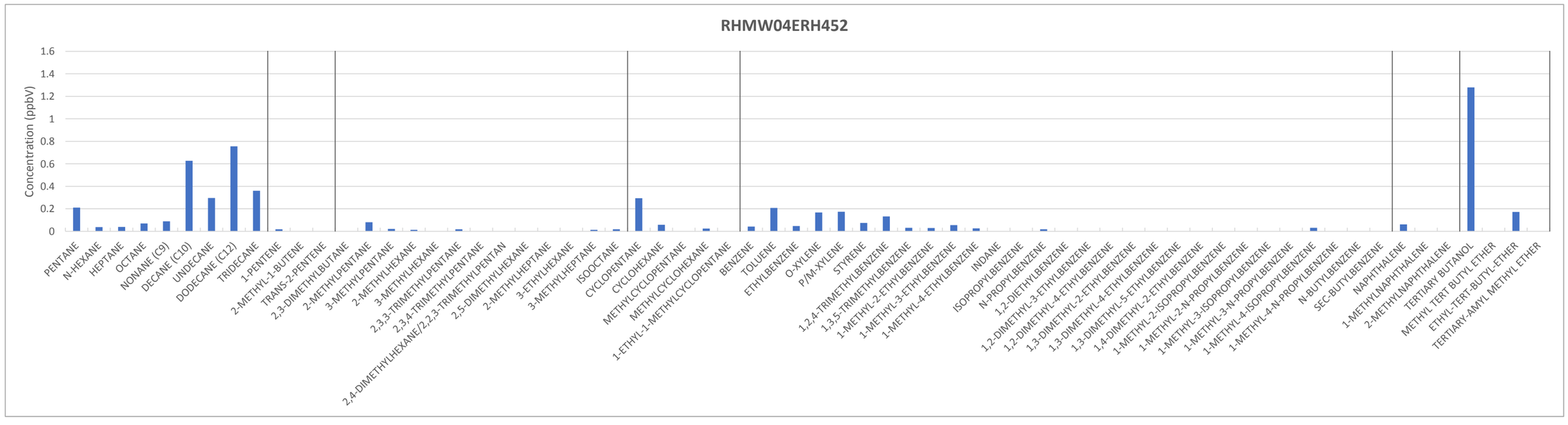

Attachment B.3.2:
FID Chromatograms for Soil Vapor and Groundwater Monitoring Well Headspace Samples

GSI ENVIRONMENTAL

ATTACHMENT B.3.2: FID CHROMATOGRAMS FOR SOIL VAPOR AND GROUNDWATER MONITORING WELL HEADSPACE SAMPLES

Red Hill Bulk Fuel Storage Facility, Joint Base Pearl Harbor-Hickam, O'ahu, Hawai'i

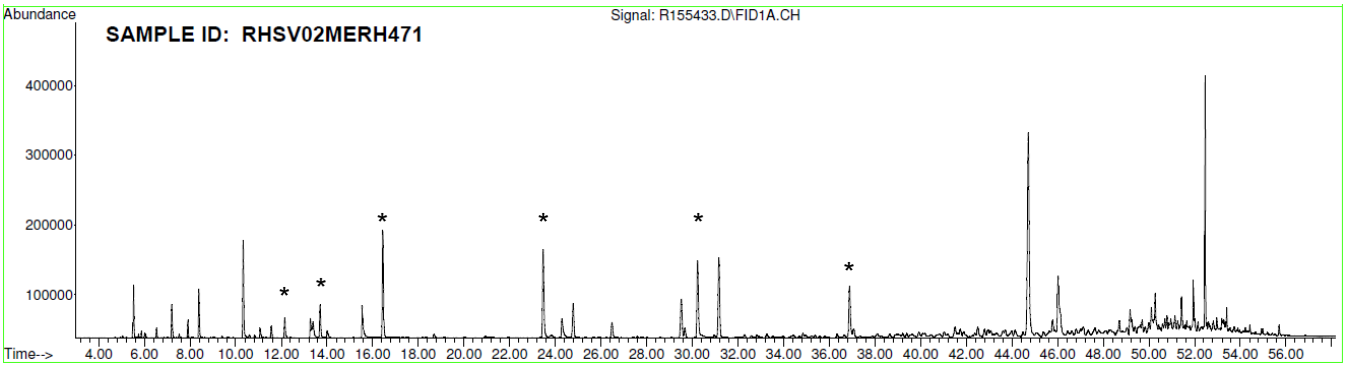

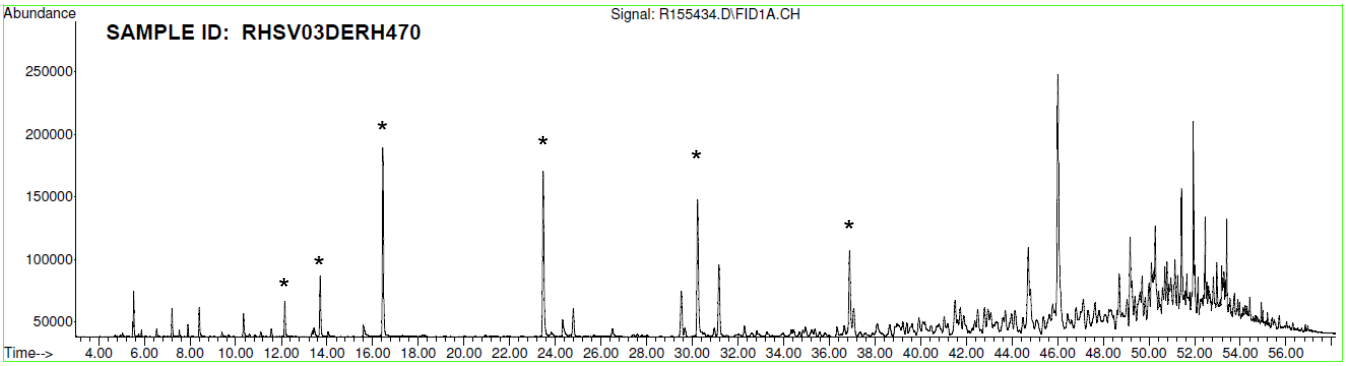

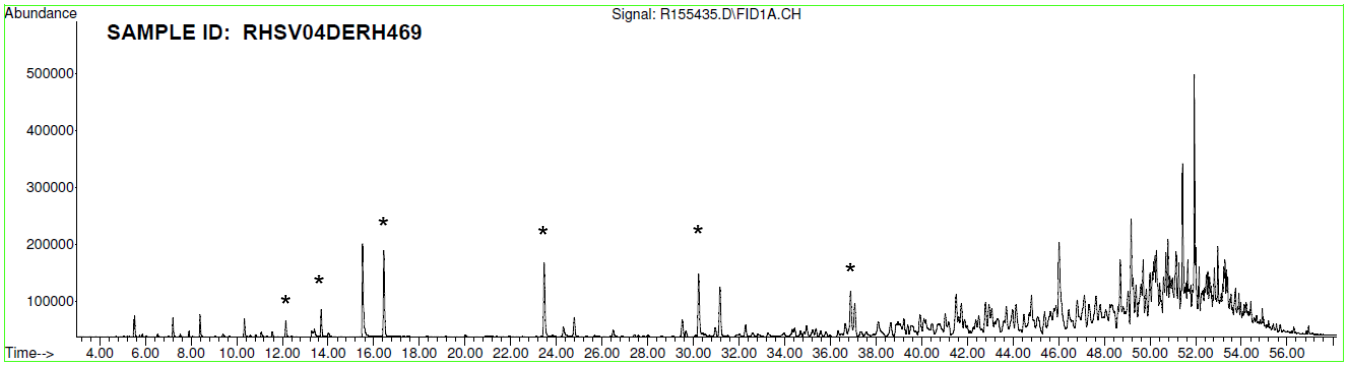

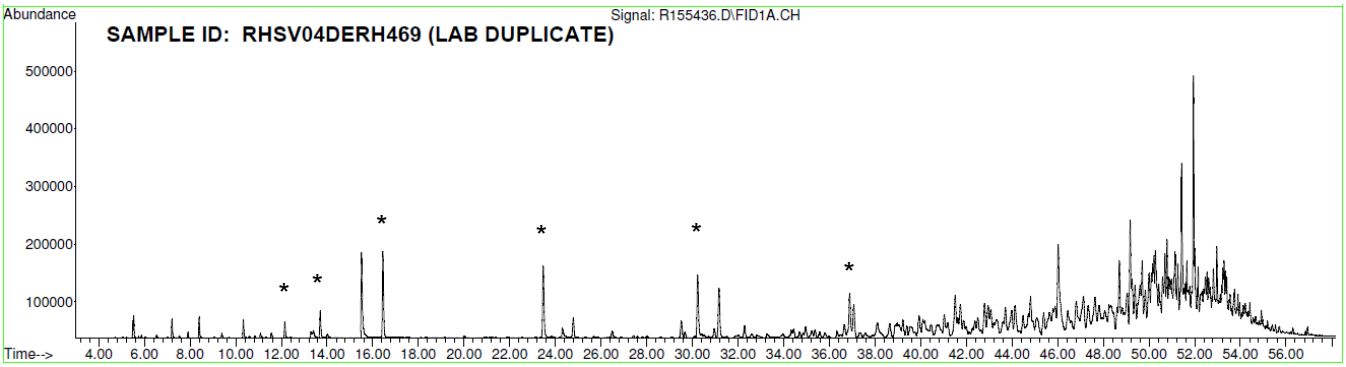

Note: Asterisk (*) = Internal Standard

GSI ENVIRONMENTAL

ATTACHMENT B.3.2: FID CHROMATOGRAMS FOR SOIL VAPOR AND GROUNDWATER MONITORING WELL HEADSPACE SAMPLES

Red Hill Bulk Fuel Storage Facility, Joint Base Pearl Harbor-Hickam, O'ahu, Hawai'i

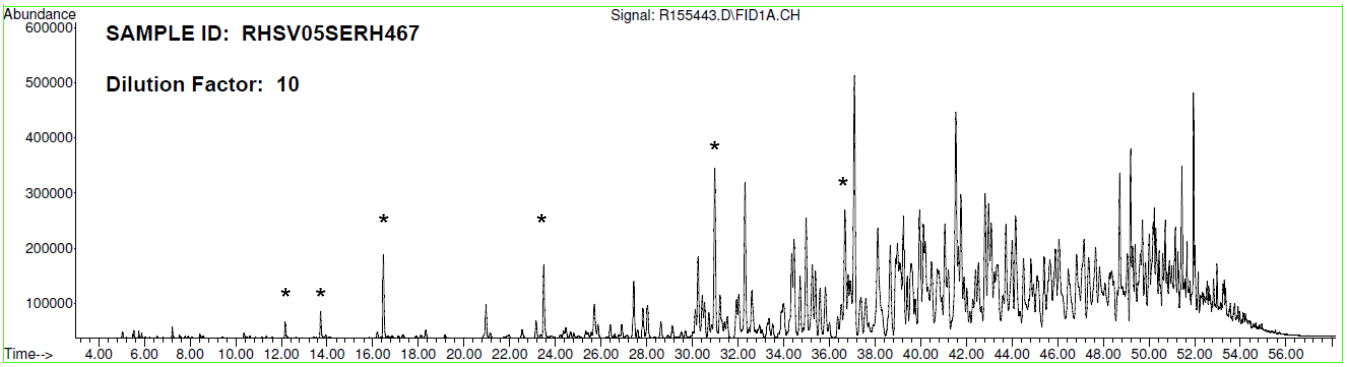

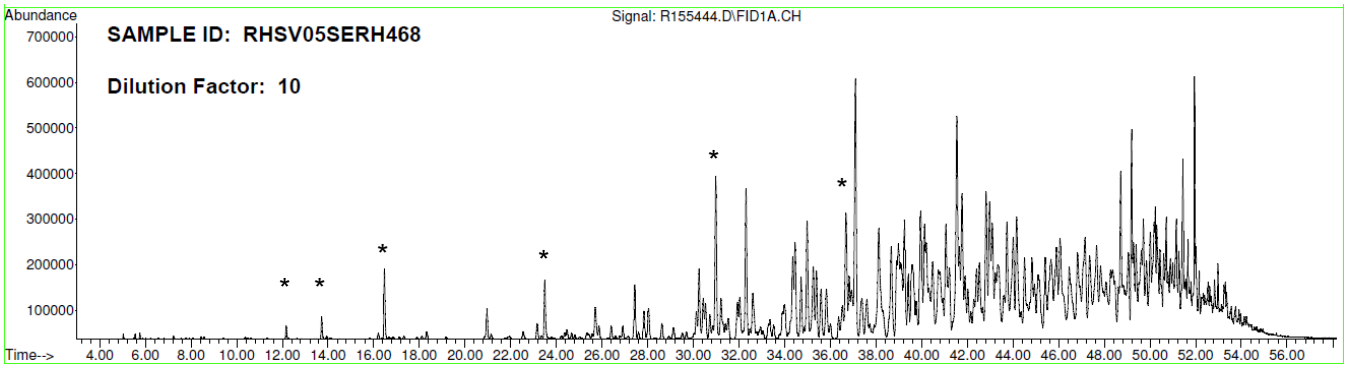

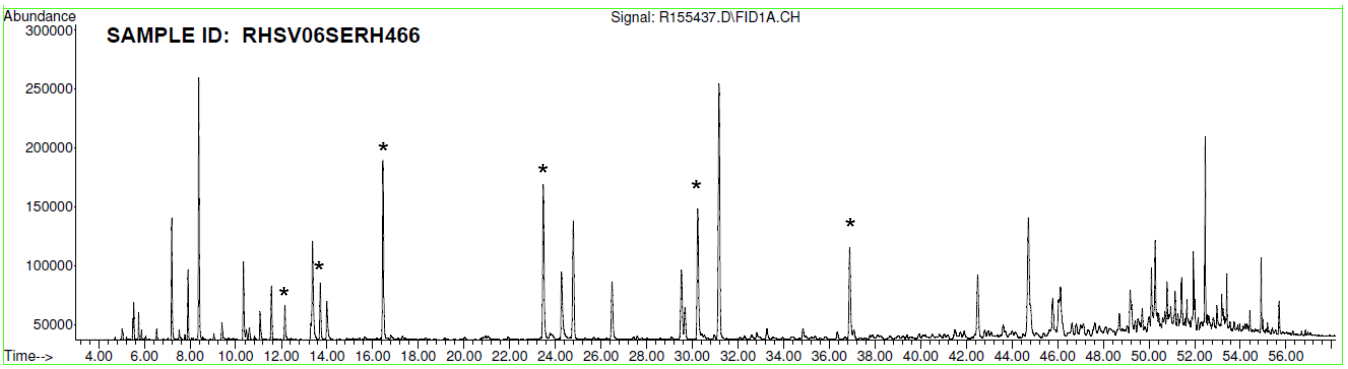

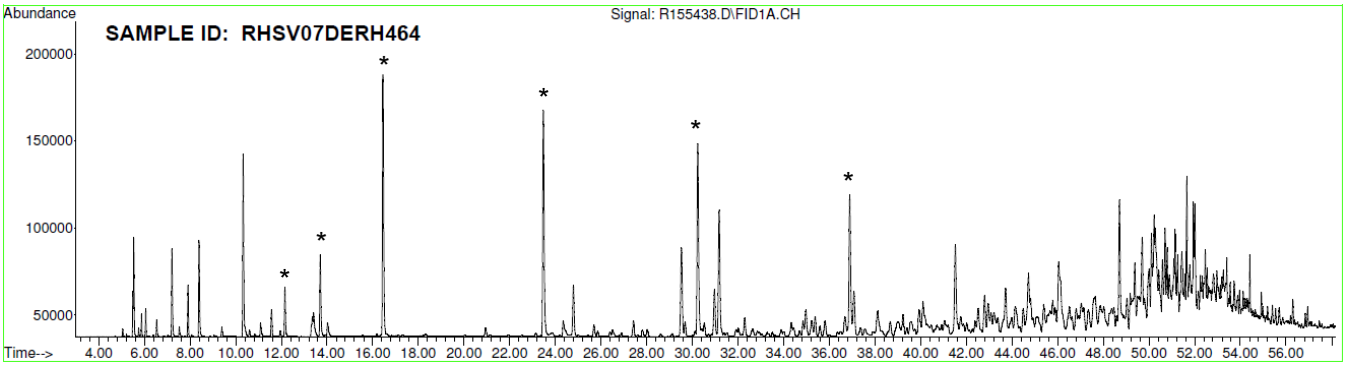

Note: Asterisk (*) = Internal Standard

GSI ENVIRONMENTAL

ATTACHMENT B.3.2: FID CHROMATOGRAMS FOR SOIL VAPOR AND GROUNDWATER MONITORING WELL HEADSPACE SAMPLES

Red Hill Bulk Fuel Storage Facility, Joint Base Pearl Harbor-Hickam, O'ahu, Hawai'i

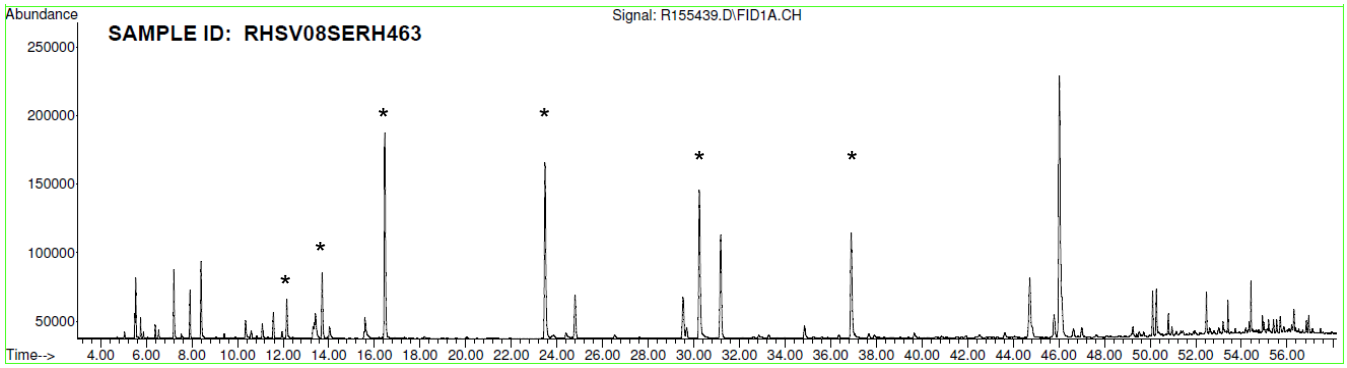

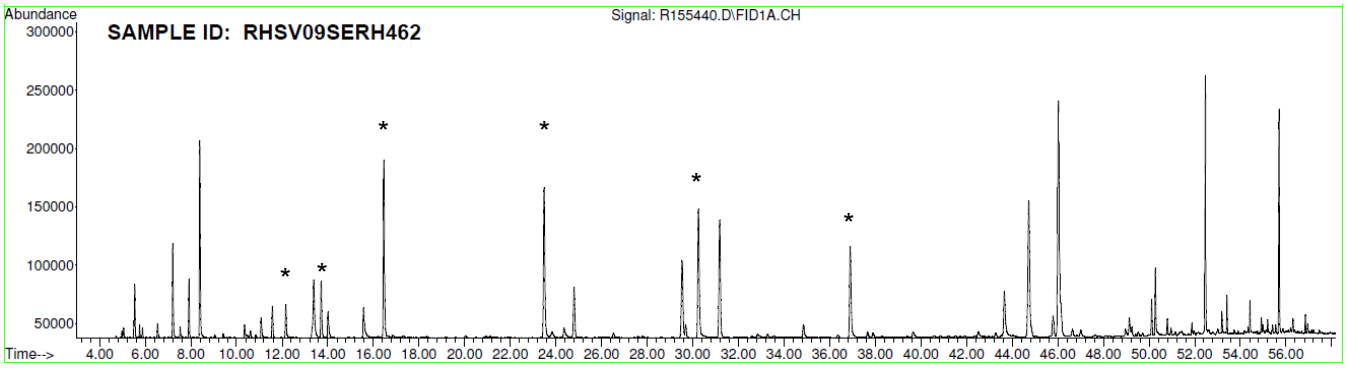

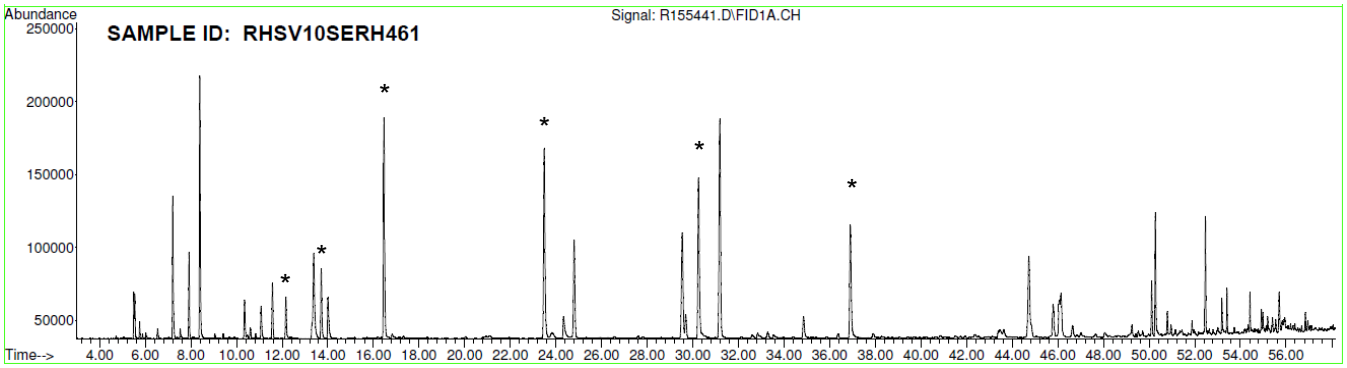

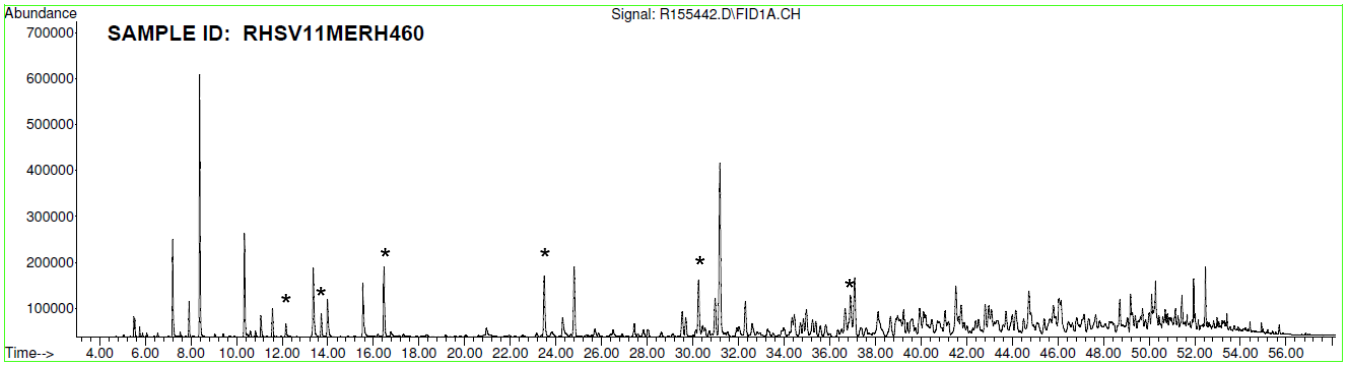

Note: Asterisk (*) = Internal Standard

GSI ENVIRONMENTAL

ATTACHMENT B.3.2: FID CHROMATOGRAMS FOR SOIL VAPOR AND GROUNDWATER MONITORING WELL HEADSPACE SAMPLES

Red Hill Bulk Fuel Storage Facility, Joint Base Pearl Harbor-Hickam, O'ahu, Hawai'i

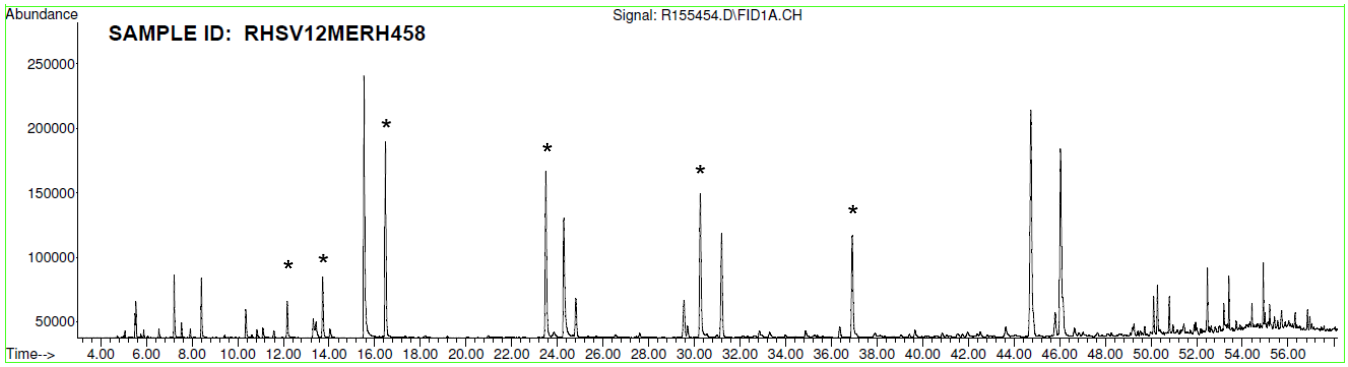

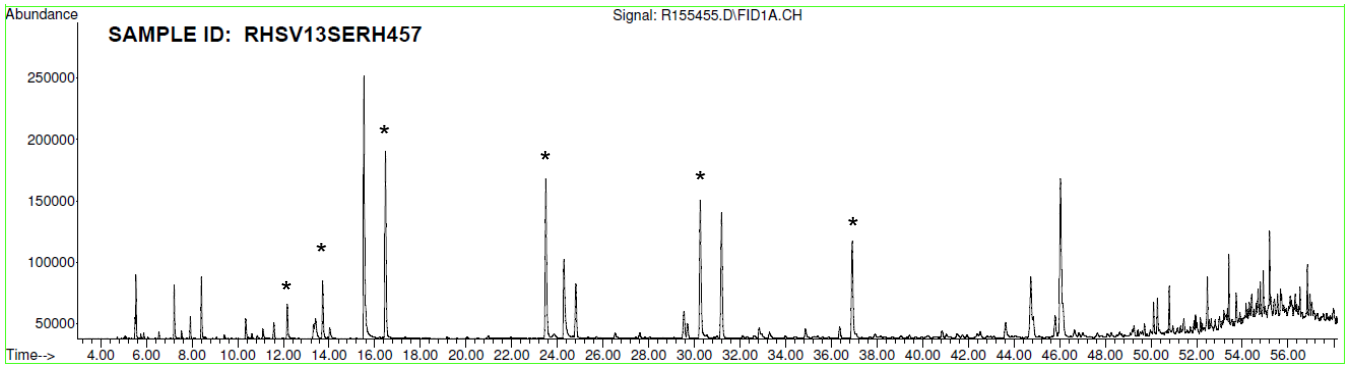

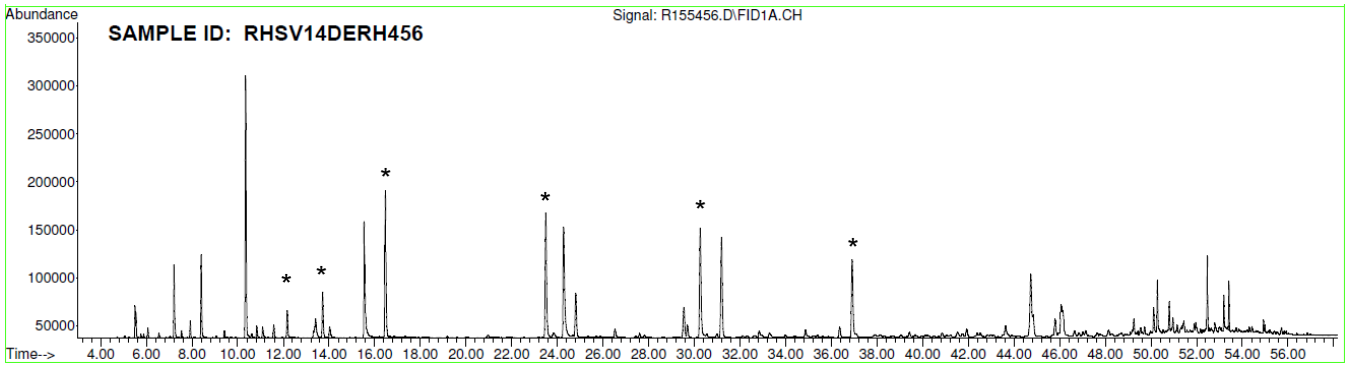

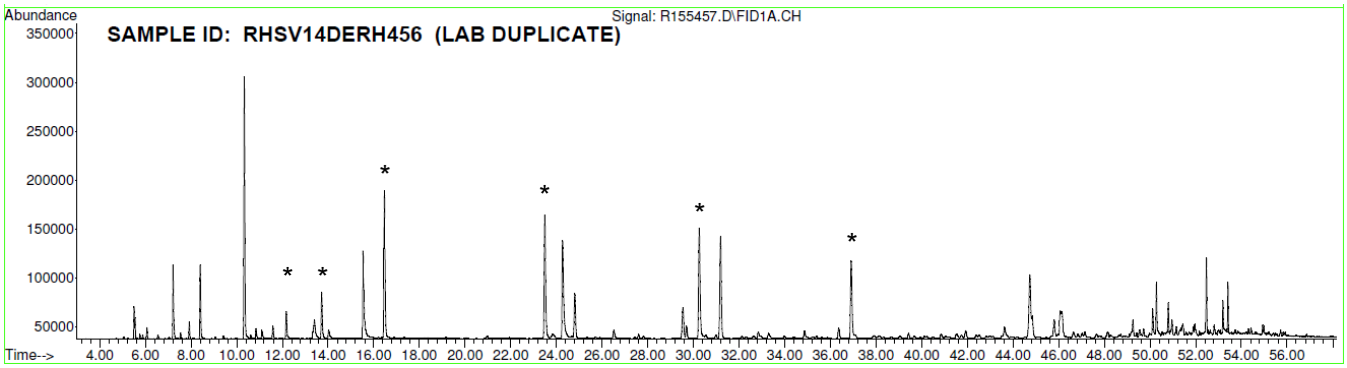

Note: Asterisk (*) = Internal Standard

GSI ENVIRONMENTAL

ATTACHMENT B.3.2: FID CHROMATOGRAMS FOR SOIL VAPOR AND GROUNDWATER MONITORING WELL HEADSPACE SAMPLES

Red Hill Bulk Fuel Storage Facility, Joint Base Pearl Harbor-Hickam, O'ahu, Hawai'i

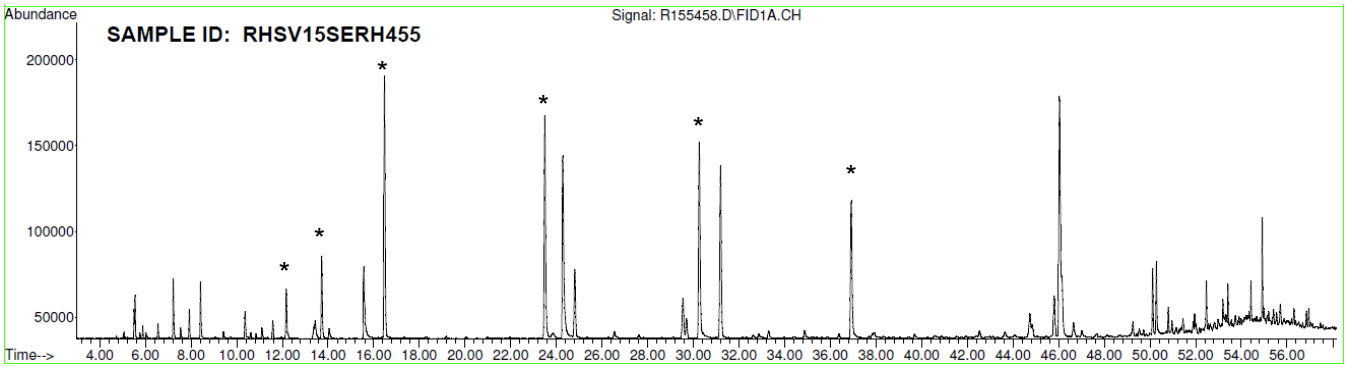

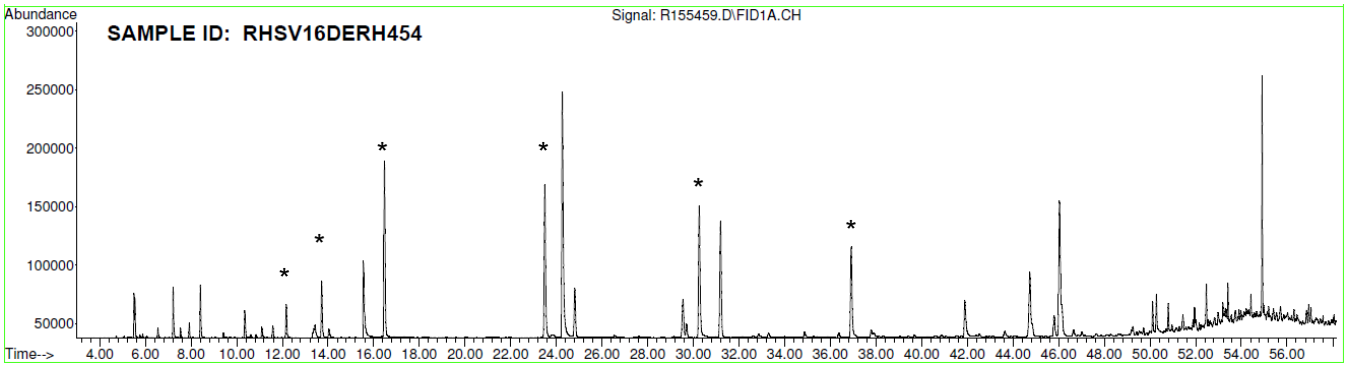

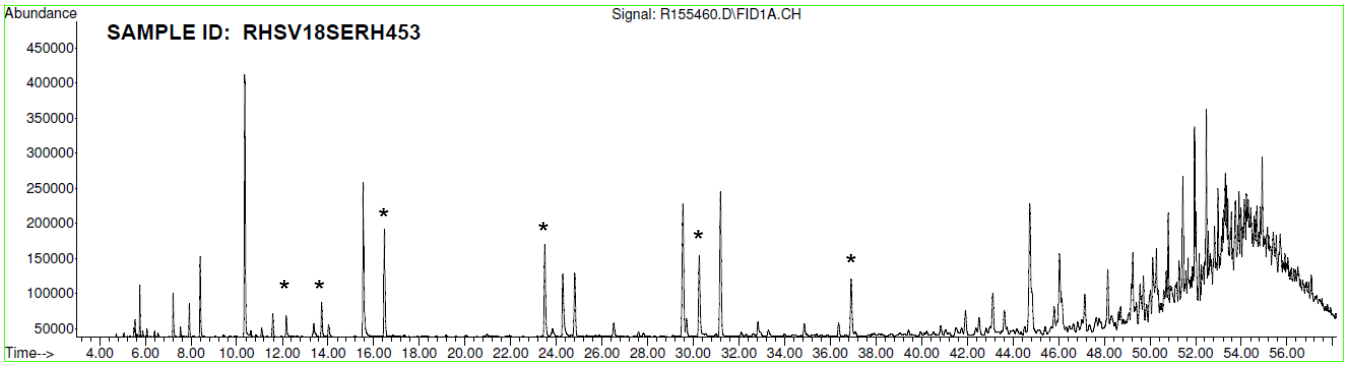

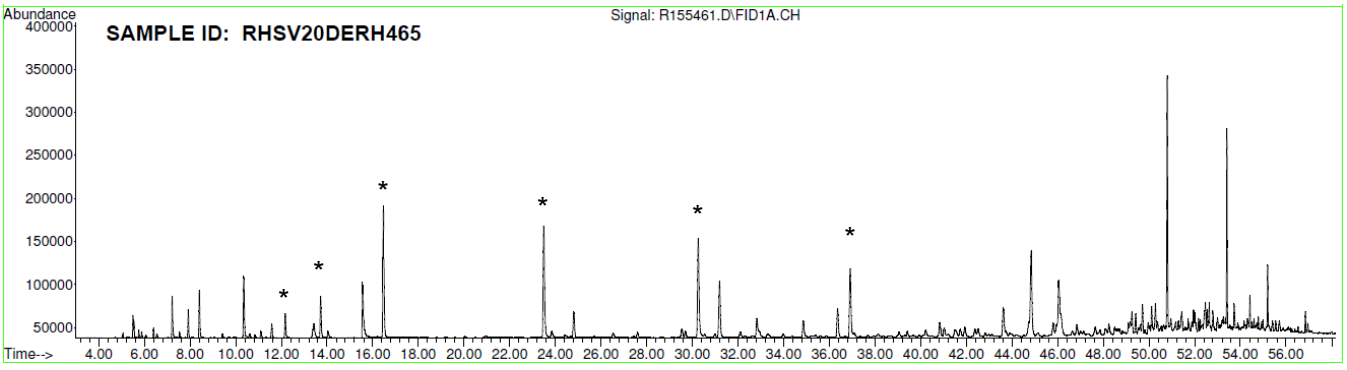

Note: Asterisk (*) = Internal Standard

GSI ENVIRONMENTAL

ATTACHMENT B.3.2: FID CHROMATOGRAMS FOR SOIL VAPOR AND GROUNDWATER MONITORING WELL HEADSPACE SAMPLES

Red Hill Bulk Fuel Storage Facility, Joint Base Pearl Harbor-Hickam, O'ahu, Hawai'i

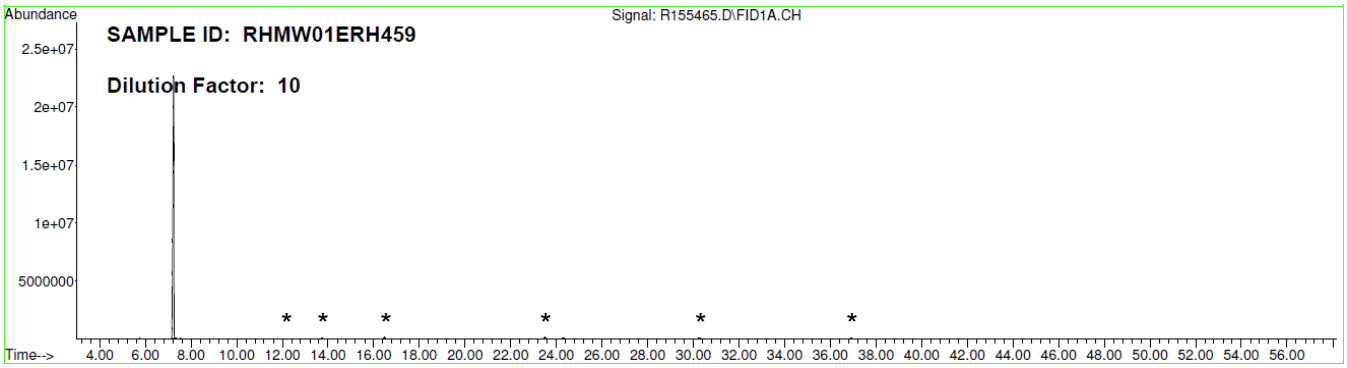

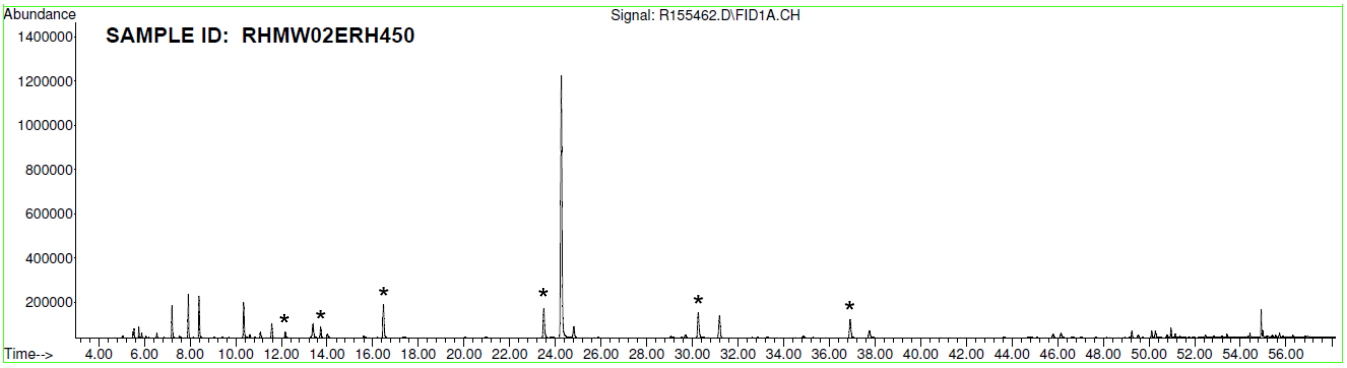

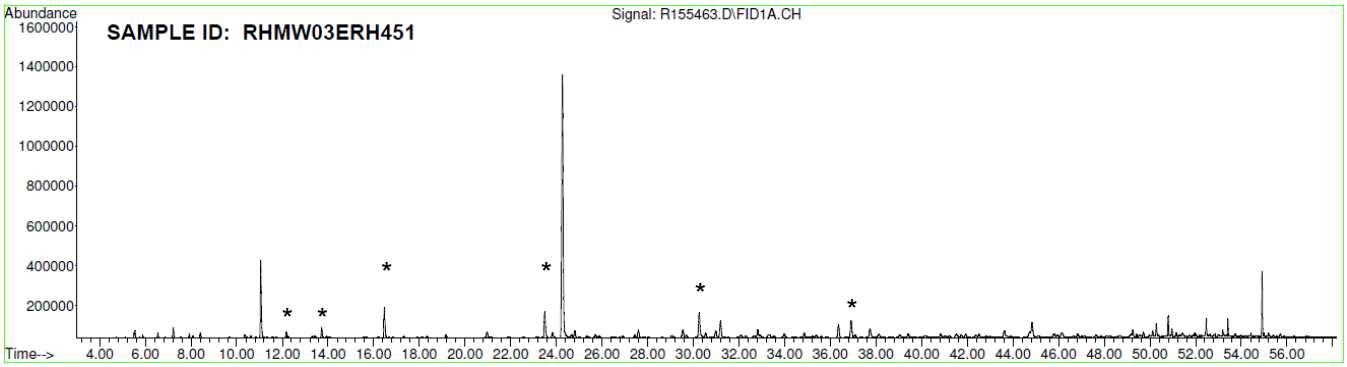

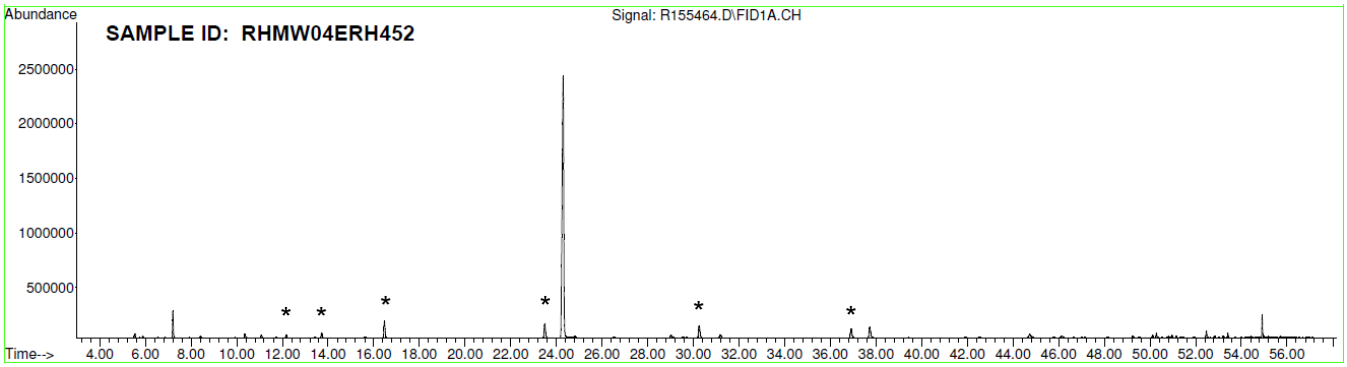

Note: Asterisk (*) = Internal Standard

ATTACHMENT B.3.2: FID CHROMATOGRAMS FOR SOIL VAPOR AND GROUNDWATER MONITORING WELL HEADSPACE SAMPLES

Red Hill Bulk Fuel Storage Facility, Joint Base Pearl Harbor-Hickam, O'ahu, Hawai'i

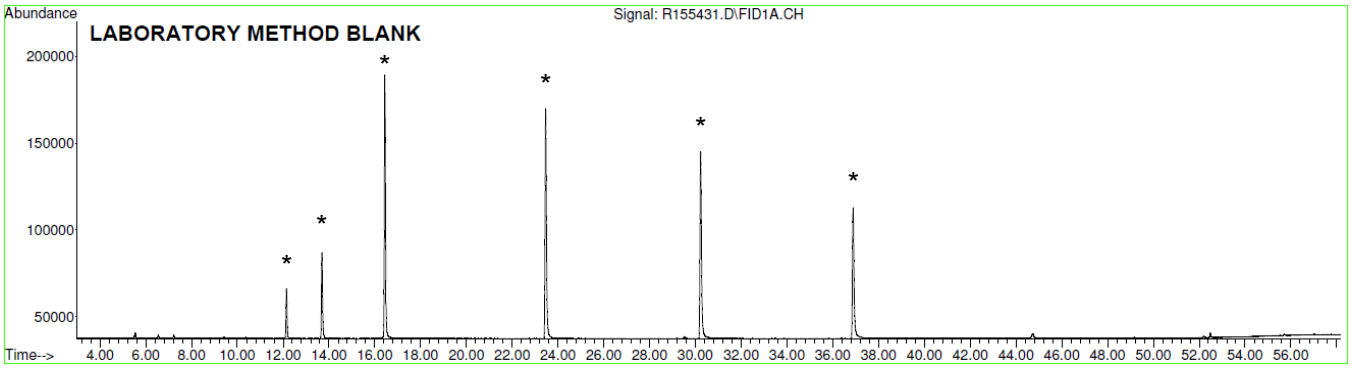

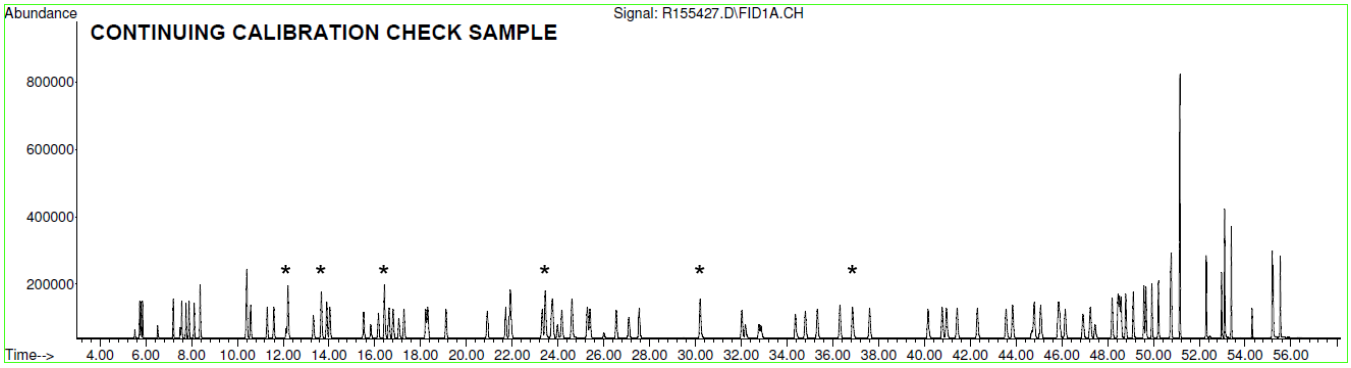

Note: Asterisk (*) = Internal Standard

Attachment B.3.3:
Soil Vapor Field Monitoring Results

GSI Job No. 4671
Issued: 22 December 2017

GSI ENVIRONMENTAL

ATTACHMENT B.3.3: SOIL VAPOR FIELD MONITORING RESULTS

Red Hill Bulk Fuel Storage Facility, Joint Base Pearl Harbor-Hickam, O'ahu, Hawai'i

	DATE	TIME	PID	OXYGEN	CO2	METHANE	BALANCE	DELTA P
LOCATION			ppb	%	%	%	%	in H20
SOIL VAPOR WELLS (Below Tanks)								
RHSV02 S	2017-10-31	11:30	608	19.5	0.7	0	79.8	0.176
RHSV02 M	2017-10-31	11:35	980	19.6	0.2	0	80.2	0.179
RHSV02 D	2017-10-31	11:40	405	19.4	0.8	0	79.8	0.164
RHSV03 S	2017-10-31	10:53	360	19	0.3	0	80.8	0.113
RHSV03 M	2017-10-31	10:57	365	20.2	0.1	0	79.7	0.225
RHSV03 D	2017-10-31	11:02	408	20.2	0.2	0	79.6	0.113
RHSV04 S	2017-10-31	10:10	340	19.5	0.7	0	79.9	0.116
RHSV04 M	2017-10-31	10:15	322	19.5	0.8	0	79.7	0.095
RHSV04 D	2017-10-31	10:20	340	19.4	0.9	0	79.7	0.095
RHSV05 S	2017-10-31	9:10	19000	18.7	0.9	0	80.5	0.035
RHSV05 M	2017-10-31	9:16	5300	18.1	1.3	0	80.6	-3.1
RHSV05 D	2017-10-31	9:27	9600	19.5	0.5	0	80	0.003
RHSV06 S	2017-10-31	8:40	12000	18.8	1.1	0	80.1	-0.036
RHSV06 M	2017-10-31	8:30	2500	19.3	0.6	0	80.1	-0.022
RHSV07 S	2017-10-30	13:58	240	20.2	0.3	0	79.5	-0.006
RHSV07 M	2017-10-30	14:01	250	19.7	0.4	0	79.9	-0.591
RHSV07 D	2017-10-30	14:07	468	13.7	3.2	0	83	0.006
RHSV08 S	2017-10-30	13:22	190	19.9	0.6	0	79.5	0.071
RHSV08 M	2017-10-30	13:25	122	19.8	0.7	0	79.5	0.016
RHSV08 D	2017-10-30	13:28	112	19.8	0.8	0	79.4	0.016
RHSV09 S	2017-10-30	12:40	1500	20	0.4	0	79.6	0
RHSV09 M	2017-10-30	12:50	385	19.8	0.6	0	79.7	0.03
RHSV09 D	2017-10-30	12:55	240	19.8	0.6	0	79.6	0.003
RHSV10 S	2017-10-30	11:15	580	19.9	0.3	0	79.8	0.019
RHSV10 M	2017-10-30	11:20	160	19.9	0.4	0	79.7	0.162
RHSV11 M	2017-10-30	10:32	31090	19.1	1	0	79.9	0.038
RHSV11 D	2017-10-30	10:43	9780	19.9	0.2	0	79.8	0.115
RHSV12 S	2017-10-27	13:41	1344	19.1	0.6	0	80.3	0.151
RHSV12 M	2017-10-27	13:48	16890	20.1	0.4	0	79.5	0.214
RHSV12 D	2017-10-27	13:56	10890	20.2	0.3	0	79.5	0.246
RHSV13 S	2017-10-27	13:00	495	19.6	0.7	0	79.8	0.204
RHSV13 M	2017-10-27	13:05	336	19.6	0.7	0	79.8	0.192
RHSV13 D	2017-10-27	13:12	396	19.7	0.6	0	79.8	0.199
RHSV14 S	2017-10-27	12:25	3286	16.4	1.5	0	82.1	0.031
RHSV14 M	2017-10-27	12:28	2938	15.7	2.4	0	81.9	0.165
RHSV14 D	2017-10-27	12:33	9154	19.8	0.4	0	79.8	0.245
RHSV15 S	2017-10-27	10:58	160	20	0.2	0	79.8	0.172
RHSV15 M	2017-10-27	11:00	Line plugged - no sample possible.					
RHSV15 D	2017-10-27	11:08	44	19.7	0.3	0	79.9	0.139
RHSV16 S	2017-10-27	10:12	1200	18.5	0.6	0	79.7	0.033
RHSV16 M	2017-10-27	10:25	2019	17.5	1.6	0	80.9	0.252
RHSV16 D	2017-10-27	10:28	5030	18.5	1.1	0	80.4	0.229
RHSV17 S	Not sampled. Access blocked by equipment.							
RHSV17 M	Not sampled. Access blocked by equipment.							
RHSV17 D	Not sampled. Access blocked by equipment.							
RHSV18 S	2017-10-27	9:15	40000	19.9	0.2	0	79.9	0.153
RHSV18 D	2017-10-27	9:11	5500	20	0.2	0	79.8	0.154
RHSV20 S	2017-10-30	14:44	580	20.6	0.1	0	79.3	0.14

GSI Job No. 4671
Issued: 22 December 2017

GSI ENVIRONMENTAL

ATTACHMENT B.3.3: SOIL VAPOR FIELD MONITORING RESULTS

Red Hill Bulk Fuel Storage Facility, Joint Base Pearl Harbor-Hickam, O'ahu, Hawai'i

	DATE	TIME	PID	OXYGEN	CO2	METHANE	BALANCE	DELTA P
LOCATION			**ppb**	**%**	**%**	**%**	**%**	**in H20**
RHSV20 M	2017-10-30	14:50	700	20.6	0.1	0	79.3	-0.007
RHSV20 D	2017-10-30	14:54	800	20.5	0.1	0	79.4	0.048
MONITORING WELL HEADSPACE								
RHMW01	2017-10-30	9:15	23200	19.1	0.7	0	80.2	0
RHMW02	2017-10-26	10:15	250	6.6	8.5	0	84.7	0.125
RHMW03	2017-10-26	11:40	200	17	2.1	0	NR	0.165
RHMW04	2017-10-26	15:10	400	20.6	0.1	0	79.3	0.47
UPPER TUNNEL VAPOR PINS								
RHVPT05	2017-10-26	12:25	75	20.3	0.3	0	79.4	0.185
RHVPT11	2017-10-26	12:37	1000	20.5	0.1	0	79.4	0.111
HILL TOP SOIL GAS POINTS								
T2 SGP	2017-10-31	12:56	329	18.7	1	0	80.3	NM
T6 SGP	2017-10-31	1:10	296	18.6	1.1	0	80.3	NM
AMBIENT AIR (mostly inside Lower Tunnel)								
Tank 2 Ambient	2017-10-31	11:30	600	20.4	0.1	0	79.5	NM
Tank 3 Ambient	2017-10-31	10:50	645	20.3	0.1	0	79.7	-0.001
Tank 4 Ambient	2017-10-31	10:07	660	20.3	0.2	0	79.5	0.002
Tank 5 Ambient	2017-10-31	9:04	970	20.1	0.4	0	79.5	0.013
Tank 6 Ambient	2017-10-31	8:35	350	20.2	0.1	0	79.7	-0.002
Tank 7 Ambient	2017-10-30	13:55	380	20.7	0.2	0	79.1	-0.002
Tank 8 Ambient	2017-10-30	13:20	220	20.6	0.2	0	79.2	-0.006
Tank 9 Ambient	2017-10-30	12:40	230	20.7	0.2	0	79.1	-0.001
Tank 10 Ambien	2017-10-30	11:11	175	20.5	0.1	0	79.4	0.004
Tank 11 Ambien	2017-10-30	10:31	267	20.3	0.3	0	79.3	0.002
Tank 12 Ambien	2017-10-27	13:37	581	20.6	0.1	0	79.3	NM
Tank 13 Ambien	2017-10-27	12:56	1125	20.6	0.1	0	79.3	NM
Tank 14 Ambien	2017-10-27	12:20	1300	20.8	0.1	0	79.1	NM
Tank 15 Ambien	2017-10-27	10:54	85	20.6	0.1	0	79.3	NM
Tank 16 Ambien	2017-10-27	10:13	235	20.4	0.1	0	79.7	NM
Tank 18 Ambien	2017-10-27	9:09	1000	20.5	0.1	0	79.4	-0.001
Tank 20 Ambien	2017-10-30	14:40	2400	20.7	0.2	0	79.1	NM
MW01 Ambient	2017-10-30	9:05	163	20.3	0.1	0	79.6	0
MW02 Ambient	2017-10-26	10:15	212	20.4	0.1	0	79.6	-0.001
MW03 Ambient	2017-10-26	11:40	38	20.3	0.9	0	78.8	-0.009
MW04 Ambient	2017-10-26	15:10	0	20.5	0	0	79.5	NM
Tank 5 UT Amb	2017-10-26	12:25	500	20.3	0.3	0	79.4	0.002
Tank 11 UT Am	2017-10-26	12:37	180	20.6	0.1	0	79.3	-0.007
T6 Ambient	2017-10-31	1:15	155	18.7	0	0	NR	

Attachment B.3.4:
Soil Vapor and Groundwater Monitoring Well Headspace Sample Analytical Results

GSI ENVIRONMENTAL

ATTACHMENT B.3.4: SOIL VAPOR AND GROUNDWATER MONITORING WELL HEADSPACE SAMPLE ANALYTICAL RESULTS
Red Hill Bulk Fuel Storage Facility, Joint Base Pearl Harbor-Hickam, O'ahu, Hawai'i

		Sample ID:	RHSV02MERH471	RHSV03DERH470	RHSV04DERH469	RHSV05SERH467	RHSV05SERH468	RHSV06SERH466
		Lab Sample ID:	L1740493-01	L1740493-02	L1740493-03	L1740493-04	L1740493-05	L1740493-06
		Sample Date/Time:	2017-10-31 12:00	2017-10-31 11:25	2017-10-31 10:43	2017-10-31 9:45	2017-10-31 10:00	2017-10-31 8:57
		Matrix:	SOIL_VAPOR	SOIL_VAPOR	SOIL_VAPOR	SOIL_VAPOR	SOIL_VAPOR	SOIL_VAPOR
FIXED GASES BY USEPA METHOD 3C								
Analyte		**Units**						
Carbon Dioxide		%	0.045 J	0.196 JD	0.989D	0.9D	0.992D	1.28D
Methane		%	<0.061	<0.061D	<0.075D	<0.068D	<0.054D	<0.066D
Oxygen		%	20.8	20.6D	20.8D	19.8D	20.1D	20D
VOCs BY USEPA METHOD TO-15 (TARGET ANALYTES)								
Analyte	**Class**	**Units**						
Decane (C10)	alkane	ppbV	0.975	1.46	2.38	<0.25	<0.25	1.17
Dodecane (C12)	alkane	ppbV	0.741	1.66	1.33	1.33D	<0.5	0.942
Heptane	alkane	ppbV	0.087	0.057	0.07	2.8D	2.12D	0.157
n-Hexane	alkane	ppbV	0.084	0.053	0.048	1.5D	0.75D	0.112
Nonane (C9)	alkane	ppbV	0.312	0.451	0.705	27.6D	33.1D	0.371
Octane	alkane	ppbV	0.146	0.146	0.18	8.26D	7.85D	0.178
Pentane	alkane	ppbV	1.06	0.435	0.42	1.45D	0.57D	2.61
Tridecane	alkane	ppbV	0.105 J	0.323 J	0.429 J	<0.5	<0.5	0.287 J
Undecane	alkane	ppbV	0.43	0.792	2.61	<0.25	<0.25	0.913
1,3-Butadiene	alkene	ppbV	<0.01	<0.01	<0.01	<0.1	<0.1	0.012 J
1-Decene	alkene	ppbV	<0.025	<0.025	<0.025	<0.25	<0.25	<0.025
1-Heptene	alkene	ppbV	<0.01	<0.01	0.055	<0.1	<0.1	0.04
1-Hexene	alkene	ppbV	<0.01	<0.01	<0.01	<0.1	<0.1	<0.01
1-Nonene	alkene	ppbV	<0.01	<0.01	<0.01	<0.1	<0.1	<0.01
1-Octene	alkene	ppbV	0.032	0.016 J	<0.01	<0.1	<0.1	<0.01
1-Pentene	alkene	ppbV	0.023 J	0.013 J	0.012 J	0.17 JD	0.19 JD	0.085
2-Methyl-1-Butene	alkene	ppbV	0.011 J	<0.01	<0.01	1.24D	1.35D	0.208
cis-2-Pentene	alkene	ppbV	<0.01	<0.01	<0.01	0.34D	0.34D	<0.01
trans-2-Pentene	alkene	ppbV	0.018 J	<0.01	<0.01	0.16 JD	0.15 JD	0.065
2,2-Dimethylpentane	branched alkane	ppbV	<0.01	<0.01	<0.01	0.2 JD	0.22 JD	<0.01
2,3,3-Trimethylpentane	branched alkane	ppbV	0.141	0.039	0.058	1.63D	1.83D	0.122
2,3,4-Trimethylpentane	branched alkane	ppbV	0.027	0.018 J	0.026	3.26D	3.76D	0.053
2,3-Dimethylbutane	branched alkane	ppbV	0.035	0.014 J	<0.01	0.5D	0.31D	0.049
2,3-Dimethylhexane	branched alkane	ppbV	0.099	<0.01	<0.01	3.28D	3.56D	<0.01
2,3-Dimethylpentane	branched alkane	ppbV	<0.01	<0.01	<0.01	2.25D	2.38D	<0.01
2,4-Dimethylhexane/2,2,3-Trimethylpentar	branched alkane	ppbV	0.042 J	<0.025	0.033 J	2.38D	2.56D	0.091
2,4-Dimethylpentane	branched alkane	ppbV	<0.01	<0.01	<0.01	0.66D	<0.1	<0.01
2,5-Dimethylhexane	branched alkane	ppbV	0.018 J	0.012 J	0.015 J	1.29D	1.34D	0.033
2-Methylheptane	branched alkane	ppbV	0.039	0.041	0.05	6.03D	6.23D	<0.01
2-Methylhexane	branched alkane	ppbV	0.028	0.026	0.024 J	1.83D	1.57D	0.023 J
2-Methylpentane	branched alkane	ppbV	0.217	0.096	0.105	2.2D	1.06D	0.463
3-Ethylhexane	branched alkane	ppbV	<0.01	<0.01	0.013 J	3.43D	3.91D	<0.01
3-Methylheptane	branched alkane	ppbV	0.032	0.033	0.048	6D	6.44D	0.043
3-Methylhexane	branched alkane	ppbV	0.118	0.065	0.095	3.38D	3.23D	0.202
3-Methylpentane	branched alkane	ppbV	0.041	0.029	0.049	1.64D	0.99D	0.04
Isooctane	branched alkane	ppbV	0.033	0.024 J	0.023 J	<0.1	<0.1	0.062
Isopentane	branched alkane	ppbV	<0.01	<0.01	<0.01	<0.1	<0.1	<0.01
1-Ethyl-1-Methylcyclopentane	cycloalkane	ppbV	<0.01	<0.01	0.014 J	3.56D	4.19D	<0.01
Cyclohexane	cycloalkane	ppbV	0.052	0.025	0.042	7.71D	8.69D	0.072
Cyclopentane	cycloalkane	ppbV	<0.01	<0.01	<0.01	0.36D	0.22 JD	<0.01
Methylcyclohexane	cycloalkane	ppbV	0.103	0.08	0.132	39.4D	44.2D	0.151
Methylcyclopentane	cycloalkane	ppbV	0.032	0.025	0.029	3.65D	3.66D	0.034
1,2,4,5-Tetramethylbenzene	aromatic	ppbV	<0.025	<0.025	0.056	<0.25	<0.25	<0.025
1,2,4-Trimethylbenzene	aromatic	ppbV	0.349	0.448	0.509	2.34D	1.7D	0.537
1,2-Diethylbenzene	aromatic	ppbV	0.042 J	0.085	0.221	2.68D	3.92D	0.029 J
1,2-Dimethyl-3-Ethylbenzene	aromatic	ppbV	0.043 J	0.076	0.13	1.23D	0.88D	0.031 J
1,2-Dimethyl-4-Ethylbenzene	aromatic	ppbV	0.169	0.326	0.871	8.41D	12D	0.16
1,3,5-Trimethylbenzene	aromatic	ppbV	0.25	0.458	1.08	24.4D	36.6D	0.229
1,3-Dimethyl-2-Ethylbenzene	aromatic	ppbV	<0.025	0.04 J	0.114	0.85D	1.01D	0.026 J
1,3-Dimethyl-4-Ethylbenzene	aromatic	ppbV	0.058	0.095	0.235	0.86D	0.95D	0.09
1,3-Dimethyl-5-Ethylbenzene	aromatic	ppbV	0.094	0.157	0.358	1.94D	2.41D	0.115
1,4-Dimethyl-2-Ethylbenzene	aromatic	ppbV	0.045 J	0.072	0.163	0.57D	<0.25	0.069
1-Methyl-2-Ethylbenzene	aromatic	ppbV	0.165	0.283	0.616	14.2D	20.9D	0.138
1-Methyl-2-Isopropylbenzene	aromatic	ppbV	<0.025	0.041 J	0.11	1.95D	2.92D	<0.025
1-Methyl-2-N-Propylbenzene	aromatic	ppbV	0.106	0.2	0.48	4.68D	6.26D	0.097
1-Methyl-3-Ethylbenzene	aromatic	ppbV	0.164	0.228	0.298	4.01D	4.99D	0.222
1-Methyl-3-Isopropylbenzene	aromatic	ppbV	0.078	0.142	0.343	5.71D	8.67D	0.084
1-Methyl-3-N-Propylbenzene	aromatic	ppbV	0.095	0.149	0.303	1.9D	2.44D	0.145
1-Methyl-4-Ethylbenzene	aromatic	ppbV	0.084	0.112	0.144	1.59D	1.84D	0.116
1-Methyl-4-Isopropylbenzene	aromatic	ppbV	0.039 J	0.052	0.076	0.49 JD	0.66D	0.084
1-Methyl-4-N-Propylbenzene	aromatic	ppbV	0.035 J	0.051	0.102	0.37 JD	0.4 JD	0.063
Benzene	aromatic	ppbV	0.054	0.029	0.044	0.45D	0.25D	0.057
Ethylbenzene	aromatic	ppbV	0.117	0.118	0.126	2.47D	2.35D	0.147
Indane	aromatic	ppbV	0.058	0.075	0.1	0.79D	0.92D	0.057
Indene	aromatic	ppbV	<0.025	<0.025	<0.025	<0.25	<0.25	<0.025
Isopropylbenzene	aromatic	ppbV	0.03	0.048	0.063	1.81D	2.27D	0.043
n-Butylbenzene	aromatic	ppbV	0.026 J	0.035 J	0.059	<0.25	<0.25	0.05
N-Pentylbenzene	aromatic	ppbV	<0.025	0.03 J	<0.025	<0.25	<0.25	<0.025
n-Propylbenzene	aromatic	ppbV	0.062	0.083	0.107	1.53D	1.84D	0.082
o-Xylene	aromatic	ppbV	0.484	0.426	0.621	13.7D	17.6D	0.691
p/m-Xylene	aromatic	ppbV	0.469	0.471	0.486	3.67D	2.22D	0.64
sec-Butylbenzene	aromatic	ppbV	0.028 J	0.053	0.114	2.33D	3.33D	0.05
Styrene	aromatic	ppbV	0.042	0.069	0.046	<0.1	<0.1	0.05
Toluene	aromatic	ppbV	0.277	0.252	0.183	2.91D	2.28D	0.237
1-Methylnaphthalene	naphthalene	ppbV	<0.05	<0.05	0.057 J	<0.5	<0.5	0.054 J
2-Methylnaphthalene	naphthalene	ppbV	<0.05	0.072 J	0.113 J	<0.5	<0.5	0.099 J
Naphthalene	naphthalene	ppbV	0.11	0.157	0.2	0.3 JD	<0.25	0.194
Tertiary Butanol	alcohol	ppbV	4.14	1.46	2.29	4.15D	3.37D	13.5
Ethyl-Tert-Butyl-Ether	ether	ppbV	0.806	0.294	0.408	0.34D	0.21 JD	2.3
Isopropyl Ether	ether	ppbV	<0.01	<0.01	<0.01	<0.1	<0.1	<0.01
Methyl tert butyl ether	ether	ppbV	0.091	0.031	0.04	<0.1	<0.1	0.241
Tertiary-Amyl Methyl Ether	ether	ppbV	0.031	<0.01	0.019 J	<0.1	<0.1	0.08
2-Ethylthiophene	thiophene	ppbV	<0.01	<0.01	<0.01	<0.1	<0.1	<0.01
2-Methylthiophene	thiophene	ppbV	<0.01	<0.01	<0.01	<0.1	<0.1	<0.01
3-Methylthiophene	thiophene	ppbV	<0.01	<0.01	<0.01	<0.1	<0.1	<0.01
Benzothiophene	thiophene	ppbV	<0.05	<0.05	<0.05	<0.5	<0.5	<0.05
Thiophene	thiophene	ppbV	<0.01	<0.01	<0.01	<0.1	<0.1	<0.01
1,2-Dibromoethane	other	ppbV	<0.01	<0.01	<0.01	<0.1	<0.1	<0.01
1,2-Dichloroethane	other	ppbV	<0.01	<0.01	<0.01	<0.1	<0.1	<0.01
MMT	other	ppbV	<0.05	<0.05	<0.05	<0.5	<0.5	<0.05

ATTACHMENT B.3.4: SOIL VAPOR AND GROUNDWATER MONITORING WELL HEADSPACE SAMPLE ANALYTICAL RESULTS
Red Hill Bulk Fuel Storage Facility, Joint Base Pearl Harbor-Hickam, O'ahu, Hawai'i

			Sample ID:	RHSV02MERH471	RHSV03DERH470	RHSV04DERH469	RHSV05SERH467	RHSV05SERH468	RHSV06SERH466
			Lab Sample ID:	L1740493-01	L1740493-02	L1740493-03	L1740493-04	L1740493-05	L1740493-06
			Sample Date/Time:	2017-10-31 12:00	2017-10-31 11:25	2017-10-31 10:43	2017-10-31 9:45	2017-10-31 10:00	2017-10-31 8:57
			Matrix:	SOIL_VAPOR	SOIL_VAPOR	SOIL_VAPOR	SOIL_VAPOR	SOIL_VAPOR	SOIL_VAPOR
VOCs BY USEPA METHOD TO-15 (TENTATIVELY IDENTIFIED COMPOUNDS)									
1-Butanol	alcohol	ppbV		-	-	-	-	-	-
1-Hexanol, 2-ethyl-	alcohol	ppbV		6.84	17.3	-	-	-	-
Amylene Hydrate	alcohol	ppbV		-	-	-	-	-	-
Methyl Alcohol	alcohol	ppbV		4.38	-	-	-	-	-
Unknown	alcohol	ppbV		-	-	12.7	-	-	-
Unknown	alcohol	ppbV		-	-	-	-	-	-
Unknown	alcohol	ppbV		-	-	-	-	-	-
Unknown	alcohol	ppbV		-	-	-	-	269	-
unknown alcohol	alcohol	ppbV		-	-	-	-	-	-
unknown alcohol	alcohol	ppbV		-	-	-	-	-	-
Unknown	alcohol cycloalkane	ppbV		-	-	-	-	-	-
Propane	alkane	ppbV		-	-	-	-	-	-
Unknown	alkane	ppbV		-	-	-	-	-	-
Unknown	alkane	ppbV		-	-	-	-	-	-
unknown alkane	alkane	ppbV		-	-	-	-	-	-
Unknown	alkane	ppbV		-	-	-	-	-	-
unknown alkane	alkane	ppbV		-	-	-	-	-	-
unknown alkane	alkane	ppbV		-	-	-	-	-	-
1-Pentene, 2-methyl-	alkene	ppbV		-	-	-	-	-	-
2,4-Dimethyl-1-heptene	alkene	ppbV		-	4.45	-	-	-	-
Unknown	alkene	ppbV		-	-	-	-	-	-
Unknown	alkene	ppbV		-	-	-	-	-	-
Unknown	alkene	ppbV		-	-	-	-	282	-
Unknown	alkene	ppbV		-	4.18	-	-	-	-
Unknown	alkene	ppbV		-	-	-	-	-	-
Unknown	alkene	ppbV		-	-	-	-	233	-
Unknown	alkene	ppbV		-	-	-	-	-	-
Unknown	alkene	ppbV		-	-	-	-	-	-
Unknown	alkene	ppbV		9.21	-	7.34	-	-	17.4
Unknown	alkene	ppbV		-	-	-	-	-	-
Unknown	alkene	ppbV		-	-	-	-	-	-
Unknown	alkene	ppbV		-	-	-	-	280	-
Unknown	alkene	ppbV		-	-	-	-	-	4.2
Unknown	alkene	ppbV		-	-	-	-	-	-
Unknown	alkene	ppbV		-	-	-	223	266	-
Unknown	alkene	ppbV		-	-	-	194	-	-
unknown alkane	alkene	ppbV		-	3.76	-	-	-	-
unknown alkene	alkene	ppbV		-	-	-	-	-	4.43
unknown alkene	alkene	ppbV		-	-	-	-	-	-
Unknown	aromatic	ppbV		-	-	-	-	-	-
Unknown	aromatic	ppbV		-	-	-	224	-	-
Hexane, 2,3-dimethyl-	branched alkane	ppbV		-	-	-	-	-	10.4
Unknown	branched alkane	ppbV		-	-	-	-	-	-
Unknown	branched alkane	ppbV		-	-	-	-	-	-
Unknown	branched alkane	ppbV		-	-	-	-	-	-
Unknown	branched alkane	ppbV		-	-	-	-	-	-
unknown alkane	branched alkane	ppbV		5.26	-	-	-	-	-
unknown alkane	branched alkane	ppbV		-	-	-	-	-	-
unknown alkane	branched alkane	ppbV		-	-	-	-	-	-
Cyclohexane, 1,1,3-trimethyl-	cycloalkane	ppbV		-	-	-	296	335	-
Unknown	cycloalkane	ppbV		-	-	8.88	-	-	-
Unknown	cycloalkane	ppbV		-	-	8.34	-	-	-
Unknown	cycloalkane	ppbV		-	-	-	313	397	-
Unknown	cycloalkane	ppbV		-	-	-	-	-	-
Unknown	cycloalkane	ppbV		-	-	-	-	-	-
Unknown	cycloalkane	ppbV		-	-	-	218	256	-
Unknown	cycloalkane	ppbV		-	-	-	255	-	-
Unknown	cycloalkane	ppbV		-	-	11.6	-	-	-
Unknown	cycloalkane	ppbV		-	-	7.65	-	-	-
Unknown	cycloalkane	ppbV		-	-	-	238	-	-
Unknown	cycloalkane	ppbV		-	-	-	-	-	-
unknown alkane	cycloalkane	ppbV		-	-	-	232	-	-
unknown cycloalkane	cycloalkane	ppbV		-	-	-	-	268	-
unknown cycloalkane	cycloalkane	ppbV		-	-	-	476	-	-
unknown cycloalkane	cycloalkane	ppbV		-	-	-	-	565	-
unknown cycloalkane	cycloalkane	ppbV		-	-	-	-	-	-
Furan, tetrahydro-	furan	ppbV		2.98	-	-	-	-	-
2-Butanone	ketone	ppbV		-	-	-	-	-	-
Acetone	ketone	ppbV		-	-	-	-	-	5.55
Cyclohexanone	ketone	ppbV		-	-	-	-	-	-
Cyclopentanone	ketone	ppbV		-	-	-	-	-	5.53
Unknown	ketone	ppbV		-	-	-	-	-	-
Unknown	ketone	ppbV		-	-	-	-	-	-
Unknown	ketone	ppbV		-	6.24	-	-	-	-
Unknown	ketone	ppbV		-	-	-	-	-	-
Unknown	ketone cycloalkane	ppbV		3.11	-	-	-	-	-
Unknown	ketone cycloalkane	ppbV		-	2.95	-	-	-	-
Unknown	ketone cycloalkane	ppbV		-	-	7.13	-	-	-
Unknown	naphthalene	ppbV		3.77	7.54	20.4	217	239	-
Unknown	other	ppbV		-	-	-	-	-	-
Unknown	other	ppbV		-	-	-	-	-	-
Unknown	other	ppbV		-	-	-	-	-	-
Unknown	other	ppbV		-	-	-	-	-	-
Unknown	other	ppbV		-	-	-	-	-	-
Unknown	other	ppbV		-	-	-	-	-	-
Unknown	other	ppbV		-	-	-	-	-	-
Unknown	other	ppbV		-	-	-	-	-	-
Unknown	other	ppbV		-	-	-	-	-	-
Unknown	other	ppbV		-	-	-	-	-	-
Unknown	other	ppbV		-	-	-	-	-	-
Unknown	other	ppbV		3.01	-	-	-	-	-
Unknown	other	ppbV		-	-	-	-	-	-
Unknown	other	ppbV		-	-	-	-	-	-
Unknown	other	ppbV		-	-	-	-	-	-
Unknown	other	ppbV		-	-	-	-	-	-
Unknown	other	ppbV		-	-	-	-	-	-
Unknown	other	ppbV		-	-	-	-	-	-
Unknown	other	ppbV		-	-	-	-	-	-
Cyclotrisiloxane, Hexamethyl-	siloxane	ppbV		13.7	7.95	7.4	-	-	16.5
Silanol, Trimethyl-	siloxane	ppbV		17.1	-	-	-	-	8.16
Unknown	siloxane	ppbV		-	6.48	-	-	-	-
unknown siloxane	siloxane	ppbV		-	4.05	-	-	-	-
unknown siloxane	siloxane	ppbV		20.6	-	-	-	-	-
unknown siloxane	siloxane	ppbV		-	-	-	-	-	8.65
unknown siloxane	siloxane	ppbV		-	-	-	-	-	-
unknown siloxane	siloxane	ppbV		-	-	-	-	-	-
unknown siloxane	siloxane	ppbV		-	-	-	-	-	5.24

1. Samples collected by GSI and analyzed by Alpha Analytical.
2. Less than ("<") indicates the analyte was not found at the stated detection limit. J = estimated result between method detection limit and reporting limit.
   D = result from a dilution.

GSI ENVIRONMENTAL

ATTACHMENT B.3.4: SOIL VAPOR AND GROUNDWATER MONITORING WELL HEADSPACE SAMPLE ANALYTICAL RESULTS
Red Hill Bulk Fuel Storage Facility, Joint Base Pearl Harbor-Hickam, O'ahu, Hawai'i

		Sample ID:	RHSV07DERH464	RHSV08SERH463	RHSV09SERH462	RHSV10SERH461	RHSV11MERH460	RHSV12MERH458
		Lab Sample ID:	L1740493-07	L1740493-08	L1740493-09	L1740493-10	L1740493-11	L1740493-12
		Sample Date/Time:	2017-10-31 14:25	2017-10-31 13:44	2017-10-31 13:10	2017-10-31 11:36	2017-10-30 10:56	2017-10-27 14:11
		Matrix:	SOIL_VAPOR	SOIL_VAPOR	SOIL_VAPOR	SOIL_VAPOR	SOIL_VAPOR	SOIL_VAPOR
FIXED GASES BY USEPA METHOD 3C								
Analyte		**Units**						
Carbon Dioxide		%	3.94D	0.79D	0.495D	0.559D	1.09D	0.312D
Methane		%	<0.061D	<0.062D	<0.061D	<0.062D	<0.061D	<0.039D
Oxygen		%	13.4D	20.8D	21D	20.7D	20.4D	12.5D
VOCs BY USEPA METHOD TO-15 (TARGET ANALYTES)								
Analyte	**Class**	**Units**						
Decane (C10)	alkane	ppbV	0.516	0.365	0.437	0.438	1.05	0.97
Dodecane (C12)	alkane	ppbV	0.54	0.485	0.686	0.641	0.752	0.908
Heptane	alkane	ppbV	0.027	0.035	0.063	0.06	0.234	0.077
n-Hexane	alkane	ppbV	0.043	0.065	0.101	0.071	0.162	0.055
Nonane (C9)	alkane	ppbV	0.185	0.132	0.134	0.169	1.06	0.437
Octane	alkane	ppbV	0.071	0.07	0.089	0.119	0.42	0.211
Pentane	alkane	ppbV	1.3	1.55	2.14	2.55	3.36	0.29
Tridecane	alkane	ppbV	0.302 J	0.281 J	0.363 J	0.369 J	0.282 J	0.526 J
Undecane	alkane	ppbV	0.516	0.428	0.395	0.463	0.463	0.732
1,3-Butadiene	alkene	ppbV	<0.01	<0.01	<0.01	<0.01	<0.01	<0.01
1-Decene	alkene	ppbV	<0.025	<0.025	<0.025	<0.025	<0.025	<0.025
1-Heptene	alkene	ppbV	<0.01	<0.01	<0.01	<0.01	<0.01	<0.01
1-Hexene	alkene	ppbV	<0.01	<0.01	<0.01	<0.01	<0.01	<0.01
1-Nonene	alkene	ppbV	<0.01	<0.01	<0.01	<0.01	<0.01	<0.01
1-Octene	alkene	ppbV	<0.01	<0.01	0.017 J	0.024 J	<0.01	<0.01
1-Pentene	alkene	ppbV	0.025	0.033	0.046	0.048	0.073	0.012 J
2-Methyl-1-Butene	alkene	ppbV	0.013 J	0.02 J	0.027	0.023 J	0.07	<0.01
cis-2-Pentene	alkene	ppbV	<0.01	<0.01	<0.01	<0.01	0.085	<0.01
trans-2-Pentene	alkene	ppbV	0.02 J	0.024 J	0.04	0.042	0.064	<0.01
2,2-Dimethylpentane	branched alkane	ppbV	<0.01	<0.01	<0.01	<0.01	<0.01	<0.01
2,3,3-Trimethylpentane	branched alkane	ppbV	0.026	0.034	0.055	0.058	0.17	0.047
2,3,4-Trimethylpentane	branched alkane	ppbV	0.023 J	0.01 J	0.02 J	0.02 J	0.142	0.017 J
2,3-Dimethylbutane	branched alkane	ppbV	<0.01	<0.01	0.026	<0.01	<0.01	0.018 J
2,3-Dimethylhexane	branched alkane	ppbV	<0.01	0.01 J	<0.01	<0.01	<0.01	<0.01
2,3-Dimethylpentane	branched alkane	ppbV	<0.01	<0.01	<0.01	<0.01	0.085	<0.01
2,4-Dimethylhexane/2,2,3-Trimethylpentar	branched alkane	ppbV	0.032 J	<0.025	0.029 J	0.04 J	0.15	<0.025
2,4-Dimethylpentane	branched alkane	ppbV	<0.01	<0.01	<0.01	<0.01	<0.01	<0.01
2,5-Dimethylhexane	branched alkane	ppbV	0.014 J	<0.01	0.012 J	0.013 J	0.062	0.013 J
2-Methylheptane	branched alkane	ppbV	0.02 J	0.018 J	0.022 J	<0.01	0.165	0.058
2-Methylhexane	branched alkane	ppbV	<0.01	0.015 J	0.029	<0.01	<0.01	0.029
2-Methylpentane	branched alkane	ppbV	0.139	0.196	0.238	0.323	0.438	0.104 B
3-Ethylhexane	branched alkane	ppbV	0.04	<0.01	<0.01	<0.01	0.096	<0.01
3-Methylheptane	branched alkane	ppbV	0.016 J	0.011 J	0.026	0.023 J	0.22	0.039
3-Methylhexane	branched alkane	ppbV	0.068	0.067	0.111	0.136	0.369	0.057
3-Methylpentane	branched alkane	ppbV	0.033	0.045	0.05	<0.01	0.098	0.031
Isooctane	branched alkane	ppbV	0.031	0.03	0.051	0.047	0.114	0.026
Isopentane	branched alkane	ppbV	<0.01	<0.01	<0.01	<0.01	<0.01	<0.01
1-Ethyl-1-Methylcyclopentane	cycloalkane	ppbV	0.032	<0.01	<0.01	<0.01	0.1	<0.01
Cyclohexane	cycloalkane	ppbV	0.103	0.062	0.068	0.082	0.387	0.039
Cyclopentane	cycloalkane	ppbV	0.228	0.047	0.048	<0.01	<0.01	<0.01
Methylcyclohexane	cycloalkane	ppbV	0.309	0.032	0.037	0.056	1.16	0.104
Methylcyclopentane	cycloalkane	ppbV	0.05	0.036	0.033	0.02 J	0.111	0.035
1,2,4,5-Tetramethylbenzene	aromatic	ppbV	<0.025	<0.025	<0.025	<0.025	<0.025	<0.025
1,2,4-Trimethylbenzene	aromatic	ppbV	0.245	0.219	0.234	0.301	0.51	0.437
1,2-Diethylbenzene	aromatic	ppbV	0.025 J	<0.025	<0.025	<0.025	0.076	<0.025
1,2-Dimethyl-3-Ethylbenzene	aromatic	ppbV	<0.025	<0.025	<0.025	<0.025	0.033 J	0.038 J
1,2-Dimethyl-4-Ethylbenzene	aromatic	ppbV	0.043 J	0.034 J	0.032 J	0.04 J	0.248	0.071
1,3,5-Trimethylbenzene	aromatic	ppbV	0.066	0.05	0.052	0.067	0.729	0.11
1,3-Dimethyl-2-Ethylbenzene	aromatic	ppbV	<0.025	<0.025	<0.025	<0.025	0.028 J	<0.025
1,3-Dimethyl-4-Ethylbenzene	aromatic	ppbV	0.045 J	0.034 J	0.032 J	0.041 J	0.071	0.07
1,3-Dimethyl-5-Ethylbenzene	aromatic	ppbV	0.061	0.04 J	0.037 J	0.048 J	0.105	0.079
1,4-Dimethyl-2-Ethylbenzene	aromatic	ppbV	0.035 J	0.027 J	0.026 J	0.033 J	0.057	0.058
1-Methyl-2-Ethylbenzene	aromatic	ppbV	0.056	0.048 J	0.053	0.066	0.468	0.114
1-Methyl-2-Isopropylbenzene	aromatic	ppbV	<0.025	<0.025	<0.025	<0.025	0.052	<0.025
1-Methyl-2-N-Propylbenzene	aromatic	ppbV	0.041 J	0.031 J	0.032 J	0.037 J	0.158	0.071
1-Methyl-3-Ethylbenzene	aromatic	ppbV	0.094	0.083	0.091	0.114	0.289	0.198
1-Methyl-3-Isopropylbenzene	aromatic	ppbV	<0.025	<0.025	<0.025	0.027 J	0.178	0.051
1-Methyl-3-N-Propylbenzene	aromatic	ppbV	0.066	0.054	0.05	0.063	0.129	0.096
1-Methyl-4-Ethylbenzene	aromatic	ppbV	0.052	0.043	0.046	0.058	0.136	0.106
1-Methyl-4-Isopropylbenzene	aromatic	ppbV	0.026 J	<0.025	<0.025	0.027 J	0.09	0.044 J
1-Methyl-4-N-Propylbenzene	aromatic	ppbV	0.032 J	<0.025	<0.025	0.027 J	0.042 J	0.043 J
Benzene	aromatic	ppbV	0.076	0.34	0.304	0.062	0.09	0.053
Ethylbenzene	aromatic	ppbV	0.073	0.067	0.087	0.094	0.254	0.134
Indane	aromatic	ppbV	0.031 J	0.03 J	0.026 J	0.033 J	0.065	0.046 J
Indene	aromatic	ppbV	<0.025	<0.025	<0.025	<0.025	<0.025	<0.025
Isopropylbenzene	aromatic	ppbV	0.068	0.233	0.323	0.024 J	0.105	0.044
n-Butylbenzene	aromatic	ppbV	<0.025	<0.025	<0.025	<0.025	<0.025	0.041 J
N-Pentylbenzene	aromatic	ppbV	<0.025	<0.025	<0.025	<0.025	<0.025	<0.025
n-Propylbenzene	aromatic	ppbV	0.04	0.031	0.035	0.043	0.109	0.079
o-Xylene	aromatic	ppbV	0.699	0.681	0.847	1.1	2.82	0.411
p/m-Xylene	aromatic	ppbV	0.293	0.289	0.365	0.407	0.88	0.578
sec-Butylbenzene	aromatic	ppbV	<0.025	<0.025	<0.025	<0.025	0.08	0.034 J
Styrene	aromatic	ppbV	0.015 J	0.015 J	0.035	0.023 J	<0.01	0.026
Toluene	aromatic	ppbV	0.15	0.17	0.369	0.263	0.562	0.285
1-Methylnaphthalene	naphthalene	ppbV	0.052 J	<0.05	<0.05	<0.05	<0.05	0.061 J
2-Methylnaphthalene	naphthalene	ppbV	0.104 J	0.071 J	0.051 J	0.075 J	0.064 J	0.115 J
Naphthalene	naphthalene	ppbV	0.17	0.106	0.097	0.116	0.16	0.144 B
Tertiary Butanol	alcohol	ppbV	3.47	3.53	10.4	10.7	33.9	2.73
Ethyl-Tert-Butyl-Ether	ether	ppbV	0.678	0.739	1.35	1.91	3.44	0.297
Isopropyl Ether	ether	ppbV	<0.01	<0.01	<0.01	<0.01	<0.01	<0.01
Methyl tert butyl ether	ether	ppbV	0.092	0.083	0.144	0.193	0.335	0.032
Tertiary-Amyl Methyl Ether	ether	ppbV	<0.01	<0.01	0.048	0.069	0.141	<0.01
2-Ethylthiophene	thiophene	ppbV	<0.01	<0.01	<0.01	<0.01	<0.01	<0.01
2-Methylthiophene	thiophene	ppbV	<0.01	<0.01	<0.01	<0.01	<0.01	<0.01
3-Methylthiophene	thiophene	ppbV	<0.01	<0.01	<0.01	<0.01	<0.01	<0.01
Benzothiophene	thiophene	ppbV	<0.05	<0.05	<0.05	<0.05	<0.05	<0.05
Thiophene	thiophene	ppbV	<0.01	<0.01	<0.01	<0.01	<0.01	<0.01
1,2-Dibromoethane	other	ppbV	<0.01	<0.01	<0.01	<0.01	<0.01	<0.01
1,2-Dichloroethane	other	ppbV	<0.01	0.087	<0.01	<0.01	<0.01	<0.01
MMT	other	ppbV	<0.05	<0.05	<0.05	<0.05	<0.05	<0.05

ATTACHMENT B.3.4: SOIL VAPOR AND GROUNDWATER MONITORING WELL HEADSPACE SAMPLE ANALYTICAL RESULTS
Red Hill Bulk Fuel Storage Facility, Joint Base Pearl Harbor-Hickam, O'ahu, Hawai'i

			Sample ID:	RHSV07DERH464	RHSV08SERH463	RHSV09SERH462	RHSV10SERH461	RHSV11MERH460	RHSV12MERH458
			Lab Sample ID:	L1740493-07	L1740493-08	L1740493-09	L1740493-10	L1740493-11	L1740493-12
			Sample Date/Time:	2017-10-31 14:25	2017-10-31 13:44	2017-10-31 13:10	2017-10-31 11:36	2017-10-30 10:56	2017-10-27 14:11
			Matrix:	SOIL_VAPOR	SOIL_VAPOR	SOIL_VAPOR	SOIL_VAPOR	SOIL_VAPOR	SOIL_VAPOR
VOCs BY USEPA METHOD TO-15 (TENTATIVELY IDENTIFIED COMPOUNDS)									
1-Butanol	alcohol	ppbV		-	1.12	-	-	-	-
1-Hexanol, 2-ethyl-	alcohol	ppbV		-	17.7	17	-	-	11.8
Amylene Hydrate	alcohol	ppbV		-	-	-	2.99	7.73	-
Methyl Alcohol	alcohol	ppbV		-	2.6	2.74	-	-	-
Unknown	alcohol	ppbV		-	-	-	-	-	-
Unknown	alcohol	ppbV		3.44	-	-	-	-	-
Unknown	alcohol	ppbV		-	-	-	-	-	-
Unknown	alcohol	ppbV		-	-	-	-	-	-
unknown alcohol	alcohol	ppbV		-	-	3.25	-	-	-
unknown alcohol	alcohol	ppbV		-	-	-	-	-	-
Unknown	alcohol cycloalkane	ppbV		3.98	-	-	-	-	-
Propane	alkane	ppbV		-	-	-	-	-	-
Unknown	alkane	ppbV		-	-	-	-	-	-
Unknown	alkane	ppbV		-	-	-	-	-	-
unknown alkane	alkane	ppbV		-	-	-	-	-	-
Unknown	alkane	ppbV		-	-	-	-	-	-
unknown alkane	alkane	ppbV		-	-	-	-	-	-
unknown alkane	alkane	ppbV		-	-	-	-	-	-
1-Pentene, 2-methyl-	alkene	ppbV		-	-	-	2.95	-	-
2,4-Dimethyl-1-heptene	alkene	ppbV		-	5.82	-	-	-	-
Unknown	alkene	ppbV		-	-	-	-	-	-
Unknown	alkene	ppbV		6.69	-	-	-	-	-
Unknown	alkene	ppbV		-	-	-	-	-	-
Unknown	alkene	ppbV		-	-	2.95	4.47	-	-
Unknown	alkene	ppbV		-	-	-	-	9.32	-
Unknown	alkene	ppbV		-	-	-	-	-	-
Unknown	alkene	ppbV		-	-	-	-	-	-
Unknown	alkene	ppbV		-	-	-	-	-	-
Unknown	alkene	ppbV		5.84	-	7.76	12	34.1	6.27
Unknown	alkene	ppbV		-	-	-	-	-	-
Unknown	alkene	ppbV		-	-	-	-	-	-
Unknown	alkene	ppbV		-	-	-	-	-	-
Unknown	alkene	ppbV		-	-	-	-	-	-
Unknown	alkene	ppbV		-	1.9	-	-	-	-
Unknown	alkene	ppbV		-	-	-	-	-	-
Unknown	alkene	ppbV		-	-	-	-	-	-
unknown alkane	alkene	ppbV		-	-	-	-	-	-
unknown alkene	alkene	ppbV		-	-	-	-	-	-
unknown alkene	alkene	ppbV		-	-	-	-	-	-
Unknown	aromatic	ppbV		-	-	-	-	-	-
Unknown	aromatic	ppbV		-	-	-	-	-	-
Hexane, 2,3-dimethyl-	branched alkane	ppbV		-	-	-	-	17.4	-
Unknown	branched alkane	ppbV		-	-	-	-	-	-
Unknown	branched alkane	ppbV		-	-	-	-	-	-
Unknown	branched alkane	ppbV		-	-	4.44	-	-	-
Unknown	branched alkane	ppbV		-	-	-	-	-	-
unknown alkane	branched alkane	ppbV		-	3.33	-	-	-	3.29
unknown alkane	branched alkane	ppbV		-	-	-	-	-	-
unknown alkane	branched alkane	ppbV		-	-	-	7.27	-	-
Cyclohexane, 1,1,3-trimethyl-	cycloalkane	ppbV		-	-	-	-	8.03	-
Unknown	cycloalkane	ppbV		-	-	-	-	-	-
Unknown	cycloalkane	ppbV		3.53	-	-	-	-	-
Unknown	cycloalkane	ppbV		-	-	-	-	-	-
Unknown	cycloalkane	ppbV		-	-	-	-	-	2
Unknown	cycloalkane	ppbV		-	-	-	-	-	-
Unknown	cycloalkane	ppbV		-	-	-	-	-	-
Unknown	cycloalkane	ppbV		-	-	-	-	-	-
Unknown	cycloalkane	ppbV		-	-	-	-	-	-
Unknown	cycloalkane	ppbV		-	-	-	-	-	-
Unknown	cycloalkane	ppbV		3.57	-	-	-	-	-
unknown alkane	cycloalkane	ppbV		-	-	-	-	-	-
unknown cycloalkane	cycloalkane	ppbV		-	-	-	-	-	-
unknown cycloalkane	cycloalkane	ppbV		-	-	-	-	-	-
unknown cycloalkane	cycloalkane	ppbV		-	-	-	-	-	-
unknown cycloalkane	cycloalkane	ppbV		-	-	-	-	12.8	-
Furan, tetrahydro-	furan	ppbV		-	-	-	-	-	1.56
2-Butanone	ketone	ppbV		-	-	-	2.13	-	-
Acetone	ketone	ppbV		3.21	2.92	4.68	5.51	12.1	2.7
Cyclohexanone	ketone	ppbV		-	-	-	-	-	-
Cyclopentanone	ketone	ppbV		-	-	-	-	-	9.1
Unknown	ketone	ppbV		-	-	-	-	-	2.21
Unknown	ketone	ppbV		-	-	-	-	-	-
Unknown	ketone	ppbV		-	-	-	-	-	-
Unknown	ketone	ppbV		-	1.48	-	-	-	-
Unknown	ketone cycloalkane	ppbV		-	-	-	-	-	-
Unknown	ketone cycloalkane	ppbV		-	-	-	-	-	-
Unknown	ketone cycloalkane	ppbV		-	-	-	-	-	-
Unknown	naphthalene	ppbV		-	-	-	-	-	-
Unknown	other	ppbV		-	-	-	-	-	-
Unknown	other	ppbV		-	-	-	-	-	-
Unknown	other	ppbV		4.48	-	-	-	-	-
Unknown	other	ppbV		-	-	-	-	-	-
Unknown	other	ppbV		-	-	-	-	-	-
Unknown	other	ppbV		-	-	-	-	-	-
Unknown	other	ppbV		-	-	-	-	-	-
Unknown	other	ppbV		-	-	-	-	-	-
Unknown	other	ppbV		-	-	-	-	-	-
Unknown	other	ppbV		-	-	-	-	-	-
Cyclotrisiloxane, Hexamethyl-	siloxane	ppbV		12.4	7.29	16.2	18.5	17.6	6.4
Silanol, Trimethyl-	siloxane	ppbV		14.3	-	-	3.08	29.6	-
Unknown	siloxane	ppbV		-	-	-	-	-	-
unknown siloxane	siloxane	ppbV		-	-	-	-	-	-
unknown siloxane	siloxane	ppbV		-	1.29	10.8	-	-	2.25
unknown siloxane	siloxane	ppbV		-	-	-	-	7.7	-
unknown siloxane	siloxane	ppbV		-	-	7.93	-	-	-
unknown siloxane	siloxane	ppbV		-	-	-	3.8	-	-
unknown siloxane	siloxane	ppbV		-	-	-	-	-	-

1. Samples collected by GSI and analyzed by Alpha Analytical.
2. Less than ("<") indicates the analyte was not found at the stated detection limit. J = estimated result between method detection limit and reporting limit.
   D = result from a dilution.

ATTACHMENT C.3.4: SOIL VAPOR AND GROUNDWATER MONITORING WELL HEADSPACE SAMPLE ANALYTICAL RESULTS
Red Hill Bulk Fuel Storage Facility, Joint Base Pearl Harbor-Hickam, O'ahu, Hawai'i

		Sample ID:	RHSV13SERH457	RHSV14DERH456	RHSV15SERH455	RHSV16DERH454	RHSV18SERH453	RHSV20DERH465
		Lab Sample ID:	L1740493-13	L1740493-14	L1740493-15	L1740493-16	L1740493-17	L1740493-18
		Sample Date/Time:	2017-10-27 13:29	2017-10-27 12:48	2017-10-27 11:24	2017-10-27 10:46	2017-10-27 10:00	2017-10-30 15:08
		Matrix:	SOIL_VAPOR	SOIL_VAPOR	SOIL_VAPOR	SOIL_VAPOR	SOIL_VAPOR	SOIL_VAPOR
FIXED GASES BY USEPA METHOD 3C								
Analyte		**Units**						
Carbon Dioxide		%	0.951D	0.404D	0.428D	1.39D	0.368D	0.17 JD
Methane		%	<0.061D	<0.075D	<0.061D	<0.061D	<0.062D	<0.063D
Oxygen		%	20.1D	7.81D	20.6D	19.7D	21.1D	21.2D
VOCs BY USEPA METHOD TO-15 (TARGET ANALYTES)								
Analyte	**Class**	**Units**						
Decane (C10)	alkane	ppbV	0.855	1.14	0.331	0.559	2.88	4.98
Dodecane (C12)	alkane	ppbV	1.22	1.11	0.511	0.725	2.09	4.79
Heptane	alkane	ppbV	0.101	0.099	0.096	0.047	0.174	0.072
n-Hexane	alkane	ppbV	0.074	0.066	0.131	0.044	0.155	0.061
Nonane (C9)	alkane	ppbV	0.49	0.577	0.137	0.214	1.04	1.73
Octane	alkane	ppbV	0.253	0.272	0.142	0.106	0.406	0.362
Pentane	alkane	ppbV	0.787	0.769	0.746	0.552	2.03	1.43
Tridecane	alkane	ppbV	1.62	0.132 J	0.208 J	0.31 J	1.08	2.29
Undecane	alkane	ppbV	1	0.861	0.372	0.611	3.03	7.98
1,3-Butadiene	alkene	ppbV	<0.01	<0.01	<0.01	<0.01	<0.01	<0.01
1-Decene	alkene	ppbV	<0.025	<0.025	<0.025	<0.025	<0.025	<0.025
1-Heptene	alkene	ppbV	<0.01	<0.01	<0.01	<0.01	<0.01	<0.01
1-Hexene	alkene	ppbV	<0.01	<0.01	<0.01	<0.01	0.192	<0.01
1-Nonene	alkene	ppbV	<0.01	<0.01	<0.01	<0.01	<0.01	<0.01
1-Octene	alkene	ppbV	<0.01	<0.01	<0.01	0.043	<0.01	<0.01
1-Pentene	alkene	ppbV	0.014 J	0.019 J	0.017 J	0.013 J	0.052	0.026
2-Methyl-1-Butene	alkene	ppbV	0.025	0.018 J	0.01 J	<0.01	0.051	0.015 J
cis-2-Pentene	alkene	ppbV	<0.01	<0.01	<0.01	<0.01	<0.01	<0.01
trans-2-Pentene	alkene	ppbV	0.012 J	0.015 J	0.012 J	0.01 J	0.041	0.022 J
2,2-Dimethylpentane	branched alkane	ppbV	<0.01	<0.01	<0.01	<0.01	<0.01	<0.01
2,3,3-Trimethylpentane	branched alkane	ppbV	0.073	0.08	0.052	0.084	0.259	0.054
2,3,4-Trimethylpentane	branched alkane	ppbV	0.02 J	0.027	0.019 J	0.018 J	0.05	0.015 J
2,3-Dimethylbutane	branched alkane	ppbV	0.028	<0.01	<0.01	<0.01	0.052	<0.01
2,3-Dimethylhexane	branched alkane	ppbV	<0.01	<0.01	<0.01	<0.01	<0.01	0.018 J
2,3-Dimethylpentane	branched alkane	ppbV	<0.01	<0.01	<0.01	<0.01	<0.01	<0.01
2,4-Dimethylhexane/2,2,3-Trimethylpentar	branched alkane	ppbV	0.038 JB	0.045 JB	0.03 JB	0.03 JB	0.077 B	<0.025
2,4-Dimethylpentane	branched alkane	ppbV	<0.01	<0.01	<0.01	<0.01	<0.01	<0.01
2,5-Dimethylhexane	branched alkane	ppbV	0.021 J	<0.01	0.012 J	0.012 J	0.035	0.011 J
2-Methylheptane	branched alkane	ppbV	0.077	0.075	0.025	<0.01	0.1	0.068
2-Methylhexane	branched alkane	ppbV	0.044	0.036	0.027	<0.01	0.045	0.022 J
2-Methylpentane	branched alkane	ppbV	0.212	<0.01	0.178	0.196	0.39	0.251
3-Ethylhexane	branched alkane	ppbV	<0.01	<0.01	<0.01	<0.01	<0.01	<0.01
3-Methylheptane	branched alkane	ppbV	0.057	0.062	0.023 J	0.02 J	0.078	0.049
3-Methylhexane	branched alkane	ppbV	0.096	0.086	0.06	0.06	0.166	0.092
3-Methylpentane	branched alkane	ppbV	0.036	0.035	0.045	0.019 J	0.061	0.062
Isooctane	branched alkane	ppbV	0.027	0.038	0.028	0.022 J	0.057	0.032
Isopentane	branched alkane	ppbV	<0.01	<0.01	0.142	0.206	0.47	0.453
1-Ethyl-1-Methylcyclopentane	cycloalkane	ppbV	<0.01	<0.01	<0.01	<0.01	<0.01	<0.01
Cyclohexane	cycloalkane	ppbV	0.058	0.063	0.036	0.024 J	0.096	0.107
Cyclopentane	cycloalkane	ppbV	<0.01	<0.01	<0.01	<0.01	<0.01	<0.01
Methylcyclohexane	cycloalkane	ppbV	0.14	0.176	0.054	0.035	0.192	0.137
Methylcyclopentane	cycloalkane	ppbV	0.046	0.038	0.025	<0.01	0.089	0.057
1,2,4,5-Tetramethylbenzene	aromatic	ppbV	<0.025	<0.025	<0.025	<0.025	0.122	0.046 J
1,2,4-Trimethylbenzene	aromatic	ppbV	0.747	0.624	0.202	0.3	2	2.12
1,2-Diethylbenzene	aromatic	ppbV	0.033 J	0.03 J	<0.025	<0.025	0.205	0.099
1,2-Dimethyl-3-Ethylbenzene	aromatic	ppbV	0.073	0.054	0.027 J	0.048 J	0.503	0.237
1,2-Dimethyl-4-Ethylbenzene	aromatic	ppbV	0.137	0.089	0.039 J	0.07	0.854	0.305
1,3,5-Trimethylbenzene	aromatic	ppbV	0.194	0.173	0.047	0.073	0.626	0.46
1,3-Dimethyl-2-Ethylbenzene	aromatic	ppbV	0.025 J	<0.025	<0.025	<0.025	0.146	0.059
1,3-Dimethyl-4-Ethylbenzene	aromatic	ppbV	0.133	0.095	0.034 J	0.065	0.587	0.407
1,3-Dimethyl-5-Ethylbenzene	aromatic	ppbV	0.147	0.094	0.039 J	0.076	0.601	0.417
1,4-Dimethyl-2-Ethylbenzene	aromatic	ppbV	0.107	0.077	0.028 J	0.052	0.469	0.292
1-Methyl-2-Ethylbenzene	aromatic	ppbV	0.191	0.201	0.042 J	0.076	0.556	0.605
1-Methyl-2-Isopropylbenzene	aromatic	ppbV	<0.025	<0.025	<0.025	<0.025	0.072	0.03 J
1-Methyl-2-N-Propylbenzene	aromatic	ppbV	0.112	0.099	0.031 J	0.061	0.608	0.424
1-Methyl-3-Ethylbenzene	aromatic	ppbV	0.358	0.284	0.07	0.116	0.8	1.11
1-Methyl-3-Isopropylbenzene	aromatic	ppbV	0.07	0.066	<0.025	0.03 J	0.239	0.244
1-Methyl-3-N-Propylbenzene	aromatic	ppbV	0.163	0.117	0.042 J	0.071	0.491	0.613
1-Methyl-4-Ethylbenzene	aromatic	ppbV	0.189	0.146	0.038	0.063	0.419	0.681
1-Methyl-4-Isopropylbenzene	aromatic	ppbV	0.059	0.065	0.025 J	0.033 J	0.189	0.228
1-Methyl-4-N-Propylbenzene	aromatic	ppbV	0.071	0.057	<0.025	0.031 J	0.206	0.351
Benzene	aromatic	ppbV	0.084	0.06	0.072	0.042	0.122	0.054
Ethylbenzene	aromatic	ppbV	0.21	0.192	0.064	0.088	0.465	0.533
Indane	aromatic	ppbV	0.107	0.06	<0.025	0.045 J	0.195	0.223
Indene	aromatic	ppbV	<0.025	<0.025	<0.025	<0.025	<0.025	<0.025
Isopropylbenzene	aromatic	ppbV	0.074	0.055	0.076	0.024 J	0.171	0.158
n-Butylbenzene	aromatic	ppbV	0.064	0.044 J	<0.025	0.027 J	0.168	0.346
N-Pentylbenzene	aromatic	ppbV	0.06	<0.025	<0.025	<0.025	0.129	0.114
n-Propylbenzene	aromatic	ppbV	0.122	0.112	0.028	0.048	0.307	0.506
o-Xylene	aromatic	ppbV	0.565	0.563	0.331	0.348	1.32	1.44
p/m-Xylene	aromatic	ppbV	0.921	0.72	0.259	0.362	1.94	2.2
sec-Butylbenzene	aromatic	ppbV	0.039 J	0.047 J	<0.025	<0.025	0.11	0.154
Styrene	aromatic	ppbV	0.034	0.074	0.023 J	0.023 J	0.115	0.026
Toluene	aromatic	ppbV	0.247	0.337	0.202	0.134	0.708	0.525
1-Methylnaphthalene	naphthalene	ppbV	0.291 J	<0.05	<0.05	<0.05	0.16 J	0.126 J
2-Methylnaphthalene	naphthalene	ppbV	0.491 J	<0.05	0.064 J	0.076 J	0.289 J	0.226 J
Naphthalene	naphthalene	ppbV	0.201 B	0.148 B	0.113 B	0.135 B	0.384	0.328
Tertiary Butanol	alcohol	ppbV	3	5.18	2	2.72	6.99	3.41
Ethyl-Tert-Butyl-Ether	ether	ppbV	0.622	0.632	0.45	0.467	1.37	0.683
Isopropyl Ether	ether	ppbV	<0.01	<0.01	<0.01	<0.01	<0.01	<0.01
Methyl tert butyl ether	ether	ppbV	0.071	0.072	0.045	0.047	0.165	0.084
Tertiary-Amyl Methyl Ether	ether	ppbV	<0.01	<0.01	<0.01	<0.01	0.052	<0.01
2-Ethylthiophene	thiophene	ppbV	<0.01	<0.01	<0.01	<0.01	<0.01	<0.01
2-Methylthiophene	thiophene	ppbV	<0.01	<0.01	<0.01	<0.01	<0.01	<0.01
3-Methylthiophene	thiophene	ppbV	<0.01	<0.01	<0.01	<0.01	<0.01	<0.01
Benzothiophene	thiophene	ppbV	<0.05	<0.05	<0.05	<0.05	<0.05	<0.05
Thiophene	thiophene	ppbV	<0.01	<0.01	<0.01	<0.01	0.019 J	<0.01
1,2-Dibromoethane	other	ppbV	<0.01	<0.01	<0.01	<0.01	<0.01	<0.01
1,2-Dichloroethane	other	ppbV	<0.01	<0.01	<0.01	<0.01	0.12	<0.01
MMT	other	ppbV	<0.05	<0.05	<0.05	<0.05	<0.05	<0.05

ATTACHMENT B.3.4: SOIL VAPOR AND GROUNDWATER MONITORING WELL HEADSPACE SAMPLE ANALYTICAL RESULTS
Red Hill Bulk Fuel Storage Facility, Joint Base Pearl Harbor-Hickam, O'ahu, Hawai'i

			Sample ID:	RHSV13SERH457	RHSV14DERH456	RHSV15SERH455	RHSV16DERH454	RHSV18SERH453	RHSV20DERH465
			Lab Sample ID:	L1740493-13	L1740493-14	L1740493-15	L1740493-16	L1740493-17	L1740493-18
			Sample Date/Time:	2017-10-27 13:29	2017-10-27 12:48	2017-10-27 11:24	2017-10-27 10:46	2017-10-27 10:00	2017-10-30 15:08
			Matrix:	SOIL_VAPOR	SOIL_VAPOR	SOIL_VAPOR	SOIL_VAPOR	SOIL_VAPOR	SOIL_VAPOR
VOCs BY USEPA METHOD TO-15 (TENTATIVELY IDENTIFIED COMPOUNDS)									
1-Butanol	alcohol	ppbV		-	-	-	-	-	-
1-Hexanol, 2-ethyl-	alcohol	ppbV		10.2	-	17.2	-	-	-
Amylene Hydrate	alcohol	ppbV		-	2.49	-	1.69	-	1.87
Methyl Alcohol	alcohol	ppbV		3.23	-	-	2.16	-	-
Unknown	alcohol	ppbV		-	-	-	-	-	-
Unknown	alcohol	ppbV		-	-	-	-	-	-
Unknown	alcohol	ppbV		-	12	-	-	16.5	3.01
Unknown	alcohol	ppbV		-	-	-	-	-	-
unknown alcohol	alcohol	ppbV		-	-	-	-	-	-
unknown alcohol	alcohol	ppbV		-	-	-	-	-	-
Unknown	alcohol cycloalkane	ppbV		-	-	-	-	-	-
Propane	alkane	ppbV		-	2.26	-	-	-	-
Unknown	alkane	ppbV		-	-	-	1.93	5.14	-
Unknown	alkane	ppbV		-	-	-	-	-	-
unknown alkane	alkane	ppbV		-	2.04	-	-	-	-
unknown alkane	alkane	ppbV		2.04	-	-	-	-	-
1-Pentene, 2-methyl-	alkene	ppbV		-	-	-	-	-	-
2,4-Dimethyl-1-heptene	alkene	ppbV		-	-	-	-	-	-
Unknown	alkene	ppbV		-	-	-	-	-	1.39
Unknown	alkene	ppbV		-	-	-	-	-	-
Unknown	alkene	ppbV		-	-	-	-	-	-
Unknown	alkene	ppbV		-	-	-	-	-	-
Unknown	alkene	ppbV		-	-	3.04	-	-	-
Unknown	alkene	ppbV		-	-	-	-	-	-
Unknown	alkene	ppbV		-	-	-	-	8.16	-
Unknown	alkene	ppbV		-	-	3.56	-	-	-
Unknown	alkene	ppbV		8.02	-	12.7	-	-	-
Unknown	alkene	ppbV		-	-	-	-	12.3	-
Unknown	alkene	ppbV		-	-	-	-	-	-
Unknown	alkene	ppbV		-	-	-	-	-	-
Unknown	alkene	ppbV		-	-	-	-	-	-
Unknown	alkene	ppbV		-	-	-	-	-	-
Unknown	alkene	ppbV		-	-	-	-	-	-
Unknown	alkene	ppbV		-	-	-	-	-	-
unknown alkane	alkene	ppbV		-	-	-	-	-	-
unknown alkene	alkene	ppbV		-	-	-	-	-	-
unknown alkene	alkene	ppbV		-	6.15	-	5.99	-	3.7
Unknown	aromatic	ppbV		1.64	-	-	-	-	-
Unknown	aromatic	ppbV		-	-	-	-	-	-
Hexane, 2,3-dimethyl-	branched alkane	ppbV		-	-	-	-	-	-
Unknown	branched alkane	ppbV		-	-	-	-	7.35	-
Unknown	branched alkane	ppbV		-	-	-	-	-	1.54
Unknown	branched alkane	ppbV		-	-	-	-	-	-
Unknown	branched alkane	ppbV		-	-	-	2.09	-	1.76
unknown alkane	branched alkane	ppbV		4.69	-	6.68	-	-	-
unknown alkane	branched alkane	ppbV		-	-	-	-	14.7	-
unknown alkane	branched alkane	ppbV		-	7.45	-	7.01	-	4.83
Cyclohexane, 1,1,3-trimethyl-	cycloalkane	ppbV		-	-	-	-	-	-
Unknown	cycloalkane	ppbV		-	-	-	-	-	-
Unknown	cycloalkane	ppbV		-	-	-	-	-	-
Unknown	cycloalkane	ppbV		-	-	-	-	-	-
Unknown	cycloalkane	ppbV		-	-	-	-	-	-
Unknown	cycloalkane	ppbV		-	-	-	-	-	1.91
Unknown	cycloalkane	ppbV		-	-	-	-	-	-
Unknown	cycloalkane	ppbV		-	-	-	-	-	-
Unknown	cycloalkane	ppbV		-	-	-	-	-	-
Unknown	cycloalkane	ppbV		-	-	-	-	-	-
Unknown	cycloalkane	ppbV		-	-	-	-	-	-
Unknown	cycloalkane	ppbV		-	-	-	-	-	-
unknown alkane	cycloalkane	ppbV		-	-	-	-	-	-
unknown cycloalkane	cycloalkane	ppbV		-	-	-	-	-	-
unknown cycloalkane	cycloalkane	ppbV		-	-	-	-	-	-
unknown cycloalkane	cycloalkane	ppbV		-	-	-	-	-	-
unknown cycloalkane	cycloalkane	ppbV		-	-	-	-	-	-
Furan, tetrahydro-	furan	ppbV		-	-	-	-	-	-
2-Butanone	ketone	ppbV		-	-	-	-	-	-
Acetone	ketone	ppbV		2.42	-	-	-	-	-
Cyclohexanone	ketone	ppbV		-	-	-	-	-	-
Cyclopentanone	ketone	ppbV		6.47	-	16.4	-	-	-
Unknown	ketone	ppbV		-	-	4.14	-	-	-
Unknown	ketone	ppbV		-	-	-	-	-	-
Unknown	ketone	ppbV		-	-	-	-	-	-
Unknown	ketone	ppbV		-	-	-	-	-	-
Unknown	ketone cycloalkane	ppbV		-	-	-	-	-	-
Unknown	ketone cycloalkane	ppbV		-	-	-	-	-	-
Unknown	ketone cycloalkane	ppbV		-	-	-	-	-	-
Unknown	naphthalene	ppbV		-	-	-	-	-	-
Unknown	other	ppbV		-	-	-	2.58	8	-
Unknown	other	ppbV		-	-	-	11	9.96	5.73
Unknown	other	ppbV		-	-	-	-	-	-
Unknown	other	ppbV		-	-	-	-	-	-
Unknown	other	ppbV		-	1.69	-	-	-	-
Unknown	other	ppbV		-	-	-	-	7.15	-
Unknown	other	ppbV		-	-	-	-	-	-
Unknown	other	ppbV		-	10.9	-	19	8.49	-
Unknown	other	ppbV		-	6.9	-	1.41	-	1.55
Unknown	other	ppbV		-	2.37	-	1.43	5.21	1.52
Unknown	other	ppbV		-	-	-	-	-	-
Unknown	other	ppbV		-	-	-	-	-	-
Unknown	other	ppbV		-	2.61	-	-	-	-
Cyclotrisiloxane, Hexamethyl-	siloxane	ppbV		5.29	-	8.91	-	-	-
Silanol, Trimethyl-	siloxane	ppbV		-	-	1.55	-	-	-
Unknown	siloxane	ppbV		-	-	-	-	-	-
unknown siloxane	siloxane	ppbV		-	-	-	-	-	-
unknown siloxane	siloxane	ppbV		-	-	2.03	-	-	-
unknown siloxane	siloxane	ppbV		1.91	-	-	-	-	-
unknown siloxane	siloxane	ppbV		-	-	-	-	-	-
unknown siloxane	siloxane	ppbV		-	-	-	-	-	-
unknown siloxane	siloxane	ppbV		-	-	-	-	-	-

1. Samples collected by GSI and analyzed by Alpha Analytical.
2. Less than ("<") indicates the analyte was not found at the stated detection limit. J = estimated result between method detection limit and reporting limit.
   D = result from a dilution.

GSI ENVIRONMENTAL

ATTACHMENT B.3.4: SOIL VAPOR AND GROUNDWATER MONITORING WELL HEADSPACE SAMPLE ANALYTICAL RESULTS
Red Hill Bulk Fuel Storage Facility, Joint Base Pearl Harbor-Hickam, O'ahu, Hawai'i

		Sample ID:	RHMW01ERH459	RHMW02ERH450	RHMW03ERH451	RHMW04ERH452
		Lab Sample ID:	L1740493-19	L1740493-20	L1740493-21	L1740493-22
		Sample Date/Time:	2017-10-30 9:12	2017-10-26 10:03	2017-10-26 11:38	2017-10-26 15:03
		Matrix:	HEADSPACE	HEADSPACE	HEADSPACE	HEADSPACE
FIXED GASES BY USEPA METHOD 3C						
Analyte		**Units**				
Carbon Dioxide		%	0.908	9.13	2.08	0.094 J
Methane		%	<0.051	<0.057	<0.058	<0.058
Oxygen		%	19.9	7.8	18.7	21.8
VOCs BY USEPA METHOD TO-15 (TARGET ANALYTES)						
Analyte	**Class**	**Units**				
Decane (C10)	alkane	ppbV	<0.25	0.157	3.67	0.628
Dodecane (C12)	alkane	ppbV	<0.5	0.279	1.82	0.755
Heptane	alkane	ppbV	0.51D	0.066	0.851	0.039
n-Hexane	alkane	ppbV	1.65D	0.132	0.499	0.037
Nonane (C9)	alkane	ppbV	0.18 JD	0.083	3.53	0.089
Octane	alkane	ppbV	0.31D	0.081	2.26	0.07
Pentane	alkane	ppbV	8.69D	8.76	0.869	0.211
Tridecane	alkane	ppbV	<0.5	0.215 J	0.501 J	0.361 J
Undecane	alkane	ppbV	<0.25	0.247	2.88	0.297
1,3-Butadiene	alkene	ppbV	<0.1	<0.01	<0.01	<0.01
1-Decene	alkene	ppbV	<0.25	<0.025	<0.025	<0.025
1-Heptene	alkene	ppbV	<0.1	<0.01	<0.01	<0.01
1-Hexene	alkene	ppbV	3.28D	<0.01	<0.01	<0.01
1-Nonene	alkene	ppbV	<0.1	<0.01	<0.01	<0.01
1-Octene	alkene	ppbV	<0.1	<0.01	<0.01	<0.01
1-Pentene	alkene	ppbV	6.83D	0.151	0.031	0.019 J
2-Methyl-1-Butene	alkene	ppbV	0.57D	0.07	0.037	<0.01
cis-2-Pentene	alkene	ppbV	<0.1	<0.01	<0.01	<0.01
trans-2-Pentene	alkene	ppbV	0.19 JD	0.111	0.035	<0.01
2,2-Dimethylpentane	branched alkane	ppbV	<0.1	<0.01	<0.01	<0.01
2,3,3-Trimethylpentane	branched alkane	ppbV	<0.1	0.07	0.084	0.018 J
2,3,4-Trimethylpentane	branched alkane	ppbV	<0.1	0.017 J	0.111	<0.01
2,3-Dimethylbutane	branched alkane	ppbV	0.27D	<0.01	0.138	<0.01
2,3-Dimethylhexane	branched alkane	ppbV	<0.1	<0.01	<0.01	<0.01
2,3-Dimethylpentane	branched alkane	ppbV	<0.1	<0.01	0.205	<0.01
2,4-Dimethylhexane/2,2,3-Trimethylpentar	branched alkane	ppbV	<0.25	0.036 JB	0.112	<0.025
2,4-Dimethylpentane	branched alkane	ppbV	<0.1	<0.01	0.104	<0.01
2,5-Dimethylhexane	branched alkane	ppbV	<0.1	0.016 J	0.092	<0.01
2-Methylheptane	branched alkane	ppbV	<0.1	<0.01	0.829	<0.01
2-Methylhexane	branched alkane	ppbV	0.33D	0.044	0.236	0.014 J
2-Methylpentane	branched alkane	ppbV	1.19D	0.754	0.439	0.081 B
3-Ethylhexane	branched alkane	ppbV	<0.1	<0.01	0.099	<0.01
3-Methylheptane	branched alkane	ppbV	<0.1	0.025	0.52	0.013 J
3-Methylhexane	branched alkane	ppbV	0.52D	0.144	0.515	<0.01
3-Methylpentane	branched alkane	ppbV	0.61D	0.069	0.267	0.022 J
Isooctane	branched alkane	ppbV	0.24 JD	0.059	0.189	0.018 J
Isopentane	branched alkane	ppbV	<0.1	<0.01	1.14	<0.01
1-Ethyl-1-Methylcyclopentane	cycloalkane	ppbV	<0.1	<0.01	0.055	<0.01
Cyclohexane	cycloalkane	ppbV	16.4D	0.175	0.464	0.059
Cyclopentane	cycloalkane	ppbV	0.43D	<0.01	0.176	0.295
Methylcyclohexane	cycloalkane	ppbV	0.93D	0.08	1.88	0.025
Methylcyclopentane	cycloalkane	ppbV	0.52D	0.058	0.533	<0.01
1,2,4,5-Tetramethylbenzene	aromatic	ppbV	<0.25	<0.025	0.036 J	<0.025
1,2,4-Trimethylbenzene	aromatic	ppbV	0.31 JD	0.133	2.04	0.133
1,2-Diethylbenzene	aromatic	ppbV	<0.25	<0.025	0.085	<0.025
1,2-Dimethyl-3-Ethylbenzene	aromatic	ppbV	<0.25	<0.025	0.157	<0.025
1,2-Dimethyl-4-Ethylbenzene	aromatic	ppbV	<0.25	<0.025	0.27	<0.025
1,3,5-Trimethylbenzene	aromatic	ppbV	0.11 JD	0.03	0.605	0.032
1,3-Dimethyl-2-Ethylbenzene	aromatic	ppbV	<0.25	<0.025	0.061	<0.025
1,3-Dimethyl-4-Ethylbenzene	aromatic	ppbV	<0.25	<0.025	0.303	<0.025
1,3-Dimethyl-5-Ethylbenzene	aromatic	ppbV	<0.25	<0.025	0.274	<0.025
1,4-Dimethyl-2-Ethylbenzene	aromatic	ppbV	<0.25	<0.025	0.236	<0.025
1-Methyl-2-Ethylbenzene	aromatic	ppbV	<0.25	0.026 J	0.679	0.029 J
1-Methyl-2-Isopropylbenzene	aromatic	ppbV	0.73D	<0.025	0.032 J	<0.025
1-Methyl-2-N-Propylbenzene	aromatic	ppbV	<0.25	<0.025	0.316	<0.025
1-Methyl-3-Ethylbenzene	aromatic	ppbV	<0.25	0.047 J	1.08	0.055
1-Methyl-3-Isopropylbenzene	aromatic	ppbV	<0.25	<0.025	0.259	<0.025
1-Methyl-3-N-Propylbenzene	aromatic	ppbV	<0.25	<0.025	0.39	<0.025
1-Methyl-4-Ethylbenzene	aromatic	ppbV	<0.1	0.023 J	0.532	0.026
1-Methyl-4-Isopropylbenzene	aromatic	ppbV	<0.25	0.051	0.234	0.031 J
1-Methyl-4-N-Propylbenzene	aromatic	ppbV	<0.25	<0.025	0.179	<0.025
Benzene	aromatic	ppbV	0.44D	0.071	0.229	0.043
Ethylbenzene	aromatic	ppbV	0.24 JD	0.061	0.969	0.048
Indane	aromatic	ppbV	<0.25	<0.025	0.185	<0.025
Indene	aromatic	ppbV	<0.25	<0.025	<0.025	<0.025
Isopropylbenzene	aromatic	ppbV	0.1 JD	<0.01	0.289	<0.01
n-Butylbenzene	aromatic	ppbV	<0.25	<0.025	0.166	<0.025
N-Pentylbenzene	aromatic	ppbV	<0.25	<0.025	0.051	<0.025
n-Propylbenzene	aromatic	ppbV	<0.1	<0.01	0.495	0.019 J
o-Xylene	aromatic	ppbV	0.63D	0.612	1.76	0.167
p/m-Xylene	aromatic	ppbV	0.89D	0.24	3.53	0.174
sec-Butylbenzene	aromatic	ppbV	<0.25	<0.025	0.213	<0.025
Styrene	aromatic	ppbV	<0.1	0.063	0.125	0.074
Toluene	aromatic	ppbV	2.94D	0.266	1.68	0.208
1-Methylnaphthalene	naphthalene	ppbV	<0.5	<0.05	0.061 J	<0.05
2-Methylnaphthalene	naphthalene	ppbV	<0.5	<0.05	0.121 J	<0.05
Naphthalene	naphthalene	ppbV	<0.25	0.066 B	0.266	0.061 B
Tertiary Butanol	alcohol	ppbV	3.88D	11.3	1.65	1.28
Ethyl-Tert-Butyl-Ether	ether	ppbV	0.56D	2.48	0.361	0.173
Isopropyl Ether	ether	ppbV	<0.1	<0.01	<0.01	<0.01
Methyl tert butyl ether	ether	ppbV	<0.1	0.352	0.038	<0.01
Tertiary-Amyl Methyl Ether	ether	ppbV	<0.1	0.06	<0.01	<0.01
2-Ethylthiophene	thiophene	ppbV	<0.1	<0.01	<0.01	<0.01
2-Methylthiophene	thiophene	ppbV	<0.1	<0.01	<0.01	<0.01
3-Methylthiophene	thiophene	ppbV	<0.1	<0.01	<0.01	<0.01
Benzothiophene	thiophene	ppbV	<0.5	<0.05	<0.05	<0.05
Thiophene	thiophene	ppbV	<0.1	<0.01	<0.01	<0.01
1,2-Dibromoethane	other	ppbV	<0.1	<0.01	<0.01	<0.01
1,2-Dichloroethane	other	ppbV	<0.1	<0.01	<0.01	<0.01
MMT	other	ppbV	<0.5	<0.05	<0.05	<0.05

ATTACHMENT B.3.4: SOIL VAPOR AND GROUNDWATER MONITORING WELL HEADSPACE SAMPLE ANALYTICAL RESULTS
Red Hill Bulk Fuel Storage Facility, Joint Base Pearl Harbor-Hickam, O'ahu, Hawai'i

			Sample ID:	RHMW01ERH459	RHMW02ERH450	RHMW03ERH451	RHMW04ERH452
			Lab Sample ID:	L1740493-19	L1740493-20	L1740493-21	L1740493-22
			Sample Date/Time:	2017-10-30 9:12	2017-10-26 10:03	2017-10-26 11:38	2017-10-26 15:03
			Matrix:	HEADSPACE	HEADSPACE	HEADSPACE	HEADSPACE
VOCs BY USEPA METHOD TO-15 (TENTATIVELY IDENTIFIED COMPOUNDS)							
1-Butanol	alcohol	ppbV		-	-	-	-
1-Hexanol, 2-ethyl-	alcohol	ppbV		-	-	-	-
Amylene Hydrate	alcohol	ppbV		-	3.75	-	-
Methyl Alcohol	alcohol	ppbV		-	4.2	2.21	3.69
Unknown	alcohol	ppbV		-	-	-	-
Unknown	alcohol	ppbV		-	-	-	-
Unknown	alcohol	ppbV		-	-	-	-
Unknown	alcohol	ppbV		-	-	-	-
unknown alcohol	alcohol	ppbV		-	-	-	-
unknown alcohol	alcohol	ppbV		-	6.39	-	-
Unknown	alcohol cycloalkane	ppbV		-	-	-	-
Propane	alkane	ppbV		-	-	-	-
Unknown	alkane	ppbV		-	-	-	-
Unknown	alkane	ppbV		-	2.41	-	-
unknown alkane	alkane	ppbV		-	-	2.03	-
unknown alkane	alkane	ppbV		-	-	-	-
1-Pentene, 2-methyl-	alkene	ppbV		-	-	-	-
2,4-Dimethyl-1-heptene	alkene	ppbV		-	-	-	-
Unknown	alkene	ppbV		-	-	-	-
Unknown	alkene	ppbV		-	-	-	-
Unknown	alkene	ppbV		-	-	-	-
Unknown	alkene	ppbV		-	-	-	-
Unknown	alkene	ppbV		-	-	-	-
Unknown	alkene	ppbV		-	-	-	-
Unknown	alkene	ppbV		-	-	-	-
Unknown	alkene	ppbV		-	-	-	-
Unknown	alkene	ppbV		-	5.91	-	-
Unknown	alkene	ppbV		-	-	4.28	-
Unknown	alkene	ppbV		-	-	-	-
Unknown	alkene	ppbV		-	-	-	-
Unknown	alkene	ppbV		-	-	-	-
Unknown	alkene	ppbV		-	-	-	-
Unknown	alkene	ppbV		-	-	-	-
unknown alkane	alkene	ppbV		-	-	-	-
unknown alkene	alkene	ppbV		-	-	-	-
unknown alkene	alkene	ppbV		-	-	-	-
Unknown	aromatic	ppbV		-	-	-	-
Unknown	aromatic	ppbV		-	-	-	-
Hexane, 2,3-dimethyl-	branched alkane	ppbV		-	-	-	-
Unknown	branched alkane	ppbV		-	-	-	-
Unknown	branched alkane	ppbV		-	-	-	-
Unknown	branched alkane	ppbV		-	-	-	-
Unknown	branched alkane	ppbV		-	-	-	-
unknown alkane	branched alkane	ppbV		-	-	5.11	-
unknown alkane	branched alkane	ppbV		-	8.25	-	2.37
unknown alkane	branched alkane	ppbV		-	-	-	-
Cyclohexane, 1,1,3-trimethyl-	cycloalkane	ppbV		-	-	-	-
Unknown	cycloalkane	ppbV		-	-	-	-
Unknown	cycloalkane	ppbV		-	-	-	-
Unknown	cycloalkane	ppbV		-	-	-	-
Unknown	cycloalkane	ppbV		-	-	-	-
Unknown	cycloalkane	ppbV		-	7.71	1.94	-
Unknown	cycloalkane	ppbV		-	-	-	-
Unknown	cycloalkane	ppbV		-	-	-	-
Unknown	cycloalkane	ppbV		-	-	-	-
Unknown	cycloalkane	ppbV		-	-	-	-
Unknown	cycloalkane	ppbV		-	-	-	-
Unknown	cycloalkane	ppbV		-	-	-	-
unknown alkane	cycloalkane	ppbV		-	-	-	-
unknown cycloalkane	cycloalkane	ppbV		-	-	-	-
unknown cycloalkane	cycloalkane	ppbV		-	-	-	-
unknown cycloalkane	cycloalkane	ppbV		-	-	-	-
unknown cycloalkane	cycloalkane	ppbV		-	-	-	-
Furan, tetrahydro-	furan	ppbV		-	-	-	-
2-Butanone	ketone	ppbV		-	-	-	-
Acetone	ketone	ppbV		-	-	-	-
Cyclohexanone	ketone	ppbV		-	-	-	2.98
Cyclopentanone	ketone	ppbV		-	-	-	-
Unknown	ketone	ppbV		-	-	-	-
Unknown	ketone	ppbV		-	-	-	3.87
Unknown	ketone	ppbV		-	-	-	-
Unknown	ketone	ppbV		-	-	-	-
Unknown	ketone cycloalkane	ppbV		-	-	-	-
Unknown	ketone cycloalkane	ppbV		-	-	-	-
Unknown	ketone cycloalkane	ppbV		-	-	-	-
Unknown	naphthalene	ppbV		-	-	-	-
Unknown	other	ppbV		-	-	-	-
Unknown	other	ppbV		-	-	2.23	-
Unknown	other	ppbV		-	-	-	-
Unknown	other	ppbV		-	-	-	-
Unknown	other	ppbV		-	-	-	-
Unknown	other	ppbV		-	-	2.1	-
Unknown	other	ppbV		-	3.72	-	-
Unknown	other	ppbV		-	94.1	94.6	212
Unknown	other	ppbV		8220	13	39.8	20.6
Unknown	other	ppbV		-	2.29	2.29	-
Unknown	other	ppbV		-	-	2.31	-
Unknown	other	ppbV		-	-	-	3.3
Unknown	other	ppbV		-	-	-	-
Cyclotrisiloxane, Hexamethyl-	siloxane	ppbV		-	-	-	-
Silanol, Trimethyl-	siloxane	ppbV		-	-	-	-
Unknown	siloxane	ppbV		-	-	-	-
unknown siloxane	siloxane	ppbV		-	-	-	-
unknown siloxane	siloxane	ppbV		-	-	-	-
unknown siloxane	siloxane	ppbV		-	-	-	-
unknown siloxane	siloxane	ppbV		-	-	-	-
unknown siloxane	siloxane	ppbV		-	-	-	-
unknown siloxane	siloxane	ppbV		-	-	-	-

1. Samples collected by GSI and analyzed by Alpha Analytical.
2. Less than ("<") indicates the analyte was not found at the stated detection limit. J = estimated result between method detection limit and reporting limit. D = result from a dilution.

Attachment B.3.5:
LNAPL Indications from Drilling Fluids and Boring Logs for Borings Completed Below Fuel Storage Tanks (Most Borings Completed 1998–2001)

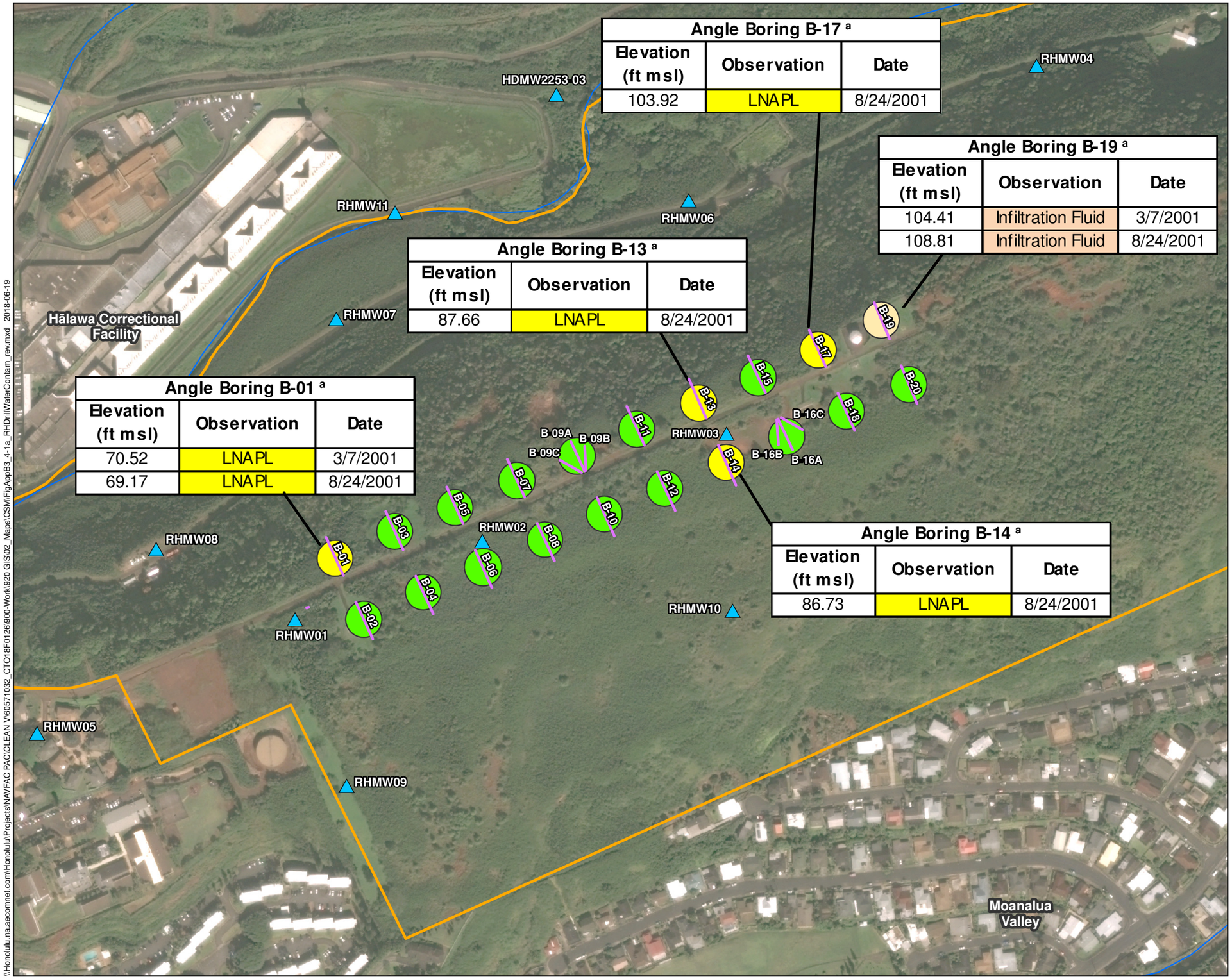

Key Map

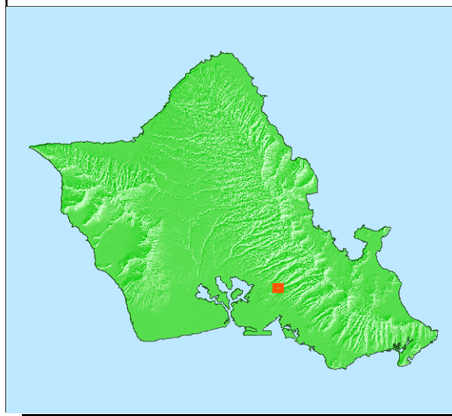

Legend

- Red Hill Fuel Storage Tank - LNAPL contamination noted
- Red Hill Fuel Storage Tank - Infiltration fluid noted
- Red Hill Fuel Storage Tank - No evidence of contamination noted
- Groundwater Monitoring Well- No evidence of contamination observed in boring log
- Angle Boring
- Stream
- Red Hill Facility Boundary
- Groundwater Model Area

Notes

1. Map projection: NAD 1983 UTM Zone 4N
2. DigitalGlobe, Inc. (DG) and NRCS. Publication_Date: 2015
3. Reference:
   a. Red Hill Bulk Fuel Storage Facility Investigation Report (Final) for Fleet Industrial Supply Center (FISC), Oahu, Hawaii. 2002. Prepared by AMEC Earth and Environmental, Inc. for NAVFAC Pacific. August.

N

0 200 400 800 Feet

Figure 4-1a
LNAPL Indications in Drilling Fluids While Drilling Angle Borings, 1998–2002
Red Hill Bulk Fuel Storage Facility
JBPHH, O'ahu, Hawai'i

\\Honolulu.na.aecomnet.com\Honolulu\Projects\NAVFAC PAC\CLEAN V\60571032_CTO18F0126\900-Work\920 GIS\02_Maps\CSM\FigAppB3_4-1a_RHDrillWaterContam_rev.mxd 2018-06-19

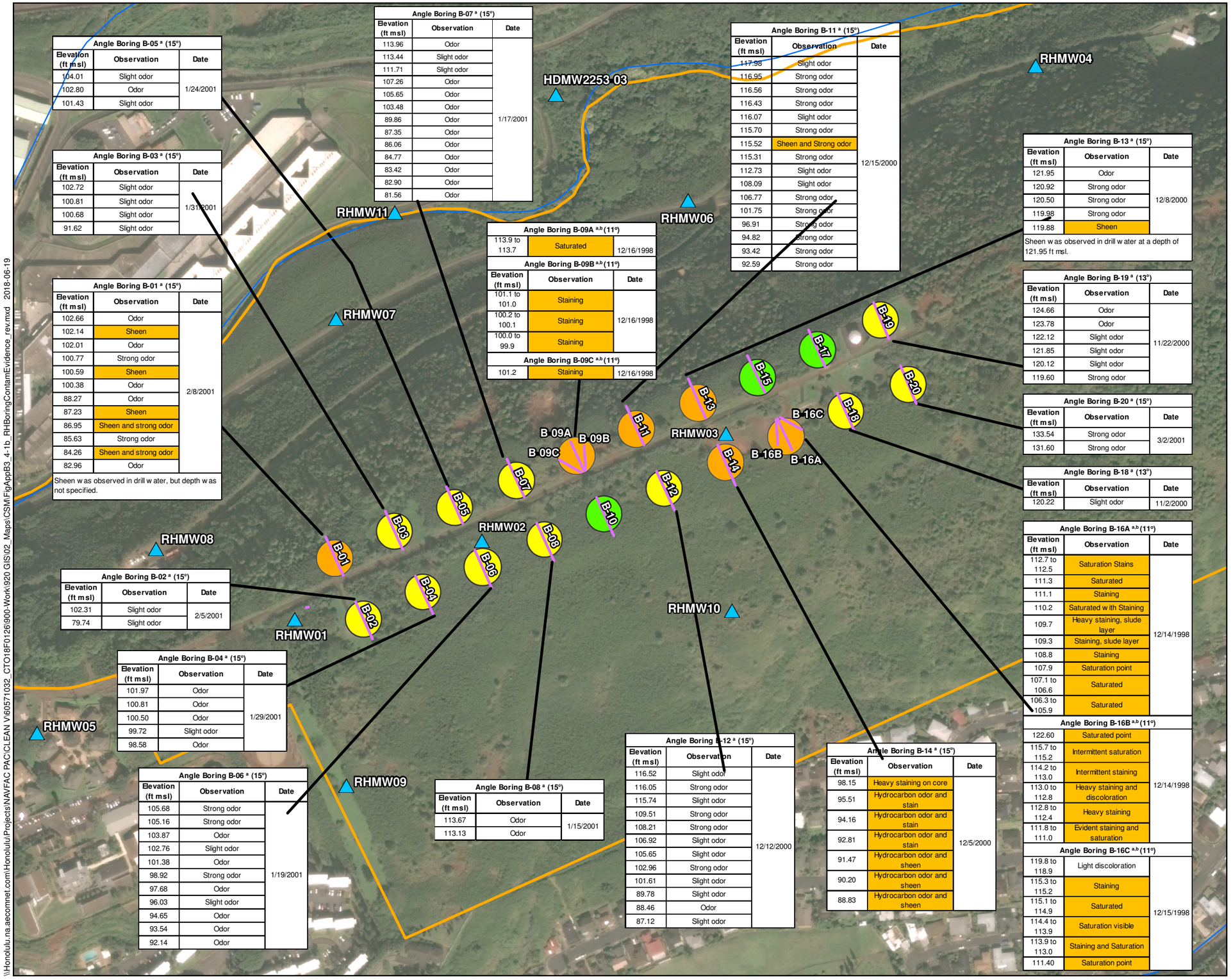

Angle Boring B-05 [a] (15°)

Elevation (ft msl)	Observation	Date
104.01	Slight odor	1/24/2001
102.80	Odor	
101.43	Slight odor	

Angle Boring B-03 [a] (15°)

Elevation (ft msl)	Observation	Date
102.72	Slight odor	1/31/2001
100.81	Slight odor	
100.68	Slight odor	
91.62	Slight odor	

Angle Boring B-01 [a] (15°)

Elevation (ft msl)	Observation	Date
102.66	Odor	2/8/2001
102.14	Sheen	
102.01	Odor	
100.77	Strong odor	
100.59	Sheen	
100.38	Odor	
88.27	Odor	
87.23	Sheen	
86.95	Sheen and strong odor	
85.63	Strong odor	
84.26	Sheen and strong odor	
82.96	Odor	

Sheen was observed in drill water, but depth was not specified.

Angle Boring B-07 [a] (15°)

Elevation (ft msl)	Observation	Date
113.96	Odor	1/17/2001
113.44	Slight odor	
111.71	Slight odor	
107.26	Odor	
105.65	Odor	
103.48	Odor	
89.86	Odor	
87.35	Odor	
86.06	Odor	
84.77	Odor	
83.42	Odor	
82.90	Odor	
81.56	Odor	

Angle Boring B-11 [a] (15°)

Elevation (ft msl)	Observation	Date
117.98	Slight odor	12/15/2000
116.95	Strong odor	
116.56	Strong odor	
116.43	Strong odor	
116.07	Slight odor	
115.70	Strong odor	
115.52	Sheen and Strong odor	
115.31	Strong odor	
112.73	Slight odor	
108.09	Slight odor	
106.77	Strong odor	
101.75	Strong odor	
96.91	Strong odor	
94.82	Strong odor	
93.42	Strong odor	
92.59	Strong odor	

Angle Boring B-09A [a,b] (11°)

Elevation (ft msl)	Observation	Date
113.9 to 113.7	Saturated	12/16/1998

Angle Boring B-09B [a,b] (11°)

Elevation (ft msl)	Observation	Date
101.1 to 101.0	Staining	12/16/1998
100.2 to 100.1	Staining	
100.0 to 99.9	Staining	

Angle Boring B-09C [a,b] (11°)

Elevation (ft msl)	Observation	Date
101.2	Staining	12/16/1998

Angle Boring B-13 [a] (15°)

Elevation (ft msl)	Observation	Date
121.95	Odor	12/8/2000
120.92	Strong odor	
120.50	Strong odor	
119.98	Strong odor	
119.88	Sheen	

Sheen was observed in drill water at a depth of 121.95 ft msl.

Angle Boring B-19 [a] (13°)

Elevation (ft msl)	Observation	Date
124.66	Odor	11/22/2000
123.78	Odor	
122.12	Slight odor	
121.85	Slight odor	
120.12	Slight odor	
119.60	Strong odor	

Angle Boring B-20 [a] (15°)

Elevation (ft msl)	Observation	Date
133.54	Strong odor	3/2/2001
131.60	Strong odor	

Angle Boring B-18 [a] (13°)

Elevation (ft msl)	Observation	Date
120.22	Slight odor	11/2/2000

Angle Boring B-16A [a,b] (11°)

Elevation (ft msl)	Observation	Date
112.7 to 112.5	Saturation Stains	12/14/1998
111.3	Saturated	
111.1	Staining	
110.2	Saturated with Staining	
109.7	Heavy staining, slude layer	
109.3	Staining, slude layer	
108.8	Staining	
107.9	Saturation point	
107.1 to 106.6	Saturated	
106.3 to 105.9	Saturated	

Angle Boring B-16B [a,b] (11°)

Elevation (ft msl)	Observation	Date
122.60	Saturated point	12/14/1998
115.7 to 115.2	Intermittent saturation	
114.2 to 113.0	Intermittent staining	
113.0 to 112.8	Heavy staining and discoloration	
112.8 to 112.4	Heavy staining	
111.8 to 111.0	Evident staining and saturation	

Angle Boring B-16C [a,b] (11°)

Elevation (ft msl)	Observation	Date
119.8 to 118.9	Light discoloration	12/15/1998
115.3 to 115.2	Staining	
115.1 to 114.9	Saturated	
114.4 to 113.9	Saturation visible	
113.9 to 113.0	Staining and Saturation	
111.40	Saturation point	

Angle Boring B-02 [a] (15°)

Elevation (ft msl)	Observation	Date
102.31	Slight odor	2/5/2001
79.74	Slight odor	

Angle Boring B-04 [a] (15°)

Elevation (ft msl)	Observation	Date
101.97	Odor	1/29/2001
100.81	Odor	
100.50	Odor	
99.72	Slight odor	
98.58	Odor	

Angle Boring B-06 [a] (15°)

Elevation (ft msl)	Observation	Date
105.68	Strong odor	1/19/2001
105.16	Strong odor	
103.87	Odor	
102.76	Slight odor	
101.38	Odor	
98.92	Strong odor	
97.68	Odor	
96.03	Slight odor	
94.65	Odor	
93.54	Odor	
92.14	Odor	

Angle Boring B-08 [a] (15°)

Elevation (ft msl)	Observation	Date
113.67	Odor	1/15/2001
113.13	Odor	

Angle Boring B-12 [a] (15°)

Elevation (ft msl)	Observation	Date
116.52	Slight odor	12/12/2000
116.05	Strong odor	
115.74	Slight odor	
109.51	Strong odor	
108.21	Strong odor	
106.92	Slight odor	
105.65	Slight odor	
102.96	Strong odor	
101.61	Slight odor	
89.78	Slight odor	
88.46	Odor	
87.12	Slight odor	

Angle Boring B-14 [a] (15°)

Elevation (ft msl)	Observation	Date
98.15	Heavy staining on core	12/5/2000
95.51	Hydrocarbon odor and stain	
94.16	Hydrocarbon odor and stain	
92.81	Hydrocarbon odor and stain	
91.47	Hydrocarbon odor and sheen	
90.20	Hydrocarbon odor and sheen	
88.83	Hydrocarbon odor and sheen	

Key Map

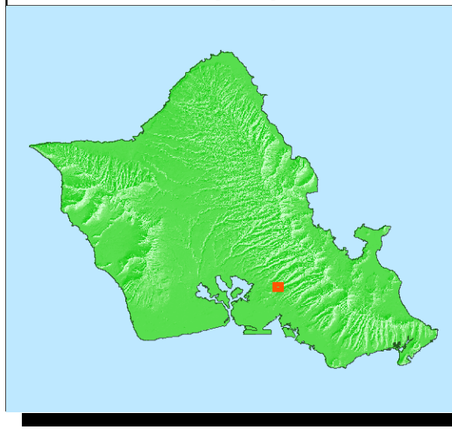

Legend

- Red Hill Fuel Storage Tank- Fuel Odor Noted in Boring Log
- Red Hill Fuel Storage Tank- Sheen or Staining Observed in Boring Log
- Red Hill Fuel Storage Tank- No Evidence of Contamination Observed in Boring Log
- Groundwater Monitoring Well- No evidence of contamination observed in boring log
- Angle Boring
- Stream
- Red Hill Facility Boundary
- Groundwater Model

Notes

1. Map projection: NAD 1983 UTM Zone 4N
2. DigitalGlobe, Inc. (DG) and NRCS. Publication_Date: 2015
3. References:
   a. Boring logs from DON 2002. Red Hill Bulk Fuel Storage Facility Investigation Report (Final) for Fleet Industrial Supply Center (FISC), Oahu, Hawaii. Prepared by AMEC Earth and Environmental, Inc. for NAVFAC Pacific. August.
   b. Boring logs from DON 1999. Initial Phase II Site Characterization Report, Fleet Industrial Supply Center Bulk Fuel Storage Facility at Red Hill. Prepared by Ogden Environmental and Energy Services Co., Inc. for NAVFAC Pacific. March.

* Elevations presented as "~100" are approximations made based on boring logs and notes in the text.

N

0 200 400 800 Feet

Figure 4-1b
LNAPL Indications from Boring Logs While Drilling Angle Borings, 1998–2002
Red Hill Bulk Fuel Storage Facility
JBPHH, O'ahu, Hawai'i

\\Honolulu.na.aecomnet.com\Honolulu\Projects\NAVFAC PAC\CLEAN V\60571032_CTO18F0126\900-Work\920 GIS\02_Maps\CSM\FigAppB3_4-1b_RHBoringContamEvidence_rev.mxd 2018-06-19

Attachment B.3.6:
Laboratory Report and EDD for Soil Vapor Samples Analyzed by Alpha Analytical: Laboratory Job Number L1740493 (Available electronically by request from GSI Environmental, email Tom McHugh at temchugh@gsi-net.com)

Appendix B.4:
MNA Primary Lines of Evidence and Rate Calculations

CONTENTS

Acronyms and Abbreviations iii

1. Introduction 1-1

1.1 Technical Background 1-1
1.2 Study Objectives 1-1

2. Methods 2-1

2.1 Data Handling and Consolidation 2-1
2.2 Plume Duration: Point Attenuation (C vs. t) Rate Coefficient 2-2
2.3 Plume Attenuation: Bulk Attenuation (C vs. d) Rate Coefficient 2-3
2.4 Plume Attenuation: Biodegradation Rate Coefficient (**λ**) 2-4
2.5 Plume Attenuation: RHMW02 to Red Hill Shaft 2-5

3. Results 3-1

3.1 Plume Duration: Point Attenuation (C vs. t) Rate Coefficients 3-1
3.2 Plume Attenuation: Bulk Attenuation (C vs. d) Rate Coefficients 3-3
3.3 Plume Attenuation: Biodegradation Rate Coefficients 3-4
3.4 Plume Attenuation: RHMW02 to RHMW01 Attenuation Rate Coefficients for TPH-d with Silica Gel Cleanup 3-5
3.5 Plume Attenuation: RHMW02 to Red Hill Shaft 3-6

4. Conclusions 4-1

5. References 5-1

FIGURES

1-1 Location of RHMW01 and RHMW02 in Relation to Tank Farm 1-2

2-1 Concentration vs. Time Attenuation Rate Coefficient and Half-Life 2-2

2-2 Concentration vs. Distance Attenuation Rate Coefficient (k) and Half-Life 2-3

3-1 Linear and Natural Log Scale Plots of 1-Methylnaphthalene Concentrations from September 2005 to April 2018 at Monitoring Well RHMW02 3-2

3-2 Linear and Natural Log Scale Plots of 2-Methylnaphthalene Concentrations from September 2005 to April 2018 at Monitoring Well RHMW02 3-2

3-3 Linear and Natural Log Scale Plots of Naphthalene Concentrations from September 2005 to April 2018 at Monitoring Well RHMW02 3-3

TABLES

2-1 Appropriate Uses for Point (C vs. t), Bulk (C vs. d), and Biodegradation Attenuation Rate Coefficients 2-1

2-2 Number of COPC Data Pairs Used to Calculate C vs. d Rate Coefficients 2-4

3-1 C vs. t Coefficients, Half-Lives, and First-Order Model Fit Parameters for the COPCs at RHMW02 (September 2005 to April 2018) 3-1

3-2 C vs. d Rate Coefficients and Half-Lives for the COPCs Along RHMW02–RHMW01 Transect (Includes Detected COPCs at Both Wells Only) 3-3

3-3 C vs. d Rate Coefficients and Half-Lives for the COPCs Along RHMW02–RHMW01 Transect (Includes Detected COPCs at One or More Wells Only) 3-4

3-4 Biodegradation Rate Coefficients and Half-Lives for the COPCs Along RHMW02–RHMW01 Transect (Includes Detected COPCs At Both Wells Only) 3-4

3-5 Biodegradation Rate Coefficients and Half-Lives for the COPCs Along RHMW02-RHMW01 Transect (Includes Detected COPCs At One or More Wells Only) 3-5

3-6 C vs. d Rate Coefficients and Half-Lives for TPH-d, TPH-d (with silica gel cleanup) and TOC Along RHMW02-RHMW01 Transect 3-5

3-7 Biodegradation Rate Coefficients and Half-Lives for TPH-d, TPH-d (with silica gel cleanup) and TOC Along RHMW02-RHMW01 Transect 3-6

3-8 RHMW02 to Red Hill Shaft Attenuation Rate Coefficients Using All Naphthalene Detects at Red Hill Shaft (2005 to 2018) 3-7

ACRONYMS AND ABBREVIATIONS

α_x	longitudinal dispersivity
λ	biodegradation rate coefficient
µg/L	micrograms per liter
1-MNAPH	1-methylnaphthalene
2-MNAPH	2-methlynaphthalene
b	thickness of the LNAPL source area at the Facility
BTEX	benzene, toluene, ethylbenzene, and xylenes
C vs. d	concentration vs. distance
C vs. t	concentration vs. time
C	concentration of COPC at time t
C_o	concentration of COPC at t=0
COPC	chemical of potential concern
C_{RHMW02}	COPC concentration at RHMW02
C_{RHS-BD}	COPC concentration at Red Hill Shaft before dilution
CSM	conceptual site model
d	day
d^{-1}	per day
DL	detection limit
EPA	Environmental Protection Agency, United States
ft	foot/feet
ft/d	feet per day
ft^3/day	cubic feet per day
k	first-order rate coefficient
k/u	the negative of the slope of a line obtained from a log-linear plot of the (center-line) COPC concentration
k_{point}	concentration vs. time attenuation rate coefficient
LNAPL	light non-aqueous-phase liquid
LOD	limit of detection (i.e., the quantitation limit for laboratory analytical results)
L_p	plume length
MGD	million gallons per day
MNA	monitored natural attenuation
n	number of samples
NAPH	naphthalene
PAH	polynuclear aromatic hydrocarbon
Q_{RHS}	average pumping rate at Red Hill Shaft
R^2	coefficient of determination
t	time
$t_{1/2}$	half-life for a given COPC
TOC	total organic carbon
TPH-d	total petroleum hydrocarbons – diesel-range organics
U.S.	United States
USGS	United States Geological Survey
v_{gw}	seepage velocity
w	width of the LNAPL source area at the Facility
yr	year
yr^{-1}	per year

1. Introduction

This subappendix is summarized in Section 7.3.2.4 of the Conceptual Site Model (CSM) main document.

1.1 TECHNICAL BACKGROUND

The United States (U.S.) Environmental Protection Agency (EPA) defines monitored natural attenuation (MNA) as:

> … the reliance on natural attenuation processes (within the context of a carefully controlled and monitored clean-up approach) to achieve site-specific remedial objectives within a time frame that is reasonable compared to other methods. The "natural attenuation processes" that are at work in such a remediation approach include a variety of physical, chemical, or biological processes that, under favorable conditions, act without human intervention to reduce the mass, toxicity, mobility, volume, or concentration of contaminants in soil and ground water. These in-situ processes include, biodegradation, dispersion, dilution, sorption, volatilization, and chemical or biological stabilization, transformation, or destruction of contaminants (EPA 1999).

A lines-of-evidence approach is commonly used to demonstrate that natural attenuation processes are occurring at a given site. Primary and secondary lines of evidence to evaluate MNA (EPA 1999; Newell et al. 2002; Wiedemeier, Wilson, et al. 1999; Wiedemeier, Rifai, et al. 1999) are:

- **Primary:** Rate of change in dissolved phase contaminant concentrations, both spatially and temporally, as a metric for plume behavior/status (i.e., stable, shrinking, expanding). Site-specific attenuation rate coefficient calculations can be used to evaluate the contribution of attenuation processes and estimate the time required to achieve remediation objectives.
- **Secondary:** Hydrogeologic and geochemical data as an indirect measure of active natural attenuation processes that support primary evidence/observations (e.g., decrease in parent contaminant concentrations). For example, changes in electron acceptor concentrations can be strong evidence for in-situ degradation of the parent compounds. Secondary lines of evidence are discussed in CSM Appendix B.5.

1.2 STUDY OBJECTIVES

The objective of this study was to evaluate natural attenuation processes at the Red Hill Bulk Fuel Storage Facility (the "Facility") using primary lines of evidence (i.e., temporal and spatial contaminant concentrations) from the Facility groundwater monitoring network. First-order rate coefficients and associated half-lives were calculated for the monitoring wells RHMW01 and RHMW02 at the Facility. Chemicals of potential concern (COPCs) considered for this study were diesel-range total petroleum hydrocarbons (TPH-d), 1-methylnaphthalene (1-MNAPH), 2-methylnaphthalene (2-MNAPH), and naphthalene (NAPH). For TPH-d, concentration vs. time rate coefficients were not calculated due to issues with the laboratory analysis for this parameter (discussed further in Section 2.2 and CSM Appendix B.7).

Benzene, toluene, ethylbenzene, and xylenes (BTEX) data were not analyzed in this study, given their low concentrations in Facility groundwater (mostly less than 1 microgram per liter [µg/L]) and/or limited datasets of detected results (i.e., the majority of BTEX concentrations were below respective

detection limits) at wells RHMW01 and RHMW02. Beginning in 2017, the EPA co-sampled some wells during the Navy sampling events. Because this co-sampling covers only a small portion of the monitoring timeframe, EPA analytical results have not been included in this analysis.

Figure 1-1 provides the locations of monitoring wells RHMW01 and RHMW02 in relation to the tank farm. Historical groundwater data from February 2005 to present (April 25, 2018) (DON 2018) were used to calculate first-order rate coefficients and half-lives for the COPCs. Descriptions of the first-order attenuation calculations are provided in Section 2.

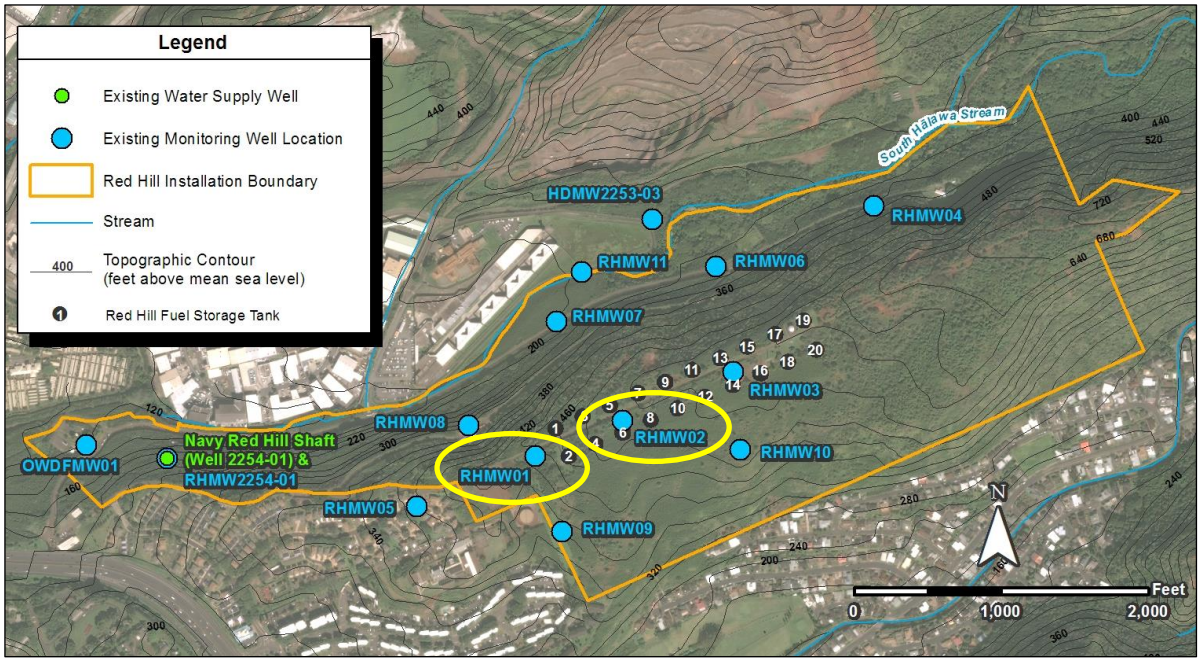

Figure 1-1: Location of RHMW01 and RHMW02 in Relation to Tank Farm

2. Methods

Three types of first-order attenuation rate coefficients were calculated to evaluate MNA processes at the Facility for this analysis: Point attenuation rate (Concentration vs. Time [C vs. t]), Bulk attenuation rate (Concentration vs. Distance [C vs. d]), and Biodegradation rate coefficients (λ). The point attenuation (C vs. t) rate describes the *plume duration* at a single monitoring well location while the bulk attenuation rate (C vs. d) rate describes the *plume attenuation* and spatial distribution of COPCs from the source area at a given time. The biodegradation rate describes *plume attenuation* resulting from the effects of biodegradation only (exclusive of advection, dispersion and other attenuation mechanisms). Each is described further in Sections 2.2, 2.3, and 2.4, respectively.

Specific applications of these rate coefficients include:

- **Plume Duration:** Based on analysis of COPC concentrations over time, evaluate concentration trends (increasing, stable, or decreasing) and effects of attenuation processes on plume duration at a given monitoring well location.
- **Plume Attenuation:** Based on changes in COPC concentrations between different monitoring locations, evaluate COPC attenuation within the groundwater flow system.

Importantly, each rate coefficient describes a specific attenuation process and, as a result, estimated rates and half-lives cannot be directly compared to each other. Table 2-1 summarizes the significance of each rate coefficient and their appropriate application for assessing natural attenuation processes (Newell et al. 2002).

Table 2-1: Appropriate Uses for Point (C vs. t), Bulk (C vs. d), and Biodegradation Attenuation Rate Coefficients

Rate Coefficient	Method of Analysis	Significance	Use of Rate Constant		
			Plume Attenuation?	Plume Trends?	Plume Duration?
Point Attenuation Rate (k_{point}, time per year)	C vs. t Plot (Figure 2-1; Equation 1)	Reduction in contaminant concentration over time at a single point	NO*	NO*	YES
Bulk Attenuation Rate (k; time per year)	C vs. d Plot (Figure 2-2; Equations 2 & 3)	Reduction in dissolved contaminant concentration with distance from source	YES	NO*	NO
Biodegradation Rate (λ, time per year)	C vs. d Plot; Calculations (Equations 4 & 5)	Biodegradation rate for dissolved contaminants after leaving source, exclusive of advection, dispersion, etc.	YES	NO	NO

* Note: Although assessment of an attenuation rate constant at a single location does not yield plume attenuation information, or plume trend information, an assessment of general trends of multiple wells over the entire plume is useful to assess overall plume attenuation and plume trends.
(Source: Newell et al. 2002, Table 2-1)

2.1 Data Handling and Consolidation

To calculate these attenuation rates, historical data from 2005 to April 2018 were considered, with the following modifications to the dataset:

- COPC concentrations reported by the laboratory as non-detect were assigned a concentration equal to the laboratory-reported limit of detection (LOD) (e.g., < 0.1 µg/L = 0.1 µg/L). The LOD is the lowest COPC concentration that must be present in a sample in order to be detected at the detection limit (DL) with 99% confidence.

- Qualified data (e.g., "J" flag) were assigned the reported COPC concentration (e.g., 12 J µg/L = 12 µg/L). Note that when a COPC is detected at a concentration below the LOD, the laboratory reports the result as detected, but the result is flagged with a "J" flag to indicate that the detected concentration was less than the LOD.
- For sampling events where duplicates were collected, the average of the primary concentration and duplicate concentration was used.

2.2 PLUME DURATION: POINT ATTENUATION (C VS. T) RATE COEFFICIENT

The Point Attenuation (C vs. t) Rate Coefficient (k_{point}) describes the behavior of the COPC at one point in space and provides information regarding the potential plume duration at that location (Newell et al. 2002). This rate coefficient, expressed in units of inverse time (e.g., per year), is calculated from the slope of the natural logarithm (log) concentration vs. time curve measured at a selected monitoring location (Figure 2-1; Equation 1). The rate coefficient and half-life (Equation 1) provide information regarding the potential plume duration at the single monitoring location, largely due to changes in strength of the plume source. Note that a rate coefficient calculated from C vs. t data at a single location cannot be used to estimate the trend of an entire plume or bulk attenuation (Table 2-1).

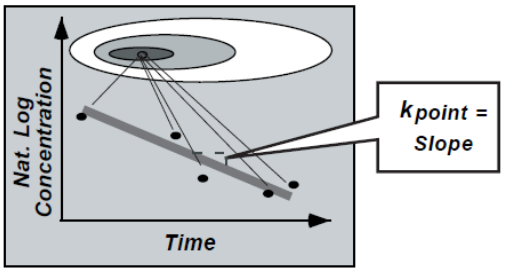

$$t = \frac{\ln(C/C_o)}{k_{point}};\ t_{1/2} = \frac{\ln(2)}{k_{point}} \quad (1)$$

where:
$t_{1/2}$ = Half-life for a given COPC (yr)
C = Concentration of COPC at time t (mg/L)
C_o = Concentration of COPC at t=0 (mg/L)
k_{point} = Concentration vs. time attenuation rate coefficient (yr^{-1})

(From Newell et al. 2002)

Figure 2-1: Concentration vs. Time Attenuation Rate Coefficient and Half-Life

C vs. t rate coefficients and half-lives were calculated for 1-MAPH, 2-MNAPH, and NAPH at RHMW02 only. For well RHMW01, the majority (> 50%) of concentration data for 1-MNAPH, 2 MNAPH, and NAPH were below respective detection limits. For both wells, C vs. t rate coefficients were not calculated for TPH-d due to issues with the laboratory analysis for this parameter. As discussed in CSM Appendix B.7, during the monitoring period of 2005–2018, several different laboratories were used for analysis of groundwater samples. Some of the increases and decreases in TPH-d concentrations over time appear to be an artifact of analytical differences between laboratories (see CSM Appendix B.7 for more information). As a result, a C vs. t attenuation rate for this parameter would not accurately reflect the true rate of COPC concentration change over time in individual monitoring wells.

For each COPC, natural log-transformed concentration data were plotted vs. time and fit to a linear trendline (using Microsoft Excel's built-in trendline and linear regression features) to estimate the first-order attenuation coefficient. Fit parameters of the linear regression model—coefficient of determination (R^2) and p-value from the F-test of overall significance—were used to evaluate the degree of variation explained by the model and the fit of the model relative to an intercept-only model (slope = 0; no predictors) at a significance level of 95%, respectively. COPC half-lives were calculated using Equation 1.

2.3 PLUME ATTENUATION: BULK ATTENUATION (C VS. D) RATE COEFFICIENT

The Bulk Attenuation (C vs. d) Rate Coefficient (k) describes the behavior of the COPC spatially within groundwater at one point in time (Newell et al. 2002). This rate coefficient, expressed in units of inverse time, is calculated by multiplying the slope of a line obtained from a log-linear plot of COPC concentration vs. distance downgradient by the estimated groundwater seepage velocity (Figure 2-2; Equation 2). The rate coefficient and half-life (Equation 3) provide information on how quickly dissolved contaminants are attenuated within groundwater as they migrate from the source, indicating if a plume is expanding, showing relatively little change, or shrinking. As such, C vs. d attenuation rates are not directly comparable to C vs. t rates (which reflect the plume duration at a single location; see Section 2.2 and Table 2-1).

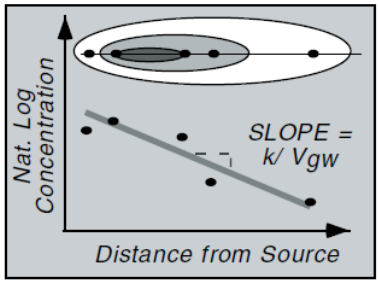

$$k = slope \times v_{gw} \quad (2)$$

$$t = \frac{\ln\left(C/C_o\right)}{k};\ t_{1/2} = \frac{\ln(2)}{k} \quad (3)$$

where:
k = Concentration vs. distance attenuation rate coefficient (d^{-1})
v_{gw} = Seepage velocity (ft/d)

(From Newell et al. 2002)

Figure 2-2: Concentration vs. Distance Attenuation Rate Coefficient (k) and Half-Life

For this study, data from monitoring wells RHMW01 and RHMW02 were used, based on the approximate west-southwesterly direction of groundwater flow through the tank farm and particle tracking indicating that these two monitoring wells fall along the same flow path. Well RHMW05 was excluded from the analysis because preliminary particle tracking model results suggested that RHMW05 lies outside of the groundwater flow path connecting RHMW02 and RHMW01 (based on investigation's interim groundwater flow modeling). In addition, the majority of COPC concentrations were below respective detection limits at RHMW05. Wells RHMW02 and RHMW01 are located approximately 620 feet (ft) apart, with RHMW02 representing the area of highest COPC concentrations and RHMW01 representing the downgradient location. This analysis assumes that RHMW02 and RHMW01 are in the same flow path (i.e., the COPCs present in RHMW01 originated in the vicinity of RHMW02).

First-order rate coefficients and half-lives were calculated for TPH-d, 1-MNAPH, 2-MNAPH, and NAPH using two modified datasets:

- **Detected COPCs at Both Wells:** a dataset including only sampling events where concentrations of a COPC above the LOD were reported at *both* RHMW01 and RHMW02.
- **Detected COPCs at One or Both Wells:** a dataset including sampling events where concentrations of a COPC above its detection limit were reported at *one or both* of the wells. COPC concentrations below the LOD were assigned a concentration equal to the respective LOD.

The purpose of the two datasets was to assess the effect of including/excluding qualified data (non-detects) on the resulting attenuation rate coefficients and half-lives. For both datasets, the following data were excluded: (1) sampling events where a given COPC was below its LOD at *both* wells and (2) sampling events where only one well was sampled (e.g., RHMW01 data collected before RHMW02 was installed). The numbers of data pairs for the COPCs for each dataset are presented in Table 2-2.

For each data pair, the slope of the natural log-linear plot of COPC concentration vs. distance was calculated using Microsoft Excel's built-in trendline feature. The average slope for each COPC was then multiplied by the estimated groundwater seepage velocity to calculate the first-order attenuation coefficient. COPC half-lives were calculated using Equation 3.

A groundwater seepage velocity of 12.4 ft per day was used based on preliminary particle tracking model results conducted for the investigation's interim groundwater flow modeling effort. Groundwater seepage velocity at the Facility is highly uncertain due to the complex geology and flat water table (i.e., very low hydraulic gradient). Efforts to develop an improved understanding of groundwater flow at the Facility are ongoing.

Table 2-2: Number of COPC Data Pairs Used to Calculate C vs. d Rate Coefficients

	Detected COPCs At *Both* Wells			Detected COPCs At *One or Both* Wells		
		No. of Non-detects			No. of Non-detects	
COPC	No. of Data Pairs	RHMW01	RHMW02	No. of Data Pairs	RHMW01	RHMW02
TPH-d	57	0	0	63	6	0
1-Methylnaphthalene	11	0	0	62	51	0
2-Methylnaphthalene	14	0	0	62	48	0
Naphthalene	26	0	0	63	37	0
TPH-d (silica gel cleanup)				5	3	0
TOC				1	1	0

TOC total organic carbon

C vs. d attenuation rates were also calculated for variations of the TPH-d analysis (i.e., TPH-d with silica gel cleanup and total organic carbon [TOC]) to identify differences in attenuation rates for petroleum hydrocarbons vs. polar metabolites (Table 2-2). This information supports CSM Appendix B.7 and is discussed further in Section 3.4.

2.4 PLUME ATTENUATION: BIODEGRADATION RATE COEFFICIENT (λ)

The Biodegradation Rate Coefficient (λ) describes the effect of biodegradation on COPC migration at one point in time and is expressed in units of inverse time. Biodegradation rate coefficients are generally smaller (and half-lives longer) than C vs. d attenuation rate coefficients, which reflect the combined effects of biodegradation, dispersion, and any other attenuation processes. For this study, biodegradation rate coefficients for each COPC were calculated using Equation 4 (Buscheck and Alcantar 1995) and Equation 5 (Xu and Eckstein 1995), as follows:

$$\lambda = (v_{gw}/4\alpha_x)\ \{[1 + 2\ \alpha_x(k/u)]^2 - 1\} \qquad (4)$$

$$\alpha_x = 2.72 \cdot [\log_{10}(L_p/3.28)]^{2.414} \qquad (5)$$

where:
λ = Biodegradation rate coefficient (d^{-1})
v_{gw} = Seepage velocity (ft/d)
α_x = Longitudinal dispersivity (ft)
k/u = The negative of the slope of a line obtained from a log-linear plot of the (center-line) COPC concentration versus distance downgradient along the flow path
L_p = Plume length (ft) (assumed to be the distance between RHMW01 and RHMW02)

Equation 4 (Buscheck and Alcantar 1995) assumes that (1) the plume is at steady-state, (2) monitoring wells are located along the centerline of groundwater flow, and (3) horizontal and vertical transverse dispersion are negligible. For purposes of this study, the distance between RHMW02 and RHMW01 (620 ft) was used as an estimate of plume length (L_p) to calculate longitudinal dispersivity. For a given COPC, the resulting biodegradation rate coefficient was calculated using the average slope of all data pairs and the estimated groundwater seepage velocity (12.4 ft per day; as discussed in Section 2.2). The same data pairs for each COPC (listed in Table 2-2) were used for this analysis. As with C vs. d rates, biodegradation rate coefficients were calculated for TPH-d (with silica gel cleanup) and TOC (Section 3.4).

2.5 PLUME ATTENUATION: RHMW02 TO RED HILL SHAFT

Similar to the analysis of COPC concentrations in RHMW02 and RHMW01, the change in COPC concentration between RHMW02 and Red Hill Shaft can be used to estimate COPC attenuation rates (Equation 6). However, because Red Hill Shaft is a pumping well that captures groundwater flow from a large area, a modified evaluation method is required to account for dilution of COPCs caused by mixing of the plume with clean water. In addition, the attenuation rate is calculated based on travel time from RHMW02 to Red Hill Shaft rather than seepage velocity because the seepage velocity increases close to Red Hill Shaft (i.e., seepage velocity is not constant along the flow path). Groundwater seepage velocity and travel time at the Facility are highly uncertain due to the complex geology and flat water table (i.e., very low hydraulic gradient). Efforts to develop an improved understanding of groundwater flow at the Facility are ongoing. For a given concentration relationship, a faster travel time yields a faster attenuation rate.

$$k = -\frac{Ln\left(C_{RHS-BD}/C_{RHMW02}\right)}{t} \quad (6)$$

where:
- k = First-order attenuation rate coefficient (d^{-1})
- C_{RHS-BD} = COPC concentration at Red Hill Shaft before dilution (Equation 7, µg/L)
- C_{RHMW02} = COPC concentration at RHMW02 (µg/L)
- t = Travel time from RHMW02 to Red Hill Shaft (Base case model = 95 days; Base with clinker model = 45 days, based on investigation's interim groundwater flow modeling)

The COPC concentration entering Red Hill Shaft before dilution due to mixing with clean groundwater can be determined based on the volume of water pumped from Red Hill Shaft and the volume of water flowing through source area at the Facility (Equation 7):

$$C_{RHS-BD} = C_{RHS} \times \frac{Q_{RHS}}{V_d \times b \times W} \quad (7)$$

where:
- C_{RHS-BD} = COPC concentration at Red Hill Shaft before dilution (µg/L)
- C_{RHS} = Measured COPC concentration at Red Hill Shaft (i.e., after dilution, µg/L)
- Q_{RHS} = Average pumping rate at Red Hill Shaft ([redacted])
- V_d = Darcy velocity of groundwater in the Facility source area (0.5 ft/d for base model; 1.4 ft/d for base model with clinker; based on investigation's interim groundwater flow modeling)
- b = Thickness of the light non-aqueous-phase liquid (LNAPL) source area at the Facility (2 m; 6.56 ft; assumed value from Connor, Newell, and Malander 1996)
- W = Width of the LNAPL source area at the Facility (300 ft; assumed value based on width between rows of tanks)

In other words, the decrease in COPC concentration at Red Hill Shaft due to dilution with clean water is a function of the fraction of water that originates from the source area. Based on the input values used in Equation 7, 0.2% of the water captured by Red Hill Shaft flow through the source area at the Facility and the remaining 99.8% of the water does not contact the source area. As a result, before dilution, the COPC concentrations entering Red Hill Shaft are 620 times higher than the diluted COPC concentrations measured through the monitoring program.

3. Results

3.1 PLUME DURATION: POINT ATTENUATION (C VS. T) RATE COEFFICIENTS

Table 3-1 presents the C vs. t first-order attenuation coefficients, half-lives, number of data points, R^2 value, and the p-value (significance level of 0.05) for the first-order model for each COPC at monitoring well RHMW02. For 1-MNAPH, an attenuation rate of 0.05 yr^{-1} (or half-life of 14.6 yrs) was estimated. Half-lives for 2-MNAPH and NAPH are not reported in Table 3-1 because the slope of the resulting trend line was slightly positive (this results in a negative half-life). At RHMW01, meaningful trendlines could not be developed for 1-MNAPH, 2-MNAPH, and NAPH since the majority (> 50%) of concentration data were below respective detection limits.

Table 3-1: C vs. t Coefficients, Half-Lives, and First-Order Model Fit Parameters for the COPCs at RHMW02 (September 2005 to April 2018)

COPC	k (yr^{-1})	$t_{1/2}$ (yr)	n	R^2	p-value
1-Methylnaphthalene	-0.05	14.6	63	0.0161	0.322
2-Methylnaphthalene	0.03	**	63	0.0032	0.658
Naphthalene	0.03	**	63	0.0085	0.472

** Half-lives are not reported for 2-methylnaphthalene and naphthalene because attenuation rates were positive (Figure 3-2 and Figure 3-3).

k first-order rate coefficient
n number of samples
$t_{1/2}$ half-life
yr year
yr^{-1} per year

Figure 3-1 to Figure 3-3 present the linear and natural log scale plots for each COPC at monitoring well RHMW02. Concentrations of 1-MNAPH, 2-MNAPH, and NAPH generally decreased during the initial 6 years of the monitoring period (2005–2011), followed by greater data scatter over the remainder. The observed scatter contributed to poor model fits and the resulting slopes were not statistically different than zero (p>0.05; Table 3-1); i.e., these COPCs show no statistically significant long-term concentration trend over the monitoring period.

The lack of a consistent trend in the C vs. t data for 1-MNAPH, 2-MNAPH, and NAPH is not unexpected given the complexity of the light non-aqueous-phase liquid (LNAPL) source at the Facility. Since jet fuel is a complex mixture of aliphatic hydrocarbons (straight, branched, and cyclic alkanes), polynuclear aromatic hydrocarbons (PAHs, especially naphthalene and methylnaphthalenes), and heterocyclic compounds, each with different solubilities and biodegradation potential, it can be very difficult to clearly assess the rate of LNAPL depletion based solely on the C vs. t trends of individual components. As LNAPL weathers, the proportion of less water soluble COPCs remaining in the residual fuel increases, resulting in a proportional increase in the effective solubilty of these COPCs. This phenomenon has been observed at other sites such as the U.S. Geological Survey (USGS) Bemidji, MN research site (Baedecker et al. 2011). As a result, dissolved-phase concentrations of COPCs from the source can vary considerably as the composition of the LNAPL source changes over time (see CSM Appendix B.7 for further discussion). Stable or increasing dissolved concentrations of less-soluble COPCs such as NAPH may, in fact, reflect significant depletion of the LNAPL source material.

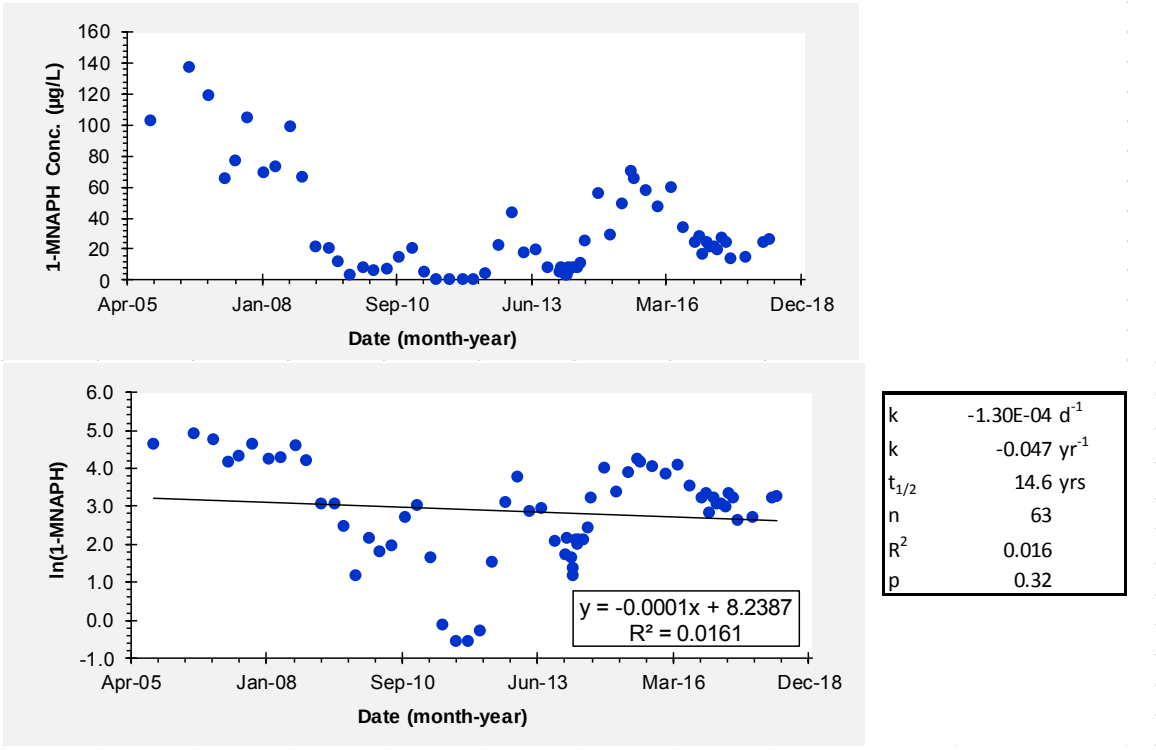

Figure 3-1: Linear and Natural Log Scale Plots of 1-Methylnaphthalene Concentrations from September 2005 to April 2018 at Monitoring Well RHMW02

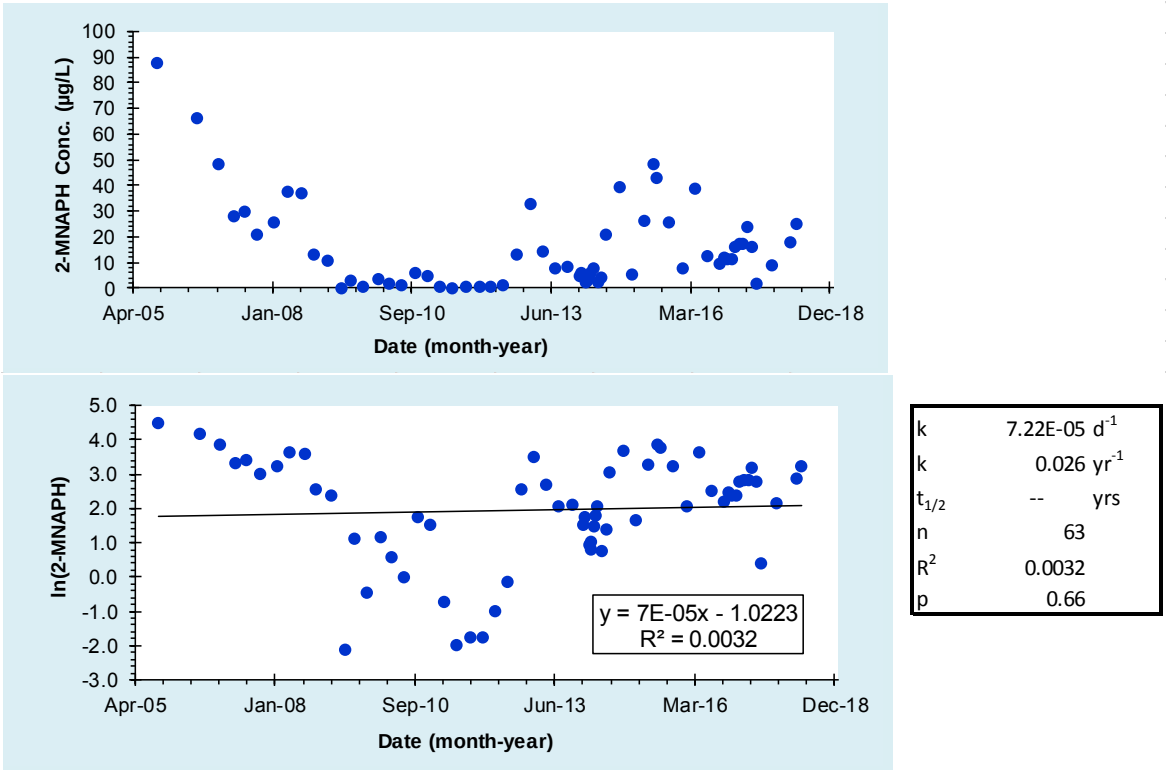

Figure 3-2: Linear and Natural Log Scale Plots of 2-Methylnaphthalene Concentrations from September 2005 to April 2018 at Monitoring Well RHMW02

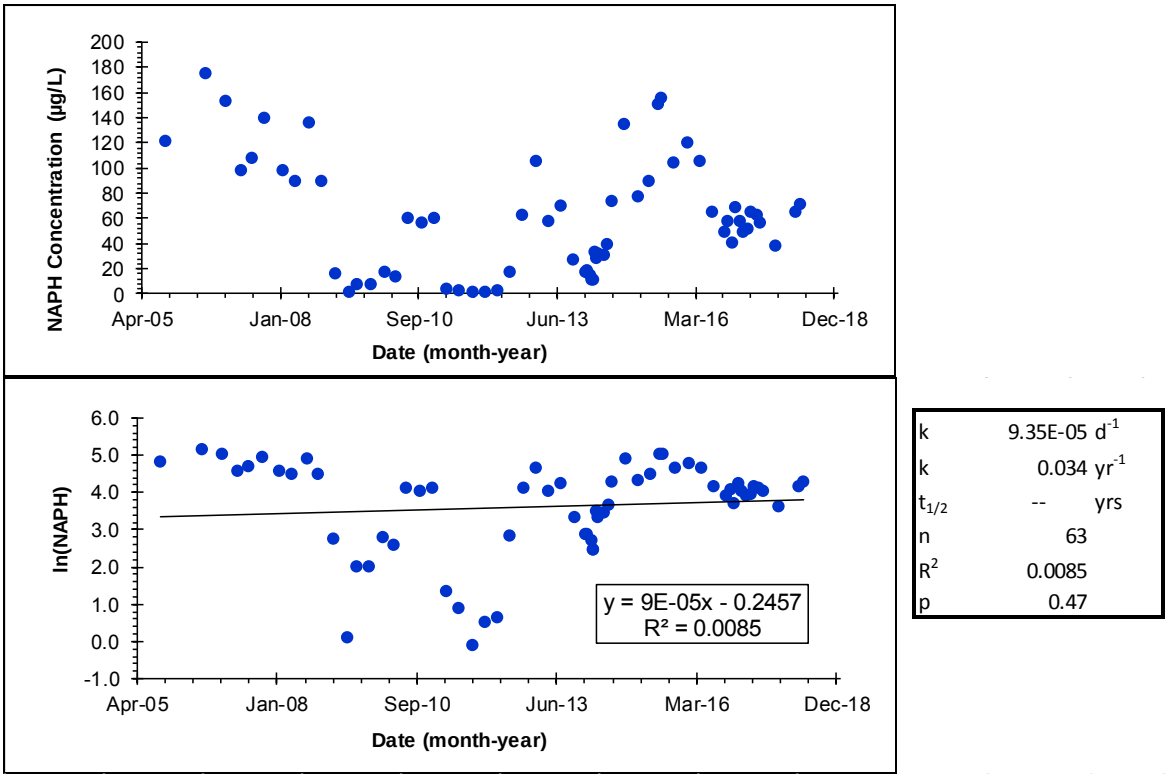

Figure 3-3: Linear and Natural Log Scale Plots of Naphthalene Concentrations from September 2005 to April 2018 at Monitoring Well RHMW02

3.2 PLUME ATTENUATION: BULK ATTENUATION (C VS. D) RATE COEFFICIENTS

A C vs. d attenuation rate was calculated for each data pair (i.e., each paired RHMW02–RHMW01 concentration measurement) for each COPC. Table 3-2 and Table 3-3 present the number of data pairs and the average first-order attenuation coefficient and corresponding half-life for each COPC. The results presented in Table 3-2 include data from sampling events where COPC concentrations above the detection limit were reported at *both* RHMW01 and RHMW02. The results presented in Table 3-3 include data from sampling events where COPC concentrations above the detection limit were reported at *one or both* of the wells. Attenuation rates and half-lives are reported in days in Table 3-2 and Table 3-3.

Table 3-2: C vs. d Rate Coefficients and Half-Lives for the COPCs Along RHMW02–RHMW01 Transect (Includes Detected COPCs at Both Wells Only)

COPC	n	k (d^{-1}) *	$t_{1/2}$ (d)
TPH-d	57	-0.05 ± 0.01	13.8
1-Methylnaphthalene	11	-0.13 ± 0.05	5.1
2-Methylnaphthalene	14	-0.12 ± 0.05	5.6
Naphthalene	26	-0.11 ± 0.04	6.2

* Attenuation rates are presented as mean ± standard deviation.
d day
d^{-1} per day

Table 3-3: C vs. d Rate Coefficients and Half-Lives for the COPCs Along RHMW02–RHMW01 Transect (Includes Detected COPCs at One or More Wells Only)

COPC	n	k (d^{-1})	$t_{1/2}$ (d)
TPH-d	63	-0.05 ± 0.01	13.6
1-Methylnaphthalene	62	-0.11 ± 0.03	6.2
2-Methylnaphthalene	62	-0.10 ± 0.04	7.2
Naphthalene	63	-0.12 ± 0.03	5.9

Major findings/observations are summarized below:

1. C vs. d first-order attenuation rate coefficients ranged from 0.05 d^{-1} to 0.13 d^{-1}, corresponding to half-lives of approximately 5–14 days (Table 3-2 and Table 3-3). These C vs. d rate coefficients (and associated half-lives) provide supporting evidence of COPC attenuation; however, these rates do reflect some uncertainty inherent in the calculations (e.g., limited number of well locations; uncertainty about the centerline of the plume and groundwater seepage velocity).

1. Throughout the monitoring period, COPC concentrations at RHMW01 are 1–2 orders of magnitude (or more) lower than at RHMW02, suggesting that attenuation processes are potentially active and consistent along the groundwater flow path. This is also reflected in the relatively low variation in C vs. d attenuation rates over the monitoring period (i.e., small standard deviation). This observation suggests that the attenuation processes limiting migration of COPCs away from the area of RHMW02 have generally remained stable over the entire monitoring period (2005 to April 2018).

2. Attenuation rate coefficients and associated half-lives for all COPCs were not appreciably different between the two datasets (i.e., excluding data pairs with one non-detect and including data pairs with one non-detect). This indicates that the C vs. d attenuation analysis is not sensitive to the laboratory analytical sensitivity for these COPCs.

3.3 PLUME ATTENUATION: BIODEGRADATION RATE COEFFICIENTS

Table 3-4 and Table 3-5 present the average first-order biodegradation rate coefficients, half-lives, and number of data pairs for the first-order model for each COPC along the RHMW02–RHMW01 transect. As discussed in Section 2.4, these biodegradation rates were calculated using the Buscheck and Alcantar (1995) method to separate the contributions of biodegradation and dispersion in the overall C vs. d attenuation rates. The results presented in Table 3-4 include data from sampling events where COPC concentrations above the detection limit were reported at *both* RHMW01 and RHMW02. The results presented in Table 3-5 include data from sampling events where COPC concentrations above the detection limit were reported at *one or both* of the wells.

Table 3-4: Biodegradation Rate Coefficients and Half-Lives for the COPCs Along RHMW02–RHMW01 Transect (Includes Detected COPCs At Both Wells Only)

COPC	n	λ (d^{-1})	$t_{1/2}$ (d)
TPH-d	57	-0.05 ± 0.01	15.0
1-Methylnaphthalene	11	-0.11 ± 0.05	6.5
2-Methylnaphthalene	14	-0.10 ± 0.05	7.0
Naphthalene	26	-0.09 ± 0.04	7.6

λ Biodegradation rate coefficient (d^{-1})

Table 3-5: Biodegradation Rate Coefficients and Half-Lives for the COPCs Along RHMW02-RHMW01 Transect (Includes Detected COPCs At One or More Wells Only)

COPC	n	λ (d^{-1})	$t_{1/2}$ (d)
TPH-d	63	-0.05 ± 0.01	14.8
1-Methylnaphthalene	62	-0.09 ± 0.04	7.6
2-Methylnaphthalene	62	-0.08 ± 0.04	8.5
Naphthalene	63	-0.09 ± 0.03	7.3

First-order biodegradation rate coefficients ranged from 0.05 d^{-1} to 0.11 d^{-1}, corresponding to half-lives of approximately 7–15 days (Table 3-4 and Table 3-5). The biodegradation rates for all COPCs were only slightly (8–22%) smaller than the respective C vs. d attenuation rates. This suggests that biodegradation is the primary attenuation process responsible for the reduction in COPC concentration from RHMW02 to RHMW01.

3.4 PLUME ATTENUATION: RHMW02 TO RHMW01 ATTENUATION RATE COEFFICIENTS FOR TPH-D WITH SILICA GEL CLEANUP

The laboratory analytical method for TPH-d measures both diesel-range petroleum hydrocarbons and polar metabolites (see CSM Appendix B.7 for a more detailed discussion of issues associated with TPH-d analyses). In order to identify potential differences in attenuation rates for petroleum hydrocarbons vs. polar metabolites, C vs. d attenuation rates and biodegradation rates were determined for variations of the TPH-d analysis (Table 3-6 and Table 3-7):

- **TPH-d (63 paired measurements, 2005 to 2018):** The TPH-d analysis measures extractable organic matter that is measured by gas chromatography in the diesel range. It can include diesel-range petroleum hydrocarbons, polar metabolites and other naturally occurring organic matter.
- **TPH-d with Silica Gel Cleanup: (5 paired measurements, 2017 to 2018):** Silica gel cleanup removes the polar metabolites and other naturally occurring organic matter while retaining the diesel-range petroleum hydrocarbons.
- **Total Organic Carbon (TOC; 1 paired measurement, October 2017):** TOC measures all organic material in the sample including some polar metabolites not extracted by the TPH-d extraction procedure.

Table 3-6: C vs. d Rate Coefficients and Half-Lives for TPH-d, TPH-d (with silica gel cleanup) and TOC Along RHMW02-RHMW01 Transect

COPC	n	k (d^{-1})	$t_{1/2}$ (d)
TPH-d	63	-0.05 ± 0.01	13.6
TPH-d (silica gel)	5	-0.05 ± 0.01	13.7
Total Organic Carbon	1*	-0.04	15.8

* Represents one data pair (one detection at RHMW02 and a qualified result at RHMW01) on 10/25/2017.

Table 3-7: Biodegradation Rate Coefficients and Half-Lives for TPH-d, TPH-d (with silica gel cleanup) and TOC Along RHMW02-RHMW01 Transect

COPC	n	λ (d^{-1})	$t_{1/2}$ (d)
TPH-d	63	-0.05 ± 0.01	14.8
TPH-d (silica gel)	5	-0.05 ± 0.01	15.0
Total Organic Carbon	1*	-0.04	17.0

* Represents one data pair (one detection at RHMW02 and a qualified result at RHMW01) on 10/25/2017.

As shown in Table 3-6 and Table 3-7, the C vs. d attenuation rates and the biodegradation rates are similar for the analyses that include or exclude the polar metabolites. This suggests that the diesel-range petroleum hydrocarbons and the polar metabolites are attenuating at similar rates within the groundwater at the Facility.

3.5 PLUME ATTENUATION: RHMW02 TO RED HILL SHAFT

The C vs. d attenuation rate coefficient for COPC migration from RHMW02 to Red Hill Shaft was evaluated only for NAPH because, to date, it has been the most commonly detected individual COPC at Red Hill Shaft (detections for 12 of 63 monitoring events from 2005 to March 2018). The very low detection frequency for other COPCs results in too much uncertainty regarding COPC concentration. For NAPH, the average concentration over the monitoring period was used to determine the C vs. d attenuation rate coefficient. Use of the average concentration was considered appropriate because:

- The C vs. t analysis indicates little overall concentration trend at RHMW02 (slope of the trendline ≈ 0) over the monitoring period (Figure 3-3).
- The travel time from RHMW02 to Red Hill Shaft (95 days for the base model and 45 days for the base with clinker model, based on the investigation's interim groundwater flow modeling) makes it difficult to pair individual measurements at RHMW02 and Red Hill Shaft.
- During some parts of the monitoring period, the sampling frequency at RHMW02 has been higher than for Red Hill Shaft (e.g., 2014).

The average NAPH concentration at Red Hill Shaft was calculated by averaging the detected results and ignoring the non-detect results (Average C = 0.047 µg/L). For Red Hill Shaft, all 12 of the detected results were J-flagged (i.e., the detected concentration was less than the LOD). As a result, calculating an average concentration by using the LOD for non-detect results would have resulted in a higher average concentration than calculated using only the detected results. For RHMW02, NAPH has been detected during all 63 monitoring events from 2005 to April 2018 (Average C = 61 µg/L). Two attenuation rates were calculated based on two estimates of travel time from RHMW02 to Red Hill Shaft: (1) the travel time from the base case groundwater flow model (95 days) and (2) the travel time for the base case model including a clinker zone connecting the Facility source area to the Red Hill Shaft (45 days) (Table 3-8).

A second analysis of plume attenuation to Red Hill Shaft was conducted using data from the March 2015 to June 2016 period. During this period, all NAPH results at Red Hill Shaft were non-detect with a LOD of 0.005 µg/L. The LOD was used as the proxy value for the NAPH concentration at Red Hill Shaft. For RHMW02, NAPH was detected during all six monitoring events during this period (Average C = 116 µg/L).

Table 3-8: RHMW02 to Red Hill Shaft Attenuation Rate Coefficients Using All Naphthalene Detects at Red Hill Shaft (2005 to 2018)

COPC	n (RHMW02)	n (RH Shaft)	C_{RHMW02} (µg/L)	C_{RHS-BD} (µg/L)	t (d)	k (d^{-1})	$t_{1/2}$ (d)
Naphthalene (base case model)	63	12	61	30	95	0.0075	92
Naphthalene (base model with clinker)	63	12	61	11	45	0.038	18

Note: The concentration entering Red Hill Shaft before dilution (C_{RHS-BD}) was calculated using Equation 7 above using the average measured naphthalene concentration in Red Hill Shaft for detected results of 0.047 µg/L.

Table 3-9: RHMW02 to Red Hill Shaft Attenuation Rate Coefficients Using Naphthalene Results from March 2015 to June 2016

COPC	n (RHMW02)	n (RH Shaft)	C_{RHMW02} (µg/L)	C_{RHS-BD} (µg/L)	t (d)	k (d^{-1})	$t_{1/2}$ (d)
Naphthalene (base case model)	6	6	116	3	95	0.038	18
Naphthalene (base model with clinker)	6	6	116	1.1	45	0.10	7

Note: The concentration entering Red Hill Shaft before dilution (C_{RHS-BD}) was calculated using Equation 7 above using the naphthalene detection limit in Red Hill Shaft of 005 µg/L for the time period of March 2015 to June 2016.

Based on this range of analyses, the plume attenuation half-life for NAPH from RHMW02 to Red Hill Shaft was between 7 days (based the 2015/2016 monitoring period and travel time for the base case groundwater flow model with the clinker zone) and 92 days (based the NAPH detects during the full monitoring period and travel time for the base case groundwater flow model without the clinker zone).

4. Conclusions

Groundwater monitoring data from the Facility over the monitoring period of 2005 to April 2018 were used to evaluate Plume Duration and Plume Attenuation. These evaluations support the following observations:

- **Plume Duration:** COPC concentrations at individual monitoring locations vary over time exhibiting both increases and decreases in concentration. At RHMW02, the monitoring location with the highest COPC concentrations, most of the COPCs show little or no long-term concentration trend due to high data variability over the monitoring period. The observed variability in COPC concentration reflects the complexity of the LNAPL source (i.e., complex mixture of individual compounds, each with different solubilities and biodegradation potential) and the changing composition of the LNAPL source over time. As a result of the changing LNAPL composition during weathering, stable or increasing dissolved concentrtations of less-soluble COPCs such as NAPH may, in fact, reflect significant depletion of the LNAPL source material. This phenomenon has been observed at other sites such as the USGS Bemidji, MN research site (Baedecker et al. 2011).
- **Plume Attenuation:** COPC concentrations generally decrease from the source area (represented by RHMW02) to downgradient monitoring locations (RHMW01 and Red Hill Shaft). C vs. d attenuation half-lives range from 5 to 14 days for the analysis of concentration changes from RHMW02 to RHMW01 while half-lives range from 7 to 92 days for the analysis of concentration changes from RHMW02 to Red Hill Shaft. Although both analyses support the conclusion that biodegradation is contributing to the natural attenuation of COPCs within groundwater, the estimated rate of attenuation varies by an order of magnitude depending on the data set and assumptions used. Both evaluations of C vs. d attenuation rates depend on important assumptions:
  - **RHMW02 to RHMW01:** This analysis assumes that RHMW02 and RHMW01 are in the same flow path (i.e., the COPCs present in RHMW01 originated in the vicinity of RHMW02). If the COPCs in RHMW01 actually originate from a different lower strength source (or a more distant source) than the analysis would overestimate the true attenuation rate.
  - **RHMW02 to Red Hill Shaft:** This analysis assumes that the very low NAPH concentrations detected in Red Hill Shaft (i.e., <0.1 µg/L) reflect the actual NAPH concentration in the Red Hill Shaft water rather than false-positive artifacts of laboratory analysis. For example, for a number of sample events in 2013 and 2014, low concentrations of NAPH (<0.1 µg/L) were detected in most or all of the groundwater samples, including those from wells upgradient of the Facility source area (see CSM Appendix B.7 for additional discussion of the uncertainty associated with the low concentration detections of NAPH). If the actual NAPH concentrations in Red Hill Shaft are lower than those indicated by the laboratory detections, then the analysis would underestimate the true attenuation rate.
- **Groundwater Seepage Velocity:** Groundwater seepage velocity at the Facility is highly uncertain due to the complex geology and flat water table (i.e., very low hydraulic gradient). Efforts to develop an improved understanding of groundwater flow at the Facility are ongoing.

Taken together, analysis of RHMW02 to RHMW01 and RHMW02 to Red Hill Shaft represents the probable range of plume attenuation rates for COPCs in groundwater at the Facility (i.e., an attenuation half-life of 5–14 days or 7–92 days). Based on the current available information, it is difficult to conclude which estimate is more reliable.

5. References

Baedecker, M. J., R. P. Eganhouse, B. A. Bekins, and G. N. Delin. 2011. "Loss of Volatile Hydrocarbons from an LNAPL Oil Source." *Journal of Contaminant Hydrology* 126: 140–152.

Buscheck, T. E., and C. M. Alcantar. 1995. "Regression Techniques and Analytical Solutions to Demonstrate Intrinsic Bioremediation." In *Intrinsic Bioremediation (Proceedings from the Third International In Situ and On-Site)*. Columbus, OH: Battelle Press.

Connor, J. A., C. J. Newell, and M. W. Malander. 1996. *Parameter Estimation Guidelines for Risk-Based Corrective Action (RBCA) Modeling*. National Ground Water Association Petroleum Hydrocarbons Conference, Houston, TX, November.

Department of the Navy (DON). 1999. *Initial Phase II Site Characterization Report, Fleet Industrial Supply Center Bulk Fuel Storage Facility at Red Hill*. Prepared by Ogden Environmental and Energy Services Co., Inc., Honolulu, HI. Pearl Harbor, HI: Pacific Division, Naval Facilities Engineering Command. March.

———. 2002. *Red Hill Bulk Fuel Storage Facility Investigation Report (Final) for Fleet Industrial Supply Center (FISC), Oahu, Hawaii*. Prepared by AMEC Earth & Environmental, Inc., Huntsville, AL. Pearl Harbor, HI: Pacific Division, Naval Facilities Engineering Command. August.

———. 2018. *Final First Quarter 2018 - Quarterly Groundwater Monitoring Report, Red Hill Bulk Fuel Storage Facility, Joint Base Pearl Harbor-Hickam, O'ahu, Hawai'i*. Prepared by AECOM Technical Services, Inc. JBPHH HI: Naval Facilities Engineering Command, Hawaii. June [in prep].

Environmental Protection Agency, United States (EPA). 1999. *Use of Monitored Natural Attenuation at Superfund, RCRA Corrective Action, and Underground Storage Tank Sites*. OSWER 9200.4-17P. Office of Solid Waste and Emergency Response. April.

Newell, C. J., H. S. Rifai, J. T. Wilson, J. A. Connor, J. A. Aziz, and M. P. Suarez. 2002. *Calculation and Use of First-Order Rate Constants for Monitored Natural Attenuation Studies*. Ground Water Issue. EPA/540/S-02/500. Cincinnati: EPA National Risk Management Research Laboratory. November.

Wiedemeier, T. H., H. S. Rifai, C. J. Newell, and J. T. Wilson. 1999. *Natural Attenuation of Fuels and Chlorinated Solvents in the Subsurface*. New York: John Wiley & Sons, Inc.

Wiedemeier, T. H., J. T. Wilson, D. H. Kampbell, R. N. Miller, and J. E. Hansen. 1999. *Technical Protocol for Implementing Intrinsic Remediation with Long-Term Monitoring for Natural Attenuation of Fuel Contamination Dissolved in Groundwater. Vols. I & II*. San Antonio, TX: Air Force Center for Environmental Excellence, Technology Transfer Division. March.

Xu, Moujin, and Yoram Eckstein. 1995. "Use of Weighted Least-Squares Method in Evaluation of the Relationship Between Dispersivity and Field Scale." *Ground Water* 33 (6): 905–8. https://doi.org/10.1111/j.1745-6584.1995.tb00035.x.

Appendix B.5:
MNA Secondary Lines of Evidence

CONTENTS

Acronyms and Abbreviations iii

1. Introduction 1-1

1.1 Technical Background 1-1
1.2 Study Objectives 1-1

2. Methods 2-1

2.1 Data Handling and Consolidation 2-1

3. Results 3-1

3.1 Spatial Concentrations of Geochemical Indicators 3-1
3.2 Temporal Concentrations of Geochemical Indicators 3-6
3.3 Key Relationships Between COPCs and Geochemical indicators 3-8

4. Conclusions 4-1

5. References 5-1

ATTACHMENTS

B.5.1 Time-Series Plots for Alkalinity, NO_3^-, SO_4^{2-}, Cl, Fe^{2+}, CH_4, and COPCs at All Monitoring Well Locations

B.5.2 X-Y Plots for Alkalinity, NO_3^-, SO_4^{2-}, Cl, Fe^{2+}, CH_4, and COPCs at All Monitoring Well Locations

FIGURES

1-1 Location of the Facility Monitoring Wells in Relation to Tank Farm Area 1-2

3-1 Concentrations of O_2, NO_3^-, SO_4^{2-}, Fe^{2+}, CH_4 and ORP from the Facility Groundwater Monitoring Network on April 23–25, 2018 3-2

3-2 Contour Plot of O_2 Concentrations from the Facility Groundwater Monitoring Network (April 23–25, 2018) 3-3

3-3 Contour Plot of SO_4^{2-} Concentrations from the Facility Groundwater Monitoring Network (April 23–25, 2018) 3-4

3-4 Contour Plot of CH_4 Concentrations from the Facility Groundwater Monitoring Network (April 23–25, 2018) 3-5

3-5 Time-Series Plots of NO_3^- (Left Panel) and SO_4^{2-} (Right Panel) Concentrations at Monitoring Wells RHMW01, RHMW02, RHMW03, and RHMW05 3-7

3-6 Time-Series Plots of Fe^{2+} (Left Panel) and CH_4 (Right Panel; y-axis: log-scale) Concentrations at Monitoring Wells RHMW01, RHMW02, RHMW03, and RHMW05 3-7

3-7 X-Y Plots for TPH-d Concentrations vs. NO_3^- (Left Panel) and SO_4^{2-} (Right Panel) Concentrations at Monitoring Wells RHMW01, RHMW02, RHMW03, and RHMW05 3-9

3-8 X-Y Plots for TPH-d Concentrations vs. Fe^{2+} (Left Panel) and CH_4 (Right Panel) Concentrations at Monitoring Wells RHMW01, RHMW02, RHMW03, and RHMW05 3-9

ACRONYMS AND ABBREVIATIONS

µg/L	micrograms per liter
1-MNAPH	1-methylnaphthalene
2-MNAPH	2-methlynaphthalene
CH_4	methane
CO_2	carbon dioxide
COPC	chemical of potential concern
CSM	conceptual site model
DL	detection limit
DO	dissolved oxygen
EPA	Environmental Protection Agency, United States
Fe^{2+}	ferrous iron
LOD	limit of detection
mg/L	milligrams per liter
MNA	monitored natural attenuation
mV	millivolt
NAPH	naphthalene
NO_3^-	nitrate as nitrogen
ORP	oxidation-reduction potential
SO_4^{2-}	sulfate
TEA	terminal electron acceptor
TPH-d	total petroleum hydrocarbons – diesel-range organics

1. Introduction

This subappendix is summarized in Section 7.3.2.4 of the Conceptual Site Model (CSM) main document.

1.1 TECHNICAL BACKGROUND

The United States Environmental Protection Agency (EPA) defines monitored natural attenuation (MNA) as:

> …the reliance on natural attenuation processes (within the context of a carefully controlled and monitored clean-up approach) to achieve site-specific remedial objectives within a time frame that is reasonable compared to other methods. The "natural attenuation processes" that are at work in such a remediation approach include a variety of physical, chemical, or biological processes that, under favorable conditions, act without human intervention to reduce the mass, toxicity, mobility, volume, or concentration of contaminants in soil and ground water. These in-situ processes include, biodegradation, dispersion, dilution, sorption, volatilization, and chemical or biological stabilization, transformation, or destruction of contaminants (EPA 1999).

A lines-of-evidence approach is commonly used to demonstrate that natural attenuation processes are occurring at a given site. Primary and secondary lines of evidence to evaluate MNA are:

- **Primary:** Rate of change in dissolved-phase contaminant concentrations, both spatially and temporally, as a metric for plume behavior/status (i.e., stable, shrinking, expanding). Site-specific attenuation rate coefficient calculations can be used to evaluate the contribution of attenuation processes and estimate the time required to achieve remediation objectives. Primary lines of evidence are discussed in CSM Appendix B.4.
- **Secondary:** Hydrogeologic and geochemical data as an indirect measure of active natural attenuation processes that support primary evidence/observations (e.g., decrease in parent contaminant concentrations). For example, changes in electron acceptor concentrations can be strong evidence for in-situ biodegradation of the parent compounds. Under aerobic conditions, oxygen serves as a terminal electron acceptor (TEA), while under anaerobic conditions, nitrate, sulfate, and carbon dioxide may serve as a TEA for the microbially mediated redox reactions (McCarty, Rittman, and Bouwer 1984).

1.2 STUDY OBJECTIVES

The objective of this study is to evaluate natural attenuation processes at the Red Hill Bulk Fuel Storage Facility (the "Facility") using secondary lines of evidence (e.g., geochemical data, electron acceptor concentrations) from the Facility groundwater monitoring network. The following analytes were considered in this study: total alkalinity, nitrate as nitrogen (NO_3^-), ferrous iron (Fe^{2+}), sulfate (SO_4^{2-}), and methane (CH_4). In addition, field measurements of dissolved oxygen (O_2) and oxidation-reduction potential (ORP) were incorporated. Where sufficient data were available, relationships between electron acceptor concentrations (and field parameters) and concentrations of chemicals of potential concern (COPCs) were identified for all monitoring wells. COPCs include diesel-range total petroleum hydrocarbons (TPH-d), 1-methylnaphthalene (1-MNAPH), 2-methylnaphthalene (2-MNAPH), and naphthalene (NAPH). Figure 1-1 provides the locations of the Facility monitoring wells in relation to the tank farm. Data analysis/interpretation methods are described in Section 2.

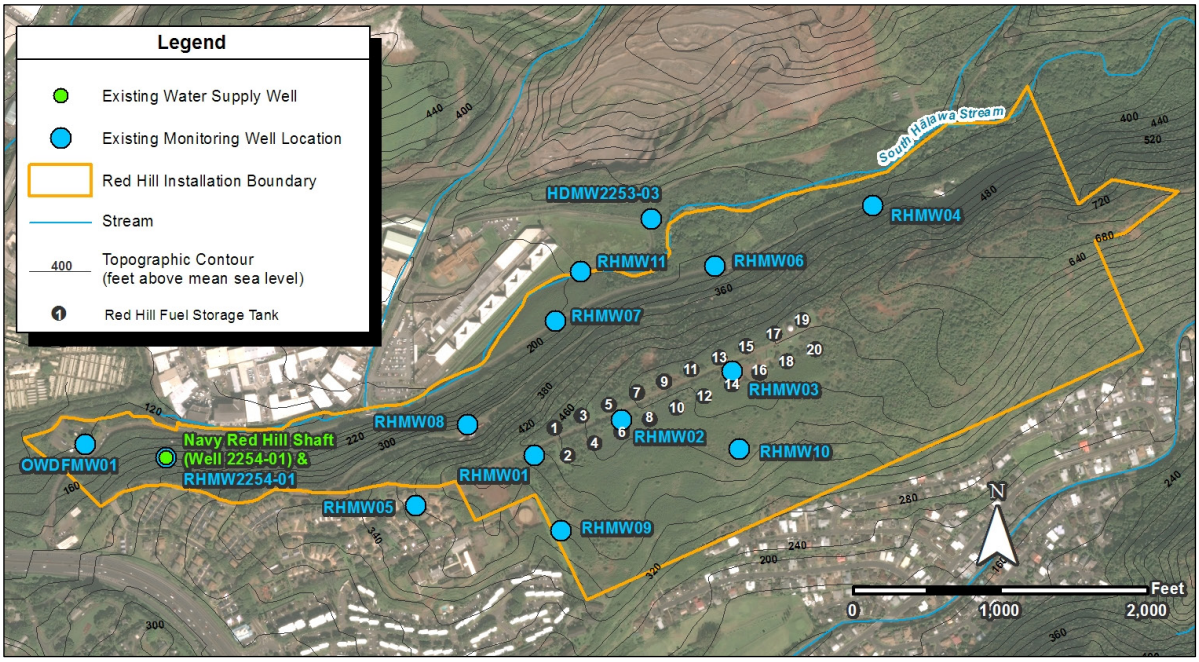

Figure 1-1: Location of the Facility Monitoring Wells in Relation to Tank Farm Area

2. Methods

Groundwater data from October 2016 to present (April 2018) were evaluated for all monitoring wells in the Facility network. Limited data from 2005 and 2006 were also included for monitoring wells RHMW01, RHMW02, RHMW03, and RHMW04, which were installed in 2001 (RHMW01) and 2005 (RHMW02, RHMW03, and RHMW04).

Two key lines of secondary evidence used to support MNA processes at the Facility, specifically biodegradation of COPCs, are summarized below (Beck and Mann 2010):

- **Depletion of TEAs:** Reduction of oxygen (O_2), nitrate (NO_3^-), and sulfate (SO_4^{2-}), in combination with declining COPC concentrations, provide strong evidence that COPC mass is being biodegraded, rather than simply attenuated by other mechanisms (e.g., volatilization, sorption, dilution).
- **Production of byproducts:** Detection and/or increasing concentrations of ferrous iron (Fe^{2+}), methane (CH_4), and carbon dioxide (CO_2; measured as alkalinity) provide supporting evidence of microbially mediated redox reactions. When all the soluble electron acceptors (i.e., dissolved oxygen, nitrate, ferric iron, and sulfate) are depleted, groundwater conditions become conducive to fermentation and methane is generated by methanogenesis. When evaluated alongside depressed dissolved oxygen concentrations, the presence of methane is a strong line of evidence of anaerobic biodegradation.

Based on well-established MNA guidance (Newell, McLeod, and Gonzales 1996; EPA 1999; Wiedemeier, Wilson, et al. 1999; Wiedemeier, Rifai, et al. 1999), time-series plots, spatial contour maps, and X-Y plots (COPC concentrations vs. TEA or byproduct concentrations) were developed to improve interpretation and analysis of the dataset.

2.1 Data Handling and Consolidation

For this analysis, historical data from 2005 to April 2018 were considered, with the following modifications to the dataset:

- COPC concentrations reported by the laboratory as non-detect were assigned a concentration equal to the laboratory-reported limit of detection (LOD) (e.g., < 0.1 microgram per liter [µg/L] = 0.1 µg/L). The LOD is the smallest COPC concentration that must be present in a sample to be detected at the detection limit (DL) with 99% confidence.
- Qualified data (e.g., "J" flag) were assigned the reported COPC concentration (e.g., 12 J µg/L = 12 µg/L). When a COPC is detected at a concentration below the LOD, the laboratory reports the result as detected, but the result is flagged with a "J" flag to indicate that the detected concentration was less than the LOD.
- For sampling events where duplicates were collected, the average of the primary concentration and duplicate concentration was used for each COPC.

3. Results

3.1 SPATIAL CONCENTRATIONS OF GEOCHEMICAL INDICATORS

Figure 3-1 presents concentrations of electron acceptors (O_2, NO_3^-, SO_4^{2-}), metabolic byproducts (Fe^{2+}, CH_4), and ORP for the most recent groundwater sampling event (April 23–25, 2018) at the Facility. In addition, Figure 3-2, Figure 3-3, and Figure 3-4 provide groundwater concentration contours for O_2, SO_4^{2-}, and CH_4, respectively, from the same sampling event. Major findings/observations are summarized below:

- Spatial patterns observed for this most recent sampling event (April 2018) are consistent with those observed for prior sampling events for TEAs (O_2, NO_3^-, SO_4^{2-}) and metabolic byproducts (Fe^{2+}, CH_4). As shown on Figure 3-1 to Figure 3-4, concentrations of O_2, NO_3^-, and SO_4^{2-} at monitoring wells RHMW01 and RHMW02 are much lower than concentrations in wells outside of the tank farm area. In addition, higher concentrations of Fe^{2+} and CH_4 are observed at these wells, relative to rest of the monitoring network. These observations strongly suggest that microbially mediated reactions are responsible for degradation of petroleum hydrocarbons (electron donor), depletion of available TEAs, and generation of anaerobic conditions (i.e., low O_2 and negative ORP values) at monitoring wells RHMW01 and RHMW02. At RHMW04 (located upgradient of the tank farm), SO_4^{2-} concentrations are consistently lower than might be expected (compared to the SO_4^{2-} distribution for the rest of the monitoring network [Figure 3-3]). This observation is not consistent with other geochemical indicators (O_2, NO_3^-, Fe^{2+}, CH_4, ORP), which appear to be more in line with neighboring wells. As a result, the SO_4^{2-} concentration at RHMW04 was excluded from the groundwater contouring in Figure 3-3.
- For the most recent sampling event (April 2018), concentrations of O_2 were very low (< 1 milligram per liter [mg/L]) at RHMW01 and RHMW02 compared to the wells located outside of the tank farm area (where O_2 concentrations were generally greater than 4 mg/L). Likewise, ORP values consistent with mildly reducing conditions were reported at these wells. ORP values for wells located outside of the tank farm area were greater than 100 millivolts (mV), consistent with aerobic conditions.
- During the most recent sampling event (April 2018), the highest concentrations of Fe^{2+} and CH_4 and lowest concentrations of O_2, NO_3^-, and SO_4^{2-} were observed at RHMW02 (where COPC concentrations are greatest). A similar relationship (depletion of TEAs, increase in byproducts, presence of TPH-d) was observed at RHMW01. These observations are consistent with active hydrocarbon biodegradation in this area. At RHMW03, depletion of TEAs and production of metabolic byproducts were not observed to the same extent (with the exception of low dissolved oxygen [DO]), despite the presence of detectable concentrations of TPH-d. This is potentially due to the influx of groundwater from upgradient of RHMW03.

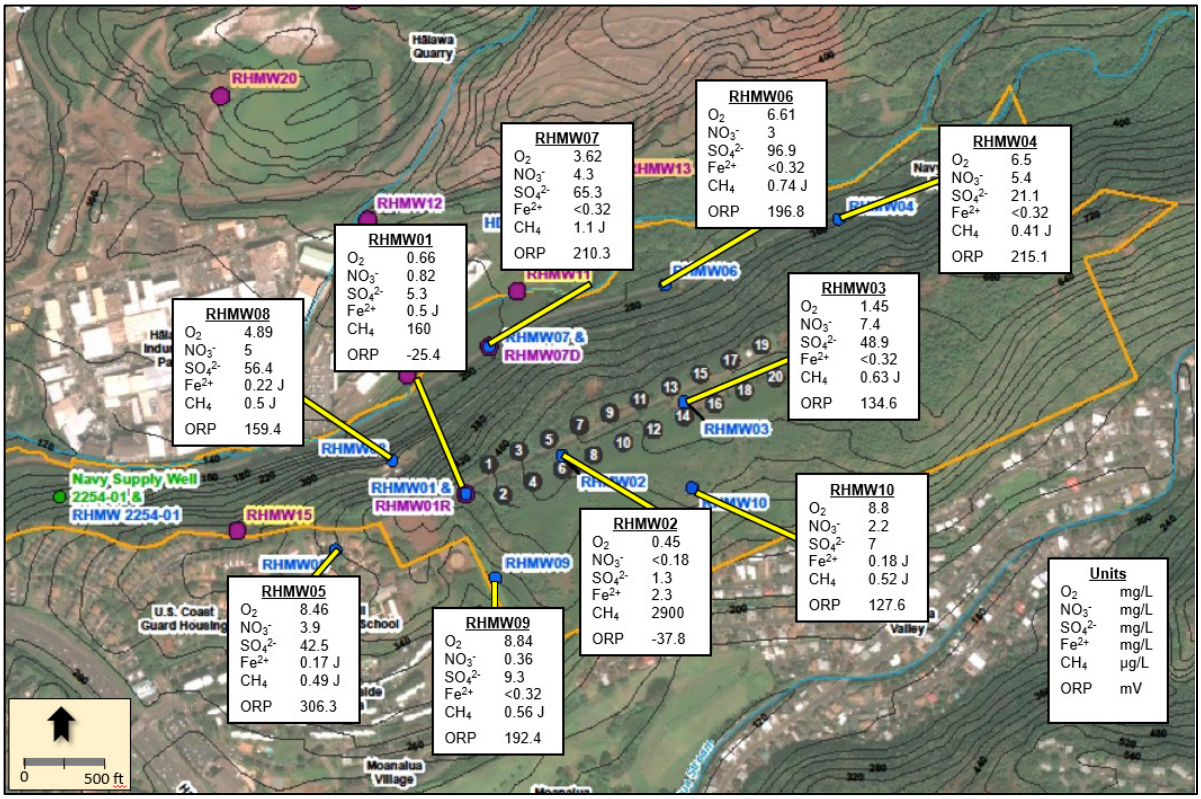

Figure 3-1: Concentrations of O_2, NO_3^-, SO_4^{2-}, Fe^{2+}, CH_4 and ORP from the Facility Groundwater Monitoring Network on April 23–25, 2018

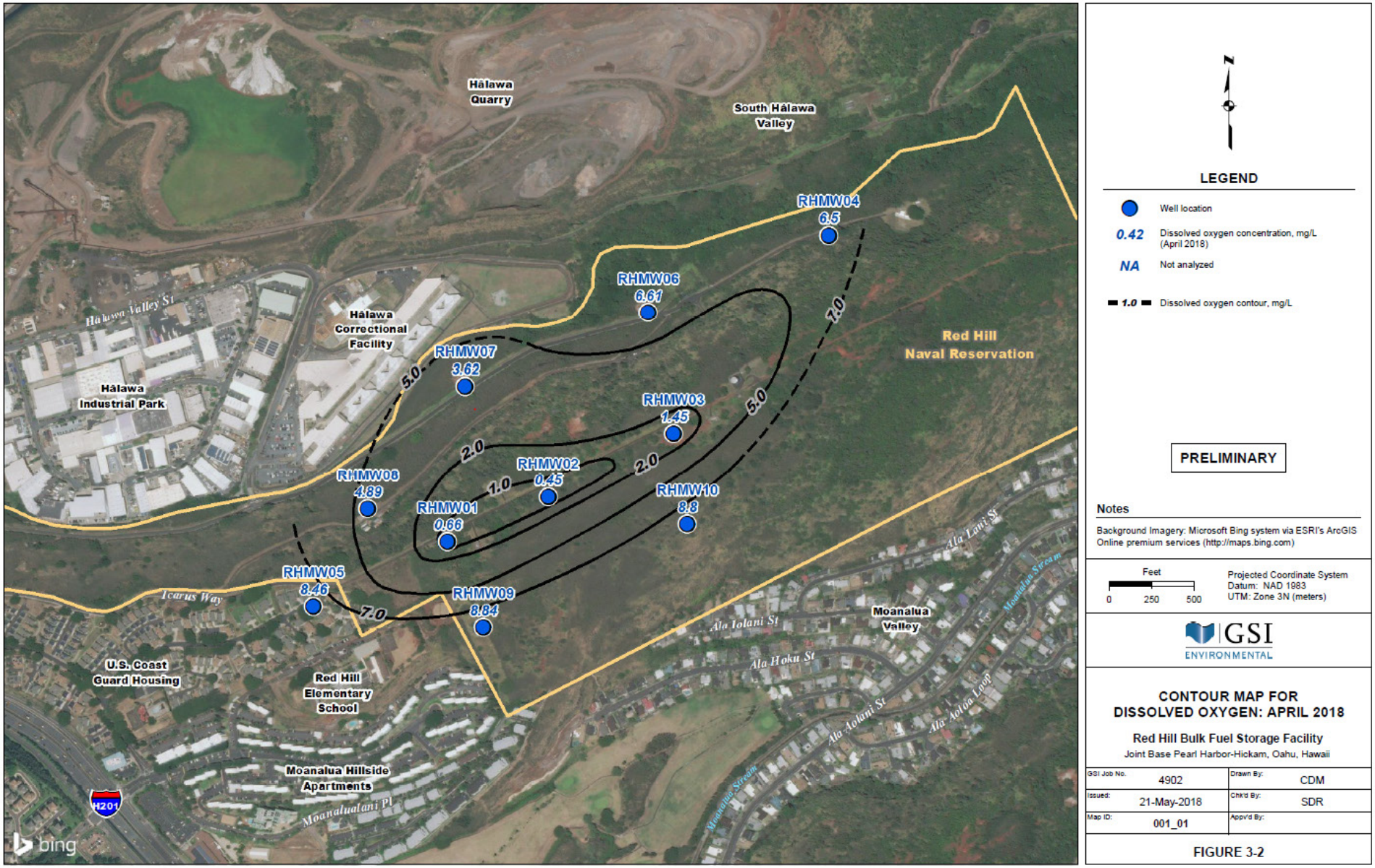

Figure 3-2: Contour Plot of O_2 Concentrations from the Facility Groundwater Monitoring Network (April 23–25, 2018)

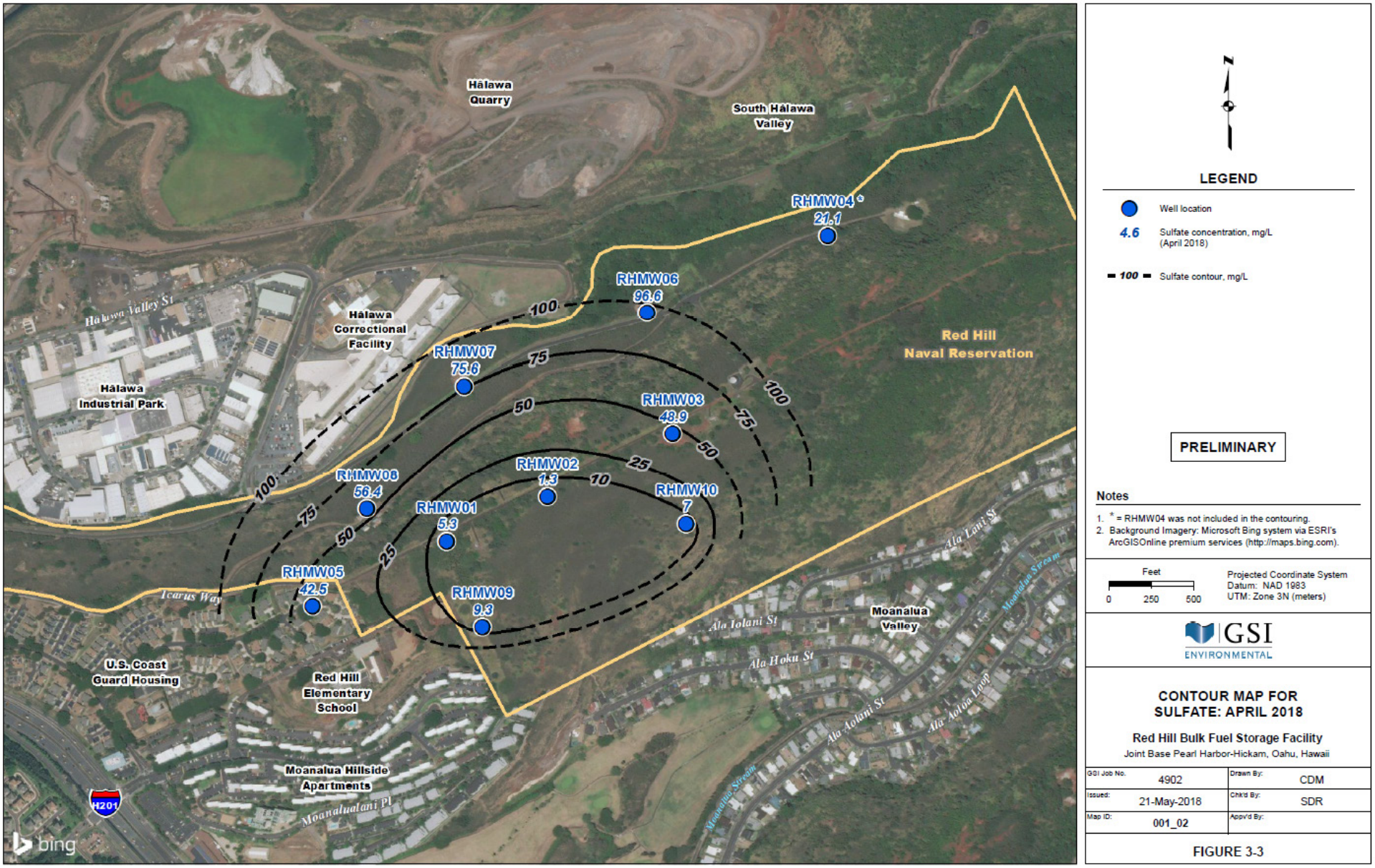

Figure 3-3: Contour Plot of SO_4^{2-} Concentrations from the Facility Groundwater Monitoring Network (April 23–25, 2018)

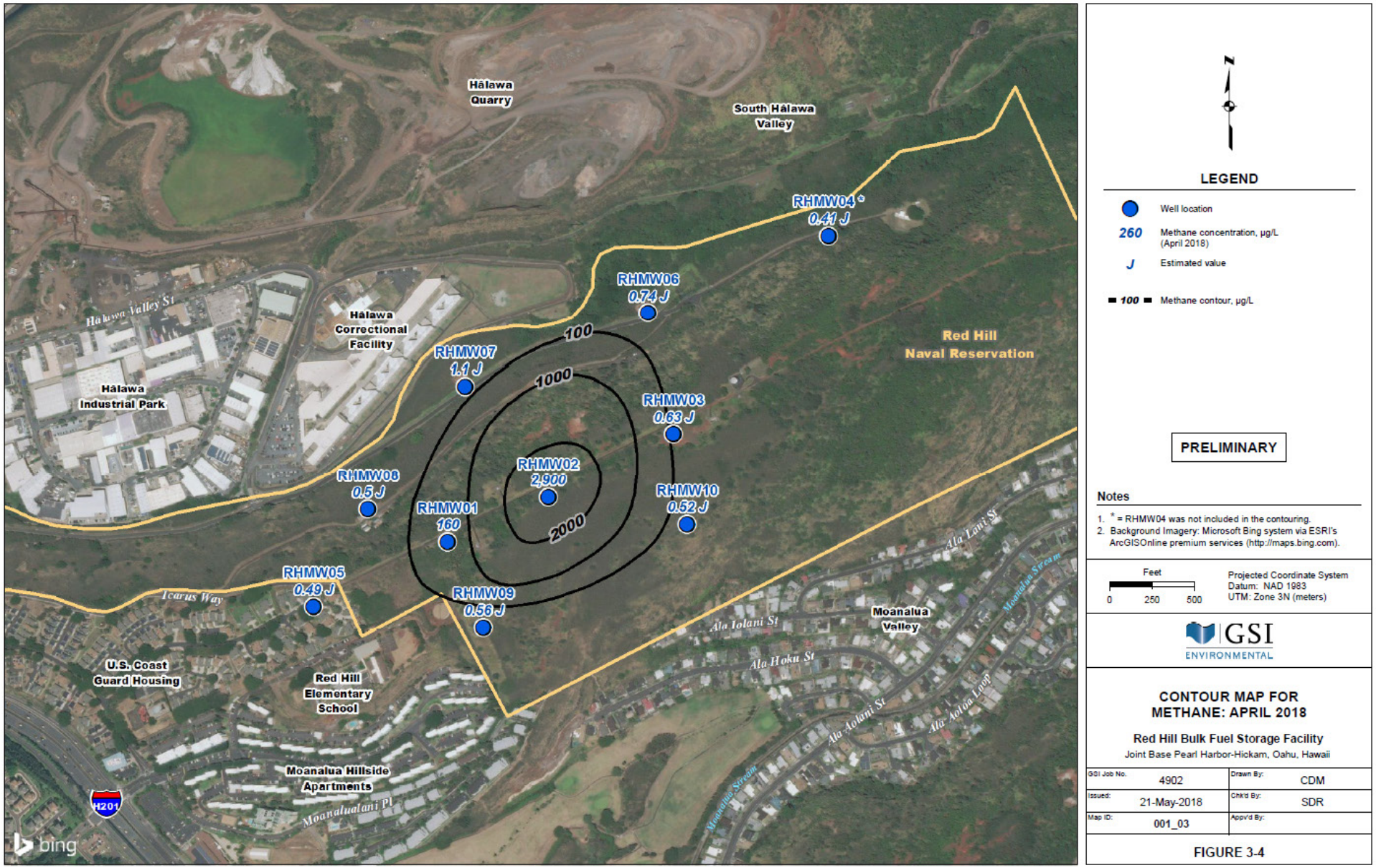

Figure 3-4: Contour Plot of CH_4 Concentrations from the Facility Groundwater Monitoring Network (April 23–25, 2018)

3.2 TEMPORAL CONCENTRATIONS OF GEOCHEMICAL INDICATORS

Attachment B.5.1 presents time-series plots for COPCs, electron acceptors, and metabolic byproducts at all Facility monitoring locations. For each analyte, three plots are presented: (1) all available data from September 2005 to April 2018 for all wells, (2) data from October 2016 to April 2018 for all wells, and (3) data from October 2016 to April 2018 for wells RHMW01, RHMW02, RHMW03, and RHMW05. In general, concentrations of electron acceptors and metabolic byproducts at each well have remained stable over the monitoring period (2016–2018), with a few exceptions (as discussed below).

Figure 3-5 and Figure 3-6 present NO_3^-, SO_4^{2-}, Fe^{2+}, and CH_4 concentrations from October 2016 to April 2018 for four monitoring wells RHMW01, RHMW02, RHMW03, and RHMW05. These wells were selected for analysis based on the assumption that primary groundwater flow direction is towards Red Hill Shaft (generally from RHMW03 to RHMW05). Efforts to develop an improved understanding of groundwater flow at the Facility are ongoing.

Major findings/observations are summarized below:

- Concentrations of NO_3^-, Fe^{2+}, and SO_4^{2-} have remained fairly stable (with only minor fluctuations) at these monitoring wells from October 2016 to April 2018. Methane concentrations at RHMW01 and RHMW02 have decreased over the same period. Specifically, CH_4 concentrations at RHMW01 have decreased from 7,500 µg/L (November 2016) to 160 µg/L (April 2018); at RHMW02, concentrations have declined from 47,000 µg/L (October 2016) to 2,900 µg/L (April 2018). In 2005 and 2006, concentrations of CH_4 at RHMW01 were 811 and 5,530 µg/L, respectively; at RHMW02, concentrations were 1,400 and 3,160 µg/L, respectively. However, in 2005–2006, the groundwater samples were collected using a bailer (rather than a bladder pump from 2016 to present). The 2005/2006 methane concentration results are likely biased low due to loss of methane from the bailer during sample collection. As a result, these older methane results are not included in Attachment B.5.1.
- As discussed in Section 3.1, concentrations of electron acceptors (O_2, NO_3^-, SO_4^{2-}) are greatest at monitoring wells RHMW03 and RHMW05, located generally upgradient and downgradient respectively, of RHMW02. In the case of SO_4^{2-}, concentrations at RHMW03 and RHMW05 are very similar (Figure 3-5), supporting that geochemical conditions are re-established along the presumed direction of groundwater flow within the tank farm area (i.e., toward Red Hill Shaft). Low to non-detect concentrations of Fe^{2+} and CH_4 (Figure 3-6) at these wells further support this conclusion.

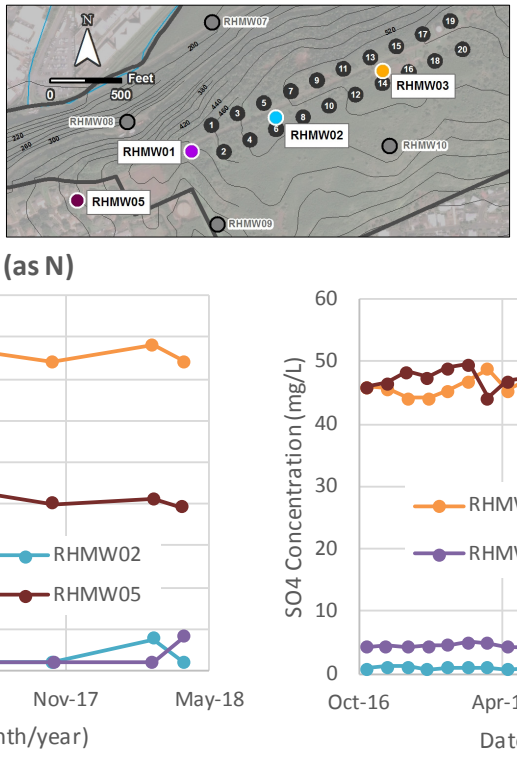

Figure 3-5: Time-Series Plots of NO_3^- (Left Panel) and SO_4^{2-} (Right Panel) Concentrations at Monitoring Wells RHMW01, RHMW02, RHMW03, and RHMW05

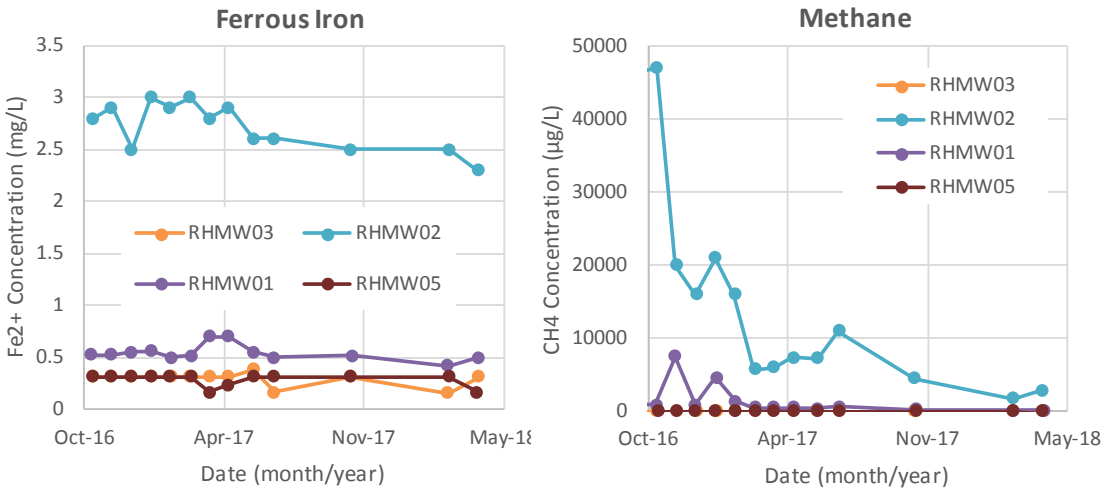

Figure 3-6: Time-Series Plots of Fe^{2+} (Left Panel) and CH_4 (Right Panel; y-axis: log-scale) Concentrations at Monitoring Wells RHMW01, RHMW02, RHMW03, and RHMW05

3.3 KEY RELATIONSHIPS BETWEEN COPCS AND GEOCHEMICAL INDICATORS

Attachment B.5.2 presents X-Y plots for all COPCs (TPH-d, TPH-g, TPH-o, 1-MAPH, 2-MAPH, NAPH) relative to concentrations of electron acceptors and metabolic byproducts at all Facility monitoring locations. For the X-Y graphs, the x-axis represents COPC concentrations; y-axis represents electron acceptor or metabolic byproduct concentrations. Since COPCs are detected primarily at RHMW02 (with some detections and qualified detections of select COPCs at RHMW01 and RHMW03) over the monitoring period, these X-Y plots clearly highlight the distinct difference in geochemistry and COPC concentrations at RHMW02 compared to the rest of the monitoring network (i.e., grouping of RHMW02 data stands apart from other wells). For cases where a COPC is also detected at RHMW01 and RHMW03 (i.e., TPH-d), some general trends are observed on the plots. For example, as shown on Figure 3-7 and Figure 3-8, the highest TPH-d concentrations (at RHMW02) are generally related to decreasing NO_3^- and SO_4^{2-} concentrations and increasing Fe^{2+} and CH_4 concentrations. This finding is consistent with microbially mediated degradation of petroleum hydrocarbons (electron donor) within the tank farm. However, during the monitoring period 2005–2018, several different laboratories were used for analysis of groundwater samples. Some of the increases and decreases in TPH-d concentrations over time appear to be an artifact of analytical differences between laboratories (see CSM Appendix B.7 for further discussion). Due to the laboratory uncertainty associated with the TPH-d analysis, apparent changes in TPH-d concentration over time may not directly correlate with true changes in the magnitude of impact.

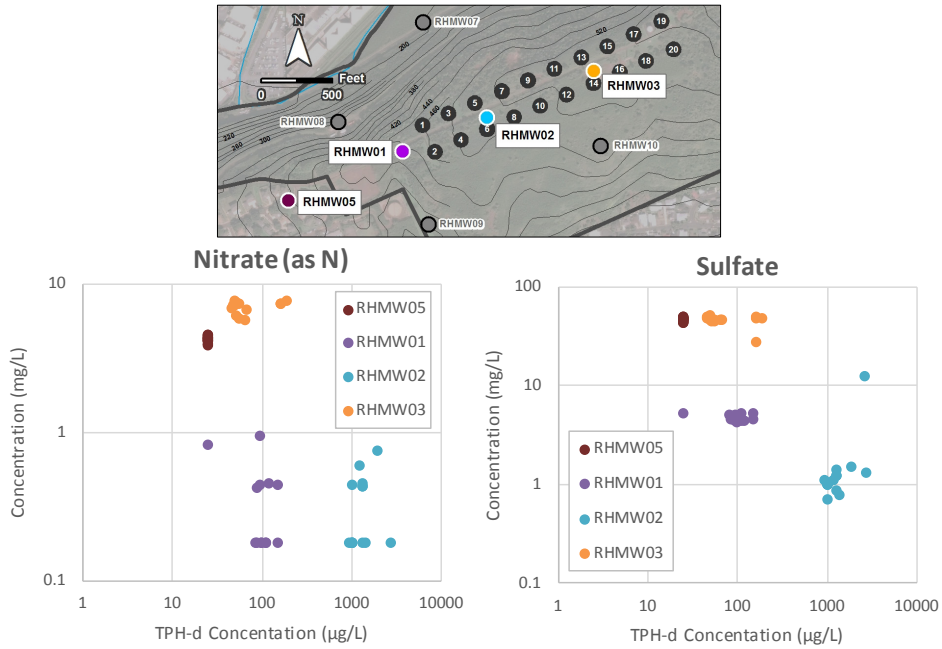

Figure 3-7: X-Y Plots for TPH-d Concentrations vs. NO_3^- (Left Panel) and SO_4^{2-} (Right Panel) Concentrations at Monitoring Wells RHMW01, RHMW02, RHMW03, and RHMW05

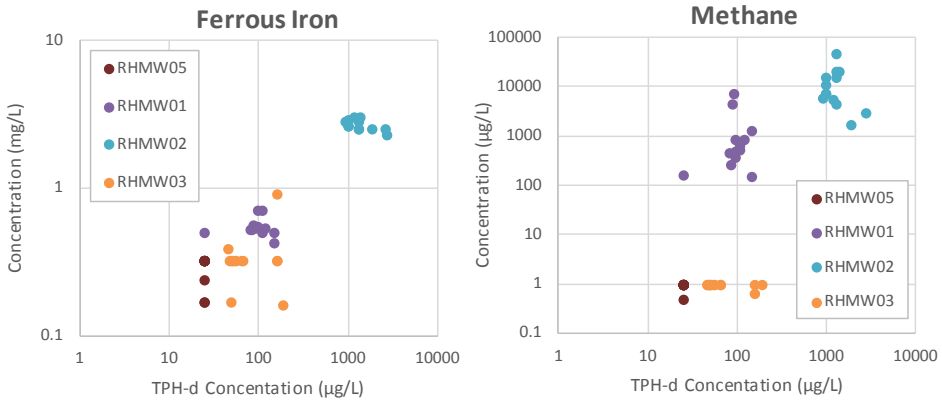

Figure 3-8: X-Y Plots for TPH-d Concentrations vs. Fe^{2+} (Left Panel) and CH_4 (Right Panel) Concentrations at Monitoring Wells RHMW01, RHMW02, RHMW03, and RHMW05

4. Conclusions

Time series, spatial contour maps, and X-Y plots were developed to evaluate natural attenuation processes at the Facility using secondary lines of evidence (i.e., geochemical indicators, electron acceptor concentrations). Historical groundwater data from October 2016 to present (April 2018) were evaluated for all monitoring wells in the Facility network; limited data from 2005 and 2006 were also included for select monitoring wells.

Spatial and temporal concentration trends for TEAs (O_2, NO_3^-, SO_4^{2-}) and metabolic byproducts (Fe^{2+}, CH_4) provide strong evidence for aerobic and anaerobic petroleum hydrocarbon degradation within the tank farm. In the area of highest COPC concentration (RHMW02), electron acceptors (O_2, NO_3^-, SO_4^{2-}) are depleted (or have low concentrations) and concentrations of metabolic byproducts (Fe^{2+}, CH_4) are elevated relative to the monitoring locations outside of the tank farm area. Low DO concentrations and negative ORP values further support anaerobic conditions in this area. These secondary lines of evidence strongly indicate that active and robust biodegradation of COPCs is occurring within the tank farm.

5. References

Beck, P., and B. Mann. 2010. *A Technical Guide for Demonstrating Monitored Natural Attenuation Of Petroleum Hydrocarbons in Groundwater*. CRC CARE Technical Report No 15, CRC Contamination Assessment and Remediation of the Environment. Adelaide, Australia.

Environmental Protection Agency, United States (EPA). 1999. *Use of Monitored Natural Attenuation at Superfund, RCRA Corrective Action, and Underground Storage Tank Sites*. OSWER 9200.4-17P. Office of Solid Waste and Emergency Response. April.

McCarty, P. L., B. E. Rittman, and E. J. Bouwer. 1984. "Microbial Processes Affecting Chemical Transformations in Groundwater." In *Groundwater Pollution Microbiology*. G. Britton and C. P. Gerba (Eds), Pp. 89–115. New York: John Wiley & Sons.

Newell, C. J., R. K. McLeod, and J. R. Gonzales. 1996. *BIOSCREEN Natural Attenuation Decision Support System User's Manual, Ver. 1.3*. Prepared for Air Force Center for Environmental Excellence (AFCEE) Technology Transfer Division at Brooks Air Force Base, by Groundwater Services, Inc., Houston.

Wiedemeier, T. H., H. S. Rifai, C. J. Newell, and J. T. Wilson. 1999. *Natural Attenuation of Fuels and Chlorinated Solvents in the Subsurface*. New York: John Wiley & Sons, Inc.

Wiedemeier, T. H., J. T. Wilson, D. H. Kampbell, R. N. Miller, and J. E. Hansen. 1999. *Technical Protocol for Implementing Intrinsic Remediation with Long-Term Monitoring for Natural Attenuation of Fuel Contamination Dissolved in Groundwater. Vols. I & II*. San Antonio, TX: Air Force Center for Environmental Excellence, Technology Transfer Division. March.

Attachment B.5.1: Time-Series Plots for Alkalinity, NO_3^-, SO_4^{2-}, Cl, Fe^{2+}, CH_4, and COPCs at All Monitoring Well Locations

Attachment B.5.1 – Time-series plots for Alkalinity, NO_3^-, SO_4^{2-}, Cl, Fe^{2+}, CH_4, and COPCs at all monitoring well locations

September 2005 - April 2018 (all wells)

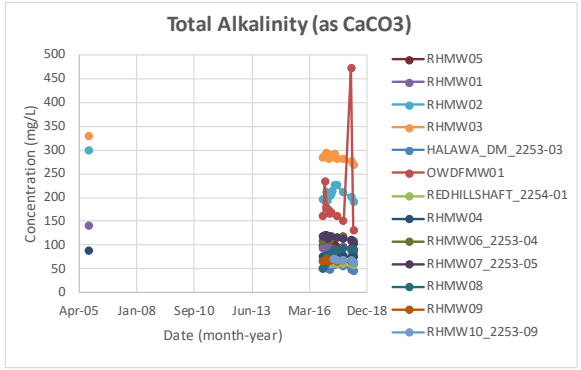

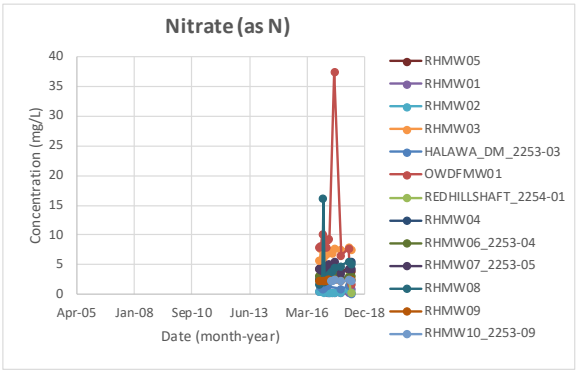

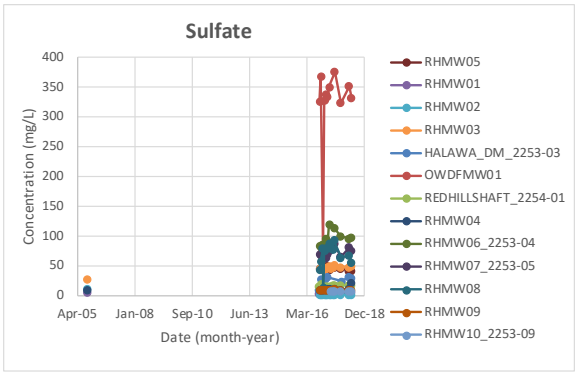

October 2016 - April 2018 (all wells)

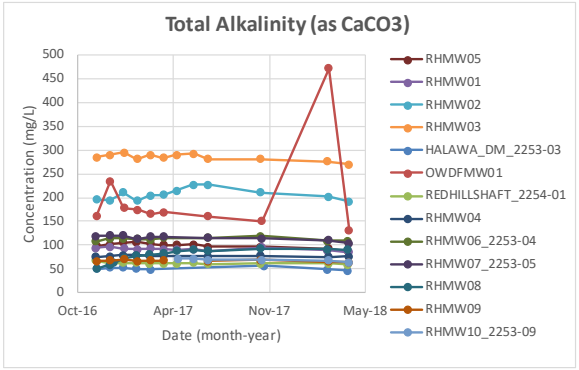

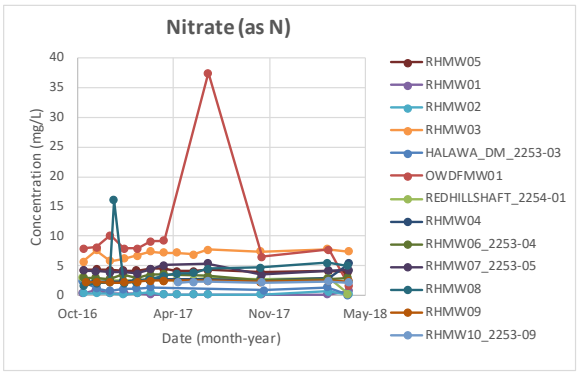

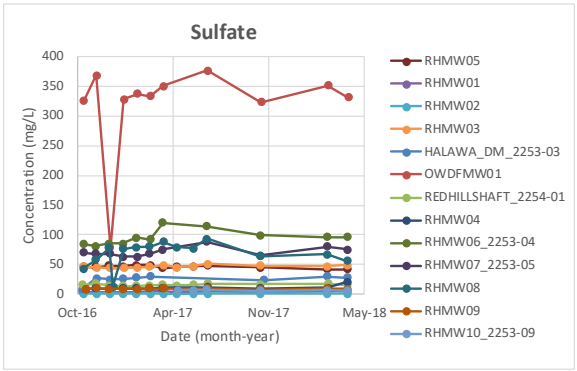

October 2016 - April 2018 (RHMW01, RHMW02, RHMW03, RHMW05)

Note: scale of y-axis may be different than plots to the left

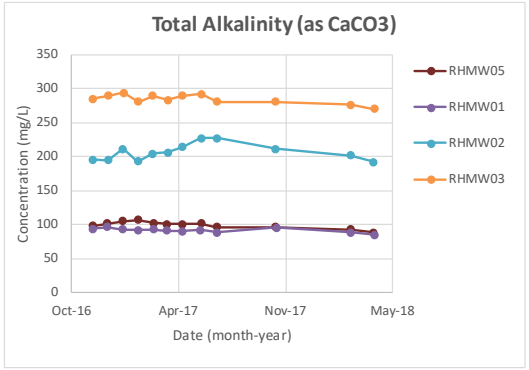

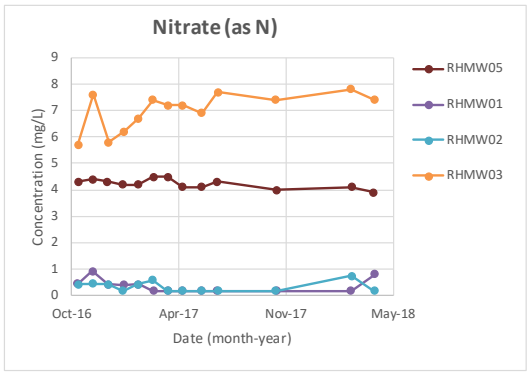

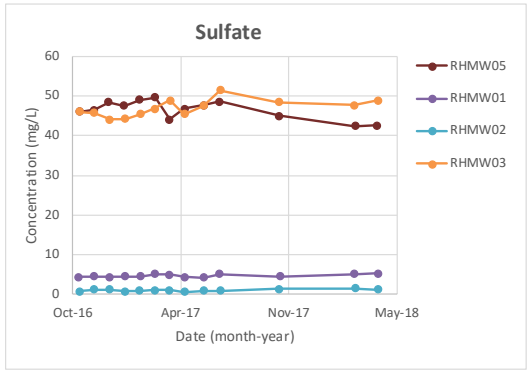

Attachment B.5.1 – Time-series plots for Alkalinity, NO_3^-, SO_4^{2-}, Cl, Fe^{2+}, CH_4, and COPCs at all monitoring well locations (continued)

September 2005 - April 2018 (all wells)

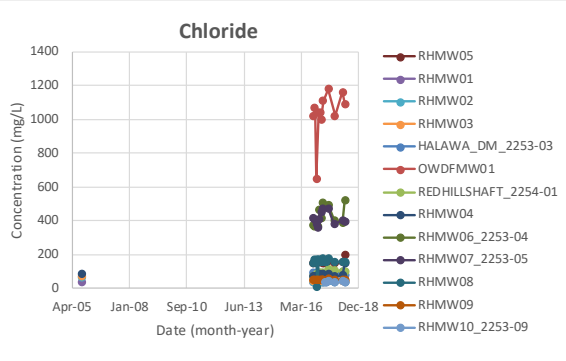

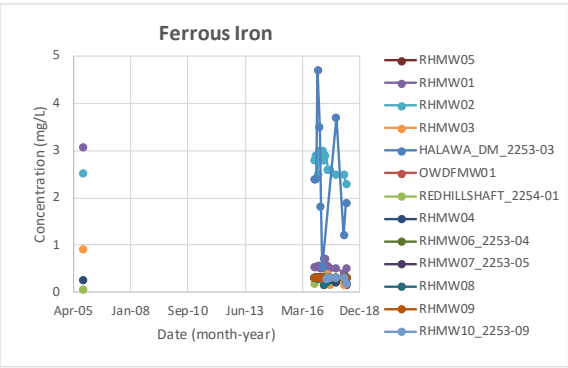

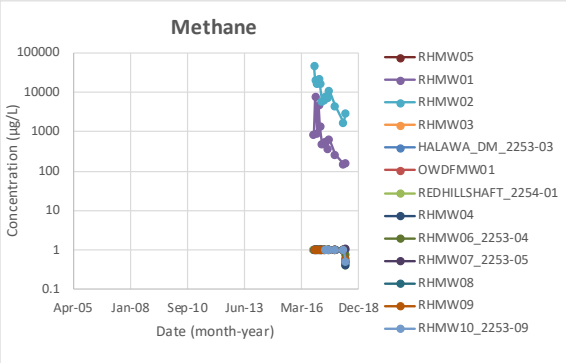

October 2016 - April 2018 (all wells)

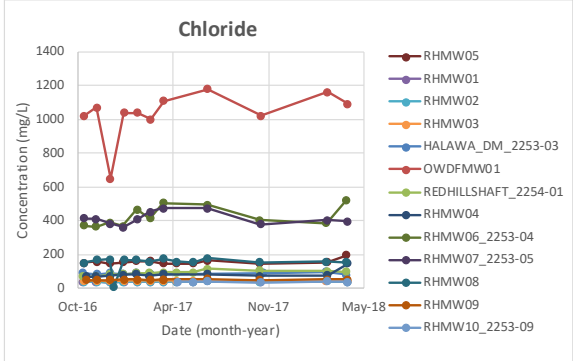

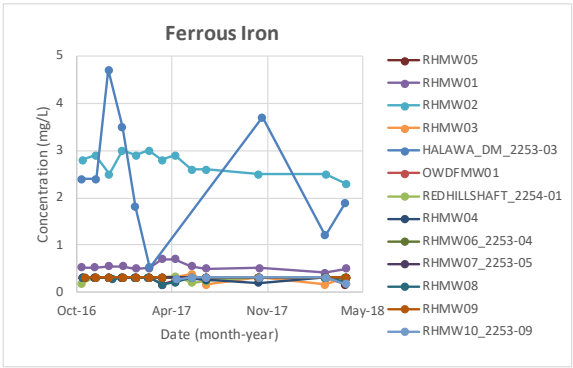

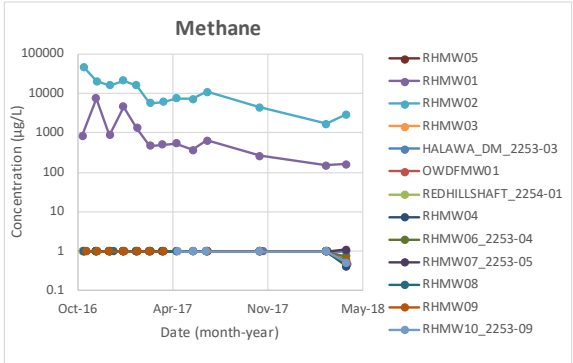

October 2016 - April 2018 (RHMW01, RHMW02, RHMW03, RHMW05)

Note: scale of y-axis may be different than plots to the left

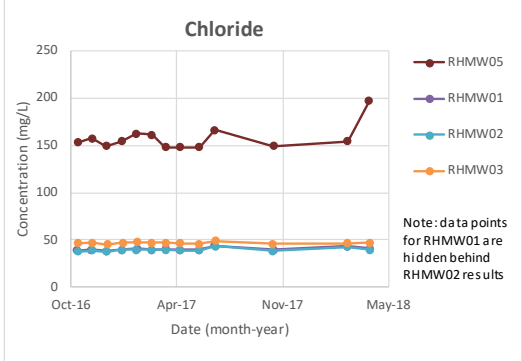

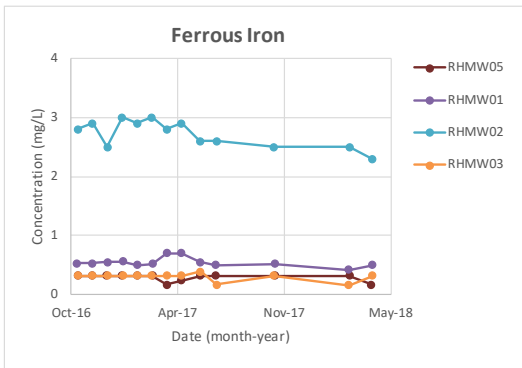

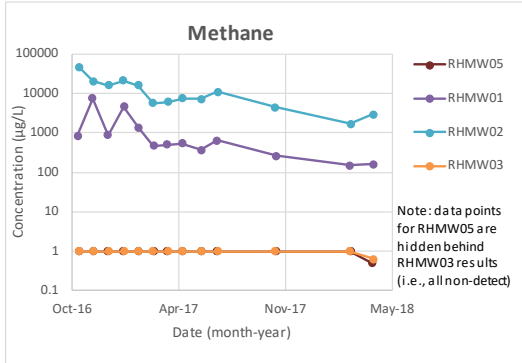

Attachment B.5.1 – Time-series plots for Alkalinity, NO_3^-, SO_4^{2-}, Cl, Fe^{2+}, CH_4, and COPCs at all monitoring well locations (continued)

September 2005 - April 2018 (all wells)

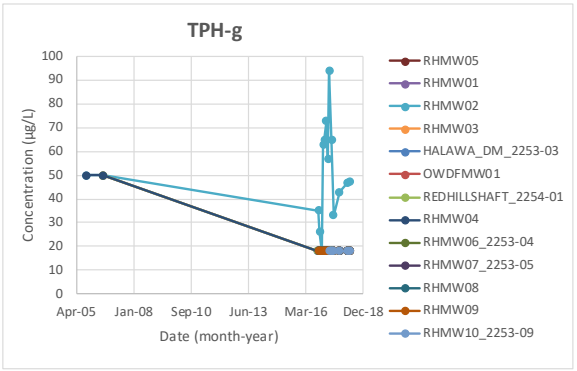

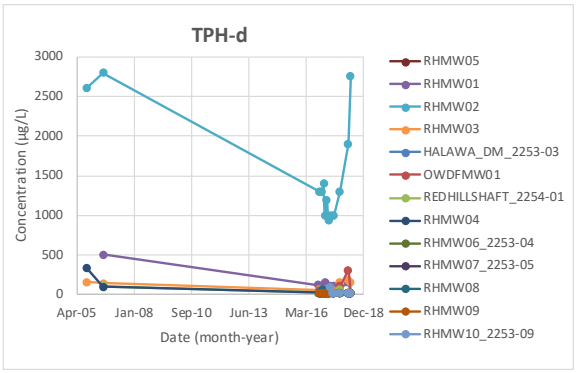

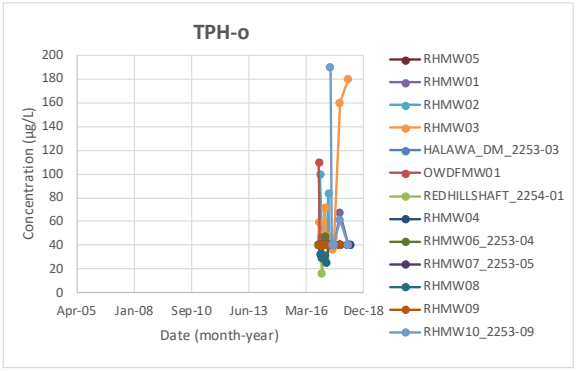

October 2016 - April 2018 (all wells)

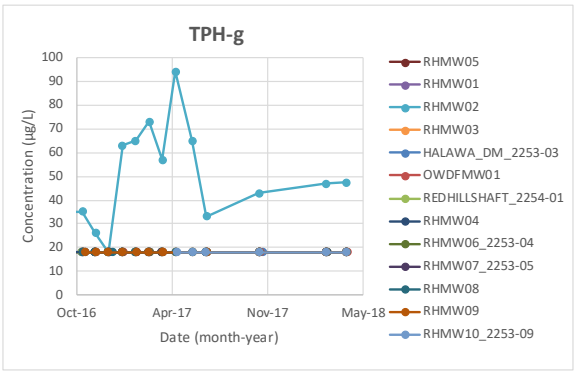

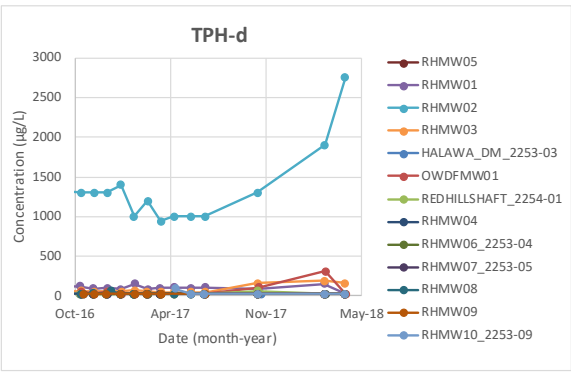

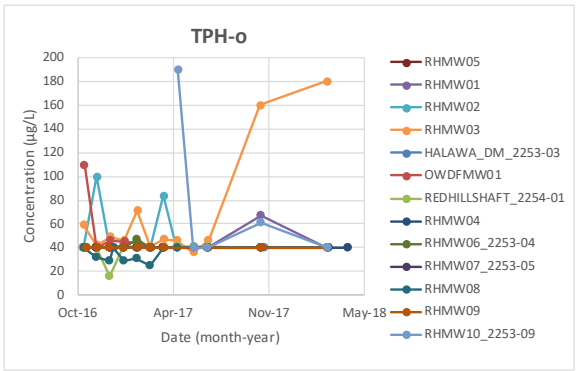

October 2016 - April 2018 (RHMW01, RHMW02, RHMW03, RHMW05)

Note: scale of y-axis may be different than plots to the left

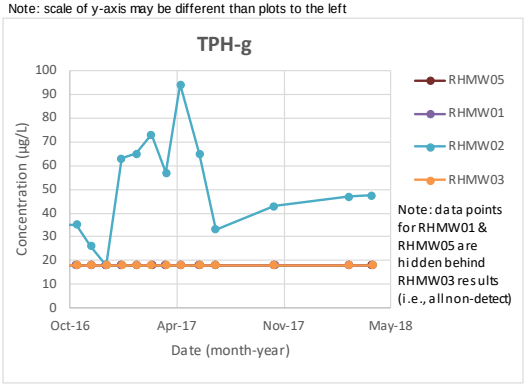

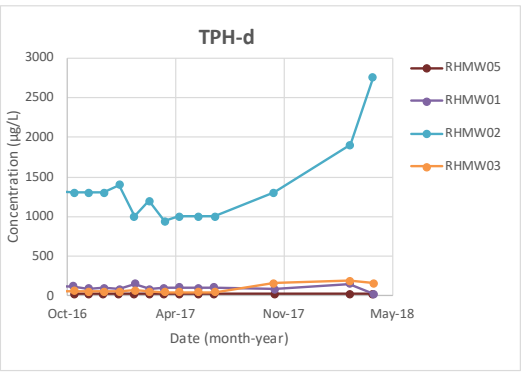

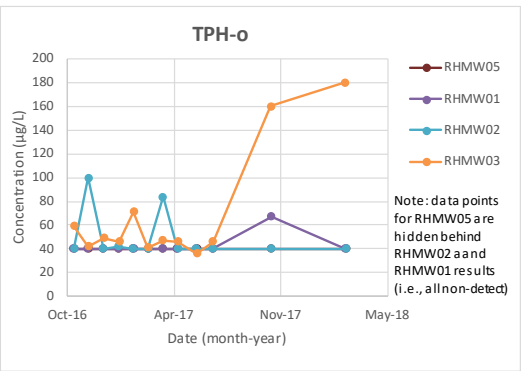

Attachment B.5.1 – Time-series plots for Alkalinity, NO_3^-, SO_4^{2-}, Cl, Fe^{2+}, CH_4, and COPCs at all monitoring well locations (continued)

September 2005 - April 2018 (all wells)

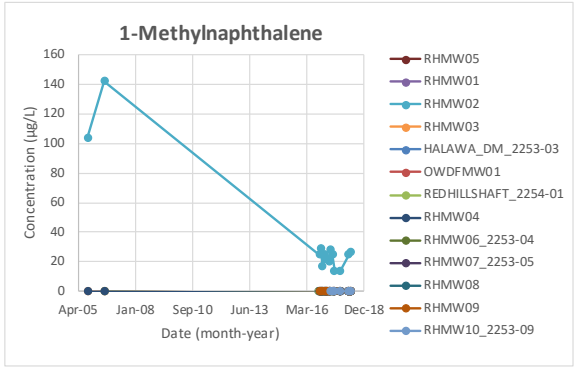

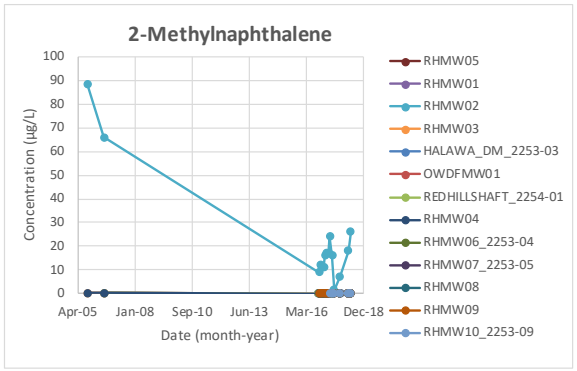

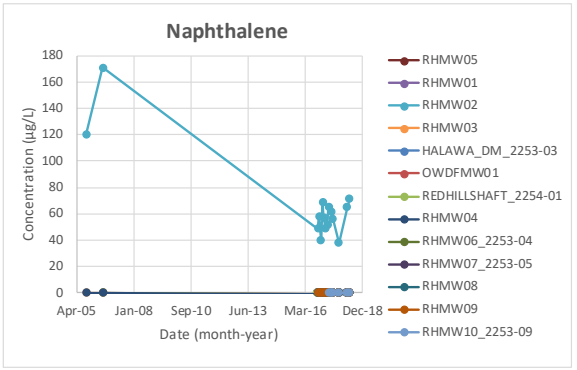

October 2016 - April 2018 (all wells)

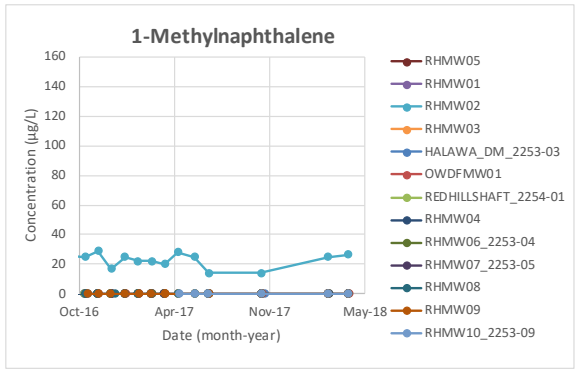

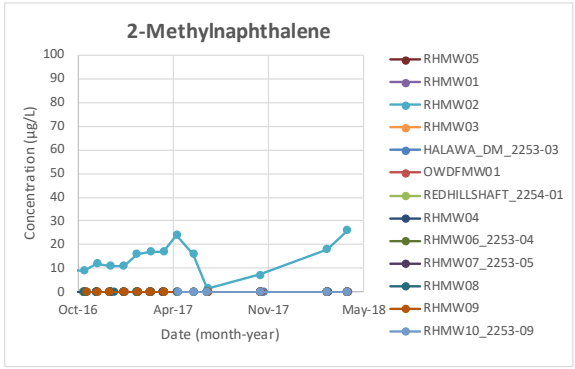

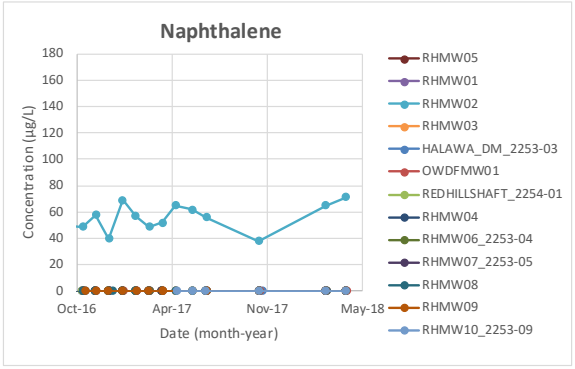

October 2016 - April 2018 (RHMW01, RHMW02, RHMW03, RHMW05)

Note: scale of y-axis may be different than plots to the left

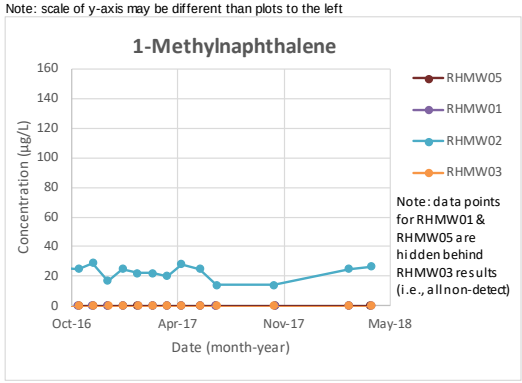

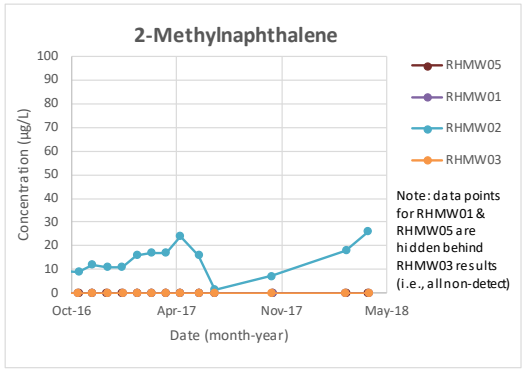

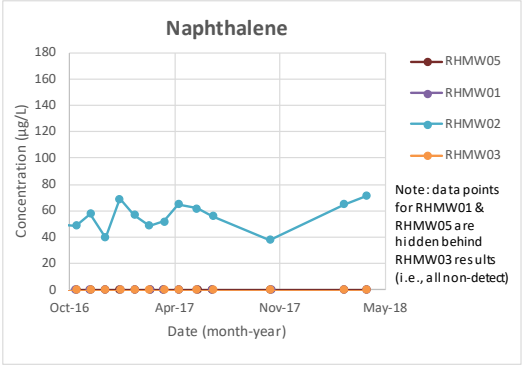

Attachment B.5.2:
X-Y Plots for Alkalinity, NO_3^-, SO_4^{2-}, Cl, Fe^{2+}, CH_4, and COPCs at All Monitoring Well Locations

Attachment B.5.2 – X-Y plots for Alkalinity, NO_3^-, SO_4^{2-}, Cl, Fe^{2+}, CH_4, and COPCs at all monitoring wells locations

TPH-d

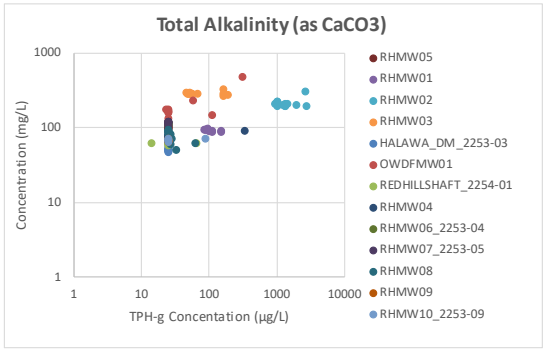

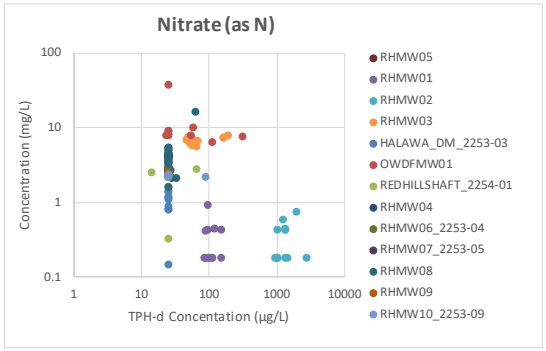

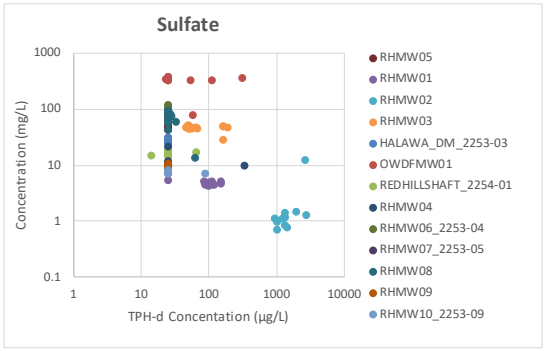

TPH-g

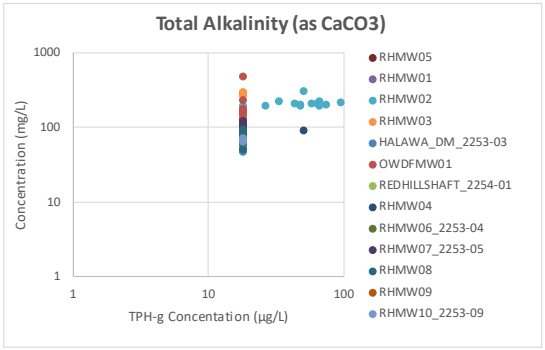

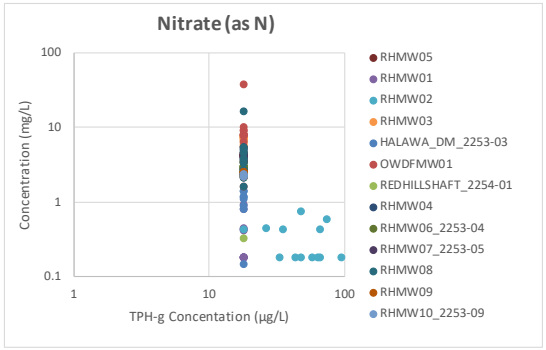

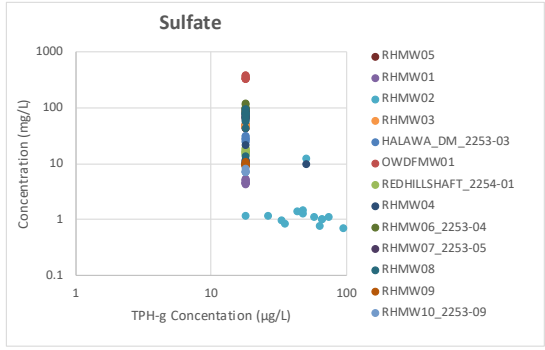

TPH-o

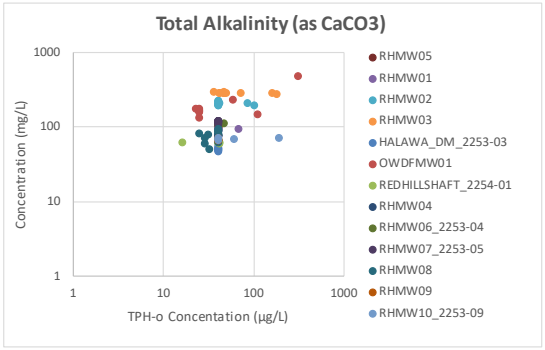

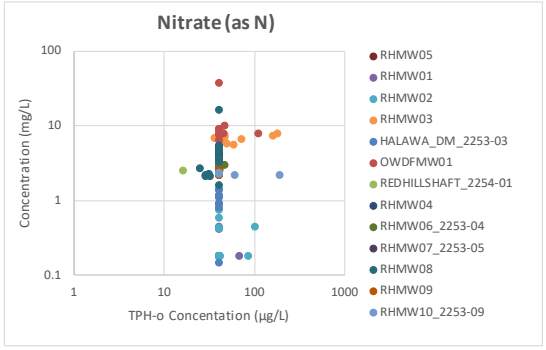

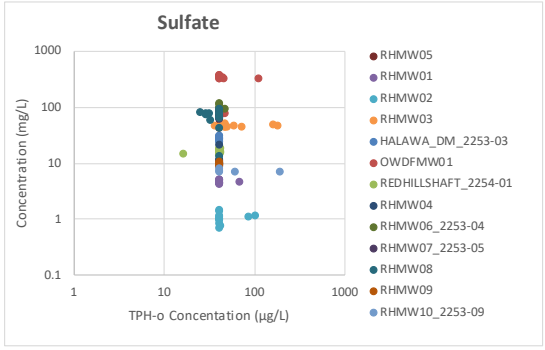

Attachment B.5.2 – X-Y plots for Alkalinity, NO_3^-, SO_4^{2-}, Cl, Fe^{2+}, CH_4, and COPCs at all monitoring wells locations (continued)

TPH-d

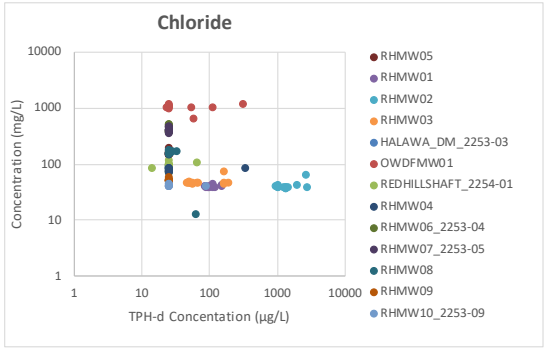

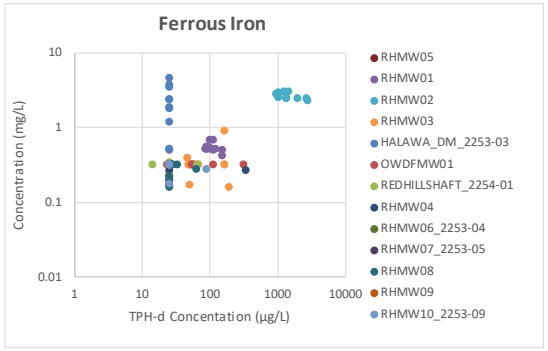

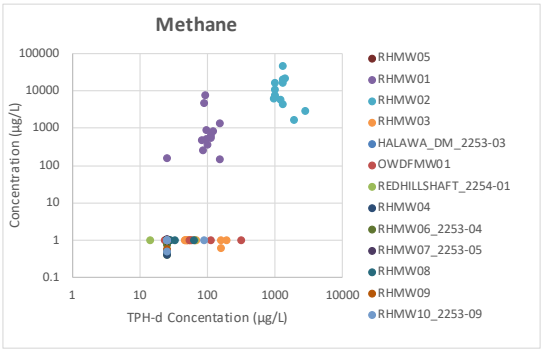

TPH-g

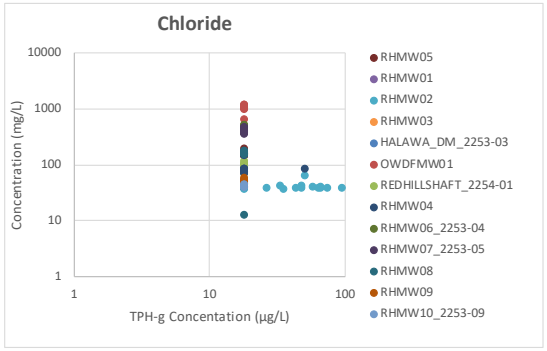

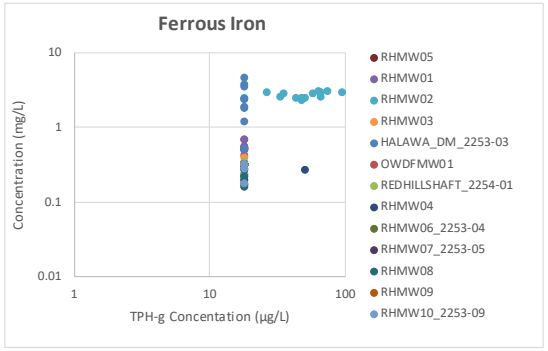

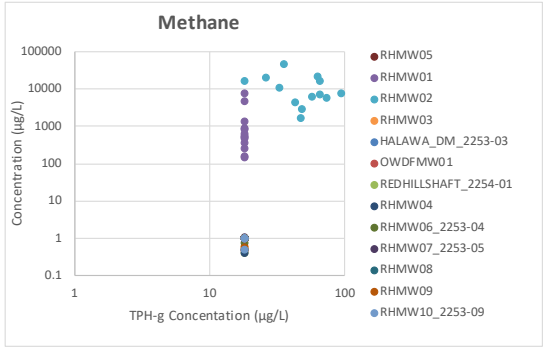

TPH-o

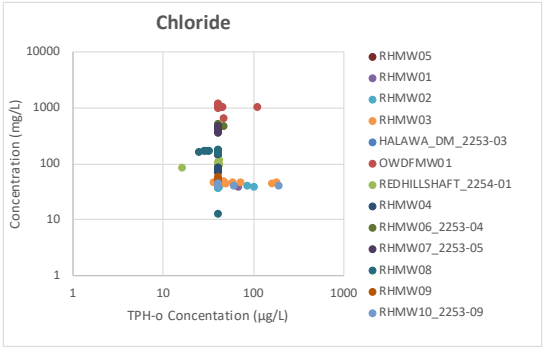

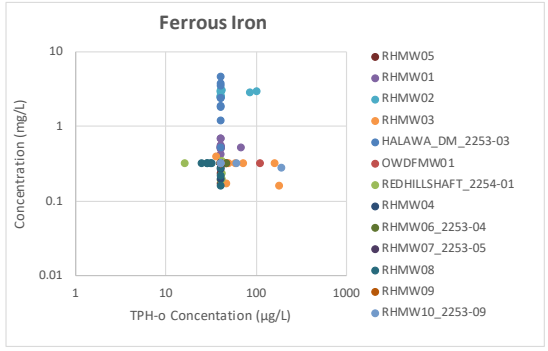

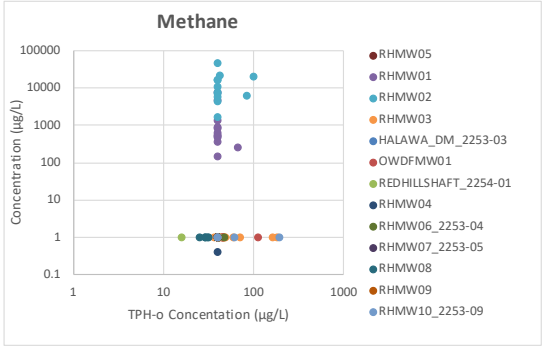

Attachment B.5.2 – X-Y plots for Alkalinity, NO_3^-, SO_4^{2-}, Cl, Fe^{2+}, CH_4, and COPCs at all monitoring wells locations (continued)

1-MNAPH

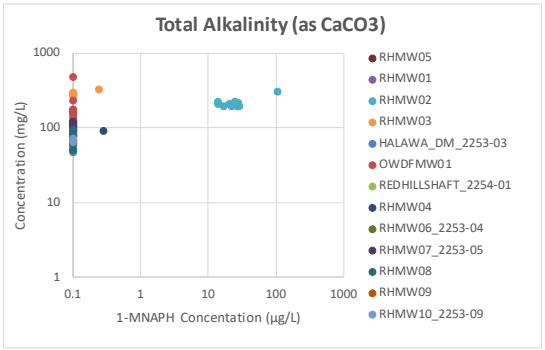

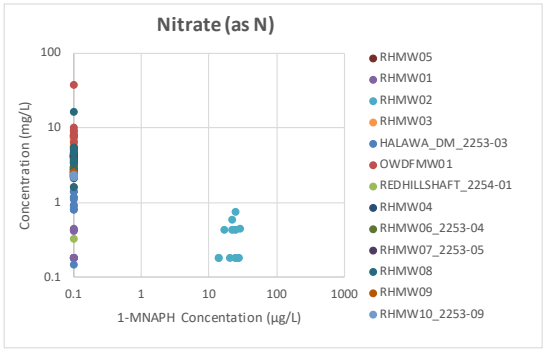

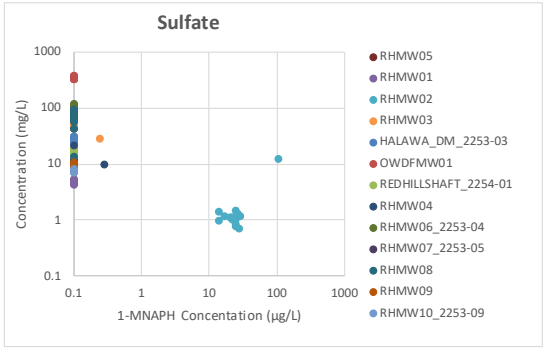

2-MNAPH

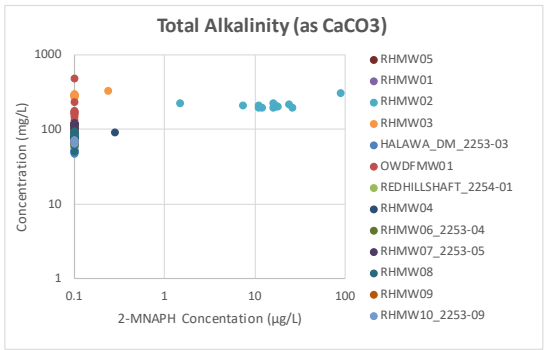

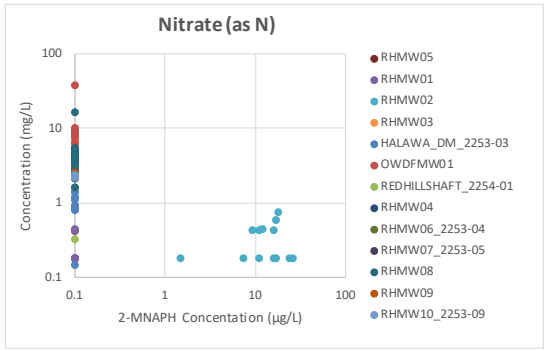

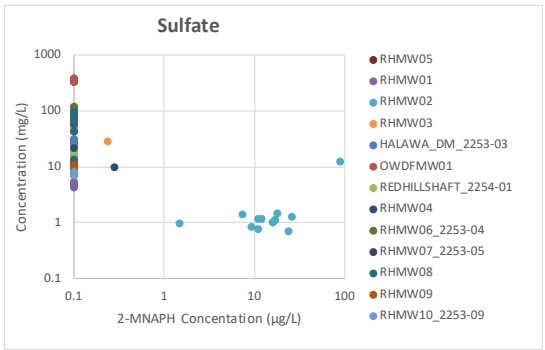

NAPH

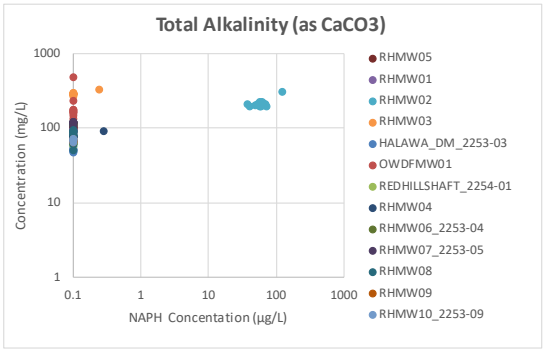

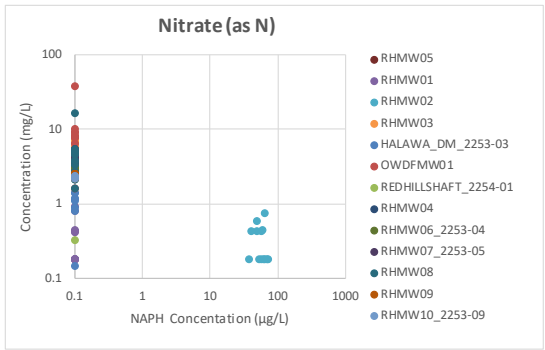

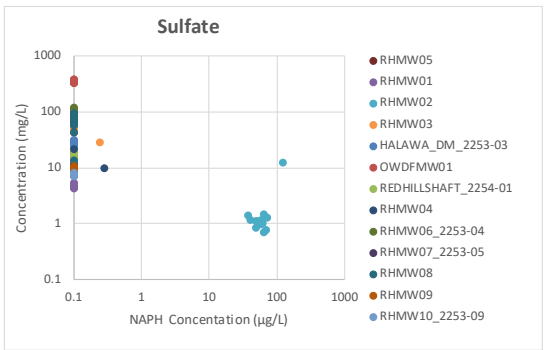

Attachment B.5.2 – X-Y plots for Alkalinity, NO_3^-, SO_4^{2-}, Cl, Fe^{2+}, CH_4, and COPCs at all monitoring wells locations (continued)

1-MNAPH

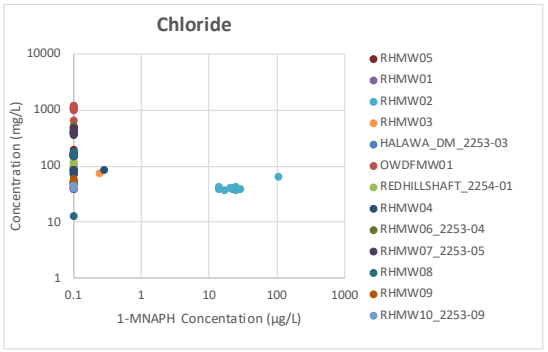

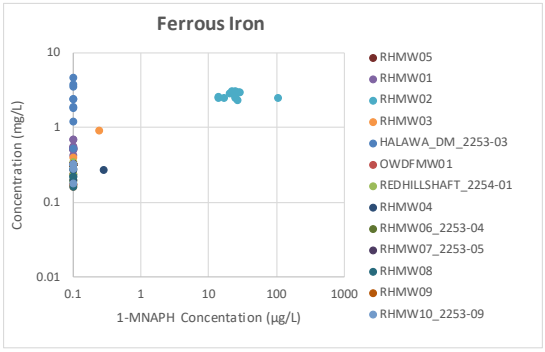

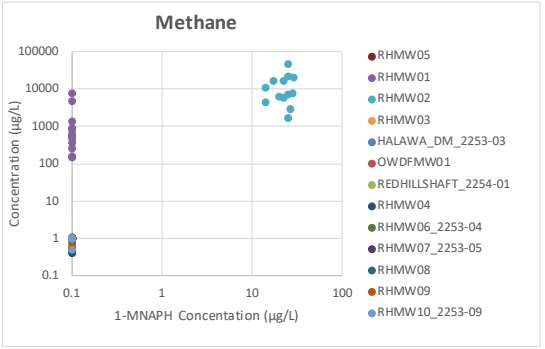

2-MNAPH

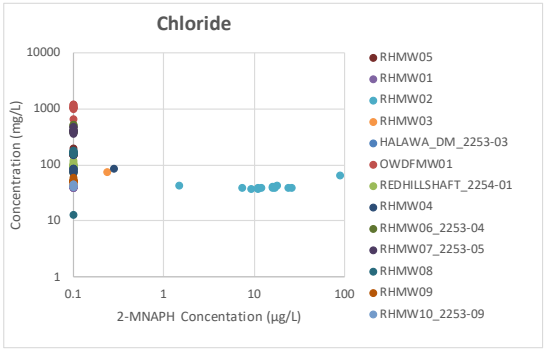

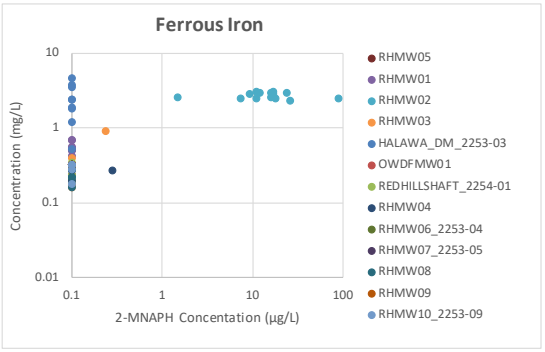

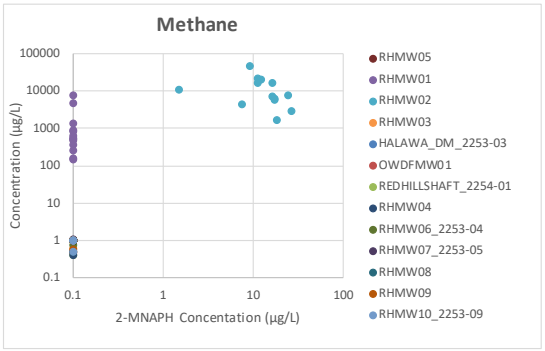

NAPH

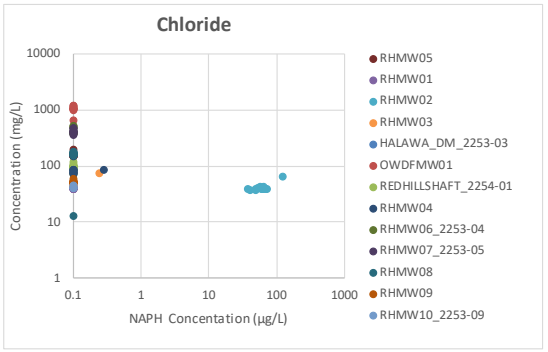

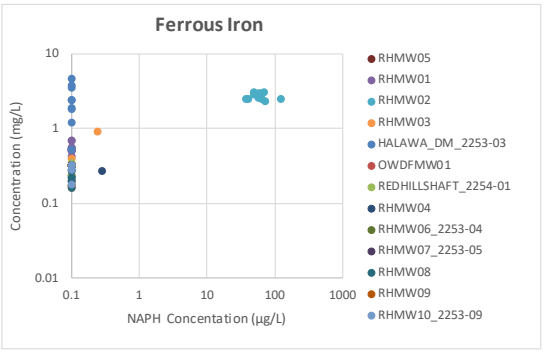

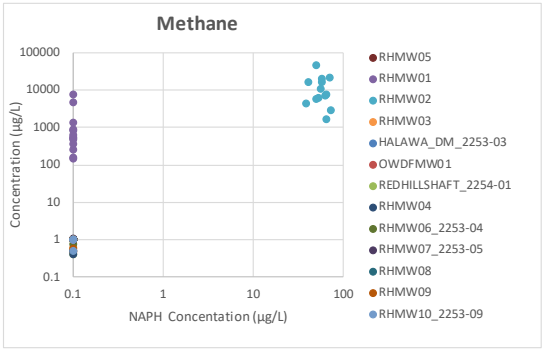

Appendix B.6:
Microcosm Study and Microbial Parameter Analysis

CONTENTS

Acronyms and Abbreviations ii

1. Introduction 1-1

2. Methods 2-1

2.1 Test Design 2-1
2.1.1 Microcosm Study 2-1
2.1.2 Microbial Parameters 2-2
2.2 Field Protocols for Sample Collection 2-3
2.2.1 Microcosm Study 2-3
2.2.2 Microbial Parameters 2-3
2.3 Laboratory Protocols for Analysis 2-4
2.3.1 Microcosm Study 2-4
2.3.2 Microbial Parameters 2-5

3. Results 3-1

3.1 Microcosm Study 3-1
3.2 Microbial Parameters 3-3

4. Conclusions 4-1

5. References 5-1

ATTACHMENTS

B.6.1 Summary of Current Data from Microcosm Study - Volatile Organic Compounds

B.6.2 Summary of Microbial Parameter Data

FIGURES

2-1 Location of Facility Wells Included in Microcosm Study (White Circles) and Microbial Parameter Analysis (Yellow Circles) 2-3

2-2 Bio-filters Used During Sample Collection for Microbial Parameter Analysis 2-4

3-1 Results of Microcosm Study: Benzene and Toluene 3-5

3-2 Results of Microcosm Study: Xylenes 3-6

3-3 Results of Microcosm Study: 1,2,4-Trimethylbenzene and 1-Methylnaphthalene 3-7

3-4 Results of Microcosm Study: 2-Methylnaphthalene and Naphthalene 3-7

TABLES

2-1 Summary of Target Initial Concentrations for Microcosm Study 2-2

2-2 Treatments and Controls for Microcosm Study 2-5

3-1 Constituent-Specific Rate Coefficients Based on Currently Available Data from Microcosm Study 3-1

ACRONYMS AND ABBREVIATIONS

µg/L	microgram per liter
1,2,4-TMB	1,2,4-trimethylbenzene
ANAT	anaerobic natural attenuation treatment
BCR	benzoyl-coenzyme A reductase
BTEX	benzene, toluene, ethylbenzene, and xylenes
COPC	chemical of potential concern
DHG	dissolved hydrogen gases
LNAPL	light non-aqueous-phase liquid
mL	milliliter
MTBE	methyl tert-butyl ether
mV	millivolt
NGS	Next Generation Sequencing
ONAT	oxygen-amended natural attenuation treatment
ORP	oxidation-reduction potential
PAH	polynuclear aromatic hydrocarbon
PCR	polymerase chain reaction
QA/QC	quality assurance / quality control
qPCR	quantitative polymerase chain reaction
TPH	total petroleum hydrocarbons
TPH-d	total petroleum hydrocarbons – diesel-range organics
VOC	volatile organic compound

1. Introduction

This subappendix, summarized in Section 7.2.6 of the Conceptual Site Model main document, describes preliminary results from two studies that are being used to assess natural attenuation capacity at the Red Hill Bulk Fuel Storage Facility (the "Facility").

- A ***microcosm study*** is being completed to provide an estimate of the bulk attenuation rate due to biodegradation for several constituents of concern under aerobic and anaerobic conditions. These are laboratory-based tests where the temporal concentrations of these constituents are monitored in bottles constructed using site material to understand the relative biodegradation kinetics. These tests started in October 2017 and will be continuing over the next several months to further evaluate anaerobic biodegradation, but preliminary data are available and discussed within this subappendix.
- A series of ***microbial parameters***, including QuantArray-Petro and Next Generation Sequencing (NGS), have been employed to quantify particular biomarkers of petroleum hydrocarbon degradation. These tests involve analyses of site groundwater using quantitative polymerase chain reaction (qPCR)-based techniques to provide a snapshot of the microbial community present at the Facility, including those capable of petroleum hydrocarbon degradation. Data from a single sampling event (October 25, 2017) are available and discussed within this subappendix.

Collectively, the results of these test help to establish if key organisms are present, active, and degrading hydrocarbons at rates that help to limit migration. These data serve not only as a line of evidence for attenuation but also as site-specific input values for subsequent fate and transport modeling.

2. Methods

2.1 TEST DESIGN

2.1.1 Microcosm Study

For the microcosm study, the primary design considerations were sampling locations, the test conditions, and the constituents to be monitored.

For the sampling locations, monitoring wells RHMW01 and RHMW02 were selected for further assessment (Figure 2-1). The primary rationale for this selection was that the recent monitoring data showed that these wells exhibited the highest concentrations of total petroleum hydrocarbon (TPH) constituents. Consequently, understanding biodegradation potential and rates at these locations is the highest priority and directly supports the decision-making process for the Facility. The concentration history at the locations also suggests that there is an active microbial community, and the microcosm study (as well as the molecular biological tests) serve as supporting evidence that biodegradation is a contributing factor to observed concentration trends.

Conditions tested during microcosm study included both anaerobic and aerobic conditions. Anaerobic conditions were selected to provide measurements of intrinsic degradation activity without amendments. In general, the geochemical conditions around RHMW01 and RHMW02 are reducing, such that the anaerobic microcosms could be considered most representative of conditions in the immediate vicinity of the wells. However, groundwater containing small amounts of oxygen and other electron acceptors may flow into the areas around the wells, such that strictly anaerobic microcosms might underestimate activity. Consequently, a parallel set of aerobic microcosms were also included to assess biodegradation in conditions where oxygen availability was not limited. Because oxygen is supplied to maintain aerobic conditions in the microcosms, this set of tests provides a best-case scenario for natural attenuation in these wells. However, data from the aerobic microcosms were also designed to show how contaminants entering the downgradient portions of the aquifer—which are highly oxidizing—might be degraded.

Constituents that were included in the monitoring program for the microcosm study are listed in Table 2-1. These constituents were selected because each meets one or more of the following criteria: (1) it is a known or suspected constituent within the light non-aqueous-phase liquid (LNAPL) present at the Facility; (2) it has been detected in monitoring wells; and (3) the constituent is a potential risk driver (i.e., even if it is not currently detected). It is important to note that the initial concentrations of these constituents were either extremely low or below reporting limits in the samples collected from RHMW01 and RHMW02 for microcosm construction. Therefore, each of these constituents had to be added (spiked) to the microcosms. In this case, the goal was to achieve a concentration that was slightly below the effective solubility of each constituent assuming water was in equilibrium with JP-8 (i.e., a potential source material). These concentrations, which are listed in Table 2-1, were calculated using available literature studies, and the spiking procedure is described in Section 2.3.

Table 2-1: Summary of Target Initial Concentrations for Microcosm Study

Constituent	Target Concentration (µg/L)
Benzene	150
1,2,4-Trimethylbenzene	500
1-Methylnaphthalene	60
2-Methylnaphthalene	60
Naphthalene	60
Xylene, m,p-	1,000
Xylene, o-	500
Toluene	600

µg/L microgram per liter

2.1.2 Microbial Parameters

For the microbial parameters study, the primary design considerations were sampling locations and the type of molecular biological tools to be employed.

Samples from monitoring wells RHMW01, RHMW02, RHMW03, and RHMW04 were selected to be part of this assessment (Figure 2-1). These wells were chosen on the basis that they include the wells that exhibited the highest concentrations of TPH constituents during recent monitoring events (RHMW01 and RHMW02) but also several wells with low and/or non-detectable levels of TPH (RHMW03 and RHMW04). The former two wells can be used to establish the microbial community that is present within the plume core, while the latter two wells provide information on the microbial community in areas where current exposure to petroleum hydrocarbons is more limited. Note that RHMW04 is outside of the footprints of the tanks and thus is the most representative of background conditions (of the wells tested).

The two molecular biological tools that are part of the current microbial parameter analysis are QuantArray-Petro and NGS. QuantArray-Petro is a proprietary qPCR-based method (from Microbial Insights) that provides information on the abundance of specific biomarkers for petroleum hydrocarbon degradation. Genetic material (DNA) is extracted from environmental samples and then qPCR is used to amplify and quantify copies of specific target genes. Rapid quantification is aided by the use of plates containing grids of immobilized genetic material (microarrays) that bind to the genes of interest. NGS has a similar goal of providing information on community structure, but it generally provides a more comprehensive picture and does not require any previous knowledge of what populations may be present at a site. The method used for this study was developed by Microbial Insights and involves a step-wise procedure to fragment genetic material into a series of smaller identifying segments. Each of these segments can then be sequenced and quantified to relate to overall community structure. Note that a series of other molecular biological tools (e.g., Stable Isotope Probing, Compound-Specific Isotope Analysis) are also planned in support of the overall assessment of natural attenuation for this study, but these were not ready for inclusion in this report.

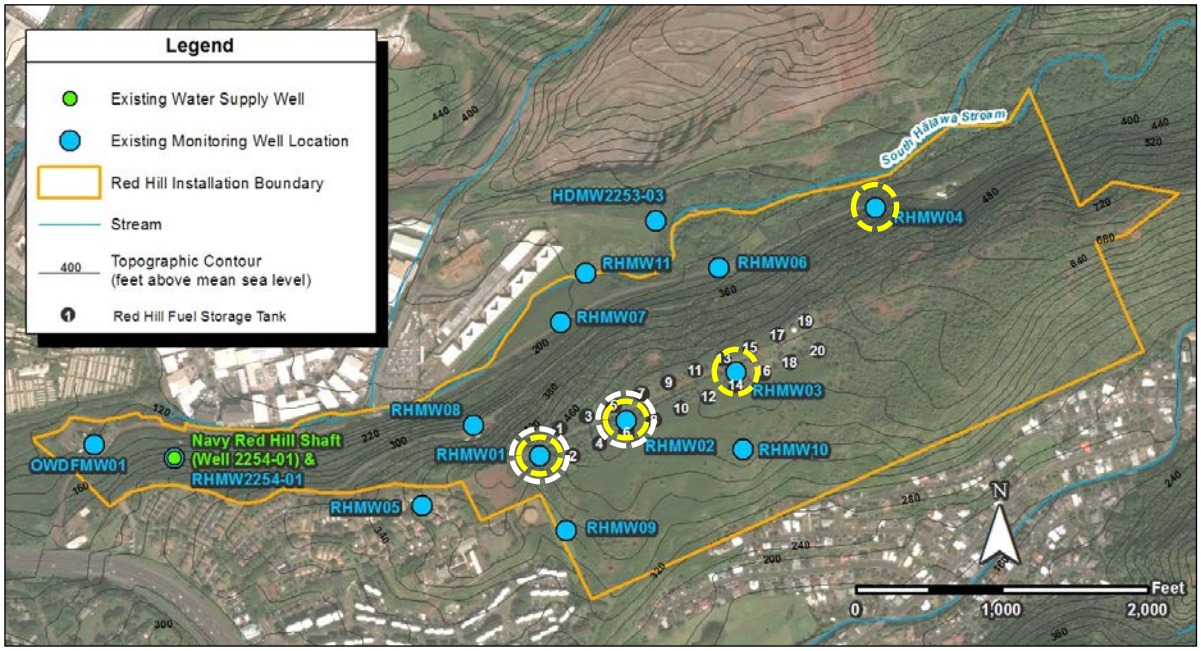

Figure 2-1: Location of Facility Wells Included in Microcosm Study (White Circles) and Microbial Parameter Analysis (Yellow Circles)

2.2 FIELD PROTOCOLS FOR SAMPLE COLLECTION

The following subsection summarizes the field sampling protocols for the tests described in this subappendix. A comprehensive summary of methods (including quality assurance / quality control [QA/QC] procedures) will be provided as part of a later submission once all tests are complete.

2.2.1 Microcosm Study

Site material (groundwater) from monitoring wells RHMW01 and RHMW02 was used to construct microcosms. Twelve liters of groundwater was collected from RHMW02 on September 19, 2017, and 9 liters of groundwater was collected from RHMW01 on September 26, 2017. In each case, samples were pumped from the well after surging to ensure that significant sediment was entrained in the groundwater. The inclusion of sediment helped ensure that sufficient initial biomass was available for the subsequent treatability tests. However, the amount of sediment was relatively small (<1% by volume) compared to amounts present in porous media. Samples were collected in polyethylene bottles with no headspace and no preservative per laboratory protocol. Samples were shipped in coolers on ice to the laboratory.

2.2.2 Microbial Parameters

Groundwater samples were collected from monitoring wells RHMW01, RHMW02, RHMW03, and RHMW04 during October 20–25, 2017 for microbial parameter analysis. In each case, 1–2 liters of groundwater was pumped from the well and then passed through a laboratory-supplied filter apparatus (bio-filter, Figure 2-2). The purpose of these filters is to collect and concentrate biomass from individual samples and thus eliminate the need to ship groundwater. Once filtering was complete, each bio-filter was capped, and the entire set shipped to the laboratory in coolers on ice.

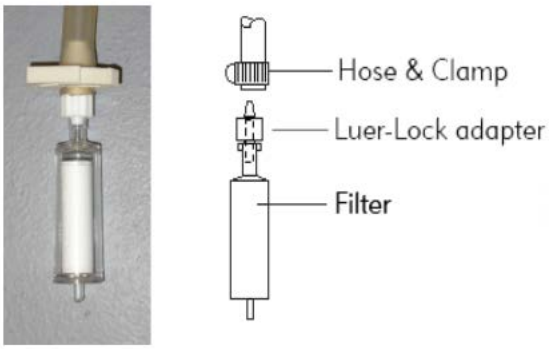

Figure 2-2: Bio-filters Used During Sample Collection for Microbial Parameter Analysis

2.3 LABORATORY PROTOCOLS FOR ANALYSIS

The following subsection summarizes the methodology used by the commercial labs that are performing this work. As noted above, a more comprehensive summary of these procedures will be provided at a later date once testing is complete.

2.3.1 Microcosm Study

A series of microcosms were constructed to assess degradation under various conditions (Table 2-2). Microcosm construction was initiated immediately after field samples were received by the laboratory (SiREM). Note that field samples from the two different site locations were handled separately. Each microcosm consisted of a 250-milliliter (mL) glass bottle filled with 200 mL of site groundwater. In addition, sediment that was collected with the field sample and then distributed in approximately equal amounts to each bottle. The bottles were sealed with Mininert valves to allow repetitive sampling of each microcosm, as well as the addition of oxygen in the aerobic treatments (labeled ONAT in Table 2-2). Given that the various analyses being included in the study required significant liquid volumes, sufficient sacrificial microcosms were constructed for each treatment condition.

Microcosms were constructed in disposable anaerobic glove bags to ensure that redox conditions within each bottle could be controlled during set up. This included a set of sterile control microcosms that were constructed using material from one location (RHMW02). The control bottles were autoclaved and amended with mercuric chloride and sodium azide to inhibit microbial activity. Anaerobic reactors (labeled ANAT in Table 2-2) and the sterile controls were then transferred to a permanent anaerobic chamber, while reactors intended for aerobic treatment were maintained on a benchtop.

Representative samples were collected prior the start of the test to determine the initial concentrations of specific chemicals of potential concern (COPCs). Concentrations of the majority were either below reporting limits or too low to reasonably test, and the decision was made to amend each reactor with representative petroleum hydrocarbons. Therefore, each reactor was spiked at the start of the study with an aliquot of neat solutions of saturated stock solutions of several hydrocarbons. In each case, the volume added was based on reaching the target concentrations listed in Table 2-1.

The ANAT and sterile control microcosms are being incubated over a period of 8–12 months. Aqueous samples are being collected from the ANAT and sterile control microcosms at seven sampling events, approximately every 4–6 weeks for analysis of benzene, toluene, ethylbenzene and xylenes (BTEX), dissolved hydrogen gases (DHG; methane, ethene, ethane), anions (i.e., sulfate, nitrate, chloride, and phosphate), pH, and oxidation-reduction potential (ORP). Naphthalene, methylnaphthalene, and trimethylbenzene samples will be collected from the sterile controls at the beginning and end of the study and from the ANAT microcosms at the beginning of the study, at least one point during the incubation period, and the end of the incubation period.

The ONAT microcosms are being incubated over a shorter period of 3–4 months. Aqueous samples are being collected over seven sampling events approximately every 1–3 weeks for analysis of BTEX, DHGs, anions, pH and ORP. Naphthalene, methylnaphthalene, and trimethylbenzene analysis samples are being collected at the beginning of the incubation period, during at least one point during the incubation period, and at the endpoint of the study. When a measurement for a particular constituent suggests that it has been completely degraded, bottles are respiked with that constituent to confirm continued biodegradation capacity. ONAT microcosms are also periodically re-amended with oxygen to sustain aerobic conditions throughout the test.

Naphthalene, methylnaphthalene, and trimethylbenzene analyses are being completed at ALS Environmental in Waterloo, ON, Canada. All other analyses are being completed by SiREM.

Sampling intervals for individual treatments may be modified (either shorter or longer intervals) during the study. Given that these tests are ongoing, only a portion of the data from these treatments is currently available and described within this subappendix.

Table 2-2: Treatments and Controls for Microcosm Study

Condition	Number of Locations	Description	Number of Replicates for Location 1 (RHMW01)	Number of Replicates for Location 2 (RHMW02)
1. ONAT	2	Amended with gaseous oxygen and incubated aerobically	2	2
2. ANAT	2	No amendments and incubated anaerobically	2	2
3. Sterile Control	1	Autoclaved and amended with mercuric chloride and sodium azide	0	2

2.3.2 Microbial Parameters

A detailed description of laboratory procedures for QuantArray-Petro and NGS was not available at the time this subappendix was prepared. These will be provided in a later submittal along with results from additional testing.

3. Results

3.1 MICROCOSM STUDY

The evaluation period for all microcosms started on October 24, 2017. As of this writing, data are available for the first 161 days of monitoring (Attachment B.6.1). However, the sampling frequency for the various treatments varies widely, such that the ONAT have more data available for the current evaluation than the ANAT or sterile controls. Similarly, not all constituents are analyzed at each time point, in part because an external laboratory is used for certain analyses. The external laboratory (ALS Environmental) also has longer turnaround times for analyses than SiREM.

Rate coefficients were calculated for individual constituents using available time-series concentration data and assuming that degradation fit a first-order relationship. In other words, the rate coefficient is equal to the slope of the best fit regression line for concentration data plotted on a logarithmic axis (Figure 3-1 to Figure 3-4). For the purposes of this calculation, the reporting limit was used as a substitute value for any instance when the concentration fell below the reporting limit (note that this is a conservative assumption). These values are summarized in Table 3-1.

Table 3-1: Constituent-Specific Rate Coefficients Based on Currently Available Data from Microcosm Study

Well Location	Condition	Benzene (1/day)	Toluene (1/day)	Xylenes, o- (1/day)	Xylenes, m-, p- (1/day)	1,2,4-TMB (1/day)	1-Methyl-naphthalene (1/day)	2-Methyl-naphthalene (1/day)	Naphthalene (1/day)
RHMW01	OANT	0.029	0.06	0.072	0.088	0.077	0.111	0.227	0.204
	ANAT	0.0008	0.011	0.0006	0.003	—	—	—	—
RHMW02	OANT	0.111	0.196	0.184	0.195	0.26	0.268	0.80	0.80
	ANAT	0.002	No degradation observed to date	No degradation observed to date	No degradation observed to date	—	—	—	—
	Sterile Control	0.003	No degradation observed to date	No degradation observed to date	No degradation observed to date	—	—	—	—

Notes: (1) Rate coefficient for aerobic condition at RHMW02 includes data from the initial spike (Day 0–28), not the respike on Day 28; (2) "No degradation observed to date" is used for treatments where concentrations were unchanged or increased over the current monitoring period.
— no data available to date

The major findings based on the early results of the microcosm study are summarized below:

- Rapid biodegradation under aerobic conditions was observed in the microcosms from RHMW02. If the rate coefficients in Table 3-1 are converted to equivalent half-lives, then all constituents were degraded with half-lives of less than 1 week, and several were less than 1 day. The data indicate that strong degradation capacity can be stimulated at this location when oxygen is present.
- Slower biodegradation rates were observed in the aerobic microcosms from RHMW01, though all constituents exhibited a concentration decrease and have been completely removed by the end of current the monitoring period. Current half-life estimates for the constituents included in the test range from 3 days (2-methylnaphthalenene) to 25 days (benzene). The slower rates observed in the microcosms from this well relative to RHMW02 are consistent with the molecular data discussed in the next section.

- Rapid biodegradation of naphthalene has been observed in aerobic microcosms from both RHMW01 (half-life of 3.4 days) and RHMW02 (half-life of 0.9 day).
- Little or no biodegradation was observed under anaerobic conditions in microcosms from either RHMW01 or RHMW02 over the first 5 months of monitoring. To date, the only volatile organic compound (VOC) data available for these microcosms are benzene, toluene, and xylenes. Concentrations for this set of microcosms were relatively unchanged and generally followed similar trends as the sterile controls.
- The lack of initial activity in anaerobic microcosms likely reflects a lag period as the microbial cultures acclimated to the reactor conditions. While these microcosms were constructed in anaerobic conditions, the ORP measured at the start of the test (Day 0) was 155 millivolts (mV) for the RHMW01 microcosms and 166 mV for the RHMW02 microcosms. This reflects the introduction of oxygen during field sampling, which cannot be easily prevented. These oxidizing conditions are generally unfavorable for growth and activity of anaerobic organisms. However, the mass of oxygen and other oxidants in these bottles was relatively small, and utilization of oxygen was expected to eventually shift redox levels downwards. By Day 28, the ORP had dropped to -149 mV in the RHMW01 microcosms and -229 mV in the RHMW02 microcosms. These reducing conditions should prove more favorable for anaerobic activity, and this may lead to more significant degradation of petroleum hydrocarbons in these microcosms during future monitoring events.

Another factor that may have contributed to the relatively stable concentrations in the anaerobic microcosms was a low supply of electron acceptors to stimulate degradation. Degradation of petroleum hydrocarbons under anaerobic conditions is an oxidation reaction (i.e., releases electrons) that generally proceeds faster when electron acceptors such as nitrate or sulfate are available. Several of these parameters are included in the monitoring program for the microcosm study, and the data collected (to date) confirm that little sulfate (<0.07–4.0 mg/L) and nitrate (< 0.09 mg/L) are present in the Facility groundwater. These geochemical conditions will limit the type of anaerobic degradation pathways (and rates) that can occur, particularly in microcosms with a finite amount of electron acceptors (as opposed to the aquifer underlying the Facility where groundwater flow helps replenish the supply of electron acceptors).

The biodegradation rate coefficients generated from the aerobic microcosms are generally comparable to published values for petroleum hydrocarbons. For example, Kao et al. (2006) evaluated natural attenuation of a petroleum hydrocarbon spill in an aquifer with a background oxygen concentration of 2.4 mg/L, and reported in situ first-order attenuation rates ranging from 0.051 per day (benzene) to 0.189 per day (1,2,4-trimethylbenzene). Xylenes and toluene were also evaluated and fell within this range. The range reported by Kao et al. (2006) is similar to the range obtained for this same set of compounds in the microcosm for RHMW02 (0.11–0.18 per day). In a study of natural attenuation of aromatic hydrocarbons, Landmeyer et al. (1998) reported a much wider range for aerobic benzene and toluene biodegradation (0.03–0.84 per day), but notably was able to establish rapid aerobic biodegradation of naphthalene (0.88 per day) at a rate that was nearly identical to the RHMW02 microcosm (0.80 per day). Aerobic biodegradation rates from the RHMW01 microcosm were slightly slower than the rates from RHMW02 but are still comparable to the ranges of rates reported in these published studies. Collectively, these early microcosm results are consistent with literature studies and guidance documents that consider dissolved-phase petroleum hydrocarbons readily degradable under aerobic conditions (Chapelle 1999; EPA 1999; Das and Chandran 2011).

3.2 MICROBIAL PARAMETERS

Results from analysis of microbial parameters are available for a single sampling event (October 20–25, 2017). The QuantArray-Petro and NGS data are tabulated in Attachment B.6.2. Because the laboratory has yet to provide an interpretative report for either dataset yet, the QuantArray-Petro results are discussed only briefly here, while the NGS results will be discussed in a later submission.

The major findings based on an initial interpretation of the QuantArray-Petro data are summarized below:

- Samples from all wells showed evidence of aerobic and anaerobic petroleum hydrocarbon degrading capabilities. This is based on the presence of measurable levels of one or more functional genes associated with the aerobic and anaerobic degradation of BTEX, alkane, and/or polynuclear aromatic hydrocarbon (PAH) degradation.
- RHMW02 and RHMW04 generally had the highest levels of biomarkers for aerobic biomarkers, including *PM1,* which is associated with BTEX and MTBE degradation. RHMW04 is screened in an aerobic portion of the basalt aquifer based on the high dissolved oxygen levels (5.35 mg/L) observed in the October 2017 monitoring event. RHMW02 is screened in an apparently much more reducing portion of the basalt aquifer based on low dissolved oxygen levels (historically below 1 mg/L) and elevated methane levels (4.5 mg/L during the October 2017 monitoring event). In addition, the microcosm study showed that the RHMW02 microbial community could be easily stimulated to degrade petroleum hydrocarbons aerobically when oxygen was added to the bottles. Collectively, these data indicate that a population of aerobic petroleum hydrocarbon degraders is present at RHMW02.
- RHMW01 and RHMW03 generally had lower levels of most aerobic biomarkers than RHMW02 and RHMW04, with some exceptions (e.g., *PHE* in RHMW03, which is associated with BTEX and MTBE degradation). This pattern is consistent with the existing geochemical data that suggest that the wells are screened in groundwater zones that are more reducing.
- Samples from all four wells had moderate to high levels of *BCR* (benzoyl-coenzyme A reductase), which is a biomarker of anaerobic BTEX degradation.
- RHMW01 and RHMW02 had measurable levels of biomarkers associated with anaerobic PAH degradation (e.g., naphthalenes).
- RHMW01 and RHMW02 also had the highest levels of eubacteria, which can be used as a bulk indicator of microbial abundance. This is consistent with the diversity of aerobic and anaerobic biomarkers measured in samples from these wells. As a result, there is significant evidence that biodegradation of petroleum hydrocarbon can occur at these locations.
- RHMW04 had the lowest levels of biomarkers for anaerobic petroleum hydrocarbon degradation of the four wells tested. This is consistent with the relatively oxidizing conditions in the groundwater at this location, as well as lower potential exposure to petroleum hydrocarbons (based on the historic groundwater monitoring data).
- The field blank also contained low but detectable levels of total eubacteria (a general bulk indicator of microbial abundance) and PM1 (a biomarker for BTEX and MTBE degradation). The level of total eubacteria measured in the field blank (9,960 cells/mL) was

only 6–20% of the levels measured in the four monitoring wells, confirming that the well samples contained significant biomass even after correcting for the levels in the field blank. The level of PM1 measured in the field blank (939 copies/mL) was similar or higher than the levels measured in samples from wells RHMW01 and RHMW03, meaning that the presence of elevated levels of this biomarker could not be confirmed in these wells. However, PM1 was present at 4×– 5× higher levels in samples from wells RHMW02 and RHMW04 relative to the field blank. These results are consistent with the other lines of evidence that suggest stronger aerobic biodegradation activity at wells RHMW02 and RHMW04.

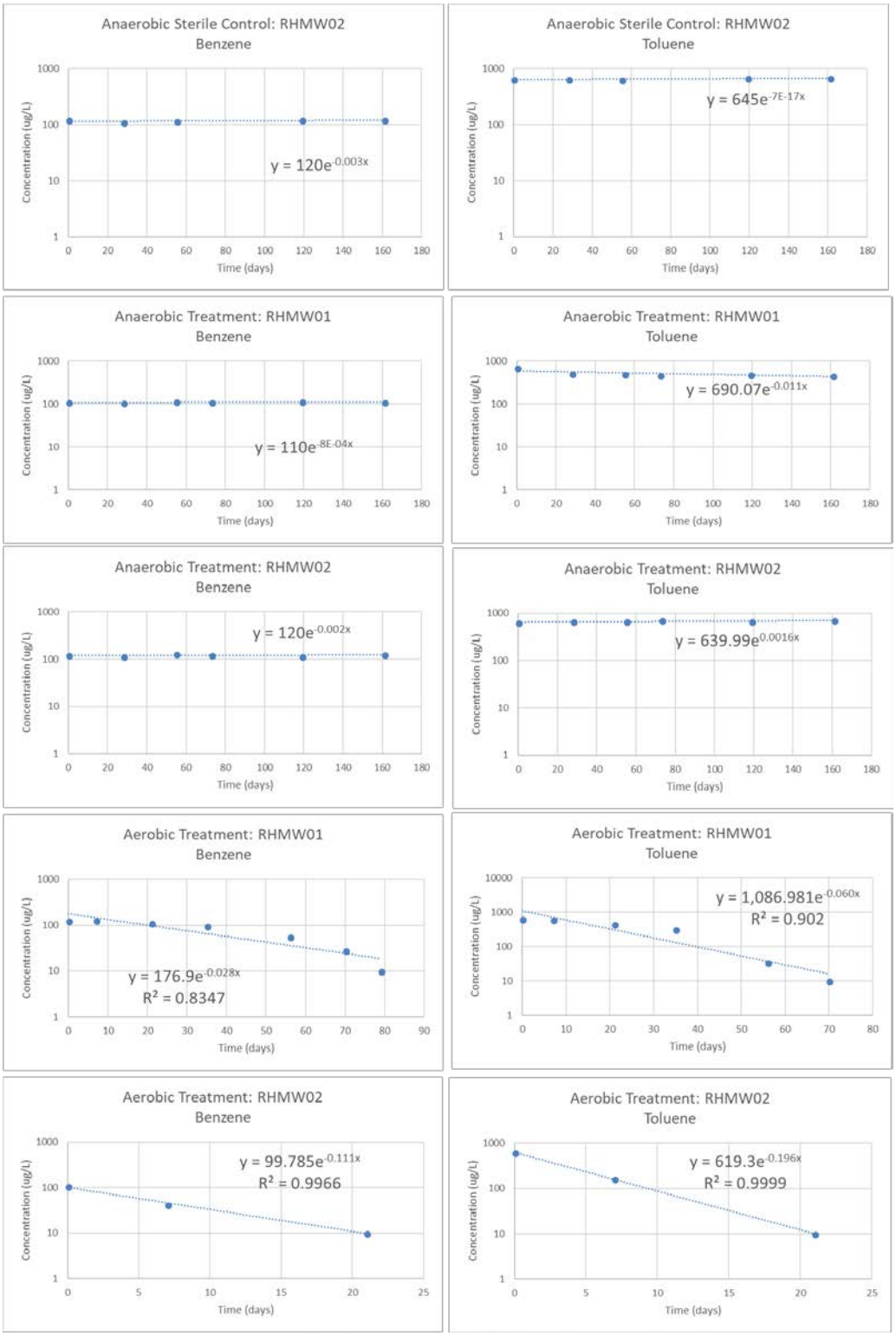

Note: In the regression equation for each set of data, the number in front of the x-variable represents the rate coefficient reported in Table 3-1.

Figure 3-1: Results of Microcosm Study: Benzene and Toluene

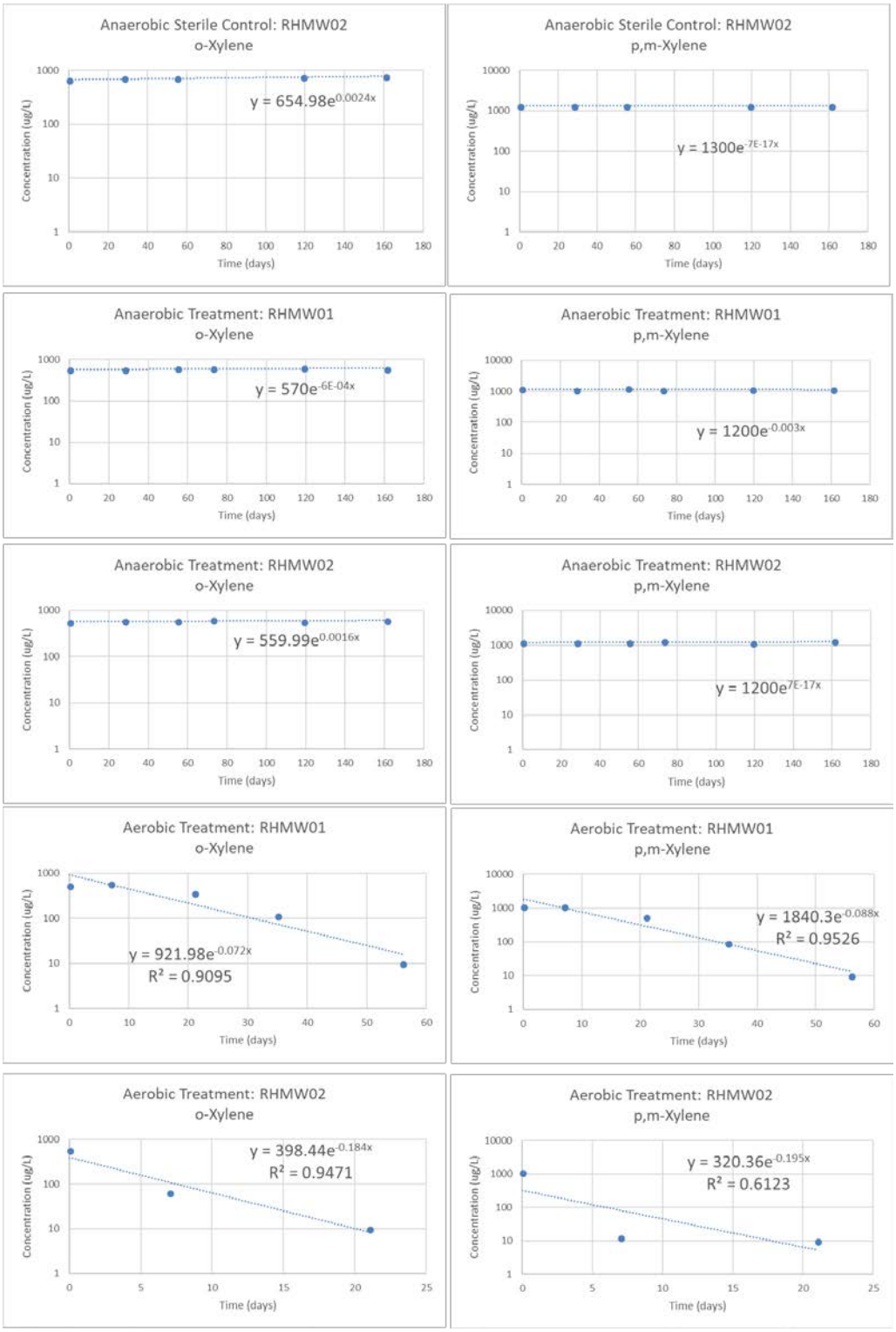

Note: In the regression equation for each set of data, the number in front of the x-variable represents the rate coefficient reported in Table 3-1.

Figure 3-2: Results of Microcosm Study: Xylenes

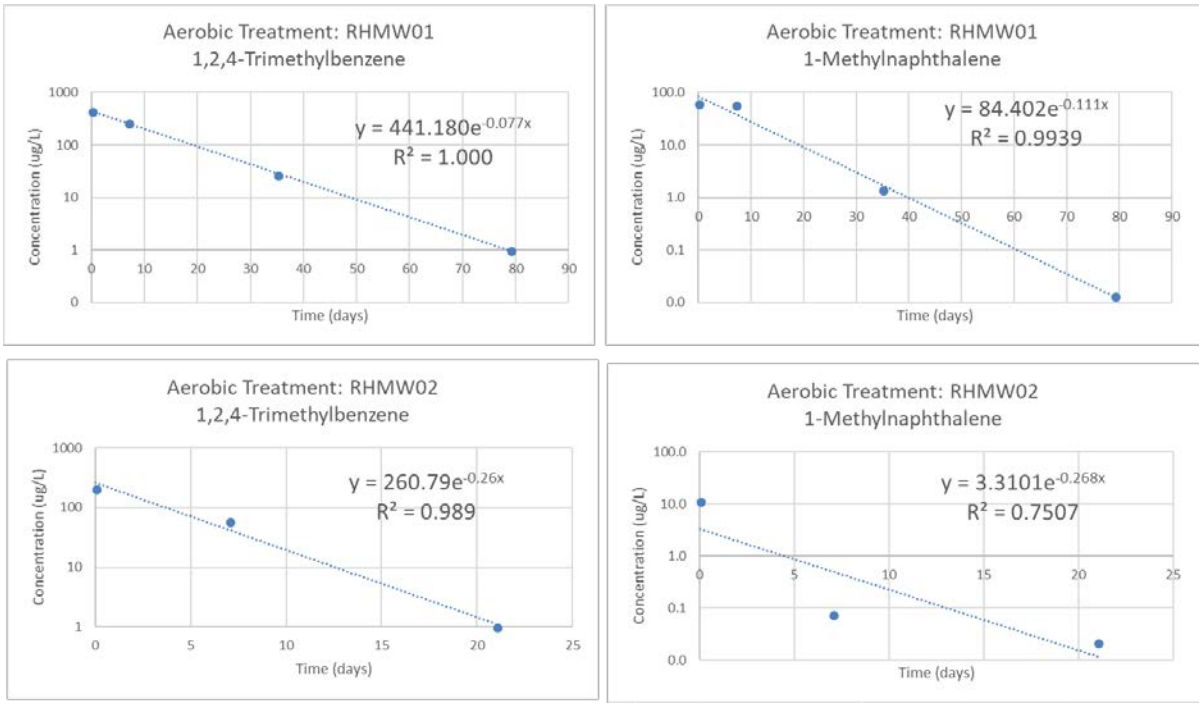

Note: In the regression equation for each set of data, the number in front of the x-variable represents the rate coefficient reported in Table 3-1.

Figure 3-3: Results of Microcosm Study: 1,2,4-Trimethylbenzene and 1-Methylnaphthalene

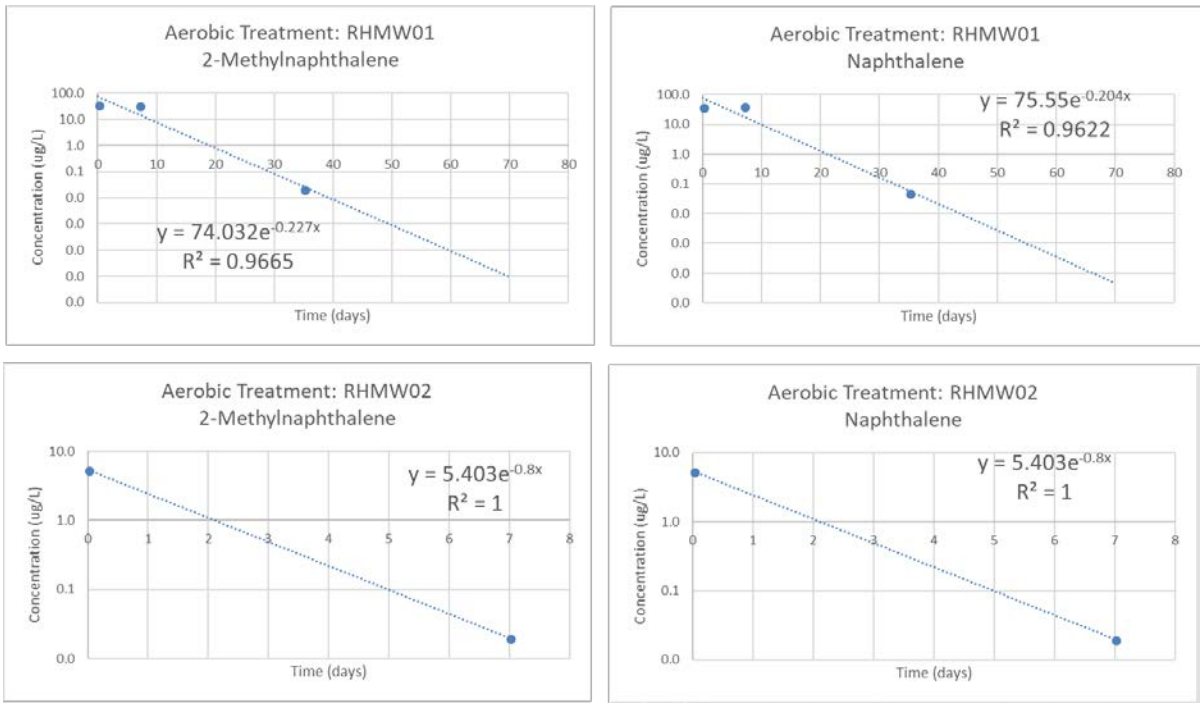

Note: In the regression equation for each set of data, the number in front of the x-variable represents the rate coefficient reported in Table 3-1.

Figure 3-4: Results of Microcosm Study: 2-Methylnaphthalene and Naphthalene

4. Conclusions

Results are presented from two different studies to better understand biodegradation potential at the Facility. An ongoing microcosm study is being used to understand the biodegradation rates for selected petroleum hydrocarbons at RHMW01 and RHMW02, while molecular biological tools have been used to analyze for several microbial parameters in a larger set of wells.

Based on the early microcosm results, degradation of these petroleum hydrocarbons is non-conclusive under anaerobic conditions, with few changes in concentration over the first 5 months of testing. This may be a laboratory artifact; oxidizing conditions were initial present in these bottles (positive ORP) because oxygen was introduced during field collection of the groundwater. The ORP readings have since decreased, and conditions are now more favorable for anaerobic growth and degradation.

In microcosms maintained under aerobic conditions, rapid degradation of all constituents was observed in RHMW02 (half-life < 7 days for all constituents, including benzene, toluene, xylenes, and PAHs). Slower aerobic degradation was observed in RHMW01 (half-lives currently on the order of 3–25 days).

A suite of different functional genes associated with both aerobic and anaerobic petroleum hydrocarbon degradation was detected in samples from all four wells (RHMW01, RHMW02, RHMW03, and RHMW04). The presence of functional genes for degradation of petroleum hydrocarbons confirms that aerobic and anaerobic microorganisms are both present and active (i.e., the genes would not be expressed if the microorganisms were not active).

The microbial data are largely consistent with concentration trends and geochemical conditions at the Facility. Specifically, petroleum hydrocarbon concentrations are relatively high at RHMW02 and then attenuate significantly moving away from this well. The molecular data suggest that a combination of anaerobic and aerobic processes is responsible for this attenuation, although the potential for rapid aerobic degradation (as observed in the microcosms) is restricted somewhat by the low availability of oxygen. Degradation rates are apparently lower at RHMW01 based on the available microcosm data, but the molecular data provide another line of evidence that biodegradation within the plume is contributing to the attenuation observed at the Facility.

RHMW03 and RHMW04 are located in areas with low or non-detectable levels of most petroleum hydrocarbon constituents. However, there is significant biodegradation potential at these locations due to the presence of abundant dissolved oxygen and multiple biomarkers for aerobic and anaerobic degradation. This would help attenuate any contaminants that migrate beyond the current plume boundary.

5. References

Chapelle, F. H. 1999. "Bioremediation of Petroleum Hydrocarbon-Contaminated Ground Water: The Perspectives of History and Hydrology." *Groundwater* 37 (1): 122–132.

Das, N., and P. Chandran. 2011. *Microbial Degradation of Petroleum Hydrocarbon Contaminants: An Overview*. DOI: 10.4061/2011/941810. Biotechnology Research International.

Environmental Protection Agency, United States (EPA). 1999. *Monitored Natural Attenuation of Petroleum Hydrocarbons*. EPA Remedial Technology Fact Sheet. EPA/600/F-98/021. May.

Kao, C. M., W. Y. Huang, L. J. Chang, T. Y. Chen, H. Y. Chien, and F. Hou. 2006. "Application of Monitored Natural Attenuation to Remediate A Petroleum-Hydrocarbon Spill Site." *Water Science & Technology* 53 (2): 321–328.

Landmeyer, J. E., F. H. Chapelle, M. D. Petkewich, and P. M. Bradley. 1998. "Assessment of Natural Attenuation of Aromatic Hydrocarbons in Groundwater Near A Former Manufactured-Gas Plant, South Carolina, USA." *Environmental Geology* 34 (4): 279–292.

Attachment B.6.1: Summary of Current Data from Microcosm Study - Volatile Organic Compounds

ATTACHMENT B.6.1: SUMMARY OF CURRENT DATA FROM MICROCOSM STUDY - VOLATILE ORGANIC COMPOUNDS
Red Hill Facility, Hawai'i

Treatment	Date	Day	Replicate	Bottle Set	SiREM: Volatile Organic Compounds						ALS: Volatile Organic Compounds				Comment
					Methane	CB	Benzene	Toluene	o-Xylene	p,m-Xylene	1,2,4-Trimethylbenzene	1-methylnaphthalene	2-methylnaphthalene	naphthalene	
					µg/L	µg/L	µg/L	µg/L	µg/L	µg/L	µg/L	µg/L	µg/L	µg/L	
Anaerobic															
Anaerobic Sterile Control RHMW02	24-Oct-17	0													Poisoned wth mecuric chloride and sodium azide.
															Amended the first replicate with 100 µL of resazurin.
															Spiked with BTX and naphthalene compounds.
			ANSC RHMW02-1	1	510	<10	120	650	620	1400	326	64.9	32.8	40.9	
			ANSC RHMW02-2	2	510	<10	120	640	690	1200	341	60.4	32.6	39.5	
			Average Concentration (µg/L)		**510**	**ND**	**120**	**645**	**655**	**1300**	**334**	**62.7**	**32.7**	**40.2**	
	21-Nov-17	28	ANSC RHMW02-1	1	410	<10	110	670	670	1400					
			ANSC RHMW02-2	2	430	<10	110	620	730	1200					
			Average Concentration (µg/L)		**420**	**ND**	**110**	**645**	**700**	**1300**					
	18-Dec-17	55	ANSC RHMW02-1	1	310	<10	110	650	650	1400					
			ANSC RHMW02-2	2	480	<10	120	610	760	1200					
			Average Concentration (mg/L)		398	**ND**	115	630	705	1300					
	20-Feb-18	119	ANSC RHMW02-1	1	250	<10	120	680	680	1400					
			ANSC RHMW02-2	2	370	<10	120	660	810	1200					
			Average Concentration (mg/L)		310	**ND**	120	670	745	1300					
	03-Apr-18	161	ANSC RHMW02-1	1	250	<10	120	690	710	1400					
			ANSC RHMW02-2	2	380	<10	120	660	810	1200					
			Average Concentration (mg/L)		315	**ND**	120	675	760	1300					
Anaerobic Natural Attenuation Treatment RHMW01	24-Oct-17	0													Amended the first replicate with 100 µL of resazurin.
															Spiked with BTX and naphthalene compounds.
			ANAT RHMW01-1	3	110	<10	120	760	580	1200	355	64.7	34.1	38.6	
			ANAT RHMW01-2	4	120	<10	100	620	560	1200	1,890	60.6	34.7	40.1	
			Average Concentration (µg/L)		**115**	**ND**	**110**	**690**	**570**	**1200**	**1,123**	**62.7**	**34.4**	**39.4**	
	21-Nov-17	28	ANAT RHMW01-1	3	57	<10	95	410	520	1000					
			ANAT RHMW01-2	4	110	<10	120	600	600	1200					
			Average Concentration (µg/L)		**84**	**ND**	**107.5**	**510**	**560**	**1100**					
	18-Dec-17	55	ANAC RHMW01-1	3	91	<10	110	470	580	1300					
			ANAC RHMW01-2	4	110	<10	120	540	610	1200					
			Average Concentration (mg/L)		100	**ND**	115	505	595	1250					
	05-Jan-18	73	ANAC RHMW01-1	3	81	<10	110	430	620	1100					
			ANAC RHMW01-2	4	69	<10	110	510	600	1100					
			Average Concentration (mg/L)		75	**ND**	110	470	610	1100					
	20-Feb-18	119	ANAC RHMW01-1	3	98	<10	110	420	610	1100					
			ANAC RHMW01-2	4	140	<10	120	560	650	1200					
			Average Concentration (mg/L)		119	**ND**	115	490	630	1150					
	03-Apr-18	161	ANAC RHMW01-1	3	130	<10	100	380	560	970					
			ANAC RHMW01-2	4	190	<10	120	540	610	1200					
			Average Concentration (mg/L)		160	**ND**	110	460	585	1135					
Anaerobic Natural Attenuation Treatment RHMW02	24-Oct-17	0													Amended the first replicate with 100 µL of resazurin.
															Spiked with BTX and naphthalene compounds.
			ANAT RHMW02-1	5	370	<10	120	660	520	1200	5,730	56.7	31.2	38.9	
			ANAT RHMW02-2	6	340	<10	120	620	610	1200	691	59.1	35.5	37.6	
			Average Concentration (µg/L)		**350**	**ND**	**120**	**640**	**560**	**1200**	**3211**	**57.9**	**33.4**	**38.3**	
	21-Nov-17	28	ANAT RHMW02-1	5	400	<10	110	650	560	1200					
			ANAT RHMW02-2	6	520	<10	120	690	610	1300					
			Average Concentration (µg/L)		**460**	**ND**	**115**	**670**	**585**	**1200**					
	18-Dec-17	55	ANAC RHMW02-1	5	820	<10	140	640	520	1100					
			ANAC RHMW02-2	6	910	<10	120	690	660	1300					
			Average Concentration (mg/L)		865	**ND**	130	665	590	1200					
	05-Jan-18	73	ANAC RHMW02-1	5	860	<10	120	720	630	1300					
			ANAC RHMW02-2	6	890	<10	120	690	630	1300					
			Average Concentration (mg/L)		875	**ND**	120	705	630	1300					
	20-Feb-18	119	ANAC RHMW02-1	5	860	<10	110	640	540	1100					
			ANAC RHMW02-2	6	880	<10	120	690	610	1200					
			Average Concentration (mg/L)		870	**ND**	115	665	575	1150					
	03-Apr-18	161	ANAC RHMW02-1	5	920	<10	120	700	600	1300					
			ANAC RHMW02-2	6	880	<10	130	710	630	1300					
			Average Concentration (mg/L)		900	**ND**	125	705	615	1300					

ATTACHMENT B.6.1: SUMMARY OF CURRENT DATA FROM MICROCOSM STUDY - VOLATILE ORGANIC COMPOUNDS
Red Hill Facility, Hawai'i

Treatment	Date	Day	Replicate	Bottle Set	SiREM: Volatile Organic Compounds						ALS: Volatile Organic Compounds				Comment
					Methane	CB	Benzene	Toluene	o-Xylene	p,m-Xylene	1,2,4-Trimethylbenzene	1-methylnaphthalene	2-methylnaphthalene	naphthalene	
					µg/L	µg/L	µg/L	µg/L	µg/L	µg/L	µg/L	µg/L	µg/L	µg/L	
Aerobic															
Oxygen Amended Natural Attenuation Treatment RHMW01	24-Oct-17	0													Amended the first replicate with 100 µL of resazurin.
															Spiked with BTX and naphthalene compounds.
															Amended with neat oxygen gas to target a headspace of 21% oxygen.
			ONAT (RHMW01)-1	7	150	<10	130	630	500	1100	539	65	34.6	35.3	
			ONAT (RHMW01)-2	8	160	<10	120	620	560	1100	343	61.4	40.1	43	
			Average Concentration (µg/L)		**155**	**ND**	**125**	**625**	**530**	**1100**	**441**	**63.2**	**37.4**	**39.2**	
	31-Oct-17	7	ONAT (RHMW01)-1	7	100.00	<0.010	140	610	590	1100	263	62.6	34.6	41.9	
			ONAT (RHMW01)-2	8	99	<0.010	120	600	570	1100	276	55.7	36.5	40.0	
			Average Concentration (µg/L)		**100**	**ND**	**130**	**605**	**580**	**1100**	**270**	**59.2**	**35.6**	**41.0**	
															Amended with neat oxygen gas to target a headspace of 21% oxygen.
	14-Nov-17	21	ONAT (RHMW01)-1	7	80	<10	110	440	350	540					
			ONAT (RHMW01)-2	8	81	<10	110	470	370	560					
			Average Concentration (µg/L)		**80.5**	**ND**	**110**	**455**	**360**	**550**					
	28-Nov-17	35	ONAT (RHMW01)-1	7	36	<10	94	290	94	87	54.6	2.90	0.045	<0.050	
			ONAT (RHMW01)-2	8	58	<10	98	350	120	98	<1	<0.020	<0.020	<0.050	
			Average Concentration (µg/L)		**47**	**ND**	**96**	**320**	**112**	**92**	27	**1.45**	**0.023**	**ND**	
															Amended with neat oxygen gas to target a headspace of 21% oxygen.
	08-Dec-17	45													Amended with neat oxygen gas to target a headspace of 21% oxygen.
	19-Dec-17	56	ONAT (RHMW01)-1	7	10	<10	32	<10	<10	<10					
			ONAT (RHMW01)-2	8	47	<10	81	58	<10	<10					
			Average Concentration (mg/L)		**28.5**	**ND**	**56.5**	**34**	**ND**	**ND**					
	02-Jan-18	70	ONAT (RHMW01)-1	7	10	<10	<10	<10	<10	<10					
			ONAT (RHMW01)-2	8	33	<10	46	<10	<10	<10					
			Average Concentration (mg/L)		**22.5**	**ND**	**28**	**ND**	**ND**	**ND**					
															Amended with neat oxygen gas to target a headspace of 21% oxygen.
	11-Jan-18	79	ONAT (RHMW01)-1	7	13	<10	<10	<10	<10	<10	<1	0.027	<0.020	<0.050	
			ONAT (RHMW01)-2	8	34	<10	<10	<10	<10	<10	<1	<0.020	<0.020	<0.050	
			Average Concentration (mg/L)		**23.5**	**ND**	**ND**	**ND**	**ND**	**ND**	ND	**0.014**	**ND**	**ND**	
Oxygen Amended Natural Attenuation Treatment RHMW02	24-Oct-17	0													Amended the first replicate with 100 µL of resazurin.
															Spiked with BTX and naphthalene compounds.
															Amended with neat oxygen gas to target a headspace of 21% oxygen.
			ONAT (RHMW02)-1	9	320	<10	100	580	560	980	197	7.96	2.54	3.70	
			ONAT (RHMW02)-2	10	130	<10	110	640	570	1200	220	15.1	8.18	7.12	
			Average Concentration (µg/L)		**225**	**ND**	**105**	**610**	**565**	**1120**	**209**	**11.5**	**5.4**	**5.4**	
	31-Oct-17	7	ONAT (RHMW02)-1	9	16	<10	<10	<10	<10	<10	<2.0	0.059	<0.020	<0.050	
			ONAT (RHMW02)-2	10	11	<10	0.075	310	120	15	59	0.096	<0.020	<0.050	
			Average Concentration (µg/L)		**13.5**	**ND**	**8.75**	**160**	**65**	**12.5**	**59**	**0.078**	**ND**	**ND**	
															Amended with neat oxygen gas to target a headspace of 21% oxygen.
	14-Nov-17	21	ONAT (RHMW02)-1	9	13	<10	<10	<10	<10	<10	<1	0.021	<0.020	<0.050	
			ONAT (RHMW02)-2	10	12	<10	<10	<10	<10	<10	<1	0.023	<0.020	<0.050	
			Average Concentration (µg/L)		**12.5**	**ND**	**ND**	**ND**	**ND**	**ND**	ND	**0.022**	**ND**	**ND**	
	14-Nov-17	22													Prepared samples for external analysis.
	20-Nov-17	27													Re-Spiked with BTX and naphthalene compounds.
															Amended with neat oxygen gas to target a headspace of 21% oxygen.
	21-Nov-17	28	ONAT (RHMW02)-1	9	<10	<10	240	680	600	1200	<1	6.90	2.34	4.22	
			ONAT (RHMW02)-2	10	<10	<10	170	920	480	900	<1	4.26	1.32	2.82	
			Average Concentration (µg/L)		**ND**	**ND**	**205**	**800**	**540**	**1050**	ND	**5.58**	**1.83**	**3.52**	
	11-Dec-17	48	ONAT (RHMW02)-1	9	11	<10	<10	<10	<10	<10	<1	<0.020	<0.020	<0.050	
			ONAT (RHMW02)-2	10	10	<10	<10	<10	<10	<10	<1	<0.020	<0.020	<0.050	
			Average Concentration (µg/L)		**11**	**ND**	**ND**	**ND**	**ND**	**ND**	ND	**ND**	**ND**	**ND**	

Notes:
µL - microliters
ANAT - anaerobic natural attenuation treatment
ANSC - anaerobic sterile control
BTX - benzene, toluene and xylenes
CB - chlorobenzene
mg/L - milligrams per leter
mmoles - millimoles
ONAT - oxygen amended natural attenuation
o-xylene - ortho-xylene
p+m-xylene - para and meta xylene

Attachment B.6.2: Summary of Microbial Parameter Data

ATTACHMENT B.6.2: SUMMARY OF MICROBIAL PARAMETER DATA
Red Hill Facility, Hawai'i

	Sample ID	ERH438	ERH439	ERH440	ERH441	ERH406
	Collected	2017-10-25	2017-10-23	2017-10-23	2017-10-24	2017-10-20
	Sample Type	Biofilter	Biofilter	Biofilter	Biofilter	GW Equipment
	Well Name	RHMW01	RHMW02	RHMW03	RHMW04	Field
Analyte	**Units**	**Result Q**	**Result Q**	**Result Q**	**Result Q**	**Result Q**
QuantArray-Petro Results						
- Aerobic BTEX&MTBE Degradation: Toluene/Benzene Dioxygenase [TOD]	cells/mL	< 2.5 U	**130**	**135**	**72.3**	< 1.3 U
- Aerobic BTEX&MTBE Degradation: Phenol Hydroxylase [PHE]	cells/mL	**202**	**213**	**919**	**407**	< 1.3 U
- Aerobic BTEX&MTBE Degradation: Toluene 2 Monooxygenase/Phenol Hyroxylase [RDEG]	cells/mL	**50**	**366**	**399**	**410**	< 1.3 U
- Aerobic BTEX&MTBE Degradation: Toluene Ring Hydroxylating Monooxygenases [RMO]	cells/mL	**0.087 J**	< 1.8 U	< 3.4 U	< 2.5 U	< 1.3 U
- Aerobic BTEX&MTBE Degradation: Xylene/Toluene Monooxygenase [TOL]	cells/mL	< 2.5 U	< 1.8 U	< 3.4 U	**18**	< 1.3 U
- Aerobic BTEX&MTBE Degradation: *Methylibium petroleiphilum* PM1 [PM1]	cells/mL	**1,000**	**4,200**	**628**	**4,490**	**939**
- Other Aerobic BTEX&MTBE Degradation Markers	cells/mL	< 2.5 U	< 1.8 U	< 3.4 U	< 2.5 U	< 1.3 U
- Aerobic PAHs&Alkanes Degradation: Naphthalene-inducible Dioxygenase [Nid A]	cells/mL	< 2.5 U	< 1.8 U	< 3.4 U	**32.3**	< 1.3 U
- Aerobic PAHs&Alkanes Degradation: Phenanthrene Dioxygenase [PHN]	cells/mL	< 2.5 U	**96.4**	< 3.4 U	< 2.5 U	< 1.3 U
- Aerobic PAHs&Alkanes Degradation: Alkane Monooxygenase [ALK]	cells/mL	< 2.5 U	< 1.8 U	< 3.4 U	**65.4**	< 1.3 U
- Other Aerobic PAHs&Alkanes Degradation Markers	cells/mL	< 2.5 U	< 1.8 U	< 3.4 U	< 2.5 U	< 1.3 U
- Anaerobic BTEX Degradation: Benzoyl Coenzyme A Reductase [BCR]	cells/mL	**11,400**	**9,130**	**25,300**	**2,460**	< 1.3 U
- Anaerobic BTEX Degradation: Benzylsuccinate Synthase [BSS]	cells/mL	**63.8**	**89.9**	< 3.4 U	< 2.5 U	< 1.3 U
- Anaerobic BTEX Degradation: Benzene Carboxylase [ABC]	cells/mL	< 2.5 U	< 1.8 U	< 3.4 U	< 2.5 U	< 1.3 U
- Anaerobic PAHs&Alkanes Degradation: Naphthylmethylsuccinate Synthase [MNSSA]	cells/mL	**465**	**641**	< 3.4 U	< 2.5 U	< 1.3 U
- Other Anaerobic PAHs&Alkanes Degradation Markers	cells/mL	< 2.5 U	< 1.8 U	< 3.4 U	< 2.5 U	< 1.3 U
- Other: Total Eubacteria	cells/mL	**173,000**	**131,000**	**54,900**	**50,700**	**9,960**
- Other: Sulfate Reducing Bacteria	cells/mL	**2,070**	**4,520**	**1,960**	< 2.5 U	< 1.3 U
Next Generation Sequencing (NGS) Results						
- Phylum: Actinobacteria	% Total Reads	3.5%	3.4%	4.0%	8.9%	0.3%
- Phylum: Bacteroidetes	% Total Reads	–	2.7%	1.0%	3.6%	0.2%
- Phylum: Chloroflexi	% Total Reads	2.3%	–	1.1%	–	–
- Phylum: Cyanobacteria	% Total Reads	3.8%	7.4%	–	0.6%	0.1%
- Phylum: DNA	% Total Reads	–	–	–	–	0.0%
- Phylum: Euryarchaeota	% Total Reads	–	4.4%	–	–	–
- Phylum: Firmicutes	% Total Reads	10.4%	9.3%	11.6%	4.5%	0.3%
- Phylum: Nitrospirae	% Total Reads	–	–	4.6%	1.1%	–
- Phylum: Planctomycetes	% Total Reads	–	–	1.7%	–	–
- Phylum: Proteobacteria	% Total Reads	16.7%	20.4%	30.0%	44.5%	69.3%
- Phylum: Spirochaetes	% Total Reads	3.4%	–	–	–	–
- Phylum: Thermi	% Total Reads	–	–	–	–	0.0%
- Phylum: Thermodesulfobacteria	% Total Reads	2.8%	3.0%	–	–	–
- Phylum: Verrucomicrobia	% Total Reads	–	–	–	0.3%	–
- Phylum: Unclassified at Phylum Level	% Total Reads	41.4%	36.0%	41.0%	35.0%	29.6%
- Genus: Acinetobacter	% Total Reads	–	–	–	3.7%	–
- Genus: Aquabacterium	% Total Reads	–	–	–	7.8%	–
- Genus: Arcobacter	% Total Reads	–	–	–	–	0.2%
- Genus: Bacillus	% Total Reads	–	–	1.2%	2.5%	–
- Genus: Brevibacterium	% Total Reads	–	–	–	3.7%	–
- Genus: Calothrix	% Total Reads	2.9%	6.3%	–	–	0.1%
- Genus: Candidatus Scalindua	% Total Reads	–	–	1.5%	–	–
- Genus: Caulobacter	% Total Reads	–	–	–	–	1.1%
- Genus: Comamonas	% Total Reads	–	–	–	5.0%	–
- Genus: Crenothrix	% Total Reads	–	1.4%	–	–	–
- Genus: Dehalogenimonas	% Total Reads	1.4%	–	–	–	–
- Genus: Desulfovibrio	% Total Reads	–	–	3.7%	–	–
- Genus: Flavobacterium	% Total Reads	–	–	–	–	0.1%
- Genus: Geobacillus	% Total Reads	1.2%	–	–	–	–
- Genus: Hydrogenophaga	% Total Reads	–	–	–	–	0.1%
- Genus: Marinospirillum	% Total Reads	–	–	4.2%	–	–
- Genus: Methylobacterium	% Total Reads	–	–	–	–	67.7%
- Genus: Microbacterium	% Total Reads	–	–	–	2.8%	–
- Genus: Pelotomaculum	% Total Reads	1.5%	2.1%	3.4%	–	–
- Genus: Pseudomonas	% Total Reads	–	–	2.2%	7.8%	–
- Genus: Rastonia	% Total Reads	–	–	–	–	0.1%
- Genus: Sulfuricurvum	% Total Reads	–	1.2%	–	–	–
- Genus: Thermodesulfatator	% Total Reads	2.8%	3.0%	–	–	–
- Genus: Thermodesulfovibrio	% Total Reads	2.0%	1.8%	3.8%	–	–
- Genus: Treponema	% Total Reads	2.9%	2.4%	–	–	–
- Genus: Unclassified at Genus Level	% Total Reads	55.2%	49.7%	50.3%	40.6%	30.0%

Appendix B.7: Forensics and Data Evaluation - Groundwater

CONTENTS

Acronyms and Abbreviations iv

1. Introduction 1-1

2. Study Objectives 2-1

3. Jet Fuel Chemistry 3-1

- 3.1 General Jet Fuel Fingerprinting and Chemistry 3-1
- 3.2 Solubility of Jet Fuel in Water 3-4
  - 3.2.1 Calculated Effective Solubilities of Site COPCs 3-6
- 3.3 Biodegradation of Jet Fuel 3-11
  - 3.3.1 Polar Compounds/Metabolites 3-12
  - 3.3.2 Evidence of Biodegradation of Site Jet Fuel 3-13

4. Evaluation of TPH-d in Groundwater 4-1

- 4.1 Composition of TPH-d in Groundwater and Evidence of Natural Attenuation 4-1
  - 4.1.1 Evaluation of Hydrocarbon and Polar Metabolite Concentrations in Groundwater 4-1
  - 4.1.2 Evaluation of Hydrocarbon and PAH Concentrations in Groundwater 4-3
- 4.2 Evaluation of Non-COPC Components of TPH-d in Groundwater 4-6
- 4.3 Natural Attenuation Parameters in Groundwater 4-7

5. Likelihood of LNAPL in Groundwater and Evidence of Impact to Groundwater from the 2014 JP-8 Release 5-1

- 5.1 Likelihood of LNAPL in Groundwater 5-1
  - 5.1.1 Absence of LNAPL in Monitoring Wells 5-1
  - 5.1.2 Composition and Concentration of Dissolved Constituents 5-1
  - 5.1.3 Is LNAPL Likely Present in Groundwater in the Vicinity of Red Hill Monitoring Wells? 5-2
- 5.2 Evidence of Impact to Groundwater from the 2014 JP-8 Release 5-2
  - 5.2.1 TPH-d 5-3
  - 5.2.2 Naphthalenes 5-6
  - 5.2.3 TPH-g 5-9
  - 5.2.4 BTEX 5-10
  - 5.2.5 Soil Vapor 5-16
  - 5.2.6 Evaluation of Analytical Data from RHMW2254-01, RHMW04, and of Low-Level Detections of Naphthalenes in all Wells 5-17
  - 5.2.7 Did the 2014 JP-8 Tank 5 Release Event Result in an Increased Impact to Groundwater? 5-17

6. Conclusions 6-1

7. References 7-1

ATTACHMENTS

Attachment B.7.1: Summary of Concentrations and Calculated Effective Solubilities

Attachment B.7.2: Review of Analytical Results for RHMW2254-01 – Red Hill Shaft

Attachment B.7.3: Review of Analytical Results for RHMW04

Attachment B.7.4: Evaluation of Low-Level Naphthalene Detections over Time and Laboratory Changes

FIGURES

3-1 Primary Types of Hydrocarbon Compound Classes in Petroleum and Petroleum Products 3-1

3-2 Chromatograms of JP-5 and JP-8 and Jet-A 3-3

3-3 Comparison of Analysis of a Jet A Sample by (a) GC/MS and (b) HPLC 3-4

3-4 Water Solubilities of n-Octane and Xylenes 3-4

3-5 Normalized Relative Distribution of Hydrocarbon Types 3-6

3-6 Combined Calculated Ideal Effective Solubility Ranges from the Data Tabulated in Table 3-3 and Attachment B.7.1 3-9

3-7 Combined Calculated Ideal Effective Solubility Ranges from the Data Tabulated in Table 3-3 and Attachment B.7.1, including Two FISC JP-5 Samples 3-9

3-8 Petroleum Fraction Composition of JP-8 (Seven Samples) 3-11

3-9 Examples of Polar and Nonpolar Compounds 3-12

3-10 Examples of Degradation Pathways for Toluene, Ethylbenzene, Xylenes, n-Propylbenzene, Naphthalene, and 2-Methylnaphthalene 3-13

3-11 "Fingerprinting" of Fresh and Biodegraded Jet and Diesel—Comparison to a Site Groundwater Sample 3-14

4-1 % Polar Metabolites of TPH-d for Samples from RHMW02 4-2

4-2 Chromatographic Fingerprints of TPH-d Before and After SGC in Groundwater from RHMW02 4-3

4-3 Extended PAH Analysis of October 2017 Samples from RHMW02 4-4

4-4 Extended PAH Analysis of a Jet Fuel Sample 4-5

5-1 RHMW02 TPH-d Results 5-5

5-2 RHMW02 TPH-d Results over Time with Laboratories Identified 5-5

5-3 RHMW01 TPH-d Results 5-6

5-4 RHMW02 Naphthalene Results 5-7

5-5 RHMW01 Naphthalene Results 5-7

5-6 Naphthalene and Sum of 1-Methylnaphthalene and 2-Methylnaphthalene Results for RHMW02 - Ratio of the Sum of the Methylnaphthalene to Naphthalene 5-8

5-7 TPH-d Chromatograms and Naphthalene Ratios for Selected Samples 5-9

5-8 RHMW02 TPH-g Results 5-10

5-9 RHMW01 TPH-g Results 5-10

5-10 Reporting Criteria for DoD QSM 5-11

5-11 RHMW02 Benzene Results 5-12

5-12 RHMW01 Benzene Results 5-12

5-13 RHMW02 Toluene Results 5-13

5-14 RHMW01 Toluene Results 5-13

5-15 RHMW02 Ethylbenzene Results 5-14

5-16 RHMW01 Ethylbenzene Results 5-14

5-17 RHMW02 Xylenes Results 5-15

5-18 RHMW01 Xylenes Results 5-15

5-19 Soil Vapor Measurements 5-16

TABLES

3-1 Typical Distribution of Compound Classes for Jet A, JP-8, and JP-5 3-2

3-2 Analysis of Water-Soluble Fraction of Kerosene 3-5

3-3 Calculated Ideal Effective Solubility in Water of Selected Compounds in Jet Fuels, Diesel, and F-76 3-8

3-4 Solubility Properties of Hydrocarbon Fractions 3-10

4-1 Results from Analysis of TPH-d Before and After SGC for Select Samples of RHMW02 4-2

4-2 Ratios of Sum of Methylnaphthalenes to Naphthalene in Fuel and Calculated for Water 4-5

4-3 Detected Volatile and Semivolatile Organic Analytes in RHMW02 4-6

4-4 NAPs for RHMW02 and RHWW04 4-8

5-1 Evidence of Impact to Groundwater from 2014 Release: Summary of Lines of Evidence 5-18

ACRONYMS AND ABBREVIATIONS

(n)	number of samples
µg/L	micrograms per liter
AFRL	Air Force Research Laboratory
API	American Petroleum Institute
BTEX	benzene, toluene, ethylbenzene, xylenes
CI/LI	corrosion inhibitor/lubricity improver
COPC	chemical of potential concern
CSM	conceptual site model
DL	detection limit
DoD QSM	Department of Defense *Quality Systems Manual*
DOH	Department of Health, State of Hawai‘i
EAL	Environmental Action Level
EC	equivalent carbon number
EHE Guidance	*Evaluation of Environmental Hazards at Sites with Contaminated Soil and Groundwater*
EPA	Environmental Protection Agency, United States
F-76	Diesel Fuel-Marine
FISC	Fleet Industrial Supply Center
FSII	fuel system icing-inhibitor
g/g-mole	grams per gram-mole
GC/MS	gas chromatography with mass spectrometry detection
GCXGC	two-dimensional gas chromatography
HPLC	high-pressure liquid chromatography
J	estimated value
JP	Jet Fuel Propellant
LCS	laboratory control sample
LNAPL	light non-aqueous-phase liquid
LOD	limit of detection
LOQ	limit of quantitation
mg/L	milligrams per liter
NAP	natural attenuation parameter
NATO	North Atlantic Treaty Organization
NIST	National Institute of Standards and Technology
NSZD	natural source-zone depletion
PAH	polynuclear aromatic hydrocarbon
PID	photoionization detector
ppb	parts per billion
ppm	parts per million
SDA	static dissipater
SGC	silica gel cleanup
SVMP	soil vapor monitoring point
SVOC	semivolatile organic compound
TIC	tentatively identified compound
TPH	total petroleum hydrocarbons
TPH-d	total petroleum hydrocarbons – diesel range organics
TPH-g	total petroleum hydrocarbons – gasoline range organics
TPH-o	total petroleum hydrocarbons – residual range organics (i.e., TPH-oil)
TPHCWG	Total Petroleum Hydrocarbon Criteria Working Group

1	UD	University of Dayton
2	USAF	United States Air Force
3	VOC	volatile organic compound
4	vol%	percent by volume
5	WAF	water equilibrated fraction
6	wt%	percent by weight

1. Introduction

This subappendix is summarized in the Conceptual Site Model (CSM) main document, Sections 7.1.3 and 7.2.

Petroleum and petroleum-based products are unique in environmental site assessment and management because these are complex mixtures of compounds with wide-ranging physical and chemical properties. Following release into the environment, these complex mixtures are subject to change due to a multitude of processes commonly referred to as weathering (e.g., volatilization, dissolution, biodegradation, oxidation). Light-molecular-weight hydrocarbons can be lost from the original fuel release by evaporation. Depending on molecular structure, some compounds partition into water. Volatilization and biodegradation are the most important degradation mechanisms for middle distillates such as jet and diesel fuels, which are the main types of fuels stored at the site. Aerobic and anaerobic biodegradation produce intermediate metabolites that are more polar and thus more water-soluble than the parent hydrocarbon. Thus, evaluation or fingerprinting of contamination from fuel releases in the environment must take into consideration the fuel chemistry to assess potential source, degree of weathering, and composition of any dissolved or residual material in light non-aqueous-phase liquid (LNAPL), air, water, and soil.

Assessment of these mixtures in air, soil, and water is through the estimation of total petroleum hydrocarbons (TPH), an analytical parameter that is defined by the method used to measure it. The analytical methods are variable (e.g., different extraction solvents, extraction methods, calibration standards, and reported carbon ranges are variable and sometimes overlap). Non-petroleum materials may also be measured.

In accordance with the State of Hawai'i *Evaluation of Environmental Hazards at Sites with Contaminated Soil and Groundwater, Volume 1* ("EHE Guidance," DOH 2017), the term "TPH" is defined as the sum total of parent petroleum hydrocarbons, as well as petroleum hydrocarbon-related metabolites and other degradants. The latter includes alcohols, phenols, ketones, aldehydes, and organic acids (Mohler et al. 2013; Zemo et al. 2013, 2017). The toxicity of parent petroleum hydrocarbon compounds and related degradants is assumed to be similar for initial screening purposes (DOH 2017, Vol 1).

Understanding the properties of hydrocarbons is essential in sampling and analysis and fate and transport considerations for developing CSMs for appropriate management of TPH in environmental media.

This document includes description of jet fuel composition, partitioning into water, and biodegradation, as well as an assessment of what composes the TPH in groundwater from monitoring location RHMW02, the only well with current concentrations of TPH-d (hydrocarbons within the middle distillates or diesel range) exceeding State of Hawai'i Department of Health (DOH) Environmental Action Levels (EALs). Also included is a thorough review of available groundwater data to assess potential presence of LNAPL at or near the water table and evidence of impact to groundwater after the 2014 Jet Fuel Propellant (JP)-8 release from Tank 5.

2. Study Objectives

In this study, the objectives were to assess:

- Type of released fuel likely responsible for the observed dissolved groundwater plume
- Properties of chemicals of potential concern (COPCs) that are part of the Red Hill risk-based decision criteria (DON 2017b)
- Evidence of attenuation of the dissolved constituents in groundwater
- Presence of LNAPL at the Facility at or near the groundwater table
- Assessment of impact to groundwater after the 2014 JP-8 release

3. Jet Fuel Chemistry

3.1 General Jet Fuel Fingerprinting and Chemistry

Kerosenes/jet fuels are middle distillates from crude oil. Middle distillates (e.g., kerosene, diesel, home heating fuel, JP-5, JP-8, Jet A) are characterized by a wide variety of aliphatic hydrocarbons (straight, branched, and cyclic alkanes), polynuclear aromatic hydrocarbons (PAHs, especially naphthalene and methylnaphthalenes), and heterocyclic compounds with carbon ranges of approximately nine carbons (C9) to C25. A small component of C5–C8 aliphatics and benzene, toluene, ethylbenzene, and xylene (BTEX) aromatics are also present (DOH 2017 Vol. 2, App. 1). The exact composition of chemicals in a fuel depends on the crude oil source and on the refinery processes used for production. Irrespective of this, kerosenes/jet fuels consist predominantly of hydrocarbons in the approximate C7–C18 range:

- Approximately 80% aliphatic hydrocarbons (paraffins or straight and branched alkanes and naphthenes or cycloalkanes)
- Approximately 20% aromatic hydrocarbons (mainly alkylbenzenes and alkylnaphthalenes)
- Less than 5% alkenes (olefins)

The primary types of hydrocarbon compound classes are shown on Figure 3-1.

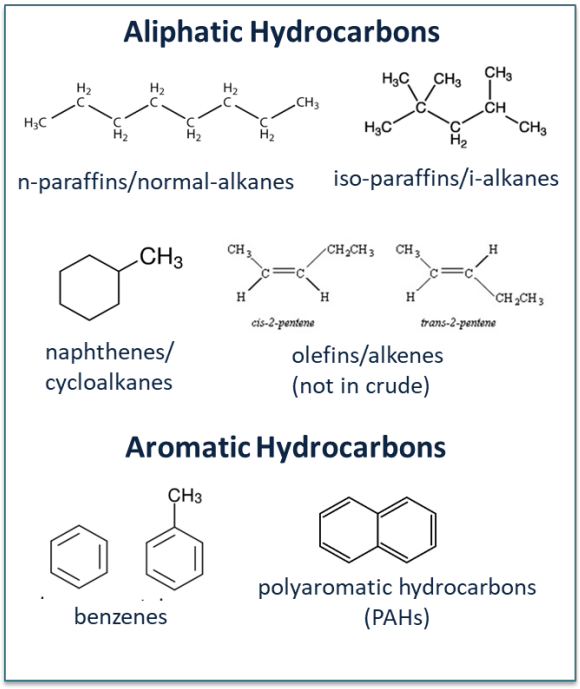

Figure 3-1: Primary Types of Hydrocarbon Compound Classes in Petroleum and Petroleum Products

Information on distribution of hydrocarbon types in Jet A, JP-8, and JP-5 is included in Table 3-1. Jet A is the primary kerosene-based fuel used by commercial airlines. It is governed by ASTM D1655, the standard specification for aviation turbine fuels. JP-8 (governed by military specifications document MIL-T-83139) is similar to Jet A except that JP-8 contains an additive package: static dissipater (SDA), fuel system icing-inhibitor (FSII), and corrosion inhibitor/lubricity improver (CI/LI). Both Jet A and JP-8 contain hydrocarbons in the C7–C18 range. Jet A with the additive package required by JP-8 can be designated as F-24 (governed by NATO Standard AFLP-3747). JP-5 is a higher-flash-point jet fuel developed by the Navy (MIL-T-5624) used on aircraft aboard ships, with hydrocarbons in the C8–C17 range. The data presented in Table 3-1 clearly show that Jet A, JP-8, and JP-5 are essentially equivalent in terms of hydrocarbon composition.

Table 3-1: Typical Distribution of Compound Classes for Jet A, JP-8, and JP-5

Compound Class	Unit	Jet A (n=13)	JP-8 (n=11)	JP-5 (n=2)
Total Saturates (Aliphatics)	vol%	80	79	78
Total Aromatics	vol%	20	21	22
- Monoaromatics (benzene and substituted benzenes)	*vol%*	*18*	*19*	*19*
- Diaromatics (naphthalene and substituted naphthalenes)	*vol%*	*3*	*2*	*3*

Source: CRC Report No. 647 (Hadaller and Johnson 2006).
vol% percent by volume
(n) number of samples

A small portion of the jet fuel, mainly the aromatic hydrocarbons, is water soluble with effective overall water solubility of approximately 5 milligrams per liter (mg/L) with about 3 mg/L from BTEX. Substituted benzenes, naphthalene and substituted naphthalenes make up the rest of the dissolved components. See Section 3.2 for detailed discussion of solubility.

Most fuels are analyzed by gas chromatographic methods in a laboratory to fingerprint the fuel signature. Figure 3-2 shows the chromatographic profiles of fingerprints of JP-5, JP-8, and Jet A. It is evident that JP-5, JP-8, and Jet A are very similar. The large peaks in JP-5, JP-8, and Jet A profiles are primarily the n-alkanes that are the most abundant types of compounds in these fuels.

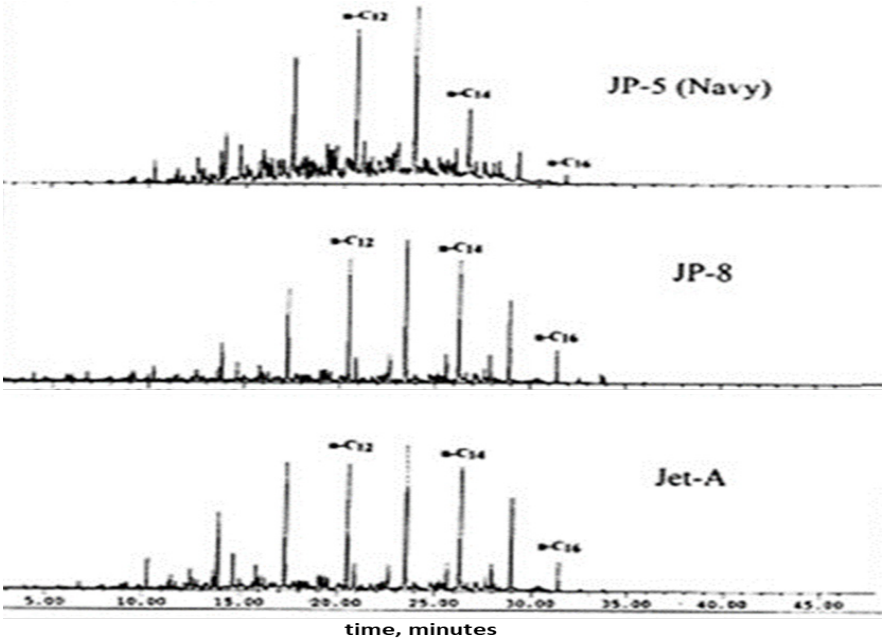

Source: Maurice et al. 2001.

Figure 3-2: Chromatograms of JP-5 and JP-8 and Jet-A

Hydrocarbon molecular structure is important in partitioning into water and weathering of the fuels once released to the environment. Examples of this importance include the following:

- The transport and dispersion of JP-5, JP-8, and Jet A fuels are dependent on the water solubility and volatility of the component hydrocarbon fractions.
- Lower-molecular-weight aliphatic hydrocarbons such as n-alkanes may volatilize relatively quickly from both water and soil, while larger aliphatics may be sorbed to organic particles in water or soil.
- Aromatic hydrocarbons will be dissolved in the aqueous phase in both vadose and saturated zones and may undergo some volatilization. Figure 3-3 shows the relative distribution of aromatics in Jet A (similar to JP-8). This figure illustrates the proportion of Jet A that is composed of saturates (aliphatics) and aromatics. The aromatic compounds are more water soluble.
- n-Alkanes can biodegrade under aerobic condition and are essentially insoluble in water for molecules with greater than six carbons.
- Cycloalkanes are more resistant to biodegradation and are practically insoluble in water.
- Aromatics are more water-soluble, particularly ones with low molecular weight. These can be readily biodegraded.
- In general, the larger the number of carbons in a molecule, the less soluble and less volatile the molecule.

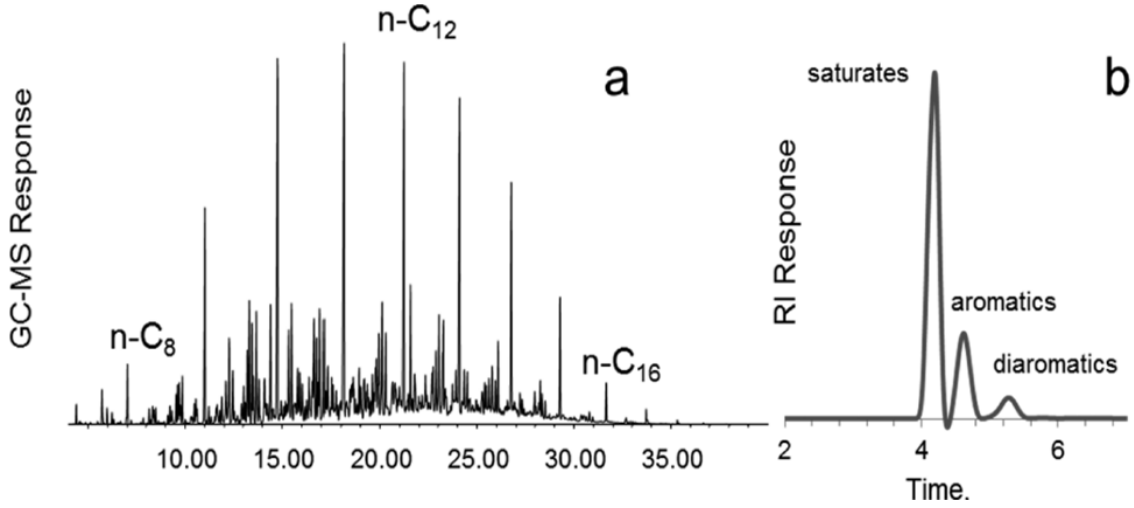

Source: CRC Report No. 647 (Hadaller and Johnson 2006).
GC/MS gas chromatography/mass spectrometry
HPLC high-pressure liquid chromatography

Figure 3-3: Comparison of Analysis of a Jet A Sample by (a) GC/MS and (b) HPLC

3.2 SOLUBILITY OF JET FUEL IN WATER

The main fuels currently stored at the Facility are the jet fuels JP-5 and F-24. Marine diesel fuels (i.e., F-76) are also stored at the Facility. As discussed in the previous section, the jet fuels are kerosene-type fuels with similar hydrocarbon composition.

Numerous studies indicate that kerosene-type fuels, which include Jet A, JP-5, and JP-8, have a water solubility of approximately 5,000 micrograms per liter (µg/L) (5 mg/L). Correspondingly, the EHE Guidance (DOH 2017) states that "*The solubility of diesel range and heavier fuels is assumed to be approximately 5,000 µg/L.*" The guidance also includes jet fuels as a subset of middle distillates and provides one set of regulatory criteria.

Water solubility values vary by orders of magnitude for the individual hydrocarbon constituents making up hydrocarbon-derived fuels. For individual compounds, both molecular weight and chemical structure influence the degree of solubility. Saturated/aliphatic hydrocarbons have relatively very low water solubility with respect to aromatic hydrocarbons. For instance, pure xylenes are greater than 200 times more soluble in water than pure n-octane (Figure 3-4). These compounds both have eight carbons, but the molecular structures are quite different.

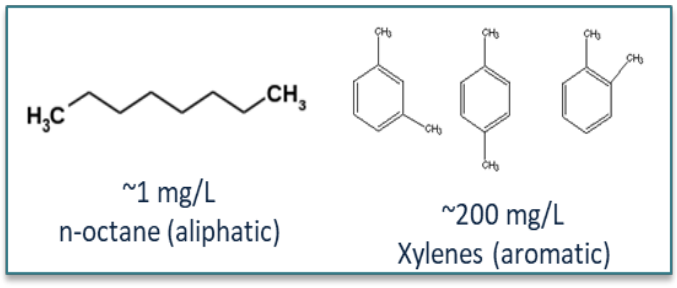

Figure 3-4: Water Solubilities of n-Octane and Xylenes

Aliphatic hydrocarbons in the jet fuel range are essentially insoluble in water, whereas aromatic hydrocarbons have pure compound solubilities ranging from 500 mg/L (toluene) to 25 mg/L (methylnaphthalenes). Effective solubilities are even more variable, as these are proportional to the concentration of the individual aromatic hydrocarbons in the fuel, the average molecular weight of the fuel, and the inherent uncertainties with prediction of mole fraction in multicomponent fuels. Furthermore, component interactions within the organic phase result in deviations from ideality. Mixtures containing compounds that are different in structure (i.e., aliphatics and aromatics) deviate from ideal behavior, and the oil-to-water ratio has significant difference in the "effective solubility" (Bobra 1992). Furthermore, as the fuel weathers by evaporation, solubilization, and biodegradation, the remaining hydrocarbons have higher mole fractions and corresponding higher effective solubilities than the unweathered fuel (Baedecker et al. 2011, 2017). In summary, the effective solubility in groundwater of each component in fuels depends on the component structure, mole fraction in the fuel, loading rates of water to oil, and presence of other hydrocarbons, as well as temperature, ionic strength, and the amount of dissolved organic carbon in groundwater.

The ideal effective solubility in water of individual chemicals can be calculated from the mass fraction of the individual chemical in the fuel as follows:

Effective Solubility $C_w = x_o S$

C_w = *effective solubility*
x_o = *mole fraction (of chemical in fuel)*
S = *solubility*

Mole Fraction $x_o = MF_x MW_o / MW_x$

MF_x = *mass fraction of selected chemical in fuel*
MW_o = *average molecular weight of fuel*
MW_X = *molecular weight of selected chemical*

Table 3-2 and Figure 3-5 show the summary of a study by Coleman et al. (1984) on the partitioning of kerosene (the primary constituent of JP-5 and JP-8) into water. Although the Coleman et al. study used kerosene that as a whole product contained approximately 70% of aliphatic hydrocarbons (i.e., alkanes and cycloalkanes) and approximately 20% aromatic hydrocarbons (i.e., benzene, substituted benzenes, naphthalene and substituted naphthalenes), the water-soluble fraction contained primarily aromatic constituents (greater than 93%). This is expected, as aliphatic hydrocarbons with more than five carbons are essentially insoluble in water. In contrast, a wider range of aromatic hydrocarbons in the fuel have some water solubility, and these compounds partition into water depending on the effective solubility of the individual aromatic compound and its concentration in the fuel.

Table 3-2: Analysis of Water-Soluble Fraction of Kerosene

Kerosene Constituents	Estimated Weight % in Whole Product [a]	Water-Soluble Fraction [b]	
		0.5 hour	17 hours
Alkanes + Cycloalkanes	68.6	4.5	0.5
Benzene - Substituted Benzenes	13.7	63.5	53.2
Naphthalene + Substituted Naphthalenes	5.7	29.6	44.8

Source: Coleman et al. 1984.
[a] Estimated weight percent in unweathered kerosene.
[b] Estimated weight percent of constituents dissolved in water after 0.5 or 17 hours of incubation.

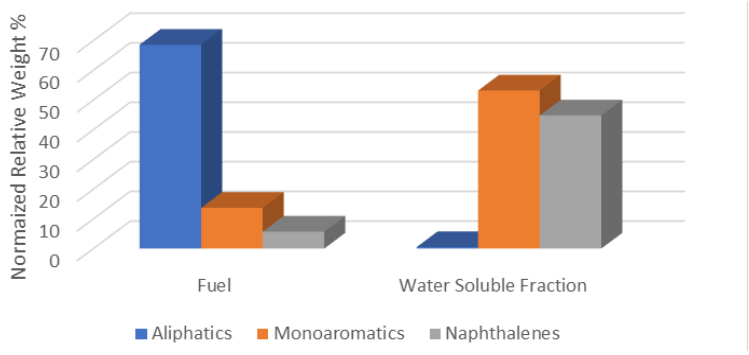

Source: Coleman et al. 1984.

Figure 3-5: Normalized Relative Distribution of Hydrocarbon Types

3.2.1 Calculated Effective Solubilities of Site COPCs

The main composition of the dissolved jet fuel from a recent release is primarly dissolved BTEX. As the fuel weathers by evaporation, solubilization, and biodegradation, the remaining residual fuel, in general, should be less water-soluble as the residual aromatics are larger molecules. However, the effective solubility of the remaining aromatic hydrocrabons would proportionally increase with increasing mole fractions (Baedecker et al. 2011, 2017). The absence of BTEX components, particularly the absence of xylenes, indicates no recent fuel releases and/or the active evaporation and biodegradation of released fuel.

Reliable data on the concentrations of individual fuel components are limited. Attachment B.7.1 presents the results from the analysis of benzene, naphthalene, 1-methylnaphthalene, and 2-methylnaphthalene for jet fuels (Jet A, JP-8, and JP-5), diesel, and F-76 from studies by the University of Dayton Research Instititute and the Air Force Research Laboratory (Shafer and Edwards 2011). These four compounds were analyzed by gas chromatography/mass spectrometry (GC/MS), a highly reliable method for identification and quantitation. Attachment B.7.1 also presents results from analysis of the same fuel types using two-dimensional gas chromatography (GCXGC), a group type analysis. Toluene is reported individually, but ethylbenzene and xylenes are combined as C2-benzenes. Individual concentrations for ethylbenzene and xylenes were estimated from assumed relative proportions of these compounds (pers. comm., J. T. Edwards, CIV USAF, Air Force Research Laboratory, January 2018). API data for 14 Jet A samples and 12 diesel samples are also presented in Attachment B.7.1. These data were used to calculate effective solubilites for seven of the site COPCs.

Table 3-3 summarizes the calculated ideal effective solubilities from multiple sources. Table 3-3 includes information on maximum and minimum concentrations per fuel or combined fuels. Standard deviations were calculated for each COPC when possible (API data were available only as average, maximum, and minimum, thus it was not possible to calculate standard deviation). There is significant variability in effective solubilities for all compounds because of natural variability in concentration of individual components in the fuels. Nevertheless, the main difference among the jet fuels is the significantly lower benzene content in JP-5. This is expected for JP-5, since it is required to have less-volatile components because it is used on shipboard aircraft, where the risk of fire is an important consideration. Figure 3-6 clearly shows that all COPCs other than benzene in JP-5 are comparable for all jet fuels. Toluene, ethylbenzene, and xylenes may appear to be lower in JP-5, but data for these COPCs are limited to two samples.

Table 3-3 also includes results from analysis of two samples of JP-5 and two samples of F-76 from the Fleet and Industrial Supply Center (FISC) Pearl Harbor (currently known as the NAVSUP Fleet Logistics Center Pearl Harbor). These samples are included in the averaged data. Results are shown individually for comparion to samples from throughout the United States. The two FISC JP-5 samples are included in the data set plotted on Figure 3-7 along with other jet fuels; these are plotted separately for comparison to the average results for all samples.

Table 3-3: Calculated Ideal Effective Solubility in Water of Selected Compounds in Jet Fuels, Diesel, and F-76

Compound	Benzene (mg/L)	Naphthalene (mg/L)	1-Methyl-naphthalene (mg/L)	2-Methyl-naphthalene (mg/L)	Toluene (mg/L)	Ethylbenzene (mg/L)	Xylenes (mg/L)
Jet A & JP-8 - API & UD/AFRL	0.29	0.065	0.064	0.085	1.02	0.35	2.20
Number of Samples	*57*	*57*	*57*	*57*	*37*	*37*	*37*
Jet A - API	0.36	0.070	0.088	0.11	1.25	0.34	2.35
Number of Samples	*14*	*14*	*14*	*14*	*14*	*14*	*14*
Jet A (23), Jet A-1 (2) UD/AFRL	0.26 ± 0.24	0.067 ± 0.024	0.058 ± 0.015	0.081 ± 0.025	1.23 ± 0.74	0.29 ± 0.11	2.02 ± 0.73
Number of Samples	*25*	*25*	*25*	*25*	*13*	*13*	*13*
JP-8 UD/AFRL	0.27 ± 0.13	0.060 ± 0.021	0.053 ± 0.015	0.072 ± 0.024	0.93 ± 0.43	0.32 ± 0.13	2.21 ± 0.87
Number of Samples	*18*	*18*	*18*	*18*	*10*	*10*	*10*
JP-5 - UD/AFRL	0.028 ± 0.021	0.083 ± 0.045	0.068 ± 0.026	0.091 ± 0.040	0.27 ± 0.24	0.13 ± 0.07	0.88 ± 0.024
Number of Samples	*13*	*13*	*13*	*13*	*2*	*2*	*2*
FISC JP-5 - UD/AFRL	0.018	0.103	0.074	0.110	NA	NA	NA
FISC JP-5 - UD/AFRL	0.041	0.070	0.063	0.087	NA	NA	NA
Diesel on road <500ppm Sulfur - API	0.36	0.029	0.067	0.10	0.69	0.13	1.02
Number of Samples	*12*	*12*	*12*	*12*	*12*	*12*	*12*
Diesel - UD/AFRL	0.28 ± 0.13	0.021 ± 0.012	0.025 ± 0.016	0.044 ± 0.027	NA	NA	NA
Number of Samples	*39*	*39*	*39*	*39*	*NA*	*NA*	*NA*
F-76 - UD/AFRL	0.14 ± 0.077	0.076 ± 0.041	0.075 ± 0.032	0.118 ± 0.060	0.40 ± 0.13	0.10 ± 0.05	0.69 ± 0.31
Number of Samples	*18*	*18*	*18*	*18*	*9*	*9*	*9*
FISC F76 - UD/AFRL	0.080	0.030	0.047	0.061	NA	NA	NA
FISC F76 - UD/AFRL	0.204	0.028	0.049	0.060	NA	NA	NA

Notes: ppm: parts per million
UD/AFRL: University of Dayton and Air Force Research Laboratory (Shafer and Edwards 2011)
API samples: Analysis by GC/MS (ASTM D5769)
UD/AFRL samples: Analysis by GC/MS for benzene and all naphthalenes. Analysis by GCXGC for toluene, ethylbenzene and xylenes. Data output is for C2-benzenes. Ethylbenzene and xylenes were calculated from the sum using 16% E and 84% X on advice from Tim Edwards, AFRL, Jan 2018 (emails).
Individual samples of JP-5 and F-76 from Pearl Harbor from Shafer and Edwards (2011) included for comparison to averaged data.
Effective Solubilities calculated by I. Rhodes, GSI Environmental.
Average molecular weight for JP-8 from GCXGC analysis (Striebich et al. 2014; pers. comm., J.T. Edwards, CIV USAF, Air Force Research Laboratory, January 2018): 160 g/mole.
Average molecular weight for JP-8 from GCXGC analysis (pers. comm., J. T. Edwards, CIV USAF, Air Force Research Laboratory, January 2018): 200 g/mole.
Solubility from TPHCWG Series, Vol. 3 (Gustafson, Tell, and Orem 1997).
Data sources: API (2010); API (2012); Shafer (2011); Striebich et al. (2014); pers. comm., J. T. Edwards, CIV USAF, Air Force Research Laboratory, January 2018.

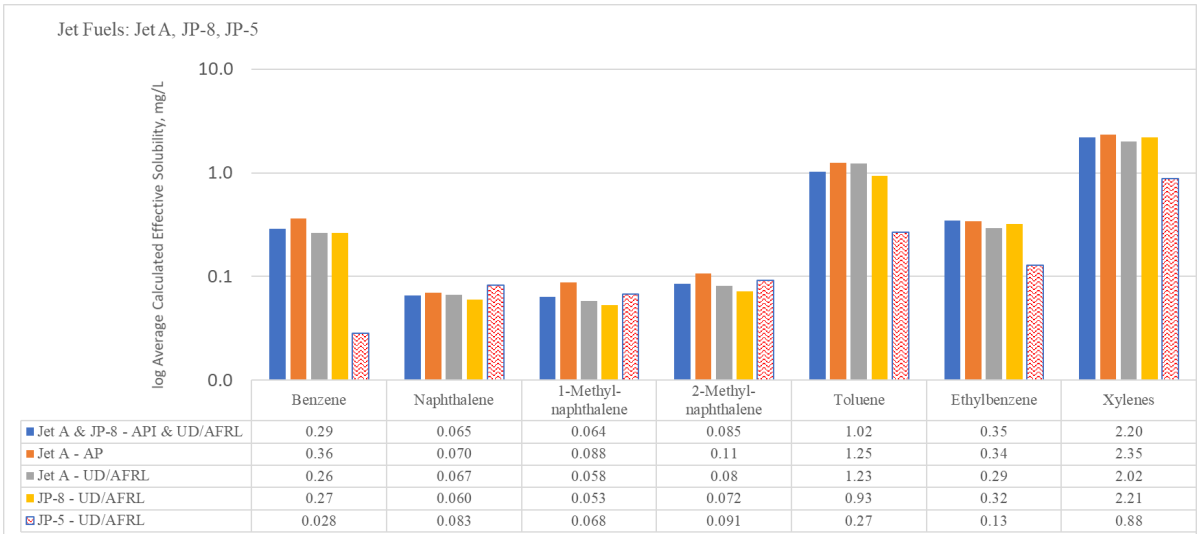

	Benzene	Naphthalene	1-Methyl-naphthalene	2-Methyl-naphthalene	Toluene	Ethylbenzene	Xylenes
Jet A & JP-8 - API & UD/AFRL	0.29	0.065	0.064	0.085	1.02	0.35	2.20
Jet A - AP	0.36	0.070	0.088	0.11	1.25	0.34	2.35
Jet A - UD/AFRL	0.26	0.067	0.058	0.08	1.23	0.29	2.02
JP-8 - UD/AFRL	0.27	0.060	0.053	0.072	0.93	0.32	2.21
JP-5 - UD/AFRL	0.028	0.083	0.068	0.091	0.27	0.13	0.88

Figure 3-6: Combined Calculated Ideal Effective Solubility Ranges from the Data Tabulated in Table 3-3 and Attachment B.7.1

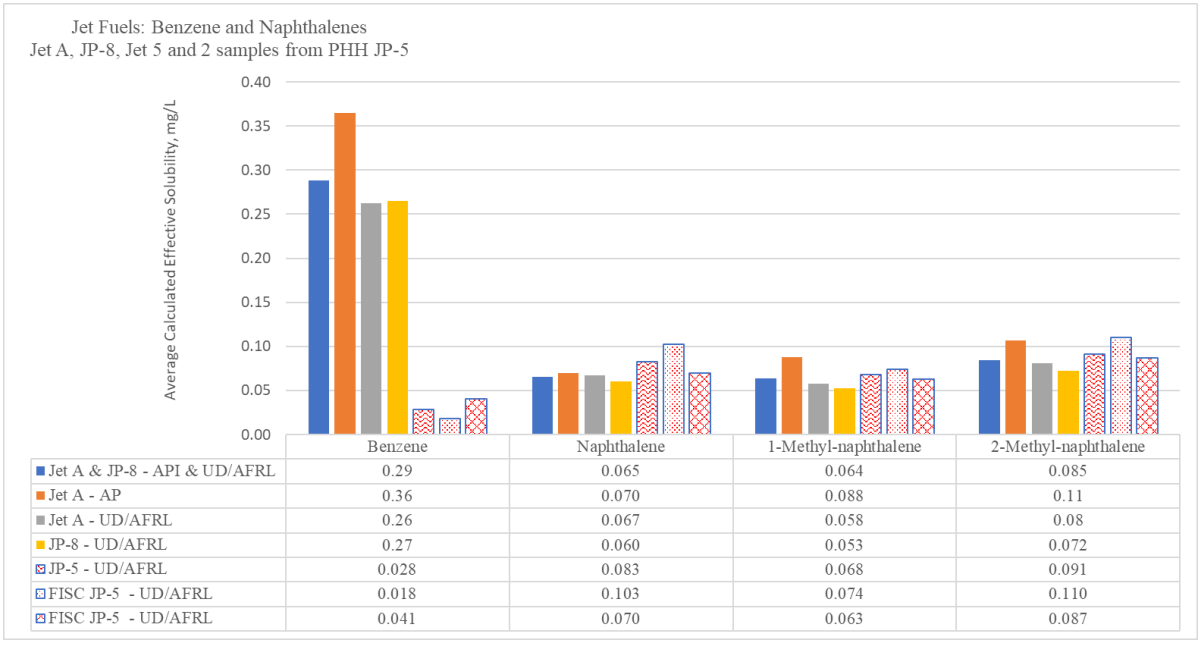

	Benzene	Naphthalene	1-Methyl-naphthalene	2-Methyl-naphthalene
Jet A & JP-8 - API & UD/AFRL	0.29	0.065	0.064	0.085
Jet A - AP	0.36	0.070	0.088	0.11
Jet A - UD/AFRL	0.26	0.067	0.058	0.08
JP-8 - UD/AFRL	0.27	0.060	0.053	0.072
JP-5 - UD/AFRL	0.028	0.083	0.068	0.091
FISC JP-5 - UD/AFRL	0.018	0.103	0.074	0.110
FISC JP-5 - UD/AFRL	0.041	0.070	0.063	0.087

Figure 3-7: Combined Calculated Ideal Effective Solubility Ranges from the Data Tabulated in Table 3-3 and Attachment B.7.1, including Two FISC JP-5 Samples

Additional concentration data and calculated effective solubilities for Jet A, JP-5, JP-8, diesel, and F-76 are included in Attachment B.7.1.

Other COPCs considered at the Facility include gasoline-, diesel-, and residual (oil)-range TPH (TPH-g, TPH-d, and TPH-o) (Section 4). These parameters are intended to be representative of gasoline, middle distillates (e.g., kerosene, jet, and diesel fuels), and heavy oils (e.g., motor oil). The results are dependent on the analytical methods used to measure them. A rough estimation of the effective solubility of these COPCs for jet fuel was done based on the data included in Table 3-4.

Table 3-4 includes the estimated solubility of equivalent carbon number (EC) fractions of aliphatic and aromatic hydrocarbons defined by the *Total Petroleum Hydrocarbon Criteria Working Group* (TPHCWG) *Series*, Vol. 3 and Vol. 5 (Gustafson, Tell, and Orem 1997; Vorhees, Weisman, and Gustafson 1999) for risk assessment, as well as data from analysis of seven samples of JP-8. Jet fuels do not have hydrocarbons extending to the TPH-o range.

Only aromatic hydrocarbons in the fuel have significant solubility to partition into water. The types of compounds expected to be dissolved in groundwater are those indicated in Table 3-3, the aromatic fraction indicated in Table 3-4, and metabolites. The weight percentages from Figure 3-8 were visually estimated for use in the calculations in Table 3-4.

Table 3-4: Solubility Properties of Hydrocarbon Fractions

Equivalent Carbon Number Fraction (EC) [b]	EC	Molecular Weight (g/g-mole)	Solubility (mg/L)	Data for JP-8 (7 samples) - (wt% from Vorhees, Weisman, and Gustafson [1999], Figure 7, p. 11)		
				Average Aliphatic (wt%)	Average Aromatic (wt%)	Calculated Average Ideal Effective Solubility [a] (mg/L)
C5–C6 Aliphatic	5.5	80	36	1	—	0.72
>C6–C8 Aliphatic	7	100	5	2	—	0.16
>C8–C10 Aliphatic	9	130	0.4	13	—	0.064
>C10–C12 Aliphatic	11	160	0.03	39	—	0.012
>C12–C16 Aliphatic	14	200	8.00E-04	25	—	1.60E-04
>C16 Aliphatic	19	270	3.00E-06	4	—	7.10E-08
>C_6–C7 Aromatic [d]	6.5	78	1,780	—	0.0073	0.27
>C_7–C_8 Aromatic [e]	7.6	92	520	—	0.14	1.3
>C8–C10 Aromatic	9	120	65	—	2	1.7
>C10–C12 Aromatic	11	130	25	—	7	2.2
>C12–C16 Aromatic	14	150	6	—	6	0.38
>C16–C21 Aromatic	18.5	190	0.7	—	2	0.012
>C21 Aromatic	28	240	7.00E-03	—	3	0.00014
JP-8, Jet A	7 - 18	160[c]	—	—	—	—
Combined TPH Defined Equivalent Carbon Ranges [a,b]						
TPH-g (>C_6 to C_{10})						3.5
TPH-d (>C_{10} to C_{24})						2.6
TPH-o (C_{24+})						0

Source: TPHCWG Series, Vol. 5 (Vorhees, Weisman, and Gustafson 1999).
g/g-mole grams per gram-mole
Notes: Fraction composition data for JP-8 were used to calculate the effective solubility of the JP-8 fractions and estimate the effective solubility of TPH-g and TPH-d for JP-8 (Figure 3-7).
[a] Calculated by I. Rhodes, GSI Environmental.
[b] Equivalent Carbon Number (EC): Carbon number correlated with the retention time of constituents in a boiling point gas chromatography column, normalized to the n-alkanes.
[c] Average molecular weight for JP-8 from GCXGC analysis (Striebich et al. 2014; pers. comm., J.T. Edwards, CIV USAF, Air Force Research Laboratory, January 2018): 160 g/mole.
[d] Benzene is the only aromatic hydrocarbon in this range. Benzene average concentration from Shafer and Edwards (2011) 2011 (Attachment B.7.1).
[e] Toluene is the only aromatic hydrocarbon in this range. Toluene average concentration from Table 3-3.

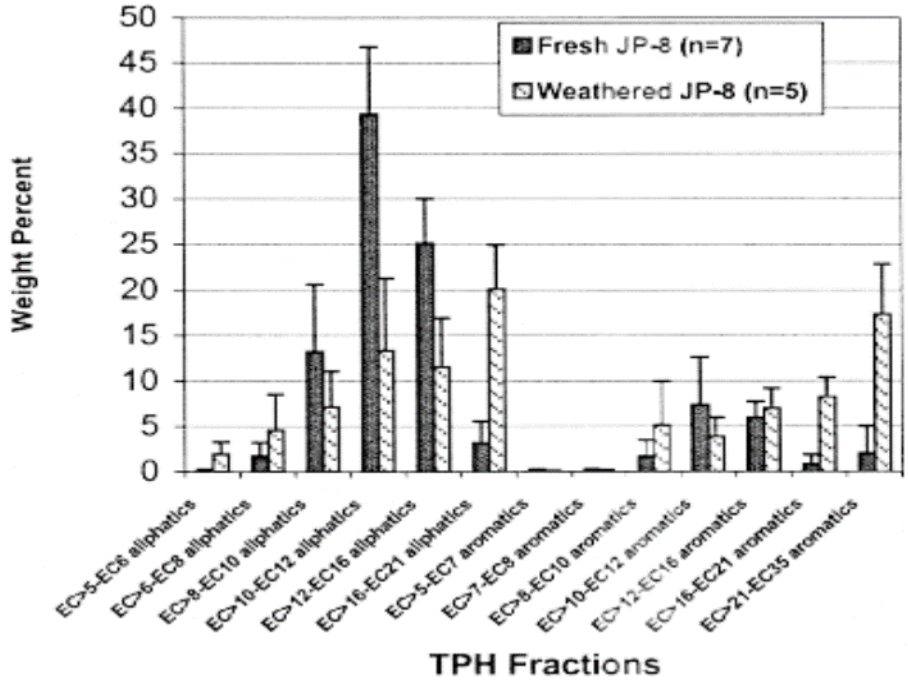

Source: TPHCWG Series, Vol. 5, pg. 11 (Vorhees, Weisman, and Gustafson 1999).

Figure 3-8: Petroleum Fraction Composition of JP-8 (Seven Samples)

The estimated ideal effective solubility in these studies is for fresh fuel. In general, it is not typical to analyze for individual compounds in groundwater beyond BTEX, naphthalenes, and selected PAHs. The concentration of dissolved fuel in water is usually measured as TPH-d (as further discussed in Section 4). It is possible to have dissolved TPH at concentrations exceeding the effective solubility of the fuel and not necessarily be indicative of the presence of free product. The TPH-d concentration may include both dissolved nonpolar hydrocarbons as well as metabolites from biodegradation of the dissolved aromatic components and from residual fuel. Metabolites are further discussed in Section 3.3.

The EHE Guidance (DOH 2017) indicates that the EAL for TPH-d assumes that petroleum-related compounds reported in this range will be dominated by non-volatile degradation compounds or "metabolites" of biogenic origin (Zemo et al. 2013, 2017). The resulting EAL is based on ingestion only and does not incorporate an inhalation pathway. Petroleum-related degradation compounds are assumed to have a similar toxicity as the parent hydrocarbon compounds for the purpose of this document, as it has not been otherwise demonstrated in a site-specific risk assessment (refer to EHE Guidance Vol. 1, Section 2.5.1 [DOH 2017]).

In summary, the compound types and the distribution of dissolved hydrocarbons in water from jet fuel releases are significantly different from the actual composition of the fresh and weathered jet fuel.

3.3 BIODEGRADATION OF JET FUEL

Biological weathering or biodegradation refers to chemical reactions catalyzed by microorganisms that alter and degrade hydrocarbons in the environment through actions of enzymes (biological

catalysts). Enzymes are highly sensitive to the structure of the molecules they are binding and processing. Therefore, hydrocarbons with different structural elements (e.g., aliphatic, aromatic, cyclic/alicyclic, aromatic and/or aliphatic polycyclic, open-chain or branched) require different enzymes and microorganisms for biodegradation to occur. Hydrocarbons generally degrade most readily under aerobic conditions. Smaller aliphatic hydrocarbons are preferentially removed from the mixture by volatilization. Hydrocarbons can also biodegrade anaerobically. Anaerobic processes are predominant in the subsurface and in groundwater where biodegradation has depleted the available oxygen.

Different strains or types of microorganisms (e.g., bacteria, archaea, and fungi) differ in their ability to activate and/or process certain molecular features of hydrocarbons (e.g., position of functional groups or side chains, carbon chain length). That can explain, for example, why alkylbenzenes like toluene more readily degrade than a plain benzene molecule, or why a larger hydrocarbon (longer aliphatic chain) may be more degraded than a small one (Alvarez, Heathcote, and Powers 1998; Baedecker et al. 2011, 2017), or why there are differences in biodegradation rates of isomers of the same molecule. Factors that affect biodegradation include total mass of the release, oxygen levels, availability of other electron acceptors (especially in anaerobic conditions), water chemistry (pH, salinity, availability of nutrients), availability of hydrocarbons to microorganisms (affected by soil type and site geology), soil moisture, soil organic matter (competition for electron acceptors), and temperature.

Anaerobic biodegradation is quite complex. The most substantial differences in biodegradability of hydrocarbons are observed under anaerobic conditions. Under these conditions, some PAHs become almost impossible to degrade. For example, naphthalenes and alkylbenzenes can be recalcitrant when oxygen is not present.

Aerobic and anaerobic biodegradation produces intermediate metabolites that are more polar and thus more water-soluble than the parent hydrocarbon. Compared to aerobic degradation, anaerobic processes are both more diverse and more complex, thus anaerobic biodegradation occurs more slowly and is more prone to accumulation of metabolites.

3.3.1 Polar Compounds/Metabolites

Polar molecules are asymmetric molecules with electrons not shared equally in some of the bonds. Polar compounds can exist in nature as naturally occurring organic matter (e.g., humic material, organic acids) or these may also be formed by biodegradation of petroleum hydrocarbons (i.e., metabolites). Figure 3-9 illustrates polar versus nonpolar bonds.

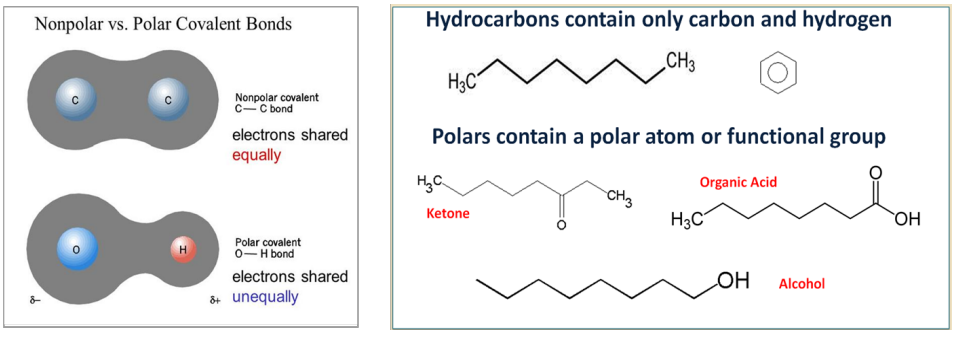

Figure 3-9: Examples of Polar and Nonpolar Compounds

Metabolites are polar molecules derived from chemicals that are undergoing or have undergone changes catalyzed by enzymes in living cells. Biodegradation of hydrocarbons is ubiquitous in soil and groundwater. Intermediate oxidation steps can result in acids/esters, alcohols, phenols, ketones, and aldehydes. Complete biodegradation ultimately converts hydrocarbons to carbon dioxide and water. Figure 3-10 shows examples of degradation pathways for several aromatic compounds common in jet fuels. These aromatic compounds partition into water from jet fuels and can biodegrade, resulting in formation of intermediate polar compounds or metabolites (Widdel and Rabus 2001); Figure 3-10 shows the bonds being broken and incorporation of oxygen into the molecules. The more polar intermediate biodegradation products have higher water solubility than the parent hydrocarbons.

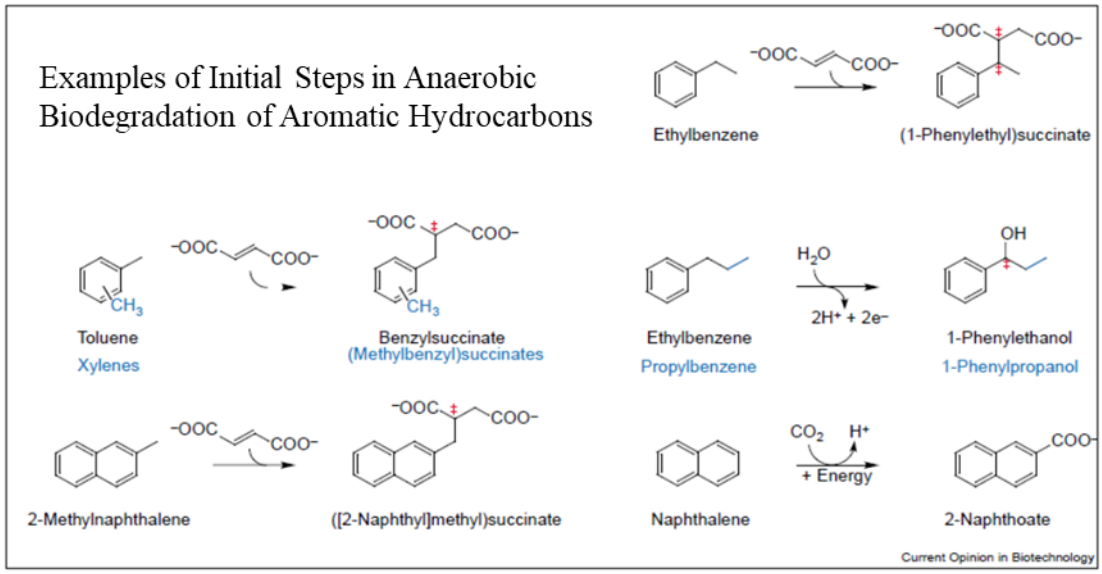

Source: Widdel and Rabus 2001.

Figure 3-10: Examples of Degradation Pathways for Toluene, Ethylbenzene, Xylenes, n-Propylbenzene, Naphthalene, and 2-Methylnaphthalene

3.3.2 Evidence of Biodegradation of Site Jet Fuel

Figure 3-11 shows the chromatograms from analysis of fresh and biodegraded jet and diesel fuels as well as the chromatogram obtained from TPH-d analysis from a sample of groundwater from the Facility (from monitoring well RHMW02). As discussed in Section 3.1, the chromatographic profile or fingerprint of jet and diesel fuels show the predominance of n-alkanes (Figure 3-2 and Figure 3-11). The n-alkanes are relatively easy to biodegrade under aerobic conditions. The chromatograms from analysis of biodegraded jet and diesel fuels show profiles that are characteristic of fuels that have depleted n-alkanes and predominance of highly branched alkanes and cycloalkanes, which are seen as unevenly distributed discrete peaks and the unresolved complex mixture or "hump." In comparison, the chromatogram from the analysis of the extracted dissolved material from RHMW02 has a very different profile. It is dominated by a "hump" and a few resolved peaks. A significant portion of the "hump" in the RHMW02 groundwater sample is heavier than the biodegraded jet fuel "hump." This profile is indicative of aromatic hydrocarbons from dissolved jet fuel (resolved peaks) and metabolites. Analysis of selected target compounds for this sample indicates that the largest resolved peaks are naphthalene, the two isomers of methylnaphthalene (C1-naphthalenes) and isomers with higher number of alkyl side chains substitution

(C2-naphthalenes, C3-naphthalenes). Analysis of the extract after silica gel cleanup (SGC) eliminates the "hump," confirming that it is due to polar metabolites or biogenic matter (discussed in Section 4 and shown on Figure 4-2 and Figure 4-3).

The chromatograms provide evidence that the dissolved TPH-d in RHMW02 is from a jet fuel release that has weathered based on the aromatic hydrocarbons found in the water and the predominance of metabolites.

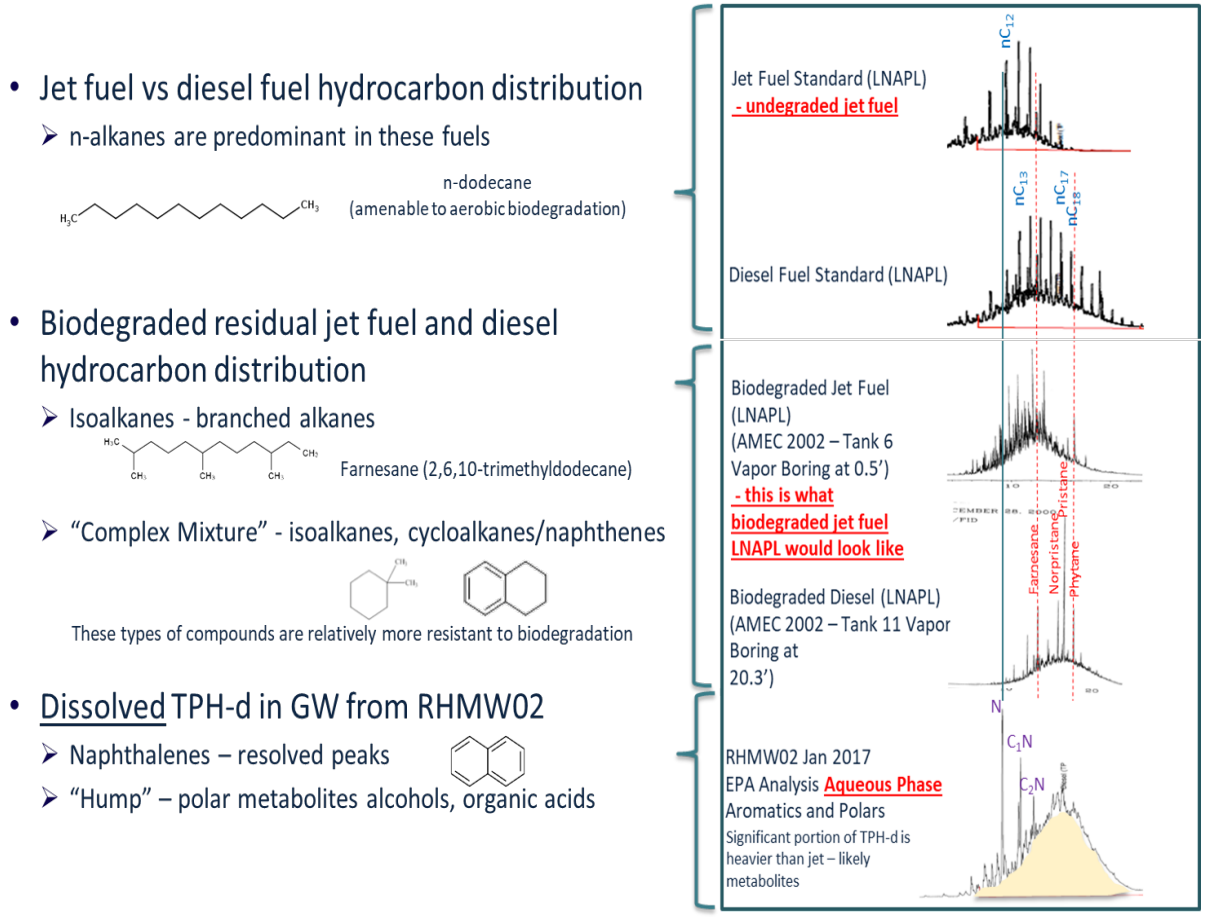

Figure 3-11: "Fingerprinting" of Fresh and Biodegraded Jet and Diesel—Comparison to a Site Groundwater Sample

4. Evaluation of TPH-d in Groundwater

4.1 COMPOSITION OF TPH-D IN GROUNDWATER AND EVIDENCE OF NATURAL ATTENUATION

As discussed in more detail in Section 5.1.1 below, LNAPL has not been detected in the groundwater monitoring wells at the Facility. The focus of this evalution is to (1) characterize extractable organics in water for monitoring wells with detectable TPH-d, (2) correlate the TPH results to a type of source fuel, and (3) assess natural attenuation in the groundwater at the Facility.

As discussed in Section 3.2, the main components of jet fuels are aliphatic compounds that are not significantly water-soluble. The aromatic compounds in jet fuels partition from the fuel into water based on their effective solubilities. Therefore, the chromatographic profile or fingerprint of jet fuel is quite different from the corresponding fingerprint of dissolved jet fuel in water.

Per the EHE Guidance (DOH 2017), TPH-d is defined as anything that is extracted by methylene chloride solvent from water, detected by gas chromatography with flame ionization eluting between nC10 and nC24, and quantitated with respect to a diesel standard.

EHE Guidance Vol.1 (DOH 2017) states, "*The term "TPH" is defined for use in this guidance as the sum of total parent petroleum hydrocarbons as well as petroleum hydrocarbon-related metabolites and other degradants*." Furthermore, "*Petroleum-related degradation compounds are assumed to have similar toxicity as the parent hydrocarbon compounds for the purpose of this document, unless demonstrated in a site-specific risk assessment."* This means that reported TPH-d concentrations are not only the soluble components of the original fuel, but all detectable matter in the specified analysis window (nC10 to nC24), which would include the soluble components of the fuel plus metabolites of degradation of the dissolved aromatics and possible metabolites of degradation of aliphatics and aromatics of any residual fuel in soil nearby.

4.1.1 Evaluation of Hydrocarbon and Polar Metabolite Concentrations in Groundwater

The relative concentrations of hydrocarbons in water vs. polar metabolites can be evaluated using SGC methods to separate and remove polar compounds from environmental media extracts to minimize misidentification and inclusion of metabolites in the reported TPH concentration. Certain chemicals related to well construction and sampling equipment (e.g., grease used for the water pump used during drilling activities) may also contribute to TPH detections. Thus, the TPH chromatograms should be evaluated to determine if there are other sources of TPH than fuels or degraded fuels.

Results from analysis of TPH-d before and after SGC for samples from RHMW02 are summarized in Table 4-1. It is clear that the bulk of the TPH-d is due to polar material, likely metabolites generated from biodegradation of dissolved petroleum compounds and potentially biodegradation of the source LNAPL. Variations in TPH-d results are expected since these methods rely on quantification of mixtures that spread over a relatively large retention time window and can be affected by baseline variations. In addition, polar compounds are not very compatible with gas chromatographic techniques that rely on vaporization of the compounds. Polar compounds do not partition well between the vapor and liquid stationary phases of the chromatographic column, thus hampering the compound's ability to reach the detector. This leads to chromatograms showing unresolved humps (where polar metabolites do not give sharp peaks and tend to tail [i.e., appear in the chromatographic pattern as wide peaks or humps extending past the expected retention time window]), which make metabolites more difficult to quantify because these can have significantly different responses in the flame ionization detector compared to the diesel standard used to calibrate the gas chromatograph. Though not typically an issue with hydrocarbon analysis, samples analyzed

later the same day may also have more peak tailing because more active sites may be present in the gas chromatograph injection system or instrument column due to nonvolatile residues from previous samples. Limitations of TPH measurements are further discussed in Section 5.2.1.2.

Results from split samples analyzed by the United States Environmental Protection Agency (EPA) Region 9 laboratory and the Navy-contracted laboratory (APPL) also showed how the unresolved polar metabolite hump led to different reported TPH-d concentrations between laboratories (see Table 4-1) despite use of the same analytical method. Following evaluation of the split sampling results, APPL laboratory implemented changes to match EPA Region 9 extraction protocols. The low recovery of TPH-d at APPL laboratory is likely due to differences in extraction efficiency of polar metabolites. Figure 4-1 presents the relative amount of polar metabolites as a portion of the TPH-d. Since TPH-d is greater than 40–85% polar matter, it is difficult to achieve consistent TPH results in biodegraded samples between laboratories.

Table 4-1: Results from Analysis of TPH-d Before and After SGC for Select Samples of RHMW02

	May-2017	Jun-2017	Jul-2017	Oct-2017		Mar-2018		Apr-2018
Laboratory >	APPL	APPL	APPL	APPL	EPA	APPL	EPA	APPL
Analyte	µg/L	µg/L	µg/L	µg/L	µg/L	µg/L	µg/L	µg/L
TPH-d	1,000	1,000	1,000	1,300	3,300	1,900	2,900	2,700
TPH-d with Silica Gel Cleanup	< 480 U	570	250	230 J	550	640	430	510
TPH-d (Dup.)	—	—	—	1,600	—	1,800	—	2,800
TPH-d with Silica Gel Cleanup (Dup.)	—	—	—	230	—	460	—	420

(Dup.) Duplicate Sample
Notes: APPL non-detect results reported as < the limit of detection (< LOD U) in accordance with the DoD *Quality Systems Manual*, Version 5.1 (DoD and DOE 2017). EPA non-detect results are reported as less than the detection limit (< DL U).
J estimated value
U undetected

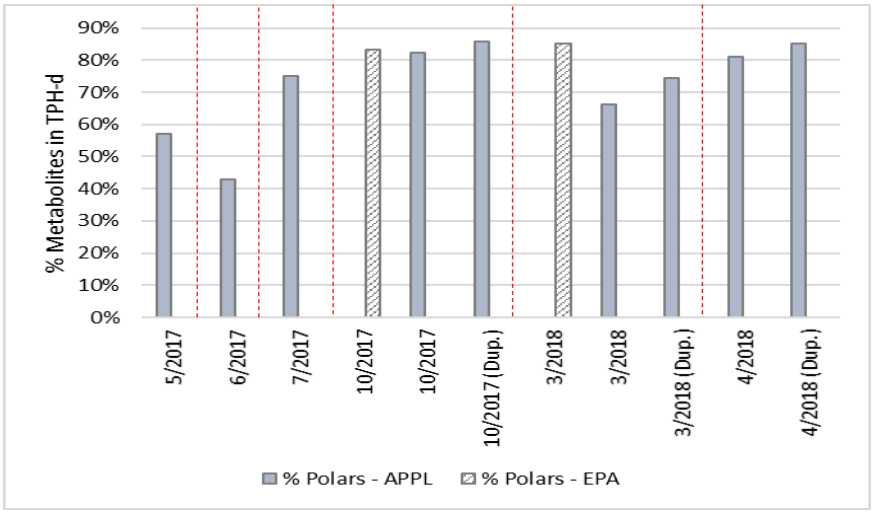

Figure 4-1: % Polar Metabolites of TPH-d for Samples from RHMW02

Figure 4-2 shows the chromatograms for analysis of dissolved material in RHMW02 (March 2018 sample event) for TPH-d before and after SGC. These chromatographic profiles are consistent with dissolved aromatic hydrocarbons in a weathered jet fuel, showing the presence of substituted benzenes (C3+), naphthalene, and substituted naphthalenes (C1+). The chromatographic profile of TPH-d before SGC shows the additional presence of metabolites.

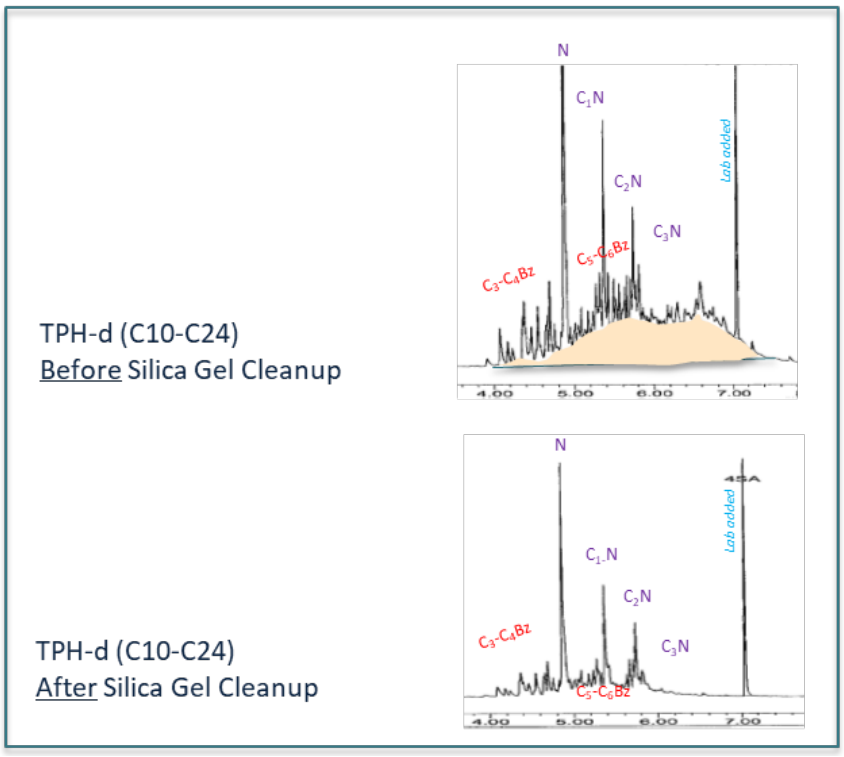

Figure 4-2: Chromatographic Fingerprints of TPH-d Before and After SGC in Groundwater from RHMW02

4.1.2 Evaluation of Hydrocarbon and PAH Concentrations in Groundwater

The March 2018 groundwater sample from RHMW02 contained 1,900 µg/L of "TPH-d" before SGC, and 640 µg/L of TPH-d after removal of polar compounds by SGC. The concentrations of naphthalene (65 µg/L), 1-methylnaphthalene (25 µg/L), and 2-methylnaphthalene (18 µg/L) in the sample were quantified by EPA Method 8270, and, therefore, the contribution of these constituents to the TPH-d result can be quantified. Based on these measurements and knowledge of other compounds in jet fuel, the likely estimated composition of "TPH-d" after removal of polar compounds is as follows:

- Naphthalene and methylnaphthalenes: 108 µg/L, which is approximately 1/6 of the 640 µg/L TPH-d w/ SGC result
- C3+ benzenes and C2+ naphthalenes: remaining bulk of the TPH-d w/ SGC result

Naphthalene concentrations in RHMW02 exceed naphthalene's effective solubility for unweathered fuel by a factor of approximately 2. The higher-than-expected concentrations of naphthalene are

consistent with a weathered source that has lost lighter ends, such that naphthalene is relatively more concentrated than in the original fuel.

Naphthalene, 1-methylnaphthalene, and 2-methylnaphthalene are routinely analyzed in the groundwater samples from the Facility. The October 2017 samples for some of the Facility wells were also analyzed for an extended list of PAHs to better understand the composition of the dissolved hydrocarbon portion of the TPH-d. Figure 4-3 shows the distribution of parent and alkylated PAHs for two samples from RHMW02. Visual comparison of the bar graph on Figure 4-3 and the bottom chromatogram shown on Figure 4-2 confirms the identity of heavier substituted naphthalenes (C2+) and indicates the presence of decalins and benzothiophenes in RHMW02.

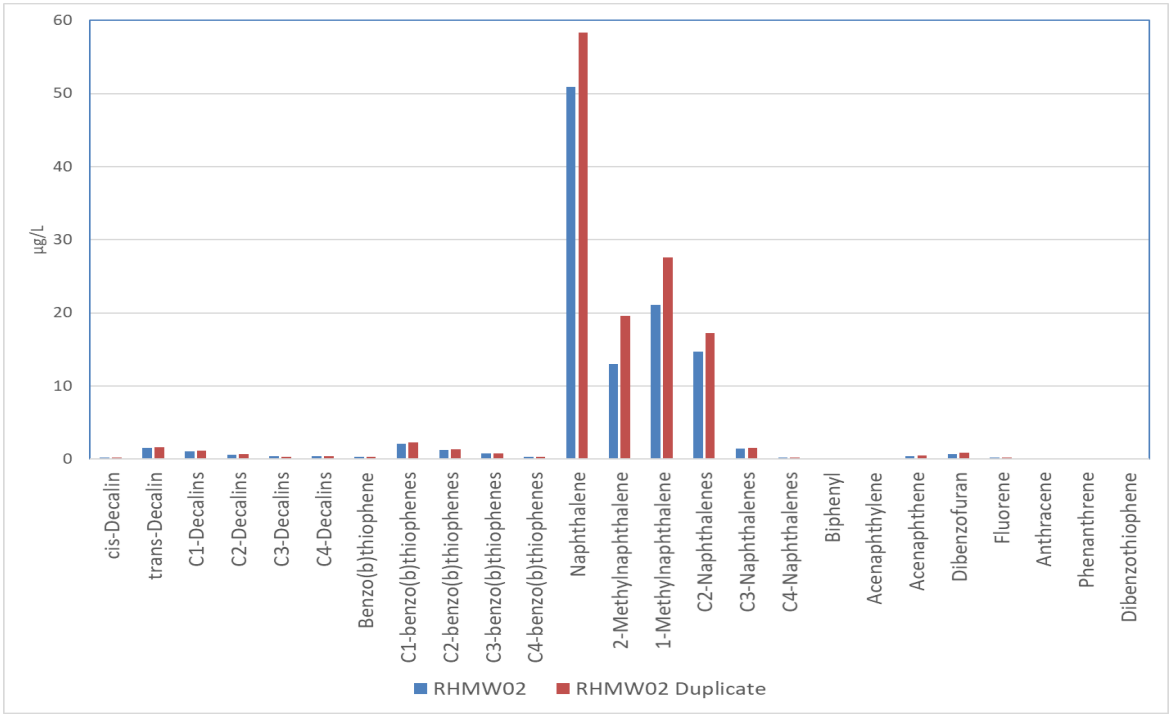

Figure 4-3: Extended PAH Analysis of October 2017 Samples from RHMW02

The distribution of naphthalenes in groundwater from RHMW02 is not consistent with the typical composition of jet fuel. Specifically, the methylnaphthalene to naphthalene ratio in RHMW02 groundwater is much lower than expected. The RHMW02 naphthalene concentration is higher than the methylnaphthalenes, and 1-methylnaphthalene is higher than 2-methylnaphthalene. In contrast, unweathered petroleum-sourced fuels have alkylated naphthalenes that are more abundant than the parent naphthalene; furthermore, 2-methylnaphthalene is more abundant than 1-methylnaphthalene. A typical distribution of PAHs in JP-8 is shown in Figure 4-4. Naphthalene is less abundant than the methylnaphthalenes (Bernabei et al. 2003). The average concentrations of methylnaphthalene and naphthalene (Shafer and Edwards 2011 and Attachment B.7.1) for the types of fuels stored at the Facility are:

JP-5: methylnaphthalenes 0.54 wt%, naphthalene 0.22 wt%
JP-8: methylnaphthalenes 0.42 wt%, naphthalene 0.16 wt%
F-76: methylnaphthalenes 0.53 wt%, naphthalene 0.16 wt%

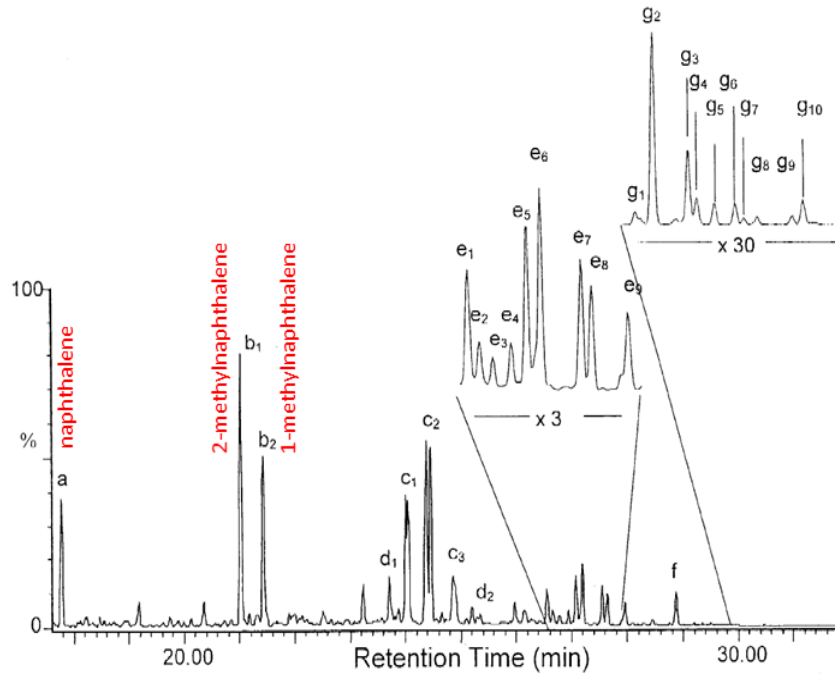

(a) naphthalene, (b) methylnaphthalenes, (c) dimethylnaphthalenes, (d) ethylnaphthalenes, (e) C_3-naphthalenes, (f) laboratory-added internal standard, (g) C_4-naphthalenes

Figure 4-4: Extended PAH Analysis of a Jet Fuel Sample

Although the samples used in the Shafer and Edwards 2011 study are not from the Facility, the average concentrations presented in the study are representative of the relative distribution of these compounds in JP-8 and of any petroleum-sourced middle distillates.

Forensics investigations often use ratios of target compounds rather than absolute concentrations to normalize sample variability and take advantage of properties and/or biodegradation differences among the different compounds that can be diagnostic of particular changes in the samples. Since the pure solubility of naphthalene (31 mg/L) and methylnaphthalenes (28–25 mg/L) are similar, the ratio of naphthalene to methylnaphthalene in fuel and in water should be relatively similar. Using the calculated ideal effective solubility estimates presented in Section 3.2.1, the ratio of the sum of methylnaphthalenes (1-methylnaphthalene and 2-methylnaphthalene) to naphthalene (Table 4-2) in the fuels and in water are approximately 2 for JP-8 (F-24), JP-5, and F-76 (diesel marine fuel). In contrast, the ratio of methylnaphthalenes to naphthalene in samples from RHMW02 is typically less than 1, further indicating that TPH-d in RHMW02 is from biodegraded fuel. This is discussed further in Section 5.2.2.

Table 4-2: Ratios of Sum of Methylnaphthalenes to Naphthalene in Fuel and Calculated for Water

JP-5 (average, 13 samples)		JP-8 (average, 18 samples)		F-76 (average, 18 samples)	
Fuel	Water	Fuel	Water	Fuel	Water
2.5	1.9	2.7	2.1	3.3	2.5

In summary, the dissolved TPH-d in RHMW02 is composed of metabolites and aromatic hydrocarbons consistent with a jet fuel source that has undergone significant biological weathering. This is also consistent with the EHE Guidance (DOH 2017), which recommends to "*use SGC to assess petroleum degradation and to optimize remedial options*." The EHE Guidance also states that "*comparison of non-SGC data for groundwater indicates significant degradation of compounds outside of areas with LNAPL*."

4.2 EVALUATION OF NON-COPC COMPONENTS OF TPH-D IN GROUNDWATER

In addition to analysis for COPCs like BTEX, naphthalene, and methylnaphthalenes that have specific EALs, some samples have been analyzed by the Navy and by EPA Region 9 for extended lists of compounds as part of the split sampling and attenuation evaluation sampling conducted in 2017 (EPA 2017; DON 2017a). The analyses were done using EPA Method 8260 for volatile organic compounds (VOCs) and EPA Method 8270 for semivolatile organic compounds (SVOCs). Both of these methods use gas chromatograph and mass spectrometer to identify and quantify compounds. A list of detected target compounds that are quantitated against standards of those compounds is included as a summary in Table 4-3. Most of the detected compounds are aromatic hydrocarbons expected to partition from jet fuel to water and are consistent with the chromatographic patterns seen in the TPH analysis after SGC. The phthalate detected is likely a plasticizer from sampling equipment or lab contamination.

Table 4-3: Detected Volatile and Semivolatile Organic Analytes in RHMW02

Target Compounds
C2 Substituted Benzenes
Ethylbenzene [a]
Xylenes [a]
C3 Substituted Benzenes
i-Propylbenzene
n-Propylbenzene
C4 Substituted Benzenes
tert-Butylbenzene
sec-Butylbenzene
n-Butylbenzene
PAHs
Naphthalene [a]
1-Methynaphthalene [a]
2-Methylnapathalene [a]
Acynaphthalene
Acenaphthene
Fluorene
Others
Dibenzofuran
Bis(2-Ethtylhexyl)phthalate

Examples of Tentatively Identified Compounds (TICs)
C4–C6 Substituted Benzenes
Tetramethylbenzenes
Diethylbenzenes
Ethyldimethylbenzenes
Methylpropylbenzenes
Dimethylstyrene
Methylbytylbenzene
Dimethylbutenylbenzene
Naphthenobenzenes
Indane
Methylindan
Ethylindan
Dimtheylindane
Tetralin
C2 Substituted Naphthalenes
Dimethylnaphthalenes
Organic Acids
PhenylPentanoic Acid
MePhPropenoic Acid
Naphthalenecarboxylic acid

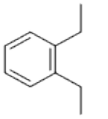

1,2-Dethylbenzene

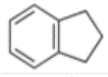

Indane

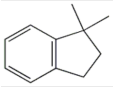

Dimethylindane

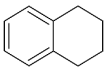

Tetralin

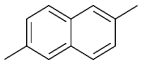

Dimethylnaphthalene

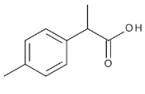

3-(4-Methylphenyl)propanoic acid

[a] Compounds with EALs.

Table 4-3 also includes a summary of tentatively identified compounds (TICs). Unlike target compounds that are identified and quantitated against standards, the identification of TICs is performed by doing a library search of the mass spectrum of each compound compared to those in the National Institute of Standards and Technology (NIST) Mass Spectrometry Data Center library. Mass spectrum detectors alone cannot differentiate isomers. For example, the mass spectra of ethylbenzene and the three isomers of xylenes are essentially the same. Most of those COPCs can be identified and quantitated individually because the actual compounds are included in the laboratory standards and have different retention times in the gas chromatograph, so that the analyst can verify the time of elution of each compound and report them. In the case of the TICs, the laboratory is identifying unknown peaks by performing a library search of the peak's mass spectrum. However, identification using mass spectra alone as well as quantitation without a calibration standard for the specific compound results in a reported TIC concentration that is not reliable. Nevertheless, TICs can provide general information on the types of compounds that can also be present in the samples.

The TICs listed in Table 4-3 are also consistent with aromatic compounds that are present in jet fuels (Lovestead et al. 2016). Of particular significance is the identification of naphtheno-benzenes, such as indane and tetralin and some of their substituted homologues. These compounds are present in fuels at relatively low concentrations, but these become more abundant as the dissolved fuel components biodegrade. As shown in Table 4-3, naphtheno-benzenes are bi-cyclic compounds, with one benzene ring and the other non-aromatic ring attached to two carbons of the benzene ring. These types of compounds are relatively resistant to biodegradation. Some of the TICs also indicate aromatic organic acids that are likely metabolites. The relative abundance of naphtheno-benzenes and organic acids provide additional evidence of natural attenuation.

4.3 NATURAL ATTENUATION PARAMETERS IN GROUNDWATER

Biodegradation depletes the groundwater of dissolved oxygen and other electron acceptors (e.g., nitrate, ferric iron, and sulfate), and subsequently increases ferrous iron and alkalinity concentrations of the groundwater. When all the soluble electron acceptors (i.e., dissolved oxygen, nitrate, ferric iron, and sulfate) are depleted, groundwater conditions become conducive to fermentation and methane is generated by methanogenesis. When evaluated alongside depressed dissolved oxygen concentrations, methane is a strong line of evidence of anaerobic biodegradation. These natural attenuation parameters (NAPs) are indirect (or secondary) lines of evidence for biodegradation of COPCs and are discussed further in CSM Appendix B.5.

From October 2016 through March 2017, dissolved methane concentrations were:

- 1.9–47 mg/L in RHMW02
- 0.15–7.5 mg/L in RHMW01
- Not detected in all other wells

Methane concentrations were also available from samples collected in September 2005 and July 2006 (DON 2007). However, these water samples were collected using a bailer; therefore, the concentration results are likely biased low due to loss of methane during the sample collection. The samples from 2016 and 2017 monitoring events were collected using a downhole bladder pump using low-flow techniques, minimizing loss of volatile compounds. Due to the difference in sample collection methods, only the more recent data have been considered in the natural attenuation evaluation.

Table 4-4 summarizes available data for these parameters as well as TPH-d before and after SGC. The presence of methane and TPH-d composed mostly of metabolites (material removed by SGC), along with the relative depletion of dissolved oxygen, nitrate, ferric ion, and sulfate, are clear evidence that natural attenuation is significant and sustained in RHMW02. Issues with TPH variability are discussed in Section 5.2.1.2, and the relative proportion of metabolites is shown on Figure 4-1. Additional information pertaining to natural attenuation is presented in the CSM main document, Section 7.4 MNA.

Table 4-4: NAPs for RHMW02 and RHWW04

Date	Nitrate (mg/L)	Sulfate (mg/L)	Ferrous Iron (mg/L)	Chloride (mg/L)	Alkalinity (mg/L)	Dissolved Oxygen (mg/L)	Methane (mg/L)	TPH-d Max (µg/L)	TPH-d w/ SGC Max (µg/L)
RHMW02									
2016-10-17	0.43	0.85	2.8	38	—	0.61	47	1,300	300
2016-11-14	0.45	1.2	2.9	39	196	0	20	1,300	—
2016-12-12	0.43	1.2	2.5	38	195	0.7	16	1,300	—
2017-01-09	< 0.18	0.79	3.0	39	211	1.05	21	1,400	—
2017-02-06	0.44	1.0	2.9	40	193	0.1	16	1,000	—
2017-03-06	0.6	1.1	3.0	39	204	0.25	5.7	1,200	—
2017-04-03	< 0.18	1.1	2.8	40	206	0.32	6.0	940	—
2017-05-01	< 0.18	< 0.71	2.9	39	214	0.17	7.4	1,000	460
2017-06-05	< 0.18	1.0	2.6	39	227	0.93	7.2	1,000	570
2017-07-04	< 0.18	0.98	2.6	44	227	0.1	11	1,000	250
2017-10-23	< 0.18	1.4	2.5	38	211	0.26	4.5	1,300	230
2018-03-13	0.75	1.5	2.5	43	202	0.53	1.9	1,900	640
2018-04-23	< 0.18	1.3	2.3	40	192	0.45	2.9	2,800	510
RHMW04									
Background ranges	2.4–2.8	9.5–11.9	<0.32–0.27	70.8–86.2	75.2–79.3	4.62–9.04	< 0.001	< 25	< 40

5. Likelihood of LNAPL in Groundwater and Evidence of Impact to Groundwater from the 2014 JP-8 Release

The historical groundwater monitoring data (i.e., 2005 to March 2018) have been reviewed to answer two questions:

1. Is LNAPL likely present in groundwater in the vicinity of Red Hill monitoring wells?
2. Did the 2014 JP-8 Tank 5 release event result in an increased impact to groundwater?

5.1 LIKELIHOOD OF LNAPL IN GROUNDWATER

The likelihood of LNAPL in groundwater is determined by (1) the presence or absence of LNAPL in individual monitoring wells, and (2) the composition and concentration of dissolved COPCs in the monitoring wells.

5.1.1 Absence of LNAPL in Monitoring Wells

The presence or absence of LNAPL in individual monitoring wells has been evaluated through (1) use of an oil/water interface probe during each monitoring well sampling event and (2) visual inspection of samples and purge water for a sheen or other evidence of LNAPL.

- *Interface Probe:* Interface probe measurements have never yielded definitive evidence of LNAPL in any monitoring well. In January 2008, the interface probe measurements at RHMW01 and RHMW02 were recorded as <0.01 foot; however, this is believed to be a nomenclature issue (i.e., reflecting the detection limit of the probe [0.01 foot]) rather than an indication of a positive result from the probe.
- *Visual Observation:* Visual observation of samples and purge water has not provided evidence of LNAPL in any of the monitoring wells since the January 2014 release.

In summary, for the available monitoring history to date, there has been no direct measurement of LNAPL in any monitoring well.

5.1.2 Composition and Concentration of Dissolved Constituents

Dissolved-phase concentrations of COPCs in groundwater and chromatographic profiles of TPH analysis may be useful as indirect indicators in evaluating the presence of LNAPL in groundwater or in close proximity to specific monitoring wells when used collectively as multiple lines of evidence. Based on the visual evaluation of the chromatograms, there is no evidence that LNAPL was present in any of the groundwater samples collected from monitoring wells at the Facility. For the four in-tunnel monitoring wells located nearest to the tanks, the dissolved-phase COPC concentrations support the following observations:

- In monitoring well RHMW03, total dissolved-phase concentrations of fuel constituents are relatively low (less than 0.5 mg/L since 2005), with limited depletion of groundwater electron acceptors (oxygen, nitrate, and sulfate) and no measurable methane production. The groundwater data in this area suggest the presence of a low-concentration dissolved plume, potentially one that is driven by infiltration/leaching processes and do not indicate the presence of LNAPL in the saturated zone in the vicinity of RHMW03.

- Monitoring well RHMW02 exhibits the highest total dissolved-phase fuel constituent concentrations among the Facility monitoring wells (approximately 2–7 mg/L since 2005). Much of these concentrations are in the form of polar compounds associated with the biodegradation of petroleum. The concentrations of naphthalene, 1-methylnaphthalene, and 2-methylnaphthalene are equal to or greater than the expected concentration based on the effective solubilities of these compounds in jet fuel. However, BTEX concentrations are very low (generally less than 1 µg/L). Although COPC concentrations have varied over time, the observed concentration ranges are similar for the monitoring periods before and after the 2014 Tank 5 release. The NAP results indicate high levels of biodegradation occurring in the vicinity of this well, as key electron acceptors are depleted and high concentrations of dissolved methane are present (sometimes greater than 10 mg/L). Evaluated together, these data suggest the presence of weathered LNAPL (i.e., pre-2005 release) in the immediate vicinity of RHMW02 or within the saturated zone upgradient from this well. Based on visual and analytical observations of petroleum contamination in subsurface angle borings advanced during investigations conducted during 1998–2002 (DON 1999, 2002), this LNAPL may have originated from releases from Tank 9, 11, or 13. The groundwater monitoring data indicate it is likely that the 2014 Tank 5 release did not impact groundwater and more likely that impacts to groundwater are the result of historical leaks.
- Monitoring well RHMW01 exhibits the next highest concentrations of dissolved-phase fuel constituents (approximately 0.1–1 mg/L since 2005); RHMW01 may have some hydraulic connection to monitoring well RHMW02. Electron acceptors are depleted, and methane is present in the 0.2–7 mg/L range since 2005. These data are consistent with the natural attenuation of dissolved constituents in groundwater and do not suggest the presence of LNAPL within the vicinity of RHMW01.
- Monitoring well RHMW05 is located between the tank farm and the Red Hill Shaft water development tunnel. Groundwater at this location exhibits low concentrations of fuel hydrocarbons (typically less than 0.05 mg/L). These data do not suggest the presence of LNAPL within the saturated zone between RHMW01 and RHMW05.

5.1.3 Is LNAPL Likely Present in Groundwater in the Vicinity of Red Hill Monitoring Wells?

Based on available data, LNAPL is likely present in the vicinity of Red Hill monitoring wells. During the monitoring period from 2005 to present (March 2018), LNAPL has not been measured in any monitoring well. However, the available data suggest the presence of weathered LNAPL (i.e., pre-2005 release) in the immediate vicinity of RHMW02 or within the saturated zone near this well. Based on the angle boring investigations conducted in 1998–2002, this LNAPL may have originated from Tank 9, 11, or 13.

5.2 EVIDENCE OF IMPACT TO GROUNDWATER FROM THE 2014 JP-8 RELEASE

In January 2014, a release of 27,000 gallons of JP-8 occurred from Tank 5. The thermal natural source-zone depletion (NSZD) investigation conducted in Fall 2017 suggests that most of this LNAPL release was retained in the vadose zone within the top 30 feet below the lower tunnel (see CSM Appendix B.1). Following the release event, LNAPL was not observed on groundwater in any of the Facility monitoring wells. Therefore, a multiple-lines-of-evidence approach has been used to evaluate whether the release caused an increased impact to groundwater.

5.2.1 TPH-d

Numerical results of dissolved TPH-d alone are not suitable as a diagnostic tool to assess the presence of LNAPL in groundwater, based on the chemistry of fuels as discussed in detail in Sections 3.1 and 3.2 and as further complicated by biodegradation of the fuels that produces polar/metabolites that tend to be more water soluble than the aliphatic parent compounds (Sections 3.3 and 4.1.1). A portion of the polar material can be extracted by the solvent (methylene chloride), and those compounds have significant differences in responses to the detectors used to measure TPH-d. Multiple lines of evidence should be evaluated to determine if an apparent change in TPH concentration based on previous results is due to a release and/or the presence of LNAPL. Changes in TPH-d concentrations should be carefully evaluated as they can be due to changes in laboratory (methods and laboratory to laboratory) and inherent limitations of TPH measurement. These are discussed in Section 5.2.1.2, Variability in TPH Measurements.

5.2.1.1 CHROMATOGRAMS

Typically, non-dissolved jet fuel would have a chromatographic "fingerprint" or profile similar to the one shown on Figure 3-2, Figure 3-3 (left), and Figure 3-11 (top). These profiles are dominated by multiple resolved peaks that are primarily n-alkanes and isoalkanes. These compounds have extremely low water solubilities. Non-dissolved biodegraded jet fuels have chromatographic profiles consistent with those shown on Figure 3-11 (middle). These profiles are characteristic of fuels that have depleted n-alkanes and predominance of highly branched alkanes and cycloalkanes, which are seen as unevenly distributed discrete peaks and the unresolved complex mixture or "hump." In comparison to fresh and biodegraded jet fuel, the chromatogram from the analysis of the extracted dissolved material from RHMW02 has a very different profile. It is dominated by a "hump" and few resolved peaks. A significant portion of the "hump" is heavier than the biodegraded jet "hump." This profile is indicative of aromatic hydrocarbons from dissolved jet fuel (resolved peaks) and metabolites. Analysis of selected target compounds for this sample indicates that the largest resolved peaks are naphthalene and the two isomers of methylnaphthalene. Analysis of the extract after SGC eliminates the "hump," confirming that the "hump" is due to polar metabolites or biogenic matter (discussed in Section 4 and shown on Figure 4-2 and Figure 4-3) and not from LNAPL.

Review of available chromatograms for RHMW02 and RHMW01 has not revealed the presence of LNAPL in these two wells. It is evident that the dissolved TPH-d is from a jet fuel release that has weathered over time based on the aromatic hydrocarbons found in the water and the predominance of metabolites. Sections 3 to 4.2 include more detailed discussions of what the likely composition of the aromatic hydrocarbons and metabolites is. These metabolites have been observed as high as 85% of the TPH-d numerical results.

Historical laboratory reports indicate that the reported TPH-d chromatographic profiles do not match a fuel pattern, and that TPH-d results are based on any material detected within the carbon range of diesel as defined by TPH-d analytical methods. Review of the TPH-d chromatograms from RHMW02 from 2012 to 2014 (i.e., the monitoring events bracketing the 2014 release) concluded that chromatograms of groundwater samples from RHMW02 did not significantly differ between each event, and did not match a standard chromatogram of JP-8 in water (DON 2015).

In summary, there is no fingerprint evidence of entrained/emulsified LNAPL seen in available chromatograms, and no evidence of change following the 2014 release.

5.2.1.2 VARIABILITY IN TPH MEASUREMENTS

Fuels are complex mixtures of hydrocarbons with a range of physical and chemical properties that are subject to weathering by such processes as volatilization, dissolution, and biodegradation. Assessment of these mixtures is through the estimation of TPH, an analytical parameter that is defined by the method used to measure it. There are many methods that can vary from state to state and even laboratory to laboratory. There can be multiple extraction solvents, instrument calibration protocols and standards, and reportable carbon ranges used in the procedures. Non-petroleum materials and metabolites are also measured as part of TPH. Numerical results and apparent trends should be interpreted with caution and with other lines of evidence.

The variability of TPH results is expected to be significantly higher than for single-component measurements like BTEX. This is reflected in relatively wide ranges of acceptance criteria for laboratory controls and calibration standards. The Department of Defense *Quality Systems Manual* (DoD QSM) Version 5.1 specifies control limits for the TPH-d laboratory control sample (LCS) of 36% to 132% of the expected value (DoD and DOE 2017). The LCS control limits for BTEX are tighter, in the range of 78% to 121%. Performance testing samples from vendors have acceptance criteria of 30% to 125% of the spiked concentrations.

The LCS is a laboratory control that is used to determine status of the calibration. For instance, if the LCS has an actual concentration of 100 parts per billion (ppb) and it is measured at 40 ppb on a given day, a field sample with the same concentration as the LCS may also be reported around 40 ppb. If another sample from the same well is analyzed on another day by the same laboratory but with the LCS measured at the time of analysis as 130 ppb, that sample may be also be measured as 130 ppb. Both results are acceptable and equivalent as the LCS's recovered within the control limits of 36% to 132%. Therefore, comparative analysis of hydrocarbon data should consider the large error inherent in TPH methods. In addition to lack of precision, variability in methods and polar/metabolites quantitation issues for TPH-d and TPH-o prevent valid trend analysis based on TPH alone. It is essential to understand what is really being measured as "TPH." Most site investigations focus on individual compounds, which are more definitive and reliable.

Switching to a different analytical laboratory also significantly affects evaluation of TPH on the basis of the numerical results alone. This is particularly important in determining trends with time.

Figure 5-1 shows the historical TPH-d concentration in RHMW02 with time; there is scatter in the data as expected for this type of analysis. Figure 5-2 shows the same data with the laboratories identified; there is more clearly variability dependency on absolute TPH results with laboratory than with time. These figures show that it is not feasible to evaluate trends on solely TPH without understanding the limitations of this parameter.

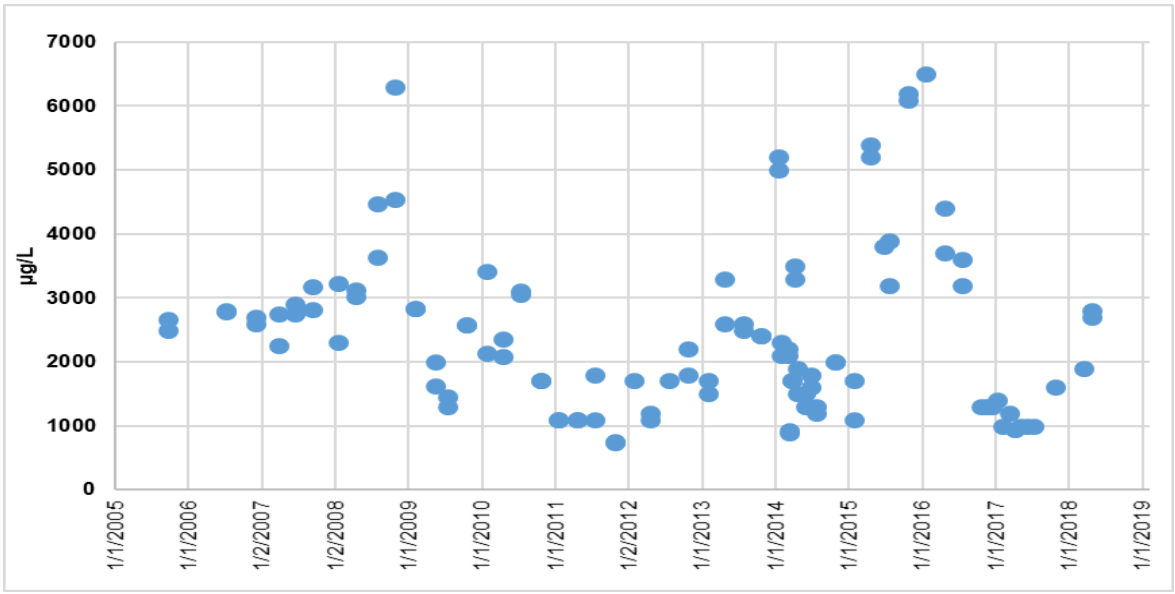

Figure 5-1: RHMW02 TPH-d Results

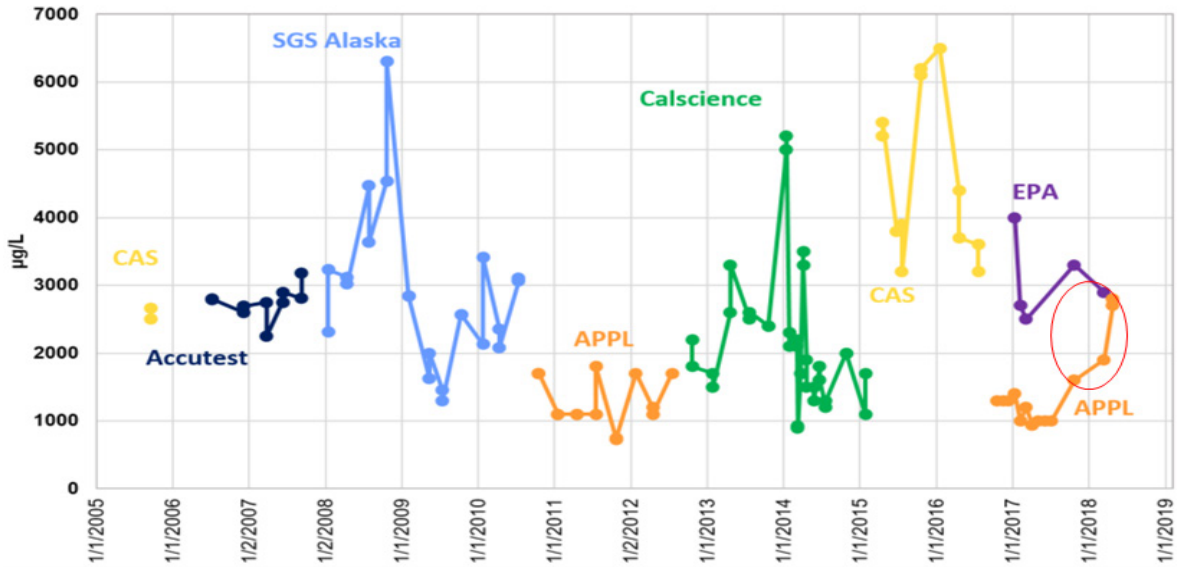

Results from samples analyzed after APPL changes in TPH-d procedure to match EPA Region 9 laboratory protocols are indicated by the circle

Figure 5-2: RHMW02 TPH-d Results over Time with Laboratories Identified

Split samples of selected wells from January, February, and March of 2017 were analyzed both by APPL (the current Navy laboratory for the Facility) and the EPA Region 9 laboratory for an extended suite of analytes including TPH-d and TPH-o. Results from these sampling events showed that APPL results were significantly different from those from EPA for analytes present at high concentrations (EPA Region 9 and DOH 2017). The differences were not random. Performance samples were analyzed by both laboratories, and it was evident that APPL was not extracting as much material from groundwater compared to the EPA laboratory. The issues were due to differences in extraction protocols (EPA Region 9 and DOH 2017; DON 2017c) exacerbated by the

predominance of polars/metabolites in the samples. As discussed in Sections 3.3 and 4.1.1, polars/metabolites are not hydrocarbons, are not the target of the TPH analysis, and are more susceptible to tailing in the gas chromatogram among other issues. In addition, TPH quantitation, as defined by the method, is with respect to a diesel standard, which is unweathered fuel and has a significantly different response in the detector used for quantitation than the polar/metabolites. APPL started modification of the extraction protocol toward the end of 2017. Figure 5-2 shows that the TPH-d results (in red circle) from APPL for the October 2017 to April 2018 samples are closer to EPA results. These higher results are due not to changing conditions in the groundwater at the Facility, but to changes in the laboratory's TPH extraction and analysis protocols.

Figure 5-3 shows the corresponding TPH-d results for RHMW01. It is clear that whatever is measured as TPH-d in RHMW02 does not extend to RHMW01. Figure 5-3 also shows that TPH-d can be found in field blanks and/or laboratory method blanks at low levels.

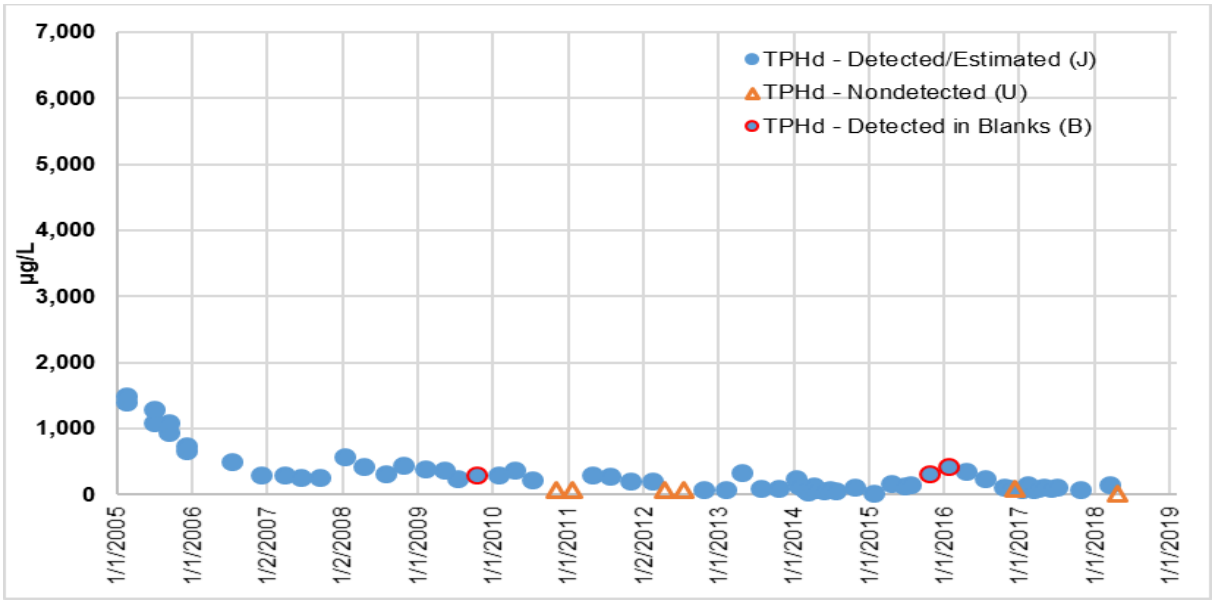

Figure 5-3: RHMW01 TPH-d Results

In summary, variability for TPH-d from one laboratory to another precludes reliable trend analyses. There are no definitive indications of changes in TPH-d in groundwater, and, consequently, additional impact from the 2014 release to groundwater is inconclusive based on the observed TPH-d concentrations.

5.2.2 Naphthalenes

Figure 5-4 shows the results for naphthalene for RHMW02. In general, there is lack of precision in naphthalene results for duplicate samples. As is done for TPH-d, naphthalene is extracted from water, and the extract is concentrated by evaporation before analysis. The DoD QSM (DoD and DOE 2017) lists an acceptance criterion for LCS in the same range as TPH-d (40% to 121%). Variability of naphthalene results may be due to partial loss in the concentration step, due to naphthalene's relative volatility. There is also a correlation with laboratory changes. Similar to TPH-d, trend analysis based solely on naphthalene results can be unreliable. There are higher levels of naphthalene before and after the 2014 release. Tank 5 was out of service from early 2011 to a short time before the 2014 release. Figure 5-5 shows the results for RHMW01. Like with TPH-d, it is clear that dissolved naphthalene plume in RHMW02 does not extend to RHMW01.

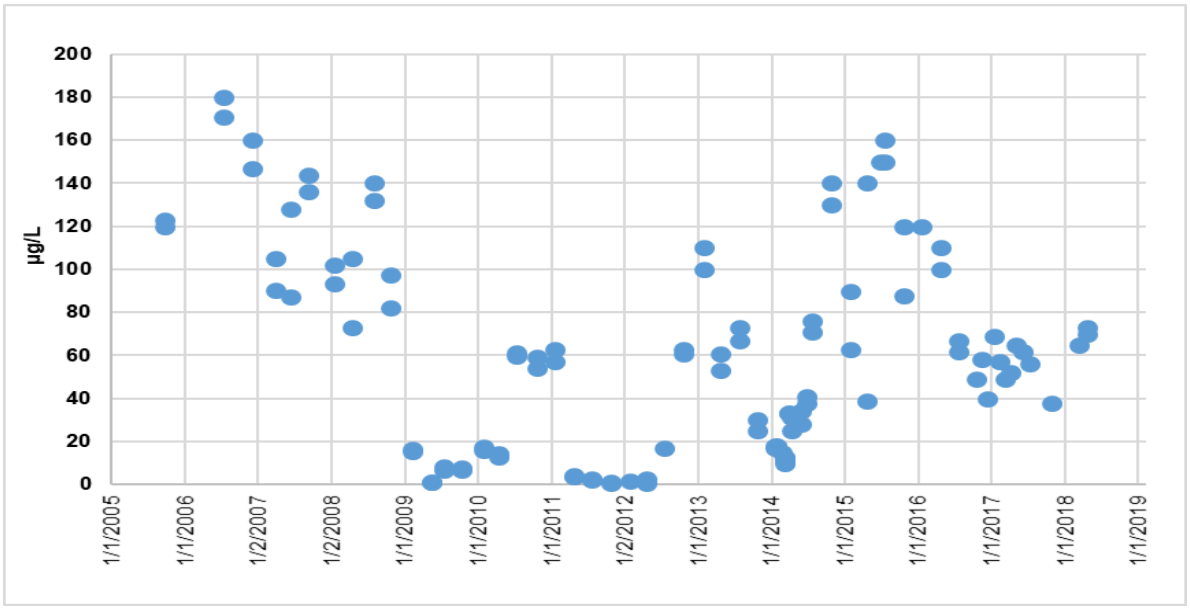

Figure 5-4: RHMW02 Naphthalene Results

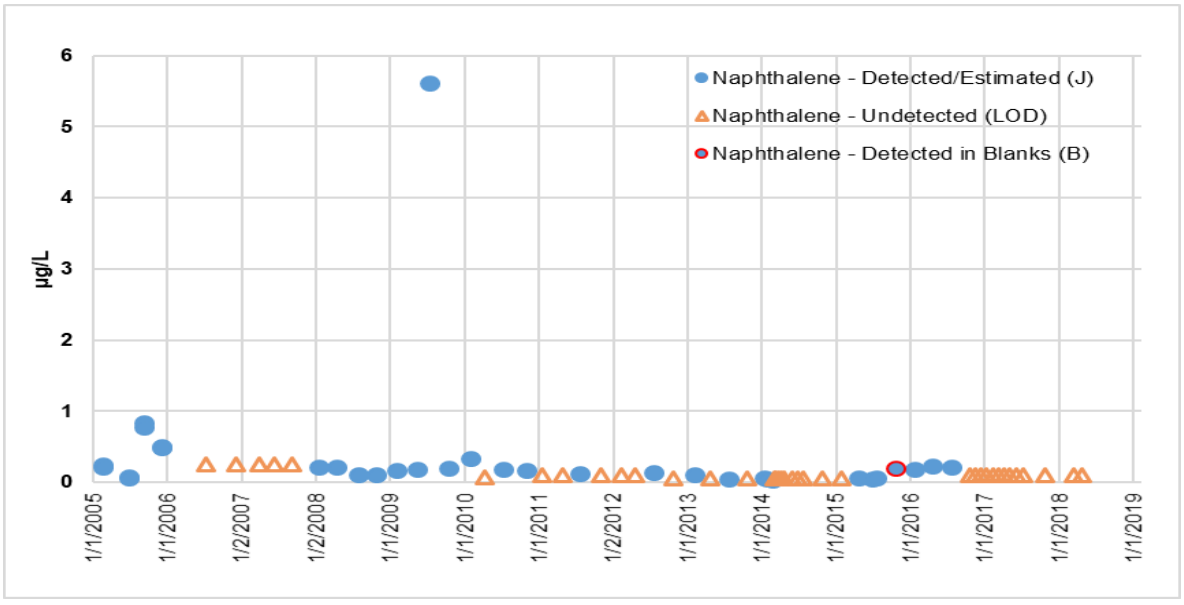

Figure 5-5: RHMW01 Naphthalene Results

Dissolved-phase concentrations of naphthalene and methylnaphthalenes in RHMW02 are within a factor of 2 or less than their effective solubilities for unweathered jet fuel (Table 3-3). It is possible that the relatively high concentrations of these constituents may further indicate a fuel source with higher than expected concentrations and/or consistent with a weathered source, such that the naphthalenes are relatively more concentrated than in the original fuel. The likelihood of a weathered source is more evident when diagnostic ratios of the naphthalenes are examined further (Section 4.1.2) as well as from review of the chromatographic fingerprints (Figure 3-11 and Figure 4-2).

As discussed in Section 4.1.2, forensics investigations often use ratios of target compounds rather than absolute concentrations to normalize sample variability and take advantage of properties and/or biodegradation differences among the different compounds that can be diagnostic of particular changes in the samples. The ratio of the sum of methylnaphthalenes to naphthalene is typically approximately 2 for unweathered sources. This ratio is less than 1 for RHMW02 samples.

Figure 5-6 is a plot of naphthalene and the sum of 1-methylnaphthalene and 2-methylnaphthalene results for RHMW02 as well as the ratio of the sum of the methylnaphthalene to naphthalene. The ratio is generally less than 1 for all samples and is less variable than the concentrations of the individual compounds. The only exceptions where the ratio is greater than 2 are for a few samples in 2009 where the individual concentrations were low. The fact that the ratio is consistently less than 2 strongly suggests that no new impact from unweathered fuels was observed at RHMW02 and, more specifically, no new impact was observed from the 2014 release event.

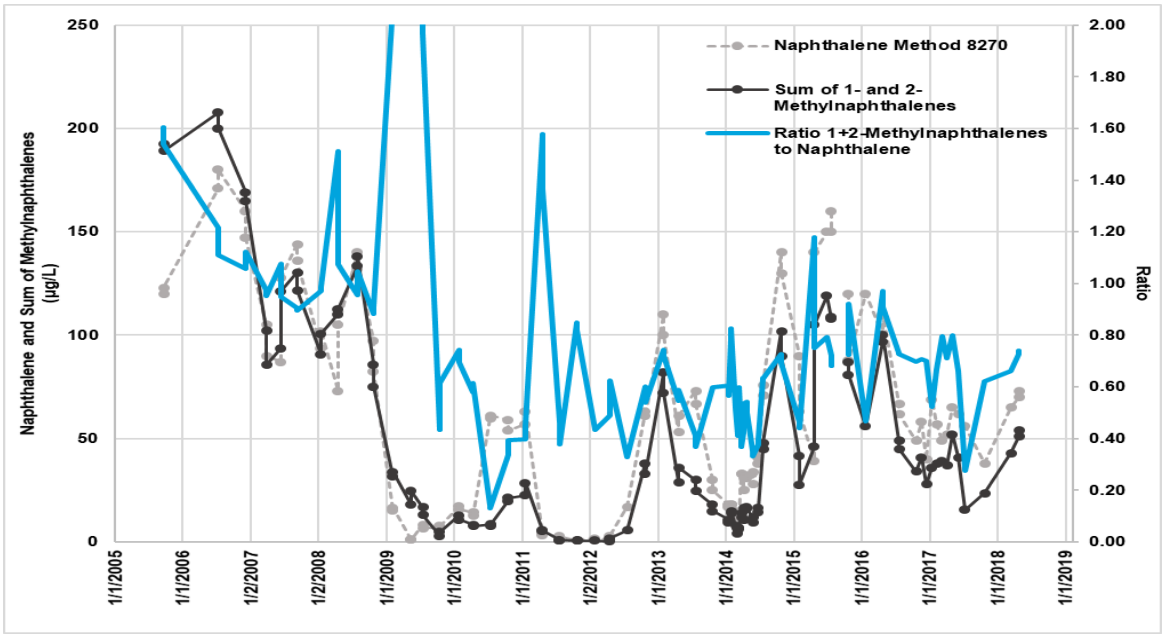

Figure 5-6: Naphthalene and Sum of 1-Methylnaphthalene and 2-Methylnaphthalene Results for RHMW02 - Ratio of the Sum of the Methylnaphthalene to Naphthalene

Figure 5-7 combines TPH-d chromatograms and naphthalene ratios for selected samples after 2012. It is evident that all of the samples contained dissolved biodegraded material. Neither the chromatograms nor the naphthalene ratios show any evidence of unweathered fuel releases.

In summary, chromatographic profiles and naphthalene ratios show weathered material regardless of concentration changes.

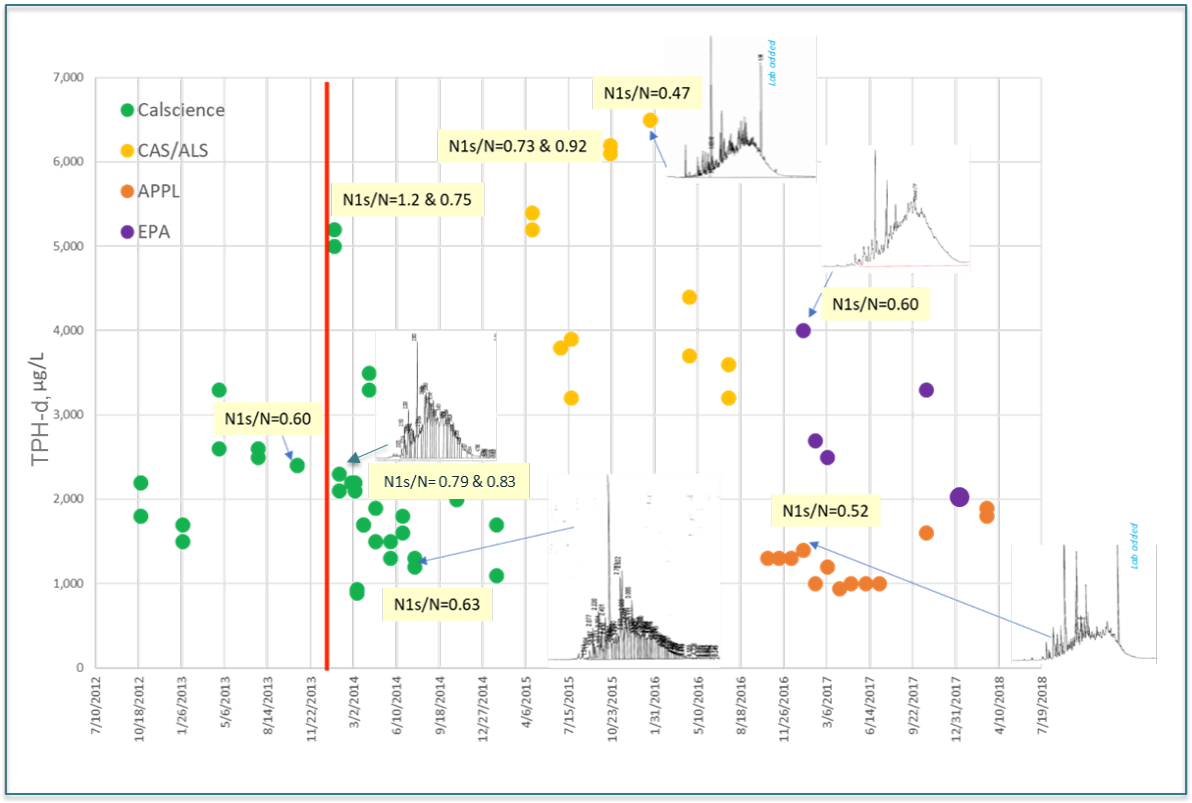

Red line indicates the date of the 2014 release.

Figure 5-7: TPH-d Chromatograms and Naphthalene Ratios for Selected Samples

5.2.3 TPH-g

Figure 5-8 shows the results from analysis of TPH in the gasoline range (C6 to C10) for RHMW02. In general, TPH-g has been detected at levels less than 100 µg/L with no evidence of significant changes over time other than for an apparent spike in late 2012/early 2013. The other COPCs did not have equivalent increases at the same time. The slight "increase" in 2017 coincides with a laboratory change and method change from EPA Method 8015 to EPA Method 8260. This is expected for any TPH measurement, that it is defined by the method used to analyze the samples and not indicative in itself of a change in conditions. Figure 5-9 shows the TPH-g data for RHMW01 with few detections, all below the limit of detection (LOD), and with some method field blanks with similar values.

In summary, there is no significant change in TPH-g concentrations at RHMW01 and RHMW02 after the 2014 release; variability coincides with change in lab and method, not unexpected for TPH measurements.

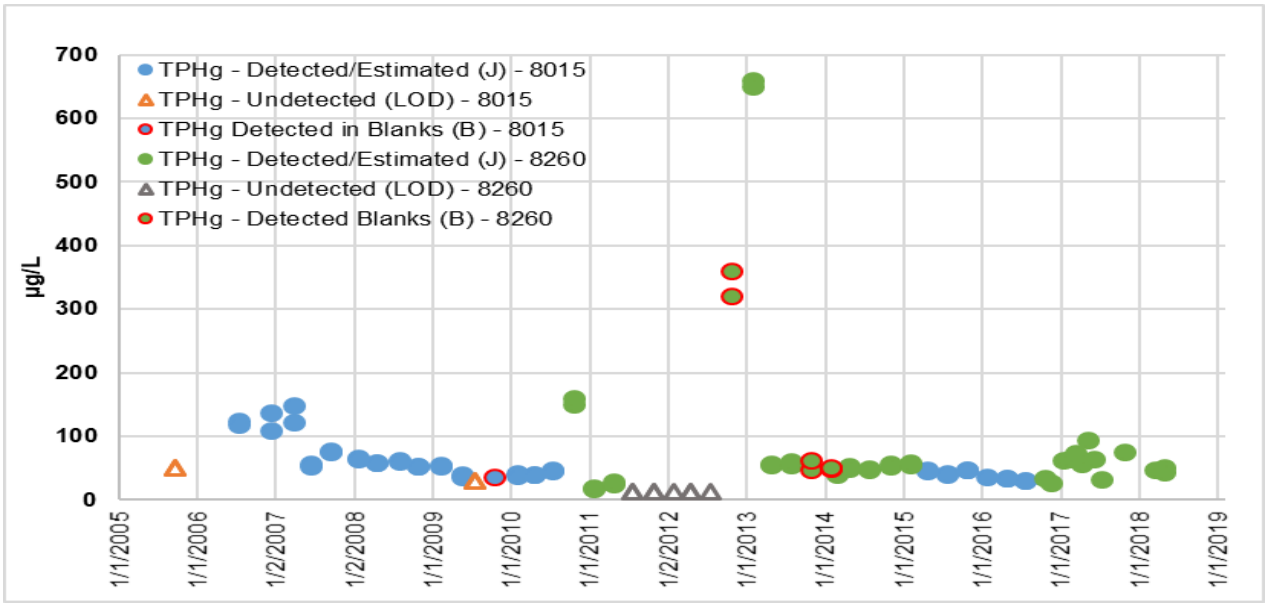

Figure 5-8: RHMW02 TPH-g Results

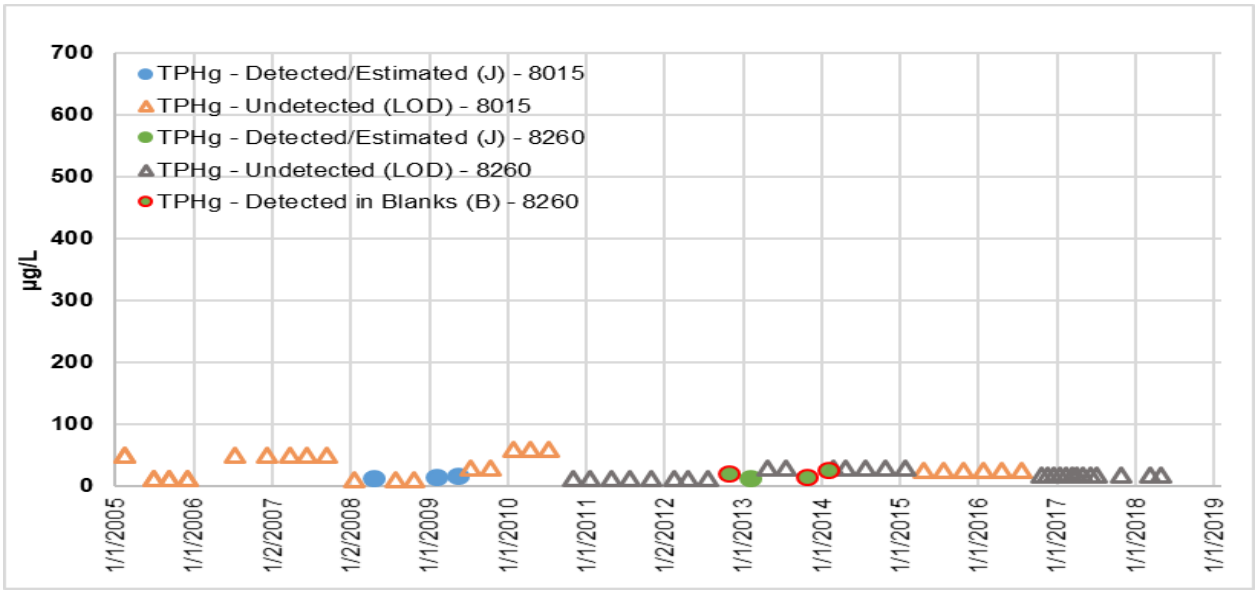

Figure 5-9: RHMW01 TPH-g Results

5.2.4 BTEX

These COPCs can be identified accurately and quantitated with better precision in groundwater. The DoD QSM LCS control limits for these compounds are 79% to 121% (DoD and DOE 2017). BTEX compounds are the most water-soluble components in jet fuels, and input from unweathered sources or recent releases is expected to increase their concentrations in groundwater. The ideal effective solubilities of BTEX in the types of fuels stored at the Facility are summarized in Table 3-3 and on Figure 3-6 and Figure 3-7. JP-8 equilibrated with water has an approximate average sum of BTEX of 3+ mg/L.

Most of these compounds are either not detected or detected at very low estimated concentrations. DoD QSM reporting criteria for analytical data require that detected results be reported down to the detection limit (DL), which is lower than the LOD and the limit of quantitation (LOQ) (DoD and DOE 2017). Figure 5-10 presents a summary of data quality characteristics below and above the DL, LOD, and LOQ as well as an example of how data should be reported.

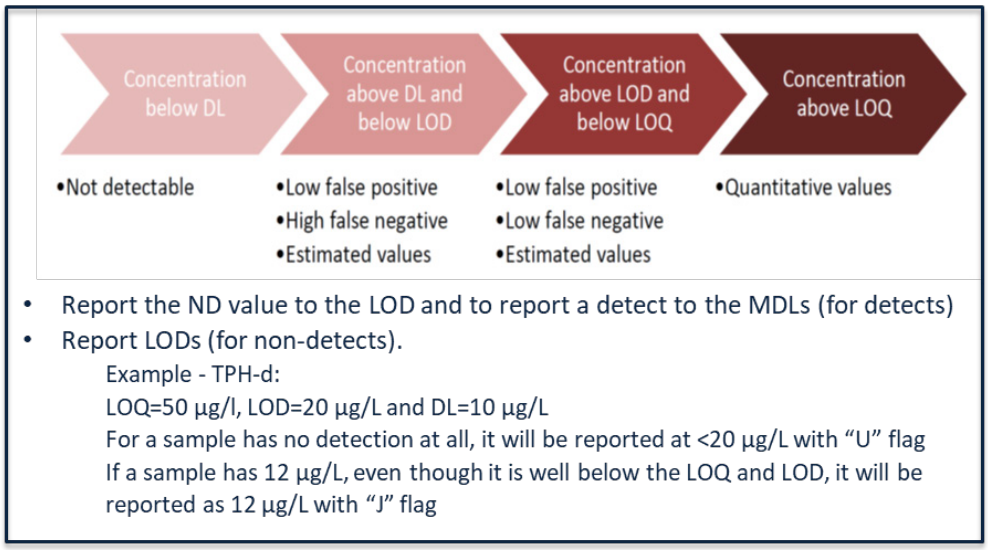

Source: DoD and DOE 2017.

Figure 5-10: Reporting Criteria for DoD QSM

In the evaluation of BTEX results over time, no distinction was made in the time series plots for results above the DL and below the LOD ("J" or estimated values) and results above the LOQ. All numerical results (estimated values and quantitative values were presented and interpreted as "detects." In many cases, non-detect values (reported as less than the LOD) are higher than the numerical values of estimated results. These limits are laboratory- and instrument-dependent and have changed with changes in laboratory. For instance, the laboratory used from April 2015 to July 2016 had LODs 5× lower than the laboratory used previously and about 3× lower than the laboratory used afterward. These changes in reporting limits are the likely cause of appearance of chemicals not observed in previous sampling events and are not due to new releases.

5.2.4.1 BENZENE

Figure 5-11 shows the benzene results for all samples from RHMW02. The majority of the RHMW02 samples do not have detectable benzene. The few benzene detections are below the laboratory LOQ and are reported as estimated values. Figure 5-12 shows the corresponding results for RHMW01. It is evident that there has not been significant benzene input to groundwater in these two wells over time.

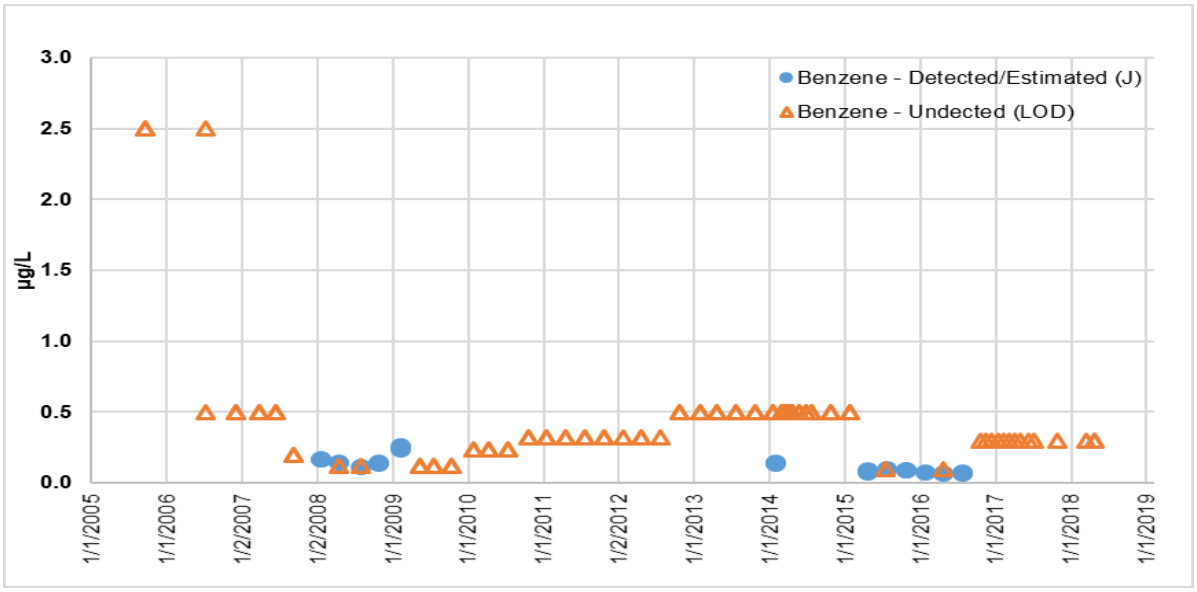

Note: The average ideal calculated effective solubility of benzene in water in contact with JP-8 is ~300 µg/L (Table 3-3).

Figure 5-11: RHMW02 Benzene Results

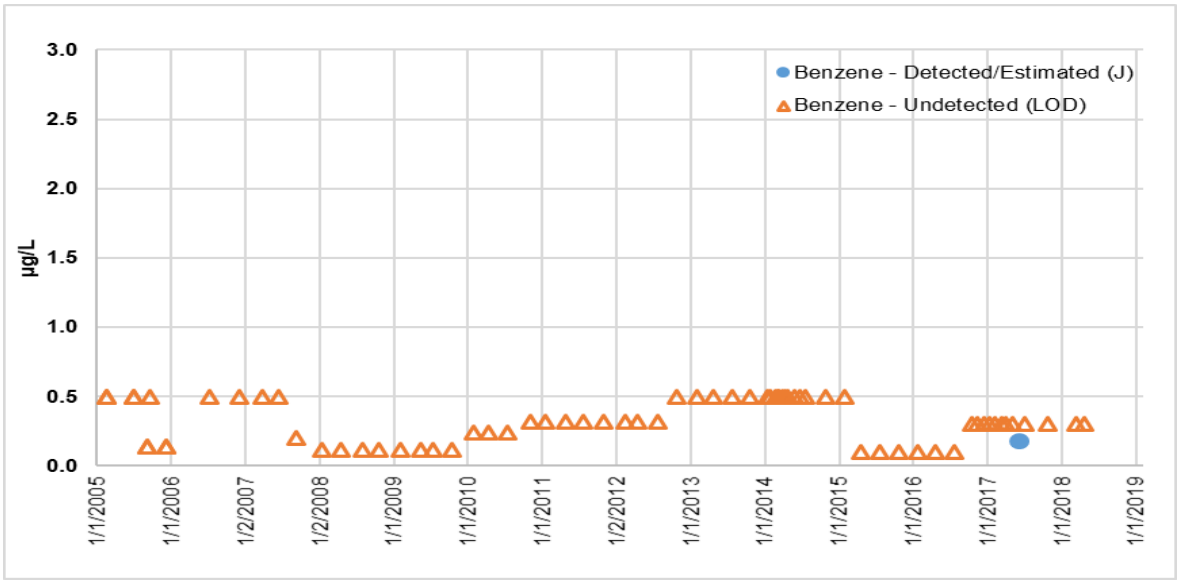

Figure 5-12: RHMW01 Benzene Results

5.2.4.2 TOLUENE

Figure 5-13 and Figure 5-14 are plots for toluene for RHMW02 and RHMW01, respectively. There are essentially no detections of toluene in these wells. Toluene was sometimes detected in the method and field blanks at similar low concentrations by the laboratory that had lower reporting limits.

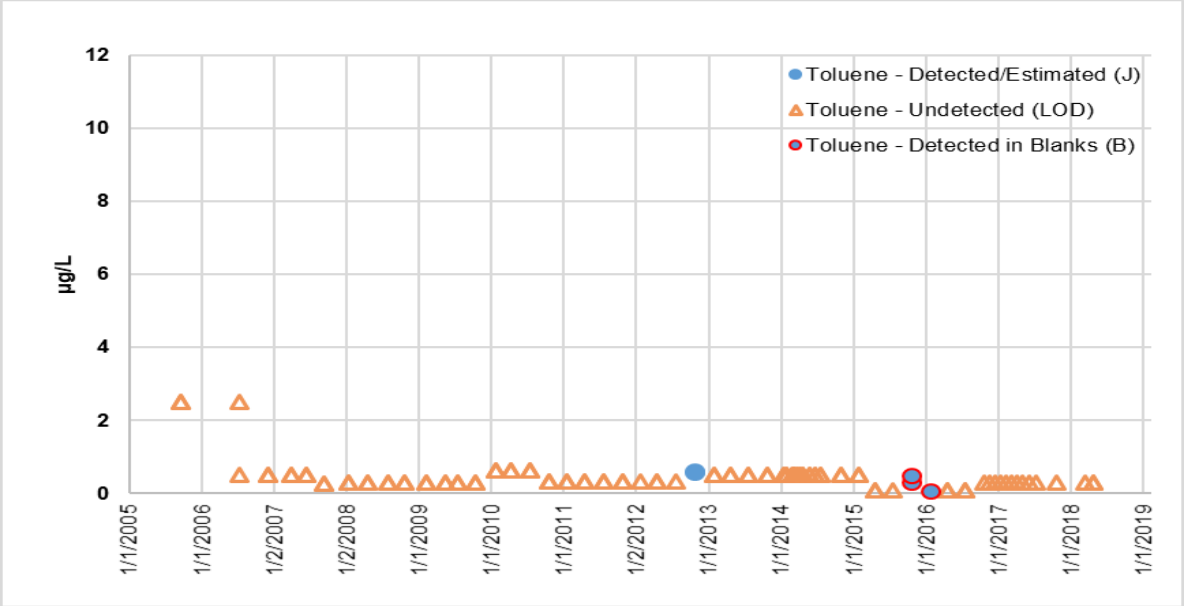

Note: The average ideal calculated effective solubility of toluene in water in contact with JP-8 is ~900 µg/L (Table 3-3).

Figure 5-13: RHMW02 Toluene Results

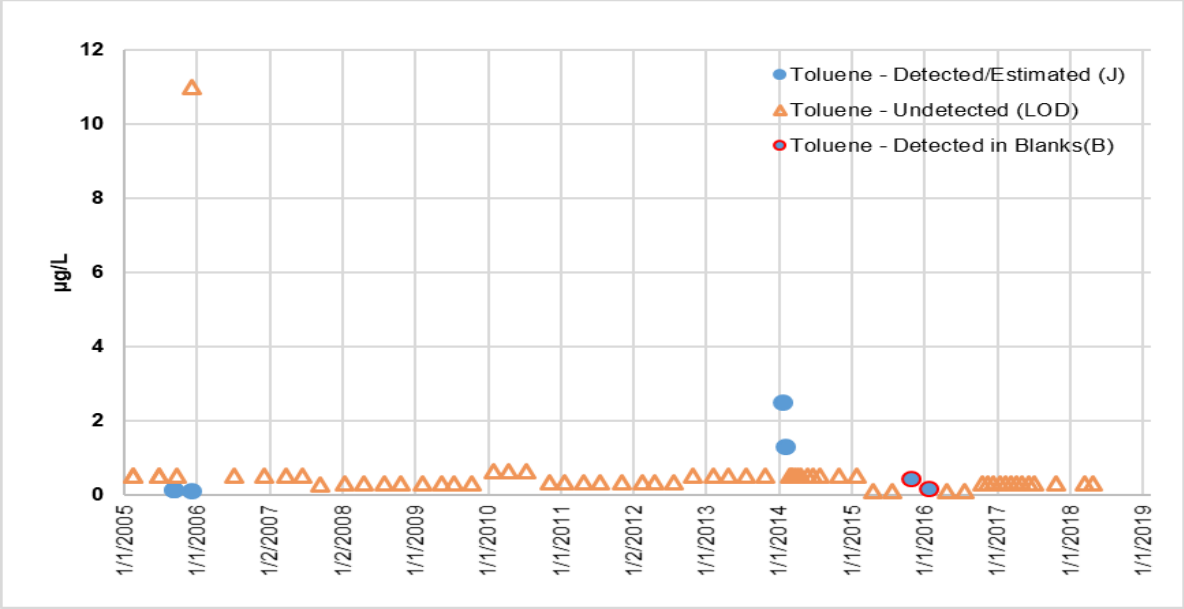

Figure 5-14: RHMW01 Toluene Results

5.2.4.3 ETHYLBENZENE

Figure 5-15 shows ethylbenzene data for RMMW02 with time. Ethylbenzene has been detected at low levels but mostly below the LOD. RHMW01 (Figure 5-16) has had no detections of ethylbenzene.

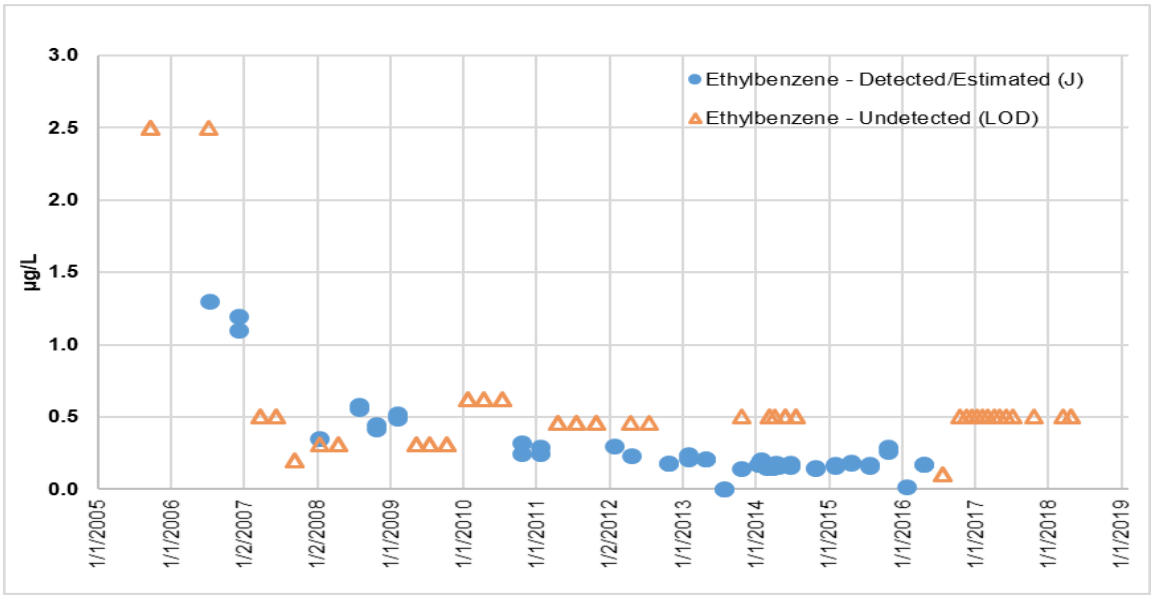

Note: The average ideal calculated effective solubility of ethylbenzene in water in contact with JP-8 is ~300 µg/L (Table 3-3).

Figure 5-15: RHMW02 Ethylbenzene Results

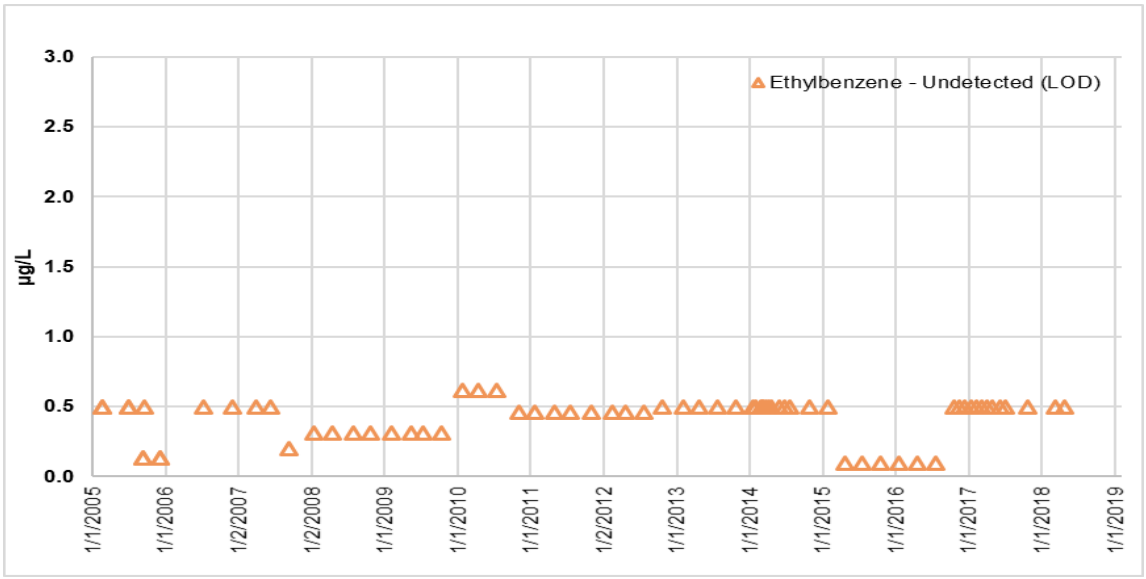

Figure 5-16: RHMW01 Ethylbenzene Results

5.2.4.4 XYLENES

There are low levels of xylenes in RHMW02 (Figure 5-17) with a general slight decrease of the detected concentrations over time. There have been no detections of xylenes in RHMW01 (Figure 5-18).

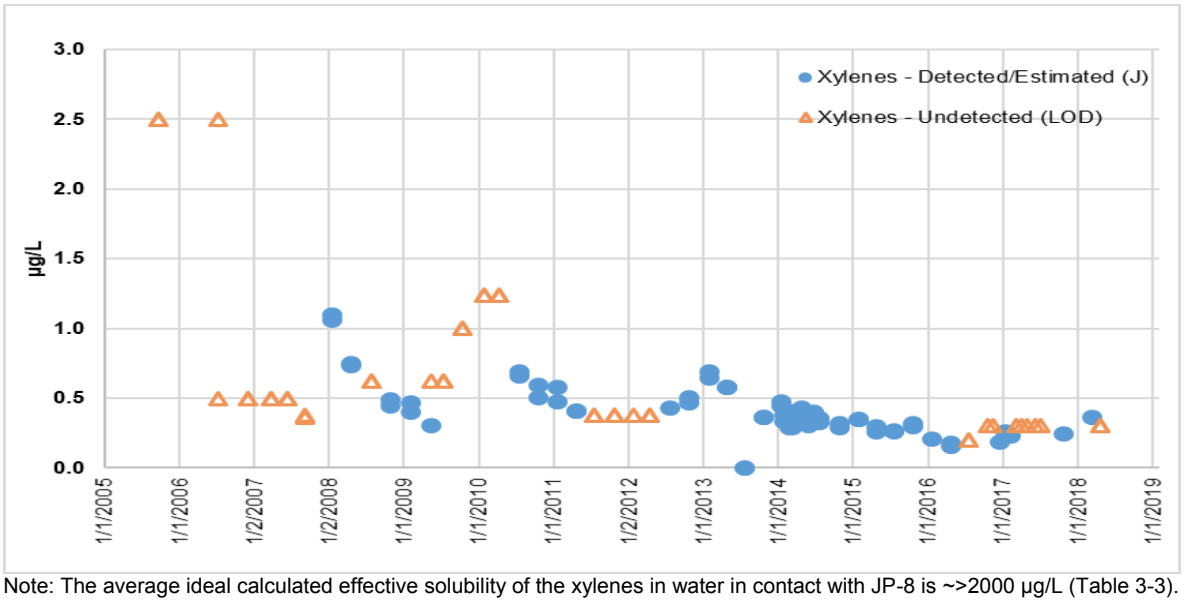

Note: The average ideal calculated effective solubility of the xylenes in water in contact with JP-8 is ~>2000 µg/L (Table 3-3).

Figure 5-17: RHMW02 Xylenes Results

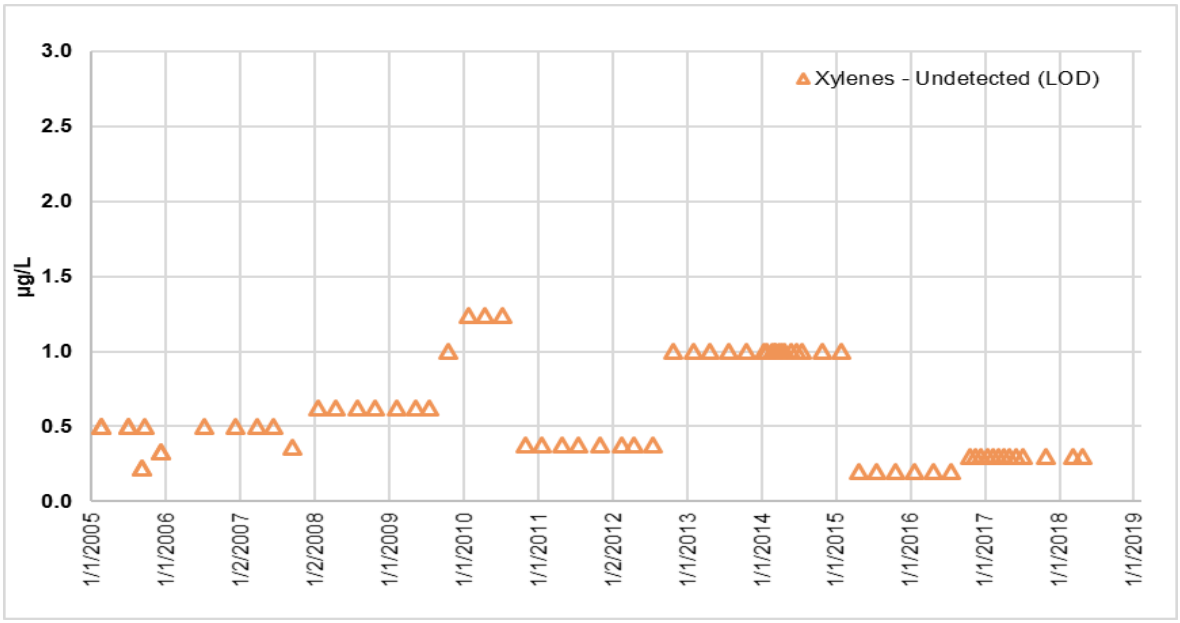

Figure 5-18: RHMW01 Xylenes Results

In summary, BTEX results for RHMW02 do not show evidence that would support groundwater impact from the 2014 release. The data do not indicate evidence of any releases after the well was installed.

5.2.5 Soil Vapor

Since 2008, monthly soil vapor monitoring using a photoionization detector (PID) has been conducted at two to three soil vapor monitoring points (SVMPs) installed below each active tank (see CSM Appendix B.3 for additional details concerning these monitoring points). Figure 5-19 includes a compilation of soil vapor measurements with time from SVMPs. For each monitoring event, the figure shows the highest PID reading for the SVMPs below each tank. A more detailed presentation of the PID monitoring data is provided in CSM Appendix B.3 (e.g., Figure 4-3 in CSM Appendix B.3). For 2008 to 2013, the PID readings showed a gradual decreasing trend over time consistent with the natural attenuation of historical fuel releases. There is an obvious sharp increase in the PID reading at Tank 5 immediately after the 2014 release of approximately 27,000 gallons of JP-8, with smaller increases in PID readings at the adjacent tanks. The soil vapor data indicate that LNAPL from the 2014 release is likely confined to the area immediately surrounding Tank 5.

No similar large and persistent increases in PID readings have been observed at any other tanks or at any other times from 2008 to present (March 2018). This indicates that the 2014 Tank 5 release was the only significant release of fuel from any tank during this monitoring period.

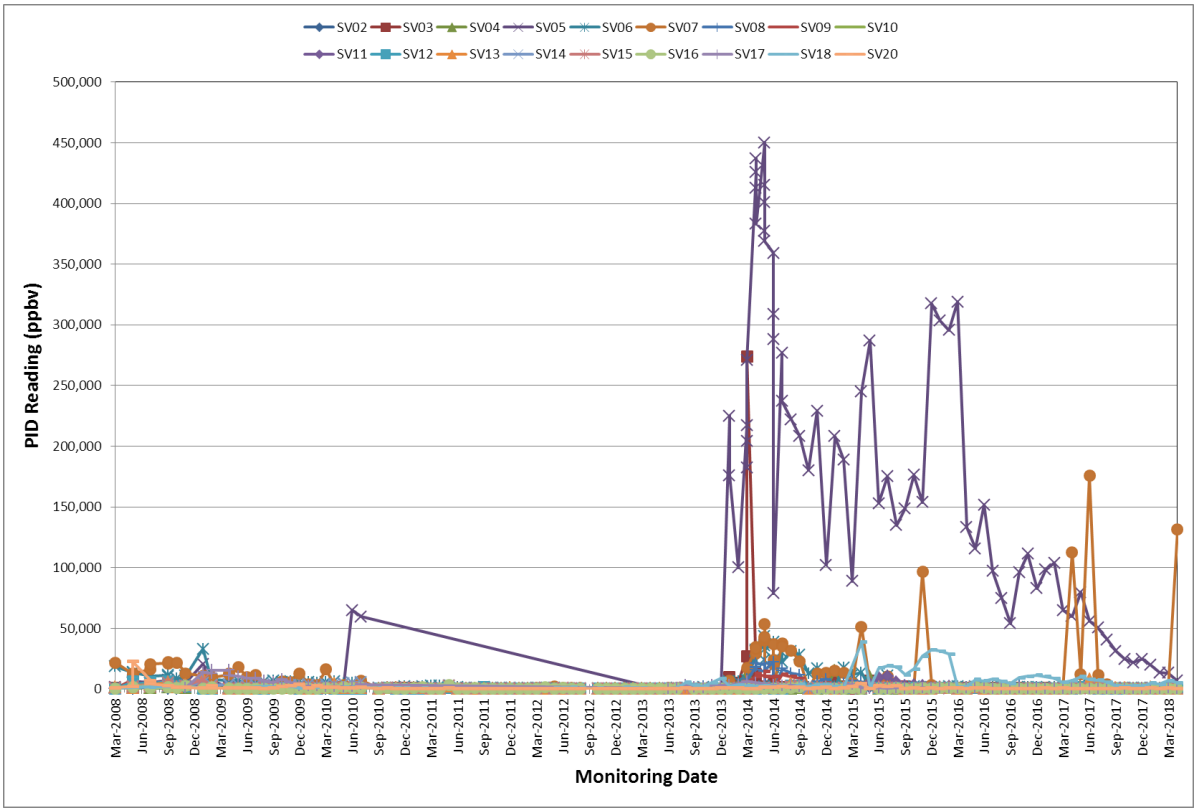

Figure 5-19: Soil Vapor Measurements

5.2.6 Evaluation of Analytical Data from RHMW2254-01, RHMW04, and of Low-Level Detections of Naphthalenes in all Wells

In addition to the evaluation discussed in the subsections above, possible impacts of the 2014 JP-8 Tank 5 release were evaluated for groundwater at Red Hill Shaft (Navy Supply Well 2254-01) and the background well (RHMW04). Attachment B.7.2 presents the evaluation of groundwater data from the monitoring point in Red Hill Shaft, and Attachment B.7.3 presents the evaluation of groundwater data from the background well (RHMW04).

Attachment B.7.4 presents an evaluation of low-level detections of naphthalene that seem to be in many wells (except for RHMW02 and RHMW01) around the same time. These naphthalene detections occurred when SGS Alaska (January 2008 to July 2010) and Calscience (October 2012 to January 2015) laboratories were used (LOD 0.05 µg/L). Most of the samples analyzed afterward January 2015 were non-detect for naphthalene The laboratory used after January 2015 was CAS/ALS, which had a lower LOD (0.005 µg/L) and reported fewer detections at the lower level in most wells than did SGS Alaska and Calscience.

These sporadic low-level detections are most likely explained by laboratory artifacts. Low-level detections (i.e., less than 0.1 µg/L) of naphthalene in outlying wells are not consistent with LNAPL transport through either the vadose or saturated zones. Due to the uncertainty associated with these low-level detections, the available monitoring record is not suitable for evaluating the presence or absence of COPCs in individual monitoring wells at concentrations of less than 0.1 µg/L. However, the available monitoring record does support a more reliable evaluation of the presence or absence of COPCs at concentrations above 0.1 µg/L. Therefore, detections of less than 0.1 µg/L for naphthalenes (i.e., 1-methylnaphthalene, 2-methylnaphthalene, and/or naphthalene) do not necessarily indicate impacts from the Facility without additional supporting lines of evidence.

Additionally, the EPA Region 9 Laboratory analyzed split samples for all existing monitoring wells during January to March 2017 (all wells except RHMW10 and RHMW11, which were installed after March 2017). 1-Methylnaphthalene, 2-methylnaphthalene, and naphthalene were detected only in RHMW01 and RHMW02 with a reporting limit of 0.05 µg/L.

5.2.7 Did the 2014 JP-8 Tank 5 Release Event Result in an Increased Impact to Groundwater?

An evaluation of COPC concentrations and multiple lines of evidence do not indicate that the 2014 JP-8 release from Tank 5 impacted groundwater and impacts to groundwater are more likely attributable to historical leaks. Evaluation of COPC results with time including TPH-d, TPH-g, BTEX, and naphthalenes along with review of the chromatographic profiles from TPH analysis, diagnostic ratios, and biodegradation indicators in groundwater at the Facility indicates that strictly weathered material is present in groundwater, and COPC concentrations have generally remained within recent historic ranges. Multiple lines of evidence do not indicate additional impact to groundwater associated with the 2014 release occurred. Table 5-1 includes a summary of lines of evidence investigated.

Table 5-1: Evidence of Impact to Groundwater from 2014 Release: Summary of Lines of Evidence

Description		Key Points	Evidence of Impact to Groundwater from 2014 Release
TPH-d	Laboratory changes	Variability for TPH-d from laboratory to laboratory precludes reliable trend analyses.	Unreliable
	Chromatographic profiles	Primarily polar/metabolites and naphthalenes consistent with dissolved weathered material.	Not Apparent
	Chromatographic profiles and naphthalene ratios	Chromatographic profiles and naphthalene ratios show weathered material regardless of concentration changes.	Not Apparent
Naphthalenes and naphthalene ratios		Ratios of 1+2 methylnaphthalenes to naphthalene < 2 indicate a weathered source. Imprecision in naphthalene results have been observed in previous data validation reports.	Not Apparent
TPH-g		No significant change in TPH-g after 2014 release, some variability coincides with lab changes and method variability, not unexpected for TPH measurements.	Not Apparent
Benzene		No significant changes in benzene after 2014 release.	Not Apparent
Toluene		No significant change in toluene after 2014 release.	Not Apparent
Ethylbenzene		No significant changes in ethylbenzene after 2014 release.	Not Apparent
Xylenes		No significant changes in xylenes after 2014 release.	Not Apparent

6. Conclusions

Impacts to groundwater from jet fuel seem to be localized in the area of RHMW02. Multiple lines of evidence were identified as supporting the conclusion that natural attenuation is occurring at the site, specifically looking at groundwater COPC NAP concentrations at monitoring well RHMW02 and, to a lesser extent, at monitoring wells RHMW01 and RHMW03.

The RHMW02 TPH-d chromatographic patterns show:

- Presence of naphthalene, C1-naphthalenes, as well as C2+naphthalenes. The chromatograms are consistent among the samples from RHMW02 and among kerosenes (JP-5 and JP-8 are kerosenes with special additives).
- Evidence of C3+benzenes from the analysis of TPH-g, VOCs, and TICs in both VOCs and SVOC analyses. Lighter components are partially lost in the extraction and concentration of the extract prior to analysis in TPH-d.
- Presence of a "hump" that extends beyond the end of the jet/kerosene carbon range (C16+). This is likely due to polar matter that may be metabolites of biodegradation. SGC removes 40–75% of the TPH-d, indicating that the hydrocarbons in RHMW02 are degrading.
- Some of the compounds detected as TICs are more recalcitrant to biodegradation (naphtheno-benzenes, for example). These are typically low in concentration in the fuel, and the fact that these are detected as TICs indicates that they are relatively concentrated in the residual hydrocarbons more than in a fresh release. The presence of organic acids is also indicative of biodegradation.

Other indications of natural attenuation include:

- Methane production in RHMW01 and RHMW02.
- Relative depletion of nitrate, sulfate, and dissolved oxygen in RHMW02 with respect to other wells.
- Relatively higher iron and alkalinity in RHMW02 with respect to other wells.

Taken together, the available data suggest the presence of weathered LNAPL (i.e., pre-2005 release) in the immediate vicinity of RHMW02 or within the saturated zone upgradient from this well. Based on the angle boring investigations conducted in 1998 to 2002, this LNAPL may have originated from Tank 9, 11, or 13. An evaluation of multiple lines of evidence does not indicate any additional impact associated with the 2014 Tank 5 release.

In summary, assessment of groundwater analytical data using multiple lines of evidence indicates that petroleum-related chemicals in groundwater are weathered and that COPC concentrations have generally remained within recent historic ranges.

7. References

Alvarez, P. J. J., R. C. Heathcote, and S. E. Powers. 1998. "Caution Against Interpreting Gasoline Release Dates Based on BTEX Ratios in Water." *Groundwater Monitoring & Remediation* 18 (4): 69–76.

American Petroleum Institute (API). 2010. *Kerosene/Jet Fuel Category Assessment Document*. API Petroleum HPV Testing Group. Submitted to the U.S. EPA. Consortium Registration # 1100997. September 21.

———. 2012. *Gas Oils Category Analysis Document and Hazard Characterization*. API Petroleum HPV Testing Group. High Production Volume (HPV) Chemical Challenge Program. Submitted to the U.S. EPA. Consortium Registration # 1100997. October 24.

Baedecker, M. J., R. P. Eganhouse, B. A. Bekins, and G. N. Delin. 2011. "Loss of Volatile Hydrocarbons from an LNAPL Oil Source." *Journal of Contaminant Hydrology* 126: 140–152.

Baedecker, M. J., R. P. Eganhouse, H. Qi, I. M. Cozzarelli, J. Trost, and B. A. Bekins. 2017. "Weathering of Oil in a Surficial Aquifer." *Groundwater*, [Epub ahead of print, Nov. 29]. https://doi.org/10.1111/gwat.12619.

Bernabei, M., R. Reda, R. Galiero, and G. Bocchinfuso. 2003. "Determination of Total Polycyclic Hydrocarbons in Aviation Jet Fuel." *Journal of Chromatography A*, January 24, 985 (1–2): 197–203.

Bobra, M. 1992. *Solubility Behaviour of Petroleum Oils in Water*. Study Funded by United States Minerals Management Service and Environment Canada, Emergencies Science Division. Ottawa: Consultchem.

Coleman, W. E., J. W. Munch, R. P. Streicher, H. P. Ringhand, and F. C. Kopfler. 1984. "The Identification and Measurement of Components in Gasoline, Kerosene, and No. 2 Fuel Oil That Partitions into the Aqueous Phase after Mixing." *Archives of Environmental Contamination and Toxicology* 13 (2): 171–178. https://doi.org/10.1007/BF01055874.

Department of Defense and Department of Energy, United States (DoD and DOE). 2017. *Department of Defense (DoD) and Department of Energy (DOE) Consolidated Quality Systems Manual (QSM) for Environmental Laboratories*. DoD QSM Ver. 5.1; DOE Quality Systems for Analytical Services Ver. 3.1. Prepared by DoD Environmental Data Quality Workgroup and DOE Consolidated Audit Program Operations Team.

Department of Health, State of Hawaii (DOH). 2017. *Evaluation of Environmental Hazards at Sites with Contaminated Soil and Groundwater, Hawai'i Edition*. Hazard Evaluation and Emergency Response. Revised 2017. Fall.

Department of the Navy (DON). 1999. *Initial Phase II Site Characterization Report, Fleet Industrial Supply Center Bulk Fuel Storage Facility at Red Hill*. Prepared by Ogden Environmental and Energy Services Co., Inc., Honolulu, HI. Pearl Harbor, HI: Pacific Division, Naval Facilities Engineering Command. March.

———. 2002. *Red Hill Bulk Fuel Storage Facility Investigation Report (Final) for Fleet Industrial Supply Center (FISC), Oahu, Hawaii*. Prepared by AMEC Earth & Environmental, Inc., Huntsville, AL. Pearl Harbor, HI: Pacific Division, Naval Facilities Engineering Command. August.

———. 2007. *Red Hill Bulk Fuel Storage Facility Final Technical Report, Pearl Harbor, Hawaii*. Prepared by TEC Inc., Honolulu, HI. Pearl Harbor, HI: Naval Facilities Engineering Command, Pacific. August.

———. 2015. *Final First Quarter 2015 – Quarterly Groundwater Monitoring Report, Inside Tunnel Wells, Red Hill Bulk Fuel Storage Facility, Joint Base Pearl Harbor-Hickam, Oahu, Hawaii*. Prepared by Environmental Science International, Inc., Kailua, HI. JBPHH HI: Naval Facilities Engineering Command, Hawaii. March.

———. 2017a. *Sampling and Analysis Plan Addendum 01, Investigation and Remediation of Releases and Groundwater Protection and Evaluation, Red Hill Bulk Fuel Storage Facility, Joint Base Pearl Harbor-Hickam, O'ahu, Hawai'i; September 1, 2017, Revision 00*. Prepared by AECOM Technical Services, Inc., Honolulu, HI. Prepared for Defense Logistics Agency Energy, Fort Belvoir, VA, under Naval Facilities Engineering Command, Hawaii, JBPHH HI.

———. 2017b. *Risk-Based Decision Criteria Development Plan, Investigation and Remediation of Releases and Groundwater Protection and Evaluation, Red Hill Bulk Fuel Storage Facility, Joint Base Pearl Harbor-Hickam, O'ahu, Hawai'i; December 11, 2017, Revision 00*. Prepared by AECOM Technical Services, Inc., Honolulu, HI. Prepared for Defense Logistics Agency Energy, Fort Belvoir, VA, under Naval Facilities Engineering Command, Hawaii, JBPHH HI.

———. Letter from R. D. Hayes III to Bob Pallarino (EPA Region 9) and Steven Y. K. Chang (DOH). 2017c. "Navy's Response to Split Sampling Results from First Quarter 2017, Administrative Order on Consent Statement of Work Section 6 and Section 7, Red Hill Bulk Fuel Storage Facility (Red Hill), Joint Base Pearl Harbor-Hickam, Oahu, Hawaii," October 11, 2017.

Environmental Protection Agency, United States (EPA). 2017. *Split Sampling and Analysis Plan, Red Hill Fueling Facility, Honolulu, Hawai'i – Groundwater Monitoring, January 2017*. U.S. EPA Region 9 Land Division and Quality Assurance Office.

Environmental Protection Agency, United States, Region 9; and Department of Health, State of Hawaii (EPA Region 9 and DOH). Letter from Bob Pallarino (EPA Region 9 Project Coordinator) and Steven Chang (DOH Project Coordinator) to: Mark Manfredi, Red Hill Project Coordinator, Naval Facilities Hawaii. 2017. "Split Sampling Results from First Quarter 2017," September 12, 2017.

Gustafson, J. B., J. G. Tell, and D. Orem. 1997. *Total Petroleum Hydrocarbon Criteria Working Group Series, Volume 3: Selection of Representative TPH Fractions Based on Fate and Transport Considerations*. Amherst, MA: Amherst Scientific Publishers.

Hadaller, O. J., and J. M. Johnson. 2006. *World Fuel Sampling Program*. CRC Report No. 647. Alpharetta, GA: Coordinating Research Council, Inc. June.

Lovestead, T. M., J. L. Burger, N. Schneider, and T. J. Bruno. 2016. "Comprehensive Assessment of Composition and Thermochemical Variability by High Resolution GC/QToF-MS and the Advanced Distillation-Curve Method as a Basis of Comparison for Reference Fuel Development." *Energy & Fuels* 30 (12): 10029–044.

Maurice, L. Q., H. Lander, T. Edwards, and W. E. Harrison III. 2001. "Advanced Aviation Fuels: A Look Ahead via a Historical Perspective." *Fuel* 80 (5): 747–756. https://doi.org/10.1016/S0016-2361(00)00142-3.

Mohler, R. E., K. T. O'Reilly, D. A. Zemo, A. K. Tiwary, R. I. Magaw, and K. A. Synowiec. 2013. "Nontargeted Analysis of Petroleum Metabolites in Groundwater Using GC×GC–TOFMS." *Environ. Sci. & Technol.* 47 (18): 10471–476. https://doi.org/10.1021/es401706m.

Shafer, L. M., and T. Edwards. 2011. *Speciated Naphthalene Analysis in Liquid Transportation Fuels*. IASH 2011, The 12th International Conference on Stability, Handling and Use of Liquid Fuels, Sarasota, Florida USA, 16–20 October 2011.

Striebich, R. C., L. M. Shafer, R. K. Adams, Z. J. West, M. J. DeWitt, and S. Zabarnick. 2014. "Hydrocarbon Group-Type Analysis of Petroleum-Derived and Synthetic Fuels Using Two-Dimensional Gas Chromatography." *Energy & Fuels*, no. 28: 5696–706. https://doi.org/dx.doi.org/10.1021/ef500813x.

Vorhees, D. J., W. H. Weisman, and J. B. Gustafson. 1999. *Total Petroleum Hydrocarbon Criteria Working Group Series, Volume 5: Human Health Risk-Based Evaluation of Petroleum Release Sites: Implementing the Working Group Approach*. Amherst, MA: Amherst Scientific Publishers.

Widdel, Friedrich, and Ralf Rabus. 2001. "Anaerobic Biodegradation of Saturated and Aromatic Hydrocarbons." *Current Opinion in Biotechnology* 12 (3): 259–276. https://doi.org/10.1016/S0958-1669(00)00209-3.

Zemo, D. A., K. T. O'Reilly, R. E. Mohler, R. I. Magaw, C. E. Devine, S. Ahn, and A. K. Tiwary. 2017. "Life Cycle of Petroleum Biodegradation Metabolite Plumes, and Implications for Risk Management at Fuel Release Sites." *Integrated Environmental Assessment and Management* 13 (4): 714–727. https://doi.org/10.1002/ieam.1848.

Zemo, D. A., K. T. O'Reilly, R. E. Mohler, A. K. Tiwary, R. I. Magaw, and K. A. Synowiec. 2013. "Nature and Estimated Human Toxicity of Polar Metabolite Mixtures in Groundwater Quantified as TPHd/DRO at Biodegrading Fuel Release Sites." *Groundwater Monitoring & Remediation* 33 (4): 44–56. https://doi.org/10.1111/gwmr.12030.

Attachment B.7.1: Summary of Concentrations and Calculated Effective Solubilities

Attachment B.7.1: Summary of Concentrations and Calculated Effective Solubilities

			Fuel	Water	Fuel	Water	Fuel	Water	Fuel	Water	Fuel	Water	Fuel	Water	Fuel	Water	Fuel
	~MW of Fuel[2,3]	Fuel Type	Benzene	Calculated Effective Solubility[1]	Naphthalene	Calculated Effective Solubility[1]	1-Methyl-naphthalene	Calculated Effective Solubility[1]	2-Methyl-naphthalene	Calculated Effective Solubility[1]	Toluene	Calculated Effective Solubility[1]	Ethyl-benzene	Calculated Effective Solubility[1]	Xylenes	Calculated Effective Solubility[1]	Density
	g/mole		ppmwt	mg/L	ppmwt	mg/L	ppmwt	mg/L	ppmwt	mg/L	ppmwt	mg/L	ppmwt	mg/L	ppmwt	mg/L	kg/L
MW[4]			78.1		128.2		142.2		142.2		92.1		106.2		106.2		
Solubility[4]			1780		31		28		25		515		152		200		
API Jet A																	
Avg	160	Jet A	100	0.36	1800	0.070	2800	0.088	3800	0.11	1400	1.25	1500	0.34	7800	2.35	0.810
Max	160		200	0.73	3000	0.12	3700	0.12	5700	0.16	5000	4.47	2600	0.60	17600	5.30	0.820
Min	160		ND	ND	700	0.027	1300	0.041	1800	0.051	600	0.54	800	0.18	3500	1.05	0.800
Count			14		14		14		14		14		14		14		14
UD/AFRL Jet A and Jet A-1																	
Avg	160	Jet A (23), Jet A-1 (2)	72	0.26	1731	0.067	1831	0.058	2878	0.081	1370	1.23	1280	0.29	6700	2.02	0.810
STDV	160		66	0.24	621	0.024	470.2	0.015	876	0.025	836	0.75	460	0.11	2420	0.73	0.016
Max	160		250	0.91	3292	0.13	2793	0.088	5219	0.15	3496	3.13	1930	0.44	10380	3.13	0.880
Min	160		2	0.007	695	0.027	870	0.027	1375	0.039	312	0.28	340	0.08	1770	0.53	0.796
Count			25		25		25		25		13		13		13		25
UD/AFRL JP-8																	
Avg	160	JP-8	73	0.27	1555	0.060	1674	0.053	2573	0.072	1038	0.93	1400	0.32	7330	2.21	0.805
STDV	160		35	0.13	540	0.021	488	0.015	861	0.024	484	0.43	551	0.13	2892	0.87	0.007
Max	160		124	0.452	2580	0.10	2430	0.077	4080	0.11	1713	1.53	2530	0.58	13600	4.10	0.822
Min	160		15	0.054	642	0.025	304	0.0096	710	0.020	358	0.32	50	0.01	280	0.08	0.79
Count			18		18		18		18		10		10		10		18
UD/AFRL JP-5																	
Avg	160	JP-5	7.8	0.028	2147	0.083	2147	0.068	3244	0.091	297	0.27	560	0.13	2920	0.88	0.816
STDV	160		5.8	0.021	1166	0.045	836	0.026	1434	0.040	269	0.24	292	0.067	1533	0.46	0.024
Max	160		21.1	0.077	3906	0.15	3144	0.099	5050	0.14	487	0.44	760	0.17	4100	1.24	0.893
Min	160		<1	ND	394	0.015	345	0.0109	502	0.014	106	0.09	350	0.08	1840	0.55	0.802
Count			13		13		13		13		2		2		2		11
UD/AFRL + API Jets Combined																	
Avg	160	JetA, JetA1, JP8,JP5	66	0.24	1777	0.069	2043	0.064	3052	0.086	1097	0.98	1461	0.33	7063	2.13	0.810
Max	160		250	0.91	3905	0.15	3700	0.12	5700	0.16	5000	4.47	2600	0.60	16950	5.11	0.893
Min	160		ND	ND	394	0.015	304	0.0096	502	0.014	106	0.09	50	0.01	280	0.08	0.79
Count			70		70		70		70		39		39		14		70
UD/AFRL + API Jets Combined MINUS JP-5																	
Avg	160	JetA, JetA1, JP8	79	0.29	1692	0.065	2019	0.064	3007	0.085	1140	1.02	1509	0.35	7287	2.20	0.808
Max	160		250	0.91	3292	0.13	2793	0.09	5219	0.15	5000	4.47	2600	0.60	17600	5.30	0.893
Min	160		ND	ND	642	0.025	304	0.0096	710	0.020	312	0.28	50	0.01	280	0.08	0.790
Count			57		57		57		57		37		37		37		57

Attachment B.7.1: Summary of Concentrations and Calculated Effective Solubilities (cont.)

			Fuel	Water	Fuel	Water	Fuel	Water	Fuel	Water	Fuel	Water	Fuel	Water	Fuel	Water	Fuel
	~MW of Fuel[2,3]	Fuel Type	Benzene	Calculated Effective Solubility[1]	Naphthalene	Calculated Effective Solubility[1]	1-Methyl-naphthalene	Calculated Effective Solubility[1]	2-Methyl-naphthalene	Calculated Effective Solubility[1]	Toluene	Calculated Effective Solubility[1]	Ethyl-benzene	Calculated Effective Solubility[1]	Xylenes	Calculated Effective Solubility[1]	Density
	g/mole		ppmwt	mg/L	ppmwt	mg/L	ppmwt	mg/L	ppmwt	mg/L	ppmwt	mg/L	ppmwt	mg/L	ppmwt	mg/L	kg/L
MW[4]			78.1		128.2		142.2		142.2		92.1		106.2		106.2		
Solubility[4]			1780		31		28		25		515		152		200		
API Diesel																	
Avg	200	Diesel, on-road, <500ppm Sulfur	80	0.36	600	0.029	1710	0.067	2750	0.097	620	0.69	470	0.13	2700	1.02	
STDV	200																
Max	200		250	1.14	1790	0.09	8240	0.32	14260	0.50	1780	1.99	700	0.20	9350	3.52	
Min	200		ND	ND	210	0.010	280	0.01	400	0.014	ND	ND	160	0.05	1010	0.38	
Count			12		12		12		12		12		12		12		
UD/AFRL Diesel																	
Avg	200	Diesel	62	0.28	430	0.021	639	0.025	1263	0.044							0.847
STDV	200		29	0.13	239	0.012	408	0.016	774	0.027							0.005
Max	200		124	0.56	1339	0.065	2538	0.100	4678	0.164							0.859
Min	200		8.8	0.040	102	0.005	116	0.005	184	0.006							0.837
Count			39		39		39		39								39
UD/AFRL + API Diesel Combined																	
Avg	200	Diesel	66	0.30	471	0.023	927	0.036	1620	0.057	620	0.69	470	0.13	2700	1.02	
Max	200		250	1.14	1790	0.087	8240	0.32	14260	0.501	1780	1.99	700	0.20	9350	3.52	
Min	200		8.8	ND	102	0.005	116	0.005	184	0.006	ND	ND	160	0.05	1010	0.38	
Count			50		50		50		50		12		12		12		
UD/AFRL F-76 Only																	
Avg	200	F76	31	0.14	1568	0.076	1906	0.075	3346	0.118	355	0.40	346	0.10	1819	0.69	0.848
STDV	200		17	0.077	854	0.041	813	0.032	1767	0.062	118	0.13	159	0.046	833	0.31	0.007
Max	200		64	0.29	3537	0.171	4125	0.162	8472	0.298	519	0.58	569	0.16	3060	1.15	0.864
Min	200		3	0.014	480	0.023	678	0.027	1037	0.036	177	0.20	146	0.04	769	0.29	0.839
Count			18		18		18		18		9		9		9		16
UD/AFRL Data for Pearl Harbor Samples Only: JP-5																	
FISC Pearl Harbpr 4117506	160	JP-5	4.9	0.018	2651	0.103	2343	0.074	3921	0.110							0.811
FISC Pearl Harbpr 4117532	160	JP-5	11.2	0.041	1808	0.070	2000	0.063	3083	0.087							0.824
UD/AFRL Data for Pearl Harbor Samples Only: F-76																	
FISC Pearl Harbor 500065	200	F-76	17.5	0.080	611	0.030	1199	0.047	1723	0.061							0.859
FISC Pearl Harbor 4129218	200	F-76	44.8	0.204	575	0.028	1238	0.049	1698	0.060							0.848

UD/AFRL: University of Dayton and AirForce Research Laboratory, Shafer and Edwards 2011

1. Calculated by I. Rhodes

2. Average molecular weight for JP-8 from GCXGC analysis (Striebich 2014 and Edwards 2018): 160 g/mole

3. Average molecular weight for JP-8 from GCXGC analysis (Edwards 2018): 200 g/mole

4. Solubility from TPHCWG, Vol. 3, 1997

Ethylbenzene and Xylenes for USAF data: From GCXGC (wt%). Output is for C2-Benzenes. E and X were calcaulated from the sum using 16% E and 84% X on advices from Tim Edwards, AFRL, Jan 2018 (emails)

Data Sources:

API, 2010, API HPV Testing Group, Kerosene/Jet Fuel Category Assessment Document, #1100997, Report to USEPA 2010.
http://www.petroleumhpv.org/petroleum-substances-and-categories/~/media/37A083A569294403AD230CB504AB17A6.ashx

API, 2012, High Production Volume (HPV) Chemical Challenge Program Gas Oils Category Analysis Document and Hazard Characterization,
Submitted to USEPA 2012. http://www.petroleumhpv.org/~/media/PetroleumHPV/Documents/2012_nov15_Gas%20Oils%20CAD%20Final%20Standard%2010_24_2012.pdf

UD/USAF, Shafer L.M. and Edwards T., Speciated Naphthalene Analysis in Liquid Transportation Fuels, IASH 2011, The 12th International Conference on Stability, Handling and Use of Liquid Fuels, Sarasota, Florida USA, 16-20 October 2011

UD/USAF, Striebich R.C., Shafer L.M., Adams R.K., West Z.J., DeWitt M.J., and Zabarnick S., Hydrocarbon Group-Type Analysis of Petroleum-Derived and Synthetic Fuels Using Two-Dimensional Gas Chromatography
Energy & Fuels, 2014, 28, 5696-5706, dx.doi.org/10.1021/ef500813x

Edwards J.T, (CIV USAF, Air Force Research Laboratory), personal communications with Ileana Rhodes (GSI Environmental), January 2018

Attachment B.7.2:
Review of Analytical Results for RHMW2254-01 – Red Hill Shaft

CONTENTS

Acronyms and Abbreviations ii

1. Summary 1

2. Data Evaluation 1

- 2.1 2005 1
- 2.2 July 2006 to September 2007 1
- 2.3 January 2008 to July 2010 2
- 2.4 October 2010 to July 2012 2
- 2.5 October 2012 to January 2015 2
- 2.6 April 2015 to July 2016 2
- 2.7 October 2016 to April 2018 2
- 2.8 Evaluation of Results 2

3. Conclusions 6

4. References 6

FIGURES

B.7.2-1 RHMW2254-01 Toluene Results 3

B.7.2-2 RHMW2254-01 Ethylbenzene Results 3

B.7.2-3 RHMW2254-01 TPH-g Results 4

B.7.2-4 RHMW2254-01 TPH-d Results 4

B.7.2-5 RHMW2254-01 TPH-o Results 4

B.7.2-6 RHMW2254-01 Naphthalene Results 5

B.7.2-7 RHMW2254-01 1-Methylnaphthalene Results 5

B.7.2-8 RHMW2254-01 2-Methylnaphthalene Results 5

ACRONYMS AND ABBREVIATIONS

µg/L	micrograms per liter
APPL	Agriculture & Priority Pollutants Laboratories
CAS	Columbia Analytical Services
COPC	chemical of potential concern
LOD	limit of detection
LOQ	limit of quantitation
TPH-d	total petroleum hydrocarbons – diesel range organics
TPH-g	total petroleum hydrocarbons – gasoline range organics
TPH-o	total petroleum hydrocarbons – residual range organics (i.e., TPH-oil)

1. Summary

RHMW2254-01 is a sampling point located inside the water development tunnel of Navy Supply Well 2254-01 (Red Hill Shaft). Detections of total petroleum hydrocarbons-gasoline range organics (TPH-g), -diesel range organics (TPH-d), -residual range organics (TPH-o), ethylbenzene, toluene, 1-methylnaphthalene, 2-methylnaphthalene, and naphthalene occurred occasionally during monitoring events since this sampling point was installed in 2005. However, chemicals of potential concern (COPCs) have not been detected above the screening criteria, and the COPC detections have been relatively sporadic. The highest TPH-d concentration (67 micrograms per liter [µg/L]) was detected during the June 2005 monitoring event (the second sampling event performed at this sampling point), much lower than the screening criterion (400 µg/L). The highest naphthalene reported was 0.085 µg/L in 2005. Naphthalenes have not been detected since March 2014. Toluene was detected during three monitoring events, but may be attributed to field or laboratory artifact, based on reported trip blank contamination during the October 2015 and January 2016 events.

Review of available laboratory and quarterly reports that include results from analysis of samples from RHMW2254-01 does not indicate that this sampling point was impacted by the January 2014 release and any impacts to groundwater are likely attributable to historical leaks.

2. Data Evaluation

Very few COPCs have been detected at RHMW2254-01; most detections reported were below quantitation limits and some were also found in corresponding field and laboratory method blanks. Groundwater chemistry data can be affected by various sampling and analytical issues that need to be considered when evaluating the data, particularly regarding field and laboratory detections in the blanks and varying limits of detection (LODs) from laboratory to laboratory with time. COPCs detections or lack thereof do not necessarily indicate a trend and must be evaluated along with differences in laboratory reporting limits.

The data tables typically include assessment of the validity of the results with qualifiers. However, qualifiers are not seen in graphically displayed data, and data issues (e.g., blank contamination) are not evident. Laboratory and quarterly groundwater monitoring reports were reviewed to gain a better understanding of groundwater results from RHM2254-01. The evaluation was performed by separating periods during which a specific laboratory performed the analyses. This is particularly important for TPH analysis, as discussed in Appendix B.7. Details are discussed below.

2.1 2005

The laboratory used during this period was Columbia Analytical Services (CAS). Traces of toluene were detected during the initial sampling event at RHMW2254-01 at concentrations (0.81–1.2 µg/L) below the screening criterion of 40 µg/L. Low detections of toluene are not uncommon in groundwater analyses, as it is a common solvent in many glues, adhesives, and piping material. There also were some low-level detections of TPH-d, TPH-o, 2-methylnaphthalene, and naphthalenes in subsequent sampling events; the LODs were 50, 100, 0.02, and 0.02 µg/L, respectively.

2.2 JULY 2006 TO SEPTEMBER 2007

The laboratory used during this period was Accutest Laboratories. No COPCs were detected; however, the TPH-d and naphthalene LODs (100 and 0.26 µg/L, respectively) were higher than for the previous laboratory. TPH-o was not analyzed during this period.

2.3 JANUARY 2008 TO JULY 2010

The laboratory used during this period was SGS Environmental Services (Alaska). Low-level detections each of TPH-g, 1-methylnaphtalene, 2-methylnaphthalene, and naphthalene were reported, but the analytes were detected at separate events; the LODs were 10 µg/L, 0.015, 0.015, and 0.031, respectively, which were lower than Accutest LODs for the previous 2006–2007 period.

2.4 OCTOBER 2010 TO JULY 2012

The laboratory used during this period was Agriculture & Priority Pollutants Laboratories (APPL). No COPCs were detected. The LODs were higher than those of CAS and SGS Alaska for most analytes. The LODs for TPH-d, TPH-g, 1-methylnaphthalene, 2-methylnaphthalene, and naphthalene were 80, 12, 0.12, 0.12, and 0.1 µg/L, respectively.

2.5 OCTOBER 2012 TO JANUARY 2015

The laboratory used during this period was Eurofins Calscience (Calscience). There were a few detections of TPH-d and TPH-g and several detections of naphthalene, all at estimated values. TPH-g was also detected in the laboratory method blanks during the events when TPH-g was detected in the groundwater samples. The LODs for TPH-d, TPH-g, 1-methylnaphthalene, 2-methylnaphthalene, and naphthalene were 20, 30, 0.05, 0.05, and 0.050 µg/L, respectively. The isolated detections of naphthalenes seen at RHMW2254-01 were also reported at similar concentrations at other monitoring wells (RHMW03, RHMW05, OWDFMW01, and HMW2253-03) sampled during the same period. RHMW04 was not sampled during this time.

These low-level naphthalene detections occurred before and after the January 2014 release, and no marked increase in concentration was seen after the release. Naphthalene has not been detected in RHMW5543-01 since March 2014. TPH was not detected during sampling events when naphthalene was detected.

2.6 APRIL 2015 TO JULY 2016

The laboratory used during this period was ALS Environmental (formerly CAS). Very low levels of TPH-d and TPH-o were detected, but similar concentrations were also found in the laboratory method blanks. There was one detection of ethylbenzene and two detections of toluene, but the toluene detections were also reported in trip blanks at similar concentrations. Due to the blank contamination, COPC detections during this period are validated as unreliable. No naphthalenes were reported during this period, which is significant because this laboratory had the lowest LODs for naphthalenes (0.005 µg/L), and for all other COPCs, of all the laboratories used.

2.7 OCTOBER 2016 TO APRIL 2018

The laboratory used during this period was APPL. The only COPCs detected were TPH-d and TPH-o in December 2016 at 14 J µg/L (LOD of 25 µg/L) and 16 J µg/L (LOD of 40 µg/L), respectively. TPH-d was also detected in October 2017 at 65 J µg/L; however, the duplicate sample was non-detect.

2.8 EVALUATION OF RESULTS

Figure B.7.2-1 to Figure B.7.2-8 show the results for all samples taken from RHMW2254-01 for most COPCs over time. These figures provide a clear visual display of the data and perspective of occurrence over time as well as caveats regarding contamination in the corresponding blanks and the differences in reporting limits for the laboratories used.

After careful review of the available data and reports and evaluation of each value reported, the few detections of naphthalene occurred when samples were analyzed by Calscience (Figure B.7.2-5). Due to the uncertainty associated with these low-level detections, the available monitoring record is not suitable for evaluating the presence or absence of naphthalenes in individual monitoring wells at concentrations of less than 0.1 µg/L. Refer to Attachment B.7.4 for more detailed discussion on low-level detections of naphthalenes. In addition, Calscience had recurrent issues with TPH-g in the method blanks (Figure B.7.2-3). TPH-d and TPH-o were mostly detected during the time that ALS/CAS laboratory was performing the analysis (Figure B.7.2-4). ALS/CAS laboratory appeared to have frequent issues with method blanks for toluene and TPH-d for some of the sampling events.

These issues with the data were investigated in the data validation report within the *Third Quarter 2016 - Quarterly Groundwater Monitoring Report, Inside Tunnel Wells* (DON 2016, Appendixes D and G). In general, detections below the limit of quantitation (LOQ) in primary samples, laboratory method blanks, and trip blanks may be false low-level hits resulting from positive interference from laboratory analytical processes (i.e., laboratory contamination), and do not necessarily indicate a trend of true groundwater concentrations without further investigation. This may indicate a systemic issue with the laboratory background contamination, and it may have been a result of ALS/CAS laboratory's very low reporting limits, which were lower than limits from any other laboratory used during other periods.

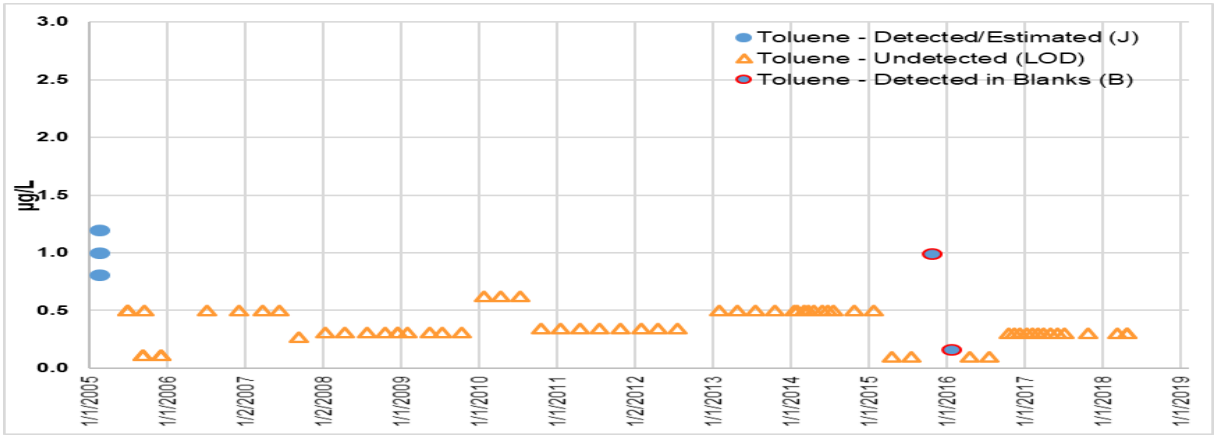

Figure B.7.2-1: RHMW2254-01 Toluene Results

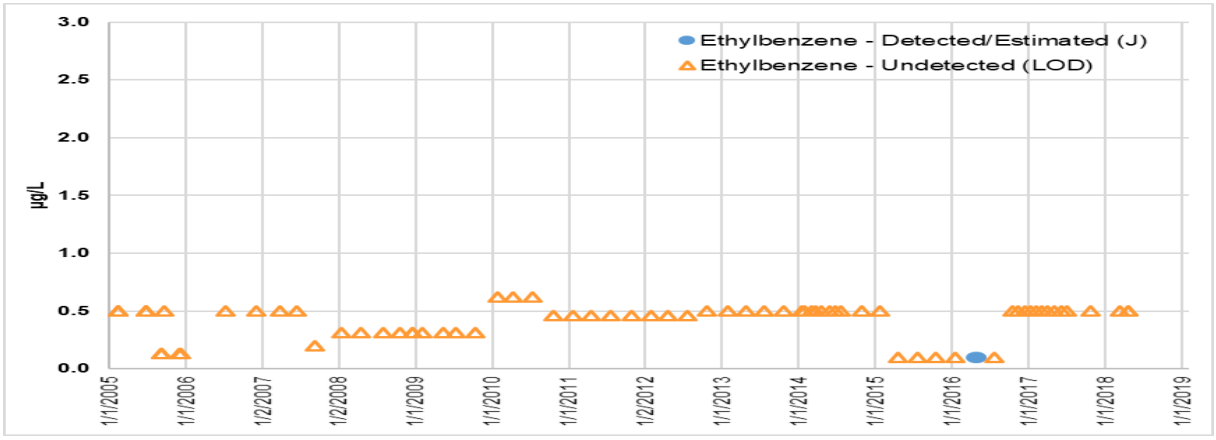

Figure B.7.2-2: RHMW2254-01 Ethylbenzene Results

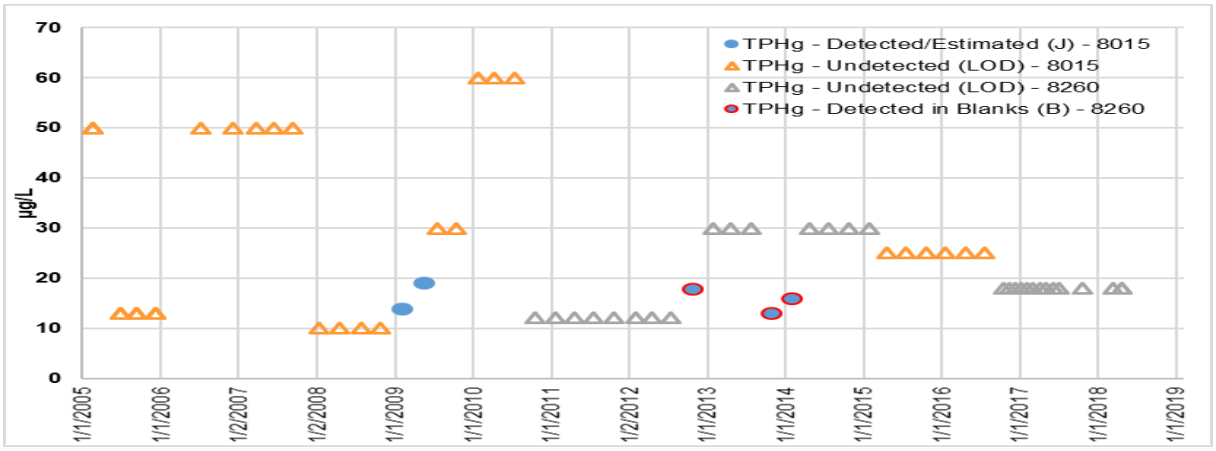

Figure B.7.2-3: RHMW2254-01 TPH-g Results

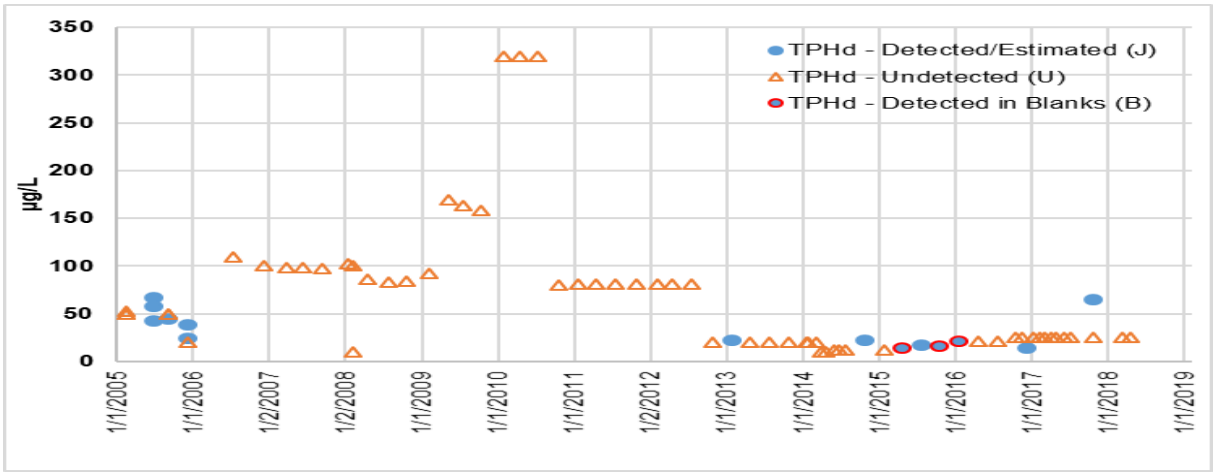

Figure B.7.2-4: RHMW2254-01 TPH-d Results

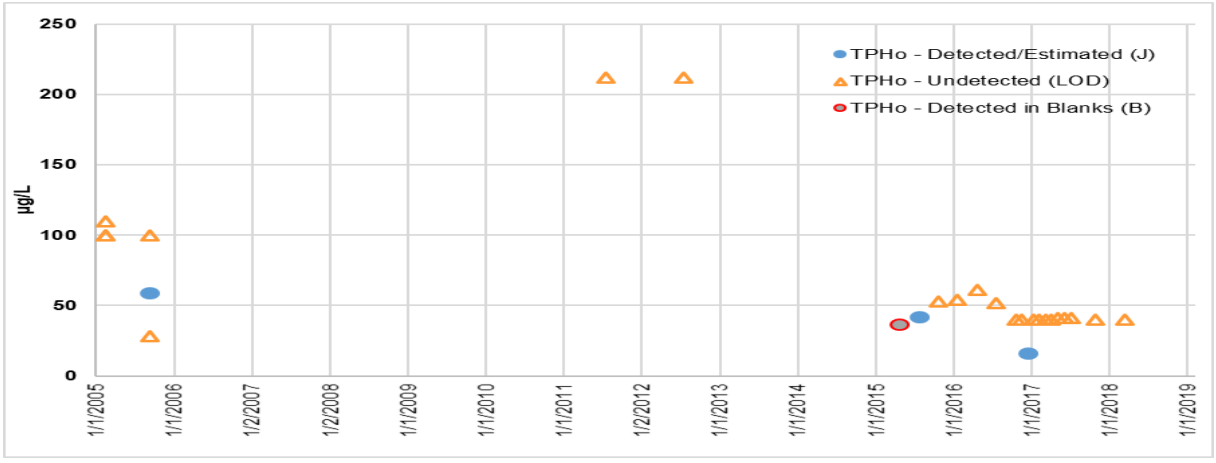

Figure B.7.2-5: RHMW2254-01 TPH-o Results

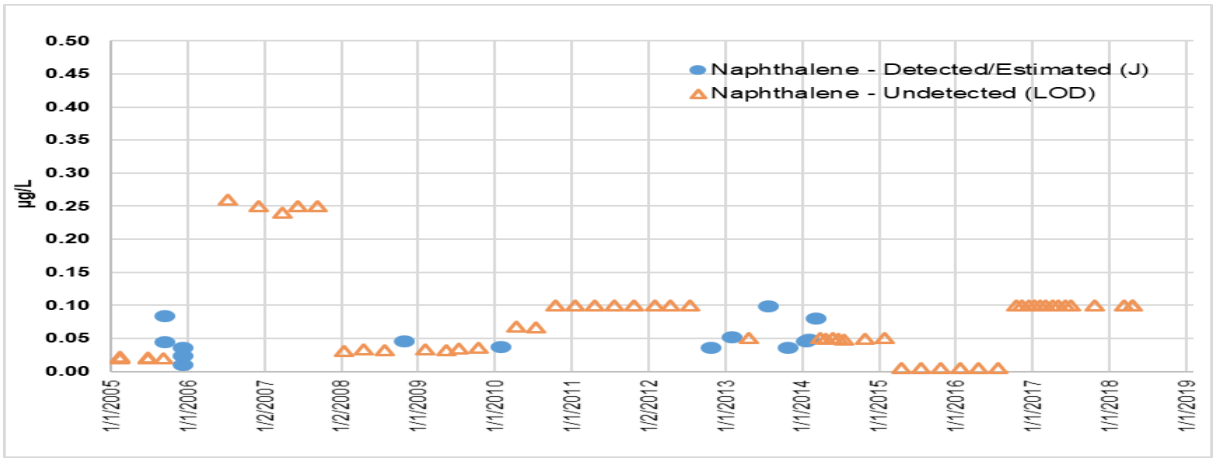

Figure B.7.2-6: RHMW2254-01 Naphthalene Results

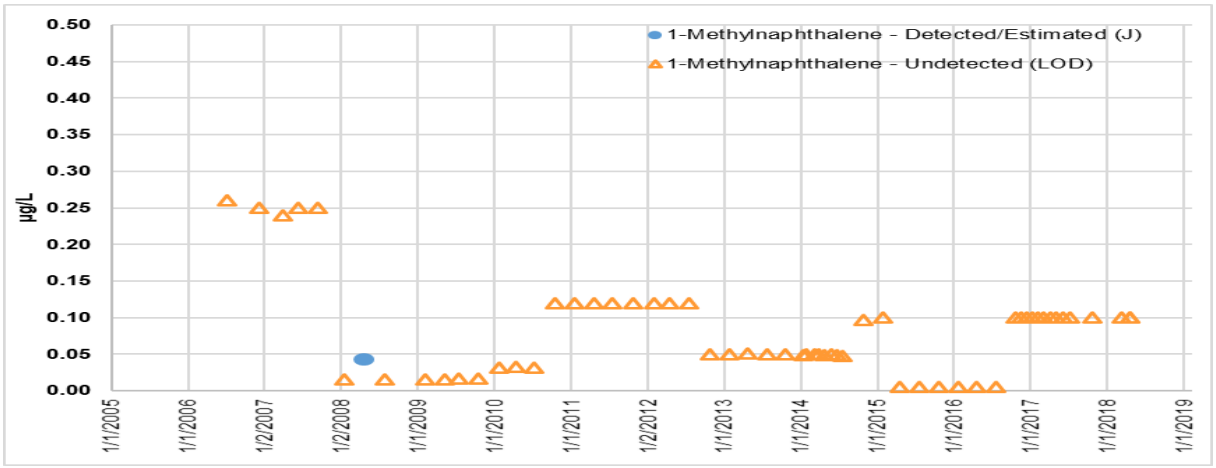

Figure B.7.2-7: RHMW2254-01 1-Methylnaphthalene Results

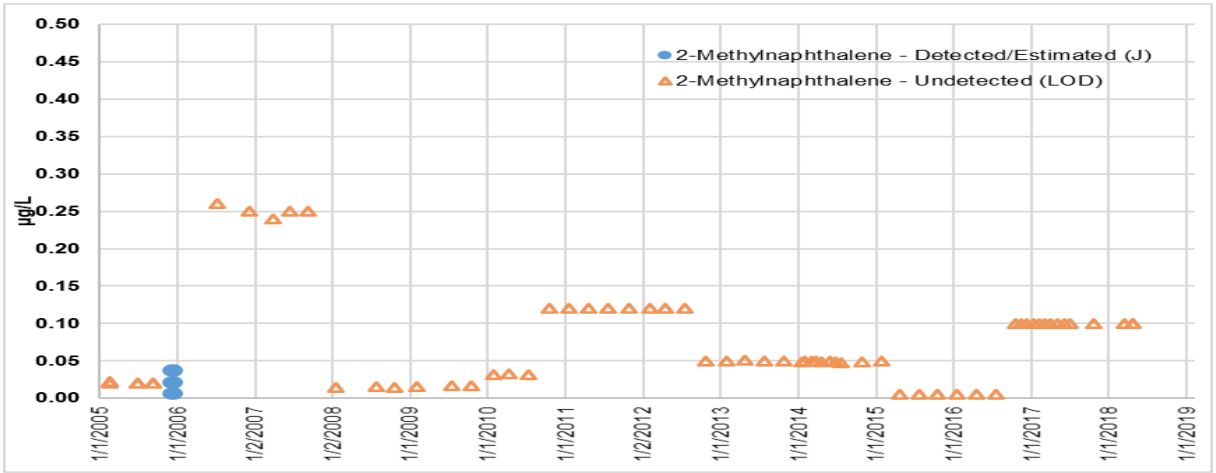

Figure B.7.2-8: RHMW2254-01 2-Methylnaphthalene Results

3. Conclusions

A review of the historical data does not indicate that RHMW2254-01 was impacted by the 2014 release and any impacts to groundwater are likely attributable to historical leaks. Very few COPCs were detected, and most detections were below quantitation limits. Additionally, COPCs were also found in corresponding laboratory and field blanks, indicating potential sample contamination from other sources. Detections of BTEX and naphthalenes did not correlate with TPH detections. There are indications that detections may be dependent on the variability in limits of detections from laboratory to laboratory rather than from a fuel release at the Facility.

4. References

Department of the Navy (DON). 2016. Final Third Quarter 2016 - Quarterly Groundwater Monitoring Report, Inside Tunnel Wells, Red Hill Bulk Fuel Storage Facility, Joint Base Pearl Harbor-Hickam, Oahu, Hawaii. October. Prepared by Element Environmental, LLC, Aiea, HI. Prepared for Naval Supply Systems Command Fleet Logistics Center Pearl Harbor, JBPHH, HI.

Attachment B.7.3:
Review of Analytical Results for RHMW04

CONTENTS

Acronyms and Abbreviations ii

1. Summary 1

2. Data Evaluation 1

    2.1 2005 to 2010 1
    2.2 July 2014 to January 2015 1
    2.3 April 2015 to July 2016 4
    2.4 October 2016 to April 2018 7

3. Conclusions 10

4. References 10

FIGURES

B.7.3-1 RHMW04 TPH-d Chromatograms from July 2014 and January 2015 Samples 2

B.7.3-2 RHMW04 TPH-d Chromatograms from April 2015 Sample 5

B.7.3-3 RHMW04 TPH-d Chromatograms from January 2016 Sample 5

B.7.3-4 RHMW04 Benzene Results 8

B.7.3-5 RHMW04 Toluene Results 8

B.7.3-6 RHMW04 TPH-d Results 9

B.7.3-7 RHMW04 TPH-o Results 9

B.7.3-8 RHMW04 Naphthalene Results 10

TABLES

B.7.3-1 RHMW04 Analytical Results, 2005–2018 3

ACRONYMS AND ABBREVIATIONS

µg/L	micrograms per liter
CAS	Columbia Analytical Services
COPC	chemical of potential concern
LOD	limit of detection
LOQ	limit of quantitation
RL	reporting limit
TPH-d	total petroleum hydrocarbons – diesel range organics
TPH-g	total petroleum hydrocarbons – gasoline range organics
TPH-o	total petroleum hydrocarbons – residual range organics (i.e., TPH-oil)

1. Summary

RHMW04 is an outside-tunnel monitoring well located northeast of the tank farm. Historical groundwater monitoring data from RHMW04 showed detections of total petroleum hydrocarbons – diesel range organics (TPH-d), TPH-residual range organics (TPH-o), benzene, toluene, 1-methylnaphthalene, 2-methylnaphthalene, and naphthalene below respective screening criteria (400, 500, 5, 40, 10, 10, and 17 micrograms per liter [µg/L]). TPH-gasoline range organics (TPH-g), ethylbenzene, and xylenes have never been detected. Review of available lab and quarterly reports does not indicate that RHMW04 is impacted by the January 2014 release and any impacts to groundwater are likely attributable to historical leaks or other potential sources (e.g., residual material from drilling).

2. Data Evaluation

Very few chemicals of potential concern (COPCs) have been detected at RHMW04, most below quantitation limits and many also found in corresponding in field and laboratory blanks. Some of these instances coincided with analysis at a laboratory with very low reporting limits. As discussed in Attachment B.7.2, groundwater chemistry data can be affected by various sampling and analytical issues that need to be considered when evaluating the data. The data tables typically include assessment of the validity of the results with qualifiers. However, qualifiers are not seen in graphically displayed data and data issues, such as blank contamination for instance, are not evident. Table B.7.3-1 includes the available data for RHMW04 and a more in-depth evaluation of laboratory controls that should be considered before determining possible impacts to groundwater in the vicinity of a well. Laboratory and quarterly groundwater monitoring reports were reviewed to get a better understanding of groundwater results from RHMW04. The evaluation was performed by separating periods during which a specific laboratory performed the analyses. This is particularly important for TPH analysis, as discussed in Appendix B.7. Details are discussed below.

2.1 2005 TO 2010

During 2005–2010, groundwater monitoring samples from RHMW04 were analyzed at the analytical laboratories Accutest and SGS Alaska. These laboratories had reporting limits ranging from 100 to 352 µg/L. The first sample from RHMW04 was collected on 9/19/2005, with TPH-d detected at 338 µg/L. This TPH-d result may have been due to possible residual material from drilling of the well rather than from fuels stored at the Facility. No TPH-d or any other COPCs were detected after this initial sample during this period other than a trace of benzene (0.25 J µg/L).

No samples were collected at RHMW04 from May 2010 to June 2014.

2.2 JULY 2014 TO JANUARY 2015

Eurofins Calscience, Inc. laboratory (Calscience) analyzed the groundwater samples for three sampling events. Calscience had reporting limits approximately 10 times lower than limits reported by the previous laboratories. Traces of TPH-d were detected and reported as estimated values (17 J and 10 J µg/L, July 2014 and January 2015, respectively). Review of the chromatograms shown on Figure B.7.3-1, seen in an expanded y-scale, revealed a series of discrete peaks in the July 2014 sample that do not resemble any type of fuel pattern, dissolved fuel components, or biodegraded matter. The sample from January 2015 shows over-integration of a very small signal at the LOD. The laboratory report for both of these samples indicates that TPH-d was also detected in the blanks.

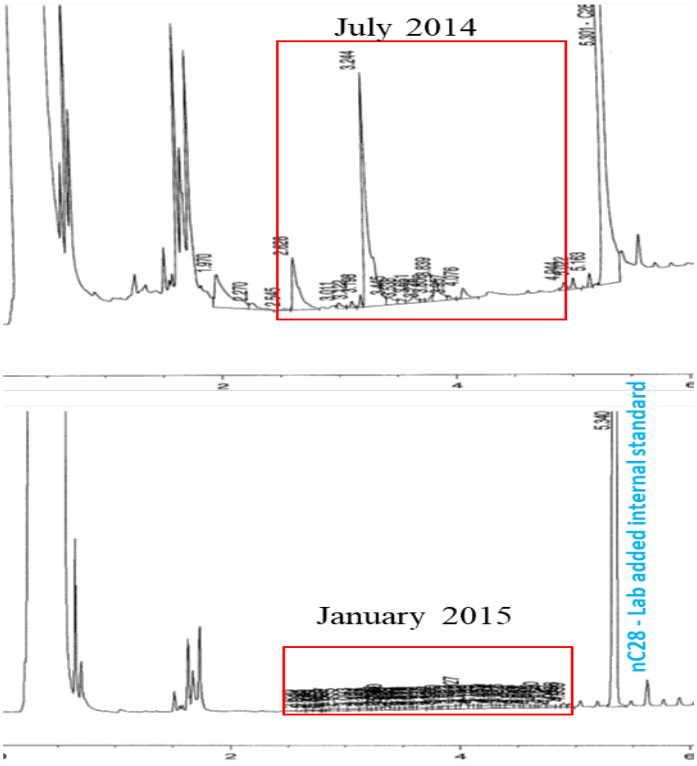

Figure B.7.3-1: RHMW04 TPH-d Chromatograms from July 2014 and January 2015 Samples

Table B.7.3-1: RHMW04 Analytical Results, 2005–2018

		µg/L:	TPH-d					TPH-o					PAHs									BTEX				
Lab	Sample ID	Date Sampled	RHMW04	RHMW04 (ND)	Method Blank	Equipment Blank	Rinseate Water	RHMW04	RHMW04 (ND)	Method Blank	Equipment Blank	Rinseate Water	1-Methylnaphthalene	1-Methylnaphthalene (ND)	2-Methylnaphthalene	2-Methylnaphthalene (ND)	Naphthalene	Naphthalene (ND)	Naphthalene - Method Blank	Naphthalene - Equipment Blank	Naphthalene - Rinseate Water	Benzene	Benzene (ND)	Toluene	Toluene (ND)	Toluene - Trip Blank
Accuttest	RHMW04W01	9/19/2005	**338**											<0.28		<0.28		<0.28					<0.05		< 0.50	
Accuttest	RHMW04-GW02	7/10/2006		<100										<0.26		<0.26		<0.26					<0.05		< 0.50	
SGS Alaska	RHMW04-WG-01	8/4/2009		<157										<0.0162		<0.0162		<0.0335					0.12		< 0.31	
SGS Alaska	RHMWA01-WG-01	8/4/2009		<161										<0.0167		<0.0167		<0.0344				**0.25J**			< 0.31	
SGS Alaska	RHMW04-WG-02	10/13/2009		<169										<0.0172		<0.0172		<0.0356					<0.12		< 0.31	
SGS Alaska	RHMWA01-WG-02	10/13/2009		<174										<0.0169		<0.0169		<0.0348					<0.12		< 0.31	
SGS Alaska	RHMW04-WG-03	1/26/2010		<334										<0.0326		<0.0326		<0.0674					<0.24		< 0.62	
SGS Alaska	RHMWA01-WG-03	1/26/2010		<330										<0.0338		<0.0338		<0.0696					<0.24		< 0.62	
SGS Alaska	RHMW04-WG-04	4/26/2010		<348										<0.0352		<0.0352		<0.073					<0.24		< 0.62	
SGS Alaska	RHMWA01-WG-04	4/26/2010		<352										<0.0352		<0.0352		<0.073					<0.24		< 0.62	
Calscience	ES112	7/23/2014	**17J**											<0.052		<0.052		<0.052					< 0.50		< 0.50	
Calscience	ES119	10/29/2014		<12										<0.099		<0.050		<0.050					< 0.50		< 0.50	
Calscience	ES129	1/29/2015	**10J**											<0.10		<0.052		<0.052					< 0.50		< 0.50	
ALS/CAS	ES139	4/22/2015		<21				**25JB**		**28JB**				<0.005		<0.005		<0.005					<0.10		< 0.10	
ALS/CAS	ES156	8/20/2015	**24JB**		**16JB**			**40JB**		**50JB**				<0.005	**0.0059J**		**0.0075J**							<0.10		< 0.10	
ALS/CAS	ERH006	10/19/2015		<22B					<53				**0.0043J**		**0.0047JB**		**0.0051JB**					**0.08J**		**0.42J**		
ALS/CAS	ERH019	1/19/2016	**36JB**		**19JB**			**52JB**		**40JB**				<0.005		<0.005		<0.005					<0.10		<0.10	
ALS/CAS	ERH020	1/19/2016	**29JB**						<53B					<0.005		<0.005		<0.005					<0.10	**0.11JTb**		**0.19JTb**
ALS/CAS	ERH034	4/19/2016		<20B					<33B					<0.005		<0.005		<0.005					<0.10		<0.10	
ALS/CAS	ERH048 - after data validation	7/19/2016		<22F					<55BF																	
	ERH048 - lab sheet	7/19/2016	**23JF**			**12JF**		**54JF**		**43JF**	**36JF**	**30JF**	**0.007J**		**0.0068J**		**0.18 BF**		**0.0045JB**	**0.0098JBF**	**0.0082JBF**		<0.10		<0.10	
APPL	ERH096	10/25/2016		<25					<40					<0.10		<0.10		<0.10					< 0.30		< 0.30	
APPL	ERH128	11/14/2016		<25					<40					<0.10		<0.10		<0.10					< 0.30		< 0.30	
APPL	ERH138	12/13/2016		<25					<40					<0.10		<0.10		<0.10					< 0.30		< 0.30	
APPL	ERH166	1/9/2017		<25					<40					<0.10		<0.10		<0.10					< 0.30		< 0.30	
APPL	ERH208	2/6/2017		<25					<40					<0.10		<0.10		<0.10					< 0.30		< 0.30	
APPL	ERH260	3/6/2017		<25					<40					<0.10		<0.10		<0.10					< 0.30		< 0.30	
APPL	ERH295	4/3/2017		<25					<40					<0.10		<0.10		<0.10					< 0.30		< 0.30	
APPL	ERH381	7/5/2017		<25					<40					<0.10		<0.10		<0.10					< 0.30		< 0.30	
APPL	ERH421	10/24/2017		<25					<40					<0.10		<0.10		<0.10					< 0.30		< 0.30	
APPL	ERH552	3/14/2018		<25					<40					<0.10		<0.10		<0.10					< 0.30		< 0.30	
APPL	ERH598	4/25/2018		<25					<40					<0.10		<0.10		<0.10					< 0.30		< 0.30	

Notes: Detected values are shown in **bold text**.
Non-detect values are reported as less than the reporting limit (<RL) or less than the limit of detection (<LOD).
B analyte also detected in the laboratory method blank
F analyte also detected in the field blank (i.e., decontamination source water or equipment rinsate)
J estimated value; detected value reported below the laboratory's reporting limit (RL) or limit of quantitation (LOQ)
Tb analyte also detected in the trip blank

2.3 APRIL 2015 TO JULY 2016

Samples were analyzed by ALS Environmental, formerly Columbia Analytical Services (CAS), with significantly lower reporting limits for polynuclear aromatic hydrocarbons (PAHs). There were seven sampling events in this time range. Five of the seven sampling events have detections, and these events have blank contamination issues:

- **Benzene and Toluene:** ALS/CAS had reporting limits that were five times lower than the previous laboratory, Calscience. Benzene (0.08 J µg/L) and toluene (0.42 J µg/L) were reported at concentrations below the quantitation limits (J-flagged as estimated values) for the October 2015 sample. Toluene (0.11 J µg/L) was also reported in the January 2016 sample, but toluene was also detected in the trip blanks at a higher estimated concentration (0.19 J µg/L) than in the groundwater sample.
- **TPH-d:** Three of the events have TPH-d detections with estimated values in the range of 24 J to 36 J µg/L. However, results from these sampling events are questionable because the laboratory method blanks and/or field blanks also have TPH-d (11–19 µg/L). One of these events (July 2016) was reported as undetected after data validation. Data validation conducted for that sampling event considered the presence of the same COPCs in the blanks and deemed that result as undetected (DON 2016). Review of some of the chromatograms from April 2015 (Figure B.7.3-2) shows very small peaks that are not likely associated with soluble components. The chromatogram from the January 2016 sample (Figure B.7.3-3) does not show much of a signal to integrate, but values were reported and there were detections in the corresponding blanks.
- **TPH-o:** TPH-o was reported at estimated values in the range of 25 J – 52 J µg/L for three samples. However, results from these sampling events are questionable because the laboratory method blanks and/or field blanks also had detections of TPH-o (28 J – 50 J µg/L). One of these events (July 2016) was reported as undetected after data validation. Data validation considered the presence of the same COPCs in the blanks and deemed that result as undetected. Figure B.7.3-2 and Figure B.7.3-3 do not show significant signals to quantitate.
- **Naphthalene and Methylnaphthalenes:** Three of the events have some naphthalenes reported, with estimated values in the range of 0.0043 J – 0.18 µg/L. Only one result for naphthalene was at the quantitation limit (0.18 µg/L), but this result was also flagged due to detection of naphthalene in the laboratory method blank as well as the field blank and equipment rinsate (0.0045–0.0098 µg/L). Some of these detections are possibly due to laboratory or field contamination. Additionally, reporting limits by ALS/CAS for naphthalenes and methylnaphthalenes are 10–20 times lower than limits by other laboratories (i.e., for samples analyzed before and after the April 2015 to July 2016 period). Due to the uncertainty associated with these low-level detections, the available monitoring record is not suitable for evaluating the presence or absence of naphthalenes in individual monitoring wells at concentrations of less than 0.1 µg/L. Refer to Attachment B.7.4 for more detailed discussion on low-level detections of naphthalenes.

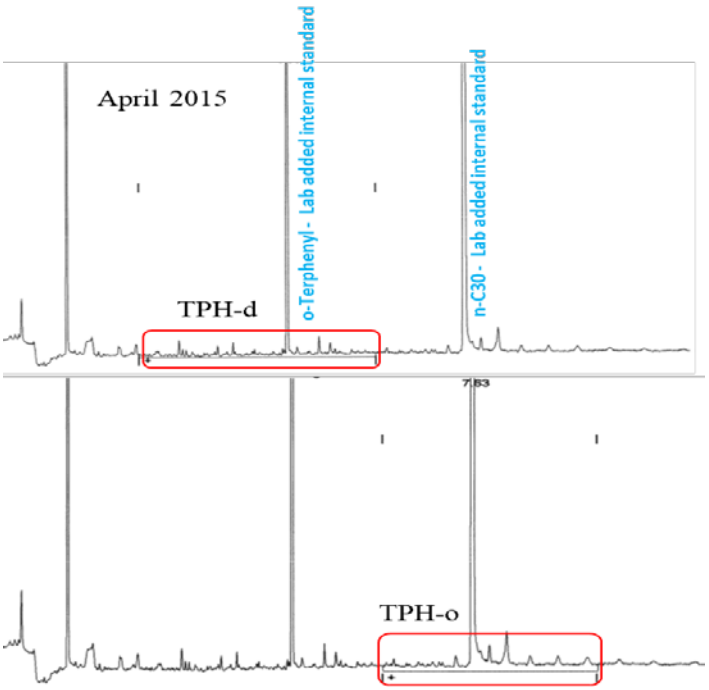

Figure B.7.3-2: RHMW04 TPH-d Chromatograms from April 2015 Sample

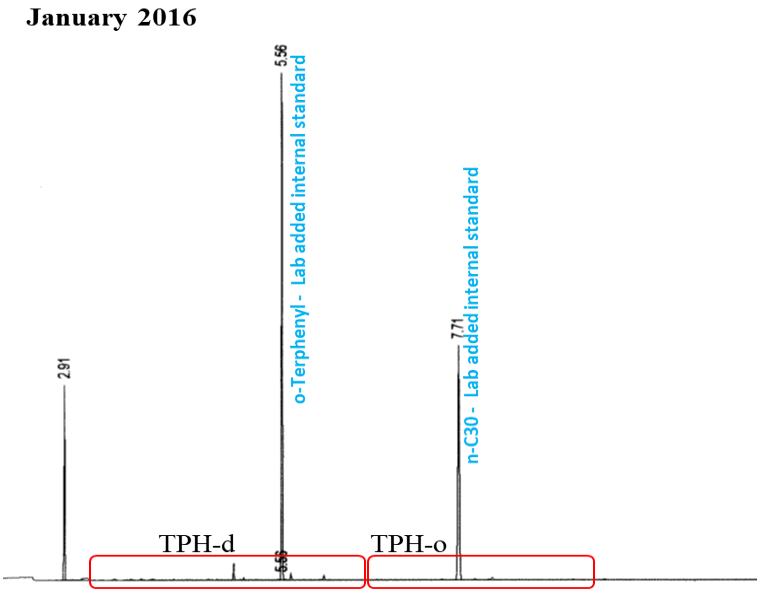

Figure B.7.3-3: RHMW04 TPH-d Chromatograms from January 2016 Sample

The following text is reproduced from the *Third Quarter 2016 - Groundwater Monitoring Report – Outside Tunnel Wells* (DON 2016), which includes the July 2016 data validation information presented above.

- Text from Section 4 – Summary, Conclusions and Recommendations:

  RHMW04 – No analytes were detected in groundwater above the laboratory LOQs or the applicable DOH Tier 1 EALs. TPH-d, TPH-o, and naphthalene were positively identified by the laboratory at levels below the LOQ, but are considered ND at these concentrations due to the presence of these contaminants in the associated source blank and subsequent equipment rinseate (TPH-d, TPH-o, and naphthalene) and laboratory method blank (TPH-o and naphthalene). No contaminants were detected above the laboratory detection limits, with the exception of polycyclic aromatic hydrocarbons (PAHs): 1-methylnaphthalene (0.0070 µg/L), 2-methylnaphthalene (0.0068 µg/L), and naphthalene (0.18 µg/L).

- Text from Section 2.3 Groundwater Contaminant Trends:

  RHMW04 – Concentrations of TPH-d, TPH-o, and naphthalene were detected in this well below the laboratory LOQs and the respective DOH Tier 1 EALs. These detections were most likely the result of source water contamination (TPH-d, TPH-o, and naphthalene) and lab contamination (TPH-o and naphthalene) and were flagged as ND by the data validators. Concentrations of all other COPCs detected during this round of quarterly sampling were below the laboratory detection limits.

- Text from Section 3.1 Data Validation and Assessment:

  Data Validation Items of Concern

  - *The fairly large error inherent to the analysis of TPH-d and TPH-o by EPA Method 8015 should be considered when results are compared to each other, to action levels, and to results from previous sampling events. Any comparative analysis of the results should take into consideration the fairly wide method acceptance limits (36-132%) as per DoD QSM Version 5.0 (DoD, 2013).*

  - *TPH-o was detected in the method blank at a concentration below its respective LOQ. Presence of this compound at comparable levels in project samples likely indicate positive interference from laboratory procedures (laboratory contamination). Subsequently, detections for compounds identified in the method blank were flagged "U (B)" by the data validators and in project sample summaries provided in Tables 2.1 and 3.1. The data validation report indicates that samples associated with this method blank should be considered as ND. The U flag added to the data by the data validator indicates that "the compound or analyte was analyzed for and positively identified by the laboratory; however, the compound or analyte should be considered non-detected at the reported concentration due to the presence of contaminants detected in the associated blank(s)".*

  - *The source blank water (ozonated, micro-filtered bottled drinking water) used for decontamination of the portable bladder pump was found to contain trace levels of TPH- o, naphthalene, ethylbenzene, and xylenes. Subsequently, similar levels of TPH-o, naphthalene, ethylbenzene, and xylenes were found in the rinseate sample as well as several primary samples. Details are included in the DVR report in Appendix D.*

- *The equipment rinseate sample was found to contain trace levels of TPH-d. Subsequently, similar levels of TPH-d were found in several primary samples. Details are included in the DVR report in Appendix D.*
- *The significantly lower reporting limits should be considered when results are compared to data from previous events. Additionally, during the April 2015 event, TPH-o was added to the analyte list. There are very few previous TPH-o results to compare this data to.*

• Text from Section 3.2 Data Assessment and Usability Conclusions:

Data Assessment and Usability Conclusions

It should be noted that analytical MDLs, LODs, and LOQs decreased beginning with the April 2015 sampling event compared to monitoring data from previous events due to a change of laboratories and the utilization of alternative methods. Analytes that were detected during the current event and were ND at or above the higher MDLs during past events include 1-methlynaphthelene, 2-methlynaphthelene, and naphthalene in RHMW04. Consequently, these analytes may have been present at the currently detected concentrations during previous events without being detected and do not necessarily indicate any trend. These compounds were also identified in the method blank and may indicate that at these very low levels, laboratory contamination may lead to false low-level hits. Furthermore, it should be noted that, in general, detections below the LOQ in primary samples, laboratory method blanks, and trip blanks should be subject to scrutiny as they could be false low-level hits resulting from positive interference from laboratory analytical processes (i.e., laboratory contamination).

The data assessment concludes that all data generated during this event are usable for the intended purpose, with the limitations described above.

2.4 OCTOBER 2016 TO APRIL 2018

No COPCs have been detected in RHMW04 from October 2016 onward.

Figure B.7.3-4 to Figure B.7.3-8 show the results for all RHMW04 samples for most COPCs. These figures provide a clear visual display of the data and perspective of occurrence over time with caveats regarding detections in the corresponding blanks and the differences in reporting limits for the laboratories used.

After careful review of the available data and reports, evaluation of the values reported (mostly estimates) in the RHMW04 samples and the COPC contamination in some of the blanks, it is evident that the few RHMW04 COPC detections were almost always during April 2015 to July 2016, the period when ALS/CAS was performing the analysis. This laboratory appeared to have frequent issues with method blank contamination for toluene, TPH-d, TPH-o, and naphthalene. This indicates a systemic issue, which may be a result of that laboratory's low reporting limits, which are lower than any other laboratory used before or after. In general, detections below the LOQ in primary samples, laboratory method blanks, and trip blanks should be subject to scrutiny as they could be false low-level hits resulting from positive interference from laboratory analytical processes (i.e., laboratory contamination) and field artifacts.

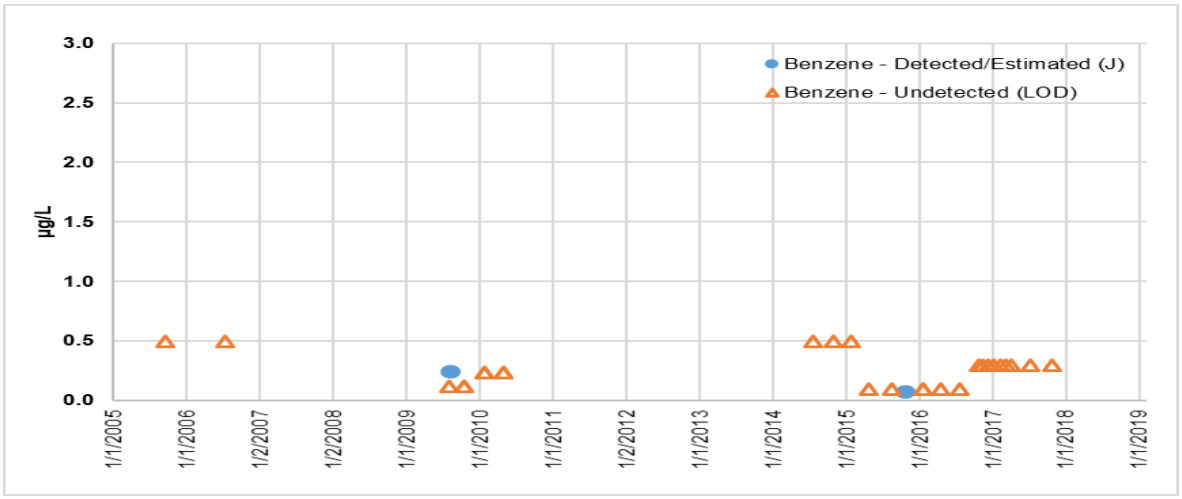

Figure B.7.3-4: RHMW04 Benzene Results

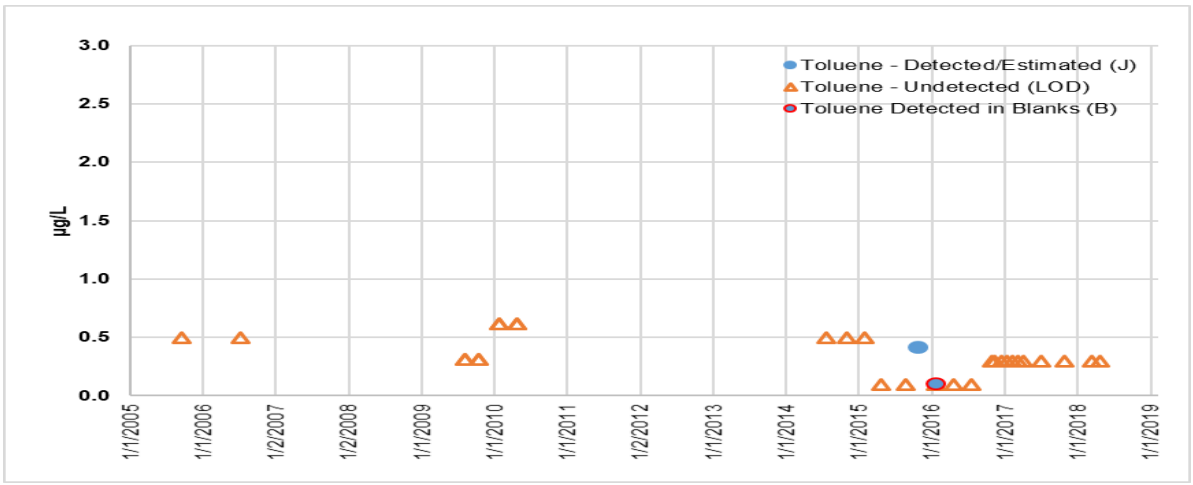

Figure B.7.3-5: RHMW04 Toluene Results

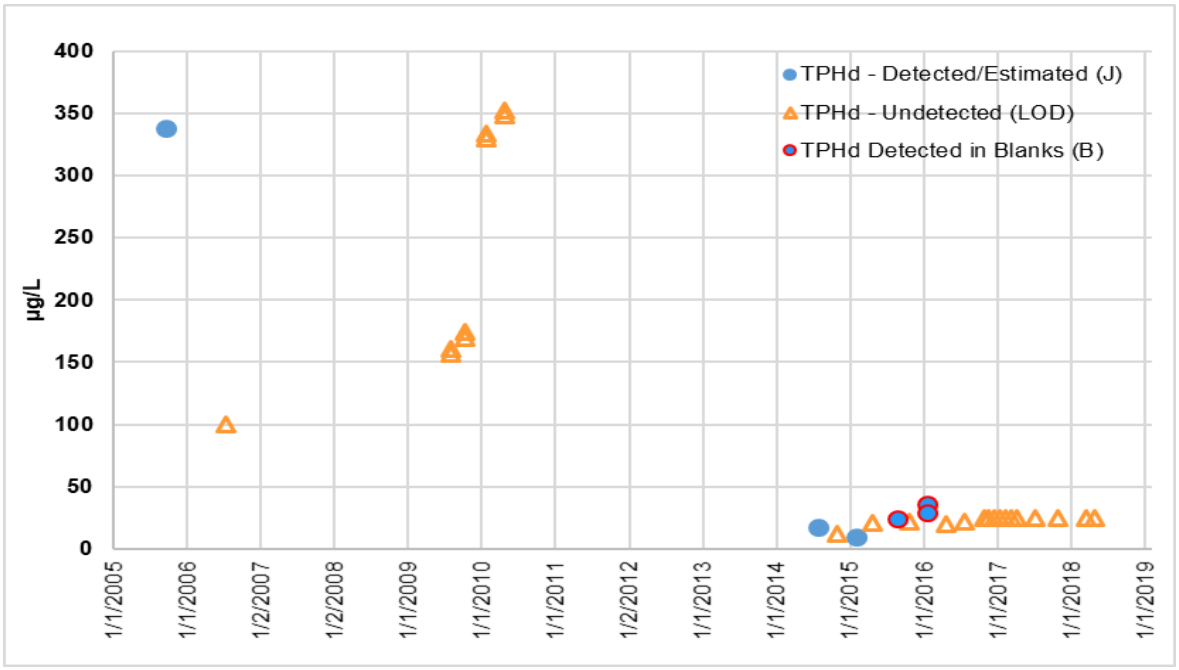

Figure B.7.3-6: RHMW04 TPH-d Results

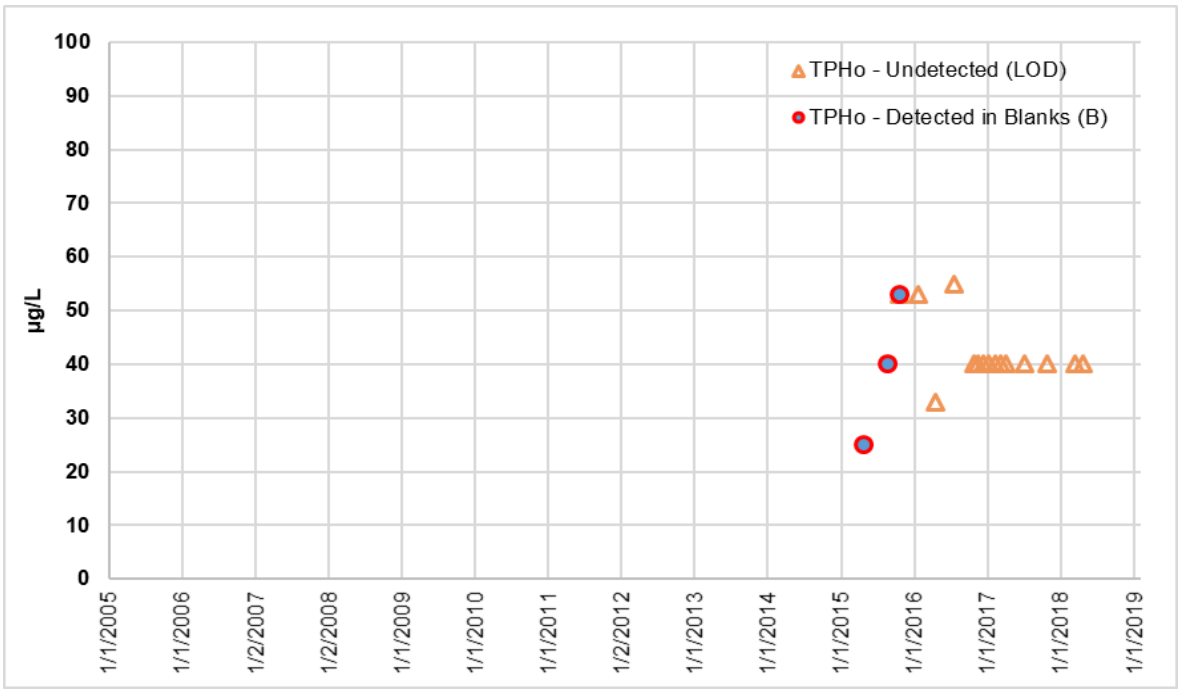

Figure B.7.3-7: RHMW04 TPH-o Results

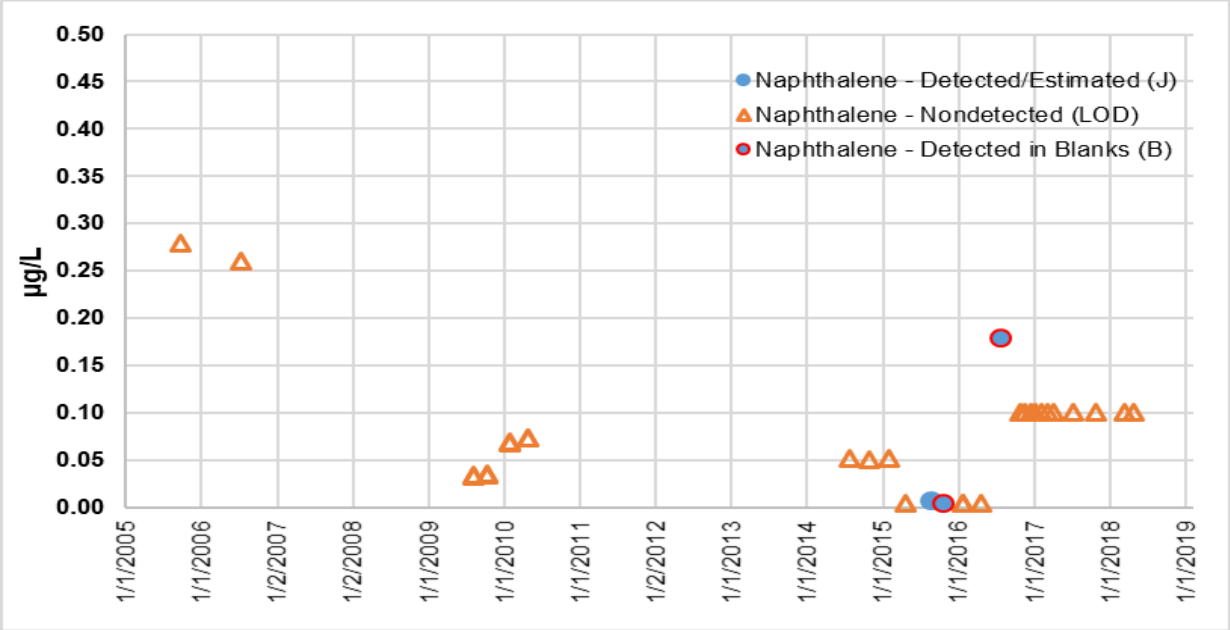

Figure B.7.3-8: RHMW04 Naphthalene Results

3. Conclusions

There is no evidence that would support that RHMW04 was impacted by the 2014 release from the Facility. There are very few COPCs reported, most below quantitation limits, and many are also found in corresponding laboratory and field blanks, indicating potential sample contamination. These few instances coincided with analysis at a laboratory with unusually low reporting concentration levels (April 2015 to July 2016).

4. References

Department of Defense, United States (DoD). 2013. *Department of Defense Quality Systems Manual (QSM) for Environmental Laboratories*. Version 5.0. Final. Prepared by DoD Environmental Data Quality Workgroup and Department of Energy Consolidated Audit Program Operations Team. July.

Department of the Navy (DON). 2016. *Final Third Quarter 2016 - Quarterly Groundwater Monitoring Report, Outside Tunnel Wells, Red Hill Bulk Fuel Storage Facility, Joint Base Pearl Harbor-Hickam, Oahu, Hawaii*. October. Prepared by Element Environmental, LLC, Aiea, HI. Prepared for Naval Supply Systems Command, Fleet Logistics Center Pearl Harbor, JBPHH, HI.

Attachment B.7.4: Evaluation of Low-Level Naphthalene Detections over Time and Laboratory Changes

Evaluation of Low-Level Naphthalene Detections over Time and Laboratory Changes

An evaluation was performed on the low-level detections of naphthalene present in many wells (except for RHMW02 and RHMW01) around the same periods of time. These naphthalene detections occurred when SGS Alaska (January 2008 to July 2010) and Calscience (October 2012 to January 2015) laboratories were used (limit of detection [LOD] 0.05 microgram per liter [µg/L]). Most of the samples analyzed after January 2015 were non-detect for naphthalene. The laboratory used after January 2015 was Columbia Analytical Services (CAS)/ALS, which had a lower LOD (0.005 µg/L) and reported fewer detections at the lower level in most wells than SGS Alaska and Calscience.

These sporadic low-level detections are potentially explained by laboratory artifacts. Low-level detections (i.e., less than 0.1 µg/L) of naphthalene in outlying wells are not consistent with transport of light non-aqueous-phase liquid (LNAPL) through either the vadose or saturated zones. Due to the uncertainty associated with these low-level detections, the available monitoring record is not suitable for evaluating the presence or absence of chemicals of potential concern (COPCs) in individual monitoring wells at concentrations of less than 0.1 µg/L. However, the available monitoring record does support a more reliable evaluation of the presence or absence of COPCs at concentrations above 0.1 µg/L. Therefore, detections of less than 0.1 µg/L for naphthalenes (i.e., 1-methylnaphthalene, 2-methylnaphthalene, and/or naphthalene) do not necessarily indicate impacts from the Facility without additional supporting lines of evidence.

Additionally, EPA Region 9 Laboratory analyzed split samples for all existing monitoring wells during January to March 2017 (all wells except RHMW10 and RHMW11, which were installed after March 2017). 1-Methylnaphthalene, 2-methylnaphthalene, and naphthalene were detected only in RHMW01 and RHMW02. There have been no detections in wells other that RHMW02 since 2016.

Figure B.7.4-1, Figure B.7.4-2, and Table B.7.4-1 present in graphic and tabular format the detections of naphthalenes in many of the monitoring well locations with respect to the analytical laboratory used.

Naphthalene detections do not correlate with the January 2014 release.

Table B.7.4-1: Number of Detections of Naphthalenes at Concentrations >0.10 µg/L

Groundwater Monitoring Location	Number of Detections > 0.10 µg/L			Date(s) of Detections
	Naphthalene	1-Methylnaphthalene	2-Methylnaphthalene	
RHMW2254-01 RHS	0	0	0	—
RHMW01	19	2	3	16: 2008–2012 3: 2015–2016
RHMW02	64	63	64	2005–2018
RHMW03	5	0	0	2008–2014
RHMW04	1	0	0	July 2016 (also detected in the laboratory method blank)
RHMW05	1	0	0	October 2013
RHMW06	0	0	0	—
RHMW07	0	0	0	—
RHMW08	0	0	0	—
RHMW09	0	0	0	—
RHMW10	0	0	0	—
RHMW11	0	0	0	—
HDMW2253-03	1	0	0	April 2013
OWDFMW01	1	0	0	July 2013

Note: RHMW06 and RHMW07 were first sampled in October 2014. RHMW08 and RHMW09 were first sampled in October 2016. RHMW10 was first sampled in May 2017. RHMW11 was first sampled in March 2018.

Figure B.7.4-1. Evaluation of Naphthalene Detections Over Time and Laboratory Changes

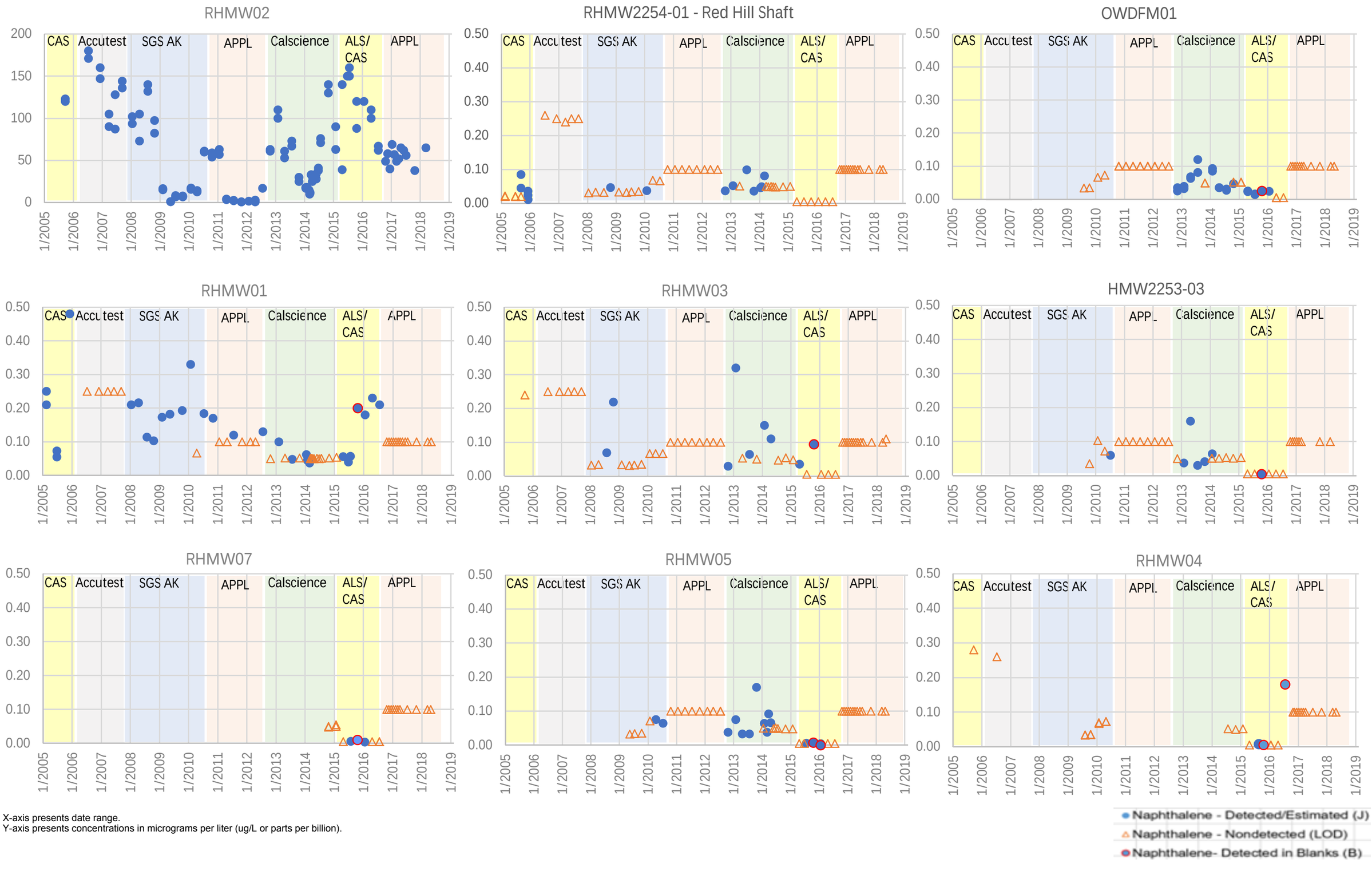

X-axis presents date range.
Y-axis presents concentrations in micrograms per liter (ug/L or parts per billion).

Figure B.7.4-2. Evaluation of Detections of Naphthalene 1-Methylnaphthalene, and 2-Methylnaphthalene Over Time and Laboratory Changes

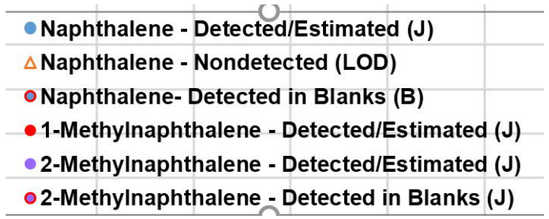

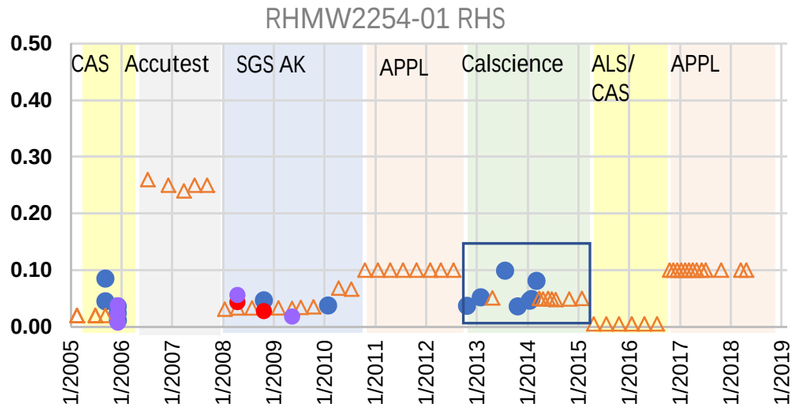

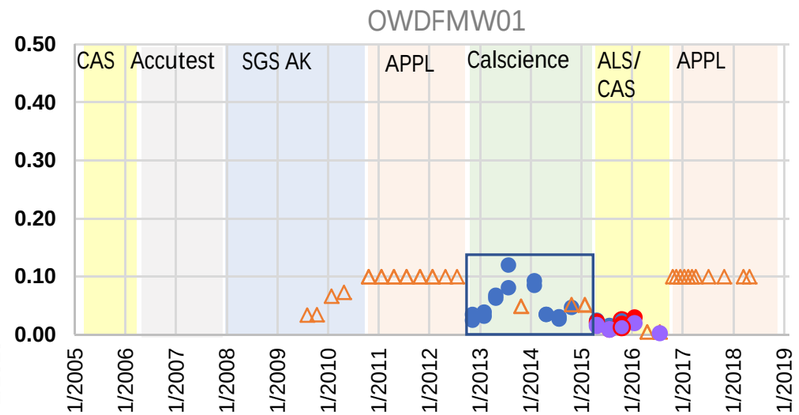

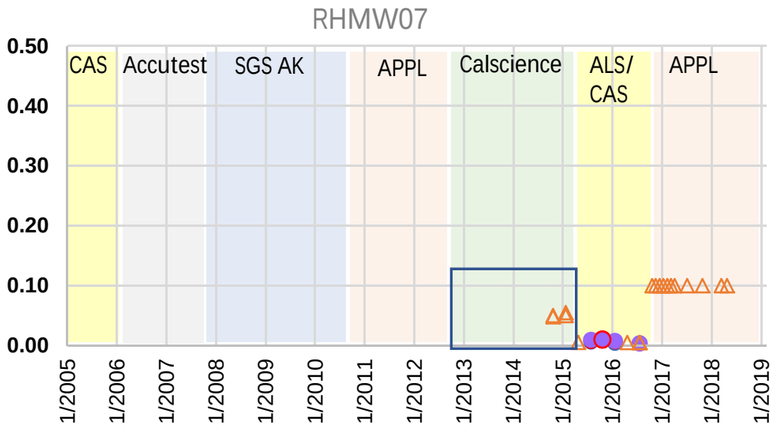

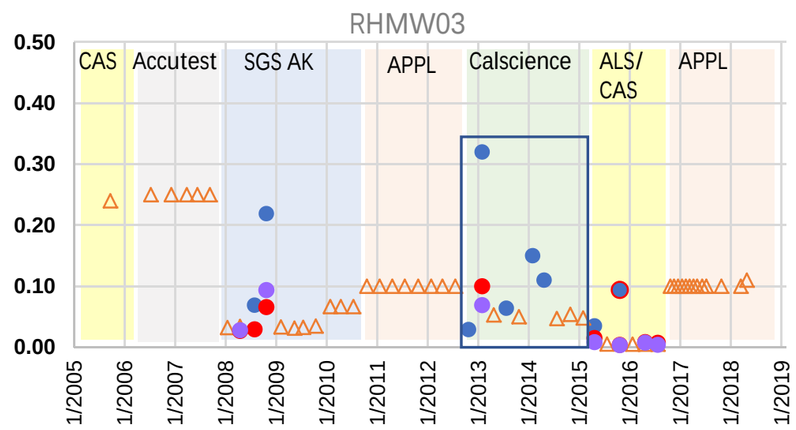

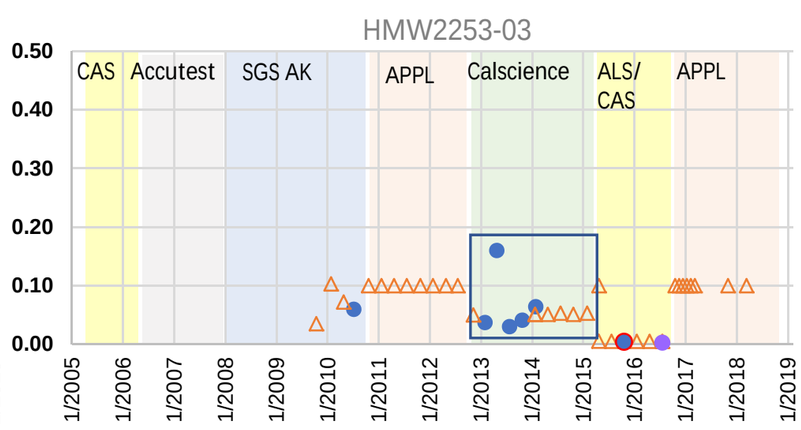

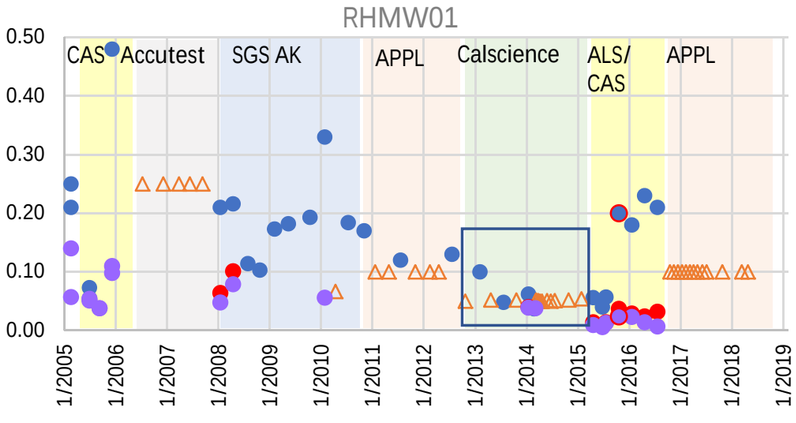

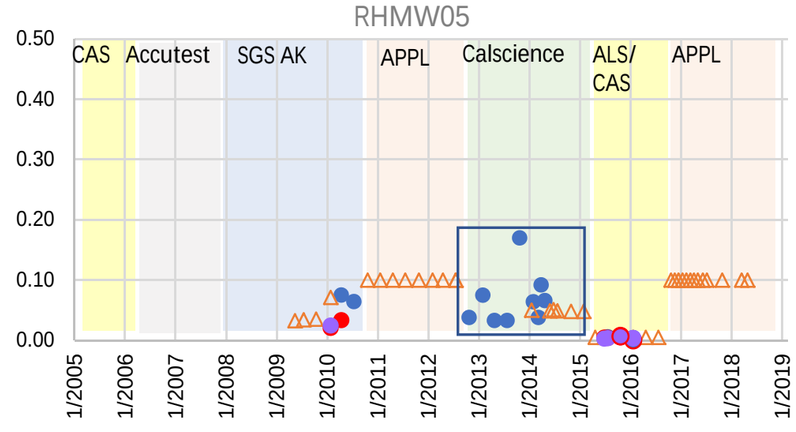

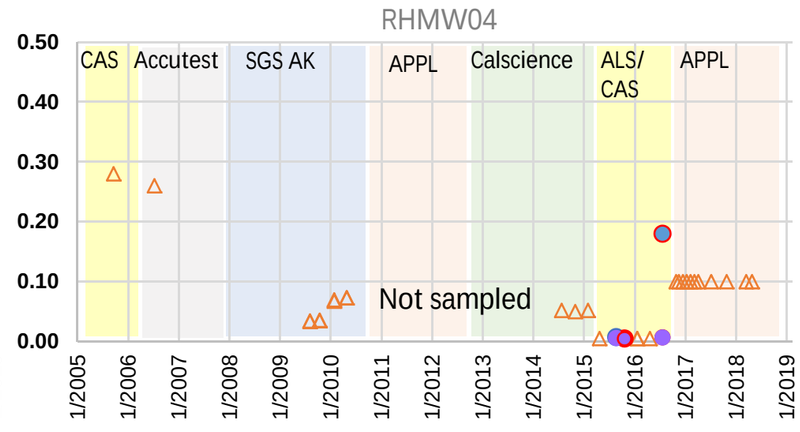

X-axis presents date range.
Y-axis presents concentrations in micrograms per liter (ug/L or parts per billion).